




PALEOGEOGRAPHY, PALEOCLIMATE, AND SOURCE ROCKS

Edited by
Alain-Yves Huc



AAPG Studies in Geology #40

Paleogeography, Paleoclimate, and Source Rocks

Edited by
A.-Y. Huc

AAPG Studies in Geology, No. 40



Published by
The American Association of Petroleum Geologists
Tulsa, Oklahoma, U.S.A.
Printed in the U.S.A.

Copyright © 1995
By the American Association of Petroleum Geologists
All Rights Reserved
Published July 1995

ISBN: 0-89181-048-X

AAPG grants permission for a single photocopy of an item from this publication for personal use. Authorization for additional copies of items from this publication for personal or internal use is granted by AAPG provided that the base fee of \$3.00 per copy is paid directly to the Copyright Clearance Center, 222 Rosewood Drive, Danvers, Massachusetts 01923. Fees are subject to change. Any form of electronic or digital scanning or other digital transformation of portions of this publication into computer-readable and/or transmittable form for personal or corporate use requires special permission from, and is subject to fee charges by, the AAPG.

Association Editor: Kevin T. Biddle
Science Director: Richard Steinmetz
Publications Manager: Kenneth M. Wolgemuth
Special Projects Editor: Anne H. Thomas
Production: Custom Editorial Productions, Inc., Cincinnati, Ohio
Cover illustration adapted from a design by M. Maguet. Adaptation by Rusty Johnson, AAPG Graphics Designer.

**THE AMERICAN ASSOCIATION OF PETROLEUM GEOLOGISTS (AAPG)
DOES NOT ENDORSE OR RECOMMEND ANY PRODUCTS AND SERVICES
THAT MAY BE CITED, USED OR DISCUSSED IN AAPG PUBLICATIONS OR
IN PRESENTATIONS AT EVENTS ASSOCIATED WITH AAPG.**

This and other AAPG publications are available from:
The AAPG Bookstore
P.O. Box 979
Tulsa, OK 74101-0979
Telephone (918) 584-2555; (800) 364-AAPG (USA—book orders only)
FAX: (918) 584-0469; (800) 898-2274 (USA—book orders only)

AAPG
*Wishes to thank the following
for their generous contributions
to*

***Paleogeography, Paleoclimate, and
Source Rocks***



Mobil Exploration & Producing
Technical Center



*Contributions are applied against the production
costs of the publication, thus directly reducing the
book's purchase price and making the volume
available to a greater audience.*

About the Editor



Alain-Yves Huc is currently Head of the Organic Geochemistry group at the Institut Français du Pétrole (also known as IFP, or French Petroleum Institute).

Dr. Huc was educated at the University of Nancy (France) and received his Ph.D. in Organic Geochemistry from the University of Strasbourg (France) in 1978. He spent a year and a half as a postdoctoral fellow at Woods Hole Oceanographic Institution (Woods Hole, Massachusetts) and two years as a CNRS researcher at the Applied Geology Department of the University of Orléans (France). Following that, he joined IFP.

Dr. Huc spent three years on research devoted to the chemical structure of asphaltenes in crude oils. For the next six years, his research interest focused on the study of the sedimentology of organic matter and its application to oil exploration. During the past three years, his main scientific concern has been reservoir geochemistry.

Acknowledgments

I am most grateful to the many individuals who have helped to make this volume possible. In particular, I thank the contributing authors; the reviewers (E. Barron, M. M. Blanc-Valleron, J. Calvert, J. Connan, J. Curiale, H. Cook, T. Cross, W. Dean, J. Dercourt, K. Emeis, A. Fleet, H. Ganz, D. Hollander, J. Golonka, J.-P. Herbin, G. Isaksen, B. Katz, K. Kelts, J. Kriest, M. Mello, P. A. Meyers, M. Moldowan, G. Moore, M. Pasley, J. Rullkotter, M. Stefani, N. Telnaes, F. van Buchem, W. Visser); C. Williams, former AAPG Publications Manager, for guiding us in the volume elaboration; M. F. Bellenoux for secretarial assistance; and M. Maguet for designing the pictorial project on the cover.

Alain-Yves Huc

Table of Contents

| | |
|--|------------|
| Preface | vii |
| Chapter 1 Paleogeography of C _{org} -Rich Rocks and the Preservation Versus Production Controversy <i>Judith Totman Parrish</i> | 1 |
| Chapter 2 Paleoceanography of Marine Organic-Carbon-Rich Sediments <i>William W. Hay</i> | 21 |
| Chapter 3 Factors Controlling the Development of Lacustrine Petroleum Source Rocks—An Update <i>Barry Jay Katz</i> | 61 |
| Chapter 4 Organic Geochemistry of Paleodepositional Environments with a Predominance of Terrigenous Higher-Plant Organic Matter <i>Gary H. Isaksen</i> | 81 |
| Chapter 5 Effect of Late Devonian Paleoclimate on Source Rock Quality and Location <i>Allen R. Ormiston and Robert J. Oglesby</i> | 105 |
| Chapter 6 The Effects of Paleolatitude and Paleogeography on Carbonate Sedimentation in the Late Paleozoic <i>D. A. Walker, J. Golonka, A. Reid, and S. Reid</i> | 133 |
| Chapter 7 Kimmeridgian (Late Jurassic) General Lithostratigraphy and Source Rock Quality for the Western Tethys Sea Inferred from Paleoclimate Results Using a General Circulation Model <i>George T. Moore, Eric J. Barron, and Darryl N. Hayashida</i> | 157 |
| Chapter 8 Paleoclimatic Controls on Neocomian–Barremian (Early Cretaceous) Lithostratigraphy in Northern Gondwana’s Rift Lakes Interpreted from a General Circulation Model Simulation <i>George T. Moore, Eric J. Barron, Karen L. Bice, and Darryl N. Hayashida</i> | 173 |
| Chapter 9 Depositional Controls on Mesozoic Source Rocks in the Tethys <i>François Baudin</i> | 191 |
| Chapter 10 Cenomanian–Turonian Source Rocks: Paleobiogeographic and Paleoenvironmental Aspects <i>Wolfgang Kuhnt and Jost Wiedmann</i> | 213 |
| Chapter 11 The Hydrocarbon Source Potential in the Brazilian Marginal Basins: A Geochemical and Paleoenvironmental Assessment..... <i>M. R. Mello, N. Telnaes, and J. R. Maxwell</i> | 233 |

| | |
|---|-----|
| Chapter 12 | |
| Source Rock Occurrence in a Sequence Stratigraphic Framework: | |
| The Example of the Lias of the Paris Basin..... | 273 |
| <i>G. Bessereau, F. Guillocheau, and A.-Y. Huc</i> | |
| Chapter 13 | |
| The Organic Carbon Distribution in Mesozoic Marine Sediments and the Influence of | |
| Orbital Climatic Cycles (England and the Western North Atlantic) | 303 |
| <i>F. S. P. van Buchem, P. L. de Boer, I. N. McCave, and J.-P. Herbin</i> | |
| Index | 337 |

Preface

A research conference on paleogeography, paleoclimate, and source rocks was held in Paris in July 1992 as a special meeting co-sponsored by the American Association of Petroleum Geologists (AAPG) and the Institut Français du Pétrole (IFP). It was co-convened by Alain-Yves Huc of IFP and Nahum Schneidermann of Chevron Overseas Petroleum. Following the conference, the convenors were asked to make the proceedings available to the public. The convenors duly organized an AAPG Research Symposium on the topic at the 1993 AAPG Annual Meeting and began preparing this volume for publication.

The goal of the research conference was to evaluate current understanding of source rocks as a guide for petroleum exploration. One of the purposes of the conference was to bring together researchers working separately in the fields of climate modeling, paleogeographic reconstruction, and source rock sedimentology. The intent was to ensure cross-disciplinary discussions and to encourage contributions reflecting the various approaches of scientific endeavor involved in the exciting task of studying the occurrence and formation of organic-rich strata. This conference also proposed to create an opportunity for a privileged exchange of ideas among scientists, from both academia and industry, concerning how accumulated experience and existing technology related to source-rock assessment could be transferred to the new needs of the oil industry.

During the course of the conference, special emphasis was placed on paleoplates and paleogeographic reconstructions, paleoclimate recreation and modeling, global source rock distribution, depositional setting of organic-rich sediments, sequence stratigraphy, cyclostratigraphy, and molecular fossils.

The discussions that were led by senior oil industry representatives G. Demaison (consultant), D. Irwin (Texaco), N. Schneidermann (Chevron), B. Tissot (IFP), and C. Tranter (Mobil) identified three main points to be carefully considered for future collaboration with the oil industry.

1. *Interest trends in oil companies:* Because of past intensive worldwide exploration, proved reserves have substantially increased in the last several decades and new discoveries of economically attractive giant fields will become more and more problematic. In view of new producing opportunities worldwide, as well as emphasis on creation of value rather than on finding reserves, reservoir management and reserve

additions in mature basins have become increasingly important. This situation limits the need for deeper knowledge of source rocks and suggests that we transfer and adapt our technology to finer-scale problems. In spite of these developments, however, oil companies continue to explore for additional value in a variety of basin types. This activity is necessary in order to maintain stable and trained teams of exploration geologists and geophysicists in spite of the current adverse economic situation. Accompanying research is consequently still required.

2. *Reduction of risk in exploration:* With respect to the last statement, petroleum explorers need to improve understanding of several points: the scale of investigation (basin scale, field scale, play scale), and the maturity of the considered province.

In very mature basins, the distribution of the source rock, its quality, and its characteristics are usually known. However, in addition, it is important to quantify the generated oil and the trapped oil, and to compare these quantities to the amount of oil that has been discovered. More research effort must be devoted to the development of oil-generation modeling and transfer from source rock to traps, and to quantification of loss during secondary migration.

In less mature basins, the stratigraphic location of the source rock is usually known, but research is required to determine its vertical/lateral extension and quality change. Sequence stratigraphy and cyclicity are promising areas of research. Moreover, this approach is likely to decipher the geometrical and regional relationship between source rocks and reservoir strata and to provide guides for understanding hydrocarbon migration behavior.

In frontier basins, presence or absence of source rocks and a working petroleum system are often unknown. In such instances, the only available guides for predicting the regional presence of organic-rich strata in the sedimentary column are based on paleogeography and paleoclimatic considerations and on geologic analogs. Improvement in paleoclimatology and climate and oceanic circulation modeling is needed, and related research should be supported.

3. *Data and information transfers from oil companies to academia:* In order to efficiently address the research areas identified above, academia needs access to hard data to constrain their results and their models. Unfortunately, academic researchers usually lack money to obtain such data directly. Oil companies currently have a considerable amount of invaluable information, but the data are not easy to collect and sort because they are often not well organized.

Researchers working in climate modeling face specific problems in obtaining global information. The oil companies that may have such data are increasingly organized according to geographical zones, must meet the stringent requirements of their own budgets, and may have little interest in global scale studies. A great effort should be made to ensure that industry data are available in a usable format for academic researchers.

Most of the papers in this volume were presented at the conference. However, a few were solicited later in order to fill in what were believed to be critical gaps in the original list of contributions. The first three chapters address the factors controlling the deposition of organic-rich sediments in marine environments (J. T. Parrish, W. W. Hay) and in lacustrine settings (B. J. Katz). Chapter 4 reviews the specificity of biomarkers related to paleodepositional environments with a predominance of terrigenous higher-plant input (G. H.

Isaksen). Chapters 5 through 11 attempt to integrate the occurrence of source rocks and their geochemical characteristics within a paleogeographic, paleoclimatic (eventually using global climate models), and paleoenvironmental framework. They cover the Late Devonian (A. R. Ormiston and R. J. Óglesby), the late Paleozoic (Walker et al.), the Kimmeridgian in the Western Tethys Sea (Moore et al.), the Neocomian–Barremian in the Northern Gondwana rift (Moore et al.), the Mesozoic of the Tethys realm (F. Baudin), the Cenomanian–Turonian (W. Kuhnt and J. Wiedmann), and on a more regional petroleum theme, the Brazilian margin (M. R. Mello et al.). The final two chapters consider the source rocks in the sedimentary column according to sequential stratigraphy perspective (G. Bessereau et al., F. van Buchem et al.).

Alain-Yves Huc
Nahum Schneidermann

Chapter 1

Paleogeography of C_{org} -Rich Rocks and the Preservation Versus Production Controversy

Judith Totman Parrish
*University of Arizona
Tucson, Arizona, U.S.A.*

ABSTRACT

New analyses of previously examined data sets had the following results: (1) Nearly half of organic-carbon- (C_{org} -) rich units were deposited in geographic settings that do not have modern analogs. (2) If upwelling associated with western boundary currents is included, predicted upwelling zones can explain up to 93% of oil-prone, C_{org} -rich deposits through the Phanerozoic. The remaining deposits occur in only three settings—rift basins; low-latitude, enclosed, epicontinental seaways; and mid-latitude shelves. (3) Thirty-four phosphate deposits can be identified in the literature that are part of the Si-P-C association, which is widely regarded to be indicative of high productivity. Another 100 deposits had one of the pairs of adjacent facies, phosphate-glaucinite or phosphate- C_{org} -rich rock, which occur together in upwelling zones. Together, these account for 82% of the 164 phosphate deposits identified in the literature.

These results support conclusions that high biologic productivity has strongly influenced sedimentation of organic carbon. Although mechanisms for the genesis of anoxia have been widely discussed, mechanisms for the genesis of high biologic productivity have not; it is suggested that consideration be given to mechanisms, in addition to localized upwelling, that might promote high productivity in the oceans and the resulting high organic accumulation in sediments.

INTRODUCTION

One of the most intractable problems in sedimentology concerns the mechanisms by which organic matter accumulates in the geologic record. Numerous papers have been written on the subject, and the discussion has become known informally as the “preservation versus production controversy.” One school of thought, represented by Tyson (Tyson, 1987) and Tyson and Pearson (Tyson and Pearson, 1991), holds that organic matter will accumulate wherever sedi-

ment and/or bottom-water conditions are anoxic, and that biologic productivity, that is, the rate of production of organic matter, is irrelevant, except perhaps in determining the overall organic-carbon (C_{org}) richness. The other school of thought, represented by Calvert, Pedersen, and their colleagues (e.g., Calvert et al., 1992a), holds that organic matter will accumulate wherever biologic productivity in the water column is high—subject to the constraints of water depth—and, further, that the oxygen content of the water above the sediments is irrelevant. The problem

with both these schools of thought is that their conclusions depend strongly on observations in the modern oceans of features that are not preserved in the geologic record, most notably, the oxygen content of the water. Correlations between sedimentary features and conditions in the water column can be observed directly in modern systems (e.g., Savrda et al., 1984), but none of these sedimentary features is unique to a particular set of conditions, so it is very difficult to extrapolate water-column conditions from the features in sedimentary rocks.

Why is this important? The reason is that by delineating the mechanisms whereby C_{org} -rich sediments accumulate, we increase our ability to predict the distribution of such units, with obvious implications for petroleum exploration. For example, if anoxia, independent of productivity, can be shown to be the most important factor in the distribution of C_{org} -rich rocks, then exploration might be concentrated on paleogeographic settings in which stagnant basins were most likely to have occurred. On the other hand, if productivity can be shown to be the dominant factor, then exploration can be concentrated in regions where productivity was likely to have been high.

Anoxia is assumed in discussions of many, if not most, C_{org} -rich, oil-producing, and/or finely laminated, fine-grained dark or black rocks (e.g., Demaison and Moore, 1980; Tyson, 1987; and many others). Discussions of C_{org} -rich rocks and anoxia have shown a strong tendency to be circular because even the simple act of choosing rock units for discussion requires making assumptions about the connections. Almost always, ancient anoxic environments are identified by the presence of finely laminated, fine-grained rocks that are dark in color; commonly, C_{org} - and/or hydrogen-richness are included as criteria. The same studies will sometimes then circle back and discuss the purported genetic relationship between anoxia and C_{org} -rich rocks, with no discussion of independent indicators of anoxia that would potentially falsify the hypothesis that anoxia and C_{org} -rich rocks are related.

In this paper, evidence is presented that the assumption of the connection between anoxia and the deposition of C_{org} -rich rocks is weak, and that more evidence exists for the relationship of C_{org} -rich rocks and high biologic productivity. This paper is structured as follows:

1. The distribution of C_{org} -rich rocks is discussed in two contexts, the distribution of anoxia and the distribution of upwelling (high-productivity) zones in the oceans. This section includes two new analyses: (1) a brief summary of how the data on C_{org} -rich rocks from Parrish (1982) and Parrish and Curtis (1982) fit into a classification of the geographic settings for anoxic water masses and (2) a re-analysis of some of these data for correspondence of oil-prone, C_{org} -rich rocks with predicted upwelling zones.

2. Sedimentary and paleontologic indicators of anoxia and high productivity are discussed in terms of their effectiveness as indicators and to review the limitations on the methods. This section includes a new compilation from the literature of deposits that contain some of those indicators.

3. The preservation versus production controversy is discussed in light of the above, and the suggestion is made for further research on high biologic productivity in ancient oceans.

Discussion will be limited to marine environments, as the processes that operate in lacustrine environments may be substantially different (see papers in Fleet et al., 1988).

METHODS AND RESULTS

Geography of C_{org} -Rich Sediments and Rocks

Background

The geographic settings in which anoxic water masses occur today include four types: (1) open continental shelves; (2) enclosed or semi-enclosed, silled basins floored by oceanic or transitional crust; (3) enclosed or semi-enclosed, silled coastal basins floored by continental crust; and (4) basins that are combinations of these, such as silled basins perched on open continental shelves. One of the few modern epeiric seas, the Baltic Sea, contains anoxic water in the deep basins, but the anoxia is probably related to input of anthropogenic nutrients (Demaison and Moore, 1980), so the Baltic Sea will be excluded from this discussion. Anoxic open oceans, in which oceanic anoxic events are thought to have occurred, and epeiric seaways are not included at this point because they have no modern analogs and the evidence cited for anoxia in those settings is commonly limited to the presence of C_{org} -rich rocks. Thus, to cite these as settings for anoxia is to create a circular argument. I return to the problems of organic accumulation in epeiric seaways and open oceans in the discussion.

On modern, open continental shelves, anoxic water masses occur in upwelling zones, where biologic productivity is high; examples are Peru-Chile (Burnett et al., 1983), Namibia (Brongersma-Sanders, 1948; Calvert and Price, 1971), and the Arabian Sea (Demaison and Moore, 1980; Banse, 1968). Basins floored by oceanic or transitional crust that have anoxic water masses include the Gulf of California, where biologic productivity is high (Calvert, 1966), and the Black Sea (Shimkus and Trimonis, 1974; Glenn and Arthur, 1985), which is stratified. Saanich Inlet and similar basins (see citations in Calvert, 1987) exemplify silled, coastal basins containing anoxic water masses. Anoxic water masses also occur in settings that are combinations of the above, including the Cariaco Trench (Fukuoka et al., 1964) and the borderland basins of southern California (Emery, 1960), which are silled basins perched on open continental shelves. The Cariaco Trench and the California borderland basins experience upwelling, but also are resistant to overturn and oxygenation by virtue of the basin sills (Emery et al., 1962). The Orca Basin is a density-stratified basin (e.g., Leventer et al., 1983) perched on an open continental shelf within a large, semi-enclosed basin (the Gulf of Mexico).

Methods and Results

Paleogeography of C_{org}-Rich Rocks

A global survey of C_{org}-rich rocks (≥ 0.5 wt% total organic carbon) that included much proprietary industry data was compiled by Parrish (1982) and Parrish and Curtis (1982). Their data included 426 localities of C_{org}-rich rocks, with "locality" defined as all such deposits for a particular age within 5° latitude-longitude (thus giving more weight to very widespread deposits; see Parrish, 1982, for further discussion). This is a large and widespread data set and provides the opportunity for a crude first pass at examining the paleogeography of environments in which significant amounts of organic matter accumulated.

The paleogeographic analysis presented here has two limitations. First, continental shelves were much wider at times in the past than they are today, and a wide continental shelf that has free water exchange with the open ocean could, in some paleogeographic configurations, be hard to distinguish from an epeiric seaway. Moreover, the boundaries of the shelves and seaways changed markedly even during intervals represented by single paleogeographic maps, and because these boundaries were not determined for each C_{org}-rich unit by Parrish (1982) and Parrish and Curtis (1982), an arbitrary geographic cutoff for defining open shelf, as opposed to epeiric seaway, was established at 1000 km from the paleogeographic shelf edge (Scotese et al., 1979; Ziegler et al., 1983). Second, distinguishing small, silled, coastal basins might be difficult in the geologic record; they might be reconstructed as part of the open-shelf setting.

Only half (171, 51%) of the localities for C_{org}-rich rocks occurred in paleogeographic settings that might be regarded as analogs to the modern anoxic settings, that is, on open continental shelves (including perched, silled basins), or in enclosed or semi-enclosed, silled basins floored by ocean crust (off the shelf edge in tectonically restricted seaways). Twenty-four (7%) localities were in the deep sea, that is, off the shelf edge in unrestricted oceans (a number that would be considerably higher if the data were compiled now, owing to new data gathered by the Ocean Drilling Project). These are nearly all Cretaceous in age and were deposited during so-called oceanic anoxic events. The remaining 138 localities (41%) were deposited in epeiric seaways, either >1000 km from the shelf edge or in epicontinental marine basins isolated from the open ocean by land.

C_{org}-Rich and Oil-Prone Rocks and Predicted Upwelling

The distribution of high biologic productivity through geologic time has been predicted using climate models. Unlike the distribution of anoxia through geologic time, predictions of the distribution of high biologic productivity through geologic time are independent of the data (Parrish and Curtis, 1982; Parrish, 1982; Kruijs and Barron, 1990). The climate models have predicted the distribution of upwelling in the oceans, which has then been taken to be the distribution of high biologic productivity. As discussed

at length by Parrish (1982), upwelling zones are not necessarily highly productive, so equating upwelling and high productivity is not an ideal approach, but model capabilities do not permit greater sophistication at present.

In the forgoing analysis and in the original studies by Parrish (1982, 1987a) and Parrish and Curtis (Parrish and Curtis, 1982), all C_{org}-rich rocks that plotted in marine settings on the paleogeographic maps were included, whether or not information about the type, quality, and environment of deposition of the organic matter was available. In the following analysis, only the data on rocks that were interpreted to be oil prone were included. The interpretation of quality for most of the data was made by the oil companies who compiled the data and was based principally on hydrogen index; hydrogen-richness has been stressed as important in the discussion of petroleum source rocks (Demaison, 1991). Additional data on hydrogen-rich rocks were added from the literature to the original data compiled by Parrish (1982, 1987a) and Parrish and Curtis (Parrish and Curtis, 1982). A total of 167 localities (as defined above and in Parrish, 1982) are analyzed here; these rocks have total organic carbon values ≥ 0.5 wt% and either were interpreted as oil prone by the original workers or have hydrogen indices ≥ 350 (Tissot and Welte, 1978).

The data were plotted on paleogeographic maps produced by Scotese and Golonka (1992) (Figures 1–10). The paleogeographic reconstructions for most of the Paleozoic and for the early Mesozoic are significantly different from the ones used by Parrish (1982, 1987a; Parrish and Curtis, 1982). For these time periods, new predictions of upwelling were generated; these are available on request from the author. The distribution of data on oil-prone, C_{org}-rich rocks was compared with the distribution of predicted upwelling zones, generally after the methods of Parrish (1982). The one departure from the method of Parrish (1982) was that, for this study, the predictions of wind-driven upwelling were relaxed to include all shelf area that might have experienced upwelling, depending on (1) the bathymetry of the shelves and (2) the intrusion of high-latitude divergence on the shelves. By contrast, Parrish (1982) took the much more conservative approach of assuming that upwelling would occur only at the shoreline. However, as she pointed out, this would not necessarily be the case on a broad continental shelf. Parrish (1982) and Parrish and Curtis (1982) were not consistent in their predictions of high-latitude divergence.

The results of the new analysis are presented in Table 1. Of 167 oil-prone, C_{org}-rich rocks, 144 (86%) corresponded to predicted upwelling, another 9 (5%) were possibly explained by upwelling by virtue of their proximity to predicted upwelling zones, and 14 (8%) could not be explained by upwelling. Thus, limiting the analysis to oil-prone, C_{org}-rich rocks results in a far higher "success" rate for upwelling predictions than originally reported (55%; Parrish, 1987a). There are two explanations for this increase. First, the paleogeographic reconstructions are better, and








| | | |
|---|---|--|
|  | oil-prone rocks that can be explained by predicted upwelling | Continents: AA Antarctica + Australia An Antarctica Au Australia Af Africa As Asia B Baltica (western Europe) E western Europe G Gondwana Gr Greenland I India La Laurentia (North America) Lr Laurussia (North America + western Europe) N North America P Pangea Pe western European portion of Pangea Pg Greenland portion of Pangea Pn North American portion of Pangea Ps Siberian portion of Pangea S Siberia SA South America |
|  | oil-prone rocks that might be explained by predicted upwelling | |
|  | oil-prone rocks that might be explained by upwelling associated with a western boundary current | |
|  | oil-prone rocks that cannot be explained by predicted upwelling | |
|  | predicted upwelling zones | |
|  | shoreline | |
|  | edge of continental shelf | |

Figure 1. Symbols and abbreviations used in Figures 2–10. In all figures, only those regions and predicted upwelling zones that are relevant to the plotted data are shown. The paleogeographic reconstructions are plotted on Mollweide equal-area projections (Scotese and Golonka, 1992), and the map edges are illustrated as curved boundaries where appropriate. Distortion of the shapes of the continents is common close to the sides of the projections; for example, in Figure 2, Gondwana is distorted because of its proximity to the edge of the projection. Refer to Table 1 for the dates of the paleogeographic reconstructions.

therefore the climate-model and resulting upwelling predictions are better. Second, much of the non-oil-prone data in the original analysis could have come from marginal marine or even continental rocks that were not identified as such and that plotted in marine environments because of limitations on the resolution of the global paleogeographic maps. Such rocks would not be expected to correspond with upwelling zones.

Of the 14 deposits that did not correspond to predictions of wind-driven upwelling, 12 occurred in three types of environments. These are: (1) rift basins—6 in the Jurassic and Cretaceous; (2) low-latitude, mostly enclosed, epicontinental seaways—5 in the Devonian, Permian, and Late Cretaceous; and (3) mid-latitude shelves—1 in the Cretaceous. Two deposits in the middle Eocene did not correspond with wind-driven upwelling, but did occur in an area very likely affected by a western boundary current such as the Gulf Stream. Such settings have upwelling and high productivity, but the upwelling is not wind driven (see discussion in Parrish, 1982). For the purposes of this paper, which focuses on productivity, these deposits are regarded as explained by high productivity.

Sedimentologic Signatures of High Biologic Productivity

Background and Methods

The sediments in many well-developed modern upwelling zones have a unique combination of authigenic components that is partly controlled by the oxygen gradient (Burnett et al., 1983; Baturin, 1983; Calvert and Price, 1983). In addition to the C_{org} -rich sediment, these are phosphorite, glauconite, and biogenic silica. The siliceous component is pervasive in the system and is especially abundant in the C_{org} -rich and phosphatic facies. By contrast, the phosphate and glauconite form distinct zones rimming a central zone of C_{org} -rich sediment, phosphate in the inner zone and glauconite in the outer zone (Burnett et al., 1983; Baturin, 1983; Bremner, 1983). This array of facies should be preserved in the geologic record. Indeed, the few ancient C_{org} -rich deposits whose interpretation as upwelling deposits is undisputed have most of these features. Thus, it is worthwhile examining the distribution of these types of deposits.

Of the four lithologies—phosphorite, C_{org} -rich rock, glauconite, and biogenic siliceous rock (hereafter referred to by the less precise but shorter term,

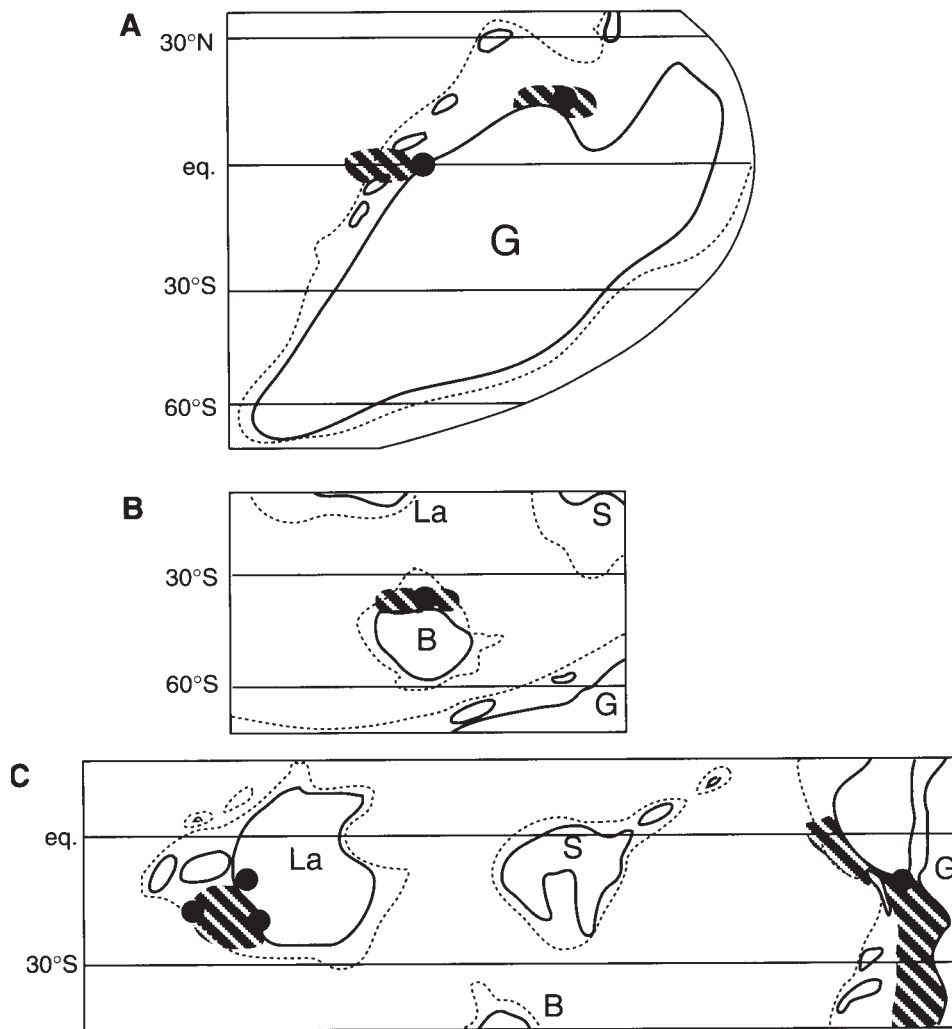


Figure 2. Data on C_{org} -rich rock and predicted upwelling zones for (A) Early Cambrian, (B) Late Cambrian, (C) Early Ordovician. See Figure 1 for symbols and notes.

chert)—chert and phosphorite are most closely tied to high productivity in the literature (Sheldon, 1964; McKelvey, 1967; Cook and McElhinny, 1979; Burnett and Lee, 1980; Burnett et al., 1980, 1983; Cook et al., 1990; Hein and Parrish, 1987). The association of chert, phosphate, and C_{org} -rich rock is sometimes referred to as the Si-P-C association and is widely regarded to be an excellent indicator of high productivity (Cook, 1976; Parrish et al., 1983). Glauconite is not an indicator of productivity, but its formation as an authigenic mineral is favored by the conditions that are created by the high flux of organic matter to the sediments (Mullins et al., 1985).

Extensive databases on chert and phosphate deposits and their associated lithologies have been collected by Parrish et al. (1983, 1986), Parrish (1983, 1990), and Hein and Parrish (1987). Although chert may record high biologic productivity in deep ocean basins (Hein and Parrish, 1987; Lisitsyn, 1977), phosphorite does not form in the deep ocean. For the purposes of this study, then, the search for ancient upwelling deposits was limited to the databases on phosphate deposits, supplemented with information from Parrish (1987b) and Parrish and Gautier (1993).

Results and Discussion

One hundred sixty-four (164) phosphate deposits are associated with either glauconite, chert, C_{org} -rich rock, or a combination of these three (Figure 11). Eleven units (including, in some cases, their lateral equivalents) had all four lithologies and another 23 units had the Si-P-C association, lacking only glauconite. Thus, 34 units, 21% of the total, can be confidently interpreted as upwelling deposits.

Although the association of C_{org} -rich sediment, phosphate, and glauconite occurs in distinct facies in upwelling zones, this association can be difficult to interpret from the literature owing to a lack of detail about geographic and stratigraphic relationships. Some deposits have a minor phosphatic phase (e.g., the Monterey Formation; Mew, 1980) that might be overlooked, or the lateral, correlative upwelling facies might not have been identified. This might be especially true for deposits known only from core or limited outcrops. It is noteworthy, therefore, that the combinations of phosphate- C_{org} -rich rock (without chert) and phosphate-glauconite (with or without chert) make up another 100 (61%) of the phosphate

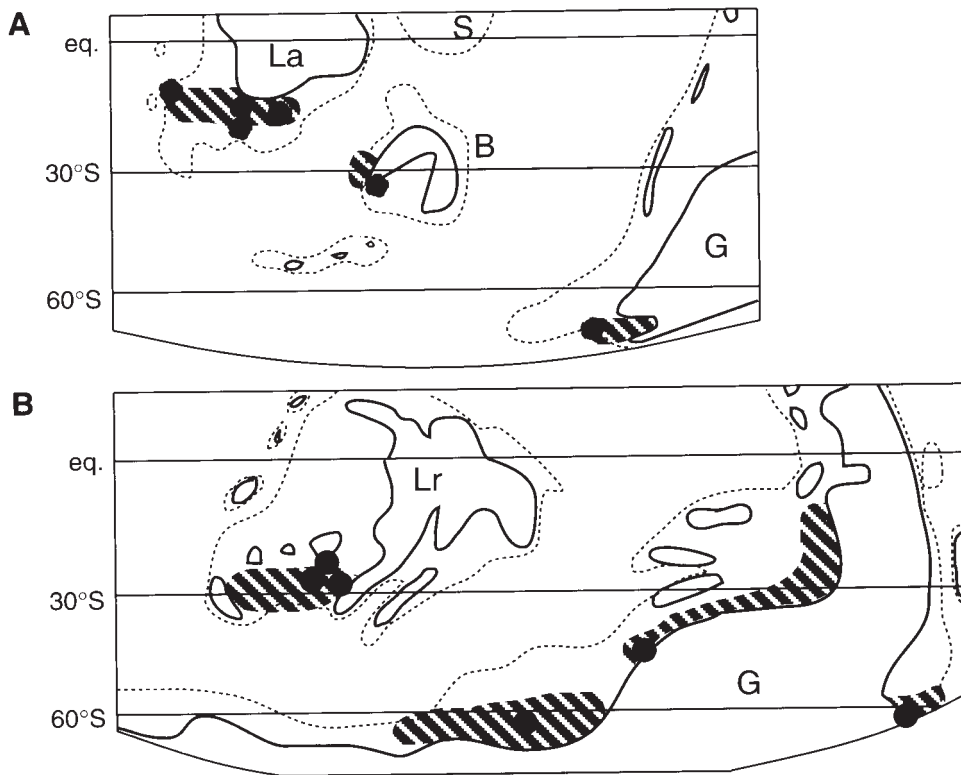


Figure 3. Data on C_{org} -rich rock and predicted upwelling zones for (A) Middle Ordovician, and (B) middle Silurian. See Figure 1 for symbols and notes.

deposits. This is significant because if only part of the upwelling deposit is preserved, one should find only those lithologies that were deposited adjacent to each other. The absence of chert merely reflects the fact that silica-secreting plankton were not always the most productive in ancient upwelling zones (e.g., Jarvis, 1980). The remaining 30 deposits were ones in which phosphorite occurred only with chert.

The Miocene Monterey Formation of California and the Permian Phosphoria Formation of the Rocky Mountains have so far remained relatively unquestioned as ancient counterparts to modern upwelling zones. Parts of the Monterey Formation were deposited in settings similar or identical to the southern California borderland basins and the margin of Peru (Pisciotta and Garrison, 1981; Soutar et al., 1981). The Monterey contains minor amounts of phosphate (Mew, 1980; Pisciotta and Garrison, 1981), but is notable for its thick units of finely laminated and C_{org} -rich diatomite (Ingle, 1981).

By contrast, the Phosphoria Formation was deposited on a shelf whose exact paleogeographic configuration and setting relative to the open ocean are not well understood. Nevertheless, the Phosphoria is one of the largest phosphate deposits in the world, and no reasonable mechanism other than upwelling has been proposed to supply the requisite amount of phosphate to such a limited area over such a short time, within the late Guadalupian (Wardlaw, 1980), certainly <5 m.y. and perhaps as short as ~1 m.y. (Harland et al., 1982). The Phosphoria also contains thick, bedded chert and C_{org} -rich rock (McKelvey et al., 1967; Maughan, 1980). During deposition of the Meade Peak

Member, when relative sea level was highest (Wardlaw, 1980), segregated facies of C_{org} -rich rock, phosphate, and glauconite were formed, similar to those observed in modern upwelling zones (Wardlaw, 1980; J. T. Parrish, field observations).

The major objection raised to the use of phosphorite as an indicator of high productivity has come from work by O'Brien and Heggie (1988; also O'Brien et al., 1988; Heggie et al., 1988), who noted that iron- and phosphate-rich nodules off southeastern Australia (Cook and Marshall, 1981; O'Brien and Veeh, 1983) form by the concentration of both iron and phosphate in the sediments through a series of oxidation-reduction reactions. The significance of this mechanism is that it can function in the absence of abundant C_{org} -rich and biogenic siliceous sediments (Heggie et al., 1988) and requires that the iron- and phosphate-bearing minerals form in the same place (O'Brien et al., 1988). Productive upwelling zones, on the other hand, commonly have C_{org} -rich and biosiliceous sediments and the phosphate and glauconite occur as spatially distinct facies (Burnett et al., 1983).

Glenn and Arthur (1990) invoked a chemical mechanism similar to O'Brien and Heggie's (1988) to explain the Cretaceous glauconitic and phosphatic (as well as C_{org} -rich and cherty) sediments of Egypt because they did not find upwelling over a wide continental shelf plausible (see discussion of nutrient supply and upwelling over wide continental shelves in Parrish, 1982). However, unlike the sediments on the Australian shelf, the glauconitic and phosphatic facies in the Egyptian deposits are segregated vertically and laterally (Glenn and Arthur, 1985), forming an associa-

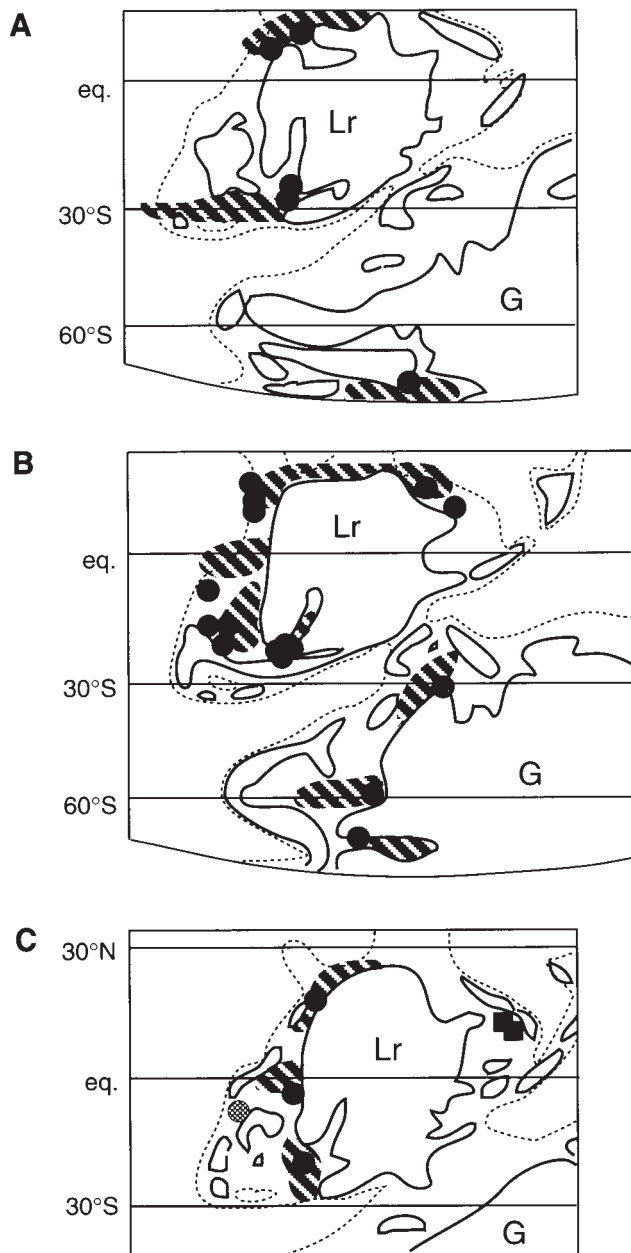


Figure 4. Data on C_{org} -rich rock and predicted upwelling zones for (A) Early Devonian, (B) Middle Devonian, (C) Late Devonian. See Figure 1 for symbols and notes.

tion very similar to that of the Meade Peak Member of the Phosphoria or the Triassic Shublik Formation of Alaska (Parrish, 1987b). If the two phases formed contemporaneously or nearly contemporaneously, as suggested by Glenn and Arthur (1990), it is difficult to see how the sorting mechanisms that they invoked could segregate the minerals so effectively.

DISCUSSION

The results of the three analyses presented here can be summarized as follows:

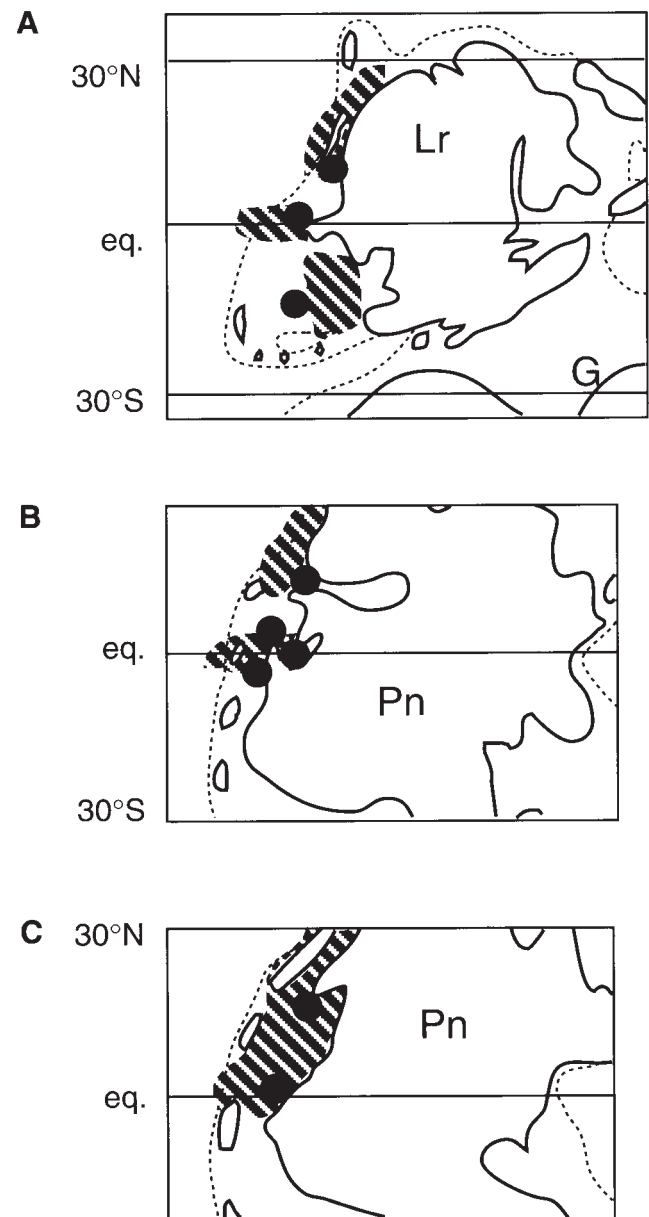


Figure 5. Data on C_{org} -rich rock and predicted upwelling zones for (A) Early Carboniferous, (B) Late Carboniferous, (C) Early Permian. See Figure 1 for symbols and notes.

1. Anoxia occurs in several geographic settings today, and some of these settings have paleogeographic counterparts in which C_{org} -rich rocks occur. However, nearly half of C_{org} -rich rocks occur in paleogeographic settings that do not have modern analogs as settings for anoxia.

2. More than 90% of C_{org} -rich rocks correspond with, or are near, predicted ancient upwelling zones.

3. The facies assemblage that is characteristic of highly productive upwelling zones today is much more common in the geologic record than has been previously reported.

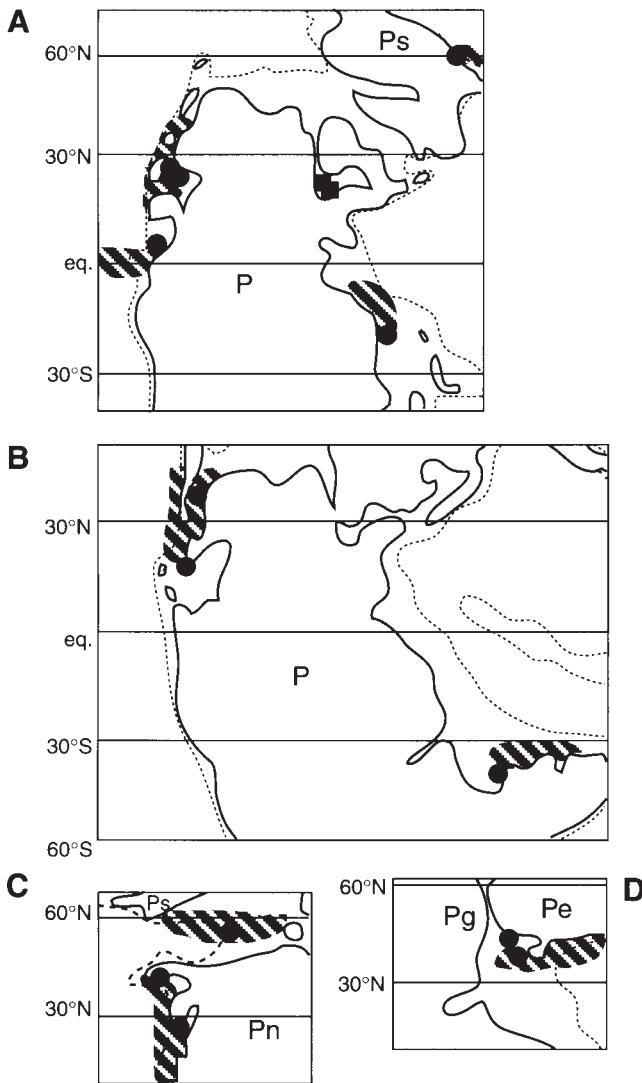


Figure 6. Data on C_{org} -rich rock and predicted upwelling zones for (A) Late Permian, (B) Early Triassic, (C) Late Triassic, (D) Early Jurassic. See Figure 1 for symbols and notes.

What are the implications of these results for the preservation versus production controversy and the deposition of C_{org} -rich rocks? First, no model currently in use has predicted the distribution of anoxia in the past; studies of anoxia in the past have always been based on the assumption that laminated, dark, C_{org} -rich rocks were deposited in anoxic settings. No independent method of determining anoxia in the geologic record has been devised apart from the use of modern analogs, and, as shown here, nearly half of C_{org} -rich rocks occur in paleogeographic settings that have no modern analogs as settings for anoxia. This study has quantified what was recognized implicitly in the establishment of the concept of oceanic anoxic events. Because so many deposits do not have modern analogs, the distribution of C_{org} -rich rocks has ended up being used as *a priori* evidence for anoxia. Any

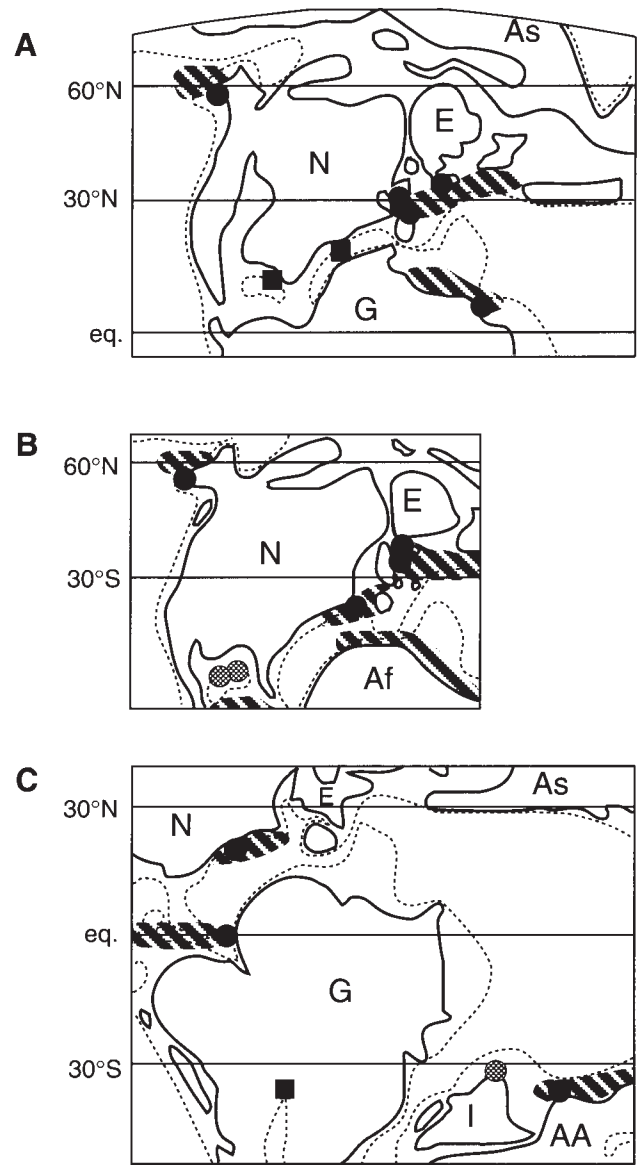


Figure 7. Data on C_{org} -rich rock and predicted upwelling zones for (A) Middle Jurassic, (B) Late Jurassic, (C) early Early Cretaceous. See Figure 1 for symbols and notes.

attempts, therefore, to discuss the influence of anoxia on organic accumulation in the past have been forced to fall back on circular arguments.

By contrast, the distribution of upwelling zones can be predicted with independent models (Parrish and Curtis, 1982; Parrish, 1982; Kruijs and Barron, 1990). The predictions are subject to revision as both the climate models and the paleogeographic maps that are put into the models are revised, but they retain their independence. Revisions of previously published models have resulted in upwelling predictions that can explain the distribution of as much as 93% of oil-prone, C_{org} -rich rocks. The second implication of this study for the preservation versus production contro-

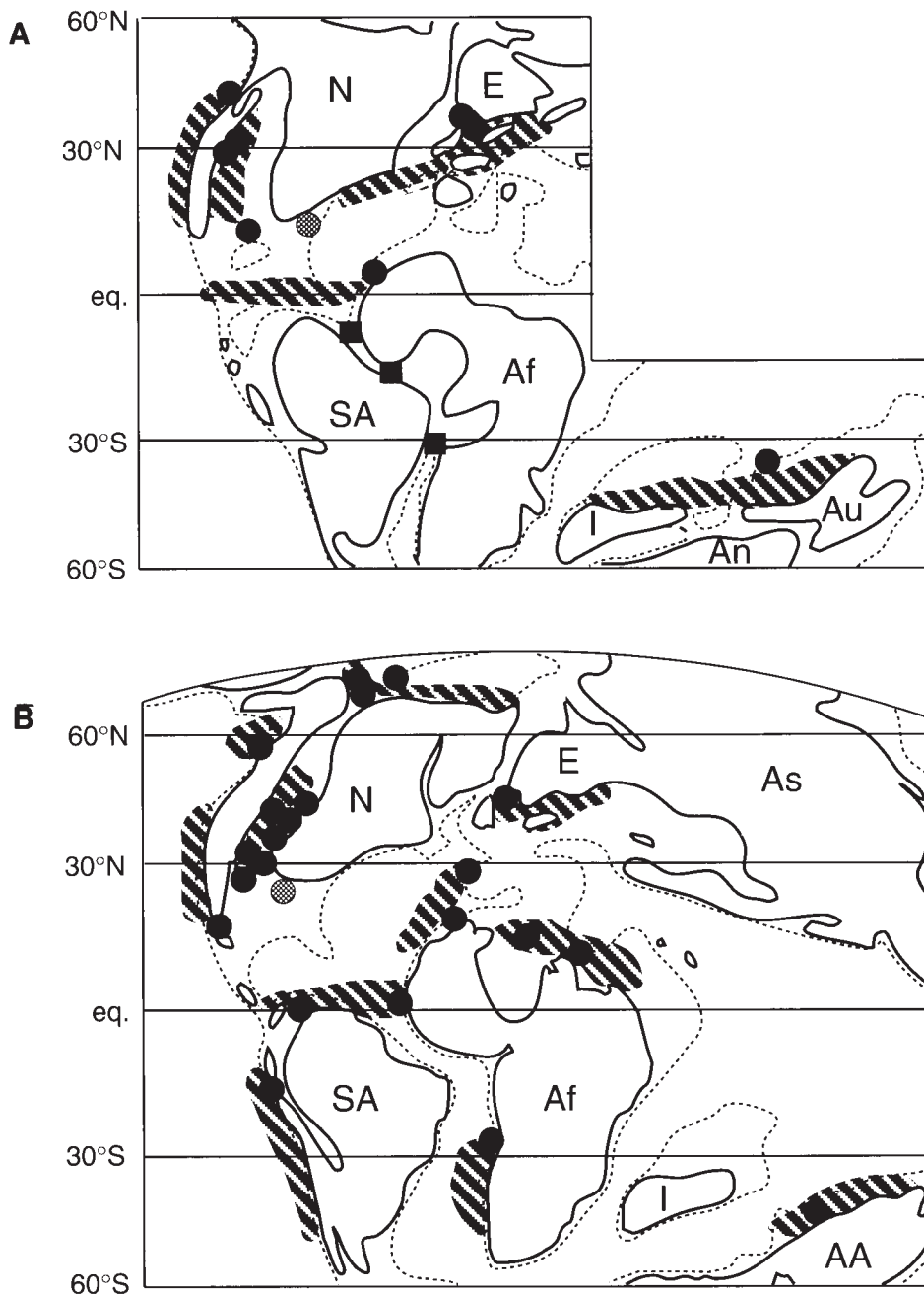


Figure 8. Data on C_{org} -rich rock and predicted upwelling zones for (A) late Early Cretaceous, (B) early Late Cretaceous. See Figure 1 for symbols and notes.

versy, then, is that upwelling and high productivity might have played a larger role in the accumulation of C_{org} -rich rocks than previously thought. Revisions of the paleogeography and limitation of the study to oil-prone rocks has resulted in a much higher correspondence between the distribution of such deposits and predicted upwelling than in previous studies.

Despite the success of the upwelling models, some C_{org} -rich rocks are not explained by the upwelling models. The task is to explain those deposits that do not correspond with upwelling predictions. The best way to study the importance of productivity in the deposition of C_{org} -rich rocks would be some method of calculating paleoproductivity. Direct geologic evi-

dence is always the best way to study processes in the geologic record; models are a relatively poor substitute because of the inherent problems of model construction and verification (Oreskes et al., 1994). However, although calculations of productivity based on organic matter accumulation appear to work well in modern and submodern sediments, they are either inapplicable or questionable for older deposits (Müller and Suess, 1979; Bralower and Thierstein, 1984, 1987; Schrader, 1992; Sarnthein et al., 1992; Abrantes, 1992; see discussion in Parrish and Gautier, 1993). Alternatively, indicators, other than the C_{org} -rich rock, of productivity or anoxia not related to productivity also would be helpful. The following is a brief review of

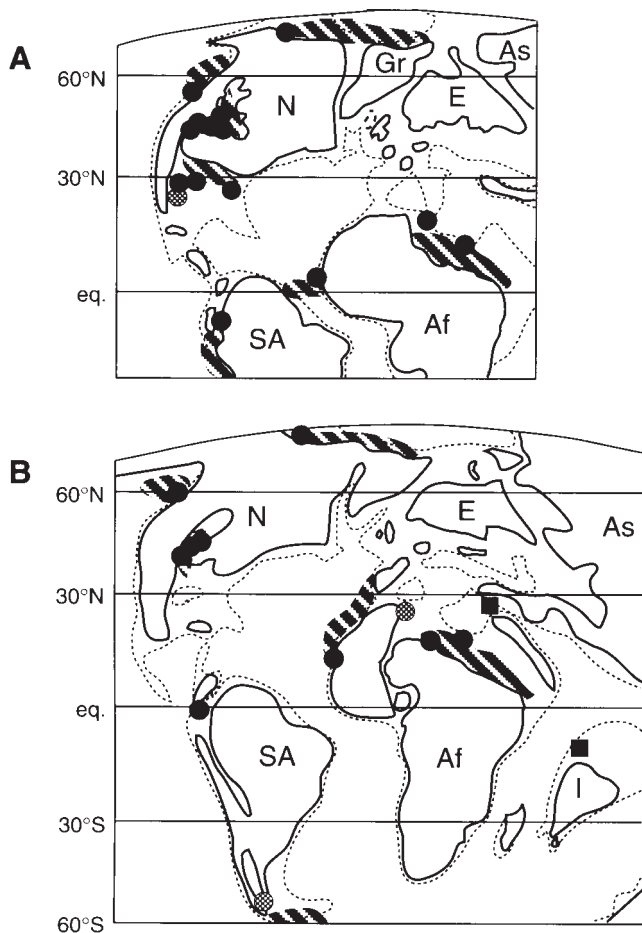


Figure 9. Data on C_{org} -rich rock and predicted upwelling zones for (A) middle Late Cretaceous, (B) late Late Cretaceous. See Figure 1 for symbols and notes.

some of the types of information that have been applied to the study of C_{org} -rich rocks.

Geologic Indicators of High Productivity or Anoxia

The results of the analysis of phosphate deposits in this paper show that the facies assemblage typical of the most productive, modern coastal upwelling zones is common in the geologic record. However, such assemblages have not been documented for most of the C_{org} -rich deposits analyzed here. Lacking such information, what other criteria might be used to distinguish high-productivity deposits in the geologic record? Like C_{org} -richness itself, many criteria have been cited as indicative of anoxia or of high productivity, depending on the preferred interpretation. Criteria discussed below are summarized in Table 2.

Indicators of High Productivity

In addition to the facies assemblage of C_{org} -rich rock, chert, phosphate, and glauconite, many other characteristics of modern high-productivity environments can be used as indicators of high productivity in the geologic record (Table 2). These include abundant fish scales and

bones (Diester-Haass, 1978; Suess, 1981), remains of higher vertebrates (Brongersma-Sanders, 1948; Parrish and Parrish, 1983) or other animals high on the food chain, and abundant, C_{org} -rich fecal pellets (Bremner, 1983; Pilskaln and Honjo, 1987). Intact, living algae may be found in fecal pellets or on the sediment surface in high-productivity settings (Porter, 1975; see also references in Morris, 1987), and the fecal pellets are C_{org} -rich compared with those in less productive environments (Pilskaln and Honjo, 1987; Porter and Robbins, 1981; Honjo, 1982). These criteria were cited by Parrish and Gautier (1993) and Hudson and Martill (1991) as indicative of high productivity in the Lower Oxford Clay (Jurassic, England) and the Sharon Springs Member of the Pierre Shale (Cretaceous, Western Interior Seaway, North America), respectively. Hudson and Martill (1991) also cited abundant hydrogen-rich organic matter; abundant geoporphyryns and coccoliths; extremely abundant ammonites and other cephalopods, which, like higher vertebrates, are high in the food chain; high diversity and complex trophic structure of the vertebrate fauna; and presence of *Leedsichthys*, a large filter-feeder, which would have depended on enormous food resources and therefore was likely to have been limited to high-productivity environments, as are baleen whales today (see also Parrish and Parrish, 1983).

Indicators of Anoxia

Of the criteria listed in Table 2, only three might be regarded as more indicative of a non-upwelling anoxic environment—laminated rocks, abundant type III kerogen, and the limitation of C_{org} -rich rock to the deepest part of the basin. The latter two criteria were suggested and discussed by Parrish and Gautier (1993), and otherwise have received little attention in the literature; they will not be discussed further here. By contrast, the presence of laminated rocks is commonly cited as the single most important indicator of anoxia because bioturbating organisms are excluded from a system that has an anoxic and, especially, sulfidic water column (Rhoads and Morse, 1971).

It does not follow from the presence of laminations that the accumulation of organic matter in these environments occurs because of the anoxia and not because of high productivity, as is commonly assumed. It has been shown repeatedly, for example, that anaerobic bacteria are efficient at degrading organic matter (as discussed by Calvert, 1987). Thus, the assumption has commonly been made that the concentration of organic matter is high owing to the absence of meio- and macrofauna, and, conversely, that degradation by meio- and macrofauna is the dominant process of organic degradation in sediments, as suggested by the theoretical studies of Pelet (1987). However, direct evidence for this mode of degradation is lacking and, indeed, is contradicted by some studies (e.g., Sun et al., 1993).

Laminations are much more complex in origin than indicated by their use as indicators of anoxia. Laminated rocks are implicitly assumed to exhibit primary sedimentological texture, which then allows the inter-

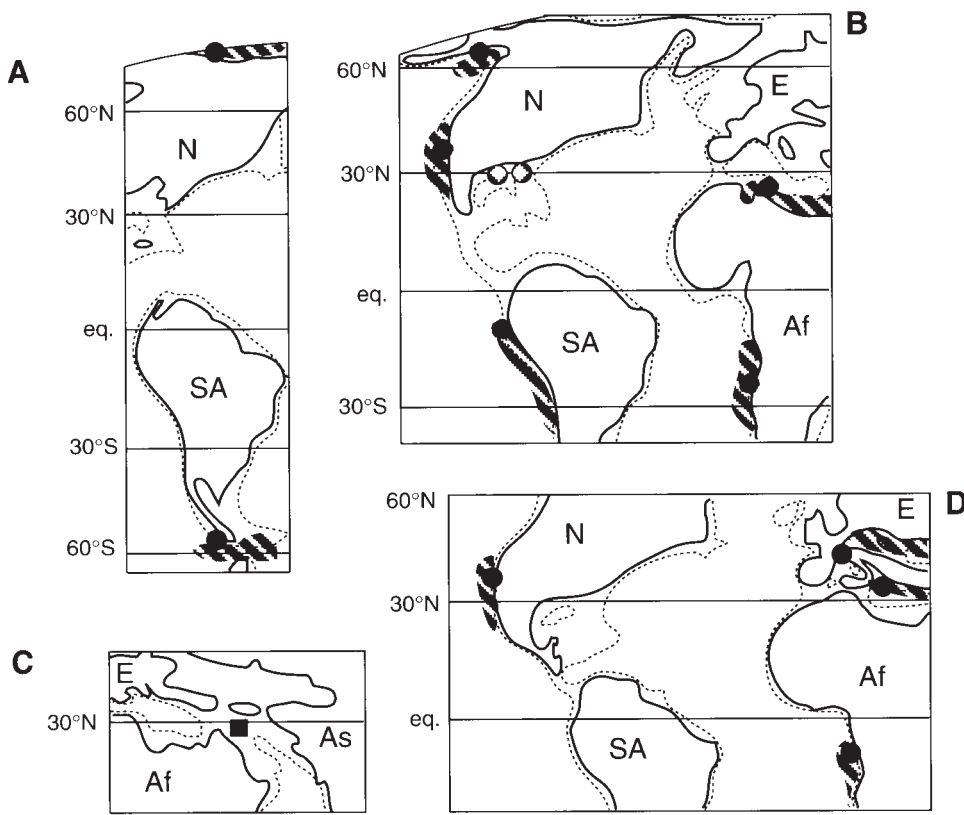


Figure 10. Data on C_{org} -rich rock and predicted upwelling zones for (A) late Paleocene, (B) middle Eocene, (C) late Oligocene, (D) late Miocene. See Figure 1 for symbols and notes.

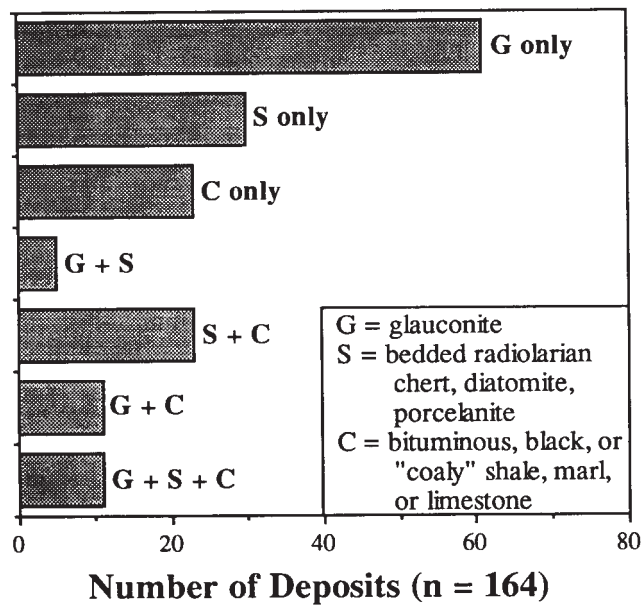


Figure 11. Phosphate deposits and their associated lithologies. Data from Parrish (1990), Parrish et al. (1983, 1986), and Parrish and Gautier (1993). Each bar represents the number of phosphate deposits associated with each lithology or combination of lithologies. Widespread phosphate deposits—those covering an area larger than 5° latitude/longitude—may be counted more than once, depending on the size of the area covered. This method is discussed in the references cited and in Parrish (1982).

pretation of anoxia. However, as pointed out by Cuomo and Bartholomew (1991), for example, lamination in rocks is not necessarily primary. They cited examples of rocks composed largely of flattened fecal pellets, which impart a lamination to the rock that was not originally part of the texture of the sediment. This kind of lamination is observed in the Sharon Springs Member of the Pierre Shale (Parrish and Gautier, 1993); in that unit, early diagenetic carbonate nodules preserve the original texture, which is massive. The appearance of lamination also may be imparted by the presence of very thin mollusk shells. This type of lamination was illustrated by Littke et al. (1991, their fig. 4) in the Posidonia Shale (Jurassic, Germany) and is observed in the C_{org} -rich facies of the Shublik Formation (Parrish, 1987b). The Posidonia Shale also has through-going sedimentological laminae, but, in the Shublik, all of the observed laminae are shells.

Bertrand and Lallier-Vergès (1993) studied a section of the Jurassic Kimmeridge Clay (England) that is finely laminated throughout. Total organic carbon (TOC), however, varies substantially from 1.8% to 9.5%. They ruled out variations in dilution as controlling the TOC; indeed, though carbonate varied, the variations were not related to variations in TOC. They concluded that the variations in TOC were related to changes in productivity and supported their conclusions with data on the reduction of sulfate, which tracked TOC closely.

Finally, not all sediments deposited in anoxic bottom waters are laminated. C_{org} -rich sediments in some marine anoxic settings, especially upwelling

Table 1. Correspondence of the distribution of predicted upwelling zones and oil-prone, C_{org}-rich rocks. Dates are those of Scotese and Golonka (1992).

| Time of Deposition | Total Deposits | Number of Deposits* | | |
|-----------------------------------|----------------|------------------------|---------------------------------|----------------------------|
| | | Explained by Upwelling | Possibly Explained by Upwelling | Not Explained by Upwelling |
| Early Cambrian (547.0 Ma) | 2 | 2 | | |
| Late Cambrian (514.0 Ma) | 1 | 1 | | |
| Early Ordovician (497.0 Ma) | 4 | 4 | | |
| Middle Ordovician (458.0 Ma) | 6 | 6 | | |
| late Middle Silurian (425.0 Ma) | 6 | 6 | | |
| Early Devonian (390.0 Ma) | 5 | 5 | | |
| Middle Devonian (377.0 Ma) | 16 | 16 | | |
| Late Devonian (363.0 Ma) | 6 | 3 | 1 | 2 |
| Early Carboniferous (342.0 Ma) | 3 | 3 | | |
| Late Carboniferous (306.0 Ma) | 4 | 4 | | |
| Early Permian (277.0 Ma) | 2 | 2 | | |
| Late Permian (255.0 Ma) | 7 | 5 | | 2 |
| Early Triassic (237.0 Ma) | 3 | 3 | | |
| Late Triassic (216.0 Ma) | 3 | 3 | | |
| Early Jurassic (195.0 Ma) | 2 | 2 | | |
| Middle Jurassic (166.0 Ma) | 8 | 6 | 2 | 2 |
| Late Jurassic (152.2 Ma) | 6 | 4 | 2 | |
| early Early Cretaceous (130.2 Ma) | 5 | 3 | 1 | 1 |
| late Early Cretaceous (118.7 Ma) | 12 | 8 | 1 | 3 |
| early Late Cretaceous (94.0 Ma) | 23 | 22 | 1 | |
| middle Late Cretaceous (88.0 Ma) | 15 | 14 | 1 | |
| late Late Cretaceous (69.4 Ma) | 14 | 10 | 2 | 2 |
| latest late Paleocene (59.2 Ma) | 2 | 2 | | |
| middle Eocene (50.3 Ma) | 7 | 5 | | 2 |
| late Oligocene (27.7 Ma) | 1 | | | 1 |
| Miocene (14.0 Ma) | 4 | 4 | | |
| | 167 | 144 86.2% | 9 5.4% | 14 8.4% |

* See text for explanation.

zones, may not be particularly well laminated (Arthur et al., 1984; Savrda et al., 1984; Savrda and Bottjer, 1988; Calvert et al., 1992a). In addition, laminated beds are not necessarily more C_{org}-rich than their homogeneous counterparts in the same deposit (e.g., Gulf of California; Calvert, 1987; Calvert et al., 1992a), although a relationship between the degree of lamination/bioturbation and TOC has been demonstrated for other deposits (e.g., Pratt et al., 1986; Emeis et al., 1991).

To summarize, good, possibly definitive indicators of high productivity can be found in the geologic record, whereas definitive indicators of anoxia not related to productivity are not. The first step in dealing with the C_{org}-rich deposits that do not correspond to predicted upwelling is to find out if they have indicators of high biologic productivity. Such a survey is beyond the scope of this paper, and probably the information is not available for all those deposits. Let us assume that such indicators do *not* occur in all of those

deposits. Where does that leave the preservation versus production controversy?

Preservation Versus Production

The major controversy in the formation of C_{org}-rich sediments is whether, all other things being equal, accumulation of significant amounts of oil-prone organic matter is principally dependent on high productivity (e.g., Calvert, 1987; Morris, 1987) or on anoxic bottom waters (Demaison and Moore, 1980; Tyson, 1987; Zimmerman et al., 1987), although some authors prefer the notion of multiple, interacting mechanisms (e.g., Arthur et al., 1984; Stow, 1987; Summerhayes, 1987). Because resolution of the debate is most critically important for the predictability of oil source-rock distribution, most workers would add that the sediments must be hydrogen-rich as well as C_{org}-rich (Demaison and Moore, 1980; Demaison, 1991; Arthur et al., 1984).

Table 2. Sedimentological and paleontological features of modern upwelling zones and non-upwelling anoxic deposits.

| Feature | Anoxic Deposits | Upwelling Zones |
|--|-----------------------|-----------------|
| <i>Sedimentologic constituents</i> | | |
| laminated sediments | ++ | + |
| dark-colored sediments | ++ | ++ |
| phosphate nodules, pellets, etc. | — | ++ |
| glauconite | + | ++ |
| bedded, biogenic chert | — | ++ |
| <i>Geochemistry</i> | | |
| organic-rich sediments | + | ++ |
| organic-carbon accumulation rates (g/cm ² /k.y.) | 0.225–0.875* | 0.96–3.98** |
| hydrogen-rich organic matter | § | ++ |
| anoxic/sulfidic bottom waters | ++ | ++ |
| abundant Type III kerogen | § | — |
| distribution of C _{org} -rich rock | deepest part of basin | side of basin |
| <i>Biologic constituents</i> | | |
| depauperate benthic macrofauna | ++ | ++ |
| abundant fish scales and bones | + | ++ |
| abundant remains of animals high in the food chain (predators) | — | ++ |
| abundant, organic-rich fecal pellets | + | ++ |

Adapted from Parrish and Gautier (1993).

Symbols: ++, very characteristic of this setting; +, sometimes present in this setting; §, sometimes present in this setting, but dependent on many outside factors (see text); —, not characteristic of this setting.

* Data from the Black Sea (Glenn and Arthur, 1985).

** Data from the Peru shelf and southern California (Bralower and Thierstein, 1987).

Demaison and Moore (1980) classified marine anoxic environments—with the assumption that these are environments in which C_{org}-rich sediments were deposited—into three types, based on the genetic mechanisms for anoxia. These were upwelling zones, density-stratified silled basins, and oceanwide oxygen-minimum zones associated with oceanic anoxic events (Schlanger and Jenkyns, 1976). Distinguishing between the effects of the anoxia and the effects of the input of organic matter in upwelling zones might be very difficult, so the controversy does not center around those environments. Rather, silled anoxic basins, such as the Black Sea and the Orca Basin, and the mechanisms that gave rise to oceanic anoxic events are focal points for the controversy.

Silled, Anoxic Basins

In density-stratified basins, the existence of a stably stratified water column reduces the supply of oxygen to the bottom waters, which become anoxic from input of organic matter and consumption of available oxygen. Stratification occurs where the surface water is less dense than the water at depth. The “type” example of such a basin is the Black Sea (Glenn and Arthur,

1985). Another example is the Orca Basin, which is perched on the continental shelf in the Gulf of Mexico, and which contains hypersaline bottom waters that may be sourced from an underlying salt diapir (Leventer et al., 1983; Shokes et al., 1977).

Recently, an impressive body of evidence has been compiled that strongly supports the idea that anoxia is not sufficient for accumulation of hydrogen-rich organic matter (Calvert, 1987, 1990; Pedersen and Calvert, 1990; Calvert et al., 1991, 1992a, b; Calvert and Pedersen, 1992, 1993). Their analyses have included work on silled, anoxic basins and on upwelling zones. In addition to work showing that the Black Sea and Mediterranean sapropels accumulated under oxic, not anoxic conditions (Calvert et al., 1987, 1992b; Calvert, 1990; see also Morris, 1987) and that the modern Black Sea sediments are not particularly C_{org}-rich (Calvert et al., 1991), they have summarized work showing that sediments in Saanich Inlet, which has anoxic bottom waters, are less rich in organic matter than sediments in adjacent basins that are oxic and, similarly, that the inner anoxic and outer oxic basins in fjords in Norway have sediments that are comparable in organic content. In Oslo Fjord, the organic matter in the anoxic basin is less hydrogen

rich than that in the oxic basin and is derived mostly from terrestrial organic matter (Calvert, 1987; Calvert and Pedersen, 1992). Work in the upwelling zones of the Gulf of California and the Oman margin has shown that sediments underlying the oxygen-minimum zone are no less C_{org} -rich than those underlying oxic waters outside the oxygen-minimum zone (Calvert et al., 1992a; Pedersen et al., 1992). The conclusion of the irrelevance of anoxia is supported by work on the Orca Basin, a silled, anoxic basin in the Gulf of Mexico (Leventer et al., 1983). These sediments have only 2–3% TOC and the organic matter is not hydrogen rich (Dinkelman and Curry, 1987; Fang et al., 1989).

Thus, the strongest support for anoxia as a mechanism for the accumulation of C_{org} -rich sediments is the circular reasoning that has led to the equation of C_{org} -richness with anoxia. This has had its best expression in discussions of oceanic anoxic events.

Oceanic Anoxic Events

The genesis of oceanic anoxic events, usually described as anoxia in oceanwide, thick oxygen-minimum zones (Arthur et al., 1984; Stow, 1987), is speculative because there is no modern analog. In general, the mechanism for the genesis of anoxia in oceanic anoxic events is assumed to be a combination of high productivity and low oxygen solubility during times of global warmth (Fischer and Arthur, 1977; Arthur and Jenkyns, 1981; Arthur et al., 1984; but see Bralower and Thierstein, 1984). Interestingly, anoxia is rarely invoked without reference to high productivity.

Demaison and Moore (1980) pointed out one possible clue to oceanic anoxic events from the modern oceans. In the Pacific, a strong oxygen-minimum zone (<0.5 mL/L O_2) can be traced several thousand kilometers to the west from its peak intensity off the western coast of the Americas (Demaison and Moore, 1980, their fig. 14). Although the oxygen minimum is most intense in the upwelling zones, its extent may be at least partly due to relatively sluggish midwater circulation (Demaison and Moore, 1980). It is not difficult to imagine that a small change in circulation vigor (Bralower and Thierstein, 1984; Fischer and Arthur, 1977), carbon supply (Tissot et al., 1980), or oxygen solubility (owing to higher water temperature and/or salinity; Fischer and Arthur, 1977; Brass et al., 1982) would allow an oxygen-minimum zone of this type to become completely anoxic and to extend across an entire ocean. An important, if not critical, element of these hypotheses is the initial requirement for high productivity, which potentially raises the question of the need for anoxia as a mechanism for organic accumulation. However, the oxygen minimum in the Pacific is generated by productivity close to the continents, so the key question is the effect of the oxygen minimum if it were to intersect shelfal areas where productivity might not necessarily be expected to be high, as the Cenomanian–Turonian oxygen minimum is supposed to have done (Thiede et al., 1982).

The Cenomanian–Turonian oceanic anoxic event is arguably the most carefully studied interval in the geologic record (Arthur et al., 1987; Pratt, 1985; Leckie,

1985; Schlanger et al., 1987; Jarvis et al., 1988; Corfield et al., 1990; Gale et al., 1993; and many others). The lower boundary of organic accumulation was on the continental slope and in oceanic basins down to about 2.5 km depth, and the upper boundary was as shallow as 100–200 m (Schlanger et al., 1987). In addition, black bands deposited during the event are found in epeiric seaways (Western Interior Seaway of North America, epeiric seaways of Europe and Africa) and on open continental shelves (Peru, Guyana, northwestern Africa, and many other sites; Schlanger et al., 1987, their fig. 13). Although many of these sites, for example, Peru, northern South America, northern Africa, and northwestern Africa, may have been upwelling zones (Parrish, 1982), the brevity and geographic range of the Cenomanian–Turonian oceanic anoxic event would appear to preclude upwelling, which today is a local phenomenon (Parrish and Curtis, 1982; Koblenz-Mishke et al., 1970), as the sole driving mechanism. However, the widespread distribution of C_{org} -rich rock should not be taken as *a priori* evidence that anoxia was involved.

Regional oceanic turnover leading to higher primary productivity oceanwide and triggered by the passing of some paleogeographic threshold during the opening of the Atlantic (Summerhayes, 1987) or by displacement of nutrient-rich deep waters during warm, saline bottom-water formation (Brass et al., 1982; Arthur et al., 1987; Funnell, 1987) has been suggested as a mechanism for the genesis of oceanic anoxic events. Thus, although the tendency toward anoxia may be enhanced by local conditions, such as a possible freshwater cap in the Western Interior Seaway (Arthur et al., 1987; Pratt, 1984) or upwelling in Venezuela (Parrish, 1982; Brass et al., 1982; Arthur et al., 1987), larger-scale processes may exert the dominant control. The process has been assumed to have been expansion of an oxygen-minimum zone, but many of the units deposited during oceanic anoxic events show evidence of high productivity in addition to C_{org} -rich rock. Thus, it might be that oceanic anoxic events were in fact oceanic productivity events. Because localized upwelling is a relatively well-understood and well-modeled phenomenon, little work has been done on possible mechanisms for oceanic productivity events. This would be a fruitful area of research.

SUMMARY AND CONCLUSIONS

New information presented here includes the following:

1. Nearly half of C_{org} -rich units were deposited in paleogeographic settings that do not have modern analogs among settings for anoxia, suggesting that significant numbers of C_{org} -rich deposits may not be subject to direct comparison with modern anoxic settings.

2. If only oil-prone C_{org} -rich rocks are considered and Gulf Stream-type upwelling is included, predicted upwelling zones can explain up to 93% of C_{org} -rich deposits through the Phanerozoic. The remaining deposits occur in three types of environments—rift

basins; low-latitude, enclosed, epicontinental seaways; and mid-latitude shelves.

3. High-productivity systems such as are found in well-developed upwelling zones would appear to be easiest to identify because of the many geologic features by which they may be recognized. Chief among these criteria is the association of biogenic siliceous rock, C_{org}-rich rocks, phosphate, and glauconite (Hein and Parrish, 1987; Parrish et al., 1983) and the distinct facies relationships among the latter three. A literature search for such associations turned up 34 deposits that have the Si-P-C association, which is widely regarded to be indicative of high productivity. Another 100 deposits had one of the pairs of adjacent facies, phosphate-glauconite or phosphate-C_{org}-rich rock.

In earlier work, I assumed that multiple mechanisms can cause high organic accumulation, and that wind-driven upwelling and associated high productivity is just one of those mechanisms (e.g., Parrish, 1982; Parrish and Curtis, 1982). As a result of this and other work, I now feel that the weight of evidence is on productivity as the cause of high organic accumulation, and that wind-driven upwelling is just one, albeit a very important, mechanism for achieving high productivity. Thus, the question arises, under what other conditions can productivity be raised? Already well established are the connection between upwelling and western boundary currents, such as the Gulf Stream, and cyclonic oceanic gyres, such as the Costa Rica Dome (Yentsch, 1974; see discussion in Parrish, 1982). Oceanic divergences, which are wind driven but which today occur only over deep water and thus were largely ignored by me (Parrish, 1982; Parrish and Curtis, 1982), may have been more important in the past, when ocean basins were narrower (Summerhayes, 1987). Likewise, seasonal and transitory divergences and their associated high productivity (Hidaka, 1955; Hidaka and Ogawa, 1958) might have played a greater role in narrow and large, shallow basins. Other observed or proposed mechanisms include (1) increased productivity with influx of nutrient-laden river water (Diester-Haass, 1983; Hudson and Martill, 1991; but see Ryther et al., 1967); (2) upwelling caused by entrainment as river water is expelled into the ocean (Emery and Milliman, 1978); (3) widespread increase of nutrient fluxes to the photic zone (Arthur et al., 1987), especially in narrow basins such as rift basins; (4) bathymetric upwelling (Blanton et al., 1981; Atkinson and Targett, 1983); and (5) ice-edge effects (Buckley et al., 1979; Greisman, 1979). Modeling studies that specifically address these mechanisms might help determine which are the most likely to have supplemented wind-driven upwelling in the past.

Although the relationship between C_{org} accumulation and anoxia is probably tenuous, anoxia is still a real phenomenon. Unless independent models or information demonstrate the relationship between anoxia and C_{org} accumulation, however, anoxia should be disassociated from carbon accumulation as a cause. C_{org}-rich rock should not be taken as *a priori* evidence for anoxia.

ACKNOWLEDGMENTS

The author bears sole responsibility for the conclusions herein, but is grateful to the following people for collegial discussion and thoughtful formal and informal reviews of this paper: Stephen E. Calvert, Kay-Christian Emeis, Eric Force, Kurt Grimm, Julie Kennedy, Thomas F. Pedersen, and Glen S. Tanck. The original data were provided by Amoco Production Co., whose contribution is gratefully acknowledged. This work was supported in part by Chevron International Oil Co., Mobil Exploration and Producing Services, Amoco Production Company, Conoco, and NSF grant EAR-9023558.

REFERENCES CITED

- Abrantes, F., 1992, Palaeoproductivity oscillations during the last 130 ka along the Portuguese and NW African margins, in C.P. Summerhayes, W.L. Prell and K.C. Emeis, eds., *Upwelling Systems: Evolution Since the Early Miocene*: Geological Society of London Special Publication 64, p. 499–510.
- Arthur, M.A., and H.C. Jenkyns, 1981, Phosphorites and paleoceanography, in W.H. Berger, ed., *Chemical Cycles in the Ocean*: *Oceanologica Acta*, v. 4 (Supplement), p. 83–96.
- Arthur, M.A., W.E. Dean, and D.A.V. Stow, 1984, Models for the deposition of Mesozoic–Cenozoic fine-grained organic-carbon-rich sediment in the deep sea, in D.A.V. Stow and D.J.W. Piper, eds., *Fine-Grained Sediments: Deep-Water Processes and Facies*: Geological Society of London Special Publication 15, p. 527–559.
- Arthur, M.A., S.O. Schlanger, and H.C. Jenkyns, 1987, The Cenomanian–Turonian oceanic anoxic event, II—Paleoceanographic controls on organic-matter production and preservation, in J. Brooks and A.J. Fleet, eds., *Marine Petroleum Source Rocks*: Geological Society of London Special Publication 26, p. 401–420.
- Atkinson, L.P., and T.E. Targett, 1983, Upwelling along the 60-m isobath from Cape Canaveral to Cape Hatteras and its relationship to fish distribution: *Deep-Sea Research*, v. 30, p. 221–223.
- Banse, K., 1968, Hydrography of the Arabian Sea shelf of India and Pakistan and effects on demersal fishes: *Deep-Sea Research* 26, p. 45–79.
- Baturin, G.N., 1983, Some unique sedimentological and geochemical features of deposits in coastal upwelling regions, in J. Thiede and E. Suess, eds., *Coastal Upwelling: Its Sediment Record*, Part B: New York, Plenum Press, p. 11–27.
- Bertrand, P., and E. Lallier-Vergès, 1993, Past sedimentary organic matter accumulation and degradation controlled by productivity: *Nature*, v. 364, p. 786–788.
- Blanton, J.O., L.P. Atkinson, L.J. Pietrafesa, and T.N. Lee, 1981, The intrusion of Gulf Stream water across the continental shelf due to topographically-induced upwelling: *Deep-Sea Research*, v. 28A(4), p. 393–405.

- Bralower, T.J., and H.R. Thierstein, 1984, Low productivity and slow deep-water circulation in mid-Cretaceous oceans: *Geology*, v. 12, p. 614–618.
- Bralower, T.J., and H.R. Thierstein, 1987, Organic carbon and metal accumulation rates in Holocene and mid-Cretaceous sediments: palaeoceanographic significance, in J. Brooks and A.J. Fleet, eds., *Marine Petroleum Source Rocks: Geological Society of London Special Publication 26*, p. 345–369.
- Brass, G.W., J.R. Southam, and W.H. Peterson, 1982, Warm saline bottom water in the ancient ocean: *Nature*, v. 296, p. 620–623.
- Bremner, J.M., 1983, Biogenic sediments on the South West African (Namibian) continental margin, in J. Thiede and E. Suess, eds., *Coastal Upwelling: Its Sediment Record, Part B: New York, Plenum Press*, p. 73–104.
- Brongersma-Sanders, M., 1948, The importance of upwelling water to vertebrate paleontology and oil geology: *Koninkl. Nederlandse Akad. Wetensch. Verh. Afd. Natuurk.*, v. 45, p. 1–112.
- Buckley, J.R., T. Gammelsrød, J.A. Johannessen, O.M. Johannessen, and L.P. Røed, 1979, Upwelling: oceanic structure at the edge of the Arctic ice pack in winter: *Science*, v. 103, p. 165–167.
- Burnett, W.C., and A.I.N. Lee, 1980, The phosphate supply system in the Pacific region: *GeoJournal*, v. 45, p. 423–436.
- Burnett, W.C., H.H. Veeh, and A. Soutar, 1980, U-series, oceanographic and sedimentary evidence in support of recent formation of phosphate nodules off Peru, in Y.K. Bendor, ed., *Marine Phosphorites: Society of Economic Paleontologists and Mineralogists Special Publication 29*, p. 61–72.
- Burnett, W.C., K.K. Roe, and D.Z. Piper, 1983, Upwelling and phosphorite formation in the ocean, in E. Suess and J. Thiede, eds., *Coastal Upwelling: Its Sediment Record, Part A: New York, Plenum Press*, p. 377–397.
- Calvert, S.E., 1966, Accumulation of diatomaceous silica in the sediments of the Gulf of California: *Geological Society of America Bulletin*, v. 77, p. 569–596.
- Calvert, S.E., 1987, Oceanographic controls on the accumulation of organic matter in marine sediments, in J. Brooks and A.J. Fleet, eds., *Marine Petroleum Source Rocks: Geological Society of London Special Publication 26*, p. 137–152.
- Calvert, S.E., 1990, Geochemistry and origin of the Holocene sapropel in the Black Sea, in V. Ittekkot, S. Kempe, W. Michaelis, and A. Spitzky, eds., *Facets of Modern Biogeochemistry: Festschrift for E. T. Degens: Berlin, Springer-Verlag*, p. 326–352.
- Calvert, S.E., and T.F. Pedersen, 1992, Organic carbon accumulation and preservation in marine sediments: how important is anoxia?, in J.K. Whelan and J.W. Farrington, eds., *Productivity, Accumulation and Preservation of Organic Matter in Recent and Ancient Sediments: New York, Columbia University Press*, p. 231–263.
- Calvert, S.E., and T.F. Pedersen, 1993, Geochemistry of Recent oxic and anoxic marine sediments: implications for the geological record: *Marine Geology*, v. 113, p. 67–88.
- Calvert, S.E., and N.B. Price, 1971, Upwelling and nutrient regeneration in the Benguela Current, October, 1968: *Deep-Sea Research*, v. 18, p. 505–523.
- Calvert, S.E., and N.B. Price, 1983, Geochemistry of Namibian shelf sediments, in E. Suess and J. Thiede, eds., *Coastal Upwelling: Its Sediment Record, Part A: New York, Plenum Press*, p. 337–375.
- Calvert, S.E., J.S. Vogel, and J.R. Southon, 1987, Carbon accumulation rates and the origin of the Holocene sapropel in the Black Sea: *Geology*, v. 26, p. 918–921.
- Calvert, S.E., R.E. Karlin, L.J. Toolin, D.J. Donahue, J.R. Southon, and J.S. Vogel, 1991, Low organic carbon accumulation rates in Black Sea sediments: *Nature*, v. 350, p. 692–695.
- Calvert, S.E., R.M. Bustin, and T.F. Pedersen, 1992a, Lack of evidence for enhanced preservation of sedimentary organic matter in the oxygen minimum of the Gulf of California: *Geology*, v. 20, p. 757–760.
- Calvert, S.E., B. Nielsen, and M.R. Fontugne, 1992b, Evidence from nitrogen isotope ratios for enhanced productivity during formation of eastern Mediterranean sapropels: *Nature*, v. 359, p. 223–225.
- Cook, P.J., 1976, Sedimentary phosphate deposits, in K.H. Wolfe, ed., *Handbook of Strata-Bound and Stratiform Ore Deposits*, v. 7: Amsterdam, Elsevier Scientific Publishing Co., p. 505–535.
- Cook, P.J., and J.F. Marshall, 1981, Geochemistry of iron and phosphorus-rich nodules from the east Australian continental shelf: *Marine Geology*, v. 41, p. 205–221.
- Cook, P.J., and M.W. McElhinny, 1979, A reevaluation of the spatial and temporal distribution of sedimentary phosphate deposits in the light of plate tectonics: *Economic Geology*, v. 74, p. 315–330.
- Cook, P.J., J.H. Shergold, W.C. Burnett, and S.R. Riggs, 1990, Phosphorite research: a historical overview, in A.J.G. Notholt and I. Jarvis, eds., *Phosphorite Research and Development: Geological Society of London Special Publication 52*, p. 1–22.
- Corfield, R.M., M.A. Hall, and M.D. Brasier, 1990, Stable isotope evidence for foraminiferal habitats during the development of the Cenomanian/Turonian oceanic anoxic event: *Geology*, v. 18, p. 175–178.
- Cuomo, M.C., and P.R. Bartholomew, 1991, Pelletal black shale fabrics: their origin and significance, in R.V. Tyson and T.H. Pearson, eds., *Modern and Ancient Continental Shelf Anoxia: Geological Society of London Special Publication 58*, p. 221–232.
- Demaison, G., 1991, Anoxia vs. productivity: What controls the formation of organic-carbon-rich sediments and sedimentary rocks?: Discussion: *AAPG Bulletin*, v. 75, p. 499–500.
- Demaison, G.J., and G.T. Moore, 1980, Anoxic environments and oil source bed genesis: *AAPG Bulletin*, v. 64, p. 1179–1209.
- Diester-Haass, L., 1978, Sediments as indicators of upwelling, in R. Boje and M. Tomczak, eds., *Upwelling Ecosystems: Berlin, Springer-Verlag*, p. 261–281.

- Diester-Haass, L., 1983, Differentiation of high oceanic fertility in marine sediments caused by coastal upwelling and/or river discharge off northwest Africa during the late Quaternary, *in* J. Thiede and E. Suess, eds., *Coastal Upwelling: Its Sediment Record*, Part B: New York, Plenum Press, p. 399–419.
- Dinkelman, M.G., and D.J. Curry, 1987, Significance of anoxic slope basins to occurrence of hydrocarbons along flexure trend, Gulf of Mexico: a reappraisal (abs.): *AAPG Bulletin*, v. 71, p. 548–549.
- Emeis, K.-C., J.K. Whelan, and M. Tarafa, 1991, Sedimentary and geochemical expressions of oxic and anoxic conditions on the Peru Shelf, *in* R.V. Tyson and T.H. Pearson, eds., *Modern and Ancient Continental Shelf Anoxia: Geological Society of London Special Publication 58*, p. 155–170.
- Emery, K.O., 1960, *The sea off southern California: a modern habitat of petroleum*: New York, Wiley and Sons, 366 p.
- Emery, K.O., and J.D. Milliman, 1978, Suspended matter in surface waters: influence of river discharge and of upwelling: *Sedimentology*, v. 25, p. 125–140.
- Emery, K.O., J. Hülsemann, and K.S. Rudolfo, 1962, Influence of turbidity current upon basin waters: *Limnology and Oceanography*, v. 7, p. 439–455.
- Fang, J., R. Sassen, H. Roberts, and J. Nunn, 1989, Organic geochemistry of sediments of the deep-water Gulf of Mexico Basin (abs.): *Organic Geochemistry*, v. 14, p. 679.
- Fischer, A.G., and M.A. Arthur, 1977, Secular variations in the pelagic realm, *in* H.E. Cook and P. Enos, eds., *Deep-Water Carbonate Environments: Society of Economic Paleontologists and Mineralogists Special Publication 25*, p. 19–50.
- Fleet, A.J., K. Kelts, and M.R. Talbot, 1988, Lacustrine petroleum source rocks: *Geological Society of London Special Publication 40*, 391 p.
- Fukuoka, J., A. Ballester, and F. Cervigon, 1964, An analysis of hydrographical condition in the Caribbean Sea (III)—especially about upwelling and sinking: *Studies in Oceanography*, v. 1964, p. 145–149.
- Funnell, B.M., 1987, Anoxic non-events: alternative explanations, *in* J. Brooks and A.J. Fleet, eds., *Marine Petroleum Source Rocks: Geological Society of London Special Publication 26*, p. 421–422.
- Gale, A.S., H.C. Jenkyns, W.J. Kennedy, and R.M. Corfield, 1993, Chemostratigraphy versus biostratigraphy: data from around the Cenomanian–Turonian boundary: *Journal of the Geological Society of London*, v. 260, p. 29–32.
- Glenn, C.R., and M.A. Arthur, 1985, Sedimentary and geochemical indicators of productivity and oxygen contents in modern and ancient basins: the Holocene Black Sea as the “type” anoxic basin: *Chemical Geology*, v. 48, p. 325–354.
- Glenn, C.R., and M.A. Arthur, 1990, Anatomy and origin of a Cretaceous phosphorite-greensand giant, Egypt: *Sedimentology*, v. 37, p. 123–154.
- Greisman, P., 1979, On upwelling driven by the melt of ice shelves and tidewater glaciers: *Deep-Sea Research*, v. 26A, p. 1051–1065.
- Harland, W.B., A.V. Cox, P.G. Llewellyn, C.A.G. Pickton, A.G. Smith, and R. Walters, 1982, *A geologic time scale*: Cambridge, Cambridge University Press, 131 p.
- Heggie, D.T., G.W. Skyring, G.W. O’Brien, C.E. Reimers, D.J. Moriarty, A. Hertzeg, and P.D. Nichols, 1988, Organic carbon cycling and modern phosphorite formation: east Australian continental margin (abs.): *International Geological Correlation Programme, Project 156 Phosphorites, 11th International Field Workshop and Symposium, September 1988*, Oxford, England.
- Hein, J.R., and J.T. Parrish, 1987, Distribution of siliceous deposits in space and time, *in* J.R. Hein, ed., *Siliceous Sedimentary Rock-Hosted Ores and Petroleum*: New York, Van Nostrand Reinhold Company, p. 10–57.
- Hidaka, K., 1955, Divergence of surface drift currents in terms of wind stresses, with special application to the location of upwelling and sinking: *Japan Journal of Geophysics*, v. 1, p. 47–56.
- Hidaka, K., and K. Ogawa, 1958, On the seasonal variations of surface divergence of the ocean currents in terms of wind stresses over the oceans: *Records of Oceanographic Works in Japan*, v. 4, p. 124–169.
- Honjo, S., 1982, Seasonality and interaction of biogenic and lithogenic particulate flux at the Panama Basin: *Science*, v. 218, p. 883–884.
- Hudson, J.D., and D.M. Martill, 1991, The Lower Oxford Clay: production and preservation of organic matter in the Callovian (Jurassic) of central England, *in* R.V. Tyson and T.H. Pearson, eds., *Modern and Ancient Continental Shelf Anoxia: Geological Society of London Special Publication 58*, p. 363–379.
- Ingle, J.C., 1981, Origin of Neogene diatomites around the north Pacific rim, *in* R.E. Garrison and R.D. Douglas, eds., *The Monterey Formation and Related Siliceous Rocks of California: Pacific Section, Society of Economic Paleontologists and Mineralogists Special Publication*, p. 159–179.
- Jarvis, I., 1980, The initiation of phosphatic chalk sedimentation—the Senonian (Cretaceous) of the Anglo-Paris Basin, *in* Y.K. Bendor, ed., *Marine Phosphorites—Geochemistry, Occurrences, Genesis: Society of Economic Paleontologists and Mineralogists Special Publication 29*, p. 167–192.
- Jarvis, I., G.A. Carson, M.K.E. Cooper, M.B. Hart, P.N. Leary, B.A. Tocher, D. Horne, and A. Rosenfeld, 1988, Microfossil assemblages and the Cenomanian–Turonian (late Cretaceous) oceanic anoxic event: *Cretaceous Research*, v. 9, p. 3–103.
- Koblenz-Mishke, O., V.V. Voldovinsky, and J.G. Kabanova, 1970, Plankton primary production of the world ocean, *in* W.S. Wooster, ed., *Symposium on the Scientific Exploration of the South Pacific: National Academy of Science*, p. 183–193.
- Kruijs, E., and E. Barron, 1990, Climate model prediction of paleoproductivity and potential source-rock distribution, *in* A.-Y. Huc, ed., *Deposition of Organic Facies: AAPG Studies in Geology 30*, p. 195–216.

- Leckie, R.M., 1985, Foraminifera of the Cenomanian–Turonian boundary interval, Greenhorn Formation, Rock Canyon anticline, Pueblo, Colorado, in L.M. Pratt, E.G. Kauffman, and F.B. Zelt, eds., *Fine-Grained Deposits and Biofacies of the Cretaceous Western Interior Seaway: Evidence of Cyclic Sedimentary Processes*: Society of Economic Paleontologists and Mineralogists Field Trip Guide Book, p. 139–150.
- Leventer, A., D.F. Williams, and J.P. Kennett, 1983, Relationships between anoxia, glacial meltwater and microfossil preservation in the Orca Basin, Gulf of Mexico: *Marine Geology*, v. 53, p. 23–40.
- Lisitsyn, A.P., 1977, Biogenic sedimentation in the oceans and zonation: *Lithology and Mineral Resources*, v. 1, p. 3–24.
- Littke, R., D.R. Baker, D. Leythaeuser, and J. Rullkötter, 1991, Keys to the depositional history of the Posidonia Shale (Toarcian) in the Hils syncline, northern Germany, in R.V. Tyson and T.H. Pearson, eds., *Modern and Ancient Continental Shelf Anoxia*: Geological Society of London Special Publication 58, p. 311–333.
- Maughan, E.K., 1980, Relation of phosphorite, organic carbon, and hydrocarbons in the Permian Phosphoria Formation, western United States of America, in *International Conference on Comparative Geology of Phosphate and Oil Deposits*, Orleans, France, 6–7 Nov. 1979; Bureau de Recherches Géologique et Minéralogique, v. 24, p. 63–91.
- McKelvey, V.E., 1967, Phosphate deposits: U.S. Geological Survey Bulletin 1252-D, p. D1–D21.
- McKelvey, V.E., J.S. Williams, R.P. Sheldon, E.R. Cressman, T.M. Cheney, and R.W. Swanson, 1967, The Phosphoria, Park City, and Shedhorn formations in Western Phosphate Field, in L.A. Hale, ed., *Anatomy of the Western Phosphate Field: Salt Lake City*, Intermountain Association of Geologists Fifteenth Annual Field Conference, p. 15–34.
- Mew, M.C., ed., 1980, *World survey of phosphate deposits*, 4th ed.: London, British Sulphur Corporation, 238 p.
- Morris, R.J., 1987, The formation of organic-rich deposits in two deep-water marine environments, in J. Brooks and A.J. Fleet, eds., *Marine Petroleum Source Rocks*: Geological Society of London Special Publication 26, p. 153–166.
- Müller, P.J., and E. Suess, 1979, Productivity, sedimentation rate and sedimentary organic matter in the oceans. I—Organic carbon preservation: *Deep-Sea Research*, v. 26A, p. 1347–1362.
- Mullins, H.T., J.B. Thompson, K. McDougall, and T.L. Vercoutere, 1985, Oxygen-minimum zone edge effects: Evidence from the central California upwelling system: *Geology*, v. 13, p. 491–494.
- O'Brien, G.W., and D. Heggie, 1988, East Australian continental margin phosphorites: *Eos*, v. 69.
- O'Brien, G.W., and H.H. Veeh, 1983, Are phosphorites reliable indicators of upwelling?, in E. Suess and J. Thiede, eds., *Coastal Upwelling: Its Sediment Record*, Part A: New York, Plenum Press, p. 399–419.
- O'Brien, G.W., A.R. Milnes, H.H. Veeh, D.T. Heggie, D.J. Cullen, and J.F. Marshall, 1988, East Australian continental margin phosphorites: depositional and post-depositional controls on petrography, mineralogy and composition (abs.): *International Geological Correlation Programme, Project 156 Phosphorites*, 11th International Field Workshop and Symposium, September 1988, Oxford, England.
- Oreskes, N., K. Shrader-Frechette, and K. Belitz, 1994, Verification, validation, and confirmation of numerical models in the earth sciences: *Science*, v. 263, p. 641–646.
- Parrish, J.M., and J.T. Parrish, 1983, Were Mesozoic marine reptiles analogs of whales? (abs.): *Geological Society of America Abstracts with Programs*, v. 26, p. 659.
- Parrish, J.T., 1982, Upwelling and petroleum source beds, with reference to the Paleozoic: *AAPG Bulletin*, v. 66, p. 750–774.
- Parrish, J.T., 1983, Upwelling deposits: nature of association of organic-rich rocks, chert, chalk, phosphorite, and glauconite (abs.): *AAPG Bulletin*, v. 67, p. 529.
- Parrish, J.T., 1987a, Palaeo-upwelling and the distribution of organic-rich rocks, in J. Brooks and A.J. Fleet, eds., *Marine Petroleum Source Rocks*: Geological Society of London Special Publication 26, p. 199–205.
- Parrish, J.T., 1987b, Lithology, geochemistry, and depositional environment of the Shublik Formation (Triassic), northern Alaska, in I.L. Tailleux and Weimer, P., eds., *Alaskan North Slope Geology*, v. 1: Alaska Geological Society and AAPG, p. 391–396.
- Parrish, J.T., 1990, Paleogeographic and paleoclimatic setting of the Miocene phosphogenic episode, in W.C. Burnett and S.R. Riggs, eds., *Phosphate Deposits of the World, Vol. 3, Genesis of Neogene to Recent Phosphorites*: Cambridge, Cambridge University Press, p. 223–240.
- Parrish, J.T., and R.L. Curtis, 1982, Atmospheric circulation, upwelling, and organic-rich rocks in the Mesozoic and Cenozoic Eras: *Palaeogeography, Palaeoclimatology, Palaeoecology*, v. 40, p. 31–66.
- Parrish, J.T., and D.L. Gautier, 1993, Sharon Springs Member of Pierre Shale: upwelling in the Western Interior Seaway?, in W.G.E. Caldwell and E.G. Kauffman, eds., *Evolution of the Western Interior Basin*: Geological Association of Canada Special Paper 39, p. 319–332.
- Parrish, J.T., A.M. Ziegler, and R.G. Humphreville, 1983, Upwelling in the Paleozoic Era, in J. Thiede and E. Suess, eds., *Coastal Upwelling: Its Sediment Record*, Part B: New York, Plenum Press, p. 553–578.
- Parrish, J.T., A.M. Ziegler, C.R. Scotese, R.G. Humphreville, and J.L. Kirschvink, 1986, Early Cambrian palaeogeography, palaeoceanography, and phosphorites, in P.J. Cook and J.H. Shergold, eds., *Phosphate Deposits of the World, Vol. 1. Proterozoic and Cambrian Phosphorites*: Cambridge, Cambridge University Press, p. 280–294.
- Pedersen, T.F., and S.E. Calvert, 1990, Anoxia vs. productivity: what controls the formation of organic-carbon-rich sediments and sedimentary rocks?: *AAPG Bulletin*, v. 74, p. 454–466.

- Pedersen, T.F., G.B. Shimmiel, and N.B. Price, 1992, Lack of enhanced preservation of organic matter in sediments under the oxygen minimum on the Oman margin: *Geochimica et Cosmochimica Acta*, v. 56, p. 545–551.
- Pelet, R., 1987, A model of organic sedimentation on present-day continental margins, in J. Brooks and A.J. Fleet, eds., *Marine Petroleum Source Rocks: Geological Society of London Special Publication 26*, p. 167–180.
- Pilskaln, C.H., and S. Honjo, 1987, The fecal pellet fraction of biogeochemical particle fluxes to the deep sea: *Global Biogeochemical Cycles*, v. 1, p. 31–48.
- Pisciotta, K.A., and R.E. Garrison, 1981, Lithofacies and depositional environments of the Monterey Formation, California, in R.E. Garrison and R.G. Douglas, eds., *The Monterey Formation and Related Siliceous Rocks of California: Pacific Section Society of Economic Paleontologists and Mineralogists Special Publication*, p. 97–122.
- Porter, K.G., 1975, Viable gut passage of gelatinous green algae ingested by *Daphnia*: *Verh. Internat. Verein. Limnol.*, v. 19, p. 2840–2850.
- Porter, K.G., and E.I. Robbins, 1981, Zooplankton fecal pellets link fossil fuel and phosphate deposits: *Science*, v. 212, p. 931–933.
- Pratt, L.M., 1984, Influence of paleoenvironmental factors on preservation of organic matter in the Middle Cretaceous Greenhorn Formation of Pueblo, Colorado: *AAPG Bulletin*, v. 68, p. 1146–1159.
- Pratt, L.M., 1985, Isotopic studies of organic matter and carbonate in rocks of the Greenhorn marine cycle, in L.M. Pratt, E.G. Kauffman, and F.B. Zelt, eds., *Fine-Grained Deposits and Biofacies of the Cretaceous Western Interior Seaway: Evidence of Cyclic Sedimentary Processes: Society of Economic Paleontologists and Mineralogists Field Trip Guide Book*, p. 38–48.
- Pratt, L.M., G.E. Claypool, and J.D. King, 1986, Geochemical imprint of depositional conditions on organic matter in laminated-bioturbated interbeds from fine-grained marine sequences: *Marine Geology*, v. 70, p. 67–84.
- Rhoads, D.C., and J.W. Morse, 1971, Evolutionary and ecological significance of oxygen-deficient marine basins: *Lethaia*, v. 4, p. 413–428.
- Ryther, J.H., D.W. Menzel, and N. Corwin, 1967, Influence of the Amazon River outflow on the ecology of the western tropical Atlantic. I. Hydrography and nutrient chemistry: *Journal of Marine Research*, v. 25, p. 69–83.
- Sarnthein, M., U. Pflaumann, R. Ross, R. Tiedemann, and K. Winn, 1992, Transfer functions to reconstruct ocean palaeoproductivity: a comparison, in C.P. Summerhayes, W.L. Prell, and K.C. Emeis, eds., *Upwelling Systems: Evolution Since the Early Miocene: Geological Society of London Special Publication 64*, p. 411–427.
- Savrda, C.E., and D.J. Bottjer, 1988, The exaerobic zone, a new oxygen-deficient marine biofacies: *Nature*, v. 327, p. 54–56.
- Savrda, C.E., D.J. Bottjer, and D.S. Gorsline, 1984, Development of a comprehensive oxygen-deficient marine biofacies model: evidence from Santa Monica, San Pedro, and Santa Barbara basins, California continental borderland: *AAPG Bulletin*, v. 68, p. 1179–1192.
- Schlanger, S.O., and H.C. Jenkyns, 1976, Cretaceous oceanic anoxic events: causes and consequences: *Geologie en Mijnbouw*, v. 55, p. 179–184.
- Schlanger, S.O., M.A. Arthur, H.C. Jenkyns, and P.A. Scholle, 1987, The Cenomanian–Turonian oceanic anoxic event, I. Stratigraphy and distribution of organic carbon-rich beds and the marine $\delta^{13}\text{C}$ excursion, in J. Brooks and A.J. Fleet, eds., *Marine Petroleum Source Rocks: Geological Society of London Special Publication 26*, p. 371–400.
- Schrader, H., 1992, Peruvian coastal primary palaeoproductivity during the last 200,000 years, in C.P. Summerhayes, W.L. Prell, and K.C. Emeis, eds., *Upwelling Systems: Evolution Since the Early Miocene: Geological Society of London Special Publication 64*, p. 391–409.
- Scotese, C.R., and J. Golonka, 1992, Paleogeographic atlas: PALEOMAP Project, Dept. of Geology, University of Texas—Arlington.
- Scotese, C.R., R.K. Bambach, C. Barton, R. Van der Voo, and A.M. Ziegler, 1979, Paleozoic base maps: *Journal of Geology*, v. 87, p. 217–277.
- Sheldon, R.P., 1964, Paleolatitudinal and paleogeographic distribution of phosphorite: United States Geological Survey Professional Paper 501-C, p. C106–C113.
- Shimkus, K.M., and E.S. Trimonis, 1974, Modern sedimentation in the Black Sea, in E.T. Degens and D.A. Ross, eds., *The Black Sea—Geology, Chemistry, and Biology: AAPG Memoir 20*, p. 249–278.
- Shokes, R.G., P.K. Trabant, B.J. Presley, and D.F. Reid, 1977, Anoxic hypersaline basin in the northern Gulf of Mexico: *Science*, v. 196, p. 1443–1446.
- Soutar, A., S.R. Johnson, and T.R. Baumgartner, 1981, In search of modern depositional analogs to the Monterey Formation, in R.E. Garrison and R.G. Douglas, eds., *The Monterey Formation and Related Siliceous Rocks of California: Pacific Section Society of Economic Paleontologists and Mineralogists Special Publication*, p. 123–147.
- Stow, D.A.V., 1987, South Atlantic organic-rich sediments: facies processes and environments of deposition, in J. Brooks and A.J. Fleet, eds., *Marine Petroleum Source Rocks: Geological Society of London Special Publication 26*, p. 287–300.
- Suess, E., 1981, Phosphate regeneration from sediments of the Peru continental margin by dissolution of fish debris: *Geochimica et Cosmochimica Acta*, v. 45, p. 577–588.
- Summerhayes, C.P., 1987, Organic-rich Cretaceous sediments from the North Atlantic, in J. Brooks and A.J. Fleet, eds., *Marine Petroleum Source Rocks: Geological Society of London Special Publication 26*, p. 301–316.
- Sun, M.-Y., C. Lee, and R.C. Aller, 1993, Laboratory studies of oxic and anoxic degradation of chlorophyll-*a* in Long Island Sound sediments: *Geochimica et Cosmochimica Acta*, v. 57, p. 147–157.
- Thiede, J., W.E. Dean, and G.E. Claypool, 1982, Oxygen-deficient depositional paleoenvironments in

- the mid-Cretaceous tropical and subtropical central Pacific Ocean, *in* S.O. Schlanger and M.B. Cita, eds., *Nature and Origin of Cretaceous Carbon-Rich Facies*: New York, Academic Press, p. 55–78.
- Tissot, B.P., and D.H. Welte, 1978, *Petroleum formation and occurrence*: Berlin, Springer-Verlag, 538 p.
- Tissot, B., G. Demaison, P. Masson, J.R. Delteil, and A. Combaz, 1980, Paleoenvironment and petroleum potential of middle Cretaceous black shales in Atlantic basins: *AAPG Bulletin*, v. 64, p. 2051–2063.
- Tyson, R.V., 1987, The genesis and palynofacies characteristics of marine petroleum source rocks, *in* J. Brooks and A.J. Fleet, eds., *Marine Petroleum Source Rocks*: Geological Society of London Special Publication 26, p. 47–67.
- Tyson, R.V., and T.H. Pearson, 1991, Modern and ancient continental shelf anoxia: an overview, *in* R.V. Tyson and T.H. Pearson, eds., *Modern and Ancient Continental Shelf Anoxia*: Geological Society of London Special Publication 58, p. 1–24.
- Wardlaw, B.R., 1980, Middle–Late Permian paleogeography of Idaho, Montana, Nevada, Utah, and Wyoming, *in* T.D. Fouch and E.R. Magathan, eds., *Paleozoic Paleogeography of West-Central United States*, West-Central United States Paleogeography Symposium 1: Rocky Mountain Section Society of Economic Paleontologists and Mineralogists, p. 353–361.
- Yentsch, C.S., 1974, The influence of geostrophy on primary production: *Tethys*, v. 6, p. 111–118.
- Ziegler, A.M., C.R. Scotese, and S.F. Barrett, 1983, Mesozoic and Cenozoic paleogeographic maps, *in* P. Brosche and J. Sündermann, eds., *Tidal Friction and the Earth's Rotation, II*: Berlin, Springer-Verlag, p. 240–252.
- Zimmerman, H.B., A. Boersma, and F.W. McCoy, 1987, Carbonaceous sediments and paleoenvironment of the Cretaceous South Atlantic Ocean, *in* J. Brooks and A.J. Fleet, eds., *Marine Petroleum Source Rocks*: Geological Society of London Special Publication 26, p. 271–286.

Chapter 2

Paleoceanography of Marine Organic-Carbon-Rich Sediments

William W. Hay

GEOMAR

Kiel, Federal Republic of Germany

and

University of Colorado

Boulder, Colorado, U.S.A.

ABSTRACT

Marine organic-carbon-rich deposits occur where there is an ample rain of organic particulate material to the sea floor and conditions favorable to its preservation. It was originally thought that the accumulation of organic carbon (C_{org}) was dependent mostly on anoxic conditions at the site of deposition; two such environments, the stagnant basin and the O_2 minimum, were often cited as models. High productivity in the overlying waters has become recognized to be of greater importance. In an overall evaluation of burial of C_{org} in marine sediments, it is apparent that terrigenous input of organic matter is the largest source, followed by marine organic matter fixed in highly productive coastal areas receiving nutrients from land. In terms of rich accumulations of marine organic matter most likely to generate petroleum, areas of ocean upwelling along continental margins are most significant.

Upwelling and nutrient availability in the upwelled waters are two different aspects of oceanographic conditions. Coastal upwelling is only one of a number of different mechanisms that bring deeper waters to the surface. High-latitude convective motions upwell and downwell large volumes of water rapidly, so that only part of the nutrients can be utilized by phytoplankton. Equatorial upwelling produces high productivity over the ocean basins but rarely impinges on continental margins. Other upwelling modes in the open ocean, such as that associated with ice margins, currents, thermocline domes, cyclonic eddies, and Ekman pumping, may have been significant in the past, but little is known about their geologic record. Wind-driven and Kelvin wave-driven coastal upwelling occurs on the eastern margins of the ocean basins in the tropics and subtropics, but the upwelled water is not everywhere nutrient rich. The upwelling is locally enhanced by favorable bathymetry offshore or orographic conditions on land.

In considering how the ocean may have operated in the past, it is necessary to consider how the structure of the ocean may have differed in the past. Other processes, such as caballing, the sinking of denser water produced by mixing waters of equal density but of different temperatures and salinities,

may have been important in producing the large accumulations of C_{org} of the Mesozoic. Finally, the accumulation of C_{org} during the Phanerozoic has taken place in the context of changing levels of atmospheric O_2 .

To take these factors into account, it is necessary to know the paleolatitude of the area at the time the source rock was formed, the orientation of the coastline at that time, the general configuration of the ocean basins and nature of their interconnections, the detailed paleobathymetry of the region being examined, the wind directions and speeds, and the general features of the oceanic circulation.

INTRODUCTION

Ideas about conditions leading to the formation of organic-carbon-rich (C_{org} -rich) sediments have changed as more becomes known about the modern distribution of C_{org} -rich sediments and about the myriad controls on the production, fluxes, and accumulation of organic matter in marine deposits. Large-scale burial of C_{org} has occurred at certain times in the past, particularly in the Ordovician, Late Devonian, Early Carboniferous, Jurassic, Early Cretaceous, and Miocene (Tissot, 1979; Ronov, 1982; Fleet and Brooks, 1987), but it is not always obvious to which, if any, modern analog the deposits of earlier ages correspond. Initially it was thought that C_{org} deposition reflects anoxic conditions in the waters, which prevented or slowed decomposition of organic matter settling through the water column and at the sediment-water interface. More recently, it has become evident that productivity in the surface waters may actually be the most important factor in the formation of C_{org} -rich sediments. In addition, grain size and accumulation rate of the enclosing sediment may also play a major role.

As more is learned about how the ocean behaves as a system, it becomes evident that sites of maximal accumulation of pelagic organic matter in marine sediments, and the form of C_{org} most likely to result in generation of petroleum, are intimately related to the physical oceanographic conditions controlling nutrient regeneration and upwelling of nutrient-rich waters into the euphotic zone. This paper reviews the oceanographic conditions that control the formation of C_{org} -rich sediment, particularly that of marine origin.

Anoxic Environments

Until a decade ago, C_{org} deposition was explained through analogy with modern anoxic environments (Schlanger and Jenkyns, 1976; Ryan and Cita, 1977; Fischer and Arthur, 1977; Thiede and van Andel, 1977; Arthur and Schlanger, 1979; Demaison and Moore, 1980a, b; de Graciansky et al., 1986). Demaison and Moore (1980a, b) emphasized the important role of anaerobic bacterial activity in enriching the organic matter in lipids leading to petroleum formation. Two anaerobic environments are usually cited: (1) deposi-

tion under stagnant conditions in a silled basin (the "Black Sea model"), or (2) deposition in an intensified O_2 -minimum zone impinging on the continental slope or shelf. To these two modern analogs, a third anoxic category with no modern analog, stagnant warm saline bottom waters formed by intense evaporation in arid regions, was added during the last decade (Brass et al., 1982a, b). The stagnant basin and warm saline bottom water models correspond to different conditions of freshwater balance.

Freshwater Balance

Because of gain or loss of fresh water from precipitation, runoff from land, and evaporation, all marginal seas and many oceanic areas have salinities significantly different from the oceanic mean of 34.5. The deficit or excess of salt is caused by a positive or negative freshwater balance. In the case of positive freshwater balance, precipitation + runoff > evaporation, and the salinity of the water is reduced. In the case of negative freshwater balance, precipitation + runoff < evaporation, and the salinity of the water is increased.

The density differences between more and less saline waters will force opposite vertical circulations for positive and negative freshwater balance, as shown in Figure 1. Because less saline water is less dense, an equivalent weight of low-salinity water occupies more volume than higher-salinity water. As a result, the surface of low-salinity water above an internal horizontal surface of equal pressure (geopotential = isobar) will be higher than the surface of higher-salinity water, as shown in Figure 2. The slope on the surface and the internal horizontal pressure gradients will force surface flow from the lower toward the higher salinity, and flow from the higher salinity toward the lower salinity at depth. The former is termed estuarine flow, and the latter is termed lagoonal or anti-estuarine flow, as indicated in Figure 1. This two-way flow will always occur if the bottom of the strait connecting the two bodies of water is below sea level. The volume of the flow depends on both the freshwater balance and the salinity contrast between the two bodies of water. If the salinity contrast is 10%, the volume of the exchanges with the ocean will be about 10 times the freshwater excess or deficit; if the salinity contrast is

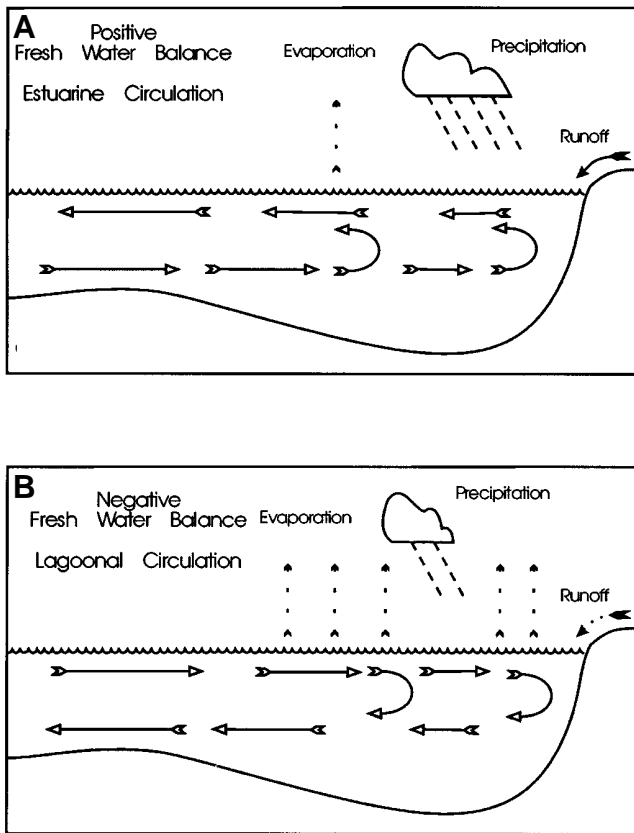


Figure 1. Freshwater balance and circulation. Open arrows indicate the flows of water. (A) Positive freshwater balance (precipitation + runoff > evaporation) results in estuarine circulation, with outflow at the surface and inflow at depth. Nutrients are introduced by rivers, upwelled, and internally recycled, resulting in high productivity. (B) Negative freshwater balance (precipitation + runoff < evaporation) results in lagoonal or anti-estuarine circulation, with inflow at the surface and outflow at depth. Nutrients are downwelled from the surface and flushed from the basin, resulting in low productivity.

20%, the volume of the exchanges with the open ocean will be about 5 times the magnitude of the freshwater balance (see Brown et al., 1989, p. 170).

Positive and negative freshwater balances play a major role in the circulation of marginal seas and some oceanic areas. As will be discussed below, estuarine circulation acts to trap nutrients introduced by runoff from land and marine inflows, resulting in high productivity. Lagoonal circulation flushes nutrients and results in low productivity.

Stagnant Basins

Three areas are generally given as examples of the stagnant basin model: the Black Sea, the Cariaco Trench, and silled Norwegian fjords. All of these basins have a positive freshwater balance. In positive freshwater balance seas that have isolated depressions extending below the mixed surface layer, density strat-

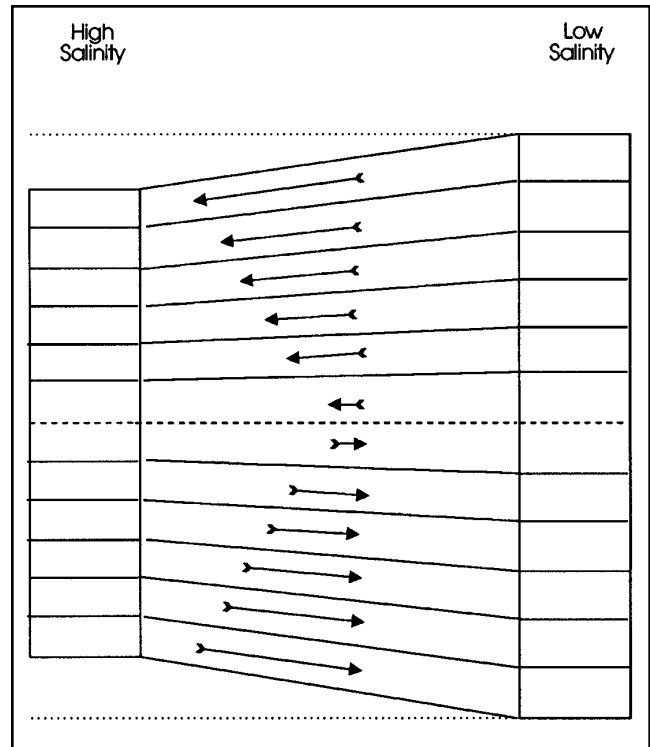


Figure 2. Flows between higher and lower-salinity bodies of water connected through a restricted strait or lying in the equatorial region where there is no Coriolis Force. The relationship of geopotentials (surface along which the acceleration due to gravity is everywhere the same; i.e., horizontal surfaces), shown as dotted lines, and isobars (surfaces of equal pressure), shown as solid lines. Low-salinity water, being less dense than high-salinity water, has a higher specific volume, that is, occupies more space, so that the isobars are more widely spaced. The surface of the low-salinity water is higher than that of the higher-salinity water; the slope of the surface and the slope of the isobars indicate the direction of flow induced by the pressure gradient. Flows are shown by arrows, with the length of the arrow corresponding to the velocity. The phenomenon of two-way flow occurs everywhere the bottom of the channel connecting the two bodies of water is below the level of the surface of the high-salinity layer. The heavy dashed line is the level of coincidence of a geopotential and an isobar, sometimes termed the "level of no motion."

ification can develop between lighter, less saline surface waters and denser, more saline subsurface waters. The density stratification can restrict vertical mixing and result in anoxia of the entire subsurface water column if the organic particle flux from the surface waters remains high as a result of nutrient input from rivers and upward mixing of the subsurface waters.

The first of these analogs, the Black Sea (Ross and Degens, 1974; Murray, 1991) is the most frequently cited and is represented schematically in Figure 3. The Black Sea has been invoked as a model for the deposi-

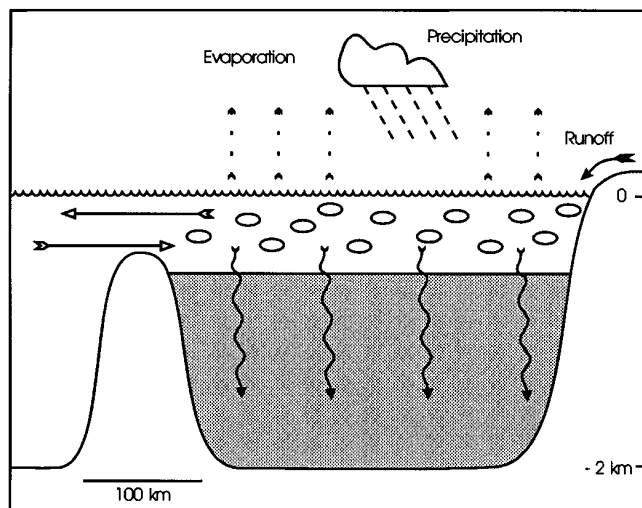


Figure 3. The stagnant basin model for deposition of C_{org} -rich sediments in an anoxic environment ("Black Sea model"). Inflow and outflow are indicated by open arrows. Ellipses represent phytoplankton, vertical wavy arrows represent the sinking organic particulate flux, shaded area indicates dysaerobic-anoxic conditions. The stagnant basin requires input of nutrients to the surface waters, and a positive freshwater balance (runoff + precipitation > evaporation). In the Black Sea, evaporation exceeds precipitation, but the freshwater contribution from runoff is very large; the nutrient supply to the Black Sea is mostly from rivers.

tion of Mesozoic bituminous shales in the North Atlantic and adjacent seas (Fischer and Arthur, 1977; Arthur and Natland, 1979; Arthur et al., 1984; Demaison and Moore, 1980a, b). Although it lies in a region where evaporation exceeds precipitation, the Black Sea is a hyposaline marginal sea; the salinity of its surface waters is only 17, half that of normal marine waters. It has a strong positive freshwater balance because it is almost completely landlocked and receives inflow from rivers draining much of the northern temperate and subtropical regions of central and eastern Europe, where precipitation \gg evaporation. The ratio of its surface area, $0.4 \times 10^6 \text{ km}^2$, to the area of land draining into it, $2 \times 10^6 \text{ km}^2$, is 1:5. It is isolated from the Sea of Marmara, which has more normal marine salinities, by the Bosphorus, a 30 km long passage that narrows to 1 km width and shallows to 60 m depth. This narrow constriction restricts the exchange with the Mediterranean (via the Sea of Marmara and Dardenelles), allowing the great degree of differentiation of the Black Sea waters. The flow through the Bosphorus into the Black Sea is approximately equal to the freshwater excess, and the outflow is twice as large. The Black Sea has been anoxic for only about 7000 years. The sediments forming today are not unusually enriched in C_{org} (Calvert, 1987). However, there was an episode of high C_{org} deposition that coincided with the development of salinity strati-

fication as salt waters began to flow into the basin at the end of the rise in sea level following the last deglaciation. According to Calvert (1990), the deposition of this C_{org} -rich sapropel took place while the basin was still oxic.

A fully marine stagnant basin analog, the Cariaco Trench, is about 1400 m deep. It is a narrow rift graben probably formed during the Quaternary by differential motion of the Caribbean plate relative to South America. It is isolated from the Venezuelan Basin by a shallow (<200 m) shelf (Richards and Vaccaro, 1956; Edgar et al., 1973). It is filled with denser, more saline waters that form on the Venezuelan shelf and flow into the basin during the northern hemisphere winter. During the remainder of the year, the shelf waters and those overlying the trench are freshened by the outflow of the Orinoco and other rivers. The Cariaco Trench has a longer history of C_{org} deposition than the Black Sea but is a hundred times smaller ($0.004 \times 10^6 \text{ km}^2$) than the Black Sea and is an even poorer analog for Mesozoic and earlier C_{org} burial over extensive areas.

The Norwegian fjords (Richards, 1965; Grasshoff, 1976) are smaller than the Cariaco Trench. The fjords, which have a sill, usually a moraine, near their mouths, have contained anoxic water only since the retreat of the glaciers. The temporal and spatial scales of the C_{org} accumulations in these modern anoxic basins are very different from those of petroleum source rocks.

The Baltic Sea (Magaard and Reinheimer, 1974) is a large positive freshwater balance sea with a shallow connection to the North Sea. It is mostly very shallow (mean depth 55 m), but has some depressions, such as the Gotland, Fårö, and Landsort Deeps, that extend to 200 m below the mean depth and contain anoxic waters (Grasshoff, 1974, 1976).

Although at present the Mediterranean has a strong negative freshwater balance (Tchernia, 1980), it has been suggested that at the times of sapropel formation in the Quaternary it had, at least regionally, a positive freshwater balance due to increased inflow from the Nile (Rossignol-Strick, 1985, 1987) and from increased precipitation in the eastern Mediterranean borderlands (Rohling and Hilgen, 1991).

Kauffman (1984) and Pratt (1985), on the basis of analysis of molluscan communities and stable isotopes, suggested that deposition of C_{org} -rich shales in the Cretaceous Western Interior Seaway of North America was in response to stratification resulting from development of a low-salinity surface water layer. This hypothesis invokes positive freshwater balance as the critical factor in inducing stagnation and input of nutrients from rivers to increase productivity.

In contrast, the Early Cretaceous South Atlantic had an area of about $9 \times 10^6 \text{ km}^2$, more than double the area of the modern Mediterranean and about 20 times larger than the Black Sea. It was oriented north-south across the arid zone. The area draining into it was probably $<6 \times 10^6 \text{ km}^2$, and most rivers were directed away from it. It had a strong negative freshwater balance, documented by extensive salt deposition (Sibuet et al., 1984; de Jesus Conceicao et al., 1988). Hence, it

was not an analog of the modern stagnant basins, which depend on positive freshwater balance to maintain a stratified condition.

O₂ Minimum

The O₂ minimum is most intensely developed along the eastern margins of the ocean basins in the tropics and subtropics (Wyrski, 1962), as shown schematically in Figure 4. In the modern ocean, the O₂ minimum reflects the balance between the ocean's two O₂ sources and the O₂ demand resulting from respiration and decomposition of sinking organic particles. The O₂ sources for waters in the tropics and subtropics are the air-sea interface there, where O₂ is carried down by turbulent mixing of the surface layer, and the air-sea interface in high latitudes where deep water is formed and subsequently advected equatorward. Water in the O₂ minimum acquired its original O₂ when it was last at the sea's surface. It subsequently loses up to 90% (or more) of its original O₂ to respiration and decomposition of organic matter. Replenishment of O₂ to the O₂ minimum can take place only through the inefficient process of turbulent mixing of waters from below and above and through the negligible process of diffusion. As discussed below, the water of the present-day O₂ minimum in the tropics and subtropics sinks along fronts in the mid-latitudes.

The idea that the O₂ minimum is closely related to the deposition of C_{org}-rich sediments came from studies of the water-column chemistry and sediments in the Gulf of Mexico (Richards and Redfield, 1954). The C_{org} content of sediments in the Gulf of Mexico is highest in the upper continental slope, at the same depth as the O₂ minimum in the waters (Dow, 1978). Coincidentally, the upper slope is also the environment where the grain size of the sediments is finest and the C_{org} is most likely to be preserved, because fine-grained material inhibits diffusion of O₂ from the overlying waters into the sediment. The O₂-minimum hypothesis of the origin of C_{org}-rich sediments was reinforced by studies along the western margin of India (Marchig, 1972; von Stackelberg, 1972; Cloos et al., 1974), where a strong O₂ minimum and high C_{org} content in the sediments approximately coincide. Levitus (1982) has shown that the O₂ minimum is most extensively developed in the northeastern Pacific Ocean, where O₂ saturation levels at the O₂ minimum are <10% (>0.5 mL/L = 22 μmol/kg). Saturation at the ocean surface is always slightly greater than 100% (<4.5 mL/L = 194 μmol/kg in the >28°C waters of the equatorial region; >8.5 mL/L = 367 μmol/kg in the <-1°C waters of the polar regions). The saturation level of bottom waters is highest in the North Atlantic (69%, 5.35 mL/L = 231 μmol/kg) and lowest in the North Pacific (49%, 3.71 mL/L = 160 μmol/kg). Along the west coast of the Americas from 30°N to 30°S, the O₂ saturation levels are <5% (0.25 mL/L = 11 μmol/kg). In the western North Pacific, O₂ saturation levels at the O₂ minimum rise to 25% (>1.0 mL/L = >43 μmol/kg). Except along the margin of South America, the O₂ minimum is not well developed in the South Pacific. In the Indian Ocean, the O₂ minimum

becomes progressively more intense from south to north; it is most strongly developed in the northern Arabian Sea and northern Bay of Bengal, where O₂ saturation levels fall below 5% (0.5 mL/L = 22 μmol/kg). The highest O₂ saturation levels (20%, 1.5 mL/L = 65 μmol/kg) in an O₂ minimum beneath a productive coastal upwelling region are off northwest Africa, between 8 and 18°N.

The area of the modern O₂ minimum off northwest Africa is almost as large as the entire Early Cretaceous North Atlantic and is developed at the same latitude. Although this might suggest that the deposition of black shales there took place in an O₂ minimum, most of the C_{org} deposition occurred in the deeper parts of the basins rather than in the shallower margin settings where the O₂ minimum intercepts the sea floor (Brass et al., 1982a, b).

Warm Saline Bottom Waters

Broecker (1969) argued that it is impossible for an ocean basin to become anoxic. The present thermohaline circulation introduces so much O₂ into the deep sea that unrealistically large increases in ocean productivity are required to expand the area of the ocean floor bathed by anoxic waters. At present, the ocean contains about 300 × 10¹⁵ mol. of O₂ (Broecker and Peng, 1982), but only 130 × 10¹⁵ mol. of C_{org} (Holser et al., 1988). If all the living biota in the ocean were killed, the ocean could completely oxidize all of the organic matter and still remain fully oxic. Just as Broecker's (1969) abstract was published, Leg 1 of the Deep Sea Drilling Project (DSDP) recovered C_{org}-rich black shales from the deep ocean basin in the western North

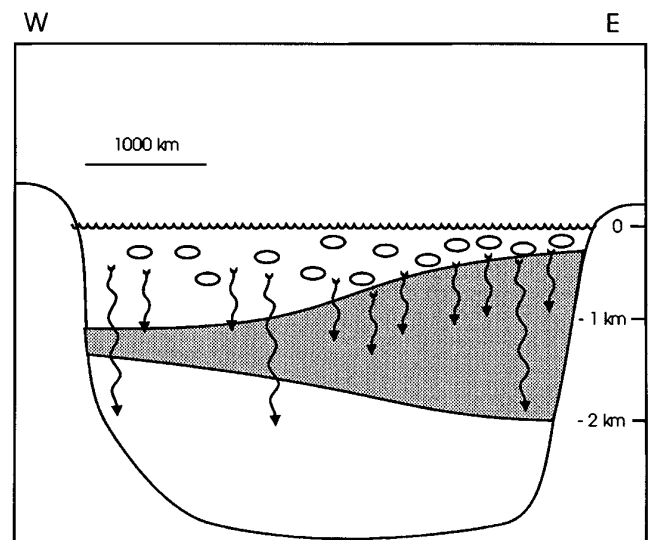


Figure 4. The O₂-minimum model for deposition of C_{org}-rich sediments in an anoxic environment where it impinges on the continental margin. Symbols as in Figure 3. The O₂ minimum is produced by decomposition of organic particulate matter. It is most strongly developed on the eastern margin of the tropical subtropical gyres.

Atlantic off the Bahamas (Ewing et al., 1969). This and subsequent discoveries of C_{org} -rich black shales in the North and South Atlantic spurred interest in the possibility that the bottom waters had been anoxic. Brass et al. (1982a, b) developed the idea that dense warm saline waters, formed by high evaporation in marginal seas surrounded by arid land, may have flowed down the continental slope and filled the deep basins as bottom water, as shown schematically in Figure 5. If this water were only supplied periodically, it would become stagnant, allowing its O_2 to be consumed. The hypothesis of warm saline bottom waters became a third possibility for producing anoxia and enhancing the preservation of C_{org} .

There are several modern examples of small basins filled with warm saline bottom waters in the modern ocean. The Orca Basin on the northwestern margin of the Gulf of Mexico is an example of a basin filled by highly saline waters that cause stratification and anoxia. It is the same size as the Cariaco Trench. It differs from the model proposed by Brass et al. (1982a, b) in that the high salinity results from dissolution of salt in surrounding diapirs, not from evaporation. The Orca Basin and similar depressions in the Mediterranean (Rossignol-Strick, 1987) and Red seas are special cases that depend on dissolution of previously deposited salt to produce the saline waters. However, on a small scale and with extreme salinities, they have the characteristics of anoxic basins filled with warm saline bottom water that may have existed in the Mesozoic and earlier times. Conditions leading to the hypothesized more extensive development of warm saline bottom waters in the past would require a negative freshwater balance.

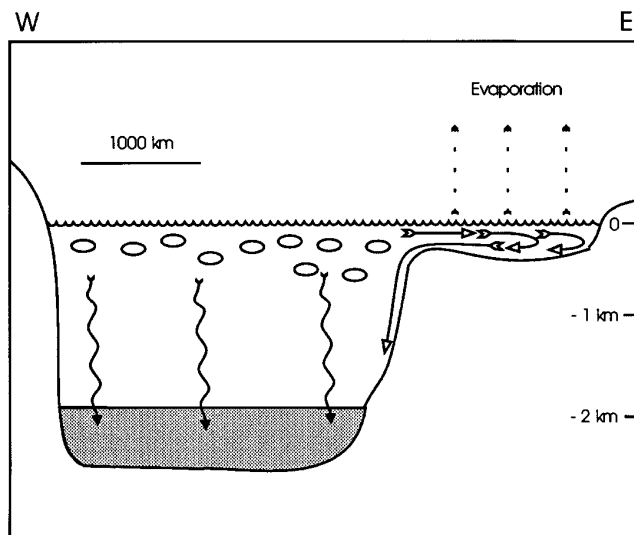


Figure 5. The warm saline bottom water hypothesis for deposition of C_{org} -rich sediments beneath anoxic bottom waters. Symbols as in Figure 3. The warm saline bottom water is formed by evaporation in a shallow marginal sea in the arid zone.

High Productivity

The importance of high productivity in response to upwelling of nutrient-rich waters along eastern subtropical coasts of the ocean basins to sedimentation of C_{org} has long been recognized (Brongersma-Sanders, 1948, 1957; Morris, 1987; Calvert, 1987). Parrish (1982), Parrish and Curtis (1982), and Barron (1985) have demonstrated that both analog and numerical climate models show that upwelling should have occurred along the eastern subtropical coasts of the ocean basins throughout geologic history, and that many of these hindcasts of upwelling correspond to known occurrence of black shales or petroleum source beds.

Nutrient regeneration and the development of the O_2 minimum are the result of the process of decomposition of organic matter. Hence, nutrient levels are highest where the O_2 content of the water is lowest; the inverse relationship is such that the amount of nutrients can be considered to be an estimate of the amount of O_2 depletion. Although the relation between O_2 consumption and nutrient levels has long been known, the relation between productivity and development of the O_2 minimum or anoxic conditions first became evident from modeling studies by Wyrski (1962) and Southam et al. (1982). They described the ocean as a three-layer model, with a surface layer with O_2 content in equilibrium with the atmosphere, an intermediate layer nutrient-rich O_2 minimum, and a deep layer that receives O_2 by advection from a high-latitude source in communication with the atmosphere. The formation of the tropical-subtropical O_2 minimum is shown schematically in Figure 6. Nutrients introduced into the surface layer from the intermediate layer are utilized by phytoplankton and ultimately sink back into deeper waters as an organic particulate flux. They demonstrated that because the O_2 content of the deep water and nutrient supply to the surface waters are coupled, a stagnant ocean will not become anoxic. Stagnation would prevent nutrients from being supplied to the surface waters. Without nutrients there can be no new primary productivity, and hence no export of organic matter from the surface to the deep layer. They found that anoxia in the deep layer required vigorous circulation that would bring large quantities of nutrients from the deep sea into the surface layer and create high productivity.

Oeschger et al. (1984) noted that ocean surface waters become nutrient depleted only where the ocean is stratified. At high latitudes, where convective overturning affects the ocean to depths well below the base of the euphotic zone, nutrients do not remain in the euphotic layer long enough to be completely utilized by the phytoplankton. As a result, the surface waters contain unused ("preformed") nutrients.

De Boer (1986) noted that there are two possible states of the ocean leading to burial of C_{org} -rich sediments. The first has rapid vertical circulation with the high O_2 supply overwhelmed by a large organic particle flux as a result of high nutrient supply to the surface waters. The second has slow circulation with a low rate of O_2 supply to the deep waters but additional

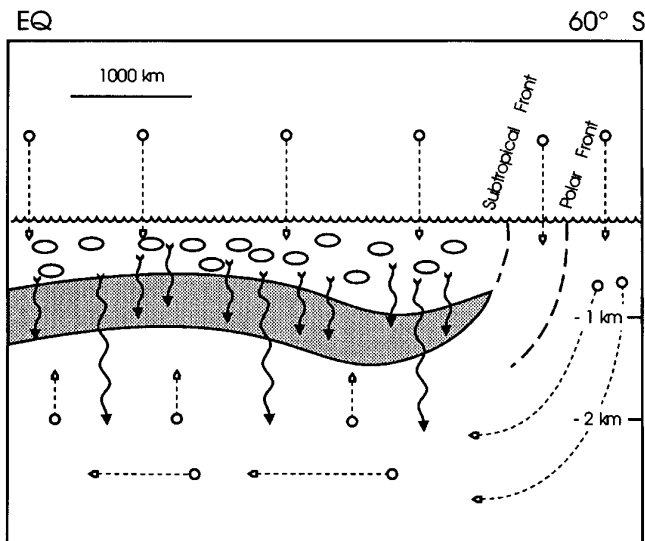


Figure 6. The origin of the O_2 minimum. O_2 flux indicated by arrows with " O_2 " tails; other symbols as in Figure 3. O_2 diffuses into the warm surface ocean in the subtropical seas. More diffuses into the cold polar seas where it is fed into the deep water of the ocean by bottom water formation. From the deep water it diffuses upward. The O_2 minimum represents the balance between O_2 supply from above and below, and O_2 demand for decomposition of settling organic particles.

nutrient supply from land. De Boer cited the productivity estimates for the Cretaceous made by Bralower and Thierstein (1984), that indicate productivity then was significantly lower than today. De Boer concluded that the paradox of C_{org} accumulation in early and middle Cretaceous sediments and low productivity is best explained by assuming that the high temperatures and decreased vertical circulation of the ocean led to a marked decrease in supply of O_2 to the bottom waters, enhancing the accumulation of C_{org} . He suggested that the nutrients required by the oceanic phytoplankton were introduced from land as sea level rose. He also noted that the burial of C_{org} would result in higher levels of atmospheric CO_2 , further increasing the temperature and providing a positive feedback for additional C_{org} burial. Finally, from analysis of $\delta^{13}C$ data, he concluded that the increased burial of C_{org} during the early and middle Cretaceous was only ~20% greater than the long-term global average of $80 \times 10^{12} \text{ gCyr}^{-1}$.

Sarmiento et al. (1988) described the behavior of an ocean box model with coupled nutrient supply and O_2 demand, but with two different surface ocean areas (Figure 7). Their model consisted of a mixed low-latitude surface ocean completely depleted in nutrients, a high-latitude ocean containing preformed nutrients and mixed to depths well below the base of the euphotic zone, and a nutrient-rich deep ocean. They assumed that nutrient utilization by phytoplankton is complete in the low-latitude surface ocean, but only

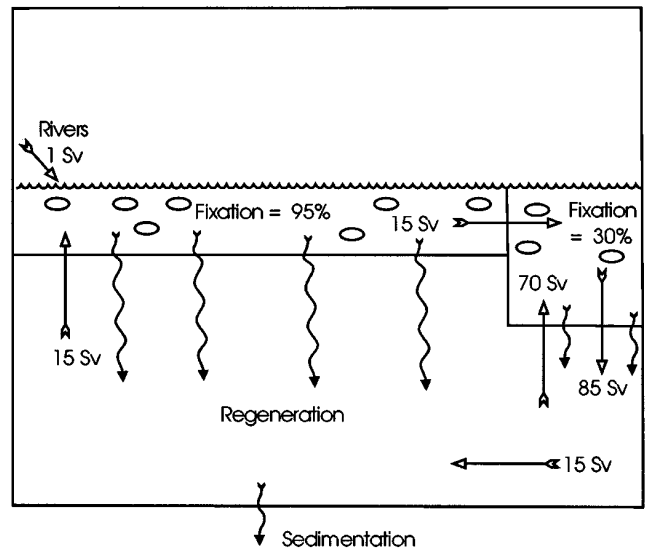


Figure 7. The Sarmiento et al. (1988) box model. Symbols as in Figure 3. The surface ocean consists of two regions, a low-latitude area corresponding to the subtropical gyres and a high-latitude region corresponding to the oceans poleward of the Subtropical Fronts. The high-latitude surface ocean communicates with the deep ocean by convective upwelling and downwelling (small arrows). The oceanic thermohaline convection, shown by large open arrows, involves formation of bottom water from the high-latitude surface ocean, advection beneath the low-latitude surface ocean, upwelling into the high-latitude surface ocean completing the loop. The nutrients upwelled into the low-latitude surface ocean are completely utilized by phytoplankton-producing organic matter that sinks as particles into the deep ocean where nutrients are regenerated. Nutrients are introduced into the high-latitude surface ocean by convective motion of the water, but are only partially utilized by phytoplankton there. A rain of organic particulate material from the high-latitude surface ocean into the deep sea completes the nutrient cycle there. O_2 levels in the deep sea depend on the proportion of the nutrients upwelled into the high-latitude surface ocean utilized by the phytoplankton.

partial in the high-latitude ocean. Nutrient regeneration takes place in the deep ocean through oxidation of sinking organic particulate material. The high-latitude ocean was assumed to be connected to the deep ocean by convective overturn. The thermohaline circulation consisted of water sinking from the high-latitude ocean into the deep ocean, being returned to the low-latitude surface ocean by upwelling and then advected back to the high-latitude ocean. With this model, they found that stagnation of the convective overturn of the high-latitude ocean, that is, reducing the rate of convective overturn and hence allowing a greater proportion of the nutrients to be utilized while at the same

time reducing the ventilation of the deep water, led to lower O_2 levels in the deep water. However, stagnation of the thermohaline circulation had the opposite effect. Because productivity of the low-latitude surface waters depends on upwelling of nutrient-rich waters, only an increase in the rate of thermohaline circulation can cause a decrease in the O_2 levels in the deep water.

A new and potentially important factor, presence of a deep chlorophyll maximum beneath the pycnocline, has been suggested by Rohling and Gieskes (1989) and Rohling (1991) to explain the Pliocene and Quaternary Mediterranean sapropels. They suggested that the sapropels may have formed in response to a decrease in the rate of formation of intermediate and deep water as well as an increased supply of nutrients from increased river flow. They proposed that the water balance of the Mediterranean need not have completely reversed from negative to positive, but that sharp reduction of the formation of interior waters would allow the pycnocline to rise. They reasoned that a shallower pycnocline would allow the nutrient-rich waters beneath it to come into the lower part of the photic zone. This would result in a highly productive deep chlorophyll maximum and a concomitant increase in the downward flux of organic matter (export production) from the euphotic layer. Parsons et al. (1984) estimated that 10–40% of the total carbon fixation integrated over the euphotic zone comes from the chlorophyll maximum. The increased productivity of both the surface waters and the deep chlorophyll maximum would increase the export flux of organic particulate matter to the bottom, forming the sapropels.

There has been much discussion recently over the relative significance of productivity and anoxia in the preservation of organic matter in sediments. The classic view that stagnation and anoxia are essential to the preservation of C_{org} in sediments has been eloquently summarized by Demaison and Moore (1980a, b). The supply of oxidants (essentially SO_4^{2-} since O_2 is absent) in euxinic sediments is restricted. Bioturbation is unavailable to enhance transport of oxidants into the sediment from the overlying water, and the oxidation of C_{org} becomes oxidant limited.

This view has been challenged after studies of the conditions along margin of India (Pedersen and Calvert, 1990), along the Oman margin (Shimmield et al., 1990; Pedersen et al., 1992), and in the Gulf of California (Calvert et al., 1992) failed to confirm the expected relation between C_{org} accumulation and the O_2 minimum. Calvert et al. (1992) noted that sediments from the Guaymas Basin of the Gulf of California having similar bulk composition also have similar total organic carbon (TOC) contents, independent of whether they are laminated and bioturbated. The laminated sediments occur where the bottom waters represent an intense O_2 minimum ($<5 \mu\text{mol/kg}$), and there are no burrowing infauna. The bioturbated sediments occur beneath waters with O_2 levels around $30 \mu\text{mol/kg}$. They conclude that the accumulation is related to productivity and to the resulting increased particulate flux to the bottom, not to the concentrations of dissolved O_2 in the bottom waters.

Other recent studies have continued to emphasize the role of anoxic conditions in retarding the decomposition of organic matter in the water column for formation of C_{org} -rich Holocene sediments (Canfield, 1989, 1992; Lee, 1992) and their presumed ancient rock counterparts (Ingall et al., 1993). Canfield (1989) has noted that the decomposition of C_{org} is the result of oxic respiration and sulfate reduction. He found that in rapidly accumulating nearshore sediments, these two sources of O_2 were approximately equal contributors to decomposition of organic matter. In the more slowly accumulating sediments of the deep sea, oxic respiration becomes 100 to 1000 times more important than sulfate reduction. Sulfate reduction is the dominant process in euxinic sediments. He described the efficiency of C_{org} burial as independent of the level of bottom-water oxygenation at very high sediment accumulation rates ($>0.1 \text{ g cm}^{-2} \text{ yr}^{-1}$), but stated that at lower sedimentation rates higher preservation of C_{org} is observed for deposition beneath O_2 -depleted waters. Paradoxically, Canfield (1989) found that as much organic matter was oxidized by sulfate reduction in euxinic sediments as is oxidized by oxic respiration and sulfate reduction combined in more normal marine sediments deposited at the same rate. Canfield (1992) concluded that O_2 -respiring fungi and bacteria are important for efficient decomposition of organic matter, particularly the aromatic compounds. These organisms are not available in euxinic environments; although decomposition also proceeds there, the rate is much slower. Lee (1992) suggested that under anoxic conditions the decomposed organic matter is converted into bacterial biomass which, in the absence of organisms that graze on bacterial remains, accumulates in the sediment rather than being recycled. Ingall et al. (1993) examined the carbon/phosphorus (C/P) ratio in Paleozoic black shales, and found that in laminated shales, C_{org} is enriched and P depleted when compared to bioturbated shales. Again, Ingall et al. attributed this to efficiency of decomposition in more oxic environments, suggesting that under anoxic conditions bacteria have a limited ability to store P, that P is preferentially regenerated from the organic matter, and that C_{org} is preferentially preserved.

The arguments have been discussed recently in exchanges of views in the *AAPG Bulletin* (Demaison, 1991; Pedersen and Calvert, 1991) and in *Geology* (van Cappelen and Canfield, 1993; Calvert et al., 1993). Demaison (1991) noted that oil source rocks have characteristics in addition to being rich in C_{org} . They must also be hydrogen-rich (type I or type II kerogen), a factor not discussed by Pedersen and Calvert (1990). Demaison (1991) also observed that black shales or oil shales containing type I or type II kerogen always display sedimentologic and paleontologic indications of O_2 -deficient water above the sediment-water interface. Finally, Demaison (1991) challenged the idea that the Black Sea sapropel was deposited under oxic conditions, stating that the sapropel was deposited in saline water with low iodine/ C_{org} (I/C_{org}) ratios and low manganese contents, similar to those measured in modern anoxic Black Sea sediments. Pedersen and

Calvert (1991) responded that their 1990 and other papers had been concerned with the general problem of C_{org} burial, not with source rock formation, which requires burial and preservation of specific types of organic matter. Pedersen and Calvert also noted that laminated sediments do not necessarily reflect anoxic conditions in the water column, but may result from seasonality of planktonic and terrigenous inputs. Pedersen and Calvert cited the Peru margin as a place where laminated sediments form beneath an oxic water column. Pedersen and Calvert concluded by arguing that the I/C_{org} ratio is high in the upper part of the Black Sea sapropel, but decreases with depth. The high ratio is characteristic of oxic conditions, and the decrease of the I/C_{org} ratio with depth was a response to the very high O_2 demand associated with the large flux of organic matter that produced the sapropel. In the second exchange, Van Cappelen and Canfield (1993) argued that laminated ancient sediments often have higher concentrations of C_{org} (2–13%) than do closely associated bioturbated shales (0.1–3%). They believe that the studies of Calvert et al. (1992) and other studies of very young sediments reflect conditions at the beginning of the diagenetic process, but that the enhanced preservation under anoxic conditions only becomes apparent after long periods of time. Calvert et al. (1993) responded that it had not been demonstrated that the supply rates of C_{org} to the ancient sediments had been the same. They observed that recent data from the Black Sea indicate sulfate reduction rates to be much higher than Canfield (1989) had assumed, making the burial efficiency of C_{org} much less than Canfield's estimate.

Sediments

The enclosing sediments play an important role in the preservation of organic matter and its transformation into petroleum. The positive correlation of C_{org} content with sedimentation rate has long been known (Trask, 1939). It was documented in Neogene deep sea sediments recovered in the Pacific by the DSDP by Heath et al. (1977), and in Holocene sediments by Müller and Suess (1979). Southam and Hay (1981), in analysis of the DSDP record of sedimentation in the global ocean, found that whereas total sedimentation rates appeared to vary by one order of magnitude through time, those of C_{org} varied through two orders of magnitude, suggesting an exponential relationship. Ibach (1982) analyzed the DSDP record in greater detail, and found that the TOC content expressed as weight percent first increases with sedimentation rate, reflecting more rapid passage of the sediment through the surficial zone of intense organic degradation. Rapid burial limits the diffusion of O_2 from the overlying waters into the sediment. Replenishment of O_2 in the pore water is required by aerobic bacteria if they are to maintain efficiency in decomposition of the organic matter. Ibach also found that at inorganic sedimentation rates between 15 cm kyr^{-1} (calcareous) and 40 cm kyr^{-1} (black shale), the TOC decreases because of dilution by the increasing clastic sediment flux. He

also found that in deep sea sediments, TOC increases systematically from calcareous through calcareous-siliceous to siliceous sediments, reaching the highest values in black shale. In a study of sediment offshore the northwestern United States, Keil et al. (1994) found that discrete organic matter, mostly in the form of plant debris, formed more than 95% of the TOC in the sand-size fraction. However, <10% of the TOC in the silt- and clay-size fractions (<64 μm) was discrete organic matter. The remainder was inseparable from the inorganic sediment, consistent with the hypothesis that it was sorbed onto the mineral surfaces as a monolayer. Keil et al. concluded that the TOC concentration was largely controlled by the surface area of the particles comprising the sediment. It has also been evident that C_{org} is more readily preserved in pelitic rather than more coarse grained deposits, but the cause of this phenomenon has remained elusive. Once the organic matter is enclosed in sediment, the development of anoxia in the pore waters retards degradation by aerobic bacteria and promotes the activity of the anaerobes. Development of anoxia in the pore waters is promoted by lesser porosity and permeability. Stein (1986) has discussed the combined effects of oxic and anoxic bottom waters and sediment accumulation rates on the burial and preservation of C_{org} .

THE PALEOCEANOGRAPHY OF C_{ORG} ACCUMULATION

This section discusses the introduction of organic matter and nutrients into the marine environment, and the interplay of productivity, O_2 depletion, nutrient regeneration, and ocean circulation to sedimentation of C_{org} in the ocean.

Sources of Organic Matter

There are two major sources of organic matter accumulating in marine sediments: (1) terrestrial plant material brought to the sea by rivers, and (2) organic particulate matter resulting from phytoplankton (primary) productivity in the ocean (Romankevich, 1984; Tissot et al., 1979). The major sites of input of organic matter are shown in Figure 8. At present, terrigenous plant material is by far the largest source, estimated by Berner (1982) to account for over 80% of the C_{org} buried in marine sediments. Terrestrial organic matter is more structured, kerogen-rich, and resistant to decomposition; organic matter originating from ocean phytoplankton is amorphous, has a higher lipid content, and is more susceptible to bacterial degradation (Tissot and Welte, 1978).

Supply of Terrigenous Organic Matter from Land

Terrigenous organic matter from land is supplied to the sea by rivers draining forested areas. The total amount of C_{org} delivered to the sea as particulate organic matter by rivers is estimated to be $180 \times 10^9 \text{ kg yr}^{-1}$ by Meybeck (1982) or $240 \times 10^9 \text{ kg yr}^{-1}$ by Lee and Wakeham (1989). About half of the particulate C_{org}

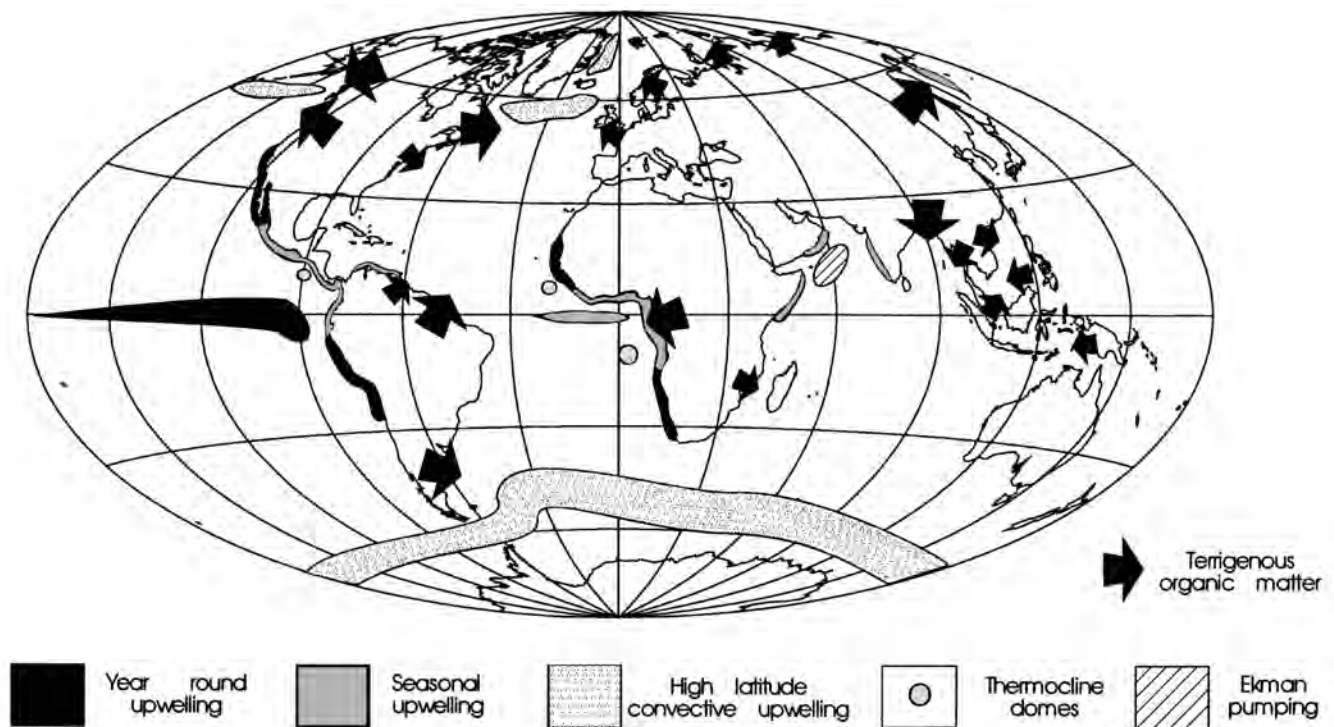


Figure 8. Sources of C_{org} in the ocean. Terrigenous sources are shown by arrows. Marine sources resulting from different types of upwelling are shown with different patterns. Estuaries and shallow coastal productivity, resulting mostly from nutrient input from land, are not shown.

brought to the sea by rivers is eaten or decomposed, and the remainder is buried in the sediments accumulating along the continental margins. As a result of the post-glacial rise in sea level, most river-borne detritus accumulates in estuaries or deltas, but this is an ephemeral situation and the suspended loads of rivers may have been more evenly distributed over larger areas of the continental shelves in the past. Berner (1982) estimated that 130×10^9 kg of terrigenous C_{org} is buried annually in shelf sediments, and that 10% of this is subsequently destroyed during diagenesis. The largest forests supplying C_{org} to rivers occur in the humid belts that lie along the equator and in the northern high-latitude temperate-subpolar region. Meybeck (1982) reported that the rate of export of total C_{org} (particulate and dissolved) reaches its maximum, about $10,000 \text{ kg km}^{-2} \text{ yr}^{-1}$, in both equatorial and temperate rain forests. It is much lower, $400 \text{ kg km}^{-2} \text{ yr}^{-1}$, in semiarid regions. Forests also occur on mountains at all but the most arid latitudes. Along the equator, the vegetation is supplied with large amounts of water by the Intertropical Convergence between the northern and southern hemisphere trade-wind systems. Meybeck (1982) indicated that almost half of the particulate C_{org} carried to the sea is transported by rivers draining tropical rain forests. The high temperatures and humidity of the tropics speed decomposition, so that most of the organic matter carried by equatorial rivers, such as the Amazon, Niger, and Congo, can be expected to be relatively resistant to further degradation (Lee and Wakeham, 1989). At high latitudes there is ample moisture for luxuriant plant

growth, but, because of the cooler temperatures, decomposition proceeds more slowly and the organic matter carried by rivers is relatively fresh. In northeastern Asia, the Amur River carries large quantities of terrigenous organic matter into the Sea of Okhotsk, making the sediments there extraordinarily rich in methane (E. Suess, 1993, personal communication). The rivers carrying organic detritus need not necessarily flow zonally, so that they may transport their loads to coastal areas not bordered by forests. If the rivers flow through extensive arid areas, their load of organic matter may be reduced through oxidation and degradation. Organic matter is also supplied by the numerous small rivers that drain mountains along equatorial and temperate coasts.

Since the Early Carboniferous, the supply of organic matter from land is likely to have occurred in the equatorial region and off the high-latitude forests. The supply of organic matter from mountains near the coast is also important geologically. The western margin of the North Atlantic received mostly terrigenous organic matter from the adjacent Appalachians during its early history (Tissot et al., 1979; Herbin and Deroo, 1982; Summerhayes, 1987). This is why the C_{org} -rich sediments of the western North Atlantic have been source rocks for gas, but little petroleum. Meyers et al. (1983) concluded that the majority of the organic matter that had accumulated in the southern Angola Basin off the southwest African margin during the Cretaceous was also of terrestrial origin. At the time, the southern Angola Basin was about 45°S , so that the onshore source would have been high-latitude forests.

Productivity and Supply of Marine Biogenic C_{org} to the Sediments

McLean (1978) estimated that 27.2% (135×10^{12} kgCyr⁻¹) of global productivity takes place on land. Of the remainder, ~67% (332×10^{12} kgCyr⁻¹) takes place in the open ocean, 5.4% (26.6×10^{12} kgCyr⁻¹) on the continental shelves, 0.28% (1.4×10^{12} kgCyr⁻¹) in estuaries, 0.12% (0.6×10^{12} kgCyr⁻¹) in algal beds and reefs, and 0.08% (0.4×10^{12} kgCyr⁻¹) in upwelling zones. Subsequent studies have shown that McLean overestimated productivity of the open ocean by an order of magnitude. Total productivity in the ocean, expressed in terms of the mass of C fixed annually, is estimated to be 23×10^{12} kg by Romankevich (1984) and 30×10^{12} kg by Berger et al. (1989). Romankevich (1984) concluded that about half of the primary productivity in the sea takes place in marginal areas and half in the open ocean. The compilation of inventories by Sundquist (1985) supports these later estimates but also illustrates the large uncertainties remaining.

Wefer (1991) reviewed the state of knowledge of how organic matter sinks through the water column. He noted that the sinking rates of clay- and silt-size particles and of coccolithophores range between a few centimeters and a few meters per day. Convective motions in the ocean prevent them from reaching the bottom unless they are aggregated into larger, more rapidly sinking particles by flocculation or packaging into fecal pellets. Diatoms and planktonic foraminifera have settling velocities high enough to be able to sink directly to the bottom. Wefer found that with a primary productivity of 30 gCm⁻²yr⁻¹, 10% of that amount leaves the euphotic zone as sinking particles, 90% of these are decomposed before reaching the bottom, and only 3% of the organic matter reaching the bottom is incorporated into the sediment, for an accumulation rate of 0.01 gCm⁻²yr⁻¹. With a primary productivity of 120 gCm⁻²yr⁻¹, 10% sinks but 75% of that is decomposed in the water column and 87% at the sea floor, for an accumulation rate of 1.2 gCm⁻²yr⁻¹.

Berner (1982) estimated the total amount of marine biogenic C_{org} buried in marine sediments to be 27×10^9 kg yr⁻¹. He estimated that half of this is buried beneath upwelling systems, a quarter is buried in shallow-water carbonates, and a quarter is buried in fine-grained pelagic sediments away from the productive upwelling areas. The supply of C_{org} to the sediments in coastal and shallow waters occurs as a result of the growth of shallow-water benthic algae and reefs, but is from phytoplankton in estuaries and over the deeper continental shelf. The major open-ocean source of C_{org} is ultimately from the pelagic primary producers, the phytoplankton.

At present, primary productivity of oceanic phytoplankton ranges through an order of magnitude, from ~500 gCm⁻²yr⁻¹ in coastal upwelling areas (e.g., Peru margin) to ~50 gCm⁻²yr⁻¹ or less in the middle of an oceanic gyre (e.g., central North Pacific) as shown in the maps compiled by Berger (1989).

Quantitative Description of the C_{org} Flux from the Surface Ocean to the Sediment

Having been fixed by the primary producers, the C_{org} enters the food chain and is eaten by herbivores that are in turn eaten by carnivores. Dead organic matter and fecal material falls as a particulate rain through the water column exporting material from the euphotic zone. The primary productivity, P , is much larger than the export production, P_{exp} . According to Eppley and Peterson (1979), $P_{exp} = P^{2/3}/400$ if the P is less than 200 gCm⁻²yr⁻¹, and $P_{exp} = P/2$ if P is greater than 200 gCm⁻²yr⁻¹. Berger and Wefer (1990) simplified this to

$$P_{exp} = 2\sqrt{P}$$

with units of gCm⁻²yr⁻¹.

As the particles sink, aerobic bacteria decompose the organic matter, releasing the nutrients for reuse by the phytoplankton. The rain rate of organic particles decreases with depth as more and more particles are decomposed (Suess, 1980), consuming O₂. Concomitant with the decrease in particulate rain in the upper part of the ocean is an increase in dissolved nutrients, which reaches a maximum at about 1 km in the tropical-subtropical ocean. Below the nutrient maximum, oceanographic factors cause the decreasing particulate rain to correspond to decreasing nutrient levels with depth. As the particles sink, most of their mass is lost through decomposition. The amount of organic matter reaching the deep-sea floor is on the order of 1% of that leaving the photic zone (Broecker and Peng, 1982). Further decomposition takes place at the sediment surface and subsequently within the sediment, so that the fraction ultimately surviving is very small compared to the original primary productivity.

The use of C_{org} as an indicator of oceanic productivity was suggested by Pedersen (1983), who found increased amounts of C_{org} in sediment of the last glacial maximum in the eastern equatorial Pacific. He noted two possibilities for this, either an increased flux of particles to the sea floor as a result of greater productivity in the surface waters, or enhanced preservation as a result of more rapid burial of the organic matter. He used the I/C_{org} ratio to distinguish between these two possibilities. Iodine is almost exclusively associated with organic matter in marine sediments, but it is preferentially lost relative to carbon at lower sediment accumulation rates. He found no evidence for significant changes in the glacial/interglacial sedimentation rate from the I/C_{org} ratios, and concluded that productivity must have been higher during the glacial.

Müller and Suess (1979) described the relations between productivity, bulk sedimentation rate, and C_{org} preservation in young sediments in terms of a preservation factor, equal to the C_{org} accumulation rate divided by the primary production rate. They found the preservation factor to vary by more than four orders of magnitude, from 0.004% to 18% in Holocene sediments, but also found it to be related to

the accumulation rate of the bulk sediment. They developed a formula to relate %C_{org} to primary productivity, sedimentation rate, sediment bulk density, and porosity:

$$\%C_{org} = \frac{0.0030PS^{0.30}}{\rho_s(1-\Phi)}$$

where P is the primary productivity, S is the sedimentation rate, ρ_s is the density of the sediment, and Φ is the porosity, so that the terms

$$\frac{S}{\rho_s(1-\Phi)}$$

convert sedimentation rate (myr⁻¹) to sediment accumulation rate (kg m⁻²yr⁻¹). This formulation neglects the difference between primary and export productivity and does not take into account the decrease in particle flux with water depth.

Bralower and Thierstein (1984) expanded the database and demonstrated that the C_{org} accumulation rate of the sediment increases exponentially with bulk accumulation rate according to the relationship

$$C_A = 0.008S_B^{1.50}$$

where C_A is the accumulation rate of C_{org} (gCm⁻²kyr⁻¹) and S_B is the bulk sediment accumulation rate (gCm⁻²kyr⁻¹). Bralower and Thierstein applied this to the Müller and Suess (1979) relation to investigate the role of oceanic primary productivity in the formation of Cretaceous deposits, including the black shales. They concluded that productivity was generally an order of magnitude less than it is today, even during deposition of black shales.

Berger et al. (1989) related the water-depth dependent C_{org} flux (F_C) to primary production by the formula

$$F_C = 17 \frac{P}{z} + \frac{P}{100}$$

where z is the depth in meters. Sarnthein and Winn (1988) and Sarnthein et al. (1987) further developed the method of estimating paleoproductivity, proposing a transfer function

$$C_A = kF_C S_{B-Corg}^a$$

relating the C_{org} accumulation rate, C_A , to a water-depth dependent flux of C_{org}, F_C (gCm⁻²kyr⁻¹), and a C_{org}-free sedimentation rate, S_{B-Corg} (cmkyr⁻¹), with two constants, a and k . The relation to primary productivity then becomes:

$$P = 15.9C^{0.66}S_B^{0.66}[\rho(1-\Phi)]^{0.66}S_{B-Corg}^{-0.71}z^{0.32}$$

where $C^{0.66}S_B^{0.66}[\rho(1-\Phi)]$ is the C_{org} accumulation rate, C_A , in gCm⁻²kyr⁻¹ and S_{B-Corg} is in units of cm kyr⁻¹, but P is in units of gCm⁻²yr⁻¹. Sarnthein et al. (1992) used these relations and data from Sarnthein and

Winn (1988) to produce an estimate of the water-depth dependent C_{org} flux to the sea floor

$$F_C = \frac{20.563P_{exp}^{0.665}}{z^{0.554}}$$

where z is the water depth.

Sarnthein et al. (1992) also used new data to develop two new transfer equations relating the accumulation of C_{org} to primary productivity, P , and export productivity, P_{exp}

$$P = 61.390C_A^{0.250}S_{B-Corg}^{-0.049}z^{0.150}$$

$$P_{exp} = 9.354C_A^{0.493}S_{B-Corg}^{-0.105}z^{0.300}$$

Again, C_A is in units of gCcm⁻²kyr⁻¹, and S_{B-Corg} is in units of cmkyr⁻¹, but P is in units of gCm⁻²yr⁻¹. These transfer functions were developed from Holocene data from the eastern North Atlantic and applied to Quaternary sediments off northwestern Africa. They suggest Holocene P levels of 95 gCm⁻²yr⁻¹ and P_{exp} levels of 25 gCm⁻²yr⁻¹ are much lower than those of the last glacial maximum, $P = 230$ gCm⁻²yr⁻¹ and $P_{exp} = 120$ gCm⁻²yr⁻¹. Applied to the Cretaceous data of Bralower and Thierstein (1979), the transfer functions indicate productivities lower than today's. The enigma of lower productivity and greater preservation remains (Thierstein, 1989).

A variety of other proxies have been used as estimators of paleoproductivity during the Quaternary: foraminiferal assemblages (Mix, 1989), the relative abundance of the planktonic foraminifer *Globigerina bulloides* (Prell and Curry, 1981; Brock et al., 1992); the abundance of benthic foraminifers (Lutze and Coulbourn, 1984; Herguera and Berger, 1991; Berger et al., 1994; Schnitker, 1994); biogenic silica (Barron and Baldauf, 1989; Herguera, 1992), $\delta^{13}C$ (Broecker and Peng, 1982; Arthur et al., 1985), and barium (Dymond et al., 1992; Shimmield et al., 1994). Of these, biogenic silica, especially the opaline silica of diatom frustules, might be the best indicator of high productivity for Neogene sediments (Diester-Haass, 1978), but diagenetic changes make it highly suspect for older rocks (Archer et al., 1993). Application of barium as a paleoproductivity indicator to rocks older than late Quaternary has yet to be attempted. $\delta^{13}C$ shows promise, but difficulties arise because many oceanographic processes influence it (Wefer and Berger, 1991).

Although the reliability of C_{org} as a quantitative indicator of paleoproductivity is degraded by contamination with terrigenous organic matter and enhanced C_{org} preservation in an anoxic environment, it may be the best qualitative indicator for ancient sediments.

Primary (phytoplankton) productivity in the sea depends on two factors: light and a supply of nutrients. Light is limited by the declination of the sun and by the turbidity of the water. The supply of nutrients depends on whether nutrients are already present in the water, or whether they must be introduced from land or by upwelling nutrient-rich deeper waters.

Light

Where the sun angle is high, light adequate for photosynthesis penetrates oligotrophic (sterile) ocean waters to a depth of about 100 m, as shown in Figure 9. At higher latitudes, the sun angle is lower and the depth of penetration is less. The refractive index of water with respect to air is about 1.33, so that when the sun is less than 41.5° above the horizon over a calm ocean surface, total reflection of the direct rays occurs and only the light of the diffuse radiation enters the water. The ocean surface is rarely calm, and the surfaces of waves may be 30° or more off the horizontal, so that some light will enter. However, it is clear that high-latitude regions are affected by low light levels in winter well equatorward of the polar circles. Light is also attenuated by the phytoplankton and other particles in the water. In eutrophic (highly productive) waters, the penetration of light adequate for photosynthesis may be reduced to 20 m or less in the tropics.

Although the base of the euphotic zone and the pycnocline, the oceanic layer where density increases rapidly with depth, may coincide in some areas, they are generally at different levels. The pycnocline is shallowest in the tropics where light penetrates deepest. At high latitudes, where the penetration of light is shallowest, the pycnocline may not exist. Adequate light levels for the growth of marine phytoplankton may penetrate only part of the way through the ocean mixed layer, to the pycnocline, or into ocean layers beneath the pycno-

cline. If the light penetrates into nutrient-rich deeper water beneath the pycnocline, it can produce a deep phytoplankton bloom, or deep chlorophyll maximum.

Light levels, especially at high latitudes, change with the orbital parameters. The intensity and global seasonal penetration of light into the ocean will vary $>10\%$ at high latitudes with the precession of the equinoxes and by up to 15% globally with the eccentricity of the orbit. However, obliquity redistributes the light at high latitudes changing light levels by $>25\%$ and may be expected to have the greatest effect on high-latitude phytoplankton growth. Light levels are also dependent on reflection and absorption of light within the atmosphere by aerosols and clouds; these may also have changed with geologic time.

Supply of Nutrients to the Euphotic Zone in the Ocean

The nutrients required for plant growth in the sea are H_2PO_4^- , NO_3^- , H_4SiO_4 , and dissolved Fe. All are present in river water, although Fe, on entering the sea, is rapidly converted to an almost insoluble form. Larger rivers may flow directly onto the continental shelf or even over the shelf edge, but most smaller rivers empty into estuaries. Many estuaries exist today, having been formed by flooding of river mouths as sea level rose after the last glaciation. As discussed above, estuaries reflect a positive freshwater balance, with runoff and precipitation exceeding evaporation. The estuarine circulation mixes the lighter river water with denser ocean water flowing in along the bottom to produce a surface outflow of hyposaline water. Both the river water and the upwelling ocean water may contain nutrients, and the phytoplankton that bloom in the estuary produce particulate organic matter that sinks into the inflowing sea water and is continuously recycled, as shown in Figure 10. The estuary becomes an effective trap for nutrients. In many areas, where precipitation and runoff are high, the continental shelf behaves like an estuary, as illustrated in Figure 11. Its waters are isolated from those of the open ocean by a front that develops above the shelf break. Nutrients that eventually escape from the coastal estuarine traps are caught and recycled in the continental shelf trap. Because of this isolation of many coastal areas, most of the C_{org} produced in the sea is buried in deltaic, estuarine, and shelf sediments. Storms may break down the front that separates shelf and ocean waters ("brown" and "blue" waters, respectively, in oceanographic parlance), and allow the nutrients brought from land to enter the ocean proper.

On a global scale, the low-salinity surface waters of the equatorial and high-latitude oceans force a form of oceanic estuarine circulation. The positive freshwater balance in these areas contrasts with the negative freshwater balance of the tropical-subtropical gyres. Because fresher water is less dense than saltier water, the ocean surface is higher in the positive areas than it is in the negative areas. The resulting salinity-driven circulation is superposed on the wind-driven circulation, exporting water from the regions with positive

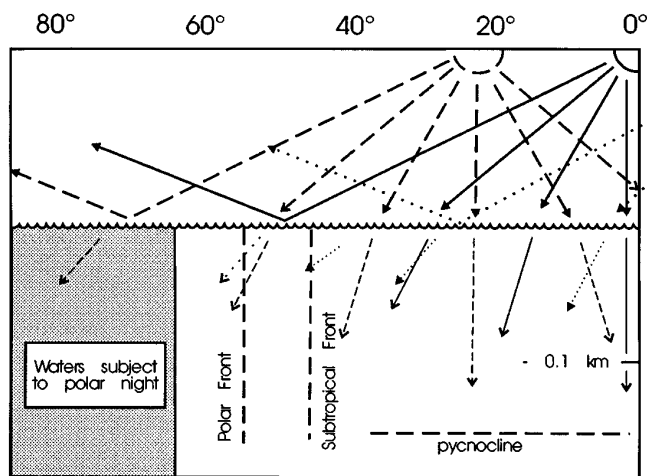


Figure 9. Light penetration into the ocean as a function of latitude. Solid lines represent conditions at the equinoxes, dashed lines represent conditions at the summer solstice, dotted lines represent conditions at the winter solstice. The critical angle for water is 41.5° . Above this latitude, the light penetrating the water is diffuse skylight and direct sunlight entering through waves. The thickness of the euphotic zone becomes shallower and more seasonal at high latitudes. Note that the critical angle of water is reached at a position between the Subtropical and Polar Fronts.

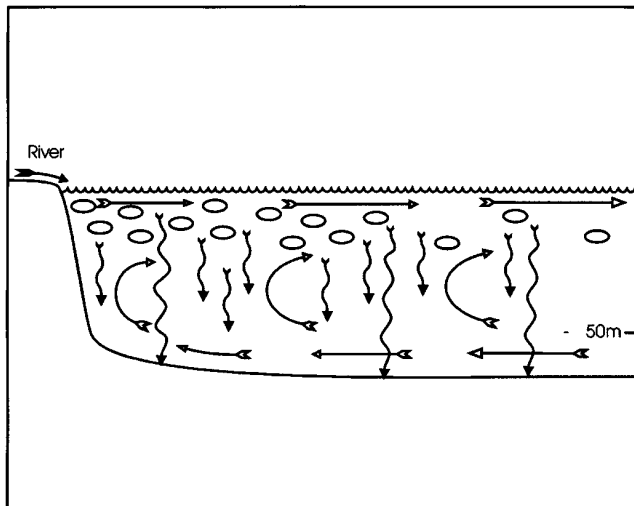


Figure 10. An estuary as a nutrient trap. Symbols as in Figure 3. Nutrients are introduced from land and are utilized by phytoplankton to produce a particulate rain that settles into the deeper sea water flowing in along the bottom of the estuary. The effect is to trap and recycle nutrients in the estuary making them highly productive.

freshwater balance. Conservation of mass requires that there be equatorial and high-latitude upwelling to compensate for the flow of lower-salinity water toward the higher-salinity areas.

In the latitudes between about 10 and 35° on the eastern sides of the ocean basins, wind-driven coastal upwelling can cause local breaks in the shelf front, allowing nutrient-rich subsurface oceanic water to flow onto the shelf, as shown in Figure 12. Again, once on the shelf, the nutrients are recycled and can become concentrated in the shelf waters.

For the ocean, two nutrients, PO_4^{3-} and NO_3^- , are usually considered to be limiting. The PO_4^{3-} has two possible sources: from the weathering of rocks on land and from hydrothermal alteration of ocean crust. The largest source is probably from land, and most of the PO_4^{3-} is brought to the sea by rivers. Meybeck (1982) was unable to detect any clear pattern relating the delivery of PO_4^{3-} by rivers to relief, climate, or geology of the drainage basin, other than to suggest that the highest values are from Iceland, a volcanic area. It may be that PO_4^{3-} is most readily supplied by weathering of volcanic rocks. Rivers also bring NO_3^- that was fixed by land plants. Meybeck (1982) found that the total amount of dissolved phosphorus delivered to the sea (as phosphate) is about $0.45 \times 10^9 \text{ kg yr}^{-1}$, and the amount of dissolved nitrogen (as nitrate) is $11 \times 10^9 \text{ kg yr}^{-1}$. The ratios of these two nutrients vary widely in river water, but average about 1:24.

Berner and Rao (1994) suggest that the river input of phosphorus to the ocean may be underestimated because only phosphorus in solution is considered. In a study of the lower Amazon, its estuary, and the adjacent continental shelf, they found that the dissolved P

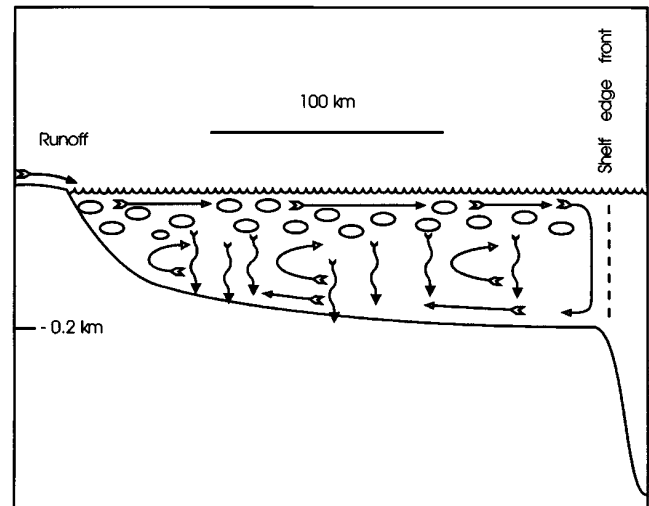


Figure 11. The continental shelf on the west side of the ocean basin as a nutrient trap. Symbols as in Figure 3. Again, nutrients are introduced from land and are utilized by phytoplankton to produce a particulate rain that settles onto the shelf. Shelf waters are isolated from open ocean waters by a front that develops above the shelf break. The circulation of water on the shelf recycles nutrients making it a highly productive region.

flux is supplemented by P from bacterial decomposition of river-transported organic matter and by desorption of P from iron oxides and hydroxides. They estimate that the total flux may be 3 times that of the dissolved P alone.

It is possible that the inputs of PO_4^{3-} from land and hydrothermal sources have varied with time. Wold and Hay (1990) have shown that during the Phanerozoic the level of volcanic activity on the continental blocks has varied by a factor of ten, with the present level of activity being average. Larson (1991) has suggested that episodes of large-scale submarine volcanism, such as occurred during the Early Cretaceous, may have introduced nutrients directly into seawater through hydrothermal alteration and weathering of volcanic products. Coffin and Eldholm (1993) have tried to estimate the dimensions of large igneous provinces, and their work might serve as a guide for exploring the hypothesis that volcanic areas can alter the rate of PO_4^{3-} input.

The concentrations of nutrients in deep ocean water and in river water differ by a factor of 2. The average concentration of phosphate is about $2.3 \mu\text{mol kg}^{-1}$ in the deep ocean (Broecker and Peng, 1982), and about half that in convecting high-latitude surface waters (Sarmiento et al., 1988); in the O_2 minimum it may reach levels $>3 \mu\text{mol kg}^{-1}$. It is about $1.3 \mu\text{mol kg}^{-1}$ in rivers (Broecker and Peng, 1982). However, the rate of return of deep ocean water to the surface is more than ten times the rate of discharge of rivers. Although the ultimate source of nutrients is the land, the major nutrient sources for the surface waters of the open

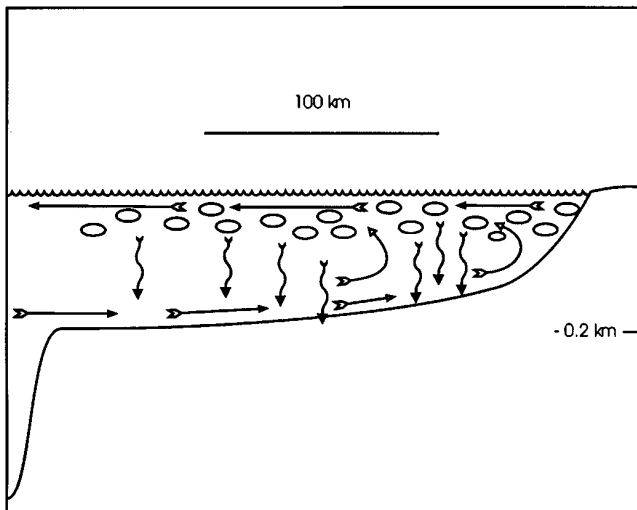


Figure 12. The continental shelf on the east side of the ocean basin as a nutrient trap. Symbols as in Figure 3. Nutrients are introduced by upwelling that draws in offshore nutrient-rich subsurface ocean waters. The nutrients are utilized by phytoplankton to produce a particulate rain that settles onto the shelf. Surface waters of the shelf are relatively isolated from open ocean waters by a divergence that develops above the shelf break. Again, the circulation of water on the shelf recycles and concentrates the nutrients making the eastern shelves highly productive regions.

ocean are the intermediate and deep waters. Phosphate is almost wholly depleted in low-latitude surface waters except near rivers and sites of nutrient upwelling.

Presently introduced by rivers in a ratio of 1:24, PO_4^{3-} and NO_3^- , respectively, are used by most phytoplankton in the ratio 1:15 (the "Redfield Ratio"). They occur in intermediate and deep ocean water in the same 1:15 ratio almost everywhere. Although it was originally hypothesized that ocean phytoplankton might have evolved to use these nutrients in the ratio in which they are present in deep waters, it has become apparent that the ratio in deep waters simply reflects regeneration of the nutrients from oxic decomposition of phytoplankton. There are no areas of the open ocean where the NO_3^- exceeds PO_4^{3-} by a factor of more than 15. The excess nitrate brought by rivers is rapidly reduced in dysaerobic environments. When most or all of the O_2 has been utilized in decomposition of organic matter, nitrate is reduced to allow the decomposition to proceed further. One notable region where this occurs is the deep waters of the Arabian Sea, where the ratio of PO_4^{3-} to NO_3^- is 1:5. When this water is upwelled to the surface it is nitrate deficient. In the sea, nitrogen (N) fixation, resulting in production of organic N from dissolved N_2 , is accomplished by cyanobacteria (blue-green algae). If there is an excess of phosphate relative to nitrate, as is the case for upwelled water in the Arabian Sea, a large proportion of the phytoplankton population will be cyanobacteria.

Iron represents a special case for nutrients. It is required for synthesis of chlorophyll, nitrate-reduction, and fixation of dissolved N_2 (Martin, 1990). Iron is brought to the sea in rivers mainly as hydrous Fe^{3+} oxides in colloidal dispersion stabilized by humic acids. It is particularly abundant in rivers rich in humic acids draining equatorial rain forests and high-latitude coniferous forests. At the river mouth, the iron colloids flocculate in brackish water removing the iron to the sediment and preventing it from entering the sea (Boyle et al., 1977). Hence, its concentrations in sea water are very low. Iron is also introduced by atmospheric transport, being carried as a component of dust. There is evidence that in some regions of the ocean, particularly in the northeast Pacific (Martin and Fitzwater, 1988) and the Circumantarctic region (Martin et al., 1990; Martin, 1990), iron is depleted and may be the limiting nutrient. It may be limiting in the Arabian Sea. It is introduced into the surface waters of Oman as ferruginous coatings on wind-blown sand grains and dust (Sirocko and Sarnthein, 1989).

Martin et al. (1990) have suggested that high-latitude productivity is enhanced during glacials by increased winds and the resulting increased dust transport of iron to the ocean. If the iron fertilization hypothesis of Martin et al. (1990) is correct, the long-term history of global dust flux (Rea et al., 1985) may hold clues to trends in oceanic productivity.

Dissolved silicon (Si) is required by a major phytoplankton group, the diatoms. It is particularly high in rivers draining basins with active silicate weathering. Typically these are warm, humid regions in the tropics and areas with extensive exposures of volcanic rocks (Hay and Southam, 1977). It is also supplied by hydrothermal alteration of ocean crust. In most upwelling regimes, it is the first nutrient to be depleted. Its depletion does not limit phytoplankton productivity as a whole, but determines the relative level of diatom productivity versus that of the non-siliceous phytoplankton groups, such as dinoflagellates and coccolithophores.

Nutrient Recycling and the O_2 Minimum

Most nutrients entering the surface waters of the ocean were regenerated by decomposition of organic matter in the intermediate and deep waters. The modern ocean can be thought of as consisting of four main parts, shown schematically in Figure 13: (1) a warm, saline tropical-subtropical surface mixed layer, underlain and meridionally bounded by (2) the main pycnocline, in which the density of the water increases due to a temperature decrease, underlain and bounded meridionally by (3) low-salinity, cold intermediate water, which is in turn underlain and bounded meridionally by (4) high-salinity cold deep water. The base of the surface mixed layer is the top of the pycnocline. Between the Subtropical Fronts at about 45°N and S , the pycnocline is a thermocline. Each of these bodies of water, except the main pycnocline, is relatively homogeneous and is internally mixed. The main pycnocline is stratified and movement of the water takes place mostly along, rather than across, the isopycnals.

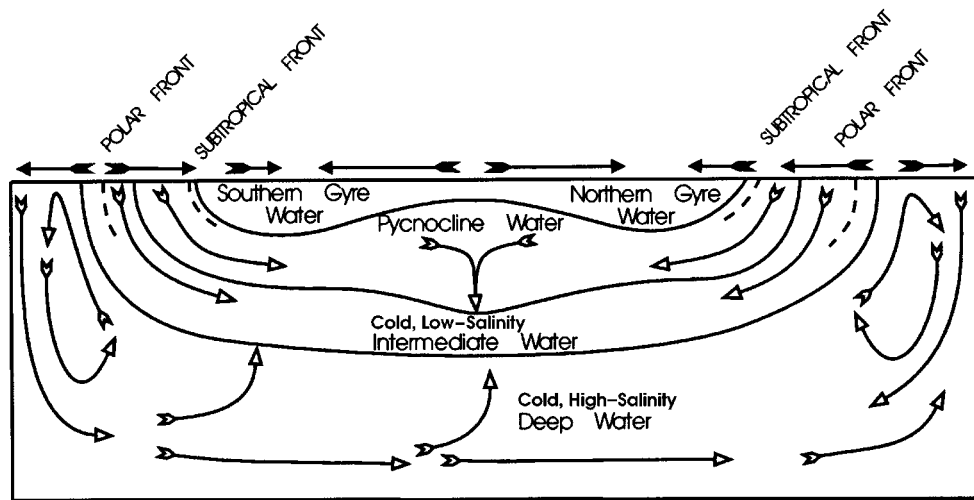


Figure 13. Idealized general structure of the ocean. The meridional components of the surface winds are indicated by solid arrows. Meridional flows of water in the interior of the ocean are indicated by open arrows. Thermocline mixing is shown in the equatorial region.

Dissolved nutrients are removed from the surface waters of the ocean by phytoplankton. Phytoplankton production in the photic zone and grazing by zooplankton result in a rain of particulate organic matter. Starting in the surface layer, the organic matter is decomposed through oxidation and nutrients are released. Once the sinking particles have fallen below the photic zone, the nutrients released by their decomposition can no longer be utilized by the phytoplankton until they have been mixed or upwelled back into the photic zone. Over the continental shelf, this particulate rain may fall through a mixed layer underlain directly by the sea floor. In this case, the nutrients can be recycled into the same mixed water mass over and over again. Off the shelf, in the open ocean, the particles sink from the surface water through the pycnocline into the deeper water masses. When the particles enter the pycnocline, the mixing with the surface water ceases, but upwelling may occur at specific sites. The most intense nutrient regeneration takes place in the intermediate water which, consequently, contains the O_2 minimum. A lesser degree of nutrient regeneration also takes place in the deep water.

The O_2 minimum in the ocean is also a nutrient maximum. This concentration of nutrients in the pycnocline and deeper waters depends on (1) the rate of supply of particulate organic matter from above and (2) the amount of dissolved O_2 available for oxidation of the organic matter, regenerating nutrients. The rate of supply of organic matter from above is a function of the productivity of the overlying waters. Productive upwelling regions will supply large amounts of organic matter, whereas the centers of the oceanic gyres, being almost sterile, will provide little. Thus, the nutrient content will be greater in subsurface waters that have passed beneath sites of upwelling of nutrient-rich waters. O_2 is supplied to the ocean only at the surface, but its solubility is strongly temperature dependent, with cold $0-2^\circ\text{C}$ water containing about $350 \mu\text{mol kg}^{-1}$

while warm 30°C waters are saturated with $<200 \mu\text{mol kg}^{-1}$. After leaving the surface, the amount of dissolved O_2 that remains in water in the interior of the ocean is a function of the intensity of the rain of organic particles from above. Because the effect of O_2 consumption is cumulative and there is no mechanism for regeneration of O_2 in the interior of the ocean, the O_2 content of the waters is a function of the length of time that has elapsed since the water was at the surface.

Because of changes in the horizontal pressure gradient with depth, the circulation below the surface is often opposite to the surface flow, as has been illustrated in Figure 2. Between the flows in opposite directions is a horizon which has been termed the "surface of no motion" (Sverdrup, 1938b; Tolmazin, 1985). Because at the surface of no motion the horizontal pressure gradient is 0 in all directions, it has been considered to be a natural reference surface for the dynamics of both surface and deep ocean currents. One of the methods of locating the surface of no motion was to assume that it would coincide with the O_2 minimum, the level where the water had the greatest age (Dietrich, 1937). In reality, the effect of lateral differences in the particle rain in upper levels of the ocean is much greater than the effect of age of the water on the development of the O_2 minimum.

The relation between the O_2 minimum, nutrient regeneration, upwelling of nutrient-rich waters, and productivity leading to a large biogenic carbon flux to the sediments becomes clear when considered in the context of the global structure of the ocean. Figure 14 shows the major features and water masses as defined by temperature and salinity.

Structure of the Ocean

The ocean can be thought of as consisting of several water masses separated by surfaces of density change. The density gradients can be horizontal (pycnoclines) or

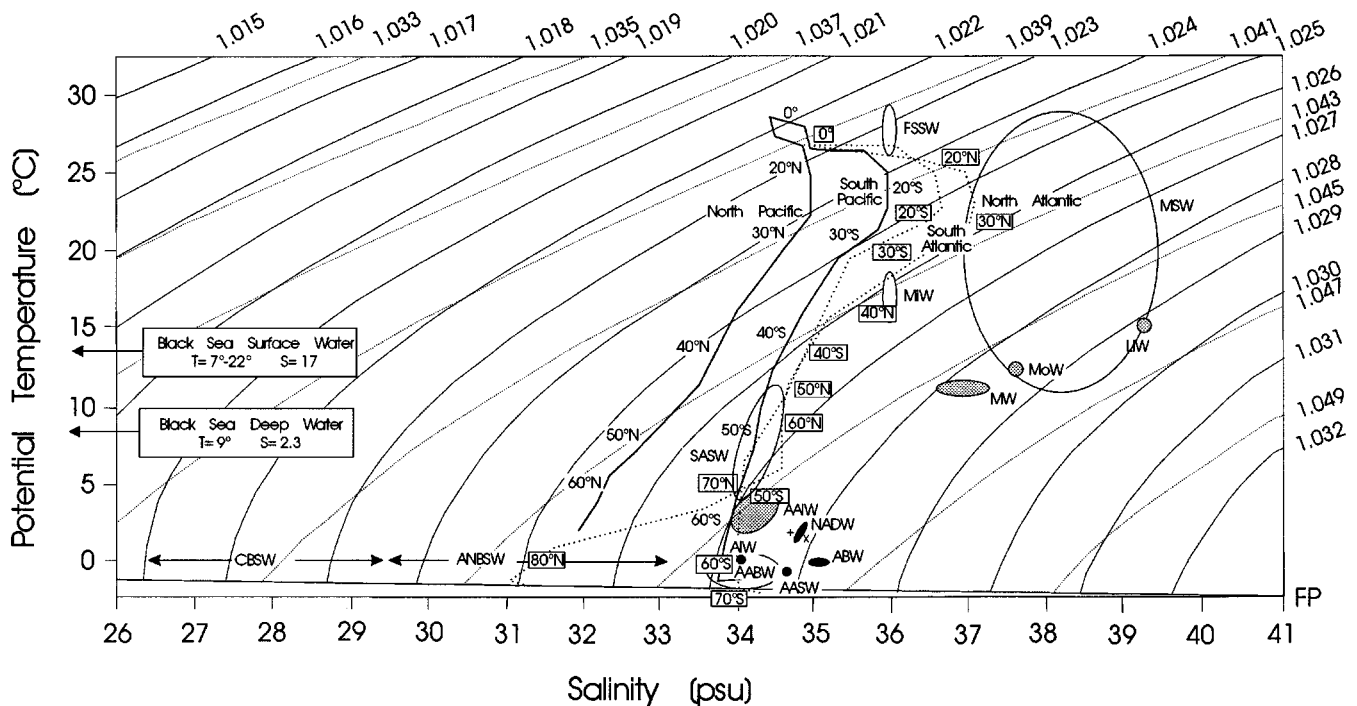


Figure 14. Relation between temperature, salinity, and density, and some major water masses. Two sets of density lines are shown: thin solid curves show the density at the surface; dotted curves show the density at a pressure of 400 bars (approximately equal to a depth of 4000 m). Densities are in g/cm^3 or kg/L . Annual averages for surface waters of the Pacific are shown by the solid line, with latitudes indicated alongside it; annual averages for the Atlantic by the dotted line, with latitudes indicated in boxes alongside it (Levitus, 1982). AABW = Antarctic Bottom Water; AAIW = Antarctic Intermediate Water; AASW = Antarctic Surface Water; ABW = Arctic Bottom Water; AIW = Arctic Intermediate Water; ANBW = Amundsen–Nansen Basin Surface Water; CBSW = Canadian Basin Surface Water; FSSW = Florida Straits Surface Water; LIW = Levantine Basin Intermediate Water (Eastern Mediterranean); MiW = Mediterranean Inflow Water; MoW = Mediterranean Outflow Water; MSW = Mediterranean Surface Water; MW = Mediterranean Water (in the Atlantic); NADW = North Atlantic Deep Water; \times = Water overflowing the Greenland–Scotland Ridge through the Denmark Strait; $+$ = World Average Water.

vertical (fronts). The fronts are narrow zones of convergence at the ocean surface, and are sites of downwelling of ocean waters from the surface into the interior.

The Major Oceanic Fronts

The general circulation of the tropical-subtropical ocean is forced by the winds and continental boundaries into basinwide anticyclonic gyres in the northern and southern hemispheres. The gyres of the northern and southern hemispheres are separated from each other by the equatorial current system and are bounded meridionally by the subtropical fronts that form in the ocean beneath the extremes of zonal wind stress. Surface layers of warm water in the tropics and subtropics lie above and adjacent to the much larger body of cold water. The warm and cold surface layers are separated from each other by oceanic fronts, where water converges from both sides and sinks. These convergences are induced by increasing meridional Ekman transport resulting from increased zonal wind stress (Rooth, 1982).

Ocean surface waters have their temperature maximum of 28–29°C in the western equatorial Pacific, but

are almost as warm, 27–28°C, in the western equatorial Atlantic. Polewards across the tropical-subtropical gyres of the Atlantic, the temperatures decline to 12°C at the Subtropical Front near 45°S and its northern hemisphere counterpart.

Salinities are lowest on the equator and in the polar regions (see Figure 14). They increase systematically in the tropical-subtropical gyres from <33.5 in the eastern equatorial Pacific to 35.5 in the center of the North Pacific gyre, 36.3 in the center of the South Pacific, 37.2 in the center of the South Atlantic, and >37.2 in the North Atlantic gyre. A body of water of intermediate temperature (12° to 4°C) and salinities of 34.0–34.5, termed Subantarctic Surface Water (SASW), occupies the region between the Subtropical and Antarctic Fronts. The Antarctic Polar Front separates the SASW from the cold, nearly isothermal (–1° to 3°C), low-salinity (<34.4) Antarctic Surface Water (AASW) that surrounds the continent. The circumglobal oceanic frontal systems of the southern hemisphere effectively isolate the water surrounding the Antarctic continent from the rest of the world's surface waters. During the winter the circumantarctic water becomes very cold

(down to -2°C) and salinities increase to 34.5 or more as it develops an extensive cover of sea ice. The sea ice breaks up and melts during the summer, producing a layer of AASW that may be up to 200 m thick.

The Subtropical and Polar Oceanic Fronts develop in response to the changing zonal wind stress of the mid-latitude westerlies. It is likely that these features have always existed, but the latitudes at which they develop may have changed through geologic time.

The Surface Mixed Layer

The surface waters of the ocean and seas are mixed by winds, waves, and currents. The mixed layer extends to the floor of shallow shelf seas. The mixed layer of shallow seas is separated from the mixed layer of the open ocean by fronts that form above the shelf break. At present, the open ocean between the Subtropical Fronts is thermally stratified and the thermocline forms the base of the mixed layer. Between the Subtropical Fronts and the equator, the water in each ocean basin circulates as an anticyclonic gyre. The rotation of anticyclonic gyres (clockwise in the southern hemisphere, counterclockwise in the northern hemisphere) forces the water in the center of the gyre downward, effectively precluding upwelling. In response to the winds, the depth of the base of the mixed layer increases from 10 m on the eastern sides of the ocean basins to 50 m on the western sides (Figure 4). The tropical-subtropical mixed layer includes a band of very light, low-salinity warm water along the equator; its thickness varies seasonally from 10 to 50 m. Beneath the western boundary currents (Gulf Stream, Kuroshio), the mixed layer thickness may reach >250 m (Levitus, 1982). The ocean thermocline and intermediate water masses crop out on the surface between the subtropical fronts and the polar fronts at about $55\text{--}60^{\circ}\text{N}$ and S. Here a surface mixed layer ~ 100 m thick overlies the outcrops of the main pycnocline, intermediate, and deep waters, but the pycnocline underlying it is weakly developed. The rotational motion of the gyres poleward of the Subtropical Fronts tends to be cyclonic, promoting upwelling in the gyre centers. Between the Subtropical and Polar Fronts large volumes of water convect from the ocean surface to the bottom. At higher latitudes, beyond the Polar Fronts in the Arctic and Antarctic, runoff from land and melting of sea ice during the summer produce a thin (10–50 m), lower-salinity mixed layer (see Figure 14) underlain by a pycnocline caused by the increase of salinity with depth (halocline).

Where the ocean's mixed surface layer is thin and separated from deeper waters by a strong pycnocline, as in the tropics and subtropics, phytoplankton utilize all available nutrients. If the ocean convects to great depths, as in the high latitudes, the mixed layer is very thick. The phytoplankton, restricted to the surface waters by their need for light, are unable to utilize all of the nutrients before they are returned to the depths. Unutilized nutrients that return to deeper waters are termed "preformed nutrients"; they did not originate from decomposition of organic matter and were not involved in depletion of O_2 from the subsurface waters.

Because it is largely controlled by the winds, variations in the thickness of the mixed layer have probably been minimal in the past. The major possibility for change in the thickness of the mixed layer with time lies in the western boundary currents, which may have varied considerably depending on configuration and degree of climatic differentiation of the ocean basins (Maier-Reimer et al., 1990; Mikolajewicz et al., 1993).

The position of the base of the mixed layer with reference to the continental shelves has changed significantly with the long-term eustatic rise and fall of sea level. When, as during the Late Cretaceous, the water over the shelf break reached a certain depth, probably about 200 m greater than it is today, the fronts separating the open ocean and shelf sea mixed layers broke down and the entire mixed layer became a homogeneous unit. Pelagic plankton then spread into the shelf seas. This must have radically altered the way in which nutrients were supplied to and distributed in the surface ocean. Nutrients from land could enter the oceanic surface mixed layer directly. Heat exchange between the open ocean and epeiric seas would have been more efficient, perhaps contributing to the "equable" climate of the time.

The Pycnocline

The pycnocline beneath the subtropical gyres is due to the increase in density of sea water with decreasing temperature. The top of the pycnocline (base of the surface mixed layer) lies between 10 and 250 m. It may be below, coincide with, or be above the base of the euphotic zone. The base of the pycnocline lies at about 500 m in the equatorial region and shallows toward the Subtropical Fronts (Levitus, 1982). Below the euphotic zone, the pycnocline can become enriched in nutrients as sinking organic matter decays. It can also be supplied with nutrients by upward mixing of the underlying intermediate waters. Hence, the pycnocline is commonly also a nutricline. The subsurface waters most susceptible to wind-induced upwelling are those of the pycnocline. The density contrast across the pycnocline at different latitudes can be estimated from Figure 14.

Although the intensity of the pycnocline is the main measure of the stratification of the ocean, the pycnocline is paradoxically responsible for a significant part of ocean mixing. The density of the water is determined by its salinity (S) and temperature (T). In a T/S diagram (Figure 14), the isopycnals are curved lines. On such a diagram, a mixing line between two water masses is a straight line. This means that if any two waters having the same density but different temperatures and salinities mix, they will form a third water mass that will always have a greater density than either of the parents. In the ocean, the isopycnals are concave upward and more or less symmetrical about the equator. They crop out on the ocean surface in the northern and southern hemispheres. Although the waters in both hemispheres have the same density where the isopycnals come to the surface, they rarely if ever have the same temperature and density. This means that somewhere in the equatorial region the different

waters representing the northern and southern parts of the isopycnal will meet, mix, become denser, and sink. This causes more water to be drawn in from the surface. At present, the salinity of the surface waters in the North Atlantic is about 0.5 greater than the waters of the South Atlantic. South Atlantic waters are in turn about 0.5 more saline than waters of the South Pacific, which are in turn 0.5 more saline than the waters of the North Pacific. The present salinity differentiation of the ocean guarantees that the waters of a given isopycnal will have different temperatures and salinities, and ensures active cross-pycnocline mixing. The phenomenon of pycnocline mixing serves both to mix waters in the interior of the ocean and to reduce the residence time of waters in the pycnocline. Rates of inflow and mixing on the pycnocline are not well known, but the residence time of water in the pycnocline must be on the order of years to a few decades.

How has the pycnocline changed with time? Assuming that there is always a meridional temperature gradient, it is likely that there has always been a thermocline beneath the tropical-subtropical gyres. However, the temperature and density gradients may have been significantly less in the past than they are at present, facilitating wind-driven upwelling. Studies of the effects of opening and closing passages between ocean basins (Maier-Reimer et al., 1990; Mikolajewicz et al., 1993) indicate that the degree of salinity differentiation of the Atlantic and Pacific was different in the past. This would have important implications for the residence time of water in the pycnocline, for the rate of pycnocline mixing, and for the thickness and overall density contrast in the pycnocline. In a less differentiated ocean, pycnocline mixing would become a less important process and the residence time of water in the pycnocline would increase. This should have resulted in a steeper nutricline, with waters having a high nutrient content occurring at shallower levels.

Intermediate Water

Most of the intermediate water in the ocean sinks along the polar fronts. At present, the intermediate water production in the ocean is dominated by the cold, low-salinity water that sinks at the Antarctic Polar Front and spreads northward beneath the main thermocline as Antarctic Intermediate Water (AAIW). Much of the water that sinks along the Antarctic Polar Front is SASW involved in circulation of the Circumantarctic Current (West Wind Drift). The prevailing westerly winds at 50°S carry these waters from west to east. The Circumantarctic Current girdles the Antarctic continent and extends from the surface to the ocean floor (Nowlin and Klinck, 1986). The rapid vertical motions mean that nutrient-rich waters have a short residence in the euphotic zone, and, consequently, only a small fraction of the nutrients (30%) are utilized by phytoplankton (Oeschger et al., 1984). The remaining preformed nutrients are returned to the depths by downwelling. The rate of production of AAIW is on the order of 10 Sv (1 Sv = 1 Sverdrup = $10^6 \text{m}^{-3}\text{s}^{-1}$) (Gordon and Taylor, 1975). The residence time of AAIW is on the order of decades. Having an intermediate tem-

perature at its source, AAIW sinks along the Polar Front with an O_2 concentration between those of the warm gyre tropical-subtropical waters and cold polar waters. It contains preformed nutrients introduced at the source. Lying just beneath the pycnocline, it acquires nutrients released by oxidation of particulate organic matter settling from above. It becomes the main reservoir of nutrients available for upwelling into the surface waters. Between the Subtropical Fronts the O_2 minimum lies within the intermediate water almost everywhere.

Marginal seas having a lagoonal circulation as a result of negative freshwater balance are another source of intermediate water in the ocean. In such seas, evaporation exceeds the freshwater input from precipitation and runoff from land. The surface waters become more saline and sink, resulting in surface inflow from the ocean and deep, more saline outflow to the ocean. Because lagoonal marginal seas draw their ocean water from the nutrient-depleted subtropical mixed layer, their outflow waters are nutrient depleted. Because the lagoonal waters were relatively warm when they sank below the surface, they contain less O_2 than intermediate waters formed along the Polar Front. The most important marginal seas supplying intermediate water at the present time are the waters that flow from the Mediterranean and Greenland-Iceland-Norwegian (GIN) seas. In both cases their outflows are more saline than the overlying waters and are nutrient depleted. As shown in Figure 14, Mediterranean Outflow Water (MOW) is the densest water entering a major ocean basin (Kraus et al., 1978). As it flows down the slope from the Straits of Gibraltar, it entrains Atlantic interior water and the mixture spreads out at a depth of about 1.5 km as Mediterranean Water (MW). Some of this relatively warm saline water combines with the cold saline waters overflowing the Greenland-Scotland Ridge from the GIN seas to form North Atlantic Deep Water (NADW) in the interior of the North Atlantic (Reid, 1979; Peterson and Rooth, 1976; Broecker and Takahashi, 1980).

With two very different potential sources of intermediate water in the ocean, the polar fronts, where lower-salinity waters are rich in nutrients, and the lagoonal marginal seas, where the higher-salinity outflowing waters are nutrient depleted, it is clear that the nutrient supply related to upward mixing of intermediate water may well have changed with time. At present, MW occupies the intermediate levels of the Atlantic as far south as Cap Blanc on the African margin. Hay and Brock (1992) and Hay (1993b) have suggested that during glacials increased volumes of MOW and reduced production of AAIW may have resulted in a shift of the boundary between nutrient-poor and nutrient-rich intermediate waters from its present location off northwestern Africa to as far south as Walvis Ridge off southwestern Africa. They attributed the decrease in productivity off southwestern Africa during Pliocene and Pleistocene glacial stages to changing intermediate water sources. They suggested that during the glacials nutrient-depleted MW

was upwelled and during the interglacials this was replaced by nutrient-rich AAIW.

Deep Water

Stommel (1962) remarked that although the thermohaline vertical circulation of the ocean is one of its major features, the sites of sinking of ocean deep waters are quite small. The thermohaline circulation is driven by formation of dense water in small regions where isolation and transformation of the water masses can occur.

Deep-water formation is initiated by an increase in the density of surface water masses. Sinking of the denser water to the ocean floor is most likely to occur where vertical convection can penetrate to the bottom. On reaching the bottom, the dense waters entrain ambient waters to form deep water. A relatively small amount of water modified to become denser can entrain a much larger volume of unmodified ocean water and produce a large flux of dense water.

Hay (1993a) reviewed deep-water formation in the context of changing climate, concluding that both modes and rates of deep-water formation may change markedly with different conditions. At present, ocean deep waters are cold and saline, as shown in Figure 14. They also contain preformed nutrients. Because of the low temperatures at their sites of formation, they are also O₂ rich. Most oceanic deep water forms at a few sites around the Antarctic, with much of the salinization being in response to sea-ice formation. The rate of formation is about 38 Sv. NADW forms from mixture of MW and Greenland-Scotland Ridge overflow waters from the GIN seas. It occupies both deep and intermediate levels in the North Atlantic, and its rate of production is about 22 Sv. As it flows into the South Atlantic, it is underridden by Antarctic Bottom Water (AABW) and comes to occupy an intermediate depth between AABW and AAIW. Broecker et al. (1985) and Hay (1993a) have observed that the production of

NADW is particularly vulnerable to freshwater input into the North Atlantic.

Deep water receives the “leftovers” of the rain of organic particles. Because of the lesser particle rain and the higher O₂ content at its source, O₂ levels remain higher and nutrient levels remain lower than in intermediate waters. The residence time of deep waters is hundreds to perhaps a thousand years. The effect of aging becomes important in determining the nutrient content of deep waters.

During earlier geologic ages, when the polar regions were warmer, the deep waters of the ocean may not have been the cold, saline waters that form at high latitudes today. Instead, deep-water formation may have taken place in low-latitude marginal seas in the arid zones through evaporation, resulting in warm, saline deep waters filling the ocean basins (Brass et al., 1982a, b), as illustrated diagrammatically in Figure 15. Much more energy is required to increase salinity through evaporation than through formation of sea ice. Hence, the process of salinization would have been less effective during times of global warmth. Except in enclosed marginal seas, the salinity contrasts may have been less than they are today. With smaller temperature and salinity contrasts, the density differences in the ocean would have been less, so that less energy would be required to drive the vertical circulation. If deep water forms at low latitudes, where would it return to the surface? The most arid marginal seas would be on the eastern sides of the ocean basins. The Coriolis force (CorF) would direct the dense waters flowing down the continental slope to the right in the northern hemisphere and to the left in the southern hemisphere, that is, poleward. This water would then return to the surface in the regions where the density contrasts are least and where the ocean convects to great depths: the polar oceans beyond the subtropical fronts. The halothermal circulation of the Cretaceous would thus force high-latitude upwelling, as indicated

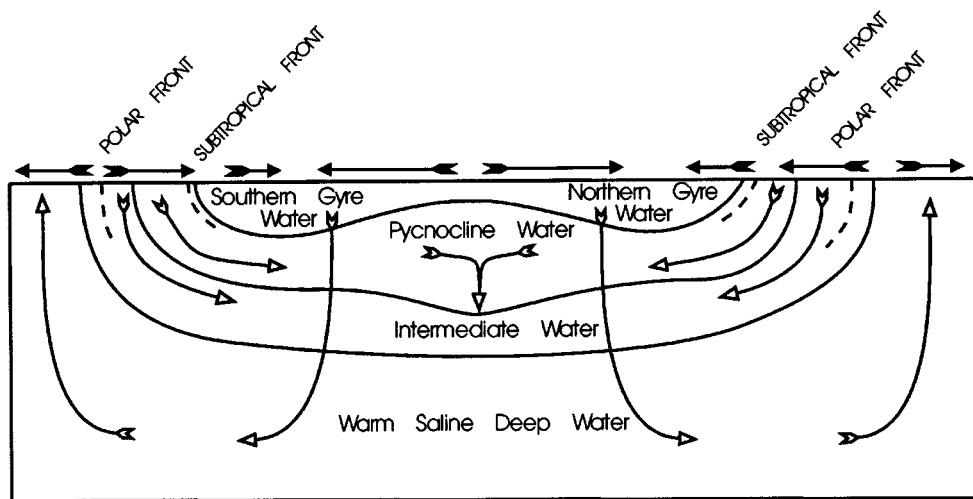


Figure 15. Idealized general structure of the ocean. The meridional components of the surface winds are indicated by solid arrows. Meridional flows of water in the interior of the ocean are indicated by open arrows. Thermocline mixing is shown in the equatorial region.

in Figure 15. The resulting large-scale heat transport to the polar regions may be responsible for the warm polar temperatures of the Cretaceous.

Being much warmer when they left the surface, the deep waters of the Late Cretaceous may have contained only half as much dissolved O_2 as do today's cold deep waters. Assuming the same biomass as today, the lower O_2 content of the deep waters would have allowed mass death of marine life, from whatever cause, to bring the ocean to the verge of anoxia.

Global Ocean Structure in the Past

Has the ocean always had a global structure similar to that at present? This is perhaps the most critical question in understanding how sedimentation of marine biogenic carbon may have changed through time. Clearly, during the Neogene and probably since the Eocene, the structure has been essentially the same as at present, although the temperatures, salinities, and relative volumes of the water masses have changed. However, for the Eocene and older ages, too little is known to be sure what structure the ocean had. There needs to be an effort to determine whether there were Subtropical and Polar Fronts like those that presently separate the tropical-subtropical ocean from the high-latitude ocean today. Much of the required evidence probably exists, but has not been organized in a form that would allow us to answer this question. More needs to be known, especially about high-latitude oceans of the past, to have a definitive answer. However, I believe that as long as there is a meridional temperature gradient (e.g., since the Oligocene), the general structure of the ocean will always have a global structure analogous to that at present.

Upwelling

Upwelling is the phenomenon whereby denser waters are brought to a higher level and mixed into less dense waters. In the upper ocean, intermediate waters are brought to the surface. In the ocean interior, deep waters are brought to intermediate levels. Most discussions of upwelling assume that the upwelled water is rich in nutrients, although this need not be the case. Upwelling is a physical phenomenon that can occur whether or not the upwelled waters contain dissolved nutrients. In fact, upwelling of nutrient-depleted water occurs in many areas, but because the upwelled waters do not display the usual characteristics—lower temperature, lower salinity, and enrichment in PO_4^{3-} , NO_3^- , H_4SiO_4 —their origin is overlooked. In the open ocean, upwelling is the major source of nutrients for the surface water. Upwelling also plays a large role in coastal areas, but rivers may also be significant suppliers of nutrients.

Two major areas of upwelling can be distinguished, the open ocean and the ocean margins. Romankevich (1984) suggested that about 3.1×10^{12} kgC are fixed annually in the equatorial upwelling system. Martin (1990) estimated that 0.9×10^{12} kgCyr⁻¹ are fixed in the Circumantarctic Current system. Coastal Zone Color Scanner (CZCS) imagery suggests that about a third as much (0.3×10^{12} kgCyr⁻¹) is fixed in the North Atlantic

and North Pacific. Herzog and Hay (in preparation) estimate that 1.0×10^{12} kgCyr⁻¹ are fixed in the Angola and Guinea Domes; including the Costa Rica Dome would add another 0.5×10^{12} kgCyr⁻¹ to the productivity of thermocline domes. The total productivity in open ocean areas is then 5.8×10^{12} kgCyr⁻¹. The productivity of the coastal upwelling system off southwest Africa has been estimated at 0.2×10^{12} kgCyr⁻¹ (Schulz, 1982). There are five such areas, so that the coastal upwelling can be estimated to be about 1.0×10^{12} kgCyr⁻¹.

Upwelling in the open ocean results from the interaction of the winds on the ocean surface or from motions of the water in the ocean interior. Upwelling occurring along the ocean margins is the result of interactions between at least two of four possible factors: wind, water, bathymetric configuration, and topography of the adjacent land.

Surface Upwelling in Response to the Wind Stress

Most upwelling at the ocean surface results from the drag of the wind (wind stress) over the water. The wind stress increases as the square of the wind speed. It is greatest where the winds are most vigorous: the easterly trade winds between 10 and 25°N and S, and the westerlies between 35 and 55°N and S (Peixoto and Oort, 1992). Except near the equator, the direct effect of the wind stress on the water is altered by the CorF, as shown in Figure 16.

Shear between the wind and the water and between successively deeper layers of water and the CorF combine to produce a net transport of the water 90° cum sole of the downwind direction. The net movement of water 90° cum sole off the direction of the wind was derived mathematically by Ekman (1905) to explain Nansen's (1902) observations of the motion of ice in the Arctic, and is therefore termed Ekman transport. Because, except near the equator, the net motion of the water is 90° off the wind, a convergence of the winds will cause a divergence of the water and vice versa.

Geologic evidence of atmospheric dust transport (Petit et al., 1981; Rea et al., 1985; De Angelis et al., 1987) and climate models (Barron, 1985; Moore et al., 1992a, b; Chandler et al., 1992; Wilson et al., 1994) suggest that wind speeds and, consequently, the wind stress on the ocean surface may vary significantly with time. The changes in wind speed are intertwined with other factors affecting climate, most notably the sensible and latent heat transport, evaporation rate, and CO_2 content of the atmosphere. It has been suggested that during the Quaternary glacials global upwelling rates were enhanced by increased wind speeds. As a result, the rate of C_{org} burial increased, depleting CO_2 from the ocean surface waters and causing atmospheric CO_2 levels to decline (Sarnthein and Fenner, 1988).

Open Ocean Upwelling

Oceanic upwelling encompasses a group of processes that operate strictly in the open ocean but account for 80% of the high productivity in the ocean. Because these processes act only in the open ocean, they contribute little to accumulations of C_{org} -rich sediments that may eventually become petroleum source

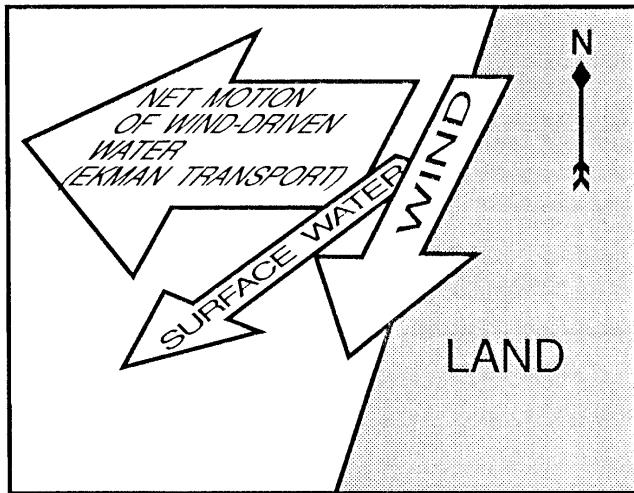


Figure 16. The phenomenon of upwelling illustrated by the effect of a wind blowing equatorward along a coast with NNE–SSW orientation in the northern hemisphere. Motion of the surface water is about 30° to the right of the wind. Net motion of the water forced by the wind is 90° to the right of the wind.

rocks. There are three possible exceptions. (1) In a few areas, oceanic upwelling may result in deposition of C_{org} -rich sediments on the lower slope and rise of continental margins. (2) C_{org} -rich sediments deposited on the ocean floor can become incorporated into accretionary margins through obduction. (3) Deep marginal seas, such as those in back-arc basins, may behave as extensions of the open ocean but later become incorporated into the continents.

It is possible that oceanic processes may have acted over continental margins and even in epeiric seas on the continental blocks at times of high sea level in the past. As discussed above, today's shelf and shallow epeiric seas tend to be discrete bodies of water, separated from the open ocean by fronts that develop above the shelf break. However, if the water in these seas were deep enough, they could behave as extensions of the open ocean. At times of global high sea level such as the Late Cretaceous, epicontinental seas could have become deep enough that the fronts above the shelf break disappeared, and the epicontinental seas became integral parts of the open ocean. Examination of modern shelves and consideration of the situation in the Cretaceous suggest that loss of the front between shelf and open ocean waters requires that the shelf break be submerged to a depth >300 m. Once the front between the shelves and open ocean has broken down, oceanic upwelling processes can occur in seas on the continental blocks.

High-Latitude Convection. High-latitude convection differs from upwelling in the stratified tropical and subtropical ocean in that the vertical circulation extends from the surface to great depths or even to the sea floor. High-latitude convection accounts for about 20% of the productivity of open ocean upwelling areas. High-latitude convective circulation is markedly different in the

two hemispheres because of their geographic asymmetry, with an ocean basin almost enclosed by landmasses at the North Pole, and a continent located on the South Pole and surrounded by a circumglobal seaway. Runoff from land freshens the surface of the Arctic Ocean so that deep convection cannot take place. The high-latitude convergence of the atmospheric Polar and Ferrel Cells in the northern hemisphere occurs mostly over land. However, over the northeast Pacific, it induces an Arctic Divergence, upwelling water along the Aleutians and in the Bering Sea. The complex geography and oceanographic conditions in the GIN Sea prevent development of a major divergence there. In the southern hemisphere, the atmospheric convergence induces the Antarctic Divergence (Dietrich, 1957). Along this divergence, nutrient-rich water upwells into the Circumantarctic Southern Ocean.

The upwelled water associated with the Antarctic divergence is part of the larger convective system between the subtropical and polar fronts. Under the influence of the westerly winds that blow around the world at 50°S uninterrupted by topographic obstructions, the Antarctic Circumpolar Current (West Wind Drift) circles the Antarctic continent, carrying the waters from west to east and mixing from the surface to the ocean floor. It has a zonal transport of about 150 Sv and a vertical convective transport of 70 Sv (Nowlin and Klinck, 1986). Such rapid vertical motion ensures that the nutrient-rich waters have a short residence in the photic zone. This short residence time, combined with light limitation on phytoplankton growth, limits nutrient utilization to only about a third of the supply (Oeschger et al., 1984). The remaining preformed nutrients are returned to the depths by mixing. Martin (1990) believes that the productivity of the Circumantarctic Current is limited today by the lack of iron as a nutrient. He suggested that during the last glacial, higher winds speeds allowed dust-transported iron to fertilize the Southern Ocean, enhancing productivity. As in the case of increased low-latitude upwelling proposed by Sarnthein and Fenner (1988), the resultant increased burial of C_{org} would cause a decrease in the level of atmospheric CO_2 .

Has high-latitude convective upwelling changed over time? The model of Sarmiento et al. (1988) is based on the assumption that it has varied with time, allowing greater and lesser utilization of upwelled nutrients (see Figure 7). In their model, increased nutrient utilization in the high-latitude ocean is the critical factor causing anoxia in the ocean interior. The Warm Saline Bottom Water (WSBW) scenario for vertical circulation (Figure 15) suggests that upwelling forced by the halothermal circulation would have slowed the high-latitude convective upwelling, resulting in greater nutrient utilization and higher productivity at high latitudes.

Ice Margin Upwelling. Ice margin upwelling is a special case of forcing that may contribute significantly to the general convective motion of waters at high latitudes. Buckley et al. (1979) and Hakkinen (1987) have described how upwelling occurs in response to the differential effect of the wind stress on the ice and

water along the edge of the Arctic Ice Pack and in the GIN Sea. The presence of sea ice isolates the ocean from the wind, but the margin of the ice acts as though it were land, providing a form of pseudo-coastal upwelling. Divergence may involve large volumes of upwelled water where the ice margin is sharply defined and the wind stress is large. The upwelling is best developed when the ice does not move. Fast ice, grounded over polar shelf seas, may force coastal upwelling offshore.

Because the distribution of sea ice is restricted to the ocean poleward of the Polar Front, this upwelling mechanism affects only the polar oceans. Ice margin upwelling is more likely to bring up nutrient-rich waters in the fall, as the ice freezes and salinization of the surrounding water enhances the likelihood of convective overturn. In the spring, when the sea ice melts, it forms a fresher, lighter surface layer that inhibits upwelling. Although nutrients introduced by upwelling in the fall and winter might not be immediately utilized by the phytoplankton because of the low light levels, the surface ocean is fertilized and ready to produce a massive spring bloom when the light returns.

Both sea ice formation and ice margin upwelling enhance convection of nutrient-rich waters at high latitudes. Ice margin upwelling would have occurred whenever sea ice was present in the past. Frakes et al. (1992) cite data to suggest that sea ice has been present in the polar regions throughout much of earth history, and may have been demonstrably absent only during the warmest times, such as during the Late Cretaceous and Eocene. The significance of ice margin upwelling in the oceans today remains to be assessed, but it is a factor that should be considered in thinking about upwelling in the polar regions in the past.

Equatorial Upwelling. It can be expected that diffuse upwelling must occur along the equator in response to the change in sign of the CorF. Under the influence of the easterly trade winds in each hemisphere, the waters in the northern hemisphere should move north and those in the southern hemisphere move south, producing divergence. However, at present and probably throughout much of geologic history, the equatorial upwelling system has been more complex, as shown schematically in Figure 17. Neumann and Pierson (1966) described the dynamics of the present equatorial upwelling system and speculated changes with relocation of the Intertropical Convergence Zone (ITCZ). Today, the northeasterly and southeasterly trade winds converge at the ITCZ at 6°N (mean annual position), with the result that the oceanic divergence associated with the ITCZ lies generally north of the equator. South of about 5°S, the water beneath the southeasterly trade winds is affected by the CorF, and its net transport is to the southwest. As the southeasterly trade winds approach the equator, they are no longer affected by the CorF and continue across the equator as southeasterly winds. Beneath them, the surface waters move directly downwind, that is, to the northwest, with the result that the water diverges along and just south of the equator. This complex sys-

tem accounts for about half of the productivity in oceanic upwelling areas.

It can be argued that if the ITCZ were located directly over the equator, there would be no oceanic divergence associated with it. Rather, there would be an equatorial convergence in the water as the downwind-driven waters meet. However, the climate of the earth seems to have rarely, if ever, been symmetrical about the equator. The global paleogeographic-lithofacies atlases of Ronov et al. (1984, 1989) suggest that the distribution of climate-sensitive sediments on the surface of the Earth has always been asymmetrical. The ITCZ may never be located over the equator for any length of time. The difference between distribution of land and sea in the two hemispheres is usually cited as the reason why the ITCZ lies north of the equator at present. Flohn (1983) suggested another cause: the inequality of the meridional temperature gradient at mid levels in the troposphere. The meridional gradient from the pole to equator is about 30°C greater in the southern than in the northern hemisphere, because of the colder temperatures at the 2 km high surface of the Antarctic Ice Sheet at the South Pole compared with relatively warmer temperatures at the same elevation above the floating sea ice covering the North Pole. Flohn (1983) indicated that when there was unipolar glaciation (Miocene), the ITCZ may have been pushed further into the nonglaciated (northern) hemisphere, and suggested that this might have resulted in increased upwelling on a global scale.

Current Divergence. Divergence resulting in upwelling may occur within currents in the open ocean because of changes in wind stress across the cur-

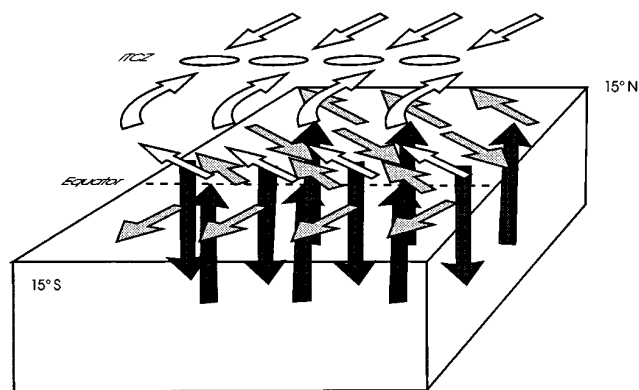


Figure 17. Schematic view of equatorial upwelling. Open arrows indicate the path of the trade winds approaching the Intertropical Convergence Zone (ITCZ) located north of the equator and marked by ellipses. Light gray arrows show the direction of Ekman transport in the surface ocean mixed layer. Dark arrows show upwelling and downwelling from the ocean interior to the surface and vice versa. Upwelling occurs along the equator in response to the divergence created as the CorF goes to 0. A second upwelling zone lies north of the equator, beneath the ITCZ.

rent (curl of the wind stress). The Ekman transport will diverge and cause upwelling if the velocity of the wind (and wind stress on the water) increases to the right in the northern hemisphere or to the left in the southern hemisphere. For the divergence to be effective in bringing up deep waters, the wind stress must change rapidly over short lateral distances. Divergence within the Benguela Current system has been indicated by Schott (1943), Dietrich (1957), and Moroshkin et al. (1970). The causes of these divergences vary, but many are related to the wind stress at the time the observations were made. Current divergence accounts for only a very small part of the productivity of the ocean, but could be locally important in the geologic past.

Upward Ekman Pumping. Ekman pumping is vertical motion of the water in response to curl of the wind stress (illustrated schematically in Figure 18). It is well documented in the Arabian Sea (Luther and O'Brien, 1985). Although the onset of the summer monsoon, with winds blowing across the Arabian Sea from southwest to northeast, is marked by coastal upwelling along the southern margin of Arabia, the later development of intense oceanic upwelling depends on another oceanographic phenomenon, Ekman pumping. As the monsoon develops, a strong southwest-northeast wind jet forms over the central Arabian Sea (Findlater, 1969). Winds along the axis of the jet are strong but decline sharply to the northwest and southeast. The resultant differential wind shear over the water, the curl of the wind stress, is positive to the northeast of the axis of the jet and negative to the southeast of the axis of the jet. The increase in positive vorticity (tendency of the water to move counterclockwise, or cyclonically in the northern hemisphere) to the northeast of the axis creates divergence and results in oceanic upwelling throughout a broad region of the northwestern Arabian Sea. The increase in negative vorticity (tendency of the water to move clockwise) to the southeast of the axis results in convergence and promotes downwelling in the southeastern Arabian Sea (Brock et al., 1992). The resultant overall effect—oceanic upwelling and downwelling induced by curl of the wind stress—is known as Ekman pumping. Ekman pumping can result from cyclonic and anticyclonic wind circulation associated with weather systems, but because of their rapid drift, their effects on the ocean are usually short lived.

Ekman pumping may also affect upwelling along the southwest African coast. If the axis of the equatorward wind jet were exactly along the shoreline, and the wind speeds decreased offshore, the effect would be to cause downward Ekman pumping over the shelf. The result would be that upwelling would be concentrated along the shore. At present, the axis of the equatorward wind jet lies offshore (Hastenrath and Lamb, 1977; Shannon, 1985). Because the wind speed decreases toward the shore, a region of upward Ekman pumping develops between the axis of the wind jet and the shore. The maximum offshore Ekman transport occurs beneath the maximum velocity of the wind jet, creating an offshore divergence. This is why

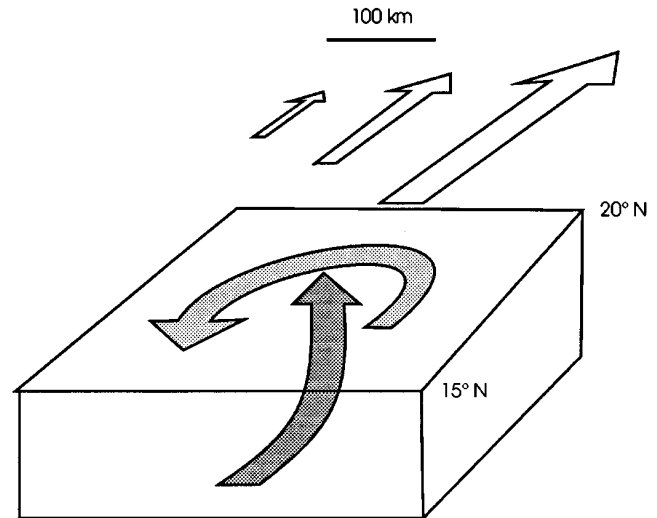


Figure 18. Schematic diagram illustrating upward Ekman pumping. Open arrows indicate the winds, which diminish to the left. Light gray arrow indicates the cyclonic rotary motion imparted by the winds to the water. Darker gray arrow shows the upwelling induced by the cyclonic motion of the water.

the upwelling presently occurs both along the shore and near the shelf break. The axis of the wind jet is offshore because the coast is bordered by desert, which creates a thermal front, and by the Great Escarpment of the Kalahari Plateau, which forms an orographic boundary and causes frictional drag.

Although regionally important, Ekman pumping is responsible for only a small fraction of the productivity due to upwelling in the open ocean. It depends on co-occurrence of geographic accidents: for the Arabian Sea, strong monsoonal circulation and uplift along the northwest African coast help to focus the monsoonal winds into a low-level jet. This was a set of conditions characteristic of many of the margins of Pangaea during much of the Permian–Jurassic (Moore et al., 1992a, b; Wilson et al., 1994).

Ocean Margin Upwelling

Although it accounts for only 20% of the high productivity in the ocean (Romankevich, 1984), upwelling along the ocean-continent margins is the most important process leading to C_{org} burial in sediments. Fine-grained sediments accumulate along the continental margins, particularly on the upper slope where the O_2 minimum impinges on the sea floor. Ocean margin upwelling occurs over large areas, but the sites of highest concentration of upwelled nutrients and primary productivity are determined by local features.

Coastal Upwelling. Coastal upwelling is the phenomenon most familiar to geologists. Along with equatorial upwelling, it is highly predictable. Conditions favorable for it exist along the western margins of continents between latitudes of 15 and 30°. It is the form of upwelling that has been most extensively investigated with climate models (Parrish, 1982; Parrish and Curtis, 1982; Barron, 1985; Moore et al., 1992a), and many

petroleum source beds are attributed to coastal upwelling (Brongersma-Sanders, 1948; Dow, 1978; Demaison and Moore, 1980a, b; Parrish, 1982). In terms of global significance, it accounts for about 20% of high productivity due to upwelling (Romankevich, 1984).

The explanation of coastal upwelling was suggested by Thorade (1909) and elaborated by Sverdrup (1938a). Conditions favorable to coastal upwelling are best developed along north-south-trending coasts, on the eastern sides of the ocean basins in the latitudes of the subtropical highs. There, the high-pressure systems over the ocean and low-pressure systems that develop over the continents generate winds that blow equatorward along the coasts, resulting in offshore Ekman transport and upwelling. The offshore Ekman transport of water is directly proportional to the wind stress, but inversely proportional to the Coriolis parameter (Pond and Pickard, 1983; Apel, 1987). As a consequence, wind-driven coastal upwelling is well developed in two bands, between 10 and 30°N and S, on the eastern sides of ocean basins where the coasts have a meridional orientation. It also occurs where the ocean basin is bordered to the south by a zonal (east-west) coast in the northern hemisphere, as in the case of the Caribbean, or to the north by a zonal coast in the southern hemisphere. Under these conditions, the net transport of water is offshore. The sea surface near the shore is depressed and the water being driven away from the shore is replaced by upwelled deeper water. The pattern of currents in a wind-driven upwelling system is illustrated schematically in Figure 19.

In the southern hemisphere, the regular longitudinal alternation of land and ocean results in an atmospheric circulation pattern more stable than that of the northern hemisphere. This pattern, termed the Walker circulation, consists of persistent highs over the ocean and lows over the continents. These vary much less with the seasons than the atmospheric pressure systems of the northern hemisphere, many of which move or reverse with the seasons, with lows forming over the ocean during the winters and highs during the summers. Because of the Walker circulation, wind-driven upwelling in the southern hemisphere tends to have less seasonal variability than that in the northern hemisphere.

Upwelled water is not necessarily nutrient-rich, hence wind-driven coastal upwelling does not always result in increased productivity. The directly upwelled water generally comes from depths of 50–200 m, but this directly upwelled water may, in turn, be replaced by a mixture of deep pycnocline and intermediate water. The degree to which deeper water can be mixed upward is a function of the density gradient and difference between the water masses. Only where the pycnocline separating the surface mixed layer from nutrient-rich deeper waters is shallow can nutrients be introduced into the surface waters in quantities large enough to increase productivity. Off the southwestern margin of Africa, the pycnocline and top of the AAIW descend to reach a maximum depth off the Cape Peninsula (Hay and Brock, 1992). Then, they slowly ascend gently toward the north. Off Lüderitz (25°S),

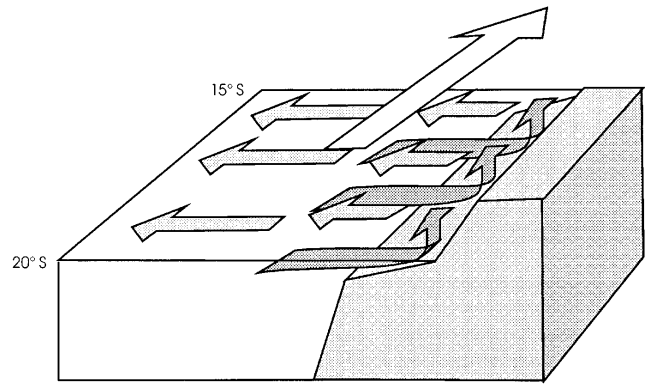


Figure 19. Upwelling along a steep coast with a narrow continental shelf, such as the active margins along the western side of South America or southern Africa.

they are shallow enough to be strongly affected by the surface upwelling processes. Thus, although waters are upwelled along the entire margin from Cape Agulhas (34°S) to Cabo Frio (18°S), the northern third of the upwelling region receives the most nutrient-rich waters. Deposition of diatomaceous oozes and C_{org} -rich sediments is concentrated there (Calvert, 1983). A similar phenomenon takes place off northwestern Africa. The nutrient-rich AAIW and nutrient-poor MW meet at Cap Blanc. Although the best wind conditions for upwelling occur north of Cap Blanc, the region between Cap Blanc and Cape Verde is much more productive because of the higher nutrient content of the waters upwelled there. The western margin of Australia lies at the same latitude as the highly productive Benguela and Peru–Chile upwelling systems of southwest Africa and South America. The western Australian margin has the same NNW–SSE orientation as the southwest African margin. The winds are favorable for coastal upwelling but productivity is low. The reason lies in the nature of the intermediate waters off western Australia. The O_2 minimum lies within the intermediate water at a depth of 500–1000 m, too deep to contribute water directly to the upwelling. Furthermore, the O_2 minimum is poorly developed, with O_2 saturation ranging from 35 to 50% (Levitus, 1982), so that the nutrient levels of the intermediate waters are low ($PO_4 \sim 2.4 \mu\text{mol kg}^{-1}$). The thickness of the mixed layer off western Australia is also much greater than in productive upwelling areas.

Because the trade winds are one of the most stable parts of the climate system, the sites of coastal upwelling in the geologic past are highly predictable. Coastal upwelling can occur from extremes of 5 to 35°N and S where the coast is oriented so that the winds will drive offshore Ekman transport. Less predictable is whether the water upwelled in the past would have contained nutrients; this depends on the source of the intermediate waters and their flow path to the site of upwelling. Although coastal upwelling occurs over a broad latitudinal belt, other features

such as Kelvin waves, bathymetry, currents, orography, and river outflows act to concentrate upwelling at particular sites.

Upwelling Driven by Factors Other Than the Direct Influence of the Wind

The localization of upwelling at particular sites can be caused by special conditions. Upwelling can be enhanced by changes in the winds in areas remote from the sites of upwelling (equatorial Kelvin waves) and can be forced indirectly by the wind (cyclonic gyres and eddies; thermocline domes). Upwelling can also be enhanced by bathymetry of the sea floor and by river discharge.

Kelvin Wave-Driven Coastal Upwelling

Coastal upwelling also occurs on the eastern sides of the tropical oceans. There, it is a seasonal response to the passage of Kelvin waves trapped by the coast. Picaut (1985) and Brown et al. (1989) have summarized the phenomenon.

Kelvin waves are long-wavelength gravity waves acted upon by the CorF. The most familiar example of Kelvin waves are the tides. As a wave moves poleward along a coast to its east, the CorF acts on it, increasing the amplitude of the wave along the coast. The Kelvin wave thus appears to be trapped along the coast; its amplitude decays away from the coast. At a distance known as the Rossby radius of deformation, it is hardly discernible. The Rossby radius of deformation is equal to the wave speed divided by the Coriolis parameter, f . Typically, the Rossby radius of deformation, infinite at the equator, decreases to the order of 100 km at 10°N or S and to 25 km in the mid-latitudes. The significance of equatorial Kelvin waves to upwelling is that they form high-amplitude internal waves in the pycnocline. The upward motion of the pycnocline brings nutrient-rich waters close enough to the surface so that they can be upwelled to the surface by wind forcing. The internal waves may even break, causing mixing across the pycnocline. As the Kelvin waves move away from the equator, the Rossby radius of deformation decreases. When this becomes less than the width of the shelf, the oceanic pycnocline can no longer be affected. Hence, this phenomenon is only effective in enhancing upwelling within about 10° of the equator.

Figure 20 is a schematic view of Kelvin waves in the eastern equatorial Atlantic and along the coast of Africa. The equator acts as a wave guide for Kelvin waves. Long waves traveling from west to east in the northern and southern hemisphere in the equatorial region experience the CorF to the right and left, respectively, locking them onto the equator and causing them to have their greatest amplitude there. The west-to-east propagating Kelvin waves trapped by the equator are generated by perturbation of the atmospheric forcing in the western part of the ocean.

The trade winds produce an east-to-west upward slope of the sea surface in the equatorial region. In the Atlantic, seasonal variation of the trade winds results in the production of equatorial Kelvin waves that cause the thermocline to move up and down, causing

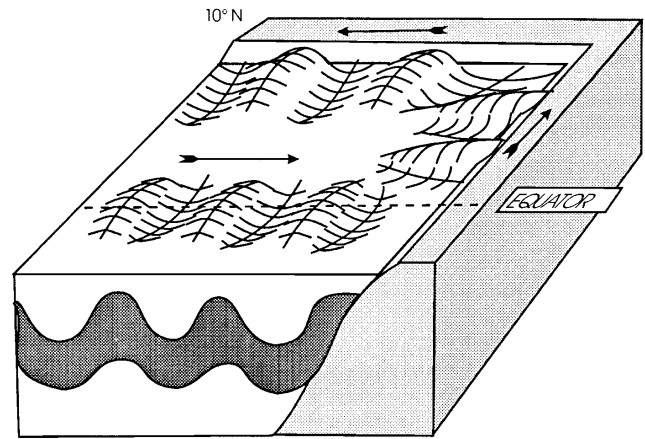


Figure 20. Schematic view of Kelvin wave-driven upwelling in the eastern equatorial Atlantic. The equatorial wave guide of the eastern tropical is also shown.

variations in the intensity of equatorial upwelling. On reaching the African margin, the Kelvin waves split and move poleward bringing the thermocline near the surface as they move along the coast, resulting in productive upwelling in the Gulf of Guinea and along the coast of Gabon (McCreary et al., 1984; Picaut, 1985). In the Pacific, relaxation of the trade winds removes the force supporting the sea surface slope and induces an internal equatorial Kelvin wave that depresses the thermocline and moves from west to east across the ocean. Upon reaching the eastern side of the ocean, the equatorial Kelvin wave splits into two poleward-moving Kelvin waves trapped by the coast. In the Pacific, this phenomenon occurs on an interannual time scale. Depression of the thermocline in the eastern Pacific prevents upwelling of nutrient-rich water to the surface, causing the reduction of biological productivity known as El Niño.

Kelvin wave-driven upwelling is likely to occur on the eastern equatorial margins of the ocean basins between 10°N and 10°S as long as there is a seasonal change in the equatorial winds. The seasonal change in equatorial winds results from migration of the ITCZ, and the effect could have been greatly enhanced if there were stronger monsoonal circulation at times in the past, as suggested by some climate models (e.g., Parrish, 1982; Parrish et al., 1982; Wilson et al., 1994).

Cyclonic Circulation

Cyclonic circulation (counterclockwise in the northern hemisphere, clockwise in the southern hemisphere) induces an upward motion in the center of the vortex. Cyclonic vortices bring deeper water upward into the mixed layer on a global scale. Cyclonic vortices are sites of divergence at the sea surface and convergence at depth, as shown in Figure 21. Anticyclonic circulation has the opposite effect.

The large tropical-subtropical gyres of the surface of the Atlantic, Pacific, and South Indian oceans are anticyclonic. Cyclonic gyres develop seasonally in the

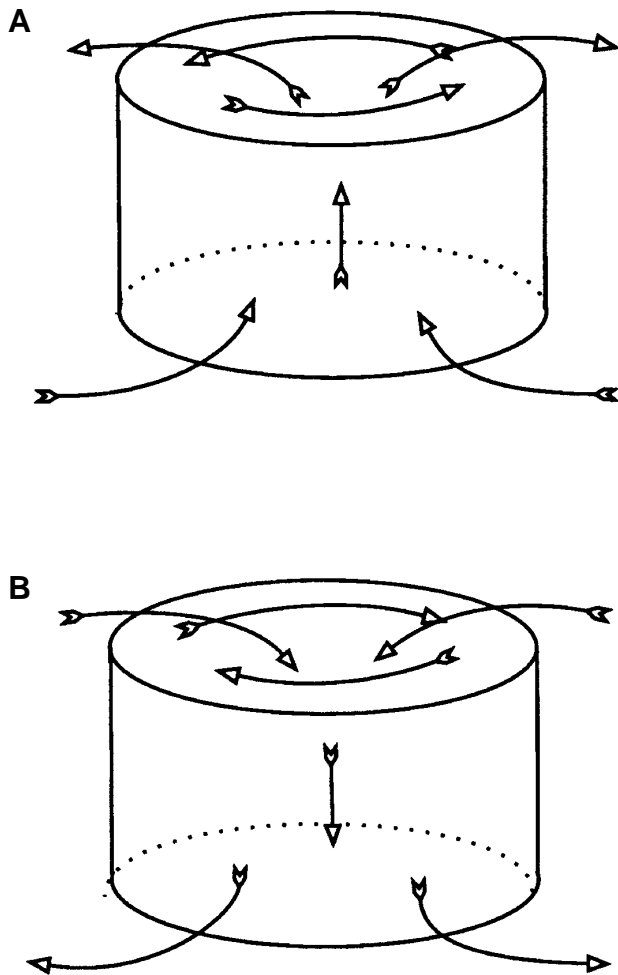


Figure 21. Effect of rotation of vortices. (A) A cyclonic gyre. Water is drawn in at the bottom of the gyre, upwelled in the center, and flows outward. The surface of the water in the center of the gyre, where upwelling takes place, is depressed below the margin. The gyre is shown rotating counterclockwise, which is cyclonically in the northern hemisphere. (B) An anticyclonic gyre. All of the features are reversed, and the rotation forces downwelling in the center. The gyre is rotating clockwise or anticyclonically in the northern hemisphere.

Arabian Sea and the Bay of Bengal, and there is a permanent cyclonic gyre in the eastern tropical South Atlantic off Zaire-Angola (Peterson and Stramma, 1991; Gordon and Bosley, 1992), associated with the Angola thermocline dome discussed below. Ocean circulation is cyclonic between the Subtropical and Polar Fronts, which encourages the deep convection. Poleward of the Polar Fronts, much of the circulation is cyclonic, as in the GIN Sea, over the Amundsen-Nansen Basin of the Arctic Ocean, and in the Weddell Sea. Although cyclonic gyres are mostly a high-latitude oceanic phenomenon today, they may have existed in the extensive marginal seas of the past.

Smaller than the major gyres are mesoscale eddies. These are vortices having diameters of a few hundred

kilometers. Smaller still are submesoscale vortices, on the order of 100 km or less. The eddies are a form of turbulence in the ocean and are best developed downstream from the western boundary currents after they have left the coasts. Although most mixing in the ocean takes place along isopycnals, the mesoscale and submesoscale vortices juxtapose waters of different densities at the same horizontal level so that other turbulent processes may induce them to mix. Eddies may be significant in mixing the surface and deeper layers of the ocean on a global scale (Kerr, 1985). In the North Atlantic, mesoscale eddies associated with the Gulf Stream commonly extend to depths of 1 km, and some raise or depress isohalines all the way to the sea floor (see salinity profiles in Fuglister, 1960). The largest mesoscale eddies in the South Atlantic are introduced from the Indian Ocean where the Agulhas Current rounds South Africa. They are among the most energetic eddies in the world (Olson and Evans, 1986) and can be seen on Fuglister's (1960) salinity profiles. However, they are spun off the north side of the Agulhas Current; hence, they are anticyclonic and do not upwell. Again, mesoscale eddies are most important in the open ocean today, but in the geologic past they may have been characteristic of currents in epicontinental seas.

Vortex motion is very important in the ocean interior. To maintain continuity of volume in the ocean, the water that sinks as deep water must be returned to the surface. At present, deep water is formed at high latitudes at a rate of about 40 Sv. This is the net volume of water that has sunk to the ocean bottom and moved equatorward of the polar fronts. It must return to the surface from beneath the tropical-subtropical gyres. This occurs through diffusion and turbulent mixing. The turbulent mixing is performed by eddies and gyral circulation in the ocean interior. Cyclonic circulation in the interior of the ocean plays an important role in returning deeper waters toward the surface. The mechanism works best where the density differences are small. When the water is introduced to the base of the pycnocline, a stronger forcing mechanism must bring it to the surface.

Large subsurface cyclonic gyres develop in the eastern parts of the ocean basins in response to internal pressure gradients. Bogorov et al. (1973) observed that these bring nutrients near to the surface and are important in enhancing the effectiveness of upwelling along the eastern sides of the ocean basins in the subtropics. One such subsurface cyclonic gyre off southwest Africa has been well documented (Moroshkin et al., 1970; Gorshkov, 1977). It brings nutrient-rich water to shallow depths immediately beneath the thin surface Benguela Current.

A poleward undercurrent beneath the equatorward surface flow is characteristic of all major productive coastal upwelling regimes (Smith, 1983). The undercurrent is usually the coastal side of a subsurface cyclonic gyre that introduces deeper nutrient-rich waters to shallower levels where they can be readily upwelled under the influence of the wind.

In the geologic past, when the polar regions were warmer, the overall density contrast in the ocean was

less than it is today. The polar waters were warmer ($> 5^{\circ}\text{C}$) so that their thermal expansion and contraction played a large role in controlling their density. Sea-ice formation, if it occurred, was restricted to much smaller areas. The dense waters had a higher salinity which they acquired through evaporation in shallow marginal seas. With a lesser density contrast, upwelling and mixing of water in the ocean interior may have occurred more readily.

Thermocline Domes

The term "thermal dome" is applied by physical oceanographers to subsurface domes of the thermocline that bring cold deep waters closer to the surface. The term "thermocline dome" is more appropriate and used here because the domes are filled with cold rather than warm water. Three thermocline domes form in the tropics, centered at 10°N and S , several hundred kilometers off the eastern margins of the ocean basins: the Costa Rica Dome in the Pacific at 10°N off Central America (Wyrki, 1964), and the Guinea Dome at the same latitude off Africa in the Atlantic (Mazeika, 1967; Voiturez, 1981). Although the existence of a Peru Dome had been suggested by Mazeika (1967), it has not been found. The Angola Dome, located beneath the cyclonic gyre of the eastern South Atlantic at 10°S , is a perennial feature. It is the most obvious of these features in CZCS satellite imagery (Herzog and Hay, in preparation). It is the only one of the thermal domes known to leave a distinct signature in the underlying sediments, which are enriched in opal and C_{org} (Gorshkov, 1977; Udintsev, 1990).

The physical oceanography of the tropical thermal domes has been reviewed by Picaut (1985). They were originally thought to form in response to the poleward deflection of the North and South Equatorial Counter-currents as they meet the eastern margins of the ocean basins, as shown diagrammatically in Figure 22. The cyclonic flow of the currents causes deep water to be brought close to the surface, but an additional impetus is required to cause the waters of the dome to upwell to the surface.

Although deep currents may be critical in creating the thermocline domes, the winds must be involved in upwelling the waters to the surface. Voiturez (1981)

suggested that upwelling would be most likely to occur when the ITCZ is located over a thermocline dome. At these times, the atmospheric pressure is low and the curl of the wind stress becomes favorable for upwelling. Hofmann et al. (1981) found the location of the Costa Rica Dome to be fixed by the curl of the wind stress. Picaut (1985) reported that the Guinea Dome is located in a region of cyclonic wind stress curl from May to October and that the Angola Dome is also located in a region where the wind stress curl is favorable most of the year.

The three well-known thermocline domes, off Costa Rica, Guinea, and Angola, play a major role in oceanic upwelling in the eastern tropical Pacific and Atlantic. They account for more than 25% of the productivity in response to open ocean upwelling. It seems likely that analogs have existed in the past, and that these features are a characteristic of the eastern sides of ocean basins. They may occur close enough to the continent to make a significant contribution to the C_{org} of continental rise sediments.

Bathymetry-Driven Upwelling

In order for a given volume of water in an ocean current to pass over a shallow ridge, it must speed up. Because the CorF acting on the current is proportional to the velocity of the water, the acceleration of the current as it crosses the ridge causes it to deviate *cum sole* (Defant, 1961). On entering the deeper water on the other side of the ridge, it will deviate *contra solem*, or turn to the left in the northern hemisphere and to the right in the southern hemisphere. This will induce clockwise (cyclonic in the southern hemisphere) circulation on the right side of the current, accompanied by upwelling. This upwelling between the current and the coast need not be confined to the shallow depths to which wind-induced upwelling is restricted. It is this effect that localizes the major upwelling centers at sites where the shelf is narrowest (Preller and O'Brien, 1980). The wider shelf just north of these sites causes the current to accelerate, producing cyclonic circulation which causes upwelling inshore. Along the southwest African margin, upwelling is most intense where the shelf is narrowest (Nelson and Hutchings, 1983; Shannon, 1985).

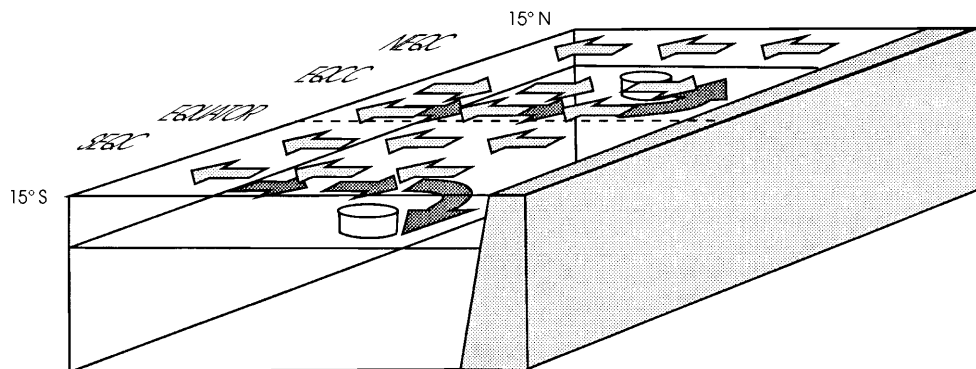


Figure 22. Schematic view of thermocline domes (shown as cylinders) in the eastern side of an ocean basin.

Zonal (east-to-west or west-to-east) flow across a shallow bank responds to the conservation of vorticity. The potential vorticity is the sum of the planetary vorticity f (i.e., the vorticity associated with the rotation of the Earth, which is identical with the Coriolis parameter $2\Omega\sin\phi$) and the relative vorticity of the water mass divided by the depth, D . Because planetary vorticity is always much larger than the relative vorticity of the moving water, the potential vorticity is closely approximated by f/D . As D decreases over a shallow bank, f must also decrease to conserve potential vorticity. Hence, as water flows zonally across a shallow bank it will move equatorward, toward lower values of planetary vorticity. Succinct discussions of this effect have been presented by Pond and Pickard (1983) and Brown et al. (1989). It would surely have been an important factor in circulation in the large epicontinental seas of the past.

Current-Induced Upwelling

A geostrophic ocean current impinging on a shelf may cause bottom Ekman transport onto the shelf, forcing weak upwelling on the shelf. Hsueh and O'Brien (1971) proposed that this phenomenon occurs in response to the strong flow of the loop current in the Gulf of Mexico. O'Brien (1975) suggested that Bang's (1971) description of upwelling on the southwest African margin indicated that current-induced upwelling also occurs there.

Orographic Upwelling

Orographic upwelling results when the onshore topography directly influences the winds blowing over the water. The best-known example of this is in

the Gulf of Tehuantepec, off Mexico. Easterly winds are funneled to the sea through a saddle in the mountains along the coast, creating a wind jet across the surface of the water. The resulting divergence of the water causes upwelling in the Gulf of Tehuantepec that results in high productivity (Barton et al., 1993).

Outflow-Induced Upwelling

Rivers that discharge large volumes of water as plumes onto narrow shelves or directly onto the surface of the ocean may induce upwelling. The freshwater discharge must mix with much larger volumes of salt water to acquire oceanic salinity. This process may draw in large volumes of ocean water (>20 times the river outflow), and if conditions are right, may result in the upwelling and incorporation of nutrient-rich waters into the plume. Such conditions occur where the Congo River discharges into the South Atlantic. The river plume directly overlies the shallow pycnocline and draws up nutrient-rich water as it is salinized (van Bennekom and Berger, 1984).

CABALLING

Caballing is a process that presently serves to ventilate the ocean interior in several regions. It might also be a means by which organic matter could be introduced into the deep sea at a rate much larger than the normal particulate rain. When two waters having the same density but different temperatures and salinities mix, the resulting water is always more dense, as shown in Figure 23. The rapid to catastrophic downwelling induced by the increase in density is termed

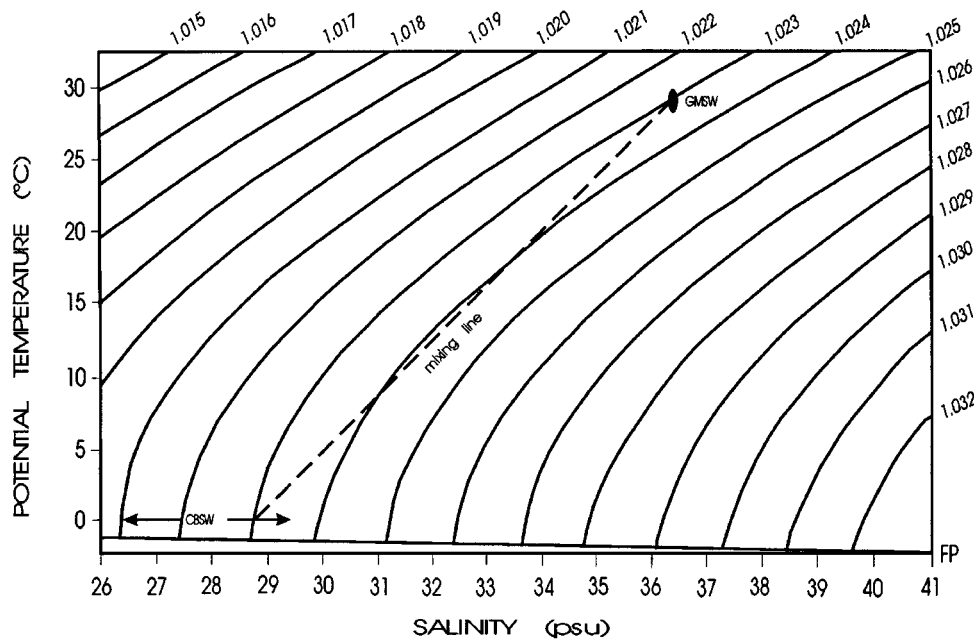


Figure 23. Temperature-salinity-density diagram showing a mixing line for surface waters in the Gulf of Mexico (GMSW) and Canadian Basin of the Arctic (CBSW). Densities are for surface waters and are given in g/cm^3 or kg/L . The mixed water can be more than 0.001 g/cm^3 denser than the parent waters.

caballing (alternate spellings: cabaling, cabelling), shown diagrammatically in Figure 24. Originally proposed to explain the formation of AABW (Brennecke, 1921), it has been shown to be involved in bottom-water formation both in shelf areas and in the open ocean (Killworth, 1983). Caballing of the denser mixed water allows it to reach the ocean bottom. The high-latitude caballing waters contain relatively little plankton, probably because of the low light levels. Caballing also occurs on a large scale in the Sea of Japan, where an arm of the warm saline Kuroshio Current that passes through the Tsushima Strait meets the colder, fresher, but equally dense water flowing south from the Tatarskiy Strait (Oba, 1991; J. Ingle, personal communication). Neither of these water masses is highly productive, and the caballing hyperventilates the Japan Sea with O_2 -rich Japan Sea Proper Water. However, if the waters mixing to produce caballing were highly productive, the process would carry large amounts of organic matter into the ocean interior.

Hay (1989) and Hay et al. (1993) have proposed that caballing in meridional epicontinental seaways might explain the formation of the widespread bituminous shales and synchronous "ocean anoxic events" (OAE). They suggested that, in the confines of the Western Interior Seaway, the catastrophic downwelling of the caballing water would cause massive kills of the plankton and entrained nekton, introducing much greater quantities of C_{org} into the deep waters than would the normal particulate flux. The mixed waters would thus have a very high O_2 demand and the bottom waters could be dysoxic or anoxic beneath their source; a situation which does not occur on Earth today. If formed in quantity, these waters would flow out of the seaway to form intermediate or deep waters in the ocean.

To understand how caballing might occur and what its effects might be, consider what would happen if the Western Interior Seaway were to come into existence today. Figure 23 shows the effect of mixing Gulf of Mexico and Canadian Basin waters. Although they have very different temperatures and salinities, the surface waters of both seas have the same density. The mixed water has a much greater density and would sink, drawing in more water from the Gulf of Mexico and the Arctic. Hay et al. (1993) assumed Cretaceous paleogeography and a moderate meridional temperature gradient. They speculated that waters of the Arctic and Gulf of Mexico would have a lesser temperature and salinity difference than today. Although they did not assume equal density of the two seas, they found that the modification of the waters by evaporation and precipitation in the Western Interior would act to cause the northern and southern water masses in the seaway to acquire the same density. Assuming the water at the southern end of the Seaway might have a temperature of 30°C and a salinity of 35, its corresponding density would be 1021.7 kg m^{-3} . The water at the northern end would be cooler and less saline with a temperature of 10°C (Parrish and Spicer, 1988) and a salinity of 30; its density would be 1023.0 kg m^{-3} . The waters would be modified by evaporation and precipitation as they move into the Seaway. Freshwater balance must have been positive in the northern and negative in the southern part of the Sea-

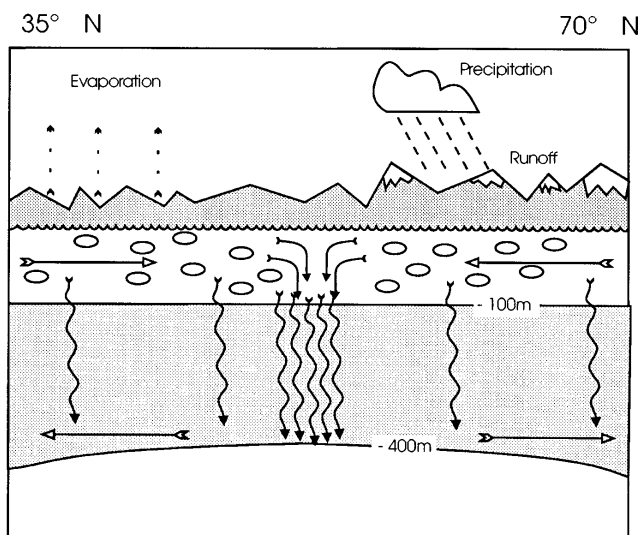


Figure 24. Schematic diagram of caballing in the Cretaceous Western Interior Seaway of North America. Waters of equal density, but different temperatures and salinities, flow in from the north and south and meet along a mixing front. The mixed water, being denser, sinks catastrophically, carrying the plankton with it.

way. The modifications would make the water in the south more dense and the water in the north less dense. Using reasonable values for the Cretaceous latitudinal precipitation-evaporation balance, the waters could be expected to have the same density (1022.0 kg m^{-3}) at about $40\text{--}50^\circ\text{N}$. At this latitude, where the southern water mass would have a temperature of 30°C and salinity of 35.4; the northern water mass would have a temperature of about 15°C and a salinity of 29.8. Assuming mixing in equal proportions, the resulting mixed water would have a temperature of 22.5°C , a salinity of 32.6, and a density of 1022.3 kg m^{-3} . The mixed water, being less dense than the Arctic water, would not flow out the north end of the seaway but, being more dense than the Gulf of Mexico water, would flow out to the south. On leaving the Seaway it would become an intermediate water mass in the Gulf of Mexico. It would be directed to the right by the CorF and flow at depth along the margin of Central America, pass through the opening to the Pacific, and mix with the O_2 -depleted waters that should have existed along the western margins of Central and North America.

There is geologic evidence that may indicate the existence of such a front. Bramlette and Ruby (in Moore, 1949) described an abrupt facies change in Cenomanian–Turonian strata northwest of the Black Hills of South Dakota. The lithology changes from calcareous shales in the southeast to noncalcareous shales in the northwest. Kauffman (1984) and Eicher and Diner (1985) demonstrated that this facies change corresponds to a major paleobiogeographic boundary. Fisher (1991) showed that the calcareous facies contains abundant planktonic foraminifera, calcareous nannoplankton, and a rich benthic foraminiferal assemblage, while the noncalcareous

facies contains an arenaceous benthic foraminiferal assemblage. The paleontologic contrasts across the facies change indicate that it marks the position of an oceanic front in the Seaway. A front is a site of downwelling, hence the presence of a front supports the caballing hypothesis.

Because of its greater density, the downwelling water along the proposed Front in the Seaway would produce strong bottom currents and cause erosion of pre-existing sediment. Extensive areas of hiatus development associated with the peak transgressive deposits of the Greenhorn and Niobrara cycles in the United States portion of the Seaway (Cobban and Reeside, 1952; Sharp, 1963; Hattin, 1975; Fisher et al., 1985; Merewether and Cobban, 1986) may reflect this process, although they are also certainly related to sediment starvation in basinal settings during late Cretaceous transgression and maximum flooding intervals.

During sea level rise, the outflow of Seaway Bottom Water formed by caballing would increase, because both the threshold depth and the width of the entrance increased. As the outflow increased, its buoyancy flux, the product of the volume flux times the density difference, would increase. Because the downwelling plume with the largest buoyancy flux becomes the deep water of the ocean (Peterson, 1979), the outflow plume might shift from spreading at shallow depth as intermediate water to become a deep-water source for the ocean. With an adequate buoyancy flux, the Seaway Bottom Water source might fill the ocean basins from the bottom up with dysaerobic or anaerobic water. This would provide a new mechanism for upwelling in the ocean interior. Filling the basins from the bottom up would greatly increase the rate of abyssal upwelling in the ocean from deep to intermediate levels. As the buoyancy flux reaches its maximum on a high sea level stand, the older deep ocean waters would be forced upward into the photic zone, resulting in a global bloom of oceanic plankton. Hay et al. (1993) hypothesized that such a global plankton bloom, producing a large flux of organic debris settling into aerobic deep waters, could be the cause of the thin widespread layer that marks the climax of the Cenomanian-Turonian OAE (~93 Ma). If the flux of anoxic Seaway Bottom Water to the deep ocean were 10 Sv, it would take about 40,000 yr for the ocean to turn over.

THE EFFECT OF BURIAL OF ORGANIC MATTER

The rise in the level of atmospheric O₂ during the Precambrian and Phanerozoic is a consequence of the development of photosynthesis but is intimately tied to the burial of C_{org}, because for every mole of carbon buried as C_{org}, a mole of O₂ is added to the atmosphere. As the concentration of atmospheric O₂ increases, it becomes more difficult to bury C_{org} both on the land and in the sea. The higher O₂ contents of the air and ocean waters make it more difficult to avoid oxidation of C_{org}. The O₂ that has already accumulated in the atmosphere can be removed from the atmosphere by

oxidation of previously buried C_{org} or by oxidation of other elements, such as Fe²⁺ to produce Fe₂O₃.

During the Phanerozoic, there have been episodes of massive burial of organic matter that must have changed the level of atmospheric O₂. The first large-scale burial of C_{org} took place in the Ordovician (Hay and Wold, 1990), and the organic matter incorporated into the sediment was certainly of marine origin. If the atmospheric O₂ content were initially low at that time, the ocean could very easily become anoxic. It may have been the Ordovician burial that raised atmospheric O₂ levels high enough to allow the formation of a layer of ozone adequate to block most of the ultraviolet radiation from reaching the surface of the Earth, permitting land plants to become abundant. Wells (1986) cites an O₂ content of one-tenth that of the present as being required for land plants to become widespread, and suggests that this O₂ level was not reached until the Silurian. There are great uncertainties, however, and Rhoads and Morse (1971) had concluded that the O₂ level had reached 20% of its present value by the beginning of the Cambrian. Holland (1984) argues from the nature of marine metazoan life at the beginning of the Phanerozoic that Cambrian atmospheric O₂ levels must have been at least 10% that of present, but that an upper limit cannot be set. Berner (1989) believed that atmospheric O₂ levels in the Cambrian were equal to those of today, but suggested that over the course of the Phanerozoic they have been as low as two-thirds (Ordovician, ~480 Ma) and as high as twice (Carboniferous, ~320 Ma) the present level.

A second major episode of marine C_{org} burial took place in the Devonian, again raising the level of atmospheric O₂. Extensive plant cover of the land developed during the Carboniferous, along with massive burial of terrigenous C_{org} as coal. This resulted in the highest atmospheric O₂ levels during the Phanerozoic. During the Permian and Triassic, extensive formation of redbeds may have removed O₂ from the atmosphere without oxidation of buried C_{org}. The atmospheric O₂ levels, under which the extensive Jurassic-Early Cretaceous deposition of C_{org} took place, may have initially been significantly lower than those of today. Only in the late Mesozoic did conditions of C_{org} supply and O₂ demand come to resemble those of today. The history of formation of petroleum source rocks over time is linked to the balance between C_{org} burial and O₂ content of the atmosphere and ocean.

SUMMARY AND CONCLUSIONS

If both high productivity in the euphotic zone and dysaerobic or anoxic conditions in the water column are important for the formation of C_{org}-rich deposits, many constraints can be placed on the search for them. Although the conclusion that coastal upwelling is responsible for producing many petroleum source beds is reassuring as a restatement of uniformitarianism, it is vexing in its vagueness as to where the richest source rocks might be found. Enough is now known of the oceanographic conditions that promote C_{org} deposition that it should be possible to make

intelligent guesses about where the largest concentrations of organic matter were deposited. In thinking about where the shales richest in C_{org} might be, it is important to consider the factors that control the supply of C_{org} , O_2 , nutrients in the ocean, upwelling, caballing, and oxidants above and below the benthic boundary layer.

The controls on the supply of C_{org} to the ocean are the rates of delivery of land plant material by rivers and the rain of organic remains of marine plankton. These processes tend to be mutually exclusive, and each dominates the system at different latitudes.

The factors that affect the O_2 and nutrient content of subsurface waters are: (1) O_2 content of the subsurface water at the site where it sank from the surface and lost contact with the atmosphere, (2) the intensity of the rain of particulate organic matter from above, and (3) how long it has been since it left the surface. At present, these factors are quite different for low- and high-latitude waters. In thinking about conditions in the past, it is important to remember that the initial O_2 content may vary by a factor of two or more, depending on whether the water has a warm or cold source area. The initial O_2 content will also have varied with the changing O_2 content of the atmosphere over geologic time. The intensity of the particulate rain will depend on the productivity of the overlying waters, which is in turn dependent on the supply of nutrients and the length of time the water is beneath the surface, which in turn depends on the rates of formation of intermediate and deep water.

There are three clear knowns: (1) Anoxic basins are most likely to develop if they are isolated from the open ocean, and in any case they must be isolated from the waters of the high-latitude convecting ocean; anoxic basins generally require a positive freshwater balance. (2) O_2 minima are most intensely developed between the Subtropical Fronts on the eastern sides of the ocean basins. (3) Dense saline waters can fill depressions in the bottom and become stagnant pools; the production of warm saline bottom waters requires a negative freshwater balance.

The factors that are required for the upwelling of nutrient-rich waters that leads to high productivity should be considered carefully because they may be quite site specific. Nutrients are most likely to be available in the convecting high-latitude ocean. However, most oceanic circulation at high latitudes is cyclonic, and, with cyclonic circulation, upwelling occurs in the centers of the gyres, not on the edges. Hence, high-latitude productivity is likely to be concentrated in the open ocean and over deep basins, not on the margins of the continental blocks. Wind-driven upwelling can occur wherever the winds are favorable for inducing offshore Ekman transport and where nutrient-rich waters lie at a depth shallow enough to be upwelled. Between the Subtropical Fronts, highly productive upwelling occurs mostly on the eastern margins of the ocean basins between 5 and 35° latitude, but is concentrated at specific sites. Such specific sites are determined by bathymetry, currents, and orography of the adjacent land.

In order to take all of these factors into account and to evaluate the source rock potential of an area, it is

necessary to know the paleolatitude of the area at the time the source rock was formed, the orientation of the coastline at that time, the general configuration of the ocean basins and nature of their interconnections, the paleobathymetry of the region being examined, and to be able to make reasonable guesses about the wind directions, wind speeds, and the oceanic circulation.

ACKNOWLEDGMENTS

This work began while the author was an Alexander von Humboldt Senior Research Scientist at GEOMAR, Christian-Albrechts-University in Kiel, Germany. It continued while he was Visiting Professor at the Institute für Ostseeforschung in Warnemünde, Germany. It was completed while he was F.C. Donders Visiting Professor in the Institute of Earth Sciences, University of Utrecht, The Netherlands. I am grateful to colleagues at all of these institutions and at the University of Colorado for stimulating discussions leading to the development of ideas presented herein.

REFERENCES CITED

- Apel, J.R., 1987, Principles of ocean physics: London, Academic Press, 634 p.
- Archer, D., M. Lyle, K. Rogers, and P. Froelich, 1993, What controls opal preservation in tropical deep-sea sediments?: *Paleoceanography*, v. 8, p. 7–22.
- Arthur, M.A., and J.H. Natland, 1979, Carbonaceous sediments in the North and South Atlantic: the role of salinity in stable stratification of Early Cretaceous basins, *in* M. Talwani, W. Hay, and W.B.F. Ryan, eds., *Deep Drilling Results in the Atlantic Ocean: Continental Margins and Paleoenvironment: American Geophysical Union, Maurice Ewing Series*, v. 3, p. 375–401.
- Arthur, M.A., and S.O. Schlanger, 1979, Cretaceous “ocean anoxic events” as causal factors in development of reef-reservoired giant oil fields: *American Association of Petroleum Geologists Bulletin*, v. 63, p. 870–885.
- Arthur, M.A., W.E. Dean, and D.A.V. Stow, 1984, Models for the deposition of Mesozoic–Cenozoic fine grained organic-carbon-rich sediment in the deep sea, *in* D.A.V. Stow and D. Piper, eds., *Fine-grained Sediments: Processes and Products: Geological Society (London) Special Publication 15*, p. 527–566.
- Arthur, M.A., W.E. Dean, and S.O. Schlanger, 1985, Variations in the global carbon cycle during the Cretaceous related to climate, volcanism and changes in atmospheric CO_2 , *in* E.T. Sundquist and W.S. Broecker, eds., *The Carbon Cycle and Atmospheric CO_2 : Natural Variations, Archaean to Present: American Geophysical Union, Geophysical Monograph 32*, p. 504–529.
- Bang, N.D., 1971, The southern Benguela Current region in February 1966: part II: bathythermography and air-sea interactions: *Deep-Sea Research*, v. 18, p. 209–224.
- Barron, E.J., 1985, Numerical climate modeling, a frontier in petroleum source rock prediction: results

- based on Cretaceous simulations: American Association of Petroleum Geologists Bulletin, v. 69, p. 448–459.
- Barron, J.A., and J. Baldauf, 1989, Tertiary cooling steps and paleoproductivity as reflected by diatoms and biosiliceous sediments, *in* W.H. Berger, V.S. Smetacek, and G. Wefer, eds., Productivity of the Ocean: Present and Past: Chichester, John Wiley, p. 341–354.
- Barton, E.D., M.L. Argote, J. Brown, P.M. Kosro, M. Lavin, J.M. Robles, R.L. Smith, A. Trasviña, and H.S. Velez, 1993, Supersquirt: dynamics of the Gulf of Tehuantepec, Mexico: *Oceanography*, v. 6, p. 23–30.
- Berger, W.H., 1989, Global maps of ocean productivity, *in* W.H. Berger, V.S. Smetacek, and G. Wefer, eds., Productivity of the Ocean: Past and Present: Chichester, John Wiley, p. 429–455.
- Berger, W.H., and G. Wefer, 1990, Export production: seasonality and intermittency, and paleo-oceanographic implications: *Global and Planetary Change*, v. 3, p. 245–254.
- Berger, W.H., V.S. Smetacek, and G. Wefer, 1989, Ocean productivity and paleoproductivity—an overview, *in* W.H. Berger, V.S. Smetacek, and G. Wefer, eds., Productivity of the Ocean: Past and Present: Chichester, John Wiley, p. 1–34.
- Berger, W.H., J.C. Herguera, C.B. Lange, and R. Schneider, 1994, Paleoproductivity: flux proxies versus nutrient proxies and other problems concerning the Quaternary productivity record, *in* R. Zahn, T.F. Pedersen, M.A. Kaminski, and L. Labeyrie, eds., Carbon Cycling in the Glacial Ocean: Constraints on the Ocean's Role in Global Change: NATO ASI Series, v. 117, p. 385–412.
- Berner, R.A., 1982, Burial organic carbon and pyrite sulfur in the modern ocean: its geochemical and environmental significance: *American Journal of Science*, v. 282, p. 451–473.
- Berner, R.A., 1989, Biogeochemical cycles of carbon and sulfur and their effect on atmospheric oxygen over Phanerozoic time: *Palaeogeography, Palaeoclimatology, Palaeoecology (Global and Planetary Change Section)*, v. 75, p. 97–122.
- Berner, R.A., and J.-L. Rao, 1994, Phosphorus in sediments of the Amazon River and its estuary: implications for the global flux of phosphorus to the sea: *Geochimica et Cosmochimica Acta*, v. 58, p. 2333–2339.
- Bogorov, V.G., M.E. Vinogradov, V.N. Stepanov, K.V. Moroshkin, and R.P. Bulatov, 1973, Tropical cyclonic macrocirculation systems and their role in the formation of ocean structure (in Russian): *Transactions of the P. P. Shirshov Institute of Oceanology*, v. 95, p. 1–13.
- Boyle, E.A., J.M. Edmond, and E.R. Sholkovitz, 1977, The mechanism of iron removal in estuaries: *Geochimica et Cosmochimica Acta*, v. 41, p. 1313–1324.
- Bralower, T.J., and H.R. Thierstein, 1984, Low productivity and slow deep water circulation in mid-Cretaceous oceans: *Geology*, v. 12, p. 614–618.
- Brass, G.W., E. Saltzman, J.L. Sloan, II, J.R. Southam, W.W. Hay, W.T. Holser, and W.H. Peterson, 1982a, Ocean circulation, plate tectonics and climate, *in* W.H. Berger and J.C. Crowell, eds., *Climate in Earth History*: Washington, D.C., National Academy Press, p. 83–89.
- Brass, G.W., J.R. Southam, and W.H. Peterson, 1982b, Warm saline bottom water in the ancient ocean: *Nature*, v. 296, p. 620–623.
- Brennecke, W., 1921, Die ozeanographischen Arbeiten der deutschen Antarktischen Expedition 1911–12: *Archiv der Deutschen Seewarte*, v. 39, p. 1–214.
- Brock, J.C., C.R. McClain, D.M. Anderson, W.L. Prell, and W.W. Hay, 1992, Southwest monsoon circulation and environments of recent planktonic foraminifera in the northwestern Arabian Sea: *Paleoceanography*, v. 7, p. 799–813.
- Broecker, W.S., 1969, Why the deep sea remains aerobic: *Geological Society of America Abstracts with Programs*, v. 7, p. 20–21.
- Broecker, W.S., and T.-H. Peng, 1982, Tracers in the sea: Palisades, NY, Eldigio Press, 690 p.
- Broecker, W.S., and T. Takahashi, 1980, Hydrography of the Central Atlantic. III. The North Atlantic deep water complex: *Deep-Sea Research*, v. 27, p. 591–613.
- Broecker, W.S., D.M. Peteet, and D. Rind, 1985, Does the ocean-atmosphere system have more than one stable mode of operation?: *Nature*, v. 315, p. 21–26.
- Brongersma-Sanders, M., 1948, The importance of upwelling water to vertebrate paleontology and oil geology: *Verhandlingen Koninklijke Nederlandse Akademie van Wetenschappen (Afdeeling Natuurkunde, 2 Sect.)*, v. 45 (4), p. 1–112.
- Brongersma-Sanders, M., 1957, Mass mortality in the sea, *in* J.W. Hedgpeth, *Treatise on Marine Ecology and Paleoecology*, V. 1, Ecology: Geological Society of America Memoir 67, p. 941–1010.
- Brown, J., A. Colling, D. Park, J. Phillips, D. Rothery, and J. Wright, 1989, *Ocean Circulation*: Oxford, Open University/Pergamon, 238 p.
- Buckley, J.R., T. Gammelsrød, A. Johannessen, O.M. Johannessen, and L.P. Røed, 1979, Upwelling: oceanic structure at the edge of the Arctic ice pack in winter: *Science*, v. 203, p. 165–167.
- Calvert, S.E., 1983, Geochemistry in Namibian shelf sediments: *in* E. Suess and J. Thiede, eds., *Coastal Upwelling, Its Sedimentary Record. Part A: Responses of the Sedimentary Regime to Present Coastal Upwelling*: NATO Conference Series IV: Marine Sciences, v. 10a, New York, Plenum Press, p. 337–375.
- Calvert, S.E., 1987, Oceanographic controls on the accumulation of organic matter in marine sediments, *in* J. Brooks and A.J. Fleet, eds., *Marine Petroleum Source Rocks*: Geological Society (London) Special Publication 26, p. 137–151.
- Calvert, S.E., 1990, Geochemistry and origin of the Holocene sapropel in the Black Sea, *in* V. Ittekkot, ed., *Facets of Modern Biogeochemistry*: Berlin, Springer-Verlag, p. 327–353.
- Calvert, S.E., R.M. Bustin, and T.F. Pedersen, 1992, Lack of evidence for enhanced preservation of sedimentary organic matter in the oxygen minimum of the Gulf of California: *Geology*, v. 20, p. 757–760.

- Calvert, S.E., R.M. Bustin, and T.F. Pedersen, 1993, Lack of evidence for enhanced preservation of sedimentary organic matter in the oxygen minimum of the Gulf of California: reply: *Geology*, v. 21, p. 571–572.
- Canfield, D.E., 1989, Sulfate reduction and oxic respiration in marine sediments: implications for organic carbon preservation in euxinic environments: *Deep-Sea Research*, v. 36, p. 121–138.
- Canfield, D.E., 1992, Organic matter oxidation in marine sediments, in R. Wollast et al., eds., *NATO ASI Series 14: Interactions of C, N, P and S Biogeochemical Cycles and Global Change*: Berlin, Springer-Verlag, p. 333–363.
- Chandler, M.A., D. Rind, and R. Ruedy, 1992, Pangaean climate during the Early Jurassic: GCM simulations and the sedimentary record of paleoclimate: *Geological Society of America Bulletin*, v. 104, p. 543–559.
- Cloos, H., H. Narain, and S.C. Garde, 1974, Continental margins of India, in C.A. Burke and C.L. Drake, eds., *The Geology of Continental Margins*: New York, Springer-Verlag, p. 629–639.
- Cobban, W.A., and J.B. Reeside, Jr., 1952, Correlation of the Cretaceous formations of the western interior of the United States: *Geological Society of America Bulletin*, v. 63, p. 1011–1044.
- Coffin, M.F., and O. Eldholm, 1993, Scratching the surface: estimating dimensions of large igneous provinces: *Geology*, v. 21, p. 515–518.
- De Angelis, M., N.I. Burkov, and V.N. Petrov, 1987, Aerosol concentrations over the last climatic cycle (60 kyr) from an Antarctic ice core: *Nature*, v. 325, p. 318–321.
- de Boer, P.L., 1986, Changes in the organic carbon buried during the Early Cretaceous, in C.P. Summerhayes and N.J. Shackleton, eds., *North Atlantic Paleooceanography*: Geological Society of London Special Publication 21, p. 321–331.
- Defant, A., 1961, *Physical oceanography*: New York, Pergamon Press, v. 1.
- de Graciansky, P.C., G. Deroo, J.P. Herbin, T. Jacquin, F. Magniez, L. Montadert, C. Müller, C. Ponsot, A. Schaaf, and J. Sigal, 1986, Ocean-wide stagnation episodes in the Late Cretaceous: *Geologische Rundschau*, v. 75, p. 17–41.
- de Jesus Conceicao, J.C., P.V. Zalan, and S. Wolff, 1988, Mechanismo, evolucao e cronologia do rift Sul-Atlantico: *Boletim Geociencias Petrobras*, v. 2, p. 255–265.
- Demaison, G., 1991, Anoxia vs. productivity: what controls the formation of organic carbon-rich sediments and sedimentary rocks: discussion: *American Association of Petroleum Geologists Bulletin*, v. 75, p. 499.
- Demaison, G.J., and G.T. Moore, 1980a, Anoxic environments and source bed genesis: *American Association of Petroleum Geologists Bulletin*, v. 64, p. 1179–1209.
- Demaison, G.J., and G.T. Moore, 1980b, Anoxic environments and oil source bed genesis: *Organic Geochemistry*, v. 2, p. 9–31.
- Diester-Haass, L., 1978, Sediments as indicators of upwelling, in R. Boje and M. Tomczak, eds., *Upwelling Ecosystems*: Berlin, Springer-Verlag, p. 261–281.
- Dietrich, G., 1937, Die “dynamische” Bezugsfläche, eine Gegenwartsproblem der dynamischen Ozeanographie: *Annalen der Hydrographie und maritimen Meteorologie*, v. 65, p. 506–519.
- Dietrich, G., 1957, Ozeanographische Probleme der deutschen Forschungsfahrten im Internationalen Geophysikalischen Jahr 1957/58: *Deutsche Hydrographische Zeitschrift*, v. 10, p. 39–61.
- Dow, W. G., 1978, Petroleum source beds on continental slopes and rises: *American Association of Petroleum Geologists Bulletin*, v. 62, p. 1584–1606.
- Dymond, J., E. Suess, and M. Lyle, 1992, Barium in deep-sea sediment: a geochemical proxy for paleo-productivity: *Paleoceanography*, v. 7, p. 163–181.
- Edgar, N.T., J.B. Saunders, T.W. Donnelly, N. Schneidermann, F. Maurasse, H.M. Bolli, W.W. Hay, W.R. Riedel, I. Premoli Silva, R.E. Boyce, and W. Prell, 1973, Site 147, in N.T. Edgar, J.B. Saunders et al., ed., *Initial Reports of the Deep Sea Drilling Project*, 15: Washington, D.C., U.S. Government Printing Office, p. 169–197.
- Eicher, D.L., and S.R. Diner, 1985, Foraminifera as indicators of water mass in the Cretaceous Greenhorn sea, Western Interior, in L.M. Pratt, E.G. Kauffman, and F.B. Zelt, eds., *Fine-grained Deposits and Biofacies of the Cretaceous Western Interior Seaway: Evidence of Cyclic Sedimentary Processes*: SEPM Field Trip Guidebook No. 4, 1985 Midyear Meeting, Golden, Colorado, p. 60–71.
- Ekman, V.W., 1905, On the influence of the earth’s rotation on ocean currents: *Arkiv for Matematik, Astronomi och Fysik*, v. 12, p. 1–52.
- Eppley, R.W., and B.J. Peterson, 1979, Particulate organic matter flux and planktonic new production in the deep ocean: *Nature*, v. 282, p. 677–680.
- Ewing, M., J.L. Worzel, A.O. Beall, W.A. Berggren, D. Bukry, C.A. Burk, A.G. Fischer, and E.A. Pessagno, Jr., 1969, Site 5, in M. Ewing, J.L. Worzel et al., eds., *Initial Reports of the Deep Sea Drilling Project*, 1: Washington, D.C., U.S. Government Printing Office, p. 214–242.
- Findlater, J., 1969, A major low level air current near the Indian Ocean during the northern summer: *Quarterly Journal of the Royal Meteorological Society*, v. 95, p. 362–380.
- Fischer, A.G., and M.A. Arthur, 1977, Secular variations in the pelagic realm: *Society of Economic Paleontologists and Mineralogists Special Publication* 25, p. 19–50.
- Fisher, C.G., 1991, Calcareous nannofossil and foraminifera definition of an oceanic front in the Greenhorn Sea (late middle through late Cenomanian), northern Black Hills, Montana and Wyoming: paleoceanographic implications: Ph.D. Thesis, University of Colorado—Boulder, 324 p.
- Fisher, C.G., E.G. Kauffman, and L. Van Holdt Wilhelm, 1985, The Niobrara transgressive hemicycle in central and eastern Colorado: the anatomy of a multiple disconformity, in L.M. Pratt, E.G. Kauffman, and F.B. Zelt, eds., *Fine-grained*

- Deposits and Biofacies of the Cretaceous Western Interior Seaway: Evidence of Cyclic Sedimentary Processes: SEPM Field Trip Guidebook No. 4, 1985 Midyear Meeting, Golden, Colorado, p. 184–198.
- Fleet, A.J., and J. Brooks, 1987, Introduction, in J. Brooks and A.J. Fleet, eds., *Marine Petroleum Source Rocks*: Geological Society (London) Special Publication 26, p. 1–14.
- Flohn, H., 1983, Actual palaeoclimatic problems from a climatologist's viewpoint, in A. Ghazi, ed., *Paleoclimatic Research and Models*: Dordrecht, D. Reidel, p. 17–33.
- Frakes, L.A., J.E. Francis, and J.I. Syktus, 1992, *Climate modes of the Phanerozoic*: Cambridge, Cambridge University Press, 274 p.
- Fuglister, F.C., 1960, Atlantic Ocean Atlas, temperature and salinity profiles and data from the International Geophysical Year of 1957–1958: Woods Hole, Woods Hole Oceanographic Institution, p. 1–209.
- Gordon, A.L., and K.T. Bosley, 1992, Cyclonic gyre in the tropical South Atlantic: *Deep-Sea Research*, v. 38 (suppl. 1), p. S323–S343.
- Gordon, A.L., and H.W. Taylor, 1975, Heat and salt balance within the cold waters of the world ocean, in *Numerical Models of Ocean Circulation*: National Academy of Sciences, p. 54–56.
- Gorshkov, S.G., 1977, *Atlas Okeanov*, v. 2: Atlanticheskii i Indijskiy Okean'i: Leningrad, Ministerstvo Oborony SSSR, Voenno-Morskoe Flot, 306 + 27 p.
- Grasshoff, K., 1974, *Chemische Verhältnisse in ihre Veränderlichkeit*, in L. Magaard and G. Reinheimer, eds., *Meereskunde der Ostsee*: Berlin, Springer-Verlag, p. 85–101.
- Grasshoff, K., 1976, The hydrochemistry of landlocked basins and fjords, in J. P. Riley and G. Skirrow, eds., *Chemical Oceanography*: London, Academic Press, v. 2, p. 456–597.
- Hakkinen, S., 1987, A coupled dynamic-thermodynamic model of an ice-ocean system in the marginal ice zone: *Journal of Geophysical Research*, v. 92, p. 9469–9478.
- Hastenrath, S., and P. Lamb, 1977, *Climatic atlas of the tropical Atlantic and eastern Pacific oceans*: Madison, University of Wisconsin Press.
- Hattin, D.E., 1975, Stratigraphy and depositional environment of Greenhorn Limestone (Upper Cretaceous), Kansas: *Kansas Geological Survey Bulletin*, v. 209, p. 128.
- Hay, W.W., 1989, Marginal seas as source of an oceanic oxygen minimum and origin of organic carbon-rich deposits: *American Association of Petroleum Geologists Bulletin*, v. 100, p. 1934–1956.
- Hay, W.W., 1993a, The role of polar deep water formation in global climate change: *Annual Review of Earth & Planetary Sciences*, v. 21, p. 227–254.
- Hay, W.W., 1993b, Pliocene–Quaternary upwelling in the southeastern Atlantic may reflect changes in water mass production: *Ciências da Terra (UNL)* 1993, p. 191–201.
- Hay, W.W., and J.C. Brock, 1992, Temporal variation in intensity of upwelling off southwest Africa, in C.P. Summerhayes, W.L. Prell, and K.C. Emeis, eds., *Upwelling Systems: Evolution Since the Early Miocene*: Geological Society Special Publication 63, p. 463–497.
- Hay, W.W., and J.R. Southam, 1977, Modulation of marine sedimentation by the continental shelves, in N.A. Anderson and A. Malahoff, eds., *The Fate of Fossil Fuel CO₂ in the Oceans*: Marine Science Series, v. 6, p. 569–604.
- Hay, W.W., and C.N. Wold, 1990, Relation of selected mineral deposits to the mass/age distribution of Phanerozoic sediments: *Geologische Rundschau*, v. 79, p. 495–512.
- Hay, W.W., D.L. Eicher, and R. Diner, 1993, Physical oceanography and water masses in the Cretaceous Western Interior Seaway, in W.E.G. Caldwell and E.G. Kauffman, eds., *Geological Association of Canada Special Paper 39*, p. 297–318.
- Heath, G.R., T.C. Moore, and J.P. Dauphin, 1977, Organic carbon in deep-sea sediments, in N.R. Anderson and A. Malahoff, eds., *The Fate of Fossil Fuel CO₂ in the Oceans*: New York, Plenum Press, p. 605–626.
- Herbin, J.-P., and G. Deroo, 1982, Sedimentologie de la matière organique dans les formations du Mésozoïque de l'Atlantique Nord: *Bulletin de la Société Géologique de France*, v. 24, p. 497–510.
- Herguera, J.C., 1992, Deep-sea benthic foraminifera and biogenic opal; glacial to postglacial productivity changes in the western Equatorial Pacific: *Marine Micropaleontology*, v. 19, p. 79–98.
- Herguera, J.C., and W.H. Berger, 1991, Paleoproductivity from benthic foraminifera abundance: glacial to postglacial change in the west-equatorial Pacific: *Geology*, v. 19, p. 1173–1176.
- Hofmann, E., A.J. Busalacchi, and J.J. O'Brien, 1981, Wind generation of the Costa Rica Dome: *Science*, v. 214, p. 552–554.
- Holland, H.D., 1984, *The chemical evolution of the atmosphere and oceans*: Princeton University Press, xii + 582 p.
- Holser, W.T., M. Schidlowski, F.T. Mackenzie, and J.B. Maynard, 1988, Geochemical cycles of carbon and sulfur, in C.B. Gregor, F.T. Mackenzie, R.M. Garrels, and J.B. Maynard, eds., *Chemical Cycles in the Evolution of the Earth*: New York, Wiley-Interscience, p. 105–173.
- Hsueh, Y., and J.J. O'Brien, 1971, Steady coastal upwelling induced by an alongshore current: *Journal of Physical Oceanography*, v. 1, p. 180–186.
- Ibach, L.E.J., 1982, Relationship between sedimentation rate and total organic carbon content in ancient marine sediments: *American Association of Petroleum Geologists Bulletin*, v. 66, p. 170–188.
- Ingall, E.D., R.M. Bustin, and P. van Cappellen, 1993, Influence of water column anoxia on the burial and preservation of carbon and phosphorus in marine shales: *Geochimica et Cosmochimica Acta*, v. 57, p. 303–316.
- Kauffman, E.G., 1984, Paleobiogeography and evolutionary response dynamic in the Cretaceous western interior seaway of North America, in G.E.G. Westermann, ed., *Jurassic–Cretaceous Biochronology and Paleogeography of North America*: Geological Association of Canada Special Paper 27, p. 273–306.

- Keil, R.G., E. Tsamakis, C.B. Fuh, J.C. Giddings, and J.I. Hedges, 1994, Mineralogic and textural controls on the organic composition of coastal marine sediments: hydrodynamic separation using SPLITT-fractionation: *Geochimica et Cosmochimica Acta*, v. 58, p. 879–893.
- Kerr, R.A., 1985, Small eddies are mixing the oceans: *Science*, v. 230, p. 793.
- Killworth, P.D., 1983, Deep convection in the world ocean: *Reviews of Geophysics and Space Physics*, v. 21, p. 1–26.
- Kraus, E.B., W.H. Petersen, and C.G. Rooth, 1978, The thermal evolution of the ocean, *in* International Conference, Evolution of Planetary Atmospheres and Climatology of the Earth: Centre national d'études spatiales (France), p. 201–211.
- Larson, R.L., 1991, Geological consequences of superplumes: *Geology*, v. 19, p. 963–966.
- Lee, C., 1992, Controls on organic carbon preservation: the use of stratified water bodies to compare intrinsic rates of decomposition in oxic and anoxic systems: *Geochimica et Cosmochimica Acta*, v. 56, p. 3323–3335.
- Lee, C., and S.G. Wakeham, 1989, Organic matter in sea water: biogeochemical processes, *in* J.P. Riley, ed., *Chemical Oceanography*, 9 p. 1–51.
- Levitus, S., 1982, Climatological atlas of the world ocean: NOAA Professional Paper 13: Washington, D.C., National Oceanic and Atmospheric Administration, 173 p.
- Luther, M.E., and J.J. O'Brien, 1985, A model of the seasonal circulation in the Arabian Sea forced by observed winds: *Progress in Oceanography*, v. 14, p. 353–385.
- Lutze, G.F., and W.T. Coulbourn, 1984, Recent benthic foraminifera from the continental margin of north-west Africa: community structure and distribution: *Marine Micropaleontology*, v. 8, p. 361–401.
- Magaard, L., and G. Reinheimer, 1974, *Meereskunde der Ostsee*: Berlin, Springer-Verlag, p. 269.
- Maier-Reimer, E., U. Mikolajewicz, and T. Crowley, 1990, Ocean general circulation model sensitivity experiment with an open Central American isthmus: *Paleoceanography*, v. 5, p. 349–366.
- Marchig, V., 1972, Zur Geochemie rezenter Sedimente des indischen Ozeans: *Meteor Forschungs Ergebnisse*, v. 11, p. 1–104.
- Martin, J.H., 1990, Glacial-interglacial CO₂ change: the iron hypothesis: *Paleoceanography*, v. 5, p. 1–13.
- Martin, J.H., and S.E. Fitzwater, 1988, Iron deficiency limits phytoplankton growth in the northeast Pacific subarctic: *Nature*, v. 331, p. 341–343.
- Martin, J.H., R.M. Gordon, and S.E. Fitzwater, 1990, Iron in Antarctic waters: *Nature*, v. 345, p. 156–158.
- Mazeika, P.A., 1967, Thermal domes in the eastern tropical Atlantic Ocean: *Limnology and Oceanography*, v. 12, p. 537–539.
- McCreary, J.P., J. Picaut, and D.W. Moore, 1984, Effect of annual remote forcing in the eastern tropical Atlantic: *Journal of Marine Research*, v. 42, p. 45–81.
- McLean, D.M., 1978, Land floras: the major late Proterozoic atmospheric carbon dioxide/oxygen control: *Science*, v. 200, p. 1060–1062.
- Merewether, E.A., and W.A. Cobban, 1986, Biostratigraphic units and tectonism in the mid-Cretaceous foreland of Wyoming, Colorado, and adjoining areas, *in* J.A. Peterson, ed., *Paleotectonics and Sedimentation in the Rocky Mountain Region, United States*: AAPG Memoir 41, Tulsa, OK, American Association of Petroleum Geologists, p. 443–468.
- Meybeck, M., 1982, Carbon, nitrogen, and phosphorus transport by world rivers: *American Journal of Science*, v. 282, p. 401–450.
- Meyers, P.A., S.C. Brassell, A.Y. Huc, E.J. Barron, R.E. Boyce, W.E. Dean, W.W. Hay, B.H. Keating, C.L. McNulty, M. Nohara, R.E. Schallreuter, J.-C. Sibuet, J.C. Steinmetz, D. Stow, and H. Stradner, 1983, Organic geochemistry of sediments recovered by DSDP/IPOD Leg 75 from under the Benguela Current, *in* J. Thiede and E. Suess, eds., *Coastal Upwelling, Its Sedimentary Record, Part B: Sedimentary Records of Ancient Coastal Upwelling*: NATO Conference Series, Series IV: Marine Sciences, v. 10b, New York, Plenum Press, p. 453–466.
- Mikolajewicz, U., E. Maier-Reimer, T.J. Crowley, and K.-Y. Kim, 1993, Effect of Drake and Panamanian gateways on the circulation of an ocean model: *Paleoceanography*, v. 8, p. 409–426.
- Mix, A.C., 1989, Pleistocene paleoproductivity: evidence from organic carbon and foraminiferal species: *in* W.H. Berger, V.S. Smetacek, and G. Wefer, eds., *Productivity of the Ocean: Past and Present*: Chichester, John Wiley, p. 313–340.
- Moore, G.T., D.N. Hayashida, C.A. Ross, and S.R. Jacobson, 1992a, Paleoclimate of the Kimmeridgian–Tithonian (Late Jurassic) world. I: results using a general circulation model: *Palaeogeography, Palaeoclimatology, Palaeoecology*, v. 93, p. 113–150.
- Moore, G.T., L.C. Sloan, D.N. Hayashida, and N.P. Umrigar, 1992b, Paleoclimate of the Kimmeridgian–Tithonian (Late Jurassic) world. II: sensitivity tests comparing three different topographic settings: *Palaeogeography, Palaeoclimatology, Palaeoecology*, v. 95, p. 229–252.
- Moore, R.C., 1949, The meaning of facies, *in* C.R. Longwell, ed., *Sedimentary Facies in Geologic History*: Geological Society of America Memoir 39, p. 1–39.
- Moroshkin, K.V., V.A. Bubnov, and R.P. Bulatov, 1970, Water circulation in the eastern South Atlantic Ocean: *Oceanology*, v. 10, p. 27–37.
- Morris, R.J., 1987, The formation of organic-rich deposits in two deep-water marine environments, *in* J. Brooks and A.J. Fleet, eds., *Marine Petroleum Source Rocks*: Geological Society (London) Special Publication 26, p. 153–166.
- Müller, P.J., and E. Suess, 1979, Productivity, sedimentation rate, and sedimentary organic matter in the oceans—organic carbon preservation: *Deep-Sea Research*, v. 27A, p. 1347–1362.
- Murray, J.W., ed., 1991, *Black Sea oceanography: results from the 1988 Black Sea Expedition*: *Deep Sea Research*, v. 38, suppl. 2A, p. S655–S1266.
- Nansen, F., 1902, The oceanography of the North Polar Basin: *Norwegian North Polar Expedition 1893–1896, Scientific Results*: Longmans, Green &

- Co., v. 3, n. 9, 427 p.
- Nelson, G., and L. Hutchings, 1983, The Benguela upwelling area: *Progress in Oceanography*, v. 12, p. 333–356.
- Neumann, G., and W.J. Pierson, 1966, *Principles of physical oceanography*: Englewood Cliffs, Prentice-Hall, 545 p.
- Nowlin, W.D., Jr., and J.M. Klinck, 1986, The physics of the Antarctic Circumpolar Current: *Reviews of Geophysics and Space Physics*, v. 24, p. 469–491.
- Oba, T., 1991, Oceanic paleoenvironmental studies in Japan: *Quaternary Research*, v. 30, p. 197–202.
- O'Brien, J.J., 1975, Models of coastal upwelling, *in* *Numerical Models of Ocean Circulation*: Washington, D.C., National Academy Press.
- Oeschger, H., J. Beer, U. Siegenthaler, B. Stauffer, W. Dansgaard, and C. Langway, 1984, Late glacial climate history from ice cores, *in* J.E. Hansen and T. Takahashi, eds., *Climate Processes and Climate Sensitivity*: Geophysical Monograph 29, Maurice Ewing v. 5, Washington, D.C., American Geophysical Union, p. 299–306.
- Olson, D.B., and R.H. Evans, 1986, Rings of the Agulhas Current: *Deep-Sea Research*, v. 33, p. 27–42.
- Parrish, J.T., 1982, Upwelling and petroleum source beds, with reference to Paleozoic: *American Association of Petroleum Geologists Bulletin*, v. 66, p. 750–774.
- Parrish, J.T., and R.L. Curtis, 1982, Atmospheric circulation, upwelling, and organic-rich rocks in the Mesozoic and Cenozoic Eras: *Palaeogeography, Palaeoclimatology, Palaeoecology*, v. 40, p. 31–66.
- Parrish, J.T., and R.A. Spicer, 1988, Middle Cretaceous wood from the Nanushuk Group, central North Slope, Alaska: *Palaeontology*, v. 31, p. 19–34.
- Parsons, T.R., M. Takahashi, and B. Hargrave, 1984, *Biological oceanographic processes*, 3rd ed.: Oxford, Pergamon Press, 330 p.
- Pedersen, T.F., 1983, Increased productivity in the eastern equatorial Pacific during the last glacial maximum (19,000 to 14,000 yr B.P.): *Geology*, v. 11, p. 16–19.
- Pedersen, T.F., and S. Calvert, 1990, Anoxia vs. productivity: what controls the formation of organic-carbon-rich sediments and sedimentary rocks?: *American Association of Petroleum Geologists Bulletin*, v. 74, p. 454–466.
- Pedersen, T.F., and S.E. Calvert, 1991, Anoxia vs. productivity: what controls the formation of organic-carbon-rich sediments and sedimentary rocks?: reply: *American Association of Petroleum Geologists Bulletin*, v. 75, p. 500–501.
- Pedersen, T.F., G.B. Shimmiel, and N.B. Price, 1992, Lack of enhanced preservation of organic matter in sediments under the oxygen minimum on the Oman Margin: *Geochimica et Cosmochimica Acta*, v. 56, p. 545–551.
- Peixoto, J.P., and A.H. Oort, 1992, *Physics of Climate*: New York, American Institute of Physics, 520 p.
- Peterson, R.G., and L. Stramma, 1991, Upper level circulation in the South Atlantic: *Progress in Oceanography*, v. 26, p. 1–73.
- Peterson, W.H., 1979, A steady state thermohaline convection model: Ph.D. Thesis, Miami, Rosenstiel School of Marine and Atmospheric Sciences, University of Miami, 160 p.
- Peterson, W.H., and C. Rooth, 1976, Formation and exchange of deep water in the Greenland and Norwegian seas: *Deep-Sea Research*, v. 23, p. 273–283.
- Petit, J.-R., M. Briat, and A. Royer, 1981, Ice age aerosol content from East Antarctic ice core samples and past wind strength: *Nature*, v. 293, p. 391–394.
- Picaut, J., 1985, Major dynamics affecting the eastern tropical Atlantic and Pacific oceans: *CALCOFI Reports*, v. 36, p. 41–50.
- Pond, S., and G.L. Pickard, 1983, *Introductory dynamical Oceanography*: Oxford, Pergamon Press.
- Pratt, L.M., 1985, Isotopic studies of organic matter and carbonate in rocks of the Greenhorn Marine Cycle, *in* L.M. Pratt, E.G. Kauffman, and F.B. Zelt, eds., *Fine-grained Deposits and Biofacies of the Cretaceous Western Interior Seaway: Evidence of Cyclic Sedimentary Processes*: SEPM Field Trip Guidebook No. 4, 1985 Midyear Meeting, Golden, Colorado, p. 38–48.
- Prell, W.L., and W.B. Curry, 1981, Faunal and isotopic indices of monsoonal upwelling: western Arabian Sea: *Oceanologica Acta*, v. 4, p. 91–98.
- Preller, R., and J.J. O'Brien, 1980, The influence of bottom topography on upwelling off Peru: *Journal of Physical Oceanography*, v. 10, p. 1377–1398.
- Rea, D.K., M. Leinen, and T.R. Janacek, 1985, Geologic approach to the long-term history of atmospheric circulation: *Science*, v. 227, p. 721–725.
- Reid, J.L., 1979, On the contribution of the Mediterranean Sea outflow to the Norwegian-Greenland Sea: *Deep-Sea Research*, v. 26, p. 1199–1223.
- Rhoads, D.C., and J.W. Morse, 1971, Evolutionary and ecologic significance of oxygen-deficient marine basins: *Lethaia*, v. 4, 413–428.
- Richards, F.A., 1965, Anoxic basins and fjords, *in* P. Riley and G. Skirrow, eds., *Chemical oceanography*, v. 1: New York, Academic Press, p. 611–645.
- Richards, F.A., and A.C. Redfield, 1954, A correlation between the oxygen content of sea water and the organic content of marine sediments: *Deep-Sea Research*, v. 1, p. 279–281.
- Richards, F.A., and R.F. Vaccaro, 1956, The Cariaco Trench, an anoxic basin in the Caribbean: *Deep-Sea Research*, v. 3, p. 214–228.
- Rohling, E., 1991, Shoaling of the Eastern Mediterranean pycnocline due to reduction of excess evaporation: implications for sapropel formation: *Paleoceanography*, v. 6, p. 747–753.
- Rohling, E.J., and W.W.C. Gieskes, 1989, Late Quaternary changes in Mediterranean intermediate water density and formation rate: *Paleoceanography*, v. 4, p. 531–545.
- Rohling, E.J., and F.J. Hilgen, 1991, The eastern Mediterranean climate at times of sapropel formation: a review: *Geologie en Mijnbouw*, v. 70, p. 253–264.
- Romankevich, E.A., 1984, *Geochemistry of organic matter in the ocean*: New York, Springer-Verlag, 334 p.
- Ronov, A.B., 1982, The earth's sedimentary shell (quantitative patterns of its structure, compositions,

- and evolution): *International Geology Review*, v. 24, no. 12, p. 1365–1388.
- Ronov, A.B., V.E. Khain, and K.B. Sestlavinsky, 1984, Atlas of lithological-paleogeographical maps of the world: late Precambrian and Paleozoic of the continents: Leningrad, U.S.S.R. Academy of Science Press, 70 p.
- Ronov, A.B., V.E. Khain, and A.N. Balukhovskiy, 1989, Atlas of lithological-paleogeographical maps of the world: Mesozoic and Cenozoic of continents and oceans: Moscow, Editorial Publishing Group, p. 1–79.
- Rooth, C., 1982, Hydrology and ocean circulation: *Progress in Oceanography*, v. 11, p. 131–149.
- Ross, D.A., and E.T. Degens, 1974, Recent sediments of Black Sea, in E.T. Degens and D.A. Ross, eds., *The Black Sea—Geology, Chemistry and Biology: AAPG Memoir 20*, p. 183–199.
- Rossignol-Strick, M., 1985, Mediterranean Quaternary sapropels, an immediate response of the African monsoon to variation of insolation: *Palaeogeography, Palaeoclimatology, Palaeoecology*, v. 49, p. 237–263.
- Rossignol-Strick, M., 1987, Rainy periods and bottom water stagnation initiating brine accumulation and metal concentrations: 1. the Late Quaternary: *Paleoceanography*, v. 2, p. 333–360.
- Ryan, W.B.F., and M.B. Cita, 1977, Ignorance concerning episodes of ocean-wide stagnation: *Marine Geology*, v. 23, p. 197–215.
- Sarmiento, J.L., T.D. Herbert, and J.R. Toggweiler, 1988, Causes of anoxia in the world ocean: *Global Biogeochemical Cycles*, v. 2, p. 115–128.
- Sarnthein, M., and J. Fenner, 1988, Global wind induced change of deep sea sediment budgets, new ocean production and CO₂ reservoirs ca. 3.3–2.35 Ma B.P.: *Philosophical Transactions of the Royal Society of London, B*, v. 318, p. 487–504.
- Sarnthein, M., and K. Winn, 1988, Global variations of surface oceanic productivity in low and mid latitudes: influences on CO₂ reservoirs of the deep ocean atmosphere during the last 21,000 years: *Paleoceanography*, v. 3, p. 361–399.
- Sarnthein, M., K. Winn, and R. Zahn, 1987, Paleoproductivity of oceanic upwelling and the effect on atmospheric CO₂ and climatic change during deglaciation times, in W.H. Berger and L.D. Labeyrie, eds., *Abrupt Climatic Change: Proceedings of the NATO/NSF A.R.W. Symposium at Biviers/Grenoble, 1985*, p. 311–337.
- Sarnthein, M., U. Pflaumann, R. Ross, R. Thiedemann, and K. Winn, 1992, Transfer function to reconstruct ocean paloproductivity: a comparison, in C.P. Summerhayes, W.L. Prell, and K.C. Emies, eds., *Upwelling Systems: Evolutions Since the Early Miocene*: Geological Society of London Special Publication 63, p. 411–437.
- Schlanger, S.O., and H.C. Jenkyns, 1976, Cretaceous anoxic events: causes and consequences: *Geologie en Mijnbouw*, v. 55, p. 179–184.
- Schnitker, D., 1994, Deep-sea benthic foraminifers: food and bottom water masses, in R. Zahn, T.F. Pedersen, M.A. Kaminski, and L. Labeyrie, eds., *Carbon Cycling in the Glacial Ocean: Constraints on the Ocean's Role in Global Change: NATO ASI Series*, v. 117, p. 539–554.
- Schott, G., 1943, *Weltkarte zur Übersicht der Meeresströmungen*: *Annalen der Hydrographie und maritimen Meteorologie*.
- Schulz, 1982, A comparison of the upwelling regions off NW and SW Africa: *Rapports et P. verbaux Réunion Conseil internationale pour l'Exploration du Mer*, v. 180, p. 202–204.
- Shannon, L.V., 1985, South African ocean colour and upwelling experiment: Cape Town, S.A., Sea Fisheries Research Institute.
- Sharp, J.V.A., 1963, Unconformities within basal marine Cretaceous rocks of the Piceance Basin, Colorado: Ph.D. Thesis, University of Colorado, 170 p.
- Shimmield, G.B., N.B. Price, and T.F. Pedersen, 1990, The influence of hydrography, bathymetry and productivity on sediment type and composition of the Oman Margin and in the northwest Arabian Sea, in A.H.F. Robertson, M.P. Searle, and A.C. Ries, eds., *The Geology and Tectonics of the Oman Region: Geological Society (London) Special Publication 49*, p. 754–769.
- Shimmield, G., S. Derrick, A. Mackensen, H. Grobe, and C. Pudsey, 1994, The history of barium, biogenic silica and organic carbon accumulation in the Weddell Sea and Antarctic Ocean over the last 150,000 years, in R. Zahn, T.F. Pedersen, M.A. Kaminski, and L. Labeyrie, eds., *Carbon Cycling in the Glacial Ocean: Constraints on the Ocean's Role in Global Change: NATO ASI Series*, v. 117, p. 555–574.
- Sibuet, J.-C., W.W. Hay, A. Prunier, L. Montadert, K. Hinz, and J. Fritsch, 1984, Early evolution of the South Atlantic Ocean: role of the rifting episode: Initial Results of the Deep Sea Drilling Project, Washington, D.C., U.S. Government Printing Office, v. 75, p. 469–481.
- Sirocko, F., and M. Sarnthein, 1989, Wind-borne deposits in the northwestern Indian Ocean, record of Holocene sediments versus modern satellite data, in M. Leinen and M. Sarnthein, eds., *Paleoclimatology and Paleometeorology, Modern and Past Patterns of Global Atmospheric Transport: NATO ASI Series*, v. 282, p. 401–433.
- Smith, R.L., 1983, Circulation patterns in upwelling regimes, in E. Suess and J. Thiede, eds., *Coastal Upwelling, Its Sedimentary Record. Part A: Responses of the Sedimentary Regime to Present Coastal Upwelling: NATO Conference Series IV: Marine Sciences*, v. 10a, New York, Plenum Press, p. 13–35.
- Southam, J.R., and W.W. Hay, 1981, Global sedimentary mass balance and sea level changes, in C. Emiliani, ed., *The Sea*, v. 7: *The Oceanic Lithosphere*: New York, Wiley-Interscience, p. 1617–1684.
- Southam, J.R., W.H. Peterson, and G.W. Brass, 1982, Dynamics of anoxia: *Palaeogeography, Palaeoclimatology, Palaeoecology*, v. 40, p. 183–198.
- Stein, R., 1986, Organic carbon and sedimentation rate—further evidence for anoxic deep-water conditions in the Cenomanian/Turonian Atlantic Ocean: *Marine Geology*, v. 72, p. 199–209.

- Stommel, H., 1962, On the smallness of sinking regions in the ocean: Proceedings of the National Academy of Sciences, v. 48, p. 766–772.
- Suess, E., 1980, Particulate organic carbon flux in the oceans—surface productivity and oxygen utilization: *Nature*, v. 288, p. 260–263.
- Summerhayes, C.P., 1987, Organic-rich sediments from the North Atlantic, in J. Brooks and A.J. Fleet, eds., *Marine Petroleum Source Rocks: Geological Society (London) Special Publication 26*, p. 301–316.
- Sundquist, E.T., 1985, Geological Perspectives on carbon dioxide and the carbon cycle, in E.T. Sundquist and W.S. Broecker, eds., *The Carbon Cycle and Atmospheric CO₂: Natural Variations, Archaean to Present: American Geophysical Union, Geophysical Monograph 32*, p. 5–59.
- Sverdrup, H., 1938a, On the process of upwelling: *Journal of Marine Research*, v. 1, p. 155–164.
- Sverdrup, H.U., 1938b, On the explanation of the oxygen minima and maxima in the oceans: *Conseil Permanente Internationale pour l'Exploration de la Mer, Journal du Conseil*, v. 13, p. 163–172.
- Tchernia, P., 1980, *Descriptive regional oceanography*: Oxford, Pergamon Press, 253 p.
- Thiede, J., and Tj.H. van Andel, 1977, The paleoenvironment of anaerobic sediments of the late Mesozoic South Atlantic Ocean: *Earth and Planetary Science Letters*, v. 33, p. 301–309.
- Thierstein, H.R., 1989, Inventory of paleoproductivity records: The Mid-Cretaceous enigma: in W.H. Berger, V.S. Smetacek, and G. Wefer, eds., *Productivity of the Ocean: Past and Present*: Chichester, John Wiley, p. 355–375.
- Thorade, H., 1909, Über die Kalifornische Meereströmung: *Annalen der Hydrographie und maritimen Meteorologie*, v. 37, p. 17–34, 63–76.
- Tissot, B., 1979, Effects on prolific petroleum source rocks and major coal deposits caused by sea level changes: *Nature*, v. 277, p. 463–465.
- Tissot, B., and D. Welte, 1978, *Petroleum formation and occurrence*: Heidelberg, Springer-Verlag, 538 p.
- Tissot, B., G. Deroo, and J.-P. Herbin, 1979, Organic matter in Cretaceous sediments of the North Atlantic: contribution to sedimentology and paleogeography, in M. Talwani, W. Hay, and W.B.F. Ryan, eds., *Deep Drilling Results in the Atlantic Ocean: Continental Margins and Paleoenvironment*: Washington, D.C., American Geophysical Union, Maurice Ewing Series v. 3, p. 362–374.
- Tolmazin, D., 1985, *Elements of dynamic oceanography*: Boston, Allen & Unwin, 181 p.
- Trask, P.D., 1939, Organic content of recent marine sediments, in P.D. Trask, ed., *Recent Marine Sediments: A Symposium*: London, Thomas Murby and Co., p. 428–453.
- Udintsev, G.B., ed., 1990, *International Geological-Geophysical Atlas of the Atlantic Ocean: IOC (of UNESCO), Ministry of Geology USSR Academy of Sciences USSR, GUGK USSR*, 158 p.
- van Bennekom, A. J., and G. W. Berger, 1984, Hydrography and silica budget of the Angola Basin: *Netherlands Journal of Sea Research*, v. 17, p. 149–200.
- van Cappelen, P., and D.E. Canfield, 1993, Lack of evidence for enhanced preservation of sedimentary organic matter in the oxygen minimum of the Gulf of California: comment: *Geology*, v. 21, p. 570–571.
- Voiturez, B., 1981, Les sous-courants équatoriaux nord et sud et la formation des dômes thermiques tropicaux: *Oceanologica Acta*, v. 4, p. 497–506.
- von Stackelberg, U.V., 1972, Faziesverteilung in Seditimenten des indisch-pakistanischen Kontinentalrandes: *Meteor Forschungs Ergebnisse*, C, v. 9, p. 1–73.
- Wefer, G., 1991, Stofftransport zum Meeresboden: Eine Übersicht: *Naturwissenschaften*, v. 78, p. 1–6.
- Wefer, G., and W.H. Berger, 1991, Isotope paleontology: growth and composition of extant calcareous species: *Marine Geology*, v. 100, p. 207–248.
- Wells, N., 1986, *The atmosphere and ocean*: London, Taylor & Francis, 347 p.
- Wilson, K.M., D. Pollard, W.W. Hay, S.L. Thompson, and C.N. Wold, 1994, General circulation model simulations of Triassic climates: preliminary results, in G.D. Klein, ed., *Pangaea: Paleoclimatology, Tectonics and Sedimentation During Accretion, Zenith and Breakup of a Supercontinent*: Geological Society of America Special Paper 288, p. 91–116.
- Wyrтки, K., 1962, The oxygen minimum in relation to ocean circulation: *Deep-Sea Research*, v. 9, p. 11–23.
- Wyrтки, K., 1964, Upwelling in the Costa Rica Dome: *Fishery Bulletin*, v. 63 (2), p. 355–372.

Factors Controlling the Development of Lacustrine Petroleum Source Rocks— An Update

Barry Jay Katz
Texaco Inc.
Houston, Texas, U.S.A.

ABSTRACT

Globally, marine petroleum source rocks dominate; however, lacustrine source rocks are of regional importance. These lacustrine rocks share many common geochemical attributes with their marine counterparts, but typically produce oils which differ both chemically and physically. Their distribution in time and space has been of growing importance as exploration has shifted from known marine provinces. There are three main factors which control the distribution of these economically important rocks: (1) those factors controlling lake development and its chemistry, (2) the level of primary productivity, and (3) the efficiency of organic preservation.

Large lakes capable of producing sufficient volumes of sediment to result in economic hydrocarbon accumulations form as a result of tectonic processes in both extensional and compressional regimes. Maximum potential for source rock development is coincident with maximum subsidence rates when associated with minimum sedimentation rates. Variations in subsidence rate within and across basins is a partial explanation for facies variations within these basins.

Productivity within lake basins is largely controlled by nutrient recycling within a mature lake system. High levels of productivity may also be maintained when the drainage basin contains streams with a high chemical load, in particular phosphate. In basins with a high width/depth ratio, the level of productivity appears to be the driving force with respect to source rock development.

Preservation efficiencies are controlled by biologic and abiologic processes. In general, organic preservation is favored when the lake is stratified and anoxia develops. Such conditions are favored at low latitudes and when salinity contrasts occur. Preservation efficiency appears to be a primary driving mechanism in lakes with a low width/depth ratio.

The integration of these component factors results in a predictive qualitative model. The application of this model is then presented for western Indonesia to explain the observed distribution of lacustrine source rocks within the region, as well as the local variability of the source.

INTRODUCTION

Commercial hydrocarbon accumulations require the presence of a source, reservoir, seal, and trap. These elements must also display the correct spatial and temporal relationships. Historically, in petroleum exploration there has been an emphasis on the identification of traps and the characterization of reservoir facies. Petroleum source rocks were largely considered ubiquitous, represented by basinal marine and deltaic shales. Exploration results, however, in many frontier basins have been disappointing. Although suitable traps and reservoirs were identified, these basins lacked commercial hydrocarbons. Postmortem analyses of these exploration opportunities suggested that lack of a hydrocarbon charge or the absence of an effective hydrocarbon source was often the reason for the lack of oil and gas.

Statistical studies have shown that hydrocarbon source rocks contain above-average quantities of organic carbon with a minimum source rock threshold between 1.0 and 1.4 wt.% (Ronov, 1958; Bissada, 1982). And, more important, when not displaying advanced levels of thermal maturity, source rocks yield upon pyrolysis above-average quantities of hydrocarbons (HC) (free + generatable hydrocarbons >2.5 mg HC/g rock; Bissada, 1982), with rocks considered as good or excellent source rocks having yields in excess of 6 mg HC/g rock (Peters, 1986). The kerogens contained within the oil-prone source rocks are hydrogen enriched. This is commonly manifested by atomic H/C ratios greater than 1.15 and hydrogen index values greater than 400 mg HC/g TOC (Jones, 1987).

Such rocks have been found in numerous depositional settings including flooded continental shelves and epicontinental seas, within regions associated with active upwelling, in regions where an oxygen depleted zone impinges on the sea floor, and within isolated marine and lacustrine basins (Demaison and Moore, 1980; Meissner et al., 1984). The conditions associated with the formation of lacustrine source rocks are the focus of this paper.

Lacustrine-derived oils typically differ from their marine counterparts both chemically and physically. Unaltered lacustrine oils display higher pour points than their marine counterparts as a consequence of their generally higher wax content (i.e., greater concentrations of nC_{22+} components; Tissot and Welte, 1984). These oils also display higher concentrations of nickel when compared with vanadium than marine oils (Lewan, 1984). Lacustrine oils also exhibit differences in their biomarker compositions (Mello et al., 1988). These differences include higher pristane/phytane and hopane/sterane ratios, as well as the presence in some oils of organism-specific compounds such as botryococcane (Moldowan and Seifert, 1980). This should not be interpreted that all lacustrine oils display geochemical similarity (Fu Jiamo et al., 1990). Many of the geochemical attributes of these oils are dependent on the salinity of the lake waters (Mello et al., 1988; Mello and Maxwell, 1990).

Although an inventory of global petroleum reserves suggests that lacustrine source rocks are not a primary

contributor to the reserve base, regionally, they may dominate. For example, over 80% of the petroleum reserves of Brazil (Mello et al., 1991), China (Halbouty, 1980), and Indonesia (Katz and Kahle, 1988) can be attributed to lacustrine source rocks, while approximately half of the petroleum reserves of India appear to be lacustrine derived (Saikia and Dutta, 1980). Lacustrine source rocks may also display considerable hydrocarbon potential in the form of oil shales. Estimates of conventional and unconventional hydrocarbons associated with the Green River Shale of the western United States range upward to 1.5×10^{13} barrels of oil equivalent (National Petroleum Council, 1973). Therefore, there appears to be a clear need to understand their development and associated controlling factors.

This paper serves as an update to an earlier examination of factors controlling lacustrine source rock development (Katz, 1990). Specifically, this paper will re-examine those factors which control the quality and distribution of lacustrine source rocks: (1) the distribution of large, long-lived lacustrine sequences in time and space, (2) lacustrine primary productivity, and (3) organic preservation within lake settings. There will also be an attempt to integrate the individual controlling factors into a preliminary source rock model and an attempt to apply this model to the Tertiary of western Indonesia.

LAKE DISTRIBUTION AND SIZE

An examination of the geologic record suggests that lake sequences play only a minor role in the preserved stratigraphic column. Their relative importance decreases with increasing age (Feth, 1964; Figure 1). This is a consequence of the problems associated with their identification (Picard and High, 1981) as well as their lack of preservation. Only areally extensive, long-lived lakes have the potential to be incorporated into the stratigraphic record and, therefore, to possibly include source rock quality material.

The Collecting Basin

The presence of a lake requires a depression, sediment-starved conditions, and the availability of water. It has been suggested by Hutchinson (1957) that there are 11 basic mechanisms which may lead to the formation of a lake. An examination of the world's 25 largest lakes suggests that tectonic and glacial lakes are most likely to be preserved in the stratigraphic record and to contain volumetrically significant quantities of sediments. A further examination of these large lake bodies reveals that large glacial lakes are restricted to the higher latitudes ($>40^\circ$), whereas tectonic lakes range from the equatorial region to the subpolar zone. The importance of latitudinal position on source rock development will be discussed in the sections dealing with both lacustrine productivity and organic matter preservation.

Tectonic lakes may form either in extensional or compressional tectonic regimes. In general, lakes which form in an extensional setting display lower width/depth

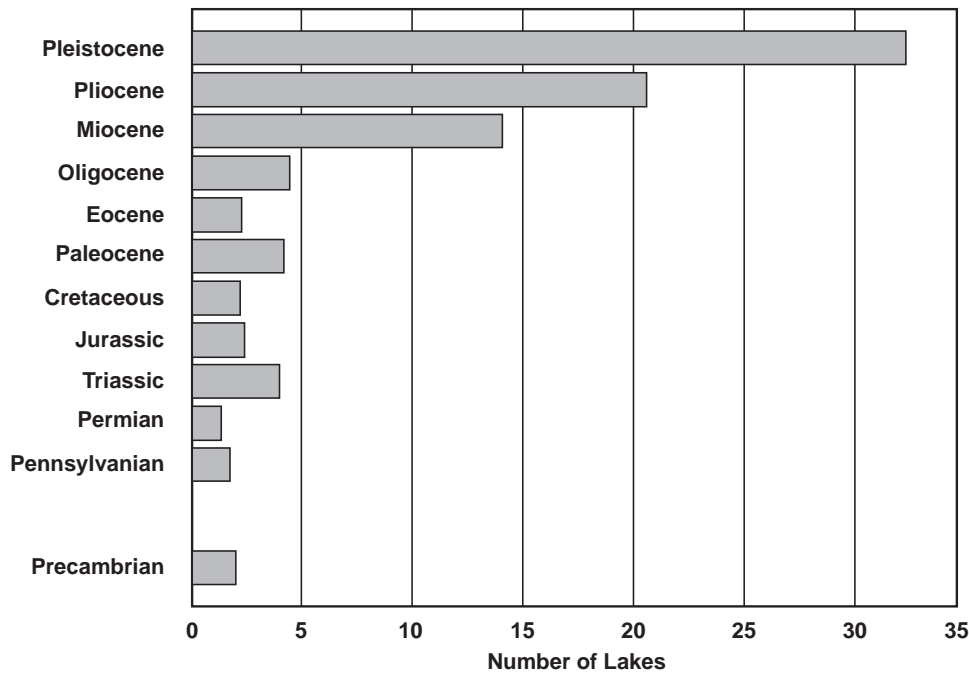


Figure 1. Number of lacustrine deposits in the western United States as a function of age (after Feth, 1964).

ratios (commonly <50) than those formed in compressional settings, where width/depth ratios typically exceed 100 and may exceed 2000. As will be discussed later, this ratio is a major factor in determining organic preservation potential and plays an important role in controlling nutrient availability by influencing the wind's ability to mix the lake water column.

These general characterizations are, in turn, overprinted by both temporal and spatial variations due to differences in the relative and absolute subsidence rates. For example, within a rift sequence, three stages of development appear to be common (Watson et al., 1987; Lambiase, 1990). The initial phase is characterized by a number of small faults, typically displaced across a broad area, leading to minor subsidence. This phase of basin development is dominated by fluvial sedimentation. If lakes are present during this period they tend to be broad and shallow. With the development of a major boundary fault system, there is an increase in the subsidence rate and deep lakes can develop. This phase of development, which is critical to source rock deposition, typically occurs between 5 and 15 m.y. after initial rifting (Watson et al., 1987). As the rate of extension decreases, so does the subsidence rate, and the lake tends to shallow as a result of sedimentary infilling.

Watson et al. (1987) also proposed a parallel evolutionary framework for foreland and flexural basins. The initial phase of development is tied to the initial collision or thrust. This results in the formation of a minor depression, typically dominated by alluvial and/or fluvial sedimentation. As the mountain belt continues to develop and the load increases, the subsidence rate increases and lacustrine sedimentation begins to dominate, with maximum lake development occurring between 20 and 30 m.y. after basin initiation. With the termination of continental collision and

thrusting, the subsidence rate decreases and the basin is filled by prograding fluvial systems.

Within individual basins there are also differences between the subsidence histories of the various sub-basins. For example, an examination of the Central Sumatra basin reveals sharp contrasts in the subsidence histories of the Kiri and Aman subbasins. The subsidence rate in the Kiri subbasin was substantially less than that of the Aman subbasin (Figure 2). As a consequence, the Kiri subbasin contains shallow lacustrine and marsh/bog facies as compared to the Aman subbasin's predominantly deep lacustrine facies (Williams et al., 1985). While within individual half-grabens, the differences in relative subsidence rate result in more lacustrine facies being developed nearer to the border fault, while coaly facies tend to develop nearer the hinge zone.

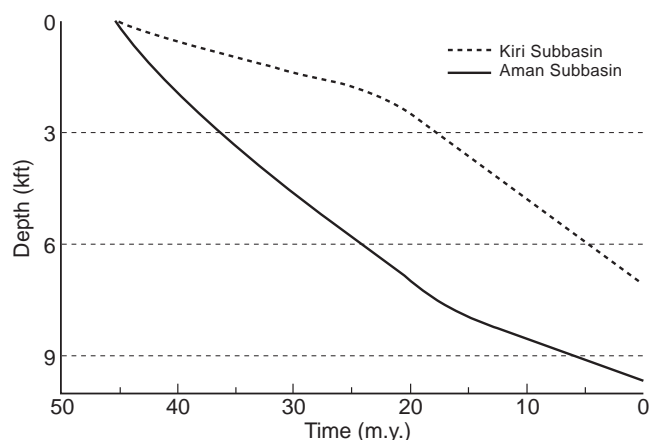


Figure 2. Comparison of subsidence rates in the Kiri and Aman subbasins in central Sumatra.

Subsidence Versus Sedimentation

A comparison of the relative rates of sedimentation and subsidence leads to three distinct depositional scenarios. The first scenario is where sedimentation exceeds subsidence. Under such conditions, the basin undergoes infilling, shallow lakes may be present, but marsh/bog deposits dominate. The second scenario is where sedimentation is equal to subsidence. Under these conditions, alluvial and fluvial deposition tends to dominate. The third scenario is where subsidence exceeds sedimentation. Under such circumstances the greatest likelihood of lacustrine sequence development occurs.

Hydrologic Factors

In addition to the presence of a sediment-starved depression, lake development requires the availability of water. Water may be supplied directly through rainfall, through surface runoff (streams and rivers), or through subsurface springs. Under most circumstances, subsurface spring discharge plays only a minor role in the hydrologic maintenance of a lake (Street and Grove, 1979). Consequently, climate is the primary control on the availability of water. Lakes tend to be better developed in those regions where there is the greatest excess of precipitation relative to evaporation. This currently exists between 15°N and 15°S, with the maximum occurring at about 5°S (Seruya and Pollinger, 1983).

The latitudinal position of this humid belt and its bounding arid regions has not been constant throughout the geologic record. This zone has expanded and contracted and migrated latitudinally, as a result of glacially related changes in atmospheric circulation patterns (Street and Grove, 1979). These changes may occur as a result of long-term factors such as continental configuration and atmospheric CO₂ levels, or with a much higher frequency driven by Milankovitch forcing factors (Olsen, 1990). These high-frequency variations in climatic conditions can, in fact, result in significant changes in lake volume. For example, Finney and Johnson (1991) suggest that between 6000 and 10,000 years ago Lake Malawi was between 100 and 150 m shallower than it currently is. The relative rates of precipitation and evaporation through time can be numerically estimated through the use of climate models (Barron, 1990).

Additional factors which appear to influence the availability of water are the size and location of continents and topographic effects. During the time of a megacontinent (e.g., Permian–Triassic) much of the precipitation would be restricted to the continental margins (Hay et al., 1990). Thus, interior lakes, when present, would commonly be saline. Topographic effects not only control the landward transport of water but may also have a direct impact on microclimate. These variations in microclimate have been used by Hay et al. (1982) to explain the presence of coals, lake deposits, and evaporites within a rift setting in a single latitudinal belt. In this type of situation, the relative humidity of an air mass is largely controlled by its

adiabatic heating and cooling as the air mass interacts with the region's topographic relief. Currently, such a topographic effect can be observed within the Ethiopian rift system. Lakes below 1700 m elevation tend to be limited and, where present, more saline, because the rate of evaporation exceeds that of precipitation. In contrast, freshwater lake bodies develop above 1700 m, where there is an excess or precipitation.

The availability of water (inflow) relative to evaporation permits a hydrologic classification scheme (Olsen, 1990). In those cases where evaporation is greater than the influx of water, shallow lakes and playas develop. These lakes, which are commonly saline, may be either permanent or ephemeral. In either case, they tend to undergo large seasonal changes in lake level. This results in cyclic sedimentation and normally an abundance of sand (e.g., Fundy basin; Olsen, 1990). In many cases, when lakes are present, they owe their existence to groundwater recharge. A second situation exists when influx is greater than evaporation. Such basins do not display desiccation features. Their persistence commonly results in the progradation of deltas into a permanent water body and the development of coal swamps around the lake margins (e.g., Richmond basin; Olsen, 1990). The third basic situation exists where influx and evaporation are in near balance. Such lakes are very sensitive to changes in precipitation, with lake levels undergoing changes of several hundred meters over geologically short periods of time. These lakes tend to be dominated by fine-grained sediments (e.g., Newark basin; Olsen, 1990).

Yet another hydrologic component is whether the lake is open or closed. A hydrologically open lake displays surface outflow, while those that lack a surface outflow are closed. In general, closed lake basins tend to fluctuate in depth, producing transgressive-regressive sequences. In contrast, open lake systems tend to result in more stable shorelines (Gore, 1989).

PRODUCTIVITY

Within lacustrine systems there are three broad classes of primary producers (Likens, 1975)—the phytoplankton which dominate in large deep lakes, the periphyton and macrophytes which tend to dominate in shallow lakes and lake margin areas, and photosynthetic and chemosynthetic bacteria which are associated with specialized ecosystems (such as meromictic lakes). It is this material which ultimately provides the precursors for the oil-prone kerogens upon which this study focuses.

Light and Turbidity

Although the measurement of lacustrine productivity levels is quite difficult, available data indicate a significant range extending over at least three orders of magnitude (Table 1; Likens, 1975). Brylinsky and Mann (1973) concluded that the availability of light was the dominant factor controlling productivity. Light availability is, in part, a function of latitude. The

Table 1. Annual lacustrine productivity levels.

| Water System | Productivity (gC/m ² /yr) |
|-----------------|--------------------------------------|
| Tropical lakes | 30–2500 |
| Temperate lakes | 2–450 |
| Arctic lakes | <1–35 |
| Antarctic lakes | 1–10 |
| Alpine lakes | <1–100 |

After Likens (1975); assumes values averaged over the “growing season” and only naturally occurring (i.e., nonpolluted) systems.

lower annual productivity levels of higher latitudes appear to be a response to the length of the day, the angle of incident radiation, and the shortening of the growing season. The growing season at higher latitudes is reduced because of the potential for snow and ice cover. Regions with limited growing seasons may also be incapable of establishing efficient populations of primary producers, thus further resulting in low carbon fixation rates.

Within latitudinally restricted zones, lacustrine productivity appears to be nutrient controlled with the possible exception of those situations where water column turbidity may be so high as to reduce the photic zone to a narrow surface layer. Such conditions may occur where stream input carries a high suspended load or where surface productivity is so high that the biomass itself may effectively reduce light penetration (Talling, 1960). Suspended load is function of drainage basin rock character and climate. Higher suspended loads are found when the drainage basin is dominated by fine-grained siliciclastic rocks and when strong seasonality exists, cycling between wet and dry seasons (Cecil, 1990).

Nutrient Supply

Nutrient availability is controlled by internal (recycling) and external sources. The dynamics of the nutrient renewal process, rather than the instantaneous absolute concentrations, appear to control the level of productivity (Bloesch et al., 1977). Dean (1981) suggested that nutrient recycling plays a more significant role in maintaining productivity, except in immature lacustrine systems that have not yet established an internal nutrient pool. Another important class of exceptions appears to be where high nutrient loads are introduced into the lake from the drainage basins. This appears to have been the case for lakes Uinta and Gosiute (Green River Formation), where high levels of productivity appear to have been maintained through the continuous supply of phosphorus from the erosion of the Phosphoria Formation (Grande, 1980). Phosphorus is typically considered the major limiting nutrient in both temperate and tropical settings (Kalff, 1983).

Higher nutrient loads are present if the drainage basin includes phosphate deposits, carbonates, and/or basalt or rhyolite flows, and where chemical weather-

ing dominates over mechanical weathering. External nutrient supply is also controlled by the drainage basin's dimensions. Consequently, external sources of nutrients tend to decrease with increasing elevation because of the more restricted size of the drainage basin (Harrison et al., 1981). Chemical weathering also dominates under semiarid conditions (Cecil, 1990).

Nutrient recycling processes not only must remineralize available organic matter, but must return the nutrient load to the photic zone. Remineralization is largely controlled by bacterial processes and occurs within both the water (Burns and Ross, 1971) and sedimentary columns, under both oxic and anoxic conditions (Håkanson and Jansson, 1983). The rate of remineralization varies among these settings. For example, the ability to release phosphorus appears to be enhanced under anoxic conditions (Ochumba and Kibaara, 1989). Because remineralization is largely controlled by bacterial processes, the rates of remineralization are highest within the tropics where temperatures permit elevated levels of bacterial activity (Serruya and Pollinger, 1983). Nutrient regeneration may be further supplemented by zooplankton grazing (Porter, 1976), as well as grazing by higher trophic levels, including flamingos (Likens, 1975).

The remineralization process is unable to foster productivity if the nutrients remain “trapped” with the hypolimnion. If such a sink exists, low levels of productivity may be anticipated (Robbins, 1983) and the lakes are commonly oligotrophic (<30 gC/m²/yr). The reintroduction of nutrients to the photic zone is largely a function of the frequency of water column overturn (Table 2). The frequency of overturn is a function of winds, basin morphology, salinity, and temperature (commonly expressed as a function of elevation and latitude). Shallow, broad lakes (i.e., large width/depth ratios) tend to be more effective in their water column mixing than deeper, more restricted or narrow lakes (i.e., low width/depth ratios; Rawson, 1955). Thus, lakes such as Victoria are more effectively able to recycle their nutrient load than Lake Tanganyika with its greater bathymetric gradient (Hecky and Kling, 1981).

The reintroduction of nutrients to the photic zone may be either continuous or seasonal. Seasonal introduction of nutrients through such processes as upwelling may result in algal blooms and a marked increase in standing phytoplankton crop (Ochumba and Kibaara, 1989) and in all successive trophic levels (Green et al., 1976).

Table 2. Classification of lake water column overturn.

| Mixing Type | Frequency of Overturn |
|-------------|----------------------------------|
| Amictic | Never circulates, remains frozen |
| Monomictic | Once per year |
| Polymictic | Frequent overturn or circulation |
| Oligomictic | Irregular and rare circulation |

From Katz (1990).

The recycling of nutrients to the photic zone need not be complete to be effective. Seasonal recycling of approximately 10% of the hypolimnion in Lakes Tanganyika and Kivu results in major changes in productivity levels (Coulter, 1963). During the periods of stable stratification (October through May), the lakes may be considered oligotrophic, while during the seasonal upwelling periods (June through September), productivity levels may become eutrophic (60–200 gC/m²/yr) or even hypertrophic (>200 gC/m²/yr), with much of the productivity associated with lake margins (Hecky and Kling, 1981).

The availability of nutrients also appears to partially control the composition of the biomass. Certain algae, such as *Desmidiaceae*, tend to be associated with nutrient-depleted oligotrophic conditions (Brook, 1965), while high nutrient levels and eutrophic conditions are commonly associated with blue-green algal blooms (Ochumba and Kibaara, 1989).

Water Chemistry

Water chemistry (salinity and ionic speciation) also influences the nature of the biomass. Water chemistry appears to have a greater influence on the nature of the primary producers rather than the absolute levels of productivity, that is, comparable levels of productivity may be observed at all salinity levels (Pearsall, 1921). For example, there is typically a decrease in species diversity with increasing salinity (Warren, 1986), although some of the highest lacustrine productivity levels are associated with saline lakes (Table 3). Within saline and hypersaline lakes macrophytes are absent, the algal population is dominated by the green alga *Dunaliella* sp., with the additional presence of halophilic or halotolerant bacteria (e.g., *Halobacterium* or *Halococcus*; Post, 1977). Such organisms can tolerate salinity levels as high as 350‰ (Borowitzka, 1981).

In freshwater lakes, ionic speciation appears to play a major role in establishing the nature of primary producers. Differences in water chemistry can be ascribed to such factors as the presence or absence of hot springs, variations in country rock, the relative importance of subsurface and riverine input, and differences in evaporation (Hecky and Degens, 1973). An examination of modern lake systems reveals that: (1) in alkali-dominated systems, green algae dominate and macrophytes are nearly absent, (2) in carbonate-dominated systems, diatoms are abundant and macrophytes are common, and (3) in those lakes that have high concentrations of dissolved organic matter, cyanobacteria (blue-green algae) dominate. Those lakes containing high levels of dissolved organic matter also tend to display acidic conditions.

Differences in both the dissolved solid load and the ionic speciation in the East African rift lakes appear to be sufficient to result in distinct algal communities (Figure 3). Such differences, if maintained, are believed to be sufficient to result in distinctly different crude oils from each lake when the organic matter is converted to kerogen and subsequently matured (Katz and Mertani, 1989).

In addition to spatial variability in the nature of the lacustrine biomass, there is evidence that such changes

Table 3. Examples of elevated saline lake productivity levels.

| Water Body | Productivity* (gC/m ² /yr) |
|------------------------------|--|
| <i>Lake Body</i> | |
| Corangamite, Australia | 759 |
| Devils, North Dakota, U.S.A. | 172 |
| Great Salt, Utah, U.S.A. | 223 |
| Humboldt, Canada | 613 |
| Mariut, Egypt | 2601 |
| Red Rock, Australia | 2201 |
| Soap, Washington, U.S.A. | 391 |
| Werowrap, Australia | 435 |
| <i>Ocean Body</i> | |
| Open ocean | 50 |
| Oceanic upwelling region | 300 |

* Lake productivity values from Hammer (1981); ocean productivity values from Krey (1970).

may occur temporally. Changes in lake level, salinity, and nutrient concentrations may result in the temporal change in organic matter character (Mello and Maxwell, 1990). Haberyan and Hecky (1987) noted distinct changes in the diatom speciation in lakes Kivu and Tanganyika during the Pleistocene and Quaternary.

ORGANIC PRESERVATION

It has been observed in marine environments that there is not always a one-to-one relationship between water column productivity and the quantity of preserved sedimentary organic matter (Demaison and Moore, 1980). Gorham et al. (1974) had earlier noted that there was an absence of any linear relationship between lacustrine algal standing crop and sedimentary organic matter. This difference between productivity and sedimentary organic carbon content is thought to be a consequence of variations in organic preservation efficiency.

Role of Free Oxygen

Among the processes acting against the preservation of organic matter is oxidation, which may occur as a result of biologic (respiration) and abiologic processes, acting in both the water and sedimentary columns. Oxygen is only one of the available oxidizing agents. Others include nitrate and sulfate.

Although there has been considerable debate on the role that free oxygen plays in the destruction or preservation of organic matter (cf. Pedersen and Calvert, 1990, 1991; Demaison, 1991), the East African rift lakes provide clear evidence that at comparable levels of productivity, both the quality (oil-proneness) and quantity of organic matter are better preserved under oxygen-depleted conditions (Katz, 1990). This may be observed best by comparing the organic geochemical attributes of lakes Edward and Albert (Mobutu).

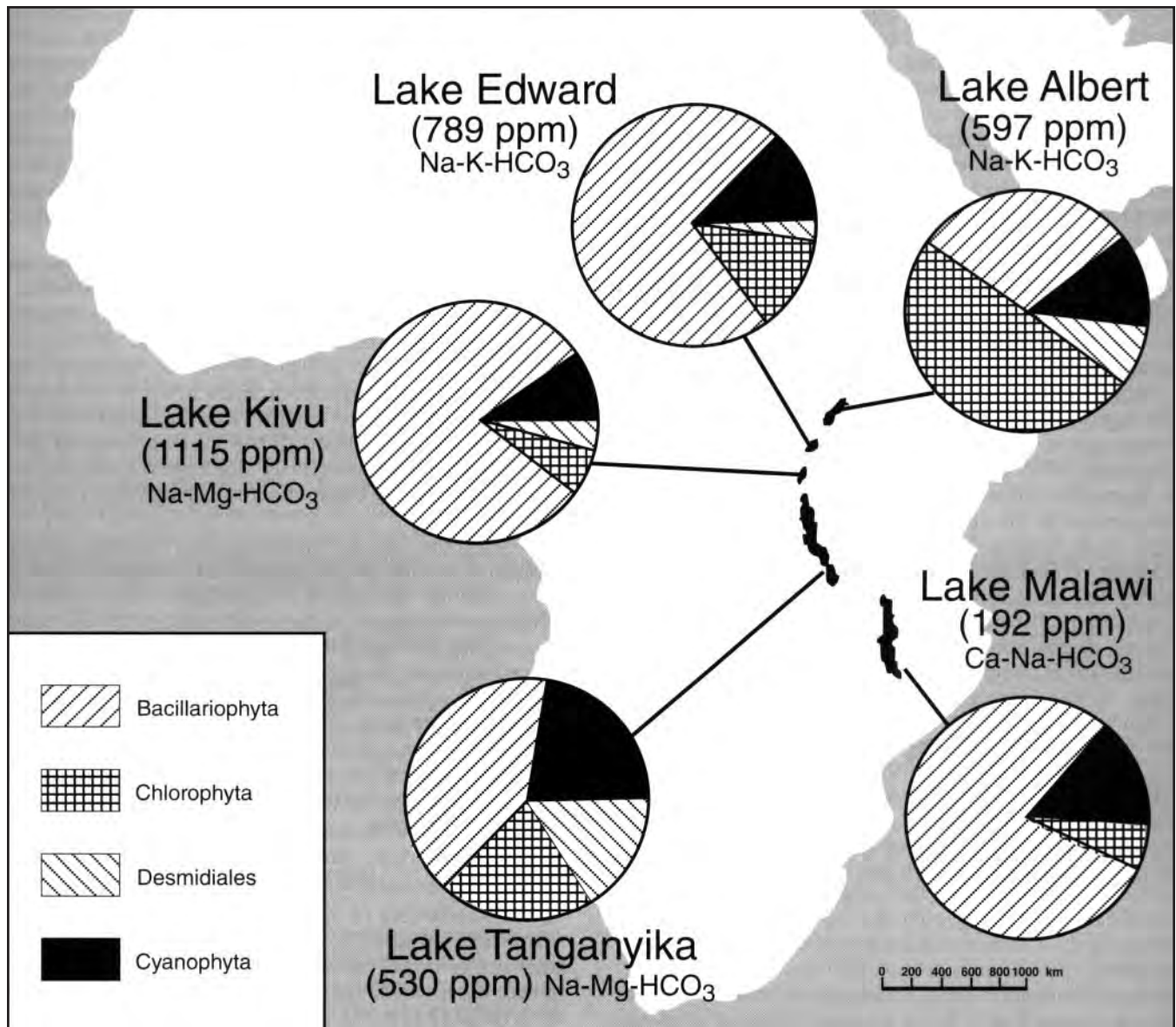


Figure 3. Algal compositions and water chemistry of East African rift lakes (data from Serruya and Pollinger, 1983).

Higher levels of organic enrichment, as well as higher hydrogen index values, were determined on sediments from Lake Edward (Katz, 1988). These differences appear to be the result of differences in the oxygen content of the water column. Lake Albert is well mixed and well oxygenated. Lake Edward undergoes seasonal overturn in August and an occasional second overturn in February (Verbeke, 1957). During nonmixing periods, the water volume is anoxic below 40 m (Serruya and Pollinger, 1983).

The availability of free oxygen is controlled by initial oxygen solubility and renewal rate. Oxygen solubility decreases with increasing temperature (Mortimer, 1956) and salinity (Kinsman et al., 1974). Under normal circumstances, oxygen solubility places an upper limit on initial availability. Supersaturation may occur infrequently during daylight periods in

regions of high productivity through photosynthesis or through the mixing of distinct water masses (Mortimer, 1956). Typically, however, because of various biologic demands, observed oxygen levels are lower than the saturation level.

Water Column Stratification

Oxygen resupply in all but the shallowest lakes is dominated by overturn and mixing rather than by molecular diffusion. Diffusion appears to be most effective near the air-water interface (Hutchinson, 1957). Several factors influence lake overturn and mixing. Overturn is an attempt by nature to establish and maintain a dynamically stable water column. In general, the potential for water column stratification is greatest at low latitudes for two primary reasons: (1) seasonal temperature

differences are minimized (Figure 4), and (2) density contrasts at higher temperatures are greater (Bradley, 1948). The reduced seasonal temperature differences at low latitudes result in changes in surface water density, which are insufficient to result in the displacement of the denser bottom waters. The density contrasts at higher temperatures require increased external energy (winds) in order to accomplish mixing. Bradley (1948) estimated that three times the amount of energy would be required to mix two water masses with temperatures at 22° and 25°C compared with two layers at 9° and 12°C, although both pairs display the same temperature difference. Water column stability is further supported if water temperatures above 4°C are maintained. Fresh water obtains its maximum density near 4°C.

Stratification may also develop as a consequence of salinity contrasts. Salinity contrasts may develop as a consequence of subsurface hydrothermal discharges (Robbins, 1983), as in Lake Kivu (Degens et al., 1973), or through nonhydrothermal subsurface spring discharges, as is the case for Green Lake (Fayetteville, New York; Brunskill and Ludlam, 1969). Salinity contrasts have also been invoked to explain stratification within the lakes associated with the deposition of the Green River Formation (Demaison and Moore, 1980). During deposition of the Green River Formation, this stratification appears to have developed through climatic cycling between humid and arid phases. During more humid phases, a fresher water cap could develop. This cap provided the necessary salinity contrast for the development of stratification. The role of salinity contrasts as a means to establish and maintain a stable water column may be greatest in lakes with high width/depth ratios and those outside of the tropics (e.g., Great Salt Lake, Utah).

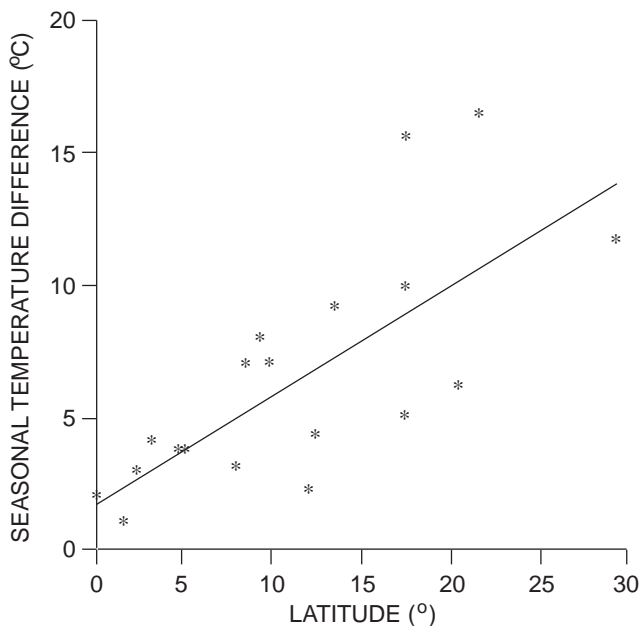


Figure 4. Seasonal lacustrine surface water temperatures as a function of latitude (data from Serruya and Pollinger, 1983).

Wind is commonly a mechanism for the disruption of stratification (Talbot, 1988) and the mixing of lake waters (Birge, 1916). Four aspects of the wind must be considered when determining whether sufficient energy is transferred to disrupt water column stratification. These are velocity, duration, frequency, and fetch. Fetch is controlled by lake basin size, the surrounding terrain, and wind direction. Greater wind speeds, longer durations, and greater fetch tend to increase mixing (Livingstone and Melack, 1984).

In broad shallow lakes (i.e., high width/depth ratios), where fetch is large (e.g., Lake Victoria), wind stresses may be sufficient to maintain a well-mixed water column even in a tropical setting. In such cases, the water column is well oxygenated and organic preservation efficiencies are low. Elevated levels of sedimentary organic matter could develop in such situations through the maintenance of elevated levels of productivity (i.e., preservation efficiency is partially compensated for by high organic matter supply).

Oxygen may also be present within the sedimentary column. The level of oxygen within the pore waters is controlled by the initial oxygen level of the waters which are entrapped in the sediments and by the rates of resupply through diffusion, as well as demand. The rate of resupply is generally higher in coarser, more permeable sediments (Krissek and Scheidegger, 1983) and in those regions where the depth and intensity of biodegradation are maximized (Wetzel, 1983). Such conditions permit better irrigation of the sediment and, hence, downward transport of potentially oxygen-bearing waters.

Oxygen Demand

The availability of oxygen is also controlled by consumptive demand (Demaison and Moore, 1980). The presence of large quantities of organic matter tends to reduce the available oxygen. This is particularly true if the available organic matter is largely labile, that is, there are greater demands associated with hydrogen-enriched, algal material than there are caused by hydrogen-poor, vitrinitic material (Waples, 1983). Supplementing the demands placed on the system by the organic matter are those introduced through the introduction of other reduced chemical species such as methane. In those cases where demands are greater than oxygen supply, anoxia develops. These demands may be temporary, resulting in brief periods of anoxia, as associated with algal blooms (Skullberg et al., 1984; Ochumba and Kibaara, 1989), or more permanent if high productivity levels are maintained, even if the water column is occasionally overturned (Green et al., 1976; Verbeke, 1957).

Euxinic conditions are not commonly associated with lacustrine systems because they lack sufficient quantities of sulfate to form free H₂S in the water column. Consequently, lacustrine sediments deposited under anoxic conditions commonly lack significant quantities of pyrite. Available iron is commonly incorporated into siderite within this anoxic setting (Bahrig, 1989).

An anoxic water column commonly results in the preservation of laminations within the sedimentary sequence. These seasonal varves, resulting from variations in the productivity cycle, appear best developed and preserved since the early Tertiary with the introduction of diatoms (Anderson and Dean, 1989). These laminations may be disrupted by the bubble discharge of gas from the organic-rich sediments.

Exposure Time

In addition to the availability of oxidizing agents, exposure time is a key element controlling preservation. In an oxic water column, exposure time includes the entire settling period, as well as the initial burial phase, and is dependent on both the sedimentation and bioturbation rates. In a partially stratified water column, exposure time is generally limited to the time spent within the oxygenated epilimnion. Exposure time not only influences the quantity of preserved organic matter but its quality (Demaison et al., 1984). Limited exposure time tends to result in both large quantities of preserved organic matter and higher levels of hydrogen enrichment (i.e., greater degree of oil-proneness).

Dysaerobic and Anaerobic Processes

Free oxygen is only one of the available oxidizing agents leading to the destruction of available organic matter. Under dysaerobic conditions, where oxygen levels approach 5% of saturation, bacterial denitrification begins (Berner, 1980). As the availability of nitrates decreases, the reduction of MnO_2 and Fe^{+3} results in the further decomposition of organic matter (Nealson, 1982). These bacterially mediated processes tend to occur within the upper tens of centimeters of the sedimentary column.

The absence of sulfate from many lacustrine systems (Berner and Raiswell, 1984) precludes sulfate reduction from taking its normal place in the diagenetic sequence. However, in saline lakes sulfate content may be quite high (Table 4). Under these conditions, the rate of organic matter destruction through sulfate reduction may be as high as that under highly oxic conditions (Kelts, 1988).

Methanogenesis further acts to reduce the amount of preserved sedimentary organic matter. Methane-producing bacteria require both anaerobic and sulfate-depleted conditions (Whiticar et al., 1986). Consequently, methane production within freshwater lakes may be quite significant. Interstitial waters may become saturated leading to bubble formation and discharge into the water column, as observed in Lake Kivu (Jannasch, 1975). Tietze et al. (1980) have estimated that Lake Kivu contains $\sim 63 \times 10^9 \text{ m}^3$ of methane at STP, although not all of this methane was derived from processes within the sedimentary column (Schoell et al., 1988).

A LACUSTRINE SOURCE ROCK MODEL

The factors noted above can be summarized and integrated into a first-order conceptual model to pre-

Table 4. Lake body sulfate levels.

| Water Body | Sulfate Concentration (mg/L) |
|---|------------------------------|
| <i>Lake Body</i> | |
| Lake Zurich, Switzerland | 5 |
| Lake Greifensee, Switzerland | 21 |
| Lake Urner, Switzerland | 23 |
| Lake Baldegg, Switzerland | 13 |
| Lake Constance, Germany | 51 |
| Lake Cadagno, Switzerland | 154 |
| Lake Kivu (surface waters/ bottom waters), Zaire | 25/220 |
| Qing Hai Lake, China | 2402 |
| Big Soda Lake, Nevada, U.S.A. | 5600 |
| Great Salt Lake, Utah, U.S.A. | 16,000 |
| Urmia, Iran | 22,000 |
| Dead Sea, Israel | 450 |
| <i>Ocean Body</i> | |
| Ocean water | 2712 |

From Kelts (1988).

dict and/or explain the distribution of lacustrine source rocks in time and space (Figure 5). The specific elements and their interrelationships are, however, insufficiently known to produce a quantitative model.

In order for a lacustrine source sequence to develop with sufficient volume to be of commercial significance, the original lacustrine basin must be of either tectonic or glacial origin. However, latitudinal restrictions on glacial lake occurrence tends to result in a reduction in their potential for source rock development and as such will not be considered. Tectonic basins in both compressional and extensional regimes have the potential for source rock development. Source rock development in lake basins which form through extension is often controlled by organic preservation (e.g., Lakes Edward and Tanganyika), while those formed in compressional settings are controlled by productivity (e.g., Lakes Gosiute and Uinta).

The existence of a tectonic basin is insufficient to ensure the presence of a lake. Water must be available. Under most circumstances this water is supplied through either surface runoff or directly through precipitation. Subsurface recharge is not normally a major contributing factor to a lake's hydrologic balance. When subsurface recharge dominates or there is a net precipitation deficit, the lakes are normally saline. Today, an excess of precipitation over evaporation occurs in a belt centered about the Intertropical Convergence Zone. The width and specific position of this region vary through time. These variations result in changes in lake level which can be significant (>100 m) and may result in changes in both the amount and type of organic matter preserved in all but the deepest basins. Talbot and Livingstone (1989) have shown that both organic carbon

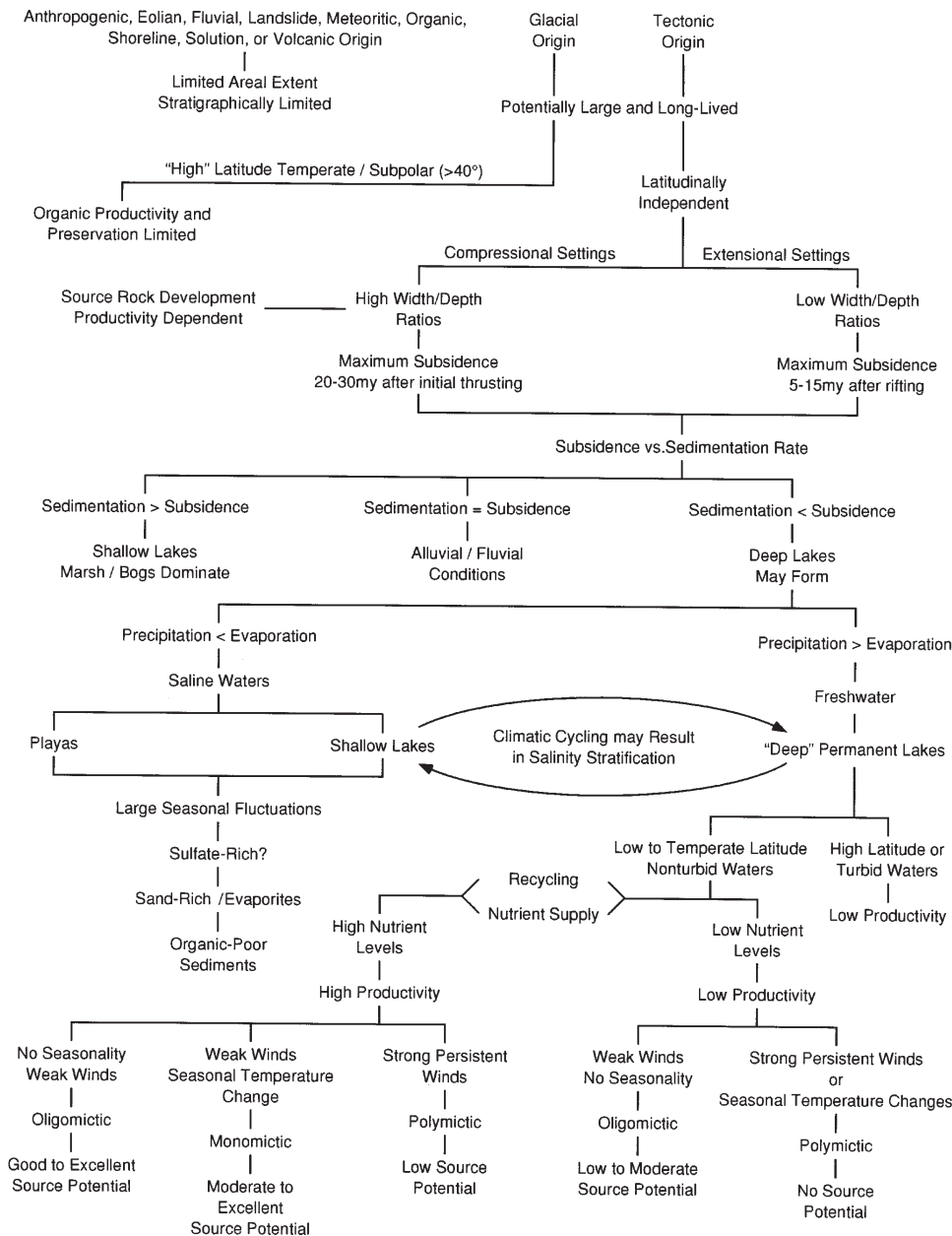


Figure 5. Schematic summary of the processes which control the development of oil-prone lacustrine source rocks.

content and the degree of oil-proneness, as measured by the hydrogen index derived from Rock-Eval pyrolysis, decrease as an exposure surface is approached. This reduction in quality and quantity occurs through both bacterial processes and inorganic oxidation. With a rise in lake level, both the amount and quality of preserved organic matter increase. They further noted that charcoal may be concentrated along the exposure surface. Thus, maximum oil source rock potential would be associated with more humid episodes.

The potential for source rock deposition is greatest during periods of maximum subsidence, particularly when associated with sedimentation rate minimums. Variations in subsidence rates within basins impact local potential for oil source rock development. Maximum source rock development

occurs farthest away from the hinge zone in either a compressional or extensional setting, and within those subbasins which display the greatest subsidence rates relative to sedimentation. In many cases, the appropriate balance between sedimentation and subsidence coincides with the maturing of a lake's nutrient pool. Consequently, the onset of elevated levels of productivity is commonly associated with maximum water depth.

Low latitudinal positions favor both organic productivity and preservation favoring lacustrine source rock development. There are conditions within temperate settings which may also permit lacustrine source rock development. Temperate lacustrine source rocks appear commonly associated with strong salinity stratification and/or eutrophic conditions, which develop as a consequence of high nutrient

loads being supplied through external sources. Both conditions are believed to have existed during the deposition of the Green River Formation (Demaison and Moore, 1980; Grande, 1980).

An examination of modern tropical East African rift lakes further suggests that within basins with low width/depth ratios, optimum conditions for lacustrine source rock development occur when lake water depths are between 60 and 400 m (Katz, 1988). Under these conditions, high levels of productivity are maintained because of nutrient renewal, and the water column can maintain stratification.

Variations in source rock quality occur through several processes including changes in lake level, preservation potential, and processes associated with the redistribution of organic matter within the basin. The redistribution of organic matter is largely controlled by depositional processes, including slumping and turbidity flows (Huc et al., 1990). Consequently, even within an apparently near-uniform depositional setting, significant organic geochemical heterogeneity may develop.

AN APPLICATION—WESTERN INDONESIA

These concepts can be applied in a case study which examines the potential for lacustrine source rock development in five basins from western Indonesia. The five basins are the North, Central, and South Sumatra basins and the Kutei and the Barito basins of Kalimantan (Figure 6).

The tectonic history of the region has been outlined by Hutchison (1989) and Daly et al. (1991). Each of the five basins formed during the Eocene. The three Sumatran basins may be considered large pull-apart basins bounded by faults to both the north and the south. These basins continued to develop through the Eocene and were inverted during the Miocene. The two basins on Kalimantan appear to be related to back-arc extension. The Kutei basin is a half-graben facing east and the Barito basin is a half-graben facing west. Rifting in these two basins appears to have been completed by the Oligocene with the onset of thermal subsidence.

The tectonic style of these basins suggests the potential for the development of long-lived, narrow, deep lakes during discrete periods of geologic time: Eocene through the Oligocene for the three Sumatra basins and Eocene for the two Kalimantan basins. However, two additional criteria need to be met. These are a positive water balance and terminations that prevent marine incursions.

Not all of these basins meet these criteria. The North Sumatra basin appears to have extended into the Andaman Sea without any apparent barriers to a marine incursion (Davies, 1984). Similarly, the two basins on Kalimantan appear to have extended directly or indirectly into the Makassar Strait to the east (Rose and Hartono, 1978) during their initial phase of development. Therefore, from a regional tectonic standpoint, only two of the five basins under examination display a paleogeographic setting which would permit lake development.

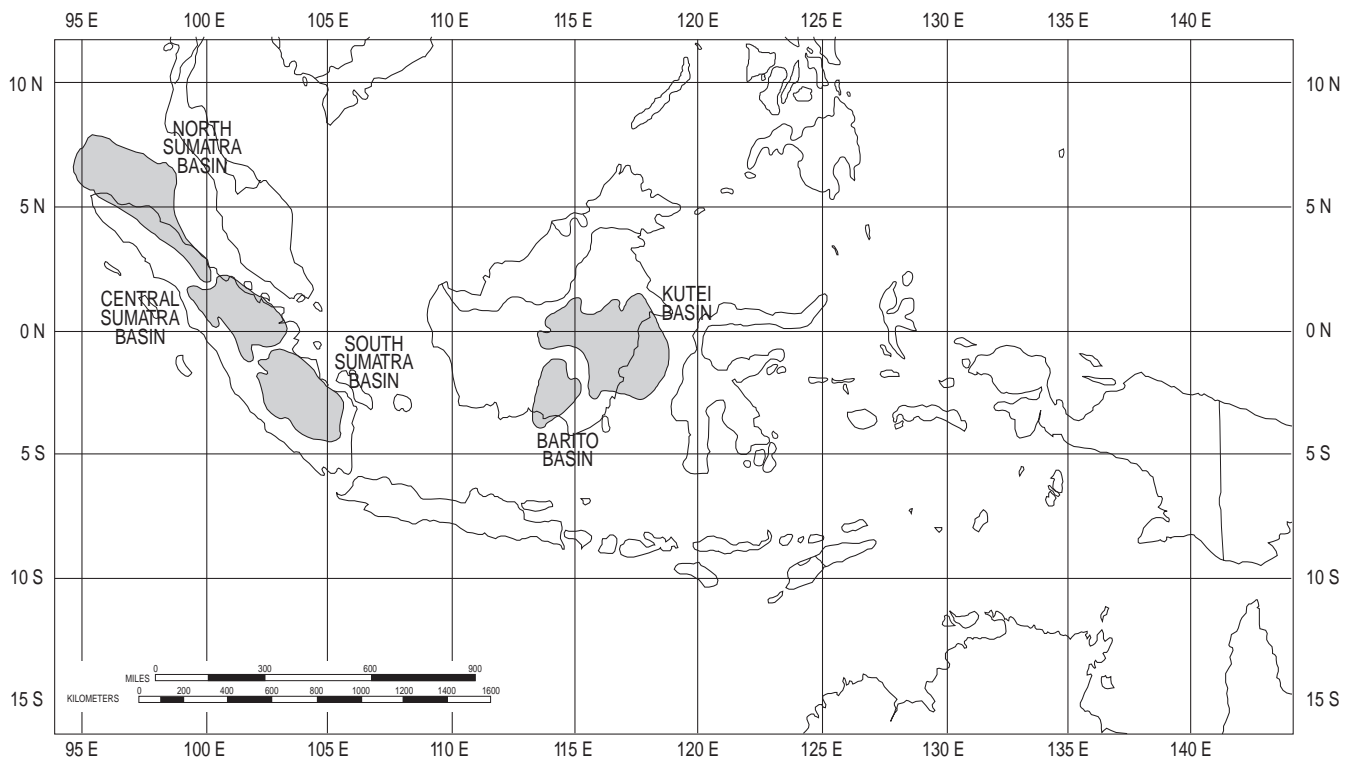


Figure 6. Index map for western Indonesia basins.

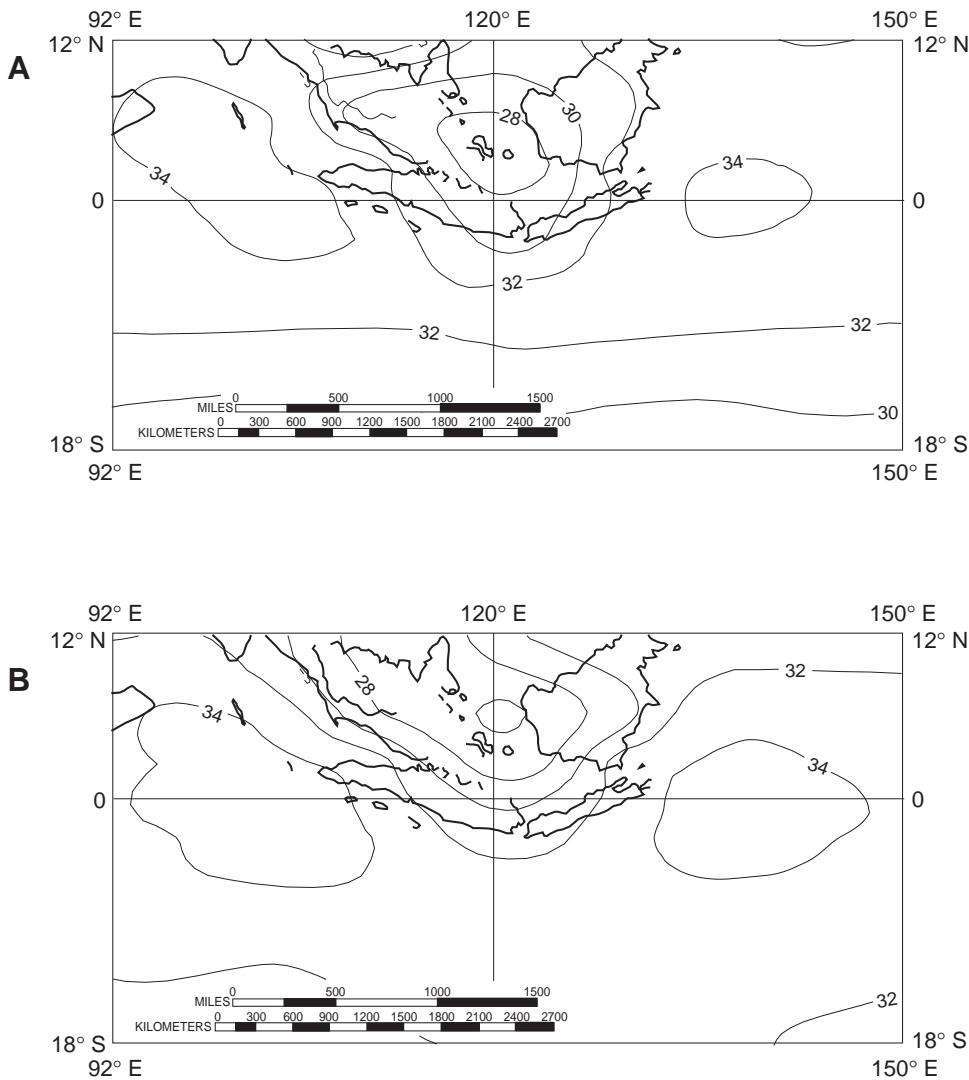


Figure 7. Surface temperature (°C) for the middle Eocene (45 Ma) during (A) June/July/August and (B) December/January/February.

The nature of the water balance as well as the influence of several other climatic factors on lacustrine source rock development can be examined through the use of numerical climate models (Barron, 1990). These models provide information on precipitation, evaporation, seasonal temperature variations, wind patterns and intensity, and storm processes. In this study the atmospheric GCM utilized is the "Community Climate Model" (CCM). This model was developed at the National Center for Atmospheric Research and has been modified for paleoclimatic investigation (Barron and Washington, 1982). The results presented in this study are from a seasonal simulation run to 15 yr. The model utilizes a $4.5^\circ \times 7.5^\circ$ latitude/longitude grid cell. The paleogeographic configurations for the early Eocene, middle Eocene, and early Oligocene were taken from Ziegler et al. (1983). The three simulations were run using atmospheric CO_2 concentrations as described by Budyko et al. (1985).

The results of these simulations indicate that several climatic factors do not provide any temporal and/or spatial discrimination for lacustrine source

rock development. For example, an examination of winter storm tracks clearly indicates that the region is not impacted by persistent storms. Also, because the study area straddles the equator, paleosurface temperatures are elevated throughout the study area (Figure 7), and there is no strong seasonal variation.

In contrast, precipitation and evaporation appear to be the most significant discriminators. This is a consequence of their spatial and temporal variability. Maps representing the difference between precipitation and evaporation are presented in Figures 8–10. Strongly positive values (>2 mm/day net excess of precipitation) persisted throughout the year over Sumatra during the early and middle Eocene. A strong seasonality began to develop by early Oligocene. This resulted in a wet June/July/August and a dry December/January/February. Although seasonality would not prevent lake development, it would spatially restrict the perennial lake and reduce organic preservation efficiencies. Consequently, it appears that most of the significant lacustrine source rock development in the Central and South Sumatra basins would be terminating during the early Oligocene.

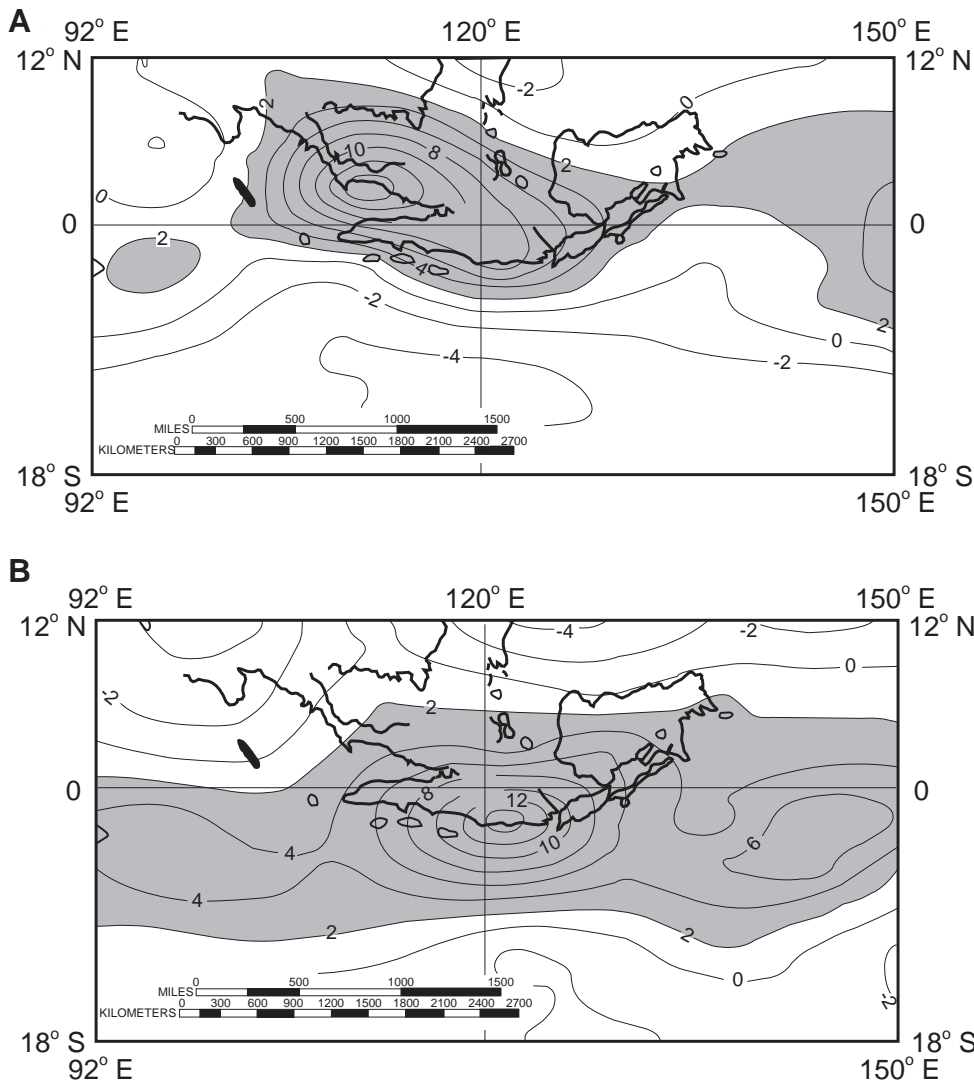


Figure 8. Difference between precipitation and evaporation (mm/day) for the lower Eocene (55 Ma) during (A) June/July/August and (B) December/January/February.

Overprinting these general climatic patterns are higher-frequency climatic oscillations caused by Milankovitch forcing factors. Modeling results (Manabe and Hahn, 1977) and palynological data (Morley and Flenley, 1987) support cyclicality across the Indonesian archipelago during the late Tertiary and Quaternary. It is, therefore, possible, if not probable, that such cyclicality also occurred during the Eocene within the study area. The modeling performed as part of this investigation did not examine the impact of Milankovitch forcing factors and assumed an insolation equivalent to today's. Longley et al. (1990), in fact, provide data which suggest cycling within the Pematang Formation of central Sumatra.

There is currently no method to quantitatively assess paleoproductivity levels. The low latitudinal position suggests the potential for high productivity. The nature of the rocks within the drainage basin does not appear to suggest a highly turbid river system, nor do they suggest unusually high nutrient loads. The drainage basin included granites and metamorphic rocks (de Coster, 1974). The lack of a major nutrient

source suggests that higher levels of productivity would occur principally during the more mature phases of lake development. This need to establish a mature nutrient pool may be a partial explanation of the limitation of the oil-prone source to the upper third of the sequence (Figure 11; Katz and Mertani, 1989).

Within the Central and South Sumatra basins, individual subbasins would probably display minor variations in water chemistry as a result of variations in such elements as basement character and the nature of spring input. Such differences would result in variations in the nature of the algal biomass and would ultimately result in variations in the character of the generated product. Katz and Mertani (1989) inferred that such variations must have existed because of the regional differences in crude oil chemistry within central Sumatra.

Another major factor influencing the character of the preserved organic matter is the nature and abundance of terrestrial material. The amount and type of allochthonous material are strongly influenced by the availability of water. Vitrinite (gas-prone material) would tend to be more abundant under humid conditions when rain for-

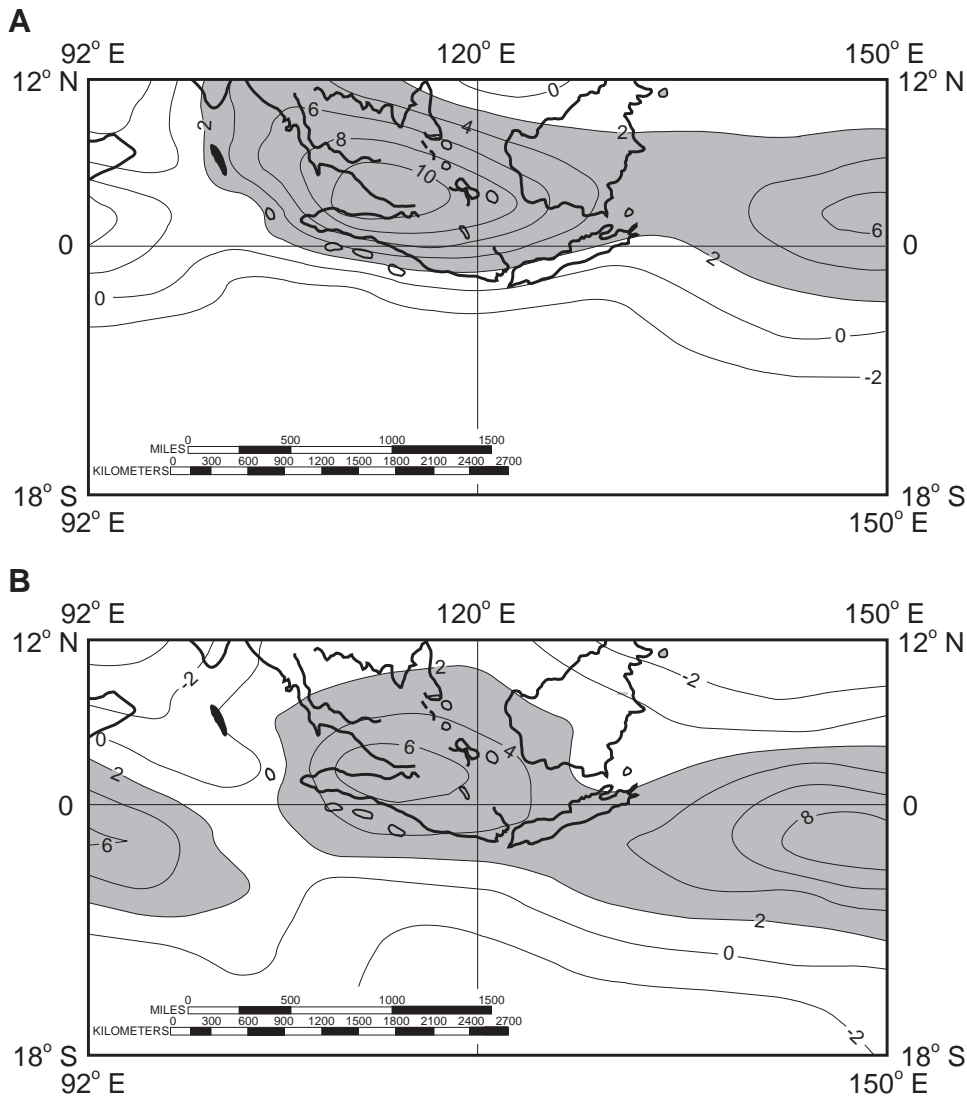


Figure 9. Difference between precipitation and evaporation (mm/day) for the middle Eocene (45 Ma) during (A) June/July/August and (B) December/January/February.

est growth would be supported. Cuticular (oil-prone material) would be more abundant if savannas or grasslands were common, while under arid conditions, the terrestrial contribution would be limited and commonly dominated by inertinite.

The paleoclimatic simulations suggest the potential for significant changes in the amount of rainfall over the island of Sumatra during the Eocene. These changes should result in changes in both the type and amount of allochthonous debris supplied to the lake systems. In general, there was a decrease in the annual rainfall and likely in the annual runoff from the early Eocene to the early Oligocene. This would result in a transition from tropical, moist rain forests to a tropical savanna. These changes would be similar to the patterns noted by Adams et al. (1991) caused by cycling between glacial and interglacial conditions. This secular trend suggests that allochthonous material in these lakes would evolve from gas-prone to oil-prone from early Eocene to early Oligocene. Such a trend is supported by the observed organic matter character in the Balam subbasin of central Sumatra (Figure 11).

CONCLUSIONS

Our current understanding of the processes which control the development of lacustrine source rocks permits a qualitative prediction of their distribution in time and space. Such a capability is particularly useful as exploration shifts from known marine provinces to those which contain significant nonmarine stratigraphic component.

The distribution of these economically important rocks is controlled first by those factors which control the distribution of lake bodies, that is, the processes which form the lake basin and those which make water available. In addition, their presence is controlled by the level of primary productivity within the water column and the organic preservation efficiency. Many of the factors which favor both are currently found within the tropics. Lacustrine source rocks have developed outside the bounds of the current tropics as a result of variations in climatic patterns through time, and as a result of other mechanisms which favor elevated rates of organic preservation. Such factors as subsidence rate, lake level, lake maturity, and sedi-

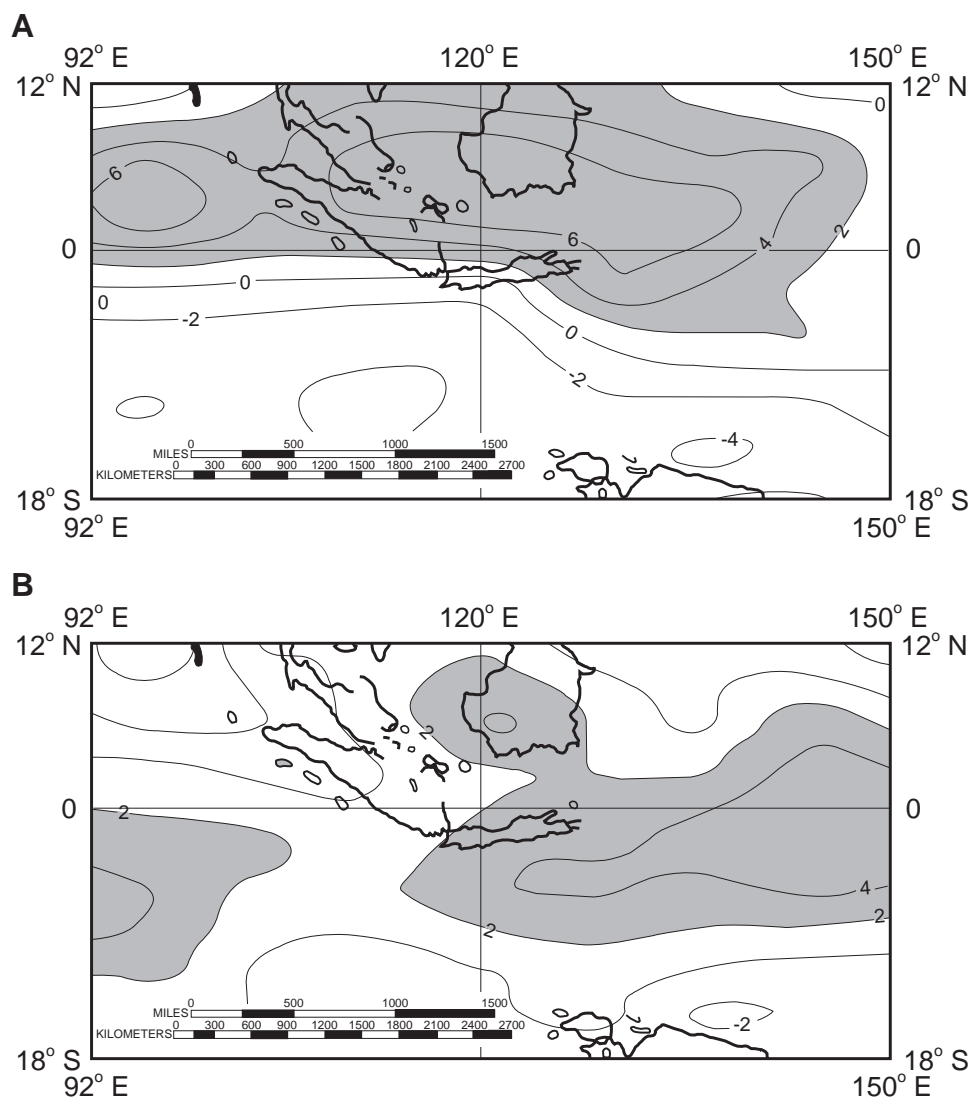


Figure 10. Difference between precipitation and evaporation (mm/day) for the lower Oligocene (35 Ma) during (A) June/July/August and (B) December/January/February.

mentation rate may influence the quality of the source rock. Consequently, there are stratigraphic variations in source rock potential within individual basins. Maximum potential for source rock development appears to be associated with lake level highstands, maximum subsidence rates, and an advanced level of lake maturity with respect to nutrient input.

The outlined model has been used to explain the temporal and spatial distribution of oil-prone lacustrine source rocks within parts of western Indonesia. The model not only provides a qualitative assessment of the region's source rock development but can account for variations in oil source rock potential within a basin, the geochemical variability of the crude oils generated across the basin, as well as the stratigraphic position of the source rock sequence.

ACKNOWLEDGMENTS

The author thanks Texaco Inc. for permission to publish this work. An early draft of this manuscript was read by M. Mello, G. Moore, and V. Robison.

Drafting was done by J. Ash, G. Novaez, and J. Mulvaney. Paleoclimate modeling assistance was provided by L. S. Kilgore.

REFERENCES CITED

- Adams, J.M., H. Faure, L. Faure-Denard, J.M. McGlade, and F.I. Woodward, 1991, Increases in terrestrial carbon storage from the last glacial maximum to the present: *Nature*, v. 348, p. 711–714.
- Anderson, R.Y., and W.W. Dean, 1989, Lacustrine varve formation through time: *Palaeogeography, Palaeoclimatology, Palaeoecology*, v. 62, p. 215–235.
- Bahrig, B., 1989, Stable isotope composition of siderite as an indicator of the paleoenvironmental history of oil shale lakes: *Palaeogeography, Palaeoclimatology, Palaeoecology*, v. 70, p. 139–151.
- Barron, E.J., 1990, Climate and lacustrine petroleum source rock prediction, *in* B.J. Katz, ed., *Lacustrine Basin Exploration—Case Studies and Modern Analogs*: AAPG Memoir 50, p. 1–18.

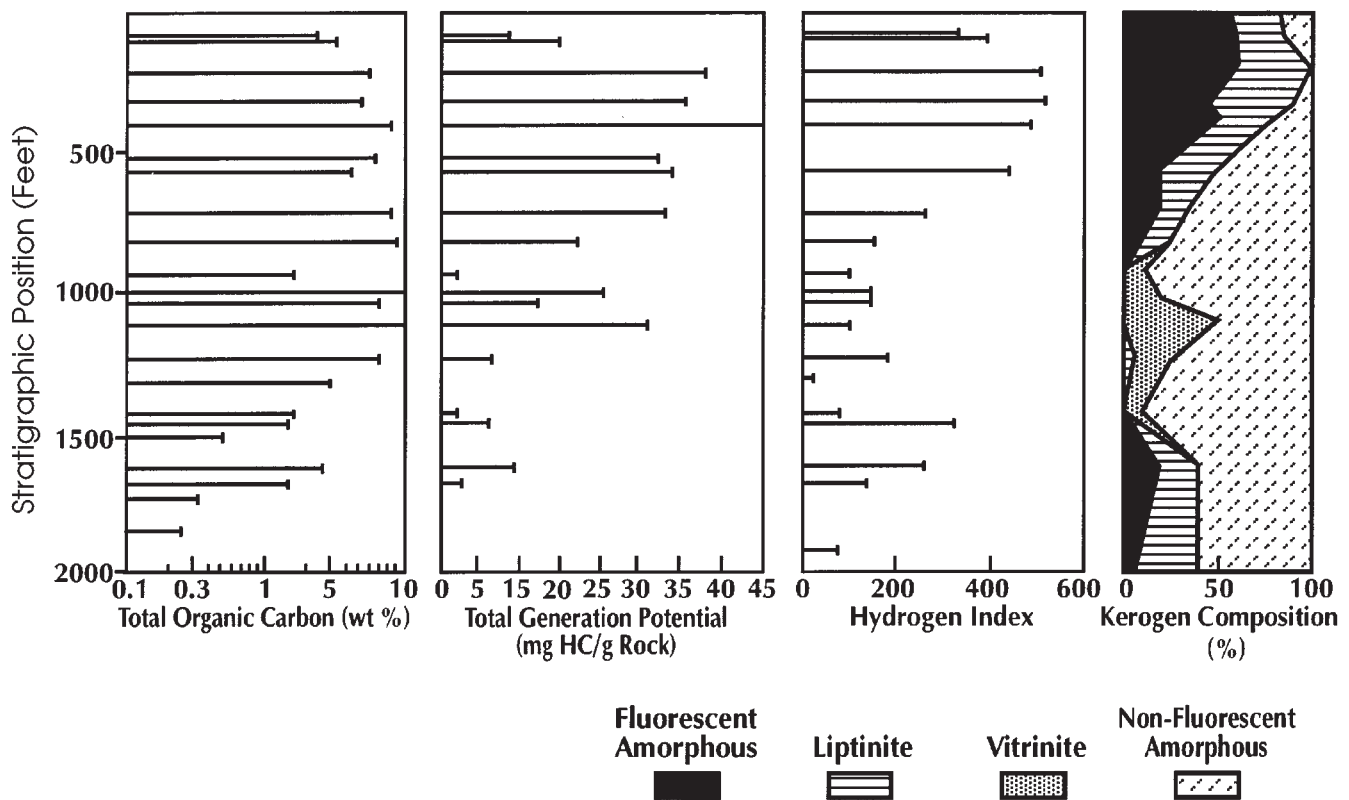


Figure 11. Geochemical log brown shale (Central Sumatra basin, Balam subbasin).

Barron, E.J., and M.W. Washington, 1982, Cretaceous climate: a comparison of atmospheric simulations with the geologic record: *Palaeogeography, Palaeoclimatology, Palaeoecology*, v. 40, p. 103–133.

Berner, R.A., 1980, *Early diagenesis—a theoretical approach*: Princeton, Princeton University Press, 241 p.

Berner, R.A., and R. Raiswell, 1984, C/S method for distinguishing freshwater from marine sedimentary rocks: *Geology*, v. 12, p. 365–368.

Birge, E.A., 1916, The work of the wind in warming a lake: *Transactions Wisconsin Academy of Science*, v. 18, p. 341–389.

Bissada, K.K., 1982, Geochemical constraints on petroleum generation and migration—a review: *Proceedings ASCOPE'81*, p. 69–87.

Bloesch, J., P. Stadelman, and H. Buhner, 1977, Primary production, mineralization, and sedimentation in the euphotic zone of two Swiss lakes: *Limnology and Oceanography*, v. 22, p. 511–526.

Borowitzka, L.J., 1981, The microflora—adaptions to life in extremely saline lakes: *Hydrobiologia*, v. 81, p. 33–46.

Bradley, W.H., 1948, *Limnology and the Eocene lakes of the Rocky Mountain region*: Geological Society of America Bulletin, v. 59, p. 635–648.

Brook, A.J., 1965, Planktonic algae as indicators of lake types, with special reference to *Desmidiaceae*: *Limnology and Oceanography*, v. 10, p. 403–411.

Brunskill, G.J., and S.D. Ludlam, 1969, Fayetteville Green Lake, New York. I. Physical and chemical

limnology: *Limnology and Oceanography*, v. 14, p. 817–829.

Brylinsky, M., and K.H. Mann, 1973, An analysis of factors governing productivity in lakes and reservoirs: *Limnology and Oceanography*, v. 18, p. 1–14.

Budyko, M.I., A.B. Ronov, and A.L. Yanshin, 1985, *History of the Earth's atmosphere*: Berlin, Springer-Verlag, 139 p.

Burns, N.M., and C. Ross, 1971, Nutrient relationships in the stratified eutrophic lake: *Proceedings 14th Conference on Great Lakes Research*, University of Michigan Great Lakes Research Division Publication, p. 749–760.

Cecil, C.B., 1990, Paleoclimate controls on stratigraphic repetition of chemical and siliciclastic rocks: *Geology*, v. 18, p. 533–536.

Coulter, G.W., 1963, Hydrological changes in relation to biological production in southern Lake Tanganyika: *Limnology and Oceanography*, v. 8, p. 463–477.

Daly, M.C., M.A. Cooper, I. Wilson, D.G. Smith, and B.G.D. Hooper, 1991, Cenozoic plate tectonics and basin evolution in Indonesia: *Marine and Petroleum Geology*, v. 8, p. 2–21.

Davies, P.R., 1984, Tertiary structural evolution and related hydrocarbon occurrences, North Sumatra basin: *Proceedings Annual Convention 13th Indonesian Petroleum Association*, v. 1, p. 19–49.

Dean, W.E., 1981, Carbonate minerals and organic matter in sediments of modern north temperate hard-water lakes, in F.G. Ethridge and R.M. Flores,

- eds., Recent and Ancient Nonmarine Depositional Environments—Models for Exploration: SEPM Special Publication 31, p. 213–231.
- de Coster, G.L., 1974, The geology of the central and south Sumatra basins: Proceedings Annual Convention 3rd Indonesian Petroleum Association, p. 77–110.
- Degens, E.T., R.P. Von Herzen, H.W. Wong, W.G. Deuser, and H.W. Jannasch, 1973, Lake Kivu—structure, chemistry and biology of an east African rift lake: *Geologische Rundschau*, v. 62, p. 245–277.
- Demaison, G., 1991, Anoxia vs. productivity: what controls the formation of organic carbon-rich sediments and sedimentary rocks?: discussion: *AAPG Bulletin*, v. 75, p. 499.
- Demaison, G.J., and G.T. Moore, 1980, Anoxic environments and source bed genesis: *AAPG Bulletin*, v. 64, p. 1179–1209.
- Demaison, G.J., A.J.J. Holck, R.W. Jones, and G.T. Moore, 1984, Predictive source bed stratigraphy. A guide to regional petroleum occurrence: Proceedings 11th World Petroleum Congress, v. 2, p. 17–29.
- Feth, J.H., 1964, Review and annotated bibliography of ancient lake deposits (Precambrian to Pleistocene) in the western states: U.S. Geological Survey Bulletin 1080, 119 p.
- Finney, B.P., and T.C. Johnson, 1991, Sedimentation in Lake Malawi (East Africa) during the past 10,000 years: a continuous paleoclimatic record from the southern tropics: *Palaeogeography, Palaeoclimatology, Palaeoecology*, v. 85, p. 351–366.
- Fu Jiamo, Sheng Guoying, Xu Jiayou, G. Eglinton, A.P. Gower, Jia Rongfen, Fan Shanfa, and Pang Pingan, 1990, Application of biological markers in the assessment of paleoenvironments of Chinese non-marine sediments: *Organic Geochemistry*, v. 16, p. 769–779.
- Gore, P.J.W., 1989, Toward a model for open- and closed-basin deposition in ancient lacustrine sequences: the Newark Supergroup (Triassic–Jurassic), eastern North America: *Palaeogeography, Palaeoclimatology, Palaeoecology*, v. 70, p. 29–51.
- Gorham, E., J.W.G. Lund, J.E. Sanger, and W.E. Dean, Jr., 1974, Some relationships between algal standing crop, water chemistry and sediment chemistry in the English lakes: *Limnology and Oceanography*, v. 19, p. 601–617.
- Grande, L., 1980, Paleontology of the Green River Formation, with a review of the fish fauna: *Geological Survey of Wyoming Bulletin* 63, 333 p.
- Green, J., S.A. Corbet, E. Watts, and O.B. Lan, 1976, Ecological studies on Indonesian lakes—overturn and restratification of Ranau Lamongan: *Journal of Zoology*, London, v. 180, p. 315–353.
- Haberyan, K.A., and R.E. Hecky, 1987, The late Pleistocene and Holocene stratigraphy and paleolimnology of Lakes Kivu and Tanganyika: *Palaeogeography, Palaeoclimatology, Palaeoecology*, v. 61, p. 169–197.
- Håkanson, L., and M. Jansson, 1983, Principles of lake sedimentology: New York, Springer-Verlag, 316 p.
- Halbouty, M.T., 1980, Methods used, and experience gained in exploration for new oil and gas in highly explored (mature) areas: *AAPG Bulletin*, v. 64, p. 1210–1222.
- Hammer, U.T., 1981, Primary production in saline lakes—a review: *Hydrobiologia*, v. 81, p. 47–57.
- Harrison, C.G.A., G.W. Brass, E. Saltzman, J. Sloan, II, J. Southam, and J.M. Whitman, 1981, Sea level variations, global sedimentation rates and the hypsographic curve: *Earth and Planetary Science Letters*, v. 54, p. 1–16.
- Hay, W.W., J.F. Behensky, E.J. Barron, and J.L. Sloan, 1982, Late Triassic–Liassic paleoclimatology of the proto-central North Atlantic rift system: *Palaeogeography, Palaeoclimatology, Palaeoecology*, v. 40, p. 13–30.
- Hay, W.W., E.J. Barron, and S.L. Thompson, 1990, Results of global atmospheric experiments on an earth with a meridional pole-to-pole continent: *Journal Geological Society (London)*, v. 147, p. 385–392.
- Hecky, R.E., and E.T. Degens, 1973, Late Pleistocene–Holocene chemical stratigraphy and paleolimnology of the rift valley lakes of Central Africa: Woods Hole Oceanographic Institution Technical Report 73–28, 93 p.
- Hecky, R.E., and H.J. Kling, 1981, The phytoplankton and protozooplankton of the euphotic zone of Lake Tanganyika: species composition, biomass, chlorophyll content and spatio-temporal distribution: *Limnology and Oceanography*, v. 26, p. 548–564.
- Huc, A.Y., J. Le Fournier, M. Vandenbroucke, and G. Bessereau, 1990, Northern Lake Tanganyika—an example of organic sedimentation in an anoxic rift lake, in B.J. Katz, ed., *Lacustrine Basin Exploration—Case Studies and Modern Analogs: AAPG Memoir* 50, p. 169–185.
- Hutchison, C.S., 1989, *Geological evolution of South-East Asia*: New York, Clarendon Press, Oxford Monograph on Geology and Geophysics, 368 p.
- Hutchinson, G.E., 1957, *A treatise on limnology—geography, physics and chemistry*: New York, John Wiley, v. 1, 1015 p.
- Jannasch, H.W., 1975, Methane oxidation in Lake Kivu (Central Africa): *Limnology and Oceanography*, v. 20, p. 860–864.
- Jones, R.W., 1987, Organic facies, in J. Brooks and D. Welte, eds., *Advances in Petroleum Geochemistry*: London, Academic Press, v. 2, p. 1–90.
- Kalff, J., 1983, Phosphorus limitation in some tropical African lakes: *Hydrobiologia*, v. 100, p. 101–112.
- Katz, B.J., 1988, Clastic and carbonate lacustrine systems—an organic geochemical comparison (Green River Formation and East African lake sediments), in A.J. Fleet, K. Kelts, and M.R. Talbot, eds., *Lacustrine Petroleum Source Rocks: Geological Society of London Special Publication* 40, p. 81–90.
- Katz, B.J., 1990, Controls on distribution of lacustrine source rocks through time and space, in B.J. Katz, ed., *Lacustrine Basin Exploration—Case Studies and Modern Analogs: AAPG Memoir* 50, p. 61–76.
- Katz, B.J., and G.M. Kahle, 1988, Basin evaluation—a supply-side approach to resource assessment: Proceedings 17th Annual Convention Indonesian

- Petroleum Association, v. 1, p. 135–168.
- Katz, B.J., and B. Mertani, 1989, Central Sumatra—a geochemical paradox: Proceedings 18th Annual Convention Indonesian Petroleum Association, v. 1, p. 403–425.
- Kelts, K., 1988, Environments of deposition of lacustrine petroleum source rocks—an introduction, in A.J. Fleet, K. Kelts, and M.R. Talbot, eds., *Lacustrine Petroleum Source Rocks: Geological Society of London Special Publication 40*, p. 3–26.
- Kinsman, D.J.J., M. Boardman, and M. Borcsik, 1974, An experimental determination of the solubility of oxygen in marine brines, in A.H. Coogan, ed., *Proceedings Fourth Symposium on Salt: Northern Ohio Geological Society*, v. 1, p. 325–327.
- Krey, J., 1970, Die urproduktion des meeres, in G. Diefrich, ed., *Erforschung des Meeres: Frankfurt, Umschau*, p. 189–195.
- Krissek, L.A., and K.F. Scheidegger, 1983, Environmental controls on sediment texture and composition in low oxygen zones off Peru and Oregon, in J. Theide and E. Suess, eds., *Coastal Upwelling—Its Sediment Record: New York, Plenum Press*, pt. B, p. 163–180.
- Lambiase, J.J., 1990, A model for tectonic control of lacustrine stratigraphic sequences in continental rift basins, in B.J. Katz, ed., *Lacustrine Basin Exploration—Case Studies and Modern Analogs: AAPG Memoir 50*, p. 265–286.
- Lewan, M.D., 1984, Factors controlling the proportionality of vanadium to nickel in crude oils: *Geochimica et Cosmochimica Acta*, v. 48, p. 2231–2238.
- Likens, G.E., 1975, Primary production of inland aquatic ecosystems, in H. Lieth and R.H. Whittaker, eds., *Primary Productivity of the Biosphere: New York, Springer-Verlag*, p. 186–215.
- Livingstone, D.A., and J.M. Melack, 1984, Some lakes of the subsaharan Africa, in F.B. Taub, ed., *Lakes and Reservoirs, Ecosystems of the World: Amsterdam, Elsevier*, p. 467–497.
- Longley, I.M., R. Barraclough, M.A. Briden, and S. Brown, 1990, Pematang lacustrine petroleum source rocks from the Malacca Strait PSC, central Sumatra, Indonesia: Proceedings 19th Annual Convention Indonesian Petroleum Association, v. 1, p. 279–297.
- Manabe, S., and D.G. Hahn, 1977, Simulation of the tropical climate of an ice age: *Journal of Geophysical Research*, v. 82, p. 3889–3911.
- Meissner, F.F., J. Woodward, and J.L. Clayton, 1984, Stratigraphic relationships and distribution of source rocks in the greater Rocky Mountain region, in J. Woodward, F.F. Meissner, and J. L. Clayton, eds., *Hydrocarbon Source Rocks of the Greater Rocky Mountain Region: Rocky Mountain Association of Geologists*, p. 1–34.
- Mello, M.R., and J.R. Maxwell, 1990, Organic geochemical and biological marker characterization of source rocks and oils derived from lacustrine environments in the Brazilian continental margin, in B.J. Katz, ed., *Lacustrine Basin Exploration—Case Studies and Modern Analogs: AAPG Memoir 50*, p. 77–97.
- Mello, M.R., P.C. Gaglianone, S.C. Brassell, and J.R. Maxwell, 1988, Geochemical and biological marker assessment of depositional environments using Brazilian offshore oils: *Marine and Petroleum Geology*, v. 5, p. 205–223.
- Mello, M.R., W.U. Mohriak, A.M. Koutsoukos, and J.C.A. Figueira, 1991, Brazilian and west African oils: Generation, migration, accumulation and correlation: Proceedings 13th World Petroleum Congress, v. 2, p. 153–164.
- Moldowan, J.M., and W.K. Seifert, 1980, First discovery of botryococcane in petroleum: *Journal of the Chemical Society, Chemical Communications*, p. 912–914.
- Morley, R.J., and J.R. Flenley, 1987, Late Cainozoic vegetational and environmental changes in the Malay Archipelago, in T.C. Whitmore, ed., *Biogeographical Evolution of the Malay Archipelago: New York, Clarendon Press, Oxford Monograph on Biogeography*, v. 4, p. 50–59.
- Mortimer, C.H., 1956, The oxygen content of air-saturated freshwaters, and aids in calculating percentage saturation, in *Verhandlungen der Internationalen Vereinigung für Theoretische und Angewandte Limnologie: Stuttgart*, E. Schweizerbart'sche Verlagsbuchhandlung, v. 6, 20 p.
- National Petroleum Council, 1973, U.S. energy outlook—oil shale availability: Oil Shale Task Group of the Other Energy Resources Subcommittee of the National Petroleum Council's Committee on U.S. Energy Outlook, 87 p.
- Nealson, K.H., 1982, Microbiological oxidation and reduction of iron, in H.D. Holland and M. Schidlowski, eds., *Mineral Deposits and the Evolution of the Biosphere: New York, Springer-Verlag*, p. 51–64.
- Ochumba, P.B.O., and D.I. Kibaara, 1989, Observations on blue-green algal blooms in the open waters of Lake Victoria, Kenya: *African Journal of Ecology*, v. 27, p. 23–34.
- Olsen, P.E., 1990, Tectonic, climatic, and biotic modulation of lacustrine ecosystems—examples from Newark Supergroup of eastern North America, in B.J. Katz, ed., *Lacustrine Basin Exploration—Case Studies and Modern Analogs: AAPG Memoir 50*, p. 209–224.
- Pearsall, W.H., 1921, A suggestion as to factors influencing the distribution of free-floating vegetation: *Journal of Ecology*, v. 9, p. 241–253.
- Pedersen, T.F., and S.E. Calvert, 1990, Anoxia vs. productivity: what controls the formation of organic-carbon-rich sediments and sedimentary rocks?: *AAPG Bulletin*, v. 74, p. 454–466.
- Pedersen, T.F., and S.E. Calvert, 1991, Anoxia vs. productivity: what controls the formation of organic-carbon-rich sediments and sedimentary rocks?: reply: *AAPG Bulletin*, v. 75, p. 500–501.
- Peters, K.E., 1986, Guidelines for evaluating petroleum source rock using programmed pyrolysis: *AAPG Bulletin*, v. 70, p. 318–329.
- Picard, M.D., and L.R. High, Jr., 1981, Physical stratigraphy of ancient lacustrine deposits, in F.G.

- Ethridge and R.M. Flores, eds., Recent and Ancient Nonmarine Depositional Environments—Models for Exploration: SEPM Special Publication 31, p. 233–259.
- Porter, K.G., 1976, Enhancement of algal growth and productivity by grazing zooplankton: *Science*, v. 192, p. 1332–1334.
- Post, F.J., 1977, The microbial ecology of the Great Salt Lake: *Microbial Ecology*, v. 3, p. 143–165.
- Rawson, D.S., 1955, Morphometry as a dominant factor in the productivity of large lakes: *Verhandlungen—Internationale Vereinigung fuer Theoretische und Angewandte Limnologie*, v. 12, p. 164–175.
- Robbins, E.I., 1983, Accumulation of fossil fuels and metallic minerals in active and ancient rift lakes: *Tectonophysics*, v. 94, p. 633–658.
- Ronov, A.B., 1958, Organic carbon in sedimentary rocks (in relation to presence of petroleum): *Geochemistry*, v. 5, p. 510–536 (English translation).
- Rose, R., and P. Hartono, 1978, Geological evolution of the Tertiary Kutei-Melawi basin, Kalimantan, Indonesia: *Proceedings 7th Annual Convention Indonesian Petroleum Association*, p. 225–251.
- Saikia, M.M., and T.K. Dutta, 1980, Depositional environments of source beds of high-wax oils in Assam basin, India: *AAPG Bulletin*, v. 64, p. 427–430.
- Schoell, M., K. Tietze, and S.M. Schoberth, 1988, Origin of methane in Lake Kivu (east-central Africa): *Chemical Geology*, v. 71, p. 257–265.
- Serruya, C., and U. Pollinger, 1983, *Lakes of the warm belt*: Cambridge, Cambridge University Press, 569 p.
- Skullberg, O.M., G.A. Codd, and W.E. Carmichael, 1984, Toxic blue-green algal blooms in Europe: a growing problem: *Ambio*, v. 13, p. 244–247.
- Street, F. A., and A.T. Grove, 1979, Global maps of lake-level fluctuations since 30,000 yr B.P.: *Quaternary Research*, v. 12, p. 83–118.
- Talbot, M.R., 1988, The origins of lacustrine oil source rocks: evidence from the lakes of tropical Africa, *in* A.J. Fleet, K. Kelts, and M.R. Talbot, eds., *Lacustrine Petroleum Source Rocks*: Geological Society of London Special Publication 40, p. 3–26.
- Talbot, M.R., and D.A. Livingstone, 1989, Hydrogen index and carbon isotopes of lacustrine organic matter as a lake level indicator: *Palaeogeography, Palaeoclimatology, Palaeoecology*, v. 70, p. 121–137.
- Talling, J.F., 1960, Self-shading effects in natural populations of a planktonic diatom: *Wetter und Leben*, v. 12, p. 235–242.
- Tietze, K., M. Geyh, H. Müller, L. Schröder, W. Stahl, and H. Wehner, 1980, The genesis of the methane in Lake Kivu (central Africa): *Geologische Rundschau*, v. 69, p. 452–472.
- Tissot, B.P., and D.H. Welte, 1984, *Petroleum formation and occurrence*: Berlin, Springer-Verlag, 699 p.
- Verbeke, J., 1957, Recherches cologiques sur la faune des grand lacs de l'Est Congo Belge, *in* *Exploration hydrobiologique des Lacs Kivu*, Edouard et Albert (1952–54)—*Résultat scientifiques*: Institut Royal des Science Naturelles, v. 3, 177 p.
- Waples, D.W., 1983, Reappraisal of anoxia and organic richness with emphasis on Cretaceous of North Atlantic: *AAPG Bulletin*, v. 67, p. 963–978.
- Warren, J.K., 1986, Shallow-water evaporite environments and their source rock potential: *Journal of Sedimentary Petrology*, v. 56, p. 442–454.
- Watson, M.P., A.B. Hayward, D.N. Parkinson, and Z. Zhang, 1987, Plate tectonic history, basin development and petroleum source rock deposition onshore China: *Marine and Petroleum Geology*, v. 4, p. 205–225.
- Wetzel, A., 1983, Biogenic sedimentary structures in a modern upwelling region: northwest African continental margin, *in* J. Theide and E. Suess, eds., *Coastal Upwelling—Its Sediment Record*: New York, Plenum Press, pt. B, p. 123–144.
- Whiticar, M.J., E. Faber, and M. Schoell, 1986, Biogenic methane formation in marine and freshwater environments—CO₂ reduction vs. acetate fermentation-isotope evidence: *Geochimica et Cosmochimica Acta*, v. 50, p. 693–709.
- Williams, H.H., P.A. Kelley, J.S. Janks, and R.M. Christensen, 1985, The Paleogene rift basin source rocks of central Sumatra: *Proceedings 14th Annual Indonesian Petroleum Association*, v. 2, p. 57–90.
- Ziegler, A.M., C.R. Scotese, and S.F. Barrett, 1983, Mesozoic and Cenozoic paleogeographic maps, *in* P. Brosche and J. Sündermann, eds., *Tidal Friction and the Earth's Rotation II*: Berlin, Springer-Verlag, p. 240–252.

Organic Geochemistry of Paleodepositional Environments with a Predominance of Terrigenous Higher-Plant Organic Matter

Gary H. Isaksen

*Exxon Production Research Company
Houston, Texas, U.S.A.*

ABSTRACT

This study examines the molecular geochemistry of depositional environments with a predominance of terrigenous higher-plant organic matter. All analyses have been performed on thermally immature to early mature rocks in order to constrain molecular observations to organic facies and minimize any overprint by higher thermal maturity. Such studies, performed on rock samples, also enable calibration to optical (lithology and kerogen) and pyrolysis data, obviously not possible from oil studies. In general, these samples are characterized by high pristane/phytane ratios, strong predominance of odd-carbon *n*-alkanes, resin signatures among tricyclics, predominance of C₂₉ regular steranes, hopane/sterane ratios up to 25, consistently low concentrations of homo-hopanes, and relatively high concentrations of oleanane in samples with high contents of angiosperm debris. Most samples were found to contain C₂₄ tetracyclic terpanes, whereas C₃₀ pentacyclic compounds, such as C₃₀ 17 α (H) diahopane, were present only in some samples. The aromatic fractions were characterized by relatively high contents of cadalene, agathalene, and retene components. P₂ pyrograms from programmed pyrolysis-GC displayed high contents of aromatics derived from the polycondensed aromatic network in lignins and tannins of higher plants. The oil-generative potential of these rocks is primarily a function of the kerogens content of high molecular weight (C₂₀₊) aliphatic hydrocarbons and hydrogen content.

INTRODUCTION

In oil and gas exploration, geochemistry can provide information on the organic matter types which have generated hydrocarbons, as well as their thermal maturity and postgenerative alteration processes. The understanding of these processes enables one to perform meaningful oil-oil or oil-source correlations.

Since each depositional environment/organic facies has characteristic geochemical properties which are controlled by physio-chemical conditions (e.g., oxygen level and salinity) and organism population, we can use biomarkers for such assessments. Studies by Moldowan et al. (1985), Philp and Gilbert (1986), Alexander et al. (1988), and Mello et al. (1988) have demonstrated the utility of biomarkers as organic

facies indicators. The objectives of this study have been to investigate the geochemical character of depositional environments with a predominance of terrigenous higher-plant organic matter. The prerequisites for this approach are:

1. All analytical work has been performed on rock samples in order to support and calibrate molecular observations with optical and bulk-pyrolysis data.

2. The rock samples were selected as "end members" with respect to their organic matter content, that is, they contain little organic matter variability.

3. The rock samples have not experienced a high degree of thermal stress. Immature to early mature samples display molecular distributions inherent with the organic matter, and have little or no overprint of maturity-related molecular conversions.

4. The rock samples are without any hydrocarbon staining.

5. Conventional core, sidewall core, or unweathered outcrop samples have been selected in favor of cuttings or weathered outcrop samples.

The observations and discussions in this report are based on the 58 rock samples listed in Table 1.

OVERVIEW OF GEOLOGICAL SETTING

The following provides a brief overview of the geology and the paleogeographic control in the areas most heavily sampled for this study.

Sumatra

Coarse clastics deposited mostly subaerially as alluvial fans and braided streams dominated the south Sumatra area during the late Eocene to early Oligocene. These sediments postdate a marked unconformity on pre-Tertiary basement. As a result of the early Oligocene regional marine transgression, delta-plain, delta-front, and marine deposits dominated the area and comprise the Upper Lahat and Talang Akar formations. Coals and shales of the Talang Akar Formation are thought to be the principal source of hydrocarbons in south Sumatra (Suseno et al., 1992). The samples in this study were collected from a lower Miocene continental delta-plain to paralic depositional environment. Time-equivalent sediments in central Sumatra belong to the Pematang Group, also deposited in a fluvio-deltaic environment (Williams et al., 1985). Further details on the geology of central and south Sumatra are documented in de Coster (1975).

Haltenbanken, Norwegian Sea

The Haltenbanken area is located between 64° and 65°30'N, approximately 250 km offshore the Norwegian mainland. During the latest Triassic through Middle Jurassic the area was dominated by regionally extensive deltaic to shallow-marine depositional environments. The samples selected for this study are from the Lower Jurassic Aare Formation, also referred to as the "coal unit." This formation is regionally extensive, up to 500 m thick, and consists of shales, coals, and

sandstones deposited in deltaic, paralic, and shallow-marine environments (Heum et al., 1986). The sediments of the Aare Formation are of similar facies and time equivalent with the Kap Stewart Formation of eastern Greenland and with the Statfjord Formation in the North Sea.

Hammerfest Basin, Southwestern Barents Sea

Samples were selected from the Late Permian strata of well 7120/12-4 on the Troms-Finnmark Platform in the southern part of the Hammerfest Basin. This area was dominated by clastic sedimentation as a result of an uplift of the land areas to the south and east (Ronnevik et al., 1982). The siltstones and silty shales selected contain woody-herbaceous and amorphous organic matter.

Jameson Land, East Greenland

Along the coast of east Greenland, outcrops of Jurassic age are widely distributed from 70°30'N to 77°N. These rocks are collectively referred to as the Jameson Land Group. The samples selected for this study are from the lowermost Sortehat Member of the Vardekloft Formation (Bajocian age) and are dominated by a very uniform sequence of dark-gray to black, finely laminated, silty micaceous shales, up to 100 m thick. They represent a shallow-marine shelf facies from a prograding shoreline and are rich in woody-herbaceous and coaly organic matter (Surlyk, 1978).

EXPERIMENTAL AND ANALYTICAL PROCEDURES

Paleogeographic knowledge of the depositional environments within various basins was the first basis for sample selection. Analytical screening through Rock-Eval pyrolysis and visual kerogen assessment allowed selection of nonstained samples rich in terrigenous higher-plant organic matter. Solvent extraction was carried out in a Tecator extraction system with a mixture of dichloromethane : methanol at a ratio of 9:1. Analytical standards (saturates and aromatics) were added to some of the samples after de-asphalting to allow quantitative biomarker analyses. Solvent extracts from samples with high sulfur contents were exposed to HCl-activated copper to remove free sulfur. The pentane-soluble fraction remaining after de-asphalting was separated into saturate, aromatic, and NSO (polar) fractions by a Waters High-Performance Liquid Chromatography (HPLC) system controlled by a Dynamic Solutions Maxima 820 datasystem and workstation. Saturate and aromatic hydrocarbon fractions were analyzed by gas chromatography (GC) on Carlo Erba Fractovap and Mega gas chromatographs equipped with an on-column injector and fitted with a 30-m Restec RTX-5 column for the saturate analyses and a 60-m Restec RTX-5 column for the aromatic analyses. Temperature programs were set to run from 75° to 305°C at a ramp rate of 2.5°C per min and held constant at 305°C for 18 min for both saturates and aromatics. Helium was employed

as a carrier gas. External standards were run at regular intervals to allow semiquantitation and instrument-performance control. Gas chromatography/mass spectrometry (GC/MS) analyses of the saturate hydrocarbon fractions were carried out on an Extrel EI/CI quadrupole with a Teknivent data system. Ionization levels were set at 70 eV, whereas the temperature program was the same as for the GC analyses mentioned above. The aromatic hydrocarbon fractions underwent GC/MS analyses on a Hewlett Packard 5970-B MSD quadrupole with an HP Chem-station. All saturate and aromatic analyses were carried out through selected ion monitoring (SIM), whereas some samples were re-run under full-scan conditions in order to identify certain compounds. Helium was employed as a carrier gas. GC/MS analyses employed external standards (all samples) and surrogate standards (selected samples) to enable quantification of biomarkers. Peak identities were established by GC retention times and mass spectral examination.

RESULTS AND DISCUSSION

Optical Analyses

Visual kerogen analyses were performed on the float-and-sink fractions of the kerogen following demineralization. Results are tabulated in Table 1. The typical view of the kerogen through transmitted light microscopy is one of larger structured woody fragments clearly showing plant cell compartments. In some cases, fungal attack on the woody debris was also observed. Most visual kerogen descriptions do not necessarily capture the broad variety in chemical properties which may exist for the different macerals. Therefore, even though two samples may be described as containing 100% woody organic matter the chemi-

cal composition from pyrolysis may be different, as discussed below. Table 1 also lists the thermal alteration indices (TAI) representative of the yellow to orange-brown to black color changes of organic matter that result from thermal alteration (Staplin, 1969; Burgess, 1974; Tissot et al., 1974). Vitrinite reflectance measurements (Table 1) on the population interpreted to be autochthonous range from 0.3% to 0.5% R_o . This corresponds to a thermally immature to early mature state prior to any significant thermal breakdown of kerogen and hydrocarbon generation.

Bulk Properties

Total organic carbon contents range upward to 19% (weight) for the carbonaceous shales and up to 55% for the coaly shales. Hydrogen indices (HI) range from 100 to 400 (Figure 1), with samples from Haltenbanken, Hammerfest Basin, and south Sumatra all displaying values in the 300–400 range. This indicates some liquid potential for these rocks upon maturation. However, the HI may not reflect the oil versus gas expulsion potential of kerogen dominated by woody and herbaceous organic matter; it is synonymous only with potential yield (Espitalié et al., 1977; Horsfield, 1984).

Molecular Geochemistry

Pyrolysis–Gas Chromatography

Pyrolysis–gas chromatography (Py-GC) of whole rock and isolated terrigenous higher-plant kerogen samples typically displays a high content of aromatic hydrocarbons (Figure 2A) in contrast to algal kerogen (Figure 2B). Higher-plant organic matter is dominated by carbohydrates and lignin. Because of its chemical structure, lignin is less susceptible to microbial degradation than carbohydrates, resulting in a high content of aromatic compounds. This was first observed by Bordenave et al.

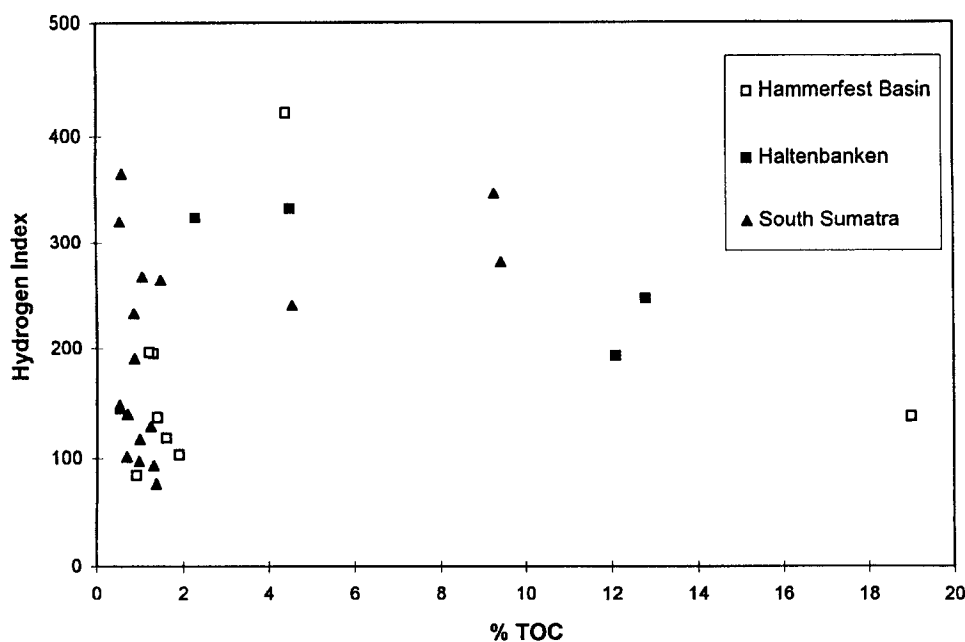


Figure 1. Organic matter quality, as measured by % total organic carbon (TOC) and hydrogen index (HI) (mg hydrocarbons/g organic carbon), for samples from Hammerfest Basin (SW Barents Sea), Haltenbanken (offshore mid-Norway), and south Sumatra.

Table 1. Location and analytical data for samples studied.

| Smpl. | Country/ Area | Basin | Well Name | Fm./ Mbr. | Age | Depth (m) | Lithology | Sample Type | TOC (% wt.) |
|-------|------------------|-----------------|------------------|--------------|----------------|--------------|-------------|----------------|----------------|
| 1 | East Greenland | Jameson Land | Shallow Drilling | Vardekloft | Bath.-Oxf. | Outcrop | Shale | Outcrop | 2.10 |
| 2 | East Greenland | Jameson Land | Shallow Drilling | Vardekloft | Bath.-Oxf. | Outcrop | Shale | Outcrop | 0.62 |
| 3 | East Greenland | Jameson Land | Shallow Drilling | Vardekloft | Bath.-Oxf. | Outcrop | Shale | Outcrop | 1.00 |
| 4 | East Greenland | Jameson Land | Shallow Drilling | Vardekloft | Bath.-Oxf. | Outcrop | Shale | Outcrop | 0.97 |
| 5 | East Greenland | Jameson Land | Shallow Drilling | Vardekloft | Bath.-Oxf. | Outcrop | Shale | Outcrop | 2.77 |
| 6 | East Greenland | Jameson Land | Shallow Drilling | Vardekloft | Bath.-Oxf. | Outcrop | Shale | Outcrop | 2.24 |
| 7 | East Greenland | Jameson Land | Shallow Drilling | Vardekloft | Bath.-Oxf. | Outcrop | Shale | Outcrop | 1.00 |
| 8 | East Greenland | Jameson Land | Shallow Drilling | Vardekloft | Bath.-Oxf. | Outcrop | Shale | Outcrop | 0.35 |
| 9 | East Greenland | Jameson Land | Shallow Drilling | Vardekloft | Bath.-Oxf. | Outcrop | Shale | Outcrop | 0.74 |
| 10 | Norway | Hammerfest | 7120/12-4 | Vardekloft | Late Permian | 1695 | Siltstone | Cuttings | 1.30 |
| 11 | Norway | Hammerfest | 7120/12-4 | | Late Permian | 1755 | Siltstone | Cuttings | 0.90 |
| 12 | Norway | Hammerfest | 7120/12-4 | | Late Permian | 1800 | Silty Shale | Cuttings | 1.60 |
| 13 | Norway | Hammerfest | 7120/12-4 | | Late Permian | 1830 | Silty Shale | Cuttings | 19.00 |
| 14 | Norway | Hammerfest | 7120/12-4 | | Late Permian | 1845 | Silty Shale | Cuttings | 1.90 |
| 15 | Norway | Hammerfest | 7120/12-4 | | Late Permian | 1950 | Silty Shale | Cuttings | 1.40 |
| 16 | Norway | Hammerfest | 7120/12-4 | | Late Permian | 1965 | Silty Shale | Cuttings | 1.20 |
| 17 | Norway | Hammerfest | 7120/10-1 | | Late Permian | 1600 | Shale | Cuttings | 4.41 |
| 18 | Norway | Haltenbanken | 6407/7-1 | Aare | Early Jurassic | 3072 | Shale | Conv. Core | 12.10 |
| 19 | Norway | Haltenbanken | 6407/7-1 | Aare | Early Jurassic | 3039 | Coaly Shale | Conv. Core | 55.10 |
| 20 | Norway | Haltenbanken | 6507/12-1 | Aare | Early Jurassic | 2708 | Shale | Conv. Core | 12.80 |
| 21 | Norway | Haltenbanken | 6407/1-2 | Aare | Early Jurassic | 3655 | Silty Shale | Cuttings | 2.30 |
| 22 | Norway | Haltenbanken | 6407/1-2 | Aare | Early Jurassic | 1600 | Silty Shale | Conv. Core | 4.50 |
| 23 | Sumatra | Central Sumatra | EK-26 | | Tertiary | 1033.0 | Shale | Conv. Core | 4.30 |
| 24 | Sumatra | Central Sumatra | EK-26 | | Tertiary | 1069.5 | Shale | Conv. Core | 3.90 |
| 25 | Sumatra | Central Sumatra | KA-1 | | Tertiary | 1078.4 | Shale | SWC | 2.10 |
| 26 | Sumatra | Central Sumatra | KA-18 | | Tertiary | 1100.3 | Shale | SWC | 7.00 |
| 27 | Sumatra | South Sumatra | Musi-10 | Talang Akar | Olig.-Miocene | 1276.5 | Silty Shale | SWC | 0.96 |
| 28 | Sumatra | South Sumatra | Musi-10 | Talang Akar | Olig.-Miocene | 1301.5 | Shale | SWC | 1.48 |
| 29 | Sumatra | South Sumatra | Musi-10 | Talang Akar | Olig.-Miocene | 1363.1 | Shale | SWC | 1.30 |
| 30 | Sumatra | South Sumatra | Musi-10 | Talang Akar | Olig.-Miocene | 1428.0 | Silty Shale | SWC | 1.36 |
| 31 | Sumatra | South Sumatra | Musi-10 | Talang Akar | Olig.-Miocene | 1480.7 | Silty Shale | SWC | 1.98 |
| 32 | Sumatra | South Sumatra | Musi-10 | Talang Akar | Olig.-Miocene | 1523.4 | Siltstone | SWC | 1.52 |
| 33 | Sumatra | South Sumatra | Musi-10 | Talang Akar | Olig.-Miocene | 1540.8 | Silty Shale | SWC | 1.54 |
| 34 | Sumatra | South Sumatra | Pabil-3 | Talang Akar | Olig.-Miocene | 678.5 | Silty Shale | SWC | 1.86 |
| 35 | Sumatra | South Sumatra | Pabil-3 | Talang Akar | Olig.-Miocene | 998.8 | Silty Shale | SWC | 1.24 |
| 36 | Sumatra | South Sumatra | Pabil-3 | Talang Akar | Olig.-Miocene | 1028.4 | Silty Shale | SWC | 1.05 |
| 37 | Sumatra | South Sumatra | Pabil-3 | Talang Akar | Olig.-Miocene | 1058.6 | Silty Shale | SWC | 1.85 |

Table 1 (continued).

| Smpl. | Country/ Area | Basin | Well Name | Fm./ Mbr. | Age | Depth (m) | Lithology | Sample Type | TOC (% wt.) |
|-------|------------------|---------------|----------------------|--------------|---------------|--------------|---------------|----------------|----------------|
| 38 | Sumatra | South Sumatra | Talang Gendum | Talang Akar | Olig.-Miocene | 1803.8 | Silty Shale | Conv. Core | 1.60 |
| 39 | Sumatra | South Sumatra | Talang Gendum | Talang Akar | Olig.-Miocene | 1478.0 | Silty Shale | Conv. Core | 9.43 |
| 40 | Sumatra | South Sumatra | Pelawe-1 | Pre-Baturaja | Olig.-Miocene | 1479.8 | Silty Shale | SWC | 4.55 |
| 41 | Sumatra | South Sumatra | Pelawe-1 | Pre-Baturaja | Olig.-Miocene | 1484.7 | Silty Shale | SWC | 9.26 |
| 42 | Sumatra | South Sumatra | Rambutan-1 | Telisa | Early Miocene | 1652.0 | Silty Shale | SWC | 0.68 |
| 43 | Sumatra | South Sumatra | Rambutan-1 | Telisa | Early Miocene | 1825.8 | Silty Shale | SWC | 0.70 |
| 44 | Sumatra | South Sumatra | Rambutan-1 | Telisa | Early Miocene | 1999.5 | Silty Shale | SWC | 0.53 |
| 45 | U.S.A. | North Slope | Pt. Thompson-4 | | Paleocene | 4119.4 | Siltstone | Conv. Core | 1.50 |
| 46 | U.S.A. | North Slope | Pt. Thompson-4 | | Paleocene | 4129.4 | Silty Shale | Conv. Core | 1.33 |
| 47 | U.S.A. | North Slope | Pt. Thompson-4 | | Paleocene | 4132.5 | Siltstone | Conv. Core | 1.40 |
| 48 | U.S.A. | North Slope | Duck Island-3 | | Paleocene | 3109.0 | Silty Shale | Conv. Core | 4.02 |
| 49 | U.S.A. | North Slope | Duck Island-3 | | Paleocene | 3200.4 | Silty Shale | Conv. Core | 6.12 |
| 50 | U.S.A. | North Slope | Alaska State F1 | | Paleocene | 3845.7 | Silty Shale | Conv. Core | 1.54 |
| 51 | U.S.A. | North Slope | Exxon G-2 | | Jurassic | 4576.3 | Silty Shale | Conv. Core | 6.40 |
| 52 | U.S.A. | North Slope | Shallow Drilling | Seabee | | | Silty Shale | Outcrop | |
| 53 | U.S.A. | Gulf Basin | Catherine (Lawrence) | Wilcox | Early Eocene | 1676.4 | Silty Shale | Cuttings | 1.42 |
| 54 | U.S.A. | Gulf Basin | Catherine (Lawrence) | Wilcox | Paleocene | 1886.7 | Coaly Siltst. | Cuttings | 26.66 |
| 55 | U.S.A. | Gulf Basin | Catherine (Lawrence) | Midway | Paleocene | 1914.1 | Silty Shale | Cuttings | 2.30 |
| 56 | U.S.A. | Gulf Basin | Nona (SE Texas) | Yegua | Late Eocene | 3011.4 | Silty Shale | Cuttings | 1.30 |
| 57 | U.S.A. | Gulf Basin | Nona (SE Texas) | Yegua | Late Eocene | 3642.4 | Silty Shale | Cuttings | 1.40 |
| 58 | U.S.A. | Wyoming | Outcrop | | Cretaceous | | Coaly Shale | Outcrop | 38.60 |

Abbreviations used: TOC: Total Organic Carbon; HI: Hydrogen Index; T_{max}: Temperature, maximum; Vitr. Refl.: vitrinite reflectance; TAI: Thermal Alteration Index; Kerogen Composition (W: Woody; H: Herbaceous; C: Coaly; F: Finely Disseminated; I: Inertinite; Am: Amorphous; Al: Algal); Sat.: Saturate Hydrocarbons; Arom.: Aromatic Hydrocarbons; NSO: Polar Heterocompounds containing nitrogen, sulfur, and oxygen functional groups; Asph.: Asphaltenes; Pr/Ph: pristane/phytane; CPI: Carbon Preference Index; C₂₇, C₂₈, and C₂₉: Regular steranes reported in percent and ppm concentrations; H/S: Hopane/Sterane ratio; C₃₀H: concentration of C₃₀ 17 α (H)21 β (H) hopane in ppm of pentane-soluble fraction; Ts/Tm: 18 α (H)-22,29,30-trisnorhopane/17 α (H)-22,29,30-trisnorhopane; MPI-1: Methyl-phenanthrene Index [1.5(3MP+2MP)/(P+9MP+IMP)]; Aga: Agathalene (1,2,5-trimethylnaphthalene); Cad: Cadalene (1,6-dimethyl-4-isopropylnaphthalene); 2MN: 2-methyl naphthalene; n.a.: not available; n.d.p.: no determination possible.

Table 1. Location and analytical data for samples studied (continued).

| Sample | HI | T _{max} (°C) | Vitr. Refl. (%) | TAI | Kerogen Comp. | Sat. (%) | Arom. (%) | NSO (%) | Asph. (%) | Pr/Ph | Pr/n-C ₁₇ | CPI | C ₂₇ (%) |
|--------|------|--------------------------|--------------------|--------|------------------|-------------|--------------|------------|--------------|-------|----------------------|-----|------------------------|
| 1 | n.a. | n.a. | 0.35 | 2 | W;H;C | 10.3 | 15.5 | 21.3 | 52.9 | 2 | 0.7 | 1.5 | 22.7 |
| 2 | n.a. | n.a. | 0.45 | 2+ | F;H;Am | 18.7 | 21.3 | 31.3 | 28.7 | 1.3 | 0.6 | 1.8 | 26.3 |
| 3 | n.a. | n.a. | 0.33 | 2+ | W;H;C | 21.2 | 18.3 | 27.3 | 33.3 | 1.9 | 0.8 | 1.9 | 26.9 |
| 4 | n.a. | n.a. | 0.39 | 2+ | W;C;H | 17.3 | 19.1 | 25.3 | 38.3 | 1.9 | 1 | 1.7 | 20.8 |
| 5 | n.a. | n.a. | 0.36 | 2+ | W;H;C | 15.1 | 22.2 | 19 | 43.6 | 2 | 0.9 | 1.7 | 26.3 |
| 6 | n.a. | n.a. | 0.40 | 2+ | W;H;Al? | 10.1 | 31.6 | 21.1 | 37.2 | 2.1 | 0.9 | 1.5 | 24.1 |
| 7 | n.a. | n.a. | 0.39 | 2+ | W;H;C | 10.9 | 29.7 | 22.7 | 36.7 | 2.2 | 1 | 1.5 | 25.7 |
| 8 | n.a. | n.a. | 0.44 | 2+ | W;H;C | 10.5 | 33.3 | 20.5 | 35.7 | 1.9 | 1.4 | 1.6 | 25.2 |
| 9 | n.a. | n.a. | 0.40 | 2+ | W;H;C | 18.5 | 20.1 | 21.8 | 39.6 | 1.8 | 1.3 | 1.5 | 27.3 |
| 10 | 195 | 434 | n.d.p. | n.d.p. | Am;W | 15.4 | 26.9 | 30.8 | 26.9 | 1.9 | 2.3 | 2 | 28.7 |
| 11 | 84 | 435 | n.d.p. | n.d.p. | W;H;Am | 31.8 | 22.7 | 27.3 | 18.2 | 2 | 2.4 | 2.1 | 27.2 |
| 12 | 118 | 433 | n.d.p. | n.d.p. | W;H | 21.4 | 35.7 | 28.6 | 14.3 | 1.9 | 2.5 | 1.9 | 26.8 |
| 13 | 137 | 436 | n.d.p. | n.d.p. | W;Am;H | 13.9 | 19.4 | 23.3 | 43.4 | 2.7 | 2.5 | 1.5 | 27.3 |
| 14 | 103 | 433 | n.d.p. | n.d.p. | W;Am;H | 15.8 | 31.6 | 39.5 | 13.1 | 2.5 | 2.5 | 1.5 | 30.0 |
| 15 | 137 | 437 | n.d.p. | n.d.p. | W;Am;H | 10 | 30 | 50 | 10 | 2.3 | 2.7 | 1.5 | 27.3 |
| 16 | 196 | 436 | n.d.p. | n.d.p. | W;Am;H | 21.9 | 28.1 | 31.3 | 18.7 | 2.3 | 1.7 | 1.6 | 25.8 |
| 17 | 421 | 435 | 0.35 | 2- | W;C;Al | 5.8 | 13.8 | 23.8 | 56.5 | 1.4 | 4.6 | 1.9 | 19.8 |
| 18 | 192 | 440 | 0.46 | 2- | W;H;Am | 21.8 | 16.5 | 38.2 | 23.5 | 2.5 | 1.5 | 1.3 | 21.8 |
| 19 | 67 | 447 | 0.40 | 2- | W;H | 18.2 | 27.2 | 33.3 | 21.3 | 2.5 | 1.2 | 1.3 | 20.4 |
| 20 | 246 | 433 | 0.47 | 2- | H;Am;W | 19.1 | 18.9 | 16.3 | 45.8 | 3.1 | 1.3 | 1.3 | 19.9 |
| 21 | 324 | 432 | n.a. | 2+ | W;F;C | 20.4 | 28.2 | 24.3 | 27 | 2.2 | 1.3 | 1.8 | 19.6 |
| 22 | 333 | 430 | n.a. | 2+ | W;H;C | 25.8 | 25.1 | 18.7 | 30.4 | 2.1 | 1.1 | 1.4 | 20.2 |
| 23 | n.a. | n.a. | n.a. | 2- | W;H;C | 4.1 | 20.7 | 11.2 | 64.0 | 2.8 | 1.9 | 2.1 | 16.5 |
| 24 | n.a. | n.a. | n.a. | 2- | W;H;C | 5.2 | 21.0 | 10.3 | 63.5 | 2.8 | 1.9 | 1.9 | 16.3 |
| 25 | n.a. | n.a. | n.a. | 2- | W;H;C | 30.9 | 12.2 | 23.5 | 33.4 | 2.8 | 2.3 | 1.8 | 17.6 |
| 26 | n.a. | n.a. | n.a. | 2- | W;H;C | 24.7 | 27.4 | 31.9 | 16.1 | 2.7 | 1.8 | 1.8 | 12.6 |
| 27 | 97 | 431 | 0.51 | 2- | W;H | 12.9 | 18.5 | 32.8 | 35.8 | 3.1 | 4.3 | 1.9 | 19.9 |
| 28 | 264 | 442 | 0.71 | 2+ | W;H;C | 14.7 | 20.5 | 16.9 | 48.0 | 2.8 | 4.1 | 2.1 | 21.4 |
| 29 | 93 | 435 | 0.52 | 2- | W;H;C | 15.1 | 23.1 | 21.9 | 39.8 | 3.7 | 4.4 | 2.3 | 17.4 |
| 30 | 76 | 439 | 0.62 | 2 | W;H;C | 5.3 | 22.1 | 15.5 | 57.1 | 3.5 | 4.9 | 2.3 | 16.2 |
| 31 | 117 | 440 | 0.62 | 2 | W;H | 6.0 | 19.1 | 13.3 | 62.2 | 3.0 | 4.3 | 2.2 | 15.6 |
| 32 | 148 | 441 | 0.60 | 2 | W;H | 4.4 | 19.3 | 30.7 | 45.6 | 2.3 | 4.0 | 1.8 | 17.9 |
| 33 | 320 | 439 | 0.64 | 2 | W;H | 12.6 | 23.7 | 19.7 | 43.9 | 2.9 | 3.9 | 1.8 | 17.1 |
| 34 | 190 | 439 | 0.64 | 2 | W;H;C | 7.6 | 26.7 | 18.5 | 47.3 | 2.8 | 4.7 | 1.9 | 15.6 |
| 35 | 129 | 433 | 0.59 | 2 | H;W;C | 13.3 | 24.8 | 18.9 | 43.1 | 2.7 | 4.5 | 2.1 | 20.6 |
| 36 | 267 | 438 | 0.60 | 2 | W;H;Am | 16.8 | 13.6 | 21.6 | 47.9 | 2.7 | 4.5 | 2.5 | 22.0 |
| 37 | 232 | 443 | 0.72 | 2+ | H;Am | 25.0 | 34.2 | 13.6 | 27.1 | 2.7 | 4.0 | 1.5 | 16.8 |

Table 1 (continued).

| Sample | HI | T _{max} (°C) | Vitr. Refl. (%) | TAI | Kerogen Comp. | Sat. (%) | Arom. (%) | NSO (%) | Asph. (%) | Pr/Ph | Pr/n-C ₁₇ | CPI | C ₂₇ (%) |
|--------|------|--------------------------|--------------------|-----|------------------|-------------|--------------|------------|--------------|-------|----------------------|-----|------------------------|
| 38 | 366 | 441 | 0.49 | 2- | W;H;C | 15.1 | 23.1 | 21.9 | 39.8 | 3.4 | 5.3 | 1.3 | 15.9 |
| 39 | 281 | 422 | 0.43 | 2- | W;H;C | 16.9 | 33.9 | 22.6 | 26.6 | 3.7 | 4.8 | 1.3 | 18.6 |
| 40 | 240 | 423 | 0.44 | 2- | W;H;C | 4.5 | 27.3 | 16.5 | 51.7 | 3.8 | 4.8 | 1.3 | 16.1 |
| 41 | 347 | 421 | 0.56 | 2 | W;H;C | 6.7 | 28.9 | 13.6 | 50.8 | 3.1 | 4.9 | 1.3 | 18.3 |
| 42 | 101 | 434 | 0.55 | 2 | W;H;C | 7.9 | 12.9 | 21.5 | 57.7 | 3.2 | 4.9 | 1.5 | 14.1 |
| 43 | 140 | 434 | 0.55 | 2 | W;H;C | 6.9 | 17.8 | 21.0 | 54.4 | 3.5 | 5.2 | 1.7 | 14.3 |
| 44 | 145 | 436 | 0.53 | 2 | W;H;C | 4.3 | 10.1 | 20.3 | 65.3 | 3.5 | 5.1 | 1.5 | 15.4 |
| 45 | n.a. | n.a. | n.a. | 2- | W;H;F | 22.9 | 15.2 | 16.8 | 45.1 | 1.2 | 1.1 | 1.2 | 15.2 |
| 46 | n.a. | n.a. | n.a. | 2- | W;H;C | 10.3 | 8.9 | 15.8 | 64.9 | 1.3 | 2.0 | 1.2 | 17.5 |
| 47 | n.a. | n.a. | n.a. | 2- | H;W;F | 15.8 | 14.7 | 32.5 | 36.9 | 1.7 | 1.2 | 1.1 | 12.5 |
| 48 | n.a. | n.a. | n.a. | 2- | Am;C | 18.7 | 36.3 | 10.2 | 34.7 | 2.0 | 1.7 | 1.5 | 17.7 |
| 49 | n.a. | n.a. | n.a. | 2- | Am;C | 17.2 | 29.7 | 15.1 | 38.0 | 2.1 | 1.7 | 1.4 | 24.1 |
| 50 | n.a. | n.a. | n.a. | 2+ | H;W | 11.4 | 31.7 | 25.9 | 31.0 | 1.7 | 1.5 | 1.3 | 21.1 |
| 51 | n.a. | n.a. | n.a. | 2- | n.a. | 25.3 | 36.1 | 26.6 | 12.0 | 1.9 | 1.4 | 1.3 | n.a. |
| 52 | n.a. | 423 | 0.43 | 2- | n.a. | 9.1 | 8.8 | 26.9 | 55.2 | 1.7 | 1.6 | 1.5 | 27.0 |
| 53 | n.a. | n.a. | n.a. | 2- | W;Am;H | 13.1 | 12.4 | 31.9 | 42.7 | 2.1 | 1.7 | 1.6 | 16.4 |
| 54 | n.a. | n.a. | n.a. | 2- | Am;W;H | 4.1 | 12.9 | 29.7 | 53.2 | 1.0 | 1.8 | 1.6 | 17.7 |
| 55 | n.a. | n.a. | n.a. | 2- | W;H;C | 8.3 | 13.3 | 37.6 | 40.8 | 1.0 | 1.4 | 1.4 | n.a. |
| 56 | n.a. | n.a. | 0.45 | 1+ | W;Al? | 14.4 | 17.8 | 30.0 | 37.8 | 0.7 | 1.3 | 3.0 | 13.4 |
| 57 | n.a. | n.a. | 0.47 | 2+ | W;Al | 16.8 | 11.1 | 19.8 | 52.3 | 0.7 | 0.9 | 2.3 | 13.9 |
| 58 | 289 | 437 | 0.53 | 2+ | n.a. | 21.2 | 21.0 | 33.6 | 24.2 | 0.6 | 0.5 | 2.5 | 15.2 |

Abbreviations used: TOC: Total Organic Carbon; HI: Hydrogen Index; T_{max}: Temperature, maximum; Vitr. Refl.: vitrinite reflectance; TAI: Thermal Alteration Index; Kerogen Composition (W: Woody; H: Herbaceous; C: Coaly; F: Finely Disseminated; I: Inertinite; Am: Amorphous; Al: Algal); Sat.: Saturate Hydrocarbons; Arom.: Aromatic Hydrocarbons; NSO: Polar Hetero-compounds containing nitrogen, sulfur, and oxygen functional groups; Asph.: Asphaltenes); Pr/Ph: pristane/phytane; CPI: Carbon Preference Index; C₂₇, C₂₈ and C₂₉: Regular steranes reported in percent and ppm concentrations; H/S: Hopane/Sterane ratio; C₃₀:H: concentration of C₃₀, 17α(H)21β(H) hopane in ppm of pentane-soluble fraction; Ts/Tm: 18α(H)-22,29,30-tris-norneohopane/17α(H)-22,29,30-trisnorhopane; MPI-1: Methyl-phenanthrene Index [1.5(3MP+2MP)/(P+9MP+1MP)]; Aga: Agathalene (1,2,5-trimethylnaphthalene); Cad: Cadalene (1,6-dimethyl-4-isopropylnaphthalene); 2MN: 2-methyl naphthalene; n.a.: not available; n.d.p.: no determination possible.

Table 1. Location and analytical data for samples studied (*continued*).

| Smpl. | C ₂₈ (%) | C ₂₉ (%) | C ₂₇ (ppm) | C ₂₈ (ppm) | C ₂₉ (ppm) | H/S | C ₃₀ H (ppm) | Oleanane (ppm) | Oleanane (%) | Gamma- cerane (%) | Ts/Tm | MPI-1 | Aga/ (Aga+Cad) | 2MN/ (2MN+Cad) |
|-------|------------------------|------------------------|--------------------------|--------------------------|--------------------------|------|----------------------------|-------------------|-----------------|----------------------|-------|-------|-------------------|-------------------|
| 1 | 20.3 | 57 | 112 | 100 | 281 | 5.3 | 1489 | 0 | 0 | 0.8 | 1.3 | n.a. | n.a. | n.a. |
| 2 | 24.1 | 49.6 | 99 | 91 | 187 | 5.2 | 981 | 0 | 0 | 0.6 | 1.78 | n.a. | n.a. | n.a. |
| 3 | 24.1 | 49.3 | 96 | 87 | 178 | 5 | 888 | 0 | 0 | 0.8 | 2.1 | n.a. | n.a. | n.a. |
| 4 | 20.8 | 58.5 | 100 | 100 | 282 | 4.4 | 1254 | 0 | 0 | 0 | 1.88 | n.a. | n.a. | n.a. |
| 5 | 15.5 | 58.2 | 115 | 68 | 255 | 5.8 | 1486 | 0 | 0 | 0 | 1.56 | n.a. | n.a. | n.a. |
| 6 | 19.1 | 56.7 | 111 | 88 | 261 | 6.4 | 1673 | 0 | 0 | 0 | 1.55 | n.a. | n.a. | n.a. |
| 7 | 23.8 | 50.4 | 98 | 91 | 192 | 8.3 | 1584 | 0 | 0 | 0 | 1.64 | n.a. | n.a. | n.a. |
| 8 | 19.0 | 55.8 | 115 | 87 | 255 | 6 | 1536 | 0 | 0 | 0 | 0.89 | n.a. | n.a. | n.a. |
| 9 | 24.3 | 48.4 | 102 | 91 | 181 | 6.6 | 1198 | 0 | 0 | 0 | 1.2 | n.a. | n.a. | n.a. |
| 10 | 28.1 | 43.3 | 102 | 100 | 154 | 7.9 | 1221 | 0 | 0 | 1.8 | 0.2 | 0.43 | 0.74 | 0.62 |
| 11 | 27.2 | 45.7 | 98 | 98 | 165 | 6 | 995 | 0 | 0 | 2.5 | 0.5 | 0.45 | 0.71 | 0.64 |
| 12 | 27.8 | 45.4 | 99 | 103 | 168 | 6 | 1008 | 0 | 0 | 1.8 | 0.4 | 0.48 | 0.73 | 0.65 |
| 13 | 24.3 | 48.4 | 111 | 99 | 197 | 7.2 | 1421 | 0 | 0 | 3 | 0.43 | 0.51 | 0.73 | 0.83 |
| 14 | 28.7 | 41.3 | 121 | 116 | 167 | 8.4 | 1399 | 0 | 0 | 2.5 | 0.35 | 0.59 | 0.72 | 0.78 |
| 15 | 28.9 | 43.8 | 108 | 114 | 173 | 6 | 1040 | 0 | 0 | 1.8 | 0.31 | 0.58 | 0.69 | 0.88 |
| 16 | 31.3 | 42.9 | 100 | 121 | 166 | 5.4 | 894 | 0 | 0 | 2.2 | 0.2 | 0.61 | 0.77 | 0.89 |
| 17 | 21.6 | 58.6 | 101 | 110 | 298 | 7.5 | 2222 | 0 | 0 | 0 | 0.96 | 0.78 | 0.75 | 0.61 |
| 18 | 26.4 | 51.8 | 138 | 167 | 328 | 4.8 | 1589 | 0 | 0 | 2.3 | 1.8 | 0.77 | 0.76 | 0.79 |
| 19 | 29.2 | 50.4 | 122 | 174 | 301 | 5.6 | 1685 | 0 | 0 | 1.8 | 0.96 | 0.79 | 0.8 | 0.77 |
| 20 | 27.9 | 52.2 | 121 | 170 | 318 | 5.3 | 1677 | 0 | 0 | 1.8 | 1.1 | 0.84 | 0.76 | 0.56 |
| 21 | 22.6 | 57.8 | 98 | 113 | 289 | 6.2 | 1800 | 0 | 0 | 0 | 0.92 | 0.88 | 0.69 | 0.64 |
| 22 | 19.0 | 60.7 | 118 | 111 | 354 | 5.9 | 2100 | 0 | 0 | 0 | 1.1 | 0.81 | 0.72 | 0.78 |
| 23 | 16.1 | 67.4 | 122 | 119 | 499 | 11.6 | 5802 | 3056 | 34.5 | 2.0 | 0.5 | 0.4 | 0.28 | 0.59 |
| 24 | 15.5 | 68.1 | 140 | 133 | 584 | 10 | 5869 | 3078 | 34.4 | 0.9 | 0.4 | 0.4 | 0.37 | 0.63 |
| 25 | 14.7 | 67.8 | 115 | 96 | 444 | 14 | 6214 | 1439 | 18.8 | 0.9 | 0.3 | 0.5 | 0.33 | 0.55 |
| 26 | 15.3 | 72.1 | 91 | 111 | 523 | 10 | 5241 | 2466 | 32.0 | 0.0 | 0.3 | 0.5 | 0.25 | 0.49 |
| 27 | 26.0 | 54.1 | 118 | 154 | 321 | 15 | 4800 | 5036 | 51.2 | 4.0 | 0.4 | 0.6 | 0.3 | 0.03 |
| 28 | 17.7 | 61.0 | 121 | 100 | 345 | 23.8 | 8200 | 4754 | 36.7 | 0.0 | 0.4 | 0.6 | 0.36 | 0.05 |
| 29 | 18.8 | 63.8 | 115 | 124 | 421 | 21.3 | 8954 | 6484 | 42.0 | 2.0 | 0.3 | 0.6 | 0.23 | 0.03 |
| 30 | 19.5 | 64.3 | 98 | 118 | 389 | 19.6 | 7623 | 8325 | 52.2 | 0.0 | 0.3 | 0.6 | 0.25 | 0.02 |
| 31 | 17.2 | 67.2 | 87 | 96 | 375 | 18.7 | 6999 | 8486 | 54.8 | 2.0 | 0.3 | 0.5 | 0.27 | 0.05 |
| 32 | 19.8 | 62.3 | 115 | 128 | 401 | 19.6 | 7854 | 4672 | 37.3 | 3.3 | 0.3 | 0.5 | 0.32 | 0.06 |
| 33 | 20.1 | 62.8 | 121 | 142 | 444 | 22.3 | 9912 | 9561 | 49.1 | 3.2 | 0.2 | 0.6 | 0.33 | 0.01 |
| 34 | 20.7 | 63.7 | 100 | 133 | 409 | 21.8 | 9932 | 9793 | 52.3 | 0.0 | 0.4 | 0.5 | 0.29 | 0.04 |
| 35 | 20.8 | 58.6 | 140 | 141 | 398 | 25.3 | 10054 | 11708 | 53.8 | 0.0 | 0.5 | 0.6 | 0.27 | 0.05 |
| 36 | 21.0 | 56.9 | 157 | 150 | 406 | 19 | 7728 | 6853 | 47.0 | 0.0 | 0.6 | 0.6 | 0.3 | 0.02 |
| 37 | 20.7 | 62.5 | 123 | 151 | 456 | 15.1 | 6891 | 5177 | 42.9 | 1.0 | 0.6 | 0.6 | 0.34 | 0.06 |

Table 1 (continued).

| Smpl. | C ₂₈ (%) | C ₂₉ (%) | C ₂₇ (ppm) | C ₂₈ (ppm) | C ₂₉ (ppm) | H/S | C ₃₀ H (ppm) | Oleanane (ppm) | Oleanane (%) | Gamma- cerane (%) | Ts/Tm | MPI-1 | Agal/ (Aga+Cad) | 2MN/ (2MN+Cad) |
|-------|------------------------|------------------------|--------------------------|--------------------------|--------------------------|------|----------------------------|-------------------|-----------------|----------------------|-------|-------|--------------------|-------------------|
| 38 | 18.1 | 66.0 | 111 | 126 | 460 | 20.3 | 9347 | 4666 | 33.3 | 1.8 | 0.5 | 0.5 | 0.34 | 0.05 |
| 39 | 19.4 | 62.1 | 97 | 101 | 324 | 22.3 | 7228 | 5342 | 42.5 | 0.0 | 0.6 | 0.6 | 0.36 | 0.04 |
| 40 | 17.3 | 66.5 | 113 | 121 | 466 | 21.3 | 9933 | 5278 | 34.7 | 0.0 | 0.5 | 0.5 | 0.29 | 0.05 |
| 41 | 17.1 | 64.6 | 142 | 133 | 501 | 20 | 10021 | 5785 | 36.6 | 0.0 | 0.4 | 0.6 | 0.3 | 0.05 |
| 42 | 15.8 | 70.2 | 100 | 112 | 499 | 18 | 8964 | 5471 | 37.9 | 0.0 | 0.6 | 0.6 | 0.31 | 0.03 |
| 43 | 17.8 | 67.9 | 89 | 111 | 423 | 26 | 10978 | 6069 | 35.6 | 0.0 | 0.6 | 0.6 | 0.33 | 0.03 |
| 44 | 20.2 | 64.4 | 92 | 121 | 385 | 23.4 | 9003 | 5732 | 38.9 | 0.0 | 0.6 | 0.5 | 0.31 | 0.04 |
| 45 | 13.6 | 71.2 | 86 | 77 | 403 | 7.8 | 3151 | 1483 | 32.0 | 0.0 | 0.6 | n.a. | n.a. | n.a. |
| 46 | 12.6 | 69.9 | 100 | 72 | 399 | 10.6 | 4222 | 1468 | 25.8 | 0.0 | 0.7 | n.a. | n.a. | n.a. |
| 47 | 13.4 | 74.1 | 56 | 60 | 331 | 11.9 | 3951 | 1248 | 24.0 | 0.0 | 0.9 | n.a. | n.a. | n.a. |
| 48 | 20.9 | 61.4 | 169 | 200 | 588 | 5.1 | 3001 | 0 | 0.0 | 0.0 | 1.3 | n.a. | n.a. | n.a. |
| 49 | 22.6 | 53.3 | 201 | 189 | 444 | 7.9 | 3521 | 0 | 0.0 | 0.0 | 1.3 | n.a. | n.a. | n.a. |
| 50 | 20.3 | 58.6 | 154 | 148 | 428 | 7 | 2999 | 0 | 0.0 | 2.3 | 1.3 | n.a. | n.a. | n.a. |
| 51 | n.a. | n.a. | n.a. | n.a. | 400 | 7 | n.a. | n.a. | n.a. | n.a. | 1.0 | n.a. | n.a. | n.a. |
| 52 | 13.9 | 69.1 | 88 | 72 | 358 | 11.5 | 4100 | 0 | 0.0 | 1.8 | 0.8 | n.a. | n.a. | n.a. |
| 53 | 27.8 | 55.8 | 118 | 200 | 401 | 11.1 | 4467 | 609 | 12.0 | 0.0 | 1.2 | 0.5 | 0.4 | 0.39 |
| 54 | 27.5 | 54.8 | 121 | 188 | 374 | 12 | 4501 | 1240 | 21.6 | 0.0 | 1.1 | 0.5 | 0.43 | 0.51 |
| 55 | n.a. | n.a. | n.a. | n.a. | n.a. | n.a. | n.a. | n.a. | n.a. | n.a. | 1.0 | 0.5 | 0.58 | 0.47 |
| 56 | 14.3 | 72.3 | 66 | 70 | 355 | 18.8 | 6671 | 3688 | 35.8 | 0.0 | 0.2 | 0.5 | 0.51 | 0.42 |
| 57 | 14.8 | 71.3 | 68 | 72 | 348 | 18.1 | 6300 | 3061 | 32.7 | 0.0 | 0.5 | 0.5 | 0.64 | 0.34 |
| 58 | 20.4 | 64.5 | 99 | 133 | 421 | 10.2 | 4286 | 482 | 10.1 | 0.0 | 0.7 | 0.9 | 0.54 | n.d.p. |

Abbreviations used: TOC: Total Organic Carbon; HI: Hydrogen Index; T_{max}: Temperature, maximum; Vittr. Refl.: vitrinite reflectance; TAI: Thermal Alteration Index; Kerogen Composition (W: Woody; H: Herbaceous; C: Coaly; F: Finely Disseminated; I: Inertinite; Am: Amorphous; Al: Algal); Sat.: Saturate Hydrocarbons; Arom.: Aromatic Hydrocarbons; NSO: Polar Hetero-compounds containing nitrogen, sulfur, and oxygen functional groups; Asph.: Asphaltenes; Pr/Ph: pristane/phytane; CPI: Carbon Preference Index; C₂₇, C₂₈ and C₂₉: Regular steranes reported in percent and ppm concentrations; H/S: Hopane/Sterane ratio; C₃₀H: concentration of C₃₀ 17 α (H)21 β (H) hopane in ppm of pentane-soluble fraction; Ts/Tm: 18 α (H)-22,29,30-tris-norneohopane/17 α (H)-22,29,30-trisnorhopane; MPI-1: Methyl-phenanthrene Index [1.5(MP+2MP)/(P+9MP+1MP)]; Aga: Agathalene (1,2,5-trimethylnaphthalene); Cad: Cadalene (1,6-dimethyl-4-isopropylnaphthalene); 2MN: 2-methyl naphthalene; n.a.: not available; n.d.p.: no determination possible.

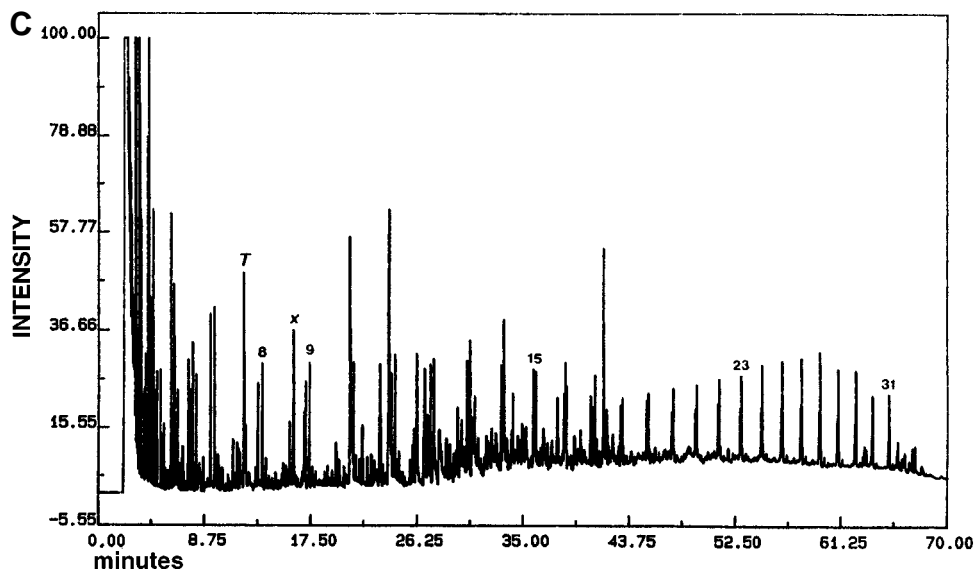
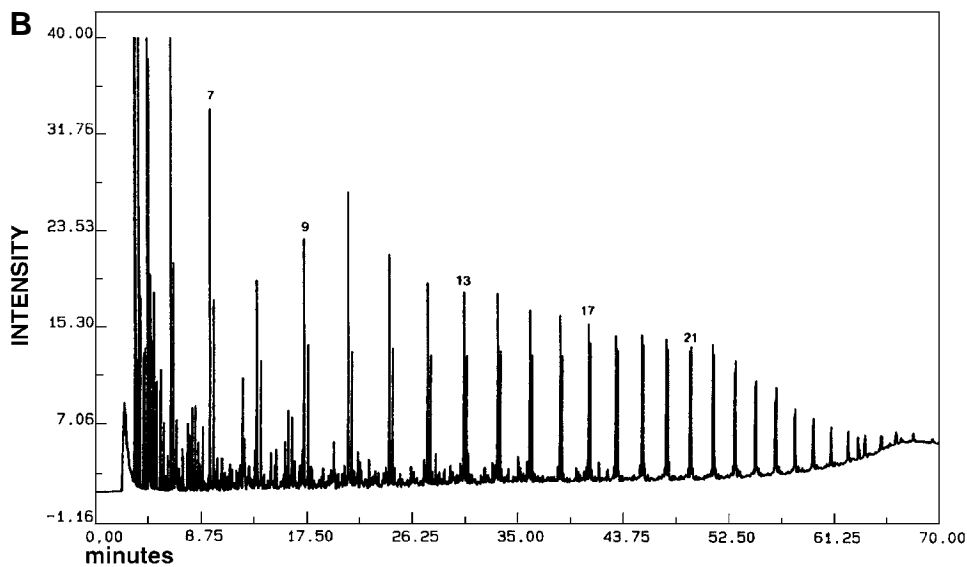
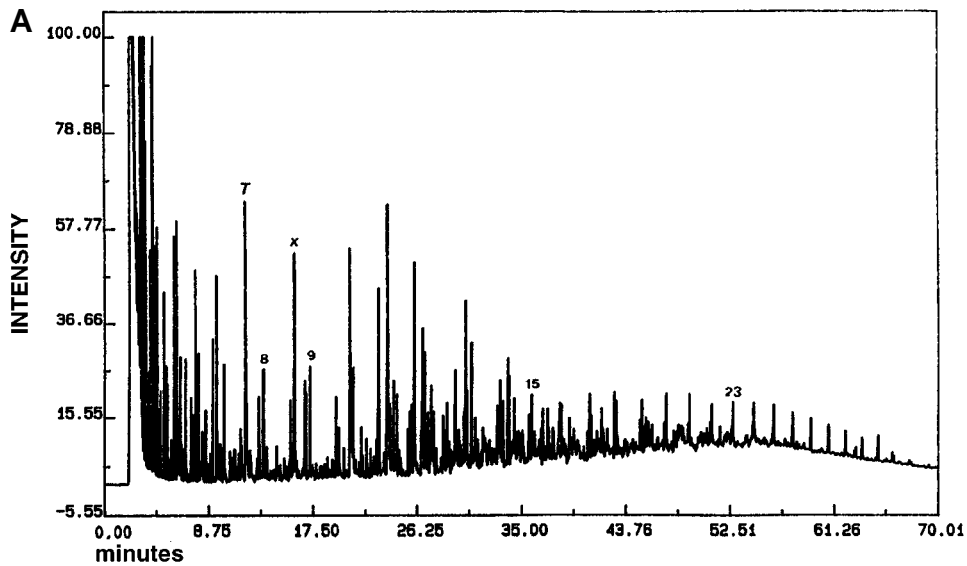


Figure 2. P_2 pyrograms from programmed py-GC of (A) silty shale (sample number 39) from the Talang Akar Formation (south Sumatra) with a predominance of terrigenous higher-plant organic matter. TOC = 9.43%; HI = 281; visual kerogen: 60% woody, 25% herbaceous, 15% coaly; age: Oligocene-Miocene; hydrocarbon potential: gas-condensate; (B) shale from the Washakie basin, Wyoming, dominated by algal organic matter; hydrocarbon potential: oil; (C) silty shale (sample 37) from the Talang Akar Formation (south Sumatra) with a mixture of terrigenous higher-plant material and algal (?) -amorphous organic matter. TOC = 1.85%; HI = 232; visual kerogen: 75% herbaceous, 25% algal(?) -amorphous; age: Oligocene-Miocene; hydrocarbon potential: gas and oil.

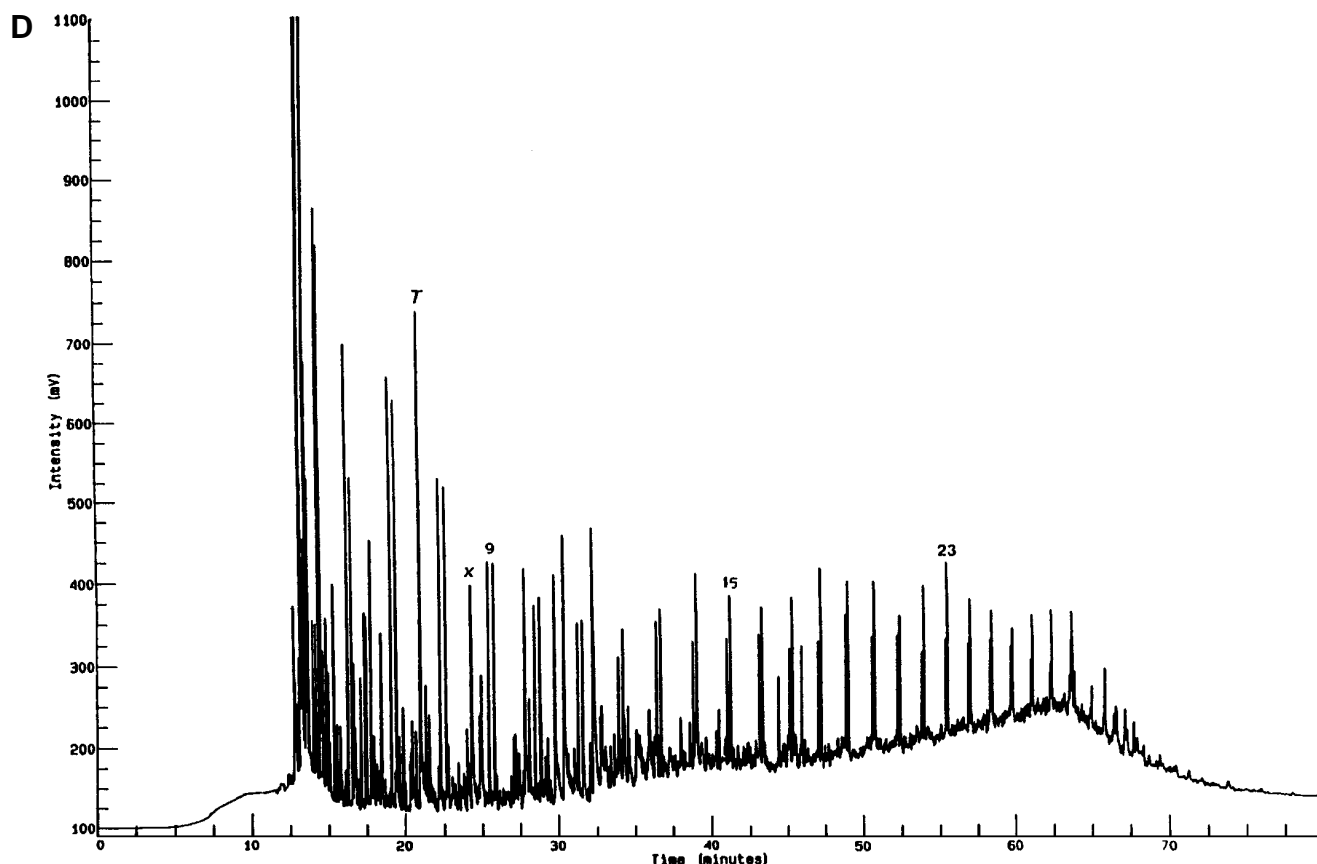


Figure 2 (continued). (D) shale (sample 20) from the Aare Formation, Haltenbanken, Norway, with a mixture of terrigenous higher-plant material and algal(?) -amorphous organic matter; TOC = 12.8%; HI = 246; visual kerogen: 70% herbaceous, 25% algal(?) -amorphous, 5% woody-inertinitic; age: Toarcian–Aalenian; hydrocarbon potential: gas and oil.

(1970) and Giraud (1970). Among the samples analyzed in this study, benzene and toluene are the most abundant compounds which, together with phenolic and methoxyphenolic compounds, are indicative of lignin precursors (Larter et al., 1978; van de Meent et al., 1980). The P_2 pyrograms from the Talang Akar Formation in south Sumatra (Figure 2C) and the Aare Formation in Haltenbanken (Figure 2D) also contain appreciable amounts of alkyl groups seen as alkene-alkane doublets. Their H/C ratios are 0.91 and 0.95, respectively. Higher H/C ratios would parallel higher contents of liptinitic material. The sample from south Sumatra, shown in Figure 3A, has an estimated H/C ratio of 0.81. This is in agreement with results from Horsfield (1984) for terrigenous type III kerogens from South Texas (H/C = 0.71) and North Africa (H/C = 0.84). Horsfield (1984) and Curry et al. (1994) note that the oil generative potential of terrigenous higher-plant material is primarily a function of the content of aliphatic groups and only secondarily a function of the hydrogen content.

Saturate Hydrocarbon Fraction

The C_{15+} saturate hydrocarbon gas chromatograms (Figure 3) demonstrate the odd-over-even carbon number preference between C_{24} and C_{34} , typical of extractable organic matter from terrigenous higher-

plant kerogens. In this sample set the carbon preference indices (CPI) range from 1.1 to 4.2 (Table 1). The major biological precursors of n -alkanes in rock extracts and oils are fatty acids, and n -alkanes of bacteria, unicellular algae, and leaf waxes. Upon diagenesis in the geological environment, the even-numbered fatty acids undergo decarboxylation to form n -alkanes with an odd number of carbon atoms (Dastillung, 1976), and, as a consequence, a high CPI. Samples from south Sumatra show the highest pristane/ n - C_{17} ratios (in spite of their slightly greater thermal maturity), whereas the CPI is similar to the other samples studied (Figure 4). The higher pristane/ n - C_{17} ratios suggest a chemically different organic facies with a greater contribution of pristane precursors. High pristane/phytane ratios, up to about 4, are also characteristic for this type of organic facies (Table 1 and Figure 3). The main source of pristane in a terrigenous higher-plant environment is from phytol (Maxwell et al., 1972), which occurs as an esterified side chain on the chlorophyll molecule. Another source of acyclic isoprenoids are archaeobacteria, where pristane can be derived from tocopherol and phytane from the *bis*-phytanyl ethers (Philp, 1994). During organic-matter diagenesis, free phytol is formed through hydrolysis of the chlorophyll side chain, followed by reduction to phytane, or

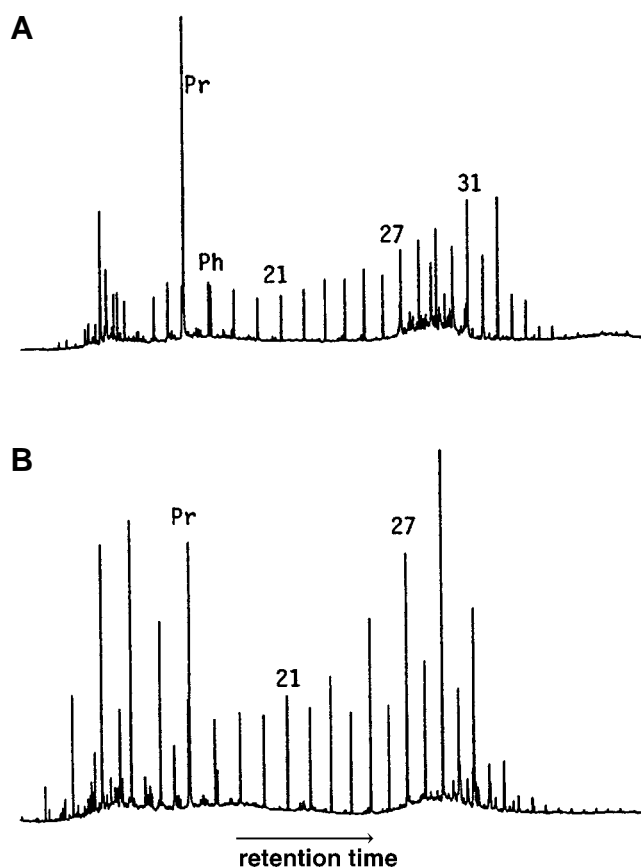


Figure 3. Typical C_{15+} gas chromatograms of the saturate hydrocarbons extracted from terrigenous higher-plant organic matter. (A) south Sumatra silty shale (sample 34) with TOC = 1.86%; HI = 190, and $\%R_o = 0.6$. (B) Haltenbanken shale (sample 20) with TOC = 12.8%, HI = 246, and $\%R_o = 0.5$. Note the high pristane/phytane (Pr/Ph) ratio and high CPI for both samples and the resin signature in the front-end of the chromatogram for the sample from south Sumatra.

oxidation of the $-OH$ group to form phytanic acid which forms pristane after loss of $-CO_2$ (Maxwell et al., 1972). Cracking from the kerogen could occur at the point of attachment with a loss of one carbon to eventually form pristane, or by formation of a double bond which subsequently reduces to form phytane.

Isolation of the branched and cyclic saturate hydrocarbon fraction through molecular sieving or urea adduction techniques revealed the presence of a homologous series of long-chain isoprenoids in samples of Hettangian age from the Aare Formation in Haltenbanken. These were monitored by their m/z 183 and m/z 253 fragment ions (Figure 5). A tentative identification made by comparison with samples analyzed by Seifert and Moldowan (1981) suggests that both regular isoprenoids with head-to-tail configurations and head-to-head configurations are present. Long-chain isoprenoids with a head-to-head linkage between smaller isoprenoid units are thought to be derived from dibiphytanyl glyceryl ethers of archaeobacteria (de Rosa et al., 1977; Moldowan and Seifert, 1979; Chappe

et al., 1982; Albaiges et al., 1985). Long-chain isoprenoids with a head-to-tail linkage may be derived from higher-plant oligo-terpenyl alcohols (Ibata et al., 1984; Philp and Gilbert, 1986; Didyk et al., 1978).

A characteristic feature of all samples is a pronounced predominance of the C_{29} regular steranes, as monitored by the m/z 217 and 218 common fragment ions (Figure 6). The corresponding C_{27} and C_{28} steranes are primarily derived from algal organic matter (Seifert and Moldowan, 1981; Huang and Meinschein, 1979) and are present in amounts of around 100 ppm of extractable organic matter (EOM) for all samples studied. Concentrations of regular C_{29} steranes, however, show greater variations and are plotted in ppm of EOM together with hopane/sterane ratios in Figure 7. Hopane/sterane ratios typically range from 5 to 30, as monitored by the m/z 191 and m/z 217 mass fragmentograms. The greatest concentration of C_{29} regular steranes and the highest hopane/sterane values were found for samples from south and central Sumatra. In their study of oils from the Gippsland Basin, Australia, Philp and Gilbert (1986) reported hopane/sterane ratios of 3 to 4. Hoffmann et al. (1984) reported similar values for Mahakam Delta, Indonesia, oils. Samples from Sumatra have hopane/sterane ratios in the range of 15 to 25. Samples from the Aare Formation in the Haltenbanken area have lower ratios of around 5 to 8. Average hopane/sterane ratios for a variety of depositional environments and organic facies have been shown by Isaksen (1991). The high content of hopanoids is most likely the result of bacterial reworking of the terrigenous higher-plant material. Note also that hopane/sterane ratios greater than about 5 typically show fragment ions of hopane with mass of 217 and 218 atomic mass units (amu).

Hopane, oleanane, and norhopane are the major triterpanes in most samples studied (Figure 8). A few samples from the Aare Formation in the Haltenbanken area are anomalous in that they contain relatively low amounts of hopane and a predominance of C_{30} $17\alpha(H)$ diahopane ("compound x") (Moldowan et al, 1991), eluting after C_{29} norhopane and C_{29} Ts. These samples are shales with predominantly woody organic matter which accumulated under oxic/suboxic conditions.

Biochemically, compounds such as β -amyryn, β -amyryn, and the corresponding acids ursolic acid and oleanolic acid, are common constituents of terrigenous higher plants (Loomis and Croteau, 1980). Early diagenetic changes in the shallow subsurface would cause reduction and minor rearrangements to form pentacyclic triterpanes with a six-membered E-ring such as oleanane, ursane, taraxerane, and lupane (Simoneit, 1986). In this sample set, the most abundant triterpane with this configuration is oleanane. This has previously also been reported by Ekweozor et al. (1979a, b), Chaffee and Johns (1983), Hoffmann et al. (1984), Strachan et al. (1988), and Czochanska et al. (1988). $18\alpha(H)$ -oleanane is a specific marker for higher flowering plants (angiosperms) and most likely derived from β -amyryn, found free and esterified in many angiosperms. The presence of $18\alpha(H)$ -oleanane in the m/z 191 mass fragmentogram can assist with age dat-

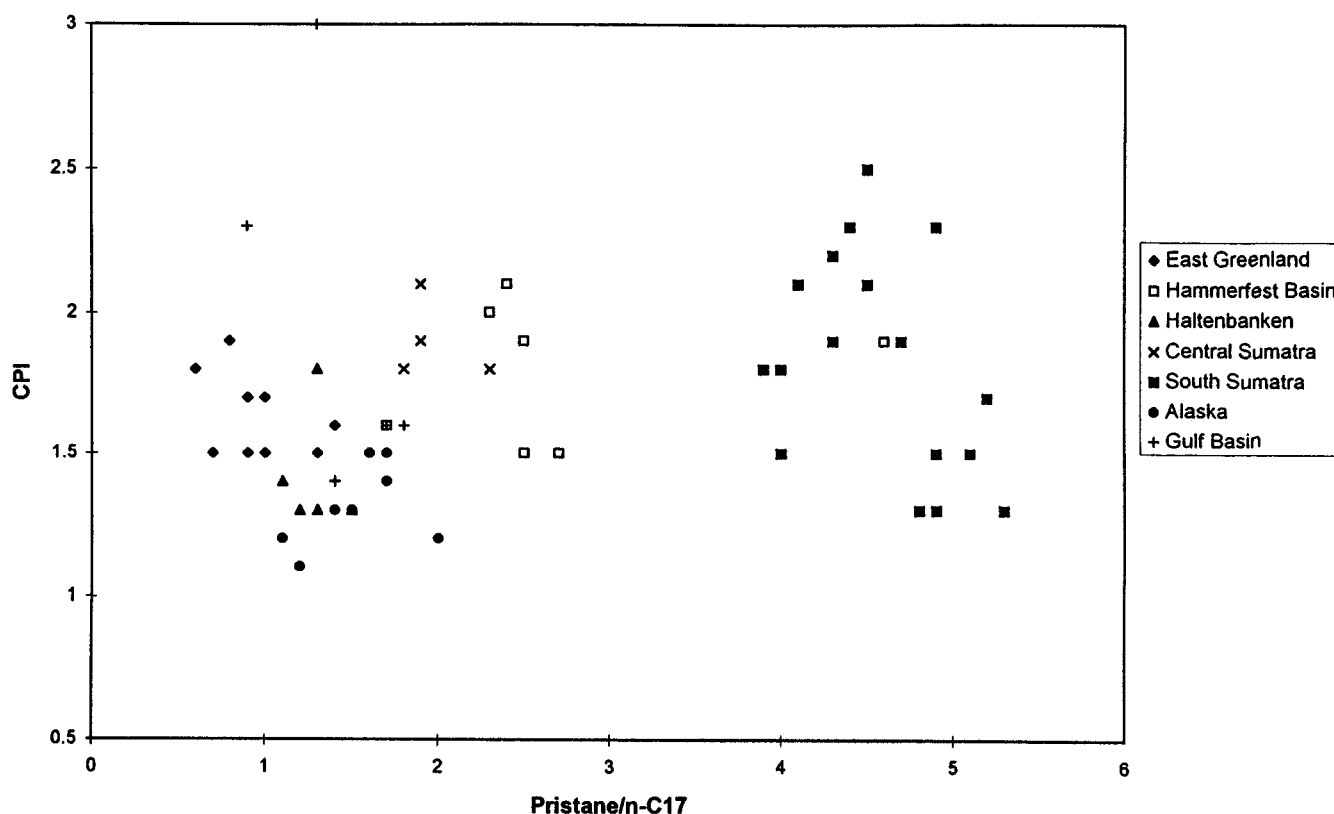


Figure 4. Crossplot of carbon preference index (CPI) and pristane/ n -C₁₇ for samples from diverse paleodepositional environments and geological ages. CPI values are relatively similar for most samples, whereas samples from south Sumatra have significantly higher pristane/ n -C₁₇ ratios even though these samples have vitrinite reflectance values up to 0.2%R_o greater than other samples (i.e., organic matter type control).

ing the organic matter. Studies of Cretaceous/Tertiary-sourced oils from Indonesia (Hoffmann et al., 1984; Grantham et al., 1983), the Philippines (Palmer, 1984), and the Niger Delta (Whitehead, 1974; Ekweozor et al., 1979a, b) have shown the presence of 18 α (H)-oleanane. Its presence is attributed to angiosperm debris in the source rock. According to Cleal (1988), angiosperms appeared no more than 200 Ma and did not become dominant until less than 100 Ma (mid-Cretaceous). The presence of the "x" (C₃₀ 17 α (H) diahopane; Moldowan et al., 1991) and "y" C₃₀ pentacyclic triterpanes was shown by Philp and Gilbert (1986) to be ubiquitous in Australian oils generated from kerogens with a predominance of terrigenous higher-plant organic matter. The absence of the "x" (C₃₀ 17 α (H) diahopane) and "y" compounds in rock extracts from south Sumatra (Figure 8) suggests that these compounds are not present in all types of higher-plant material. This is in agreement with observations made by Hoffmann et al. (1984), demonstrating the absence of these compounds in Indonesian oils proposed to be derived from a higher-plant organic facies. Actually, diahopanes may not be of higher-plant origin at all; they may be contributed by bacteria as they rework higher-plant material. Moldowan et al. (1991) show evidence of a bacterial or possibly fungal origin for diahopanes. The relatively high content of

pentacyclic triterpanes of the regular hopane-type with a five-membered E-ring is likely due to bacterial input to the organic matter. Bacteria have also contributed methyl-hopanes (m/z 205) in addition to diahopanes.

Extracts of rocks with a predominance of higher-plant organic matter typically show low homo-hopane contents (Figure 8). The main source of pentacyclic triterpanes with a five-membered E-ring is thought to be bacteria (Ourisson et al., 1979).

The reasons why relatively low concentrations of homo-hopanes are found in immature to early mature samples is not well understood. Three possible explanations follow. (1) Oxidation of the alkyl-tetrol side chain on bacteriohopane-tetrol could make it more labile during diagenesis. (2) Alternatively, high abundance of phenolic-type compounds in the organic-matter degradational environment could create aseptic conditions hostile to blooming bacterial populations and, thus, result in less contribution of bacterial hopanoids to the sedimentary organic matter. This is not indicated, in view of the high contents of hopanes derived from bacterial organic matter. (3) Oxidizing conditions in the depositional environment would preclude reduction of the bacteriohopane-tetrols. These processes could result in lower homo-hopane contents in terrigenous kerogens.

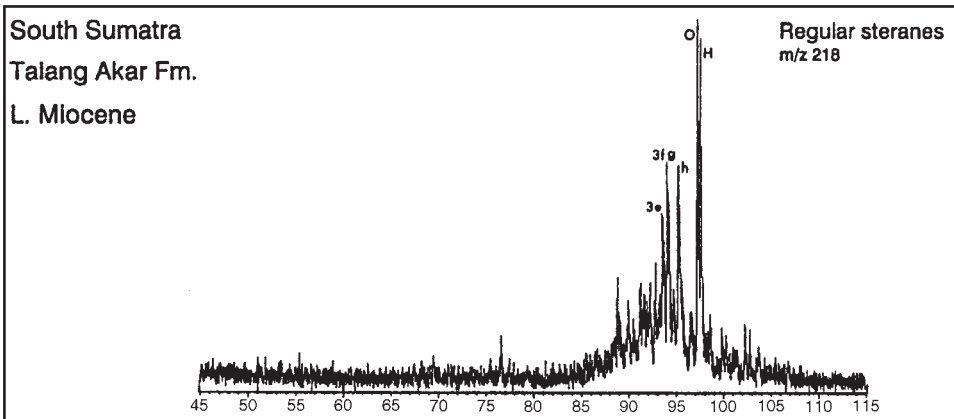
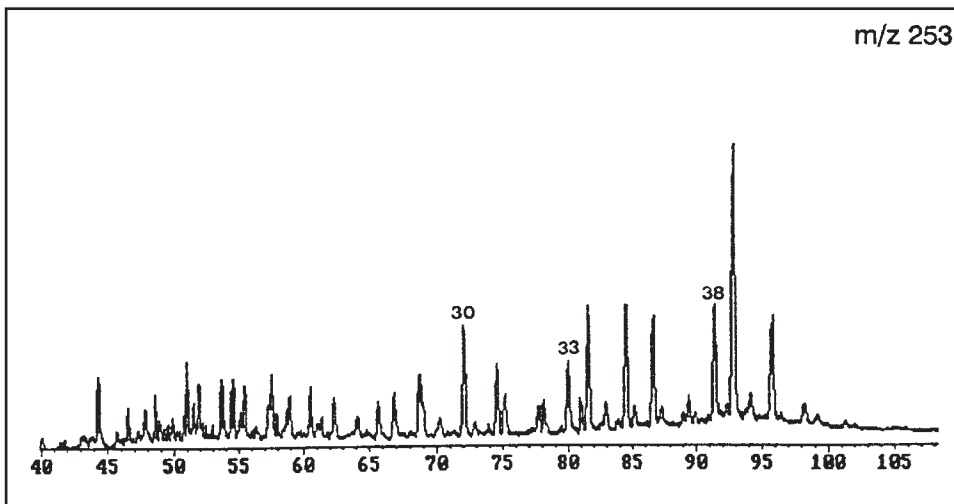
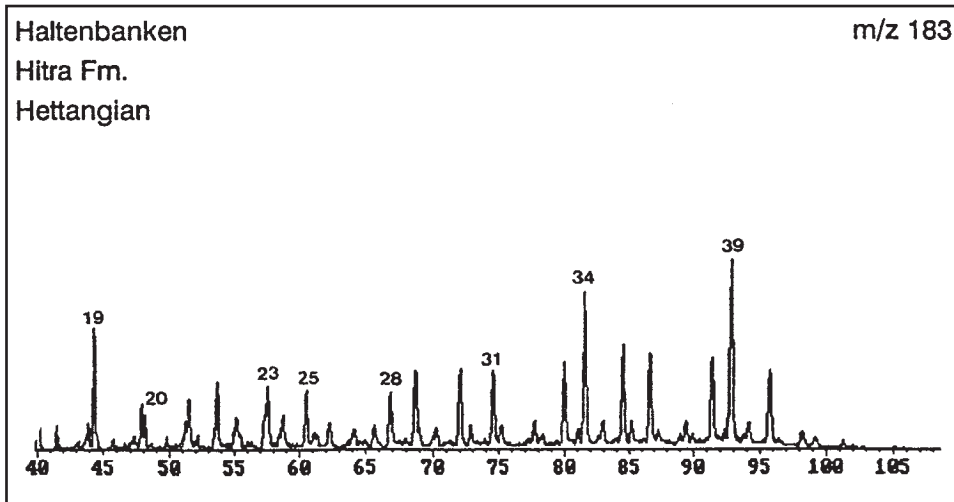


Figure 5. GC/MS fragmentograms monitoring common fragment ions m/z 183 and m/z 253 for long-chain isoprenoids. The majority of these are the head-to-tail isoprenoids. The sample is a silty shale of Hettangian age from Haltenbanken, Norway.

Figure 6. Example of regular sterane distributions from sample 34, south Sumatra, as monitored by the m/z 218 fragment ion. Steranes are dominated by the C₂₉ desmethyl steranes. When hopane/sterane ratios are high (typically greater than 5), minor fragments of triterpanes with masses 217 and 218 amu are notable. The m/z 218 was selected to show the fragments of C₃₀ 17 α (H), 21 β (H) hopane ("H") and 18 α (H) oleanane ("O"). 3e: 5 α (H), 14 β (H), 17 β (H) stigmastane 20S; 3f: 5 α (H), 14 β (H), 17 β (H) stigmastane 20R; 3g: 5 α (H), 14 α (H), 17 α (H) stigmastane 20S; 3h: 5 α (H), 14 α (H), 17 α (H) stigmastane 20R.

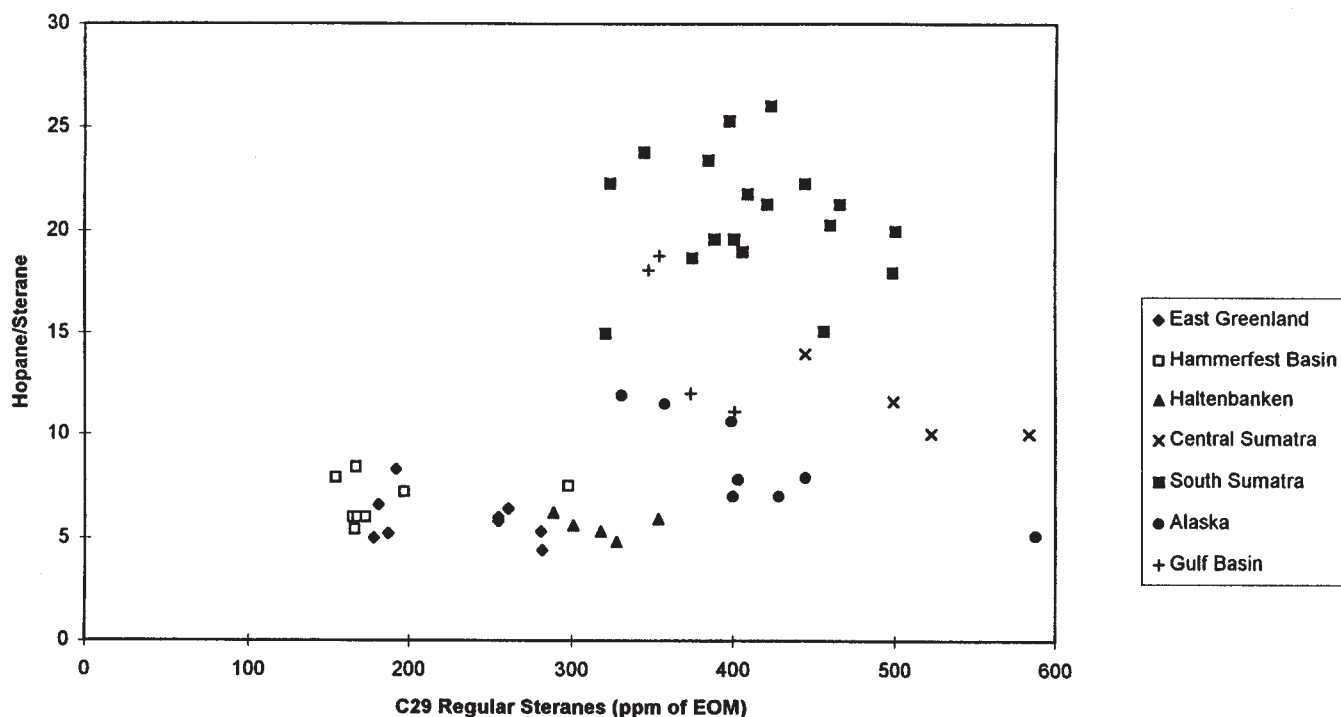


Figure 7. Comparison of biomarker relations typical of derivation from terrigenous higher-plant organic matter. Quantitatively, samples from south Sumatra have the greatest content of C_{29} regular steranes (measured in ppm of extractable organic matter), in agreement with pristane/ $n-C_{17}$, hopane/sterane, and CPI values. This suggests derivation from different types of plants in each of the environments studied.

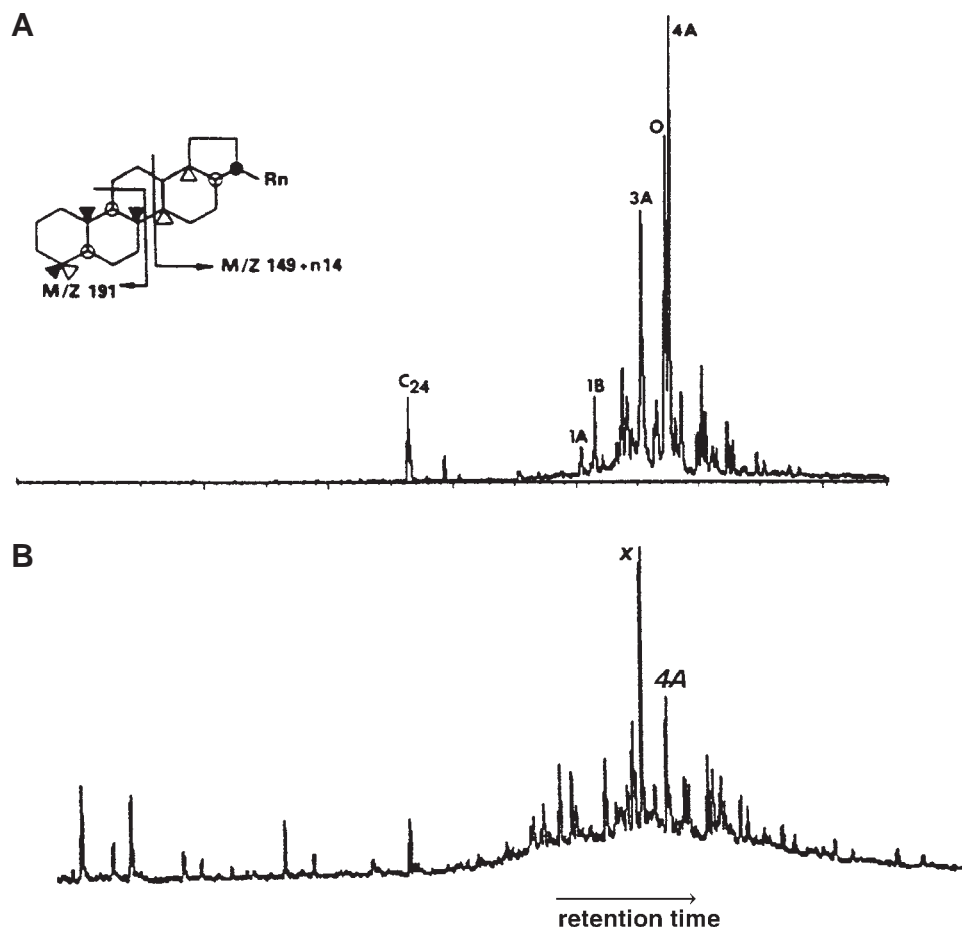


Figure 8. Typical distributions of triterpanes as monitored by their common fragment ion m/z 191 by GC/MS analysis. (A) Sample 34 from South Sumatra with high $18\alpha(H)$ oleanane ("O"), low amounts of homohopanes, and presence of C_{24} tetracyclics; (B) sample 20 from Haltenbanken, Norway, showing a predominance of C_{30} 15α methyl $17\alpha(H)27$ -norhopane (C_{30} diahopane) ("compound x"). Legend: 1A: $18\alpha(H)$ -22,29,30-trisnorhopane (Ts); 1B: $17\alpha(H)$ -22,29,30-trisnorhopane (Tm); 3A: $17\alpha(H)$, $21\beta(H)$ -30-norhopane; 4A: $17\alpha(H)$, $21\beta(H)$ hopane.

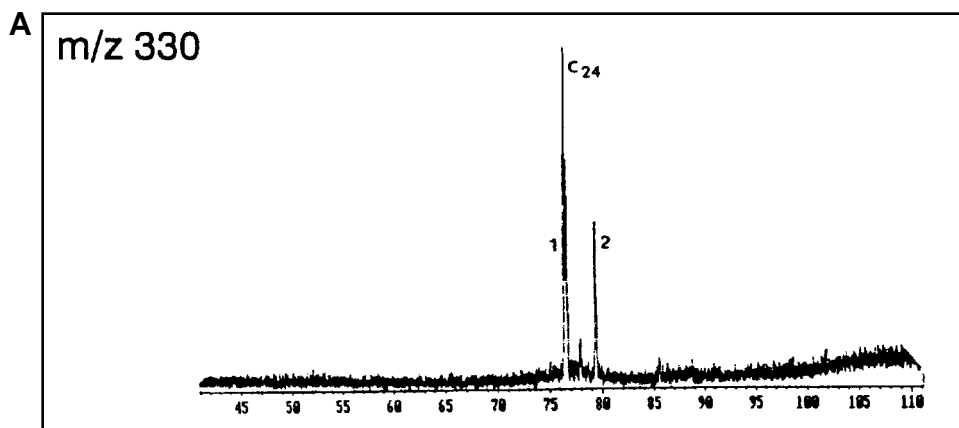
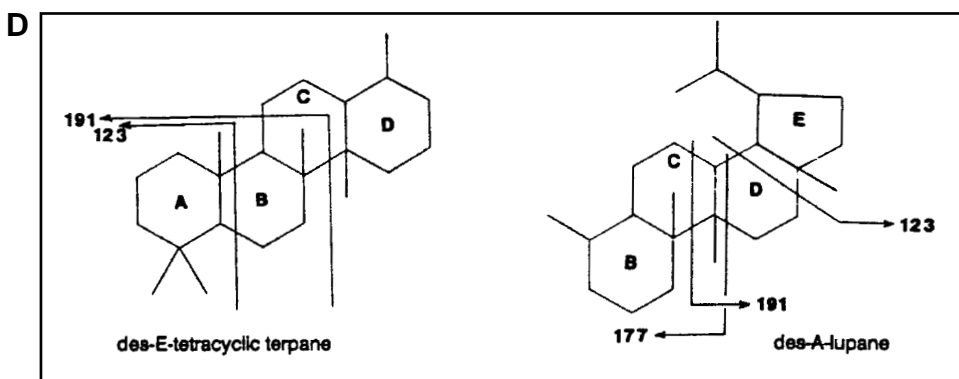
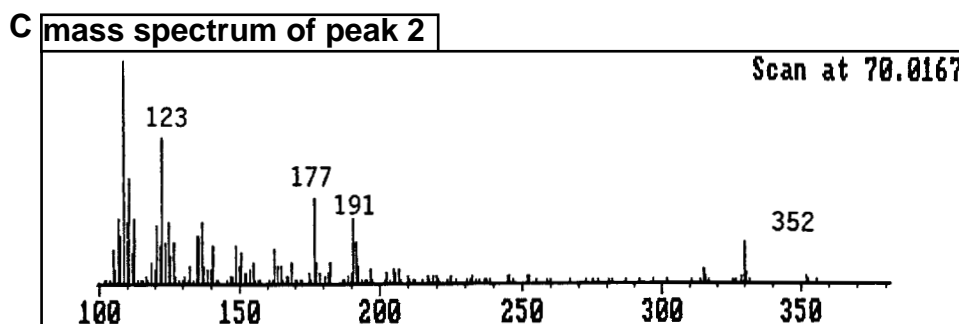
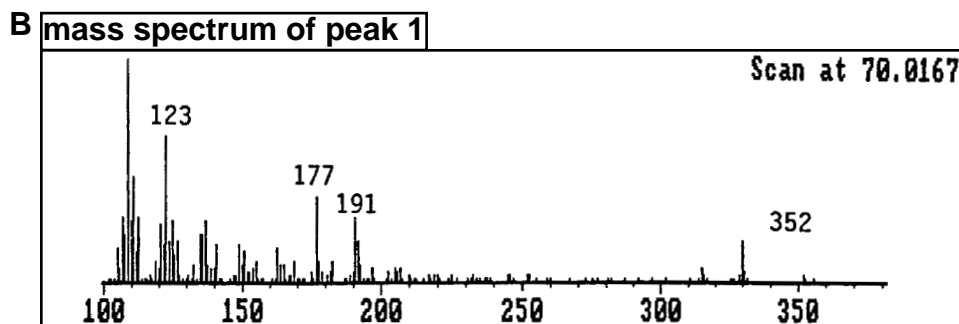


Figure 9. Identification of tetracyclics within extracts from rocks with a predominance of terrigenous higher-plant organic matter. Their common fragment ions are m/z 191 and 123, whereas their parent ion is m/z 330 (A). (B–C) The mass spectra of the two peaks labeled 1 and 2 are shown with two proposed molecular structures; des-E-tetracyclic terpane and des-A-lupane (D).



Rocks of Miocene age from south Sumatra have a relatively high content of what is thought to be a C₂₄ tetracyclic compound (eluting between the C₂₅ and C₂₆ tricyclics) in the saturate hydrocarbon fraction (Figure 9). This is based on comparisons with results obtained by Philp and Gilbert (1986) from an Australian crude oil generated from higher-plant organic matter. GC/MS analyses of the saturate fraction reveal com-

mon ions for this compound in the m/z 191 and 123 mass fragmentograms and with a parent ion m/z 330. This could be interpreted as a des-E-pentacyclic terpane, or des-A-lupane (Figure 9).

Gas chromatograms of the saturate hydrocarbon fractions show a marked resin signature in the C₁₃ to C₁₆ range (Figure 10A). These compounds are identified as diterpanes through GC/MS analyses monitor-

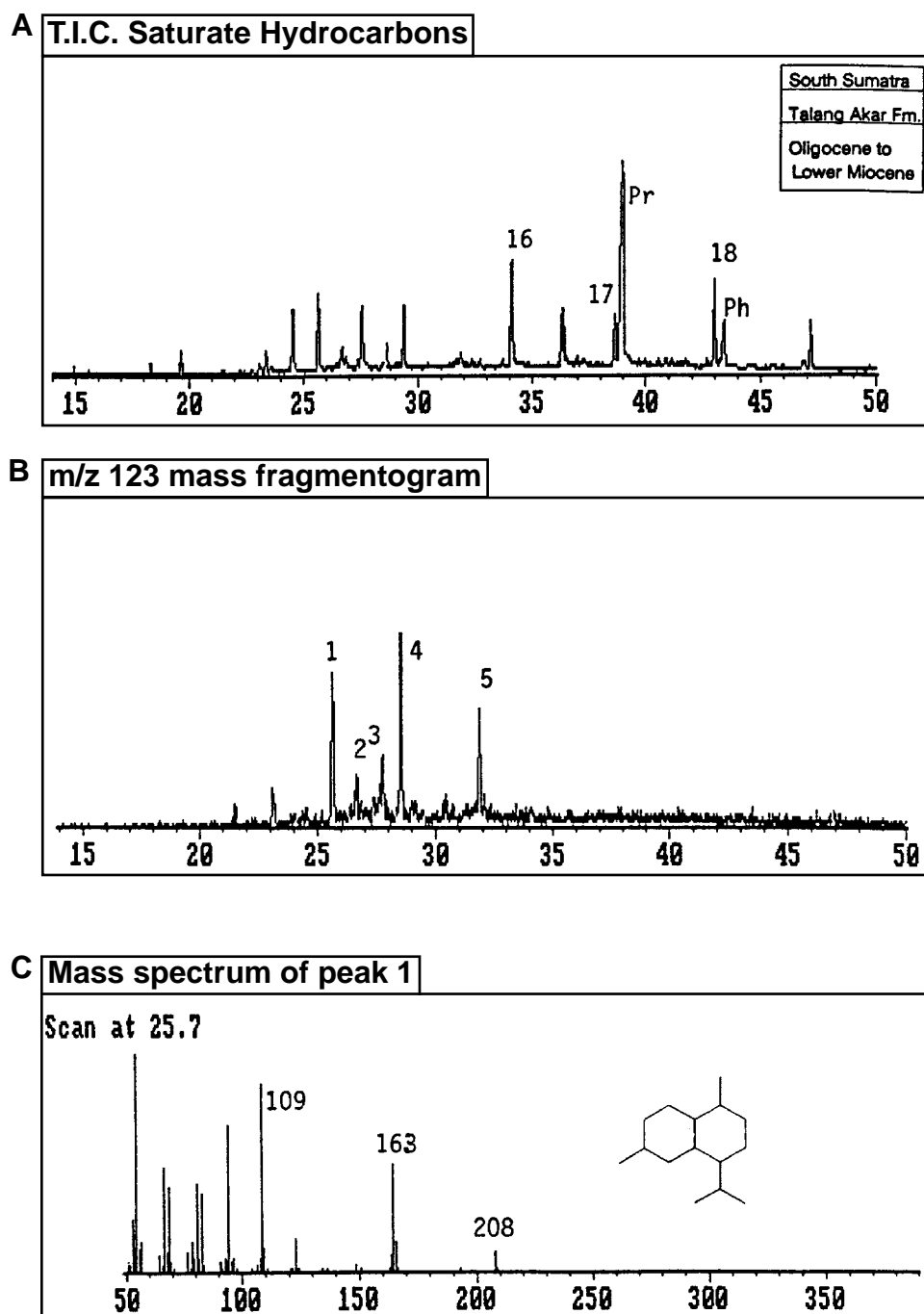


Figure 10. Diterpenoid (resin) biomarkers from terrigenous higher-plant organic matter. (A) GC trace showing diterpenoids eluting in the C_{13} – C_{16} range. (B) The diterpenoids are monitored by their common fragment ion of m/z 123. (C) The mass spectrum of the peaks labeled 1 through 5 are shown, together with the likely molecular structure for these compounds.

ing the m/z 191 and 123 common ion for diterpanes (Figure 10B). Mass spectra of the compounds and their identification are shown in Figures 10C–G and Table 2, respectively. Other diterpanes, occurring as tricyclics, are common in these samples and monitored by their m/z 233 fragment ion (Table 3). Figure 11 shows the mass fragmentograms and mass spectra for these compounds, together with their most likely molecular structure. Diterpane compounds are ubiquitous in higher plants and fungi. Sosrowidjojo et al. (1994) reported bicadinane resin markers in greater concentrations than C_{30} $17\alpha(H)$ hopane in Sumatran crude oils generated from source rocks with a predominance

of terrigenous higher-plant material. Our samples have not shown such high bicadinane concentrations.

Aromatic Hydrocarbon Fraction

Cadalene, $C_{15}H_{18}$ (1,6-dimethyl-4-isopropyl-naphthalene), is present in relatively high quantities in the aromatic fraction of the samples studied (Figure 12). Previously, studies by Bendoraitis (1974) and Simoneit (1986) have shown cadalene to be a specific marker for terrigenous higher-plant debris in sediments. The resinous portion of higher-plant material is thought to be the precursor (Grantham et al., 1983; van Aarssen et al., 1990). Cadalene has a molecular

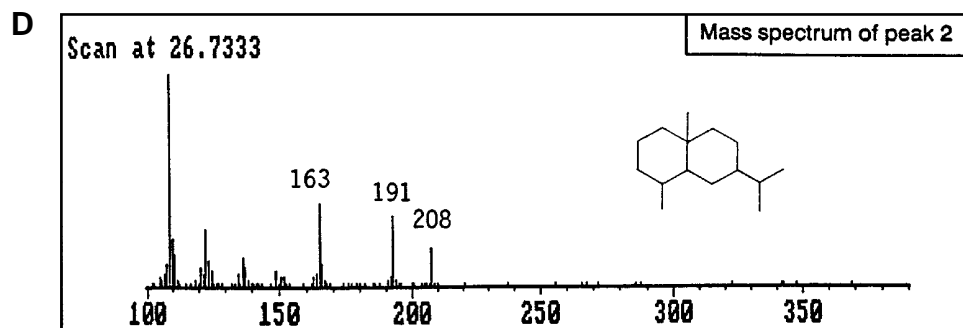
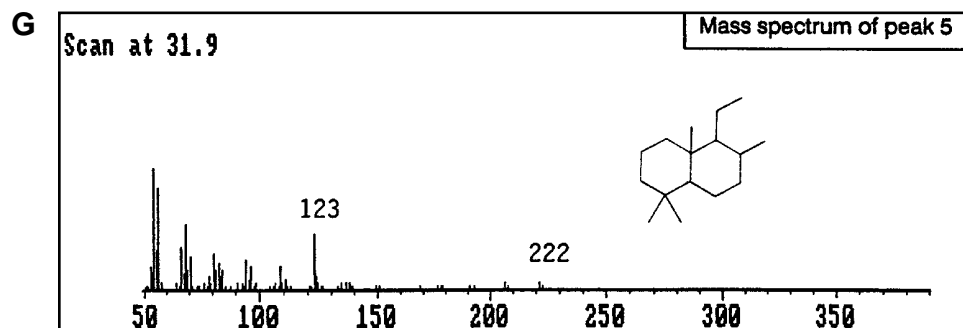
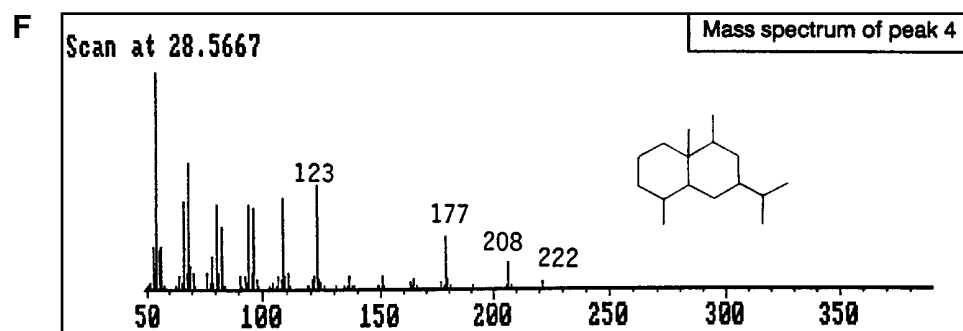
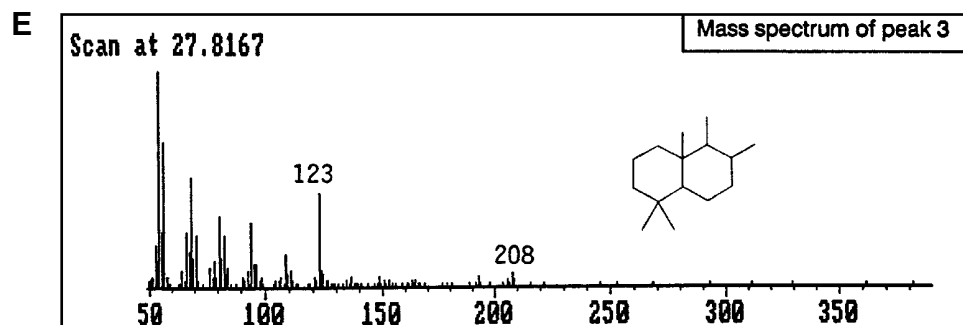


Figure 10 (continued). (D–G) The mass spectrum of the peaks labeled 2 through 5 are shown, together with the likely molecular structure for these compounds.



weight of 198 amu and an m/z 183 common fragment ion. The concentration of cadalene relative to other diaromatic, bicyclic compounds increases with increasing content of higher-plant material in the kerogen. Bendoraitis (1974) reported on the presence of cadalene in Loma Novia crude oil reservoir in the "Jackson sands" (Eocene) of South Texas. The oil

in this area is thought to have been generated from the "Jackson shale," deposited in an open-marine environment with a high input of land plant detritus (Tanner and Feux, 1988). Baset et al. (1979) found cadalene in low-rank coal extracts and suggested a possible origin from the dehydrogenation of sesquiterpene hydrocarbons, such as cadinene. Pre-

Table 2. Bicyclic compounds shown in Figure 10.

| Peak No. | Scan (Min) | Base Peak | M. Wt. | Name | Reference |
|----------|------------|-----------|--------|--|------------------------------|
| 1 | 25.7 | M/Z 109 | 208 | Cadinane | Katayama and Marumo (1983) |
| 2 | 26.73 | M/Z 109 | 208 | Eudesmane | Alexander et al. (1983) |
| 3 | 27.82 | M/Z 123 | 208 | Drimane | Alexander et al. (1983) |
| 4 | 28.56 | M/Z 123 | 222 | C ₁₆ Bicyclic Sesquiterpane | This study |
| 5 | 31.90 | M/Z 123 | 222 | C ₁₆ Bicyclic Sesquiterpane | Richardson and Müller (1982) |

Table 3. Tricyclic compounds shown in Figure 11.

| Peak No. | Scan (Min) | Base Peak | M. Wt. | Name | Reference |
|----------|------------|-----------|--------|---------------------------|------------------------------|
| 1 | 42.4 | M/Z 233 | 248 | C ₁₈ Diterpane | Richardson and Müller (1982) |
| 2 | 44.1 | M/Z 233 | 248 | C ₁₈ Diterpane | Richardson and Müller (1982) |

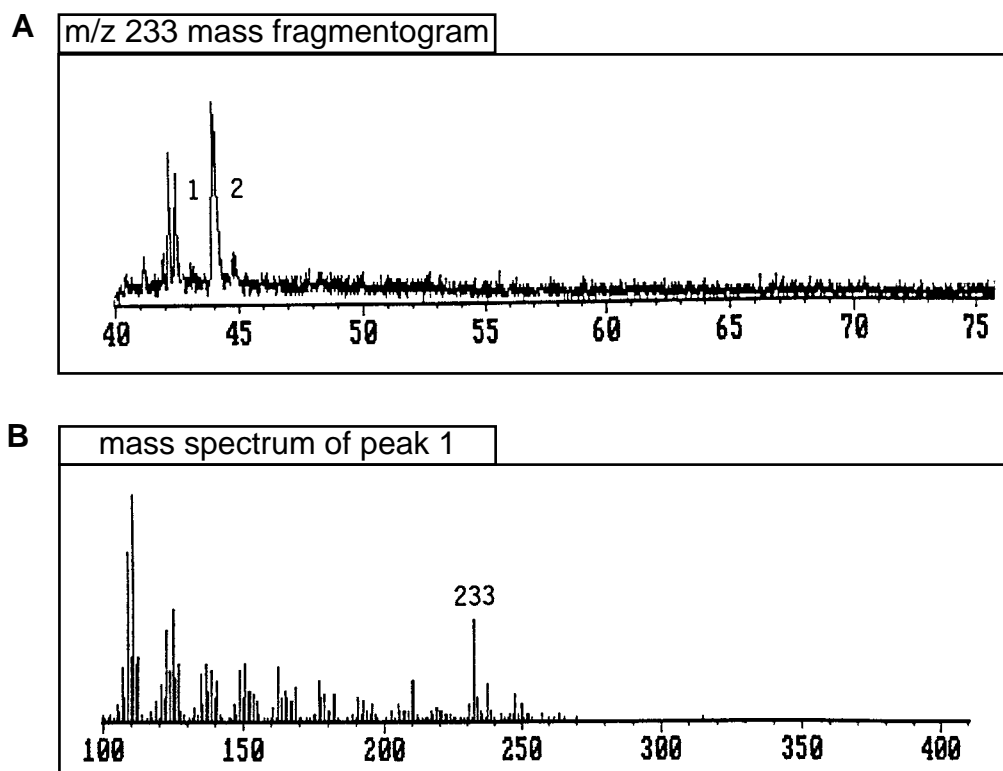


Figure 11. Tricyclic diterpane biomarkers present in relatively high quantities in some samples with a predominance of terrigenous higher-plant organic matter. (A) Their common fragment ion is shown by the m/z 233 mass fragmentogram. (B) The mass spectrum of the peak labeled 1.

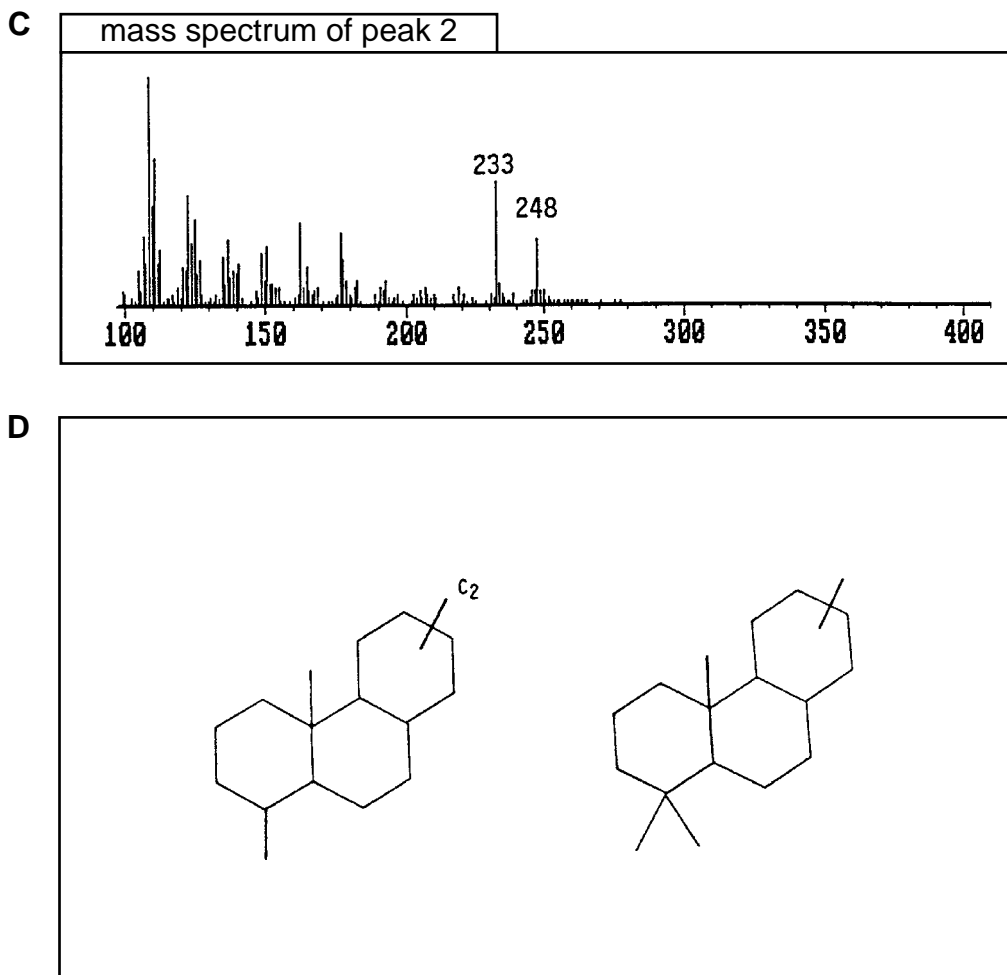


Figure 11 (continued). Tricyclic diterpane biomarkers present in relatively high quantities in some samples with a predominance of terrigenous higher-plant organic matter. (C) The mass spectrum of the peak labeled 2. (D) Two possible molecular structures. The sample is from the Talang Akar Formation of south Sumatra.

viously, Mair (1964) suggested a possible origin from cyclization of farnesol.

Concentrations of agathalene (1,2,5, trimethylnaphthalene) co-vary with the amount of higher-plant organic matter in the kerogen. Although the ratio of cadalene to agathalene may contain information about the type of higher-plant material from which it was generated, this is not yet understood. Like cadalene, agathalene also originates from the resinous portion of higher plants. Thomas (1969) reported on the presence of resinous compounds in various species of *Agathis*. These were found to be dominated by bicyclics and tricyclics. The biological precursors of agathalene are nonaromatic compounds such as agathic acid, methyl-agathate, communols, communic acid, abietic acid, sandaracopimaradienol, and sandaracopimaric acid, as suggested by Alexander et al. (1988) in their study of rocks and oils from the Cooper-Eromanga basin system in Australia. The precursor plant is thought to be the Kauri pine (*Araucariaceae*), which did not become prominent until the early to mid-Jurassic. The molecu-

lar alterations of biological precursors are mainly dehydrogenation (aromatization) and disproportionation. Aromatization of saturated precursor compounds may occur through thermal maturity-related removal of hydrogen or diagenetic aromatization in an oxidizing, peat-forming environment.

The ratio of other naphthalenes to cadalene and agathalene could assist with discerning the organic facies in the depositional environment. The ratios of 2-methyl naphthalene/cadalene and 2-methyl naphthalene/agathalene are used to assess the organic facies from which the oils could have been generated. Very high contents of cadalene are observed in samples from Sumatra (Figures 12 and 13; Table 1). The samples from a paralic depositional environment from the Jurassic Aare Formation of Haltenbanken have, by comparison, low contents of cadalene and agathalene (Figure 12). This could be due to slightly higher levels of thermal maturity or, more likely, different plant communities in the Jurassic of Haltenbanken than those found in the Miocene of Sumatra. Agatha-

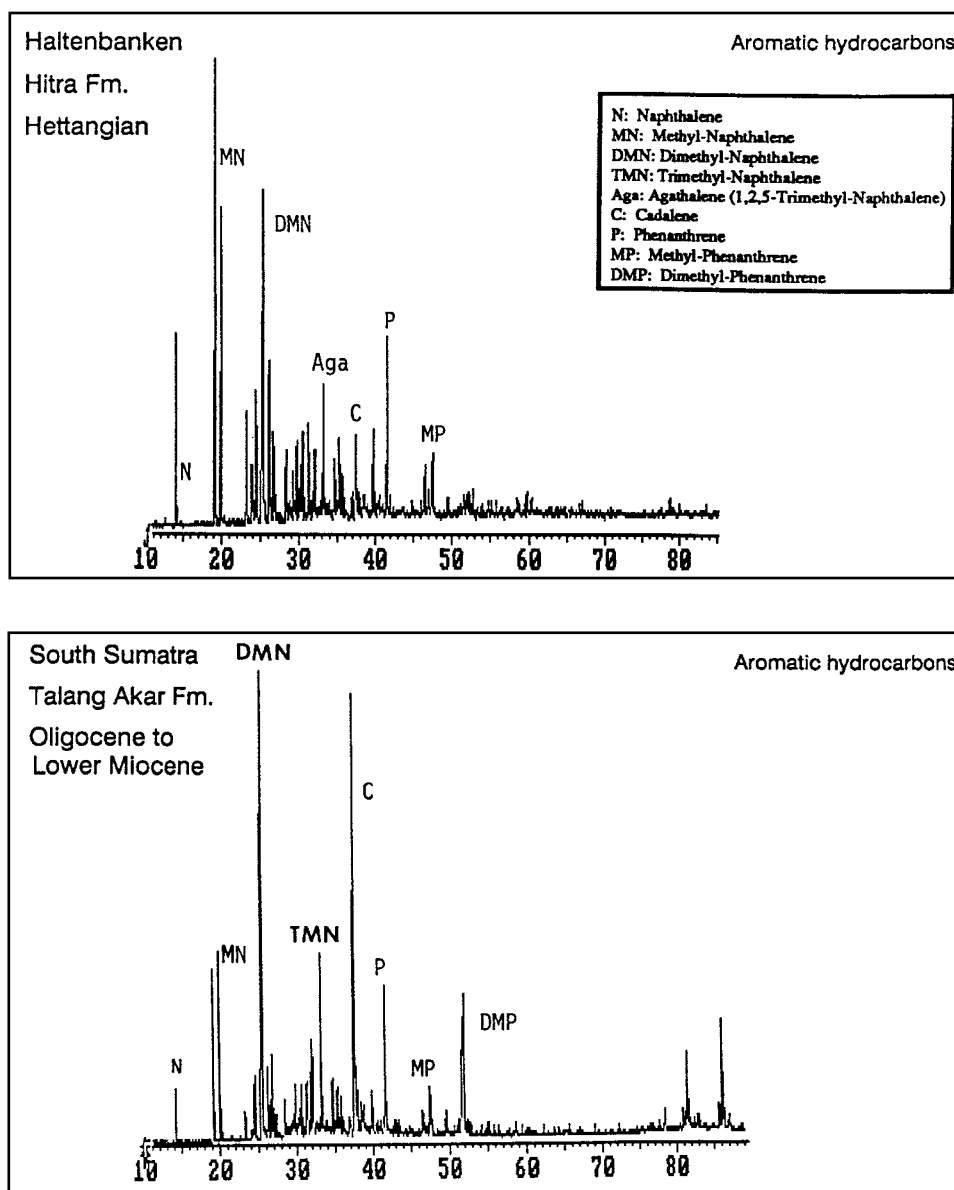


Figure 12. Gas chromatograms of the aromatic hydrocarbon fraction typical of the Hita Formation (Haltenbanken, Norway) and the Talang Akar Formation (south Sumatra).

lene/(Agathalene + Cadalene) values are low for south and central Sumatra samples and higher for the Haltenbanken samples (Figure 13). These organic facies also display differences in their relative contents of 2-methyl naphthalene and cadalene (Figure 13). Further studies are needed to tie these molecular observations to differences in plant species.

CONCLUSIONS

This study examined the organic geochemistry of rock samples with a predominance of terrigenous organic matter. The samples range in age from Late Permian to late Miocene, and represent a broad range

of paleodepositional environments and types of terrigenous higher-plant organic matter. Analyses of oils and condensates can result in conflicting data, especially if mixing of hydrocarbons from additional source rocks has taken place. These potential conflicts are better controlled through the study of rock samples, as calibrations can be made to lithology and kerogen composition (optical and pyrolytical). In summary, the samples are characterized by:

- high pristane/phytane ratios (up to 4),
- high content of long-chain isoprenoids,
- strong predominance of odd-carbon *n*-alkanes,
- resin signatures among tricyclics,

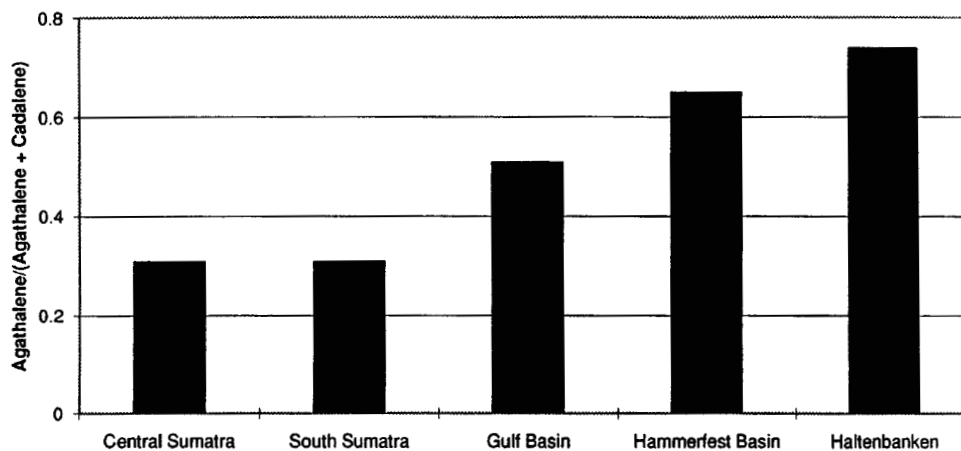


Figure 13. Comparison of cadalene and agathalene relations. Rocks of early–mid-Jurassic age from Haltenbanken, Norway, and late Permian age in the Hammerfest Basin, Norway, show the highest values of agathalene/(agathalene+cadalene). Rocks of Tertiary age from Sumatra likely contain woody material which is biochemically different (derived from different plant species) as indicated by the relatively low agathalene/(agathalene+cadalene) values.

- predominance of C_{29} regular steranes, and near-constant relative amounts of C_{27} and C_{28} regular steranes,
- hopane/sterane ratios up to 25,
- low amounts of homo-hopanes (C_{31} – C_{35} hopanes),
- relatively high concentrations of oleanane in samples with high contents of angiosperm debris,
- appreciable amounts of C_{24} tetracyclic terpanes in most samples, whereas pentacyclic compounds “x” (C_{30} $17\alpha(H)$ diahopane) and “y” were only present in some samples, probably related to oxic/suboxic depositional/diagenetic environments.
- relatively high contents of cadalene, agathalene, and retene compounds. Concentrations of cadalene and agathalene co-vary with the content of higher-plant organic matter in the kerogen. Also, the ratio of other naphthalenes to cadalene and agathalene seems useful for discerning the organic facies in the depositional environment.

ACKNOWLEDGMENTS

I thank Esso management and Exxon Production Research Company for permission to release this work. I also thank to Dave Curry at EPRCo for helpful discussions, and the technical staff of the Petroleum Geochemistry Section at EPRCo for sample analyses.

REFERENCES CITED

- Albaiges, J., Borbon, J., and Walker, II, W., 1985, Petroleum isoprenoid hydrocarbons derived from catagenic degradation of Archaeobacterial lipids: *Advances in Organic Geochemistry*, v. 8, p. 293–297.
- Alexander, R., Kagi, R., and Noble, R., 1983, Identification of the bicyclic sesquiterpanes, drimanes, and eudesmane in petroleum: *Journal of the Chemical Society, Chem. Comm.*, p. 226–228.
- Alexander, R., Larcher, A.V., Kagi, R.I., and Price, P.L., 1988, The use of plant-derived biomarkers for correlation of oils with source rocks in the Cooper/Eromanga basin system, Australia: *APEA Journal* 1988.
- Baset, Z.H., Pancirov, R.J., and Ashe, T.E., 1979, Organic compounds in coal: Structure and origins, in A.G. Douglas and J.R. Maxwell, eds., *Advances in Organic Geochemistry 1979*: Pergamon Press.
- Bendoraitis, J.G., 1974, Hydrocarbons of biogenic origin in petroleum: aromatic triterpenes and bicyclic sesquiterpenes, in B. Tissot and F. Bienner, eds., *Advances in Organic Geochemistry, 1973*: Paris, Editions Technip, p. 209–224.
- Bordenave, M., Combaz, A., and Giraud, A., 1970, Influence de l’origine des matières organiques et de leur degré d’évolution sur les produits de pyrolyse du kérogène, in G.D. Hobson and G.C. Speers, eds., *Advances in Organic Geochemistry 1966*: Pergamon Press, Oxford, p. 389–405.
- Burgess, J.D., 1974, Historical review and methods for determining thermal alteration of organic materials, in *Palynology: Proceedings Eighth Annual Meeting of the American Association Strat. Palynol.*, v. 1, p. 1–7.
- Chaffe, A.L., and Johns, R.B., 1983, Polycyclic aromatic hydrocarbons in Australian coals. I. Angularly fused pentacyclic tri- and tetraaromatic components of Victorian brown coal: *Geochimica et Cosmochimica Acta*, v. 47, p. 2141–2155.
- Chappe, B., Michaelis, W., and Albrecht, P., 1982, Polar lipids of Archaeobacteria in sediments and petroleum: *Science*, v. 217, p. 65–66.
- Cleal, C.J., 1988, Questions of flower power: *Nature*, v. 331.

- Curry, D.J., Emmett, J.K. and Hunt, J.W., 1994, Geochemistry of aliphatic-rich coals in the Cooper Basin, Australia and Taranaki Basin, New Zealand: implications for the occurrence of potentially oil-generative coals, in A.C. Scott and A.J. Fleet, eds., Coal and coal-bearing strata as oil-prone source rocks?: Geological Society Special Publication 77, p. 149–182.
- Czochanska, Z., Gilbert, T.D., Philp, R.P., Sheppard, C.M., Weston, R.J., Wood, T.A., and Woodhouse, A.D., 1988, Geochemical applications of sterane and triterpane biomarkers to a description of oils from the Taranaki Basin in New Zealand: *Organic Geochemistry*, v. 2, p. 123–135.
- Dastillung, M., 1976, Lipides de sediments recents: Thesis, University of Strasbourg, 1976.
- de Coster, G.L., 1975, The geology of the central and south Sumatra Basins: Proceedings of the Indonesian Petroleum Association, p. 77–110.
- de Rosa, M., de Rosa, S., Gambacorta, A., Minale, L., and Bullock, J.D., 1977, Chemical structure of the ether lipids of thermophilic bacteria of the Caldariella group: *Phytochemistry*, v. 16, p. 1961–1965.
- Didyk, B.M., Simoneit, B.R.T., Brassell, S.C., and Eglinton, G., 1978, Organic geochemical indicators of paleoenvironmental conditions of sedimentation: *Nature*, v. 272, p. 216–222.
- Ekweozor, C.M., Okogun, J.I., Ekong, D.E.U., and Maxwell, J.R., 1979a, Preliminary organic geochemical studies of samples from the Niger Delta (Nigeria). I. Analysis of crude oils for triterpanes: *Chemical Geology*, v. 27, p. 11–28.
- Ekweozor, C. M., Okogun, J.I., Ekong, D.E.U., and Maxwell, J.R., 1979b, Preliminary organic geochemical studies of samples from the Niger Delta (Nigeria). II. Analysis of shale for triterpenoid derivatives: *Chemical Geology*, v. 27, p. 29–37.
- Espitalié, J., Laporte, J.L., Madec, M., Marquis, F., Le Plat, P., Paulet, J., and Boutefeu, A., 1977, Méthode rapide de caractérisation des roches mères, de leur potentiel pétrolier et de leur degré d'évolution: *Rev. Inst. Fran. Petr.*, v. 32, p. 23–42.
- Giraud, A., 1970, Application of pyrolysis and gas chromatography to geochemical characterization of kerogen in sedimentary rock: *AAPG Bulletin*, v. 54, p. 439–451.
- Grantham, P.J., Posthuma, J., and Baak, A., 1983, Triterpanes in a number of Far Eastern crude oils, in M. Bjoroy et al., eds., *Advances in Organic Geochemistry 1981*: Chichester, Wiley, p. 675–683.
- Heum, O.R., Dalland, A., Meisingset, 1986, Habitat of hydrocarbons at Haltenbanken (PVT-modelling as a predictive tool in hydrocarbon exploration), in *Habitat of Hydrocarbons on the Norwegian Continental Shelf*: Norwegian Petroleum Society, p. 259–274.
- Hoffmann, C.F., Mackenzie, A.S., Lewis, C.A., Maxwell, J.R., Oudin, J.L., Durand, B., and Hollander, N.B., 1984, Geohistory and hydrocarbon evaluation of the Haltenbank area, in *Petroleum Geology of the North European Margin*: Norwegian Petroleum Society, p. 383–388.
- Hoffmann, F., Mackenzie, A.S., Lewis, C.A., Maxwell, J.R., Oudin, J.L., Durand, B., and Vandenbroucke, M., 1984, A biological marker study of coals, shales and oils from the Mahakam Delta, Kalimantan, Indonesia: *Chemical Geology*, v. 42, p. 1–23.
- Horsfield, B., 1984, Pyrolysis studies and petroleum exploration, in J. Brooks and D. Welte, eds., *Advances in Petroleum Geochemistry*, v. 1, p. 247–298.
- Huang, W.Y., and Meinschein, W.G., 1979, Sterols as ecological indicators: *Geochimica et Cosmochimica Acta*, v. 43, p. 739–745.
- Ibata, K., Kageyu, A., Takigawa, T., Okada, M., Nishida, T., Mizuno, M., Tanaka, Y., 1984, Poly prenols from conifers: multiplicity in chain length distribution: *Phytochemistry*, v. 23, p. 2517–2521.
- Isaksen, G.H., 1991, Molecular indicators of lacustrine freshwater depositional environments, in D.A.C. Manning et al., eds., *Organic Geochemistry: Advances and Applications in the Natural Environment*. 15th Meeting of EAOG: Manchester University Press, p. 361–364.
- Katayama, M., and Marumo, S., 1983, The revised structure of sclerosporin, a sporogenic substance of *Sclerotinia fructicola*. The total synthesis of (\pm)-sclerosparin: *Tetrahedron Letters*, v. 24, n. 16, p. 1703–1706.
- Larter, S.R., Solli, H., and Douglas, A.G., 1978, Analysis of kerogens by pyrolysis-gas chromatography mass spectrometry using selective ion detection: *Journal of Chromatography*, v. 167, p. 423–431.
- Loomis, D.W., and Croteau, R., 1980, Biochemistry of terpenoids, in P.K. Stumpf, ed., *The Biochemistry of Plants: A Comprehensive Treatise*, v. 4: Academic Press.
- Mair, B.J., 1964, Terpenoids, fatty acids and alcohols as source materials for petroleum hydrocarbons: *Geochimica et Cosmochimica Acta*, v. 28, p. 1303–1321.
- Maxwell, J.R., Cox, R.E., Ackman, R.G., and Hooper, S.N., 1972, The diagenesis and maturation of phytol. The stereochemistry of 2,6,10,14-tetramethylpentadecane from an ancient sediment, in H.R. von Gaertner and H. Wehner, eds., *Advances in Organic Geochemistry 1971*: Pergamon Press, p. 277–291.
- Mello, M.R., Gaglianone, P.C., Brassell, S.C., and Maxwell, J.R., 1988, Geochemical and biological marker assessment of depositional environments using Brazilian offshore oils: *Marine and Petroleum Geology*, v. 5, p. 205–223.
- Moldowan, J.M., and Seifert, W.K., 1979, Head-to-head linked isoprenoid hydrocarbons in petroleum: *Science*, v. 204, p. 169–171.
- Moldowan, M.J., Seifert, W.K., and Gallegos, E.J., 1985, Relationship between petroleum composition and depositional environment of petroleum source rocks: *AAPG Bulletin*, v. 69, n. 8, p. 1255–1268.
- Moldowan, M.J., Fago, F.J., Carlson, R.M.K., Young, D.C., VanDuyne, G., Clardy, J., Schoell, M., Pillinger, C.T., and Watt, D.S., 1991, Rearranged hopanes in sediments and petroleum: *Geochimica et Cosmochimica Acta*, v. 55, n. 11, p. 3333–3354.
- Ourisson, G., Albrecht, P., Rohmer, M., 1979, The hopanoids, paleochemistry and biochemistry of a group of natural products: *Pure Applied Chemistry*, v. 51, p. 709–729.

- Palmer, S.E., 1984, Effect of water washing on C₁₅₊ hydrocarbon fractions of crude oil from NW Palawan, Philippines: AAPG Bulletin, v. 68, p. 137–149.
- Philp, R.P., 1994, Geochemical characteristics of oils derived predominantly from terrigenous source materials, in A.C. Scott and A.J. Fleet, eds., Coal and coal-bearing strata as oil-prone source rocks?: Geological Society Special Publication 77, p. 71–91.
- Philp, R.P., and Gilbert, T.D., 1986, Biomarker distributions in Australian oils predominantly derived from terrigenous source material, in Advances in Organic Geochemistry 1985: Organic Geochemistry, v. 10, p. 73–84.
- Richardson, J.S., and Müller, D.E., 1982, Identification of dicyclic and tricyclic hydrocarbons in the saturate fraction of a crude oil by GC/MS: Analytical Chemistry, v. 54, p. 765–768.
- Ronnevik, H.C., Beskow, B., and Jacobsen, H.P., 1982, Structural and stratigraphic evolution of the Barents Sea, in A.F. Embry and H.R. Balkwill, eds., Arctic Geology and Geophysics: Canadian Society of Petroleum Geology Memoir 8, p. 431–440.
- Seifert, W.K., and Moldowan, J.M., 1981, Paleoreconstruction by biological markers: Geochimica et Cosmochimica Acta, v. 45, p. 783–794.
- Simoneit, B.R.T., 1986, Cyclic terpenoids of the geosphere, in R.B. Johns, ed., Biological Markers in the Sedimentary Record. Methods in Geochemistry and Geophysics, 24: Elsevier, p. 43–99.
- Sosrowidjojo, I.B., Alexander, R., and Kagi, R.I., 1994, The biomarker composition of some crude oils from Sumatra: Organic Geochemistry, v. 21, n. 3/4, p. 303–312.
- Staplin, F.L., 1969, Sedimentary organic matter, organic metamorphism, and oil and gas occurrence: Canadian Petroleum Geology Bulletin, v. 17, p. 47–66.
- Strachan, M.G., Alexander, R., and Kagi, R.I., 1988, Trimethylnaphthalenes in crude oils and sediments: effects of source and maturity: Geochimica et Cosmochimica Acta, v. 52, p. 1255–1264.
- Surlyk, F., 1978, Jurassic basin evolution of East Greenland: Nature, v. 274, n. 5667, p. 130–133.
- Suseno, P.H., Zakaria, Mujahidin N., and Subroto, E.A., 1992, Contributions of Lahat Formation as hydrocarbon source rock in South Palembang area, south Sumatra, Indonesia, in Proceedings of the Indonesian Petroleum Association Twenty-First Annual Convention, p. 57–90.
- Tanner, J.A., and Feux, A.N., 1988, Chemical and isotopic evidence of the origin of hydrocarbons and source potential of rocks from Vicksburg and Jackson formations of Slick Ranch area, Starr County, Texas, in Geochemistry of Gulf Coast Oils and Gases: SEPM Program Abstract, Ninth Annual Research Conference, New Orleans, Louisiana.
- Thomas, B.R., 1969, Kauri resins—modern and fossil, in G. Eglinton and M.T.J. Murphy, eds., Organic Geochemistry—Methods and Results: Berlin, Springer-Verlag, p. 599–618.
- Tissot, B., Durand, B., Espitalié, J., Combaz, A., 1974, Influence of the nature and diagenesis of organic matter in formation of petroleum: AAPG Bulletin, v. 58, p. 499–506.
- van Aarssen, B.G.K., Cox, H.G., Hoogendoorn, P., and de Leeuw, J.W., 1990, A cadinane biopolymer in fossil and extant dammar resins as a source of cadinanes and bicadinanes in crude oils from southeast Asia: Geochimica et Cosmochimica Acta, v. 54, p. 3021–3031.
- van de Meent, D., Brown, S.C., Philp, R.P., and Simoneit, B.R.T., 1980, Pyrolysis resolution gas chromatography and pyrolysis gas-chromatography mass spectrometry of kerogen precursors: Geochimica et Cosmochimica Acta, v. 44, p. 999–1014.
- Whitehead, E.V., 1974, The structure of petroleum pentacyclanes, in B. Tissot and F. Bienner, eds., Advances in Organic Geochemistry 1973: Paris, Editions Technip, p. 225–243.
- Williams, H.H., Kelly, P.A., Janks, J.S., and Christensen, R.M., 1985, The Paleogene rift basin source rocks of Central Sumatra, in Proceedings of the Indonesian Petroleum Association Fourteenth Annual Convention, p. 57–90.

Effect of Late Devonian Paleoclimate on Source Rock Quality and Location

Allen R. Ormiston
Amoco E&P Technology
Tulsa, Oklahoma, U.S.A.

Robert J. Oglesby
Purdue University
West Lafayette, Indiana, U.S.A.

ABSTRACT

Late Devonian climate was very different from the present. With most of the landmass in equatorial or high-latitude regions, there was little monsoonal activity. Precipitation maxima coincided with elevations. No perennial snowcover existed because of Gondwanan dryness. Low-latitude sea surface temperatures ranged between 17 and 34°C, high enough to kill reefs, leading to increased volume of plankton reaching epeiric seas. Upwellings explain only a minority of Upper Devonian source rocks. Far more source rocks were produced by conditions best described by the epeiric sea model. Anoxia was promoted by salinity stratification and/or low seasonality.

INTRODUCTION

A key component in understanding the occurrence and nature of Devonian source rocks is an assessment of the role of climate on physical processes responsible for source rock formation. Previous studies that assessed the relationship between climate and Upper Devonian source rocks were qualitative and concentrated on the role of upwellings (e.g., Parrish et al., 1979; Parrish, 1982). While this work demonstrated certain ways in which climatic and sedimentological processes could interact to affect deposition of source rock precursors, the work could not be quantified; that is, it could not be determined whether the proposed mechanisms could actually occur on the planet Earth during the Devonian. Furthermore, these models depend on a priori assumption of the important processes; independent assessment of other possibilities not originally anticipated cannot be undertaken.

Quantitative modeling, through the use of sophisticated general circulation models (GCMs) of climate, holds the potential to avoid both of these problems. GCMs provide a quantitative simulation of the climate for any geologic period, dependent only on the boundary conditions and external forcings that are imposed. The solution is not directly dependent on the physical processes assumed to be important for any particular scenario. This provides an independent check of any preconceived hypothesis. It also means that investigation of the runs may suggest mechanisms not previously suggested.

In this paper, we report on a study in which we have used a GCM to help evaluate existing theories and develop new theories about the role of climatic processes in source rock formation and deposition during the Devonian. We have employed a widely used atmospheric GCM, the National Center for Atmospheric Research (NCAR) "Community Climate Model," version 1 (CCM1). We made simulations with boundary

conditions (paleogeography and paleotopography) and forcings appropriate for the Devonian. We evaluate the general climate as simulated globally for the Devonian, and then we use the climate model results to assess conceptual models that relate Devonian climate to source rock formation and deposition. Our results suggest a diverse set of connections between climatic factors and source rocks, and do not support upwelling as a master control for source rock formation.

In the next section, we provide a summary of our estimation of the Devonian paleogeography and paleotopography, both to orient readers and to acquaint them with particular details we have used that may not be otherwise obtainable readily from the literature. In section 3, we describe known source rock regions for the Devonian, emphasizing the paleoenvironmental context in which they occur. In section 4, we describe existing conceptual models that have been proposed to account for Devonian source rock occurrences. In section 5, we describe the GCM we have employed, as well as our experiment strategy (including a discussion of how we have treated boundary

conditions and external forcings). In section 6, we describe the basic simulated Devonian climate. In section 7, we discuss the implications of the climate modeling results for previous, as well as new, scenarios of source rock occurrence. In section 8, we provide a summary and conclusion for the study, as well as directions for future research.

PALEOGEOGRAPHY

Sources of the Paleogeographic Reconstruction Employed in This Paper

Success of the uniformitarian application of principles of modern hydrospheric-atmospheric circulation systems to ancient reconstructions depends critically on reliable paleogeographic and topographic reconstructions. For those attempting Paleozoic interpretations, this has long been a vexatious issue because Paleozoic paleogeography is less well constrained than reconstructions of more recent geologic periods. Figure 1 shows the major sutures and component

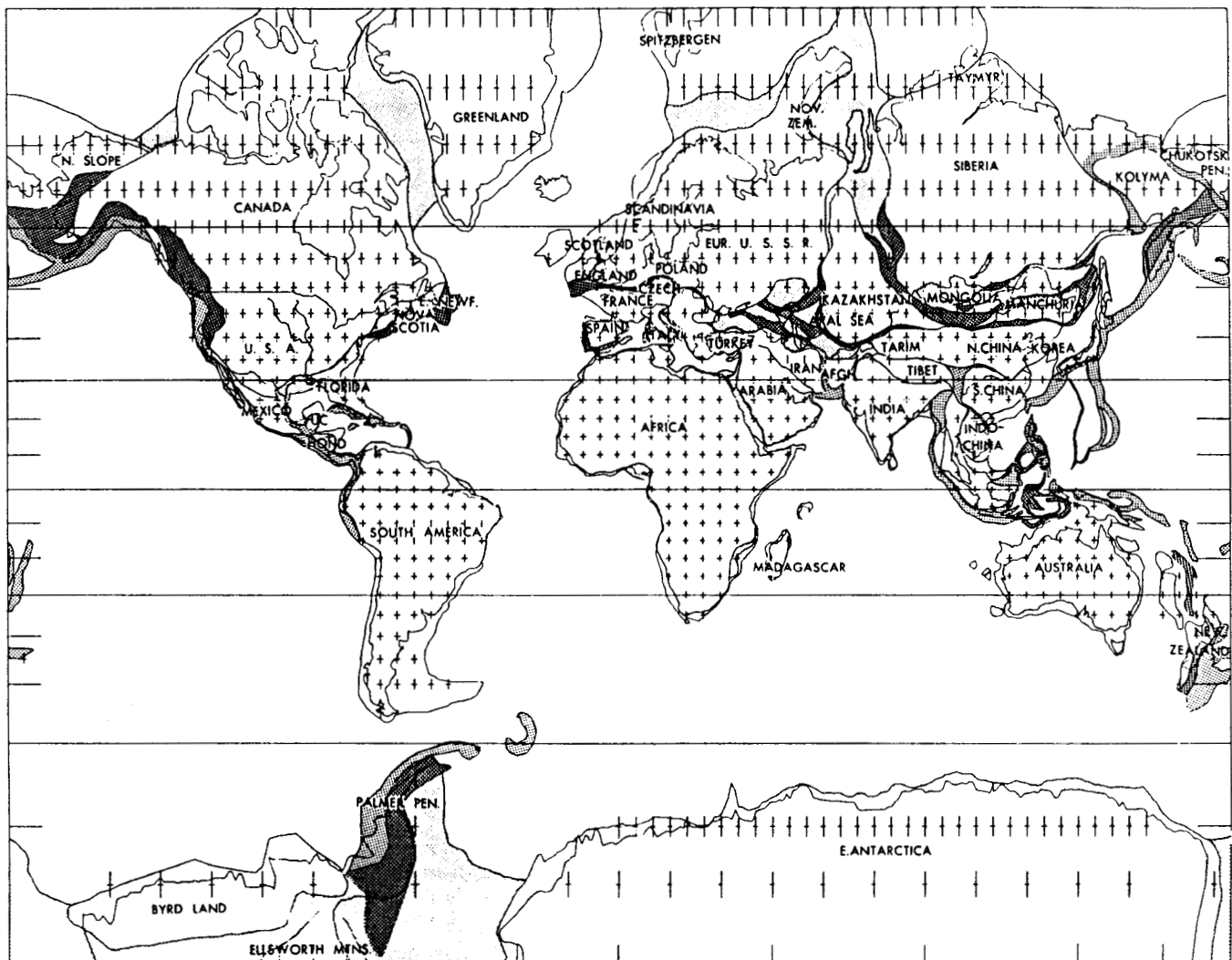


Figure 1. Map showing sutures and continental elements of paleogeographic maps used in this report. Dense shading depicts late Paleozoic and Mesozoic accreted terranes. After Ziegler et al. (1977).

paleocontinental elements of the reconstruction used by us. We discuss some specific details below.

The reinterpretation of Australian paleomagnetic data by Klootwijk and Giddings (1988) changes the high-latitude position for Australia that was used by Scotese (1986) and places Australia in low southern latitudes. Since that interpretation is far more consistent with the faunal distribution data in the Late Devonian, in particular for conodont migration, we have adopted that interpretation. The oceanic separation between Gondwana and North America shown on our map (Figure 2) is required by the vertebrate distributional data of Young (1990, p. 250). The location of Gondwana has been a very serious paleomagnetic problem for some time, because of the limited number of data points and the irreconcilable solutions which they provide. Scotese and Barrett (1990) have pointed out the quite unsatisfactory character of the paleomagnetic database and have employed lithic and biotic data to constrain the position of Gondwana. Our placement of Gondwana for the Upper Devonian is in conformity with their interpretation.

The positioning of Siberia has been a point of discussion for many years. The high-latitude placement of Siberia shown on the Upper Devonian reconstruction of Scotese (1986) is inconsistent with widespread development of carbonates and evaporites on that paleocontinent during the Upper Devonian. The paleomagnetic database (Khranov and Rodionov, 1981) on which that positioning has depended is open to serious question because of the vague age dating of the samples that was used and the absence of any field tests to establish consistent paleohorizontal determinations in the sample program. Lithic paleoclimate and biotic paleoclimate indicators, such as coral distributions and the distributions of evaporites and oolitic carbonates, require a much more southerly positioning of Siberia than shown by Scotese (1986). Thus, our positioning for Siberia centered on about 40°N latitude regards existing paleomagnetic data as unreliable and is nearly convergent with the reconstruction by Witzke and Heckel (1990). It is also convergent with the reconstruction of Burrett et al. (1990), except for the unrotated orientation (right way up) for Siberia used by them.

The positioning of the Kolyma block has been a problem because of irreconcilable paleomagnetic poles from different parts of this block. The reason may be that Kolyma was not a single unit, but a dispersed group of microplates in the Upper Devonian. The widespread development of carbonates on this block prevents locating it any further north than Siberia has been situated. We have attempted to apply the principle of "no harm" in terms of the longitudinal positioning of Kolyma, which we consider as a unit, placing it sufficiently distant from other continental masses that it would have exerted no great influence on climates of adjacent blocks. Famennian conodont faunas described from Kolyma (Gagiev, 1982) and our modeling of surface winds suggest that it lay in an area of cyclonic circulation in good communication with Siberia.

Defining Paleotopography

We may infer the existence of ancient topography by means of mapping lithofacies and recognizing that coarse siliciclastics are derived from nearby topographic highs, by noting the existence of emergent barriers which separate biogeographic provinces, by recognizing large areas of Precambrian rocks (shields) which lack any Upper Devonian stratigraphic record as having been emergent, by recognizing that continental collisions frequently produced major marginal zones of uplift, and by recognizing major tectonic displacements, such as rifts and overthrusts, as having created significant topography. This means that a global synthesis of lithofacies distributions, an analysis of biogeographic provinces, and a tectonic analysis are all required to infer paleotopography. These sorts of analyses were carried out in an Upper Devonian source rock study (Hinch et al., 1990) leading to identification of elevated emergent areas. Estimating topographic height is far more difficult. Facies analyses can provide a clue by relating volume of coarse clastics to probable minimal height of adjacent topography. The Acadian orogeny in eastern North America, produced by progressive collision in Middle and Late Devonian, led to growth of mountainous topography along the East Coast. Studies carried out at the University of Chicago by Ziegler and others have tried to relate crustal thickness maps to paleophysiography. Ziegler's further studies of conodont alteration index, fluid inclusions, and coal vitrinite values suggest that there was a deep mountain root for the Appalachians and that they had elevations of some 3000 m during the Late Devonian. From this, one can make relative comparisons of sediment wedges derived from other land areas of the globe to recreate a relative topography. Figure 2 shows our Upper Devonian topographic reconstruction derived from consideration of principles discussed above.

DISTRIBUTION OF UPPER DEVONIAN SOURCE ROCKS

North America

As shown by Figure 3, good quality marine source rocks occupy large areas of North American epicontinental basins. The major Upper Devonian source rocks in North America are among the richest sources of this age in the world. Almost all of them are epeiric sea deposits. According to geochemical data summarized by Hinch et al. (1990), 14 of the 15 highest quality source rocks of Late Devonian age are North American.

Europe (Excluding European Russia)

High-quality Upper Devonian source rocks are of limited occurrence in Europe. The richest known occurrence is the Porsquen Shales of Brittany which have an average total organic carbon (TOC) of 4.3%. Another important occurrence is in the subsurface of Poland where Famennian source rocks richer than 4%

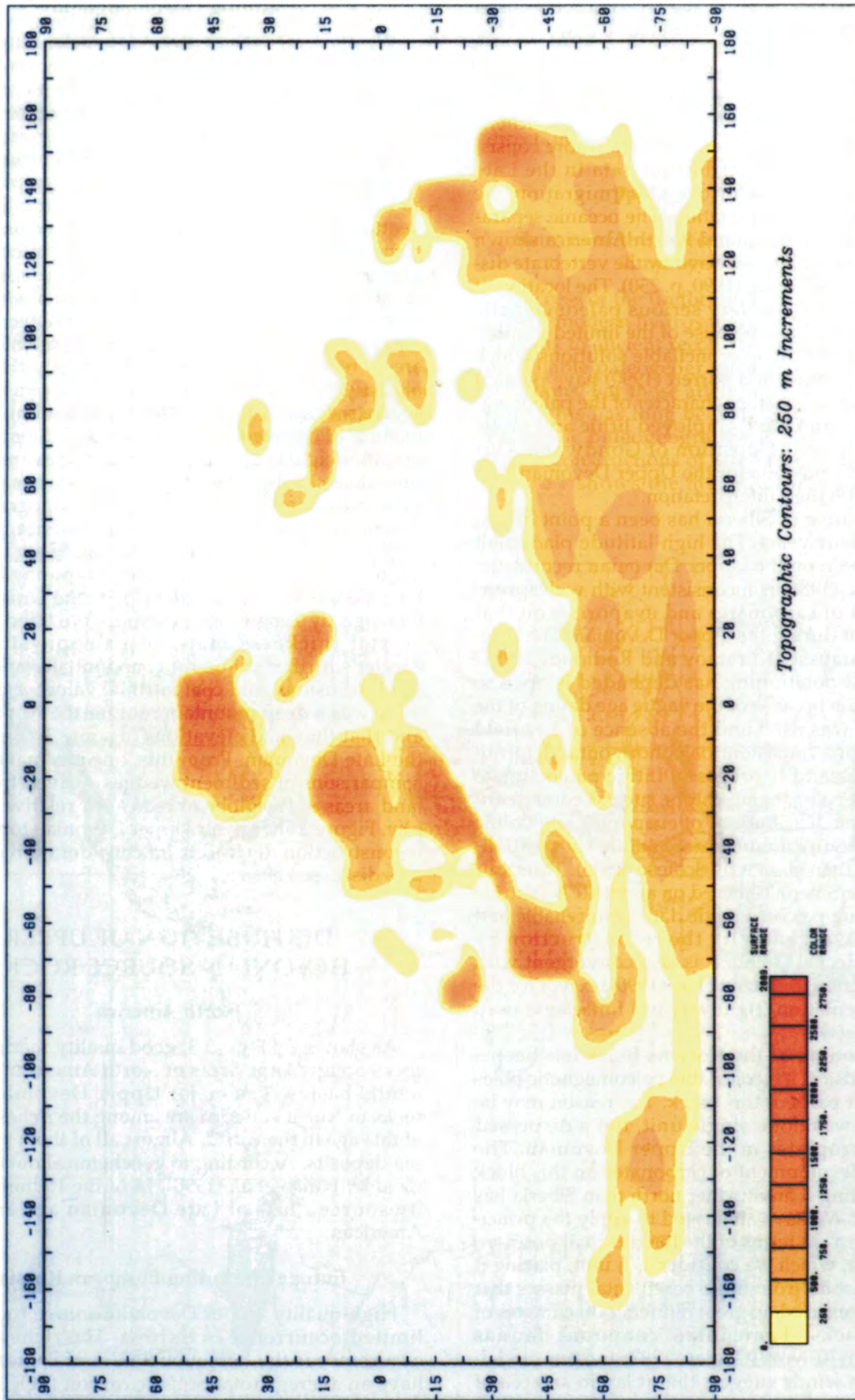


Figure 2. Late Devonian paleogeography and topography.

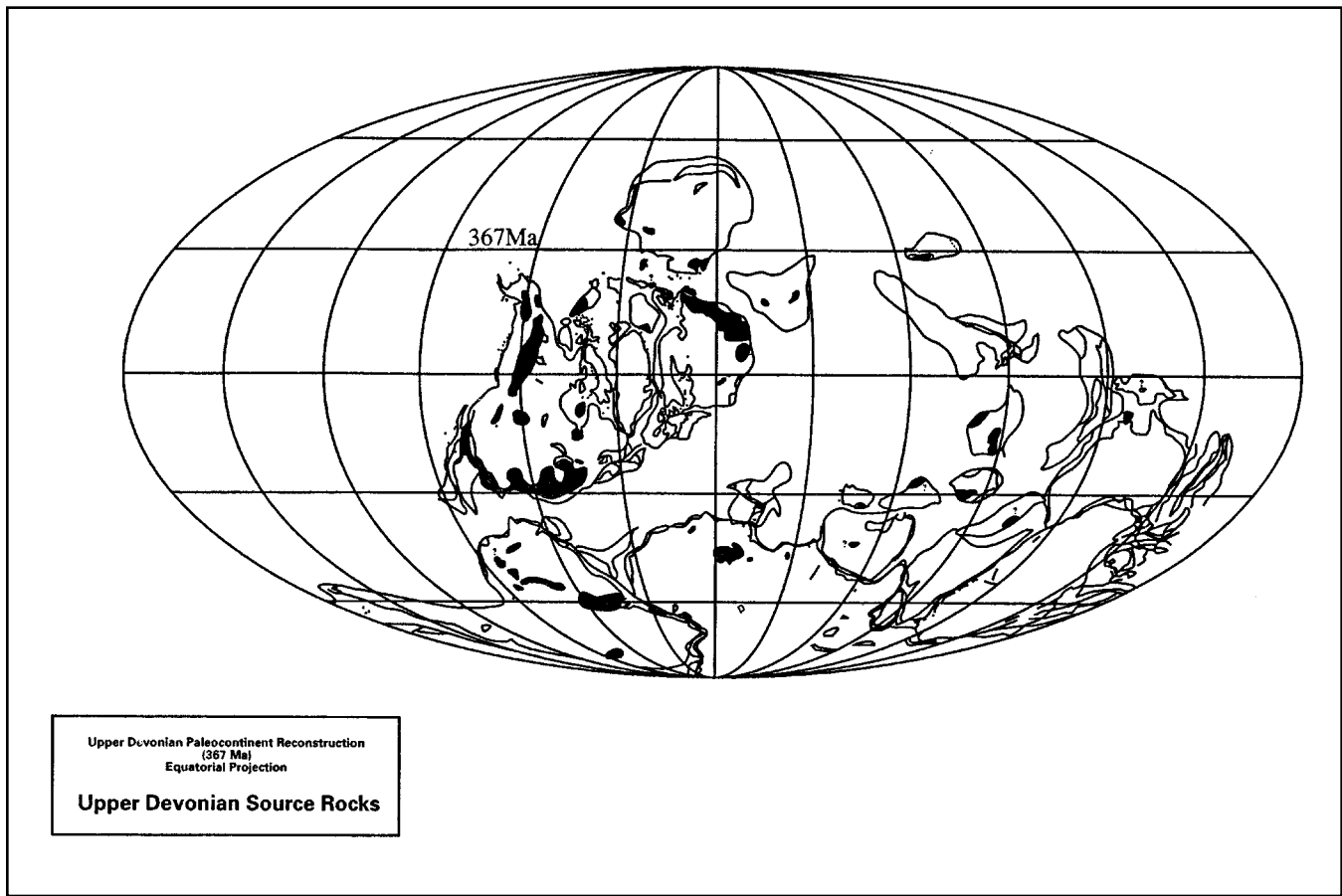


Figure 3. Distribution of Upper Devonian source rocks (>2% TOC).

occur. The source rocks of Poland and Brittany are typical epicontinental sea type. In southern France, Famennian source rocks occur in the Montagne Noire in deeper water facies and have TOCs up to 3%. Upper Devonian nonmarine source rocks are also known from the Orcadian basin of northern Scotland where TOC values as high as 5% are known, but mean TOC values are considerably smaller.

The Russian Platform

The Russian platform and basins within and peripheral to it contain extensively developed world-class source rocks localized in rifts or in basins which experienced pre-Devonian rifting but are classifiable as epicontinental source rocks. In all, an area of some 490,000 km² consists of good quality source rocks of the domank facies in the Volgo-Ural, Timan-Pechora, Pricaspian, Pripyat, and Dneiper-Donets basins. A very large area of the Pricaspian basin is underlain by potential Upper Devonian source rocks for which there is, however, insufficient geochemical data to derive reliable calculations. It is known that TOC values ranging from 1.5 up to 11% characterize rocks of this age in the Pricaspian basin (Bylinkin et al., 1984). The total area of the Pricaspian basin potentially underlain by such rocks is 290,000 km²; however, the

thickness of the source beds and their quality is inadequately known. Water depths in the Pricaspian basin somewhat exceeded those of the other Russian platform basins in the judgment of those who have carried out studies on the Pricaspian basin. For example, Anfan'sieva and Zamilatskaya (1992) interpreted the depth of water for Upper Devonian to Lower Carboniferous strata in the Pricaspian basin to have been approximately 250 m, slightly deeper than the 100 to 200 m water depth that is widely accepted for the Timan-Pechora basin. Yet, the Pricaspian basin, like the Michigan basin, although relatively deep water, was clearly cratonic in setting and not oceanic.

Siberia

The west Siberian basin contains Upper Devonian source rocks with TOC values up to 3.5% (Trofimuk, 1984). These clastic sources are closely associated with carbonate buildups which serve as reservoirs (Zapivalov and Trofimuk, 1989). The association of these source rocks with Upper Devonian buildups and their other facies characteristics suggest that they were epicontinental deposits.

A rift-related elongate trough-like Paleozoic depression in northern Taimyr accumulated source-prone facies through much of the Paleozoic. The western end

of this trough includes Upper Devonian source rocks with TOC values of 2.5% (Zharkov and Bakhturov, 1982).

Geochemical information from eastern Siberia is sparse, but even here there are several rift-related occurrences of Upper Devonian source-prone facies. By way of summary, it can be said that epeiric sea source rocks of Late Devonian age are preserved in grabens at scattered localities in Eastern Siberia. In the Pay Khoy area, which was situated on the slope of the Uralian Ocean during Late Devonian time, there are Upper Devonian source rocks whose paleobathymetry contrasts with the epeiric sea source rocks discussed above (Puchkov, 1979). Upper Devonian siliceous shales in this area are thin, bathyal deposits with TOC values up to 5% (Yudovich et al., 1985) but typically are at elevated maturation levels (Ovnatanova, 1989), suggesting thermal exposure for these rocks of 300°C or more.

North Africa

The Illizi-Ghadames basin of Algeria, an area of 81,800 km², contains Upper Devonian source rocks with TOC values in excess of 2.5%. Other Algerian basins such as the Bechar-Ahnet, Cuvette de Sbra, Grand Erg Occidental, and Depression du Mouydir contain small areas of distribution of marginal quality Upper Devonian source rocks. In the Tindouf basin of western Algeria, Upper Devonian rocks are overmature. The small Tadla basin of Morocco also contains Upper Devonian source rocks. All of these basins are examples of epeiric sea deposition in which good source rocks coincide with pronounced transgressive episodes. A single subsurface occurrence of Upper Devonian source facies is known from western Egypt in the Foram-1 well (paleoservices). Geochemical data are not available for subsurface Libyan Upper Devonian rocks, but source rocks are apparently present. The partly onshore and partly offshore Keta basin of Ghana was a platformal basin with epeiric sea deposition in Devonian time (Akpati, 1978). Famennian shales in this basin have source rock properties.

Arabian Platform

In Saudi Arabia, epeiric sea Upper Devonian strata preserved in the Widyan graben include source rocks. Hussein (1992) reports TOC values for these source rocks of up to 3.7%.

India

No geochemical data are available to support the existence of Upper Devonian source rocks on the Indian subcontinent. However, Upper Devonian black shales of epeiric sea type crop out in Bhuttan (Termier and Gansser, 1974). These rocks are apparently now overmature but may originally have had source rock attributes.

China

Frasnian rocks in the Shongshan section in Guangxi Province, China, are epeiric sea deposits that probably include source rocks. Luijiang Formation, which is described as bituminous black shales and includes four of the major transgressive episodes of Johnson et al. (1985), is especially likely to be a source rock interval. There is presently no geochemical evidence to prove this. Elsewhere in south China, Upper Devonian source rocks are known from the Chuxiong basin of Yunnan Province. Upper Devonian black shales and argillaceous, siliceous limestones from the Nanpanjiang basin in Guizhou and Guangxi provinces were identified as source rocks by Lee (1984) but without supporting geochemical data.

Australia

The Canning basin has been identified by Ulmishek and Klemme (1990) as a basin with significant Upper Devonian source rocks, but available geochemical data do not support this contention.

Only the Arafura basin in northern Australia clearly has Upper Devonian source rocks. The Arafura Group in this basin exhibits TOC values as high as 4.8% (Bradshaw et al., 1990), although the average TOC is described as being less. The Upper Devonian in several of the Australian cratonic basins, such as the Officer and Amadeus basins and others, is very sand rich and not prospective for source rocks.

South America

Many of the South American basins have limited or no development of Upper Devonian source rocks. This may partly be the result of local removal of Upper Devonian strata beneath an Early Carboniferous unconformity (Hinch et al., 1990). It is also true that several of these basins show large volumes of Upper Devonian siliciclastics which have a deleterious effect on source rock quality.

Upper Devonian rocks in the Amazon and Solimoes (formerly Upper Amazon) basins have good TOC values but do not exceed 100 m in thickness. In the Amazon basin, the Barreirinha member of the Curua Formation is known to be the source rock. In all cases, the Upper Devonian strata with elevated TOC values in South American basins have the characteristics of epeiric sea deposits.

Significance

It is evident from the preceding summary that epeiric sea source rocks (those deposited in a few hundred meters of water) were the globally dominant type during the Late Devonian. Only the Upper Devonian source rocks of Pay Khoy exhibit characteristics of deep-water deposition. Puchkov (1979, p. 66) determined that the water depth in which these Pay Khoy source rocks were deposited was between 2000 and 3000 m. Such a reconstruction is reasonable since these

rocks were deposited on the slope of the oceanic Uralian Seaway. It is difficult to find other clear-cut examples of deep-water Upper Devonian source rocks. An excellent example of facially varied, oceanic Upper Devonian strata has been described by Rotarash et al. (1982) from the margin of the Siberian continent, but no source rock facies were recognized.

It could be argued that there is a systematic underrepresentation of ancient oceanic slope facies, because such rocks are commonly subducted and either metamorphosed beyond recognition or nowhere exposed. If this is true, the argument also becomes a reason to de-emphasize the search for oceanic source rocks as they should be more likely to be of poor quality.

COMPETING MODELS OF SOURCE ROCK DEPOSITION

Two incompatible models have dominated literature discussions of source rock genesis for some time. The first of these, appropriately named the *productivity model*, assumes the applicability of modern oceanic models to ancient examples of marine source rocks. This model assumes that greatly increased bioproductivity in surface ocean waters can overwhelm the oxygen content of underlying waters with organic matter whose decay consumes oxygen. The excess unoxidized organic matter then settles into a dysaerobic or anoxic environment where it is preserved. In essence, the several available variants of upwelling models are essentially synonyms for the productivity model.

The second model is the *preservational model*, which invokes some form of water stratification that disrupts vertical circulation of the water column, eventually resulting in diminished oxygen flux between bottom waters and the upper parts of the water column. Bottom waters become anoxic eventually and preserve incoming organic matter. The commonly observed evidence for strongest anoxia in the deeper central parts of many depositional basins is viewed as supporting the operation of this model. The Michigan basin, Illinois basin, and Williston basin are good De-

vonian examples of this phenomenon, and the Black Sea basin is an excellent modern example. They all support the concept of an anoxic water body preserving organic matter as an important control on the development of source rocks. The Black Sea is a particularly persuasive example because maximum bioproductivity there is in nearshore areas, adjacent to points of entry of river waters which are transporting nutrients. Yet, the highest TOC values (Huc, 1980) are preserved in the central, deeper parts of this basin. This lack of spatial coincidence of maximum TOC values and maximum bioproductivity in the Black Sea (Figure 4) fails to support the productivity model according to which these two values should be highest at the same location.

The nature of Upper Devonian source rocks summarized above clearly suggests the operation of a third model, namely an *epeiric sea model*. Although it can be appropriately classified as a variant of the preservational model, it deserves separate naming as a way of emphasizing some important characteristics. The shallowness of the water column (often <500 m) in this model enhances its preservational capacity. Studies by Suess (1980) suggest that because of extensive consumption and degradation of particulate organic matter during its long water column residence time, a sea of 400 m depth should initially preserve ten times as much organic carbon as one 4000 m deep—the average depth of modern seas (Figure 5). In addition, further transgressions can greatly increase the areal extent. These characteristics are clearly reflected in many of the source rocks examined in this study which exhibit large areas of distribution in shallow seas and good TOC values (i.e., >2% TOC).

CLIMATE MODEL DESCRIPTION AND EXPERIMENTAL STRATEGY

Model Description

The climate model employed for this study is the NCAR CCM1, which is described by Williamson et al. (1987), combined with a description of the model

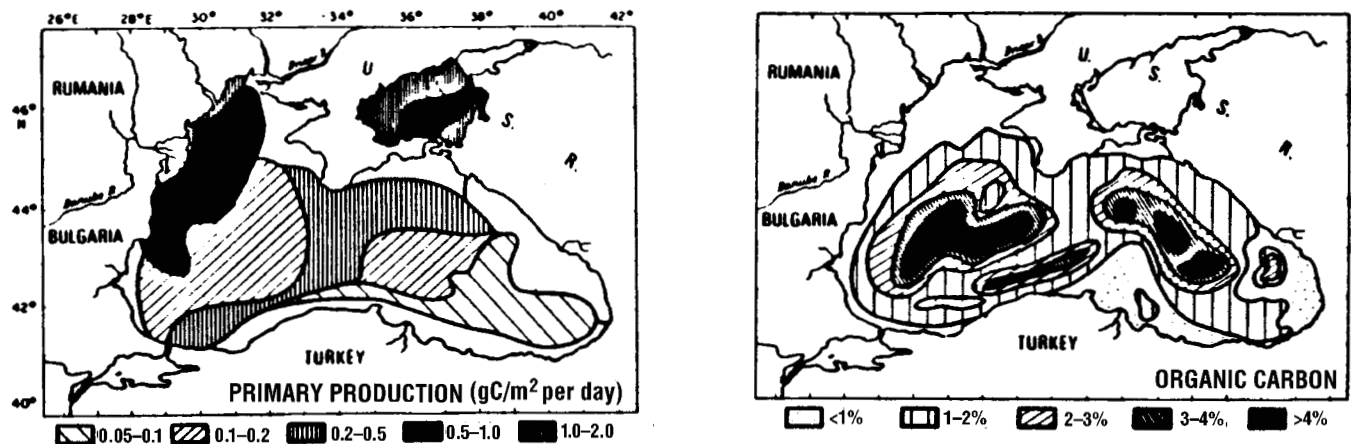


Figure 4. Noncoincidence of maximal bioproductivity and elevated TOC in the Black Sea. After Huc (1980).

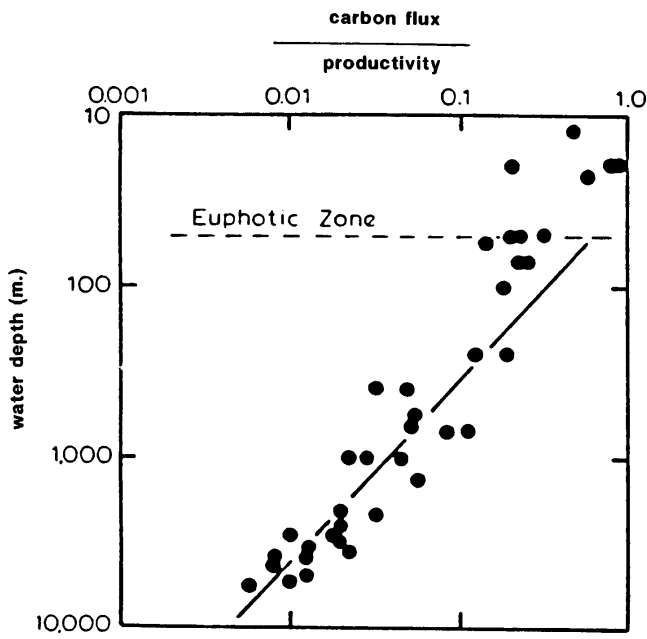


Figure 5. Relation of water depth to organic carbon survival—a key factor in the epeiric sea model. After Suess (1980).

climate statistics for the present-day given by Williamson and Williamson (1987). The CCM1 is global in domain and consists of the conservation equations for mass, momentum, energy, and moisture expressed for 12 vertical layers, with an equivalent horizontal resolution of 7.5° longitude by 4.45° latitude. Realistic topography is incorporated to the extent possible, given the coarse horizontal resolution and spectral smoothing. Using a pseudospectral scheme, one can use the model to calculate the quasi-equilibrium statistics of such quantities as the winds, temperatures, humidities, radiative fluxes, clouds, surface energy budget, and precipitation. Surface temperatures over land and sea ice (if any) are obtained via the instantaneous surface energy budget. Because of the large effective thermal inertia of the ocean, computing sea surface temperatures (SSTs) is an uncertain, computer-intensive procedure. We instead have chosen to prescribe SSTs for our simulations; how we did this is described in detail in the Experiment Strategy section. The model can be run in one of two radiation modes: perpetual season, in which radiation is held fixed at one day of the year (usually either mid-January or mid-July, in order to get mid-winter or mid-summer conditions, depending on hemisphere), or in seasonal-cycle mode, with insolation varying as to the time of year. With perpetual-season mode, a fixed surface hydrology must be used (explained more fully below). When seasonal-cycle mode is chosen, an interactive surface hydrology is employed in which soil moisture, snowcover, and, in some cases, sea ice are computed as functions of time and can thus interact with other model components.

Experiment Strategy

We have made three simulations of Late Devonian climate with CCM1: two 450 day perpetual-season simulations (one for mid-January and one for mid-July), and a 5 year seasonal-cycle run. All simulations use the paleogeography and paleotopography described earlier but differ in how they treat SSTs, snowcover, and soil moisture. Figure 2 shows the paleogeography and paleotopography we used, binned to the fairly coarse model resolution of 4.45° latitude by 7.5° longitude. The topographic elevations have undergone “spectral smoothing,” which acts to broaden and lower elevational features. For lack of more complete information on the nature of Devonian SSTs, we based the SSTs for our simulations on those computed for the Cretaceous (Barron and Washington, 1984) and subsequently modified by Oglesby and Park (1989). Further modifications were made based on scanty Amoco data for the Devonian. For instance, presence of Upper Devonian reefs at 40°S latitude was a basis for specifying a 17°C minimum SST at that latitude. The most important effect was to increase slightly the northern hemisphere meridional temperature gradient. The SSTs are all prescribed as zonally symmetric; that is, they are constant around a given latitude circle. The January and July seasonal range is that used by Oglesby and Park (1989); this range assumes a relatively “equable,” or reduced seasonality climate and is about half the present-day range. The seasonal difference is about 4°C at high latitudes, decreasing more-or-less linearly to no seasonal difference equatorward of 25°N and 25°S latitude. For the perpetual-season simulations, we of course needed only to specify the January or July SST as appropriate. For the seasonal-cycle simulation, we needed to prescribe a full seasonal cycle of SSTs; to do this we adopted the methodology used by Oglesby (1989).

We have used the interactive hydrology for the seasonal-cycle simulation, but it could not be used for the perpetual-season simulations (because continental conditions will get unrealistically dry in perpetual summer and unrealistically wet in perpetual winter). Instead, we must impose (prescribe) surface wetness (a proxy for soil moisture) and snowcover. For surface wetness, we followed Oglesby and Park (1989) and used a value of 0.25 (where this value represents the ratio of actual evaporation to evaporation from a saturated surface). This value represents most nondesert surface types in the model control; since we know little about Devonian vegetation and land covers, we use it under the principle of “least harm.” For snowcover in the perpetual-season runs, we simply specified a zero field; that is, no snowcover anywhere, at anytime, during the runs. We also needed to specify land surface albedos for both the perpetual-season and seasonal-cycle simulations; again, we followed Oglesby and Park (1989) and everywhere used a value for short grassland of 0.15 that is roughly in the middle of allowable surface type values.

Three other model parameters are of potential importance for pre-Pleistocene paleoclimatic studies

and need further explanation. These three include atmospheric CO₂ concentration, solar luminosity, and the earth's rotation rate. CO₂ concentration undergoes large natural fluctuations and has been considerably elevated in the past; for example, during the Mesozoic, values may have been up to 12 times present-day values. Going as far back in time as the Devonian, it is much less certain what CO₂ values were, although geochemical modeling does suggest they may have been higher than at present (Berner, 1990). Astronomical models of stellar evolution suggest that solar luminosity has increased by about 30% from the formation of the earth to the present. If this increase is linear, then the solar luminosity would have been about 3% less than at present during the Devonian. The earth's rotation rate has slowed through time, primarily because of gravitational interactions with the moon. Precise values are uncertain, but a "day" may have been up to an hour shorter during the Devonian. For our modeling study, we have chosen to hold all three parameters constant at present-day values. In part, this is because of the tremendous uncertainty in values of these parameters for the Devonian; in part, it is because explicit treatment of variations in them requires a tremendous amount of computer time and, hence, would be very expensive. Since a dominant effect of both CO₂ and solar luminosity changes is to modify SST, our prescribed SST can carry some implied effects of changes in these two parameters. In particular, our SSTs are based on Cretaceous modeling, are considerably warmer than at present, and, indeed, are close to those obtained by Oglesby and Saltzman using 3× present CO₂. Since reductions in solar luminosity can work to offset increases in CO₂, our prescribed SST may be reasonable given possible Devonian values for these parameters. It is unlikely that the slightly shorter Devonian day would have any significant impact on the overall simulation of the climate for that period of time.

RESULTS

The Basic Devonian Climate

In general, we show only results for the seasonal cycle, discussing differences with perpetual season as appropriate.

Surface Temperature

Figure 6 shows seasonal-cycle surface temperature for December, January, and February (DJF) and June, July, and August (JJA). (Note the zonally symmetric SST with a very steep gradient between 45° and 60°N and a somewhat less steep gradient between about 40° and 60°S.) In summertime, Siberia temperatures are relatively warm (up to 32°C) in the low-elevation south, but relatively cool (10–12°C) in the higher-elevation north. In winter, the high-elevation northeast corner is very cold (–20°C), while much of the south and west remains above freezing. Temperatures in the equatorial land regions show little seasonality;

cooler temperatures (20–25°C) coincide with higher elevations, while adjacent low-elevation basins have warm temperatures (up to 40°C). The large Southern Hemisphere landmass has summer temperatures that are fairly uniform (about 25–30°C over the interior and about 20–25°C along the coast). One noticeable exception is Australia, which is extremely hot, up to 45°C. Winter temperatures show more variations and steeper gradients. The high-latitude interiors are very cold (–35°C), while coastal regions range from just above freezing at high latitudes up to 20°C at mid-latitudes. All of Australia remains above freezing, while interior South America is a few degrees below freezing.

In general, the perpetual-season and seasonal-cycle simulations show similar behavior. The extremely hot temperatures found over portions of North America and Australia and the seasonal-cycle simulations are considerably more moderate in perpetual seasons. This is due to a soil moisture feedback present in the seasonal-cycle runs, but absent from perpetual-season runs. With the feedback, the ground dries out and then must warm up to preserve energy balance. In short, temperatures in the perpetual-season simulations are less extreme, especially in hot regions.

Sea Level Pressure

Perhaps the most noticeable overall aspect is the general lack of strong pressure gradients. A general, more-or-less zonal band of low pressure is seen in the mid-latitude Northern Hemisphere, interrupted only by high pressure over Siberia. A weaker zone of low pressure is also discernible in summer, now augmented by a fairly deep thermal low over the elevation of northeast Siberia. A less consistent zonal pattern is seen in the Southern Hemisphere. Generally, low pressure is seen between 45° and 70°S in winter; this is interrupted by high pressure over the landmass of South America and Australia. The changes, however, are generally less than 10 millibars. Summer in the Southern Hemisphere is more complicated. Low pressure is seen over South America and Australia, but gradients are very slight over most of the continental interior. A fairly consistent pattern in both hemispheres of subtropical high pressure and equatorial low pressure is seen in JJA; however, while it generally exists in DJF, the gradients are so slight that they cannot be detected on the plot. In general, the expected zonal and land-ocean patterns are seen, but the differences in mass are small. In particular, these results are suggestive of both weakened transient activities (i.e., diminished winter mid-latitude cyclones) and a weak monsoon. There are strong seasonal shifts in surface pressure over portions of Siberia, South America, and Australia, but the area involved is small compared to the total land area. Much of the large continental mass is either at too high a latitude or too equatorial for strong monsoons to develop. There is no substantial difference between perpetual-season and seasonal-cycle results for sea level pressures.

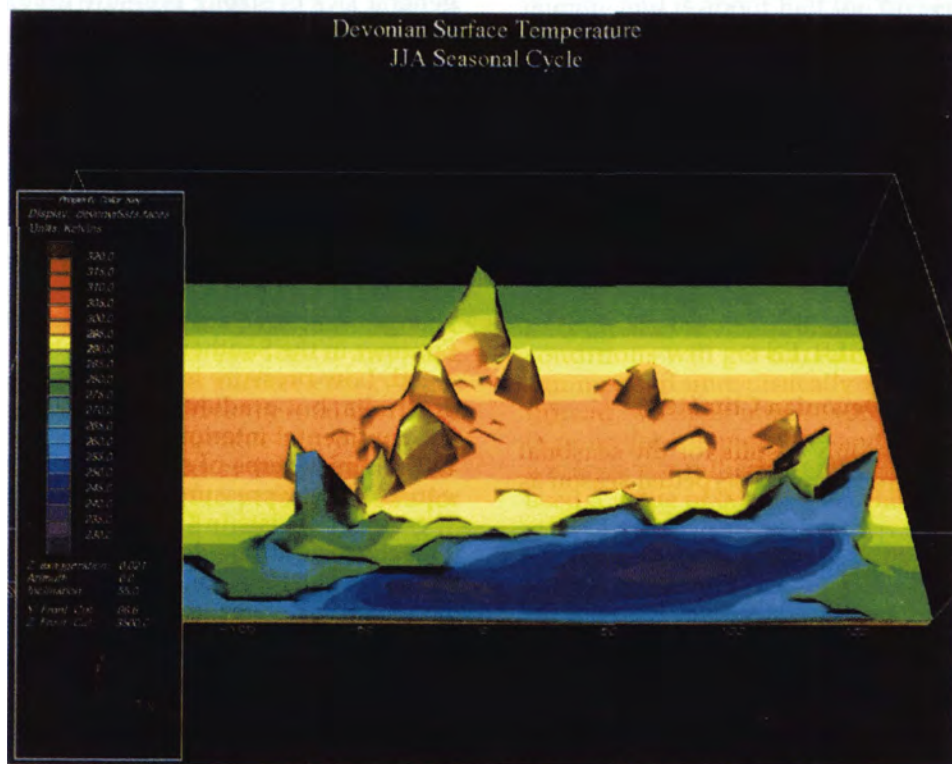
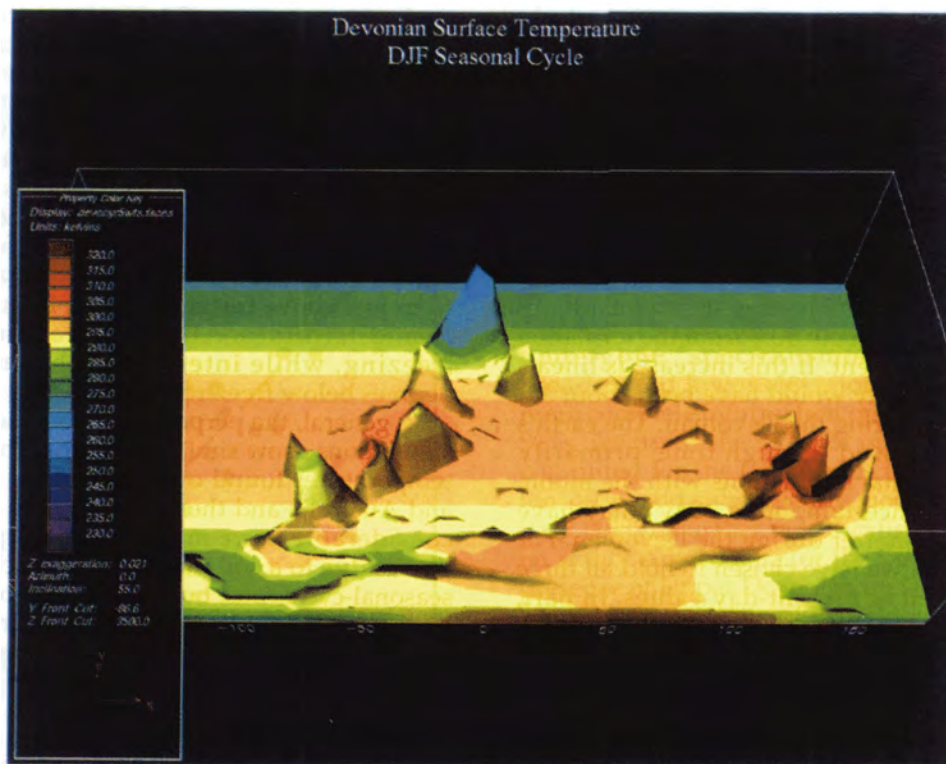


Figure 6. Seasonal cycle surface temperatures for DJF and JJA.

Surface Winds

A major feature is the strong northeasterly and southwesterly trade winds, despite the relatively weak pressure gradients (Figures 7 and 8). The mid-latitude, Northern Hemisphere Ocean shows generally cyclonic winds in both seasons (remember the trough of low pressure); in particular, a band of easterlies occupies much of the 65° to 70°N zone. Siberia shows a general cyclonic flow in winter (bringing moisture to the elevations in the northeast), and without flow from the center of the continent. In summer, a strong cyclonic flow (induced by a thermal low) continues (Figure 7), feeding more moisture to the northeast. The Southern Hemisphere winds are more complex (Figure 8). A region of southwesterly/northeasterly confluence occurs over the East Coast of North America (a region of generally high topography) in both seasons, the stronger and more extensive in summer. This elongated feature stretches from about 50°S to the equator.

Precipitation

Figure 9 shows precipitation. Perhaps the most important and intriguing result is the strong similarity in the patterns of precipitation in both seasons. This is perhaps not too unexpected for an equatorial region—though the Intertropical Convergence Zone (ITCZ) shows little seasonal shift, unlike the present-day climate—but completely unexpected in mid- and high latitudes, given a large seasonal shift in solar radiation. Apart from the dominant, but largely stationary ITCZ, the pattern of precipitation most clearly follows the pattern of topography. Precipitation maxima are invariably located over topographic heights, with adjacent, low-elevation basins that are extremely dry. Maxima are located along northeast Siberia, northern Australia, the East Coast of North America, and India. Very dry basins include the Orcadian, Hudson Bay, Williston, Norilsk, Chuy Sary Su, and Arafura.

Ocean regions have generally low precipitation with maxima coinciding with regions of weak low pressure and minima coinciding with weak regions of high pressure. One continental region that does show a seasonal shift is the high-latitude Southern Hemisphere Continent, which is quite dry in winter but relatively moist in many parts in summer. The importance of these year-round precipitation patterns cannot be overemphasized.

Precipitation Minus Evaporation

The precipitation minus evaporation (P – E) balance was modeled for both seasons of both perpetual season and seasonal cycle. Three important points can be noted at the outset:

1. Land/ocean differences. In general, continental regions have net precipitation (primarily because evaporation is restricted), while oceanic regions have net evaporation (because evaporation is unbounded; that is, an ocean is an infinite moisture source).

2. The P – E pattern is, in general, quite similar to that of the precipitation alone plots. That is, regions of

relatively high precipitation tend to have a positive P – E balance, while regions of relatively low precipitation tend to have a negative (or at best a slightly positive) P – E balance.

3. Unlike the previously discussed climatic variables, the distinction between perpetual-season and seasonal-cycle simulations now becomes important. This is because perpetual-season simulations employ the fixed surface hydrology, which means that a land grid point has a constant, specified amount of moisture available, no matter how much evaporation occurs, while seasonal-cycle simulations employ an interactive surface hydrology in which a land grid point can become drier/wetter, with resultant decrease/increase in evaporation. In particular, this means that perpetual-season simulations can help identify and highlight regions with a large net evaporative balance, by exaggerating the actual evaporation that occurs.

Two land regions are of particular interest as large evaporative basins. One of these occupies much of central North America, the other occupies much of southern and western Australia. In both cases, the basins have almost nonexistent precipitation and receive strong surface heating from insolation (year-round in North America, primarily summer for Australia). Hudson Bay is among the largest evaporative sources in the (modeled) Devonian world. Both basins are adjacent to high topographic features that receive considerable year-round precipitation; thus, runoff into these basins is likely to have been significant. These regions are of considerable importance in relating the modeled climate of the Devonian with occurrences of source rocks. Apart from these two basins, regions of generally positive and large P – E occur over topographical elevations and the ITCZ, with regions of generally large and negative P – E over the subtropical (and portions of the tropical) oceans. The oceanic region between and to the east of Siberia and northern North America is a particularly large net evaporative region. The higher-latitude ocean tends to be a region of weak net precipitation, although the pattern is not very consistent. The northeast corner of Siberia has net precipitation in both seasons, while the southern section has net evaporation in both seasons. The remainder of the landmass switches from net evaporation in summer to net precipitation in winter. The large Southern Hemisphere landmass also shows that general tendency of (relatively weak) net precipitation in winter and evaporation in summer.

Snowcover

Figure 10 shows winter snowcover for the seasonal-cycle simulation for the Northern Hemisphere (Figure 10B) and the Southern Hemisphere (Figure 10A). Not shown, but probably of greatest interest, is the complete lack of summer snowcover in either hemisphere. For the Northern Hemisphere this is not surprising, given the relatively low-latitude location and small size of Siberia, but the polar landmass in the Southern Hemisphere also is snow-free during the

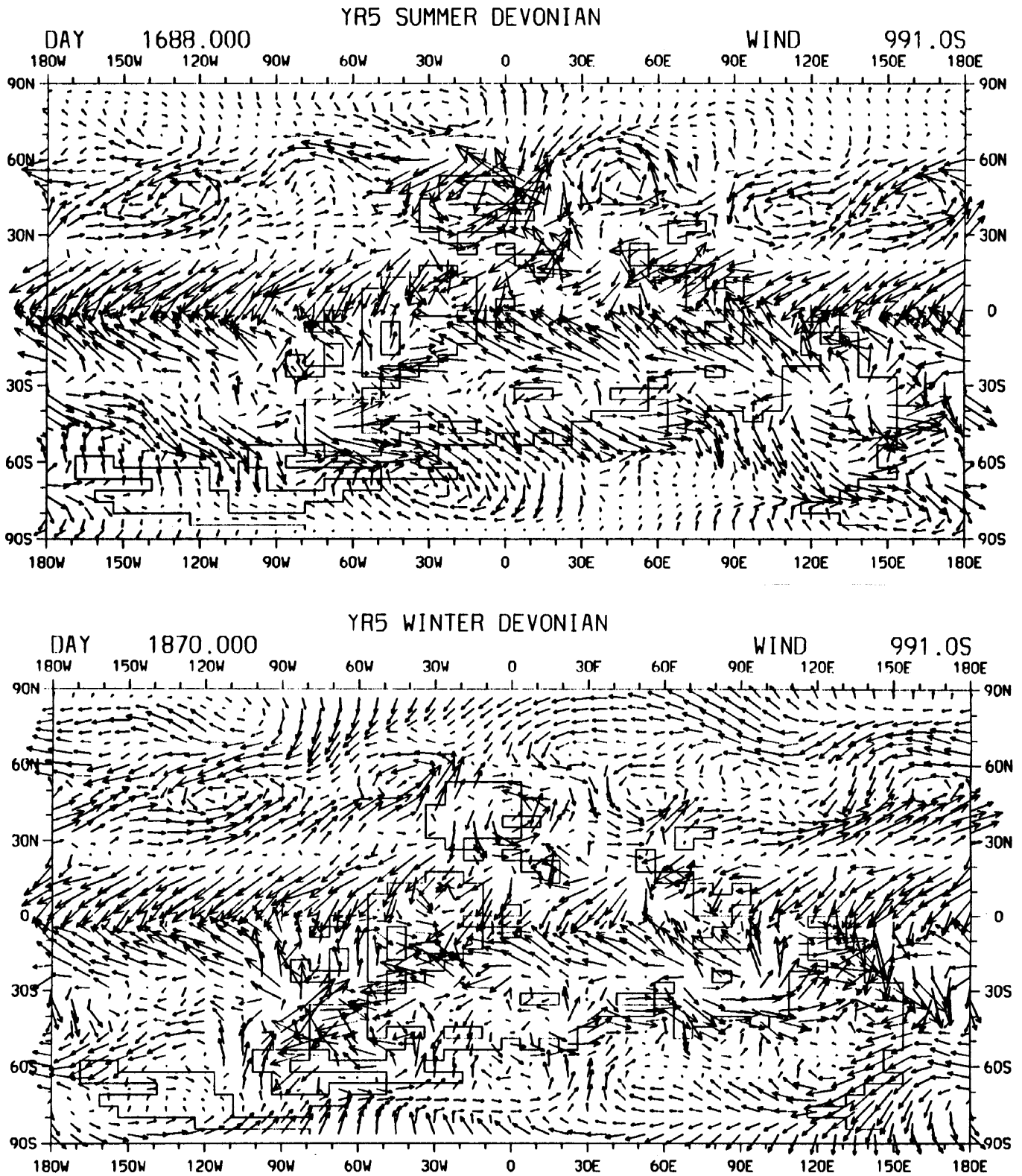


Figure 7. Surface wind vectors for the JJA (top) and DJF (bottom) seasonal cycles.

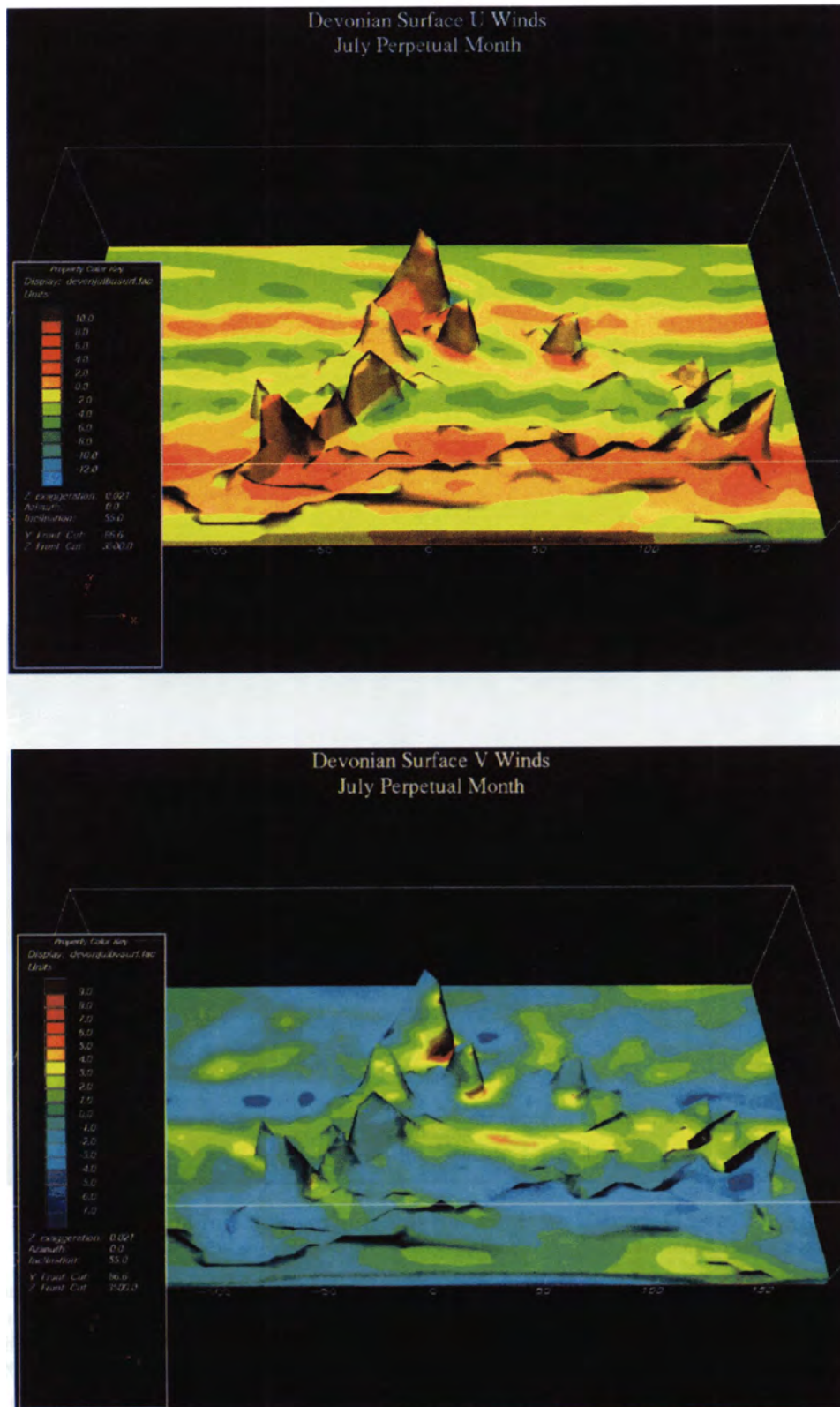


Figure 8. Upper Devonian surface zonal (U) winds and vertical (V) winds.

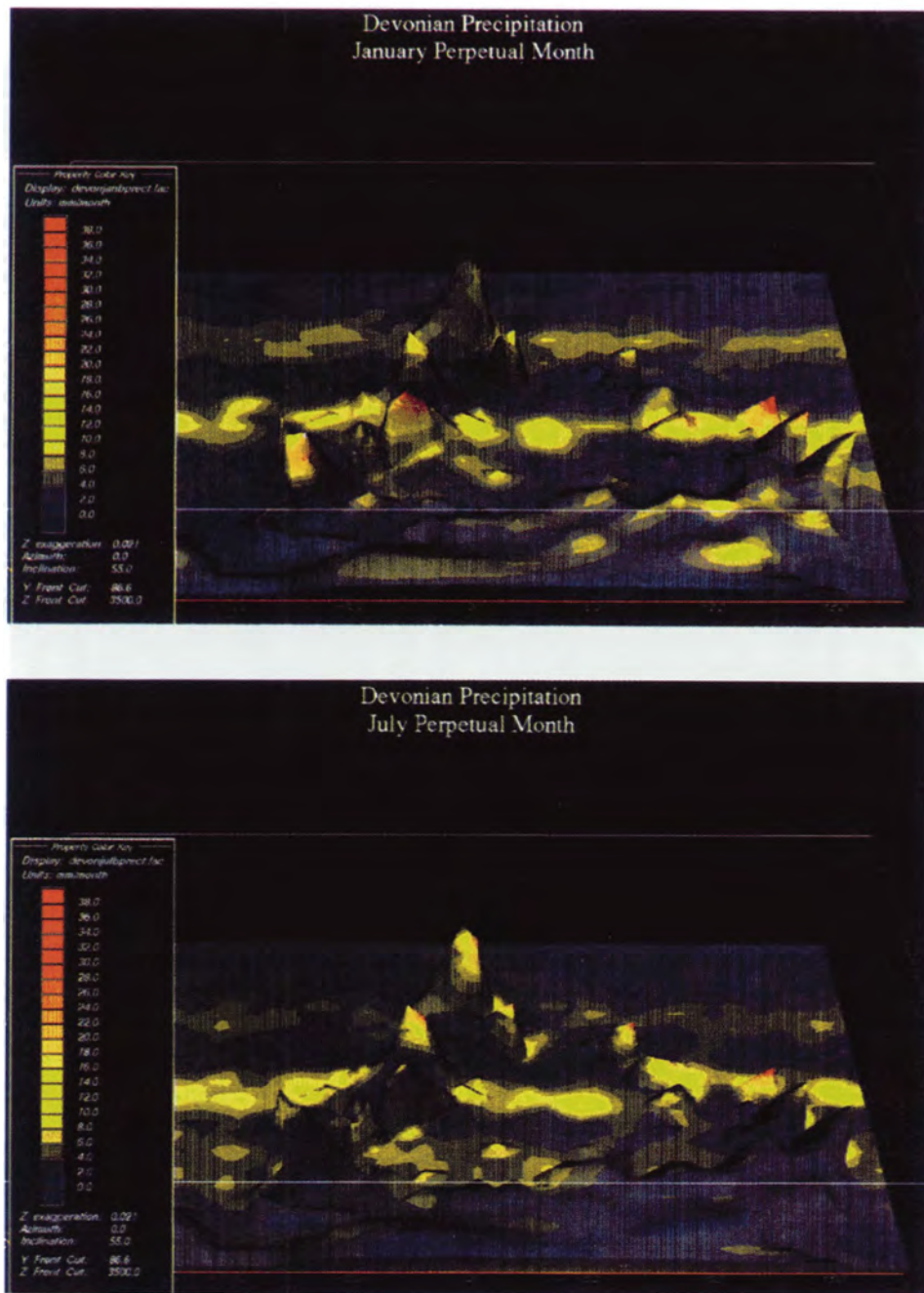


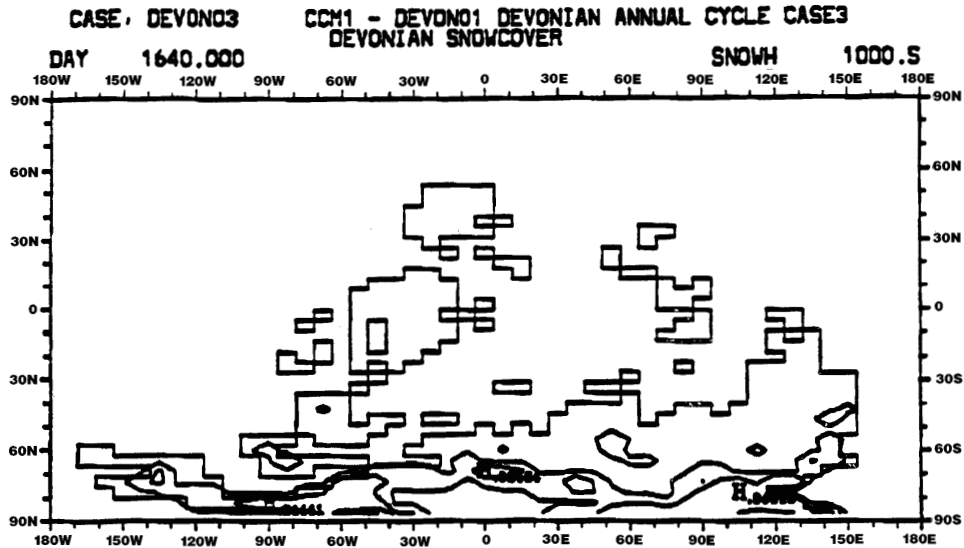
Figure 9. Upper Devonian precipitation showing marked similarity in winter and summer seasons.

summer. This is in apparent disagreement with the results of Oglesby (1989), who used CCM1 and found that present-day Antarctica tended to maintain snow-cover through the summer under a variety of imposed (paleoclimatic) conditions; he attributed this primarily to its polar position. However, Oglesby (1989) did find that when Antarctica was low and flat and surrounded by very warm sea surface temperatures, it became snow-free for about two months during summer.

Inferred Oceanic Circulation—Horizontal Surface Circulation and Vertical Upwelling

Our modeling combination did not involve the use of an interactive (either thermodynamic or dynamic) ocean; instead, we prescribed SSTs based, with appropriate modifications, on a previous model computation of SSTs. By implication, we prescribed the state of the ocean and constrained ocean-atmosphere interactions through our choice of SSTs. Nonetheless, we can

A



a.

B

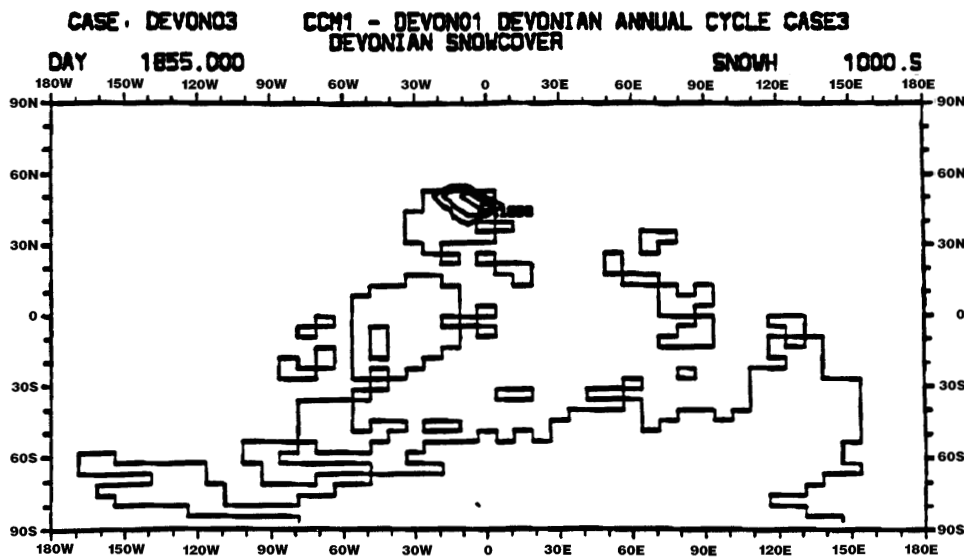


Figure 10. Winter maximum snowcover for seasonal-cycle simulation for (A) Southern Hemisphere (5 cm or less) and (B) Northern Hemisphere (18 cm or less).

infer much information on what the surface circulation of the Devonian ocean may have been like, since this circulation is largely (but not entirely) forced by the atmospheric winds. Of particular interest in this regard are the surface wind stresses, the divergence of the wind (and wind stress), and the curl (especially the zeros) of the wind-stress field. We have also computed Ekman drift explicitly, following the approach of Barron (1985), from the divergence of the wind stress. The wind-stress fields provide information on the magnitude (intensity) of oceanic circulation features or currents, the zero of the wind-stress curl can provide

information on the location and boundaries of horizontal circulation features (and help identify open-ocean upwelling and downwelling regions), while the divergence fields provide information on likely locations of coastal upwellings. Our analyses of potential upwelling areas are shown on Figures 11 and 12.

Summary of the General Devonian Climate

In summary, the Devonian climate is very different than the present-day climate. This must be due to some combination of changed paleogeography, topography, land surface type, and sea surface temperatures, since

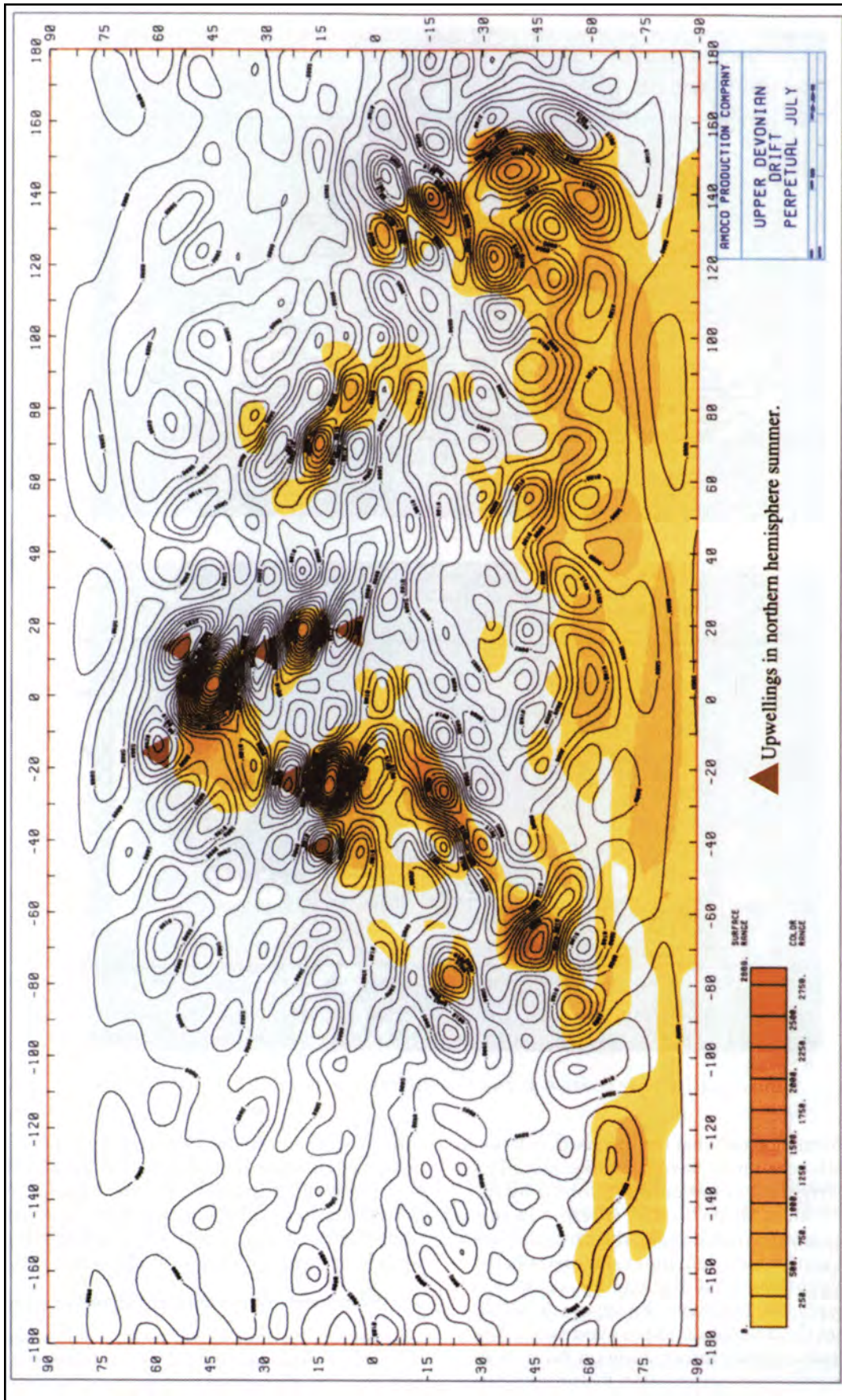


Figure 11. Late Devonian upwellings in Northern Hemisphere summer.

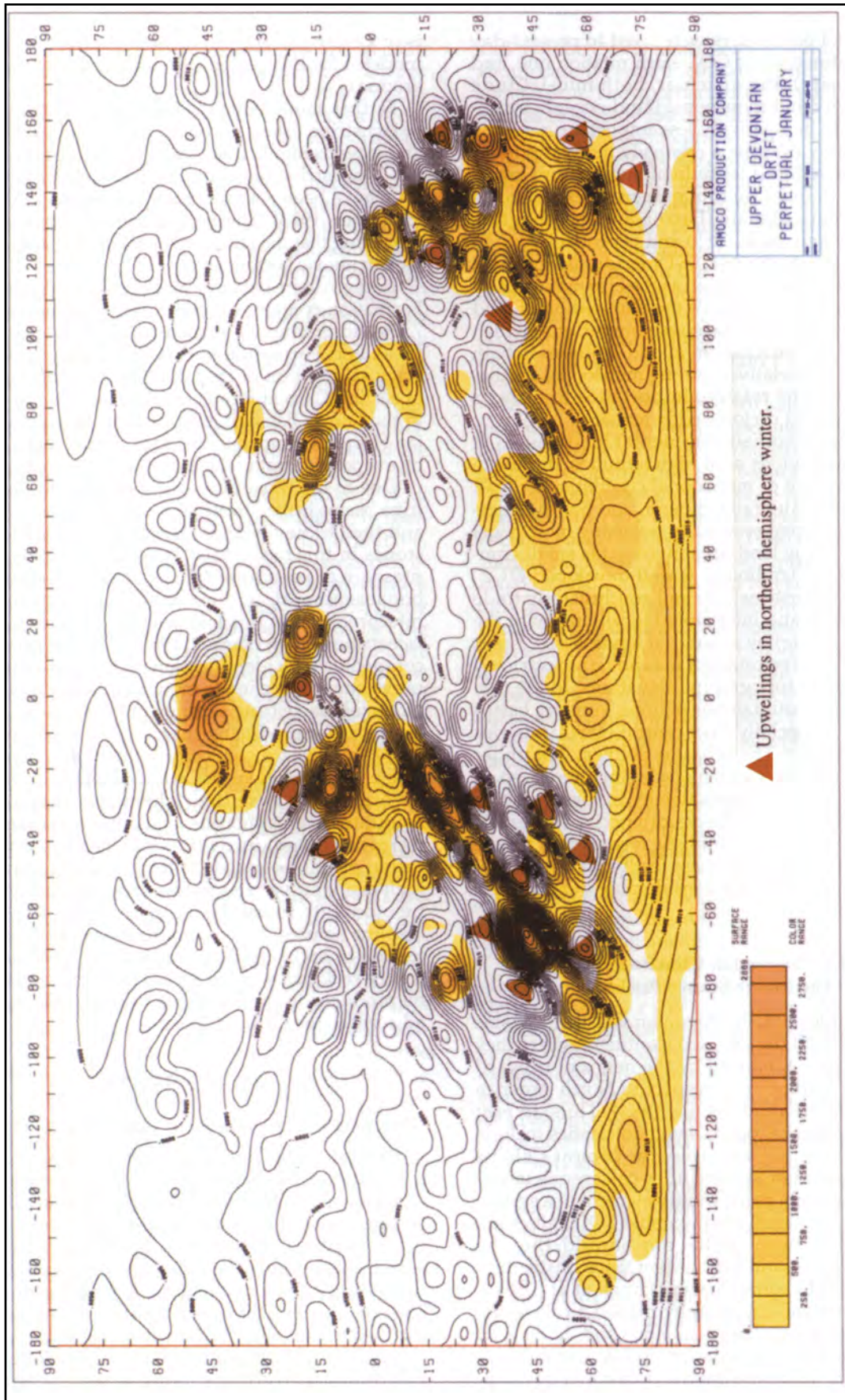


Figure 12. Late Devonian upwellings in Northern Hemisphere winter.

all other model parameters were fixed to present-day values (e.g., atmospheric CO₂, earth rotation rate, and solar luminosity). In particular, both mid-latitude cyclonic activity and monsoonal (land-ocean) circulations appear to be relatively less important, with the local topography exerting a relatively more important influence. The reduced latitudinal temperature gradient is similar to that found in numerical experiments of the Cretaceous climate (Barron and Washington, 1984; Oglesby and Park, 1989) and is probably due in large part to the prescribed SST meridional gradient (less than present-day), as well as the elimination of all sea ice (and to a lesser degree the elimination of land ice). However, these Cretaceous simulations (which have considerable landmasses at mid-latitudes in both hemispheres) had relatively strong monsoonal circulations (although the relative importance was also a function of reduced cyclonic eddy activity).

Most of the Devonian continental landmass is at equatorial land regions or at high latitudes, diminishing the importance of monsoonal circulations. Small regions, notably Australia, Siberia, and South America, do show a strong seasonally reversing monsoonal circulation, but the land area involved is small compared to the total landmass. A well-developed ITCZ, with attendant northeasterly and southeasterly trade winds, is present and interrupted locally (as with the present-day climate) by equatorial landmasses. Apart from the ITCZ, precipitation maxima are restricted almost entirely to topographic elevations. In the rain shadow of these mountainous regions, very dry basins tend to occur, especially over central North America and over Australia. These basins get very hot under high insolation in the seasonal-cycle simulations, so, in part, this is due to the interactive hydrology in which strong soil moisture feedbacks can occur. It must be noted that the relatively simplistic formulation for the hydrology may exaggerate these feedbacks. Regions of precipitation maxima have considerably more moderate temperatures.

Late Devonian Climate and Lacustrine Source Rocks

Most examples of Late Devonian lacustrine basins are associated with the Old Red Continent where they were tectonically enhanced by the major northward translation of Europe with respect to North America then underway (Faleide et al., 1984). Thus, in east Greenland the thick Upper Devonian clastics include lacustrine facies. For example, the Mount Celsius group of Famennian age includes calcareous lacustrine shales, but only as a minority element in a system that is sand dominated. No favorable TOC values are reported from these shales nor should they be expected in such a sand-rich system since clastic dilution is inimical to source rocks (Hinch et al., 1990). Clearly, climate and topography played a role in the erosion of these Greenland highlands and delivery of clastics to adjacent tectonic basins. While variability in precipitation is evident from the occasional development of lacustrine facies, the volume of coarse clastics

is in keeping with the elevated precipitation values modeled for this region (>16 mm a month for the year around).

Farther south along the Old Red Continent, a series of lacustrine basins occurs in the Canadian Maritimes and extends into Maine. The Perry Formation of Maine has a lacustrine fauna and is a dark mudstone which may have been a source rock but is now overmature (Schluger, 1973). These mudstones contain salt casts indicating that the lake system was saline and probably had an anoxic bottom layer.

In the Albert basin of New Brunswick, the Albert Formation contains alginites with an average TOC of 7.1% and produces a small amount of oil. Salt overlies the Albert Formation in this basin, indicating a late-stage salinization of the lake. The Albert Formation is of earliest Carboniferous age, but, northward offshore in the Fundy Basin, it is likely that the Upper Devonian Horton Group also includes source rocks overlain by evaporitic strata which may serve as seals.

One of the most interesting of the Old Red lacustrine basins is the Orcadian basin of northern Scotland and the Orkney Islands. Devonian calcareous mudstones in this basin have TOC values up to 5%. The presence of pseudomorphs of trona, a sodium bicarbonate mineral, in these mudstones has led to the interpretation of this lake as an evaporative alkaline lacustrine system (Parnell, 1985). This interpretation is compatible with identification of this area as an evaporative one in our climate model. An Amoco evaluation of ancient lacustrine settings in terms of their propitiousness for producing source rocks (Ormiston et al., 1988) emphasizes particularly the hydrochemistry of lake waters and identifies saline-alkaline lakes as most favorable, because their chemistry makes higher amounts of phosphorous available to plankton, thus increasing bioproductivity, while their salinity stratification promotes anoxic bottom waters. Apparently, high evaporative rates in this area were accompanied by moderate runoff bringing in and concentrating alkaline solutes. Thus, climatic elements contributed to source rocks in the Orcadian basin. A lacustrine source rock has been implicated in contributing to the oil produced in the North Sea Beatrice field which lies adjacent to the Orcadian basin.

DISCUSSION

Previous Interpretations of Late Devonian Climate

Parrish (1982) and Parrish et al. (1983) used schematic, qualitative models in early attempts to infer Late Devonian climate by mapping pressure fields. By analogy with the relationship in the modern world between pressure fields and upwellings, these pressure fields became the basis for interpreting paleo-upwellings. The conclusion was reached that up to 75% of Upper Devonian source rocks could be ascribed to upwellings (Parrish et al., 1983).

An attempt was made in Amoco to model Upper Devonian upwellings using a semiquantitative approach based on the Fujita method (Gyllenhaal et

al., 1991). The results of that analysis also fail to coincide with our quantitative assessment of Upper Devonian upwellings. For example, that attempt suggested a major upwelling existed in the area of the Alberta basin, but that conclusion is not supported by our present quantitative model. A large upwelling was also identified in the Fujita method analysis in the area of offshore west Australia, and such an upwelling is also recognized on our quantitative model, but proven Upper Devonian source rocks are absent in this area. The Fujita method identified upwellings near Antarctica/India and north of Libya which do not coincide with any upwelling identified by our quantitative model. Two upwellings recognized using the Fujita method north of Siberia and off North China are also recognized as seasonal upwellings by our quantitative analysis. Considering the numerous upwellings that have been recognized by our quantitative modeling, the degree of match between it and the semiquantitative analysis is dissatisfyingly low.

As Hay (1990) has recently re-emphasized, not all upwellings are equally effective in inducing heightened bioproductivity. In order to be effective, upwellings must draw up deep, colder waters rich in dissolved nutrients to cause increased near-surface bioproductivity. As Barron has shown (1985), many modern upwellings are situated above areas lacking deep water and are ineffective. During the Late Devonian, the extensive development of shallow epeiric seas may have made lack of development of deep water a serious limitation on the efficiency of the upwelling engine to cause elevated bioproductivity. This may explain why our quantitative model suggests the existence of four categories of upwellings in the Late Devonian. These are: (1) a minority of upwellings which coincide year round with known areas of Upper Devonian source rocks (e.g., Timan-Pechora basin); (2) upwellings which are operational for only part of the year but coincide with known areas of source rock (e.g., west Siberian basin, Amazon basin, south Kazakhstan, north Australia); (3) upwellings which operate annually but do not coincide with known source rocks (e.g., Canadian Arctic), and (4) other upwellings which do not coincide with known source rocks (e.g., west Australia, east Australia, south Antarctic, north Siberia, and offshore North America). More significant than all of these upwelling-related categories is the observation that so many areas of rich Upper Devonian source rocks are not associated with any upwelling based on our modeling. In particular, this is true for the Illizi basin, the Tadla basin, the Keta basin, the Guinea Bissau basin, the Appalachian basin, the Michigan basin, Williston basin, the Volgo-Ural basin, the south China basins, various basins in eastern Europe and western Europe, the Alberta basin, and others. In our interpretation, all of these areas developed source rock by the operation of an epeiric sea model without significant contributions from upwelling.

We know of no published quantitative paleoclimate models for the Late Devonian to directly compare with ours. However, Witzke and Heckel (1989)

and Witzke (1990) made some interesting inferences about Late Devonian climates which allow limited comparison. The approach used in both of those studies was to employ the distribution of climatically sensitive lithofacies, such as coals, evaporites, and oolites, to infer Late Devonian paleolatitudes from analogy with modern latitudinal distributions of such lithotopes. We had deliberately avoided this kind of approach, preferring to use such lithotopes to test the plausibility of our quantitative model after its completion. Elsewhere in this report there is a discussion of how the distribution of source rock-bearing evaporitic basins compares to model predictions of the occurrence of evaporites. These results are encouraging with respect to the model's ability to simulate evaporites.

In general, the Witzke (1990) Late Devonian paleo-equator is similar to our positioning but runs through the Timan-Pechora basin, whereas on our paleogeographic reconstruction that basin is at 20°N latitude. Our paleo-equator may be more consistent with the presence of Upper Devonian evaporites in the Timan-Pechora basin than Witzke's (1990) equatorial position should be. Based on the assumption of a generally zonal circulation, Witzke and Heckel (1989) suggested only weak monsoonal circulation over Euramerica, which is consistent with conclusions from our quantitative model. However, our model also shows that topography in the Late Devonian caused significant departures from simple zonal circulation as is discussed elsewhere in this report. Witzke and Heckel (1989, their figure 4c) also accepted certain Upper Devonian strata in Brazil as glacial in origin. Our modeling does not support the idea that Gondwana glaciation occurred in Late Devonian time.

Finally, the hypothesis of Thompson and Newton (1989) that the Frasnian-Famennian biotic extinction was related to elevated sea surface temperatures, a hypothesis generated without any climate model support, is compatible with the results of our Late Devonian climate model.

Our model results suggest a much more diverse set of relationships between climatic factors and Upper Devonian source rocks than has previously been proposed. Past published interpretations have strongly emphasized upwellings and have encouraged nearly exclusive attention on modeling upwelling phenomena as a predictor of source rocks. Suggestions have also been made about the role of temperature in biotic extinctions with advocacy of both lethally cold (Stanley, 1984) and lethally hot (Thompson and Newton, 1989) sea surface temperatures, but without explicit description of any relation to source rocks. A close connection of extinctions to source rock generation has recently been advocated on a basis of climatically triggered sharp changes in consumer/producer trophic relationships, and a resulting excess of unconsumed plankton (Ormiston and Klapper, 1992).

We recognize from quantitative modeling that climatic factors influenced Upper Devonian source rock development in several other ways not previously modeled. These include the enhancement of nutrient

supply to upwelling areas by orographically induced precipitation in nearby highlands, the absence of strong seasonality which tends to protect transgression-induced water stratification in epeiric basins, the development of salinity-stratified basins with highly stable stratification, and enduring anoxia in which halite and source rocks were deposited in close association. Note that these are not evaporitic source rocks, but marine and lacustrine source rocks closely associated with salt. Note also that elevated sea surface temperatures in tropical latitudes combined with transgressions to cause a net increase in plankton abundances reaching epeiric seas. We discuss more specifically below the consistency between the climate model results and the conceptual models of source rock formation.

Climatic Influence on Extinctions

Late Devonian extinctions show stacked patterns which have been related to transgressions as documented for conodonts by Klapper and Ziegler (1979), for corals by Pedder (1982), and for other groups. There is little agreement on what attributes of the transgressions are causing these stacked extinctions. SST has attracted interest as an extinction agent with proponents from both ends of the temperature spectrum. Stanley has been a vigorous advocate (1984, 1988) of the lethal influence of cold Devonian sea surface temperatures produced by Gondwana glaciers. Our quantitative modeling does not support the existence of Gondwana glaciers hypothesized by Stanley.

Thompson and Newton (1989) suggested that very high sea surface temperatures would have been even more effective in Late Devonian extinctions because

tropical organisms have more tolerance for cooling than for heating above 30°C (see Figure 13). This suggestion is interesting but unsupported by any climate model. Isotopic paleotemperatures as determined by Brand (1989) from Upper Devonian and Lower Carboniferous brachiopods, including examples from source rocks, show a temperature peak at the Frasnian–Famennian boundary (Figure 14) followed by pronounced temperature decline in the Early Carboniferous. This general pattern certainly fits the geologic evidence for progressive cooling and glaciation by middle Carboniferous time. The Upper Devonian sea surface paleotemperatures of Brand are high, averaging some 34°C. Because a correction for a progressive shift in the isotopic fractionation coefficient has to be made for pre-Permian rocks, some skepticism about the precise value of this temperature peak is probably in order. Still, the overall pattern described by Brand with a peak temperature at the Frasnian–Famennian boundary followed by cooling is compatible with available geologic evidence. Moreover, the Upper Devonian sea surface temperatures of Brand are convergent with those in our model.

One of the most dramatic results of the Frasnian–Famennian extinction was the loss of the integrated reef community at the end of Frasnian time. The brunt of this extinction was on shallow corals rather than deep-living ones (see Figure 15). This fits with the concept of elevated sea surface temperatures being implicated in the extinction of shallow corals, while those residing in deeper, cooler water survived. This loss of reef community had an immediate impact on the net amount of phytoplankton reaching epeiric seas. Reefs are major consumers of plankton. Glynn’s work (1973) showed that the plankton abundance is reduced by

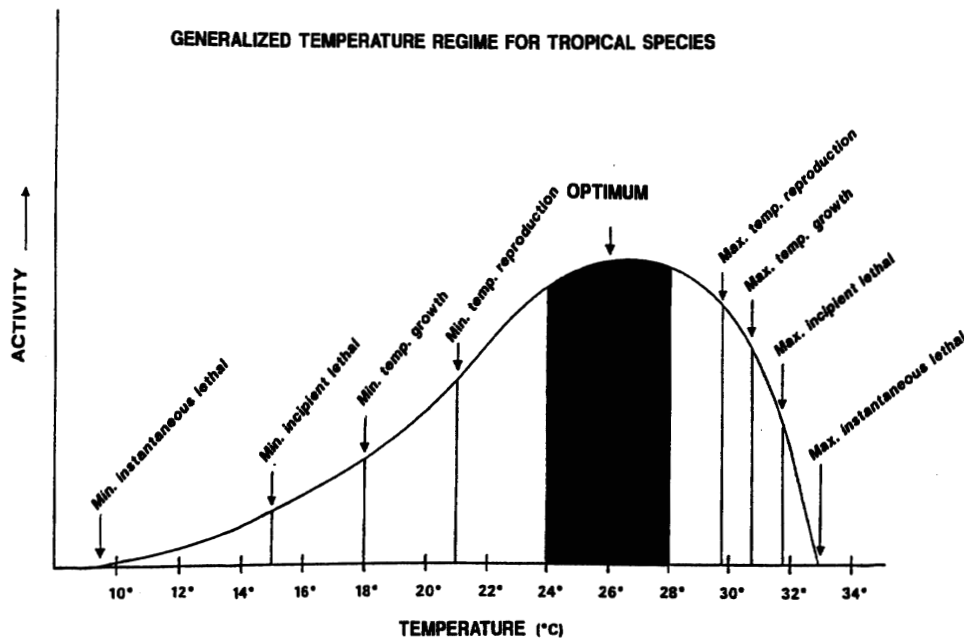


Figure 13. Effect of elevated temperatures on tropical organisms. After Thompson and Newton (1989).

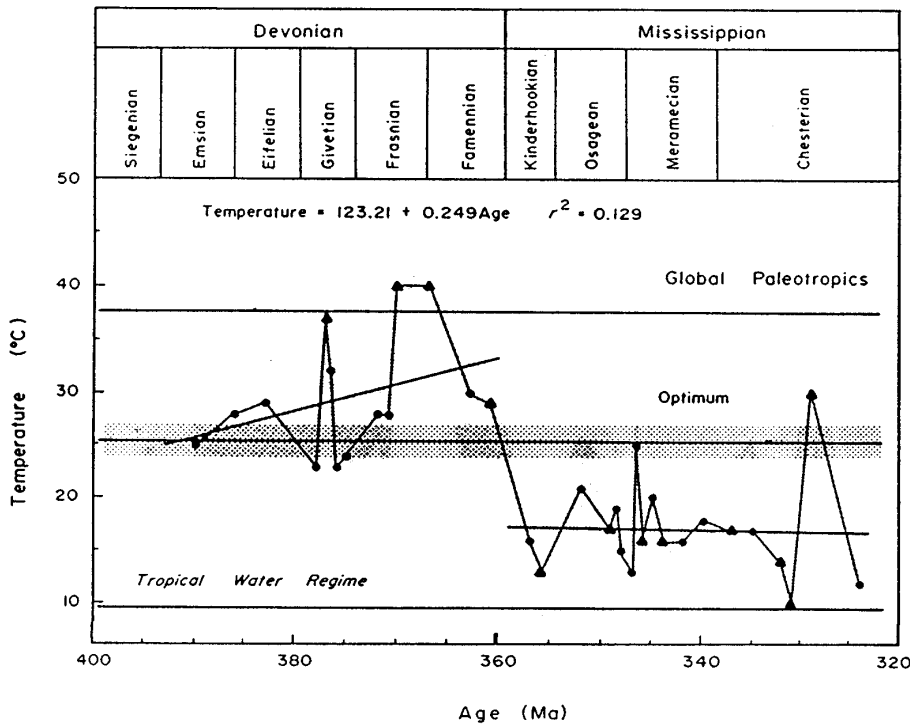


Figure 14. Isotopic paleotemperatures determined by Brand (1989).

70% in waters crossing from the oceanward to the leeward side of the Panama Reef. Thus, loss of Frasnian reefs would have led to a pronounced jump in plankton being brought into epeiric seas across the physically degraded and now nonconsuming former reef tract. There is evidence from an increase in plankton abundance in Famennian rocks as compared to Frasnian ones that this happened. Source rocks of Famennian age such as the Cleveland, Chagrin, Antrim, and Famenne shales all have elevated *Tasmanites* counts

per gram of rock (up to 8000 specimens per gram) as compared with a typical Frasnian abundance of 1000 specimens or fewer per gram. It seems plausible that elevated sea surface temperatures in the range of 30–31°C, such as obtained from our climate modeling, and the same values as temperatures which are presently killing reefs in tropical areas of the world ocean, were also implicated in the Frasnian extinction producing an increase in richness of epeiric sea source rocks.

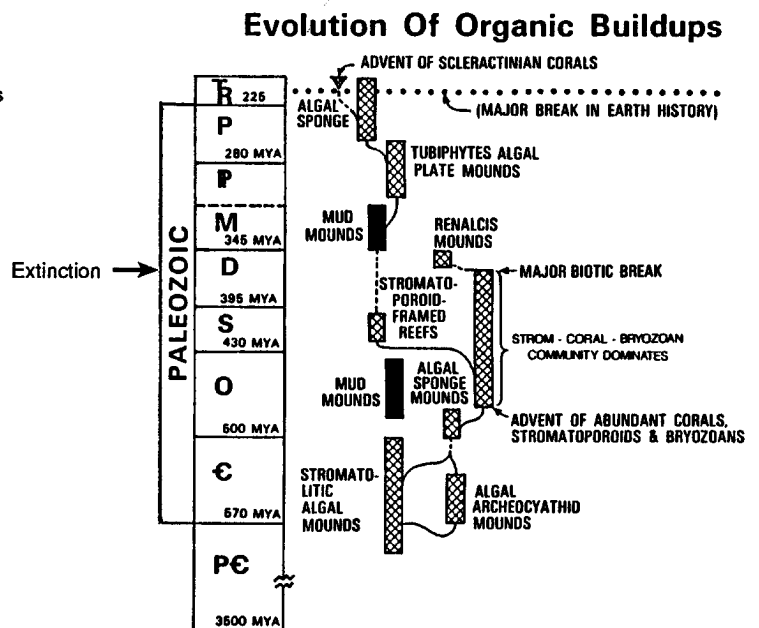
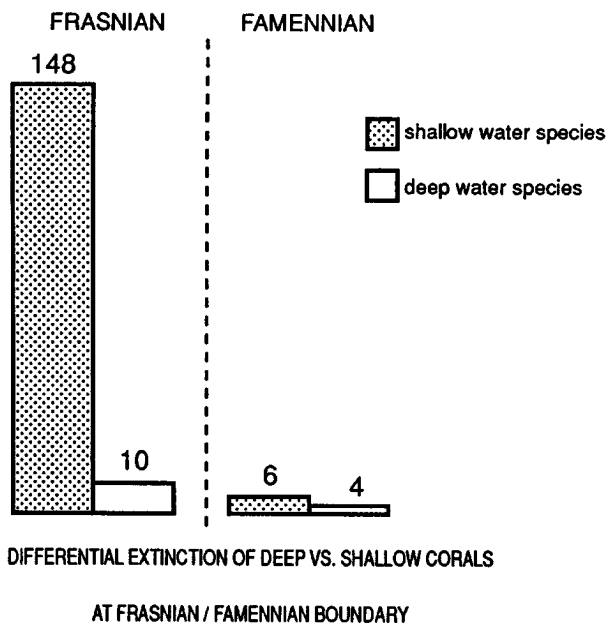


Figure 15. Coral extinction at the Frasnian–Famennian boundary. Adapted from Pedder (1982).

Climatic Features Protecting Stratified Water Columns

In many Upper Devonian epeiric basins, there is clear evidence in the form of maximal TOC values, absence of benthic organisms, and abundance of pyrite within the sediments for the development of strongest anoxia in the deeper central parts of these basins. Among the basins that serve as examples are the Michigan basin, the Williston basin, the Timan-Pechora basin, and from the modern world the Black Sea basin. The central location of this anoxic maximum is a strong argument for the operation of an anoxic water body in the preservation of organic matter as a first-order control in the development of source rocks. The Black Sea basin provides evidence that the greater depth in the central parts of the basin rather than maximum bioproductivity is the primary control on the development of anoxia. In the case of the Black Sea, maximum bioproductivity is in the marginal parts of the basin adjacent to points of entry of river waters with high concentrations of nutrients which induce that bioproductivity. The highest TOCs in the Black Sea are, however, found centrally in the deeper part of the basin, and this noncoincidence between the locus of maximal bioproductivity and the locus of maximal TOC strongly suggests that the anoxia results from physical stratification of the water. If the anoxia were induced by maximal bioproductivity, it should occur directly beneath the area of maximal bioproductivity, which, in the case of the Black Sea, is the west margin of the basin.

There are several other lines of evidence that anoxia was a primary prerequisite for the preservation of organic matter. The rapid facies changes which occur between shelf carbonates with highly diverse faunas but deposited under oxygenated conditions and having low TOCs and contemporaneous basinward deposits of fine-grained composition, dark color, and high TOCs that were deposited under anoxic conditions found in many Paleozoic epicontinental basins cannot be explained by regional variations in bioproductivity, since even on the oxygenated platform areas the bioproductivity was clearly high. A simpler explanation is rapid changes in degree of oxygenation with very modest changes in bottom depth in such settings. Another line of evidence is the virtual universal presence in source rocks of reduced-valence iron minerals such as pyrite as the dominant iron mineral species, and the existence of a positive correlation of high TOC values to reduced iron in such rocks. The conspicuous presence in the Upper Devonian of globally synchronous transgressive events (Johnson et al., 1985) with which source rocks are correlatable strongly suggests that changes of physical characteristics of the water column leading to increased anoxia were produced by those transgressive events.

Transgressive episodes such as those so typical of the Upper Devonian produced a stratified water column in many epeiric basins resulting from increased depth of the water, increased distance from shore of the central parts of the basin, reduced influx of minor turbidity flows into the central part of the basin, and

possibly reduced oxygen content of the newly introduced waters because of their elevated temperature.

Seasonality and the Maintenance of Anoxia

Once such stratified water columns developed in shallow epeiric seas, their persistence was an important preservational agent for the organic material being deposited in them. Our climate model results suggest the development of only a weak tendency toward monsoonal climates, particularly in the lower-latitude areas where many of the best Upper Devonian source rocks were being produced. Model assessment of the climate change associated with Upper Devonian seasonality shows it to be much less than, for example, what others have modeled for the Permian and Cretaceous. Strong monsoons and strong storm tracks are absent. Pressure field ranges are small, and geopotential height anomalies are about half that of the Cretaceous. This minimization of monsoonal tendencies should have served to preserve or, perhaps more accurately stated, failed to disturb the already existing stratified water columns because there was fairly steady-state runoff rather than pronounced alternations of wetter and drier periods.

Salinity Stratification

Our modeling of excess evaporation was intended to identify basins which might have very stable anoxia because of salinity stratification. Because oceans represent an essentially infinite reservoir for water, the identification of areas of excess evaporation over the ocean has no significance for this objective. We did find that in both seasons areas of excess evaporation existed over considerable land areas. Figure 16 depicts areas of excess evaporation in the southern hemisphere winter. We found these high-evaporation areas coincided in all instances with basins known to us to contain evaporites of Late Devonian age associated with source rocks of that age. This is true for the Williston basin of North America, the Hudson Bay basin, the Orcadian basin of Scotland (lacustrine), the Albert basin of the Canadian Maritimes (lacustrine), the Pripyat basin of Byelorussia, the Chu Sary Su basin of Kazakhstan, the Norilsk basin of western Siberia, and the Kempendai basin of eastern Siberia. This kind of ground truthing, demonstrating the coincidence of modeled areas of excess evaporation over land with the occurrence of evaporites in Upper Devonian basins, strongly supports the plausibility of our quantitative model with regard to localizing areas of hypersaline waters. The basins mentioned above are located in Figure 16. With regard to the relationship between source rocks and evaporites, the Pripyat basin of Byelorussia is an instructive example having source rocks sandwiched between salts (Figure 17). Accepting the circulation models proposed by Witzke (1987) for epeiric basins, it is hypothesized that areas of strong excess evaporation were characterized by shallow shelves on which hypersaline waters developed, which then, because of their elevated density, tended to flow as a bottom-hugging current into

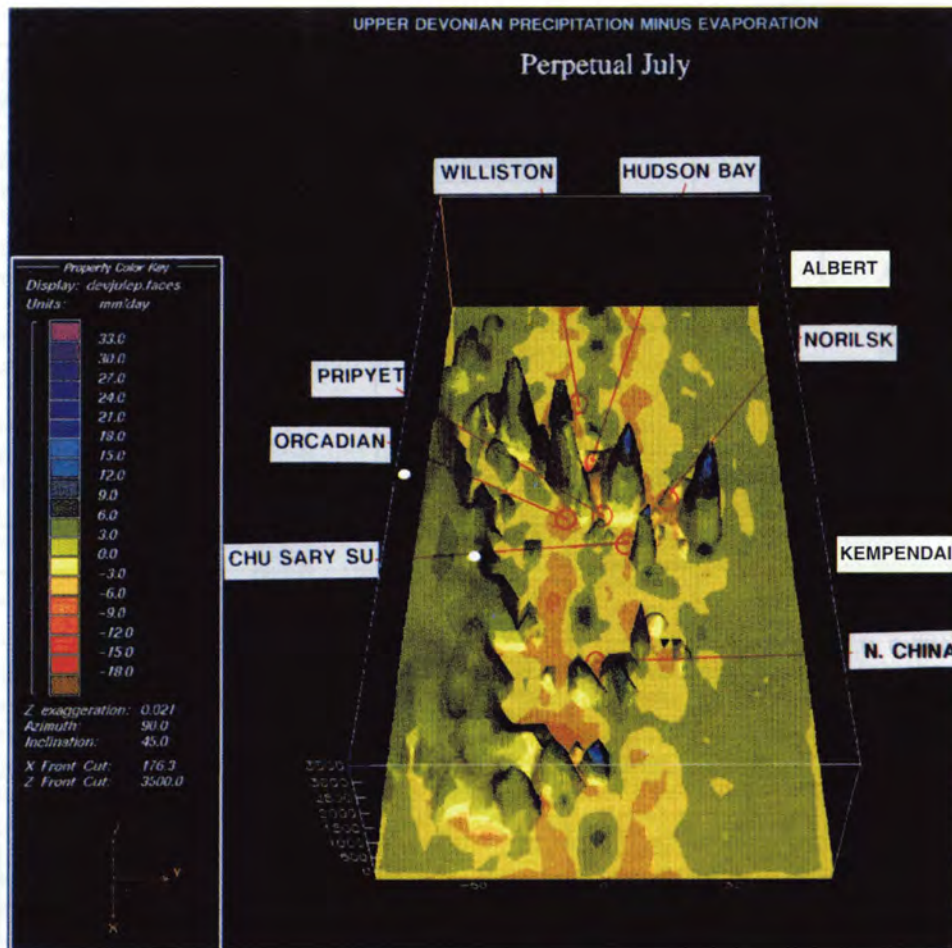


Figure 16. Basins with modeled excess evaporation which also contain evaporites in the Upper Devonian.

adjacent basinal areas to produce a lens of saline bottom water with great resistance to being disrupted because of its high density. Such a halocline can serve as an excellent maintainer of anoxic conditions on the basin bottom. The common association of Upper Devonian rocks with over- or underlying salt suggests the operation of such an anoxic bottom layer in areas of excess evaporation.

Upwellings and Source Rocks

The possible association of Upper Devonian source rocks with upwellings has been investigated by computing Ekman drift explicitly from wind-stress fields. We have chosen a minimum divergence value of $0.0025 \text{ Newtons/m}^2$ as a cutoff for significant upwelling areas. Divergence values over land have no meaning for our purpose and are ignored. The highest divergence values over water exceed $0.0050 \text{ Newtons/m}^2$ (north Australia, winter seasonal cycle), but these relative strengths of divergence have no clear relation to source proneness. We presently have no effective means to model deep-water formation and to map its distribution with respect to upwellings, but suspect that such an approach would be a better pre-

dictor of source rock occurrences than upwelling strength alone. Strength of upwelling is immaterial as a process for source rock formation if there is no cold, nutrient-rich water at depth to be brought to the surface.

As shown on Figures 10 and 11, there is a general lack of year-round upwelling in our model. Only two cases of perennial upwelling are seen. One of those is in the Canadian Arctic (Innuitian basin) where there are no known Upper Devonian source rocks and where the dominant lithotope of that age is regressive sandstones. The other occurs adjacent to Timan-Pechora, a basin with excellent Upper Devonian source rocks.

The extensive north Gondwana coast shows no Upper Devonian upwelling except for a local, moderate-strength winter upwelling which is located between Florida and northwest Africa off Morocco in both the perpetual January and seasonal cycles. This implies that the majority of North African basins, and especially the important Algerian basins, show no upwelling association. This is strongly at odds with the interpretation of Parrish et al. (1983) which inferred almost continuous Devonian upwelling across the North African coast.

| LOCATION PRIPYAT BASIN, BYELORUSSIA | | | | | | | |
|-------------------------------------|-----------------|---|---|--------------|-----------------------|--------------|--------------|
| STAGE OR SERIES | FORMATION | LITHOFACIES | CONODONT ZONE BIOFACIES | PLANKTON | STRATIGRAPHIC SECTION | THICKNESS m. | TOC |
| FAMENNIAN | LEBEDYAN-DANKOV | shaly dolomite | Retispora lepidophyta | | | up to 3,200 | |
| | | Halite & Sylvite | Cornispora varicornata | | | | |
| | ZADON-ELETS | argillaceous limestones rare ss. | p. rhomboidea PALM p. crepida PALM | RADS RADS | | up to 1,070 | 2.8% |
| | LIVEN | Halite anhydrite dolomite marls anhydritic dolomite | Hymeno. subsutus Hymeno. speciosus | | | up to 1,150 | source prone |
| FRANSIAN | EVLANOVO | | | | | 380 | |
| | VORONEZH | oolitic ls., tuffs | Archaeo. semilucensis | | | | |
| | PETIN | coralline ls., dolo., argill. ls., | | | | | |
| | SEMILUKI | ls. & dolomites | | | | | |
| GIVETIAN | LUZHSK | shales & ss. | G. eriense | | | 140 | |
| | NAROV | dolomite fine ss. & siltst. | | | | 100 | |
| EIFELIAN | | | | | | | |

Figure 17. Halite associated with Upper Devonian marine source rocks in the Pripyat basin.

Table 1 summarizes our assessment of relations between modeled upwelling and basins containing Upper Devonian source rocks. There are seven important basins for which the model supports upwelling as a likely cause of source rock development, out of a total of 37 possible basins. There are 23 basins which have source rocks but no upwelling, and another seven basins for which our model suggests upwelling but which lack source rocks. It is certainly fair to conclude that even carefully modeled upwellings are a quite imperfect predictor of source rocks. The claim of a 75% match between Upper Devonian source rocks and upwelling (Parrish, 1987) which was based on a qualitative model should, according to our quantitative model, become a 22% match (seven basins out of 37).

Runoff as a Source of Nutrients

With the development of large areas of tree fern forests in Late Devonian time, considerable amounts of phosphorus and nitrogen had to become incorporated into soils from decaying vegetation. This material is available for transport elsewhere either by contact with transgressions, as envisioned in the epeiric sea model, or by river runoff. This source re-

presents an alternative to upwelling as a transporter of critical nutrients and has been identified as an important element in source rock formation (Robison, 1992).

Our modeling has shown strong topographic forcing of precipitation in the Upper Devonian. A number of elevated areas with high runoff are contiguous with or not far removed from marine waters, with or without upwellings, and may have augmented the nutrient resupply. An example is found off the coast of mountains in west Siberia where rainfall averages 10 mm/day year-round. Nutrient enhancement by runoff from this range probably contributed to the production of west Siberian Upper Devonian (paleoeast) source rocks, whereas to the paleowest, there was a rain shadow within which red arkosic fill with gypsum stringers accreted in lacustrine basins such as the Tuva Depression.

Other precipitation maxima occur on the east coast of North America and are probably involved in the Catskill delta development. There is a marked high-precipitation area in Irian Jaya, in an area which is both elevated and lies astride the ITCZ and does coincide with Upper Devonian black shales in the Carstensz Mountains. A relationship between precipitation and these black shales for which we have no

Table 1. Relations between modeled upwellings and Upper Devonian source rocks.

Year-round upwelling—source rocks present

Timan-Pechora basin

Year-round upwelling—source rocks absent

Innuitian basin

Seasonal upwelling—source rocks present

West Siberian basin, Amazon basin, Chu Sary Su basin, Arafura basin

Seasonal upwelling—source rocks absent

Canning basin, East Australia, South Antarctic, East Antarctic, North Siberia, Offshore Appalachians

*No upwelling—source rocks present*Illizi basin, Tadla basin, Ahnet basin, Grand Erg Occidentale, Mouydir basin, Keta basin, Liberia basin, Gineau-Bissau basin, Appalachian basin, Permian basin, Anadarko basin, Volgo-Ural basin, Pripyat basin, North Slope basin, Pricaspian basin, Alberta basin, Michigan basin, Williston basin, Dneipr-Donets basin, Nanpangjiang basin, Chuxiong basin, Polish Trough, Brittany basin

TOC data and runoff may exist. In this region, up to 20 mm/day of precipitation was modeled. In areas of high-latitude parts of Gondwana, there are marked variations in precipitation from dry winter months to locally wet summer months, but no direct relation to source rocks is clear. One possibility is the long-distance transport of land-derived nutrients northward by river into the coastal area of the Arafura basin, which itself was a high-evaporation area.

Although unable to accept the upwelling version of the productivity model as a master control on the generation of source rocks, we do recognize that productivity has a relation to source richness. Thus, the peak productivity, which occurs in the near-coastal waters around all continents in the modern world, suggests that a similar situation obtained in the geologic past is a logical explanation for the richness of many epeiric seas.

CLIMATIC ENHANCEMENT OF SOURCE ROCK FOSTERING EPEIRIC SEA ATTRIBUTES

The insufficiency of upwellings revealed by our quantitative modeling to explain the distribution of Upper Devonian source rocks requires the identification of additional source rock-favoring processes. From the conclusions of Hinch et al. (1990), which have proven compatible with the climatic modeling results, we advocate the epeiric sea model, periodically rejuvenated by recurrent transgressions, to explain the majority of Late Devonian source rocks.

This conclusion has been reinforced by finding that several aspects of Upper Devonian climate serve to enhance the operation of the epeiric sea model. Our model results do not support the idea of glacioeustatic control on Late Devonian transgression history, providing no evidence for a major ice cap in Gondwana. In any case, the idea of such glaciation in the Late

Devonian is quite counter-intuitive to the very clear evidence that the Late Devonian was dominated by transgressions and sea level highstands, a fact which cannot be reconciled with a lowstand condition expectable during glacial conditions. Our climatic model leaves unexplained the ultimate cause of Upper Devonian transgressions, but their source rock effects are conspicuous.

Elevated sea surface temperatures in low-latitude waters which are inherent in our model are supported also by isotopically determined paleotemperatures (Brand, 1989). The consequences of having such warm waters transgress shelf edges into epicontinental basins are indicated by Thompson and Newton (1989). If sea surface temperatures in the range of 30-34°C existed, they would have destroyed reefs (Figure 13), producing a net increase in volume of plankton reaching epeiric seas and an increase in source rock formation. Geologic evidence exists for such a jump in plankton abundance after the Frasnian-Famennian extinction, lending credence to the role of elevated temperature waters in source rock formation. Such an elevation of temperature would also reduce the oxygen content of the transgressive waters and favor development of anoxia.

Late Devonian climate may have helped sustain epeiric sea anoxia once it was developed. Seasonal climate changes in the Late Devonian as modeled are much less than what others have modeled in the Permian and Cretaceous. The weaker development in the Upper Devonian of phenomena such as storm tracks and monsoonality means that there would have been a lesser tendency to disrupt any stratified epeiric sea water column either with sheetwash runoff or by storm winds. In short, anoxia may have been more persistent in the Upper Devonian than at other periods of geologic history.

In areas of excess evaporation over land, which the Upper Devonian modeling identifies with surprising accuracy, an even stronger protector of anoxia existed.

In bottom waters of such epeiric basins, water stratification was enhanced by development of a halocline, which is far more resistant than a thermocline to disruption by water mixing.

Although our quantitative modeling does include a specific calculation of runoff volume, it may not be fully reliable. Better appreciation of distribution of high and low runoff areas can be obtained from examination of precipitation maps and evaporation minus precipitation maps. Topographic forcing of precipitation is a conspicuous feature of these maps, which makes it easy to identify areas and direction of runoff. Runoff is important for resupply of critical nutrients to epeiric sea basins, especially because the model identifies so few areas of upwelling in proximity to epeiric sea basins. The accurate reconstruction of paleotopography is a key to such interpretations, and a more vigorous analysis of paleotopography should be a goal for future work.

The existence of tree-sized vegetation in the Upper Devonian ensured a terrestrial supply of nitrogen- and phosphate-rich decaying vegetation which could be transported to epeiric basins either by transgressive incursions or by river runoff. The wide development of Upper Devonian epeiric basins must mean efficient riparian transport of nutrients from relict highland areas in the middle and low latitudes into epeiric basins.

In summary, the operation of the epeiric basin model of source rock development was significantly abetted by Upper Devonian climatic factors such as elevated sea surface temperature, weak development of monsoonal climates and weak storm tracks, topographic forcing of precipitation to provide runoff into broad low-lying areas of epeiric basins, and development of excess evaporation in land regions where saline bottom layers were developed within basins and maintained strong anoxia which favored preservation of organic matter.

CONCLUSIONS

Climate Modeling Results and Exploration Concepts

Our results suggest that the primacy that has been accorded the upwelling model as a source rock predictor for at least the past decade should be abandoned. It should be replaced by a more balanced approach to source rock prediction which would include consideration of the epeiric sea model, transgression history, and at least such climatic elements as seasonality, storm tracks, evaporation minus precipitation maps to infer location of salinity-stratified anoxia-prone basins, runoff as a source of nutrients, climatic cycles, distribution of sea surface temperature and its relation to biotic distributions or extinctions, and upwelling possibilities.

With the exception of the assessment of climatic cycles (e.g., Milankovitch), the suggested analyses are derivable directly from a judicious combination of CCM1 perpetual-season and seasonal-cycle runs and

their results for climatic parameters such as surface temperature, precipitation minus evaporation, surface winds, 200 and 500 millibar winds, surface pressure, geopotential height, curl and divergence of the surface wind fields, and precipitation. We found it desirable to assess upwellings by specific calculation of divergence values from the wind-stress fields because of the extraordinary significance attributed to Devonian upwellings by other authors. Upwellings could be inferred almost as accurately by careful perusal of tau curl and divergence maps.

The above discussion specifically concerns source rock prediction, in keeping with the theme of this report. Of course, paleoclimatic modeling can equally well contribute to improved prediction of other important hydrocarbon exploration problems such as reservoirs, seals, and traps. To mention only a few especially viable possibilities, we could list the use of evaporation minus precipitation maps as a means of localizing possible salt seals, input of climatic parameters such as precipitation and cyclicity into computer-driven depositional models to better predict spatial and temporal facies patterns, storm track mapping to infer location of coarse clastic facies, and paleowind directions to predict localization of clastic carbonate reservoirs and siliciclastic reservoirs.

REFERENCES CITED

- Anfan'sieva, M., and Zamilatskaya, T., 1992, The paleobiogeography of the northeast Pricaspian basin and Pre-Uralian depressing in Artinskian time based on radiolaria and foraminifera: *Micropaleontology Special Publication 6*, p. 109–117.
- Akpati, B., 1978, Geologic structure and evolution of the Keta basin, Ghana, West Africa: *GSA Bulletin*, v. 89, p. 124–132.
- Barron, E., 1985, Numerical climate modeling. A frontier in petroleum source rock prediction: results based on Cretaceous simulations: *AAPG Bulletin*, v. 69(3), p. 448–459.
- Barron, E., and Washington, W., 1984, The role of geographic variables in explaining paleoclimates: results from Cretaceous climate model simulations: *Journal of Geophysical Research*, v. 80, p. 1267–1279.
- Berner, R., 1990, Atmospheric carbon dioxide levels over Phanerozoic time: *Science*, v. 249, p. 1349–1472.
- Bradshaw, J., Nicoll, R., and Bradshaw, M., 1990, The Cambrian to Permo-Triassic Arafura basin, Northern Australia: *APEA Journal 1990*, p. 107–126.
- Brand, U., 1989, Global climatic change in the Devonian–Mississippian: stable isotope biogeochemistry of brachiopods: *Palaeogeography, Palaeoclimatology and Palaeoecology*, v. 75 (1989), p. 311–329.
- Burrett, C., Long, J., and Stait, B., 1990, Early-Middle Paleozoic biogeography of Asian terranes derived from Gondwana, in *Paleozoic Palaeogeography and Biogeography: Geological Society Memoir 12*, p. 163–174.
- Bylinkin, G., Nabrotsky, O., Sidorov, I., and Oreshkin, I., 1984, Geochemical conditions of oil and gas formation

- of the subsalt beds of the southwest Caspian basin: *International Geological Review*, v. 26(7), p. 803–809.
- Faleide, J., Gudlaugsson, S., and Jacquart, G., 1984, Evolution of the Western Barents Sea: Marine and Petroleum Geology, v. 1, p. 123–150.
- Gagiev, M., 1982, Conodonts of the Upper Famennian and Tournaisian strata of the NE part of the Omolon Massif: Moscow State University Avtoreferat (in Russian).
- Glynn, P., 1973, Ecology of a Caribbean coral reef. The *Porites* reef-flat biotope. Part II. Plankton community with evidence for depletion: *Marine Biology*, v. 22, p. 1–21.
- Gyllenhaal, E., Engberts, C., Markwick, P., Smith, L., and Patzkowsky, M., 1991, The Fujita-Ziegler model: a new semiquantitative technique for estimating paleoclimate from paleogeographic maps: *Palaeogeography, Palaeoclimatology and Palaeoecology*, v. 86 (1991), p. 41–66.
- Hay, W., Barron, E., and Thompson, S., 1990, Results of global atmosphere circulation experiments on an Earth with a meridional pole-to-pole continent: *Journal of the Geological Society, London*, v. 147 (1990), p. 385–392.
- Hinch, H. H., Lewan, M. D., Ormiston, A. R., Beach, P. G., O'Reilly, C. M., 1990, A global approach to prediction of Upper Devonian–Lower Mississippian source rock occurrences and oil generating potential: Amoco Production Company Research Department Report F90-G-21, 465 p.
- Huc, A.Y., 1980, Origin and formation of organic matter in recent sediments and its relation to kerogen, in B. Durand, ed., *Kerogen, insoluble organic matter from sedimentary rocks*: Paris, Ed. Technip Publishers.
- Husseini, M., 1992, Potential petroleum resources of the Paleozoic rocks of Saudi Arabia: Thirteenth World Petroleum Congress, Buenos Aires, 1992, v. II, p. 3–13.
- Ivanov, V.L., and Nepomiluev, V.F., 1975, New data on bituminous occurrences in Paleozoic and Triassic strata of the New Siberian Islands, in *Geology and Useful Minerals of the New Siberian Islands and Wrangell Island*: Leningrad, Scientific Research Institute on the Geology of the Arctic, p. 55–60.
- Johnson, J., Klapper, G., and Sandberg, C., 1985, Devonian eustatic fluctuations in Euramerica: *GSA Bulletin*, v. 96, p. 567–587.
- Khramov, A., and Rodionov, V., 1981, Paleomagnetism and reconstruction of paleogeographic positions of the Siberian and Russian Plates during the Late Proterozoic and Paleozoic, in *Global reconstruction and the geomagnetic field during the Paleozoic*: Boston, Dredel Publishing Co., p. 23–37.
- Klapper, G., and Ziegler, W., 1979, Devonian conodont biostratigraphy, in *The Devonian System*: Palaeontological Association, London, Special Paper 23, p. 199–224.
- Klootwijk, C., and Giddings, J., 1988, An alternative APWP for the Middle to Late Palaeozoic of Australia—implications for terrane movements in the Tasman Fold Belt: Ninth Australian Geological Convention, Abstracts, v. 21, p. 219–220.
- Lee, K., 1984, Geology of the Dian-Qian-Gui foldbelt, Southwest China: U.S. Geological Survey Open-File Report 84-357, 48 p.
- Oglesby, R., 1989, A GCM study of Antarctic glaciation: *Climate Dynamics*, v. 3, p. 135–156.
- Oglesby, R., and Park, J., 1989, The effect of precessional insolation changes on Cretaceous climate and cyclic sedimentation: *Journal of Geophysical Research*, v. 94 (D12), p. 14,793–14,816.
- Ormiston, A., and Klapper, G., 1992, Paleoclimate, controls on Upper Devonian source rock sequences and stacked extinctions: Paleontological Society Special Publication 6, p. 227.
- Ormiston, A., Van Nieuwenhuise, D., and Lipke, L., 1988, An optimal lacustrine model for generation of hydrocarbon source rocks: Amoco Research Report F88-G-19.
- Ovnatanova, N., 1989, Thermal epigenesis of Paleozoic strata of Pay Khoy (Termal'nyy Epigenez paleozoyskikh otlozheniy Pay-Khoya): Komi Scientific Center, Uralian Branch ANSSR, Skytyvkar, 21 p. (in Russian).
- Parnell, J., 1985, Sedimentology of lacustrine source rocks, Orcadian basin: Abstracts of Lacustrine Petroleum Source Rocks Meeting, London, p. 45.
- Parrish, J., 1982, Upwelling and source beds with reference to the Paleozoic: *AAPG Bulletin*, v. 66(5), p. 750–754.
- Parrish, J., 1987, Palaeoupwelling and the distribution of organic-rich rocks, in Brooks and Fleet, eds., *Marine Petroleum Source Rocks*: Geological Society of London Publication 26, p. 199–205.
- Parrish, J., Hansen, K.S., and Ziegler, A.M., 1979, Atmospheric circulation and upwelling in the Paleozoic, with reference to petroleum source beds (abs.): *AAPG Bulletin*, v. 63, p. 507–508.
- Parrish, J., Ziegler, A., and Humphreyville, R., 1983, Upwelling in the Paleozoic Era, in Thiede, J., and Suess, E., eds., *Coastal Upwelling: Its Sedimentary Record*: NATO Conference Series IV, 10B, Plenum Press, p. 553–578.
- Pedder, A., 1982, The rugose coral record across the Frasnian/Famennian boundary, in Silver, L., and Shultz, P., eds., *GSA Special Paper 190*, p. 485–489.
- Puchkov, V.N., 1979, Bathyal complexes of passive margins of geosynclinal regions (Batialnye komplekсы passivnykh okrain geosynklinal'nykh oblastey): Uralian Science Center, Akad. Nauk. Nauka Press—Moscow, 128 p. (in Russian).
- Robison, V., 1992, Relative importance of runoff and upwelling as a nutrient resupply: AAPG International Research Conference, Paris.
- Rotarash, A.I., Samygin, S.G., Gredyushko, Ye.A., Keyl'man, G.A., Mileyev, V.S., and Perfil'yev, A.S., 1982, The Devonian active continental margin in the Southwestern Altay: *Geotectonics*, v. 16(1), p. 31–41.
- Schluger, P., 1973, Stratigraphy and sedimentary environments of the Devonian Perry Formation: *GSA Bulletin*, v. 84, p. 2533–2548.
- Scotese, C., 1986, Phanerozoic reconstructions: a new look at the assembly of Asia: University of Texas Institute for Geophysics Technical Report 66, p. 1–54.

- Scotese, C., and Barrett, S., 1990, Gondwana's move over the South Pole during the Paleozoic: evidence from lithologic indicators of climate, *in* Paleozoic Palaeogeography and Biogeography: Geological Society of London Memoir 12, p. 75–86.
- Stanley, S.M., 1984, Temperature and biotic crises in the marine realm: *Geology*, v. 12, p. 205–208.
- Stanley, S.M., 1988, Paleozoic mass extinctions: shared patterns suggest global cooling as a common cause: *American Journal of Science*, v. 288, p. 334–352.
- Suess, E., 1980, Particulate organic flux in the oceans—surface productivity and oxygen utilization: *Nature*, v. 288, p. 260–263.
- Termier, G., and Gansser, A., 1974, Les series devoniennes du Tang Chu (Himalaya du Bhoutan): *Ecolgae Geologica Helvetica*, v. 67(3), p. 587–596.
- Thompson, J., and Newton, C., 1989, Late Devonian mass extinction: episodic climatic cooling or warming?, *in* McMillan et al., eds., *Devonian of the World: Proceedings of the Second International Symposium on the Devonian System*, Calgary, v. 3, p. 29–34.
- Trofimuk, A., 1984, Organicheskaya Geokhimiya Paleozoyskikh otlozheniya yuga Zapadno-Sibirskoy Plity (Organic Geochemistry of the Southwest Siberian Plate): ANSSR, Siberian Branch, Trudy, v. 589, 212 p.
- Ulmishek, G., and Klemme, H., 1990, Depositional controls, distribution and effectiveness of world's petroleum source rocks: U.S. Geological Survey Bulletin 1931, 59 p.
- Williamson, G., and Williamson, D., 1987, Circulation statistics from seasonal and perpetual July and January simulations with the NCAR Community Climate Model (CCM1): NCAR Technical Note TN-302+STR, 199 p.
- Williamson, D., Kiehl, J., Ramanathan, V., Dickinson, R., and Hack, J., 1987, Description of NCAR Community Climate Model (CCM1): NCAR Technical Note TN-285+STR, 112 p.
- Witzke, B., 1987, Circulation patterns in Paleozoic epicontinental seas: *Paleoceanography*, v. 2, p. 228–248.
- Witzke, B., 1990, Paleoclimatic indicators and inferred Devonian paleolatitudes of Euramerica, *in* McMillan et al., eds., *Devonian of the World: Proceedings of the Second International Symposium on the Devonian System*, Calgary, v. 1, p. 49–63.
- Witzke, B., and Heckel, P., 1989, Palaeoclimates in Laurentia and Euramerica, *in* McKerrow and Scotese, eds., *Paleozoic Palaeogeography and Biogeography: Geological Society of London Memoir 12*, p. 57–74.
- Young, G., 1990, Devonian vertebrate distribution patterns and cladistic analysis of paleogeographic hypotheses, *in* Paleozoic Palaeogeography and Biogeography: Geological Society of London Memoir 12, p. 243–256.
- Yudovich et al., 1985, Petrochemical identification of volcanic products in the Pay Khoy Black Shales: *Geochemistry International*, 1985, p. 71–84.
- Zapivalov, N.P., and Trofimuk, A.A., 1989, Distribution of oil and gas in Devonian rocks of West Siberia: *Canadian Society of Petroleum Geologists Memoir 14*, p. 553–556.
- Zharkov, M.A., and Bakhturov, S.F., 1982, Paleozoyskie bituminoznye karbonatono-slantsevye formatsii Vostochnoy Sibiri (Paleozoic bituminous shale-carbonate formations of Eastern Siberia), *in* Yanshin, A.L., ed., *Osobennosti stroyeniya osadochnykh formatsii*. (Peculiarities of the construction of sedimentary formations): Trudy, Instituta Geologii i Geofiziki, Sibirskoe Otde 1, ANSSSR, Novosibirsk, v. 535, p. 103–115.
- Ziegler, A., Hansen, K., Johnson, M., Kelly, M., Scotese, C., and Van der Voo, R., 1977, Silurian continental distributions, paleogeography, climatology and biogeography: *Tectonophysics*, v. 40 (1977), p. 13–51.

The Effects of Paleolatitude and Paleogeography on Carbonate Sedimentation in the Late Paleozoic

D. A. Walker

*Mobil Exploration and Producing U.S.
Midland, Texas, U.S.A.*

J. Golonka

*Mobil Exploration and Producing Technical Center
Dallas, Texas, U.S.A.*

A. Reid

S. Reid

*Consulting Geologists
Midland, Texas, U.S.A.*

ABSTRACT

Facies distribution in the late Paleozoic of west Texas indicates that paleolatitude and paleogeography strongly influenced carbonate sedimentation. Placing regional facies maps into their late Paleozoic latitudes and plate orientations can assist in explaining and predicting basin sedimentation patterns. Paleogeographic reconstructions indicate that west Texas was very near the equator throughout the late Paleozoic. This produced a tropical climate that was ideal for widespread carbonate deposition. The response of Paleozoic sedimentation to prevailing winds would have been similar to that presently observed in the low latitudes. Carbonate sedimentation during the Pennsylvanian and Permian responded to these trade winds in a similar fashion as observed in the modern tropics near the equator.

The PALEOMAP and TERRAMOBILIS softwares were used to construct plate reconstructions and paleogeographic maps. These maps indicate that during the late Paleozoic North America was rotated approximately 43° northeast from its present setting. Shelf edges in the Delaware and Midland basins presently oriented 0 to 15° were in fact oriented 40 to 60° northeast during the late Paleozoic. Thin coals on the Eastern shelf indicate west Texas was located in a humid tropical climate during the Pennsylvanian. Later, during the Permian, extensive evaporites indicate this area had moved into a more arid tropical climate. This change occurred as the North American plate migrated northward at the end of the Paleozoic.

The past orientation of the carbonate shelves must be determined and combined with the direction of prevailing winds to better understand facies distribution. It is not only important to know the direction of prevailing winds, but also which portion of the shelf would have been in a windward location. The location and actual orientation of carbonate shelves are important when considering where the regional prevailing winds would have struck the platform edges during sedimentation. Understanding basin orientation and prevailing wind direction enables the prediction of the distribution of carbonate grain types and carbonate sand-body geometry and location.

INTRODUCTION

Numerous paleogeographic reconstructions of North America indicate west Texas was much farther south during the late Paleozoic than it is today (Ross, 1978; Scotese et al., 1979; Irving, 1979; Heckel, 1980; Bambach et al., 1980; Scotese, 1984; Scotese and McKerrow, 1990). Throughout the Pennsylvanian and Permian, west Texas was very near the equator (Figures 1–3).

Being located in low latitudes meant that west Texas was an ideal location for carbonate sedimentation throughout the late Paleozoic. An abundance of reef-forming organisms, a warm tropical climate, and lack of siliciclastics led to the accumulation of a consider-

able thickness of carbonate rocks. These factors contributed to the formation of broad carbonate platforms and shelves along the basin margins and atolls within the basins. Most paleogeographic maps are intended to reconstruct the positions of paleocontinents. This practice makes it difficult to accurately locate even large features such as the Midland and Delaware basins. As a result, this limits the use of most paleogeographic maps in understanding the effects that latitude and regional geography had on carbonate sedimentation during the Pennsylvanian and Permian.

The latitude and orientation of west Texas have changed greatly throughout time. Paleolatitude reconstructions show that North America (Laurentia) migrated northeastward during the late Paleozoic (Golonka, 1991). As North America drifted northeastward, changes in paleolatitude would have affected the direction that prevailing winds and ocean currents would strike the carbonate platforms and shelves. By placing west Texas in its paleolatitude and paleogeographic orientation through time, the potential influence of prevailing winds and currents on carbonate sedimentation can be determined.

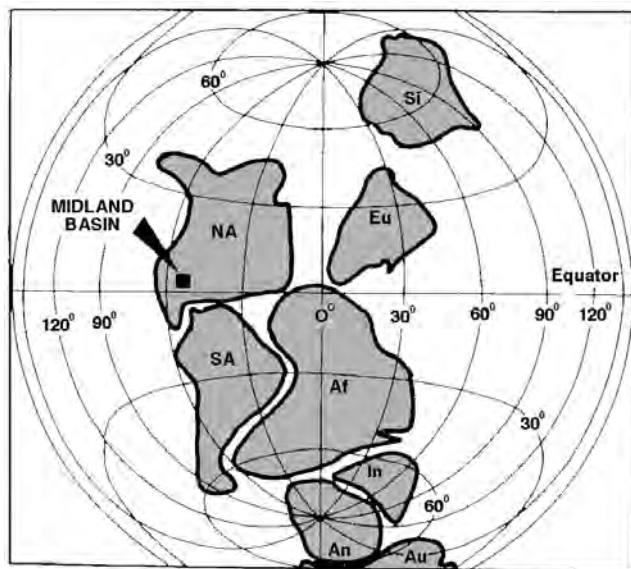


Figure 1. Generalized reconstructions of plate locations adapted from Matthews (1984, 1987) and Hamilton and Kronsley (1967) indicate that west Texas was located at a low latitude during the late Paleozoic. This places the Midland and Delaware basins very close to the equator during the Pennsylvanian and Permian. Si = Siberia; NA = North America; Eu = Europe; SA = South America; Af = Africa; In = India; An = Antarctica; Au = Australia.

METHODS

Reconstructing the positions of continental plates in the Paleozoic relies primarily on paleomagnetic data (Bambach et al., 1980). Faunal and floral communities have long been used to provide additional important information concerning paleolatitude position of the continents (Khoppen and Wegener, 1924; Du Toit, 1937; Crowell, 1978; Ziegler et al., 1981; Stanley, 1988). Paleoclimate and paleowind data are also useful in determining the location and orientation of continental plates (Wegener, 1966; Heckel, 1986; Parrish and Peterson, 1988; Peterson, 1991).

The latitude and longitude positions and orientations of the Midland basin and Horseshoe atoll during the Pennsylvanian and Permian were modeled by computer using the PALEOMAP software package. The PALEOMAP software was developed by University of Chicago Paleogeographic Atlas Project (PGAP) and University of Texas Paleogeographic Mapping Project (POMP) in cooperation with Mobil

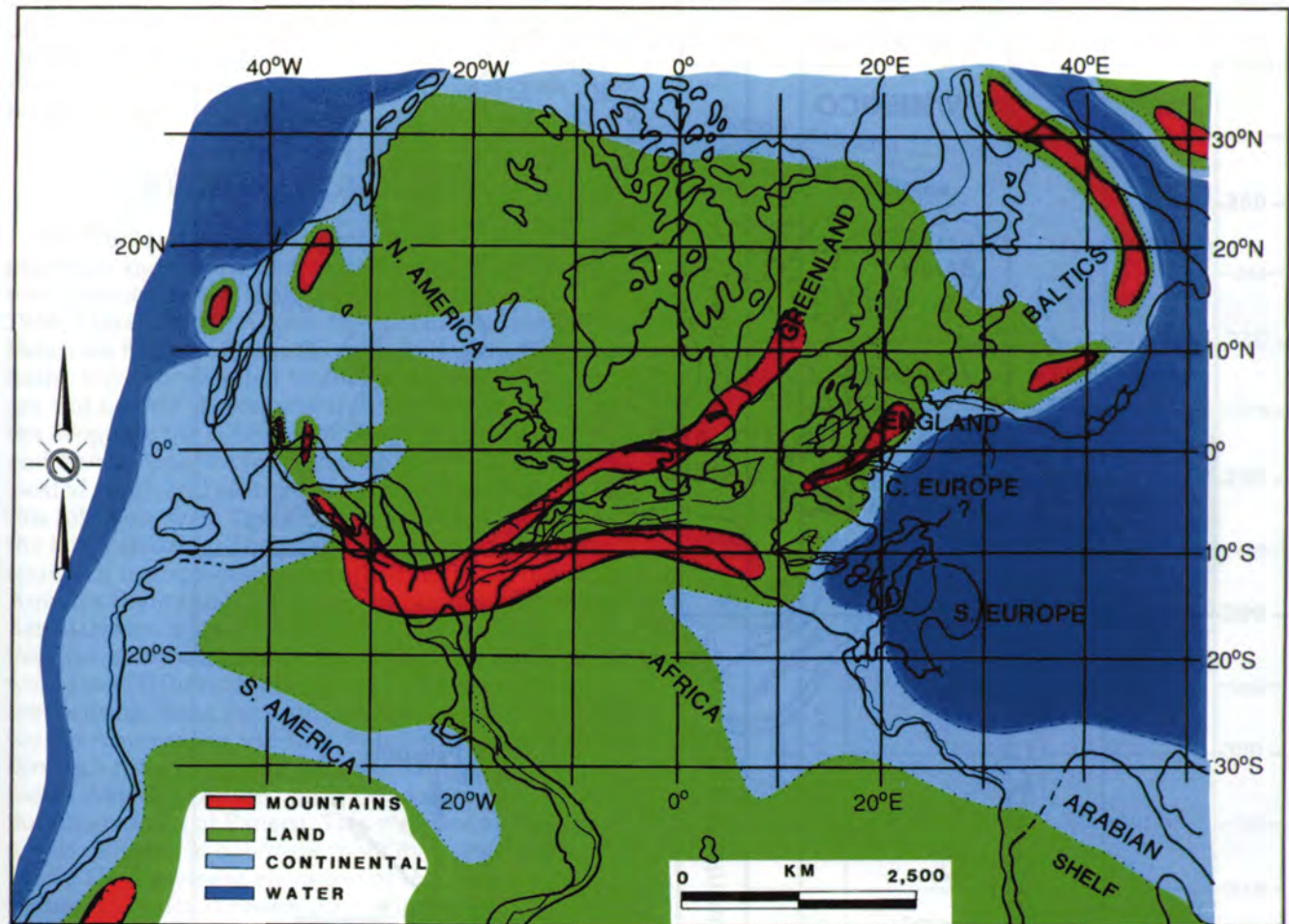


Figure 2. Detailed paleogeography and paleolatitude reconstructions for the Pennsylvanian and Permian by Golonka (1991) show the Midland basin was located between the equator and 10°N latitude and 30° to 40°W longitude. Note how the locations of major geographic features indicate that the North American plate was rotated to the northeast from its current orientation.

Corp. PALEOMAP is a digital tectonic-reconstruction program which has been used in numerous exploration projects (Golonka, 1991) to create paleo-continental base maps. It takes tectonic features in the form of digitized data files, assembles those features in accordance with user-specified rotation criteria, and creates a plot or an ASCII file. The output files yield a map of size, projection, and format selected by the user.

The first step in our studies was to encode the study area into digital form. This was done using the VAX Intergraph digitizing tablet and Mobil Surface Analysis System (MSAS) computer program. This technique converted X and Y Intergraph design file coordinates into latitude and longitude coordinates. The digital file was later introduced into the PALEOMAP and POMP version database using the MEPSITOPOMP program. The MEPSITOPOMP program, designed for Mobil by POMP researcher Lisa Gahagan, converts a file format and attaches a description of the age of the feature, the plate with which it was traveling, and a simple coded

description of the feature (e.g., BA = bathymetric contour, RI = spreading ridge, CS = coastline, etc.). For the Horseshoe atoll and Midland basin, the age and coastline for the North America (Laurentia) plate were encoded in the file.

After the file encoding, the data were manipulated using VAX PALEOMAP version and Paleozoic-Mesozoic (PZMZ) rotational database designed and modified by Scotese and others (Scotese et al., 1979; Scotese, 1984; Scotese and McKerrow, 1990). The rotation files contain lists of finite rotations between pairs of tectonic elements, at different episodes of time. Each element is described by the plate code, latitude and longitude of finite pole, angle of opening, time in millions of years of rotational stage, references, and comments. The Late Pennsylvanian and Permian orientation of Laurentia described in the rotational database is based on the combined paleoclimatic poles from all the Pangean continents (Van der Voo et al., 1984). It is similar to maps by Lottes and Rowley (1990) and shows good agreement with biogeographic

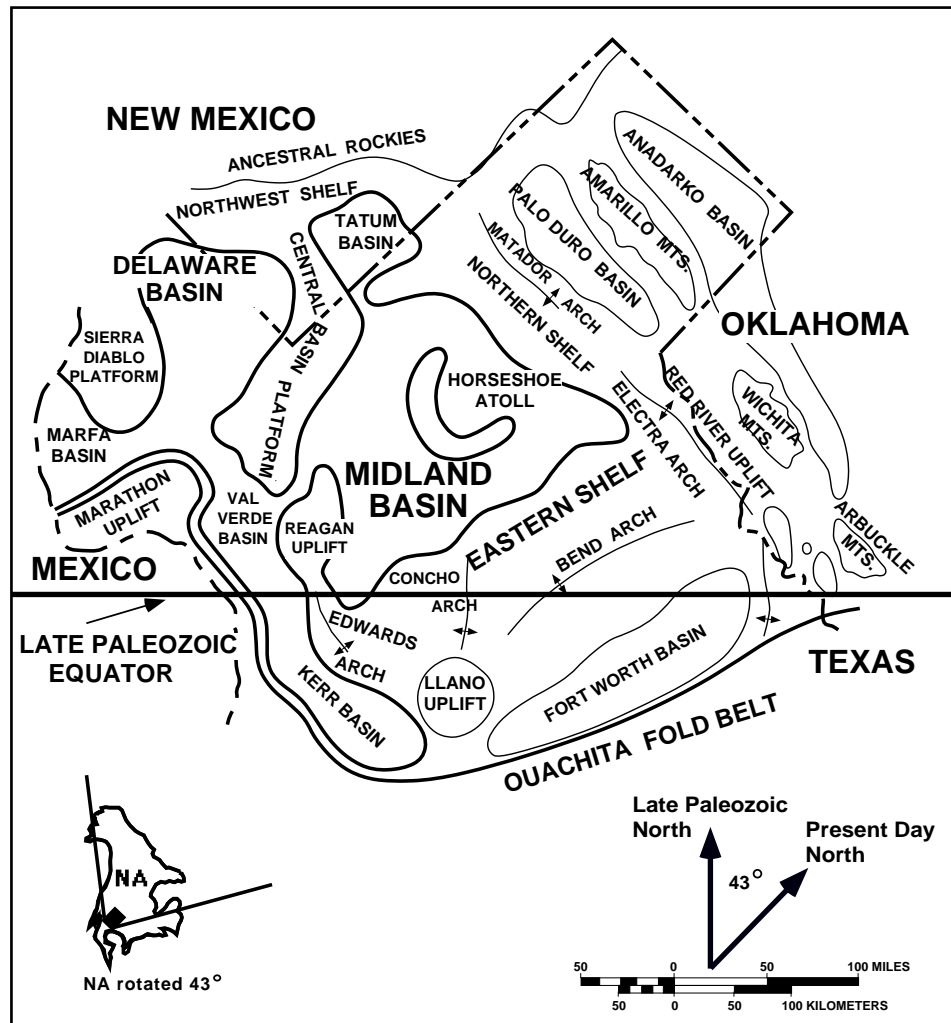


Figure 3. A late Paleozoic paleogeographic map of west Texas shows the region was oriented 43° east of present north. The Midland and Delaware basins, often collectively called the Permian basin, were surrounded by the Northwestern, Northern, and Eastern shelves. The generalized location for the equator during the Late Pennsylvanian and Early Permian is adapted from Walker et al. (1991).

and paleoclimatic indicators (Van der Voo, 1988; Witzke, 1990; Ziegler, 1990).

The PALEOMAP software changed the original present-day latitude and longitude of the Midland and Delaware basins via a digital file into its paleolatitude and paleolongitude of Pennsylvanian–Permian age (312–280 Ma). The output digital files were converted into Intergraph design files, plotted, and interpreted. For purposes of this study, the time scale and stratigraphic nomenclature (Figure 4) for Pennsylvanian and Permian in the Permian basin is from Mear (1983). The distribution of carbonate facies discussed in this study is derived from the examination and analysis of over 1700 wireline logs, well cuttings, and cores.

Comparisons of late Paleozoic and modern carbonates can be greatly enhanced by understanding some of the broad regional influences geography and latitude have on sedimentation. Studies indicate that

modern carbonate sedimentation can be influenced by geography and geomorphology (Wilson, 1975; Wilson and Jordan, 1983). The direction of modern prevailing or trade winds is directly related to latitude. These winds may have an important impact on ocean currents, which, in turn, affect the type and sedimentation patterns of carbonate facies. The orientation and geomorphology of platforms and shelves determine which edges are windward and which edges are leeward. Platform and shelf morphology place additional controls on sedimentation.

To identify the prevailing wind direction, the paleolatitude of an area must first be determined. The regional prevailing winds are in general controlled by the paleolatitude. The locations and orientations of the carbonate shelves and platforms are identified from paleogeographic and facies maps. Estimates of where windward and leeward sedimentation may occur can

then be predicted by combining the prevailing wind directions with platform and atoll orientations and shapes. The expected prevailing winds and ocean currents in the late Paleozoic can be used to estimate carbonate facies.

REGIONAL GEOLOGY

The Midland basin, Delaware basin, Central Basin platform, and Ozona arch were formed by major tectonic activity during the early Pennsylvanian (Galley, 1958; Horak, 1985; Algeo, 1992). The Midland and Delaware basins, often collectively called the Permian basin, were surrounded by the Northwestern, Northern and Eastern shelves (Figure 1). During the Hercynian orogeny, the collision of South America, Africa, and North America produced the Ouachita fold belt located south and east of the Permian basin. North of this fold belt, west Texas was in a foreland setting in the late Paleozoic. The progressive closure between southern Europe–Africa–South America and North America (Laurentia) advanced through the southern Appalachians and Ouachitas of Oklahoma during the Pennsylvanian and culminated in the Early Permian in west Texas (Horak, 1985; Algeo, 1992). This indicates the suturing along the southern continental margin of North America in the late Paleozoic progressed through time from east to west. During this time, North America collided with Gondwana, producing the supercontinent Pangea. This complex tectonic history is reflected in basement mobility analysis (Horak, 1985). The basement elevation of the Permian basin changed greatly through time (Figure 5). Basement mobility profiles of major geologic provinces through time indicate long episodes of stable tectonics interrupted by short events of rapid crustal movement.

Throughout the late Paleozoic, west Texas was in the low latitudes, making it an ideal location for carbonate sedimentation and the growth of reef-forming organisms. As a consequence of this tropical environment, broad carbonate shelves became established on the western, northern, and eastern margins of the Delaware and Midland basins as well as over portions of the Central Basin platform. Extensive reef and complex carbonate facies developed in a high-energy environment along the shelf margins. These carbonates accumulated in a series of shallowing-upward cycles that were a response to worldwide fluctuations in sea level. The most likely controls on the sea level changes were glacial eustatic (Wanless and Shepard, 1936; Crowell, 1978; von Brunn and Stratten, 1981; Boardman and Malinky, 1985; Ross and Ross, 1985, 1987; Veevers and Powell, 1987; Walker et al., 1990). These grain-dominated sediments accumulated along shelf and platform edges, restricting the circulation of marine waters into the platform interior (Horak, 1985; Bebout et al., 1987). This resulted in low-energy carbonate sediments and evaporites being deposited in the platform interiors. In addition, a large carbonate platform, called the Horseshoe atoll, consisting of multiple high-energy reefs and grainstone bars developed in the northern Midland basin (Reid et al., 1989,

| System | Global Series/Stages | | North American Series/Stages | Ma | |
|---------------|----------------------|-------------|------------------------------|---------------|------------|
| Permian | Upper | Tatarian | Ochoan | 250 | |
| | | Kazanian | Guadalupian | 255 | |
| | | Kungurian | | 260 | |
| | Lower | Artinskian | Leonardian | 265 | |
| | | Sakmarian | Wolfcampian | 270 | |
| | | Asselian | | 275 | |
| Carboniferous | Upper | Stephanian | Gzhelian | 280 | |
| | | | Kasimovian | 285 | |
| | Middle | Westphalian | Moscovian | Pennsylvanian | 290 |
| | | | | | Bashkirian |
| | | Virgilian | 300 | | |
| | | | Missourian | 305 | |
| Desmoinesian | 310 | | | | |
| | Atokan | 315 | | | |
| Morrowan | 320 | | | | |
| | | | | 325 | |
| | | | | 330 | |

Figure 4. This chart shows the chronostratigraphic units and time scale applicable to the late Paleozoic in west Texas. The absolute dates for the Pennsylvanian and Permian are from Mear (1983). Both North American and global nomenclature are shown.

1990, 1991; Walker et al., 1990, 1991). It was able to form due to the general lack of siliciclastics during the Pennsylvanian through Early Permian in this area of the basin.

Orogenic uplifts periodically shed siliciclastics into the basins as deep marine sediments. Siliciclastics were also occasionally deposited in shallow-water environments and are interbedded with the shelf carbonates. At times, the Eastern shelf, which lay east of the Midland basin, was also the site of considerable

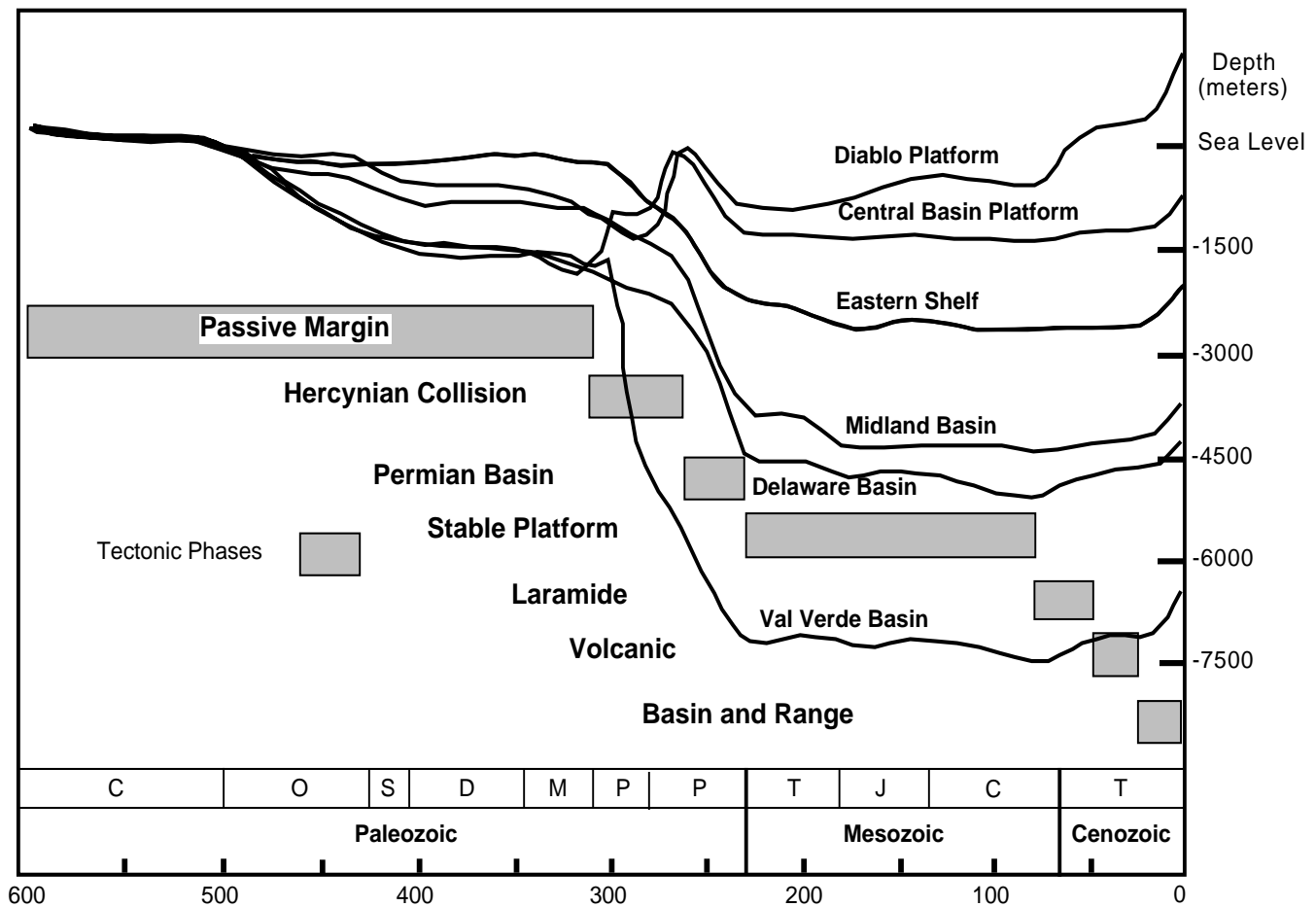


Figure 5. The mobility profiles of the primary geologic provinces of the Permian basin graphically show that basement elevation has changed through time. This figure shows the basement elevation related to specific areas through time and tectonic events. In general, there have been lengthy periods of relatively little tectonic movement interspersed by times of very rapid basement mobility. Modified from Horak (1985) and Borer and Harris (1991).

cyclic sedimentation (Brown, 1969; Brown et al., 1973; Malinky et al., 1984; Yancey, 1984; Boardman and Malinky, 1985; Yancey and McLerran, 1988; Reid and Mazzullo, 1988; Reid et al., 1988; Boardman and Heckel, 1989). These cycles have considerable amounts of siliciclastics and resemble classical cyclothems found in the Appalachian basin (Bloomer et al., 1991). The nearest major sources of Eastern shelf siliciclastics throughout the Pennsylvanian were the Ouachita Mountains in eastern Texas and the Wichita Mountains in western Oklahoma (Figure 3). Repeated sub-aerial exposure of the Eastern shelf resulted in the development of numerous paleosols in the shelf sediments (Brown et al., 1973; Yancey and McLerran, 1988; Bloomer et al., 1991).

PENNSYLVANIAN PALEOGEOGRAPHY

The Horseshoe atoll located in the northern Midland basin is an ideal location to examine the influence paleolatitude and paleogeography can have on carbonate sed-

imentation. Late Paleozoic in age, it is called the Horseshoe atoll for its paleogeomorphology. Found only in the subsurface, this large carbonate platform is the site of numerous important oil reservoirs (Figure 6; Stafford, 1955, 1956; Myers et al., 1956; Burnside, 1959; Vest, 1970).

Its fields have collectively produced over two billion barrels of oil since the discovery of the trend in 1948 (Galloway et al., 1983). One field, SACROC (also called Scurry Reef and Kelly Snyder), has produced over one billion barrels of oil (Galloway et al., 1983; Schatzinger, 1983, 1988). Some individual wells are also prolific, initially producing several thousand barrels of oil per day (Vanderhill et al., 1990). The fact that there has been considerable drilling allows for detailed examination of platform carbonates from cores, cuttings, and well logs. Reservoir development is controlled by the distribution, diagenesis, and cyclicity of carbonate facies. Thus, it is critical to understand how paleolatitude and paleogeography could have influenced carbonate sedimentation.

In addition to the probable warm tropical climate and proximity to the equator, the Midland basin

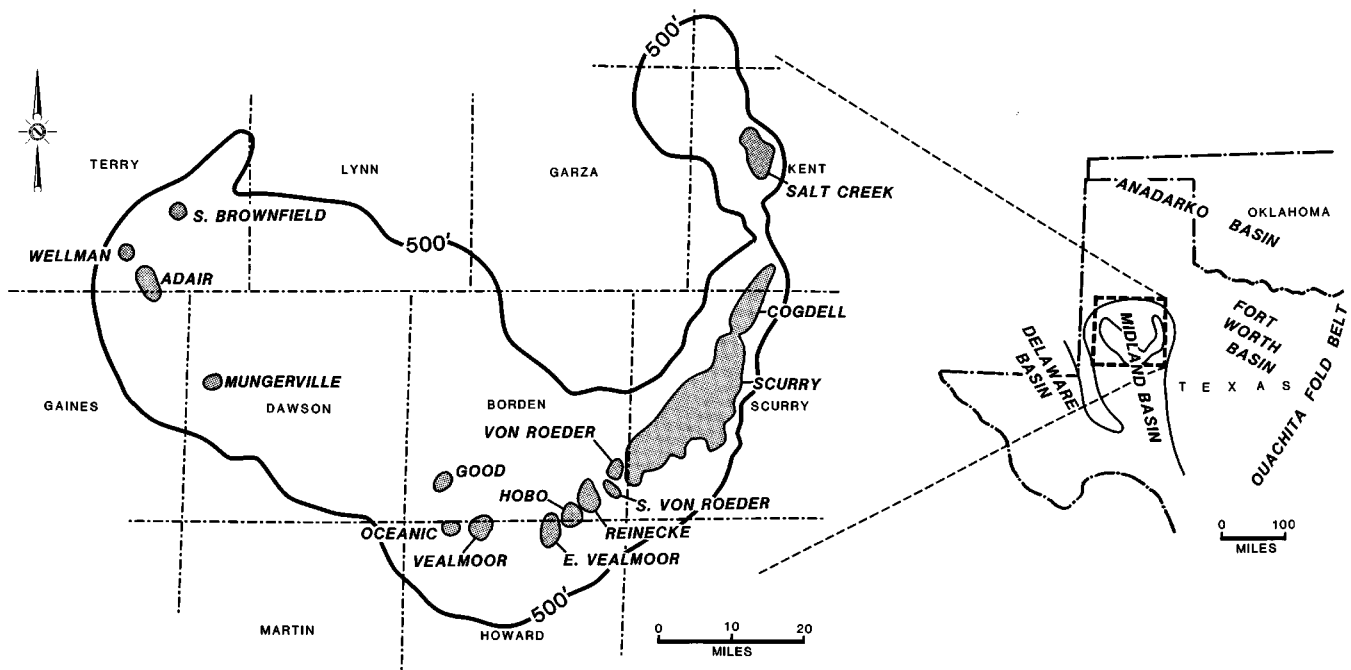


Figure 6. A generalized isopach map of the Horseshoe atoll shows the area with the thickest accumulations of carbonates. The 500 ft carbonate isopach is adapted from Vest (1970). The more significant reservoirs on the Horseshoe atoll are also identified.

received little siliciclastic sedimentation during the Pennsylvanian. Most siliciclastic sedimentation was confined to the shallow waters of the Eastern shelf east of the Midland basin. The deltas that were the site of siliciclastic sedimentation were hundreds of miles from the center of the Midland basin. The lack of siliciclastics in the Midland basin favored the rapid accumulation of carbonates because the reef organisms could grow without the interference of silt or sand. The reefs that built on the Pennsylvanian (Desmoinesian through Virgilian) platforms or atolls did not consist of frame-building organisms. Instead, in the Midland basin and elsewhere, Pennsylvanian reefs consisted primarily of phylloidal algae, bryozoans, solitary corals, crinoids, *Tubiphytes*, and encrusting foraminifera (Schatzinger, 1983, 1988; James and Macintyre, 1985; Crawford et al., 1988; West, 1988; Stanley, 1985, 1988; Peterson, 1991). In addition to boundstones, there are abundant carbonate mudstones, wackestones, and grainstones on the platform and atolls (Stafford, 1955, 1956; Myers et al., 1956; Burnside, 1959; Schatzinger, 1983, 1988). Oolitic grainstones formed when very shallow water covered the northeast area of the platform (Schatzinger, 1983, 1988; Walker et al., 1990; Reid and Reid, 1991).

The Horseshoe atoll began developing in the early Desmoinesian (Strawn) while the Midland basin was on the equator. At times, open marine waters stretched for hundreds of miles south and east of the Horseshoe atoll (Hills, 1972; Heckel, 1980, 1986; Stanley, 1985). In the middle to late Desmoinesian, carbonate sediment began to accrete vertically on the broad early Desmoinesian platform (Figures 6–9). This trend continued during the Missourian (Canyon), Virgilian (Cisco), and into the Permian (Wolfcampian). The

deposition of each successive unit was more restricted laterally and with predominantly greater vertical growth than the previous one. This may relate to the rate of subsidence of the basin. Reefs in each successive highstand had less of an area to colonize due to the increasing water depths combined with basin subsidence. Later during the Missourian, carbonates were accumulating on the platform from 1° to 2°N latitude. As North America (Laurentia) migrated northeastward, carbonate sedimentation continued during the Virgilian, occurring from 2° to 4°N latitude. Carbonate sedimentation on the platform ended during the Wolfcampian at 6°N latitude due to the influx of fine-grained siliciclastics and dark shales.

From 312 Ma (Early Desmoinesian) to 306 Ma (middle Missourian), the relative motion of the platform and basin was N63°E (Figure 7). Later, from 298 Ma (Early Virgilian) to 280 Ma (Wolfcampian), the direction of movement changed to N24°E. This change in motion indicates a major tectonic event occurred in the Late Pennsylvanian that greatly modified the movement of the Laurentia plate. At that time, Laurentia had collided with Gondwana and become part of the supercontinent Pangea. From 312 Ma to 280 Ma the North American (Laurentia) plate was oriented such that the platform and basin were rotated 43° to the northeast relative to present-day coordinates.

Previous attempts to reconstruct how the platform developed have used the present-day orientation of the atoll as a reference. Prevailing winds have been identified as coming from the south, east, or ENE (Myers et al., 1956; Schatzinger, 1983, 1988). Myers et al. (1956) felt that the accumulation of carbonates on the atoll was influenced by south prevailing winds.

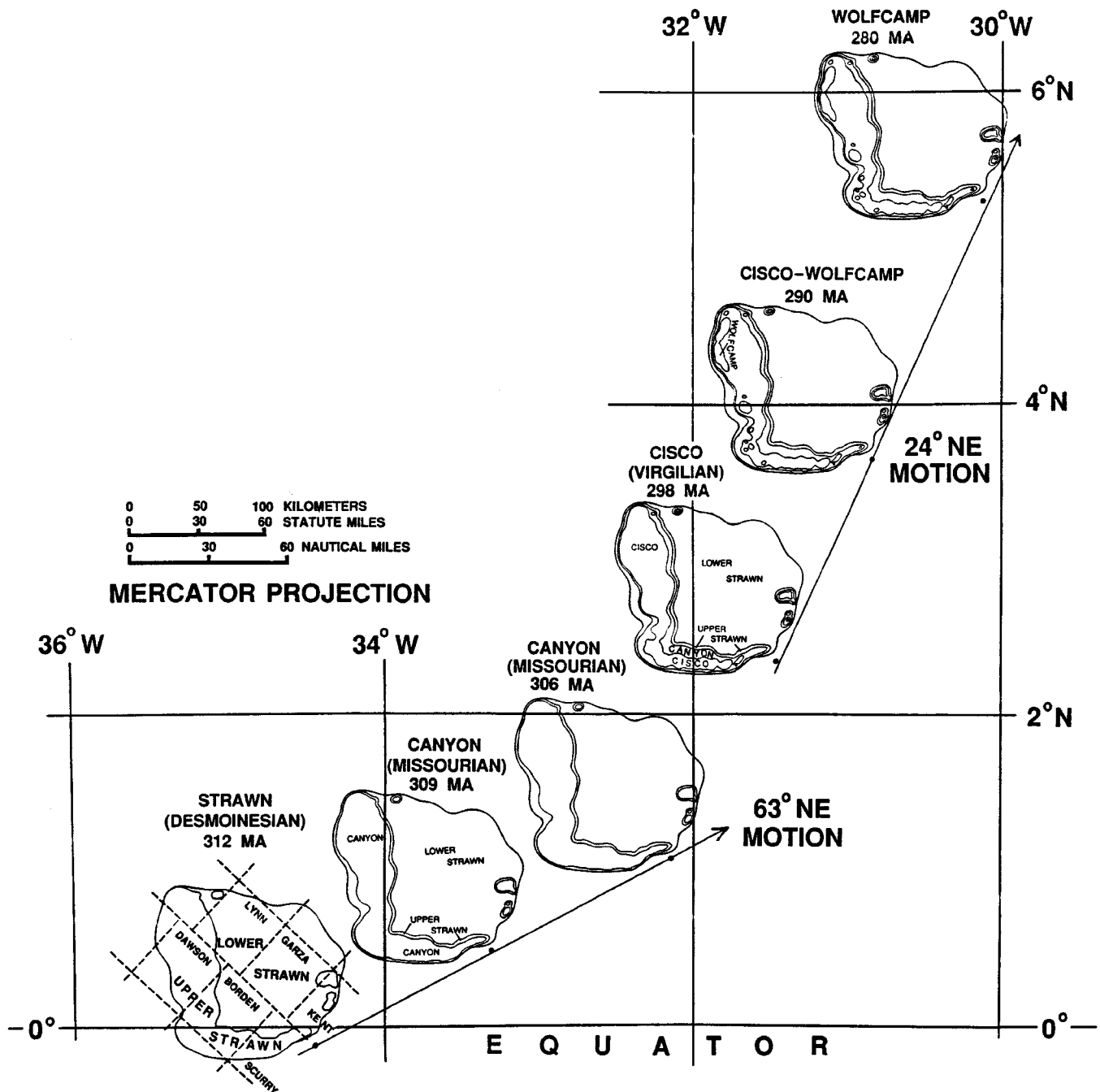


Figure 7. Carbonates began accumulating on the Horseshoe atoll during the early Desmoinesian while the Midland basin was on the equator. Missourian sedimentation was from 1° to 2°N latitude. Carbonate sedimentation on the atoll ended during the Wolfcampian near 6°N latitude. From 312 to 306 Ma the relative motion of the basin was N63°E. During the period of 298 to 280 Ma the atoll was moving N24°E. It was during the Hercynian collisional phase that the motion of the Horseshoe atoll dramatically changed from N63°E to N24°E.

According to this model, prevailing southern winds produced detrital lobes by eroding the existing lithified carbonates. The southern winds and ocean currents eroded the transverse edge of the atoll and transported the detrital sediments to leeward locations. This would produce the horseshoe shape with the detrital lobes being parallel to a south wind direction. Eventually, these detrital lobes were colonized

and stabilized by reef organisms. Later drilling has shown that these detrital lobes, as suggested by this model, do not exist. Schatzinger (1983, 1988), in a detailed examination of the SACROC field, suggested that the prevailing winds in the area were most likely from the ENE or east because of the likely tropical setting. It was suggested that facies in the field might relate to prevailing winds.

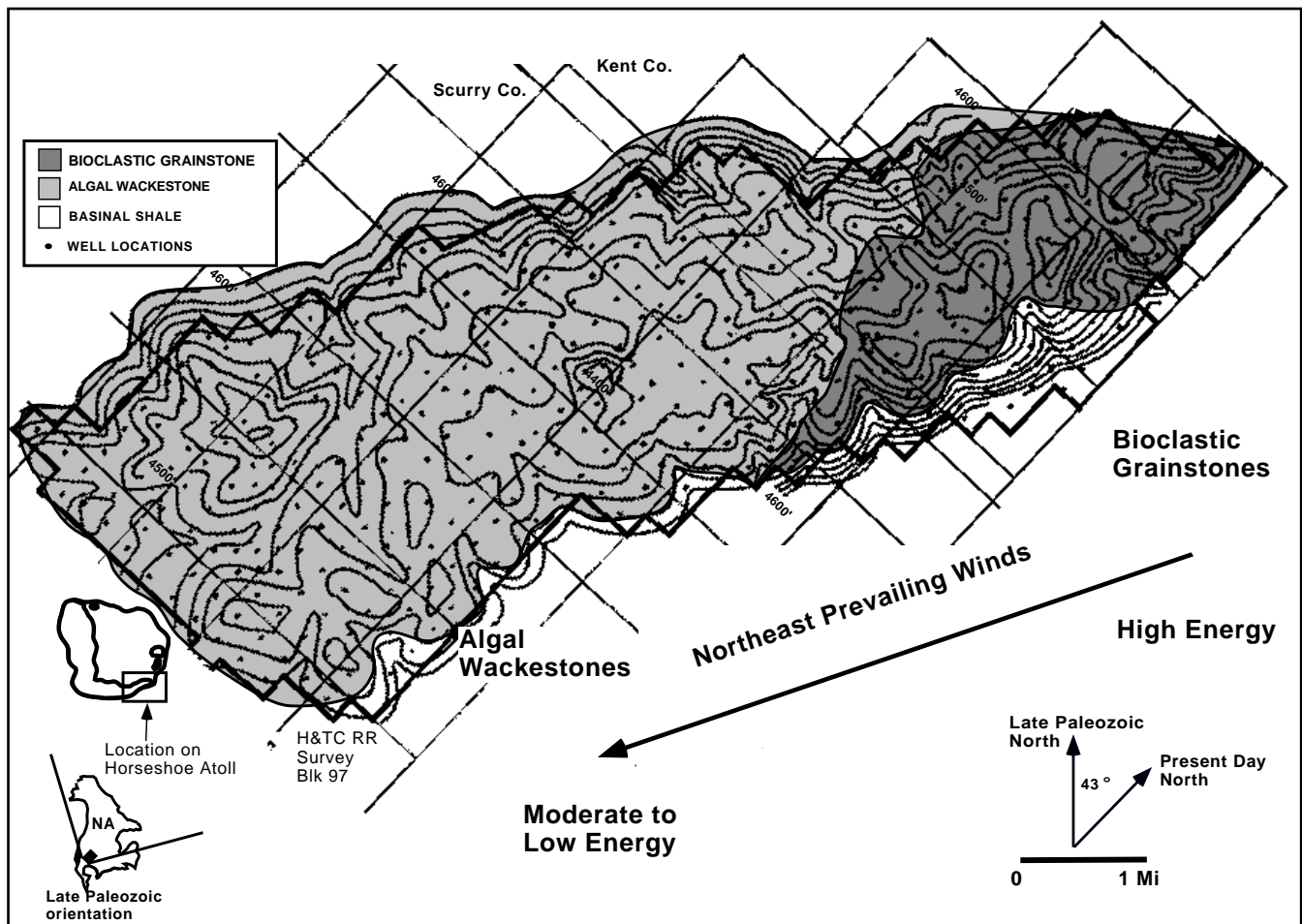


Figure 8. Upper Desmoinesian carbonates at the Cogdell field clearly demonstrate the influence of prevailing winds. Bioclastic grainstones are found in windward locations on the northeast-facing edges of the platform. Algal mudstones and wackestones formed in areas of moderate to low energy that were leeward of these high-energy deposits. Facies adapted from Reid et al. (1991). Lithofacies are superposed onto a Desmoinesian structure map that has a subsea contour interval of 20 ft.

Recent studies give better understanding of the direction of prevailing winds in the low latitudes during the Pennsylvanian and Permian. Wind directions calculated from measurements of sedimentary structures in eolian sandstones indicate that within 30° north of the equator, the prevailing winds in Pennsylvanian were from the northeast (Peterson, 1988). Also, estimates of wind directions using paleolatitude and weather patterns also predict a general northeasterly wind direction north of the equator (Hills, 1972; Heckel, 1986; Parrish and Peterson, 1988; Peterson, 1991). Within 30° south of the equator, the prevailing winds were probably from a general southeast direction (Hills, 1972; Parrish and Peterson, 1988).

The location and succession of carbonate facies in the Pennsylvanian (Desmoinesian through Virgilian) suggest paleolatitude and paleogeography played an important role in carbonate sedimentation. As the orientation and latitude of the basin changed through time, the direction of prevailing winds changed relative to the platform. This could have greatly influenced

carbonate sedimentation and depositional environments on the platform during the late Paleozoic.

Desmoinesian Sedimentation

In the early Desmoinesian, the platform that would be the base for the Horseshoe atoll began to develop near the equator (Figures 7 and 8). During this time the platform and basin were oriented approximately 43° to the northeast from their current alignment (Figures 7 and 8). By the late Desmoinesian, the platform had moved so that its northeastern edge was north of the equator. In the late Desmoinesian, oolitic and bioclastic grainstones are found on what were once northeast-facing edges of the atoll (Figure 8). During this time, it can be observed in the Cogdell field and the surrounding area that the grainstone facies grade southwestward to algal wackestones and mudstones (Figure 8).

In the late Desmoinesian when the platform was north of the equator, carbonate sedimentation was probably influenced by prevailing winds from the

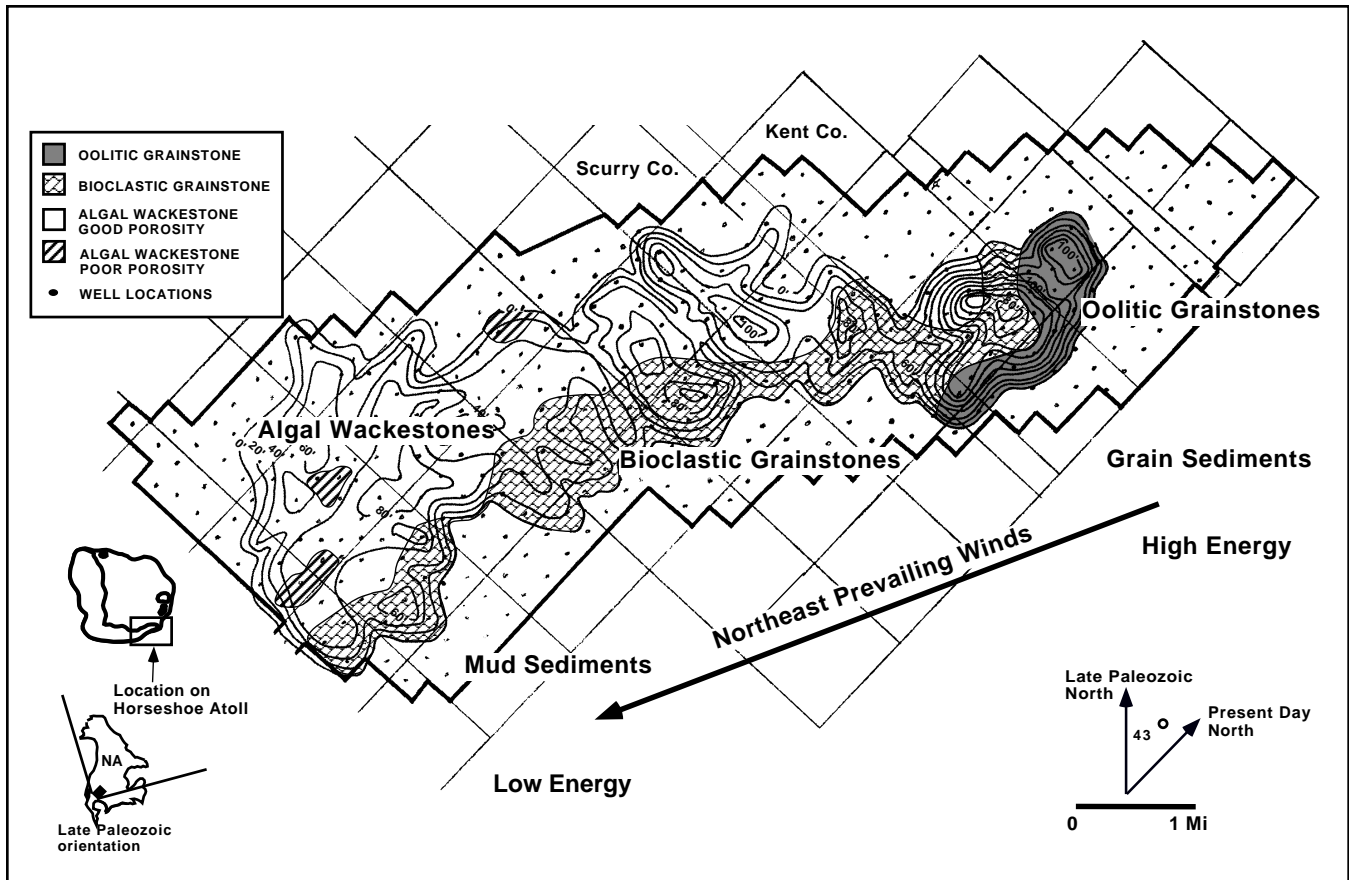


Figure 9. In the middle Missourian, oolitic grainstones are found on the windward edges of platforms. A bioclastic grainstone zone is found along the eastern edge of the Cogdell field. This is probably a beach or shoal deposit. Algal wackestones are found in southwest or leeward locations behind the grainstones. The facies demonstrate a high- to low-energy transition related to the prevailing northeast winds. Facies adapted from Reid et al. (1991). Lithofacies are superposed onto a middle Missourian isopach map that has a contour interval of 20 ft.

northeast (Hills, 1972; Stanley, 1985; Parrish and Peterson, 1988; Peterson, 1991). Rotating the platform 43° to the northeast as it was in the Pennsylvanian places what are presently the eastern and northeastern platform edges squarely in line to be struck by prevailing northeasterlies and the ocean currents driven before them.

Sedimentation at the Cogdell field demonstrates the influence that the prevailing winds and currents can play on grain type (Figure 8). The bioclastic grainstones are clearly windward deposits formed in shallow water by the turbulence of the prevailing northeasterlies striking what were once northeast-facing edges of the atoll. Wind energy was dissipated on northeast edges, so that as the weakened winds continued southwestward no grainstones formed. Behind the grainstone shoals, algal wackestone and mudstones accumulated in a leeward location. The location of the algal wackestones suggests that they accumulated in relatively quiet waters behind grainstone shoals.

The carbonate facies in and around the Cogdell field are generalized from the examination of over 300 wireline logs, well cuttings, and cores. Grainstones

have not been found in the leeward areas of the eastern edge of platform. Grainstones formed and accumulated on structurally high locations because the shallow water often found in these areas was conducive to their formation. In the area of the Cogdell field, it appears as if the northeast edge of the platform served as a point source for the formation of grainstones. Close examination of grainstones' concentration suggests longshore drift may have redistributed grainstones along a beach or shoal running roughly parallel to the prevailing winds and currents. Grainstones may have also formed and accumulated in these areas since the beach or shoal environments would have been both northeast facing and in windward locations. Contemporaneous sediments in more leeward locations east and southeast of the grainstone accumulations are predominantly mudstones and occasional thin, black shales. They are known to be contemporaneous by detailed fusulinid zonation.

In the late Desmoinesian, there is a clear relationship between carbonate facies distribution and the direction and energy level of prevailing winds. The occurrence and distribution of oolitic grainstones with

mudstones, and skeletal grainstones with algal boundstones, suggest a gradient of higher energy to lower energy from northeast to southwest. The transition from grain- to mud-dominated sediments suggests windward to leeward sedimentation. This is coincident with the predicted prevailing northeast winds. Importantly, the true direction and orientation of the carbonate facies trends are only evident after the paleolatitude reconstructions rotate the basin and platform 43° to the northeast. Otherwise, the facies trends would not parallel the predicted prevailing winds. In addition, this demonstrates how knowledge of the past orientation of the basin can be used to determine where the windward edge of the platform is located. Thus, one can predict where grainstone reservoir facies should have formed.

Missourian Sedimentation

During the Missourian, the Midland basin began slowly moving north away from the equator (Figures 7 and 9). During this time the basin was located about 1° to 2°N latitude. Its relative motion from the Desmoinesian through the Missourian was N63°E. During the Missourian, considerable accumulations of oolitic grainstones, algal wackestones, and algal boundstones were deposited on the platform (Schatzinger, 1983, 1988; Walker et al., 1990, 1991; Reid and Reid, 1991). Growth of the carbonate buildups became primarily vertical at this time.

At Cogdell, the oolitic grainstones formed shallow marine shoals and beaches (Reid and Reid, 1991). Paleogeographic maps indicate that they were deposited on the northeastern-facing edges of the platform (Figure 9). Facing the basin or open ocean, bioclastic grainstones were deposited on beaches. They are slightly behind and southwest from the oolites. In a protected and leeward location, algal wackestones and boundstones accumulated. The oolite and bioclastic grainstone shoals extend along the entire eastern edge of Cogdell field in the early Missourian. However, with time, the oolites became more localized. For example, by the middle Missourian, the oolites shoals were restricted to the extreme northeast edge of the field (Figure 9). During this time, a narrow zone of oolites that appears to have been carried southwest by long-shore drift is found on the eastern margin of the field. This suggests that there were northeast to southwest ocean currents that were probably associated with and parallel to the northeast prevailing winds. The winds and ocean currents produced a transition from grainstones to boundstones to mudstones in a northeast to southwest direction at Cogdell.

A similar facies pattern is found at the SACROC field where the depositional environments change in a northeast to southwest direction from oolite shoals, to sponge-algal mounds, to tidal mud flats (Schatzinger, 1983, 1988). It was noted that oolite shoal distribution along the eastern edge of the platform may have been due to the direction of prevailing winds. In general, the volume of oolitic and coated-grain grainstones clearly decreases in roughly a north to south direction

(present orientation) in the Cogdell to SACROC fields. Because the basin was in low latitudes, it was suggested that sedimentation was influenced by ENE prevailing winds.

The highest percentage of oolitic or coated-grain grainstones occurs in Cogdell, and they decrease both in occurrence and percentage southward into SACROC (Figure 10). Using the present orientation of the platform and anticipated prevailing winds, there would be large portions of the SACROC area that would have been in windward locations. Beach and shoal grainstones would be expected along the eastern edges of the SACROC field. Yet, there are no beach or shoal deposits along most of the SACROC area. Based on this occurrence and the previously described carbonate facies distribution, one could conclude that the prevailing winds were generally north to south. Yet, because this area of the basin was located slightly north of the equator, the winds should have been from the northeast (Hills, 1972; Stanley, 1985; Parrish and Peterson, 1988). The distribution of grainstones and the transition from grain- to mud-dominated carbonates as they appear today, in a north to south direction, do not support northeasterly prevailing winds that one would expect in the low latitudes.

However, it is important to distinguish between the depositional setting of the carbonates which is dependent on paleogeography and paleolatitude, among other factors, and their present-day geographic orientation. The importance of this trend of grainstone and carbonate facies becomes clear when the platform is rotated 43° to the northeast from its present orientation as it was during the late Paleozoic (Figures 1–3, 7, 10, and 11). Now, instead of a general north-south alignment as it is today, the facies trends are actually oriented northeast-southwest. This direction clearly parallels the prevailing northeasterly winds (Figures 10 and 11). The contoured percentage of oolitic or coated-grain grainstones also shows a clear variation with respect to wind direction (Figure 10). The greatest amount of these grainstones, exceeding 70% of the Pennsylvanian section, occurs on the northeast-facing or windward edges. They decrease in a clear and predictable fashion until they disappear to the southwest in a leeward direction. It appears that in this case, the northeast windward edges of the platform served as a point source for the formation and accumulation of massive amounts of grainstones during highstands. The present-day distribution of carbonate facies is confusing until the platform is placed in its proper paleolatitude and paleogeography. Only after the platform is rotated northeastward does the distribution of carbonates clearly indicate a northeast-southwest facies trend associated with northeasterly prevailing winds.

Regional Pennsylvanian Sedimentation

In a regional overview, the high-energy oolite facies were located on the northeast and eastern edges of the platform where maximum turbulence was produced by ocean currents associated with the northeasterly prevailing winds (Figure 11). This is clearly demon-

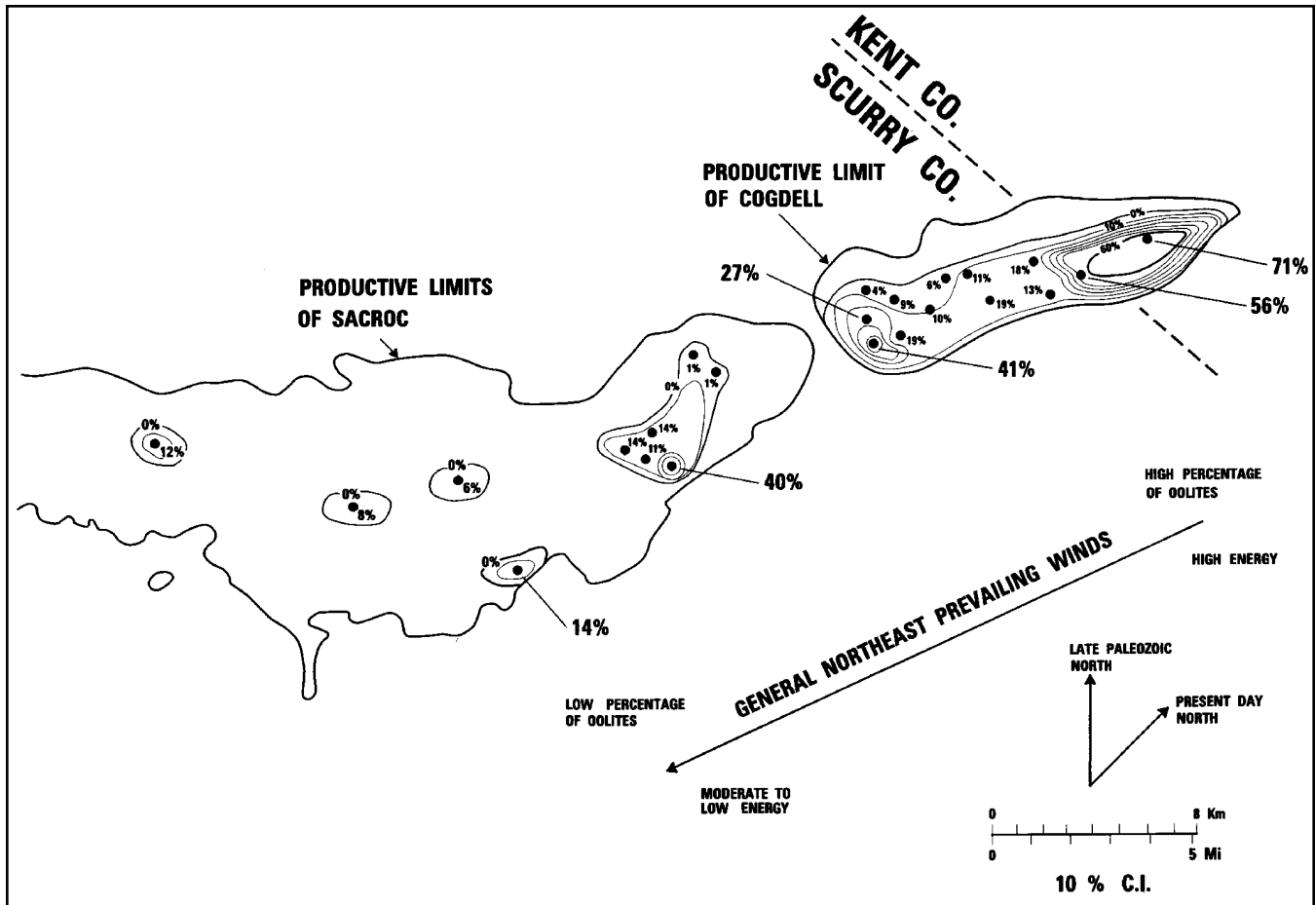


Figure 10. When the percentages of oolitic or coated-grain grainstones (values from Schatzinger, 1983, 1988) were contoured, the highest concentrations were found in windward areas of the platform. Note that the long axis of the grainstone percentages parallels the prevailing wind direction. In addition, the percentages of grainstones are highest in the northeast and decrease to the southwest. The orientation and location of grainstones suggest that the directional energy of the prevailing northeast winds and ocean currents greatly influenced sedimentation.

strated at the Cogdell field (Reid and Reid, 1991). Here, oolitic grainstones formed in highly agitated shallow water. The oolites are clearly windward deposits. As the ocean currents and winds moved to the southwest over the Missourian topographic and bathymetric highs, their energy was dissipated and progressively fewer oolites were formed away from the leading edges of the platform (Figure 11). Southwest of the oolite shoals, sponge-algal mounds grew in an intermediate-energy zone. Here, boundstones formed in areas of intermediate wind and current turbulence. Mudstones developed farther to the southwest where the water was shallowest (perhaps mud flat or subtidal) and the influence of the winds and currents was the least. The sponge-algal boundstones and mudstones are generally interpreted as leeward deposits. The tidal or mud flat environment is best observed in the southwest portions of SACROC and Diamond M fields (Figure 11).

The transition in a northeast to southwest direction from grain- to mud-dominated sediments indicates

wind and current energy was probably very important to their formation. These facies suggest that a high-energy to low-energy gradient associated with the direction of prevailing winds had a strong influence on sedimentation. In the Bahamas, prevailing winds and currents have a similar effect on modern carbonate sedimentation (Wilson, 1975; Wilson and Jordan, 1983). Here, the combined effects of Pleistocene topography and Holocene wind directions are important controls on modern carbonate facies patterns. Lime mud, packstone, and wackestone facies are found west of Andros Island in areas leeward of the prevailing winds. The area west of Andros Island lies in a turbulence shadow. Grain-dominated sediments are found in locations that have high energy associated with tidal currents and prevailing winds.

Knowing the location and distribution of oolitic, algal boundstone, and bioclastic grainstones can be very important. They are often the most prolific reservoirs in the Horseshoe atoll (Schatzinger, 1983, 1988; Walker et al., 1990; Reid and Reid, 1991). The oolitic

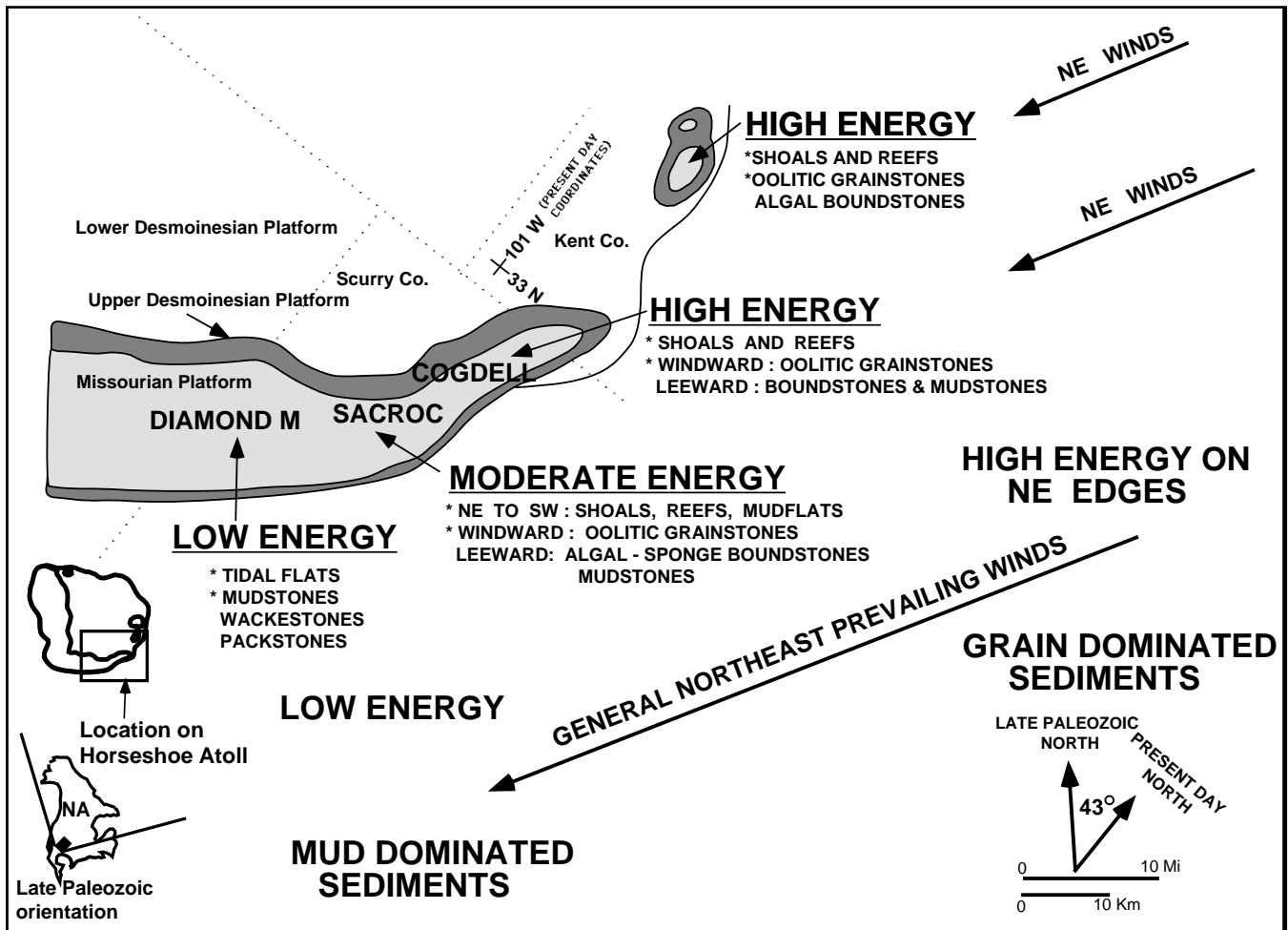


Figure 11. After placing the Midland basin in a late Paleozoic orientation, regional facies patterns appear to relate to prevailing winds and ocean currents. A generalized facies distribution map along the eastern edge of the Horseshoe atoll indicates that the northeast prevailing wind played an important role in sedimentation. Grainstones are associated with high wind and wave energy, while the algal-sponge boundstones, wackestones, and mudstones are indicative of moderate to low wind-wave energy. Generally, grain-dominated sediments are found in windward areas while mud-dominated sediments are located in leeward locations.

grainstones are often found at the top of individual shoaling-upward cycles. Typically they exhibit extensively developed oomoldic porosity which ranges from 20 to 30%. Also, they typically have good permeabilities (Schatzinger, 1988; Vanderhill et al., 1990). Porosity development probably occurred during the multiple exposures associated with glacial-eustatic regressions (Walker et al., 1990). Equant calcite cements and oomoldic porosity indicate that oolitic grainstones underwent diagenesis in the freshwater phreatic environment. These cements would be expected when the oolite shoals were exposed and significant freshwater lenses developed in the sediments (Wanless and Dravis, 1989). These conditions were probably the result of the Midland basin being in a humid tropic belt throughout the Pennsylvanian.

It becomes clear that late Paleozoic paleolatitude and paleogeography greatly influenced sedimentation on the Horseshoe atoll by controlling the interaction of

platform and shelf edges with prevailing winds and ocean currents. The previously discussed windward and leeward variations in carbonate facies distribution represent sea level highstand deposition. During sea level lowstands, the platform carbonates were exposed to erosion and underwent mechanical and chemical weathering. Drilling to the east of the platform edge has identified carbonate debris flows along the eastern edge of the atoll. Slumps or debris fans have been reported along the eastern or windward edges of SACROC (Schatzinger, 1983, 1988). They have also been observed along the eastern and northeastern edges of Cogdell (Reid and Reid, 1991). Here, carbonates slumped into the Midland basin through channels eroded into the platform edge during the sea level lowstands. These debris flows formed fans that were relatively close to their source and can be traced back to individual channels. Drilling to the west of the platform edge and associated carbonate buildups has

not encountered any major debris fans. The minor debris fans west of the platform edge are isolated and confined to local channels.

The occurrence of debris flows along the eastern edge of the platform is probably due to greater erosion in this area. Here, ocean waves were driven into exposed cliffs of carbonates by the prevailing northeasterly winds. During the middle Missourian, marine terraces formed along the eastern edge of the carbonate buildups at Cogdell. The location of erosional terraces or cliff faces along the edge of the Horseshoe atoll appears to be isolated to the eastern and north-eastern windward edges. This is to be expected, as these areas would have the maximum wind and wave energy associated with prevailing winds when the platform was partially exposed during sea level lowstands. The waves eroded the platform carbonates, producing sediment that was funneled through channels into the basin east of the platform. The western edges of the buildups, being in the lee of prevailing winds, lacked sufficient energy to produce substantial erosion which would have led to the development of the debris flows. Marine terraces have not been identified along the western edges of the carbonate buildups which ring the platform. Little evidence exists for either erosional features or major debris flows in the leeward portions of the Horseshoe atoll.

In addition, the prevailing winds may have influenced the nature of karst formation and associated erosional features during sea level lowstands (Tomlinson-Reid, 1979; Mozynski and Reid, 1992a, b; Mozynski et al., 1993). Paleolatitude reconstructions place the Midland basin in what would have been the humid tropics. The occurrence of karst features supports this interpretation. In addition, minor coals were accumulating on the Eastern shelf, providing further evidence of a humid tropical environment. The Horseshoe atoll was a large positive feature and was subaerially exposed during lowstand deposition. Its topographic relief could have influenced the effects of the prevailing winds. During the Pennsylvanian, shallow-water lowstand carbonates were deposited seaward of the Horseshoe atoll.

The morphologies of tower karst terranes were influenced by prevailing northeasterly winds and their geographic position relative to the emergent Horseshoe atoll. In the lee of the atoll, subaerial exposure produced generally symmetrical tower karst terranes. These features are analogous to those in Phang Na Bay, Thailand; Ipoh, Malaysia; or those in southern China. These karst towers have near-vertical sides with steep slopes in all directions. The Perriwinkle fields in Martin County, Texas, southwest of the atoll (Figure 6), are reservoirs that are found in such a symmetrical tower karst. In windward areas in front of the atoll margin, karst towers are similar to the mogotes of Puerto Rico. They have relatively gentle slopes on the windward side (northeast-east) and steep to near-vertical slopes on the lee side (southwest-west) of the feature. The B. C. Canyon field located in Howard County, Texas, south-southeast from the atoll (Figure 6), is found in an asymmetrical tower karst.

PERMIAN PALEOGEOGRAPHY

During the Permian, North America continued to drift northward. By the Wolfcampian, the Midland and Delaware basins were located around 6° to 8°N latitude (Figure 7). From early Desmoinesian (312 Ma) to the Missourian (306 Ma), the relative motion of west Texas was N63°E. Later, beginning in the Virgilian (298 Ma) and continuing into the Wolfcampian (280 Ma), the direction of movement changed to N24°E. This represents a major tectonic event associated with the collision and suturing of North America with the supercontinent Pangea. As during the Pennsylvanian, the North American (Laurentia) plate was oriented so that west Texas was oriented 43° to the northeast relative to current coordinates.

As a consequence of its being in the low latitudes, west Texas remained in a tropical environment. As a result, broad carbonate shelves developed on the western, northern, and eastern margins of the Delaware and Midland basins. In addition to these fringing carbonate environments, carbonates began to accumulate over portions of the Central Basin platform. During the Permian, extensive reef, grainstone shoals, and complex carbonate facies developed in a high-energy environment along the shelf margins (Figure 12). Grain-dominated sediments and reefal buildups accumulated along shelf and platform edges, restricting the circulation of marine waters into the platform interior (Horak, 1985; Bebout et al., 1987). This restriction of normal marine circulation resulted in low-energy carbonate sediments and evaporites being deposited in the platform interiors.

Wolfcampian Sedimentation

As during the Pennsylvanian, there are Permian examples where the prevailing winds, ocean currents, and platform orientation influenced carbonate sedimentation. At the Nolley Wolfcamp field located in Gaines and Andrews counties, Texas, the distribution of carbonate facies suggests that these factors played a major role in the distribution of grain-dominated sediments which make up the reservoir. These sediments were deposited during the Early Permian along the eastern edge of the Central Basin platform.

The best reservoir facies are found in bioclastic-skeletal and oolitic grainstones that were deposited in a shallow-water environment (Mesoloras, 1989). These grainstones formed in both shoal and sheet-like geometry. Vertically, the carbonate sediments formed a series of shallowing-upward cycles. The base of the cycles begins with shales and wackestones. The tops of these cycles are capped by exposure zones developed in the grainstones. The extensive leaching of the grainstones and freshwater phreatic cements suggests subaerial exposure of the carbonate rocks. The change in facies within a shoaling-upward cycle and the repetition of numerous shoaling cycles suggest that the sedimentation was a response to eustatic sea level changes (Mesoloras, 1989). During the early Permian, the Central Basin

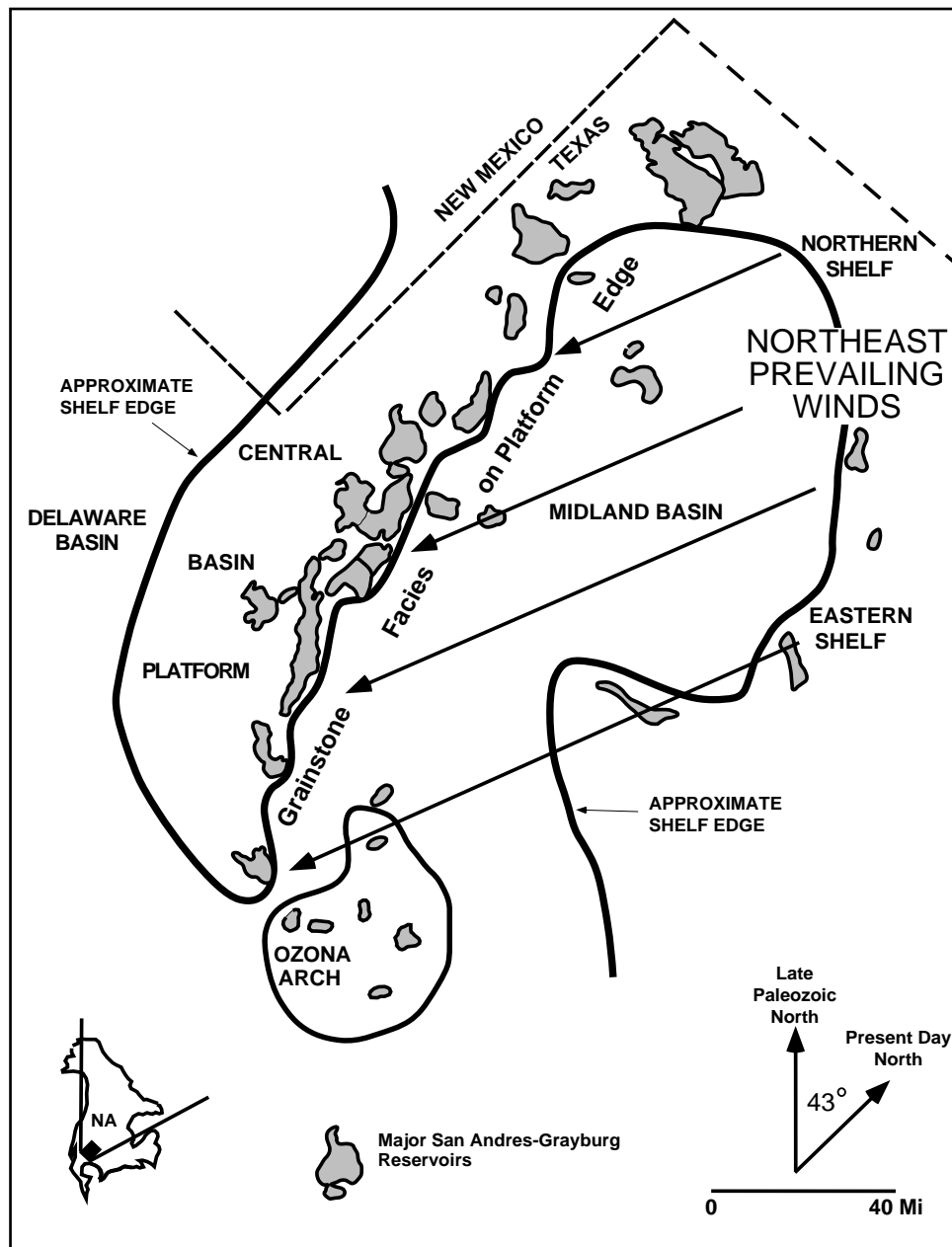


Figure 12. A generalized Upper Permian paleogeographic map indicates that the eastern portions of the Central Basin platform were in a windward location relative to regional winds. Tropical northeasterly winds and ocean currents produced a marginal high-energy zone along eastern-facing edges of the platform. Extensive grainstones were deposited in this windward environment. The more significant Guadalupian reservoirs are identified. Major San Andres-Grayburg reservoirs adapted from Bebout et al. (1987) and Galloway et al. (1983).

platform was undergoing gradual subsidence and only occasional tectonic uplift. The uplifts are not repetitive enough to account for the observed cycles, or did not occur rapidly enough to have individual cycles directly attributed to them. However, the regional tectonic events could have combined with global eustatics influencing sea levels.

Facies maps show that the thickest accumulations of grainstones are oblong in shape and are presently

oriented slightly east of a general north-south axis (Mesoloras, 1989). The approximate orientation of this axis would be 5–10°. The entire area must be rotated 43° for the relationship between sedimentation and wind-ocean current directions to become evident. After the 43° rotation is performed, the area is in its late Paleozoic setting. Now, rather than an apparent north-south orientation there is a northeast-southwest pattern to the distribution of grainstones. This is paral-

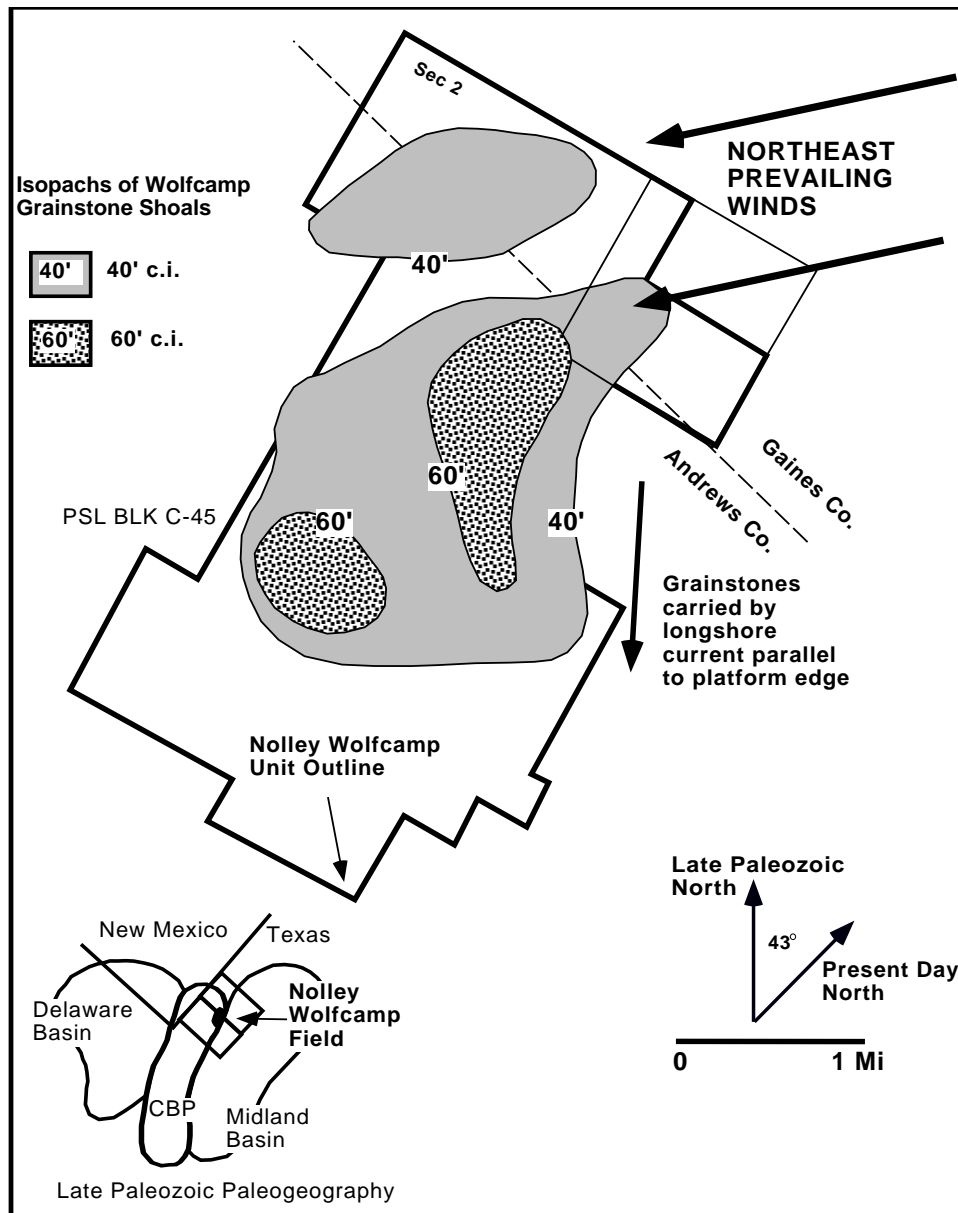


Figure 13. Oolitic and bioclastic grainstones at the Nolley Wolfcamp field demonstrate the influence of northeast prevailing winds. Isopach maps (upper zone) show the long axes of the thickest accumulations of grainstones are aligned with the prevailing winds. Some lenses of grainstones suggest that longshore currents redistributed grainstones to the south along the Wolfcampian shoreline. Carbonate facies adapted from Mesoloras (1989).

labeled to the predicted prevailing winds (Figure 13). Clearly the northeast-southwest accumulations of grainstones are directly related to their depositional setting. The grainstone shoal on the northern edge of the field best exhibits the northeast-southwest direction. In the southern shoal, longshore drift appears to have redistributed some grainstones southward.

When examining the facies in a northwest to southwest orientation, the direction and influence of wind and wave energy become clear. The grainstones accumulated in a high-energy shoal environment that was

marginal to the Central Basin platform. Northeasterly prevailing winds struck the platform edge along its eastern margin, and, where the paleobathymetry was shallow, grainstone shoals began to develop. Phylloid algal mounds developed in slightly deeper water in front of these shoals (Mesoloras, 1989). The grainstones clearly represent windward or high-energy deposits. Continuing to the southwest one finds lower-energy mud-dominated wackestones and packstones. These accumulated in a restricted marine environment that developed in a leeward position behind

the northeasterly grainstone shoals. A clear directional variation in sediment facies is evident at the Nolley Wolfcamp field. High-energy grainstones are found to the northeast along the windward-edge platform margin. These grainstones are replaced by low- to moderate-energy mudstones, wackestones, and packstones to the southwest nearer to the platform.

Guadalupian Sedimentation

During the Guadalupian, the eastern edge of the Central Basin platform became the site of extensive and complex carbonate sedimentation (Figures 14 and 15). Important oil production comes from these carbonate cycles. San Andres and Grayburg reservoirs (Figure 12) have produced over 10 billion barrels, which amounts to 42% of the oil recovered from west Texas (Bebout et al., 1987).

In the Permian basin, the San Andres and Grayburg formations represent repetitive shallowing-upward cycles. The carbonate facies in the cycles indicate that sedimentation progressed from subtidal to supratidal and a west-to-east tidal flat progradation (Lucia et al., 1990; Tyler et al., 1991; Bebout et al., 1987). Todd (1976)

suggested that oolitic grainstones in the San Andres Formation were deposited on topographic highs as a result of prevailing winds. The oolitic facies were compared to similar deposits in the Bahamas and the Persian Gulf. The grainstones were identified as forming a shallow-water facies consisting of long, linear bars or shoals.

On the eastern margin of the Central Basin platform, the San Andres and Grayburg formations in the Dune field demonstrate a transitional relationship between open-marine and tidal-flat depositional facies. In the basin east of the platform, pelletal grainstones and packstones accumulated in an open-marine environment. Fusulinid wackestones formed in bioherms that developed in the relatively shallow water. Landward, or to the west, oolitic and bioclastic grainstones formed as fringing bars or beaches. Further to the west, low-relief islands and tidal flats consisting of pisolites, laminated mudstones, and algal-laminated mudstones developed behind the fringing grainstones. Repetitive desiccation features indicate that this environment was subjected to cyclic and extensive subaerial exposure and diagenesis. When the platform was flooded, shallow-water banks developed in a low-energy environment. These banks consisted of carbon-

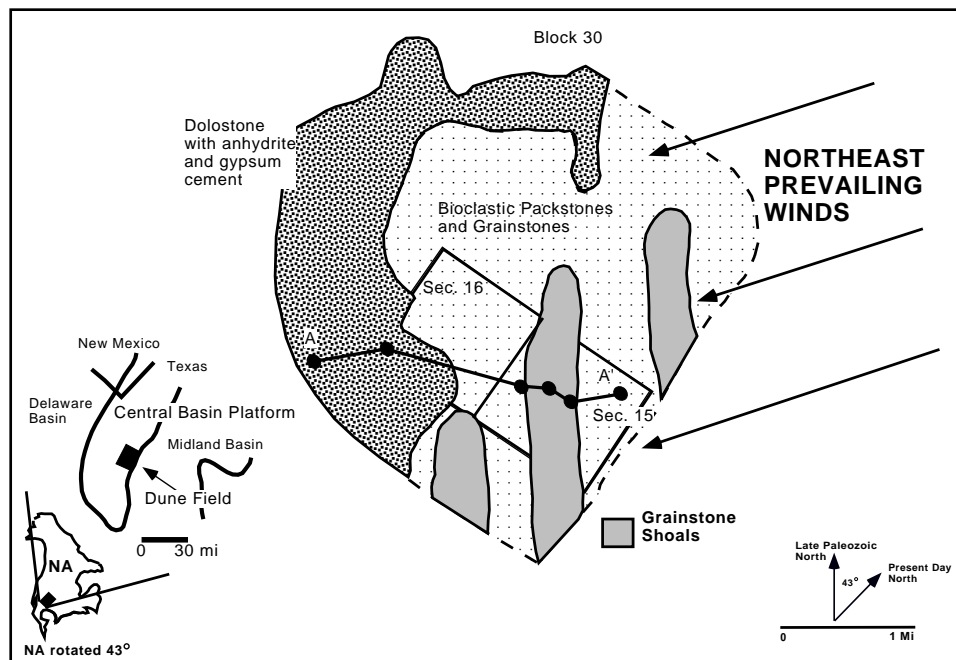


Figure 14. At the Dune field, grainstones accumulated along the eastern margin of the Central Basin platform (Bebout et al., 1987; Lucia et al., 1990). Facies maps of the Grayburg Formation (Guadalupian Series) at the Dune field suggest that prevailing winds and currents interacted with platform orientation and water depth to influence carbonate sedimentation. Concentrations of grainstones are found in linear zones that are oriented roughly parallel to the platform edge. Grainstones were most likely deposited in a shoal or beach environment and represent windward deposits. Leeward, or to the west, of the grainstone shoals there are wackestones, mudstones, and anhydrite deposited as mixed lagoon, tidal-flat, and supratidal facies. Carbonate facies of the Grayburg Formation adapted from Lucia et al. (1990).

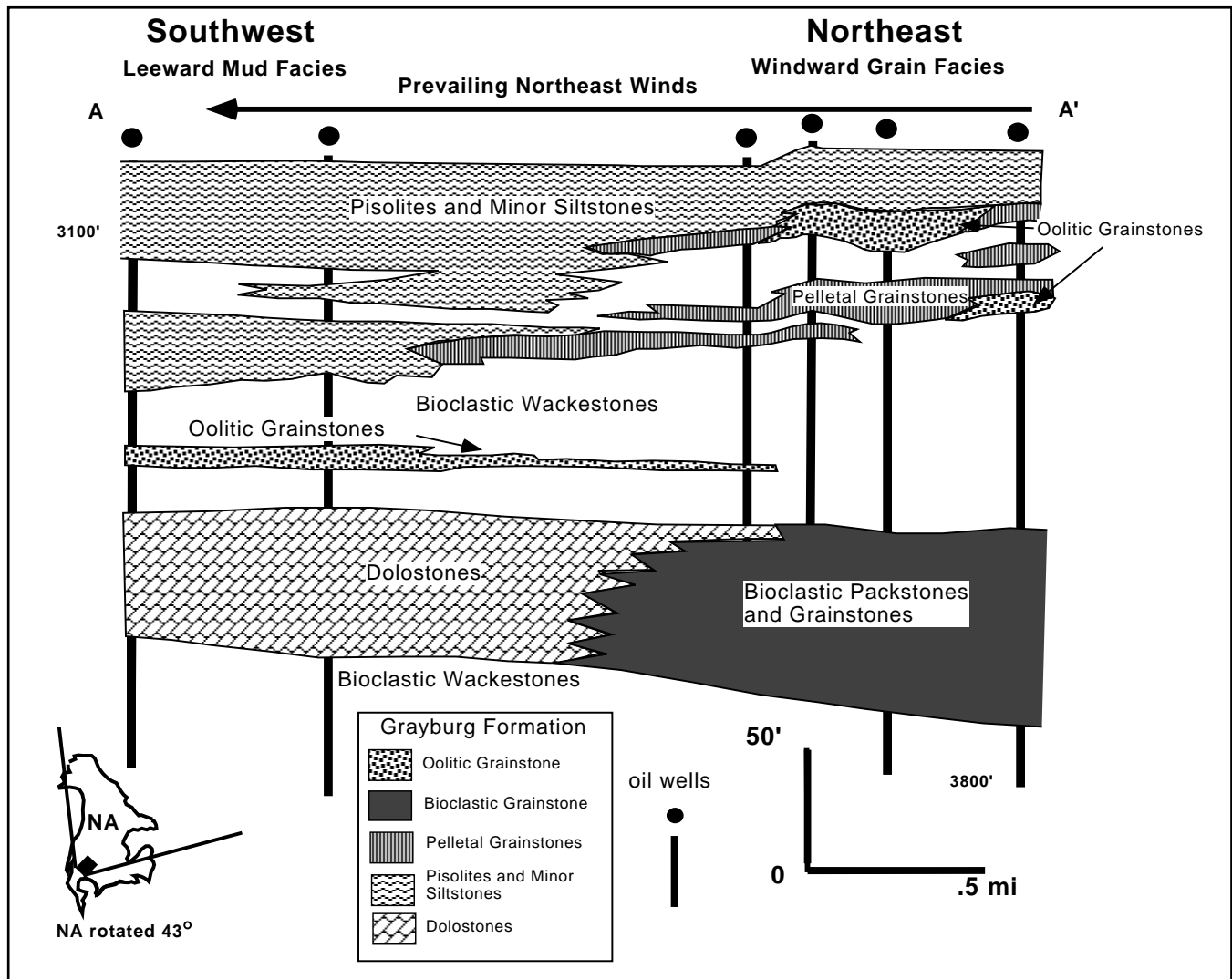


Figure 15. A cross section through the Dune field shows the relationship between carbonate facies (zone MA, Grayburg Formation, Guadalupian Series). It indicates that the prevailing winds produced a high-energy zone that consisted of grain-dominated sediments on the eastern margin of the platform. To the west, mud-dominated sediments accumulated in a leeward zone of low wind and wave energy. Well locations are identified in Figure 14. Carbonate facies adapted from Bebout et al. (1987) and Lucia et al. (1990).

ate mudstones with algal and sponge material. These sediments are now dolostone with anhydrite and gypsum cement (Bebout et al., 1987; Lucia et al., 1990; Tyler et al., 1991).

From paleotectonic reconstructions, it is clear that during the Permian both the Midland and Delaware basins were north of the equator. This would have placed them in a belt of northeasterly prevailing winds similar to those interpreted during the Pennsylvanian. The large amounts of evaporites associated with the Permian suggest that west Texas was most likely in an arid tropical environment during this time. This contrasts to the humid tropical conditions found in the Pennsylvanian.

Dune field and the Central Basin platform were rotated 43° to the northeast to determine if the carbonate sedimentation was influenced by prevailing winds

and paleogeography (Figures 14 and 15). At Dune field and on other eastern-facing edges of the Central Basin platform grainstones accumulated along the platform margin (Bebout et al., 1987; Lucia et al., 1990). After the rotation is performed, facies maps of the Grayburg Formation at Dune field suggest that prevailing winds interacted with platform orientation and water depth to influence carbonate sedimentation.

The grainstones are clearly windward deposits that run roughly parallel to the edge of the platform (Figure 14). The wind directions identified from this study support the facies interpretation of Todd (1976). After the regional rotation is performed, it appears that the prevailing winds and ocean currents would have struck the Central Basin platform at a slightly oblique angle. These prevailing winds and currents produced a moderate- or high-energy depositional zone along the east-

ern platform margin. Grainstones were deposited in this windward and marginal belt of high-energy conditions. The grainstones accumulated in the shallow waters which fringed the edge of the platform. This would have been the location of maximum wave energy produced by the ocean currents associated with the prevailing winds. In this location, the fine-grained sediments and mud would have been winnowed away leaving grainstones that formed the shoals and beaches shown in the facies maps. The grainstone shoals are very narrow and localized. This suggests that most of the energy associated with the prevailing winds was quickly dissipated on the leading edge of the platform. In addition, the oblique angle at which the winds passed over the platform would have probably produced a southwestern to southern longshore current. This could have distributed grainstones in the linear fashion observed in the facies maps.

Leeward or to the west of the grainstone shoals, there are wackestones, mudstones, and anhydrite deposited as mixed lagoon, tidal-flat, and supratidal facies. Algal-laminated mudstones were deposited in restricted ponds on the tidal flat. The sediments clearly represent low-energy deposition. The grainstone shoals and beaches would have protected the algae and sponges growing in the shallow waters. Occasionally these sediments were subaerially exposed. An arid environment is evidenced by caliche, pisolites, evaporites, and desiccation structures.

Cross sections through Dune field show an interesting geometry and relationship between the windward grainstones and leeward mudstones and wackestones (Figure 15). Once paleowind direction is accounted for, it is clear that the grain-dominated sediments thin and eventually pinch out to the west. The thickest accumulations of grainstones clearly exist on the windward edge of the platform. Contemporaneous tidal-flat sediments interfinger with the grainstones. The cross section indicates the prevailing winds produced a high-energy zone that consisted of grain-dominated sediments on the eastern margin of the platform. To the west of this windward area, mud-dominated sediments accumulated in a leeward zone of low wind and wave energy.

Paleozoic Source Rocks

A burial-history analysis of the Midland basin by Horak (1985) found that oil generation from Paleozoic rocks in the Midland basin probably occurred most rapidly during the Triassic through the Jurassic. This was determined from a detailed examination of the timing, depth, stratigraphic sources, and the generation of hydrocarbons in the basin. The most likely source rocks in the basin include Simpson shales (Ordovician), Woodford shales (Devonian), Pennsylvanian shales, and Lower Permian shales. Horak (1985) determined that oil generation initiated in the Simpson during the Late Triassic and in the Woodford during the Middle Jurassic. This analysis indicated that the generation of oil continues to the present. There is a likely middle Cretaceous timing for the gen-

eration of oil from Pennsylvanian and Permian sediments. Sediments younger than Wolfcampian are considered to be thermally immature. The amount of gas in the Midland basin is small when compared to the large volumes of oil found in late Paleozoic reservoirs. Horak (1985) indicated that the potential source rocks did not have the necessary thermal maturity to produce large volumes of gas.

Ramondetta (1982), in a study of the Northern shelf of the Midland basin, concluded that the oil in the San Andres Limestone (Guadalupian) and Clear Fork Group (Leonardian) did not form in situ. This was based on kerogen type, thermal alteration index, and vitrinite reflectance values. Ramondetta (1982) identified the Wolfcampian shales in the Midland basin as the most likely source for San Andres oil. The maturation analysis of Horak (1985) supports this conclusion by indicating that in the northern Midland basin and Northern shelf the Pennsylvanian and Permian (Wolfcamp) shales were thermally mature. Horak (1985) felt that the giant oil reserves of the Guadalupian reservoirs came from older Permian units.

Galloway et al. (1983) indicated that the source for the giant oil accumulations in the Horseshoe atoll to have been adjacent Pennsylvanian and Permian (Wolfcampian) shales and shaly limestones. They are organic-rich deposits initially formed in the sediment-starved areas of the basin. As the basin filled, Wolfcampian shales and shelf sediments prograded from the east, encasing the reservoir limestones in these probable source rocks. In addition, considerable thicknesses of these probable source rocks immediately surround the platform from nearby depocenters of the Midland basin.

CONCLUSIONS

Reconstructing the paleolatitude and paleogeography of a basin through time can assist in predicting the regional distribution of facies. This technique can apply information concerning prevailing winds, ocean currents, climate, and the orientation of carbonate platforms. These factors can have a major impact on the type and location of carbonate sediments. The past orientation of the carbonate shelf must be determined and combined with the direction of prevailing winds to better understand the distribution of facies. Together, platform and shelf orientation and prevailing winds strongly influenced the distribution of carbonate grain types. This in turn can control the distribution of facies that form potential oil and gas reservoirs.

Throughout the late Paleozoic, west Texas was very near the equator. This placed the Midland and Delaware basins in humid and arid tropical climates that contributed to the development of large carbonate shelves and platforms. During the Late Pennsylvanian, the relative motion of west Texas was N63°E. At the end of the Pennsylvanian, this changed dramatically so that by the Permian the basins were moving N24°E. This dramatic change reflects the suturing of North America to Gondwana, forming the superconti-

ment Pangea during the Hercynian orogeny. During this time, North America was rotated some 43° to the northeast from its current orientation.

Estimating the regional prevailing winds and probable ocean currents from paleolatitude reconstructions does not adequately explain observed carbonate facies. At best, it provides a partial answer. The reconstructions indicate that west Texas was slightly north of the equator, from which northeasterly or easterly prevailing winds would be expected. However, the present-day distributions of carbonate facies do not support that conclusion. They appear to support a much more northerly wind direction than one would expect for the low latitudes, as predicted from paleolatitude reconstructions. For example, the present-day orientation of carbonate facies in the Cogdell and Nolley Wolfcamp fields suggests more northerly than easterly prevailing winds. In the SACROC area, northeastern winds should have produced a beach or shoal environment along most of the present-day eastern edge of the platform. Yet, there is no high-energy sedimentation along the majority of the eastern edge of the field.

By combining the regional rotation with expected winds and ocean currents, the actual relationship between carbonate sedimentation and prevailing winds becomes much clearer. After which, the observed facies and their lateral changes parallel the expected northeasterly or easterly prevailing winds. After the rotation, the distribution of facies in Cogdell and Nolley Wolfcamp fields supports the prediction of northeast prevailing winds. Likewise, it explains that, except for the northeast edge of the SACROC area, the platform was in a leeward location. This explains why the grainstones are absent along what might previously be thought to be the windward side. After rotation, the grainstones found in the northeast portion of SACROC can be explained as windward deposits.

After the regional rotation is combined with the expected prevailing winds and currents, numerous conclusions can be drawn. During the Desmoinesian through the Virgilian, carbonate facies in the Midland basin demonstrate the influence of paleolatitude and paleogeography. On northeastward-facing edges of carbonate platforms, a directional variation is observed in the carbonate facies. The actual orientation of this variation becomes clearer after the Midland basin is rotated from its present setting 43° northeast, as it was in the late Paleozoic. Carbonate facies on these platforms indicate an environmental transition from high energy in the northeast to low energy in the southwest. This reflects the directional energy of the northeast prevailing winds and associated ocean currents as they struck the platform. Along the northeastern edges of platforms in a northeast to southwest direction, the general facies are oolitic grainstones, algal-sponge boundstones, and tidal-flat mudstones. The percentages of grainstones are highest in the northeast and decrease to the southwest where there are predominantly mud-dominated carbonate facies. During sea level lowstands, the northeast edges of the platform were subject to erosion. The location of erosional terraces also supports northeast prevailing winds. After regional rotation, the terraces are

observed to have formed in the windward locations. They are not found in leeward areas. Debris transported from these areas is found directly adjacent to the erosional terraces.

Carbonates deposited during the Wolfcampian and Guadalupian suggest that sedimentation during the Permian was also influenced by basin orientation and prevailing northeasterly winds. These prevailing winds and associated ocean currents produced a high-energy depositional zone along the eastern margin of the Central Basin platform. The grainstones were deposited in shallow waters in this windward, marginal belt of high-energy conditions. Isopach thicks of oolitic grainstones deposited during the Wolfcampian are aligned with prevailing northeasterly winds. During the Guadalupian, extensive oolitic and bioclastic grainstones were deposited along the windward margin of the Central Basin platform. To the west in a leeward direction, wackestones, algal mudstones, and anhydrite were deposited as mixed lagoon and supratidal facies. Northeast prevailing winds and currents probably struck the Central Basin platform at an oblique angle during the Permian, creating southwest-erly longshore currents.

Paleolatitude and paleogeography mapping are very useful in explaining regional facies patterns. Combining the orientation of tectonic features, ancient latitude, and prevailing winds, one can demonstrate how previously poorly understood factors can greatly influence sedimentation patterns. Once these factors are identified on ancient carbonate platforms, modern carbonate models are directly applicable to field development and regional exploration. From this, one can explain why certain facies are found in various locations about the basin. Further, it can lead to predictions of where good reservoir facies are yet to be found.

ACKNOWLEDGMENTS

W. J. Purves, L. E. Waite, and M. A. Mosely are thanked for discussing applications of paleogeographic and paleolatitude reconstructions. K. Potter provided geological technician support and assisted in mapping and computer operations. S. Brown, R. Barnhart, and J. B. Potter drafted the many maps and figures.

REFERENCES CITED

- Algeo, T. J., 1992, Continent-scale wrenching of southwestern Laurussia during the Ouachita Marathon Orogeny and tectonic escape of the Llano Block, *in* Robert F. Lindsay and C. L. Reed, eds., *Sequence Stratigraphy Applied to Permian Basin Reservoirs: Outcrop Analogs in the Caballo and Sacramento Mountains of New Mexico*, Field Seminar Guidebook: West Texas Geological Society Pub. No. 92-92, p. 115-131.
- Bambach, R. K., C. R. Scotese, and A. M. Ziegler, 1980, Before Pangea: the geographies of the Paleozoic World: *American Scientist*, v. 68, p. 26-38.
- Bebout, D. G., F. Jerry Lucia, and G. E. Fogg, 1987, Geological characterization, *in* Bebout, D. G., F. Jerry

- Lucia, G. E. Fogg, and G. W. Stoep, 1987, Characterization of the Grayburg Reservoir, University Lands, Dune Field, Crane County, Texas: Report of Investigation No. 168, Bureau of Economic Geology, The University of Texas at Austin, Austin, Texas, p. 10–78.
- Bloomer, R. R., E. R. Harrison, E. S. Hughes, and D. G. Morris, 1991, Cyclic deposition of Pennsylvanian and Permian sediments on the Eastern shelf, Texas: Abilene Geological Society Fieldtrip Guidebook, Southwest Section AAPG Convention, 30 p.
- Boardman, II, D. R., and J. M. Malinky, 1985, Glacial-eustatic control of Virgilian cyclothems in north central Texas: Southwest Section AAPG Transactions, p. 13–22.
- Boardman, II, D. R., and P. H. Heckel, 1989, Glacial-eustatic sea-level curve for early Late Pennsylvanian sequence in north-central Texas and biostratigraphic correlation with curve for midcontinent North America: *Geology*, v. 17, p. 802–805.
- Borer, J. M., and P. M. Harris, 1991, Lithofacies and cyclicity of the Yates Formation, Permian basin: implications for reservoir heterogeneity: *AAPG Bulletin*, v. 75, no. 4, p. 726–779.
- Brown, L. F., Jr., 1969, Virgil-lower Wolfcamp repetitive depositional environments in north-central Texas, in J. G. Elam and S. Chuber, eds., *Cyclic Sedimentation in the Permian Basin*: West Texas Geological Society, p. 115–134.
- Brown, L. F., Jr., A. W. Cleaves, and A. W. Erxleben, 1973, Pennsylvanian depositional systems in north-central Texas: Texas Bureau of Economic Geology Guidebook 14, 122 p.
- Burnside, R. J., 1959, Geology of part of the Horseshoe atoll in Borden and Howard Counties, Texas: U. S. Geological Survey Professional Paper 315-B, 34 p.
- Crawford, G. A., G. E. Moore, and W. Simpson, 1988, Depositional and diagenetic controls on reservoir development in Pennsylvanian phylloid algal complex: Reinecke field, Horseshoe atoll, west Texas: *Transactions Southwest Section AAPG*, p. 81–90.
- Crowell, J. C., 1978, Gondwana glaciation, cyclothems, continental positioning and climate change: *American Journal of Science*, v. 278, p. 1345–1372.
- Du Toit, A. L., 1937, *Our wandering continents*: Edinburgh, Oliver and Boyd, 336 p.
- Galley, J. E., 1958, Oil and geology in the Permian basin of Texas and New Mexico, in L. G. Weeks ed., *Habitat of Oil—a Symposium*: AAPG, p. 395–446.
- Galloway, W.E., T.E. Ewing, C.M. Garrett, N. Tyler, and D.G. Bebout, 1983, Oil and gas fields of Texas: Bureau of Economic Geology, Austin, Texas, 139 p.
- Golonka, J., 1991, Exploration application of paleogeographic reconstruction and paleoclimatic modeling maps: *AAPG Bulletin*, v. 75, no. 3, p. 583.
- Hamilton, W., and D. Krinsley, 1967, Upper Paleozoic glacial deposits of South Africa and southern Australia: *Geological Society of America Bulletin*, v. 78, p. 795.
- Heckel, P. H., 1980, Paleogeography of eustatic model for eustatic marine transgressive-regressive depositional cycles along Midcontinent outcrop belt North America: *Geology*, v. 14, p. 330–334.
- Heckel, P. H., 1986, Sea-level curve for Pennsylvanian deposition of Mid-Continent Pennsylvanian cyclothems, in T. D. Fouch and E. R. Magathan, eds., *Paleogeography of west-central United States: Rocky Mt. Section SEPM, West-Central U.S. Paleogeography Symposium 1*, p. 197–215.
- Hills, J. M., 1972, Late Paleozoic sedimentation in west Texas Permian basin: *AAPG Bulletin*, v. 56, no. 12, p. 2303–2322.
- Horak, R. L., 1985, Tectonic and hydrocarbon maturation history in the Permian basin: *Oil and Gas Journal*, v. 83, p. 124–129.
- Irving, E., 1979, Paleopoles and paleolatitudes of North America and speculations about displaced terrains: *Canadian Journal of Earth Science*, v. 16, p. 669–694.
- James, N. P., and I. G. Macintyre, 1985, Carbonate depositional environments modern and ancient. Part 1: Reefs zonation, depositional facies, diagenesis: *Colorado School of Mines Quarterly*, v. 80, no. 3, 70 p.
- Khoppen, W. P., and A. L. Wegener, 1924, *Die klimater der Geologischen Vorzeit*: Berlin, Gebrüder Borntraeger, 255 p.
- Lottes, A. L., and D.B. Rowley, 1990, Early and Late Permian reconstruction of Pangea, in C.R. Scotese and W.S. McKerrow, eds., *Paleozoic Paleogeography and Biogeography: The Geological Society of London Memoir 12*, p. 383–395.
- Lucia, F. Jerry, D. G. Bebout, and C. R. Hocott, 1990, Reservoir characterization through integration of geological and engineering methods and techniques: Dune (Grayburg) field, University Lands, Crane County, Texas, in D. G. Bebout and P. M. Harris, eds., *Geologic and Engineering Approaches in Evaluation of San Andres/Grayburg Hydrocarbon Reservoirs—Permian Basin*: Bureau of Economic Geology, University of Texas at Austin, Austin, Texas, p. 197–238.
- Malinky, J.M., D.R. Boardman, II, and T.E. Yancey, 1984, Recognition of offshore “core” shale deposition in cyclothems of Texas and northern Midcontinents: *Geol. Soc. Amer., South-Central Section Abstracts Prog.*, v. 15, p. 5.
- Matthews, R. K., 1984, *Dynamic stratigraphy*, 2nd Edition: Englewood Cliffs, N.J., Prentice-Hall, p. 373–464.
- Matthews, R. K., 1987, Eustatic controls on near-surface carbonate diagenesis, in R. B. Halley and R. K. Matthews, eds., *Carbonate Depositional Environments, Modern and Ancient, Part 6: Diagenesis 2*: Colorado School of Mines Quarterly, v. 82, no. 1 (March), p. 17–40.
- Mear, C. E., 1983, Midland basin, in A. Lindberg, ed., J. M. Hills and F. E. Kottowski, Coordinators, *AAPG Correlation of Stratigraphic Units of North America, Southwest/Southwest Mid-continent Correlation Chart*.
- Mesoloras, N., 1989, The Nolley Wolfcamp unit, Andrews and Gaines Counties, Texas—a classic shallowing-upward sequence: *Transactions Southwest Section AAPG Convention, San Angelo, Texas*, p. 67–73.

- Mozynski, D. C., A. Reid, and D. A. Walker, 1993, The effect of paleogeography on erosion of Pennsylvanian lowstand carbonates in the northern Midland basin, with modern analogies, a new view of an old trend: *AAPG Bulletin*, v. 77, no. 1, p. 141.
- Mozynski, D. C., and A. Reid, 1992a, B. C. Canyon field, Howard County, Texas: an ancient analog to modern tropical tower karst terrain: *AAPG Bulletin*, v. 76, p. 580.
- Mozynski, D. C., and A. Reid, 1992b, Perriwinkle and Perriwinkle North fields, Martin County, Texas: a Cisco-Canyon lowstand reef complex: *AAPG Bulletin*, v. 76, no. 4, p. 580–581.
- Myers, D. A., P. T. Stafford, and R. Burnside, 1956, *Geology of the late Paleozoic Horseshoe atoll in west Texas*: University of Texas Publication No. 5607, Bureau of Economic Geology, University of Texas, Austin, Texas, 113 p.
- Parrish, J. T., and F. Peterson, 1988, Wind directions predicted from global circulation models and wind directions determined from eolian sandstones of the western United States—a comparison, *in* G. Kocurek, ed., *Late Paleozoic and Mesozoic Eolian Deposits of the Western Interior of the United States: Sedimentary Geology*, v. 56, p. 261–282.
- Peterson, F., 1988, Pennsylvanian to Jurassic eolian transportation systems in the western United States, *in* G. Kocurek, ed., *Late Paleozoic and Mesozoic Eolian Deposits of the Western Interior of the United States: Sedimentary Geology*, v. 56, p. 207–260.
- Peterson, J. A., 1991, Aneth oil field, giant carbonate stratigraphic trap, Paradox basin, Utah, U.S.A.: *AAPG Bulletin*, v. 75, no. 3, p. 653.
- Ramondetta, P. J., 1982, Genesis and emplacement of oil in the San Andres Formation, Northern shelf of the Midland basin: Report of Investigation, No. 112, Bureau of Economic Geology, Univ. of Texas, 39 p.
- Reid, A. M., and S. J. Mazzullo, 1988, Paint Rock and Paint Rock Southwest fields, Concho County, Texas: Strawn analogues of modern shelf island systems: *West Texas Geological Society Bulletin*, v. 27, no. 8, p. 5–10.
- Reid, A. M., S. T. Reid, S. J. Mazzullo, and S. T. Robbins, 1988, Revised fusulinid biostratigraphic zonation and depositional sequence correlation, subsurface Permian basin: Southwest Section Meeting Abstracts, *AAPG Bulletin*, v. 72, p. 102.
- Reid, A. M., S. T. Reid, S. J. Mazzullo, and S. C. Robbins, 1989, Refined fusulinid biostratigraphic zonations of Wolfcampian and Lower Leonardian strata in the Permian basin: Southwest Section Meeting Abstracts, *AAPG Bulletin*, v. 73, p. 256.
- Reid, A. M., S. T. Reid, and S. J. Mazzullo, 1990, Lowstand carbonate reservoirs: upper Pennsylvanian sea level changes and reservoir development adjoining the Horseshoe atoll: Southwest Section Meeting Abstracts, *AAPG Bulletin*, v. 74, no. 2, p. 221.
- Reid, A. M., and S. Tomlinson-Reid, 1991, The Cogdell field study, Kent and Scurry Counties, Texas: a post mortem, *in* M. Candelaria, ed., *Tomorrow's Technology Today: West Texas Geology Society Symposium*, Pub. No. 91-89, p. 39–66.
- Ross, C. A., 1978, Late Pennsylvanian and Early Permian sedimentary rocks and tectonic setting of the Marathon geosyncline, *in* S. J. Mazzullo, ed., *Tectonics and Paleozoic Facies of the Marathon Geosyncline, West Texas: Field Conference Guidebook, Permian Basin Section SEPM, Publication 78-14*, p. 89–93.
- Ross, C. A., and J. R. P. Ross, 1985, Late Paleozoic depositional sequences are synchronous and worldwide: *Geology*, v. 13, p. 194–197.
- Ross, C. A., and J. R. P. Ross, 1987, Late Paleozoic sea levels and depositional sequences, *in* C. A. Ross and D. Haman, eds., *Timing and Depositional History of Eustatic Sequences: Constraints on Seismic Stratigraphy*: Houston, Cushman Foundation for Foraminiferal Research, Special Publication No. 24, p. 137–149.
- Schatzinger, R. A., 1983, Phylloid algal and sponge-bryozoan mound-to-basin transition: a late Paleozoic facies tract from the Kelly-Snyder field, west Texas, *in* P. M. Harris, ed., *Carbonate Buildups—A Core Workshop: SEPM Core Workshop 4*, p. 244–303.
- Schatzinger, R. A., 1988, Changes in facies and depositional environments along and across the trend in the Horseshoe atoll, Scurry and Kent Counties, Texas, *in* B. K. Cunningham, ed., *Permian and Pennsylvanian Stratigraphy, Midland Basin, West Texas: Studies to Aid Hydrocarbon Exploration: PBS-SEPM Research Seminar One, Publication 88-28*, p. 79–105.
- Scotese, C. R., R.K. Bambach, C. Barton, R. Van der Voo, and A. M. Ziegler, 1979, Paleozoic base maps: *Journal of Geology*, v. 87, no. 3, p. 217–268.
- Scotese, C. R., 1984, An introduction to this volume: Paleozoic paleomagnetism and the assembly of Pangea, *in* R. Van der Voo, C.R. Scotese, and N. Bonhommet, eds., *Plate Reconstruction from Paleozoic Paleomagnetism: American Geophysical Union Geodynamics Series 12*, p. 1–10.
- Scotese, C.R., and W.S. McKerrow, 1990, Revised World maps and introduction, *in* C. R. Scotese and W.S. McKerrow, eds., *Paleozoic Paleogeography and Biogeography: The Geological Society of London Memoir 12*, p. 1–21.
- Stafford, P. T., 1955, Zonation of the late Paleozoic Horseshoe atoll in Scurry and southern Kent Counties, Texas: U. S. Geological Survey Oil and Gas Investigations Chart OC-53.
- Stafford, P. T., 1956, *Geology of part of the Horseshoe atoll, Scurry and Kent Counties, Texas*: U. S. Geological Survey Professional Paper 315-A, 20 p.
- Stanley, S. M., 1985, *Earth and life through time*: New York, W.H. Freeman and Co., 690 p.
- Stanley, S. M., 1988, Climatic cooling and mass extinction of Paleozoic reef communities: *Palios*, v. 3, Reefs Issue, p. 228–232.
- Todd, R. G., 1976, Oolite-bar progradation, San Andres Formation, Midland basin, Texas: *AAPG Bulletin*, v. 60, no. 6, p. 907–925.

- Tomlinson-Reid, S., 1979, Karst features in Yucatan and the subsurface of Texas, geology of Cancun, Quintana Roo, Mexico: West Texas Geological Society, September 22–26 Field Trip Guidebook, Publication 79-72, p. 124–127.
- Tyler, N., D. G. Bebout, C. M. Garrett, Jr., E. H. Guevara, C. R. Hocott, M. H. Holtz, S. D. Hovorka, C. Kearns, F. J. Lucia, R. P. Majors, S. C. Ruppel, and G. W. Vander Stoep, 1991, Integrated characterization of Permian basin reservoirs, University Lands, west Texas, in *Targeting the Remaining Resource for Advanced Oil Recovery: Report of Investigation No. 203*, Bureau of Economic Geology, The University of Texas at Austin, Austin, Texas, p. 44–55.
- Vanderhill, A.L., D.K. Markley, C.E. Hansen, 1990, Salt Creek field, in *Oil and Gas Fields in West Texas, Volume V: West Texas Geological Society*.
- Van der Voo, R., 1988, Paleozoic paleogeography of North America, Gondwana and intervening displaced terranes: comparisons of paleomagnetism with paleoclimatology and biogeographical patterns: *Geological Society of America Bulletin*, v. 100, p. 311–324.
- Van der Voo, R., J. Penado, and C. R. Scotese, 1984, A paleomagnetic reevaluation of Pangea reconstruction, in R. Van der Voo, C.R. Scotese, and N. Bonhommet, eds., *Reconstruction from Paleozoic Paleomagnetism: American Geophysical Union Geodynamics Series 12*, p. 11–16.
- Veevers, J. J., and C. Powell, 1987, Late Paleozoic glacial episodes in Gondwanaland reflected by transgressive-regressive depositional sequences in Euramerica: *Geological Society of America Bulletin*, v. 98, p. 475–487.
- Vest, E. L., 1970, Oil fields of the Pennsylvanian–Permian Horseshoe atoll, west Texas, in M. T. Halbouty, ed., *Geology of Giant Petroleum Fields: AAPG Memoir 14*, p. 185–203.
- von Brunn, V., and T. Stratten, 1981, Late Paleozoic tillites of the Karoo basin of South Africa, in J. M. Hambrey and W. B. Harland, eds., *Earth's Pre-Pleistocene Glacial Record: Cambridge University Press*, p. A10.
- Walker, D. A., J. M. Jensen, S. Zody, and S. Tomlinson-Reid, 1990, Pennsylvanian cycle stratigraphy and carbonate facies control of reservoir development in the Salt Creek field, Kent County, Texas, in J.E. Flis and R.C. Price, eds., *Permian Basin Oil and Gas Fields: Innovative Ideas in Exploration and Development: West Texas Geological Society Symposium, 1–2 November, 1990*, p. 107–112.
- Walker, D. A., J. Golonka, A. Reid, and S. Tomlinson-Reid, 1991, The effects of late Paleozoic paleolatitude and paleogeography on carbonate sedimentation in the Midland basin, Texas, in M. Candelaria, ed., *Permian Basin Plays—Tomorrow's Technology Today: West Texas Geological Society Symposium, Pub. No. 91-89*, p. 141–162.
- Wanless, H. R., and F. P. Shepard, 1936, Sea level and climatic changes related to late Paleozoic cycles: *Geological Society of America Bulletin*, v. 47, p. 1177–1206.
- Wanless, H.R. and J.J. Dravis, 1989, Carbonate environments and sequences of the Caicos platform: 28th International Geological Congress, Field Trip Guidebook T 374, American Geophysical Union, 75 p.
- Wegener, A., 1966, *The Origin of Continents and Oceans; Die Entstehung der Kontinente und Ozeane, 1929*, 4th rev. edition, translated to English by J. Biram: Dover, New York, 246 p.
- West, R. R., 1988, Temporal changes in Carboniferous reef mound communities: *Palios*, v. 3, Reefs Issue, p. 152–169.
- Wilson, J. L., 1975, *Carbonate facies in geologic history*: New York, Springer-Verlag, 471 p.
- Wilson, J. L., and C. F. Jordan, 1983, Middle shelf environment, in P. A. Scholle, D. G. Bebout, and C. H. Moore, eds., *Carbonate Depositional Environments: AAPG Memoir 33*, p. 297–343.
- Witzke, B. J., 1990, Paleoclimatic constraints for Paleozoic paleolatitudes of Laurentia and Euramerica, in C. R. Scotese and W.S. McKerrow, eds., *Paleozoic Paleogeography and Biogeography: The Geological Society of London Memoir 12*, p. 57–73.
- Yancey, T.E., 1984, Cycle correlation in Late Pennsylvanian strata of the Midland basin: *Southwest Section AAPG Transactions, AAPG Bulletin*, v. 68, no. 1, p. 120.
- Yancey, T. E., and R. D. McLerran, 1988, Cyclic stratigraphy of the Late Pennsylvanian of north-central Texas, in B. K. Cunningham, ed., *Permian and Pennsylvanian Stratigraphy, Midland Basin, West Texas: Studies to Aid Hydrocarbon Exploration: PBS-SEPM Research Seminar One, Publication 88-28*, p. 65–77.
- Ziegler, A. M., R.K. Bambach, J. T. Parrish, S.F. Barrett, E. H. Gierlowski, W.C. Parker, A. Raymond, and J.J. Spkowski, Jr., 1981, Paleozoic biogeography and climatology, in K. J. Niklas, ed., *Paleobotany, Paleogeology, and Evolution: Praeger Special Studies, Praeger Scientific*, p. 231–267.
- Ziegler, A. M., 1990, Phytogeographic patterns and continental configurations during the Permian Period, in C.R. Scotese and W.S. McKerrow, eds., *Paleozoic Paleogeography and Biogeography: The Geological Society of London Memoir 12*, p. 363–377.

Kimmeridgian (Late Jurassic) General Lithostratigraphy and Source Rock Quality for the Western Tethys Sea Inferred from Paleoclimate Results Using a General Circulation Model

George T. Moore

Eric J. Barron

*The Pennsylvania State University
University Park, Pennsylvania, U.S.A.*

Darryl N. Hayashida

*Chevron Petroleum Technology Company
La Habra, California, U.S.A.*

ABSTRACT

The application of any General Circulation Model (GCM) simulation is only as valuable as: the quality of the original input boundary conditions, the computer model used and its track record for producing quality paleoclimate simulations, and the extent to which the simulation results have been tested successfully with the geologic record. We utilize a global simulation of the Kimmeridgian (Late Jurassic) to focus on an area of investigation. The simulation was tested against the geologic record. The results replicate the paleoclimate with a consistency that is acceptable, if not impressive. Therefore, the results can be utilized to map the distribution of climatically sensitive sediments within a given area.

The study area includes the western part of the Tethys Sea, which was a zonally oriented tropical sea at a paleolatitude of about 0°–25°N and isolated from the Panthalassa Ocean by an isthmus. The sea was characterized by warm tropical surface water and generally strong net evaporation creating conditions of low oxygen content and elevated salinities in the surface water mass. Much of the margin receives insufficient precipitation to maintain lasting soil moisture or generate runoff to the sea in any season, precluding development of a lush vegetative cover. The general lack of runoff improves conditions for reef growth and carbonate deposition on the continental shelves. Much of the margin possesses wind-driven coastal upwelling. As a positive correlation exists between upwelling and high primary productivity on the margins of today's World Ocean, we predict that a similar relationship occurred in the Kimmeridgian Western Tethys Sea.

The high salinities contributed to a probable negative water balance, such as the Mediterranean Sea today. This circulation would keep the main axis of the basin generally oxygenated, except for isolated, restricted local basins. In this study, model results correlate well with published regional lithofacies maps where data are available. This complement offers encouraging proof that this model generally replicates the real Late Jurassic paleoclimate by creating the proper physical conditions under which the biota existed and sediments were deposited.

INTRODUCTION

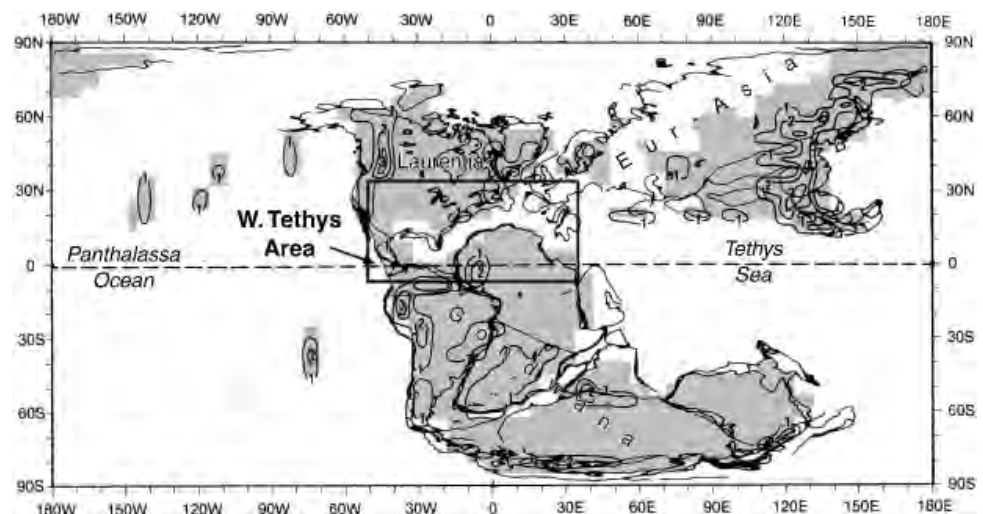
The application of any General Circulation Model (GCM) simulation is only as valuable as: the quality of the original input boundary conditions, the computer model used and its track record for producing quality paleoclimate simulations, and the extent to which the simulation results have been tested successfully with the geologic record. A global simulation of the Kimmeridgian (Late Jurassic) (154.7–152.1 Ma; Harland et al., 1990) is utilized here to present a focused area of investigation, the Western Tethys Sea (Figure 1). This simulation was selected from among several as best matching the Late Jurassic geologic record (Moore et al., 1992a, b; Ross et al., 1992). We believe the results replicate the Late Jurassic paleoclimate with a consistency that is acceptable, if not impressive. Valdes and Sellwood (1992) likewise modeled this interval using the Universities Global Atmospheric Modelling Project (Cycle 27) GCM. In the region of this study the surface temperature and precipitation results are generally similar.

The paleogeographic setting placed the Western Tethys Sea between the elevated landmasses of North America, Greenland, and northern Europe on the north and positive elements such as the Sahara platform in Africa to the south (Ziegler, 1988). Central and southern Europe were complicated by tectonic uplifts

isolated from one another by a network of shallow to moderately deep marine seaways (Ziegler, 1988). The highly irregular paleobathymetry in a warm tropical sea was an ideal setting for the extensive development of two reef varieties (demosponge/coral and demosponge/algal) characteristic of the Late Jurassic (Beauvais, 1973; Heckel, 1974; Flügel and Flügel-Kahler, 1992).

The paleogeography used in this simulation is specified for the beginning of the Kimmeridgian. By Late Jurassic time, a westward propagating rift system, that became the central Atlantic and proto-Gulf of Mexico, began fragmentation of Pangea, the megacontinent, by splitting Laurentia/Eur-Asia from Gondwana (Figure 1). For the purpose of this paper we term this the Western Tethys Sea. According to this reconstruction, the rift system had not completely separated northern Pangea from Gondwana (Figures 1 and 2). Workers also differ as to whether or not Laurentia (North America) was tectonically and physically separated from Gondwana by the Tithonian (Barron et al., 1981; Smith et al., 1981; Ziegler et al., 1983; Pindell, 1985; Scotese and Summerhayes, 1986; Salvador, 1987; Ross and Scotese, 1988; Ulmishek and Klemme, 1990; Rowley, 1991; and Scotese and Golonka, 1992). However, Ross et al. (1992) concluded from studying the ammonoid faunas that separation occurred by Tithonian (late Late Jurassic) time.

Figure 1. Late Jurassic (155 Ma) paleogeography used in this paleoclimate simulation, showing the location of the Western Tethys Sea area (outline). See Moore et al., 1992a for discussion of methodology and rationale. Land grid cells shaded. Many islands, particularly in Europe, existed in the Tethys Sea, but are too small to be represented by the coarse grid of this general circulation model. Paleotopographic contours in kilometers. © 1993, George T. Moore.



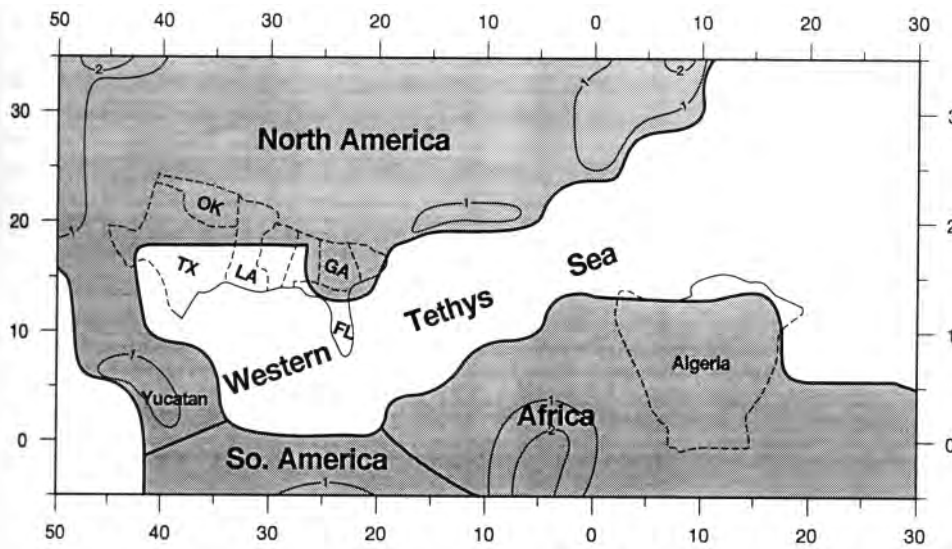


Figure 2. Paleogeography of the Western Tethys Sea showing location of U.S. Gulf states and Algeria (enlargement of outline in Figure 1). Horizontal axis shows degrees longitude, vertical axis shows degrees latitude. Land area shaded. Paleotopographic contours in kilometers. © 1993, George T. Moore.

The study area includes the western part of the Tethys Sea, which was a zonally oriented tropical sea at a paleolatitude of about 0° – 25° N. In this reconstruction, the westward propagating rift system splitting central Pangea had not completely separated North America from the Gondwana continents. Thus, we show the Mexican Yaqui, Guerrero, and Yucatan blocks as an isthmus joining the continents on the west and separating the Tethys Sea from the Panthalassa Ocean. The southern part of North America and northwest Africa border the Western Tethys Sea (Figure 2). Algeria and the U.S. Gulf states are outlined on this and succeeding maps for reference. The discussion of the paleoclimate and the inferences drawn in this report presume that the paleogeography and paleotopography are reasonably accurate.

We present the December/January/February and June/July/August seasons for each climate parameter discussed. The other seasons, while occasionally referred to, are not included in this paper. For the readers' convenience, we put two seasons in one figure using the convention of having December/January/February on top and June/July/August below.

MODEL DESCRIPTION

The atmospheric GCM utilized in this study is termed the Community Climate Model (CCM). This CCM was developed for climate studies and weather prediction at the National Center for Atmospheric Research (NCAR) in Boulder, Colorado. The evolution and characteristics of the model have been described by various authors (Barron, 1985; Sloan and Barron 1992; Moore et al., 1992a; Fawcett et al., 1994). The CCM was modified by E.J. Barron for use in the study of paleoclimates. Pre-Pleistocene intervals modeled using the CCM or the next generation, GENESIS, include the Eocene (Sloan and Barron, 1992) mid-Cretaceous (Barron, 1985), Late Jurassic (Moore et al., 1992a); mid-Jurassic and Triassic (Fawcett et al., 1994); early Late Permian (Fawcett et al., 1994; Kutzbach and

Ziegler, 1993), and mid-Silurian (Moore et al., 1993, 1994). The reader is referred to any of the above papers and references cited therein for model details or a summary.

The CCM results are from a seasonal simulation run to equilibrium. This version of the CCM is thermally and hydrologically, but not dynamically, coupled to a mixed-layer ocean 50 m deep. The ocean provides for heat storage and a moisture source, but not ocean heat transport. The lack of a dynamic coupling between the ocean boundary layer and the atmosphere renders the question of whether or not North America and Gondwana are joined by an isthmus largely academic. The model utilizes a coarse $4.5^{\circ} \times 7.5^{\circ}$ latitude/longitude, scale grid cell; however, the difference of one to two grid points would not likely affect the CCM-computed atmospheric circulation.

The simulation was run using an atmospheric CO_2 concentration of 1120 ppm, 4 \times the pre-Industrial level (Barnola et al., 1987). This is in general agreement with the range of published values by Barron (1990) and Freeman and Hayes (1992).

Paleotopography is an important boundary condition and is interpreted from highlands mapped by Ziegler et al. (1983) and Scotese and Golonka (1992). Moore et al. (1992b) compared three Late Jurassic simulations with varying paleotopographic specifications. As the paleotopographic contrasts were reduced, ultimately to a world with flat continents, the global circulation became more simplified. They showed that the location and height of mountain ranges influence surface temperature, the hydrologic cycle, zonal wind belts, and storm systems.

The hydrologic cycle employed in this model was investigated by Barron et al. (1989) using numerous simulations. They found that the CCM qualitatively reproduces present-day precipitation patterns rather well. Soil moisture in the model is based on a simple grid cell by grid cell precipitation-minus-evaporation calculation frequently described as a "bucket" hydrology. Soil texture, color, and vegetative cover are not factors in regulating soil moisture in this model. When

moisture in a grid cell accumulates to a value exceeding 15 cm, it is treated as runoff. In the model results, runoff tends to occur in areas of heavy precipitation. As the Late Jurassic landscape is rather poorly resolved, particularly on a global basis, this simplistic treatment of components in the hydrologic cycle may well approach the limits of our knowledge. The CCM and the geologic record may be compatible in terms of detail and sophistication.

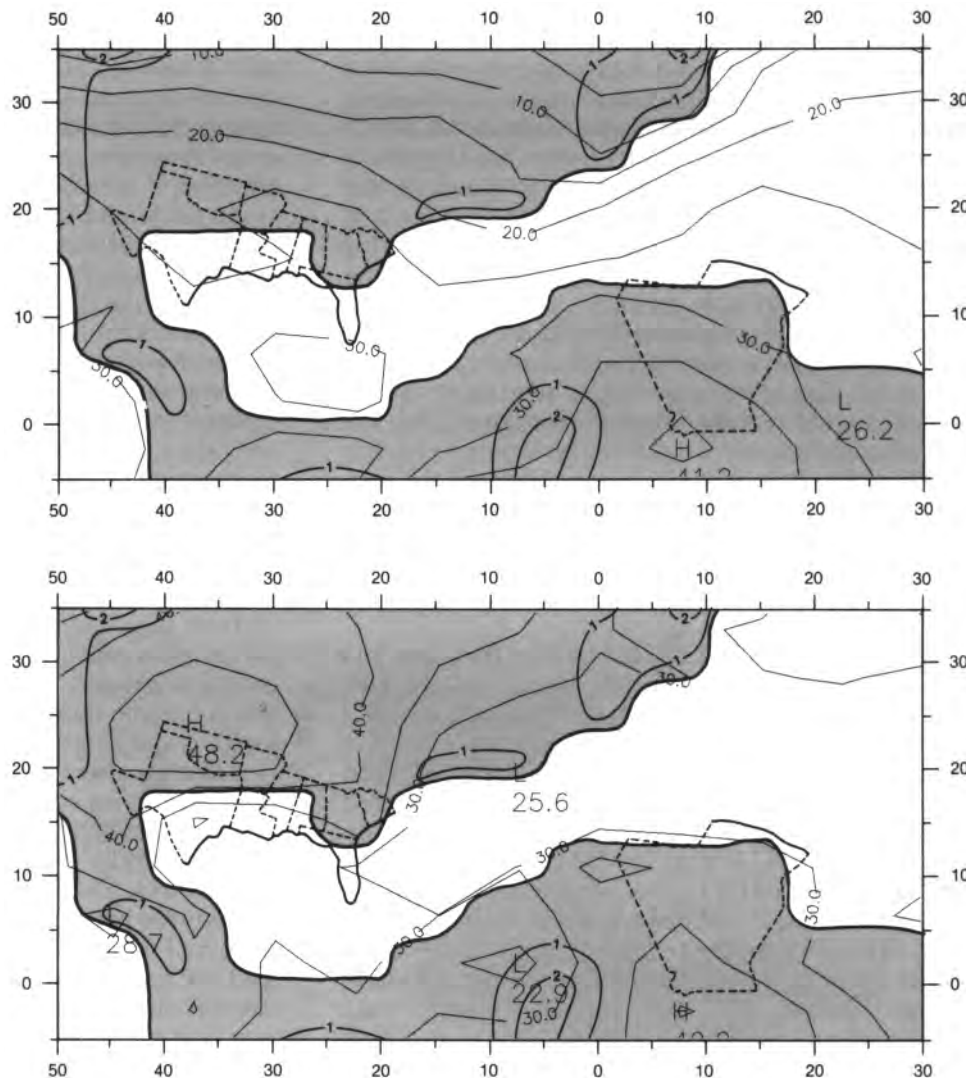
PALEOCLIMATE

Surface Temperatures

The Kimmeridgian/Tithonian sea surface temperatures (SST) reflect the low latitudinal position of the Western Tethys Sea (Figure 3). The SST ranges from about 20° to 30°C in both December/January/February and June/July/August seasons with the gradient increasing westward into the proto-Gulf of Mexico. In this paleogeographic configuration, a closed-off seaway with restricted circulation, the warm tropical surface waters contain a lower oxygen content than normal seawater (USNOO, 1967). If this water moves to a deeper

level by downwelling, the water mass would already possess a depressed oxygen level and a lowered capacity to oxidize organic matter. Such downwelling could create either a deeper thermohaline-stratified and oxygen-deficient water mass if the seaway at this time possessed complex bathymetry and individual small isolated basins or, as is more likely in this latitude, develop a negative water balance such as the present circulation in the Mediterranean Sea (Demaison and Moore, 1980). Such a circulation pattern, in view of Ziegler's (1988) paleogeography showing a continuous, curving, basinal trough, would keep the sea floor generally oxygenated. The presence of isolated, small, oxygen-depleted basins, particularly along the margins, could not be discounted completely. Such basins, though, are well below model resolution. Roth (1986) reviewed the available data from Deep Sea Drilling Program (DSDP) sites and the marginal basins of Africa and Europe, and all, except for the Kimmeridge of England and the North Sea, lack such organic-rich sediments. The negative water balance interpretation is favored and is supported by the extensive reef carbonate, evaporite, and siliciclastic deposits reported from the Western Tethys Sea region (Heckel, 1974; Locker,

Figure 3. December/January/February (upper) and June/July/August (lower) surface temperature (°C) for the Western Tethys Sea area. C.I. = 5°C. © 1993, George T. Moore.



1984; Dercourt et al., 1985; Poag, 1985; Salvador, 1987; Stephan et al., 1990; Flügel and Flügel-Kahler, 1992; Cecca et al., 1993).

The land surface temperatures generally are greater than 25° except during December/January/February in North America. In June/July/August, the land surface temperature in portions of both areas exceeds 40°C.

Precipitation and Precipitation Minus Evaporation (P – E)

Precipitation on the North American continent is restricted seasonally to the eastern part of the continent where the orographic effects of the Appalachian Mountains and June/July/August onshore flow of tropical marine air cause extensive rainfall (Figure 4). Otherwise, the continent is dry in other seasons. In the interior and along the proto-Gulf of Mexico, precipitation is too low to support anything but xerophytic vegetation in an arid landscape. The region receives <500 mm annually (Figure 5).

In the general region of northwestern Africa the continent receives little precipitation (Figure 4) and

generally less than 1000 mm annually (Figure 5). The precipitation high to the west of Algeria is associated with the orographic effects of the local highlands and the onshore flow of tropical marine air carried by the northeast trade winds (Moore et al., 1992a).

Seasonal rainfall centers in the southwestern part of the region result from the strong, well-organized northeast trade winds throughout the year and a very weak monsoonal circulation in June/July/August (and September/October/November, not shown).

The areas of greatest moisture sources, particularly the extreme western part of the Tethys, and those of net rainfall accumulation are shown in the annual P – E map (Figure 6). In general, the areas of greatest moisture accumulation (Figure 6) are those receiving the highest precipitation (Figures 4 and 5).

The model results generally are confirmed by the paleoenvironmental map of Fourcade et al. (1991), which shows a shallow carbonate platform with evaporites spanning much of the African margin in the Tithonian. These deposits are flanked to the east, beginning in the Gulf of Sirte (~25°E), and to the west, near South America, by accumulations of, or inferred, terrigenous shelf deposits.

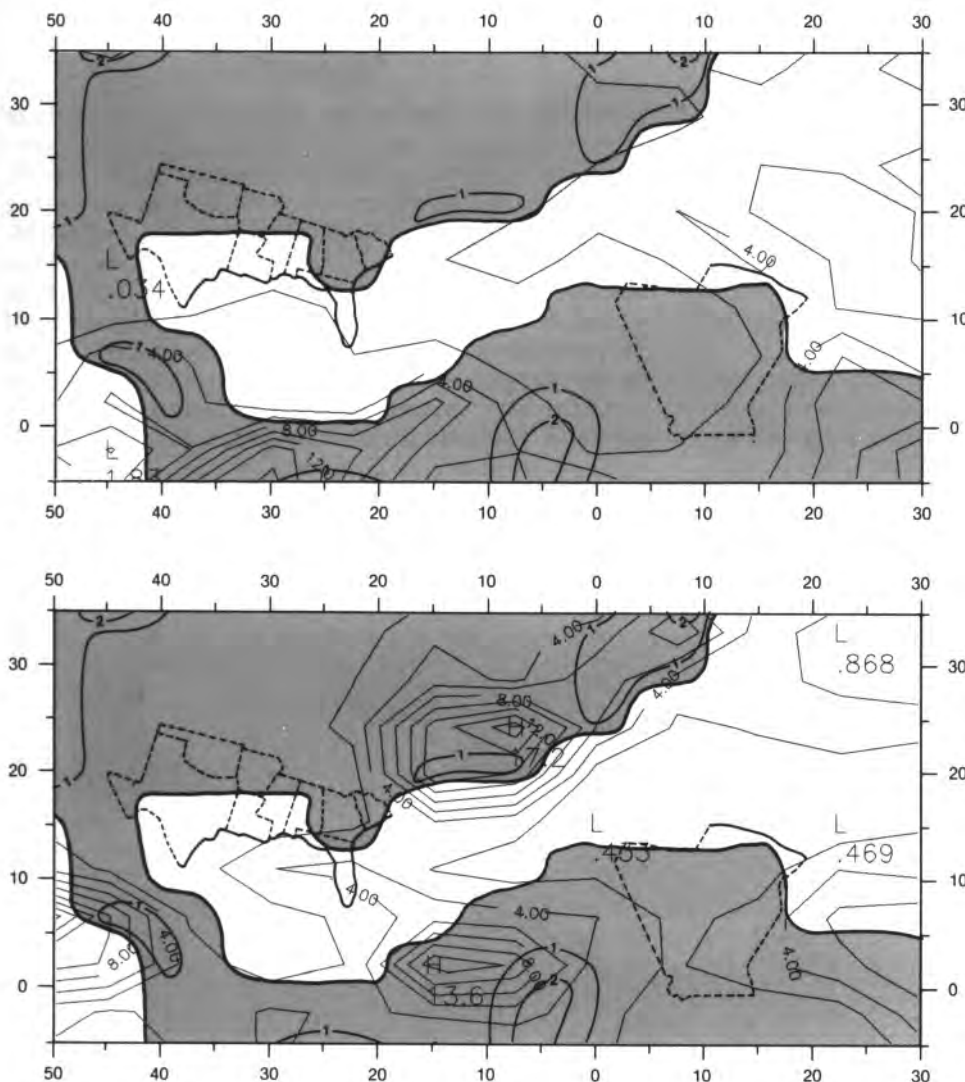
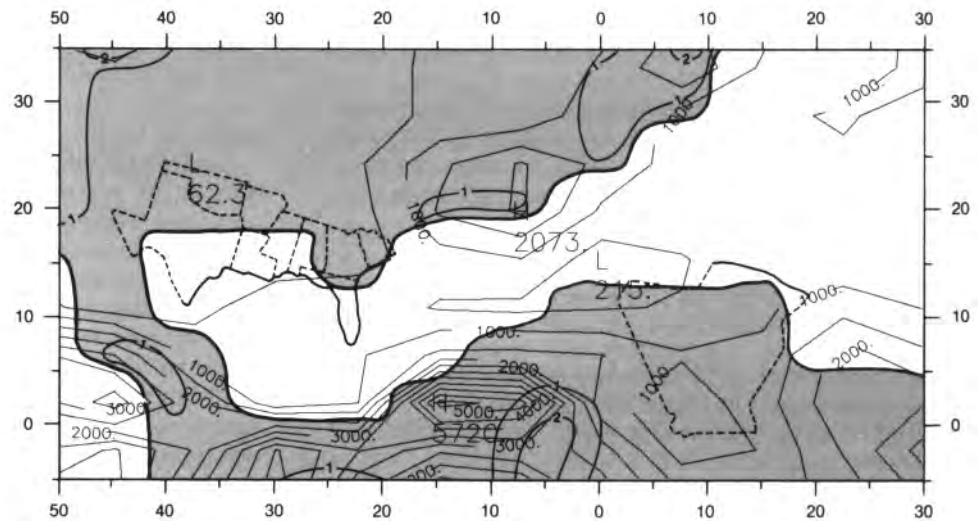


Figure 4. December/January/February (upper) and June/July/August (lower) precipitation (mm d^{-1}) for the Western Tethys Sea area. C.I. = 2 mm d^{-1} . © 1993, George T. Moore.

Figure 5. Total annual precipitation (mm) for the Western Tethys Sea region. C.I. = 500 mm. © 1993, George T. Moore.



Soil Moisture

Soil moisture is a parameterized calculation that utilizes model-derived precipitation and evaporation to simulate moisture accumulation in the soil. Each land grid cell acts as a pan with 15 cm high sides. Soil moisture is stored in a single layer of soil in each cell. When the volume of excess precipitation accumulates to 15 cm, the soil layer is considered saturated. Precipitation exceeding this height is considered runoff (Washington and Williamson, 1977).

Soil moisture exists only seasonally where extensive centers of precipitation occur (Figure 7). Evaporation rates were high enough to evaporate all the rain that fell, as the wet areas were dry by the following season. This included the heavy rainfall belt along the southwestern Tethys Sea in December/January/February. The northern Appalachians above 23°N possess soil moisture year-round.

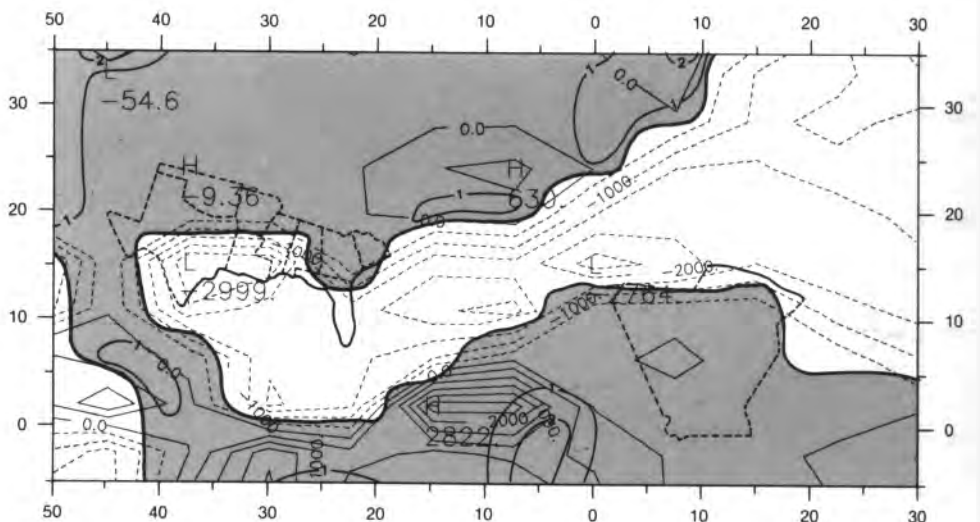
With precipitation insufficient and evaporation too high to maintain large permanent lakes, playa lakes may have existed locally for short time intervals in areas of net evaporation (Figure 6). Such lakes would likely contain siliciclastics interbedded with evapor-

ites. We would anticipate lacustrine deposits in the nonmarine continental section in depressions where annual soil moisture permanently existed (Figure 8) and/or where the $P - E$ was positive (Figure 6). Based on work by Barron (1990), the CCM can be used to interpret conditions where lakes can become stratified and probably anoxic.

Runoff

Runoff occurs when the amount of soil moisture exceeds 0.15 m (15 cm) in a grid cell. Only major seasonal precipitation centers generate runoff (Figure 9). All three major centers of rainfall, the extensive June/July/August one associated with the Appalachians and the two seasonal centers south of the Tethys Sea, are along the coasts. Rivers flowing from them would be the source of clastic material to the sea with the probable development of deltas and probable fans on the margins that are constructed on the basin floor by turbidity currents flowing through submarine canyons. The Late Jurassic delta-fan complex developed on the eastern U.S. margin mapped by Uchupi et al. (1984) fits this runoff pattern remarkably well.

Figure 6. Annual precipitation-minus-evaporation ($P - E$) (mm) for the Western Tethys Sea region. Solid contours represent a positive $P - E$; dashed contours show a negative $P - E$. C.I. = 500 mm. © 1993, George T. Moore.



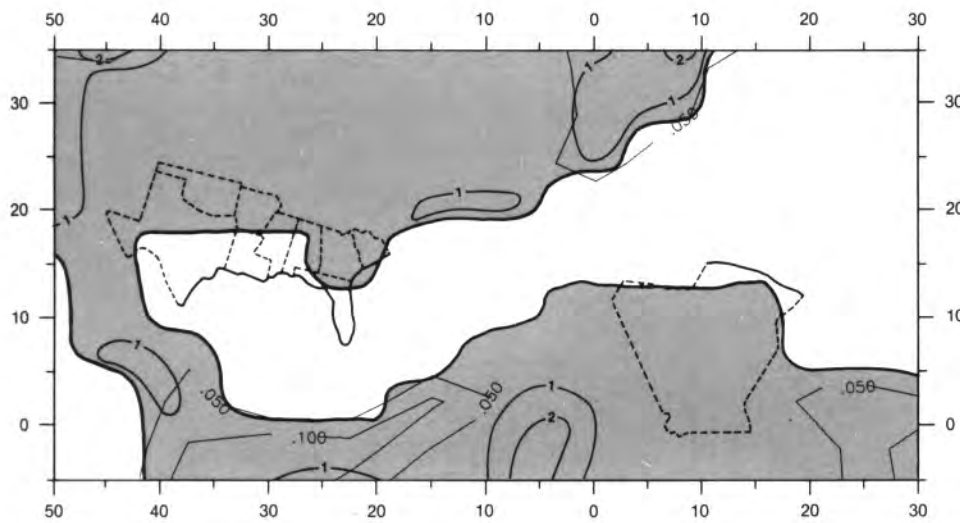


Figure 7.
December/January/February
(upper) and June/July/
August (lower) soil moisture
(m) for the Western Tethys
Sea area. C.I. = 0.05 m. ©
1993, George T. Moore.

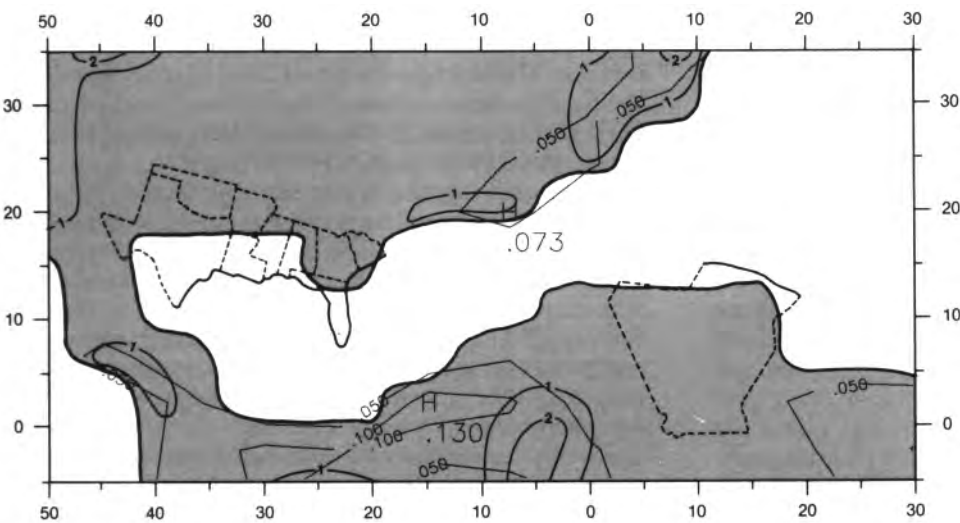
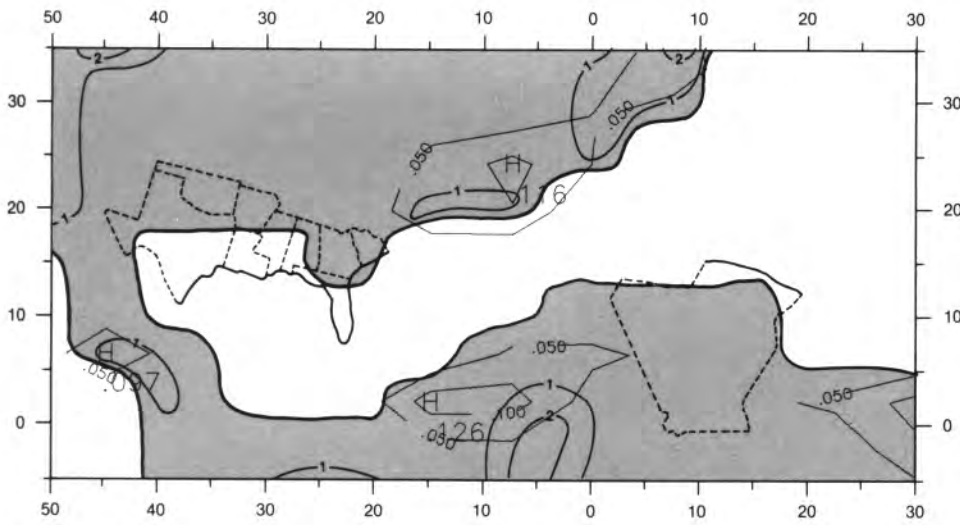


Figure 8. Annual average
soil moisture (m) Western
Tethys Sea area. © 1993,
George T. Moore.

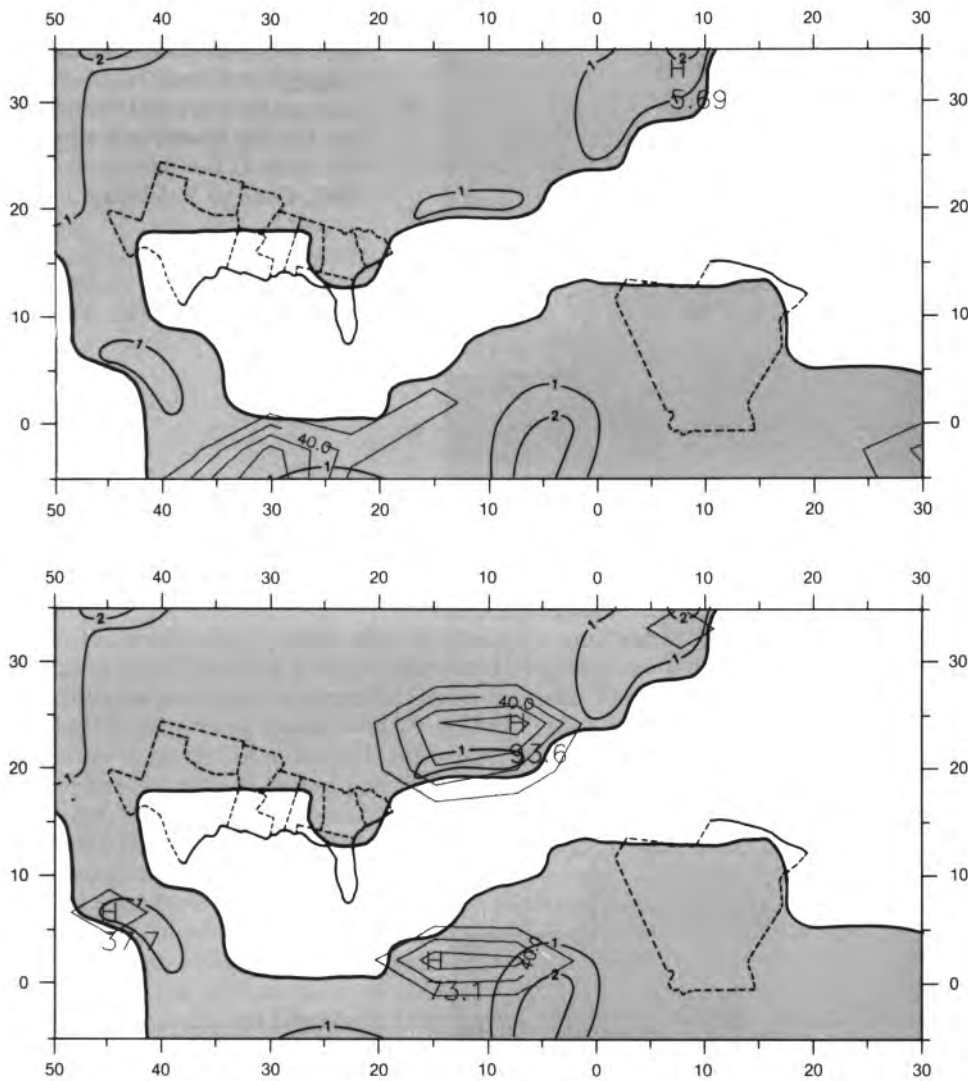


Figure 9.
December/January/February
(upper) and June/July/
August (lower) runoff (mm d^{-1})
for the Western Tethys
Sea area. C.I. = 20 mm d^{-1} .
© 1993, George T. Moore.

Depending on the paleotopography and paleodrainage, some of the June/July/August runoff associated with the southern Appalachians could flow to the southwest and/or west forming deltaic complexes in these areas. This could serve as a source for some of the fluvial clastic deposits in the eastern proto-Gulf in both the early and late Kimmeridgian (Salvador, 1987). The model results show an extremely arid region to the west in the U.S. Gulf states and northeastern Mexico. The strong, model-simulated aridity in this region is confirmed by the presence of argillaceous shelf carbonates rimming the basin, and extensive lower Kimmeridgian evaporites in southern Texas and northeastern Mexico (Salvador, 1987).

Surface Wind

The two seasonal wind maps show that the southern part of the region is under the influence of the northeast trade winds or easterlies (Figure 10). They are strongest during December/January/February and weakest during June/July/August. The northern

margin of the easterlies is influenced by the differential seasonal cooling (Figure 10, upper) and heating (Figure 10, lower) of the North American continental interior. The strongest onshore flow of marine air onto the Gondwanan continent, the isthmus, and southern Gulf states occurs in December/January/February where the wind velocities reach 15 m s^{-1} .

In the arid regions, eolian transport would be anticipated only where the winds exceed the threshold velocity of sand (0.25–0.30 mm) of 6 m s^{-1} (Fryberger, 1979). The seasonal plots show the direction of eolian transport and the potential migratory routes of dunes for any grid square. In the case of eolian transport, the sediment is moved in the direction the wind is blowing, and, by convention, wind is referred to by the direction from which it is blowing.

The easterlies blowing over northern Africa, which lacks soil moisture, can create an inland sand sea if sufficient material is present. In June/July/August, the weakened trade winds became more easterly but still have sufficient velocity to transport sand inland or along the northern coast.

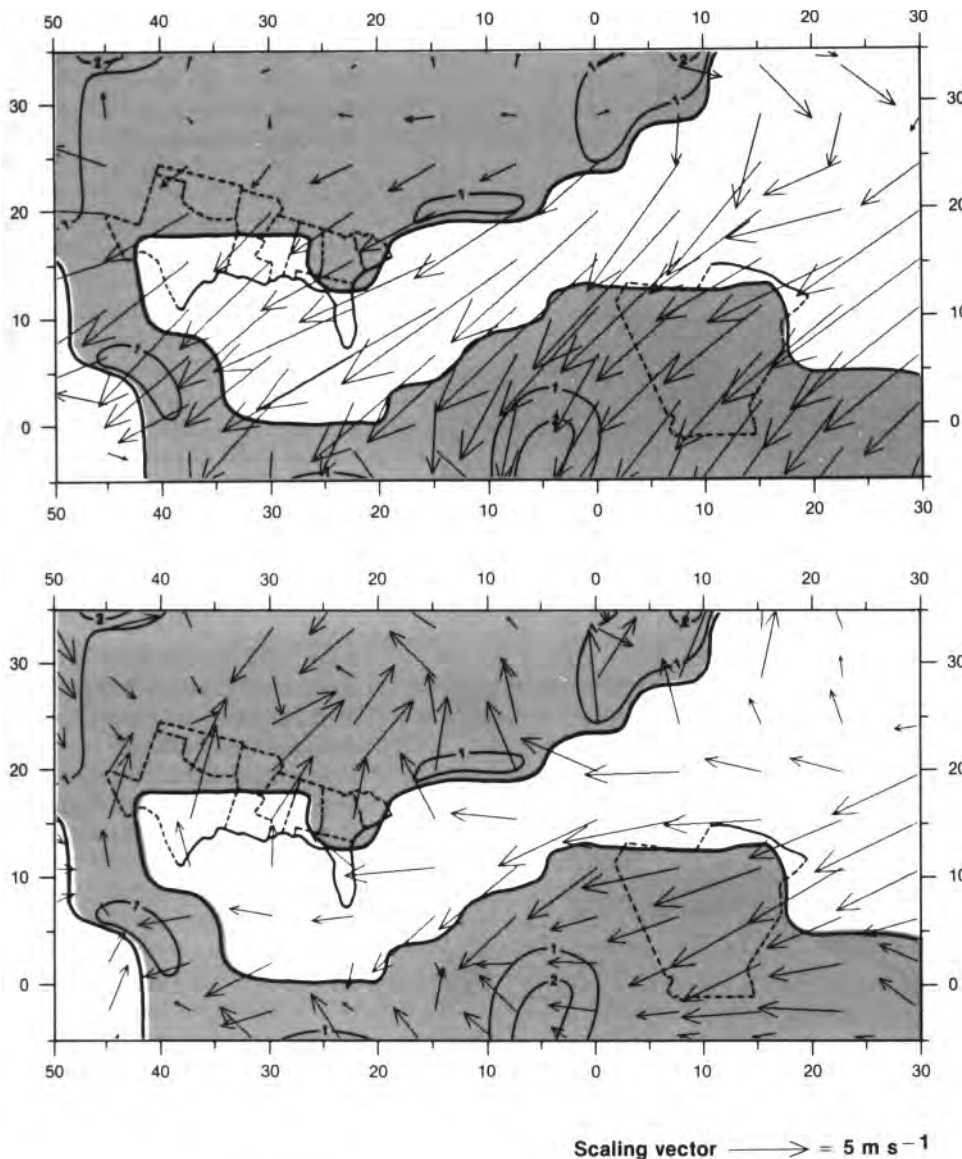


Figure 10. December/January/February (upper) and June/July/August (lower) surface wind vectors (m s^{-1}) for the Western Tethys Sea region. © 1993, George T. Moore.

Elsewhere, the seasonally variable winds make an interpretation difficult. The threshold velocity in December/January/February was barely reached by a northeasterly wind only in the grid cells covering northern Texas and Georgia. In these areas, coastal dunes might be expected. The pattern reversed seasonally in June/July/August due to a warming of the continent with several grid cells at the threshold level. The annual net surface wind direction is required to determine the direction of dune migration (Figure 11).

This lack of a strong seasonal or annual unidirectional wind pattern over the U.S. Gulf states (Figure 10) suggests that the eolian deposits in the Western Interior and in Alabama on the Gulf Coast, both indicating northwesterly winds as determined from cross-bedding (Peterson, 1988), may have been Milankovitch forced. A combination of planetary orbital variations that increased seasonality and thermal contrasts between the American continental subtropical

high cell and the Tethys Sea would strengthen seasonal winds and could offer an explanation for eolian transport. The settings for eccentricity, obliquity, and precession in this version are for the present.

Upwelling

The program UPWELL utilizes the U (east/west) and V (north/south) components of wind velocity, the Ekman effect, and the Coriolis force to compute weak and intense upwelling (Barron, 1985; Kruijs and Barron, 1990). Due to the frictional drag of the wind over the water and the Coriolis force, the surface water is displaced at 90° to the right of the direction from which the wind is blowing in the Northern Hemisphere.

Intense December/January/February, coastal upwelling occurs along the southern Tethys margin but gets progressively weaker to the west (Figure 12).

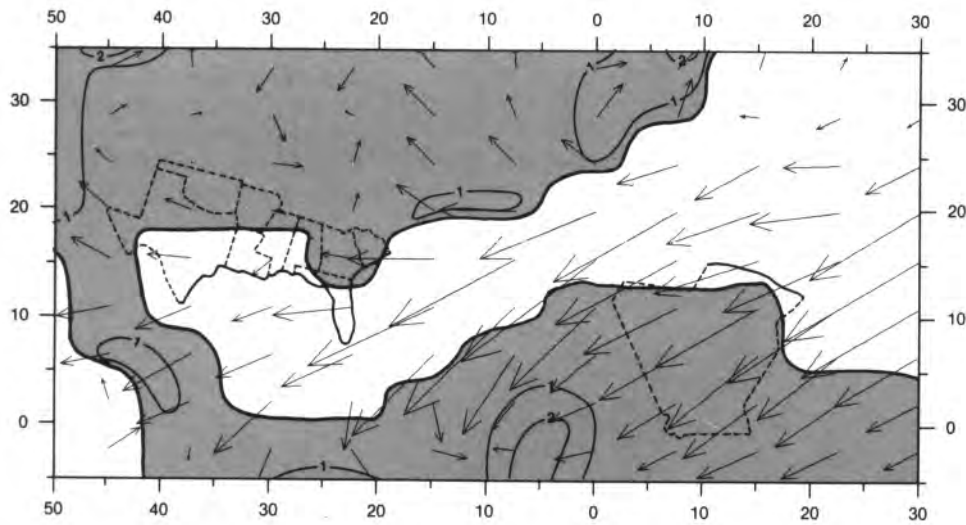


Figure 11. Annual resultant (net) surface wind direction (m s^{-1}) for the Western Tethys Sea region. © 1993, George T. Moore.

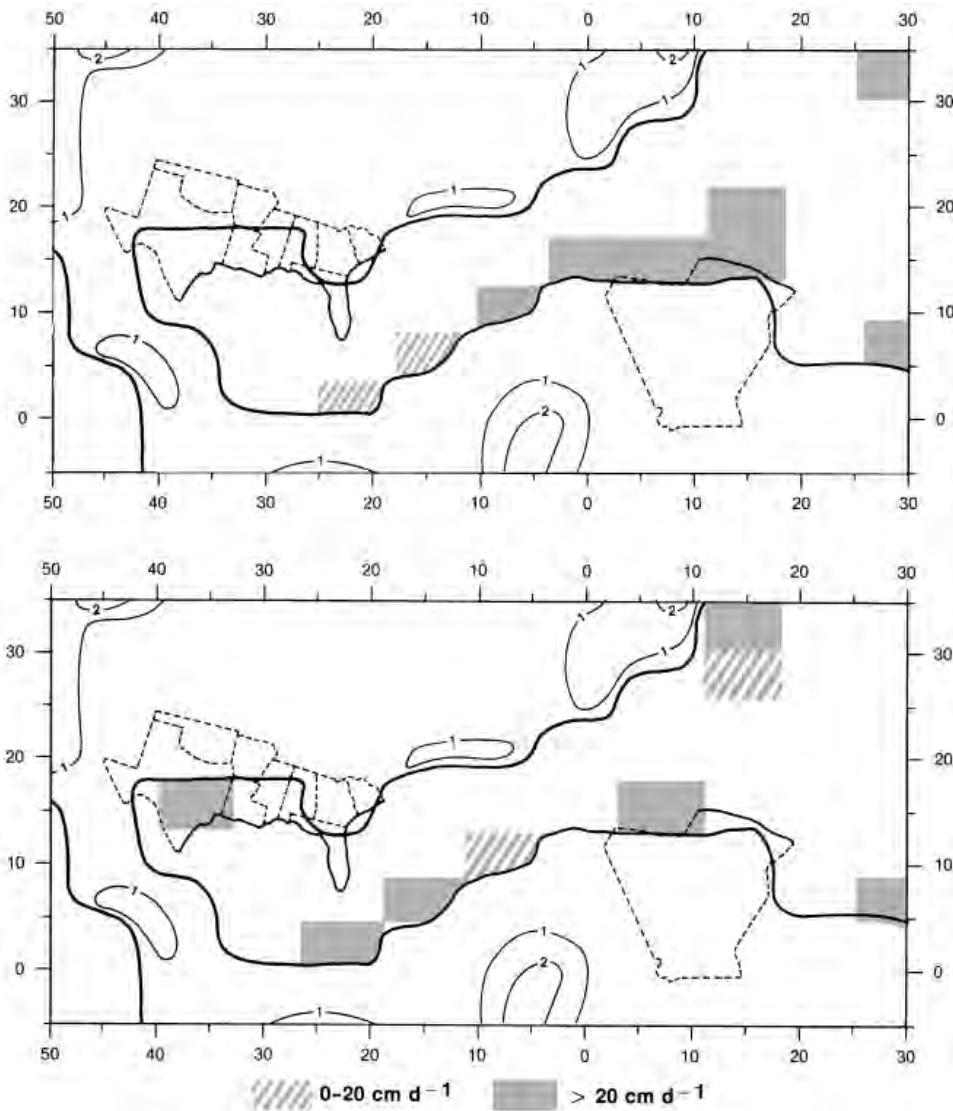


Figure 12. December/January/February (upper) and June/July/August (lower) wind-driven upwelling (cm d^{-1}) for the Western Tethys Sea region. © 1993, George T. Moore.

The northern Tethys margin lacks upwelling. In June/July/August, intense upwelling occurs in three grid cells along the African margin and one in the westernmost Tethys Sea (Texas and western Louisiana) (Figure 12). Two grid cells with upwelling occur off northern North America.

Based on the work of Kruijs and Barron (1990), we can postulate source rock occurrence and quality with results from a simulation. With sufficient rainfall that created conditions with year-round soil moisture, the paleoclimatic setting would produce areas where forests grew and organic soils developed (Figures 4–8). Where runoff to the ocean occurs (Figure 9), the drainage basins with a well-developed flora can contribute a significant terrestrial component (type III) to the coastal and marine sediments. On the other hand, where intense upwelling exists off arid or semiarid coasts, primary productivity would have been high, and the marine biologic cycle could have produced significant quantities of marine organic matter (type II).

Tropical Cyclones

Barron (1989) summarized, from existing literature, the criteria that must exist to form and sustain a cyclone. The factors that generate cyclones are dominated by SSTs that exceed 27°C and various components of the general atmospheric circulation, most of which can be deduced from the model results.

The track of cyclones is related to large-scale pressure patterns in the low to mid-latitudes. The zonal and poleward movement of these storms is controlled by the location, extent, and intensity of the subtropical high. Thus, the SST controls cyclone genesis and the large-scale atmospheric circulation guides them (Barron, 1989). As these parameters are readily obtained from a simulation, they can be combined to interpret the probable tracks of storms and their likely landfall. With such inferences, we can interpret some sedimentary structures indicative of storm deposits (Barron, 1989) and use the information to assist in developing sedimentary models.

The August/September/October temperature and sea level pressure maps respectively were combined to generate a cyclone track map (Figure 13, lower). Such storms, after making landfall, should have moved across central Algeria and dissipated as they dropped their moisture load. If any storms formed in the Gulf, they should have been small, but their track would be difficult to predict.

Source Rock Distribution

North (1985) reviewed the source rock distribution generally in his discussion of the region's petroleum potential. Cecca et al. (1993) used the organic facies concept outlined by Demaison et al. (1984) to describe the region's source rocks. In 1982, Jones and Demaison formally defined the term *organic facies* as a "mappable subdivision of a designated stratigraphic unit, distinguished from the adjacent subdivisions on the basis of the character of its organic constituents, without regard to the inorganic aspects of the sediment."

Jones (1987) detailed the geochemical parameters and limits of each specific facies, as well as various mixed ones, and the depositional environments that produce them. He further eliminated the confusion caused by using the same Roman numerals for both organic facies and kerogen types. For the purpose of this discussion we will use Jones' (1987) organic facies designations A, B, C, and D for facies dominated by kerogen types I, II, III, and IV, respectively. However, when predicting what types of kerogen will be produced and preserved in sediments we will use the Roman numeral designations of Tissot and Welte (1984).

The northeast corner of the area includes western Europe and the southern margin of the North Sea. The Kimmeridgian source rock in the North Sea is well documented (Barnard and Cooper, 1981; Cooper and Barnard, 1984; Dore et al., 1985; Thomas et al., 1985). Demaison et al. (1984) mapped the organic facies in the northern portion of the North Sea. They showed that the regional variation of the facies improved from a mixed BC and D organic facies on the margins to facies B in the central part of the basin. Organic facies B rocks of equivalent age in the Mic Mac Formation sourced the large petroleum discoveries in the Jeanne d'Arc Basin off Newfoundland; however, the facies becomes mixed and diluted with terrestrial organic and siliciclastic material toward the margin giving a BC organic facies (Demaison et al., 1984). Both localities possess seasonal upwelling and increased primary biologic productivity (Figure 12) which, if combined with the suboxic/anoxic model of Demaison et al. (1984), could account for the richness of the basinal shales.

Demaison et al. (1984) map a generally continuous (though partially question marked) Upper Jurassic band of organic facies B, BC, and C along the Canadian and United States margins to the paleolatitude of about 15°N. These facies are interpreted to be seaward of the Upper Jurassic reef/carbonate bank. However, the presence of such source rocks of Kimmeridgian age has yet to be documented. Seasonal upwelling is not predicted for the margin south of Newfoundland (Figure 12). Condensate and gas occurrences on the Scotian shelf are sourced from organic matter of terrestrial origin, organic facies C, from the Verrill Canyon Formation (Powell and Snowden, 1980; Powell, 1982). The condensate and gas encountered in the Baltimore Canyon Trough have a similar terrestrially derived source from fluvial and paralic back-reef deposits.

The remaining United States, Mexican, and most of the South American margins are largely devoid of model-predicted upwelling (Figure 12) and source rocks of this age. Known source rocks of this region, such as the Smackover Formation, are Oxfordian (Salvador, 1987). In eastern Mexico, Cecca et al. (1993) consider the Oxfordian–Kimmeridgian Taman Formation to include a lower dark shale section in the Tampico basin. However, Salvador (1987) prefers to consider this argillaceous section a separate unit below the Taman Formation, clearly older than Kimmeridgian age.

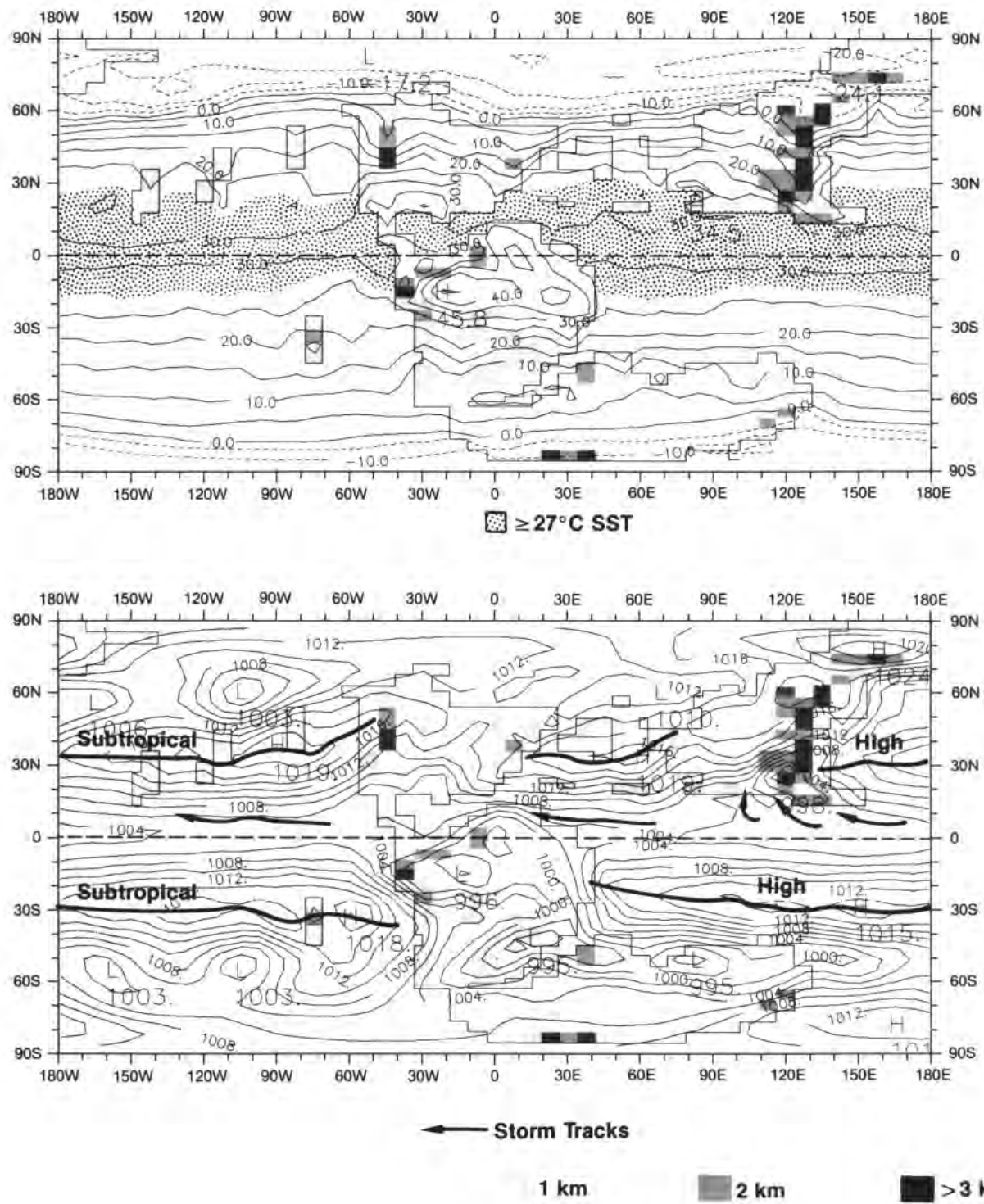


Figure 13. August/September/October cyclone season showing the sea surface temperature $>27^{\circ}\text{C}$ (dot pattern) on a surface temperature map (upper) and cyclone tracks on a sea level pressure (mb) map (lower). C.I. = 5°C (upper); 2 mb (lower). Paleotopography shown in shaded patterns. © 1993, George T. Moore.

Because of the orientation and position of the southern Tethyan shoreline (northwest and north Africa) with respect to the strong prevailing easterlies, intense upwelling is a dominant feature of this margin in all

seasons (Figure 12; March/April/May and September/October/November not shown). The presence of relatively thick sections of bituminous shales is reported in two wells drilled in Algeria (L. Skander,

1994, personal communication). These shales may represent deposition in marginal basins with restricted circulation.

Carbonate Distribution

The tropical to warm temperate oceans and seas vary widely in latitudinal position, orientation, size, configuration, chemistry, and depth. Carbonate/evaporite deposition can occur in warm tropical waters over broad, extensive banks or ramps, particularly where the SSTs are too warm for corals to grow. Coral reefs will form where the SST is in the range of 20°–30°C, the salinities are in a normal range, and the water is clear. Temperatures above 30°C cause coral bleaching and ultimate death if the high temperatures persist (Roberts, 1987). Corals appear to do well in the present-day oceans and seas where salinities reach 42‰ (CMC, 1988) to a seasonal low of 32‰ (USNOO, 1967).

Coastal upwelling generally limits the development of reefs in the present-day World Ocean (CMC, 1988). The causes are the low water temperatures (<20°C) and light limitations due to high productivity characteristically associated with nutrient-rich, upwelled water. The Tethys is isolated from any source of high-latitude water, and Late Jurassic conditions are not conducive to the formation of extensive intermediate or deep, cold, oceanic water (Moore et al., 1992a). Therefore, we do not believe that coastal upwelling played a significant role in limiting or restricting reef development.

On the assumption that the post-Triassic genera comprising reef colonies react to the same or similar physico-chemical requirements as present-day ecosystems, we can use the results of this Late Jurassic simulation to predict where coral reefs, other carbonates, and evaporites could occur (Figure 14).

In the eastern part of the sea, the SST range from 25° to 30°C is ideal for coral growth (Figure 3). However, in the proto-Gulf of Mexico, temperatures exceed 30°C. The salinities [which can be only estimated from SST (Figure 3) and P – E (Figure 6)] should be higher than normal.

Excess seasonal precipitation and river runoff from the southwestern margin of the sea and June/July/August runoff from the Appalachian region would inhibit reef development in those areas (Figures 6 and 9). However, the strong prevailing easterlies and related wind-driven circulation over the southern Tethys prevent the turbid plumes of river-borne sediment from Gondwana from moving eastward (Figures 10 and 11).

Cyclones can devastate coral reef colonies (CMC, 1988). The reef damage and recovery are usually proportional to the storm size, frequency of occurrence, and the storm landfalls. Our interpretation of tropical storm tracks predicts that only the easternmost margin of Africa would be favored sites for the landfall of cyclones (Figure 13).

From this discussion, conditions were probably not propitious for coral reefs to thrive in the proto-Gulf. However, elsewhere we predict that fringing and barrier reefs would have developed parallel to the paleoshorelines with the deposition of carbonate and probably evaporites in the back-reef lagoons due to a negative P – E (Figure 6). Any sea-floor spreading-related volcanoes, terranes, or tectonically uplifted blocks in the sea that reached the photic zone would have served as the loci for development of either fringing reefs or, with subsidence, atolls.

CONCLUSIONS

The paleogeographic setting for the Western Tethys Sea places it in the Northern Hemisphere tropics. Communication of the Tethys Sea with the Panthalassa Ocean became established in the Late Jurassic; however, workers do not agree necessarily on the precise timing of the complete event. Thus, as interpreted from the reconstruction and simulation, circulation in this part of the Tethys Sea is restricted at its western end.

The modeled Western Tethys Sea is characterized by warm tropical surface water and generally strong net evaporation (P < E). This created conditions for

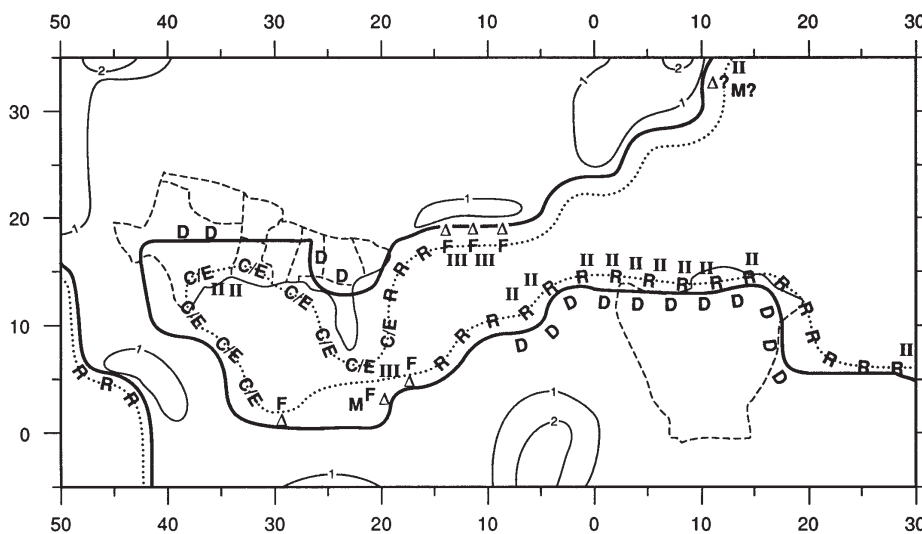


Figure 14. Source rock potential and reservoir rocks interpreted from upwelling, temperature, precipitation, soil moisture, and runoff for the Western Tethys Sea region. Dotted line = shelf break. Reservoir rocks: D = dune; DF = delta-fan complex; R = reef. Reservoir/Seal = C/E Carbonate/Evaporite. Kerogen types in source rocks: II = marine organic matter, oil prone; III = terrestrial organic matter, gas prone; M = Mixed types II and III. © 1993, George T. Moore.

low initial oxygen content (possibly 20–25% less than an average ocean) and elevated salinities. The denser water likely would sink and create a negative water balance system in which the deep water would flow eastward, flushing the deeper part of the basin.

Much of the margin receives insufficient precipitation to maintain lasting soil moisture or generate runoff to the sea in any season. The regions surrounding both northwest Africa and the northern proto-Gulf of Mexico are characterized by low precipitation and lack of soil moisture, which precluded development of a lush vegetative cover. Plant life would have been restricted to desert and semiarid xerophytic and halophytic types capable of surviving in a harsh environment. The general lack of runoff improves conditions for potential reef growth and carbonate deposition on the shelves and margins of this warm, clear, tropical sea. Marine sediments were not diluted by an influx of terrigenous sediments from land except in three localities.

Parts of the margins possess intense coastal upwelling in one season, alternating with weak periods in the other season. There is a high correlation of seasonal upwelling with high primary productivity on the margins of today's World Ocean. From this association, we predict that similar productivity rates existed in the coastal parts of the Late Jurassic Western Tethys Sea. However, due to predicted circulation patterns, except for the North Sea, offshore Newfoundland, Nova Scotia, and localities in Algeria, preservation would be limited.

In this study, model results correlate well with published regional lithofacies maps where data are available. This complement offers encouraging proof that this model generally replicates the real Late Jurassic paleoclimate by creating the proper physical conditions under which the biota existed and sediments were deposited. Because climatically sensitive sediments, as well as floras and faunas, relate to and are controlled by many physical and environmental factors, paleoclimatic data are an invaluable tool in interpreting their distribution. This includes interpolation between known outcrops or well bores in the subsurface, but also where the geologic record has been removed by erosion or destroyed by metamorphism.

ACKNOWLEDGMENTS

Much of this research was completed while GTM was employed by Chevron Oil Field Research Company at La Habra, California. We thank Chevron Petroleum Technology Company, its successor, for permission to publish this scientific material.

P.M. Harris and D.G. Morse provided helpful discussions and directed GTM to literature on reefs and dunes, respectively. The quality of the paper has been improved by the suggestions and contributions of J. Golonka and W. Visser who reviewed the manuscript.

L.F. Lynch typed the manuscript. J.L. Bube and J. Koishor prepared the figures.

REFERENCES CITED

- Barnard, P.C., and B.S. Cooper, 1981, Oils and source rocks of the North Sea area, *in* L.V. Illing and G.D. Hobson, eds., *Petroleum geology of the continental shelf of north-west Europe*: London, Heyden & Son Ltd., p. 169–175.
- Barnola, J.M., D. Raynaud, Y.S. Korotkevich, and C. Lorius, 1987, Vostok ice core provides 160,000-year record of atmospheric CO₂: *Nature*, v. 329, p. 408–414.
- Barron, E.J., 1985, Numerical climate modeling: A frontier in petroleum source rock prediction: results based on Cretaceous simulations: *AAPG Bulletin*, v. 69, p. 448–459.
- Barron, E.J., 1989, Severe storms in Earth history: *Geological Society of America Bulletin*, v. 101, p. 601–612.
- Barron, E.J., 1990, Climate and lacustrine petroleum source prediction, *in* B.J. Katz, ed., *Lacustrine basin exploration—case studies and modern analogs*: *AAPG Memoir* 50, p. 1–18.
- Barron, E.J., C.G.A. Harrison, J.L. Sloan, II, and W.W. Hay, 1981, Paleogeography. 180 million years ago to present: *Eclogae Geologicae Helvetica*, 74, p. 443–470.
- Barron, E.J., W.W. Hay, and S.T. Thompson, 1989, The hydrological cycle: a major variable during Earth history: *Palaeogeography, Palaeoclimatology, Palaeoecology*, 75, p. 157–174.
- Beauvais, L., 1973, Upper Jurassic hermatypic corals, *in* A. Hallam, ed., *Atlas of Palaeobiogeography*: New York, Elsevier, p. 317–328.
- Berner, R.A., 1990, Atmospheric carbon dioxide levels over Phanerozoic time: *Science*, 249, p. 1382–1386.
- Cecca, F., J. Azema, E. Fourcade, F. Baudin, R. Guiraud, L.-E. Ricou, and P. DeWever, 1993, Early Kimmeridgian (146 to 144 Ma), *in* J. Dercourt, L.-E. Ricou, and B. Vrielynch, eds., *Atlas Tethys Palaeoenvironmental Maps. Explanatory Notes*: BEICIP-FRANLAB, Rueil-Malmaison, p. 97–112.
- CMC (Conservation Monitoring Centre), 1988, Coral reefs of the world, Volume 2: Indian Ocean, Red Sea, and Gulf, *in* S. M. Wells, ed., *UNEP, Nairobi, Kenya, and IUCN*: Cambridge, U.K., 389 p.
- Cooper, B.S., and P.C. Barnard, 1984, Source rocks and oils of the central and northern North Sea, *in* G.J. Demaison and R. J. Murriss, eds., *Petroleum geochemistry and basin evaluation*: *AAPG Memoir* 35, p. 303–314.
- Demaison, G.J., and G.T. Moore, 1980, Anoxic environments and oil source bed genesis: *AAPG Bulletin*, v. 64, p. 1179–1209.
- Demaison, G.J., A.J.J. Holck, R.W. Jones, and G.T. Moore, 1984, Predictive source bed stratigraphy: a guide to regional petroleum occurrence—North Sea Basin and eastern North American continental margin: *Proceedings of the Eleventh World Petroleum Congress*, v. 2, London, 1983: New York, John Wiley & Sons, p. 17–29.
- Dercourt, J. (and 16 coauthors), 1985, *Présentation de 9 cartes paléogéographiques au 1/20,000,000°*

- s'étendant de l'Atlantique au Pamir pour la période du Lias à l'Actuel: Bulletin Société de France. Ser. 8, v. 1, p. 637–652, 9 maps.
- Dore, A.G., J. Vollset, and G.P. Hamar, 1985, Correlation of the offshore sequences referred to the Kimmeridge Clay Formation—relevance to the Norwegian sector, *in* B.M. Thomas et al., eds., *Petroleum geochemistry in exploration of the Norwegian Shelf*: London, Graham & Trotman, p. 27–37.
- Fawcett, P.J., E.J. Barron, V.D. Robison, and B.J. Katz, 1994, The climate evolution of India and Australia from the Late Permian to mid-Jurassic: a comparison of climate model results with the geologic record: *Geological Society of America Special Paper* 288, p. 139–157.
- Flügel, E., and E. Flügel-Kahler, 1992, Phanerozoic reef evolution: basic questions and data base—Jurassic: *Facies*, v. 26, p. 167–278.
- Fourcade, E., J. Azéma, F. Cecca, M. Bonneau, B. Peybernes, and J. Dercourt, 1991, Essai de reconstitution cartographique de la paléogéographie et des paléoenvironnements de la Tethys au Tithonique supérieur (138 à 135 Ma): *Bulletin de la Société Géologique de France*, 162, p. 1197–1208.
- Freeman, K.H., and J.M. Hayes, 1992, Fractionation of carbon isotopes by phytoplankton and estimates of ancient CO₂ levels: *Global Biogeochemical Cycles*, 6, p. 185–198.
- Fryberger, S.G., 1979, Dune forms and wind regime: *USGS Professional Paper* 1052, p. 141–169.
- Harland, W.B., R.L. Armstrong, A.V. Cox, L.E. Craig, A.G. Smith, and D.G. Smith, 1990, *Geological time scale 1989*: Cambridge University Press.
- Heckel, P.H., 1974, Carbonate buildups in the geologic record: a review, *in* L.F. Laporte, ed., *Reefs in time and space—selected examples from the recent and ancient*: Society of Economic Paleontologists and Mineralogists Special Publication 18, p. 90–154.
- Jones, R.W., 1987, Organic facies: *Advances in Petroleum Geochemistry*, v. 2, p. 1–90.
- Jones, R.W., and G.J. Demaison, 1982, Organic facies—stratigraphic concept and exploration tool, *in* A. Salvidar-Sali, ed., *Proceedings of the Second ASCOPE Conference and Exhibition*: Manila, p. 51–68.
- Kruijs, E., and E.J. Barron, 1990, Climate model prediction of paleoproductivity and potential source-rock distribution, *in* A.Y. Huc, ed., *Deposition of organic facies: AAPG Studies in Geology* 30, p. 195–216.
- Kutzbach, J.E., and A.M. Ziegler, 1993, Simulation of Late Permian climate and biomes with an atmospheric/ocean model: comparison with observations: *Philosophical Transactions of Royal Society of London, Series B* 341, p. 327–340.
- Locker, S.D., 1984, Lithofacies of Oxfordian (Upper Jurassic) rocks, *in* R.T. Buffler, S.D. Locker, W.R. Bryant, S.A. Hall, and R.H. Pilger, Jr., eds., *Ocean Margin Drilling Program, Gulf of Mexico, Atlas 6*: Woods Hole, Marine Science International, p. 27.
- Moore, G.T., D.N. Hayashida, and C.A. Ross, 1993, Late Early Silurian (Wenlockian) general circulation model—generated upwelling, graptolitic black shales, and organic-rich source rocks—an accident of plate tectonics?: *Geology*, 21, p. 17–20.
- Moore, G.T., D.N. Hayashida, C.A. Ross, and S.R. Jacobson, 1992a, Paleoclimate of the Kimmeridgian/Tithonian (Late Jurassic) World: I. Results using a general circulation model. *Palaeogeography, Palaeoclimatology, Palaeoecology*, 93, p. 113–150.
- Moore, G.T., L.C. Sloan, D.N. Hayashida, and N.P. Umrigar, 1992b, Paleoclimate of the Kimmeridgian/Tithonian (Late Jurassic) World: II. Sensitivity tests comparing three different paleotopographic settings: *Palaeogeography, Palaeoclimatology, Palaeoecology*, 95, p. 229–252.
- Moore, G.T., S.R. Jacobson, C.A. Ross, and D.N. Hayashida, 1994, A paleoclimate simulation of the Wenlockian (late Early Silurian) world using a general circulation model with implications for early land plant paleoecology: *Palaeogeography, Palaeoclimatology, Palaeoecology*, 110, p. 115–144.
- North, F.K., 1985, *Petroleum geology*: London, Allen & Unwin, 607 p.
- Peterson, F., 1988, Pennsylvanian to Jurassic eolian transportation systems in the western United States: *Sedimentary Geology*, 56, p. 207–260.
- Pindell, J.L., 1985, Alleghenian reconstruction and subsequent evolution of the Gulf of Mexico, Bahamas, and Proto-Caribbean: *Tectonics*, 4, p. 1–39.
- Poag, C.W., 1985, Depositional history and stratigraphic reference section for central Baltimore Canyon Trough, *in* C.W. Poag, ed., *Geologic evolution of the United States Atlantic Margin*: New York, Van Nostrand Reinhold Company, p. 217–264.
- Powell, T.G., 1982, Petroleum geochemistry of the Verriell Canyon Formation; a source for Scotian shelf hydrocarbons: *Bulletin of Canadian Petroleum Geology*, v. 30, p. 167–179.
- Powell, T.G. and L.R. Snowden, 1980, Geochemical controls on hydrocarbon generation in Canadian sedimentary basins, *in* A.D. Miall, ed., *Facts and Principles of World Petroleum Occurrence: Canadian Society Petroleum Geologists Memoir* 6, p. 421–466.
- Roberts, L., 1987, Coral bleaching threatens Atlantic reefs: *Science*, 238, p. 1228–1229.
- Ross, C.A., G.T. Moore, and D.N. Hayashida, 1992, Late Jurassic paleoclimate simulation—paleoecological implications for ammoniod provinciality: *Palaios*, 7, p. 487–507.
- Ross, M.I., and C.R. Scotese, 1988, A hierarchical tectonic model of the Gulf of Mexico and Caribbean region: *Tectonophysics*, 155, p. 139–168.
- Roth, P.H., 1986, Mesozoic palaeoceanography of the North Atlantic and Tethys oceans, *in* C.P. Summerhayes and N.J. Shackleton, eds., *North Atlantic Palaeoceanography: Geological Society Special Publication* 21, p. 299–320.
- Rowley, D.B., 1991, Preliminary Jurassic reconstructions of the Circum-Pacific region, *in* G. Westermann,

- ed., *The Jurassic of the Circum-Pacific: IGCT Project 171*, Cambridge University Press, p. 15–27.
- Salvador, A., 1987, Late Triassic–Jurassic paleogeography and origin of Gulf of Mexico Basin: *AAPG Bulletin*, 71, p. 419–451.
- Scotese, C.R., and J. Golonka, 1992, *Paleogeographic Atlas: PALEOMAP Project*: University of Texas at Arlington, Arlington, TX.
- Scotese, C.R., and C.P. Summerhayes, 1986, Computer model of paleoclimate predicts coastal upwelling in the Mesozoic and Cenozoic: *Geobyte*, 1, p. 28–42.
- Sloan, L.C., and E.J. Barron, 1992, A comparison of Eocene climate model results to quantified interpretations: *Palaeogeography, Palaeoclimatology, Palaeoecology*, 93, p. 183–202.
- Smith, A.G., A.M. Hurley, and J.C. Briden, 1981, *Phanerozoic paleocontinental World maps*: Cambridge University Press, 102 p.
- Stephan, J.-F., (and 14 coauthors), 1990, Paleogeodynamic maps of the Caribbean: 14 steps from Lias to Present: *Bulletin de la Société Géologique de France*, Ser. 8, v. VI, p. 915–919, 14 maps.
- Thomas, B.M., P. Moller-Pedersen, M.F. Whitaker, and N.D. Shaw, 1985, Organic facies and hydrocarbon distributions in the Norwegian North Sea, *in* B.M. Thomas et al., eds., *Petroleum geochemistry in exploration of the Norwegian Shelf*: London, Graham & Trotman, p. 3–26.
- Tissot, B.P., and H.D. Welte, 1984, *Petroleum formation and occurrence*: New York, Springer-Verlag, 699 p.
- Uchupi, E., C. Sancetta, J.D. Eusden, Jr., S.T. Bolmer, Jr., R.L. McConnell, and J.J. Lambiasi, 1984, Lithofacies of upper part of J_2/J_1 to J/J_1 sequences, *in* J.I. Ewing and P.D. Rabinowitz, eds., *Eastern North American continental margin and adjacent ocean floor, 34° to 41°N and 68°–78°W, Atlas 4*: Woods Hole, Marine Science International, 30 p.
- Ulmishek, G.F., and H.D. Klemme, 1990, Depositional controls, distribution, and effectiveness of World's petroleum source rocks: *U.S. Geological Survey Bulletin* 1931, 59 p.
- USNOO, 1967, *Oceanographic atlas of the North Atlantic Ocean, Section II, physical properties*: Washington, D.C., U.S. Naval Oceanographic Office, 300 p.
- Valdes, P.J., and B.W. Sellwood, 1992, A paleoclimate model for the Kimmeridgian: *Palaeogeography, Palaeoclimatology, Palaeoecology*, 95, p. 47–72.
- Washington, W.M., and D.L. Williamson, 1977, A description of the NCAR global circulation models, *in* J. Chang, ed., *Methods in Computational Physics*: New York, Academic Press, p. 111–169.
- Ziegler, P.A., 1988, Evolution of the Arctic-North Atlantic and the western Tethys: *AAPG Memoir* 43, 198 p.
- Ziegler, A.M., C.R. Scotese, and S.F. Barrett, 1983, Mesozoic and Cenozoic paleogeographic maps, *in* P. Brosche and J. Sündermann, eds., *Tidal Friction and the Earth's Rotation II*: Berlin, Springer, p. 240–252.

Paleoclimatic Controls on Neocomian–Barremian (Early Cretaceous) Lithostratigraphy in Northern Gondwana's Rift Lakes Interpreted from a General Circulation Model Simulation

George T. Moore

Eric J. Barron

Karen L. Bice

*The Pennsylvania State University
University Park, Pennsylvania, U.S.A.*

Darryl N. Hayashida

*Chevron Petroleum Technology Company
La Habra, California, U.S.A.*

ABSTRACT

By the earliest Cretaceous, a meridionally oriented rift system began splitting Northern Gondwana into the respective continents of South America and Africa. The system terminates abruptly against the Falkland-Agulhas transform on the south and the St. Paul–Romanche transform to the north, which give the boundaries to the present-day South Atlantic Ocean. This 5000 km long system created an elongated, segmented, complex series of rift valleys that were the settings for lakes ranging in age from Neocomian through Barremian. Various geologic factors defined the major segmentations of the margin and ultimately controlled basin dimensions. Early in the history of these basins, the lakes occupying some basins became anoxic, allowing organic-rich sediments to accumulate.

These source rocks and their generated oils have been shown through geochemistry and biomarker studies to change character north of the Rio Grande Rise–Walvis Ridge complex toward the interior of Northern Gondwana. The southern rift lake basins that evolved into the Santos, Campos, and Espirito Santo basins on the South American margin and the Angola, Congo, Cabinda basins on the African margin generated oils from source rocks originally deposited in saline to brackish water anoxic lakes. In the more continental interior basins of Sergipe-Alagoas, Potiguar (South America), and Gabon (Africa) the organic-rich sediments were deposited in freshwater lakes that were dysaerobic to anoxic. These relationships imply

evaporative conditions in the south and a net positive water balance in the interior of Northern Gondwana, far-removed from a convenient moisture source.

However, when the rift lakes are plotted on paleoclimate maps derived from a general circulation model (GCM) simulation this apparent paradox is readily explainable. The southern saline-brackish lakes are in an arid region. In contrast, the freshwater lakes are in a region affected by a massive, seasonal system of monsoonal and trade wind-dominated precipitation that covers most of the northern portion of the continent. This exemplary integration of geochemistry and paleoclimate modeling elucidates the absolute requirement of multidisciplinary approaches to resolving regional questions related to geological processes that control the formation of sedimentary rocks.

INTRODUCTION

Between the Tithonian (latest Jurassic) and Cenomanian (early Late Cretaceous) a northward-propagating rift system split Northern Gondwana into the two present continents of South America and Africa (Brice et al., 1982; Gerrard and Smith, 1982; Ojeda, 1982; Asmus and Baisch, 1983; Reyre, 1984; Edwards and Bignell, 1988; McHargue, 1990) (Figure 1). This rifting event created a series of parallel, elongate depressions along both margins in which paleoclimatic conditions favored the development of lakes.

They range in age from Neocomian (Berriasian, Valanginian, Hauterivian) to Barremian (Early Cretaceous) 145.5 to 124.5 Ma (Harland et al., 1990). Most contain organic-rich lacustrine source rocks which vary regionally in richness and kerogen content. As both margins contain these rift lake systems, a dual rift model of two propagating megafault systems proposed by Bradley (1992) for the northeastern Brazilian and Gabon basins cannot be discounted. Major rifting, which produced the initial separation of the continents, was well underway in the Berriasian (143.8 Ma) (Scotese and Golonka, 1992). The basal rocks in each

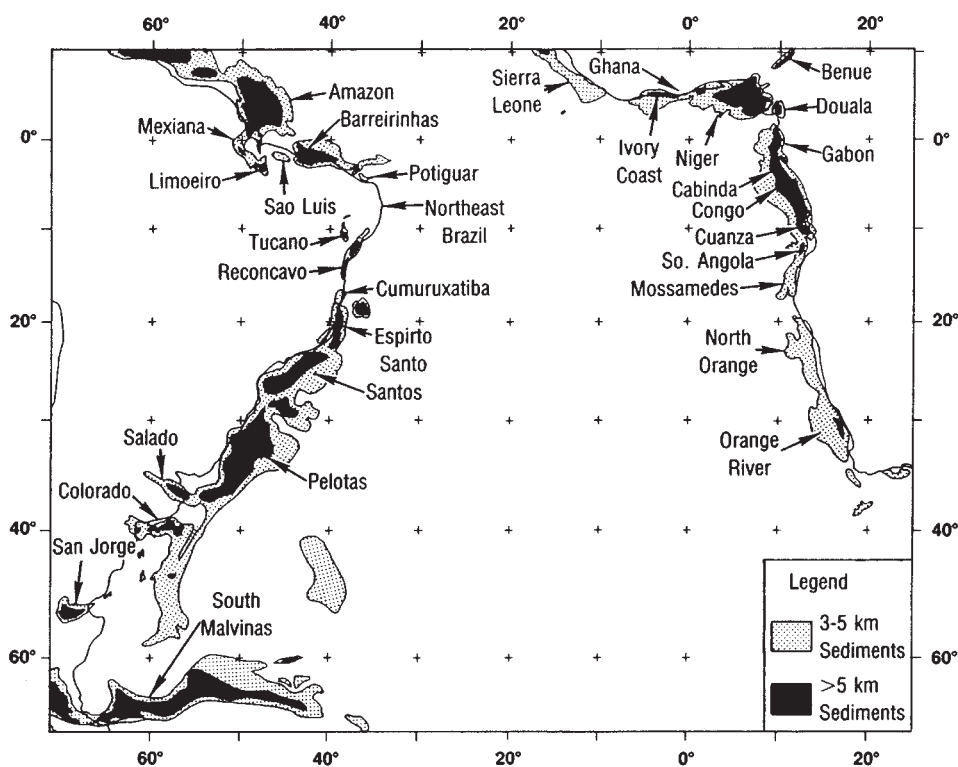


Figure 1. Distribution of syn- and post-breakup depocenters on conjugate South American and African margins. © 1993, George T. Moore.

basin are composed of siliciclastics with varying amounts of associated volcanics. Radiometric dates of the volcanics cluster around the Jurassic–Cretaceous boundary (Edwards and Bignell, 1988) at a date of 145.5 Ma (Harland et al., 1990). The rifting propagated northward and, by Aptian time, had completed the fragmentation of the region between the Falkland-Agulhas and St. Paul–Romanche transforms. In this paper we focus on the lacustrine rift basins north of the volcanic complex of the Rio Grande Rise and Walvis Ridge (Ojeda, 1982); however, similar time-equivalent, lacustrine organic-rich sediments were deposited in rift valleys of the Orange River Basin on the southern Namibia and Republic of South Africa (ROSA) margins (Muntingh, 1993; Figure 1).

The rifting event created basins suitable for development of a series of lakes beginning in the southwest region of Gondwana and continuing northeastward into the interior. The Gondwana Rift Lake System (GRLS) extended over 45° of latitude, approximately 5000 km, formed the South Atlantic ultimately, and created the coastal margins of many South American and African countries (Figure 2). Numerous local names are applied to the organic-rich lacustrine sediments, most of which are shales in these various rift basins (Table 1).

In this study we use a Kimmeridgian–Tithonian (Late Jurassic) paleoclimate simulation (Moore et al., 1992a). This does not represent the precise Neocomian–Barremian time interval under discussion, but the input boundary conditions of paleogeography and paleotopography are reasonably close and warrant its application for studying the GRLS and the regional variation in the content, quality, and concentration of organic matter. The objective of this study is to determine if the modeled paleoclimate will provide an insight into the early depositional history of these syn-rift source rocks.

Paleoclimate and paleogeography have been shown to be major factors in controlling the distribution of

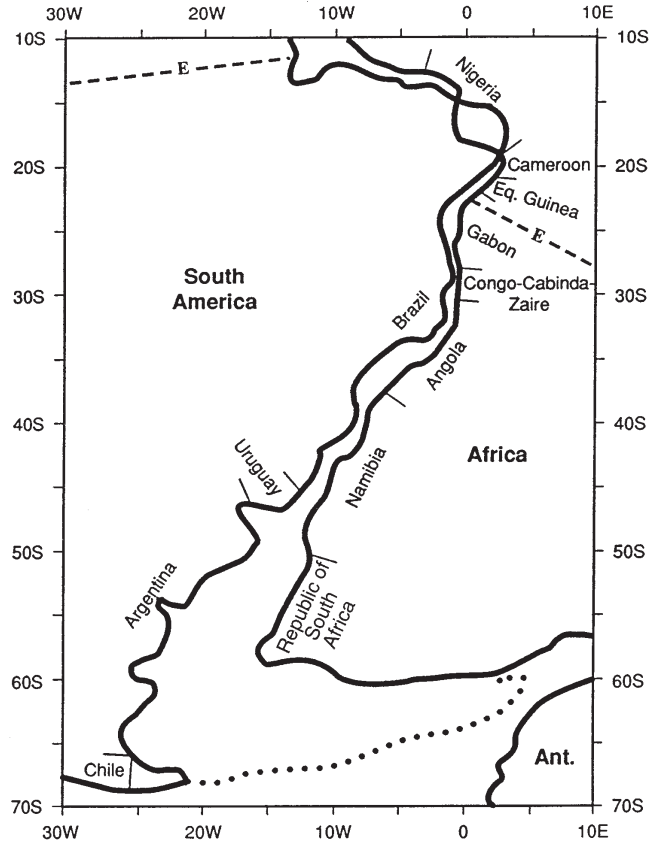


Figure 2. Detail of Gondwana Rift Lake System (GRLS) area showing approximate country boundaries along conjugate margins of South America and Africa. Dotted line = extension of Falkland Plateau. E = present-day equator. Overlap of boundaries near 15°S lat. and 0° long. is caused by the Tertiary growth of the Niger delta (southwest-pointing curve). Coastal boundaries between countries are repeated on all maps for reference. © 1993, George T. Moore.

Table 1. Formational names of Neocomian and Barremian (Early Cretaceous) lacustrine source rocks in basins on the conjugate margins of South America and Africa. Basins are shown in their approximate positions relative to one another.

| South America | | Africa | |
|-----------------|-----------------------|-----------------------|---------------------|
| Basin | Formation | Formation | Basin |
| Sergipe-Alagoas | Barra do Itiuba/Ibura | | |
| Jatoba-Tucano | L. Cretaceous shales | | |
| Reconcavo | Candeias/Lilhas | Melania/Kissenda | Gabon |
| | | Bucomazi | Cabinda |
| | | Marne de Pointe Noire | Congo |
| Espirito Santo | Jiquia | Bucomazi | Angola |
| Campos | Lagoa Feia | Cuvo | Cuanza |
| Santos | Guaratiba | | |
| | Rio Grand Rise | | Walvis Ridge |
| | | "Graben fill" | Orange River |

From: Muntingh, 1993; McHargue, 1990; Smith, 1990; Mohriak et al., 1990; Burwood et al., 1990; Teisserenc and Villemin, 1989; Talbot, 1988; Estrella et al., 1984; Reyre, 1984; Ojeda, 1982.

lakes, their water chemistry, biologic productivity, and ultimate organic matter preservation (Katz, 1990). Barron (1990) investigated the paleoclimatic variables that influence sedimentation in the lacustrine environment. He used results from a present-day GCM simulation to establish the hydrologic conditions suitable for lake formation. Then he evaluated the potential for stability and stratification of the water mass and organic preservation using temperature, water balance, precipitation-minus-evaporation ($P - E$), and storm tracks (Barron, 1989).

NATURE OF RIFT LAKES

By their nature, lakes are typically ephemeral; however, the most persistent and largest class of lakes is that of tectonic origin (Katz, 1990). The lakes in this study largely spanned the Neocomian and extended into the Barremian, a maximum interval of 21 m.y. (Harland et al., 1990). Lakes formed in a rift setting generally are elongate with a relatively low maximum width-to-depth ratio which tends to minimize wind-driven vertical mixing (Katz, 1990). The wind velocity, persistence, and its direction with respect to the orientation of the lake axis affect the mixing depth as well as complete turnover (Talbot, 1988; Katz, 1990). Talbot (1988) has shown a strong correlation between permanent stratification (or only episodic mixing) in the present rift-related African tropical lakes of significant size and high total organic carbon (TOC) values of organic matter in the bottom sediments. However, exceptions occur and, in such cases, primary productivity is a factor (Talbot, 1988).

Climate exerts a dominant role on the chemistry of lakes which, in turn, regulates the rate and type of productivity, water column stability, and the preservation of organic matter in the bottom sediments (Reyre, 1984; Powell, 1986; Mello et al., 1988a, b; Talbot, 1988; Burwood et al., 1990; Mohriak et al., 1990). The groundwater delivery of dissolved nutrients to the basin and the creation of lake margin ever-wet conditions for the growth of algal mats (De Deckker, 1988) are both conducive to increased productivity of lacustrine organic matter. Finally, productivity in lakes can also be influenced by bedrock lithology and structure.

Organic-rich lacustrine shales and carbonates have produced large reserves of oil and/or gas and, under ideal circumstances, prolific petroleum provinces (Smith, 1990). Early Cretaceous (pre-Aptian) rocks in basins on the conjugate margins of South America and Africa are related tectonically, paleoclimatically, and thereby stratigraphically. Collectively, they contain huge petroleum reserves, including ten basins that each contain in excess of 0.5 billion barrels of oil (BBO) (Moore, 1990). Although the association has long been discussed in the literature, Mello et al. (1992) were the first to provide a comprehensive organic geochemical study and overview of the lacustrine source rock and oil consanguinity. Their study revealed that 95% (20 BBO) of the oil in place on the Brazilian margin is lacustrine sourced, whereas only 10% (11 BBO) on the

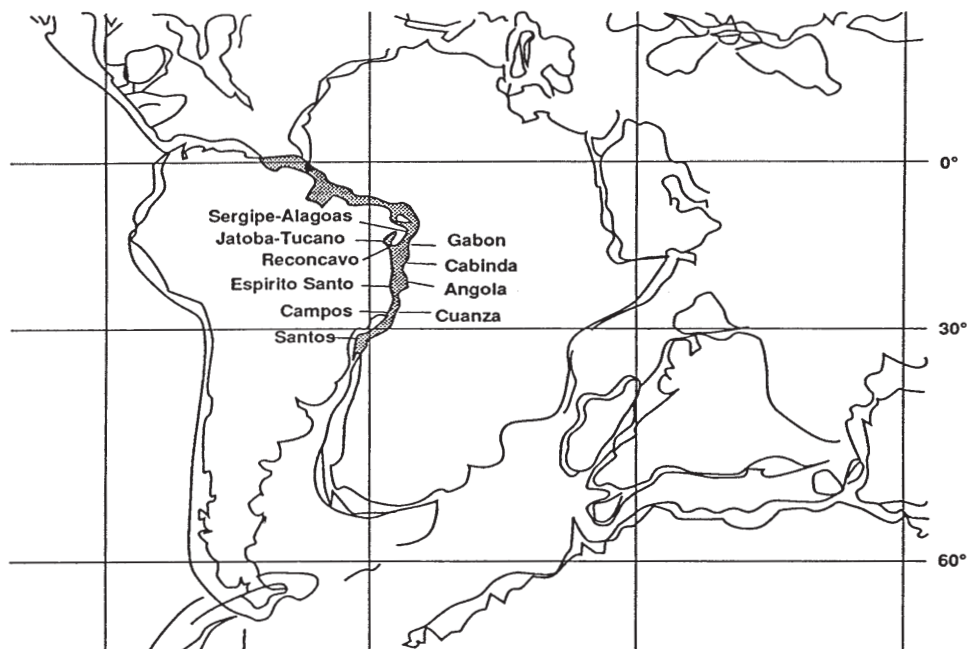
African margin is so sourced. The African figures are skewed by the major petroleum province of the Tertiary Niger delta, for which no Brazilian counterpart exists. When viewed in the context of just the lacustrine source rocks, a 2:1 ratio favoring South America does not present any paradox. As Mello et al. (1992) pointed out, this overall imbalance reflects nonsymmetrical separation between the two continents, differing maturation levels, and exploration to date. Recent deep-water discoveries in the Campos Basin add a potentially vast amount of lacustrine-sourced oil to Brazil's reserves (Franke, 1992).

DEPOSITIONAL ENVIRONMENTS FROM GEOCHEMISTRY

The rift lakes on the South American margin lie within the boundaries of one country, Brazil, and its national oil company, Petrobras, has been in the forefront of basin (Estrella et al., 1984; Mohriak et al., 1990; Trindade and Brassell, 1992) and regional (Mello et al., 1988a, b; Mello and Maxwell, 1990) geochemical studies on source rocks and oils. The published literature therefore contains a comprehensive description of the lacustrine source rock characteristics and paleolatitudinal variation in quality and kerogen type for the South American rift basins (Mello and Maxwell, 1990). The opposite African conjugate margin represents the antithesis. Until recently (Mello et al., 1992), studies on the African margin from ROSA to Gabon characteristically are country or basin specific (Gerrard and Smith, 1982; Muntingh, 1993 [ROSA]; Brice and Pardo, 1980; Brice et al., 1982; McHargue, 1990 [Angola]; Reyre, 1984; Burwood et al., 1990 [Congo]; Brice et al., 1980; Teisserenc and Villemin, 1989; Bradley, 1992 [Gabon]). As the synrift, lacustrine, organic-rich sediments were deposited in subparallel or, indeed, the same basins along the approximate 5000 km of this conjugate margin (Figure 3), the physical and paleoclimatic factors that controlled deposition on the South American margin were replicated on the African margin. Consequently, conclusions reached by the Brazilian workers can apply as well to the basins on the African margin.

A major regional variation occurs in the nature of the source rocks from south to north in the Brazilian marginal basins. The herbaceous and wood/coaly, type III kerogen content increases from the southern Campos and Espirito Santo basins (5–15%) to the Bahia Sul, Sergipe-Alagoas, and more northern basins (5–50%) (Mello and Maxwell, 1990). The regional variation in kerogen types correlates with and is related to the differing lacustrine environments of deposition from saline in the south to freshwater in the north (Mello et al., 1988b; Mello and Maxwell, 1990). Mello et al. (1988b) used geochemical biomarkers to differentiate the lacustrine and marine depositional environments of Brazilian Cretaceous source rocks and oils generated from them. On the African margin off Angola, Burwood et al. (1990) reported kerogen types I and II assemblages in a "transitional lacustrine to mainly marine" (saline) depositional environment.

Figure 3. Reconstruction at 120 Ma showing location of Early Cretaceous rift basins with lacustrine oil shale deposits in the GRLS area. Modified from Smith (1980). © 1993, George T. Moore.



Northward in Gabon, the organic-rich sediments were deposited in brackish to freshwater environments (Brice et al., 1980). These parallel the interpretation on the Brazilian margin. Rock-Eval pyrolysis data from three representative wells in basins from Angola to Gabon show a general northward decline in TOC and hydrogen index (HI) (mg HC/g TOC) values from well above 2% TOC and >300 HI to values of <0.5% TOC and 150 HI. Oxygen index (mg CO₂/g TOC) values increase to >200 in Gabon (Figure 4; and other unpublished Chevron data).

These data from both South American and African margins indicate a progressive increase in a type III kerogen component of terrigenous organic matter toward the interior of Gondwana. This regional northward change in rift lake chemistry from saline to freshwater reflects increasing availability of rainwater and higher precipitation rates toward the interior of a giant compound continent. Empirical models based on geologic data (Robinson, 1973; Hallam, 1982, 1984; Parrish et al., 1982; Parrish, 1988) as well as GCM simulations (Kutzbach and Gallimore, 1989; Moore et al., 1991) have shown that generally the interiors of large continents receive little precipitation and tend to be arid. Special factors or paleogeographical settings, however, can alter this generally valid observation. We believe that this paradox is both worthy of investigation and suitable for possible resolution using results from a GCM.

MODEL DESCRIPTION

The atmospheric GCM utilized in this study is the Community Climate Model (CCM). The CCM was developed for climate studies and weather prediction at the National Center for Atmospheric Research

(NCAR) in Boulder, Colorado. The evolution and characteristics of the model have been described by various authors (Barron, 1985a; Sloan and Barron, 1992; Moore et al., 1992a; Fawcett et al., 1994). The CCM was modified by E.J. Barron (1985b) for use in the study of paleoclimates. The reader is referred to any of the above papers and references cited therein for model details or a summary.

The hydrologic cycle employed in this model was investigated by Barron et al. (1989) using numerous simulations. They found that the CCM qualitatively reproduces present-day precipitation patterns rather well. Soil moisture in the model is based on a simple grid cell by grid cell P – E calculation frequently described as a “bucket” hydrology. Soil texture, color, and vegetative cover are not factors in regulating soil moisture in this model. When moisture in a grid cell accumulates to a value exceeding 15 cm, it is treated as runoff. In the model results, runoff tends to occur in areas of heavy precipitation. As the Late Jurassic to Early Cretaceous landscape is rather poorly understood, particularly on a global basis, this simplistic treatment of components in the hydrologic cycle may well approach the limits of our knowledge. Thus, the CCM and the geologic record may be compatible in terms of detail and sophistication.

The CCM results are from a seasonal simulation run to 17.0 yr. This version of the CCM is thermally and hydrologically, but not dynamically, coupled to a mixed-layer ocean 50 m deep. The ocean provides for heat storage and a moisture source, but not ocean heat transport. The model utilizes a 4.5° × 7.5° latitude/longitude scale grid cell.

The paleogeography (Figure 5) is set for the beginning of the Kimmeridgian. By latest Tithonian time (~145.6 Ma) communication had become established between the proto-Indian Ocean seaway (white area at

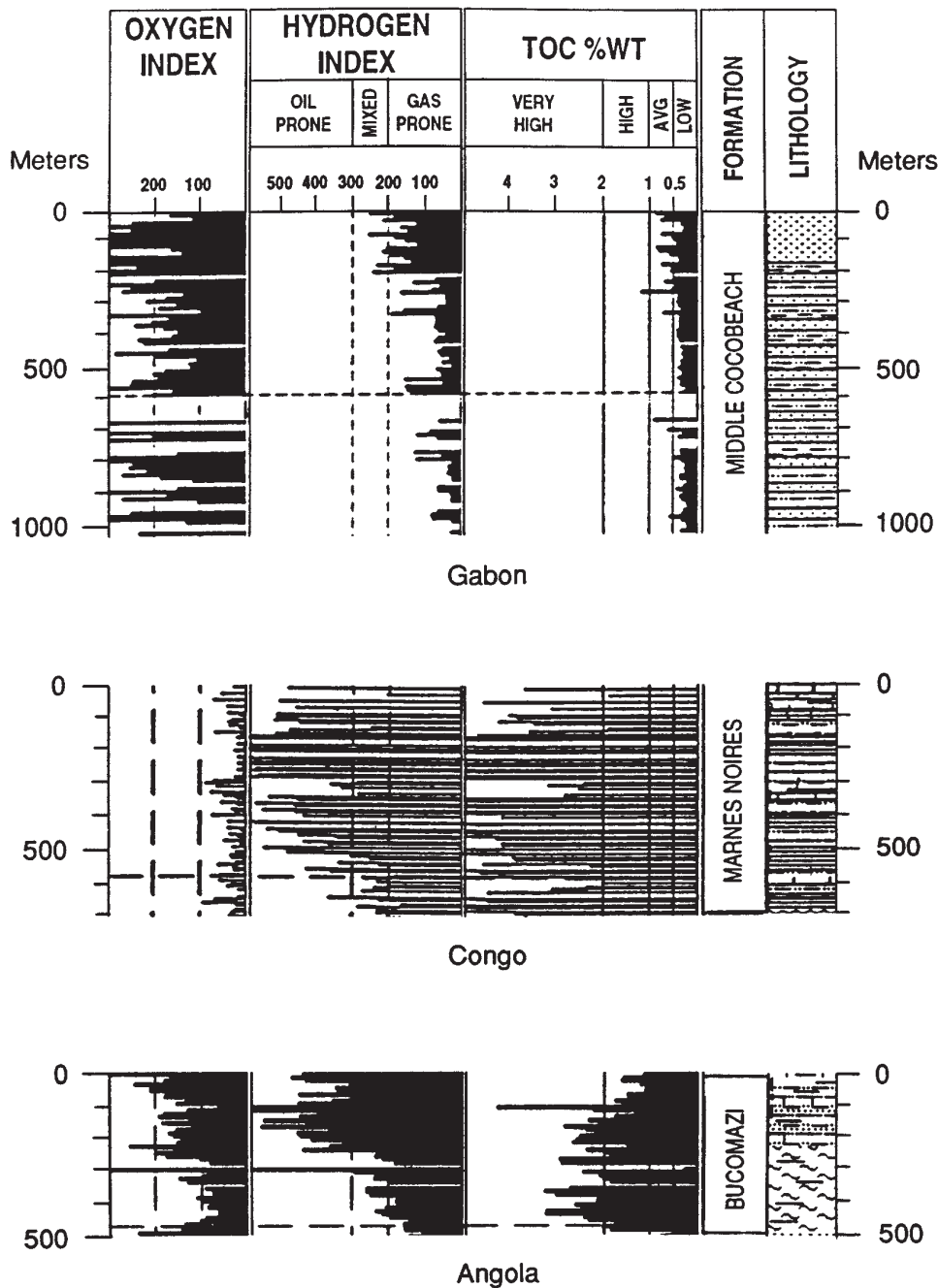


Figure 4. Change in the Neocomian–Barremian (Early Cretaceous) source rock character along GRLS trend on the African margin. Hydrogen and oxygen index values (HI, OI) derived from Rock-Eval pyrolysis and TOC weight percentages were obtained from three wells in the Chevron Overseas Petroleum Incorporated geochemical database at San Ramon, California. These portions of the geochemical logs are reproduced with Chevron's permission.

60°S, southeast corner of Figure 5) and the Panthalassa Ocean (white area in southwest corner of Figure 5). An early Neocomian reconstruction would show a continuous band of one to two rows of water grid cells near 60°–70°S. While previous studies (Ericksen and Slingerland, 1990) indicated that regional patterns generally are not affected by one grid cell-sized changes in land/water specifications, this modification could have some moderate impact on certain paleoclimate variables.

The simulation was run using an atmospheric CO₂ concentration of 1120 ppm, 4× the pre-Industrial level (Barnola et al., 1987). This is in general agreement with the range of published values by Berner (1990) and Freeman and Hayes (1992).

RESULTS AND DISCUSSION

The preservation of organic matter is adversely affected by three factors that can be readily obtained from a GCM simulation: seasonal temperature extremes, winter minimum temperature, and seasonal P – E. A large seasonal variation (>40 to 45°C) of the annual temperature cycle will promote seasonal overturn (Barron, 1990). A temperature minimum below 4°C (freezing point of fresh water) will cause seasonal overturn. A large difference (>5 mm d⁻¹) between winter and summer P – E will also promote seasonal lake overturn. High precipitation rates leading to a positive P – E can create sediment-laden turbidity currents that will oxygenate the lake bottom

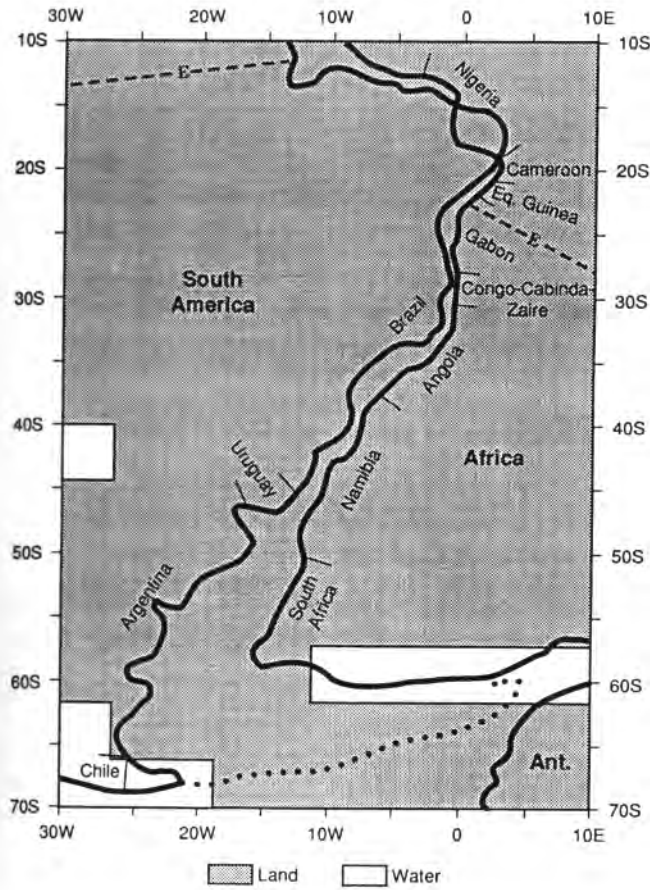


Figure 5. Distribution of land and water grid cells in model resolution for the GRLS area. © 1993, George T. Moore.

under certain conditions. However, while turbidity currents deliver oxygenated water to the lake bottom, individual gravity-flow events appear to have been short-lived in at least one anoxic Miocene basin (Anadón et al., 1988). In fact, in the anoxic bottom water of Lake Tanganyika, turbidity currents are an important control on the distribution of organic carbon-rich facies (Huc, 1988; Huc et al., 1990).

We use the following climate parameters that control the conditions under which lacustrine sediments are deposited: surface temperature, the hydrologic cycle (precipitation, P - E, soil moisture, runoff, mid-latitude storm tracks), and surface wind. The lakes contain varying thicknesses and qualities of lacustrine source rocks. The results have been used to evaluate stratigraphy along the Lower Cretaceous rift system by paleoclimate variation.

In this paper the results of the seasonal extremes December/January/February (Dec/Jan/Feb) and June/July/August (June/July/Aug) are evaluated using the criteria of Barron (1990) to examine the potential for stability of the GRLS and to examine three basins on the African margin: Angola, Congo/Cabinda, and Gabon (Figures 1 and 3; Table 1). Lacustrine sandstones are more common and organic richness appears to decrease in Gabon. Organic-rich

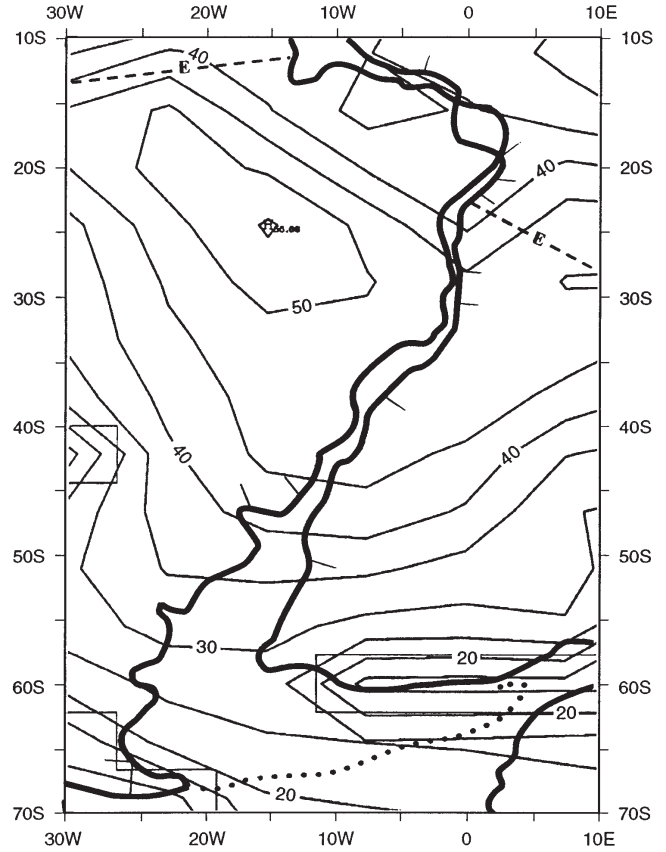


Figure 6. Dec/Jan/Feb surface temperature (°C) for the GRLS area. CI = 5°C. © 1993, George T. Moore.

shales are best developed in the Congo/Cabinda region (Figure 4).

SURFACE TEMPERATURE

Modeled surface temperatures show the changing seasonal conditions in the GRLS (Figures 6 and 7). In Dec/Jan/Feb, the summer temperature ranges from slightly under 30°C in ROSA to a high of 45°C, which peaks in the subtropics near 35°S, before progressively cooling northward. The June/July/Aug winter temperature gradient ranges from -5°C in the south to +30°C in the north. The 4°C isotherm is at the southern boundary of Angola (approximately 37°S). In the region to the south of the isotherm, lake surfaces will freeze in the winter. The associated fall and spring overturn will aerate the bottom. North of the 4°C isotherm, the lakes do not turn over and can be stable. The seasonal temperature variation does not exceed 45°C; however, in Namibia and the southern two-thirds of Angola, the seasonal range does exceed 40°C (Figure 8). Within the 40°C thermal high, predicting overturn is speculative. However, near the high's center, the likelihood of overturn due to temperature dif-

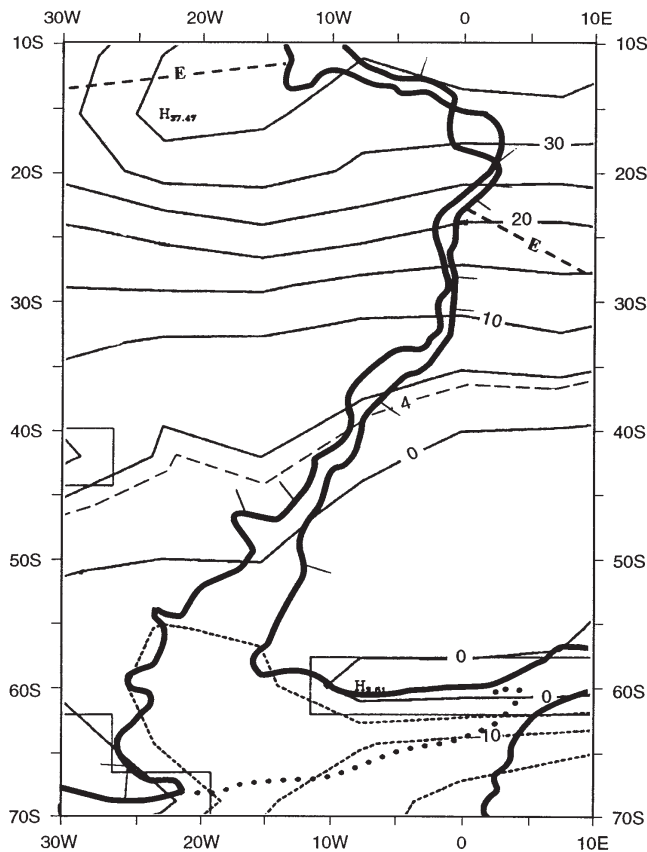


Figure 7. June/July/Aug surface temperature ($^{\circ}\text{C}$) for the GRLS area. CI = 5°C . © 1993, George T. Moore.

ferences would be probable. Thus, the rift lakes in present-day southern Angola and northern Namibia would be predicted to undergo seasonal overturn. The connection between the proto-Indian and Panthalassa oceans, which existed by latest Tithonian time, probably would tend to move the 4°C isotherm farther southward, moderate the seasonal temperature range to maintain an above-freezing winter temperature, and provide a moisture source. The presence of lacustrine source rocks containing types I and III kerogens in the Orange River Basin (Muntingh, 1993) supports the latter speculation.

HYDROLOGIC CYCLE

Introduction

Large-scale patterns of precipitation and evaporation are generally well simulated by the CCM (Barron et al., 1989). Regions of seasonal variation in precipitation, such as monsoons, where the driving mechanism is related to land-water distribution, and the seasonal state of the atmosphere likewise are well modeled. The CCM also is very good at predicting winter mid-latitude storm tracks. The location of these storm tracks is governed by the position of the jet stream. In this case, the paleogeography disrupts zonal circulation over Gondwana (Moore et al., 1992a). Where precipitation

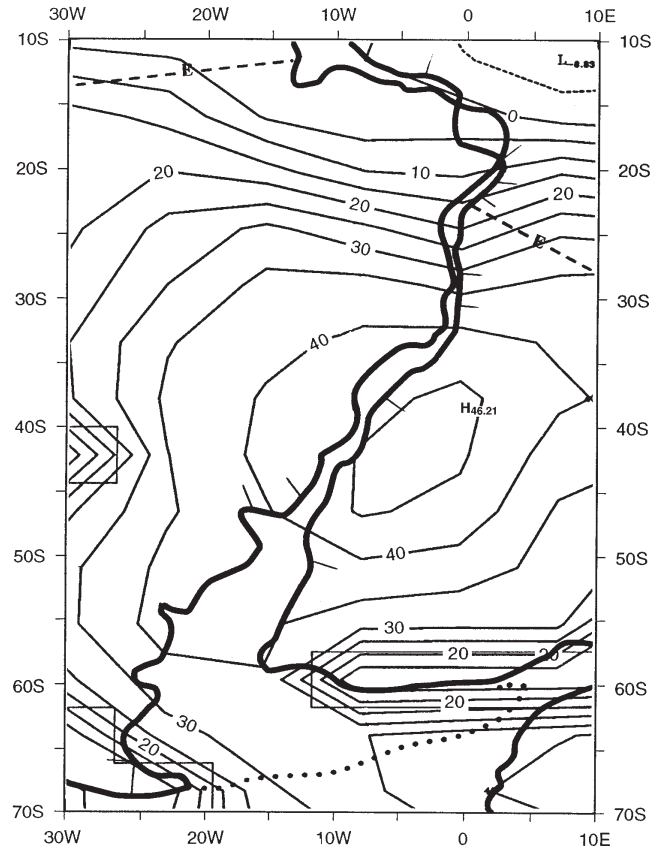


Figure 8. Seasonal temperature difference (Dec/Jan/Feb minus June/July/Aug) for the GRLS area. CI = 5°C . © 1993, George T. Moore.

is convective with high spatial and temporal variability (e.g., thunderstorms, tropical thermal cells) and at subgrid scale, the predictability of the model is poor. Paleotopography is important in defining boundary conditions because of the orographic effects caused by the uplifting and cooling of an air mass over mountains associated with the lapse rate. The CCM responds well to this phenomenon and its related precipitation (Moore et al., 1992b). In summary, the CCM is remarkable in predicting large-scale and orographic precipitation patterns; however, the magnitudes are less well quantified (Barron et al., 1989).

The hydrologic cycle-driven moisture patterns are consistent with the regional pattern of the GRLS, but the reader should bear in mind that spatial and temporal variability which occur in lacustrine deposits may be climate dependent but unresolvable with a GCM. Lake distribution, size, and structure are sensitive not only to the large-scale patterns of seasonal moisture balance simulated by the GCM, but also to local- and regional-scale variations in surface drainage patterns and groundwater flow. These parameters can change over an area smaller than an individual rift basin and within relatively short time periods. Such change could produce high variability in the horizontal and vertical distribution of saline versus freshwater lacustrine source sediments. Such variability has been documented in north African lakes during the Holocene

(Fontes et al., 1985; Fontes and Gasse, 1991) and is suggested for the Cretaceous lakes from the stratigraphy (Brice et al., 1980) and organic geochemistry (Mello et al., 1992).

Changes in surface drainage and groundwater flow patterns may also be closely tied to changes in seasonal precipitation patterns. The GCM used in the study simulates the position of the monsoon for a specified solar insolation forcing. However, insolation changes due to obliquity and precession may have produced variability in the intensity and distribution of seasonal maximum precipitation in African lakes during the Quaternary (Kutzbach and Street-Perrott, 1985; Spaulding, 1991) and in the Atlantic margin rift basins during the Cretaceous (Park and Oglesby, 1991). Energy-balance model simulations of the Milankovitch forcing on the intensity of Pangaean monsoons also compare well with inferred Triassic lake-level fluctuations (Crowley et al., 1992).

Evaporation rates reflect temperature, saturation of the air (relative humidity), and whether the grid cell is land or water (surface saturation). Evaporation from a land grid cell is limited to the amount of precipitation received or moisture stored in the soil. Regions of high continental precipitation almost always are regions of high evaporation. The surface hydrology is a simplistic P - E calculation. The P - E difference is an impor-

tant and valuable calculation in checking model results against the geologic record. Moore et al. (1992a) found an excellent correlation of evaporites with negative P - E values, and coals, as well as basins with type III kerogen source rocks, with positive P - E values in a Late Jurassic simulation. Where the moisture balance is negative, the paleoclimate is semiarid to arid. In such paleoclimatic belts, low sediment transport is to be expected (Cecil, 1990). Restricted fluvial environments improve lake conditions for organic matter preservation by limiting both sediment dilution due to river influx and oxygenation of the lake bottom by turbidity currents. In relatively saline lakes, the inflow of river water could form a freshwater cap and further promote stability of the water column.

Precipitation

To place the GRLS region in perspective, the study area is shown on the global total annual precipitation map (Figure 9). The map shows a lack of zonation. Rather, each continent forces its own pattern with moderate to high rainfall patterns on the eastern sides of continents, particularly Gondwana, and arid regions in the centers and mid-latitude western margins. These results support the conclusions of Parrish et al. (1982) and Hallam (1982, 1984) from biofacies and lithofacies data that the interiors of the continents were arid. The

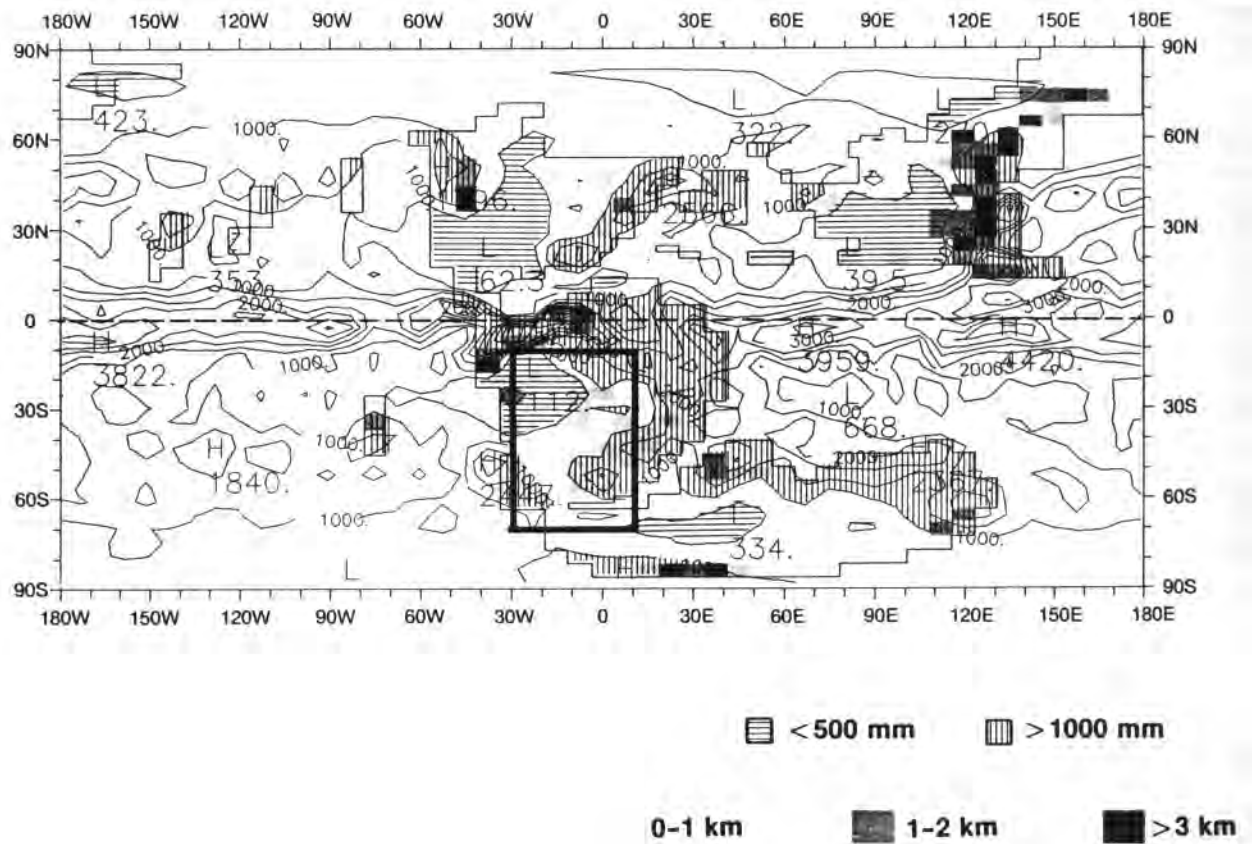


Figure 9. Total annual precipitation in mm yr⁻¹. CI = 500 mm. Continents and islands shown as outlines; elevations in patterns of grey. GRLS area outlined. Land areas with <500 mm and >1000 mm of precipitation are indicated by horizontal and vertical line patterns, respectively. © 1993, George T. Moore.

heavy precipitation (>1000 mm) in the northeast corner of the GRLS region was associated with a large center of intense monsoonal and trade wind-dominated precipitation that developed over northern Gondwana in Dec/Jan/Feb (Moore et al., 1992a).

Precipitation in the study area is shown for the changing seasonal conditions in the rift zone (Figures 10 and 11). During Dec/Jan/Feb, the northeast, north of Angola, was influenced by the northern Gondwana precipitation center (Figure 10). This center provided extensive moisture to the northeast GRLS area. South of the Congo, the region became progressively drier. In June/July/Aug, there were alternating bands of <2 mm per day (d^{-1}) and little more than 4 mm d^{-1} of precipitation (Figure 11). From southern Gabon to southern Namibia, the area was arid to semiarid.

Precipitation-Minus-Evaporation

On P - E maps the zero line divides where precipitation exceeded evaporation ($P - E > 0$: positive values and solid lines; $P - E < 0$: negative values and dashed lines). The annual P - E daily average can be used for predicting the occurrence of lakes. Any positive value would indicate moisture accumulation. Barron (1990) preferred using a minimum positive moisture balance of $>0.5 \text{ mm } d^{-1}$ for lake development and maintenance. The CCM's capability of predicting P - E for small values near zero cannot be modeled with confidence. In attempts to predict the distribution of pres-

ent-day large lakes using the GCM, regions of mean annual P - E values of $<0.5 \text{ mm } d^{-1}$ were found to include virtually all deserts, but also include some large, deep lakes fed by high volumes of seasonal precipitation, spring meltwater, and groundwater flow (Barron, 1990). The annual daily P - E average for the region showed values between 0 and $0.5 \text{ mm } d^{-1}$ over ROSA to central Namibia. Elsewhere the values ranged between 0 and $-0.5 \text{ mm } d^{-1}$ (Figure 12).

In Dec/Jan/Feb, the P - E balance was slightly negative throughout the entire GRLS region except for the extreme northeast corner from Nigeria south to northern Gabon (Figure 13). In June/July/Aug, the zero P - E contour passed through northern Angola, dividing the region from a barely negative balance to the north, to a slightly positive balance to the south (Figure 14). The principal conclusion drawn from these seasonal maps is that low regional variability characterizes both seasons. Barron (1990) suggested that regions where the difference between winter and summer P - E values was $>5 \text{ mm } d^{-1}$ would have been more likely to experience seasonal lakewater overturn. In no part of the rift lake system did the model-predicted difference between winter and summer P - E exceed $5 \text{ mm } d^{-1}$.

Soil Moisture

Soil moisture occurs where the P - E is positive. Soil moisture in Dec/Jan/Feb was associated with the large precipitation center and positive P - E area of the

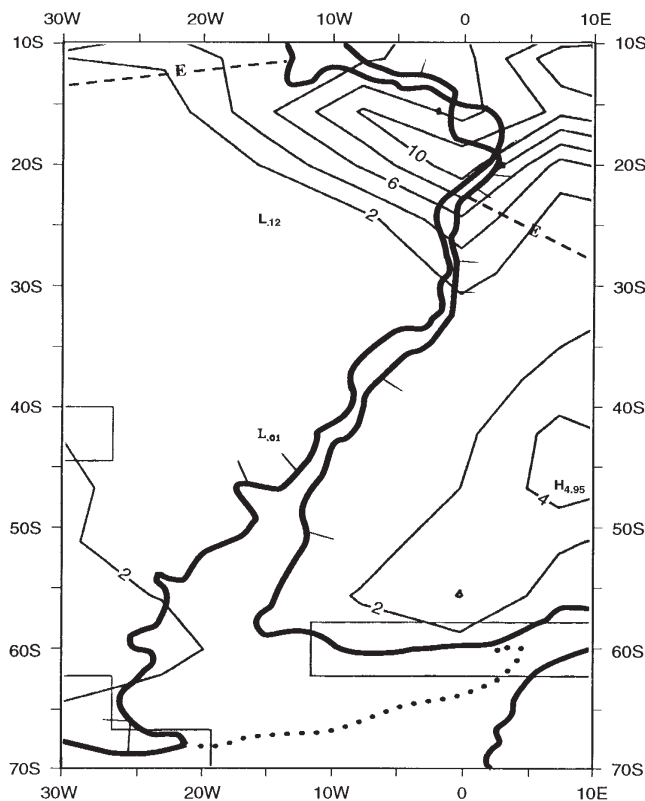


Figure 10. Dec/Jan/Feb precipitation for the GRLS area. CI = $2 \text{ mm } d^{-1}$. © 1993, George T. Moore.

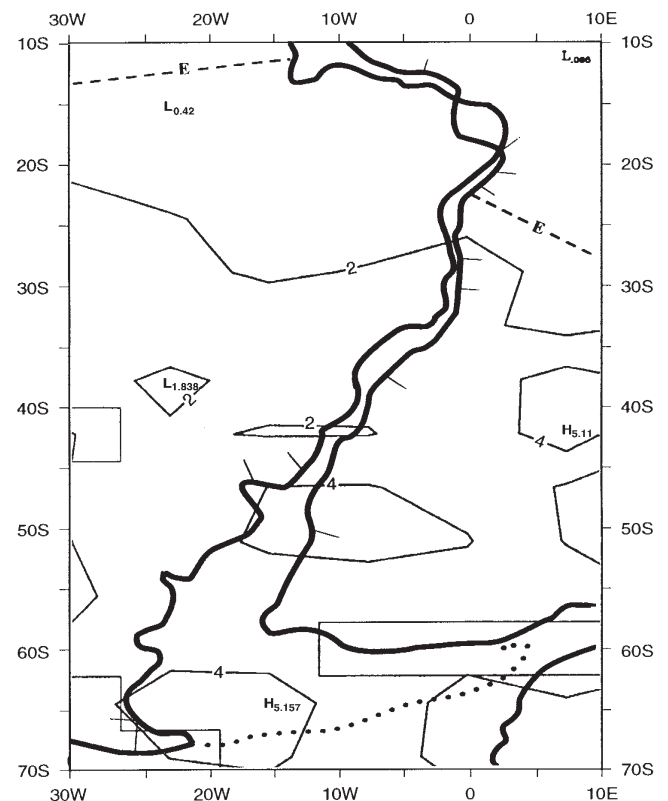


Figure 11. June/July/Aug precipitation for the GRLS area. CI = $2 \text{ mm } d^{-1}$. © 1993, George T. Moore.

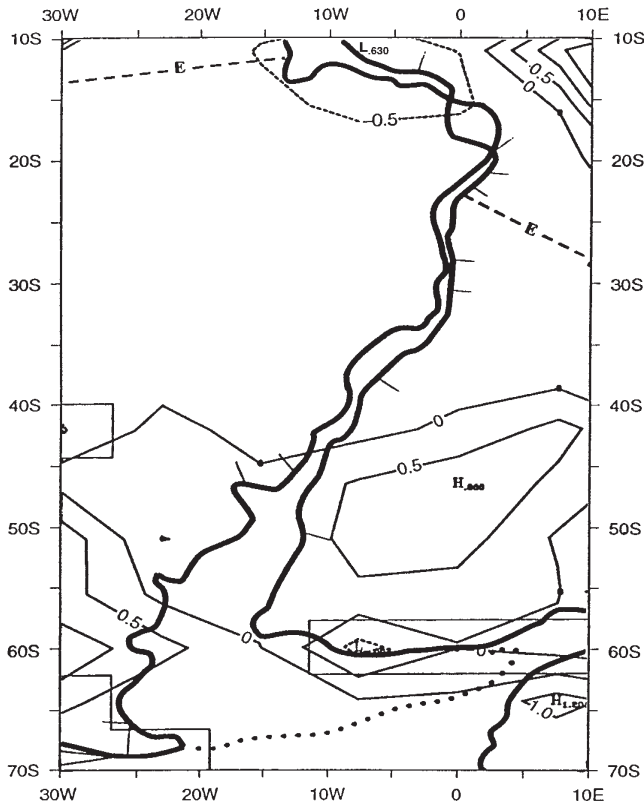


Figure 12. Mean annual P - E for the GRLS area. CI = 0.5 mm d⁻¹. Solid lines = net precipitation; dashed lines = net evaporation. © 1993, George T. Moore.

northeast (Figure 15). The winter June/July/Aug season contained soil moisture in the south (Figure 16). This reflected moderate precipitation and cooler temperatures. The results are that moisture in the soil evaporated less rapidly. Moving northward with increasing temperatures, soil moisture was progressively evaporated and the value approaches zero.

Runoff

Summer (Dec/Jan/Feb) runoff was associated with the precipitation center (Figure 17). Central Equatorial Guinea through northern Gabon received this runoff and the fluvial transport of siliciclastics into the area from the shield, probably the region of Cameroon that was to become the future Douala Basin (Figure 1). The runoff can account for the increasing amount of lacustrine sandstone and the dilution of organic matter by siliciclastics. This likewise may explain why the lacustrine source rock section of the Sergipe-Alagoas Basin has relatively low (~2%) TOC values, contains some type III kerogen, and is in a siliciclastic section (L. Trindade, 1992, personal communication). The correlation of lithostratigraphy with model results here is striking. Of equal significance is that not only do the real and simulated worlds compare well, but the actual cause of this lithostratigraphic change in the northeastern part of the GRLS area can be explained. The expan-

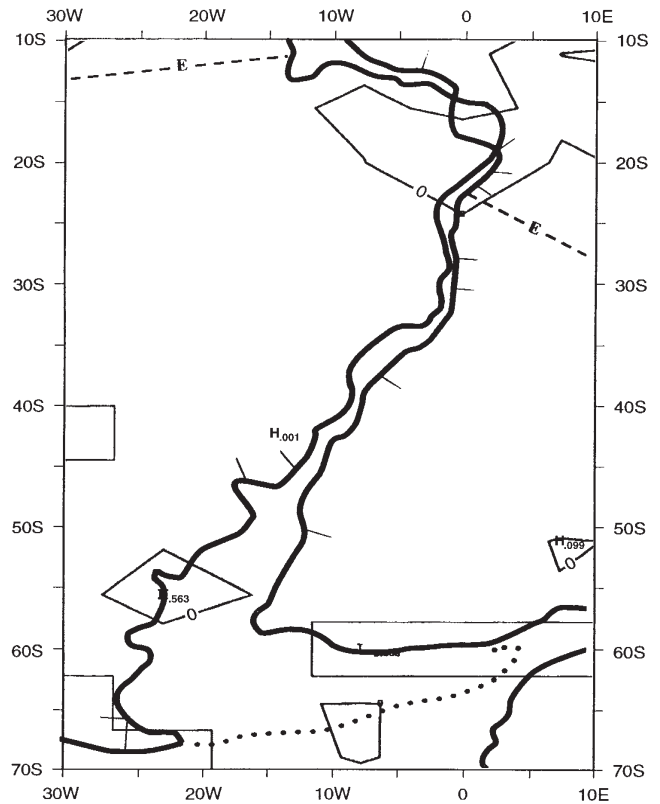


Figure 13. Dec/Jan/Feb P - E for the GRLS area. CI = 4 mm d⁻¹. Positive values = net precipitation; negative values = net evaporation. © 1993, George T. Moore.

sion of the Dec/Jan/Feb precipitation belt far into the interior of the continent is caused by three interrelated factors: (1) the extensive low-pressure system that developed over the interior of the continent; (2) the depression of the Intertropical Convergence Zone (ITCZ) to 30°S over Gondwana; and (3) the close association of Gondwana's northeast margin with the equatorially oriented, warm, tropical Tethys Sea and strong easterlies (Moore et al., 1992a). This quite remarkable correlation shows that, for large-scale phenomena, the CCM produces reliable results. During June/July/Aug there was insufficient moisture to produce runoff (Figure 18).

MID-LATITUDE WINTER STORM TRACKS

The importance of mid-latitude winter storms, the ability of the model to predict them, and their significance in the geologic record have been discussed by Barron (1989). The CCM does well at predicting these storms through the time-filtered standard deviation of the geopotential height field, the frequency of how often high- and low-pressure systems pass. Lakes positioned along these tracks would not be favored for source rock accumulation. Although the southern portion of the GRLS area lies within that latitudinal band,

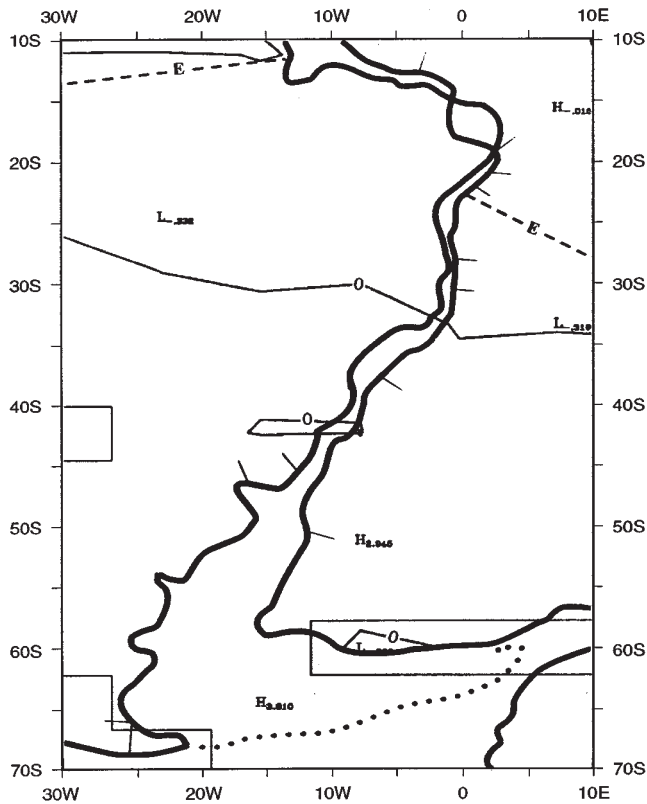


Figure 14. June/July/Aug P - E for the GRLS area. CI = 4 mm d⁻¹. Positive values = net precipitation; negative values = net evaporation. © 1993, George T. Moore.

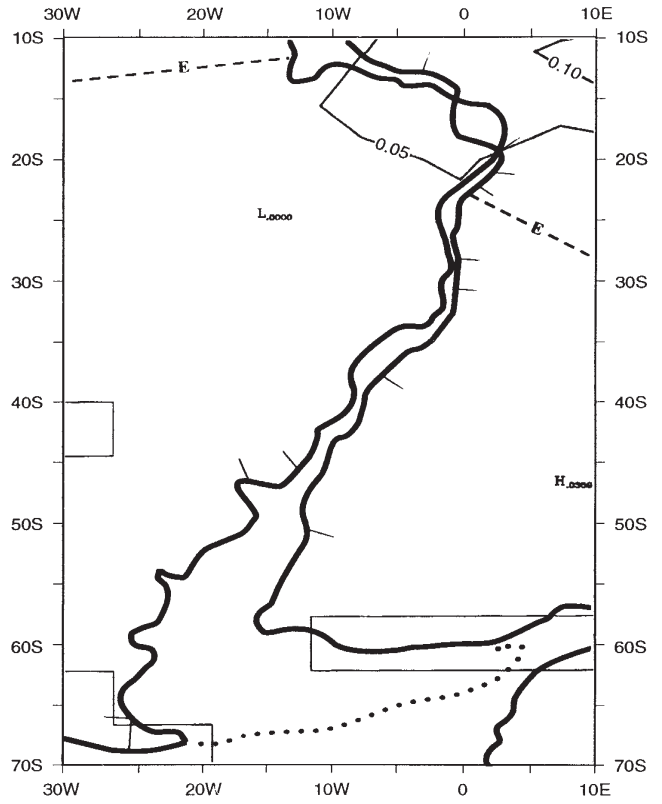


Figure 15. Dec/Jan/Feb soil moisture for the GRLS area. CI = 0.05 m. © 1993, George T. Moore.

the thermal inertia of Gondwana breaks down the zonal flow, weakens the polar front, and disrupts the storm tracks (Figure 19). Consequently, the southern GRLS area is not subjected to these storms.

SURFACE WIND

In addition to temperature and the hydrologic cycle, wind shear can play an important role in creating vertical instability in lakes (Talbot, 1988; Katz, 1990). Partial to complete mixing due to wind shear has been reported from certain African lakes (Talbot, 1988). The orientation of a lake with respect to a strong seasonal or prevailing wind will influence the rate of turnover (Livingston and Melack, 1984). Thus, to completely evaluate lakes in the geologic past, consideration must be given to the direction and velocity of seasonal as well as prevailing zonal winds. Wind vectors from a GCM simulation are the only method by which to quantify this parameter in terms of its effectiveness in causing lake turnover for the geologic past.

The northern and southern portions of the GRLS were influenced by Dec/Jan/Feb winds that reached in excess of 6 m s⁻¹ (Figure 20). Winds in excess of 6 m s⁻¹ are strong enough to move medium-sized sand and form dunes in arid regions (Fryberger, 1979). In Dec/Jan/Feb, the northern GRLS received strong

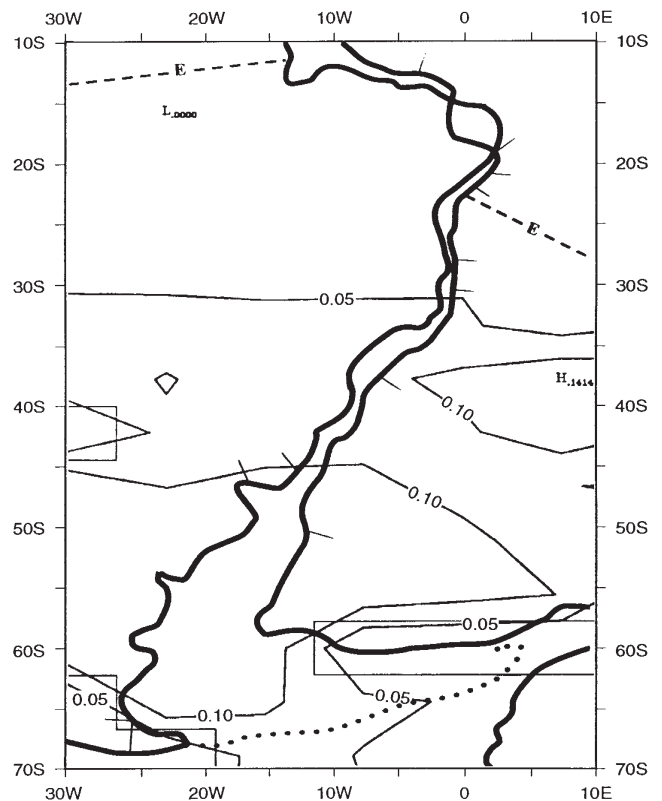


Figure 16. June/July/Aug soil moisture for the GRLS area. CI = 0.05 m. © 1993, George T. Moore.

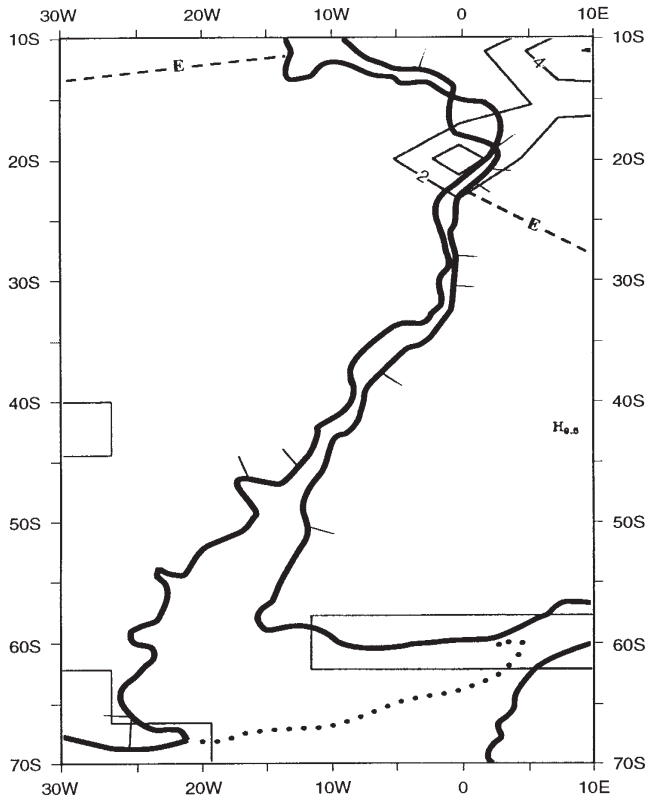


Figure 17. Dec/Jan/Feb runoff for the GRLS area. CI = 2 mm d⁻¹. © 1993, George T. Moore.

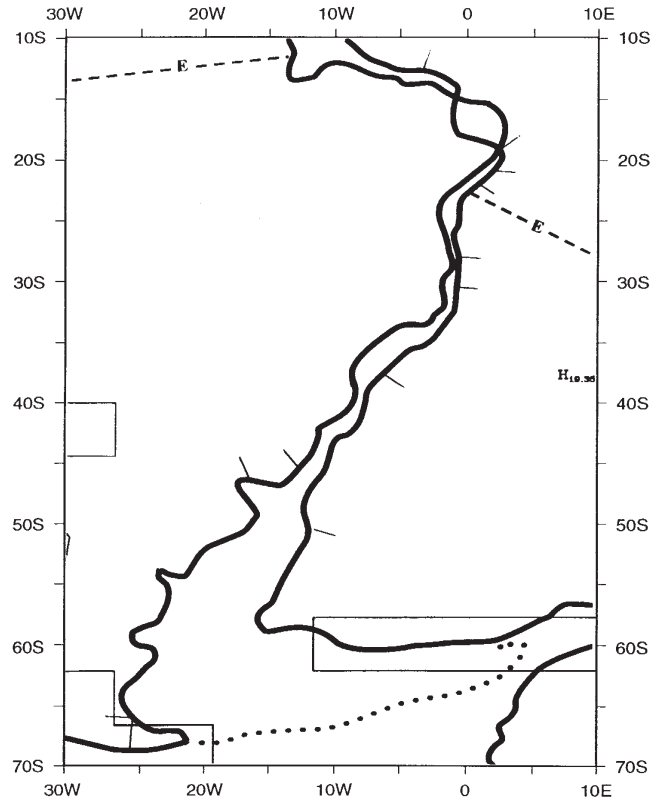


Figure 18. June/July/Aug runoff for the GRLS area. Note that there was insufficient moisture to produce runoff. © 1993, George T. Moore.

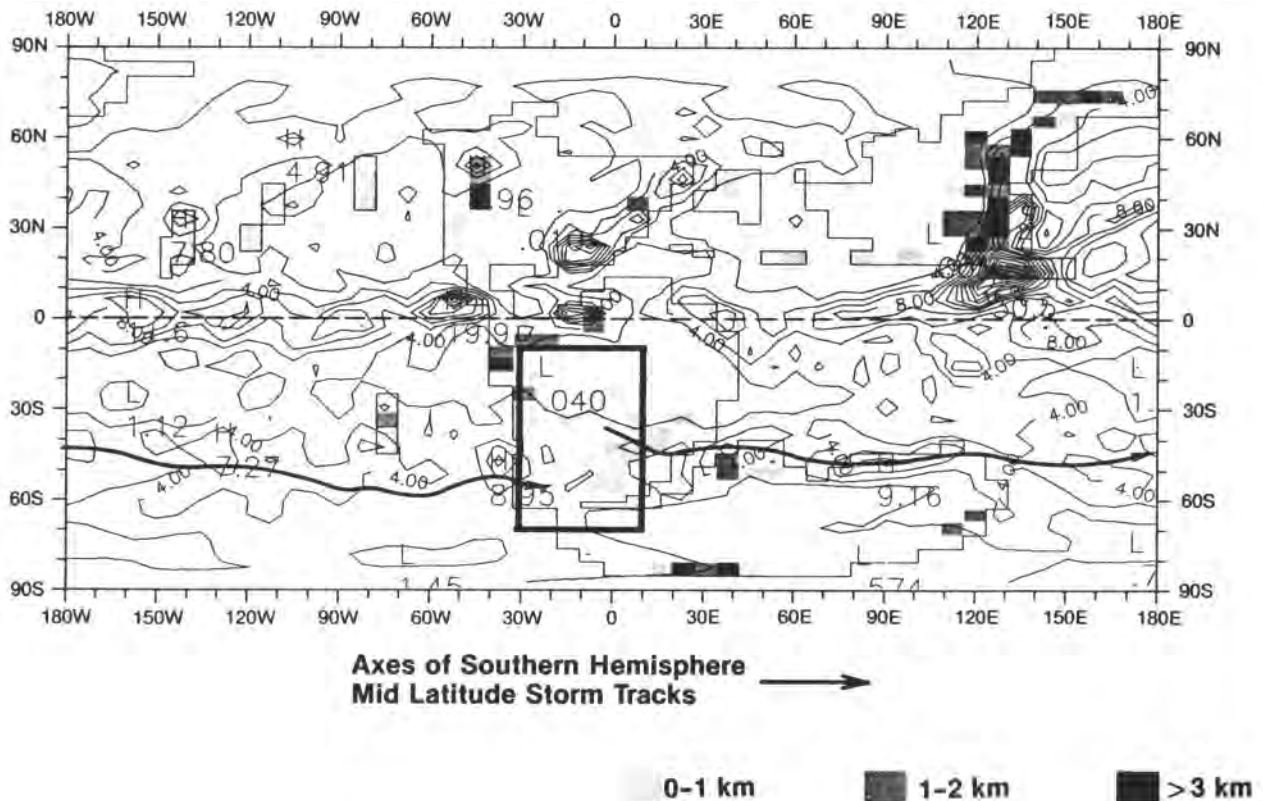


Figure 19. June/July/Aug precipitation showing position of the mid-latitude winter storm track. GRLS area outlined. © 1993, George T. Moore.

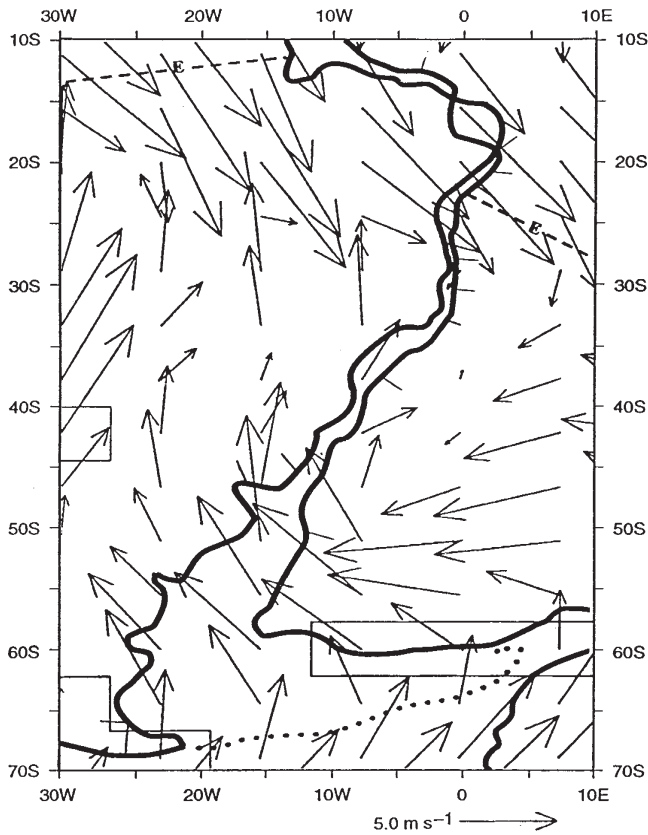


Figure 20. Dec/Jan/Feb surface wind vectors for the GRLS area. © 1993, George T. Moore.

winds from an onshore monsoonal flow due to the summer heating of interior Gondwana and the southern depression of the ITCZ (Moore et al., 1992a). The southern part of the GRLS area received the easterly to northeasterly winds reaching 6 m s^{-1} over southern Namibia and South Africa. This part of the GRLS, with virtually no Dec/Jan/Feb precipitation (Figure 10) and only about 2 mm d^{-1} in June/July/Aug (Figure 11), had a P – E balance approaching zero. This is suggestive of a semiarid to arid environment with potential dune formation. Under these wind conditions dunes would migrate northwest. In the winter months of June/July/Aug, the predictable zonal flow of the easterlies in the north and the westerlies in the south prevailed (Figure 21). The winds did not reach 6 m s^{-1} , hence, eolian sediment transport would not occur in this season.

CONCLUSIONS

The use of paleoclimate from GCM simulations has been shown to be a valuable tool in predicting the source rock potential of lacustrine deposits. Generation, deposition, and preservation of significant quality organic matter in lake bottom sediments involves a complex interplay of paleogeography and paleotopography, the factors which force paleoclimate, and lake chemistry.

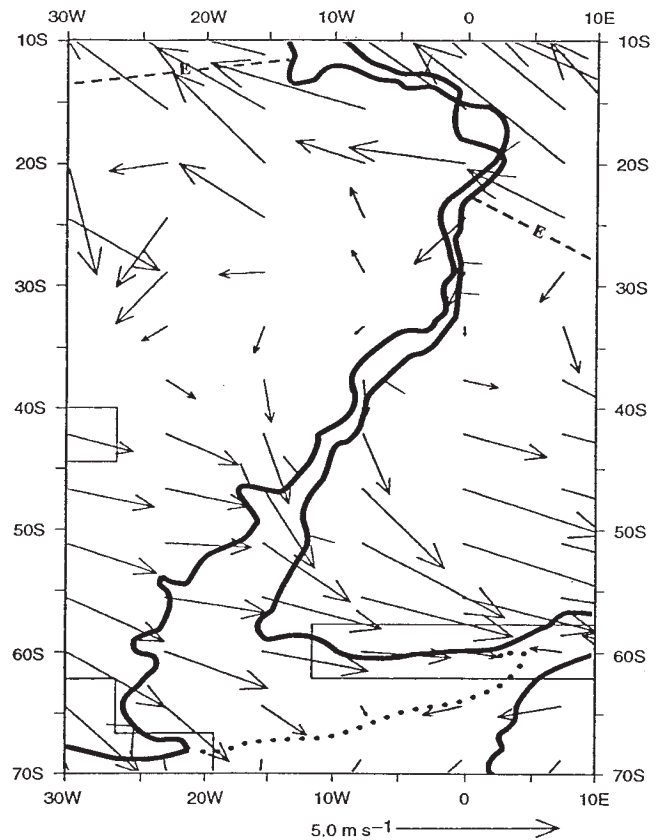


Figure 21. June/July/Aug surface wind vectors for the GRLS area. © 1993, George T. Moore.

A 5000 km long Neocomian rifting event surgically segmented central Northern Gondwana producing a generally linear, but complex, system of lakes. Many of these lakes became stratified permitting organic-rich sediments of varying quality to accumulate. The existing paleoclimate in any one segment was an important control on the nature of these source rocks. In northern Gabon and the equivalent South American Sergipe-Alagoas basins, the effects of monsoonal rains with associated soil moisture and runoff reduced the quality of the source rocks by diluting the section with a high volume of siliciclastics and seasonally oxygenating the lake bottoms with turbidity currents. The lacustrine basins of southern Gabon, Cabinda, Congo, and northern Angola lay in a region where paleoclimatic conditions favor water column stability and bottom anoxia. The June/July/Aug winter temperatures did not approach 4°C and therefore seasonal overturn did not occur. The sedimentation rate in this region was low due to lack of a major precipitation center and to not being near a storm track. The setting was ideal for developing quality source rocks.

Farther south the rift lake systems are more difficult to interpret due to altered boundary conditions between the Late Jurassic model and the Neocomian world. A trend toward aridity is suggested by a P – E balance approaching zero. This would favor red-bed development. Seasonal easterly to northeasterly winds

exceeded the threshold velocity for moving sand. Eolian deposits could have been expected in this region. Lakes that developed probably would not turn over because the minimum winter temperatures should have been moderated by the presence of the Neocomian seaway. Lakes in parts of this region could have had conditions suitable for quality source rock formation as indicated by Smith (1990).

The GCM simulates the average position of the monsoon for a specified solar insolation forcing. However, insolation change due to obliquity and precession may have produced variability in the intensity and distribution of seasonal maximum precipitation in the Neocomian–Barremian rift lakes. The simulated climate is consistent with the regional pattern of GRLS, but spatial and temporal variability in these lacustrine deposits may be climate dependent and cannot be resolved by the GCM. The large-scale climate parameters generated in this simulation could be used as boundary conditions to a mesoscale model with sub-basin-sized horizontal resolution. In addition, lake distribution, size, and structure are sensitive to local and regional scale variations in surface drainage patterns and groundwater flow. These parameters could have changed over an area smaller than an individual rift basin and within relatively short time periods.

ACKNOWLEDGMENTS

Much of this research was completed while GTM was employed by Chevron Oil Field Research Company at La Habra, California. We thank Chevron Petroleum Technology Company, its successor, for permission to publish this scientific material. The authors appreciate M.W. Boyce of Chevron Overseas Petroleum Inc. releasing for publication the proprietary geochemical data used in this paper.

A.T. Smith and T.J. McHargue reviewed an earlier version of this manuscript. The quality of the paper has been enhanced by suggestions and comments from B.J. Katz and K. Kelts.

L.F. Lynch typed the manuscript. J.L. Bube and J. Koishor prepared the figures. We thank them for their assistance.

REFERENCES CITED

- Anadón, P., L. Cabrera, and R. Julià, 1988, Anoxic-oxic cyclical lacustrine sedimentation in the Miocene Rubielos de Mora Basin, Spain, *in* A.J. Fleet, K. Kelts, and M.R. Talbot, eds., *Lacustrine Petroleum Source Rocks: Geological Society Special Publication 40*, p. 353–367.
- Asmus, H.E., and P.R. Baisch, 1983, Geological evolution of the Brazilian continental margin: Episodes, p. 3–9.
- Barnola, J.M., D. Raynaud, Y.S. Korotkevich, and C. Lorius, 1987, Vostok ice core provides 160,000-year record of atmospheric CO₂: *Nature*, 329, p. 408–414.
- Barron, E.J., 1985a, Numerical climate modeling: a frontier in petroleum source rock prediction: results based on Cretaceous simulations: *AAPG Bulletin*, 69, p. 448–459.
- Barron, E.J., 1985b, Climate models: applications for the pre-Pleistocene, *in* A.D. Hecht, ed., *Paleoclimate Analysis and Modeling: New York, John Wiley*, p. 397–421.
- Barron, E.J., 1989, Severe storms in Earth history: *Geological Society of America Bulletin*, 101, p. 601–612.
- Barron, E.J., 1990, Climate and lacustrine petroleum source prediction, *in* B.J. Katz, ed., *Lacustrine basin exploration—case studies and modern analogs: AAPG Memoir 50*, p. 1–18.
- Barron, E.J., W.W. Hay, and S.T. Thompson, 1989, The hydrological cycle: a major variable during Earth history: *Palaeogeography, Palaeoclimatology, Palaeoecology*, 75, p. 157–174.
- Berner, R.A., 1990, Atmospheric carbon dioxide levels over Phanerozoic time: *Science*, 249, p. 1382–1386.
- Bradley, C.H., 1992, Early Cretaceous paleogeography of Gabon/northeastern Brazil; a tectono-stratigraphic model based on propagating rifts: *Houston Geological Society Bulletin*, 34, p. 17.
- Brice, S.E., and G. Pardo, 1980, Hydrocarbon occurrences in nonmarine, pre-salt sequence of Cabinda, Angola: *AAPG Bulletin*, 64, p. 681.
- Brice, S.E., K.R. Kelts, and M.A. Arthur, 1980, Lower Cretaceous lacustrine source beds from early rifting phases of South Atlantic: *AAPG Bulletin*, 64, p. 680–681.
- Brice, S., M.D. Cochran, G. Pardo, and A.D. Edwards, 1982, Tectonics and sedimentation of the South Atlantic rift sequence, Cabinda, Angola, *in* J.S. Watkins and C.L. Drake, eds., *Studies in continental margin geology: AAPG Memoir 34*, p. 5–18.
- Burwood, R., P.J. Cornet, K. Jacobs, and J. Paulet, 1990, Organofacies variation control on hydrocarbon generation: a Lower Congo coastal basin (Angola) case history: *Organic Geochemistry*, 16, p. 325–338.
- Cecil, C.B., 1990, Paleoclimate controls on stratigraphic repetition of chemical and siliciclastic rocks: *Geology*, 18, p. 533–536.
- Crowley, T.J., K-Y Kim, J.G. Mengel, and D.A. Short, 1992, Modeling 100,000-year climate fluctuations in pre-Pleistocene time series: *Science*, 255, p. 705–707.
- De Deckker, P., 1988, Large Australian lakes during the last 20 million years: sites for petroleum source rocks or metal ore deposition, or both? *in* A.J. Fleet, K. Kelts, and M.R. Talbot, eds., *Lacustrine Petroleum Source Rocks: Geological Society Special Publication 40*, p. 45–38.
- Edwards, A., and R. Bignell, 1988, Hydrocarbon potential of West African salt basin: *Oil & Gas Journal*, 86, no. 50, p. 71–74.
- Ericksen, M.C., and R. Slingerland, 1990, Numerical simulations of tidal and wind-driven circulation in the Cretaceous Interior Seaway of North America: *Geological Society of America Bulletin*, 102, p. 1499–1516.
- Estrella, G., M.R. Mello, P.C. Gaglianone, R.L.M. Azevedo, K. Tsubone, E. Rossetti, J. Concha, and I.M.R.A. Brüning, 1984, The Espirito Santo Basin (Brazil) source rock characterization and petroleum habitat, *in* G. Demaison and R.J. Murriss, eds., *Petroleum geochemistry and basin evaluation: AAPG*

- Memoir 35, p. 253–271.
- Fawcett, P.J., E.J. Barron, V.D. Robison, and B.J. Katz, 1994, The climate evolution of India and Australia from the Late Permian to mid-Jurassic: a comparison of climate model results with the geologic record: Geological Society of America Special Paper 228, p. 139–157.
- Fontes, J.C., and F. Gasse, 1991, PALHYDAF (Palaeohydrology in Africa) program: objectives, methods, major results: Palaeogeography, Palaeoclimatology, Palaeoecology, 84, p. 191–215.
- Fontes, J.Ch., F. Gasse, Y. Callot, J-C. Plaziat, P. Carbonel, P.A. Dupeuble, and I. Kaczmarek, 1985, Freshwater to marine-like environments from Holocene lakes in northern Sahara: Nature, 317, p. 608–610.
- Franke, M.R., 1992, Discovered and potential petroleum resources, deep offshore Brazil: Proceedings Thirteenth World Petroleum Congress, 2, Exploration and Production, p. 71–73.
- Freeman, K.H., and J.M. Hayes, 1992, Fractionation of carbon isotopes by phytoplankton and estimates of ancient CO₂ levels: Global Biogeochemical Cycles, 6, p. 185–198.
- Fryberger, S.G., 1979, Dune forms and wind regime. USGS Professional Paper 1052, p. 141–169.
- Gerrard, I., and G.C. Smith, 1982, Post-Paleozoic succession and structure of the southwestern African continental margin, in J.S. Watkins and C.L. Drake, eds., Studies in continental margin geology: AAPG Memoir 34, p. 49–74.
- Hallam, A., 1982, The Jurassic climate, in Climate in Earth History: Washington, D.C., National Academy Press, p. 159–162.
- Hallam, A., 1984, Continental humid and arid zones during the Jurassic and Cretaceous: Palaeogeography, Palaeoclimatology, Palaeoecology, 47, p. 195–223.
- Harland, W.B., R.L. Armstrong, A.V. Cox, L.E. Craig, A.G. Smith, and D.G. Smith, 1990, Geological time scale 1989: Cambridge University Press, 263 p.
- Huc, A.Y., 1988, Aspects of depositional processes of organic matter in sedimentary basins: Organic Geochemistry, 13, p. 263–272.
- Huc, A.Y., J. LeFournier, and M. Vandenbroucke, 1990, Northern Lake Tanganyika—an example of organic sedimentation in an anoxic rift lake, in B.J. Katz, ed., Lacustrine Basin Exploration: Case Studies and Modern Analogs: AAPG Memoir 50, p. 169–185.
- Katz, B.J., 1990, Controls on distribution of lacustrine source rocks through time and space, in B.J. Katz, ed., Lacustrine basin exploration—Case studies and modern analogs: AAPG Memoir 50, p. 61–76.
- Kutzbach, J.E., and R.G. Gallimore, 1989, Pangaeon climates, megamonsoons of the megacontinent: Journal of Geophysical Research, 97, D3, p. 3341–3357.
- Kutzbach, J.E., and F.A. Street-Perrott, 1985, Milankovitch forcing of fluctuations in the level of tropical lakes from 18 to 0 kyr B.P.: Nature, 317, p. 130–134.
- Livingston, D.A., and J.M. Melack, 1984, Some lakes of subsaharan Africa, in F.B. Taub, ed., Lakes and reservoirs, ecosystems of the World: Elsevier, 23, p. 467–497.
- McHargue, T.R., 1990, Stratigraphic development of proto-South Atlantic rifting in Cabinda, Angola—a petroliferous basin, in B.J. Katz, ed., Lacustrine basin exploration—case studies and modern analogs: AAPG Memoir 50, p. 307–326.
- Mello, M.R., and J.R. Maxwell, 1990, Organic geochemical biomarker characterization of source rocks and oils derived from lacustrine environments in the Brazilian continental margin, in B.J. Katz, ed., Lacustrine basin exploration—case studies and modern analogs: AAPG Memoir 50, p. 77–97.
- Mello, M.R., P.C. Gaglianone, S.C. Brassell, and J.R. Maxwell, 1988a, Geochemical and biological marker assessment of depositional environments using Brazilian offshore oils: Marine and Petroleum Geology, 5, p. 205–223.
- Mello, M.R., N. Telnaes, P.C. Gaglianone, M.I. Chiarelli, S.C. Brassell, and J.R. Maxwell, 1988b, Organic geochemical characterization of depositional palaeoenvironments of source rocks and oils in Brazilian marginal basins: Organic Geochemistry, 13, p. 31–45.
- Mello, M.R., W.U. Mohraik, E.A.M. Koutsoukos, and J.C.A. Figueira, 1992, Brazilian and west African oils: Generation, migration, accumulation and correlation: Proceedings of the Thirteenth World Petroleum Congress, 2, Exploration and Production, p. 153–164.
- Mohriak, W.U., M.R. Mello, J.F. Dewey, and J.R. Maxwell, 1990, Petroleum geology of the Campos Basin, offshore Brazil, in J. Brooks, ed., Classic petroleum provinces: Geological Society Special Publication 50, p. 119–141.
- Moore, G.T., 1989, Comparison of sedimentary basins on conjugate margins of South America and Africa: 28th International Geologic Congress Abstracts, Washington, D.C., 2, p. 2–455.
- Moore, G.T., 1990, Sedimentary basins on the conjugate margins of South America and Africa: AAPG Bulletin, 74, p. 724.
- Moore, G.T., S.R. Jacobson, and D.N. Hayashida, 1991, A paleoclimate simulation of the Late Permian greenhouse world and its consequences: AAPG Bulletin, 75, p. 175.
- Moore, G.T., D.N. Hayashida, C.A. Ross, and S.R. Jacobson, 1992a, Paleoclimate of the Kimmeridgian/Tithonian (Late Jurassic) World: I. Results using a general circulation model: Palaeogeography, Palaeoclimatology, Palaeoecology, 93, p. 113–150.
- Moore, G.T., L.C. Sloan, D.N. Hayashida, and N.P. Umrigar, 1992b, Paleoclimate of the Kimmeridgian/Tithonian (Late Jurassic) World: II. Sensitivity tests comparing three different paleotopographic settings: Palaeogeography, Palaeoclimatology, Palaeoecology, 95, p. 229–252.
- Muntingh, A., 1993, Geology, prospects in Orange Basin offshore western South Africa: Oil & Gas Journal, 91, no. 4, p. 106–109.

- Ojeda, H.A.O., 1982, Structural framework, stratigraphy, and evolution of Brazilian marginal basins: AAPG Bulletin, 66, p. 732–749.
- Park, J., and R.J. Oglesby, 1991, Milankovitch rhythms in the Cretaceous: a GCM modeling study: Global and Planetary Change, 90, p. 329–355.
- Parrish, J.T., 1988, Pangaeon paleoclimates: EOS, 69, p. 1061.
- Parrish, J.T., A.M. Ziegler, and C.R. Scotese, 1982, Rain-fall patterns and the distribution of coals and evaporites in the Mesozoic and Cenozoic: Palaeogeography, Palaeoclimatology, Palaeoecology, 40, p. 67–101.
- Powell, T.G., 1986, Petroleum geochemistry and depositional setting of lacustrine source rocks: Marine and Petroleum Geology, 3, p. 200–219.
- Reyre, D., 1984, Petroleum characteristics and geological evolution of a passive margin. Example of the Lower Congo–Gabon Basin: Société Nationale Elf-Aquitaine (Production), 8, p. 303–332.
- Robinson, P.L., 1973, Paleoclimatology and continental drift, in D.H. Tarling and S.K. Runcorn, eds., Implications of continental drift to the earth sciences: London, Academic Press, p. 451–476.
- Scotese, C.R., and J. Golonka, 1992, Paleogeographic atlas. PALEOMAP Project: University of Texas at Arlington, Arlington, TX.
- Sloan, L.C., and E.J. Barron, 1992, A comparison of Eocene climate model results to quantified interpretations: Palaeogeography, Palaeoclimatology, Palaeoecology, 93, p. 183–202.
- Smith, M.A., 1990, Lacustrine oil shale in the geologic record, in B.J. Katz, ed., Lacustrine basin exploration—case studies and modern analogs: AAPG Memoir 50, p. 43–60.
- Spaulding, W.G., 1991, Pluvial climatic episodes in North America and North Africa: types and correlation with global climate: Palaeogeography, Palaeoclimatology, Palaeoecology, 84, p. 217–227.
- Talbot, M.R., 1988, The origins of lacustrine oil source rocks: evidence from the lakes of tropical Africa, in A.J. Fleet, K. Kelts, and M.R. Talbot, eds., Lacustrine petroleum source rocks: Geological Society Special Publication 40, p. 29–43.
- Teisserenc, P., and J. Villemin, 1989, Sedimentary basin of Gabon—geology and oil systems, in J.D. Edwards and P.A. Santogrossi, eds., Divergent/passive margin basins: AAPG Memoir 48, p. 117–199.
- Trindade, L.A.F., and S.C. Brassell, 1992, Geochemical assessment of petroleum migration phenomena on a regional scale: case studies from Brazilian marginal basins: Organic Geochemistry, 19, p. 13–27.

Depositional Controls on Mesozoic Source Rocks in the Tethys

François Baudin
CNRS-URA 1761
Université Pierre et Marie Curie
Paris, France

ABSTRACT

About 70% of the total world petroleum resources are concentrated in the Tethyan realm, the Mesozoic deposits being the most prolific source rocks of these oil and gas reserves. To understand the depositional controls of these organic-rich facies at the scale of the Tethys is a challenging problem. A recent set of paleoenvironmental maps for the Tethyan realm allows integration of source-rock mapping with other mappable geologic information. This integrated approach is attempted here for three short time intervals of the Mesozoic: Toarcian, Kimmeridgian, and Cenomanian, all of which were periods of good source-rock deposition.

The source-rock distribution during the Toarcian shows a contrast between the western European and Tethyan realms. While there are high concentrations of organic matter corresponding to thick deposits in the western European realm, there are only lower concentrations within thin sedimentary sequences in the Tethyan realm. Although the organic facies are similar in both settings, widespread anoxia must have existed in western European epicontinental seas, while the preservation of organic matter in the Tethyan realm must be related to morphological factors. During the Kimmeridgian, preservation of marine organic matter was important in epicontinental platforms as well as in newly created margins. The Cenomanian is also clearly associated with good preservation of oil-prone source rocks, especially in low latitudes. During this interval, numerous organic-rich shale deposits are preserved, whatever the environment: on platforms as well as in basins. Whereas the northern shelves seem more favorable for organic concentration than the Tethyan margins during the Toarcian—and probably also during the Kimmeridgian—the reverse is true for the black shales preserved during the Cenomanian.

During these three intervals of enhanced marine organic-carbon preservation, the distribution of source rocks was controlled both by plate movements that influenced opening or closing of seaways, basin morphologies and their evolution; and by paleocurrents and paleoclimates.

Critical to future global source-rock mapping is the refinement of stratigraphic dating, in order to identify the synchronism of source-rock deposits and to better understand their distribution in time and space.

INTRODUCTION

The causes of widespread deposition of source rocks during short time intervals are numerous, and their respective importance is the subject of controversy among specialists. Because the Tethyan realm contains about 70% of the known world petroleum resources (Bois et al., 1980; Ulmishek and Klemme, 1990), it is important to analyze the distribution of Tethyan source rocks and their depositional conditions in the context of plate tectonic and global changes.

A recent multidisciplinary work (Dercourt et al., 1993) has provided a set of paleoenvironmental maps of the Tethyan realm, from Indonesia and Australia in the east to the Caribbean in the west. These maps attempt to reconstruct the paleogeography and paleoenvironments of the Tethys Ocean and surrounding continents from the Late Permian to the Tortonian. Data from hundreds of publications on regional geology and stratigraphy have been used in the construction of every map. Each map presents (1) the present-day coastlines as a reference; (2) a paleolatitude grid; (3) 14 types of paleoenvironments, both marine and continental, selected for their depositional or bathymetric indications; and (4) the major hydrodynamic pattern, reproduced from the literature (Berggren and Hollister, 1977; Parrish and Curtis, 1982; Haq, 1984; Cottreau and Lautenschlager, 1994). These maps provide the opportunity to integrate the information on organic-rich facies in order to obtain a more coherent picture of source-rock distribution with respect to tectonic, climatic, and circulation changes.

The purpose of this paper is to describe briefly the paleogeography and paleoenvironments of the Tethyan realm for three high sea level intervals (the Toarcian, Kimmeridgian, and Cenomanian) and to discuss the depositional controls on their source rocks. The selected stages correspond to three prolific intervals for source-rock deposition which, in turn, correspond to three high sea level intervals (Tissot, 1979; Ulmishek and Klemme, 1990) and to different steps in the evolution of the Tethyan realm. The Toarcian marks the rapid initiation of the opening of the Neotethys (so called to avoid confusion with previous Paleotethys); the Kimmeridgian is an early stage of opening of the North Atlantic; the Cenomanian illustrates the beginning of closure in the Neotethys and opening of communication between the North and South Atlantic.

SOURCE ROCK DATA

Most of the data cited here are provided from the cited references, the Deep Sea Drilling Program

(DSDP) and Ocean Drilling Project (ODP) volumes, as well as from personal work of the author. The source rocks discussed in this paper include both effective (mature) and potential (immature) source rocks. Their potential to have sourced, or to source in the future, is generally based on the assessment of geochemical data (e.g., Rock-Eval pyrolysis, elemental analysis of kerogen, gas chromatography) and visual examination of kerogens. All investigated source rocks are tentatively linked with one of the kerogen types defined by Tissot et al. (1974) and reported on a map by specific symbols. Three main types of kerogen are distinguished here:

- Type I and type II kerogens are related to lacustrine or marine-reducing environments and are derived mainly from phytoplanktonic organisms or bacteria. They are generally the most prolific source rocks and are identified on our map by the same symbol, whereas their quality and quantity are reported in the tables.
- Type III kerogen is derived from terrestrial plants transported to marine or nonmarine environments with a moderate degree of degradation. Coals and type III kerogen have commonly less importance for oil generation during the Jurassic and Cretaceous than during the Tertiary. Nevertheless, they are reported on the map and interpreted in terms of global climatic pattern. It is obvious that other conditions (i.e., low drainage, sea level drop, small delta progradation) control the distribution of coals and type III kerogen; however, this must be analyzed on a finer scale than that permitted by the present base maps.
- A fourth type, sometimes called type IV, corresponds either to recycled organic matter from older sediments or to an organic matter deeply altered by subaerial weathering, extensive transport, combustion, or biological degradation. This type IV, devoid of petroleum potential, indicates good oxygenation of the depositional environment on these maps.

Precise information on the location, age, and main geochemical characteristics, as well as selected references on the source rocks, reported on the maps are furnished in the tables.

PALEOGEOGRAPHIES AND SOURCE ROCK DISTRIBUTIONS

Toarcian

The Toarcian (Figure 1 and Table 1) was marked by an active phase of breakup of the Pangea. The general

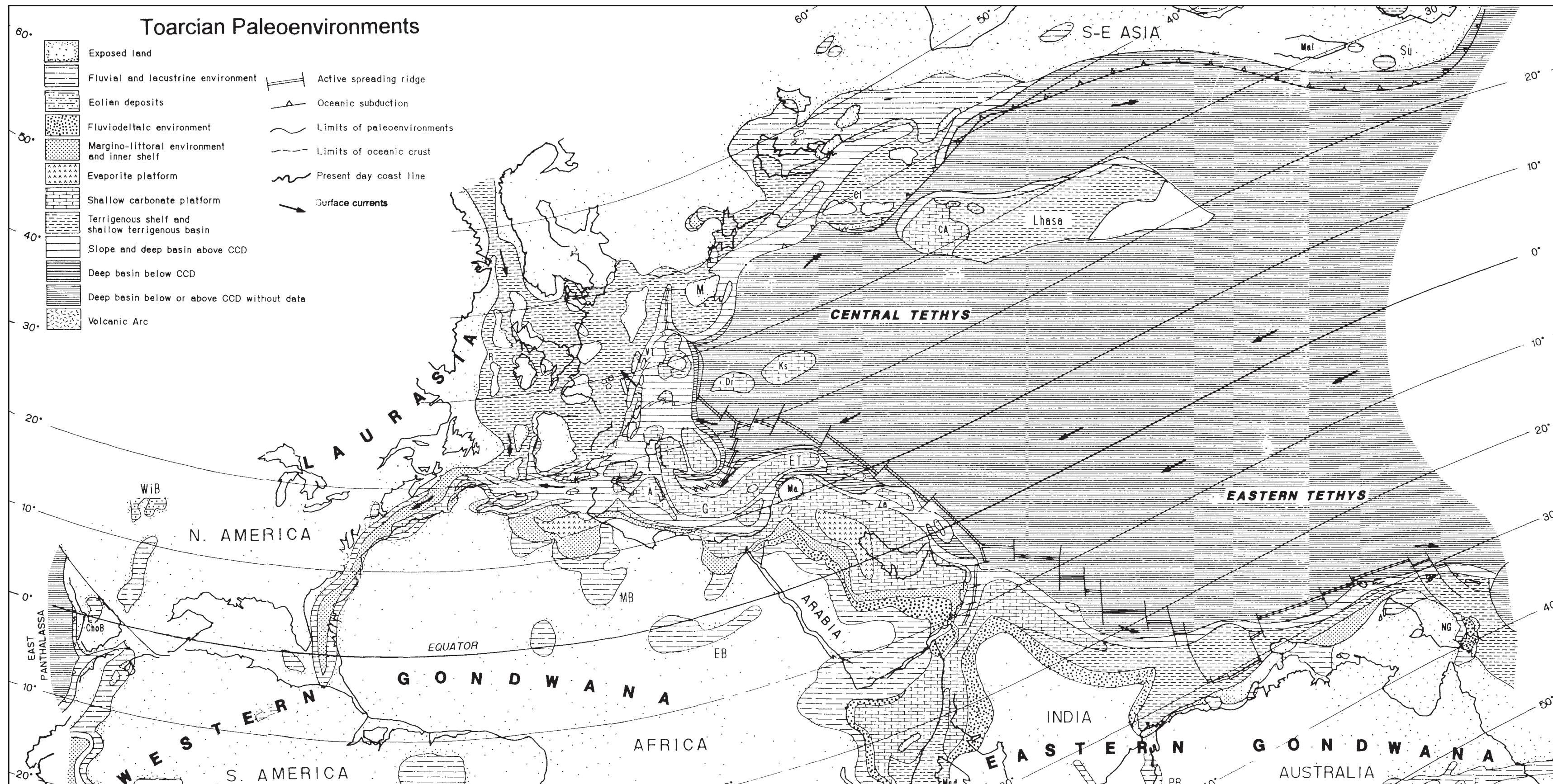


Figure 1A. Reconstructed Toarcian paleogeography and paleoenvironments of the Tethys (after Bassoulet et al., 1993), showing the progressive breakup of western Gondwana and the embryonic North Atlantic. The Eastern and Central Tethys are wide, and the Mediterranean Tethys is characterized by an intense tectonic extension and basin differentiation. Note CCD: Calcite Compensation Depth.

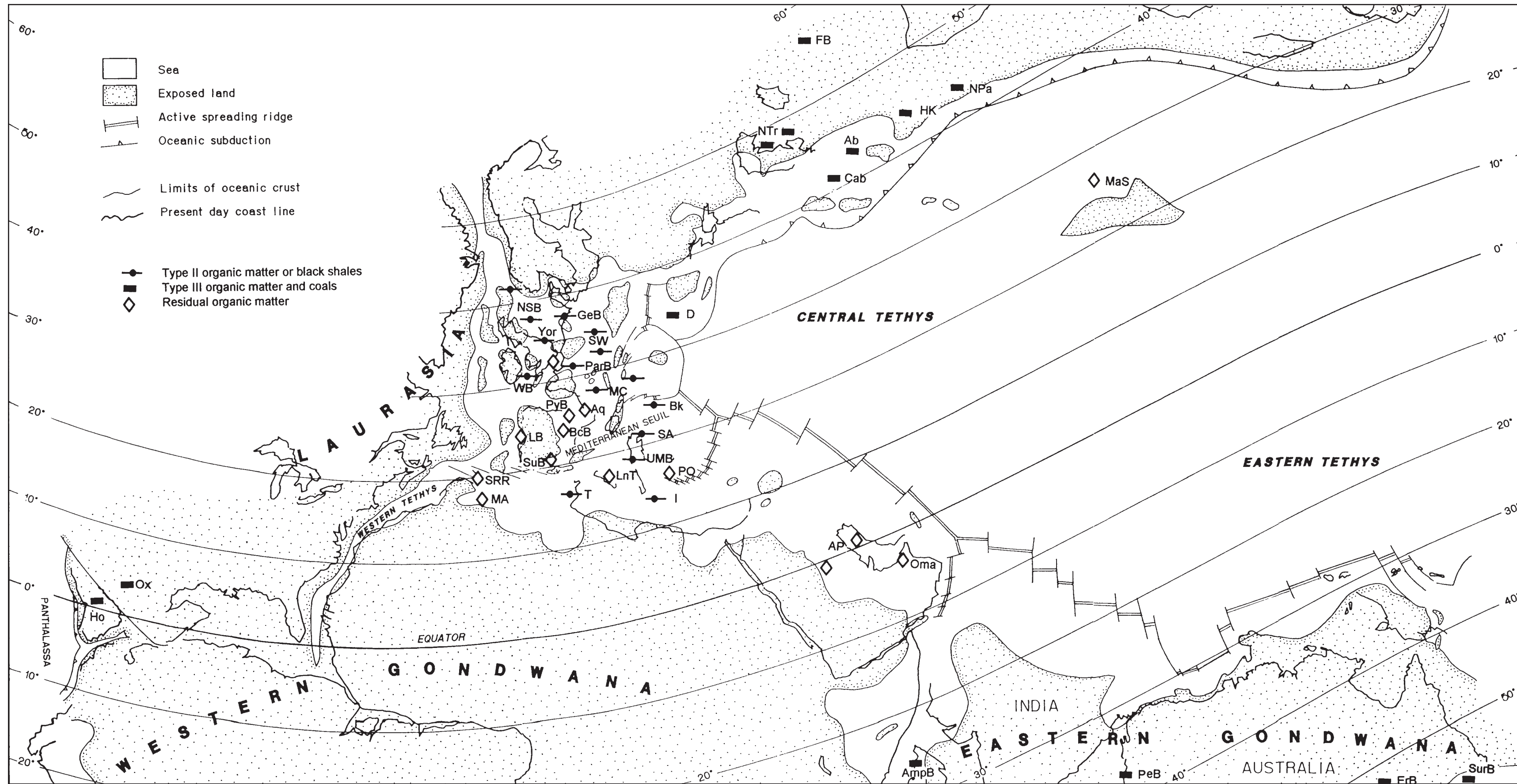


Figure 1B. Black shales and thick source rocks with type II kerogen occur on the northwestern European terrigenous shelf, whereas coeval thin black shales exist in the Mediterranean Tethys. Coal deposits are well distributed along temperate humid climatic belts and the tropical zone in the Eastern Tethyan realm, and locally in equatorial positions in the rift zone of western Gondwana.

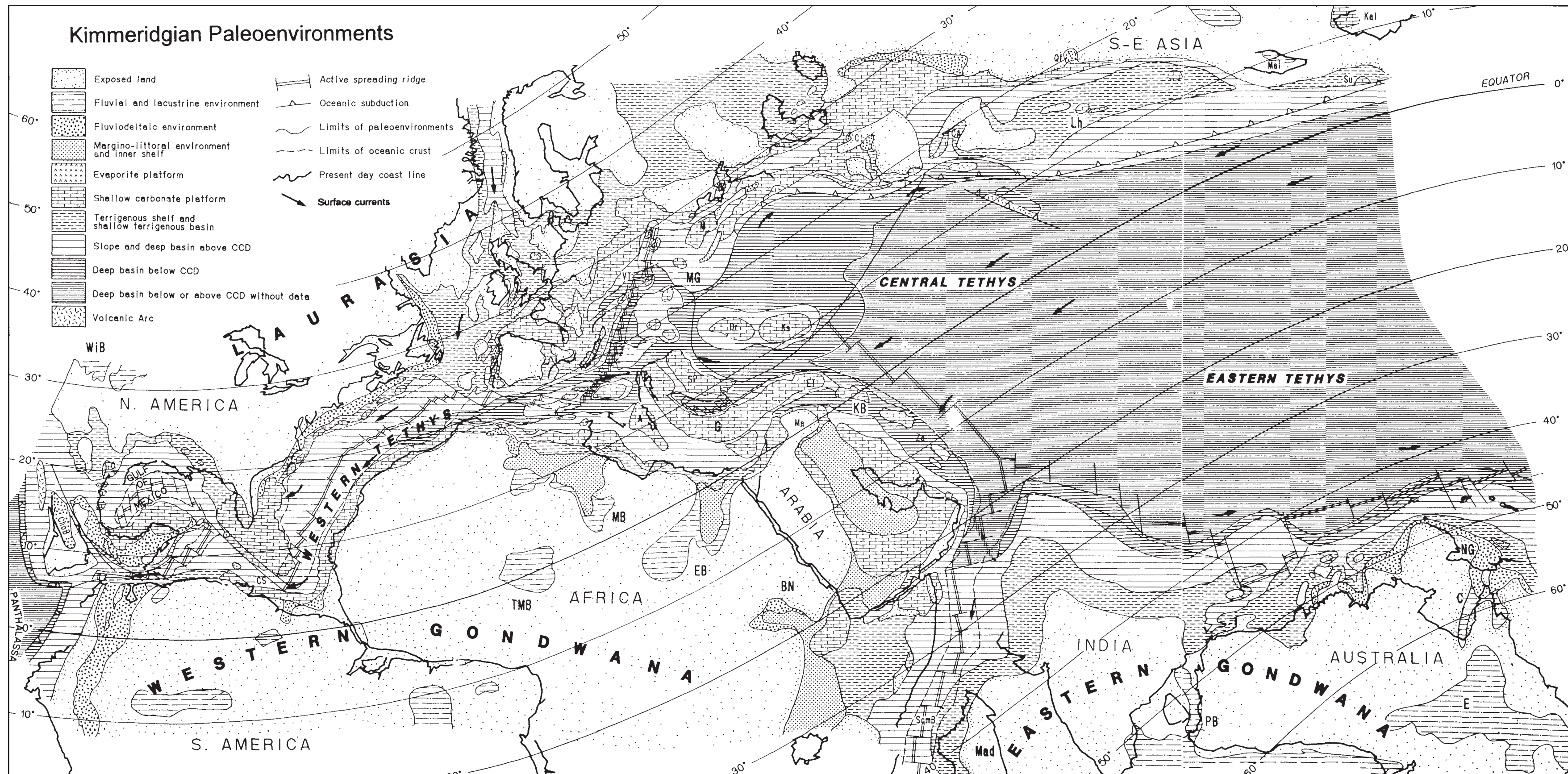


Figure 2A. Reconstructed Kimmeridgian paleogeography and paleoenvironments of the Tethys (after Cecca et al., 1993) showing the opening of the Western Tethys into the Pacific through a narrow North Atlantic seaway. This affected the bottom water circulation, which became well oxygenated and inhibited organic-carbon preservation. Note CCD: Calcite Compensation Depth.

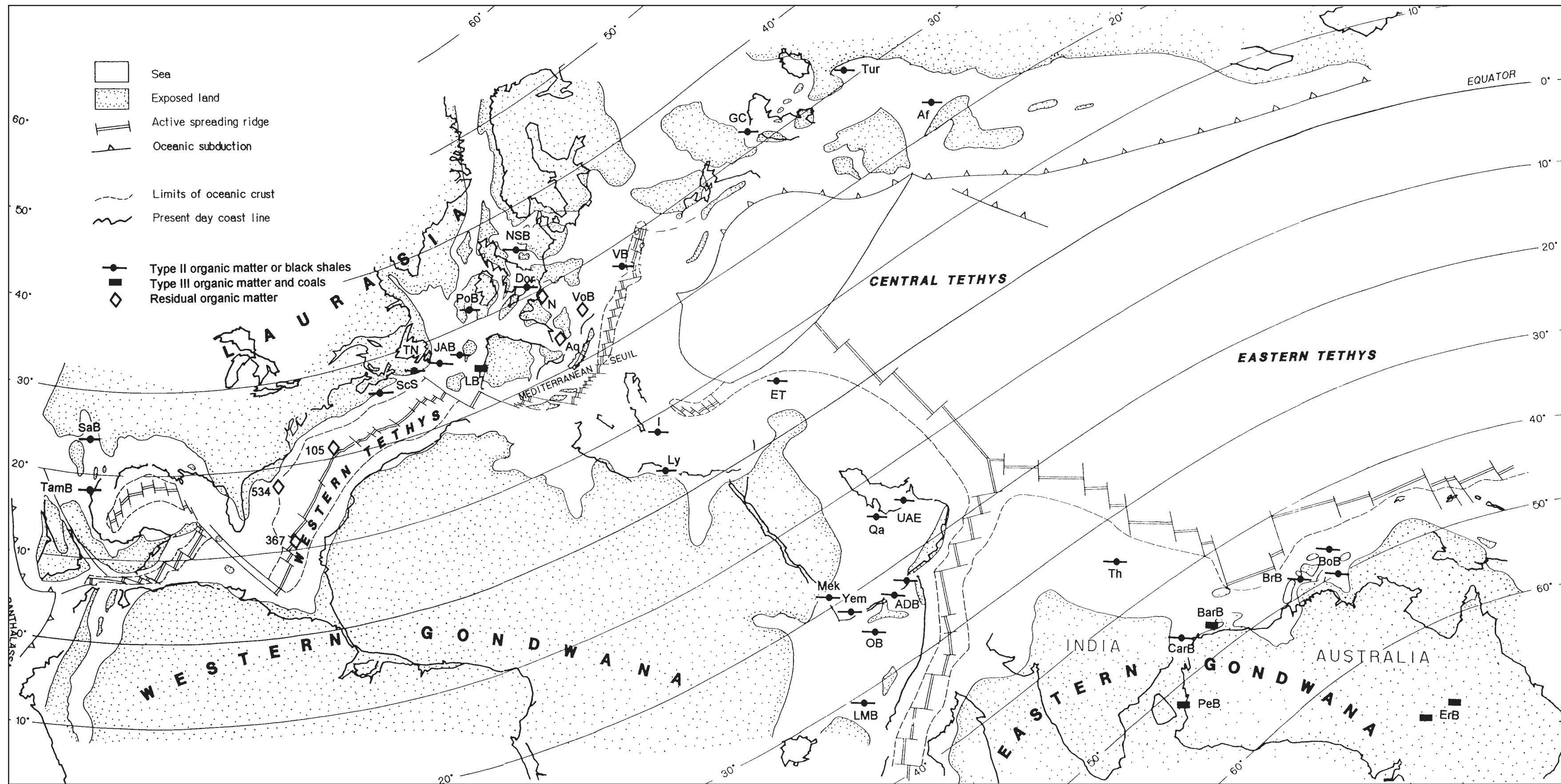


Figure 2B. Marine source rocks are still important on northern European and eastern Canadian epicontinental platforms but also occurred on newly created margins (e.g., Gulf of Mexico, northwestern Australia). Coal and type III source rocks are not abundant for the Kimmeridgian and are restricted to high paleolatitudes of the Southern Hemisphere. Their absence in low latitudes is probably due to more arid climatic conditions.

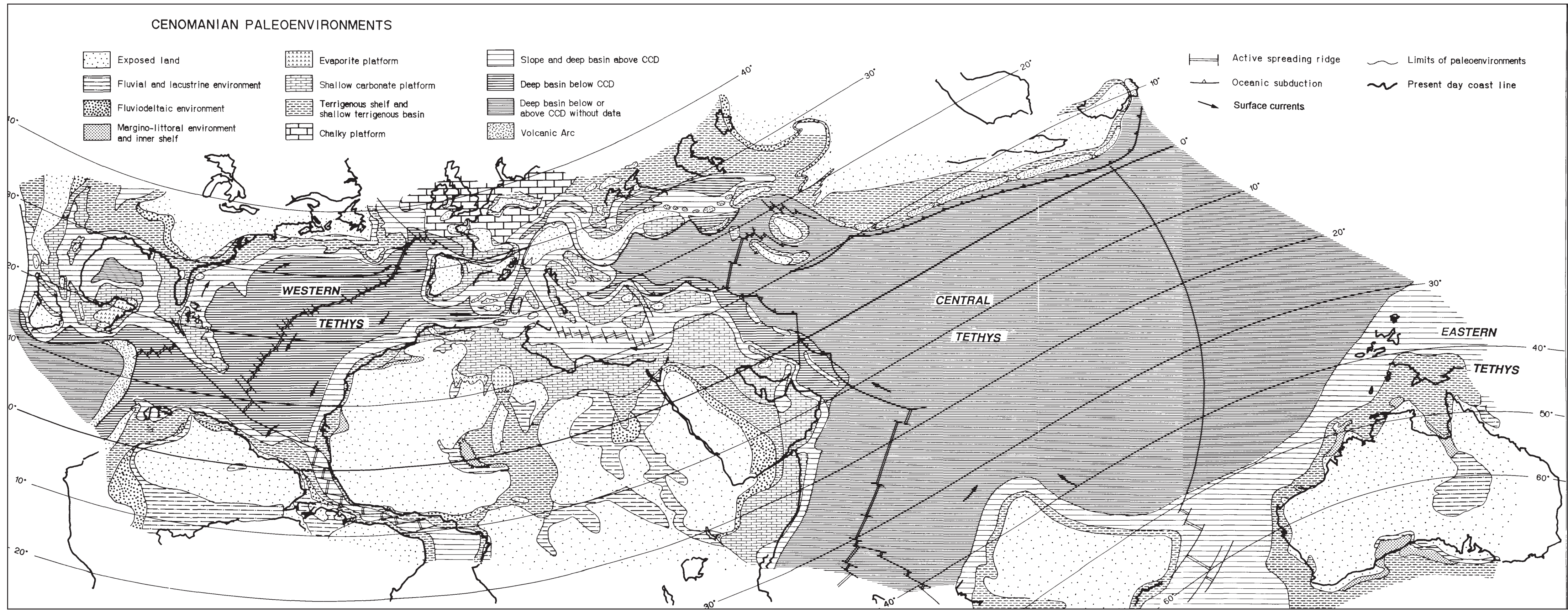


Figure 3A. Reconstructed Cenomanian paleogeography and paleoenvironments of the Tethys (after Philip et al., 1993) showing a large North Atlantic Ocean and the beginning of communication between the North and South Atlantic. In the Eastern Tethys, Madagascar, India, and Australia are now separated by large oceanic domains. Note CCD: Calcite Compensation Depth.

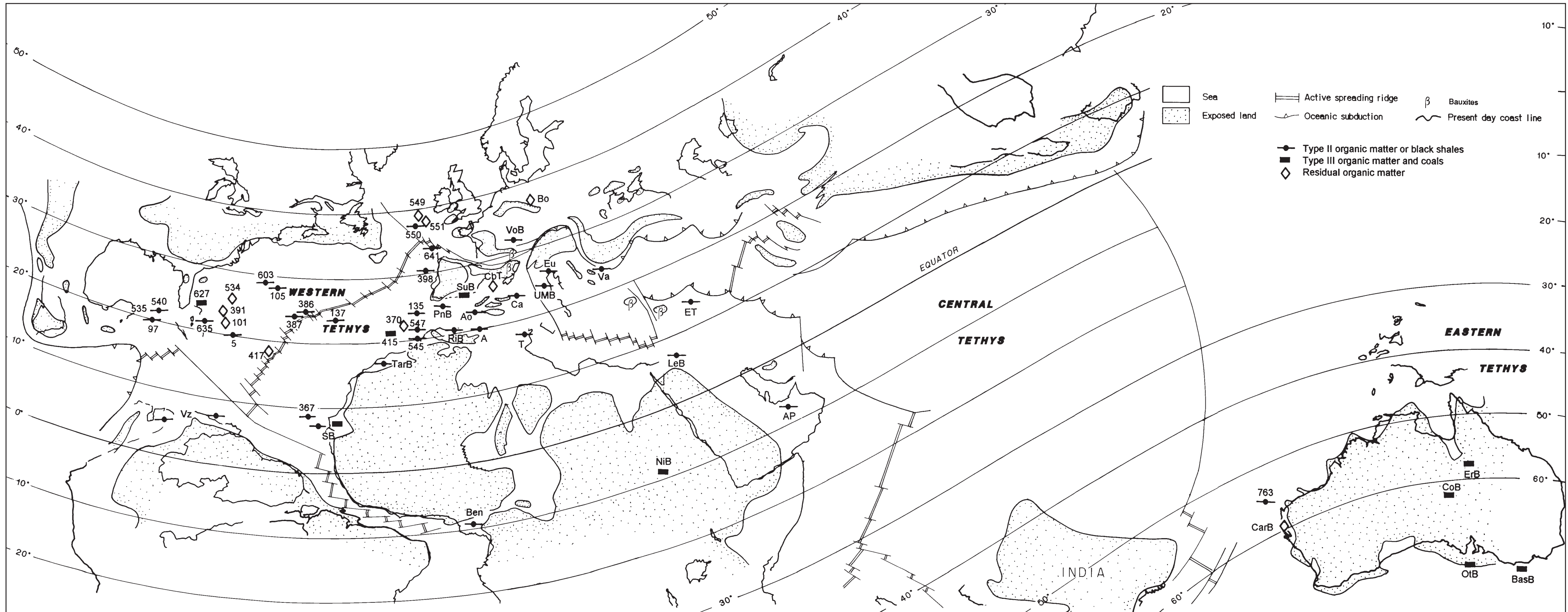


Figure 3B. Black shales and marine source rocks are well preserved—especially in low latitudes—whatever the environment: on platforms as well as in basins. Large quantities of organic matter were preserved, more often in thin levels (DSDP-ODP sites in Atlantic) but sometimes in thick deposits which contain potential or effective source rocks (e.g., Venezuela and Senegal basins). Coals and type III source rocks are less common during this time of high sea level.

paleogeographic picture shows the continental masses penetrated by a v-shaped oceanic wedge: the Neotethys. This ocean, relatively narrow in its western part (500 km in the Mediterranean Tethys), was progressively broader eastward (5000 to 6000 km along the Australian meridian). Much of the Toarcian—and even younger—oceanic crust of the Neotethys has been subducted and only a very small percentage of the remaining crust and its sedimentary cover remains as strongly metamorphosed rocks in orogenic belts. Consequently, little is known of the potential organic-richness of the Neotethys deep-sea deposits, whereas the deeper parts of the Atlantic Ocean still contain Mesozoic deposits.

Gondwanan Domain

On the southern border of this ocean, the Gondwanan shield was composed of the Australian and Indian blocks linked together, separated from the Arabo–African–South American megablock by a southern embayment between Ethiopia–Somalia and Madagascar. The Australian–Indian block, located in the southern temperate humid belt, saw the deposition of thick coal seams (age uncertain) and lacustrine organic-rich shales in the Surat basin. These terrestrial organic facies are mainly present in the Perth and Eromanga basins in Australia, as well as in northern Madagascar. On the Arabian platform, the predominance of shallow-water carbonate platform and marginolittoral environments was not suitable to source-rock deposition. Mainly type IV and sometimes type III kerogens are noted in Saudi Arabia.

Atlantic Margins

A narrow proto-Atlantic seaway is outlined between western Africa and North America. This western cul-de-sac of the Neotethys, corresponding to Iberia and northwestern Africa, was a narrow and complex zone of intense deepening. The Toarcian rocks commonly consist of cyclic alternation of carbonates and shales corresponding to shallow and restricted platform environments. These environments as the evaporitic domain in northeast Sahara were not suitable for source-rock deposition. All investigated basins in the southwest of France, Portugal, Spain and Morocco show type IV organic facies. There is no evidence of marine communication between western Neotethys and the Pacific Ocean during the Toarcian (Bassoullet et al., 1993). However, evidence of late Liassic (late Early Jurassic) rifting in the Gulf of Mexico and the Caribbean region is provided by the occurrence of thick continental beds. These deposits contain coal and plant remains as known in the Oaxaca basin in Mexico and within the Honduras basin.

Eurasian Margins

On its northern border, the Neotethys was limited by the subduction of the oceanic floor under the Eurasian plate and the continental Cimmerian block. This is composed of central Afghanistan, southern Pamir (Pakistan), southern Tibet, and western Thailand. Little information on organic carbon is available for this region. Only organic facies IV has been

recorded in the Mae Shot basin in western Thailand where marine facies were deposited. The northern margin of the Neotethys was marked by an intense arc-type volcanism which was particularly active in northern Turkey and northern Iran. This medium-latitude setting (around 40° to 50°N) promoted the formation of large deltaic complexes with numerous, thick coal beds as in the Shemshak Formation in northern Iran and Saighan series in Hindu Kouch (Afghanistan). Northward, from the western Caucasus to central Asia, important fluvio-lacustrine environments rich in plant remains and coal horizons were also developed. Nevertheless, the stratigraphic control of these facies is poor and ranges from the Sinemurian to the Toarcian.

European Platform

The southern North Sea and northwestern Europe formed a wide epicontinental terrigenous platform where the Toarcian deposits were well developed. They include the Jet Rock in Great Britain, the Posidonia Shales in the southern North Sea, the Schistes cartons in the Paris basin, and the Posidonienschiefer in Germany and Switzerland. Similar intervals are also known in southern France (Causse basin). Most of these carbon-rich shales are type II and were deposited in the *Falciferum* ammonite zone (Lower Toarcian). Development of these good source rocks was related to stagnant water density stratification (Trümpy, 1983; Farrimond et al., 1989) or to the impingement of an oxygen-minimum zone during the Toarcian transgression (Jenkyns, 1985, 1988; Fleet et al., 1987). Runoff of nutrient-rich waters from northern lands is also invoked (Loh et al., 1986). Furthermore, as mentioned by Ziegler (1990), it is also significant that these source rocks were widespread in the shallow sea of interfingering Neotethyan and Arctic waters.

Mediterranean Tethys

In the Mediterranean Tethys, the Toarcian was also a period of intense tectonic activity and strong subsidence, especially in the Alpine and Apulian domains where numerous gravity deposits testify to intense block faulting. Such a situation created a complex paleogeography with small carbonate platforms surrounded by more or less deep basins. In the newly created basins, type II or a mixture of types II and III source rocks occur, especially in northern and central Italy, western Greece, Hungary, and northern Tunisia. Nevertheless, these source rocks have lower total organic carbon contents (about 1% on average) and are thinner than in the epicontinental basins farther north. Organic-rich intervals seem restricted to the basin flanks, edges of shelf highs (Jenkyns, 1988), or to the deeper parts of the half-grabens in Greece (Baudin and Lachkar, 1990), but not to deeper sites where type IV kerogen is dominant.

Kimmeridgian

Most of the organic-rich facies of the Late Jurassic range from Oxfordian to Tithonian in age (Figure 2 and Table 2). As far as possible, only Kimmeridgian source rocks are reported on the map. Such strati-

Table 1. Location, age, environment, thickness, and main geochemical characteristics of the selected source rocks and organic-rich facies reported on the Toarcian map. The code for the basins is reported on the map.

| Code | Basin/Province (Country) | Age | Paleoenv. | Thickness (m) | % TOC Range | Kerogen Type | Selected References |
|------|-----------------------------|----------------------------|-----------|------------------|----------------|-----------------|---|
| Ab | Eastern Elbourz (Iran) | Toarcian | TS | 200 | 0.2–15 | III | Rad (1982, 1986) |
| AmpB | Ampasindava (Madagascar) | Upper Lias | TS | ? | ? | coal | Besairie and Collignon (1972) |
| AP | Marrat (Saudi Arabia) | Toarcian | ML | 10 | 0–0.9 | IV+III | Baudin et al. (1990b) |
| AP | Persian Gulf (Iran) | Toarcian | CP | 25 | 0–0.6 | IV | Baudin et al. (1990b) |
| Aq | Aquitaine (France) | Pliensbachian– Toarcian | TS | ? | 0–0.5 | IV | Carozzi et al. (1972) |
| BcB | Betic Cordillera (Spain) | Toarcian | TS | 15 | 0–0.3 | IV | Baudin et al. (1990b) |
| Bk | Bakony (Hungary) | Toarcian | PR | 20 | 1.5–4 | II+III | Polgari et al. (1989); Jenkyns (1991) |
| Cab | Central Elbourz (Iran) | Toarcian | TS | 300 | 0.2–60 | III | Baudin and Téherani (1991) |
| D | Danubian (Romania) | Upper Lias | TS | ? | ? | coal | Vinogradov (1968) |
| Dor | Dorset (Great Britain) | Toarcian | TS | 0.5–3 | ? | IV | Ebukanson and Kinghorn (1985, 1986, 1990) |
| Erb | Eromanga (Australia) | Sinemurian– Toarcian | FL | ? | 1–60 | III | Park (1976); Kantsler et al. (1984); Moore (1986) |
| FB | Fergana (Turkestan) | Sinemurian– Toarcian | FL | 3000 | ? | coal | Vinogradov (1968) |
| GeB | Westphalia, Saxe (Germany) | Toarcian | TS | 15–20 | 1–16 | II | Mann et al. (1986); Rüllkötter et al. (1987) |
| GeB | Franconia (Germany) | Toarcian | TS | 5 | 1.5–17 | II | Küspert (1983) |
| HK | Hindou Kouch (Pakistan) | Upper Lias | FL | ? | ? | coal | de Lapparent and de Lavigne (1965) |
| Ho | (Honduras) | Upper Lias | FL | ? | ? | coal | Salvador (1987) |
| I | Ionian (Greece) | Toarcian | B> | 5–75 | 0.5–5 | II+III | Baudin et al. (1988); Jenkyns (1988); Baudin and Lachkar (1990) |
| Jur | Jura (France/Switzerland) | Toarcian | TS | 5–25 | 1–12 | II | Broquet and Thomas (1979); Mettraux et al. (1986); Gorin and Feist, 1990 |
| LB | Lusitanian (Portugal) | Toarcian | B> | 50 | 0–0.5 | IV | Baudin et al. (1990a) |
| LnT | Lagonegro (Italy) | Toarcian | B< | ? | 0–0.5 | IV | Jenkyns (1988) |
| MA | Middle Atlas (Morocco) | Toarcian | B> | 40 | 0–0.5 | IV | Bassoulet et al. (1991) |
| MaS | Mae Shot (Thailand) | Toarcian | TS | 30 | 0.5–1 | IV | Baudin (unpublished) |
| MC | South-Est Basin (France) | Toarcian | TS | 5–10 | 0.5–5 | II+III | Dromart et al. (1989) |
| MC | Causses (France) | Toarcian | TS | 1–20 | 1–8 | II | Trümpy (1983) |

Table 1 (continued).

| Code | Basin/Province (Country) | Age | Paleoenv. | Thickness (m) | % TOC Range | Kerogen Type | Selected References |
|------|-----------------------------------|----------------------------|-----------|------------------|----------------|-----------------|--|
| NPa | Northern Pamir (Afghanistan) | Upper Lias | FL | ? | ? | coal | Vinogradov (1968) |
| NSB | North Sea | Toarcian | TS | 20–50 | 2–12 | II | Barnard and Cooper (1981, 1983) |
| NSB | Rijswijk (The Netherlands) | Toarcian | TS | ? | ? | II | Bodenhausen and Ott (1981) |
| NTr | North Transcaspien | Sinemurian– Toarcian | FL | ? | ? | coal | Vinogradov (1968) |
| Oma | (Oman) | Upper Lias | CP | 50 | ? | IV | Grantham et al. (1987) |
| Ox | Oaxaca (Mexico) | Upper Lias | FL | ? | ? | coal | Salvador (1987) |
| ParB | Alsace (France) | Toarcian | TS | 15 | 2–13 | II | IFP data (unpublished) |
| ParB | Lorraine (France) | Toarcian | TS | 10–70 | 4–7 | II | Huc (1976, 1977); Espitalié and Madec (1981) |
| ParB | Paris Basin (France) | Toarcian | TS | 10–60 | 2–9 | II | Espitalié et al. (1987) |
| PeB | Perth (Australia) | Sinemurian– Toarcian | FL | 1000 | 1–27 | III | Thomas (1979) |
| PO | Pindus-Olonos (Greece) | Pliensbachian– Toarcian | B> | 50 | 0–0.2 | IV | Baudin and Lachkar (1990) |
| PyB | Pyrenean (Spain) | Toarcian | TS | 15 | 0–0.5 | IV | Baudin (1989) |
| SA | Southern Alps (Italy/ Germany) | Toarcian | B> | 5–10 | 0.2–16 | II | Bitterli (1963); Farrimond et al. (1988); Baudin et al. (1990b) |
| SRR | South Rifan Ridges (Morocco) | Toarcian | B> | 60 | 0–0.5 | IV | Bassoullet et al. (1991) |
| SuB | Sub-betic (Spain) | Toarcian | B> | 15 | 0–0.3 | IV | Baudin et al. (1990b) |
| SurB | Surat (Australia) | Sinemurian– Toarcian | ML | 100 | 0.5–2.5 | II+III | Thomas (1982) |
| SW | Swabian Alb (Germany) | Toarcian | TS | 5 | 2–18 | II | Küspert (1982); Moldovan et al. (1985) |
| T | North-South Axis (Tunisia) | Toarcian | B> | 20 | 0.5–4 | II+III | Soussi et al. (1988, 1989) |
| UMB | Umbria-Marches (Italy) | Toarcian | B> | 10 | 0.2–2 | II | Jenkyns (1988); Farrimond et al. (1988); Baudin et al. (1990a) |
| WB | Wales (Great Britain) | Toarcian | TS | 90 | 0.2–1.5 | II+III | Baudin (1989) |
| Yor | Yorkshire (Great Britain) | Toarcian | TS | 30 | 3–20 | II | Morris (1979); Myers and Wignall (1987) |

Abbreviations: B> = basin above the CCD (Calcite Compensation Depth); B< = basin below the CCD; CP = carbonate platform; D = deltaic; FL = fluvial and lacustrine; ML = margino-littoral and inner shelf; PR = paleo rise; TS = terrigenous shelf.

Table 2. Location, age, environment, thickness, and main geochemical characteristics of the selected source rocks and organic-rich facies reported on the Kimmeridgian map.

| Code | Basin/Province (Country) | Age | Paleoenv. | Thickness (m) | % TOC Range | Kerogen Type | Selected References |
|------|--|----------------------------|-----------|------------------|----------------|-----------------|---|
| 105 | Site DSDP 105 (Central Atlantic) | Oxfordian– Tithonian | B> | | 0–0.5 | IV | Herbin et al. (1983); Katz (1983) |
| 367 | Site DSDP 367 (Central Atlantic) | Oxfordian– Tithonian | B> | 50 | 0–0.2 | IV | Herbin et al. (1983); Katz (1983) |
| 391 | Site DSDP 391 (Central Atlantic) | Oxfordian– Tithonian | B> | | 0–0.3 | IV | Herbin et al. (1983); Katz (1983) |
| 534 | Site DSDP 534 (Central Atlantic) | Oxfordian– Tithonian | B> | 30 | 0–1.3 | IV | Herbin et al. (1983); Katz (1983); Summerhayes (1983) |
| ADB | Al-Mado Daror (Yemen) | Oxfordian– Tithonian | B> | 230 | ? | black shales | Beydoun (1986); Haitham and Nani (1990) |
| Af | (Afghanistan-Tadzikistan) | Oxfordian– Tithonian | B> | ? | ? | black shales | Ulmishek and Klemme (1990) |
| Aq | Aquitaine (France) | Kimmeridgian | CP | | 0.1–0.5 | IV | Carozzi et al. (1972) |
| BarB | Barrow-Dampier (Australia) | Oxfordian– Tithonian | TS | ? | 1–3 | III to II/III | Osborne and Howell (1987) |
| BoB | Bonaparte (Australia) | Oxfordian– Tithonian | B> | 100 | 0.5–2 | II+III | Whibley and Jacobson (1990); Botten and Wulff (1990) |
| BrB | Browse (Australia) | Oxfordian– Tithonian | TS | ? | 0.5–2 | II to II+III | Thomas (1982); Volkman et al. (1983); Masters and Scott (1986) |
| CarB | Carnarvon (Australia) | Oxfordian– Tithonian | TS | ? | 1–2 | II to II/III | Thomas (1982) |
| GC | Great Caucasus (Armenia, Azerbaïdjan) | Oxfordian– Tithonian | TS | ? | ? | black shales | Ulmishek and Klemme (1990) |
| Dor | Dorset (Great Britain) | Kimmeridgian | TS | | <1 | II | Cox and Gallois (1981) |
| ErB | Eromanga (Australia) | Oxfordian– Tithonian | FL | ? | 1–7 | III | Kantsler et al. (1984) Hamilton et al. (1988) |
| ET | Taurus (Turkey) | Kimmeridgian | B> | 3 | 0.5–30 | II | Baudin et al. (1994) |
| I | Ionian (Greece) | Oxfordian– Kimmeridgian | B> | 50 | 0.2–3 | II+III | Danelian and Baudin (1990) |
| JAB | Jeanne d'Arc (Canada) | Kimmeridgian | TS | 75–100 | 1–9 | II | Powell (1985); Grant et al. (1988); von der Dick (1989) |

Table 2 (continued).

| Code | Basin/Province (Country) | Age | Paleoenv. | Thickness (m) | % TOC Range | Kerogen Type | Selected References |
|------|-----------------------------|----------------------------|-----------|------------------|----------------|-----------------|--|
| LB | Lusitanian (Portugal) | Kimmeridgian | D | 300 | 1-20 | III | Baudin (unpublished) |
| LMB | Lugh Mandra (Somalia) | Oxfordian- Tithonian | TS | ? | ? | black shales | Beydoun (1989) |
| Ly | (Lybia) | Oxfordian- Tithonian | TS | ? | ? | black shales | Thusu et al. (1988) |
| Mek | Mekele (Ethiopia) | Oxfordian- Tithonian | TS | 70 | ? | black shales | Beydoun (1989); Savoyat et al. (1989) |
| N | Normandie (France) | Kimmeridgian | TS | 10 | 0.1-0.5 | IV-II | Baudin (1992) |
| OB | Ogaden (Ethiopia) | Oxfordian- Tithonian | TS | ? | ? | black shales | Savoyat et al. (1989) |
| PeB | Perth (Australia) | Oxfordian- Tithonian | FL | 1000 | 0.5-2 | III | Lord (1976); Thomas (1979) |
| PoB | Porcupine (Ireland) | Kimmeridgian- Tithonian | TS | 100 | 1-4 | II | Croker and Shannon (1987) |
| Qa | (Qatar) | Oxfordian- Tithonian | CP | 100 | 1-6 | II | Murris (1980); Alsharshan and Naim (1990) |
| SaB | Sabinas (Mexico) | Kimmeridgian- Tithonian | TS | ? | ? | black shales | Longoria (1984) |
| ScS | Scotian Shelf (Canada) | Kimmeridgian | TS | ? | 1-3 | II+III | Purcell et al. (1979, 1980); Mukhopadhyay and Wade (1990) |
| TamB | Tampico-Tuxpan (Mexico) | Kimmeridgian- Tithonian | B> | 200 | 0.5-3 | II | Guzman-Vega (1991) |
| Th | Thakkhola (India) | Oxfordian- Tithonian | B> | 200 | 0.5-2 | II to III | Gradstein et al. (1989, 1991); Baudin (unpublished) |
| TN | Carson (Canada) | Kimmeridgian- Tithonian | TS | ? | 0.5-1 | II+III | Powell (1985) |
| Tur | Amu Darya (Turkestan) | Oxfordian- Kimmeridgian | CP | ? | ? | black shales | Ulmishek and Klemme (1990) |
| UAE | (United Arab Emirates) | Oxfordian- Tithonian | ML | ? | 0.2-5.5 | II | Alsharshan (1985); Beydoun (1986) |
| VB | Vienna (Austria) | Oxfordian- Tithonian | B> | | 0.3-3 | II+III | Ladwein (1988) |
| VoB | Vocontian (France) | Kimmeridgian | B> | | 0-0.3 | IV | Lever (1991) |
| Yem | (Yemen) | Oxfordian- Tithonian | TS | 20 | ? | black shales | About Ela (1987) |

Abbreviations: B> = basin above the CCD (Calcite Compensation Depth); CP = carbonate platform; D = deltaic; FL = fluvial and lacustrine; ML = margino-littoral and inner shelf; TS = terrigenous shelf.

graphic refinement is possible for certain well-known intervals and well-studied basins, but the lack of biostratigraphic information in other places, particularly in continental series, is a complex problem. The stratigraphic data of every source rock reported on the map are referenced in Table 2.

Compared to the Toarcian map, the Kimmeridgian reconstruction is characterized by a new kinematic configuration resulting in the opening of the North Atlantic Ocean.

Australian and Indian Domain

On the southern border of the Neotethys, the Indian and Australian blocks were still linked together. However, the rifting on the northern margin of Australia caused the formation of small and isolated basins suitable for deposition of the mixture of organic facies II and III or, more frequently, type III kerogen when the terrigenous supply was great. They are especially well developed at the northwestern shelf of Australia and southern Timor but their dating is often imprecise. Southward, organic facies III is known in the Perth and Eromanga basins within thick, poorly dated continental series. On the northern margin of India, organic-rich deposits are reported from the Oxfordian to Tithonian Spiti Shales and Nupra formations (Gradstein et al., 1989, 1991).

Arabian and African Margins

Rifting in Gondwana resulted in the opening of an oceanic basin between eastern Africa and the India-Madagascar block. This new corridor promoted the deposition of black shales facies on the eastern part of Africa while no organic-rich beds are described on its eastern part (western India-Madagascar).

The Arabian Peninsula had moved from the equatorial belt to the tropical arid zone as a consequence of the southeastward drift of the Africa-South America megablock. This location, suitable for deposition of type II source rocks, initiated during the Oxfordian with the Hanifa Formation and its equivalents and continued locally during the Kimmeridgian.

Atlantic Margins

The opening of the North Atlantic Ocean paralleled the opening of the western arm of the Neotethys (the Ligurian and Alboran-Penninic basins). A continuous oceanic corridor extended from the Gulf of Mexico to Indonesia and Australia. Thus, a world-circling oceanic circulation existed along the north tropical belt.

In the young and narrow North Atlantic Ocean, no good source-rock deposits are known from the Cat Gap Formation. DSDP data from Sites 105, 365, 391, and 534 indicate a type IV kerogen from each site. In the Gulf of Mexico province, Kimmeridgian-Tithonian organic-rich shales containing dominant organic facies II were deposited in the Tampico-Tuxpan and Sabinas basins in Mexico. These source rocks were deposited at the newly created continental margin in deep and isolated troughs, where circulation was restricted.

Eurasian Margins

On the northern margin of the Neotethys, the Cimmerian block was now close to collision with Asia.

Active arc-type volcanism was still present from northern Turkey to northern Himalaya. Our knowledge on organic-rich beds from Caucasus to Indonesia is poor, but Ulmishek and Klemme (1990) reported possible Upper Jurassic source rock from central Caucasus to Afghan-Tadzhik.

Eurasia had shifted from a temperate humid belt toward a north tropical belt since the Toarcian. This probably explains the disappearance of the previously abundant coal-bearing facies, and the wide occurrence of reef limestones as well as the local appearance of evaporitic basins.

European Platform

The northwestern European platform, with predominantly terrigenous deposits during the Toarcian, was now bordered by a carbonate platform along its southern margin. The Kimmeridgian deposits in the Channel and the Paris basin are dominated by type II kerogen. Organic-rich shales of Kimmeridgian and Tithonian age are well developed northward (North Sea, west Siberia, North Slope of Alaska, etc.). This widespread deposition of type II source rocks in high paleolatitudes is worth noting, although, of course, most are not shown on our map. A southern branch of these prolific northern marine source rocks is known in the Porcupine trough, Jeanne d'Arc basin, and along the Scotian shelf. Some organic facies III is known in the Lusitanian basin within the Abadia Marls Formation.

Mediterranean Tethys

In the Mediterranean Tethys, the general organization of troughs and platforms has not changed since the Early Jurassic. During the Kimmeridgian, the troughs deepened and radiolarite deposits were widespread (De Wever et al., 1994). Few basins have conditions favorable for source-rock deposition. However, there were mainly silled basins (southern Turkey) or isolated medium-deep troughs (western Greece) where organic facies II and II+III are recorded. These series, however, contain relatively thin organic-rich deposits (5 to 15 m on average). Borehole data from the substratum of Austrian Molasse basin indicate that the Kimmeridgian basinal shales are the main hydrocarbon source in the Vienna basin (Ladwein, 1988).

Cenomanian

The Cenomanian paleogeography was characterized by a wide North Atlantic Ocean and by the opening of new seaways (Figure 3 and Table 3).

Australian and Indian Domain

On the southern border of the Neotethys, the Indian and Australian blocks were separated. The change in the direction of spreading between India and Australia also corresponded to the separation of Madagascar from India. The latter started its rapid northward motion. Most of Australia, which was covered by shallow seas during the Aptian-Albian, was continental during the late Cenomanian. Thus, fluvial and lacustrine environments are well represented, especially in Great Artesian and Eromanga basins within the late Albian-Cenomanian Witton Sandstone Formation

which supported the deposition of carbonaceous shales and minor coal beds. On the southern margin of Australia, the Otway and Bass basins were also suitable to minor coal deposits. No organic-carbon-rich formation seems to have existed on the Indian plate during the Cenomanian.

Arabian and African Margins

Extensive carbonate platforms occupied the eastern and northern shelves of Africa and Arabia. Some locations corresponding to protected environments (Turkey, Israel, and Lebanon) supported the preservation of type II organic matter. On the Arabia peninsula (Iraq, United Arab Emirates, and Oman), shelf areas were dominated by the type II organic-rich Misrif Formation. In northeast Africa, a wide lacustrine to fluvial-deltaic system extended along the present Nile basin. Poorly dated sandstone and clay deposits contain a lot of plant remains but their organic content is, unfortunately, unknown.

Atlantic and Caribbean Margins

Cenomanian Atlantic deposits, well known from numerous DSDP and ODP sites, show important variation in lithology and sedimentation rates. Organic-carbon-rich layers appear at all bathymetric levels, but thickest accumulations occur in outer shelf environments and in low-latitude areas. There is a trend of decreasing organic-carbon content and of shorter duration of the organic pulse from south to north (Kuhnt et al., 1990). For instance, the record of Cenomanian organic-rich sediments in the Celtic Sea basin (Sites 549 to 551) is limited to a single 0.5 m thick black shale layer around the Cenomanian-Turonian boundary within the chalk, whereas the Senegal basin contains a 400 m thick black shale series ranging from late Albian to Turonian.

A complicated paleogeography, with numerous isolated carbonate platforms and with subduction beneath the advancing Great Antilles island arc, characterized the Caribbean domain. Organic-rich deposits are rare except in DSDP sites from the Florida Straits, where a mixture of type IV and II organic matter is recorded. The South American plate was independent from both Africa and North America. In western Venezuela, the basal part of the La Luna Formation, or its coeval, more pelagic, Querencual Formation in eastern Venezuela, consisted of organic-rich black and cherty fine-grained limestones (Talukdar et al., 1985; Tribovillard et al., 1991).

Eurasian Margins

Along the northern margin of the Neotethys, a narrow furrow, infilled by flysch, separated western Europe from the Apulia promontory. Eastward, from the Rhodope Massif to Borneo, subduction of the Tethyan ocean crust gave birth to volcanic arcs and back-arc basins. The organic content of these extensive terrigenous environments is poorly documented for the Cenomanian.

In western Europe, much of the Early Cretaceous land area was inundated. Consequently, the terrigenous influx was reduced and the deposition of the pelagic chalks series took place. Some northern sites,

such as the Bohemian basin, show low carbon content in clastic and shaly late Cenomanian deposits.

Mediterranean Tethys

In the Mediterranean Tethys, Cenomanian organic-rich facies are mainly distributed in deep environments where redeposition was frequent. Organic-rich facies consist frequently of thin, black chert or shaly limestones with radiolaria such as the famous "Livello Bonarelli" in Italy or the coeval bed in the Rif and Gibraltar arch domain (Thurrow and Kuhnt, 1986). They extend as far east as the Vocontian trough in the Alpine domain (Crumi re et al., 1990).

DEPOSITIONAL CONTROLS OF TETHYAN SOURCE ROCKS

Organic-matter accumulation in sediments is influenced by both biological and physico-chemical factors. Biological factors include primary productivity of the surface waters and biochemical degradation of organic matter after the death of primary producers. Physico-chemical factors include the mode of settling of organic matter, the sedimentation rates, the redox potential, as well as the size of particles. The relative importance of these processes varies greatly from place to place, depending on the amount of production, water depth, rate of sedimentation, and the availability of oxidants. Many authors (Bitterli, 1963; Pelet and Deroo, 1983; Demaison and Moore, 1980; Calvert, 1987; Durand, 1987; Hallam, 1987; Huc, 1980, 1988; Pedersen and Calvert, 1990, among others) have discussed the relative importance of these different processes in local, or even global, accumulation of organic matter.

At a global scale, it is obvious that factors influencing the sedimentation are indirectly controlled by the continents' configuration, atmosphere and ocean dynamics, and climate (Jansa, 1991). These factors are discussed here for source-rock deposition on the basis of their paleogeographic distribution described above.

Paleolatitude and Climate

Mesozoic climate has mainly been studied using different criteria issuing from paleontology, mineralogy, sedimentology, or geochemistry, and a strong agreement exists in favor of a more equable temperature distribution than today's. Evident polar ice caps were absent and temperature regimes corresponding to tropical and temperate belts extended much farther toward the poles (Hallam, 1975, 1984; Barron, 1983). As briefly outlined above for the Tethyan realm, the Mesozoic geography also had a large contrast to the present with significantly different continental positions and elevations. As a result, the locations of plates through climatic zones had an important influence on facies development and especially on source-rock distribution.

These maps show that the latitudinal distribution of humic organic matter (coal and type III) was roughly opposite to the distribution of type II organic matter. Several factors may interact to control such distribu-

Table 3. Location, age, environment, thickness, and main geochemical characteristics of the selected source rocks and organic-rich facies reported on the Cenomanian map.

| Code | Basin/Province (Country) | Age | Paleoenv. | Thickness (m) | % TOC Range | Kerogen Type | Selected References |
|------|---|------------|-----------|------------------|----------------|-----------------|--|
| 5 | DSDP Site 5 (western North Atlantic) | Cenomanian | B< | | ? | bitumen? | Ewing and Worzel (1969) |
| 97 | DSDP Site 97 (Gulf of Mexico) | Cenomanian | B> | | <1 | II+III | Boyce (1973) |
| 101 | DSDP Site 101 (western North Atlantic) | Cenomanian | B< | | <0.5 | IV | Philip et al. (1993) |
| 105 | DSDP Site 105 (western North Atlantic) | Cenomanian | B< | 3-5 | 2-10 | II/III-II | Herbin et al. (1986) |
| 135 | DSDP Site 135 (offshore Morocco) | Cenomanian | B< | <2 | 2-12 | II | Herbin et al. (1986) |
| 137 | DSDP Site 137 (central North Atlantic) | Cenomanian | B< | 1 | 1-4 | IV-II/III | Herbin and Deroo (1982) |
| 367 | DSDP Site 367 (offshore Senegal) | Cenomanian | B< | 4 | >5 | II | Deroo et al. (1977); Herbin and Deroo (1982) |
| 370 | DSDP Site 370 (offshore Morocco) | Cenomanian | B< | | <1 | IV | Herbin and Deroo (1982) |
| 386 | DSDP Site 386 (central North Atlantic) | Cenomanian | B< | <0.5 | 1-5 | IV-II | Herbin and Deroo (1982) |
| 387 | DSDP Site 387 (central North Atlantic) | Cenomanian | B< | <0.5 | 0.5-15 | IV-II | Herbin and Deroo (1982) |
| 391 | DSDP Site 391 (western North Atlantic) | Cenomanian | B< | | <0.5 | IV | Philip et al. (1993) |
| 398 | DSDP Site 398 (Galicia Bank) | Cenomanian | B> | 0.5 | 2-10 | II/III-II | Deroo et al. (1979); Herbin et al. (1986) |
| 415 | DSDP Site 415 (offshore Morocco) | Cenomanian | B< | | <1 | III | Herbin et al. (1986) |
| 417 | DSDP Site 417 (central North Atlantic) | Cenomanian | B< | | <0.5 | IV | Herbin and Deroo (1982) |
| 534 | DSDP Site 534 (western North Atlantic) | Cenomanian | B< | | <1 | IV | Herbin et al. (1983) |
| 535 | DSDP Site 535 (Gulf of Mexico) | Cenomanian | B> | 100 | 0.7-7 | IV-II | Herbin et al. (1984) |
| 540 | DSDP Site 540 (Gulf of Mexico) | Cenomanian | B> | | 1 | II | Patton et al. (1984) |
| 545 | DSDP Site 545 (offshore Morocco) | Cenomanian | B> | | <1 | II+III | Deroo et al. (1984) |
| 547 | DSDP Site 547 (offshore Morocco) | Cenomanian | B> | | <1 | II+III | Deroo et al. (1984) |

Table 3 (continued).

| Code | Basin/Province (Country) | Age | Paleoenv. | Thickness (m) | % TOC Range | Kerogen Type | Selected References |
|------|---|-------------------------|-----------|------------------|----------------|-----------------|---|
| 549 | DSDP Site 549 (Goban Spur) | Cenomanian | B> | <0.5 | 0.1-3 | IV-II/III | Waples and Cunningham (1985) |
| 550 | DSDP Site 550 (Goban Spur) | Cenomanian | B> | <0.5 | 0.5-1 | IV-II/III | Waples and Cunningham (1985) |
| 551 | DSDP Site 551 (Goban Spur) | Cenomanian | B> | <0.5 | 0.1 | IV | Waples and Cunningham (1985) |
| 603 | DSDP Site 603 (western North Atlantic) | Cenomanian | B< | 3-5 | 0.5-5 | IV-II/III | Herbin et al. (1987) |
| 627 | ODP Site 627 (Bahamas) | Albian- Cenomanian | B> | | <1 | III | Katz (1988) |
| 635 | ODP Site 635 (Bahamas) | Albian- Cenomanian | B> | | 1-2.5 | II/III-II | Katz (1988) |
| 641 | ODP Site 641 (Galicia Bank) | Cenomanian | B> | 0.3 | 0.2-11 | IV-II | Meyers et al. (1987); Thurow et al. (1988) |
| 763 | ODP Site 763 (Exmouth Plateau) | Cenomanian | B> | 0.5 | 0.2-20 | IV-II | Thurow et al. (1992) |
| A | (Algeria) | Cenomanian | B> | ? | 2-5 | II | Thurow and Kuhnt (1986); Herbin et al. (1986) |
| Ao | Alboran (Morocco) | Cenomanian | B< | 1-10 | 3-10 | II | Herbin et al. (1986); Bachaoui et al. (1992) |
| AP | (Abu Dhabi/Saudi Arabia) | Cenomanian | B> | 90-120 | >10 | II | Ulmishek and Klemme (1990) |
| BasB | Bass (Australia) | Albian- Cenomanian | ML | ? | ? | coal | Nicholas et al. (1981) |
| Ben | Benué (Nigeria) | Cenomanian | TS | 1-8 | 2-4 | II | Kuhnt et al. (1990) |
| Bo | Bohemian (Czech) | Cenomanian | TS | 5 | <1 | IV | Ulicny et al. (1993) |
| Ca | Calabria-Sicily (Italy) | Cenomanian | B< | 1-10 | >5 | II | Thurow and Kuhnt (1986); Herbin et al. (1986) |
| CarB | Carnarvon (Australia) | Albian- Cenomanian | FL | ? | 0.5 | IV | Thomas (1982) |
| CbT | Celtiberic (Spain) | Cenomanian- Turonian | B> | <1 | <1 | IV | Herbin et al. (1986) |
| CoB | Cooper (Australia) | Albian- Cenomanian | FL | ? | ? | coal | Khorasani (1987) |
| ErB | Eromanga (Australia) | Albian- Cenomanian | FL | 1000 | 2-16 | coal | Moore and Pitt (1984) |
| ET | Eastern Taurus (Turkey) | Cenomanian | CP | 10 | 1-9 | II | Baudin (unpublished) |
| Eu | Euganean Hills (Italy) | Cenomanian | B> | 3 | 2 | II | Herbin et al. (1986) |
| LeB | (Israel and Lebanon) | Cenomanian | CP | 100 | 0.7-2.5 | IV-II | Lipson-Benitah et al. (1990) |
| NiB | Nile (Sudan and Egypt) | Albian-Turonian | FL | ? | ? | coal | Wycisk et al. (1990) |
| OtB | Otway (Australia) | Albian- Cenomanian | ML | ? | ? | coal | Struckmeyer and Felton (1990) |

Abbreviations: B> = basin above the CCD; B< = basin below the CCD (Calcite Compensation Depth); CP = carbonate platform; FL = fluvial and lacustrine; ML = margino-littoral and inner shelf; TS = terrigenous shelf.

Continued on following page

Table 3 (continued). Location, age, environment, thickness, and main geochemical characteristics of the selected source rocks and organic-rich facies reported on the Cenomanian map.

| Code | Basin/Province (Country) | Age | Paleoenv. | Thickness (m) | % TOC Range | Kerogen Type | Selected References |
|------|-----------------------------|-------------------------|-----------|------------------|----------------|-----------------|--|
| PnB | Penibetic (Spain) | Cenomanian– Turonian | B> | 1–5 | 4–30 | II | Thurov and Kuhnt (1986) |
| RiB | Rif (Morocco) | Cenomanian | B> | 5–40 | 0.6–20 | IV–II | Kuhnt et al. (1990) |
| SB | Cesamance (Senegal) | Cenomanian | TS–B> | 400 | 3–10 | II | Herbin et al. (1986) |
| SuB | Sub-betic (Spain) | Cenomanian– Turonian | B> | 3 | <1 | III | Herbin et al. (1986) |
| T | (Tunisia) | Cenomanian | CP | 30 | 2–4 | II | Herbin et al. (1986) |
| TarB | Tarfaya (Morocco) | Cenomanian | TS | 200 | 3–15 | II | Herbin et al. (1986) |
| UMB | Umbria-Marches (Italy) | Cenomanian | B> | 1–2 | >5 | II | Herbin et al. (1986) |
| Va | Carpathian (Romania) | Cenomanian– Turonian | B> | ? | 2 | II | Philip et al. (1993) |
| VoB | Vocontian (France) | Cenomanian | B> | 150 | 0.5–2 | III–II | Crumiere et al. (1990) |
| Vz | (Venezuela) | Albian– Cenomanian | B> | 50–100 | 1–4 | II | Talukdar et al. (1985); Tribovillard et al. (1991) |

Abbreviations: B> = basin above the CCD; B< = basin below the CCD (Calcite Compensation Depth); CP = carbonate platform; FL = fluvial and lacustrine; ML = margino-littoral and inner shelf; TS = terrigenous shelf.

tion, but climate appears to have been the most influential. Coal deposits are widely accepted as good indicators of a humid climate (Parrish et al., 1982), though not of temperature. Coal and type III source rocks were more extensively distributed in the Toarcian (Figure 1) than in the Kimmeridgian or Cenomanian (Figures 2 and 3). On the Toarcian map, terrestrial organic-rich facies predominated along the northern margin of the Neotethys, ranging between 40°N and 55°N paleolatitude, from the Danubian domain to Northern Pamir. Important coal measures are noted in the Southern Hemisphere in the same range of paleolatitudes, especially in the Australian basins. The main areal distribution of Toarcian type III source rocks was limited to temperate paleolatitudes where deltaic and fluvio-lacustrine environments were dominant.

During the Kimmeridgian, coal deposits were much more restricted, occurring only in Australia and in the Lusitanian basin in Portugal. It should be noted that the coal areal distribution from the northern Tethyan margin is highly conjectural because little data has been reported from the Caucasus to Indonesia.

Nevertheless, the Late Jurassic is characterized by arid conditions as evidenced by abundant evaporitic deposits and well-developed reefs along the margin of the Tethys. These substantial deposits of evaporites provide the best indicator of an arid, warm climate, unfavorable to coal deposition. It may explain the weak distribution of coal and type III source rock evidenced in the Kimmeridgian map.

The middle Cretaceous climate is thought to have been relatively humid as suggested by the wide distribution of bauxite (Bardossy and Dercourt, 1990). However, the distribution of Cenomanian type III source rock is not significant and coal seams represent generally thin deposits with a mean organic richness (Table 3). It should be noted that the distribution of coal in the Southern Hemisphere extended to 65°S and was probably related to the expansion of the tropical and temperate climatic belts at that time (Barron, 1983).

Many lithologies from the northern Tethyan margin contain moderate amounts of terrestrial organic matter, but probably not enough to be designated as source rocks.

The tropical belt seems not suitable for type III organic-matter deposition, except in some basins during the Toarcian interval (i.e., Honduras and Mexico basins). It is well known that the present tropical rain forests sustain extremely high organic productivity, but relatively low accumulations of organic matter occur because of the high rate of decomposition. This was probably true during the Mesozoic when coals and type III kerogen in equatorial positions were deposited only in the rift basins where an important detrital input protected the organic matter from degradation.

The distribution of type II source rocks is prominent in low- and medium-latitude zones for the three studied intervals. They were mainly concentrated between 10°N and 30°N in the Mediterranean Seuil and on the European platform during the Toarcian, whereas a widespread distribution, ranging from 40°S

to 40°N, characterized the Kimmeridgian and Cenomanian. The Toarcian concentration around the Mediterranean Seuil is partly due to the nonexistence of the Atlantic at that time, and the development of fluvio-deltaic or margino-littoral environments, unfavorable to type II source-rock preservation along the southern margin of the Tethys.

The widespread distribution of marine source rocks at low paleolatitudes during the Kimmeridgian and Cenomanian is mainly managed by the existence of the Atlantic Ocean and its margins where most of the black shales accumulated. It should be noted, however, that marine source rocks were also widespread in high northern paleolatitudes during the Late Jurassic, but these regions are not covered by the Kimmeridgian map presented here. Ulmishek and Klemme (1990) have suggested that this particular northern richness in marine source rocks could be linked to the development of suitable tectonic structures in the northern subpolar regions (rift in the North Sea, circular sag in western Siberia) correlative with a possible high-latitude anoxic event. Nevertheless, several authors (Bois et al., 1980; Parrish and Curtis, 1982; North, 1985) have suggested that the low-latitude position of the Tethyan realm favored the development of anoxic conditions because of its isolation from oxygenated polar waters. The low to medium latitudes of the Tethyan realm during the Kimmeridgian and the Cenomanian probably supported high organic productivity.

Oceanic Seaways and Water Ventilation

The closing and opening of seaways has an important effect on the deposition and distribution of source rocks because they induced new circulation patterns and, hence, modifications in the local or global oxygenation of water, as well as modifications in climate. The evolution of circulation in the Tethys, intimately linked with the kinematic history, largely controlled the distribution of source rocks.

As illustrated on our maps, an important event was the opening of the oceanic corridor between the North Atlantic and the Pacific oceans. Dating of this event still remains controversial: suggested dates range from as early as the Pliensbachian to as late as the Oxfordian. In any case, this opening changed the surface hydrodynamic pattern of the central North Atlantic, which passed from a cul-de-sac system illustrated by the Toarcian map (Figure 1) to an open-channel system illustrated by the Kimmeridgian map (Figure 2).

The evidence for this change is recorded in the change from shallow restricted facies to white and red deeper facies. The absence of organic-rich deposits during the Kimmeridgian in the North Atlantic may be related to good water oxygenation induced by this latitudinal current along the northern tropical belt.

Continued expansion of the North Atlantic resulted in a widening surface circulation that permitted an equatorial countercurrent and a return flow along the southeast edge of the North Atlantic.

A second example of seaway influence is illustrated by Cretaceous Atlantic deposits. The Early Cretaceous corresponds to the first collision between Apulia and Eurasia, which induced the closure of the Ligurian deep-ocean seaway (Ricou, 1987). At the same time, landmasses or very shallow seas still separated the Atlantic and the Tethys from deep and oxygenated polar waters. The present deep north-south currents of cold and oxygenated water did not exist in the deep basins at that time. Sluggish circulation within the North Atlantic resulted from this isolation and anoxic deposition took place from the early Aptian to the Cenomanian–Turonian (Jenkyns, 1980). Weak circulation was certainly one of the main reasons for the lack of oxygen replenishment and the formation of black shales.

The disappearance of the barrier between the North and the South Atlantic during the Late Cretaceous led to a new pattern of oceanic circulation which progressively swept the sluggish water masses out of the Neotethys (Herbin et al., 1986). This may explain the disappearance of anoxic conditions and the end of black shale preservation.

Basin Morphology and Structural Evolution

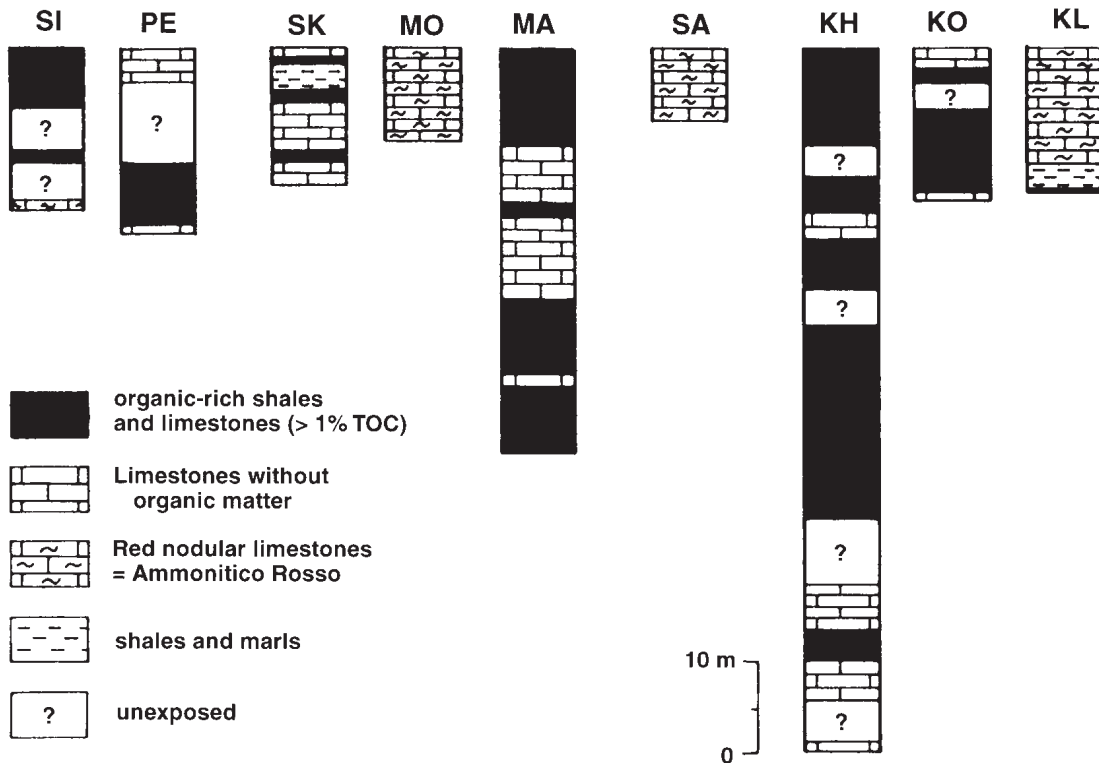
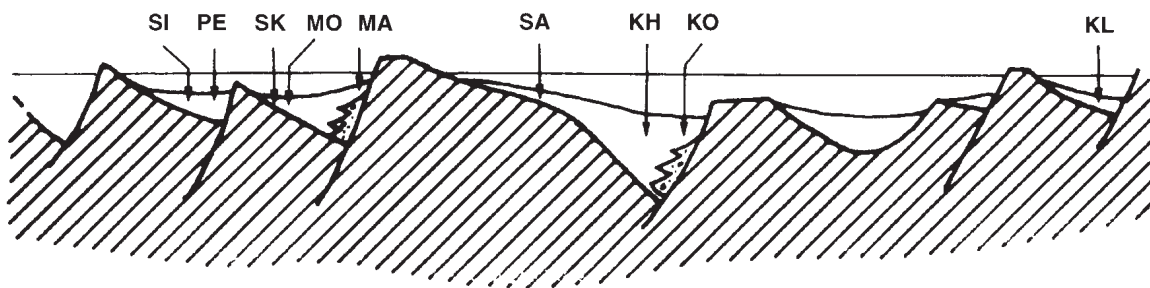
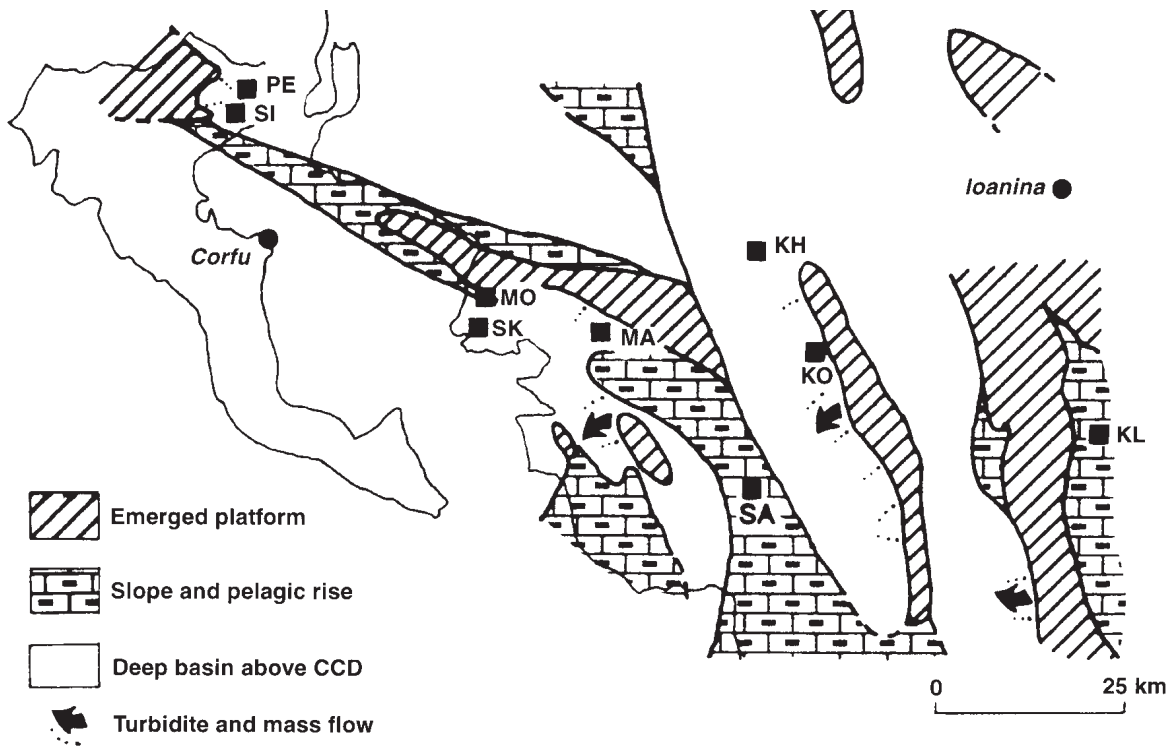
Basin morphology and structural evolution had a fundamental influence on the availability of clastic material, as well as on the rate of subsidence and sedimentation.

The distribution of type III kerogen and coals varies relatively little between different basin morphologies. They occurred in all structural settings and the critical parameters appear to have been the runoff in the land area and the clastic input into the basin. However, basin morphology primarily controlled the deposition of the type II source rocks. The anoxic or suboxic conditions occurred preferentially in silled basins and in deep, isolated troughs. The Toarcian paleogeography of the Mediterranean Tethys (Figure 1) clearly illustrates the influence of the basin morphology on the preservation of marine organic matter. An intense crustal extension of this region during the middle and late Lias created a complex paleogeography with small carbonate platforms surrounded by more or less deep basins, such as the Ionian trough (Figure 4). During the early and middle Lias, the Ionian trough was affected by important vertical movements attested to by numerous gravity

deposits. The tops of tilted blocks corresponded to areas (both subaerial and submarine) being denuded; slopes and pelagic rises were frequently characterized by the deposition of red nodular limestones, the so called "Ammonitico Rosso" facies (Aubouin, 1964; Jenkyns, 1974; Cecca et al., 1992). The resulting topography of the basin promoted the onset of water stratification that permitted the accumulation of type II organic matter in the deepest parts of the basin. Organic-carbon-rich black shales and limestones are effectively restricted to the basin flanks, edge of shelf highs (Jenkyns, 1988), as well as the deepest part of the half-graben (Baudin and Lachkar, 1990). In the closer basins, such as the Lagonegro trough or the Pindus-Olonos, more open into the oceanic oxic circulation, only type IV kerogen was present (Jenkyns, 1988; Baudin and Lachkar, 1990).

The stratigraphic distribution of source rocks from the western Tethys clearly illustrates the influence of the basin evolution. The Mesozoic breakup of western Gondwana was marked by the development of extensive rift basins which promoted a network of small and isolated depressions (Toarcian map, Figure 1). Under tropical climates, these basins were mostly dominated by fluvio-deltaic deposits and/or marsh environments. The organic matter accumulated is mainly of type III (e.g., the Oaxaca coal deposits). During the subsequent phase of extension (Kimmeridgian map, Figure 2), the former narrow basins were affected by important vertical movements which created deep and elongated troughs separated by uplifted blocks. These basins were progressively invaded by the sea where the topography promoted the onset of water stratification. The latter was maybe occasionally reinforced by an influx of saline waters from surrounding evaporitic platforms. These factors, coupled with an adequate phytoplanktonic productivity, contributed to the development of oxygen-depleted deep waters and, hence, to the preservation and accumulation of type II source rocks (i.e., the Taman Formation from the Tampico-Tuxpan basin). In the late stage of the basin evolution (Cenomanian map, Figure 3), the tectonic distension reached its maximum and the deep isolated troughs were progressively opened to marine circulation with oxygenated waters. At that time, the disappearance of topographic barriers permitted the ventilation of the basins, which terminated water stratification and extensive organic-matter preservation.

Figure 4. Paleogeography of Ionian zone (western Greece) during the Toarcian and schematic postulated west-east cross section of comparable horizontal scale (modified from IGRS-IFP, 1966, and Baudin and Lachkar, 1990). The tops of tilted blocks correspond to areas (both subaerial and submarine) being denuded. Slopes and pelagic rises promoted the deposition of red nodular limestones (Ammonitico Rosso facies), and troughs are suitable to organic-carbon-rich black shales and limestones. Coarse debris was also dumped into troughs from the steep, western flanks of tilted blocks. Note CCD: Calcite Compensation Depth. Studied sections are marked by a square. SI = Siniais, PE = Perithia, SK = Skoupitsa, MO = Mavron Oros, MA = Mavroudhi, SA = Skandhalon, KH = Khionistra, KO = Koukouloi, and KL = Kouklessi. Precise locations and full lithological details of black shale sections as well as their organic content studies may be found in Baudin and Lachkar (1990), whereas Ammonitico Rosso sections are described by Galbrun et al. (1994).



CONCLUSIONS

It is well known that periods of widespread formation of source rocks are generally nearly synchronous with major transgressions. Nevertheless, this tendency is locally or regionally reinforced by others factors which are (1) the positions of continental plates through the climatic zones that influence coal deposition; (2) the opening and closing of seaways that affect oceanic circulation patterns, water chemistry and, hence, the distribution of black shales; and (3) basin morphology that influences water stratification.

This review is, of course, limited because all the sedimentary changes within the Tethys were linked not just with Tethyan phenomena. But it also emphasizes a critical point of global source-rock mapping and environmental interpretations: except for the well-studied basins, the stratigraphic control on the age of most source rocks is weak. They generally correspond to time intervals equivalent to several ammonite zones, and frequently have a less precise dating. The result is a coeval distribution for a 2–6 m.y. time interval. However, when stratigraphic control is improved, the synchronicity of source-rock deposits is usually less evident. Consequently, the present review calls for further discussion between stratigraphers and sedimentologists in order to clarify this problem.

ACKNOWLEDGMENTS

General financial support for the Tethys Paleoenvironments Atlas comes from BP, BRGM, CNRS-INSU, Elf, IFP, IFREMER, Shell, Total, and UPMC. We also thank Jean Dercourt for his enthusiasm and his helpful comments. The figures were drafted by Michel Petzold.

REFERENCES CITED

- Aboul Ela, N.M., 1987, Palynology of Upper Jurassic black shales from northeast of Sana'a (Bani Hushaysh area), Yemen A.R.: *Neues Jahrbuch Geologische Paläontologische Monatshefte*, v. 5, p. 257–266.
- Alsharhan, A.S., 1985, Depositional environment, reservoir units evolution and hydrocarbon habitat of Shuaiba Formation, Lower Cretaceous, Abu Dhabi, United Arab Emirates: *AAPG Bulletin*, v. 69, p. 899–912.
- Alsharhan, A.S., and A.E.M. Nairn, 1990, Geology and hydrocarbon potential in the state of Qatar, Arabian Gulf: *AAPG Bulletin*, v. 74, p. 598.
- Aubouin, J., 1964, Réflexions sur le faciès "ammonitico-rosso": *Bulletin Société Géologique France*, v. 6, p. 475–501.
- Bachaoui, E.M., J-R. Disnar, and A. Desprairies, 1992, Caractérisation et diagenèse de la matière organique à la limite Cénomanién–Turonien dans le domaine externe de la chaîne rifaine (Maroc). Influence de la tectonique: *Comptes-Rendus Académie Sciences*, v. 314, p. 1211–1218.
- Bardossy, G., and J. Dercourt, 1990, Les gisements de bauxites téthysiennes (Méditerranée, Proche et Moyen-Orient): cadre paléogéographique et contrôle génétique: *Bull. Soc. Géol. France*, v. 8, p. 869–888.
- Barnard, P.C., and B.S. Cooper, 1981, Oils and source rocks of North Sea area, in I.V. Illing and G.D. Hobson, eds., *Petroleum geology of continental shelf of North-West Europe*: Institute of Petroleum, p. 169–175.
- Barnard, P.C., and B.S. Cooper, 1983, Geochemical data related to the Northwest European gas province, in J. Brooks, ed., *Petroleum geochemistry and exploration of Europe*: Geological Society Special Publication, v. 12, p. 19–33.
- Barron, E.J., 1983, The warm, equable Cretaceous: the nature of the problem: *Earth Science Review*, v. 19, p. 305–338.
- Bassoulet, J.P., G. Lachkar, F. Baudin, K. Benshili, P. Blanc, M. Boutakiout, F. Dépêche, S. Elmi, and C. Ruget, 1991, Stratigraphie intégrée dans le Toarcien du Maroc (Rides sud-rifaines et Moyen Atlas): *Bulletin Société Géologique France*, v. 162, p. 825–839.
- Bassoulet, J.P., S. Elmi, A. Poisson, L.E. Ricou, F. Cecca, Y. Bellion, R. Guiraud, and F. Baudin, 1993, Mid Toarcian (184–182 Ma), in J. Dercourt, L.E. Ricou, and B. Vrielynck, eds., *Atlas Tethys Paleoenvironmental Maps. Explanatory Notes*: Gauthier-Villars, p. 63–80.
- Baudin, F., 1989, Caractérisation géochimique et sédimentologique de la matière organique du Toarcien Téthysien (Méditerranée, Moyen-orient). Significations paléogéographiques: *Mémoire Sciences de la Terre*, v. 30, 350 p.
- Baudin, F., 1992, Étude préliminaire du contenu en matière organique du Kimméridgien normand: *Géologie de la France*, 2, p. 31–38.
- Baudin, F., and G. Lachkar, 1990, Géochimie organique et palynologie du Lias supérieur en zone ionienne (Grèce): exemple d'une sédimentation anoxique dans une paléo-marge en distension: *Bulletin Société Géologique France*, 8, p. 123–132.
- Baudin, F., and K. Téhérani, 1991, Faciès organiques et maturation thermique du Lias supérieur de la Formation de Shemshak (Elbourz central, Iran): *Ecologae Geologicae Helveticae*, v. 84, p. 727–738.
- Baudin, F., J. Dercourt, J.P. Herbin, and G. Lachkar, 1988, Le Lias supérieur de la zone ionienne (Grèce): une sédimentation riche en carbone organique: *Comptes-Rendus Académie des Sciences*, v. 307, p. 985–990.
- Baudin, F., J.P. Herbin, and M. Vandembroucke, 1990a, Mapping and geochemical characterization of the Toarcian organic matter in the Mediterranean Tethys and Middle East: *Organic Geochemistry*, v. 16, p. 677–687.
- Baudin, F., J.P. Herbin, J.P. Bassoulet, J. Dercourt, G. Lachkar, H. Manivit, and M. Renard, 1990b, Distribution of organic matter during the Toarcian in Mediterranean Tethys and Middle East, in A.Y. Huc, ed., *Deposition of Organic Facies: AAPG Studies in Geology* 30, p. 73–91.
- Baudin, F., O. Monod, V. Bégouën, F. Laggoun-Defarge, and A. Person, 1994, Caractérisation et diagenèse de la matière organique du Jurassique

- supérieur du Taurus occidental (Turquie méridionale). Reconstitution paléoenvironnementale et conséquences tectoniques: *Bulletin Société Géologique France*, v. 165, p. 135–145.
- Berggren, W.A., and C.D. Hollister, 1977, Plate tectonics and paleocirculation-commotion in the ocean: *Tectonophysics*, v. 38, p. 11–48.
- Besairie, H., and M. Collignon, 1972, Géologie de Madagascar. I. Terrains sédimentaires: *Annales Géologiques Madagascar*, v. 35, 463 p.
- Beydoun, Z.R., 1986, The petroleum resources of the Middle East: a review: *Journal of Petroleum Geology*, v. 9, p. 5–28.
- Beydoun, Z.R., 1989, The hydrocarbon prospects of the Red Sea–Gulf of Aden: a review: *Journal of Petroleum Geology*, v. 12, p. 125–144.
- Bitterli, P., 1963, Aspects of genesis of bituminous rock sequences: *Geologie en Mijnbouw*, v. 42, p. 183–201.
- Bodenhausen, J.W.A., and W.F. Ott, 1981, Habitat of Rijswijk oil province, onshore, The Netherlands, in I.V. Illing and G.D. Hobson, eds., *Petroleum geology of continental shelf of North-West Europe*: Institute of Petroleum, p. 301–309.
- Bois, C., P. Bouche, and R. Pelet, 1980, Histoire géologique et répartition des réserves d'hydrocarbures dans le monde, in 26ème Congrès Géologique International: *Revue Institut Français Pétrole*, v. 35, p. 273–298.
- Botten, P.R., and K. Wulff, 1990, Exploration potential of the Timor Gap Zone of co-operation: *Australian Petroleum Exploration Association Journal*, v. 30, p. 68–90.
- Boyce, R.E., 1973, Carbon and carbonate analysis, Leg 10: Initial Reports Deep Sea Drilling Project, v. 10, p. 637–639.
- Broquet, P., and M. Thomas, 1979, Quelques caractères géologiques et géochimiques des schistes bitumineux du Toarcien franc-comtois: *Bulletin Centre Recherche Exploration Pau*, v. 3, p. 265–280.
- Calvert, S.E., 1987, Oceanographic controls on the accumulation of organic matter in marine sediments, in J. Brooks and A.J. Fleet, eds., *Marine petroleum source rocks*: Geological Society of London Special Publication 26, p. 137–151.
- Carozzi, A.V., J. Bouroullec, R. Deloffre, and J.L. Rumeau, 1972, Microfaciès du Jurassique d'Aquitaine: *Bulletin Centre Recherche Exploration Pau*, Special v. 1, 594 p.
- Cecca, F., J. Azéma, and E. Fourcade, 1992, The disappeared of the Ammonitico-Rosso: *Palaeogeogr., Palaeoclimatol., Palaeoecol.*, v. 99, p. 55–70.
- Cecca, F., J. Azéma, E. Fourcade, F. Baudin, R. Guiraud, L.E. Ricou, and P. De Wever, 1993, Early Kimmeridgian (146–144 Ma), in J. Dercourt, L.E. Ricou, and B. Vrielynck, eds., *Atlas Tethys Paleoenvironmental Maps*. Explanatory Notes: Gauthier-Villars, p. 97–111.
- Cottureau, N., and M. Lautenschlager, 1994, Tethyan oceanic circulation during the Latest Jurassic: a GMC simulation: *Comptes-Rendus Académie des Sciences*, v. 318, p. 389–396.
- Cox, B.M., and R.W. Gallois, 1981, The stratigraphy of the Kimmeridgian Clay of the Dorset type area and its correlation with some other Kimmeridgian sequences: *Institut Geological Sciences Report*, 80/4, 44 p.
- Croker, P.F., and P.M. Shannon, 1987, The evolution and hydrocarbon prospectivity of the Porcupine basin, offshore Ireland, in J. Brooks and K. Glennie, eds., *Petroleum Geology of North West Europe*: Graham and Trotman, p. 633–642.
- Crumière, J.P., C. Crumière-Airaud, J. Espitalié, and P. Coton, 1990, Global and regional controls on potential source-rock deposition and preservation: the Cenomanian–Turonian Oceanic Anoxic Event (CTOAE) on the European Tethyan margin (Southeastern France), in A.Y. Huc, ed., *Deposition of Organic Facies*: AAPG Studies in Geology 30, p. 107–117.
- Danelian, T., and F. Baudin, 1990, Découverte d'un horizon carbonaté, riche en matière organique, au sommet des radiolarites d'Épire (zone ionienne, Grèce): le Membre de Paliambela: *Comptes-Rendus Académie Sciences*, II, v. 311, p. 421–428.
- de Lapparent, A.F., and J. de Lavigne, 1965, A propos de l'âge de la série de Saïgan et du charbon en Afghanistan: *Annales Société Géologique Nord*, v. 85, p. 105–109.
- Demaison, G., and G.T. Moore, 1980, Anoxic environments and oil bed genesis: *American Association of Petroleum Geologists Bulletin*, v. 64, p. 1179–1209.
- Dercourt, J., L.E. Ricou, and B. Vrielynck, 1993, *Atlas Tethys Paleoenvironmental Maps*: Gauthier-Villars, 307 p. and 14 maps.
- Deroo, G., J.P. Herbin, J. Roucaché, and B. Tissot, 1977, Organic geochemistry of some Cretaceous black shales from sites 367 and 368; Leg 41, Eastern North Atlantic: Initial Reports of Deep Sea Drilling Project, v. 41, p. 865–873.
- Deroo, G., J.P. Herbin, J. Roucaché, and B. Tissot, 1979, Organic geochemistry of Cretaceous shales from DSDP Site 398, Leg 47B, Eastern North Atlantic: Initial Reports of Deep Sea Drilling Project, v. 47, p. 513–522.
- Deroo, G., J.P. Herbin, and J. Roucaché, 1984, Organic geochemistry of Cenozoic and Mesozoic sediments from Deep Sea Drilling Sites 544 to 547, Leg 79, eastern North Atlantic: Initial Reports of Deep Sea Drilling Project, v. 79, p. 721–741.
- De Wever, P., J. Azéma, and E. Fourcade, 1994, Radio-laires et radiolarites, production primaire, diagenèse et paléogéographie: *Bull. Centre Rech. Explo. Pau*, v. 18, p. 315–379.
- Dromart, G., J.P. Crumière, S. Elmi, and J. Espitalié, 1989, Géodynamique et potentialités pétrolières d'une marge de bassin: le Jurassique de la bordure ardéchoise (France, Sud-Est): *Comptes-Rendus Académie Sciences*, v. 309, p. 1495–1502.
- Durand, B., 1987, Du kérogène au charbon et au pétrole: les voies et les mécanismes de transformations des matières organiques au cours de l'enfouissement: *Mémoire Société Géologique de France*, v. 151, p. 77–95.
- Ebukanson, E.J., and R.R.F. Kinghorn, 1985, Kerogen facies in the major Jurassic mudrock formations of southern England and the implication on deposi-

- tional environments of their precursors: *Journal of Petroleum Geology*, v. 8, p. 435–462.
- Ebukanson, E.J., and R.R.F. Kinghorn, 1986, Maturity of organic matter in the Jurassic of southern England and its relation to the burial history of sediments: *Journal of Petroleum Geology*, v. 9, p. 259–280.
- Ebukanson, E.J., and R.R.F. Kinghorn, 1990, Jurassic mudrock formation of southern England: lithology, sedimentation rates and organic carbon content: *Journal of Petroleum Geology*, v. 13, p. 221–228.
- Espitalié, J., and M. Madec, 1981, Les schistes bitumineux du Toarcien de la bordure orientale du Bassin de Paris: *Bulletin Centre Recherche Exploration Pau*, v. 5, p. 461–472.
- Espitalié, J., F. Marquis, L. Sage, and I. Barsony, 1987, Géochimie organique du bassin de Paris: *Revue Institut France Pétrole*, v. 42, p. 271–302.
- Ewing, M.W., and J.L. Worzel, 1969: Initial Reports of the Deep Sea Drilling Project, v. 1, 651 p.
- Farrimond, P., G. Eglinton, S.C. Brassel, and H.C. Jenkyns, 1988, The Toarcian black shale event in northern Italy: *Organic Geochemistry*, v. 13, p. 823–832.
- Farrimond, P., G. Eglinton, S.C. Brassel, and H.C. Jenkyns, 1989, Toarcian anoxic event in Europe: an organic geochemical study: *Marine and Petroleum Geology*, v. 6, p. 136–147.
- Fleet, A.J., C.J. Clayton, H.C. Jenkyns, and D.N. Parkinson, 1987, Liassic source rock deposition in western Europe, in J. Brooks and K. Glennie, eds., *Petroleum Geology of North West Europe*: Graham and Trotman, p. 59–70.
- Galbrun, B., R. Mouterde, F. Baudin, T. Danelian, and J. Dercourt, 1994, L'Ammonitico-Rosso Toarcien de la zone ionienne (Epire, Grèce): magnétostratigraphie et biostratigraphie: *Eclog. Geol. Helv.*, v. 87, p. 91–111.
- Gorin, G.E., and S. Feist, 1990, Organic facies of Lower to Middle Jurassic sediments in the Jura Mountains, Switzerland: *Revue Paleobotany Palynology*, v. 65, p. 349–355.
- Gradstein, F.M., M.R. Gibling, L.F. Jansa, M.A. Kaminski, J.G. Ogg, M. Sarti, J. Thurow, U. von Rad, and G.E.G. Westermann, 1989, Mesozoic stratigraphy of Takkhola, Central Nepal: *Special Report Centre for Marine Geology, Dalhousie University*, v. 1, 115 p.
- Gradstein, F.M., M.R. Gibling, M. Sarti, U. von Rad, J. Thurow, J.G. Ogg, L.F. Jansa, M.A. Kaminski, and G.E.G. Westermann, 1991, Mesozoic Tethyan strata of Thakkhola, Nepal: evidence for the drift and breakup of Gondwana: *Palaeogeography, Palaeoclimatology, Palaeoecology*, v. 88, p. 193–218.
- Grant, A.C., L.F. Jansa, K.D. McAlpine, and A. Edwards, 1988, Mesozoic–Cenozoic geology of the Eastern margin of the Grand Banks and its relation to Galicia Bank: *Proceedings of the Ocean Drilling Project, Scientific Results*, v. 103, p. 787–808.
- Grantham, P.J., G.W.M. Lijmbach, J. Posthuma, M.W.H. Clarke, and R.J. Willink, 1987, Origin of crude oils in Oman: *Journal of Petroleum Geology*, v. 11, p. 61–80.
- Guzman-Vega, M.A., 1991, Géodynamique sédimentaire du bassin de Tampico-Tuxpan (Est du Mexique): remplissage, subsidence et évolution de la matière organique: Thèse Université Pau et Pays de l'Adour, 304 p.
- Haitham, F.M.S., and A.S.O. Nani, 1990, The Gulf of Aden rift: hydrocarbon potential of the Arabian Sector: *Journal of Petroleum Geology*, v. 13, p. 211–220.
- Hallam, A., 1975, *Jurassic environments*: Cambridge University Press, 269 p.
- Hallam, A., 1984, Continental humid and arid zones during the Jurassic and Cretaceous: *Palaeogeography, Palaeoclimatology, Palaeoecology*, v. 47, p. 195–223.
- Hallam, A., 1987, Mesozoic marine organic-rich shales, in J. Brooks and A.J. Fleet, eds., *Marine petroleum source rocks*: Geological Society of London Special Publication 26, p. 251–261.
- Hamilton, D.S., C.B. Newton, M. Smyth, T.D. Gilbert, N. Russell, A. McMinn, and L.T. Etheridge, 1988, The petroleum potential of the Gunnedah Basin and overlying Surat Basin sequence, New South Wales: *Australian Petroleum Exploration Association Journal*, v. 28, p. 218–241.
- Haq, B.U., 1984, Paleooceanography: a synoptic overview of 200 million years of ocean history, in B.U. Haq and J.D. Milliman, eds., *Marine geology and oceanography of Arabian Sea and coastal Pakistan*: von Nostrand Reinhold Company, p. 202–231.
- Herbin, J-P., and G. Deroo, 1982, Sédimentologie de la matière organique dans les formations du Mésozoïque de l'Atlantique Nord: *Bulletin Société Géologique France*, v. 3, p. 497–510.
- Herbin, J-P., G. Deroo, and J. Roucaché, 1983, Organic geochemistry in the Mesozoic and Cenozoic formations of site 534, Leg 76, Blake-Bahama basin, and comparison with Site 391, Leg 44: *Initial Reports of Deep Sea Drilling Project*, v. 76, p. 481–493.
- Herbin, J-P., G. Deroo, and J. Roucaché, 1984, Organic geochemistry of Lower Cretaceous sediments from Site 535, Leg 77, Florida Straits: *Initial Reports of Deep Sea Drilling Project*, v. 77, p. 459–475.
- Herbin, J-P., L. Montadert, C. Müller, R. Gomez, J. Thurow, and J. Wiedmann, 1986, Organic-rich sedimentation at the Cenomanian–Turonian boundary in oceanic and costal basins in the North Atlantic and Tethys, in C.P. Summerhayes and N.S. Shackelton, eds., *North Atlantic Paleooceanography*: Geological Society Special Publication, v. 21, p. 389–422.
- Herbin, J-P., E. Masure, and J. Roucaché, 1987, Cretaceous formations from the lower continental rise off Cape Hatteras: organic geochemistry, dinoflagellate cysts, and the Cenomanian/Turonian boundary event at Sites 603 (Leg 93) and 105 (Leg 11): *Initial Reports of the Deep Sea Drilling Project*, v. 92, p. 1139–1161.
- Huc, A.Y., 1976, Mise en évidence de provinces géochimiques dans les schistes bitumineux du Toarcien de l'est du Bassin de Paris: *Revue Institut Français Pétrole*, v. 31, p. 933–953.

- Huc, A.Y., 1977, Contribution de la géochimie organique à une esquisse paléocéologique des schistes bitumineux du Toarcien de l'est du Bassin de Paris: *Revue Institut Français Pétrole*, v. 32, p. 703–718.
- Huc, A.Y., 1980, Origins and formation of organic matter in recent sediments and in relation to kerogen, in B. Durand, ed., *Kerogen: insoluble organic matter from sedimentary rocks*: Technip, p. 445–474.
- Huc, A.Y., 1988, Sedimentology of organic matter, in F.H. Frimmel and R.F. Christmas, eds., *Humic substances and their role in the environment*: John Wiley, p. 215–243.
- IGRS-IFP, 1966, *Etude géologique de l'Épire (Grèce Nord-occidentale)*: Technip, 306 p.
- Jansa, L.F., 1991, Processes affecting paleogeography, with examples from the Tethys: *Palaeogeography, Palaeoclimatology, Palaeoecology*, v. 87, p. 345–371.
- Jenkyns, H.C., 1974, Origin of red nodular limestones (ammonitico rosso, Knollenkalk) in the Mediterranean Jurassic, a diagenetic model, in K.J. Hsü and H.C. Jenkyns, eds., *Pelagic sediments: on land and under the sea*: Internat. Assoc. Sedimentologists, v. 1, p. 249–272.
- Jenkyns, H.C., 1980, Cretaceous anoxic events: from continents to oceans: *Journal of Geological Society*, v. 137, p. 171–188.
- Jenkyns, H.C., 1985, The early Toarcian and Cenomanian–Turonian anoxic events in Europe: comparisons and contrasts: *Geologische Rundschau*, v. 74, p. 505–518.
- Jenkyns, H.C., 1988, The early Toarcian (Jurassic) anoxic event: stratigraphic, sedimentary and geochemical evidence: *American Journal of Science*, v. 288, p. 101–151.
- Jenkyns, H.C., 1991, Impact of Cretaceous sea level rise and anoxic events on the Mesozoic carbonate platform of Yugoslavia: *AAPG Bulletin*, v. 75, p. 1007–1017.
- Kantsler, A.J., T.J.C. Prudence, A.C. Cook, and M. Zwigulis, 1984, Hydrocarbon habitat of the Cooper/Eromanga basin, Australia, in G. Demaison and R.J. Murriss, eds., *Petroleum Geochemistry and Basin Evaluation*: AAPG Memoir 35, p. 373–390.
- Katz, B.J., 1983, Organic geochemical character of some Deep Sea Drilling Project cores from legs 76 and 44: Initial Reports of Deep Sea Drilling Project, v. 76, p. 463–468.
- Katz, B.J., 1988, Organic-geochemical character and hydrocarbon-source potential of Site 635: Proceedings Ocean Drilling Program, Scientific Results, v. 101, p. 381–387.
- Khorasani, G.K., 1987, Australian Petroleum Exploration Association Journal, v. 27, p. 106–111.
- Kuhnt, W., J-P. Herbin, J. Thurow, and J. Wiedmann, 1990, Distribution of Cenomanian–Turonian organic facies in the Mediterranean and along the adjacent Atlantic margin, in A.Y. Huc, ed., *Deposition of organic facies*: AAPG Studies in Geology 30, p. 133–160.
- Küspert, W., 1982, Environmental change during oil-shale deposition as deduced from stable isotope ratios, in G. Einsele and A. Seilacher, eds., *Cyclic and event stratification*: Springer Verlag, p. 482–501.
- Küspert, W., 1983, Faziestypen des Posidonien-schiefers (Toarcium, Süddeutschland). Ein isotopengeologische, organisch-chemische und petrographische Studie: Doktor Dissertation, 233 p.
- Ladwein, H.W., 1988, Organic geochemistry of Vienna basin: model for hydrocarbon generation in overthrust belts: *AAPG Bulletin*, v. 72, p. 586–599.
- Levert, J., 1991, Répartition géographique des minéraux argileux dans les sédiments mésozoïques du bassin subalpin: mise en évidence d'une diagenèse complexe: Documents Laboratoires Géologie Faculté Sciences de Lyon, v. 114, 175 p.
- Lipson-Benitah, S., A. Flexer, A. Rosenfield, A. Honigstein, B. Conway, and H. Eris, 1990, Dyaerobic sedimentation in the Cenomanian–Turonian Daliyya Formation, Israel, in A.Y. Huc, ed., *Deposition of organic facies*: AAPG Studies in Geology 30, p. 27–30.
- Loh, H., B. Maul, M. Prauss, and W. Riegel, 1986, Primary production, maceral formation and carbonate species in Posidonia Shale of NW Germany: *Mitt. Geol-Paläont. Institut University Hamburg*, v. 60, p. 397–421.
- Longoria, J.F., 1984, Stratigraphic studies in the Jurassic of northeastern Mexico: evidence for the origin of the Sabinas Basin: SEPM Foundation Third Annual Research Conference Proceedings, p. 171–193.
- Lord, J.H., 1976, Perth basin W.A., Jurassic–Cretaceous, in D.M. Traves and D. King, eds., *Economic geology of Australia and Papua New Guinea 2—Coal*: The Australasian Institute of Mining and Metallurgy, p. 339–340.
- Mann, U., D. Leythaeuser, and P.J. Müller, 1986, Relation between source rock properties and wireline log parameters: an example from Lower Jurassic Posidonia Shale, NW Germany: *Organic Geochemistry*, v. 10, p. 1105–1112.
- Masters, C.D., and E.W. Scott, 1986, Some elements of Australian petroleum geology: *AAPG Bulletin*, v. 75, p. 617.
- Mettraux, M., C. Dupasquier, and P. Homewood, 1986, Conditions de dépôt et diagenèse précoce du Toarcien inférieur des préalpes médianes romandes (Suisse): Document Bureau Recherches Géologiques Minières, v. 110, p. 231–237.
- Meyers, P.A., K.W. Dunham, and E.S. Ho, 1987, Organic geochemistry of Cretaceous black shales from the Galica Margin. Ocean Drilling Program Leg 103: *Organic Geochemistry*, v. 13, p. 89–96.
- Moldovan, J.M., P. Sundararaman, and M. Schoell, 1985, Sensitivity of biomarker properties to depositional environment and/or source input in the Lower Toarcian of SW Germany: *Organic Geochemistry*, v. 10, p. 915–926.
- Moore, P.S., 1986, Jurassic and Triassic stratigraphy and hydrocarbon potential of the Poolowanna Trough (Simpson desert region), northern Australia: *Geological Society Australia Special Publication 12*, p. 39–51.
- Moore, P.S., and G.M. Pitt, 1984, Cretaceous of the Eromanga basin. Implications for hydrocarbon explo-

- ration: Australian Petroleum Exploration Association Journal, v. 24, p. 359–376.
- Morris, K.A., 1979, A classification of Jurassic marine shale sequence: an example from the Toarcian (Lower Jurassic) of Great Britain: *Palaeogeography, Palaeoclimatology, Palaeoecology*, v. 26, p. 117–126.
- Mukhopadhyay, P.K., and J.A. Wade, 1990, Organic facies and maturation of sediments from three Scotian shelf wells: *Bulletin of Canadian Petroleum Geologists*, v. 38, p. 407–425.
- Murris, R.J., 1980, Middle East: stratigraphic evolution and oil habitat: *American Association of Petroleum Geologists Bulletin*, v. 64, p. 597–618.
- Myers, K.J., and P.B. Wignall, 1987, Understanding Jurassic organic-rich mudrocks. New concepts using gamma-ray spectrometry and palaeoecology, in J.K. Legget and G.G. Zuffa, eds., *Marine clastic sedimentology*: Graham and Trotman, p. 172–189.
- Nicholas, E., K.L. Lockwood, A.R. Martin, and K.S. Jackson, 1981, Petroleum potential of the Bass Basin: *Journal of Australian Geology and Geophysics*, v. 6, p. 199–212.
- North, F.K., 1985, Episodes of source-sediment deposition: *Journal of Petroleum Geology*, v. 2, p. 199–218.
- Osborne, D.G., and E.A. Howell, 1987, The geology of the Harriet oilfield, offshore western Australia: *Australian Petroleum Exploration Association Journal*, v. 27, p. 152–163.
- Park, W.J., 1976, Tiaro district, Q, in D.M. Traves and D. King, eds., *Economic geology of Australia and Papua New Guinea 2—Coals*: Australasian Institut Mineralogy Metallurgy, 7, p. 317–318.
- Parrish, J.T., and R.L. Curtis, 1982, Atmospheric circulation, upwelling and organic-rich rocks in the Mesozoic and Cenozoic eras: *Palaeogeography, Palaeoclimatology, Palaeoecology*, v. 40, p. 31–66.
- Parrish, J.T., A.M. Ziegler, and C.R. Scotese, 1982, Rainfall patterns and the distribution of coal and evaporites in the Mesozoic and Cenozoic: *Palaeogeography, Palaeoclimatology, Palaeoecology*, v. 40, p. 67–101.
- Patton, J.W., P.W. Choquette, G.K. Guannel, A.J. Kaltenback, and A. Moore, 1984, Organic geochemistry and sedimentology of the Lower to Mid-Cretaceous deep-sea carbonates, Sites 535 and 540, Leg 77: Initial Report Deep Sea drilling Project, v. 77, p. 417–443.
- Pedersen, T.F., and S.E. Calvert, 1990, Anoxia vs. productivity: what controls the formation of organic-carbon-rich sediments and sedimentary rocks?: *American Association of Petroleum Geologists Bulletin*, v. 74, p. 454–466.
- Pelet, R., and G. Deroo, 1983, Vers une sédimentologie de la matière organique: *Bulletin Société Géologique de France*, v. 7, n. 25, p. 483–493.
- Phillip J., J.F. Babinot, G. Tronchetti, E. Fourcade, R. Guiraud, Y. Bellion, J-P. Herbin, P.J. Combes, J.J. Cornée, J. Dercourt, and L.E. Ricou, 1993, Late Cenomanian (94–92 Ma), in J. Dercourt, L.E. Ricou, and B. Vrielynck, eds., *Atlas Tethys Palaeoenvironmental Maps. Explanatory Notes*: Gauthier-Villars, p. 153–177.
- Polgari, M., B. Molak, and E. Surova, 1989, Contribution of the organo-geochemical study of the black shale-Mn-carbonate sequence Urküt (Hungary) and comparison to the Mn-carbonate sequences in Branisko Mts. (E. Slovakia): Meeting of the Czechoslovakian working group. PICG 254: “Metalliferous black-shales”, 23–25 mai 1989, 18 p.
- Powell, T.G., 1985, Paleogeographic implications for the distribution of Upper Jurassic source beds: offshore eastern Canada: *Bulletin of Canadian Petroleum Geology*, v. 33, p. 116–119.
- Purcell, L.P., M.A. Rashid, and I.A. Hardy, 1979, Geochemical characteristics of sedimentary rocks in Scotian basin: *American Association of Petroleum Geologists Bulletin*, v. 63, p. 87–105.
- Purcell, L.P., D.C. Umpleby, and J.A. Wade, 1980, Regional geology and hydrocarbon occurrences off the east coast of Canada, in A.D. Miall, ed., *Facts and Principles of the World’s Petroleum Occurrence*: Canadian Society of Petroleum Geologists Memoir 6, p. 551–566.
- Rad, F.K., 1982, Hydrocarbon potential of eastern Alborz region, NE Iran: *Journal of Petroleum Geology*, v. 4, p. 419–435.
- Rad, F.K., 1986, A Jurassic delta in the Eastern Alborz, N.E. Iran: *Journal Petroleum Geology*, v. 9, p. 281–294.
- Ricou, L.E., 1987, The Tethyan oceanic gates: a tectonic approach to major sedimentary changes within the Tethys: *Geodinamica Acta*, v. 1, p. 225–232.
- Rullkötter, J., D. Leythaeuser, B. Horsfield, R. Littke, U. Mann, P.J. Müller, M. Radke, R.G. Shaefer, H.-J. Shenk, K. Schwochau, E.G. Witte, and D. Welte, 1987, Organic matter maturation under the influence of a deep intrusive heat source: a natural experiment for quantification of hydrocarbon generation and expulsion from a petroleum source rock (Toarcian shales, northern Germany): *Advances in Organic Geochemistry*, v. 13, p. 847–850.
- Salvador, A., 1987, Late Triassic–Jurassic paleogeography and origin of Gulf of Mexico Basin: *AAPG Bulletin*, v. 71, p. 419–451.
- Savoyat, E., A. Shiferaw, and T. Balcha, 1989, Petroleum exploration in the Ethiopian Red Sea: *Journal of Petroleum Geology*, v. 12, p. 187–204.
- Soussi, M., M.H. Ben Ismail, A. M’Rabet, and C. Parris, 1988, Les roches mères potentielles des séries jurassiques en Tunisie centrale et méridionale: 1 Journées tunisiennes de Géologie Appliquée, 32 p.
- Soussi, M., A. M’Rabet, and M. Rabhi, 1989, The Jurassic series of Central Tunisia: an example of shallow to deep marine carbonate shelf (abs.): 10th IAS Regional Meeting on Sedimentology.
- Struckmeyer, H.I.M., and E.A. Felton, 1990, The use of organic facies for refining palaeoenvironmental interpretations: a case study from the Otway Basin, Australia: *Australian Journal of Earth Sciences*, v. 37, p. 351–364.
- Summerhayes, C.P., 1983, Organic facies of Cretaceous and Jurassic sediments from Deep Sea Drilling Project site 534 in the Blake-Bahama basin, Western North Atlantic: *Initial Reports of Deep Sea Drilling Project*, v. 76, p. 469–480.
- Talukdar, S., O. Gallango, and A. Ruggiero, 1985, Formaciones La Luna y Querecual de Venezuela:

- rochas madres de petroleo: 6th Congreso Geologico Venezuelano, p. 3606–3642.
- Thomas, B.M., 1979, Geochemical analysis of hydrocarbon occurrences in northern Perth basin, Australia: AAPG Bulletin, v. 63, p. 1092–1107.
- Thomas, B.M., 1982, Land plant source rocks for oil and their significance in Australian basins: Australian Petroleum Exploration Association Journal, v. 22, p. 164–178.
- Thurrow, J., and W. Kuhnt, 1986, Mid-Cretaceous of the Gibraltar Arch area, in C.P. Summerhayes and N.S. Shackleton, eds., North Atlantic Paleogeography: Geological Society Special Publication 21, p. 423–445.
- Thurrow, J., M. Moulade, H.J. Brumsak, E. Masure, J. Taugourdeau, and K. Dunham, 1988, The Cenomanian/Turonian Boundary Event (CTBE) at Hole 641A, ODP Leg 103: Proceedings Ocean Drilling Project, Scientific Results, v. 103, p. 587–634.
- Thurrow, J., H.-J. Brumsack, J. Rullkötter, R. Littke, and P. Meyers, 1992, The Cenomanian/Turonian boundary event in the Indian Ocean—a key to understand the global picture: Geophysical Monograph, v. 70, p. 253–273.
- Thusu, B., J.G.L.A. Van der Eem, A. El-Medhawi, and F. Bu-Argoub, 1988, Jurassic–Early Cretaceous palynostratigraphy in northeast Libya, in A. El-Arnauti et al., eds., Subsurface Palynostratigraphy of Northeast Libya, p. 171–213.
- Tissot, B., 1979, Effects on prolific petroleum source rocks and major coal deposits caused by sea level changes: Nature, v. 277, p. 463–465.
- Tissot, B., B. Durand, J. Espitalié, and A. Combaz, 1974, Influence of nature and diagenesis of organic matter in formation of petroleum: AAPG Bulletin, v. 58, p. 499–506.
- Tribovillard, N., J.F. Stephan, H. Manivit, Y. Reyre, P. Cotillon, and E. Jautée, 1991, Cretaceous black shales of Venezuelan Andes: preliminary results on stratigraphy and paleoenvironmental interpretations: Palaeogeography, Palaeoclimatology, Palaeoecology, v. 81, p. 313–321.
- Trümpy, D., 1983, Le Lias moyen et supérieur des Grands Causses: Cahiers Université Pau et Pays de l'Adour, v. 19, 276 p.
- Ulicny, D., J. Hladik, and L. Hradecka, 1993, Record of sea level changes, oxygen-depletion and the $\delta^{13}\text{C}$ anomaly across the Cenomanian–Turonian boundary, Bohemian Cretaceous Basin: Cretaceous Research, v. 14, p. 211–234.
- Ulmishek, G.F., and H.D. Klemme, 1990, Depositional controls, distribution, and effectiveness of world's petroleum source rocks: U.S. Geological Survey Bulletin, v. 1931, 59 p.
- Vinogradov, A.P., 1968, Atlas of the lithological and paleogeographical maps of URSS, vol. III: Triassic, Jurassic and Cretaceous: Ministry of Geology of the URSS, Academy of Sciences of the URSS.
- Volkman, J.K., R. Alexander, R.I. Kagi, R.A. Noble, and G.W. Woodhouse, 1983, A geochemical reconstruction of oil in the Barrow Subbasin of Western Australia: Geochimica et Cosmochimica Acta, v. 47, p. 2091–2105.
- von der Dick, H., 1989, Environment of petroleum source rock deposition in the Jeanne d'Arc basin off Newfoundland, in A.J. Tankard and H.R. Balkwill, eds., Extensional tectonics and stratigraphy of the North Atlantic margins: AAPG Memoir, v. 46, p. 295–303.
- Waples, D.W., and R. Cunningham, 1985, Leg 80 Shipboard organic geochemistry: Initial Report Deep Sea Drilling Project, v. 80.
- Whibley, M., and T. Jacobson, 1990, Exploration in the Northern Bonaparte Basin, Timor Sea: Australian Petroleum Exploration Association Journal, v. 30, p. 7–25.
- Wycisk, P., E. Klitzsch, C. Jas, and O. Reynolds, 1990, Intracratonal sequence development and structural control of Phanerozoic strata in Sudan: Berliner Geowissenschaft Abh. A, v. 120, p. 45–86.
- Ziegler, P.A., 1990, Geological atlas of Western and Central Europe: Shell International Petroleum Maatschappij, 238 p.

Cenomanian–Turonian Source Rocks: Paleobiogeographic and Paleoenvironmental Aspects

Wolfgang Kuhnt

*Christian-Albrechts-Universität zu Kiel
Kiel, Federal Republic of Germany*

Jost Wiedmann*

*Universität Tübingen
Tübingen, Federal Republic of Germany*

ABSTRACT

Biological proxy indicators (molluscs, planktonic and benthic foraminifera) are used in combination with estimates of organic-matter accumulation to trace mid-Cretaceous paleocirculation, paleoproductivity, and water-mass oxygenation along the eastern Atlantic margin from Nigeria to northwestern Europe. Significant changes in the paleobiogeographic distribution of some mollusc groups roughly coeval with the Cenomanian–Turonian boundary include an incursion of boreal elements into lower latitudes. These biogeographic changes may be related to climatic cooling at high latitudes and resulting upwelling of cooler deep waters at low latitudes. Changes in benthic foraminiferal biofacies which relate to latitude and paleobathymetry also correlate to variations in accumulation rates and geochemical characteristics of Cenomanian–Turonian source rocks. Assemblages which are characteristic of high productivity upwelling conditions and high organic-matter accumulation rates are dominant in paleolatitudes between the mid-Cretaceous equator and 20°N along the eastern North Atlantic margin and in outer shelf to upper slope paleobathymetries. Deep sea and Northern Temperate (Boreal) environments may allow good preservation of organic matter under oxygen-deficient conditions, but Late Cenomanian benthic foraminiferal biofacies indicate neither enhanced surface productivity nor substantially increased organic particle fluxes to the sea floor.

* Deceased.

INTRODUCTION

The environmental conditions controlling the deposition of sediments with unusually high concentrations of total organic carbon (TOC) in the North Atlantic and its marginal seas during the Cenomanian–Turonian transition have been the subject of vigorous discussion (Schlanger and Jenkyns, 1976; Summerhayes, 1981, 1987; Arthur and Premoli Silva, 1982; Einsele and Wiedmann, 1982; de Boer, 1983; Bralower and Thierstein, 1984; Busson, 1984; Pratt, 1984; Brumsack and Thurow, 1986; De Graciansky et al., 1986; Herbin et al., 1986; Kuhnt et al., 1986; Schlanger et al., 1987; Arthur et al., 1988; Thierstein, 1989; Thurow et al., 1988, 1992). Substantial debate has centered on the question of whether the accumulation of organic matter was enabled by enhanced preservation of organic matter at the sea floor as a result of oxygen-depleted deep-water masses, or by an unusually high flux of organic matter to the sea floor with the rate of burial exceeding the rate of oxidation and biogenic recycling at the sea floor and within the sediments. This discussion has been mainly based on studies of deep sea sediments encountered in DSDP/ODP (Deep Sea Drilling Project/Ocean Drilling Program) sites or pelagic deep-water sequences in the western Mediterranean basins (e.g., the Umbrian Appennines) and largely neglected shelf sequences, where not only do organic-carbon-rich sediments occur, but also organic-matter accumulation rates are sufficiently high to produce potential or effective petroleum source rocks. Environmental conditions favoring the formation of good petroleum source rocks may need elevated levels of both organic production and preservation. Primary production and

preservation of organic matter are controlled by a wide range of factors which are ultimately related to paleoclimate and paleogeography (Figure 1).

Factors controlling the nutrient budget for primary production, such as upwelling or riverine input, are directly related to paleoclimatic conditions (rainfall, light intensity, wind stress, seasonality). These conditions probably were, compared to modern tropical regions, not fundamentally different in the Cenomanian–Turonian. However, the Cenomanian–Turonian time interval generally was characterized by eustatic sea level highstand, high CO₂ levels in atmosphere, and resulting comparatively temperate polar regions (Berger and Spitzzy, 1988). Model calculations (Kruijs and Barron, 1990) demonstrated a pronounced sensitivity of oceanic deep-water formation to these climatic conditions. In the general circulation model (GCM) of these authors, an increase of CO₂ levels in the atmosphere resulted under identical paleogeographic preconditions in a fundamental shift from cool deep-water formation in high-latitude Pacific regions to salinity-driven deep-water formation within the Tethys. Lower concentrations of dissolved oxygen in mid-water and deep-water masses in the mid-Cretaceous may have been the most important factor for the enhanced preservation of organic matter. However, settling flux of organic matter to the sea floor is a still poorly understood control on the formation of organic-rich deposits. Many factors, such as the role of clustered aggregates and fecal pellets, and the presence of intermittent nepheloid layers or deep current transport which would allow lateral transport of organic matter, have not yet been fully introduced in mid-Cretaceous models of organic-matter distribution (Degens et al., 1986a). Recycling of organic matter at

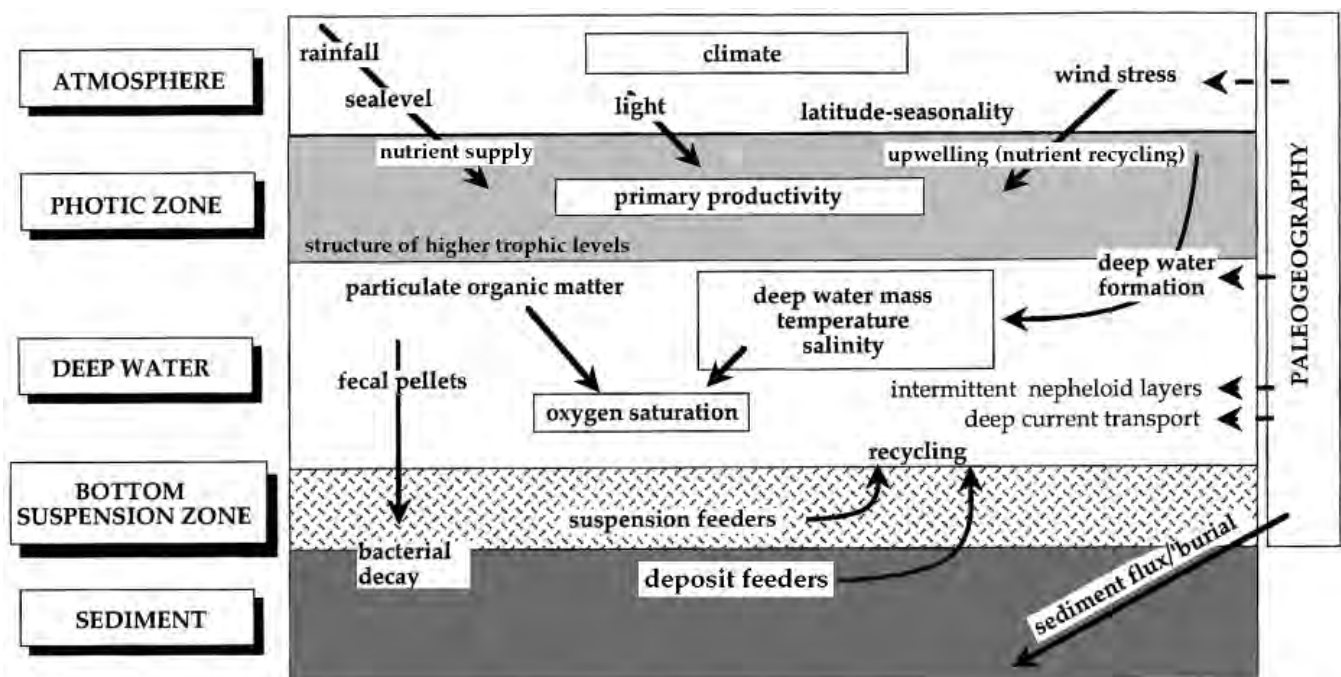


Figure 1. Factors and processes controlling organic-matter accumulation in pelagic environments.

the sediment surface and in the bottom suspension zone is another important, but poorly investigated, mechanism influencing mid-Cretaceous organic-matter distribution (Degens et al., 1986b). Benthic foraminiferal assemblages are one of the major groups feeding on particulate organic matter in modern oceans, including suspension-feeding and deposit-feeding forms. Their tests can be studied in the paleontologic record, and their life habitat and feeding strategies can be directly compared to similar modern morphotypes. We believe that comparison of the community structure of these forms in modern and fossil environments will shed some light on the paleoenvironmental conditions of the sediment surface and the bottom suspension zone in mid-Cretaceous organic-rich sedimentary accumulations.

Physically based climate models have been used in source rock prediction by correlating climatic data and key variables for organic productivity and preservation (Barron, 1985). However, the existing climate models are still insufficiently constrained by geologic data. One of the objectives of this study is to test climate model predictions for the Cenomanian–Turonian boundary by comparison with the biogeographic distribution of selected temperature- or productivity-sensitive faunal groups and the paleogeographic distribution of organic-matter accumulation. Benthic foraminiferal assemblages are excellent indicators of bottom water oxygenation and proxy indicators of phytodetritus flux rates to the sea floor. Their distribution patterns can be used to identify areas of enhanced paleoproductivity and compare them to model-predicted upwelling areas.

A major problem is the still very poor database of reliable oxygen isotope data from the Cenomanian–Turonian marine record. Most available temperature curves calculated from oxygen isotopes (e.g., Spicer and Corfield, 1992) are generated from bulk-sediment analyses which mix surface water and bottom water signals and which may also include some diagenetic bias. However, even within these somewhat biased data a significant trend of cooling, approximately beginning with the Cenomanian–Turonian boundary, is obvious. This general trend should have influenced the biogeographic distribution of temperature-sensitive surface-dwelling organisms. The paleobiogeographic distribution of nektonic molluscs (ammonoids and inoceramids) mainly reflects surface water circulation patterns and can be used as a proxy for surface water temperatures. We examined the biogeographic distribution of some selected groups of molluscs within the eastern Atlantic and its marginal basins in the late Cenomanian and early Turonian using our own collections and literature data.

One of the most controversial topics in Mesozoic and Paleogene paleoceanography is the composition and formation of deep-water masses in the world's ocean. Brass et al. (1982) proposed a Mesozoic and Paleogene deep-water mass formation mainly by down-sinking of warm, saline water masses in equatorial regions. Recent model calculations (Herbert and Sarmiento, 1991) predict that warm, saline deep-water masses must consequently lead to bottom water anoxia. Since anoxic conditions in abyssal oceanic

areas are—with the exception of the Cape Verde Basin—not recorded in sequences younger than the Cenomanian–Turonian boundary, a fundamental change of the mode of deep-water formation can be assumed for the base of the Turonian. This datum coincides with a major evolutionary turnover in deep-water agglutinated foraminifera, leading to diversified Late Cretaceous abyssal communities with many resemblances to modern abyssal communities associated with cold oxic bottom water masses (Kuhnt, 1992). Since the assemblage composition of deep-water agglutinated foraminifera is generally related to the overlying water mass, changes in assemblage composition and evolution of this group during the Cenomanian–Turonian may reflect changes in the physical properties of deep-water masses.

We used small-scale paleoecological observations to compare paleoenvironmental changes at the Cenomanian–Turonian boundary of three key areas:

1. Boreal pelagic shelf basins of Northwest Europe, with a paleogeographic position in the Northern Temperate zone and well north of the tropical zone of advection. Typical examples are the Wunstorff and Lengerich sections in northwestern Germany.

2. The Upper Cretaceous Tarfaya (Morocco) and Casamance (Senegal) coastal basins on the northwest African margin as examples for tropical shelf basins where mid-Cretaceous upwelling and extended oxygen-minimum water masses were predicted by GCMs (Kruijs and Barron, 1990).

3. The abyssal North Atlantic basin (DSDP holes 398D, 386, 603B and ODP Hole 641A) where comparatively thin layers of organic-rich, benthic-free, laminated sediments indicate unusually good preservation of organic matter and deep-water anoxia during a short period at the Cenomanian–Turonian boundary.

CENOMANIAN/TURONIAN PALEOECOLOGY AND ORGANIC- MATTER ACCUMULATION IN THREE KEY PALEOENVIRONMENTS

Boreal Shelf Basins

Black shales at the Cenomanian–Turonian boundary of boreal shelf basins were studied in the Wunstorff and Lengerich sections, northwestern Germany. Sedimentation was characterized by the following features (Figure 2):

1. Comparatively low accumulation rates of mixed terrestrial/marine organic matter. Black shale intercalations are generally thin. Representative organic-matter contents of black shales from the localities in northwestern Germany range between 0.8 and 2.5% TOC.

2. The environment during black shale sedimentation never was completely anoxic. Black bands are bioturbated and contain rich benthic foraminiferal assemblages.

3. Benthic foraminiferal assemblages of upper Cenomanian black shales are characteristic of dysaerobic environments (agglutinated forms dominate), but

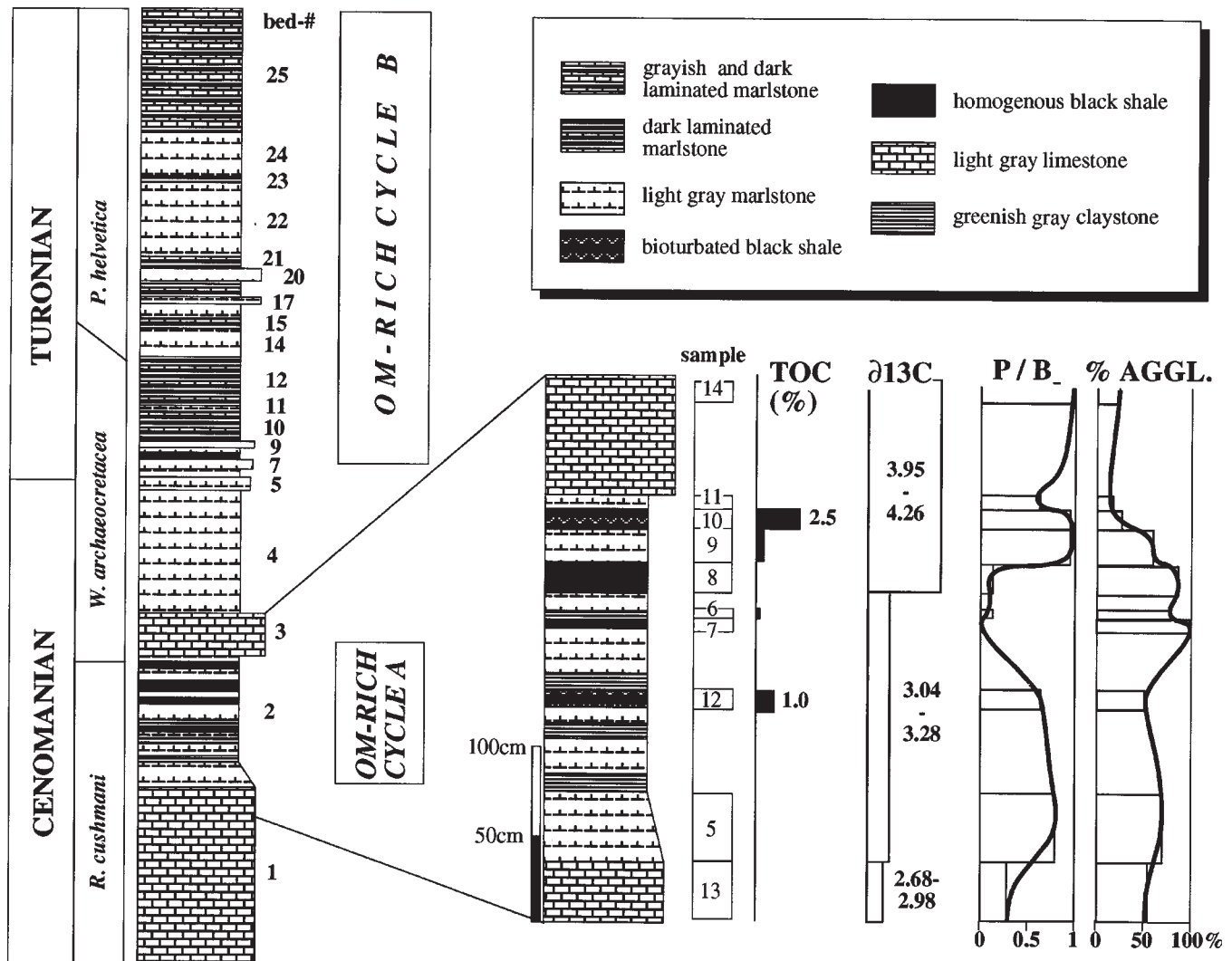


Figure 2. Paleoenvironmental changes and organic-matter accumulation at the Cenomanian–Turonian boundary in northwestern Germany (Wunstorf section). Inorganic carbon isotope data are from Hilbrecht and Hoefs (1986) and Schlanger et al. (1987); biostratigraphy is modified after Ernst et al. (1983, 1984), Hilbrecht (1986), and Hilbrecht et al. (1986). Note the low planktonic/benthic foraminifera ratio (P/B) and the high percentages of agglutinated foraminifera (%AGGL.) within the black shales of cycle A. OM is organic matter.

are rare in phytodetritus-feeding opportunists, which are indicators of enhanced surface productivity. Characteristic species of benthic foraminifera are: *Ammodiscus cretaceus*, *Bulbobaculites* sp., *Dorothia* ex gr. *filiformis*, *Glomospira charoides*, *Rhizammina indivisa*, *Saccammina* cf. *placenta*, *Haplophragmoides* cf. *concausus*, *Gavelinella* sp., *Buliminella* sp., *Lenticulina* sp.

4. Two cycles of organic-rich sedimentation are discriminated. A first cycle coincides with the last occurrence of *Rotalipora cushmani* in the uppermost Cenomanian (the "Cenomanian–Turonian boundary event"). It is characterized by low accumulation rates of organic matter and carbonate, and may be capped by a hiatus. The second cycle roughly corresponds to the main part of the *Whiteinella archaeocretacea* Zone and part of the *Helvetoglobotruncana helvetica* Zone. It differs from the first cycle mainly in significantly increased carbonate accumulation, which we relate to

enhanced productivity of calcareous planktic organisms. Benthic foraminiferal assemblages contain increased numbers of buliminid, bolivinid, and gavelinellid morphotypes, such as *Bulimina elata*, *Tappanina laciniosa*, *Bolivina* sp., and *Lingulogavelinella turonica*, which may be indicators of increased organic-matter flux rates to the sea floor.

Environmental features of Cenomanian–Turonian boundary (first cycle) black shales in boreal shelf basins favor a model of enhanced preservation of organic matter under oxygen-minimum conditions in restricted basins rather than formation of organic-rich sediments driven by excess surface productivity. This pattern may change in the early Turonian *W. archaeocretacea* Zone, where the deposition of several tens of meters of organic-rich, laminated marlstones and limestones may indicate enhanced primary productivity. Wind-driven upwelling has been recently sug-

gested as a possible mechanism for this productivity change within the earliest Turonian of the North German Basin (Hilbrecht et al., 1992).

Casamance Transect (Senegal)

Upper Cretaceous foraminiferal assemblages have been studied in 133 cuttings samples from offshore well Casamance Maritime 10 (CM10) at the outer continental shelf off Senegal, northwestern Africa (Ly and Kuhnt, 1994; Figure 3).

Upper Cenomanian/Lower Turonian bituminous limestones are free of benthic fossils and were probably deposited under anoxic conditions. The calcareous benthic foraminiferal fauna in the middle Turonian to Maastrichtian part of well CM10 is dominated by species of the genera *Afrobulimina*, *Buliminella*, *Cibicides*, *Lenticulina*, *Neobulimina*, *Præbulimina*, and *Orthokarstenia* which are known as being well adapted to dysaerobic conditions. Agglutinated assemblages are of low diversity and characterized by common *Haplophragmoides excavatus* and *Gaudryina* spp.

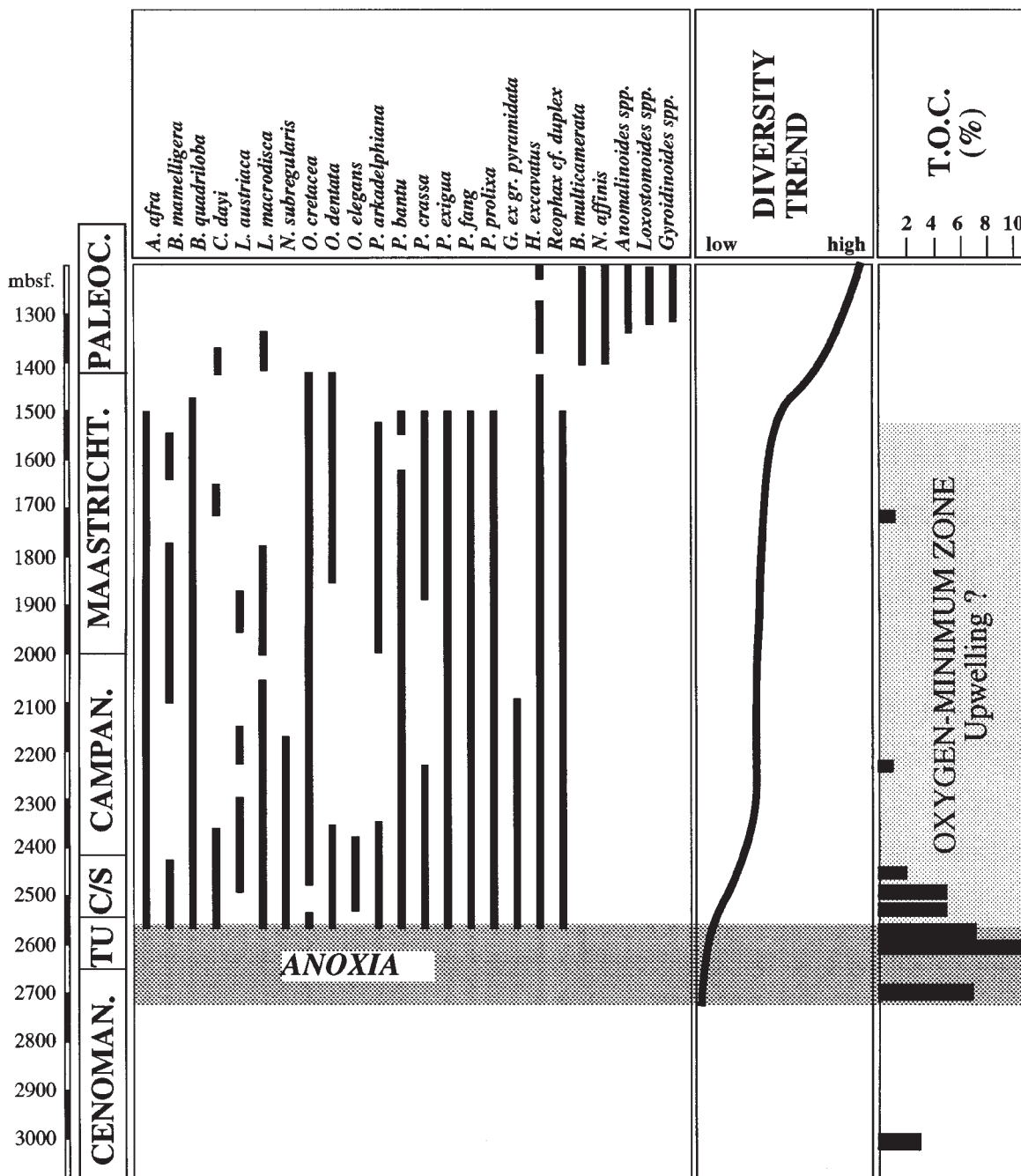


Figure 3. Benthic foraminiferal biofacies and organic carbon content in the Upper Cretaceous of well Casamance Maritime 10 (Senegal Basin). TOC data are partly from Herbin et al. (1986) and Kuhnt et al. (1990); benthic foraminiferal ranges are from Ly and Kuhnt (1994). Scale is meters below sea floor (mbsf).

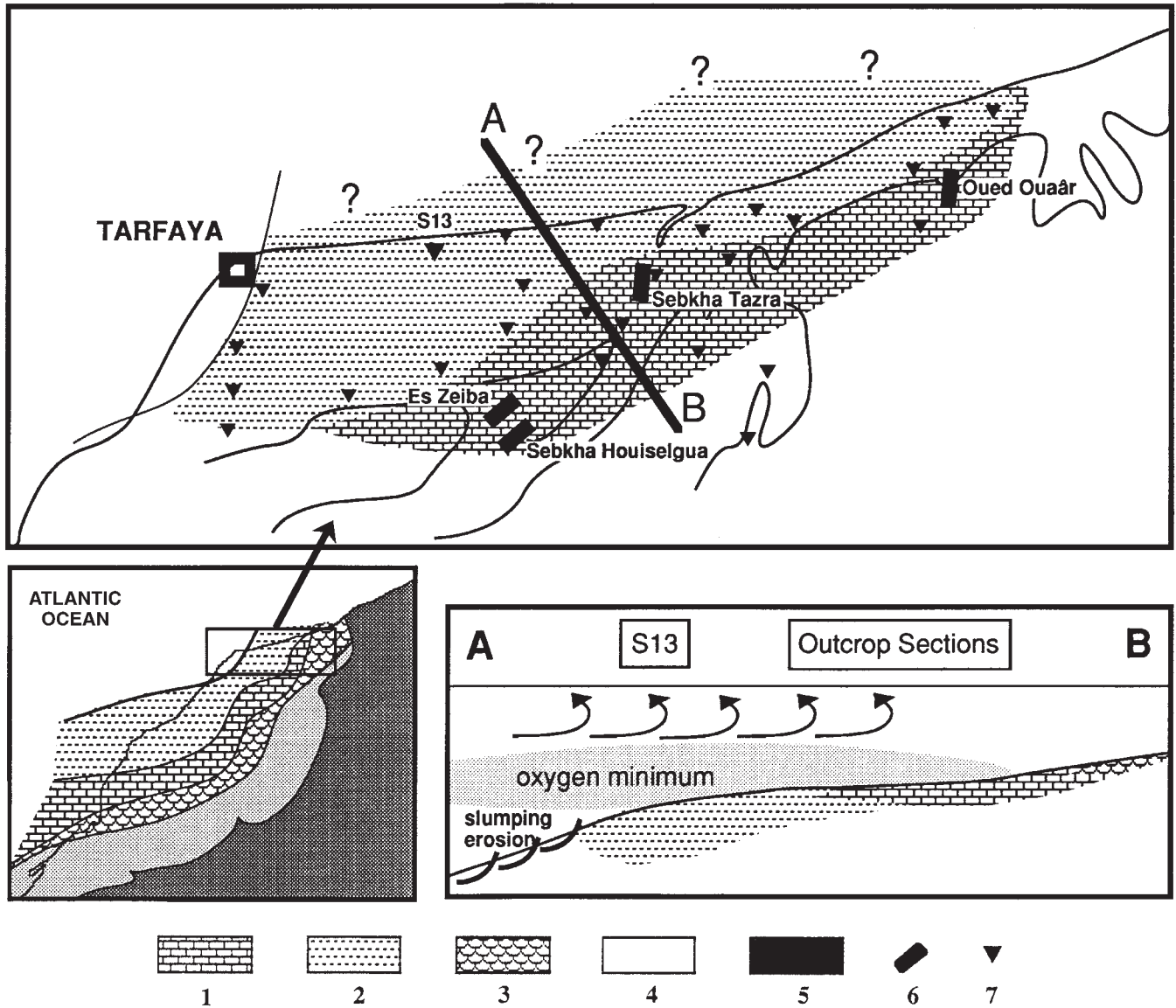


Figure 4. Facies distribution in the Tarfaya coastal basin and inferred environmental model. Legend: 1. pelagic carbonates (middle to outer shelf environments); 2. pelagic laminated marlstones with high organic-matter content (outer shelf to uppermost bathyal environments); 3. neritic limestones (inner shelf environment); 4. terrestrial sediments; 5. land; 6. outcrop sections; 7. BRPM/Shell exploration wells.

TOC content of the Upper Cretaceous dark-gray shales is generally above 1%, reaching more than 10% with marine kerogen type in the lowermost Turonian. Medium to high paleoproductivity in this area may be concluded from the comparatively high bulk-sedimentation rates of more than 40 m/m.y. for the entire Upper Cretaceous in combination with high TOC values.

We interpret the Late Cretaceous sedimentation and biofacies as indicating deposition under an oceanic oxygen-minimum layer created by upwelling conditions in an open marine, middle-outer shelf environment. The benthic foraminiferal distribution indicates cessation of the upwelling conditions, decreased surface productivity, and a diminished oxygen-minimum zone not before the late Maastrichtian.

Tarfaya Coastal Basin (Morocco)

The paleogeographic situation of the Tarfaya coastal basin is of special interest for understanding the mid-Cretaceous paleoceanography of the central North Atlantic. GCMs predict values of mean annual coastal upwelling of more than 20 cm/day for this area during the mid-Cretaceous (Krujjs and Barron, 1990). If these predictions are true, outer shelf sites in this area should have been characterized by high primary productivity and the development of an expanded and intensified oxygen-minimum layer. A first indication for the existence of a high-productivity zone and an intensified oxygen-minimum layer impinging on the shelf in the mid-Cretaceous Tarfaya

basin is given by the distribution of organic-rich sediment accumulation (Figure 4). The characteristic organic-rich laminated marlstones of the Tarfaya “oil shales” dominate in the distal part of the basin, whereas in the southeastern part of the basin, which was closer to the paleoshoreline, TOC accumulation rates are lower. In this part of the basin, which we studied in the Es Zeiba, Sebkhah Houiselgua, Sebkhah Tazra, and Oued Ouair outcrop sections, high TOC values were observed in the uppermost Cenomanian (around the *R. cushmani* last occurrence level) and within the *H. helvetica* Zone.

In the distal part of the basin (exploration well S13), two major sedimentary cycles are distinguished, covering the interval between the upper part of the *R. cushmani* Zone and most of the *W. archaeoretacea* Zone (cycle A in Figure 5) and the lower part of the *H. helvetica* Zone (cycle B). These cycles are reflected by the hydrocarbon content and the distribution of benthic foraminifers as indicators of bottom water oxygenation (Figure 5). The laminated bituminous chalks of the Turonian Tarfaya basin were not deposited under continuously anoxic conditions. Thin layers at the top of the *R. cushmani* Zone and in the upper parts of the *W. archaeoretacea* and *H. helvetica* zones contain tiny, multichambered, elongated, thin-walled benthic foraminifera (*Gabonita*,

Neobulimina). These morphotypes may be comparable to modern phytodetritus-feeding opportunists living within the fluffy layer on the sediment surface below high-productivity surface waters. Other characteristic benthic foraminiferal forms of the dysaerobic intervals in the Tarfaya section are flattened trochospiral morphotypes with high pore densities or relict apertures (*Gavelinella dakotensis*, *Cibicoides*, *Lingulogavelinella turonica*). Similar forms are characteristically associated with modern oxygen-minimum water masses.

Abyssal North Atlantic

The black shale interval at the Cenomanian–Turonian boundary was the last period in the evolution of the North Atlantic when strongly oxygen-depleted or even anoxic bottom water conditions prevailed in the abyssal parts of the ocean (De Graciansky et al., 1982; Herbin et al., 1986; Schlanger et al., 1987; Thurow et al., 1988). This anoxic interval was generally devoid of any benthic life in the deep sea and was accompanied by an important taxonomic turnover in deep-water agglutinated foraminifers in the North Atlantic (Moullade et al., 1988; Kuhnt, 1992). Many of the characterizing taxa of typical Late Cretaceous abyssal agglutinated foraminiferal assemblages are not

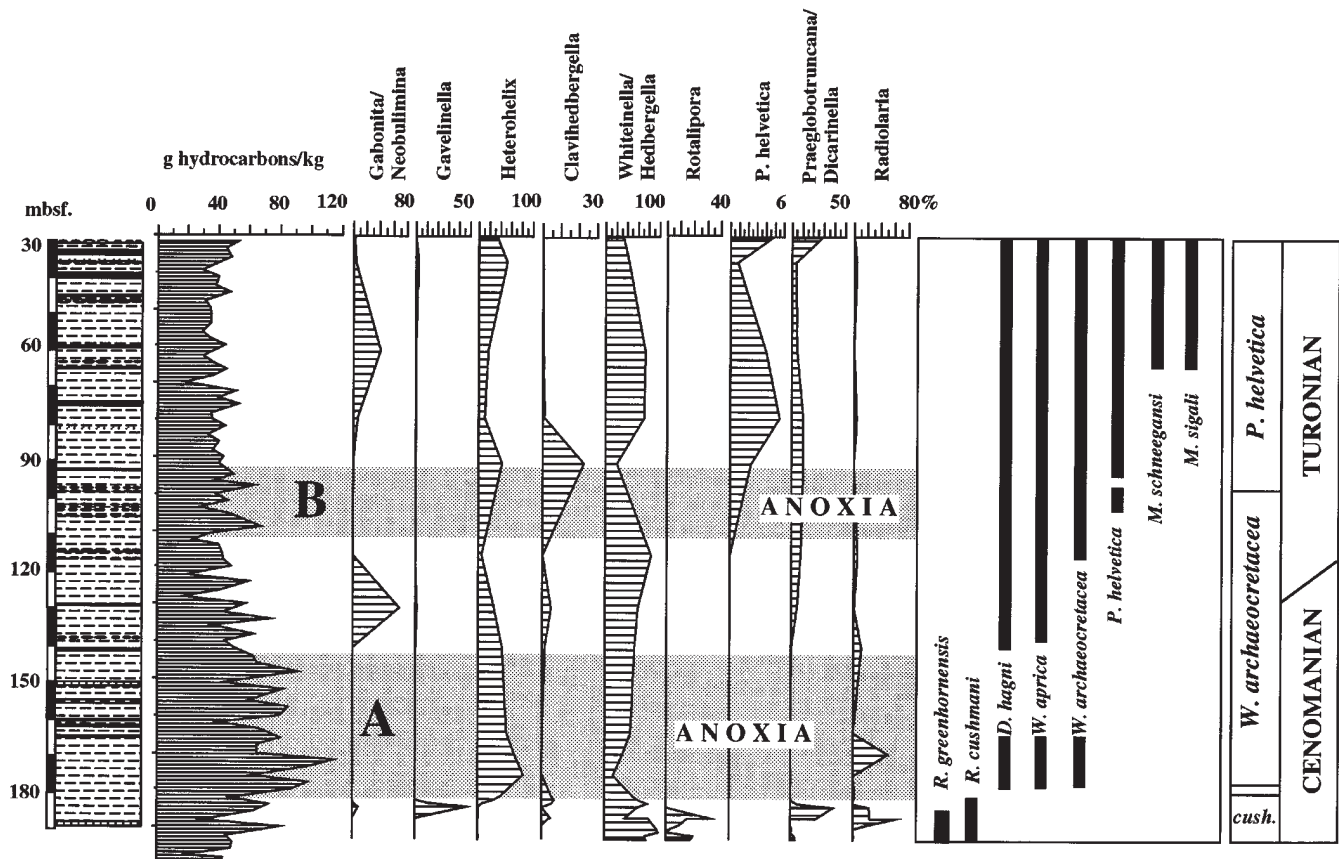


Figure 5. Paleoenvironmental changes and organic-matter accumulation at the Cenomanian–Turonian boundary in well S13 in the high-productivity zone of the Tarfaya coastal basin. Scale (mbsf) is meters below sea floor.

known from Lower Cretaceous or Cenomanian beds in the deep sea and must have evolved in a rapid radiation after the black-shale event or migrated into the deep-sea basins from shallow-water areas or marginal troughs.

Benthic foraminiferal assemblages of distinct taxonomic composition are observed at the top of benthic-free black shales which correspond to the anoxic event at the Cenomanian–Turonian boundary in North Atlantic abyssal sites (Kuhnt, 1992). These assemblages are characterized by low species diversity, variable abundance, and dominance of few taxa (i.e., of the genera *Haplophragmoides*, *Rhizammina*, and *Glomospira*). These are regarded as opportunistic species, which are suitable to survive in low-oxygen environments and to be the pioneers recolonizing the newly available niches after the cessation of bottom water anoxia. The succession of their appearance after the anoxic event was probably controlled by the continuous reoccurrence of more oxygenated bottom and interstitial water conditions. With the final installation of oxic bottom water conditions in the Turonian, a rapid radiation of deep-water agglutinated foraminifers was observed in the North Atlantic (Kuhnt, 1992). The new “modern” deep-water foraminiferal fauna after the anoxic event is comparable to actual deep-water assemblages under cool oxic deep-water conditions and low seasonal food supply of phytodetritus.

The first benthic foraminiferal assemblages observed after the anoxic event at the Cenomanian–Turonian boundary in the abyssal North Atlantic are characterized by thin-walled, minute agglutinated morphotypes generally <250 μm in maximum diameter or length (Kuhnt, 1992). Calcareous benthic foraminiferal assemblages with predominantly minute specimens are known from various mid-Cretaceous oxygen-depressed environments (Bernhard, 1986; Koutsoukos et al., 1990). Small size of benthic foraminifera in organic-rich sediments has been interpreted as a reaction to the adverse oxygen-deficient environmental conditions (Bradshaw, 1961), minimizing the oxygen consumption, and increasing the efficiency of oxygen uptake by increasing the surface to volume ratio. Phleger and Soutar (1973) and Koutsoukos et al. (1990) interpreted the dominance of dwarfed forms in dysaerobic environments as the result of enhanced reproductivity rate and early reproduction under favorable environmental conditions (high nutrient availability, low competition, and scarce predation by macrobenthos) for opportunistic species. However, the dwarfed assemblages from the oxygen-depleted deep-water environments at the Cenomanian–Turonian boundary generally show normal or even unusually low faunal density, which is at odds with inferred high reproductivity rates. Bernhard (1986) speculated that small specimens, which require less oxygen and use oxygen more efficiently, may be the only surviving individuals during an extensive and enduring anoxic period, whereas in basins with episodic or seasonally localized anoxia the seasonal increase of oxygenated water may permit larger foraminiferal specimens to

inhabit basins at least periodically. This model is in good agreement with the observations at the Cenomanian–Turonian boundary in deep-water environments, where a long period of extensive oxygen depletion resulted in dwarfed benthic foraminiferal assemblages with predominantly low-standing stocks.

PALEOBIOGEOGRAPHY DATA AND PALEOGEOGRAPHIC DISTRIBUTION PATTERNS OF ORGANIC-MATTER ACCUMULATION

Temporal and Spatial Distribution of Organic-Matter Accumulation

Deep Sea Environment

Maximum organic-matter accumulation occurred in the southern part of the North Atlantic (Cape Verde Basin, DSDP Site 367) (Figure 6). In the Gibraltar Seaway (Rif, northern Morocco and Subbetic/Penibetic zones, southern Spain) the period of the organic-matter accumulation was strongly attenuated, although the maximum TOC contents remained high. This temporal distribution is quite similar to the observations in the deep bathyal sequences of Sicily and Central Italy (Gubbio section, Umbrian Apennines). Finally, off the Galicia Margin (ODP Site 641), the preservation of organic matter is restricted to a very short interval at the Cenomanian–Turonian boundary and the maximum TOC content is only about 10%. This general trend of decreasing quantity of preserved organic matter and shorter duration of the organic pulse from south to north was confirmed by data from the Celtic Basin (DSDP sites 449 and 551) where maximum TOC contents of thin, deep-water black shale layers at the Cenomanian–Turonian boundary range between 3.5% (Site 449, core 27, section 1) and 4–10% (Site 551, core 5, section 2). In both cases, the organic matter is characterized by mixed marine and terrestrial kerogen (Herbin et al., 1986), and accumulation rates of organic matter related to marine primary production are low.

Shelf and Slope Environments

The southernmost occurrence of Cenomanian–Turonian organic-rich sediments examined for this study are the black shales of the Eke Azu formation in the Nigerian Benue trough. Here, duration of the organic-rich pulse was restricted to the lower Turonian and the measured TOC values do not exceed 5%. Highest accumulation rates of organic matter around the Cenomanian–Turonian boundary have been observed in low-latitude areas, culminating between the equator and 15°N offshore Senegal and in the Tarfaya Atlantic coastal basin. In addition, the duration of organic-matter accumulation was longest in these low-latitude areas and decreases toward the north and the south. In sections on the European continent (e.g., Vergons section in the French Alps and the sections in northwestern Germany), TOC values remain low (generally

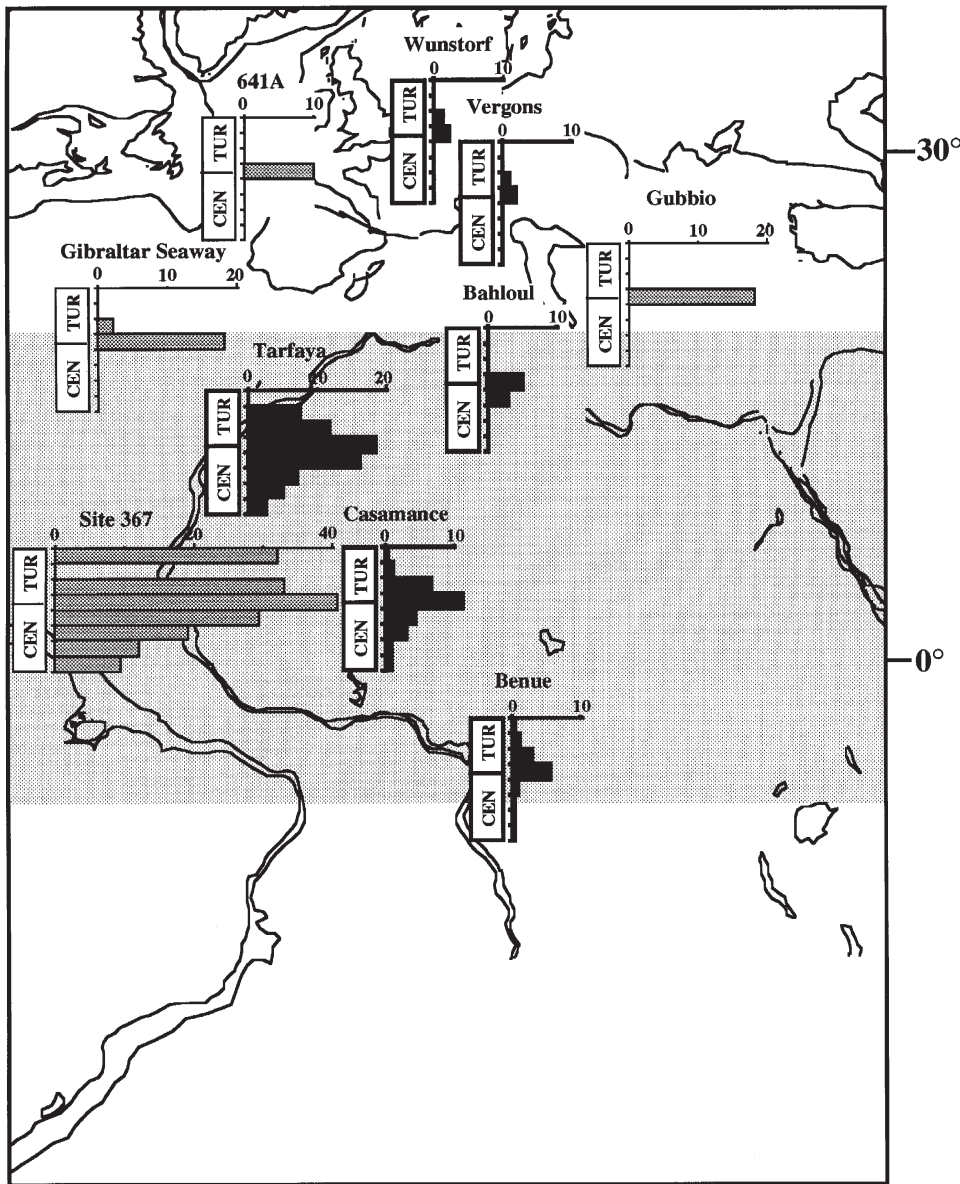


Figure 6. Latitude-dependent maximum organic carbon weight percent for eight distinct time slices. Stippled bars correspond to deep sea environments, solid bars indicate shelf environments. Shaded area corresponds to area of highest probability for high accumulation rates and long duration of organic-matter accumulation within the Cenomanian/Turonian interval.

below 3%) and organic-rich sediments were restricted to the Cenomanian–Turonian boundary interval.

Benthic Foraminifera as Monitors of Oceanic Oxygenation and Paleoproductivity

Oxygen-depleted bottom water masses are usually a result of eutrophic epipelagic conditions. High epipelagic productivity contributes to high levels of nutrient fall in the form of particulate organic material and induces oxygen deficiency on bottom waters. Deposited organic matter is the primary trophic resource for the marine meiofauna thriving under such conditions, and the community structure of benthic assemblages is thus directly dependent on water-mass oxygenation and paleoproductivity. Consequently, benthic foraminiferal communities may be useful as sensitive bioindicators for changes in paleoproductivity and oxygenation of oceanic water masses. Also, the

paleobiogeographic distribution patterns of benthic deep-water foraminifera in the ocean basins were influenced by the paleobathymetry of ocean basins and margins, surface productivity and oxygenation of bottom water masses, ocean pathway configurations, and changes in oceanic circulation. The reconstruction of paleobiogeographic distribution patterns of deep-water benthic foraminifera may be an interesting contribution to Mesozoic paleogeographic and paleoceanographic models.

A first attempt to recognize supraregional biogeographic patterns in benthic foraminiferal distribution has been made using a data set from 32 different sedimentary basins mainly located along the eastern margin of the North Atlantic from the equator to 55°N latitude. A major problem for biogeographic analyses of benthic foraminifera across the Cenomanian–Turonian boundary is a significant faunal change (mass extinction) in benthic foraminifera caused by the global

anoxic event in the latest Cenomanian. This faunal turnover resulted in faunal differences within one single section which are often more significant than the biogeographic variation. To minimize this problem we have chosen a comparatively short stratigraphical interval close to the first appearance of *H. helvetica* for our biogeographic analysis. This interval roughly corresponds to the recolonization phase after the anoxic event and the re-establishment of "normal" benthic foraminiferal communities. Data for this interval were available from 30 different sedimentary basins. For each of these basins, at least two samples have been quantitatively picked for benthic foraminifera. Multivariate statistical methods were used to define and correlate microfossil assemblages and biofacies (Imbrie and Kipp, 1971; Malmgren and Haq, 1982). R-mode principle components factor analysis (PCA) was used to examine the relationships between different faunal components. PCA (R-mode) consists of a linear transformation of the original variables to new variables (components) for better recognition of significant taxa (Brower, 1985). Eighteen species and species groups were sufficiently abundant in several of the basins and have been included in the factor analysis. Rare species and species which only occur in a few localities have been excluded from the data set; also, samples with monospecific assemblages have not been taken into account. Although our collection can not be regarded as a rigorous statistical data matrix for mid-Cretaceous benthic foraminiferal distribution, some trends in species distribution are quite obvious. Four factors account for most of the variance and are used to define four biofacies assemblages, which may mainly reflect differences in organic-matter flux to the sea floor.

Factor 1: (*Tappanina* biofacies) characteristic species with high factor score weights are *Tappanina laciniosa*, *Praebulimina elata*, and *Lingulogavelinella* spp. indicating slightly enhanced phytodetritus flux and oxic or mildly dysaerobic bottom waters.

Factor 2: (Ammodiscidae biofacies) characteristic are primitive agglutinated foraminifera of the families Ammodiscidae and Astrorhizidae. These forms are observed in recolonization faunas after anoxia in deep sea environments indicating normal (low) phytoplankton flux and possibly oxygen-deficient bottom waters.

Factor 3: Characteristic forms are *Clavulinoides* ex gr. *gaultinus* and *Pleurostomella* spp. indicating low organic-matter flux and well-oxygenated bottom waters in bathyal environments of the western Tethys.

Factor 4: (*Gabonita* biofacies) characteristic species are: *Gabonita levis*, *G. obesa*, and *Lingulogavelinella* spp. Dominant in organic-rich sediments of the Tarfaya basin, this biofacies probably indicates high phytodetritus flux and severely dysaerobic bottom waters. This biofacies is regarded as a typical assemblage of high-productivity zones.

Paleogeographic distributions of organic-matter flux-related benthic foraminiferal assemblages were plotted for a time interval roughly corresponding to the base of the *H. helvetica* planktonic foraminiferal zone, immediately following the global Cenomanian–Turonian anoxic event (Figure 7). Characteristic

species are illustrated in Figures 8A through 8C. The distribution pattern indicates that enhanced productivity and local anoxia prevailed along the northwest African continental margin. Indicative are benthic foraminiferal assemblages dominated by the genus *Gabonita* and occasional *Lingulogavelinella* and *Gavelinella dakotensis* or *Cibicidoides*. Similar assemblages have been reported from the Turonian of Gabon (de Klasz et al., 1961), the Sergipe Basin, Brazil (Koutsoukos, 1992), and from Israel (Hamaoui, 1965).

Northern Tethyan and temperate shelf biofacies may include forms indicating mild oxygen deficiency and enhanced organic flux rates such as *Praebulimina elata*, *Lingulogavelinella turonica*, and *Tappanina laciniosa* (factor 1) but are significantly different from tropical upwelling assemblages. These assemblages are observed in shelf environments of the North African margin (Morocco), shallower parts of the Basco-Cantabrian Basin (northern Spain), in slope settings of southeast France (Tronchetti and Grosheny, 1991), and in the lower Saxony Basin (North Germany). Comparatively low organic-carbon fluxes in deep sea environments and in Tethyan marginal assemblages are characterized by factors 2 and 3 (dominated by primitive agglutinated foraminifera and infaunal morphotypes such as *Clavulinoides*, *Pleurostomella*, and *Spiroplectinata*). Exclusively agglutinated assemblages are common in deep sea environments of the North Atlantic and the Alpine-Carpathian Flysch trenches, but also occur in the late Cenomanian "black band" in Northern Germany and England. In the Wunstorf section, these assemblages are replaced by a factor 1 assemblage at the base of the *W. archaeocretacea* Zone, indicating increased local primary production.

Mollusc Biogeography

The biogeographic distribution of selected species and species groups of ammonoids and inoceramids has been mapped for two times, the late Cenomanian (*Metoicoceras geslinianum* and *Neocardioceras juddii* zones) and the early Turonian (*Watinoceras coloradoense* Zone). The data were compiled from our collections from northwestern Germany, southeast France, Spain, northwestern African coastal basins, Nigeria, Tunisia, and the Middle East. Additional occurrences are compiled from Pervinqui re (1907), Greco (1915), Furon (1935), Reyment (1954a, b, 1971), Barber (1957), Freund and Raab (1969), Cobban (1972, 1984), Cobban and Scott (1972), Kennedy (1971, 1988), Cooper (1973, 1978), Kennedy and Cobban (1976, 1991), Thomel (1978), Wright and Kennedy (1981), Renz (1982), Lewy et al. (1984), Berthou et al. (1985), Zaborski (1985, 1986, 1987), and Kennedy et al. (1989). The late Cenomanian distribution is characterized by a well-defined boundary between a North Temperate bioprovince and a Tethyan bioprovince at about 30°N latitude (Figure 9A). The northern bioprovince is defined by the ammonite species *Sciponoceras gracile* and *Neocardioceras juddii*; *Euomphaloceras septemseriatum* also occurs. Most characteristic of the Tethyan late Cenomanian bioprovince are *Vascoceras* spp.,

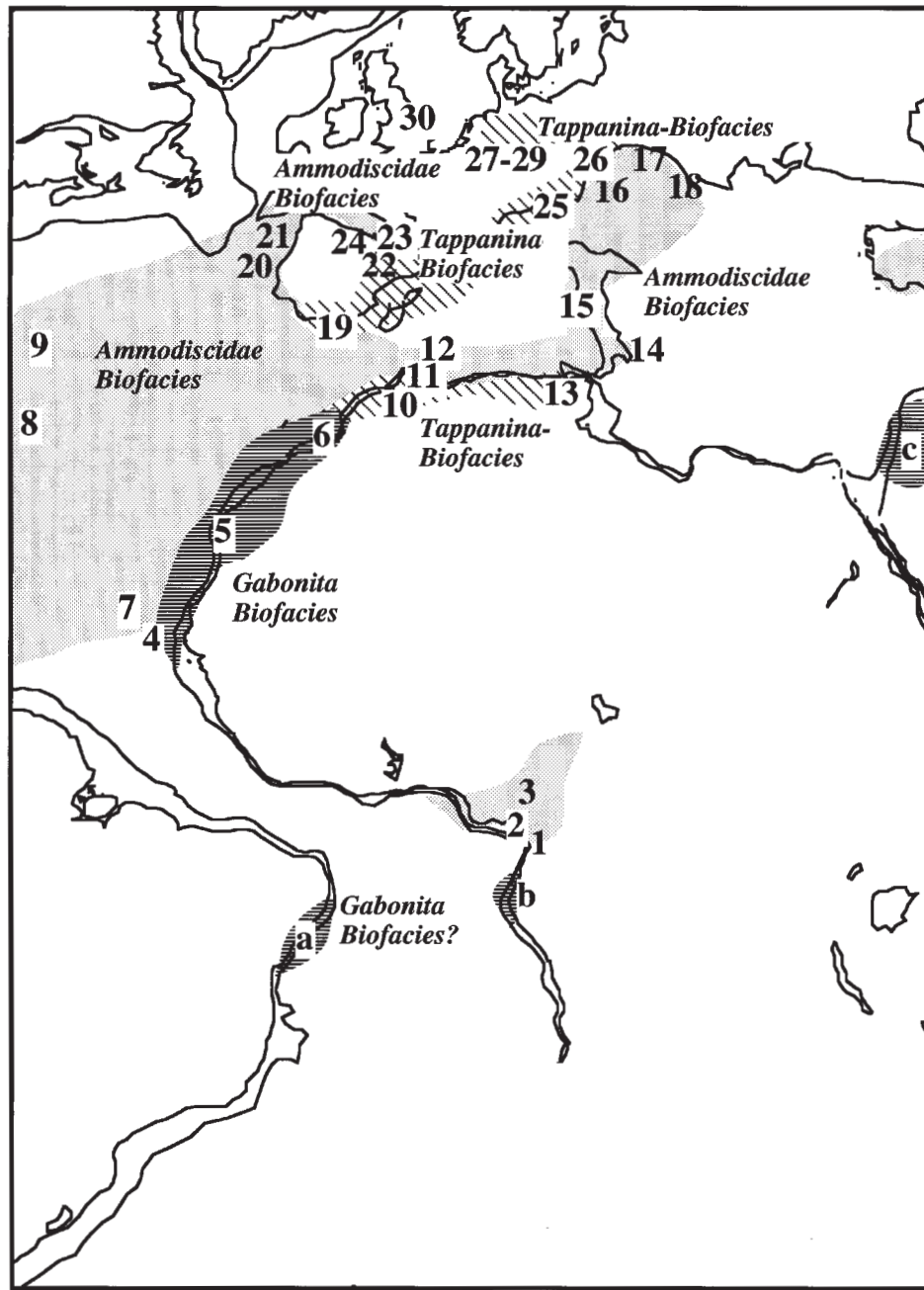


Figure 7. Distribution of early Turonian benthic foraminiferal biofacies in the North Atlantic and its marginal basins. Samples from the following localities were available for benthic foraminiferal counts. 1. Mungo River section, Cameroon; 2. Calabar flank, Nigeria; 3. Central Benue trough, Nkalagu section, Nigeria; 4. exploration well CM10, Casamance shelf, offshore Senegal; 5. exploration well S13 and outcrop sections, Tarfaya basin, Morocco; 6. Agadir section, Morocco; 7. DSDP Site 367; 8. DSDP Hole 603B; 9. DSDP Site 386; 10. Prerif sections, Morocco; 11. Mesorif sections, Morocco; 12. Intrarif sections, Morocco; 13. Bahloul section, Tunisia; 14. Oriolo section, Calabria, Italy; 15. Gubbio section, Umbrian Apennines, Italy; 16. Cismon section, southern Alps, Italy; 17. Silesian sections, Polish External Carpathians; 18. Intorsura Buzaului sections, Romanian Eastern Carpathians; 19. Penibetic and Subbetic sections, southern Spain; 20. DSDP Hole 398D; 21. ODP Hole 641A; 22. Menoyo section, northern Spain; 23. Ulzama basin sections, Western Pyrenees; 24. Zumaya section, Basque basin, northern Spain; 25. Vergons sections, Vocontian basin, southeastern France; 26. Ultrahelvetic sections; Bavarian Alps; 27. Lengerich section, northwestern Germany; 28. Wunstorf and Misburg sections, lower Saxony Basin, northwestern Germany; 29. Baddeckenstedt section, northwestern Germany; 30. Culver Cliff section, Isle of Wight, U.K. Additional literature data were used to compile the biogeographic distribution of the genus *Gabonita*: a. Sergipe basin (Brazil) (Koutsoukos, 1992); b. Gabon (de Klasz et al., 1961); c. Israel (Hamaoui, 1965).

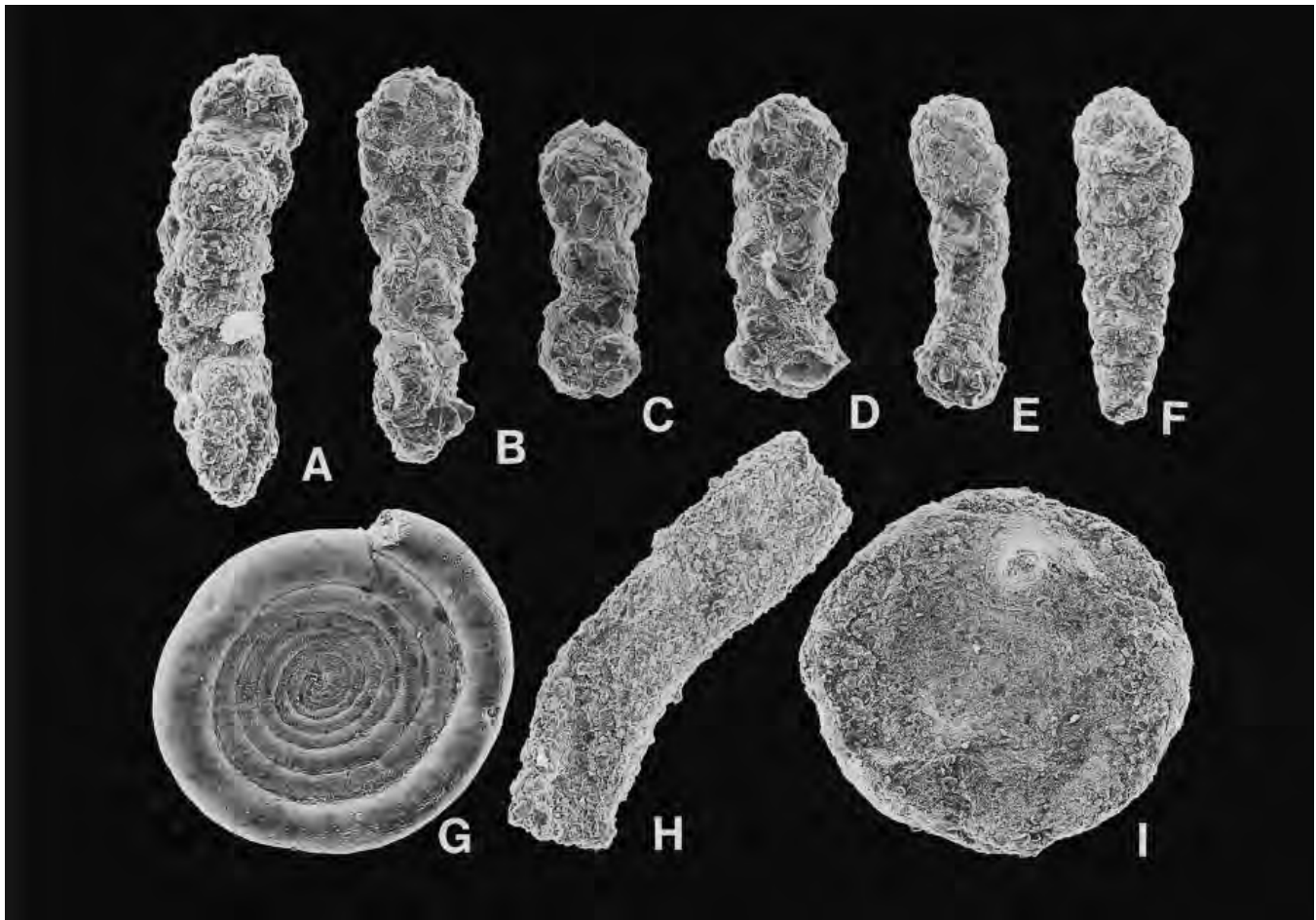


Figure 8A. Agglutinated assemblages indicating comparatively low organic-matter flux rates (factor 2). These assemblages characterize early Turonian deep sea environments and late Cenomanian temperate shelf seas with presumably low primary productivity. All figures are from late Cenomanian black shales of the Wunstorf section (Northern Germany). (A–B) *Dorothia filiformis* (elongate multichambered infaunal morphology); (C–E) *Bulbobaculites* sp.; (F) *Textularia* sp.; (G) *Ammodiscus cretaceus*; (H) *Rhizammina indivisa*; (I) *Saccamina* cf. *placenta*.

Nigericeras spp., and *Neolobites* spp. South of the Guinea fracture zone, *Euomphaloceras septemseriatum* reappears and typical Tethyan vascoceratids are absent. We interpreted this distribution as a possible indication for the presence of a South Temperate Bioprovince, reaching from the Angola Basin northward to the Sergipe Basin in Brazil. A doubtful occurrence of *Euamphaloceras septemseriatum* is also reported from the southern part of the Benue trough (Zaborski, 1987). The latitudinal distribution of ammonoids in the Late Cenomanian may indicate the presence of a stable, tropical, warm surface water mass, reaching from about 10°S to 30°N in the eastern Atlantic and its marginal basins.

The early Turonian distribution of ammonoids and inoceramids differs significantly from the late Cenomanian pattern (Figure 9B). A certain separation of a northern bioprovince and a typical Tethyan warm-water biofacies is only observed within the Mediterranean realm. The Tethyan bioprovince, defined by

the ammonite genus *Pseudotissotia*, is largely restricted to the Mediterranean shallow-water seas and the Trans-Sahara Seaway. Additional occurrences are reported from Mexico (Boese, 1920; Kummel and Decker, 1954). The well-defined boundary between a North Temperate bioprovince and a Tethyan bioprovince disappeared at least in the North Atlantic area. Northern Temperate faunas, such as the ammonites *Watinoceras* spp. and the inoceramids *Mytiloides* spp., are not restricted to the area of the previous North Temperate zone but occur all along the entire Atlantic margins.

These significant changes of the paleobiogeographic distribution of some mollusc groups roughly coincide with the Cenomanian–Turonian. An important incursion of boreal elements into lower latitudes is observed in the early Turonian. These biogeographic changes may be related to climatic cooling at high latitudes and resulting upwelling of cooler deep waters at low latitudes.

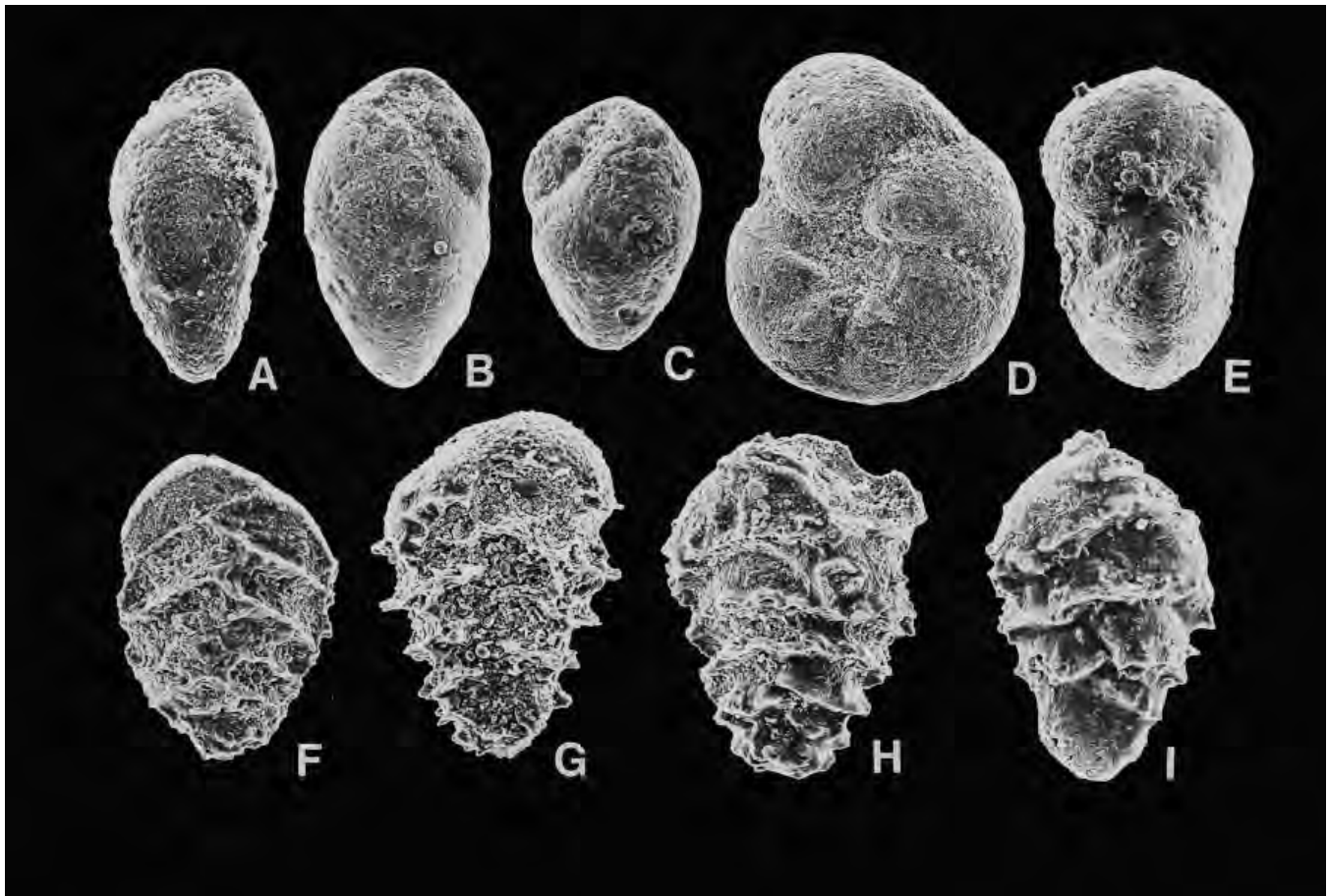


Figure 8B. Benthic foraminiferal assemblages of northern Tethyan and temperate shelf seas with increased primary productivity (factor 1) (A–C) *Praebulimina elata*; (D–E) *Lingulogavelinella* spp.; (F–I) *Tappanina laciniosa*. All specimens are from the Wunstorff section (Northern Germany).

CONCLUSIONS: TOWARD A MODEL OF CENOMANIAN–TURONIAN SOURCE ROCK FORMATION AND DISTRIBUTION

Oceanic Productivity

We attempted to reconstruct and “map” oceanic productivity during the Cenomanian–Turonian along a north-south transect in the eastern North and Western Tethys. Biologic productivity and particle flux were reconstructed using organic-carbon accumulation rates and microfossil species assemblages. Benthic foraminifera assemblages record phytodetritus/organic-matter flux rates at the time of deposition and may consequently be better proxy indicators for paleoproductivity than organic-matter accumulation rates, which only record the preserved part of the primary production. Our results point to substantially enhanced primary production mainly in a comparatively restricted area along the northwest African margin (Casamance, Tarfaya, and Agadir transects). In other areas, formation of Cenomanian–Turonian source rocks was restricted to a short time span of a few

100,000 yr in the latest Cenomanian, and organic-matter accumulation was mainly controlled by favorable preservation conditions (e.g., widespread anoxia due to warm-saline intermediate or deep-water masses).

Deep Ocean Circulation

The Cenomanian–Turonian was a period of fundamental changes in deep ocean circulation, such as changes in production of deep and intermediate waters. Evolutionary patterns of abyssal benthic foraminifera in the central North Atlantic point to a significant change of deep-water masses coeval with the cessation of deep-water anoxia in the early Turonian. We speculate that the formation of significant amounts of cold, high-latitude deep water started around this time and caused both the cessation of abyssal anoxia and the fundamental changes in benthic foraminiferal faunas toward “modern” assemblages.

Intermediate and Surface Water Circulation

Distribution patterns of molluscs suggest cooling of surface and intermediate water masses in large parts of the Atlantic Ocean (but probably not in the western

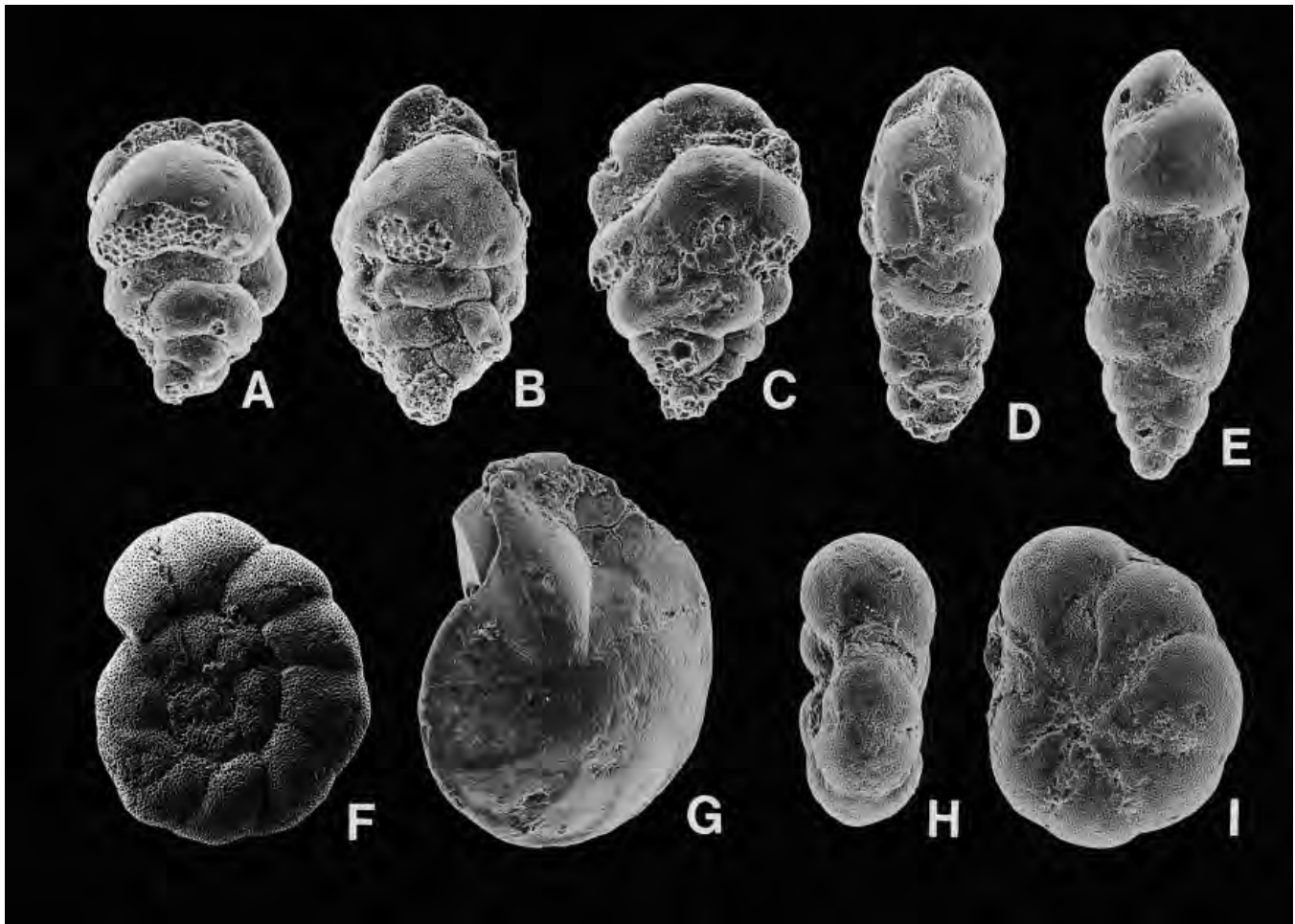


Figure 8C. Benthic foraminiferal assemblages of tropical shelf seas with high primary productivity (factor 4). (A–C) *Gabonita obesa*; (D–E) *Gabonita levis*; (F) *Gavelinella ex gr. dakotensis*; (G) *Lenticulina* sp. A; (H–I) *Lingulogavelinella globosa*. All specimens are from the Tarfaya basin.

Tethys) during the early Turonian. The occurrence of “boreal” faunal elements in low-latitude coastal basins of the North Atlantic was previously explained by upwelling of cold, deep or intermediate waters. However, a global deterioration of the climate during the early Turonian coincident with reduced atmospheric CO₂ after the peak in the latest Cenomanian (Arthur et al., 1988) may be an attractive alternative model.

Needs and Emphasis in Future Research

Better knowledge of the spatial distribution of Cenomanian–Turonian source rocks is absolutely necessary to determine potential causes of their formation. More records, especially from high latitudes, need to be analyzed using not only geochemical but also paleontological indicators. It is especially important to improve the calibration of environmental proxy records, combining geochemical (organic geochemistry, inorganic geochemistry, stable isotope data) and paleontological data (e.g., quantitative distribution of benthic foraminiferal species, and biogeographic maps

of various intermediate and surface water dwellers such as ammonites, inoceramids, radiolarians, and planktonic foraminifers).

We believe that the input of biological proxy data into Cenomanian–Turonian paleogeographic and paleoceanographic models can contribute to a better understanding of the influence of the following parameters: (1) paleogeographic distribution of paleoproductivity and organic-matter flux rates, and (2) oxygenation of bottom water masses in shelf seas and along continental margins. Agglutinated foraminifers in abyssal environments are useful as tracers of deep-water masses, and reconstructions of their distribution patterns may help monitor changes in deep oceanic circulation patterns.

ACKNOWLEDGMENTS

Field work in Cameroon, Nigeria, Morocco, Tunisia, Rumania, Italy, and Spain was supported by the Deutsche Forschungsgemeinschaft. Samples and foraminiferal data from the Casamance transect (Sene-

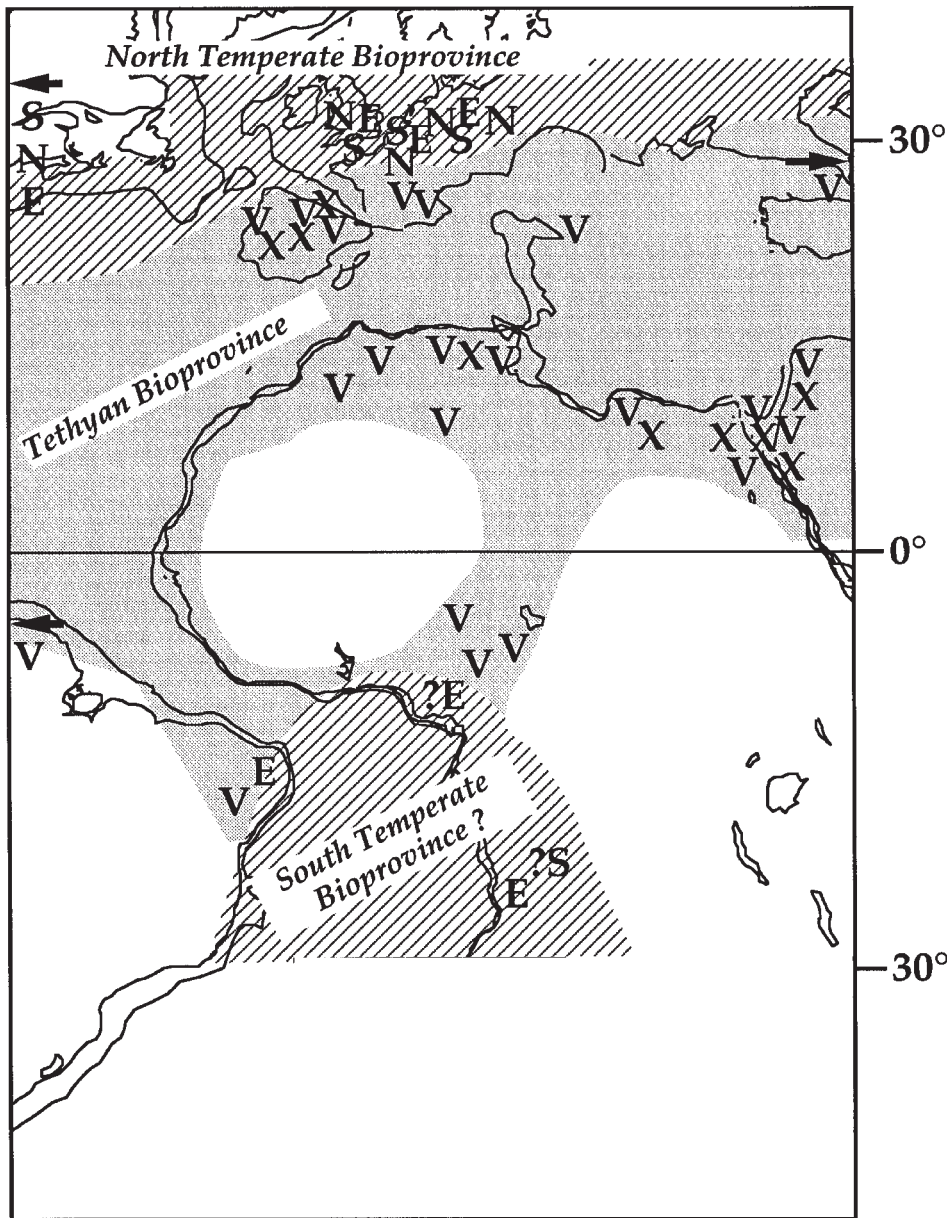


Figure 9A. Biogeographic distribution of selected mollusc species and species groups in the Late Cenomanian. Paleolatitudes according to Smith and Briden (1977) are shown.

gal) were available through Ababacar Ly (University of Dakar). Kai-Uwe Gräfe and Wolfgang Schwentke provided additional samples from Northern Spain. Various aspects of this paper benefited from discussions with Erle G. Kauffman (Boulder), Jürgen Thurow (Bochum), and Karl-Arnim Tröger (Freiberg). Careful reviews by Walter Dean and Philip Meyers significantly helped to improve an earlier version. We are especially grateful to Jean Paul Herbin (IFP, Rueil Malmaison) for Rock Eval analysis and the fruitful exchange of ideas over the years.

REFERENCES CITED

- Arthur, M. A., and I. Premoli Silva, 1982, Development of widespread organic-carbon-rich strata in the Mediterranean Tethys, in S. O. Schlanger and M. B. Cita, eds., *Nature and origin of Cretaceous carbon-rich facies*: Academic Press, p. 7–54.
- Arthur, M. A., W. E. Dean, and L.M. Pratt, 1988, Geochemical and climatic effects of increased marine organic burial at the Cenomanian/Turonian boundary: *Nature*, v. 335 (6192), p. 714–717.
- Barber, W. M., 1957, Lower Turonian ammonites from northeastern Nigeria: *Bulletin of the Geological Survey of Nigeria*, v. 26, p. 1–86.
- Barron, E. J., 1985, Numerical climate modeling: an exploration frontier in petroleum source rock prediction: *AAPG Bulletin*, v. 69, p. 448–456.
- Berger, W. H., and A. Spitzzy, 1988, History of atmospheric CO₂; constraints from the deep-sea record: *Paleoceanography*, v. 3 (4), p. 401–411.
- Bernhard, J. M., 1986, Characteristic assemblages and

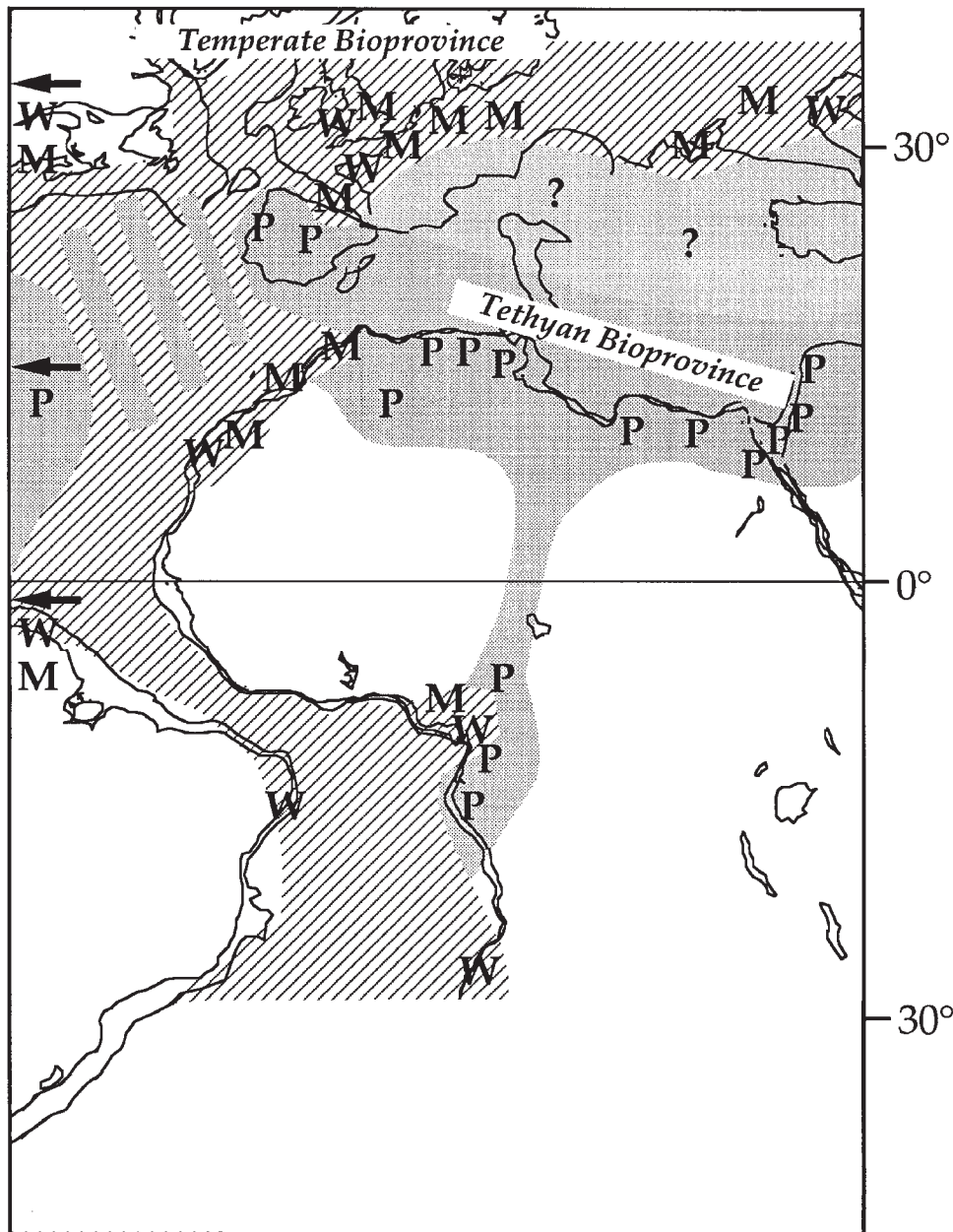


Figure 9B. Biogeographic distribution of selected mollusc species and species groups in the early Turonian. Paleolatitudes according to Smith and Briden (1977) are shown.

morphologies of benthic foraminifera from anoxic organic-rich deposits: Jurassic through Holocene: *Journal of Foraminiferal Research*, v. 16 (3), p. 207–215.

Berthou, P. Y., G. R. Chancellor, and J. Lauerjat, 1985, Revision of the Cenomanian–Turonian ammonite *Vascoceras* Choffat, 1898, from Portugal: *Comunicacoes Servico Geologico do Portugal*, v. 71, p. 55–79.

Boese, E., 1920, On a new ammonite fauna of the Lower Turonian of Mexico: *University of Texas Bulletin*, v. 1856, p. 173–257.

Bradshaw, J. S., 1961, Laboratory experiments on the ecology of foraminifera: *Contributions from the Cushman Foundation of Foraminiferal Research*, v. 12, p. 87–106.

Bralower, T. J., and H. Thierstein, 1984, Low productivity and slow deep-water circulation in mid-Cre-

taceous oceans: *Geology*, v. 12, p. 614–618.

Brass, G. W., J. R. Southam, and W.H. Peterson, 1982, Warm saline bottom water in the ancient ocean: *Nature*, v. 296, p. 620–623.

Brower, J.C., 1985, Multivariate analysis of assemblage zones, in F.M., Gradstein, F.P. Agterberg, J.C. Brower, and W.S. Schwarzacher, eds., *Quantitative Stratigraphy*: Dordrecht, Reidel, p. 65–94.

Brumsack, H.-J., and J. Thurow, 1986, The geochemical facies of black shales from the Cenomanian/Turonian boundary event, in E. T. Degens, P. A. Meyers, and C. Brassell: *Biogeochemistry of Black Shales: Mitteilungen aus dem Geologisch-Paläontologischen Institut der Universität Hamburg*, v. 60, p. 247–265.

Busson, G., 1984, Relations entre la sédimentation du Crétacé moyen et supérieur de la plate-forme du

- nord-ouest africain et les dépôts contemporains de l'Atlantique centre et nord: *Eclogae Geologicae Helveticae*, v. 77 (2), p. 221–235.
- Cobban, W. A., 1972, New and little known ammonites from the Upper Cretaceous (Cenomanian and Turonian) of the Western Interior of the United States: U.S. Geological Survey Professional Paper 699, p. 1–24.
- Cobban, W.A., 1984, Mid-Cretaceous ammonite zones, Western Interior, United States: *Bulletin of the Geological Society of Denmark*, v. 33, p. 71–89.
- Cobban, W.A., and G.R. Scott, 1972, Stratigraphy and ammonite fauna of Graneros Shale and Greenhorn Limestone near Pueblo, Colorado: U.S. Geological Survey Professional Paper 645, p. 1–108.
- Cooper, M.R., 1973, Cenomanian ammonites from Novo Redondo, Angola: *Ann. S. African. Mus.*, v. 62, p. 41–67.
- Cooper, M.R., 1978, Uppermost Cenomanian–basal Turonian ammonites from Salinas, Angola: *Ann. S. Afr. Mus.*, v. 75, p. 51–152.
- de Boer, P.L., 1983, Aspects of Middle Cretaceous pelagic sedimentation in Southern Europe: *Geologica Ultraiectina*, v. 31, p. 1–112.
- Degens, E.T., K.-C. Emeis, B. Mycke, and M.G. Wiesner, 1986a, Turbidites, the principal mechanism yielding black shales in the early deep Atlantic Ocean, *in* C. P. Summerhayes and N. J. Shackleton: *North Atlantic Palaeoceanography: Geological Society of London Special Publication 21*, p. 361–376.
- Degens, E.T., P.A. Meyers, and C. Brassell, eds., 1986b, *Biogeochemistry of black shales: Mitteilungen aus dem Geologisch-Paläontologischen Institut der Universität Hamburg*, v. 60, p. 1–421.
- De Graciansky, P.C., E. Brosse, G. Deroo, J.P. Herbin, L. Montadert, C. Müller, A. Schaaf, and J. Sigal, 1982, Les formations d'âge Crétacé dans les sites DSDP de l'Atlantique Nord: *Revue Institut Français du Pétrole*, v. 37 (3), p. 275–336.
- De Graciansky, P. C., G. Deroo, J.P. Herbin, T. Jacquin, F. Magni, L. Montadert, and C. Müller, 1986, Ocean-wide stagnation episodes in the Late Cretaceous: *Geologische Rundschau*, v. 75 (1), p. 17–41.
- de Klasz, I. P. Marie, and D. Rérat, 1961, Deux nouvelles espèces du genre *Gabonella* (Foraminifère) du Crétacé du Gabon (Afrique Equatoriale): *Revue de Micropaléontologie*, v. 4, p. 77–79.
- Einsele, G., and J. Wiedmann, 1982, Turonian black shales in the Moroccan coastal basins: first upwelling in the Atlantic Ocean?, *in* U. von Rad, K. Hinz, M. Sarntheim, and E. Seibold: *Geology of the Northwest African Continental Margin*: Berlin, Springer-Verlag, p. 396–414.
- Ernst, G., F. Schmid, and E. Seibertz, 1983, Event-Stratigraphie im Cenoman und Turon von NW-Deutschland: *Zitteliana*, v. 10, p. 531–554.
- Ernst, G., C.J. Wood, and H. Hilbrecht, 1984, The Cenomanian–Turonian boundary problem in NW Germany with comments on the north-south correlation to the Regensburg area: *Bulletin of the Geological Society of Denmark*, v. 33, p. 103–113.
- Freund, R., and M. Raab, 1969, Lower Turonian ammonites from Israel: *Palaeontology Special Paper*, v. 4, p. 1–83.
- Furon, R., 1935, Le Crétacé et le Tertiaire du Sahara Soudanais (Soudan, Niger, Tchad): *Archives du Muséum National d'Histoire Naturelle*, Paris, v. 6, n. 13, p. 1–96.
- Greco, B., 1915, Fauna cretacea dell'Egitto raccolta dal Figari Bey: *Palaeontographia Italiana*, v. 29, p. 189–231.
- Hamaoui, M., 1965, Sur la présence de *Gabonella* (Foraminifera) en Israël: *Revue de Micropaléontologie*, v. 8, p. 33–36.
- Herbert, T.D., and J.L. Sarmiento, 1991, Ocean nutrient distribution and oxygenation: Limits on the formation of warm saline bottom water over the past 91 m.y.: *Geology*, v. 19, p. 702–705.
- Herbin, J.P., L. Montadert, C. Müller, R. Gomez, J. Thurow, and J. Wiedmann, 1986, Organic-rich sedimentation at the Cenomanian–Turonian boundary in oceanic and coastal basins in the North Atlantic and Tethys, *in* C. Summerhayes and N. J. Shackleton: *North Atlantic Palaeoceanography: Geological Society Special Publication 22*, p. 389–422.
- Hilbrecht, H., 1986, On the correlation of the upper Cenomanian and lower Turonian of England and Germany (Boreal and N-Tethys): *Newsletter on Stratigraphy*, v. 15, p. 115–138.
- Hilbrecht, H., and J. Hoefs, 1986, Geochemical and palaeontological studies of the $\delta^{13}\text{C}$ anomaly in boreal and N-Tethyan Cenomanian–Turonian sediments in Germany and adjacent areas: *Palaeoecology, Palaeoclimatology, Palaeogeography*, v. 53, p. 169–189.
- Hilbrecht, H., M. A. Arthur, and S.O. Schlanger, 1986, The Cenomanian–Turonian boundary event: sedimentary, faunal and geochemical criteria developed from stratigraphic studies in NW-Germany, *in* O. Walliser, *Global Bio-Events*: Berlin, Springer-Verlag, v. 8, p. 345–351.
- Hilbrecht, H., H.-W. Hubberten, and H. Oberhänsli, 1992, Biogeography of planktonic foraminifera and regional carbon isotope variations: productivity and water masses in Late Cretaceous Europe: *Palaeogeography, Palaeoclimatology, Palaeoecology*, v. 92, p. 407–421.
- Imbrie, J., and N. Kipp, 1971, A new micropaleontological method for quantitative micropaleontology: application to a Late Pleistocene Caribbean core, *in* K.K. Turekian, ed., *The Late Cenozoic Glacial Ages*: New Haven, Conn., Yale University Press, p. 71–181.
- Kennedy, W.J., 1971, Cenomanian ammonites from southern England: *Special Papers in Palaeontology*, v. 8, p. 1–133.
- Kennedy, W.J., 1988, Late Cenomanian and Turonian ammonite faunas from North-East and Central Texas: *Special Papers in Palaeontology*, v. 39, p. 1–131.
- Kennedy, W.J., and W.A. Cobban, 1976, Aspects of ammonite biology, biogeography, and biostratigraphy: *Special Papers in Palaeontology*, v. 17, p. 1–94.
- Kennedy, W.J., and W.A. Cobban, 1991, Stratigraphy and interregional correlation of the Cenomanian–Turonian transition in the Western Interior of the United States near Pueblo, Colorado, a potential

- boundary stratotype of the Turonian stage: *Newsletters on Stratigraphy*, v. 24, p. 1–33.
- Kennedy, W.J., W.A. Cobban, J.M. Hancock, and S.C. Hook, 1989, Biostratigraphy of the Chispa Summit Formation at its type locality: a Cenomanian through Turonian reference section for Trans-Pecos Texas: *Bulletin of the Geological Institutions of the University of Uppsala, New Series*, v. 15, p. 39–119.
- Koutsoukos, E.A.M., 1992, Late Aptian to Maastrichtian foraminiferal biogeography and palaeoceanography of the Sergipe Basin, Brazil: *Palaeogeography, Palaeoclimatology, Palaeoecology*, v. 92, p. 295–324.
- Koutsoukos, E.A.M., P.N. Leary, and M.B. Hart, 1990, Latest Cenomanian–earliest Turonian low-oxygen tolerant benthonic foraminifera: a case-study from the Sergipe basin (N.E. Brazil) and the western Anglo-Paris basin (southern England): *Palaeogeography, Palaeoclimatology, Palaeoecology*, v. 77, p. 145–177.
- Kruijs, E., and E. Barron, 1990, Climate model prediction of paleoproductivity and potential source-rock distribution, in A. Y. Huc, ed., *Deposition of Organic Facies: AAPG Studies in Geology* 30, p. 195–216.
- Kuhnt, W., 1992, Abyssal recolonization by benthic foraminifera after the Cenomanian/Turonian boundary anoxic event in the North Atlantic: *Marine Micropaleontology*, v. 19, p. 257–274.
- Kuhnt, W., J. Thurow, J. Wiedmann, and J.P. Herbin, 1986, Oceanic anoxic conditions around the Cenomanian/Turonian boundary and the response of the biota, in E. T. Degens, P. A. Meyers, and S. C. Brassell, *Biogeochemistry of Black Shales: Mitteilungen aus dem Geologischen Institut der Universität Hamburg*, v. 60, p. 205–246.
- Kuhnt, W., J.P. Herbin, J. Thurow, and J. Wiedmann, 1990, Distribution of Cenomanian–Turonian organic facies in the western Mediterranean and along the adjacent Atlantic Margin, in A. Y. Huc, ed., *Deposition of Organic Facies: AAPG Studies in Geology* 30, p. 133–160.
- Kummel, B., and J.M. Decker, 1954, Lower Turonian ammonites from Texas and Mexico: *Journal of Paleontology*, v. 28 (3), p. 310–319.
- Lewy, Z., W. J. Kennedy, and G.R. Chancellor, 1984, Co-occurrence of *Metoicoceras geslinianum* (d'Orbigny) and *Vascoceras cauvinii* (Chudeau) (Cretaceous Ammonoidea) in the southern Negev (Israel) and its stratigraphic implications: *Newsletters on Stratigraphy*, v. 13, p. 67–76.
- Ly, A., and W. Kuhnt, 1994, Late Cretaceous benthic foraminiferal assemblages of the Casamance shelf (Senegal, NW Africa)—indication of a Late Cretaceous oxygen minimum zone: *Revue de Micropaléontologie*, v. 37 (1), p. 49–74.
- Malmgren, B.A., and B.U. Haq, 1982, Assessment of quantitative techniques in paleobiogeography: *Marine Micropaleontology* 7 p. 213–236.
- Moullade, M., W. Kuhnt, and J. Thurow, 1988, Agglutinated benthic foraminifera from Upper Cretaceous variegated clays of the North Atlantic Ocean (DSDP Leg 93 and ODP Leg 103), in G. Boillot, E. L. Winterer et al., *Proceedings of the Ocean Drilling Program, Scientific Results*, v. 103, p. 349–377.
- Pervinquier, L., 1907, *Études de Paléontologie Tunisienne. I. Céphalopodes des terrains secondaires*: Paris, Rudeval.
- Phleger, F.B., and A. Soutar, 1973, Production of benthic foraminifera in three east Pacific oxygen minima: *Micropaleontology*, v. 19, p. 110–115.
- Pratt, L.M., 1984, Influence of paleoenvironmental factors on preservation of organic matter in middle Cretaceous Greenhorn Formation, Pueblo, Colorado: *AAPG Bulletin*, v. 68 (9), p. 1146–1159.
- Renz, O., 1982, The Cretaceous ammonites of Venezuela: Basel, Maraven.
- Reyment, R.A., 1954a, New Turonian (Cretaceous) ammonite genera from Nigeria: *Colon. Geol. Miner. Resour.*, London, v. 4, p. 149–164.
- Reyment, R.A., 1954b, Some new Cretaceous ammonites from Nigeria: *Colon. Geol. Miner. Resour.*, London, v. 4, p. 248–270.
- Reyment, R.A., 1971, Vermuteter Dimorphismus bei der Ammonitengattung *Benuites*: *Bull. Geol. Instn. Univ. Uppsala*, (n.s.) v. 3, p. 1–18.
- Schlanger, S.O., and H.C. Jenkyns, 1976, Cretaceous anoxic events: causes and consequences: *Geol. Mijnbouw*, v. 55 (3/4), p. 179–184.
- Schlanger, S.O., M.A. Arthur, H.C. Jenkyns, and P.A. Scholle, 1987, The Cenomanian–Turonian anoxic event. I. Stratigraphy and distribution of organic carbon-rich beds and the marine $\delta^{13}\text{C}$ Excursion, in J. Brooks and A. Fleet, eds., *Marine Petroleum Source Rocks: Geological Society of London Special Publication* 26, p. 371–399.
- Smith, A.G., and J.C. Briden, 1977, *Mesozoic and Cenozoic paleocontinental maps*: Cambridge, Cambridge University Press, p. 1–63.
- Spicer, R.A., and R.M. Corfield, 1992, A review of terrestrial and marine climates in the Cretaceous with implications for modelling the 'Greenhouse Earth': *Geological Magazine*, v. 129 (2), p. 169–180.
- Summerhayes, C.P., 1981, Organic facies of middle Cretaceous black shales in deep North Atlantic: *AAPG Bulletin*, v. 65, p. 2364–2380.
- Summerhayes, C.P., 1987, Organic-rich Cretaceous sediments from the North Atlantic, in J. Brooks and A. Fleet, eds., *Marine Petroleum Source Rocks: Geological Society of London Special Publication* 26, p. 301–316.
- Thierstein, H.R., 1989, Inventory of paleoproductivity records: the mid-Cretaceous enigma, in W. H. Berger, V. S. Smetacek, and G. Wefer, *Productivity of the Ocean: Present and Past*: John Wiley, p. 355–375.
- Thomel, G., ed., 1978, *Événements de la partie moyenne du Crétacé-rapports sur la biostratigraphie des régions clefs*: *Annales du Muséum d'Histoire Naturelle de Nice*, v. 4, Editions du Centre d'Études Méditerranéennes.
- Thurow, J., M. Moullade, H.J. Brumsack, E. Masure, J. Taugourdou, and K. Dunham, 1988, The Cenomanian–Turonian Boundary Event (CTBE) at Leg 103/Hole 641A, in G. Boillot, E. L. Winterer et al.,

- Proceedings of the Ocean Drilling Program, Scientific Results, v. 103, p. 587–634.
- Thurrow, J., H.J. Brumsack, R. Littke, P. Meyers, and J. Rullkötter, 1992, The Cenomanian/Turonian boundary event in the Indian Ocean: a key to understand the global picture, *in* Indian Ocean: American Geophysical Union Geophysical Monograph, v. 70, p. 253–273.
- Tronchetti, G., and D. Grosheny, 1991, Les assemblages de foraminifères benthiques au passage Cénomanien-Turonien à Vergons, S-E France: *Geobios*, v. 24, p. 13–31.
- Wright, C.W., and W.J. Kennedy, 1981, The Ammonoidea of the Plenus Marls and the Middle Chalk: Paleontographical Society Monographs, p. 1–148.
- Zaborski, P.M.P., 1985, Upper Cretaceous ammonites from the Calabar region, south-east Nigeria: Bulletin of the British Museum of Natural History (Geology), v. 39, p. 1–72.
- Zaborski, P.M.P., 1986, Lower Cenomanian (mid-Cretaceous) ammonites from south-east Nigeria: *Journal of African Sciences*, v. 5 (4), p. 371–380.
- Zaborski, P.M.P., 1987, Lower Turonian (Cretaceous) ammonites from south-east Nigeria: Bulletin of the British Museum of Natural History (Geology), v. 41 (2), p. 31–66.

The Hydrocarbon Source Potential in the Brazilian Marginal Basins: A Geochemical and Paleoenvironmental Assessment

M. R. Mello

*Petrobrás/Cenpes/Divex
Rio de Janeiro, Brazil*

N. Telnaes

*Norsk Hydro Research Center
Bergen, Norway*

J. R. Maxwell

*University of Bristol
Bristol, U.K.*

ABSTRACT

A geochemical survey of Brazilian marginal basins using a wide selection of source rocks and oils, ranging from Early Cretaceous to Tertiary in age, has been undertaken. The aims were to review, assess, and characterize the paleoenvironment of deposition of source rocks and to correlate reservoired oils with their putative source rocks using an approach based mainly on the distribution and absolute concentrations of biological markers. The survey included evaluation of organic carbon contents, Rock-Eval pyrolysis data, vitrinite reflectance measurements, carbon isotope ratios, elemental and visual kerogen analyses and molecular studies involving liquid and gas chromatography, qualitative and quantitative biological marker investigations using gas chromatography–mass spectrometry (GC-MS) and metastable ion monitoring GC-MS of saturated hydrocarbons. The metastable ion GC-MS data were evaluated using principal component analysis.

Integration of the results with geological and paleontological data facilitates the recognition and differentiation of seven depositional regimes: lacustrine fresh/brackish water, lacustrine saline water, marine evaporitic, marine carbonate, marine deltaic with carbonate influence, open marine anoxic with a predominance of calcareous mudstone lithology, and open marine anoxic with a predominance of siliciclastic lithology.

The analyses of the oils reveal significant differences among groups which enable a correlation with putative source rocks deposited in six of the aforementioned depositional regimes. Although siliciclastic rocks derived from an open marine environment show high lipid-rich organic carbon contents,

they are immature, and are not considered source rocks in the Brazilian marginal basins. Thus, geochemical characteristics of organic-rich rocks and oils enable differentiation of depositional environments as well as oil–source rock correlations.

This study also provides a framework of bulk, elemental, and specifically biological marker characteristics which can be used to assess and characterize the paleoenvironment of deposition of organic-rich sedimentary rocks and oils.

INTRODUCTION

Sedimentary organic matter contains a complex assemblage of biological markers that reflects in a particular rock extract or oil the precursor compounds of the organisms which contributed organic matter at the time of sediment deposition. The distribution of these biological markers can, therefore, serve as diagnostic fingerprints, carrying information about the prevailing environmental conditions. Thus, biological marker analyses of oils or organic-rich rocks can assist in ascertaining the depositional environment of petroleum source rocks, as well as, in some cases, the types of organisms which prevailed in these environments. Recently, a better understanding of the distributions and concentrations of geochemical and biological marker parameters has provided the geochemist with tools for assessing and differentiating the paleoenvironment of deposition of petroleum source rocks, and for oil–oil and oil–source rock correlation.

Recently, many authors have shown that organic geochemical analyses enable differentiation of rock extracts and oils derived from a variety of depositional environments (e.g., Grantham et al., 1983; McKirdy et al., 1984; Palacas et al., 1984; Moldowan et al., 1985; Fu Jia Mo et al., 1986; McKirdy et al., 1986; Philp and Gilbert, 1986; Talukdar et al., 1986; Brooks, 1986; Powell, 1986; Albaiges et al., 1986; Connan and Dessort, 1987; Wang Tieguan et al., 1988; ten Haven et al., 1988; Mello et al., 1988a, b; Mello and Maxwell, 1990; Mello et al., 1993).

This work contributes to those studies using a multidisciplinary approach (geochemical, geological, paleontological, and statistical) in an attempt to assess the depositional environments of source rocks and to correlate them with their derived oils in the major Brazilian marginal basins. Also, it extends earlier preliminary studies of samples from some of the basins (e.g., Mello et al., 1984; Estrella et al., 1984; Babinski and Santos, 1987; Rodrigues et al., 1988; Mello et al., 1988a, b; Mello and Maxwell, 1990). Fifty oils and 200 rock samples ranging in age from lower Neocomian to Oligocene were initially analyzed.

The organic-rich rocks (TOC > 2.0%; where TOC is total organic carbon) cover a wide maturity range (0.45 to 0.9% R_o) but only those (approx. 150 samples) with R_o values between 0.45 and 0.75% are discussed herein, to minimize maturation effects on biological

marker concentrations (Rullkötter et al., 1984). Similarly, only oils (approx. 40) with medium to high API gravities and those not severely affected by biodegradation were analyzed. The samples have been discussed in more detail elsewhere (Mello, 1988; Mello et al., 1988a, b).

GENERAL GEOLOGY

The Brazilian marginal basins are directly related to the rapture of the African and South American plates. The basins originated as new accretionary plate boundaries, but once formed, they mark the junction between oceanic and continental crusts within plate interiors. The nearly 8000 km long set of basins (Figure 1) can be classified as components of a typical divergent, mature, Atlantic-type continental margin (Ponte and Asmus, 1978; Ojeda, 1982; Estrella et al., 1984). Based on their tectonosedimentary sequence, they can be linked to a single evolutionary geological history (Figures 2 and 3), which can be divided into three main stages: pre-rift, rift, and drift (gulf proto-oceanic and oceanic phases; cf. Asmus, 1975).

The Late Jurassic/Early Cretaceous pre-rift stage is associated with stretching of the continental crust and lithosphere. This phenomenon resulted in block faulting, sedimentary troughs, and localized mafic volcanism associated with thinning of the underlying crust and mantle, and with an upwelling of the asthenosphere producing a thermal anomaly (Bott, 1976).

The Neocomian rift stage (Figure 3A) is a direct result of an overall subsidence produced by the thinning of the lithosphere. The rifting process is generally associated with basement-involved block-rotated faulting, and intense and widespread mafic volcanism (Bott, 1976; Mohriak and Dewey, 1987). As a result, a thick sedimentary succession comprising continental, fluvial, and lacustrine siliciclastic and carbonate sediments was deposited (e.g., Viana et al., 1971; Bertani and Carozzi, 1985). In some areas it overlies and is intercalated with volcanic rocks, mainly basalts. After rifting, tectonic activity appears to have been restricted to subsidence and basinward tilting, with the development of gravity-sliding features (e.g., Falkenheim, 1981) and localized reactivations of faults (e.g., Ponte and Asmus, 1978). The rift phase ceased once sea-floor spreading started, with



Figure 1. Location map of the Brazilian marginal basins.

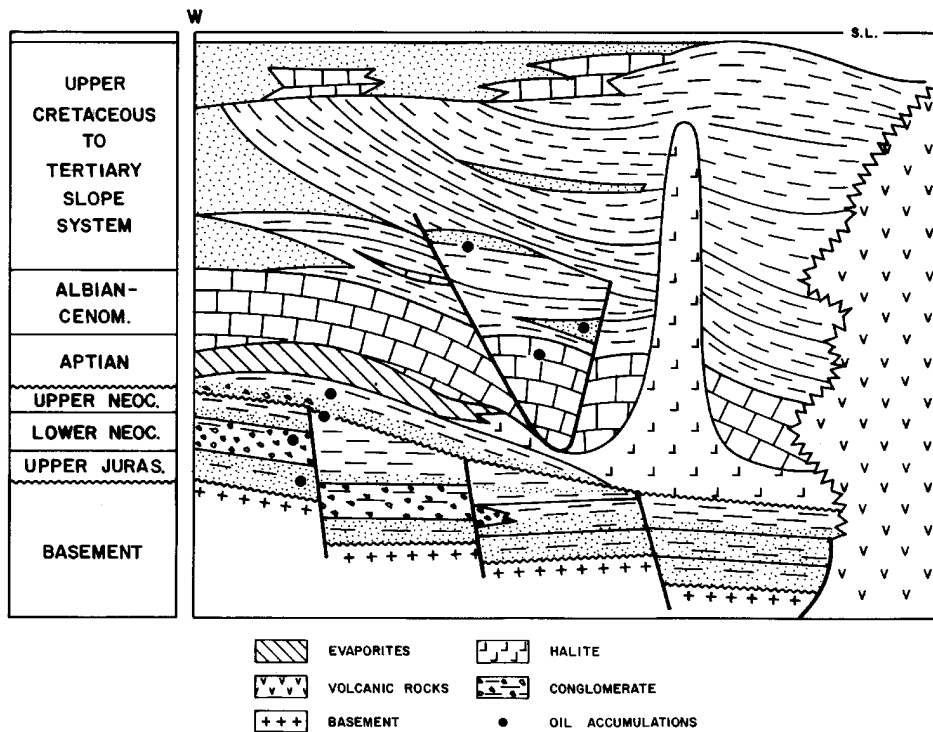


Figure 2. Schematic stratigraphic and structural section for the Brazilian marginal basins.

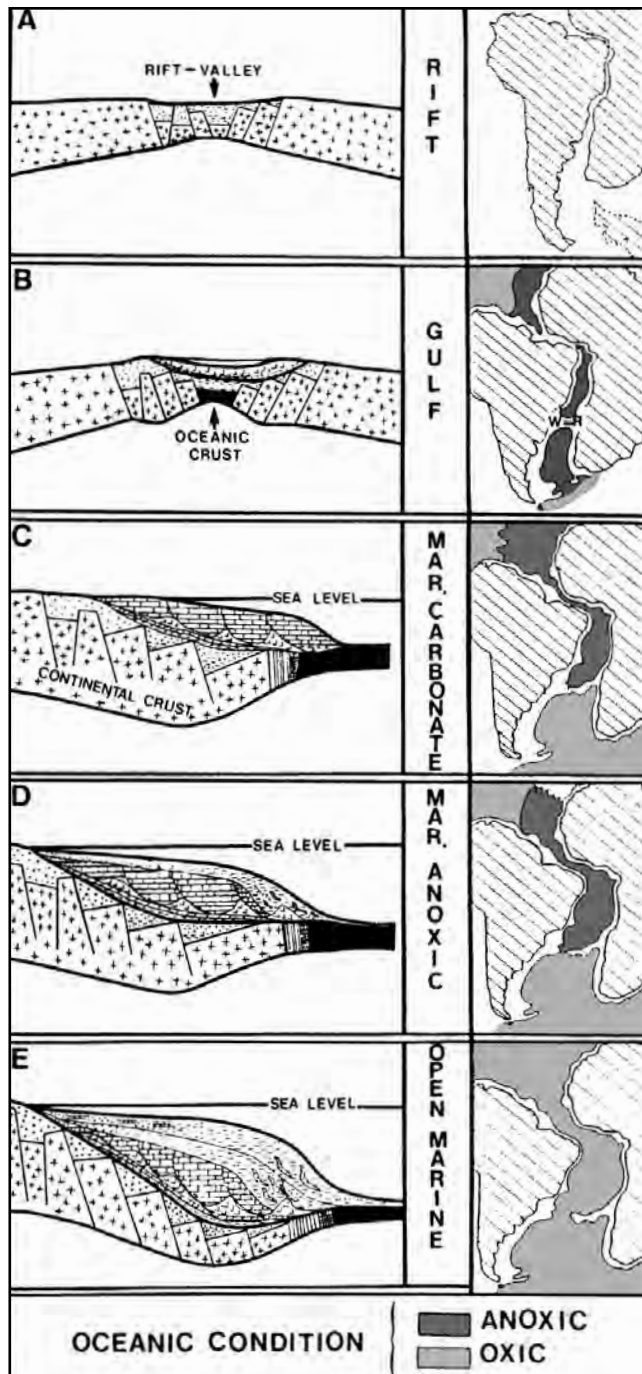


Figure 3. Evolution of the Brazilian marginal basins from Cretaceous to Tertiary showing the distribution of depositional environments (modified from Tissot et al., 1980).

the succeeding drift stage being characterized by flexural subsidence of the margin without conspicuous faulting. This phenomenon is attributed to progressive cooling and contraction of the underlying lithosphere (Bott, 1976).

The drift stage can be subdivided into two distinct phases: gulf proto-oceanic and oceanic. The gulf proto-oceanic phase (Figure 3B) is associated with the first

marine incursions into the coastal basins during the Barremian/Aptian. The combination of tectonic quiescence, topographical barriers, and arid climate led to a low clastic influx and restricted conditions appropriate for deposition of mixed carbonate and siliciclastic sediments together with evaporites in coastal, shallow continental to marine hypersaline environments (Asmus, 1975).

The oceanic phase (Figure 3C) is a consequence of increasing sea-floor spreading and the continuous subsidence of the continental margin. Differences in paleoenvironmental setting allow the subdivision of this phase into three major sequences:

1. The Albian marine carbonate sequence (Figure 3C) is characterized mainly by carbonate platform and slope sediments deposited in a neritic to upper bathyal environment, in a shallow and narrow epicontinental sea (e.g., Koutsoukos and Dias-Brito, 1987). This succession appears to have been linked with conditions of tectonic quiescence, with some adiastraphic tectonism often associated with listric detached faults soling out on the Aptian-aged salt (Figure 2).

2. The Cenomanian to Campanian–Maastrichtian open marine shelf-slope sedimentary system (Figure 3D) is characterized by predominantly siliciclastic and calcareous mudstone deposition in progressively deepening basins (e.g., Koutsoukos, 1987). Maximum water depths occurred toward the end of the period, when bathyal/abyssal conditions were established in more distal areas. In some areas, the Cenomanian section is missing due to an erosional event initiated by the effective structural and oceanographic connection between the North and South Atlantic, which occurred sometime during the Cenomanian and/or Turonian (e.g., Koutsoukos, 1984, 1987; Koutsoukos and Merrick, 1988). The deposition of widespread organic-rich calcareous mudstones and black shales in almost all the basins is an important process that occurred during the Cenomanian to Santonian (Mello et al., 1989). The preservation of organic matter is consistent with expansion of the oxygen-minimum zone, linked to periods of rising sea levels associated with enhanced primary biological productivity and/or sluggish circulation (cf. Schlanger et al., 1987; Mello et al., 1989). The worldwide occurrence of Cretaceous anoxic sediments has led to proposals of an oceanic anoxic event (see Schlanger et al., 1987, for a review).

3. The Maastrichtian to Holocene progradational sequence (Figure 3E) is generally characterized by a proximal, coarse siliciclastic facies and a distal facies with pelitic and turbidite deposits. Geochemical and micropaleontological evidence shows that oxygenated conditions have prevailed in most of the Brazilian marginal basins since the Campanian, with the accumulation of organic-poor, mixed clastic and carbonate sediments (Mello et al., 1984, 1989, and references therein).

Local basaltic flows, progressive basin subsidence, seaward tilting, and large adiastraphic growth-fault structures mark the tectono-sedimentary activity of the entire open marine sequence (e.g., Estrella et al., 1984).

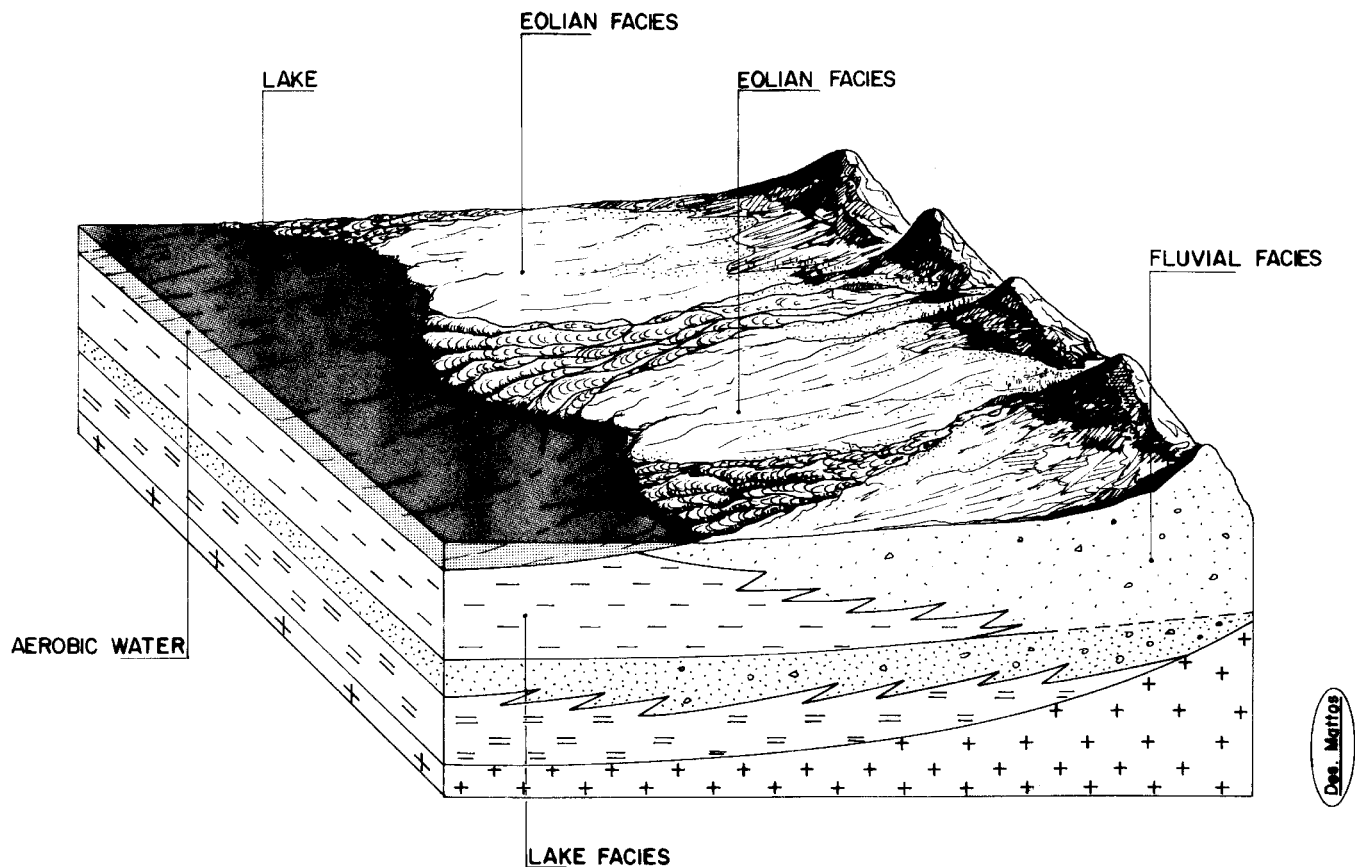


Figure 4. Schematic block diagram showing the sedimentary facies in a braided fluvial, eolian and shallow fresh- to brackish-water lacustrine depositional environment from the pre-rift stage in the Brazilian basins (modified from Medeiros and Ponte, 1981).

ASSESSMENT OF PALEOENVIRONMENT OF DEPOSITION

In order to assess and differentiate the paleoenvironments of deposition of organic-rich rocks in accordance with paleontological, sedimentological, and geochemical data, each tectonic-sedimentary stage in the Brazilian marginal basins is discussed separately, from a genetic point of view, in the following manner.

Pre-Rift Stage

The upper Jurassic–Lower Neocomian pre-rift stage is associated with a succession of continental, fluvial, and delta-lacustrine siliciclastic oxidized sediments (Figure 2; Medeiros et al., 1971; Schaller, 1969). In general, the section is composed mainly of red beds of fine to coarse clastic rocks deposited under highly oxygenated conditions in braided fluvial facies, and associated with eolian facies and shallow freshwater to saline water lake environments (Figure 4; Netto et al., 1982; de Azambuja Filho, 1987). Due to such environmental conditions, the pelitic rocks have low organic carbon contents ($\text{TOC} < 0.5\%$). The organic matter is comprised mainly of oxidized higher plant debris, and was not further investigated.

Rift Stage

Paleogeographical and paleontological evidence (e.g., Viana et al., 1971; Bertani and Carozzi, 1985) indicates that the organic-rich Neocomian rift-stage succession was deposited in lacustrine environments. The formation and behavior of such lacustrine systems are a function of a number of physical and chemical processes whose relative importance is mainly influenced by tectonic settings, lake morphology, water chemistry, and climatic conditions. Based on sedimentological, paleontological, and geochemical data (see below), it is possible to differentiate two distinct organic-rich lacustrine systems in the Brazilian marginal basins:

1. A relatively large, deep, lacustrine freshwater type, ranging in age from Lower Neocomian to Aptian.
2. A closed and shallow lower to upper Neocomian system, having saline waters of alkaline affinities.

Each lake type is discussed separately in the following sections.

Deep Lacustrine Freshwater Basins

Physical, chemical, and biological data suggest that the optimal conditions for producing organic-rich

sediments in a deep lacustrine freshwater basin are deep water conditions, a warm and wet climate without seasonal overturn, water salinities ranging from fresh to brackish, low sulfate concentration (fermentation rather than sulfate degradation), abundant dissolved nutrients (e.g., nitrates and phosphates), negative supply/demand balance of oxygen in the bottom waters (anoxic conditions), and moderate to high sedimentation rate (cf. Demaison and Moore, 1980; Kelts, 1988; Talbot, 1988). Based on sedimentological, paleontological, and geochemical interpretations, these conditions appear to have been present during the deposition of lacustrine sediments in the Brazilian basins (e.g., Ponte and Asmus, 1978; Viana et al., 1971; Schaller, 1969; Mello et al., 1984, 1988a, b; Mello and Maxwell, 1990).

Organic-rich rocks and oils derived from this group are present in the Ceará, Potiguar, Sergipe/Alagoas, and Bahia Sul basins (Figures 5 and 6). The presence of most of the Neocomian to Aptian lakes in the equatorial and central areas of the Brazilian margin indicates the timing of continental drifting, and that these areas represent the last part of the South American plate to be connected to its African counterpart (Figure 3A). Generally, the organic-rich rocks consist of thick beds of dark gray/black shales (TOC up to 13%; e.g., Figure 7) with low sulfur (~0.1%) and CaCO₃ contents (<7%). Hydrogen and oxygen indices and organic petrology data identify the organic mat-

ter as composed predominantly of type I/II kerogen (Figure 7) with significant amounts of higher plant debris (25–35% herbaceous, mainly pollen and spores) associated with lipid-rich (mainly algal) organic matter (45–60%). These data suggest that algal blooms, higher plant debris, and nutrient input in the photic and aerobic zones enhanced anaerobic bacterial activity and led to anoxic bottom waters in the deeper parts of the lakes, thus creating ideal conditions for preservation of organic matter (lipid-rich organic matter with hydrogen indices up to 900 mg HC/g organic carbon; where HC is hydrocarbon). The excellent hydrocarbon source potential (up to 40 kg of HC/ton of rock; e.g., Figure 7) of these sediments, combined with the appropriate thermal evolution conditions, indicates that they have good source rock characteristics. These rocks are the source of large accumulations of low sulfur (usually <0.1%), waxy oils (API ranging from 28–30°; Figure 8). The geochemical and biological marker data for the oils and organic-rich sediments show a set of characteristics diagnostic of lacustrine freshwater environments (cf. Moldowan et al., 1985; Powell, 1986; McKirdy et al., 1986; Philp and Gilbert, 1986; Wang Tieguan et al., 1988; Burwood et al., 1993). Details of the Brazilian samples and a discussion of the geochemical features are given by Mello et al. (1988a and 1988b) and Mello and Maxwell (1990). The most diagnostic biomarker features (high wax content with abundance of high



Figure 5. Location map of the Brazilian marginal basins showing the distribution of the organic-rich sediments in accordance with proposed depositional environment.



Figure 6. Location map of the Brazilian marginal basins showing the distribution of the oil samples investigated in accordance with proposed depositional environment of their source rocks.

| DEPTH (METERS) | ORGANIC CARBON | | | WELL DATA | | HYDROGEN INDEX | | | OXYGEN INDEX | | HC SOURCE POTENTIAL | | | | VITRINITE REFLECT. | | | |
|-------------------|----------------|-----|-----|-----------------|-------|----------------|--|-----|--------------|-----------------------|---------------------|------|------|------|--------------------|-----|------|-----|
| | WT % | | | AGE | LITHO | GAS | | OIL | | S ₃ TOC | POOR | FAIR | GOOD | EXC. | IMMAT | MAT | OVER | MAT |
| | 6 | 4 | 2 | | | mg HC/g TOC | | 50 | | | mg H/g ROCK | | | | 0.2 0.6 1.35% | | | |
| | 100 | 300 | 500 | | | | | | | | | | | | | | | |
| 1500 | | | | ALBIAN | | | | | | | | | | | | | | |
| 2000 | | | | EARLY NEOCOMIAN | | | | | | | | | | | | | | |
| 2500 | | | | EARLY NEOCOMIAN | | | | | | | | | | | | | | |
| 3000 | | | | EARLY NEOCOMIAN | | | | | | | | | | | | | | |

Figure 7. Example of a geochemical well log showing the stratigraphic position of lacustrine freshwater organic-rich sediments deposited during the early Neocomian.

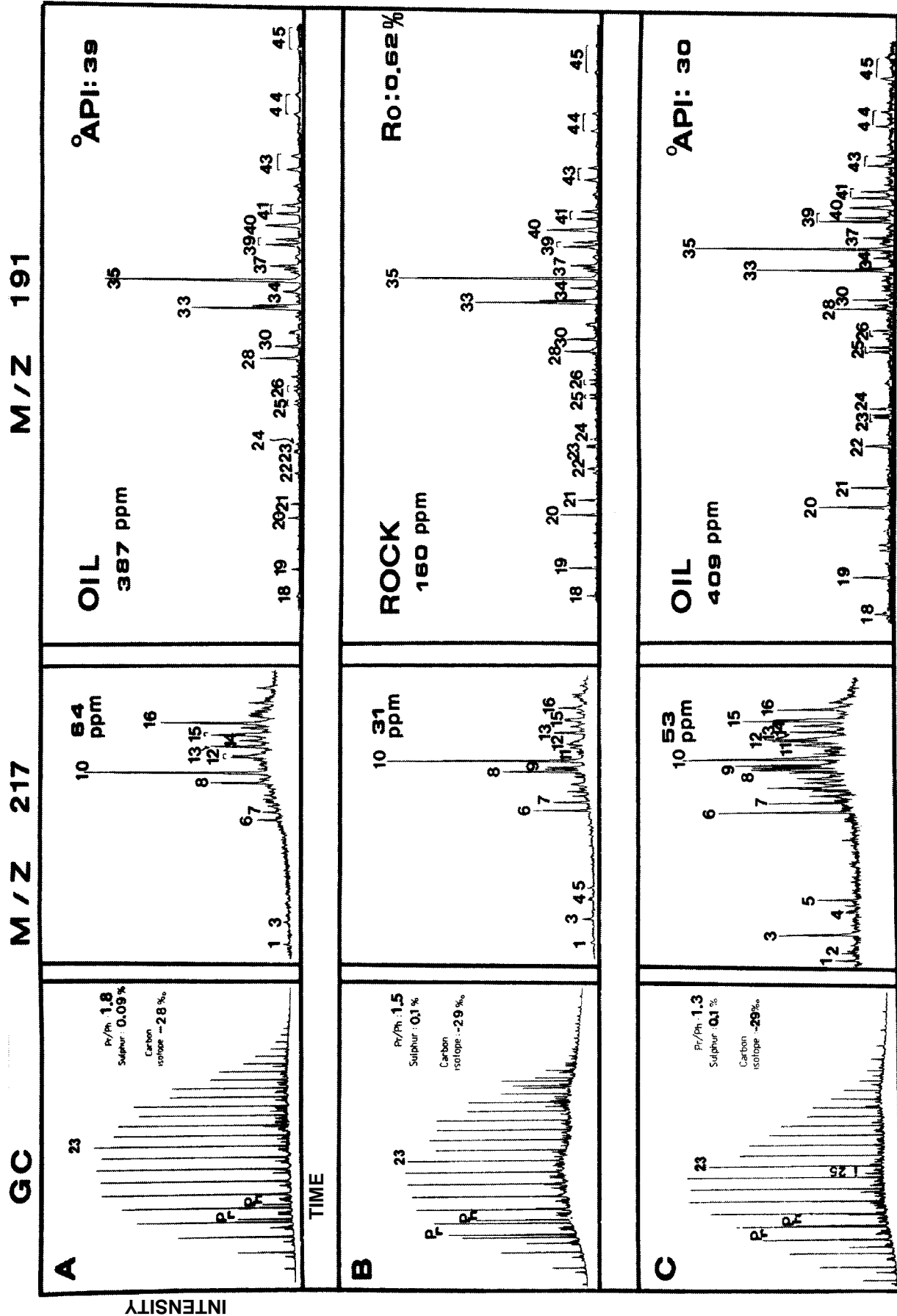


Figure 8. Oil-source rock correlation using gas chromatograms of total alkanes, bulk and elemental parameters, partial m/z 217 and m/z 191 chromatograms, and absolute concentrations of C₂₇ ααα 20S+R-steranes and C₃₀ αβ-hopane for a typical lacustrine freshwater source rock (B) versus two related oils (A and C) from the Brazilian marginal basins (for peak assignment and quantification procedure see Appendices I and II).

molecular weight *n*-alkanes with odd over even predominance, high pristane/phytane [>1.3] and hopane/sterane ratio [usually >8], and absence of C_{30} steranes and dinosteranes, etc.) of samples from this depositional environment are shown in Table 1 (cf. Figure 8 and Appendices I and II).

The integration of such data supports an origin for the organic-rich lower Neocomian and Aptian sedimentary succession studied from lacustrine anoxic fresh, perhaps brackish, water depositional environments (cf. Mello et al., 1988a and 1988b, and Mello and Maxwell, 1990).

The distributions of fossil biota are in agreement with the geochemical data, being characterized by the presence of organisms typical of freshwater lakes, such as ostracods, gastropods, and conchostraceans (Schaller, 1969; Ghignone and de Andrade, 1970). The idea of a deep-water setting comes from paleontological data, for example, shell ornamentation on ostracods with thin and delicately ornamented tests (de Deckker, 1988; Tolderer-Farmer et al., 1987), and the occurrence of particular sedimentary facies and structures, for example, large turbidite deposits associated with deep-water shales (Viana et al., 1971; Netto et al., 1982). The block diagram in Figure 9 is an illustration of the main depositional facies of the deep lacustrine freshwater environment thought to be typical of the freshwater lakes which existed during the rift stage of the Brazilian marginal basins.

The most organic-rich and thickest deposits in such a system appear to be associated with the depocenter

of the basin (deepest part of the lakes; Figure 9). Detailed descriptions of a number of analogous ancient and recent deep freshwater systems have been reported in AAPG Memoir 50, *Lacustrine Basin Exploration—Case Studies and Modern Analogs*, edited by B. J. Katz. Noteworthy ancient examples include the Songliao and Shanganning basins in China (Powell, 1986; Wang Tieguan et al., 1988; Li Desheng and Luo Ming, 1990), the Otway and Gippsland basins, Australia (e.g., McKirdy et al., 1986; Philp and Gilbert, 1986), and the pre-salt sequence in the west coast of Angola and Gabon (McHargue, 1990). Analogous modern examples appear to be lakes Tanganyika and Kivu in the East African rift system (Demaison and Moore, 1980; Cohen, 1990).

Shallow Saline Lake Systems of Alkaline Affinities

This type of lake generally occurs in areas of high evaporation (semiarid/moist climates). The large amount of nutrients available in the highly saline waters, generally associated with alkaline springs, enhances the development of well-adapted, limited aqueous species that, with little competition, show prolific productivity. The result is a high input of algal and bacterial organic matter within the lake. The differences in salinity between an upper aerobic, less saline layer and a lower anaerobic, more saline layer enhance water column stability, leading to stratification and extended periods of bottom water anoxia. These conditions, although they enhance anaerobic bacterial activity, are lethal for most other life forms. Low sulfate

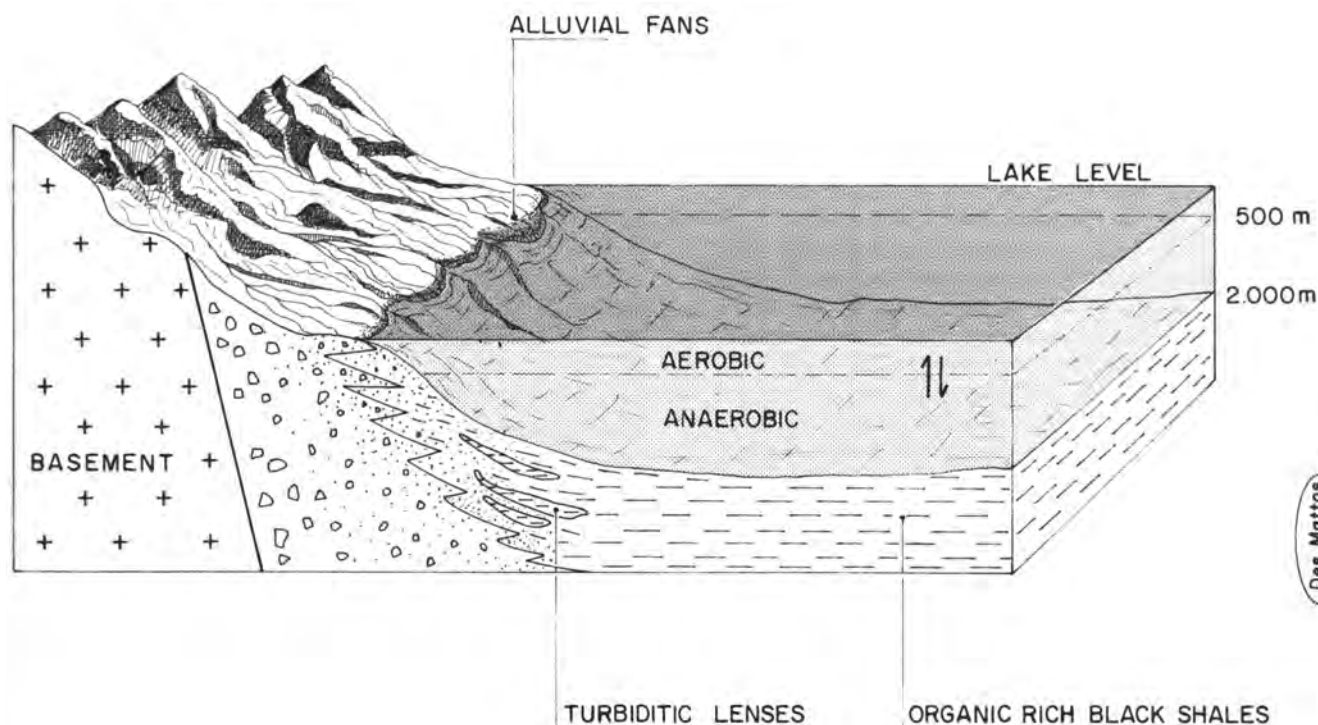


Figure 9. Schematic block diagram showing the sedimentary facies in a deep freshwater lake from the rift stage in the Brazilian marginal basins (modified from de Azambuja Filho, 1987).

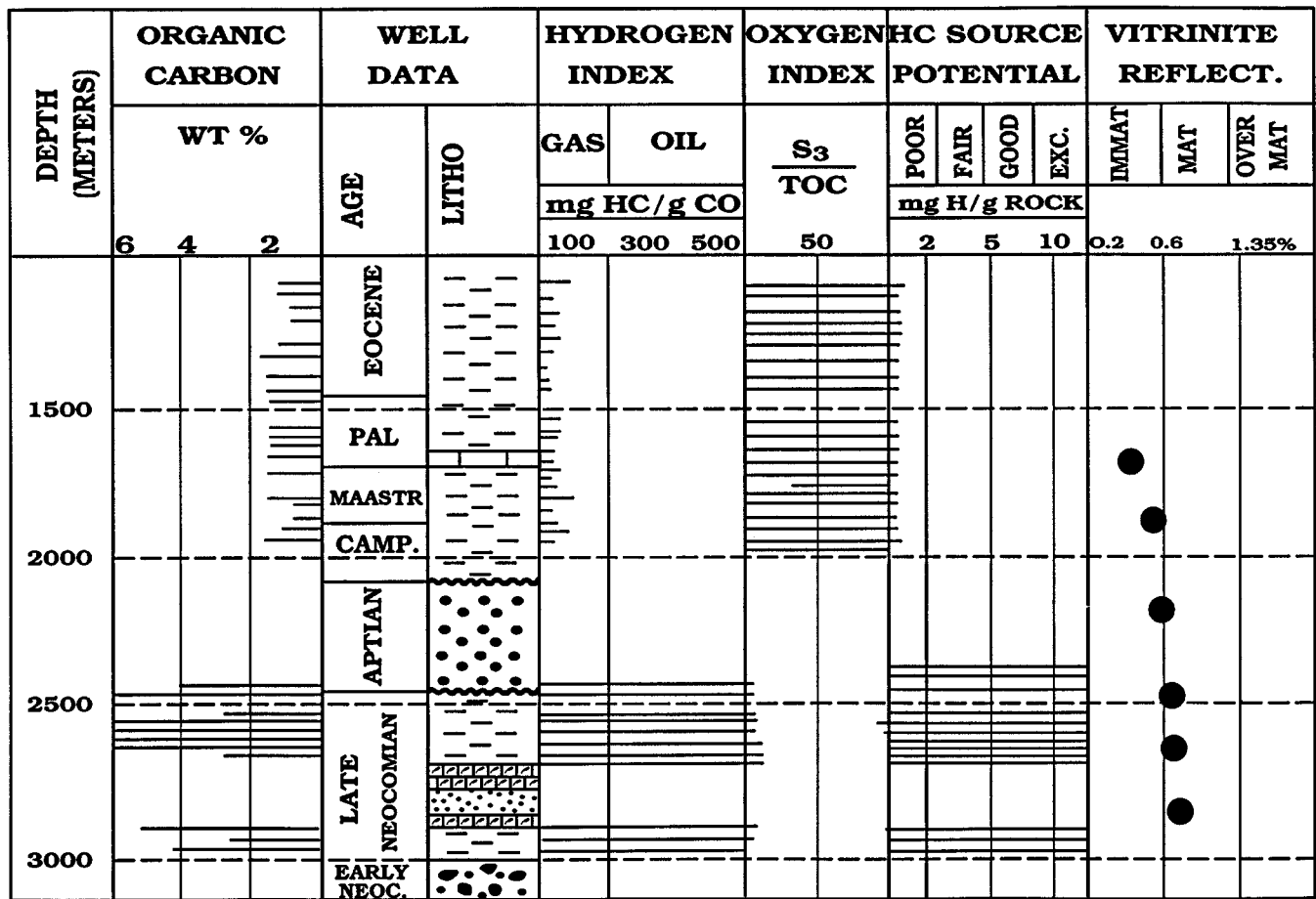


Figure 10. Example of a geochemical well log showing the stratigraphic position of lacustrine saline water organic-rich sediments deposited during the late Neocomian.

concentrations (scavenging by alkaline elements) associated with anoxic conditions in the bottom waters enhance the degree of organic matter preservation resulting in the deposition of well-laminated, organic-rich calcareous black shales (e.g., Dean and Fouch, 1983; Kelts, 1988; de Deckker, 1988; Castle, 1990).

Organic-rich rocks and oils derived from this environment are confined to the Sergipe-Alagoas, Espirito Santo, and Campos basins in the northern and southern areas of the continental margin (Figures 5 and 6). Generally, the rocks are composed of thick beds of calcareous ($CaCO_3$ up to 48%) black shales (TOC up to 9%; e.g., Figure 10), with relatively low sulfur content (<0.5%). The hydrogen index (up to 970 mg HC/g organic carbon; Figure 10) and organic petrology data identify the organic matter as predominantly type I kerogen, consisting of amorphous material (lipid-rich algal and bacterially derived). The good hydrocarbon source potential, combined with deep burial, influenced the generation of oils characterized by high API gravities (around 30°), low content of sulfur (around 0.3%), and significant quantities of alkanes (up to 70%; Figure 11). The geochemical and biological marker data from oils and organic-rich sediments show features diagnostic of nonmarine environments (cf. Moldowan et al., 1985; Powell, 1986; McKirdy et al., 1986; Philp

and Gilbert, 1986; Wang Tieguan et al., 1988; Mello et al., 1988a, b; Mello and Maxwell, 1990; Burwood et al., 1993), but differ from the lacustrine freshwater samples with respect to elemental, bulk, and biological marker features. These appear to be related to the enhanced salinity. For example, the samples show heavier $\delta^{13}C$ values for whole oil and rock extract, presence of β -carotane, and higher concentrations of tricyclic terpanes, 28, 30-bisnorhopane, 4-methyl steranes, and low molecular weight regular steranes (peaks 1–5; Table 1, Figure 11, and Appendices I and II). The most important geochemical features of the samples from this depositional environment are shown in Table 1 (cf. Figure 11 and Appendices I and II).

The fossil biota, characterized by the presence of nonmarine organisms such as ostracods with thicker and coarsely reticulated shells, secreted in extremely saturate waters, are an indication of a shallow, saline alkaline environment (Castro and de Azambuja Filho, 1980; Castro et al., 1981; Bertani and Carozzi, 1985; de Deckker, 1988). Noteworthy, and also diagnostic of the shallow, saline, and alkaline character, is the mineralogical assemblage found; for example, the widespread occurrence of gypsum and anhydrite molds, the distribution of diagenetic minerals syndepositionally formed as trioctahedral smectites, dolomite, zeo-

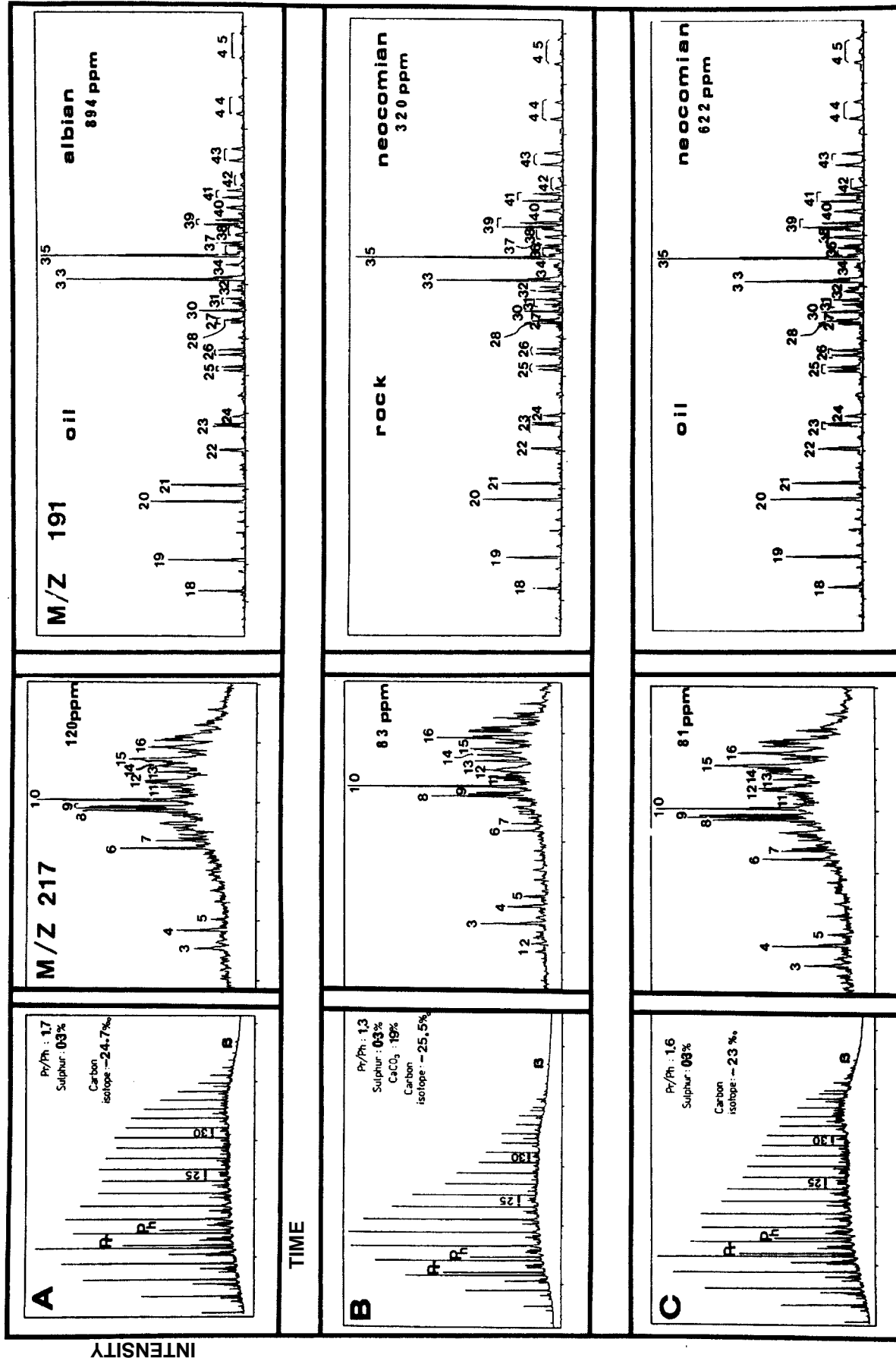


Figure 11. Oil-source rock correlation using gas chromatograms of total alkanes bulk and elemental parameters, and partial m/z 217 and m/z 191 chromatograms, and absolute concentration of C₂₇ααα+R-steranes and C₃₀ αβ-hopane for typical lacustrine saline water source rocks (B) versus two related oils from (A and C) the Brazilian marginal basins (for peak assignments and quantification procedures see Appendices I and II).

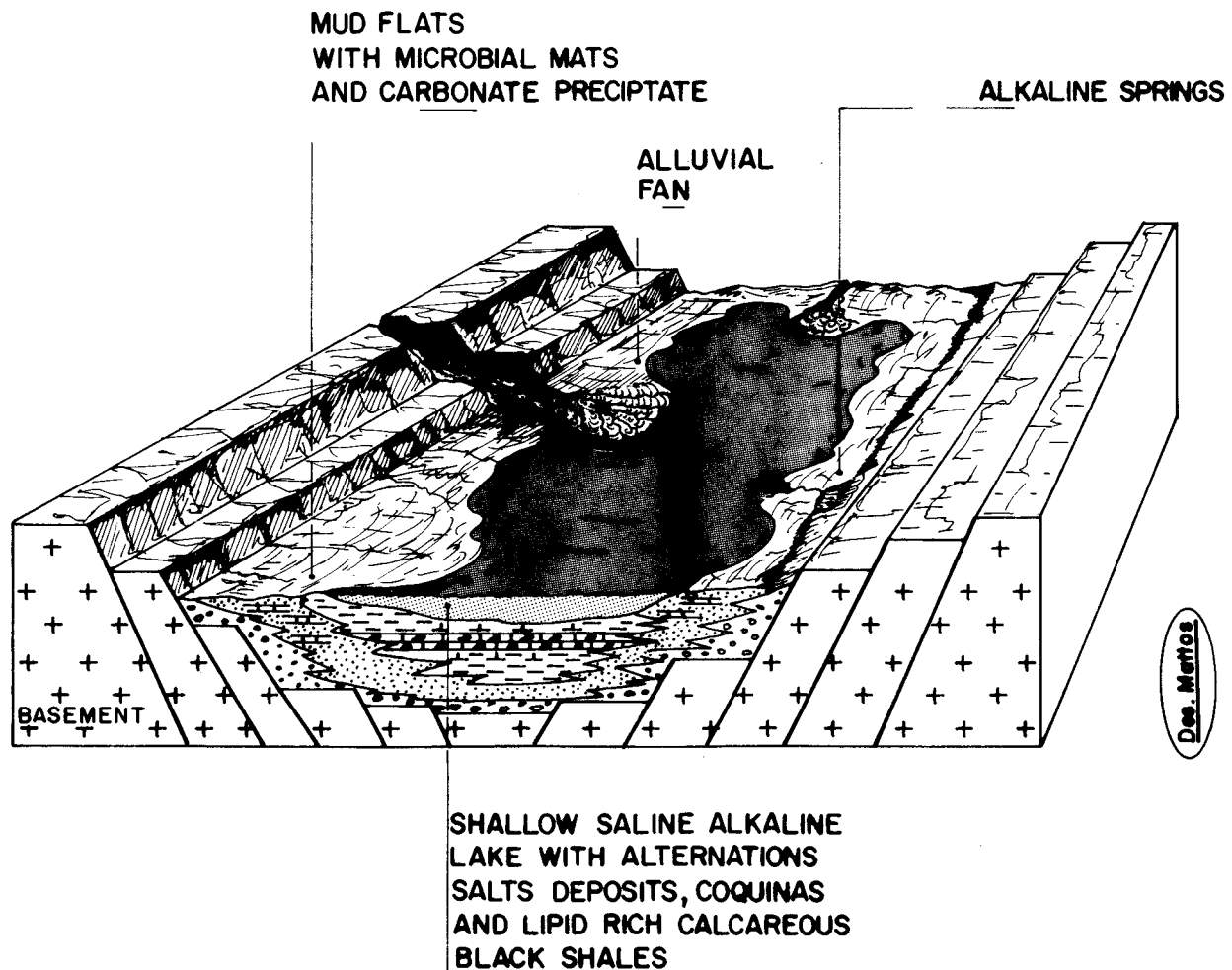


Figure 12. Schematic block diagram showing the sedimentary facies in a shallow saline to hypersaline lake with alkaline affinities from the rift stage in the Brazilian marginal basins (modified from Eugster, 1986).

lites of the heulandite-clinoptilolite type, and some authigenic minerals such as stevensite/talc/sepiolite (Bertani and Carozzi, 1985). Stable isotopic composition (carbonate of the fossils showing both $\delta^{13}\text{C}$ and $\delta^{18}\text{O}$ values between 1.0‰ and -1.0‰) also suggests saline conditions (Takaki and Rodrigues, 1984).

The block diagram in Figure 12 is an illustration of the main sedimentological facies of the shallow, saline lake system of alkaline affinities that appears to have dominated the Upper Neocomian in the rift stage of the Brazilian marginal basins. As observed for the freshwater basins, the thickest and most organic-rich deposits appear to be associated with the deeper parts of these lakes. It is noteworthy, however, that in this case the depocenter of the basin does not appear to correspond to the deep part of the lake where the organic-rich sediments were deposited.

Few analogous examples of ancient, shallow, saline lake systems of alkaline affinities have been reported. The best comparisons to the Brazilian examples appear to be the well-studied Eocene Green River Formation in Uinta Basin, USA (Tissot et al., 1978; Demaison and Moore, 1980; Dean and Fouch, 1983; Castle, 1990), the

Chaidamu and Jiangnan basins, China (Chen Changming et al., 1984; Powell, 1986; Fu Jia Mo et al., 1986), and the Officer basin in Australia (McKirby et al., 1984). Modern examples appear to be lakes Nakuru, Magady, and Bogoria in the East African rift system (Eugster, 1986; Vincens et al., 1986).

Drift Stage

The drift stage can be subdivided into two distinct phases:

1. A gulf proto-oceanic evaporitic phase (Figure 3B), normally associated with restricted marine conditions, and ideal for deposition of evaporitic sediments.
2. An oceanic phase characterized mainly by platform and slope carbonate sediments deposited in a neritic to upper bathyal environment (Figure 3C) and marine shelf-slope system (Figure 3D, E), composed of predominantly siliciclastic and calcareous mudstones deposited in neritic to bathyal conditions.

Gulf Proto-Oceanic Evaporitic Phase

The gulf proto-oceanic phase can be considered a transition between the rift continental stage and the marine phase in the Brazilian marginal basins.

With the onset of sea-floor spreading during the Aptian, evidence suggests that the topographic volcanic barrier of the São Paulo Plateau–Walvis Ridge complex was passed over (Asmus, 1975; Taylor et al., 1985; Figure 3B). As a result, intermittent transgressions from the South Atlantic invaded the lacustrine coastal basins. These marine incursions, which according to biomarkers started in the early Neocomian, were periodically cut off. Tectonic quiescence, isolation by topographical barriers, and an arid and hot climate led to a low clastic influx and restricted conditions appropriate for high evaporation, with subsequent cyclic deposition of hypersaline (halite, anhydrite, dolomite) and mixed carbonate and siliciclastic sediments in coastal, shallow continental to marine environments (Asmus, 1975; see below). Typically, deposition appears to have been as a series of narrow, shallow, and elongated embayments or lagoons, isolated from the open sea by a restricted passage (cf. Figure 3B). They were formed along the eastern margin from the Santos basin in the southeast and progressed northward via Sergipe-Alagoas basin toward the Potiguar and Ceará basins in the equatorial margin (Figures 1 and 3B). Generally, in conditions of extreme restriction, a rise in salinity was sufficient to extinguish the fauna and to allow precipitation of higher evaporites (gypsum, anhydrite, halite, etc.) which seldom contain any organic-rich material. Conversely, during periods of marine transgressions, less hypersaline conditions were established. These marine incursions resulted in an increase in basinal area and less arid conditions. This was favorable for the deposition of organic-rich, calcareous black shales and marls. The occurrence of such organic-rich sediments was due to the extensive supply of nutrients provided to a select number of species, producing a high input of algal and bacterial organic matter to the lagoons (cf. Kirkland and Evans, 1980). Furthermore, the high density of hypersaline waters resulted in water column stability, increasing the potential for stratification and permanent bottom water anoxia. Such environmental conditions, lethal for macrolife forms and benthic organisms, dramatically enhance the preservation of organic matter (e.g., Demaison and Moore, 1980; Kirkland and Evans, 1980; Taylor et al., 1985; Katz et al., 1987).

Organic-rich rocks (Aptian) and oils derived from this sequence occur mainly in the Ceará, Potiguar, and Sergipe/Alagoas basins, localized along the central and eastern areas of the margin (Figures 5 and 6).

The rocks are characterized by a set of paleontological, mineralogical, and particularly geochemical and biological marker data indicating a marine hypersaline depositional environment (e.g., Della Favera et al., 1984; Ojeda, 1982; Mello et al., 1988, 1993). Usually, the calcareous black shales and marls associated with the evaporites contain few invertebrate marine fossils. Two possible explanations are discussed below.

1. The salinity was so high that no normal marine fauna (dinoflagellates, calcareous nannoplankton and foraminifera) could flourish.

2. The marine waters which invaded the rift system from the south did not contain such fauna in abundance. Indeed, paleontological and geochemical evidence suggests that during the Aptian (when hypersaline and anoxic conditions also existed in the southern Atlantic) nannoplankton were few, benthic organisms occurred sporadically, and planktonic foraminifera were extremely rare or absent (e.g., Magniez-Janin and Jacquin, 1986). Whatever the explanation, the marine origin of this succession is supported by paleontological (rare occurrences of dinoflagellates and foraminifers in some areas), mineralogical (e.g., presence of massive halite), and biological marker evidence (presence of C_{30} steranes and dinosteranes, considered to be diagnostic features of marine organic matter; cf. Moldovan et al., 1985; Summons et al., 1987; Goodwin et al., 1988; see below). Also, the general geological features of the Brazilian examples correlate well with classical, well-described marine hypersaline examples (Kendall, 1978; Friedman, 1980; Taylor et al., 1985).

The rocks of this sequence are mainly composed of organic-rich (TOC up to 14%; e.g., Figure 13) calcareous black shales and marls ($CaCO_3$ up to 45%), generally rich in sulfur (0.5 to 2.5%). Pyrolysis Rock-Eval data and organic petrology indicate a predominance of type II kerogen (hydrogen index up to 750 mg of HC/g organic carbon; e.g., Figure 13), composed of a mixture of amorphous organic matter (45–60%) with herbaceous (15–25%) and woody plus coaly material (10–25%). Unexpected in such an environment is the significant input of higher plant debris. One possible explanation is the extreme salinity. In such conditions, the suspended organic matter would tend to float in the water column due to the high water density. This would retard its settling rate and prolong its exposure to anaerobic bacteria, which could use the high amounts of sulfates, nitrates, and phosphates to oxidize labile phytoplankton remains, thus causing a relative increase in the more resistant, herbaceous, woody, and coaly organic matter (cf. Katz et al., 1987).

The block diagram in Figure 14 shows a schematic illustration of the paleoenvironment of deposition that is thought to have dominated the Brazilian margin, from the Bahia Sul to the Ceará basins, during the Neocomian and Aptian. This model assumes that intermittent incursions of sea water account for the filling of pre-existing, deep topographic depressions (rift basins) with marine evaporitic (e.g., halite, anhydrite, and dolomite) and mixed carbonate and siliciclastic sediments accumulating in shallow-water environments (broad embayments or lagoons). The most organic-rich and thickest deposits appear to be associated with sea level rise and occurred in the deeper parts of these shallow lagoons. Several examples of analogous ancient environments have been reported. Appropriate ones appear to be represented by the lower Cretaceous sediments from Gabon; the Pliocene–Pleistocene sediments of the Dead Sea; the Pleistocene sediments of the

| DEPTH (METERS) | ORGANIC CARBON | | | WELL DATA | | HYDROGEN INDEX | | | OXYGEN INDEX | | | | VITRINITE REFLECT. | | | |
|-------------------|----------------|---|---|-----------------|-------|----------------|-------------|-------------|-------------------|------|------|------|--------------------|-------|-----|----------|
| | WT % | | | CRONO | LITHO | GAS | OIL | | $\frac{S_g}{TOC}$ | POOR | FAIR | GOOD | EXC. | IMMAT | MAT | OVER MAT |
| | 6 | 4 | 2 | | | | mg HC/g TOC | mg HC/g TOC | | | | | | | | |
| | | | | 100 | 300 | 500 | 50 | 2 | 5 | 10 | 0.2 | 0.6 | 1.35% | | | |
| 2000 | | | | TERTIARY | | | | | | | | | | ● | | |
| | | | | LATE CRETACEOUS | | | | | | | | | | ● | | |
| 2500 | | | | APTIAN | | | | | | | | | | ● | | |
| 3000 | | | | EARLY NEOCOMIAN | | | | | | | | | | ● | | |

Figure 13. Example of a geochemical well log showing the stratigraphic position of marine evaporitic organic-rich sediments deposited during the Aptian.

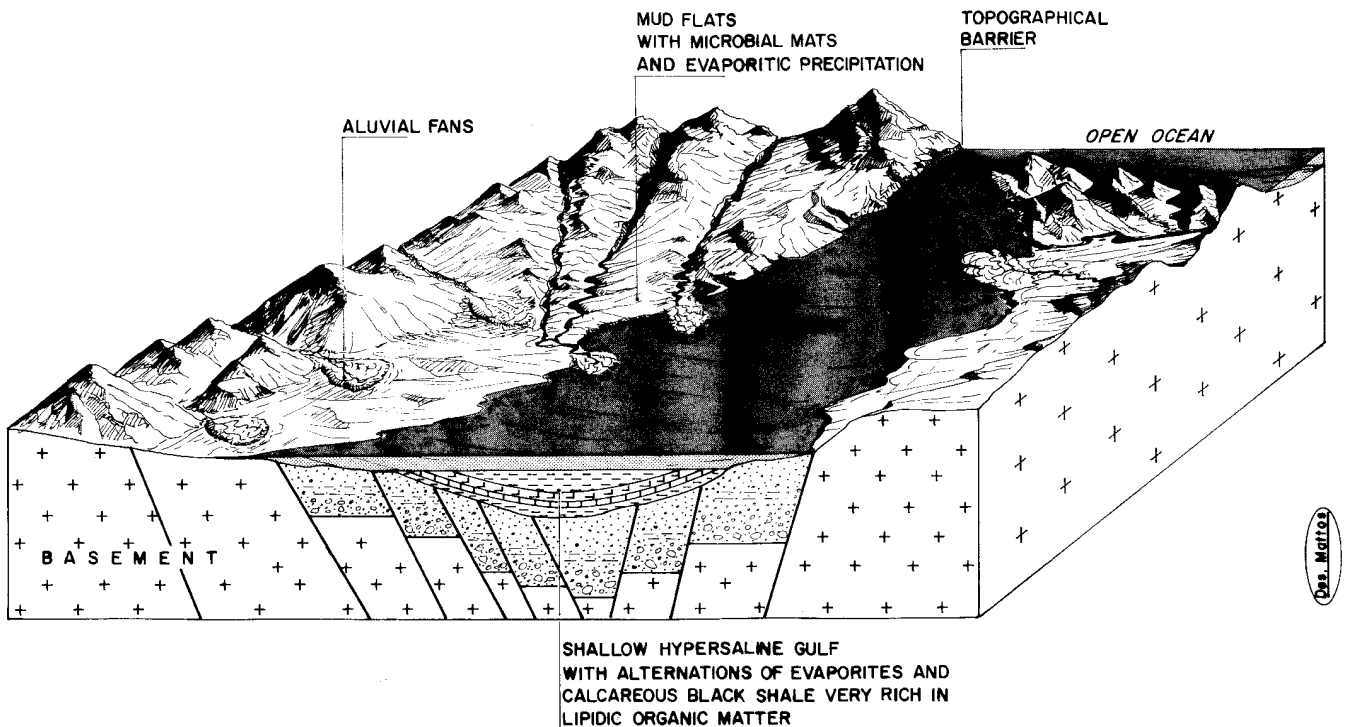


Figure 14. Schematic block diagram showing the sedimentary facies in a marine evaporitic environment from the Brazilian marginal basins.

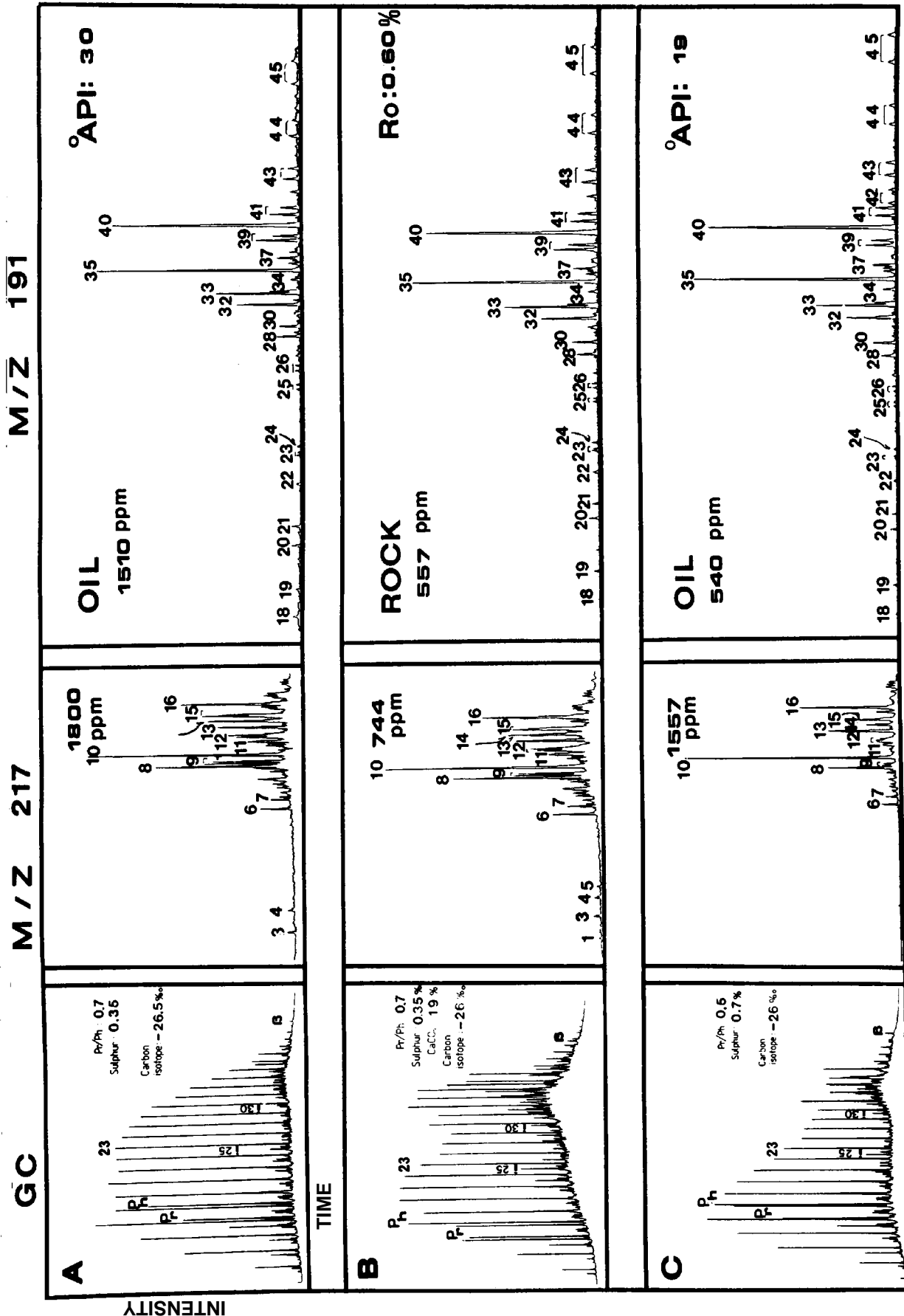


Figure 15. Oil-source correlation using gas chromatograms of total alkanes, bulk and elemental parameters, and partial m/z 217 and m/z 191 chromatograms, and absolute concentrations of C₂₇ααα, 20S+R-steranes and C₃₀ αβ-hopane for a typical marine evaporitic source rock (B) versus related oils (A and C) (see Appendices I and II).

Danakil Basin, Ethiopia (Taylor et al., 1985); the Tyro (eastern Mediterranean) and Messinian basins (northern Apennines), Italy (ten Haven, 1986; ten Haven et al., 1989); Prinos basin, Greece (e.g., Moldowan et al., 1985); Tarragona basin, Spain (Albaiges et al., 1986); Marl Slate member of the Zechstein, England (Gibbons, 1978), El Lajjun, Jordan (Abed and Bilal, 1983), and Mulhouse basin, France (Hofmann and Leythaeuser, 1993).

There are no large marine evaporite basins in existence today, although there are examples of small ones, such as the Red Sea (Friedman, 1980) and Shark Bay in Western Australia (Dunlop and Jefferies, 1985).

The oils and organic-rich rocks from this type of environment are characterized by a set of bulk, elemental, and biological marker features that in some respects give the most straightforward classification. This presumably arises from the idea that the organisms in such an environment would be expected to be largely restricted to a relatively few salinity-tolerant aquatic species. Clearly, the effects on the resulting biological marker distributions might be expected to be dramatic, leading to the occurrence of high concentrations and dominance of specific compounds, for example, those derived from precursors biosynthesized by microorganisms such as archaeobacteria (including halophiles), certain green algae, cyanobac-

teria, and sulfur-bacteria (Boon et al., 1983; Goossens et al., 1984; Connan et al., 1986; Mello, 1988).

The main diagnostic molecular features that characterize and distinguish the marine and high-salinity water of this environment are: phytane greater than pristane with even over odd *n*-alkane predominance, low hopane/sterane ratio (< 2.0), $Ts/Tm < 1$, C_{35}/C_{34} hopanes > 1 , presence of C_{30} steranes and dinosteranes, high concentrations of 28,30-bisnorhopane, β -carotane, gammacerane, regular C_{25} isoprenoid (*i*- C_{25} squalane), and (*i*- C_{30}). Other biological marker features of the samples from this type of environment are shown in Table 1 (cf. Figure 15 and Appendices I and II).

Oceanic Phase

As a result of sea-floor spreading and the progressive cooling and contraction of the underlying lithosphere, normal marine conditions developed within the marginal basins (Asmus, 1975; Ojeda, 1982). Differences in paleogeography and paleoenvironment allow subdivision of the oceanic phase into three distinct sequences:

1. Albian marine platform and slope carbonate sequence (Figure 3C) composed mainly of car-

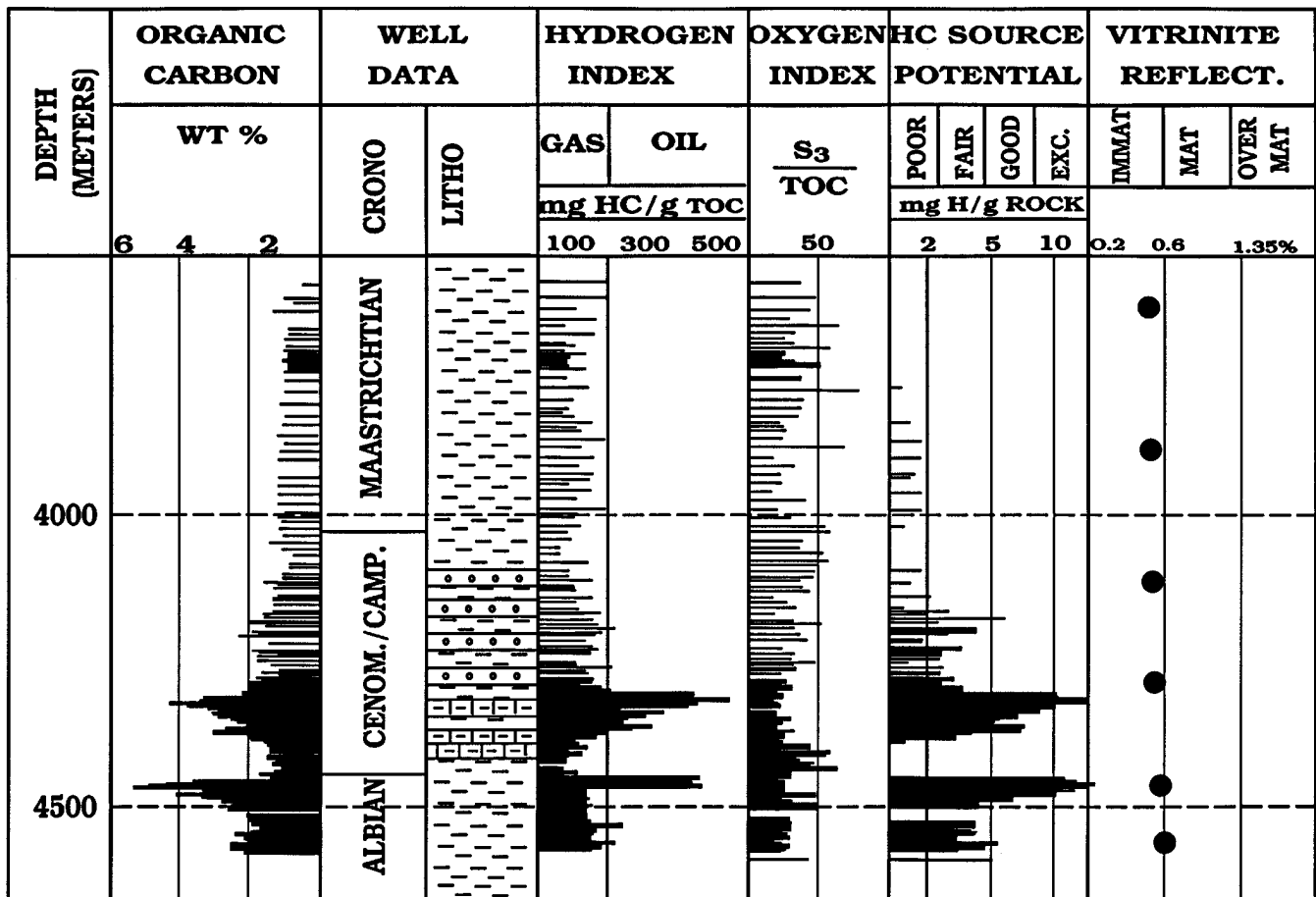


Figure 16. Example of a geochemical well log showing the stratigraphic position of marine carbonate organic-rich sediments deposited during the Albian.

- bonate sediments deposited in semirestricted neritic to upper bathyal environments.
2. Cenomanian to Campanian open marine shelf-slope sequence (Figure 3D), characterized mainly by late Cenomanian to Coniacian deposition of organic-rich calcareous mudstone and siliciclastic sediments, in middle/deep neritic and bathyal conditions (sequence of coastal onlap).
 3. Maastrichtian to Holocene open marine shelf-slope sequence (Figure 3E), characterized mainly by proximal siliciclastic facies and distal pelitic facies, and local deltaic deposits (progradational sequence of the continental margin).

Albian Marine Carbonate Sequence

As a consequence of increased sea-floor spreading and the dynamic equilibrium between subsidence and sedimentation within the continental margin, the proto-South Atlantic Ocean maintained an almost uniform paleogeographic setting during the Albian (e.g., Koutsoukos and Dias-Brito, 1987). At that time, in near-normal marine conditions (Figure 3C), fine to coarse carbonate sediments accumulated within neritic to upper bathyal environments (e.g., Koutsoukos and Dias-Brito, 1987).

Typically, the Albian ocean was a narrow and shallow semirestricted epicontinental sea, where a hot and tropical climate, semirestriction, poor circulation, and

progressively deepening conditions (in some areas to upper bathyal; cf. Koutsoukos et al., 1991a), led to deposition of organic-rich marls and calcareous mudstones (e.g., Figure 16). These rocks were deposited in hypersaline, anoxic conditions (e.g., Koutsoukos et al., 1991a, b) and mainly comprised of organic-rich (TOC up to 6%, Figure 16) gray marls (CaCO_3 up to 60%), generally possessing medium sulfur contents (0.3 to 0.7%). The Rock-Eval data and organic petrology indicate a predominance of type II kerogen (hydrogen index ranging from 200 to 720 mg HC/g organic carbon; e.g., Figure 16). The composition of organic matter is similar to marine evaporitic-derived samples, with a small increase in the woody plus coaly content (20–30%). As with the marine evaporitic environment, the occurrence of a secondary oxidation process is likely the cause for greater preservation of higher plant organic matter in this marine carbonate environment.

The organic-rich rocks of this group occur mainly in the Cassiporé, Pará-Maranhão, Sergipe/Alagoas and Bahia Sul basins (Figure 5). The oils are confined to the Pará-Maranhão, Cassiporé, and Bahia Sul basins (Figure 6). Such a distribution is not unexpected since the appropriate maturity conditions have only occurred in those basins of the continental margin (cf. Mello, 1988).

The block diagram in Figure 17 is an idealized illustration of the paleoenvironment of deposition proposed to have existed in the Brazilian margin during the Albian. This model assumes that during early mid-

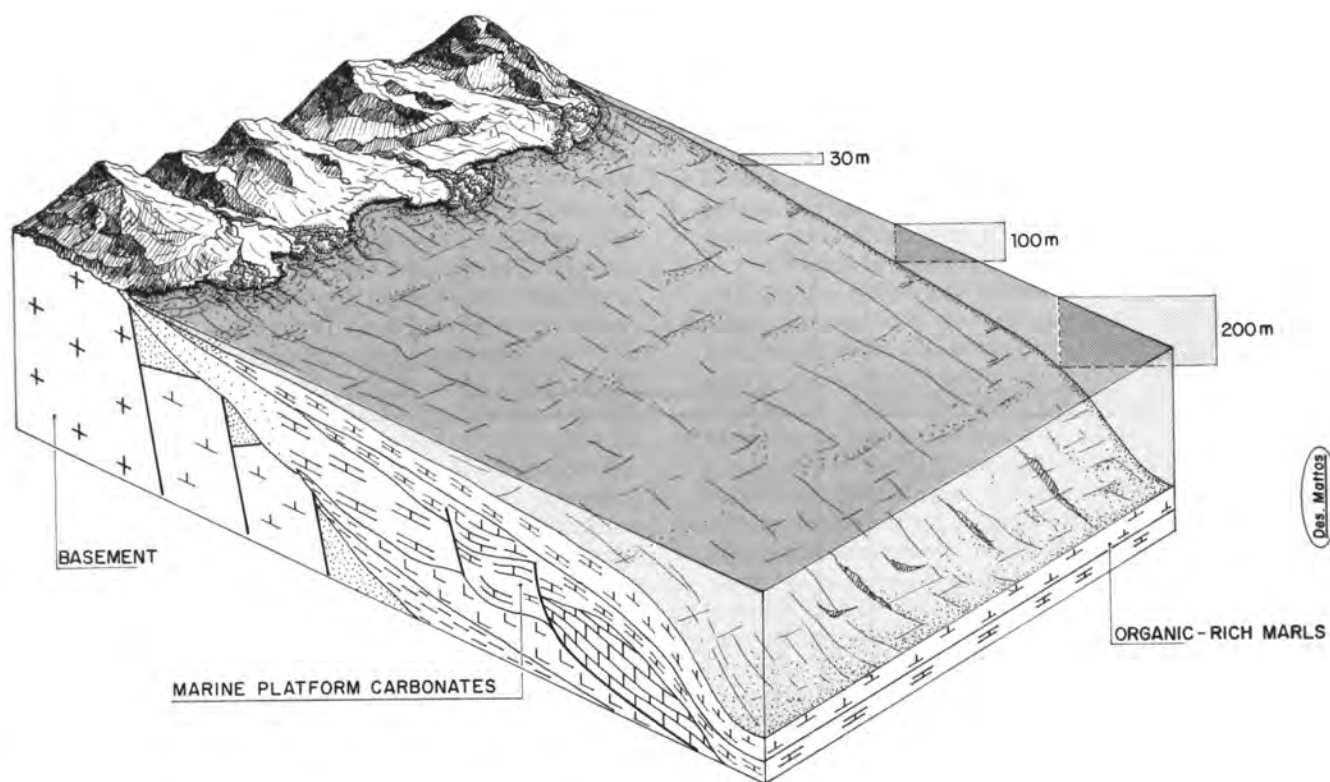


Figure 17. Schematic block diagram showing the sedimentary facies in a marine carbonate environment from the drift stage in the Brazilian marginal basins.

dle Albian time, extensive coarse carbonate deposits were primarily deposited in upper to middle neritic environments. In the late Albian, a change in oceanographic conditions, with consequent relative sea level rise, resulted in a change to a deep neritic/bathyal environment and allowed deposition of the pelitic organic-rich carbonate sediments (e.g., Mello et al., 1988a and 1988b; Koutsoukos et al., 1991).

Examples from ancient analogous environments appear to include Albian–Cenomanian marine carbonate sediments in the La Luna and Querencual formations, Venezuela (Cassani, 1986; Talukdar et al., 1986); Toolebuc Formation, Eromanga basin, Australia (Riley and Saxby, 1982); eastern Officer basin, Australia (McKirdy et al., 1984); Sunniland Formation, South Florida basin, USA (Palacas et al., 1984); and Serpiano Shale, middle Triassic Grenz bitumen zone, Switzerland (Gransch and Eisma, 1966; Rieber, 1982; Premovic et al., 1986). Recent examples are very few, but those worthy of mention are the continental margins of southwestern Puerto Rico and of Northern Belize (Rafalska-Bloch and Cunningham, 1986), and the Gulf of Aden, offshore.

Several features in the bulk, elemental, and biological marker data (Figure 18 and Table 1) are similar to those of the marine evaporitic samples. However, a distinction can be made between them. In the evaporitic samples, gammacerane, β -carotane, regular steranes, and hopanes occur in higher concentrations, while in the marine carbonate samples dinosteranes, C_{30} steranes, and tricyclic terpanes higher than C_{28} are present in higher concentrations (cf. Mello et al., 1988a and 1988b; De Grande et al., 1993). The most distinct biological marker features of samples from this type of environment are shown in Table 1 (cf. Figure 17, and Appendices I and II).

Cenomanian–Campanian Open Marine Sequence

The Cenomanian to Campanian is characterized mainly by an alternation of siliciclastic and calcareous mudstone deposition in progressively deepening basins. These basins developed bathyal conditions in distal areas. The Cenomanian succession is generally missing in some offshore areas (e.g., Koutsoukos, 1987).

During the late Cenomanian, Turonian, and locally the Santonian, the establishment of widespread anoxic conditions with deposition of organic-rich calcareous mudstones and black shales occurred in most of the marginal basins (Figure 3D; Mello et al., 1988b and 1989). Micropaleontological studies reveal a low diversity of benthic foraminifera, with a predominance of small-sized specimens in certain layers associated with a well-developed planktonic biota, such as foraminifera and radiolarians. Together with the geochemical data (see below) the micropaleontological data suggest that the organic-rich sediments were deposited in anoxic waters, perhaps in a deep neritic to middle bathyal environment (cf. Mello et al., 1989). The depositional model, based on the available data, assumes that an overall humid and warm equable climate, with periodic high sea level conditions, provided a significant increase in the supply of nutrients (e.g., marine transgressions

flooding coastal areas). Phytoplankton blooms in the upper layers, coupled with restricted circulation and perhaps enhanced salinity (Mello et al., 1989), led to the development of bottom waters markedly depleted in oxygen. In this context, both the degree of anoxia and the relative position of the anoxic water layer appear to have provided ideal conditions for the preservation of algal and bacterial material, since their exposure to aerobic conditions during their descent through the water column was minimized (cf. Schlanger and Jenkyns, 1976; Schlanger et al., 1987; Arthur et al., 1987). During times of increasing salinity (semiarid climate), deposition of predominantly calcareous mudstone occurred, containing organic matter with significant amounts of sulfur and siliceous material (cf. Mello et al., 1989). Conversely, times of improved circulation resulted in a salinity decrease, enhancing the potential for deposition of predominantly low sulfur siliciclastic sediments (black shales). Hence, these pelitic successions are made up of two distinct facies:

1. A light to dark-gray siliceous calcareous mudstone facies (11–40% $CaCO_3$), with high organic carbon contents and low to medium sulfur contents (up to 5% and 0.6% respectively; e.g., Figure 19, see marls). The pyrolysis Rock-Eval and organic petrology data (hydrogen index up to 500 mg HC/g organic carbon) indicate mainly type II kerogen, with the predominance (approx. 85%) of amorphous (algal and bacterially derived) organic matter over herbaceous and woody plus coaly material derived from higher plants.

2. A black shale facies (up to 15% $CaCO_3$) with medium to high organic carbon contents (up to 3%) and a slightly lower sulfur content (up to ~0.3%; Figure 19, see shales). The Rock-Eval and organic petrology data (hydrogen index up to 400 mg HC/g organic carbon) indicate mainly type II kerogen with a predominance (around 80%) of amorphous (algal and bacterially derived) organic matter. Organic-rich sediments from both environments are widespread on the continental margin (Figure 5). Generally, these sediments are immature in most of the Brazilian margin basins (except Santos and Espírito Santo basins), due to a combination of low geothermal gradients and shallow burial (e.g., Mello, 1988; Mello et al., 1988a, 1989). The oils of this group occur in Santos and Espírito Santo basins (Figure 6). Although the oils and mature organic extracts show characteristics diagnostic of open marine organic-rich sediments, they differ in elemental, bulk, and biological marker features compared to the immature ones (Figures 20 and 21). The differences are related to biomarkers that are degradable during the early stages of kerogen breakdown (just before the oil window). The most prominent biological marker features of this group are phytane usually greater than/equal to pristane, low hopane/sterane ratios (0.3 to 0.9), $Ts/Tm < 1$, C_{35}/C_{34} hopanes > 1 , high relative abundances and concentrations of 28,30-bisnorhopane and 25,28,30-trisnorhopane, predominance of C_{28} and C_{29} steranes relative to their C_{27} counterparts, and high concentration of tricyclic compounds up to C_{39} (Figures 20 and 21 and Table 1).

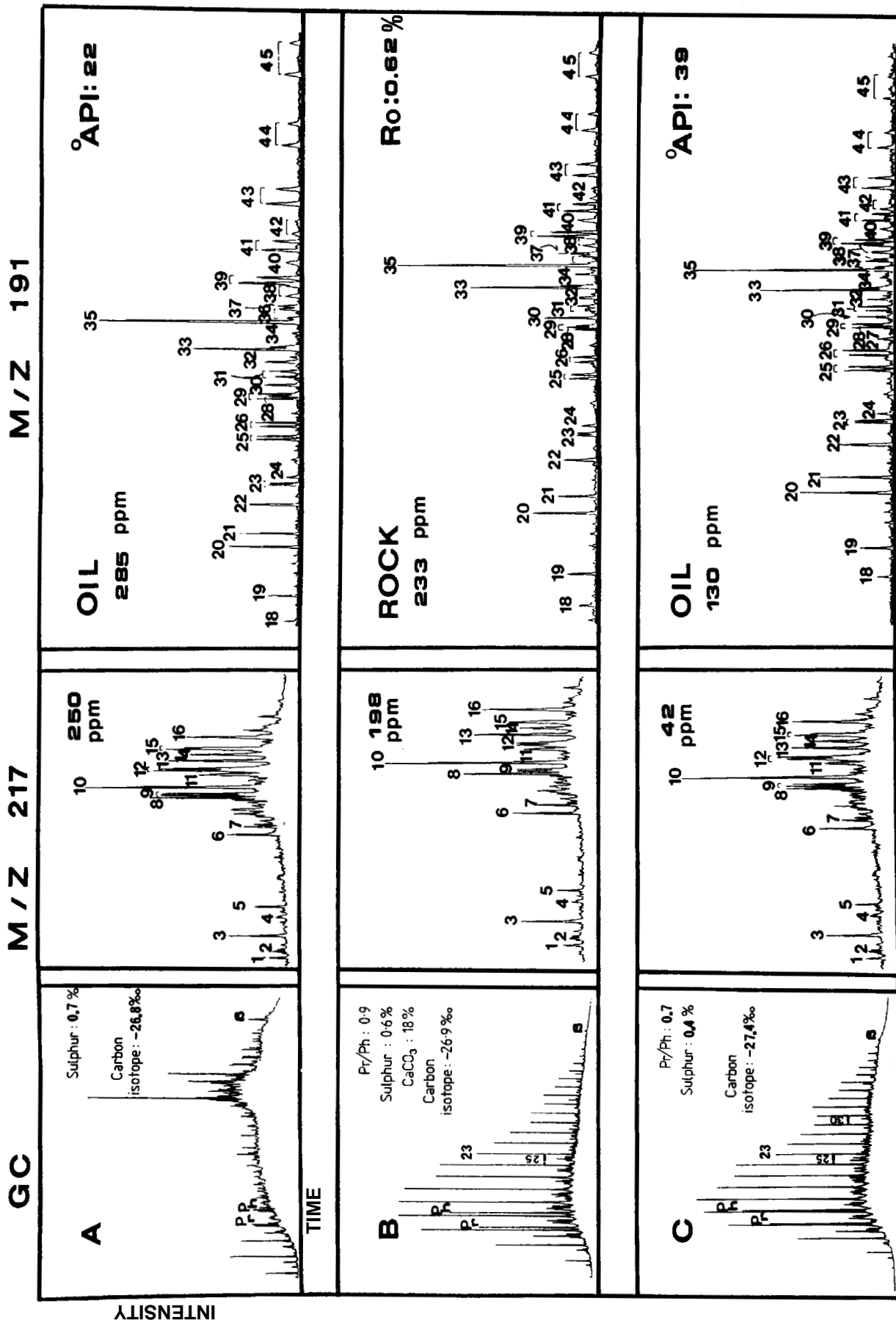


Figure 18. Oil-source rock correlation using gas chromatograms of total alkanes, bulk and elemental parameters, and partial m/z 217 and m/z 191 chromatograms, and absolute concentration of C₂₇ααα, 20S+R-steranes and C₃₀β-hopane for a typical mature carbonate source rock (B) versus related oils (A and C) from the Brazilian marginal basins (for peak assignments and quantification procedures see Appendices I and II).

Table 1. Bulk and geochemical data for Brazilian oils and sediments and their inferred depositional environment.

| | Lacustrine | | Lacustrine | | | | Marine | | | | |
|--|------------------|------------------|------------------|-----------------------------------|-----------------------------------|------------------|---------------------|--|--|--|--|
| | Fresh Water | Saline Water | Evaporitic | Carbonate | Deltaic | Calc. Lith. | Marine Silic. Lith. | | | | |
| °API (oils) | 30–39 | 24–32 | 20–30 | 25–30 | 42–44 | 34–40 | — | | | | |
| % Saturates (oils) | 60–73 | 45–65 | 30–59 | 20–60 | 60–70 | 50–80 | — | | | | |
| % Sulfur (oils) | <0.1 | 0.2–0.4 | 0.3–1.5 | 0.4–0.7 | 0.3–0.4 | 0.1–0.2 | — | | | | |
| V/Ni (oils) | <0.05 | 0.3–0.4 | 0.2–0.3 | 0.4–0.5 | 0.8–1.0 | — | — | | | | |
| % R _o (rocks) | 0.4–0.7 | 0.4–0.8 | 0.5–0.7 | 0.4–0.6 | 0.5–0.6 | 0.4–0.6 | 0.5–0.7 | | | | |
| % Saturates (rocks) | 40–60 | 25–55 | 25–40 | 20–45 | 27–30 | 22–34 | 25–44 | | | | |
| % Sulfur (rocks) | 0.2–0.3 | 0.1–0.5 | 0.3–2.5 | 0.2–0.6 | 0.6–0.7 | 0.4–0.5 | 0.3–0.7 | | | | |
| % CaCO ₃ (rocks) | <7 | 2–30 | 5–25 | 15–65 | 50–70 | 18–48 | 6–20 | | | | |
| δ ¹³ C (PDB‰; whole oil) | <–28 | –23;–27 | –25;–27 | –26;–28 | –24;–26 | –25;–27 | –26;–27 | | | | |
| <i>n</i> -alkane max. | ≈C ₂₃ | ≈C ₁₉ | ≈C ₁₈ | ≈C ₂₀ –C ₂₂ | ≈C ₂₀ –C ₂₂ | ≈C ₂₀ | ≈C ₁₇ | | | | |
| Odd/even | ≥1 | ≥1 | ≤1 | ≤1 | ≤1 | ≤1 | >1 | | | | |
| Pr/Ph | >1.3 | >1.1 | <1.0 | <1 | <1 | <1 | <1 | | | | |
| 1. i-C ₂₅ + i-C ₃₀ (ppm) | <170 | 70–700 | 300–1500 | 100–500 | 10–300 | 10–100 | 40–180 | | | | |
| 2. β-carotane (ppm) | ND | 10–200 | 100–400 | 20–60 | ND | 10–30 | ND | | | | |
| 3. C ₂₁ + C ₂₂ steranes (ppm) | Tr | 10–30 | 10–60 | 10–60 | 30–50 | 10–30 | 25–35 | | | | |
| 4. C ₂₇ steranes (ppm) | 10–50 | 50–150 | 500–4000 | 50–300 | 50–350 | 50–200 | 20–400 | | | | |
| 5. C ₂₇ + C ₂₉ steranes | 1.5–4.0 | 1.5–2.5 | 1.0–2.2 | 1.1–1.5 | 1.3–1.8 | 0.8–1.2 | 1.5–2.5 | | | | |
| 6. Diasterane index | 20–40 | 10–50 | 6–20 | 20–30 | 30–60 | 10–30 | 30–80 | | | | |
| 7. C ₃₀ steranes and dinosteranes (MS-MS) | ND | ND | Low | High | Medium | Medium | High | | | | |
| 8. 4-Me-sterane index | 30–50 | 30–150 | 30–80 | 30–80 | <10 | 20–60 | 10–20 | | | | |
| 9. Hopane/steranes | 5–30 | 5–30 | 0.4–2.0 | 0.9–3.0 | 0.5–3.0 | 0.5–5.0 | 1.5–8.0 | | | | |
| 10. Tricyclic index | 30–100 | 100–200 | 10–60 | 60–200 | 60–180 | 50–100 | 70–100 | | | | |
| 11. C ₃₄ /C ₃₅ αβ hopanes | >1 | >1 | <1 | ≤1 | <1 | ≤1 | >1 | | | | |
| 12. Bisnorhopane index | 0 | 3–15 | 15–40 | 10–30 | 0 | 20–1000 | 1–5 | | | | |
| 13. 18α(H)-oleanane index | 0 | 0 | 0 | 0 | 20–40 | 0 | 0 | | | | |
| 14. Ts/Tm | >1 | <1 | ≤1 | <1 | >1 | <1 | >1 | | | | |
| 15. C ₃₀ αβ hopanes (ppm) | 200–500 | 200–1600 | 300–2000 | 80–300 | 100–250 | 10–70 | 50–800 | | | | |
| 16. Gammacerane index | 20–40 | 20–70 | 70–120 | 10–20 | 0–5 | 0–25 | 1–5 | | | | |
| % amorphous | 55–65 | 85–90 | 45–60 | 50–60 | 60–70 | 60–70 | 85–95 | | | | |
| % herbaceous | 25–35 | 5–10 | 15–25 | 10–15 | 10–15 | 5–10 | 5–10 | | | | |
| % woody + coaly | 5–10 | 5–10 | 10–25 | 20–30 | 15–25 | 20–25 | 0–5 | | | | |

For ppm measurement, see Appendix II.
Abbreviations: Tr, trace; ND, not detected.

| DEPTH (METERS) | ORGANIC CARBON | | | WELL DATA | | HYDROGEN INDEX | | | OXYGEN INDEX | | HC SOURCE POTENTIAL | | | | VITRINITE REFLECT. | | |
|-------------------|----------------|-----|-----|---------------|-------|----------------|-------------|-----|----------------|-----|---------------------|------|------|------|--------------------|-----|----------|
| | WT % | | | CRONO | LITHO | GAS | OIL | | S ₃ | TOC | POOR | FAIR | GOOD | EXC. | IMMAT | MAT | OVER MAT |
| | 6 | 4 | 2 | | | | mg HC/g TOC | | | | | | | | | | |
| | 100 | 300 | 500 | 2 | 5 | 10 | 0.2 | 0.6 | 1.35% | | | | | | | | |
| 1700 | | | | | | | | | | | | | | | | | |
| 2000 | | | | TURON./SANTON | | | | | | | | | | ● | | | |
| 2500 | | | | ALBIAN | | | | | | | | | | ● | | | |
| 3000 | | | | APTIAN | | | | | | | | | | ● | | | |

Figure 19. Example of a geochemical well log showing the stratigraphic position of open marine anoxic organic-rich sediments with dominance of calcareous lithology deposited during the Cenomanian–Turonian.

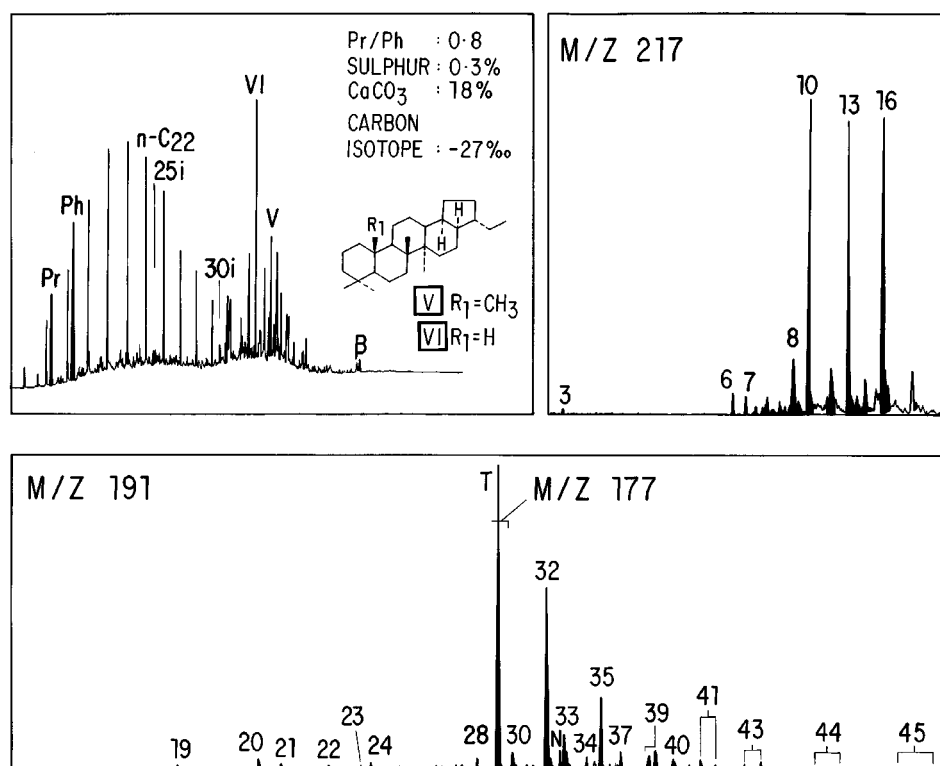


Figure 20. Gas chromatograms of total alkanes, bulk and elemental parameters, and partial m/z 191 and m/z 217 chromatograms, and absolute concentrations of C₂₇- α,α,α -20S+R-steranes and C₂₈-bisanthracene for a typical immature organic-rich sediment from the open marine highly anoxic depositional environment with predominance of calcareous mudstone lithology from the Brazilian marginal basins (for peak assignments and quantification procedures see Appendices I and II).

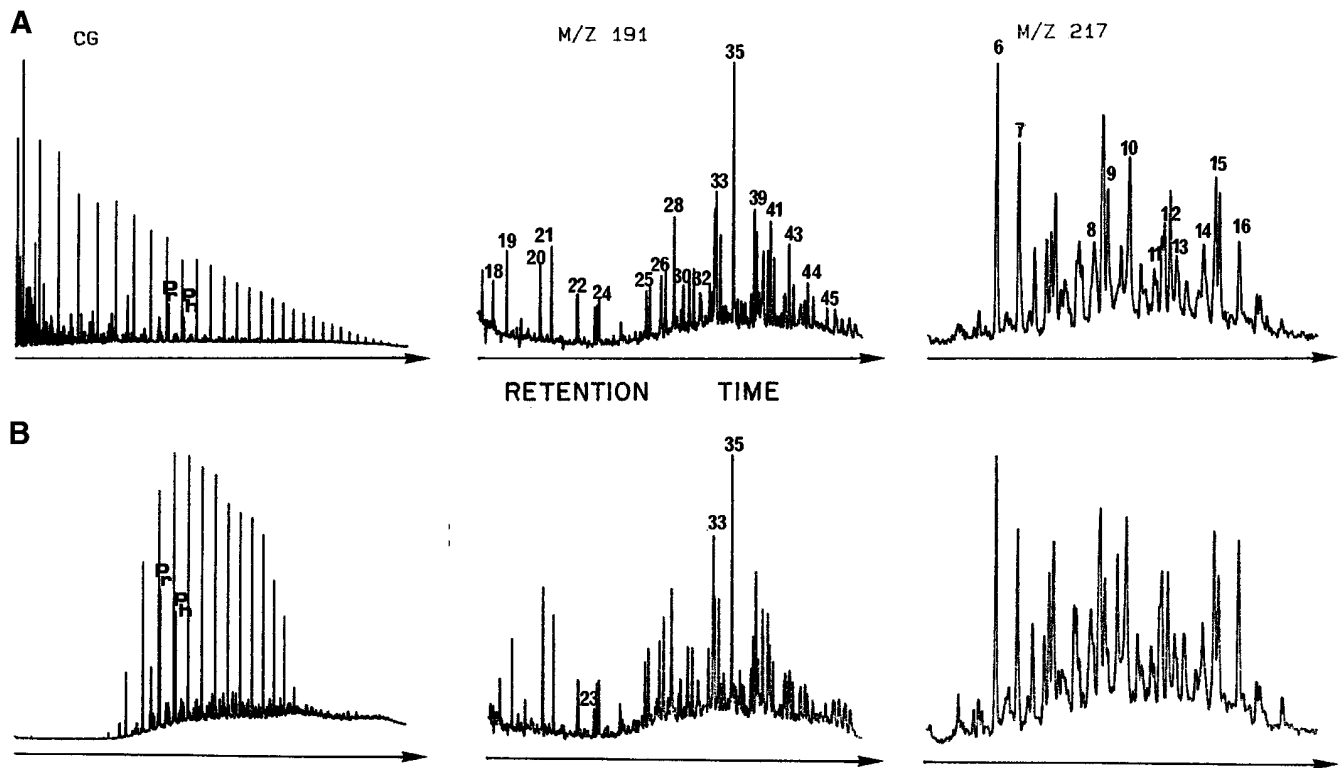


Figure 21. Gas chromatograms of total alkanes, and partial m/z 191 and m/z 217 chromatograms, for a typical organic-rich sediment and oil from the open marine anoxic depositional environment with predominance of carbonate lithology from the Santos basin (for peak assignments and quantification procedures see Appendices I and II).

Figures 22 and 23 show a proposed schematic reconstruction of the depositional paleoenvironments in the marginal basins during the late Cenomanian to Coniacian times. These models assume that most of the continental shelf and upper slope was invaded by an oxygen minimum zone, occasionally depressed in the deep waters and variable in intensity. This led to the deposition and preservation of organic-rich sediments in a deep neritic to upper bathyal, open marine, highly anoxic environment with alternation of calcareous mudstone and siliciclastic (black shale) lithology.

Descriptions of several analogous examples of ancient open marine highly anoxic environments with a dominance of calcareous lithology have been reported. Noteworthy of mention are the well-known Monterey Formation in California, USA (Katz and Elrod, 1983; Curiale et al., 1985); the late Cenomanian/Turonian sections of the La Luna and Querencual formations in Venezuela (Talukdar et al., 1986); the Nakalagu Formation, Benue Trough in Nigeria (Peters and Ekweozor, 1982a, b); the Cenomanian/Turonian sediments from the Danish Graben in the North Sea, and from Oued Bahloul in Tunisia and Monte Massenza in the Trento Plateau, Italy (Farrimond, 1987). Likewise, open marine anoxic environments with a dominance of siliciclastic lithology are represented by the Toarcian Shales, Paris Basin, and Southern Alps (Tissot et al., 1971; Mackenzie, 1980; Farrimond, 1987); Liassic and the Kimmeridge

Shale, North Sea (Mackenzie et al., 1984; Farrimond, 1987); and lower Liassic shales of southwestern Germany (Moldowan et al., 1986).

It is difficult to think of modern analogs of such depositional environments; however, reasonable suggestions could be offshore Peru and the southwest African Shelf for the marine anoxic with a dominance of calcareous/siliceous lithology, and the Black Sea and the Indian Ocean for the marine anoxic with a dominance of siliciclastic lithology (e.g., Demaison and Moore, 1980).

Maastrichtian to Holocene Open Marine Shelf-Slope Sequence

In general, the Maastrichtian to Holocene sequence in the Brazilian margin is characterized by deposition of a proximal coarse siliciclastic and distal facies with pelitic and turbiditic deposits in neritic to bathyal environments (e.g., Koutsoukos, 1987; Mello et al., 1989). Geochemical and micropaleontological evidence suggests that in the case of the Late Cretaceous South Atlantic, normal marine conditions with warm tropical waters and well-oxygenated conditions prevailed in the entire water column. This is emphasized by the deposition of organic-poor mixed clastic and carbonate sediments in most of the basins from the Campanian onward (e.g., Mello et al., 1989).

Rocks from this sequence in all the basins have been examined. Generally, they contain low to moderate

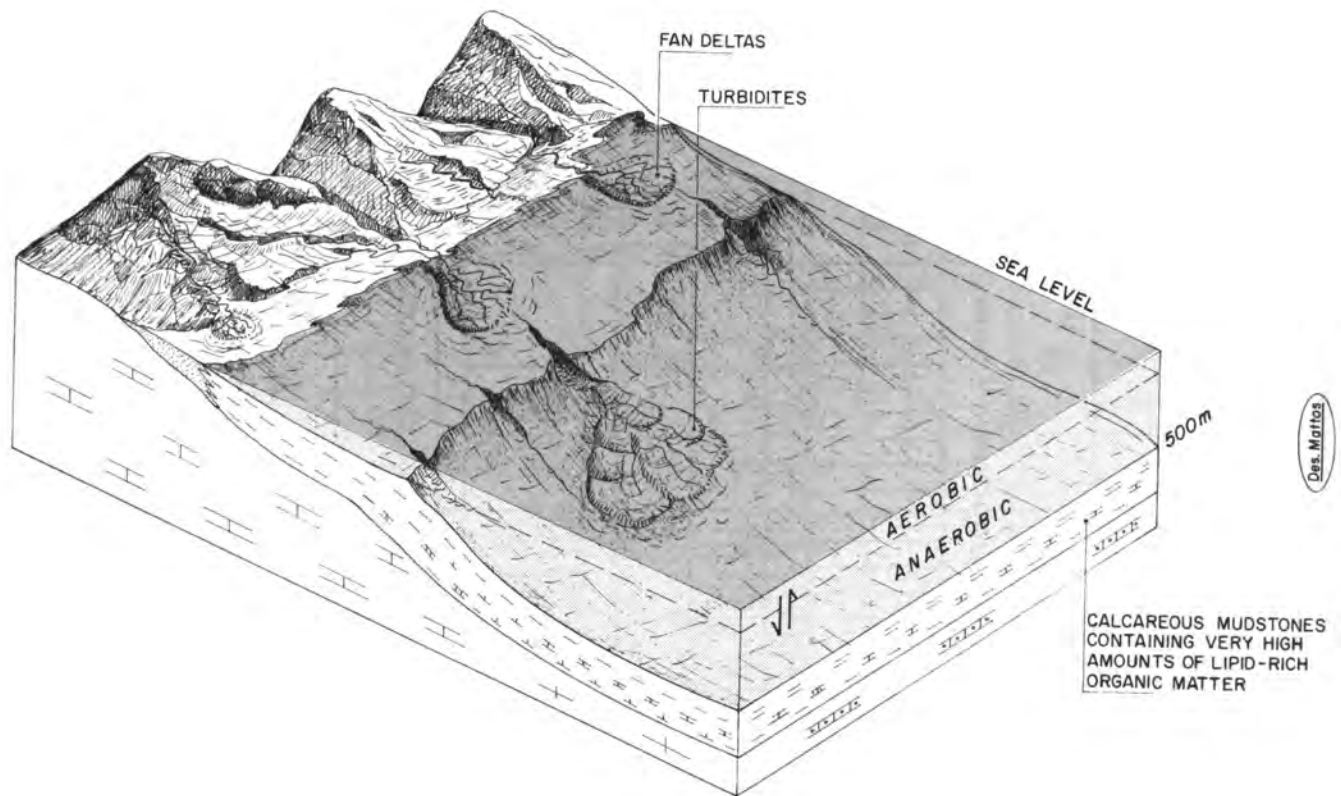


Figure 22. Schematic block diagram showing the sedimentary facies in an open marine, highly anoxic environment with dominance of calcareous mudstone lithology from the drift stage in the Brazilian marginal basins.

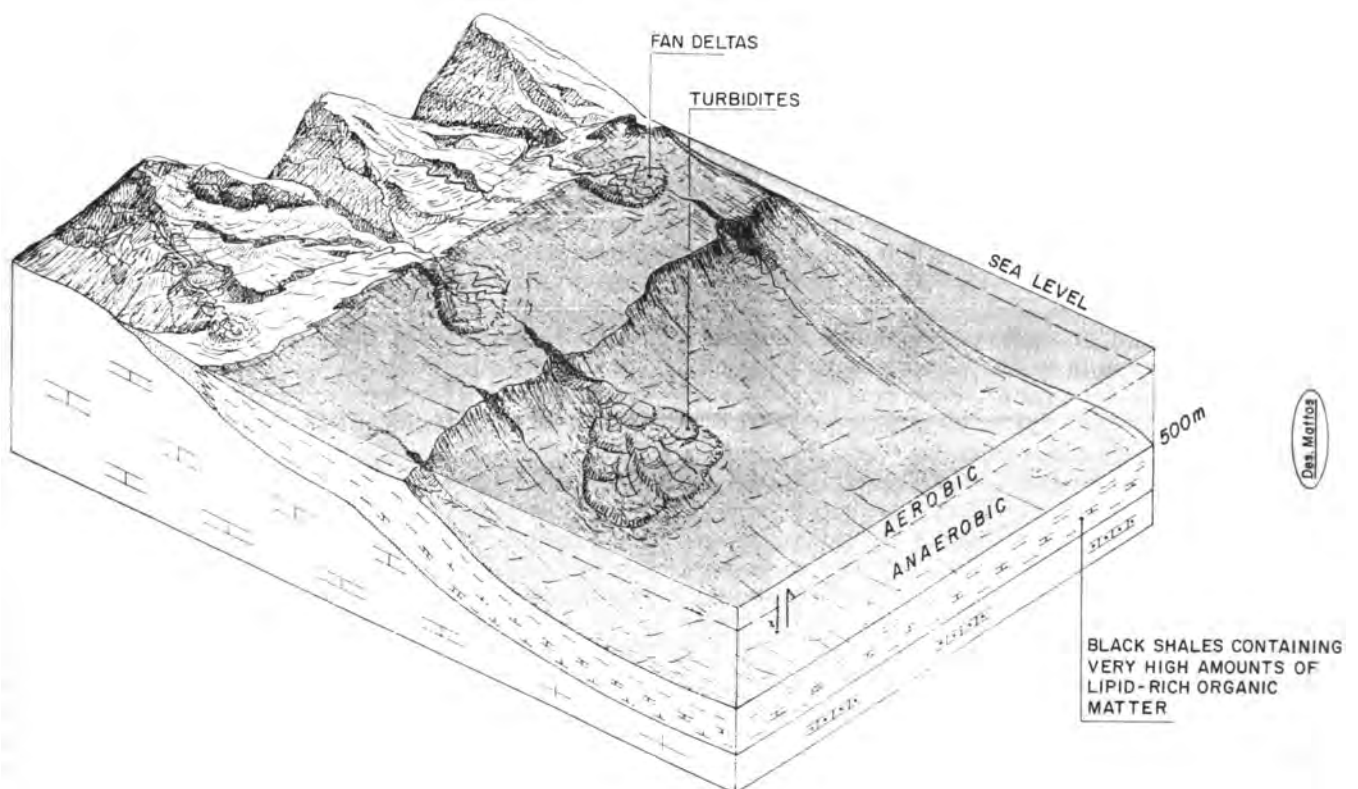


Figure 23. Schematic block diagram showing the sedimentary facies in an open marine, anoxic environment with dominance of siliciclastic lithology from the drift stage in the Brazilian marginal basins.

| DEPTH (METERS) | ORGANIC CARBON | | WELL DATA | | HYDROGEN INDEX | | | OXYGEN INDEX | | HC SOURCE POTENTIAL | | | | VITRINITE REFLECT. | | |
|-------------------|----------------|---|-----------|-------|----------------|-----|-----|-----------------------|------|---------------------|------|------|-------|--------------------|-------------|-----|
| | WT % | | AGE | LITHO | GAS | OIL | | S ₃ TOC | POOR | FAIR | GOOD | EXC. | IMMAT | MAT | OVER MAT | |
| | 4 | 2 | | | | 100 | 300 | | | | | | | | | 500 |
| | mg HC/g TOC | | | | mg H/g ROCK | | | | | | | | | | | |
| 4000 | | | MIOC. | | | | | | | | | | | | | |
| | | | OLIGOCENE | | | | | | | | | | | | | |
| 4500 | | | Eocene | | | | | | | | | | | | | |

Figure 24. Example of a geochemical well log showing the stratigraphic position of marine deltaic with carbonate influence, organic-rich sediments deposited during the Eocene–Oligocene.

organic carbon contents (up to 1%; e.g., Figure 24 except for some samples of the Eocene–Oligocene sections). Their potential to generate hydrocarbons is poor (type III kerogen; e.g., Figure 24). The prevalence of oxic conditions is supported by high oxygen indices and the presence of normal and abundant benthic foraminifera (e.g., Estrella et al., 1984; Mello et al., 1984, 1989). Exceptions to these oxic depositional conditions are marine deltaic environments associated with major river systems. Generally, the primary biological productivity offshore from deltas tends to be high, since there is a substantial nutrient influx from the rivers. The input of terrestrial organic matter is also high. This causes an impoverishment of oxygen in the oxic bottom waters from normal marine conditions due to the oxygen consumption from degradation of organic matter. Furthermore, the high sedimentation rates which characterize this type of environment play an important role, since they enhance the preservation of the organic matter at the sediment-water interface. Such features result in the deposition of marine sediments generally with an abundance of hydrogen-rich derived organic matter (e.g., Demaison and Moore, 1980). This appears to have been the case for the organic-rich sediments deposited during the Eocene–Oligocene, in the northern area of the continental margin (Mello et al., 1988a; see below).

The organic-rich rocks and related oils from this depositional environment are confined to the northern area of the Brazilian continental margin (Figures 5 and 6). The geological and biological marker data contain features consistent with the establishment of a deltaic environment with carbonate influence. The sediments are mainly organic-rich (TOC up to 5%; Figure 24) gray marls (CaCO₃ up to 70%), generally possessing medium sulfur contents (up to 0.4%). Rock-Eval data and organic petrology indicate a predominance of type II/III kerogen (hydrogen index up to 350 mg HC/g organic carbon; e.g., Figure 24), made up mainly of amorphous organic matter (up to 85%). The good hydrocarbon source potential of the sediments (S₂ up to 26 kg HC/ton of rock; e.g., Figure 24), combined with the thermal maturity level, produced low-density waxy oils (around 40° API), with significant quantities of alkanes (up to 70%). As can be observed in Figure 25, the samples from this depositional environment can be differentiated using the presence of biological markers thought to be specific for higher plant contributions, along with features thought to be diagnostic of a marine carbonate environment. The most marked features are: dominance of high molecular weight *n*-alkanes (C₂₂–C₂₄), phytane dominant over pristane, linked with even/odd *n*-alkane preference,

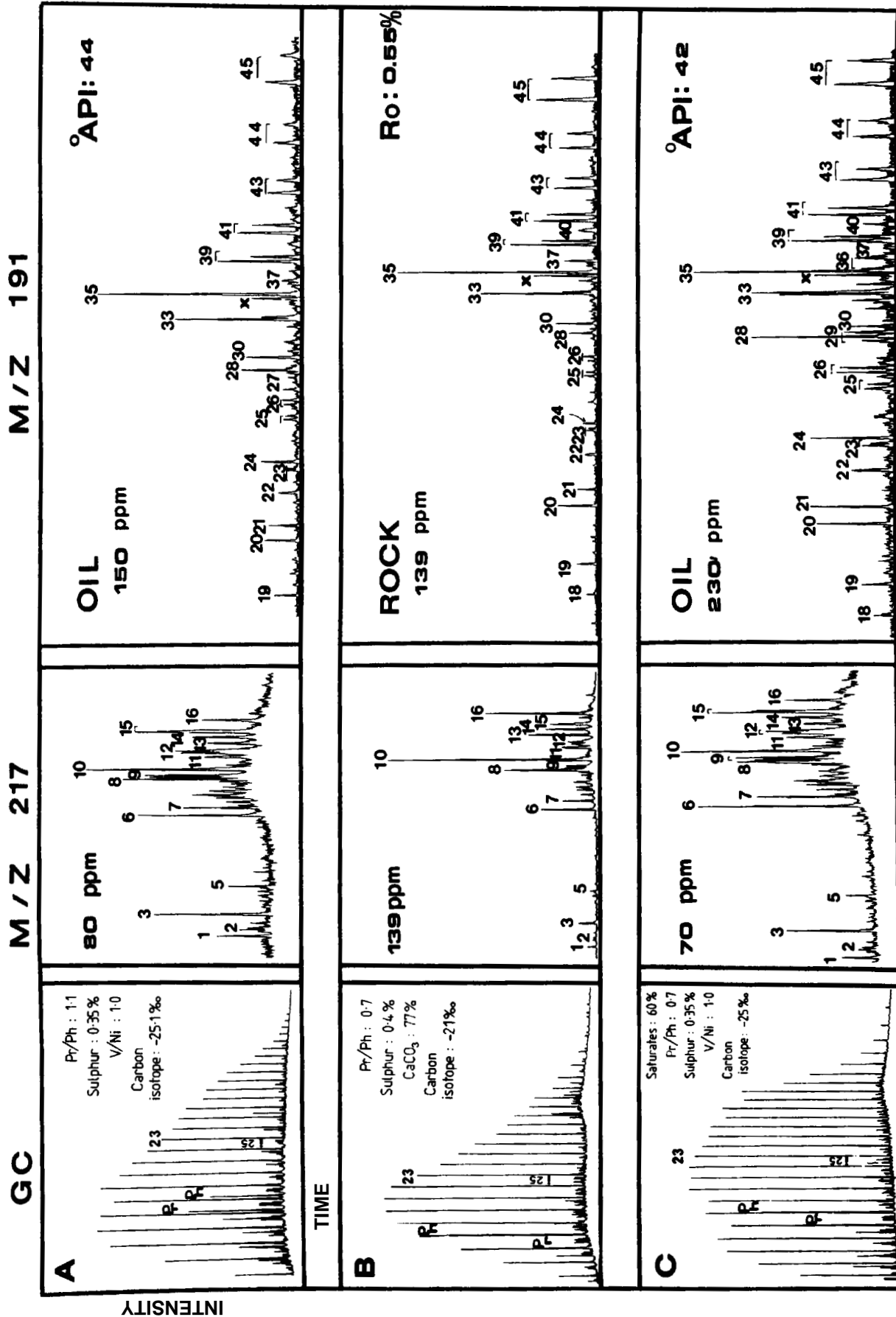


Figure 25. Oil-source rock correlation using gas chromatograms of total alkanes, bulk and elemental parameters, and partial m/z 217 and m/z 191 chromatograms, and absolute concentrations of C₂₇ steranes and C₃₀ $\alpha\beta$ -hopane for a typical marine deltaic, with carbonate influence, source rock (B) versus related oils (A and C) from the Brazilian marginal basins (for peak assignments and quantification procedures see Appendices I and II).

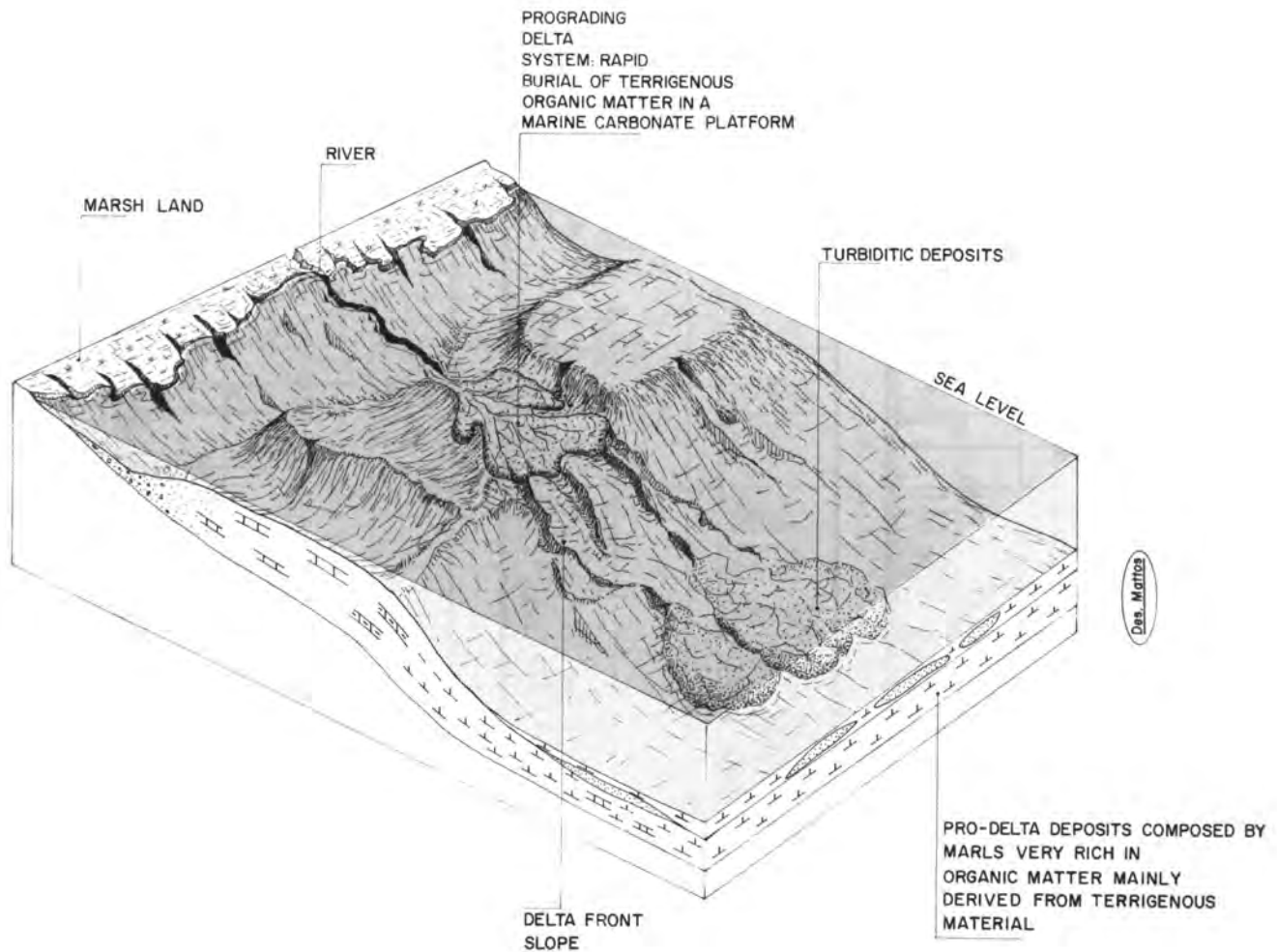


Figure 26. Schematic block diagram showing the sedimentary facies in a marine deltaic depositional environment associated with a marine carbonate platform from the drift stage in the Brazilian marginal basins.

high relative abundances of $18\alpha(H)$ -oleanane, des-E C_{24} to C_{27} tetracyclic terpanes and diasteranes, presence of regular C_{30} steranes, and C_{35} hopanes greater than their C_{34} counterparts (see Figure 25, Table 1, and Appendices I and II).

The block diagram shown in Figure 26 is an idealized illustration of the marine deltaic paleoenvironment of deposition, with a carbonate influence that appears to have developed in the northern area of the Brazilian margin, during Eocene–Oligocene times. This model assumes that thicker and more extensive proximal coarse carbonate deposits were formed in shallow to middle neritic environments. Conversely, pelitic carbonate rocks rich in organic matter occur in distal areas with a deep neritic to lower bathyal environment of deposition. This resulted in the establishment of a marine deltaic environment associated with a carbonate platform system (e.g., Mello et al., 1988a, b). A similar ancient depositional environment, but with a predominance of siliciclastic lithology, has been reported in relation to Eocene–Oligocene sequences from the Niger delta (e.g., Ekweozor et al., 1979a, b); Mahakam delta, Indonesia (e.g., Grantham et al., 1983);

and Beaufort-Mackenzie delta (Brooks, 1986). Some biological marker features similar to the Brazilian samples have, however, been reported from oils derived from the Miocene Klasafet and Klamogun shales and carbonate source rocks from the Salawati Basin, Eastern Indonesia (Poa and Samuel, 1986). Recent examples appear to be the Niger delta; the Ganges delta, Indian Ocean; the Amazon and Mississippi deltas (e.g., Demaison and Moore, 1980); and the Mahakam delta (e.g., Pilon et al., 1986).

MULTIVARIATE ANALYSIS

The concentrations and complex distribution of biological markers in oils and source rock extracts, as analyzed by GC-MS, have been shown above to be useful as diagnostic fingerprints carrying information about organic input in various depositional environments in Brazilian marginal basins. The complexity and large amounts of such data make their handling and interpretation difficult and time consuming. Multivariate data analysis provides a useful tool for studying large

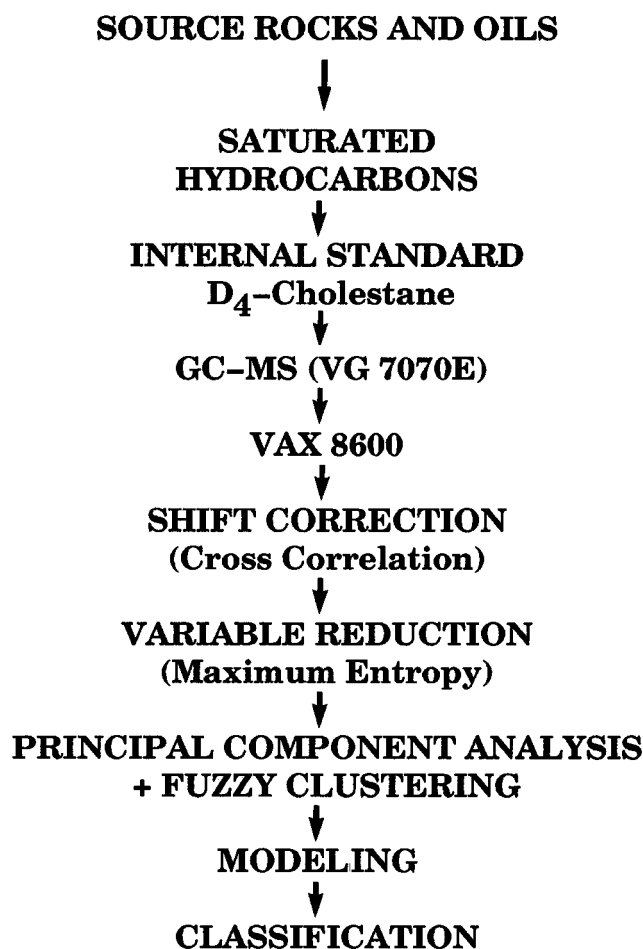


Figure 27. Show diagram for the multivariate classification and modeling.

data sets. One aspect of multivariate data analysis is model building, where patterns or processes in the real world are described in quantitative terms. In this study, the biomarker GC-MS elution profiles from the source rocks characterized above are used to establish multivariate models for specific paleodepositional environments. These models are used to predict the origin of oils produced from adjacent areas in terms of the depositional environments of the source rocks.

One major problem in oil-source rock correlation is to distinguish the effects of maturity from the inherited genetic differences in the biological marker composition. This type of problem lends itself to a multivariate data analytical approach, where complex relations between many variables may be considered together.

Quantitative biological marker data from 34 oils and 60 organic-rich rocks, selected from those studied above, were analyzed using supervised principal component analysis (PCA) and class modeling (Wold, 1976; Figure 27). For each sample, raw GC-MS time-versus-intensity data from the monitoring of 26 biomarker metastable ions, representing the transitions from the molecular ions to the main fragment ions for terpanes (m/z 191), steranes (m/z 217), and 4-methyl-

steranes (m/z 231), were transferred to a VAX 8600 computer. The intensity (relative concentration) of each of the fragments was normalized to the intensity of the fragment from the deuterated internal standard [$5\alpha(H),14\alpha(H),17\alpha(H)-2,2,4,4-d_4$ -cholestane]. Raw data from a retention-time window for each transition ion were collected sequentially to create a new file, a reconstructed biomarker elution profile.

The resulting 27,000 data points (variables) per sample (a mass spectrometric cycle time of approx. 1 sec/26 transitions and retention-time windows from 10 to 20 min) were shift-corrected using a cross-correlation function, and reduced to 962 variables by a maximum entropy method. This is a data reduction method that sums variables with little or no intensity (areas where there are no peaks), and thus conserves total intensity and full instrument resolution for the significant peaks. Such a procedure eliminates the need for peak integration, which can often introduce errors when processing very complex distributions. The biomarker elution profiles are essentially treated as spectra. Figure 28 shows the average elution profile of the resulting variables for a specific marine evaporitic organic-rich sediment extract of the Ceará basin.

Figure 29 shows the computer-reconstructed biomarker profiles, normalized to an internal standard, for a marine evaporitic source rock and an oil derived from such a source rock (samples A and B in Figure 15). Not only are the distributions similar, but the absolute concentrations are also comparable. Such elution/concentration profiles can be used as input to a PCA for each type of depositional environmental (see above), thus producing a so-called "class model." PCA calculates a few new variables that are linear combinations of the original 962 variables. A logarithmic transformation of the data is used in the PCA. This is essential because PCA is a least-squares method, making variables with large variances important in the final result. When establishing a class model from the data, it is important to obtain the correct number of principal components. The number of statistically significant principal components (PCs) calculated for each class is determined using a procedure of cross validation (Wold, 1978).

Source Rock Results

Figure 30A is a PC score plot for the eight samples numbered from 47 to 50 and from 52 to 55 comprising the class of marine carbonate organic-rich rocks. Samples 53 and 54 are analytical parallels and show a good reproducibility for this type of analysis. Samples 52 and 49 are separated from the others along the first principal component, while samples 48, 50, and 55 are separated from samples 47, 53, and 54 along the second principal component. In order to extract information about the relative importance of the various variables (loadings) in each of the principal components, a loading plot is used. Figures 30B and 30C show the loadings versus retention time variable for the first two principal components. In Figure 30B, the high negative loadings of the regular steranes suggest that the most important feature distinguishing samples 52 and 49 from the remainder in Fig-

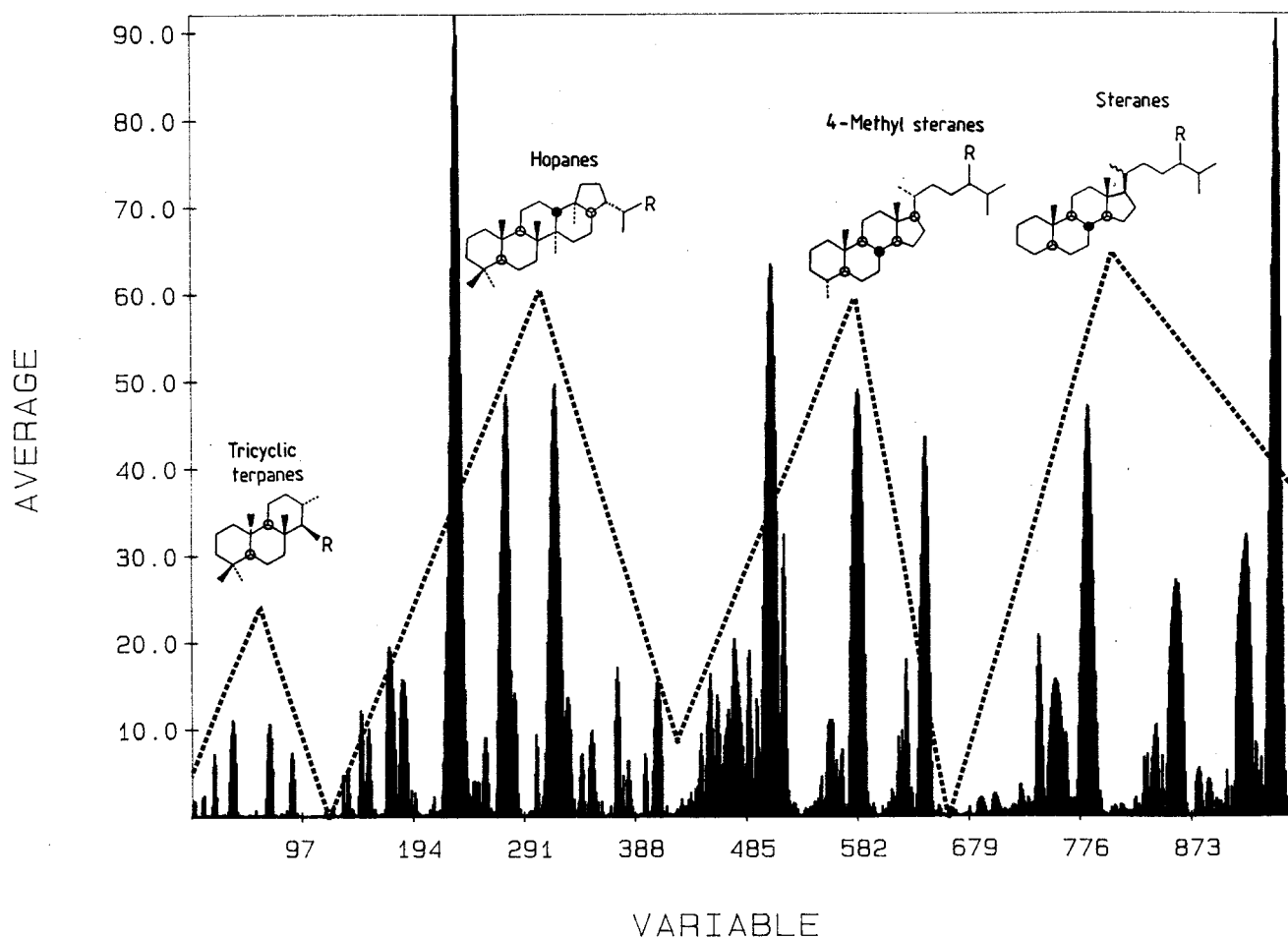


Figure 28. Computer-reconstructed biological marker distribution profile for the marine evaporitic organic-rich sediments (normalized to an internal standard average of all samples in the class).

ure 30A is the lower absolute concentration of regular steranes. Similarly, Figure 30C shows that the most important feature along the second principal component is a negative correlation between the C_{29} -regular steranes and the rest of the biological markers.

Figure 31 gives the average biomarker distribution from two source-rock classes: marine carbonate and marine evaporitic rocks. As can be observed, there is a higher absolute concentration of biological markers in the marine evaporitic organic-rich rocks, attributed mainly to the pentacyclic triterpanes (see Figure 29).

Oil–Source Rock Correlation

The same classes were also modeled using the biological markers from the oils, and in some of these classes distinct regional differences within the class could be observed. Figure 32 shows a plot of the scores on the first PC versus the scores on the second PC for lacustrine saline water oils. Three different groups have been differentiated based on fuzzy clustering of the principal component scores. These groups correspond to oils originating from two different basins (indicating that these oils are generated from source

rocks with slight differences in depositional environments), but still characterized as a lacustrine saline water environment. Indeed, geochemical and biological marker studies do suggest different salinity conditions within the depositional paleoenvironment of the source rocks that gave rise to such oils (Mello, 1988). Each of the modeled source-rock classes was compared with the others, and the modeling and discrimination power for each of the variables were calculated (Albano et al., 1981). Variables with a low modeling power are of little relevance in the class model, and the discrimination power gives a measure of the importance of a variable in separating two different classes. Since each of the source-rock classes spans a range of maturities, selecting variables with a high discrimination power ensures that these are less a function of maturity. Based on the magnitude of the discrimination powers, a new reduced data set containing only 142 variables was constructed. An example of this procedure is shown in Figure 33 where lacustrine-derived oils have been analyzed by PCA using the full data set (962 variables), and with a reduced data set consisting only of those variables which are important (i.e., have a high discrimination power), in separating the lacus-

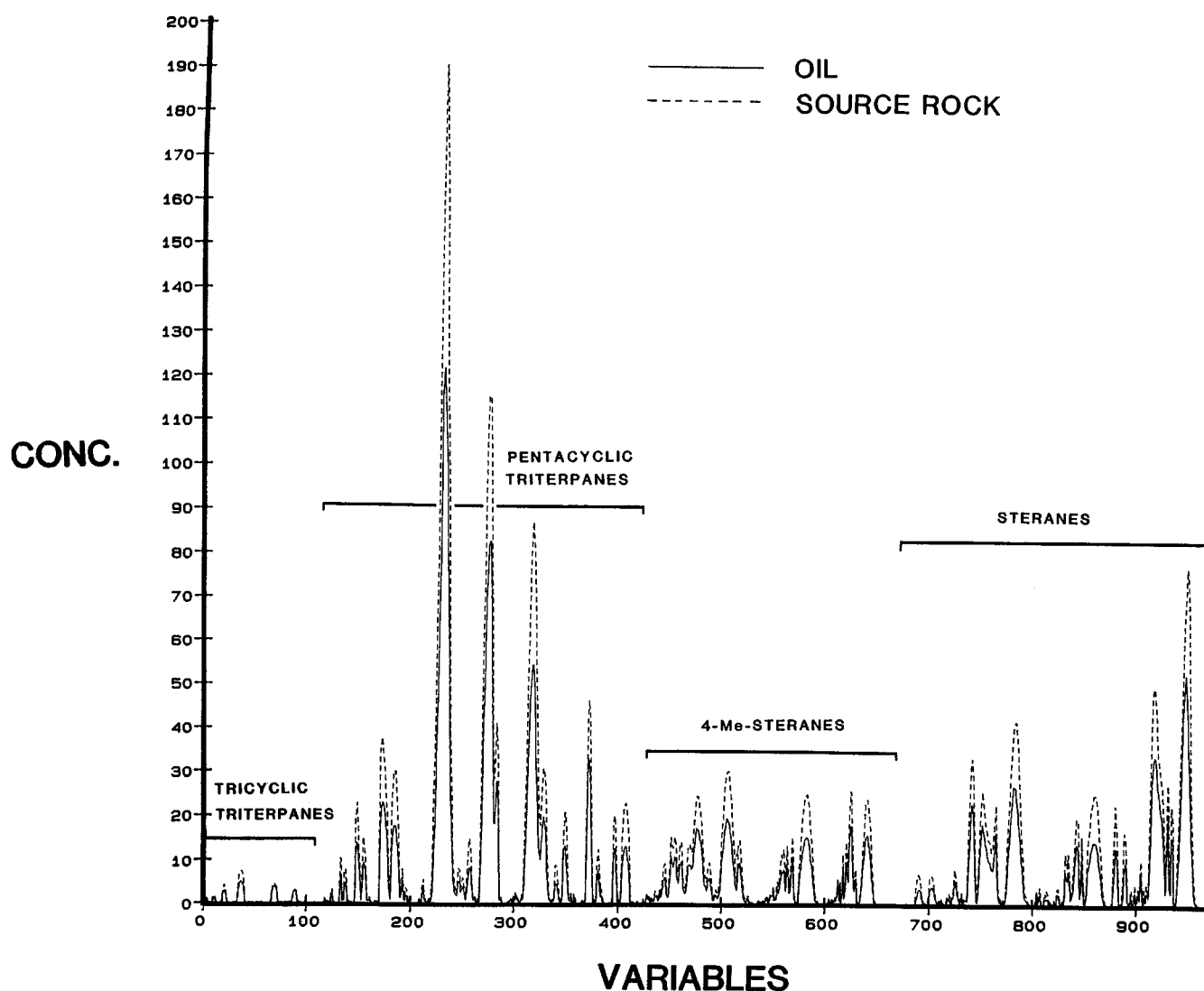


Figure 29. Computer-reconstructed biological marker distribution profile, normalized to an internal standard, for a marine evaporitic source rock and oil.

trine saline water oils (7 to 19) from the lacustrine freshwater oils (1 to 7). The figure clearly shows an improved separation between the two classes when the variables are optimized with respect to their discrimination power.

Samples from depositional environments where both source rocks and oil samples were available were analyzed by PCA as a single class, and the resulting scores on the first and second PC are plotted in Figure 34. As can be observed, the oils generally plot together with the source rocks from the same depositional environment, suggesting that the effect of maturity on the classification of biological markers has been reduced. The source-rock classes were remodeled using the reduced data set, and the oil samples were fitted to each of the resulting classes. The residual standard deviation (RSD) for each fitted item provides a measure of similarity between the item and the calibration set. If the RSD is significantly larger than that found in the calibra-

tion set, it can be concluded that the fitted object does not belong to the class. Table 2 gives the results from fitting of the oil samples to each of the source-rock classes using the reduced data set with 142 variables. The results show that, in general, the oils fit into the corresponding source-rock class suggesting that this method may be used for classifying oils according to the depositional environment of their source rocks. Mixed oils may also be classified using this method. The marine deltaic oils appear to fit into several classes because there is no class for the marine deltaic source rocks, and, thus, the features typical of these source rocks [i.e. the presence of $18\alpha(H)$ -oleanane] are not included in the reduced data set used for classification. On the other hand, the rock and oil samples from the open marine anoxic environment class were not included in the multivariate study.

It is clear from the above results that, in order to effectively classify oils in terms of the paleoenviron-

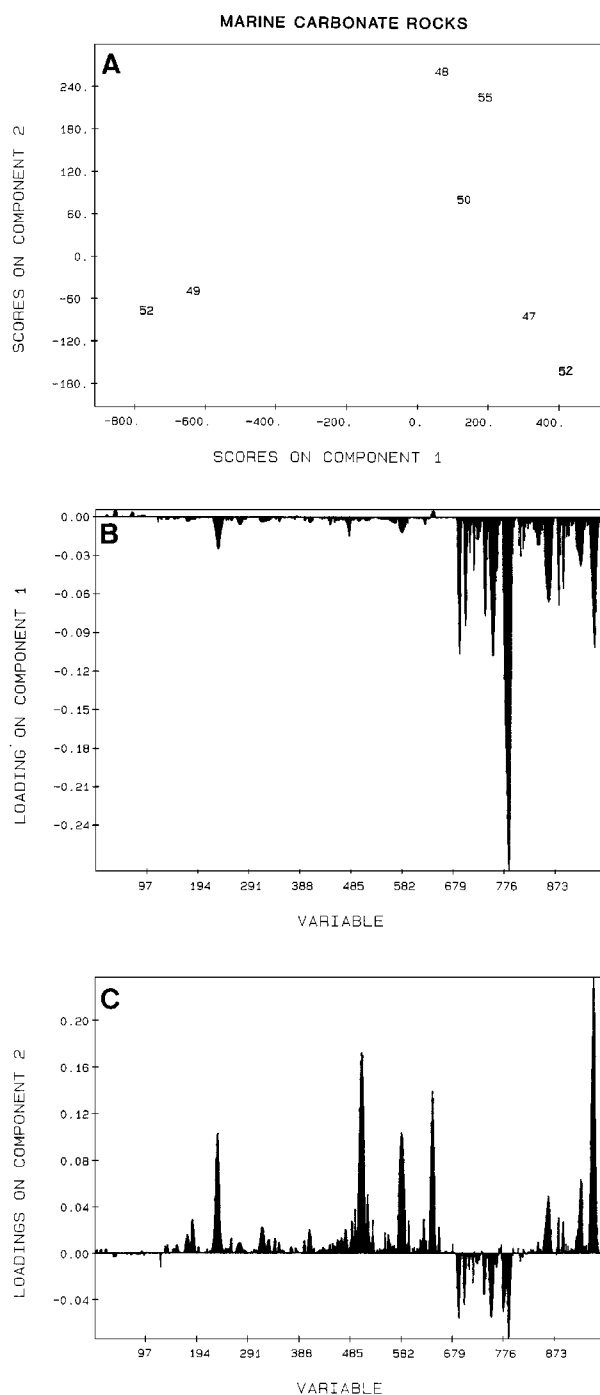


Figure 30. Results from the principal component analysis of the biological marker distribution profiles from marine carbonate organic-rich sediments. (A) The scores on principal component 1 (PC1) versus the scores on principal component 2 (PC2). (B) Loadings on PC1 versus variable. (C) Loadings on PC2 versus variable (see Figure 28 for compounds identification).

ment of deposition of their source rocks, calibration sets spanning all the possible source-rock types are required.

EXPERIMENTAL AND ANALYTICAL PROCEDURES

All oil and rock samples were submitted to bulk, elemental, and liquid chromatography analysis according to procedures described previously (Mello, 1988). The GC-MS analyses of alkanes were carried out using a Finnigan 4000 spectrometer coupled to a Carlo Erba 5160 gas chromatograph equipped with an on-column injector and fitted with a 60 m DB-1701 column. Helium was employed as the carrier gas with a temperature program of 50–90°C at 6°C/min and 90–310°C at 4°C/min. The column was led directly into the ion source (ionizer temperature around 250°C; electron energy 35 eV; emission current 350 μ A, voltage 2 kV). The scan range was typically m/z 50–550 with total scan time of 1.0 sec. The spectrometer was operated in two different modes for each sample; full data collection (FDC) and multiple ion detection (MID), monitoring only selected ions. Data were acquired and processed using an Incos 2300 data system, comprising a Data General Corporation Nova/4 computer. Relative quantification and ratios measured for hydrocarbons were performed using peak areas in appropriate mass chromatograms (cf. Appendix II).

To ensure comparable results, the analyses were performed as far as possible sequentially, under similar conditions using large batches. All the quantitative data on biological marker concentration, reported as ppm of extract or oil, were obtained for selected samples by adding a fixed amount of synthesized deuterated sterane internal standard (2,2,4,4-d₄ 5 α (H), 14 α (H), 17 α (H)-cholestane) to each alkane fraction. 20R + 20S 5 α (H), 14 α (H), 17 α (H)-cholestanes were quantified by comparing peak areas in m/z chromatograms with the peak area of the standard m/z 221 chromatograms (cf. Appendix II). Although response factors for m/z 217 in the low molecular weight steranes are expected to be different, the ppm concentrations of these components were measured in the same way. Other components were quantified by comparison of peak areas with that of the standard in the Reconstituted Ion Chromatogram (RIC) traces (cf. Appendix II). To confirm the order of concentrations of specific biological markers, quantification was also carried out using mass chromatograms (e.g., by comparison of m/z 221 for the standard with m/z 191 to obtain relative concentrations of C₃₀ $\alpha\beta$ hopane). In cases where concentrations were too low to be measured using RIC traces, quantification was obtained by comparing mass chromatograms for the standard (m/z 221) with mass chromatograms for the components in question (e.g., m/z 125 for β -carotane), and then making a correction using a derived factor obtained from analyses of samples where the components could be observed in the RIC traces. Peak identities were established by mass spectral examination, GC retention time, and, in a number of cases, coinjection of standards [18 α (H)-oleanane, gammacerane, C₂₉ $\alpha\beta$ and $\beta\alpha$ norhopanes, C₃₀ $\alpha\beta$ and $\beta\alpha$ hopanes, C₂₇ to C₂₉ 20R-5 α (H)-steranes, C₂₁ $\beta\alpha$ -diapregnane, C₂₂ $\alpha\alpha\alpha$ 4-methylhomopregnane, C₂₁ $\alpha\alpha\alpha$ -pregnane,

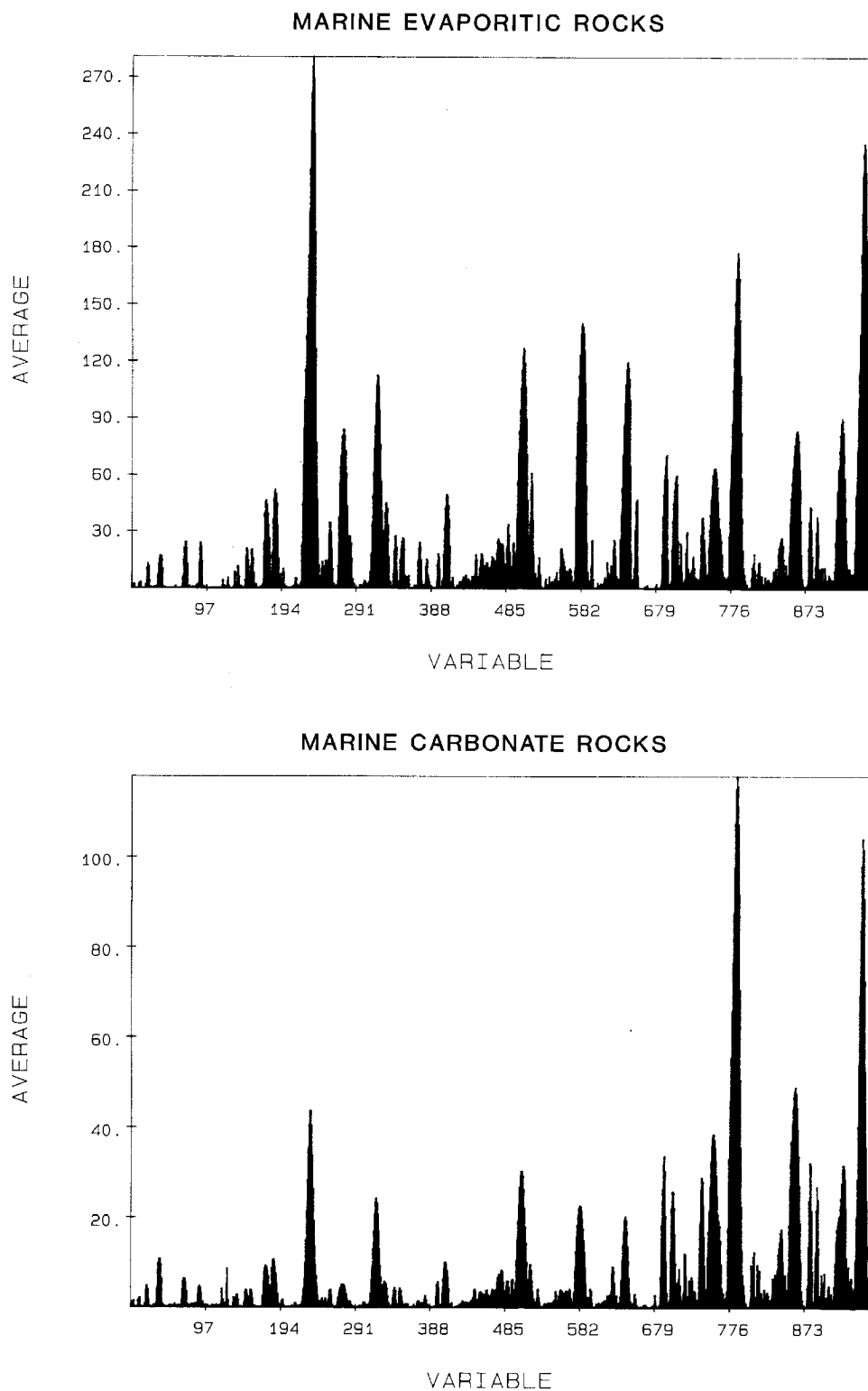


Figure 31. Computer-reconstructed biological marker elution profiles, normalized to an internal standard, for two types of depositional paleoenvironments (average of all samples in each class; see Figure 28 for compounds identification).

C_{24} des-E tetracyclic terpane, C_{25} regular isoprenoid and C_{25} irregular isoprenoid].

The metastable linked scan technique used for the multivariate statistical evaluation of biological markers

was performed by computerized GC-MS using a VG/7070E instrument coupled to an HP S790 Split/Splitless gas chromatograph fitted with a Ultra I HP cross-linked methyl silicon fused silica column (25 m,

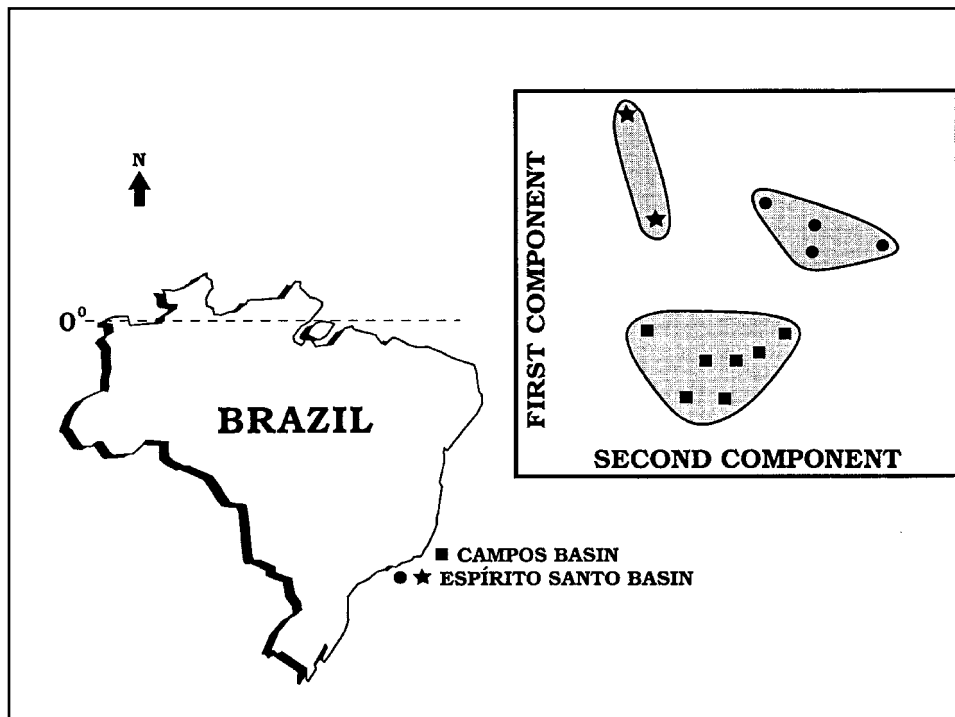


Figure 32. The scores on PC1 versus the scores on PC2 from principal component analysis of the biological marker distribution profiles for lacustrine saline water oils.

Table 2. Classification of Brazilian oils.

| Oil | Source Rock Classes | | | | |
|-------------------|---------------------|------------------|------------------------|-------------------------|----------------------|
| | Marine Evaporitic | Marine Carbonate | Lacustrine Fresh Water | Lacustrine Saline Water | Marine Siliciclastic |
| Lac. fresh water | 1.67 | 1.12 | 0.42 | 0.47 | 0.65 |
| Lac. fresh water | 1.64 | 1.26 | 0.66 | 0.47 | 1.07 |
| Lac. fresh water | 2.44 | 0.98 | 0.42 | 0.51 | 0.74 |
| Lac. fresh water | 1.78 | 1.03 | 0.28 | 0.32 | 0.52 |
| Lac. fresh water | 2.38 | 0.85 | 0.34 | 0.45 | 0.67 |
| Lac. fresh water | 1.68 | 1.01 | 0.34 | 0.42 | 0.63 |
| Lac. saline water | 1.42 | 1.62 | 0.53 | 0.33 | 0.61 |
| Lac. saline water | 2.15 | 0.85 | 0.68 | 0.39 | 0.59 |
| Lac. saline water | 1.95 | 0.84 | 0.46 | 0.34 | 0.47 |
| Lac. saline water | 1.55 | 1.30 | 0.54 | 0.31 | 0.55 |
| Lac. saline water | 1.29 | 1.41 | 0.74 | 0.23 | 0.34 |
| Lac. saline water | 1.45 | 1.48 | 0.94 | 0.42 | 0.80 |
| Lac. saline water | 1.99 | 0.97 | 0.54 | 0.44 | 0.58 |
| Lac. saline water | 1.62 | 0.94 | 0.64 | 0.31 | 0.51 |
| Lac. saline water | 1.69 | 1.12 | 0.69 | 0.33 | 0.50 |
| Lac. saline water | 1.56 | 1.01 | 0.68 | 0.31 | 0.46 |
| Lac. saline water | 1.47 | 1.13 | 0.54 | 0.26 | 0.47 |
| Lac. saline water | 1.49 | 1.16 | 0.86 | 0.49 | 0.65 |
| Lac. saline water | 1.12 | 1.91 | 0.93 | 0.38 | 0.50 |
| Marine evap. | 0.55 | 2.10 | 1.88 | 0.68 | 0.86 |
| Marine evap. | 0.44 | 2.19 | 3.21 | 1.07 | 1.07 |
| Marine evap. | 0.66 | 3.86 | 4.23 | 2.12 | 2.33 |
| Marine evap. | 0.77 | 1.49 | 2.01 | 0.69 | 0.82 |
| Marine evap. | 0.59 | 1.69 | 3.63 | 1.36 | 1.46 |
| Marine evap. | 1.52 | 0.50 | 0.88 | 0.52 | 0.59 |
| Marine carb. | 1.88 | 0.55 | 0.77 | 0.53 | 0.49 |
| Marine delt. | 2.05 | 0.55 | 0.40 | 0.37 | 0.53 |
| Marine delt. | 2.02 | 0.77 | 0.72 | 0.47 | 0.64 |
| Marine delt. | 2.38 | 0.84 | 0.52 | 0.47 | 0.66 |
| Marine delt. | 2.22 | 0.57 | 0.38 | 0.39 | 0.61 |
| RSD of class | 0.52 | 0.57 | 0.49 | 0.46 | 0.46 |

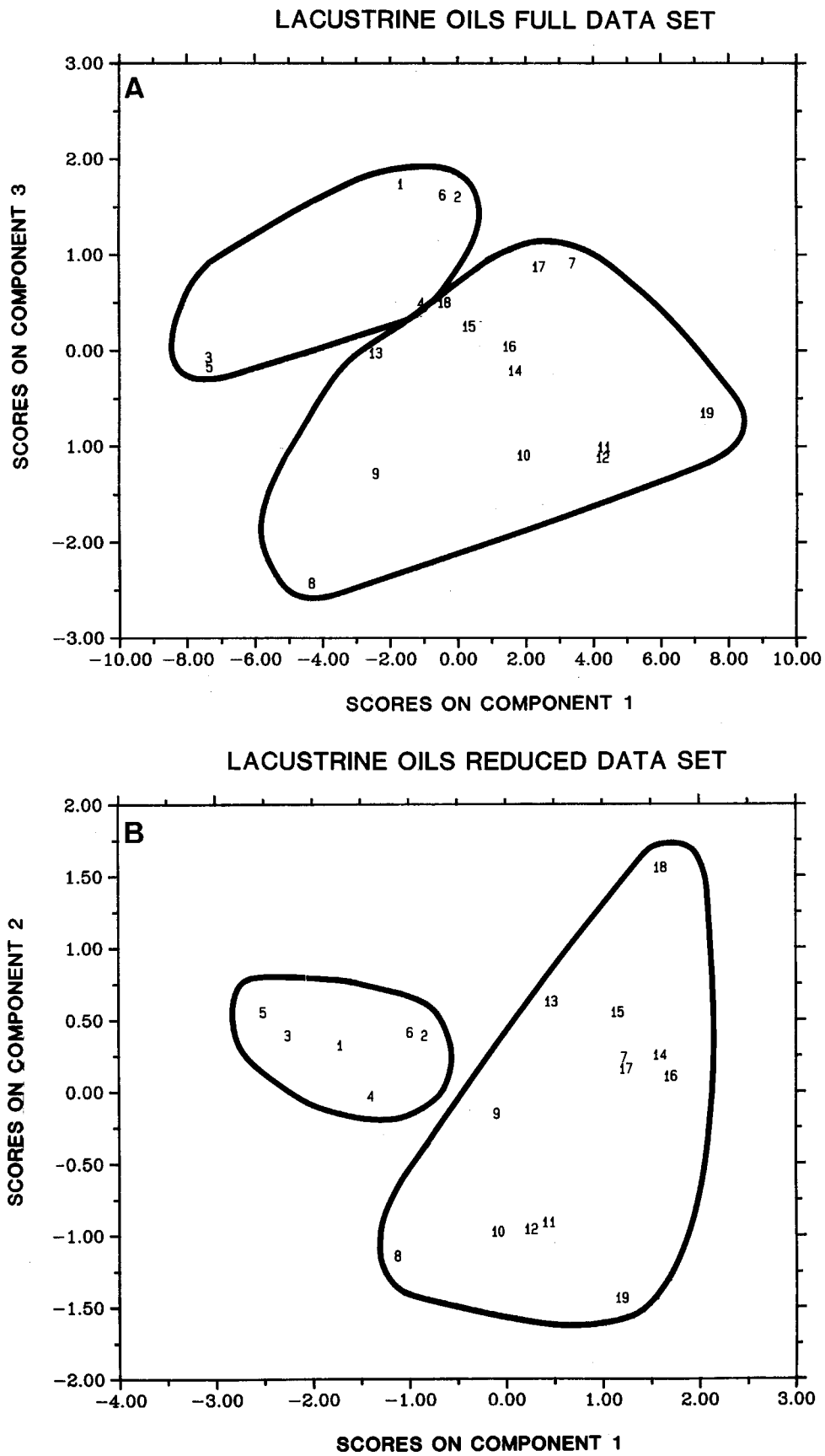


Figure 33. The scores on PC1 versus the scores on PC2 from principal component analysis of the biological marker distribution profiles for lacustrine oils. (A) Results with full data set using 962 variables. (B) Results with reduced data set using 142 variables.

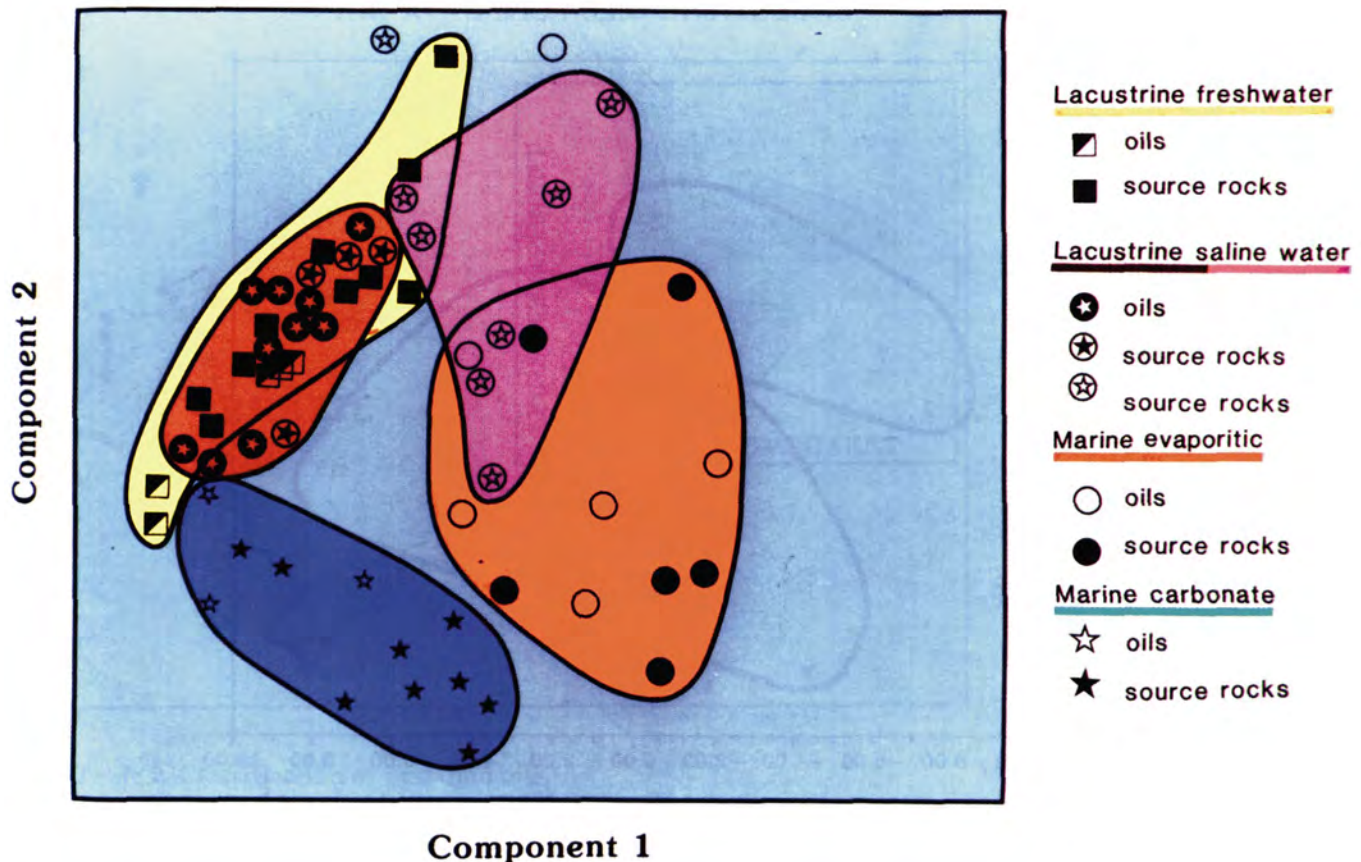


Figure 34. The scores on PC1 versus PC2 from principal component analysis of the reduced data set comprising depositional environments containing both sediment extracts and oil samples.

0.2 m, 0.33 μm). Helium was employed as the carrier gas with a temperature program of 70–150°C at 25°C/min and 150–310°C at 1.5°C/min. Metastable ions, formed in the first field free region of the mass spectrometer, were monitored using a fixed accelerating voltage (6 kV) and preselected changes in the electrostatic analyzer/magnet values (these analyses were carried out at Norsk Hydro Research Center, Norway). The presence and absence of C_{30} regular staranes were checked by monitoring the transition m/z 414–217 (cf. Moldowan et al., 1985). The program SIRUS, implemented on a VAX 8600, was used for multivariate data analysis and class modeling.

CONCLUSIONS

1. Geochemical and biological marker data, together with paleontological and sedimentological information, allowed organic-rich rocks of the Brazilian marginal basins to be classified into seven different depositional regimes: I—lacustrine fresh water; II—lacustrine saline water; III—marine evaporitic; IV—marine carbonate; V—marine deltaic with carbonate influence; VI—open marine highly anoxic with domi-

nance of calcareous lithology; and VII—open marine anoxic with dominance of siliciclastic lithology.

2. Bulk geochemical data and the distribution patterns and concentrations of biological markers of a selection of oils allowed their correlation with source rocks from six of the seven depositional regimes: I—lacustrine fresh water; II—lacustrine saline water; III—marine evaporitic; IV—marine carbonate; V—open marine anoxic with dominance of calcareous lithology; and VI—marine deltaic with carbonate influence.

3. Although in most areas of the continental margin the open marine anoxic sedimentary succession contains organic-rich sediments, they are generally immature (except Santos and Espírito Santos basins), due to a combination of low geothermal gradient and shallow burial, and are not considered effective source rocks in most of the Brazilian continental margin. The fact that the open marine oil type was identified only in Santos and Espírito Santos basins supports such an assumption.

4. Oil—source rock and rock—rock correlations based on biological marker distributions and concentrations, and using multivariate analysis, have been shown to be valid, and may be a useful tool in the assessment of paleoenvironment of deposition and in the petroleum exploration strategy for the Brazilian basins.

5. The use of the biological marker distributions and concentration in paleoenvironmental assessment is a powerful tool in order to determine the type of depositional environment of source rocks in the Brazilian marginal basins using only oil samples.

6. In most cases, no single biological marker property was sufficient to assess environment of deposition. Nevertheless, consideration of various properties in a multiparameter approach can provide diagnostic criteria. On the other hand, the presence of specific compounds, such as $18\alpha(H)$ -oleanane, can be diagnostic of a particular depositional environment (associated here with a deltaic environment).

7. The absence of diagnostic biological marker compounds can be as important as their presence. For example, the absence or low relative abundance of C_{30} steranes and dinosterane isomers appears to be diagnostic of nonmarine depositional environments.

8. The use of a deuterated sterane as an internal standard allowed a quantitative approach (ppm of extract or oil) which extended the information provided by the biological marker pattern distribution.

9. Based on the results of this investigation and previous studies, it is proposed that some biomarker properties, such as pristane/phytane ratio and high abundances of the regular C_{25} isoprenoid alkane, squalane, β -carotane and gammacerane may be considered useful indicators of the salinity of the water column in the depositional environment.

10. Hypersaline depositional conditions tend to result in the highest concentration of biological markers derived from bacterial and algal precursors.

11. Although the "end members" of specific depositional environments possess a fairly clear diagnostic group of characteristics, overlaps of a number of biological marker features do occur. Such features were mainly observed for oils and environments thought to represent enhanced salinity conditions and environmental transitions (e.g., lacustrine hypersaline/marine evaporitic and lacustrine fresh/brackish/to saline water). These "overlaps" show the difficulties that can occur in trying to characterize and distinguish depositional environments.

12. Integration of geological, paleontological, and particularly geochemical data, available from this study, provides a framework of features (e.g., biological marker characteristics) for prolific oil-prone depositional environments. These can be compared with samples from other parts of the world.

13. In relation to the quantitative biological marker approach, it is clear that care must be exercised when attempting to assess the paleoenvironment of deposition using mature rocks and oils, since the concentration of biological markers decreases considerably with increasing maturity.

ACKNOWLEDGMENTS

We thank the geochemistry section of Petrobrás research center for all the elemental and bulk analysis; Drs. G.H. Isaksen, N.C. de Azambuja Filho, W. Mohriak, C. B. Eckardt, and E. Koutsoukos for their

helpful comments and revision of the text; Mr. Baltazar F. da Silva for editing the manuscript, Mrs. A.P. Gowar and Miss L. Dias for advice during analytical work, and Mr. A. Steen of Norsk Hydro Research Center for running the metastable ion monitoring GC-MS. We thank NERC for GC-MS facilities (GR3/2951 and GR3/3758) and Petrobrás for permission to publish.

REFERENCES CITED

- Abed, A.M., and S.A. Bilal, 1983, Petrography and geochemistry of some Jordanian oil shales from north Jordan: *Journal of Petroleum Geology*, v. 513, p. 261–273.
- Albaiges, J., L. Algaba, E. Glavell, and T.J. Grimalt, 1986, Petroleum geochemistry of the Tarragona Basin (Spanish Mediterranean off-shore), *in* Leythaeuser, D., and J. Rullkötter, eds., *Advances in Organic Geochemistry 1985*, p. 441–450.
- Albano, C., G. Blomquist, D. Coomans, W.J. Dunn III, U. Edlund, B. Eliasson, S. Hellberg, E. Johansson, B. Norden, M. Sjöström, B. Söderstrom, H. Wold, and S. Wold, 1981, Pattern recognition by means of disjoint principal component models (SIMCA), philosophy and methods: *Proceedings of Symposium on Applied Statistics*, p. 44–61.
- Arthur, M.A., S.O. Schlanger, and H.C. Jenkyns, 1987, The Cenomanian–Turonian oceanic anoxic event. II. Palaeoceanographic controls on organic-matter production and preservation, *in* Brooks, J., and A.J. Fleet, eds., *Marine Petroleum Source Rocks: Geological Society Special Publication 26*, p. 401–420.
- Asmus, H.E., 1975, Controle estrutural da deposição Mesozoica nas bacias da margem continental Brasileira: *Rev. Bras. Geoc.*, v. 5, p. 160–175.
- Babinski, N.A., and R.C.B. Santos, 1987, Origem e classificação dos hidrocarbonetos da bacia Sergipe-Alagoas; *Caracterização geoquímica: B. Geociências da Petrobras*, Rio de Janeiro, v. 1, p. 87–95.
- Bertani, R.T., and A.V. Carozzi, 1985, Lagoa Feia Formation (Lower Cretaceous) Campos Basin, offshore Brazil: rift valley stage carbonate reservoirs I and II: *Journal of Petroleum Geology*, v. 8, p. 37–58.
- Boon, J.J., H. Hines, A.L. Burlingame, J. Klokk, W.I.C. Rijpstra, J.W. de Leeuw, K.E. Edmunds, and G. Eglinton, 1983, Organic geochemistry studies of Solar Lake laminated cyanobacterial mats, *in* Bjorøy, M., et al., eds., *Advances in Organic Geochemistry 1981*, p. 207–227.
- Bott, M.H.P., 1976, Formation of sedimentary basins of graben type by extension of the continental crust: *Tectonophysics*, v. 36, p. 77–86.
- Brooks, P.W., 1986, Unusual biological marker geochemistry of oils and possible source rocks, offshore Beaufort-Mackenzie Delta, Canada, *in* Leythaeuser, D., and J. Rullkötter, eds., *Advances in Organic Geochemistry 1985*, p. 401–406.
- Burwood, R., P. Leplat, B. Mycke, and J. Paulet, 1993, Rifted margin source rock deposition: a carbon isotope and biomarker study of a West African Lower Cretaceous lacustrine section, *in* Eckardt, C.B., J.R.

- Maxwell, S.R. Later, and D.A.C. Manning, eds., *Advances in Organic Geochemistry 1991*, p. 41–53.
- Cassani, F., 1986, Organic geochemistry of extra-heavy crude oils from the Eastern Venezuelan Basin: Ph.D. Thesis, University of Bristol, 226 p.
- Castle, J.W., 1990, Sedimentation in Eocene Lake Uinta (lower Green River Formation), Northeastern Uinta Basin, Utah, *in* Katz, B.J., ed., *Lacustrine Basin Exploration—Case Studies and Modern Analogs: AAPG Memoir 50*, p. 243–265.
- Castro, J., and N.C. de Azambuja Filho, 1980, Fácies análise estratigráfica e reservatório da Formação Lagoa Feia, Cretáceo inferior da bacia de Campos. Rio de Janeiro: Relatório Interno, Petrobras, 110 p.
- Castro, J., N.C. de Azambuja Filho, and A.P.G. Xavier, 1981, Fácies e análise estratigráfica da Formação Lagoa Feia, Cretáceo inferior da Campos, Brasil: VIII Congresso Geológico Argentino, San Luis, Actas II, p. 567–576.
- Chen Chang Ming, Huang Jiakuan, Chen Ingsha, and Tian Xingyou, 1984, Depositional models of Tertiary rift basins, Eastern China, and their application to petroleum prediction: *Sedimentary Geology*, v. 40, p. 73–88.
- Cohen, A.S., 1990, Tectono-stratigraphic model for sedimentation in Lake Tanganyika, Africa, *in* Katz, B.J., ed., *Lacustrine Basin Exploration—Case Studies and Modern Analogs: AAPG Memoir 50*, p. 137–151.
- Connan, J., and T.D. Dessort, 1987, Novel family of hexacyclic hopanoid alkanes (C₃₂–C₃₅) occurring in sediments and oils from anoxic palaeoenvironments: *Organic Geochemistry*, v. 11, p. 103–113.
- Connan, J., J. Bourouillec, T.D. Dessort, and P. Albrecht, 1986, The microbial input in carbonate-anhydrite facies of a sabkha palaeoenvironment from Guatemala; a molecular approach, *in* Leythaeuser, D., and J. Rullkötter, eds., *Advances in Organic Geochemistry 1985*, p. 29–50.
- Curiale, J.A., D. Cameron, and D.V. Davis, 1985, Biological marker distribution and significance in oils and rocks of the Monterey Formation, California: *Geochimica et Cosmochimica Acta*, v. 49, p. 271–288.
- Dean, W., and T.D. Fouch, 1983, Lacustrine environment, *in* Scholle, P.A., et al., eds., *Carbonate Depositional Environments: AAPG Memoir 33*, p. 97–130.
- de Azambuja Filho, N.C., 1987, Preenchimento sedimentar de bacias do tipo rift. Rifts Intra-continentais. Seminario: Petrobras; DEPEX, Rio de Janeiro, p. 644–656.
- de Deckker, P., 1988, Large Australian lakes during the last 20 million years: sites for petroleum source rocks and metal ore deposition, or both, *in* Kelts, K., A. Fleet and M. Talbot, eds., *Lacustrine Petroleum Source Rocks*, p. 45–58.
- De Grande, S.M.B., F.R. Aquino Meot, and M. R. Mello, 1993, Extended tricyclic terpanes in sediments and petroleum: *Organic Geochemistry*, v. 20, n. 7, p. 1039–1047.
- Della Favera, J.C., R.A. Medeiros, C.J. Appi, G. Beurlen, M.C. Vivier, and A.L. Hashimoto, 1984, Análise estratigráfica do Andar Alagoas na bacia do Ceará: Petrobras Internal Report, 67 p.
- Demaison, G.J., and G.T. Moore, 1980, Anoxic environments and oil source bed genesis: *AAPG Bulletin*, v. 64, p. 1179–1209.
- Dunlop, R.W., and P.R. Jefferies, 1985, Hydrocarbons of the hypersaline basins of Shark Bay, Western Australia: *Organic Geochemistry*, v. 8, p. 313–320.
- Ekweozor, C.M., J.I. Okogun, D.E.U. Ekong, and J.R. Maxwell, 1979a, Preliminary organic geochemical studies of samples from the Niger delta (Nigeria). I. Analyses of crude oils for triterpanes: *Chemical Geology*, v. 27, p. 11–29.
- Ekweozor, C.M., J.I. Okogun, D.E.U. Ekong, and J.R. Maxwell, 1979b, Preliminary organic geochemical studies of samples from the Niger delta (Nigeria). II. Analyses of shale for triterpenoid derivatives: *Chemical Geology*, v. 27, p. 29–37.
- Estrella, G., M.R. Mello, P.C. Gaglianone et al., 1984, The Espirito Santo Basin—Brazil. Source rock characterization and petroleum habitat, *in* Demaison, G., and R.J. Murriss, eds., *Petroleum Geochemistry and Basin Evaluation: AAPG Memoir 35*, p. 253–271.
- Eugster, H.P., 1986, Lake Magady, Kenya: a model for rift valley hydrochemistry and sedimentation, *in* Frostick, L.E., R.W. Renaut, I. Reid, and J.J. Tiercelin, eds., *Sedimentation in the African Rifts: Geological Society Special Publication 25*, p. 177–191.
- Falkenheim, F.U.H., 1981, Carbonate microfacies of the Macaé Formation (Lower Cretaceous), Campos Basin, offshore Brazil: Ph.D. Dissertation, University of Illinois, 160 p.
- Farrimond, P., 1987, The Toarcian and Cenomanian/Turonian oceanic anoxic events: an organic geochemical study: Ph.D. Thesis, University of Bristol, 382 p.
- Friedman, G.M., 1980, Review of depositional environments in evaporite deposits and the role of evaporites in hydrocarbon accumulation: *AAPG Bulletin*, v. 56, p. 1072–1086.
- Fu Jia Mo, S. Guoying, P. Pinoan, S.C. Brassell, G. Eglinton, and J. Jigang, 1986, Peculiarities of salt lake sediments as potential source rocks in China, *in* Leythaeuser, D., and L. Rullkötter, eds., *Advances in Organic Geochemistry 1985*, p. 119–127.
- Ghignone, J.I., and G. de Andrade, 1970, General geology and major oil fields of Reconcavo Basin, Brazil: *AAPG Memoir 14*, p. 337–358.
- Gibbons, M., 1978, The geochemistry of sabkha and related deposits: Ph.D. Thesis, University of Newcastle, 260 p.
- Goodwin, N.S., A.L. Mann, and R.L. Patience, 1988, Structure and significance of C₃₀ 4-methylsteranes in lacustrine shales and oils: *Organic Geochemistry*, v. 12, p. 495–506.
- Goossens, H., J.W. De Leeuw, P.A. Schenck, and S.C. Brassell, 1984, Tocopherols as likely precursors of pristane in ancient sediments and crude oils: *Nature*, v. 312, p. 440–442.
- Gransch, J.A., and E. Eisma, 1966, Geochemical aspects of the occurrence of porphyrins in west Venezuelan

- mineral oils and rocks, *in* Hobson, G.P., and G.C. Speers, eds., *Advances in Organic Geochemistry* 1965, p. 69–88.
- Grantham, P.J., J. Posthuma, and A. Baak, 1983, Triterpanes in a number of Far Eastern crude oils, *in* Bjorøy, M., et al., eds., *Advances in Organic Geochemistry* 1982, p. 675–683.
- Hofmann, P.M., and D. Leythaeuser, 1993, Sedimentological and geochemical conditions for the accumulation of organic matter in Oligocene evaporite sediments of the Mulhouse basin, *in* Oygard, K., ed., *Advances in Organic Geochemistry* 1993, p. 393–398.
- Katz, B.J., ed., 1990, Lacustrine basin exploration—case studies and modern analogs: AAPG Memoir 50, 340 p.
- Katz, B.J., and L.W. Elrod, 1983, Organic geochemistry of DSDP site 467, offshore California. Middle Miocene to lower Pliocene strata: *Geochimica et Cosmochimica Acta*, v. 47, p. 389–396.
- Katz, B.J., K.K. Bissada, and J.W. Wood, 1987, Factors limiting potential of evaporites as hydrocarbon source rocks (abs.): AAPG Annual Convention, Los Angeles.
- Kelts, K., 1988, Environments of deposition of lacustrine petroleum source rocks: an introduction, *in* Kelts, K., A. Fleet, and M. Talbot, eds., *Lacustrine Petroleum Source Rocks*, p. 3–26.
- Kendall, A.C., 1978, Facies models 12. Subaqueous evaporites: *Geosci. Can.*, v. 5, p. 124–139.
- Kirkland, D.W., and R. Evans, 1980, Source-rock potential of evaporitic environment: AAPG Bulletin, v. 69, p. 181–190.
- Koutsoukos, E.A.M., 1984, Evolução paleoecológica do Albiano ao Maestrichtiano na área noroeste da Bacia de Campos, Brasil, com base em foraminíferos: XXXIII Congresso Brasileiro de Geologia, Anais, 2, p. 685–698.
- Koutsoukos, E.A.M., 1987, Área noroeste da Bacia de Campos, Brasil, do Mesocretáceo ao Neocretáceo: Evolução paleoambiental e paleogeográfica através de estudos de foraminíferos: IX Congresso Brasileiro de Paleontologia, Anais, p. 970–978.
- Koutsoukos, E.A.M., and E. Dias-Brito, 1987, Paleobatimetria da margem continental do Brasil durante o Albiano: IX Congresso Brasileiro de Paleontologia, Anais, p. 1019–1026.
- Koutsoukos, E.A.M., and K. Merrick, 1988, Foraminiferal paleoenvironments from the Barremian–Maestrichtian of Trinidad, West Indies: *Transaction of the First Geological Conference of the Geological Society of Trinidad & Tobago*, p. 85–101.
- Koutsoukos, E.A.M., M.R. Mello, N.C. de Azambuja Filho, J.R. Maxwell, and M.B. Hart, 1991a, The Albian succession of Sergipe basin, Brazil: an integrated palaeoenvironmental assessment: AAPG Bulletin, v. 75, p. 479–498.
- Koutsoukos, E.A.M., M.R. Mello, N.C. de Azambuja Filho, J.R. Maxwell, and M.B. Hart, 1991b, Micropaleontological and geochemical evidence of mid-Cretaceous dysoxic-anoxic palaeoenvironments in the Sergipe basin, northeastern Brazil, *in* Tyson, R.V., and T.H. Pearson, eds., *Modern and Ancient Continental Shelf Anoxia: Geological Society of London Special Publication* 58, p. 427–447.
- Li Desheng and Luo Ming, 1990, Hydrocarbon accumulation in Meso-Cenozoic lacustrine remnant petroliferous depressions and basins, Southeastern China, *in* B.J. Katz, ed., *Lacustrine Basin Exploration—Case Studies and Modern Analogs: AAPG Memoir* 50, p. 327–335.
- Mackenzie, A.S., 1980, Applications of biological marker compounds to subsurface geological processes: Ph.D. Thesis, University of Bristol, 376 p.
- Mackenzie, A.S., J.R. Maxwell, M.L. Coleman, and C.E. Deegan, 1984, Biological marker and isotope studies of North Sea crude oils and sediments: *Proceedings of the 11th World Petroleum Congress*, vol. 2, *Geology Exploration Reserves*, p. 45–56.
- Magniez-Jannin, F., and T. Jacquin, 1986, Foraminifères et séquences sédimentaires: vers une meilleure compréhension des environnements anoxiques de Crétacé dans l'Atlantique Sub, *in* BENTHOS'86—Third International Symposium on Benthic Foraminifera, September 22–28, 1986, Geneva, Abstracts, p. 47.
- McHargue, T.R., 1990, Stratigraphic development of Proto-South Atlantic Rifting in Cabinda, Angola—a petroliferous lake basin, *in* B.J. Katz, ed., *Lacustrine Basin Exploration—Case Studies and Modern Analogs: AAPG Memoir* 50, p. 307–327.
- McKirdy, D.M., A.J. Kantsler, J.K. Emmett, and A.K. Aldridge, 1984, Hydrocarbon genesis and organic facies in Cambrian carbonates of the eastern Officer Basin, South Australia, *in* Palacas, J.G., ed., *Petroleum Geochemistry and Source Rock Potential of Carbonate Rocks: AAPG Studies in Geology* 18, p. 13–32.
- McKirdy, D.M., R.E. Cox, J.K. Volkman, and V.G. Howell, 1986, Botryococane in a new class of Australian non-marine crude oils: *Nature*, v. 320, p. 57–59.
- Medeiros, R.A., and F.G. Ponte, 1981, Roteiro geológico da Bacia de Recôncavo, Bahia: *Internal Report, Petrobras*, 56 p.
- Medeiros, R.A., H. Schaller, and G.M. Friedman, 1971, Facies sedimentares: análise e critérios para o reconhecimento de ambientes deposicionais: *Ciência-Técnica-Petróleo*, v. 5, 123 p.
- Mello, M.R., 1988, Geochemical and molecular studies of the depositional environments of source rocks and their derived oils from the Brazilian marginal basins: Ph.D. Thesis, Bristol University, 240 p.
- Mello, M.R., and J.R. Maxwell, 1990, Organic geochemical and biological marker characterization of source rocks and oils derived from lacustrine environments in the Brazilian continental margin, *in* Katz, B.J., ed., *Lacustrine Basin Exploration—Case Studies and Modern Analogs: AAPG Memoir* 50, p. 77–99.
- Mello, M.R., G.O. Estrella, and P.C. Gaglianone, 1984, Hydrocarbon source potential in Brazilian marginal basins (abs.): AAPG Annual Convention, San Antonio, Texas.

- Mello, M.R., P.C. Gaglianone, S.C. Brassell, and J.R. Maxwell, 1988a, Geochemical and biological marker assessment of depositional environment using Brazilian offshore oils: Marine and Petroleum Geology, v. 5, p. 205–203.
- Mello, M.R., N. Telnaes, P.C. Gaglianone, M.I. Chicareli, S.C. Brassell, and J.R. Maxwell, 1988b, Organic geochemical characterisation of depositional palaeoenvironments of source rocks and oils in Brazilian marginal basins, in Mattavelli, L., and L. Novelli, eds., Advances in Organic Geochemistry 1987, p. 31–45.
- Mello, M.R., E.A.M. Koutsoukos, M.B. Hart, S.C. Brassell, and J. R. Maxwell, 1989, Late Cretaceous anoxic events in Brazilian continental margin: Organic Geochemistry, v. 14, n. 5, p. 529–542.
- Mello, M.R., E.A.M. Koutsoukos, E.V. Santos Neto, and A. Silva Telles, Jr., 1993, Geochemical and micropaleontological characterization of lacustrine and marine hypersaline environments from Brazilian basins, in Katz, B.J., and L. Pratt, eds., Source Rocks in a Sequence Stratigraphic Framework: AAPG Studies in Geology 38, p. 17–34.
- Mohriak, W.U., and F.F. Dewey, 1987, Deep seismic reflectors in the Campos Basin, offshore Brazil: Geophys. J. R. Astr. Soc., v. 89, p. 133–140.
- Moldowan, J.M., W.K. Seifert, and E.J. Gallegos, 1985, Relationship between petroleum composition and depositional environment of petroleum source rocks: AAPG Bulletin, v. 69, p. 1255–1268.
- Moldowan, J.M., P. Sundaraman, and M. Schoell, 1986, Sensitivity of biomarker properties of depositional environment and/or source input in the lower Toarcian of SW Germany, in Leythaeuser, D., and J. Rullkötter, eds., Advances in Organic Geochemistry 1985, p. 915–926.
- Netto, A.S.T., et al., 1982, Projeto Andar Dom João: Rel.Petrobras, Depex., 1726 p.
- Ojeda, H.A., 1982, Structural framework, stratigraphy and evolution of Brazilian margin basins: AAPG Bulletin, v. 77, p. 732–749.
- Palacas, J.G., D.E. Anders, and J.D. King, 1984, South Florida Basin—a prime example of carbonate source rocks of petroleum, in Palacas, J.G., ed., Petroleum Geochemistry and Source Rock Potential of Carbonate Rocks: AAPG Studies in Geology 18, p. 71–96.
- Peters, S.W., and C.M. Ekweozor, 1982a, Origin of Mid-Cretaceous black shales in the Benue Trough, Nigeria: Palaeogeography, Palaeoclimatology, Palaeoecology, v. 40, p. 311–319.
- Peters, S.W., and C.M. Ekweozor, 1982b, Petroleum geology of Benue Trough and southeastern Chad Basin, Nigeria: AAPG Bulletin, v. 66, p. 1114–1149.
- Philp, R.P., and T.D. Gilbert, 1986, Biomarker distributions in Australian oils predominantly derived from terrigenous source material, in Leythaeuser, D., and J. Rullkötter, eds., Advances in Organic Geochemistry 1985, p. 73–84.
- Pillon, P., L. Jocteur-Monrozier, C. Gonzale, and A. Saliot, 1986, Organic geochemistry of Recent equatorial deltaic sediments, in Leythaeuser, D., and J. Rullkötter, eds., Advances in Organic Geochemistry 1985, p. 711–716.
- Poa, R.S.K., and L. Samuel, 1986, Problems of source rock identification in the Salawati basin. Irianjaya: Proc. Indian Petroleum Assoc., 15th Annual Convention, p. 403–421.
- Ponte, F.C., and H.E. Asmus, 1978, Geological framework of the Brazilian continental margin: Geol. Rundsch., v. 68, p. 201–235.
- Powell, T.O., 1986, Petroleum geochemistry and depositional settings of lacustrine source rocks: Marine and Petroleum Geology, v. 3, p. 200–219.
- Premovic, P.I., M.S. Pavlovic, and N.Z. Pavlovic, 1986, Vanadium in ancient sedimentary rocks of marine origin: Geochimica et Cosmochimica Acta, v. 50, p. 1923–1931.
- Rafalska-Bloch, J., and R. Cunningham, Jr., 1986, Organic facies in Recent sediments of carbonate platforms: Southwestern Puerto Rico and Northern Belize, in Leythaeuser, D., and J. Rullkötter, eds., Advances in Organic Geochemistry 1985, p. 717–724.
- Rieber, H., 1982, Cyclic and event stratification, p. 527–541.
- Riley, K.W., and J.D. Saxby, 1982, Organic matter and vanadium in the Toolebuc Formation of the Eromanga Basin: Chemical Geology, v. 37, p. 265–275.
- Rodrigues, R., L.A.F. Trindade, J.N. Cardoso, and F.R. Aquino Neto, 1988, Biomarker stratigraphy of the lower Cretaceous of Espirito Santo Basin, Brazil, in Mattavelli, L., and L. Novelli, eds., Advances in Organic Geochemistry 1987, p. 707–714.
- Rullkötter, J., A.S. Mackenzie, D. Welte, D. Leythaeuser, and D. Radke, 1984, Qualitative gas chromatography-mass spectrometry analysis of geological samples, in Schenck, P.A., J.W. DeLeeuw, and C.W.M. Lijmbach, eds., Advances in Organic Geochemistry 1983, p. 817–827.
- Schaller, H., 1969, Revisão bioestratigráfica da bacia de Sergipe-Alagoas: Bol. Téc. Petrobrás, v. 12, p. 21–86.
- Schlanger, S.O., and H.C. Jenkyns, 1976, Cretaceous oceanic anoxic events: causes and consequences: Geol. Mijnbow, v. 55, p. 179–184.
- Schlanger, S.O., M.A. Arthur, H.C. Jenkyns, and P.A. Scholle, 1987, The Cenomanian–Turonian oceanic anoxic event. I. Stratigraphy and distribution of organic-rich beds and the marine $\delta^{13}\text{C}$ excursion, in Brooks, J., and A.J. Fleet, eds., Marine Petroleum Source Rocks: Geological Society Special Publication 26, p. 371–400.
- Summons, R.E., J.K. Volkman, and C.J. Boreham, 1987, Dinosterane and other steroidal hydrocarbons of dinoflagellate origin in sediments and petroleum: Geochimica et Cosmochimica Acta, v. 51, p. 3075–3082.
- Takaki, T., and R. Rodrigues, 1984, Isotopos estáveis do carbono e oxigênio dos calcários como indicadores paleoambientais-Bacias de Campos, Santos e Espírito Santo: Anais XXXIII Congresso Brasileiro de Geologia, p. 4750–4762.
- Talbot, M.R., 1988, The origins of lacustrine oil source rocks: evidence from the lakes of tropical Africa, in Fleet, A.J., K. Kelts, and M. Talbot, eds., Lacustrine Petroleum Source Rocks, p. 29–44.
- Talukdar, S., O. Gallango, and M. Chin-a-uen, 1986,

- Generation and migration of hydrocarbons in the Maracaibo Basin, Venezuela: an integrated basin study, *in* Leythaeuser, D., and J. Rullkötter, eds., *Advances in Organic Geochemistry 1985*, p. 261–280.
- Taylor, J.C.M., et al., 1985, The role of evaporites in hydrocarbon exploration: Courses Notes 39, JAPEC (UK).
- ten Haven, H.L., 1986, Organic and inorganic geochemical aspects of Mediterranean late Quaternary sapropels and Messinian evaporitic deposits: Ph.D. Thesis, Geological Ultraiectina Instituut voor Sardwetenschappen der Rijksuniversiteit Utrecht, 203 p.
- ten Haven, H.L., J.W. De Leeuw, J.S. Sinninghe Danste, P.A. Schenck, S.E. Palmer, and J.E. Zumberge, 1988, Application of biological marker in the recognition of paleo hypersaline environments, *in* Kelts, K., A. Fleet, and M. Talbot, eds., *Lacustrine Petroleum Source Rocks*, p. 123–131.
- Tissot, B.P., Y. Califet-Debyser, G. Deroo, and J.L. Oudin, 1971, Origin and evolution of hydrocarbons in early Toarcian shales, Paris basin, France: *AAPG Bulletin*, v. 55, p. 2177–2193.
- Tissot, B., G. Deroo, and A. Hood, 1978, Geochemical study of the Uinta basin: formation of petroleum from the Green River Formation: *Geochimica et Cosmochimica Acta*, v. 42, p. 1469–1485.
- Tissot, B., G. Demaison, P. Masson, J.R. Delteil, and A. Combaz, 1980, Paleoenvironment and petroleum potential of mid-Cretaceous black shales in Atlantic basins: *AAPG Bulletin*, v. 64, p. 2051–2063.
- Tolderer-Farmer, M., J.C. Coimbra, J.A. Moura, and H.M.N. Gilson, 1987, Paleoenvironmental reconstruction of the Reconçavo basin (Lower Cretaceous, Brazil) based on ostracod assemblages—preliminary study: *Resumo das Comunicações. X Cong. Bras. de Paleontologia*, 53 p.
- Viana, C.F., E.G. Gama, Jr., I.A. Simões, J.A. Moura, J.R. Fonseca, and R.J. Alves, 1971, Revisão estratigráfica da bacia do Recôncavo-Tucano: *Bol.Tec. Petrobras*, v. 14(3/4), p. 157–192.
- Vincens, A., J. Casanova, and J.J. Tiercelin, 1986, Palaeolimnology of Lake Bogoria (Kenya) during the 4500 BP high lacustrine phase, *in* Frostick, L.E., R.W. Renaut, I. Reid, and J.J. Tiercelin, eds., *Sedimentation in the African Rifts: Geological Society Special Publication 25*, p. 323–331.
- Wang Tieguan, Fan Pu, and F.M. Swain, 1988, Geochemical characteristics of crude oil and source rocks beds in different continental facies of four oil bearing basins, China, *in* Fleet, A., K. Kelts, and M. Talbot, eds., *Source Rocks*, p. 309–326.
- Wold, S., 1976, Pattern recognition by means of disjoint principal components models: *Pattern Recognition*, v. 8, p. 127–139.
- Wold, S., 1978, Cross validatory estimation of the number of components in factor and principal components models: *Technometrics*, v. 20, p. 397–406.

APPENDIX I.

PEAK ASSIGNMENTS FOR CHROMATOGRAMS IN THIS CHAPTER

- Pr—2,6,10,14-tetramethylpentadecane (pristane)
 Ph—2,6,10,14-tetramethylhexadecane (phytane)
 β—β-Carotane
 6—13β(H),17α(H)-diacholestane,20S (C₂₇-diasterane)
 7—13β(H),17α(H)-diacholestane,20R (C₂₇-diasterane)
 8—5α(H),14α(H),17α(H),20S (C₂₇-cholestane)
 9—5α(H),14β(H),17β(H),20R + 20S (C₂₇-cholestane)
 10—5α(H),14α(H),17α(H),20R (C₂₇-cholestane)
 11—5α(H),14α(H),17α(H),20S (C₂₈-methylcholestane)
 12—5α(H),14β(H),17β(H),20R + 20S (C₂₈-methylcholestane)
 13—5α(H),14α(H),17α(H),20R (C₂₈-methylcholestane)
 14—5α(H),14α(H),17α(H),20S (C₂₉-ethylcholestane)
 15—5α(H),14β(H),17β(H),20R + 20S (C₂₉-ethylcholestane)
 16—5α(H),14α(H),17α(H),20R (C₂₉-ethylcholestane)
 17—C₁₉ tricyclic terpene
 18—C₂₀ tricyclic terpene
 19—C₂₁ tricyclic terpene
 20—C₂₃ tricyclic terpene
 21—C₂₄ tricyclic terpene
 22—C₂₅ tricyclic terpene
 23—C₂₆ tricyclic terpene
 24—C₂₄ tetracyclic (Des-E)
 Te—C₂₄ tetracyclic (Des-A)
 25—C₂₈ tricyclic terpanes
 26—C₂₉ tricyclic terpanes
 27—C₂₅ tetracyclic
 28—C₂₇ 18α(H)-trisorneohopane(Ts).
 29—C₃₀ tricyclic terpanes
 T—C₂₇^{25/28,30}-trisorhopane
 30—C₂₇ 17α(H)-trisorhopane(Tm).
 32—17α(H),18α(H),21β(H)-28,30-bisorhopane(C₂₈).
 N—25-norhopane (C₂₉)
 33—C₂₉ 17α(H),21β(H)-norhopane.
 34—C₂₉ 17β(H),21α(H)-norhopane.
 35—C₃₀ 17α(H),21β(H)-hopane.
 37—C₃₀ 17β(H),21α(H)-hopane
 38—C₃₄ tricyclic terpanes
 39—C₃₁ 17α(H),21β(H)-homohopane (22S + 22R).
 40—C₃₀ gammacerane.
 41—C₃₂ 17α(H),21β(H)-bishomohopane (22S + 22R).
 42—C₃₅ tricyclic terpanes
 43—C₃₃ 17α(H),21β(H)-trishomohopane (22S + 22R).
 44—C₃₄ 17α(H),21(H)-tetrakishomohopane (22S + 22R).
 45—C₃₅ 17α(H),21β(H)-pentakishomohopane (22S + 22R).
 46—C₃₈ tricyclic terpanes
 47—C₃₉ tricyclic terpanes

APPENDIX II.

QUANTIFICATION PROCEDURES FOR CHROMATOGRAMS IN THIS CHAPTER

| | |
|--|---|
| 1. $i\text{-C}_{25} + i\text{-C}_{30}$ | Sum of 2, 6, 10, 14, 18- and/or 2, 6, 10, 15, 19-pentamethyleicosane ($i\text{-C}_{25}$) and squalane ($i\text{-C}_{30}$) peak areas in RIC trace and normalized to added sterane standard. |
| 2. β -carotane | Peak area (β) in RIC trace and normalized to added sterane standard. |
| 3. Low molecular weight steranes | Sum of peak area (1+2+3+5) in m/z 217 chromatogram and normalized to added sterane standard (m/z 221 chromatogram). |
| 4. Sterane concentration | Sum of peak areas for 20R 5 α (H), 14 α (H), 17 α (H)-cholestane m/z 217 chromatogram and normalized to added sterane standard (m/z 221 chromatogram). |
| 5. C_{27}/C_{29} sterane | Peak areas of 20R 5 α (H), 14 α (H), 17 α (H)-cholestane (10) over peak area of 20R 5 α (H), 14 α (H), 17 α (H)-ethylcholestane (16) in m/z 217 chromatogram. |
| 6. Diasterane index | Sum of peak areas of C_{27} 20R 13 β , 17 α (H)-diasteranes (6+7) in m/z 217 chromatogram over sum of peak areas of C_{27} 20R and 20S 5 α (H), 14 α (H), 17 α (H)-cholestane (8+10) \times 100. Low, <30; Medium, 30–100; High, >100. |
| 8. 4-Methyl sterane index | Sum of peak areas of all C_{30} 4-methyl sterane in m/z 217 chromatogram recognized using mass spectra and m/z 414 chromatogram over sum of peak areas of C_{27} 20R and 20S 5 α (H), 14 α (H), 17 α (H)-cholestane (8+10) \times 100. Low, <60; Medium, 60–80; High, >80. |
| 9. Hopane/sterane | Peak areas of C_{30} 17 α (H), 21 β (H)-hopane (35) in m/z 191 chromatogram over sum of peak areas of C_{27} 20R and 20S 5 α (H), 14 α (H), 17 α (H)-cholestane (8+10) in m/z 217 chromatogram. Low, <4; Medium, 4–7; High, >7. |
| 10. Tricyclic index | Sum of peak areas of C_{19} to C_{29} (excluding C_{22} , C_{27}) tricyclic terpanes (18–23, 25, 26) m/z 191 chromatogram over peak areas of C_{30} 17 α (H), 21 β (H)-hopane (35) \times 100. Low, <50; Medium, 50–100; High, >100. |
| 11. C_{34}/C_{35} Hopane | Peak areas of C_{34} 22R and 22S 17 α (H), 21 β (H)-hopanes (44) in m/z 191 chromatogram over peak areas of C_{35} counterparts (45). Low, <1; High, >1. |
| 12. Bisnorhopane index | Peak areas of C_{28} 28, 30-bisnorhopane (32) over peak of C_{30} 17 α (H), 21 β (H)-hopanes (35) \times 100 in m/z 191 chromatogram. Low, <10; Medium, 10–50; High, >50. |
| 13. Oleanane index | Peak areas of 18 α (H)-oleanane (X) in m/z 191 chromatogram over peak area of C_{30} 17 α (H), 21 β (H)-hopanes (35) \times 100 in m/z 191 chromatogram. |
| 14. Ts/Tm | Peak areas of 18 α (H)-trisorneohopane (Ts) (28) over peak area of C_{30} 17 α (H), 21 β (H)-trisorhopane (Ts) (30) in m/z 191 chromatogram. |
| 15. Hopane concentration | Peak areas of C_{30} 17 α (H), 21 β (H)-hopane (35) measured in RIC and normalized to added standard. |
| 16. Gammacerane index | Peak areas of gammacerane (40) in m/z 191 chromatogram over peak area of C_{30} 17 α (H), 21 β (H)-hopane (35) \times 100. Low, <50; Medium, 50–60; High, >60. |
| Bisnorhopane concentration | Peak areas of peak 32 measured in RIC and normalized to added standard. |
| Trisorhopane concentration | Peak areas of C_{27} trisorhopane "T" measured in RIC and normalized to added standard. |
| Tetracyclic index | Peak areas of C_{24} tetracyclic over peak of C_{30} 17 α (H), 21 β (H)-hopanes (35) \times 100 in m/z 191 chromatogram. |

Source Rock Occurrence in a Sequence Stratigraphic Framework: The Example of the Lias of the Paris Basin

G. Bessereau

*Institut Français du Pétrole
Rueil Malmaison, France*

F. Guillocheau

*Université de Rennes
Rennes, France*

A.-Y. Huc

*Institut Français du Pétrole
Rueil Malmaison, France*

ABSTRACT

The appraisal of the petroleum potential of a sedimentary basin requires a good evaluation of its source rocks. Sequence stratigraphy appears as a powerful tool for the study of basin-fill histories and is, at present, used for reservoir characterization purposes. Here, we demonstrate that this approach is also a powerful tool for predicting the organic matter distribution by providing a chronostratigraphic framework in which the role of the main parameters controlling its accumulation can be approached.

The study was performed at the basin scale and covers a period of 25 m.y. where different orders of superimposed sequences were identified. It investigated the Lias (Lower Jurassic) of the Paris basin, an interval which is known as the bulk source rock for the oil pools in this basin. It used two methods, both applied on wireline logs: (1) the Carbolog method, which estimates the in-situ organic carbon content of the series, showed that the Liassic series was characterized by strong vertical and lateral variations of total organic carbon (TOC), and by the occurrence of several organic-rich intervals besides the well-known Schistes Carton; and (2) the "stacking pattern" method, which produced a consistent framework of three superimposed sequences which are in keeping with the global transgressive-regressive (T-R) Lias cycle. These are the genetic units (0.1 to 0.4 m.y.) of possible climatic origin, the genetic unit sets (0.6 to 1 m.y.) which might be of eustatic origin, and four minor T-R cycles (5 to 8 m.y.; i.e., the "stage scale") of clearly tectonic origin. The study showed a correlation between the distribution of the organic matter and the sequence stratigraphic framework, at the different sequence orders evidenced

here, and at the basin scale: (1) the organic-rich intervals are associated with the maximum flooding surface (MFS) and more widely with the end of the retrogradation (upper part of the transgressive systems tract [TST]) and the beginning of the progradation (lower part of the highstand systems tract [HST]), *as long as these occur below the storm-wave base (SWB)*; (2) a hierarchy in the organic content of the organic-rich intervals is observed, from the upper sequence order to the lower sequence order; that is, the T-R cycles, where the organic-richest intervals are located; and (3) the organic content of an organic-rich interval is generally correlated to its thickness—there is no condensation of this interval basinward. The study also showed that some exceptions, however, may exist in these documented features. The analysis of these results emphasized the predominant role of factors involved in preservation of the organic matter as well as the role of the hydrodynamic processes, which partly accounted for its lateral distribution. Its complex vertical distribution has been related to the superimposition of the different orders of the depositional sequences. Tectonics was of predominant importance at the T-R cycle scale, in controlling the physiographic patterns and the sedimentation accumulation rates. Consequently, we consider that the application of these “rules” for the prediction of organic matter distribution is probably more or less restricted to the same tectonic settings as the Paris basin; that is, the intracratonic basins.

INTRODUCTION

Understanding source rock distribution is of primary importance in the appraisal of the petroleum potential of a sedimentary basin. However, even in mature basins available data are often fragmentary and unrepresentative. It is now well established that the organic content of sediments is highly variable in time and space. One approach to increase quality and representativeness of information was to develop tools based on wireline log information in order to avoid the bias introduced by sampling policy—for example, outcrops and cuttings (Herron, 1986; Meyer and Nederlof, 1984; Carpentier et al., 1991; Passey et al., 1990; Herron and Le Tendre, 1990). Another approach was to investigate the factors controlling the organic matter sedimentology, one final aim being to decipher the critical factors involved in the deposition of source beds; the roles of preservation (Demaison and Moore, 1980) and productivity (Calvert and Pedersen, 1992) are still widely debated.

Developed over the last few years, sequence stratigraphy appears as a powerful tool for the study of basin-fill histories. The sequences are interpreted as forming in response to the interactions among eustasy, subsidence, and sediment supply (Posamentier et al., 1988; Van Wagoner et al., 1988). This interpretative methodology provides a chronostratigraphic framework for the interpretation of the succession in the sedimentary record. It allows the reservoir geometries to be predicted, and, thus, it is now commonly used for reservoir characterization purposes at various scales.

Up to now, few studies have been devoted to the field of source rocks in a sequence stratigraphic approach. Among the studies including this approach, most refer to high-frequency sequences (Barlow and Kauffman, 1985; Weedon and Jenkins, 1990; Herbin et al., 1991, 1992; Carpentier et al., 1993; Van Buchem et al., 1994). Very few have investigated the organic matter distribution at lower-frequency sequence orders, the problem of the condensed section being one of the main purposes of these studies (Curiale et al., 1992; Pasley et al., 1991; Wignall, 1991). A recent paper proposed a global model for the occurrence of marine and lacustrine source rocks (Creaney and Passey, 1993).

This study examines the distribution of organic matter in terms of sequence stratigraphy at a basin scale and for a period encompassing several tens of millions of years where different orders of superimposed sequences can be identified. It investigates the Liassic sedimentary series in the Paris basin (Figure 1), a typical intracratonic basin essentially of Mesozoic age. The Liassic series is known as the major source rock for the oil pools of the basin (Espitalié et al., 1987). A previous study (Bessereau et al., 1992) showed that it is characterized by strong vertical variations of the total organic carbon (TOC) with several occurrences of organic-rich intervals besides the well-known Schistes Carton of early Toarcian age. This study, by way of a 3-D investigation, evaluates how the organic matter distribution is in keeping in the different sequence orders considered. Concomitantly, it tries to identify and classify the key parameters controlling the organic

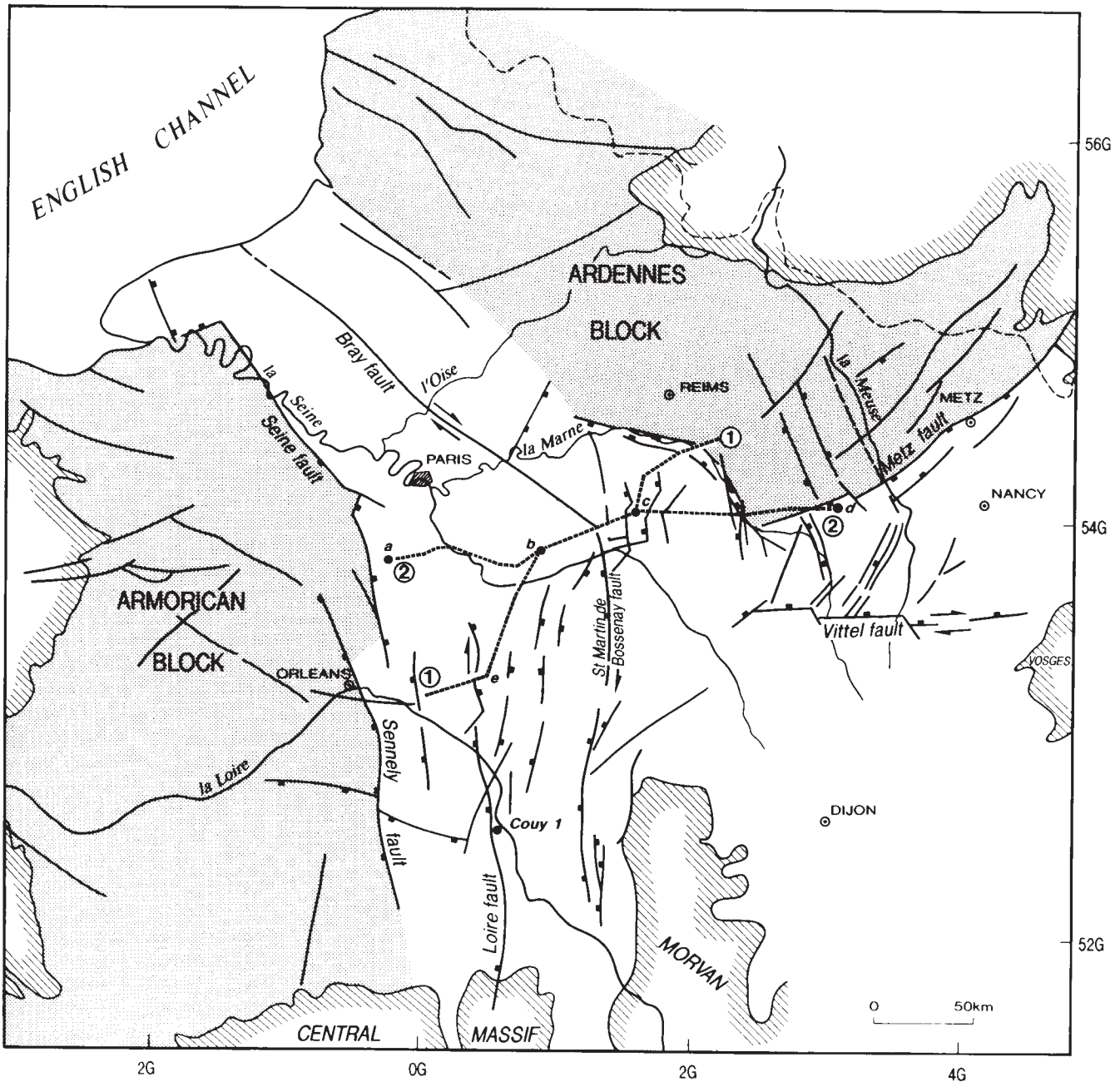


Figure 1. Paris basin: major structural elements; location of the cross sections and the wells of the Figures 6, 10, and 12.

facies in sediments at these different orders of sequences and in this *specific tectonic context*; that is, in an intracratonic basin. Successful approach to such problems might greatly contribute to a more accurate prediction of the organic matter location vertically in the series as well as laterally in the basin.

METHODOLOGY

To obtain a reliable distribution of organic matter in terms of sequence stratigraphy, it is necessary to compare two sets of data of the same resolution. This was achieved using the Carbolog method to estimate the

organic carbon content and the stacking pattern method to identify and classify the different orders of superimposed sequences.

The Carbolog Method

The Carbolog method (Carpentier et al., 1991) estimates the in-situ organic carbon content of the sediment from the combination of two conventional logs, the sonic and the resistivity, assuming that organic matter is characterized by high sonic transit time and high resistivity. To be applied on a basin scale, it requires a calibration based on analytical data in a few wells. The results are presented as continuous logs of

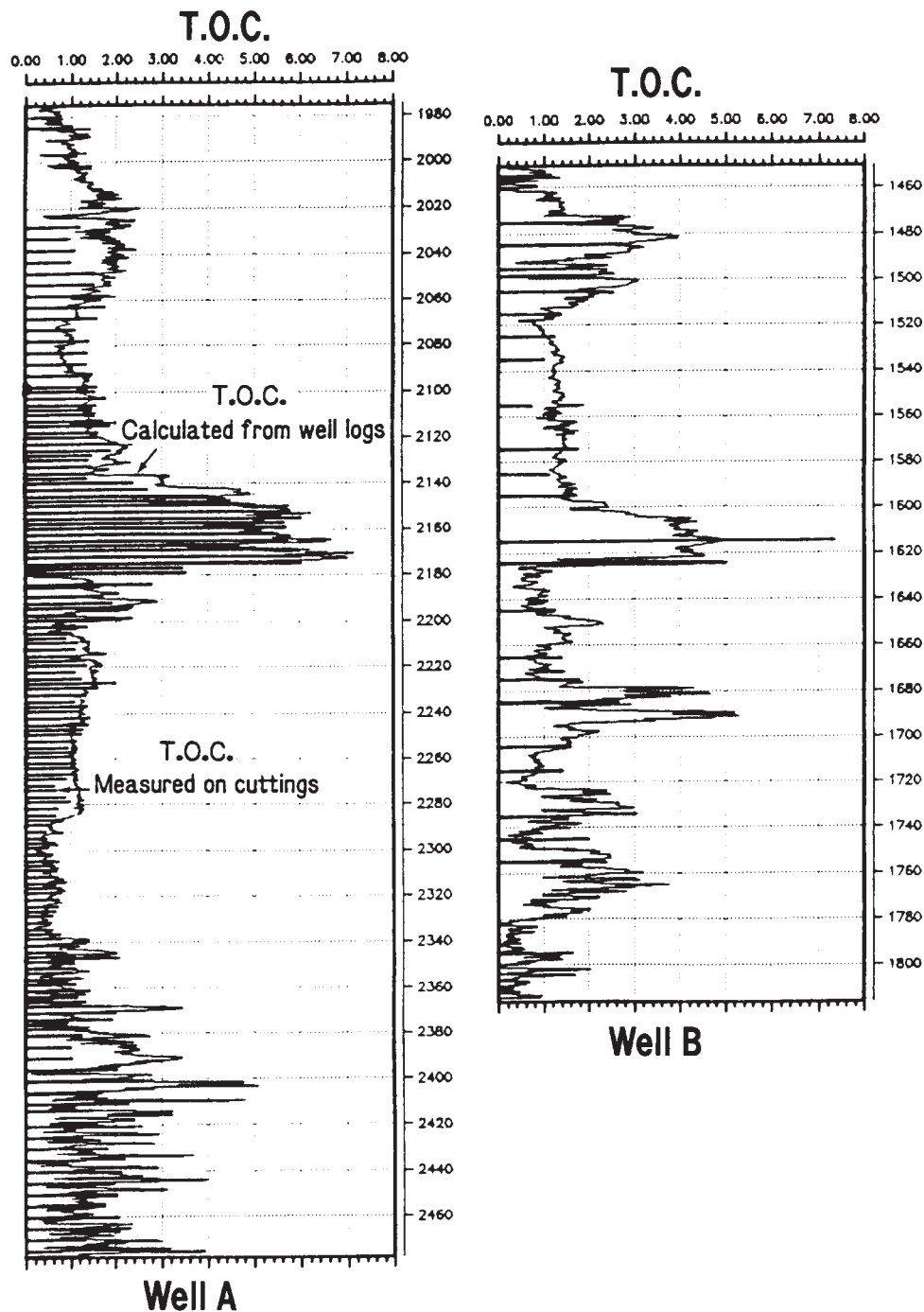


Figure 2. Carbolog method: comparison of the TOC calculated by Carbolog to the TOC measured on cuttings in two representative wells exhibiting very different sampling rates. Scale is in meters.

TOC (in weight percent) (Figure 2). Regardless of which wireline log is used, the density of data from wireline logs is always much higher than that provided by cuttings, on which geochemical analyses (Rock-Eval pyrolysis, for example) are most often performed.

Application of the Carbolog Method to the Paris Basin and Problems Related to Maturity

The TOC calculated from wireline logs is the present-day TOC. In mature areas, a fraction of the

organic matter has been transformed into oil and possibly expelled. Thus, the present-day TOC will not necessarily correspond to the TOC initially deposited; it will have to be corrected if data pertinent to organic sedimentology purpose are required. Furthermore, it has been noticed by some authors (Meisner, 1978; Mann and Muller, 1987) that the organic matter maturation level could affect the wireline log response: for instance, oil present within the source rock increases resistivity and would be

interpreted as an increase of the organic content by Carbolog.

In the Paris basin, it has been demonstrated (unpublished data) that, in the central zone where the lower part of the Liassic series is mature (T_{\max} values up to 450—Espitalié et al., 1987), the calculated TOC values could be considered as corresponding to present-day TOC values. It has also been demonstrated (Bessereau et al., 1992) that only the very central zone of the basin was significantly affected by the present-day/initial TOC correction.*

The Stacking Pattern Method

The stacking pattern method is among the best tools to obtain geometries of depositional sequences by correlation of well data. This method is based on the identification of the smallest stratigraphic units which can be defined on wireline logs and on their vertical stacking. These so-called “genetic units”** (Homewood et al., 1992; Cross et al., 1993) record a full cycle of relative sea level variation. The stratigraphic response is a progradational-retrogradational cycle; that is, in marine environments, a shallowing-upward followed by a deepening-upward variation. Because of well-log resolution and sedimentation rate variations, genetic unit thickness varies, ranging in the Paris basin from 4 to 10 m, and their duration is between tens of thousands and a few hundreds of thousands of years. The genetic units are defined on sedimentological criteria between two deeper facies or two more seaward facies; that is, two maximum flooding surfaces (MFSs). These surfaces can be assumed to be isochronous as they correspond to turn-around periods between progradation and retrogradation at the basin scale.

A stacking pattern study is subdivided into three steps (Figure 3).

1. *Facies characterization and well-log response of genetic units according to the type of sedimentary environment.* These well-log signatures can be deduced from both theoretical models of genetic units (Homewood et al., 1992; Cross et al., 1993) and, mainly, calibrations on cores and outcrops (see below).

2. *1-D stacking pattern of the genetic units.* This is limited by two MFSs (corresponding to two deeper [seaward] facies). Their vertical stacking leads to the definition of lower-order sequences and, thus, to the definition of the general trends—seaward stepping (progradation), vertical stacking (aggradation), and landward stepping (retrogradation)—(Cross, 1988; Michum and Van Wagoner, 1991; Homewood et al., 1992).

* The TOC profiles in this study are either present-day TOC profiles when qualitative approach is sufficient (Figure 10), or initial TOC profiles for more quantitative approaches (Figures 11, 12, 14b and 15a). It must be noticed from the comparison of the most “mature” well (c) in Figure 10 and Figure 12 that the general TOC profiles are very similar.

** These units have not been called genetic sequences as this term has been defined for lower order sequences by Galloway (1989). They are synonymous with parasequences in the common sense of the word (Van Wagoner et al., 1988, 1990) but the parasequences are bounded by flooding surfaces and, thus, are retrogradational-progradational cycles.

3. *Correlation of the 1-D stacking patterns.* Correlation of the 1-D stacking patterns (i.e., the vertical profiles) implies classifying the different orders of depositional sequences and their significant boundaries (MFS, flooding surfaces [FS], and unconformities). These correlations also have to be validated by biostratigraphical information. However, the resolution of these data is less than that from stacking pattern of genetic units.

Application of the Stacking Pattern Method to the Paris Basin and Problems Caused by Occurrence of Organic Matter

Facies identification and calibration with well logs was based on both cores and outcrops. The outcrops are located east and south of the Paris basin as are most of the cores available, including the fully cored Couy 1 well (Gely and Lorenz, 1991; Guillocheau et al., 1992) located south of the basin but which correlates with well e (Figure 1). In the central part of the Paris basin, very few cores are available and the only tools for facies identification were well logs (mainly gamma ray [GR], sonic, and resistivity). Nevertheless, sedimentary facies generally have no direct characteristic well-log signatures. It is only at the genetic unit scale that well-log trends can be assumed to be characteristic of sedimentary environments. This well-log response at the genetic scale differs according to the type of rock (marine or continental) preserved during different periods of relative sea level change (progradational or retrogradational). This is called volumetric partitioning (Cross et al., 1993). Consequently, there is a tendency for increased sediment preservation during progradation in marine environments and during retrogradation in continental environments.

Within the studied area, the marine environments from the shoreface to the lower offshore (i.e., below storm-wave base [SWB]) were dominant from early Sinemurian to late Toarcian. These genetic units are dominated by progradational shallowing-upward trends. In the lower offshore, they are essentially made up of clays with slightly increasing upward marl content with occasional limestone condensed strata on top. This is recorded in well logs as a homogeneous trend of high radioactivity and low resistivity (Figure 4, log A). In upper offshore (below fair-weather wave base), the genetic units consist of thickening-upward marl/clay alternations of storm deposits. They are clay-rich in the lower or distal part and limestone dominated in the shallow or proximal part. On well logs, they exhibit a typical funnel-shaped pattern on the GR, sonic, and resistivity logs (Figure 4, logs B and C). In the shoreface, sediments are only made up of more or less terrigenous bioclastic sands due to permanent wave winnowing. A homogeneous trend of low radioactivity with small vertical variations in porosity is generally related to this facies (Figure 4, log E). In the Liassic series, the MFSs, which correspond to maximum water depth are, thus, expressed by maximum shale content.

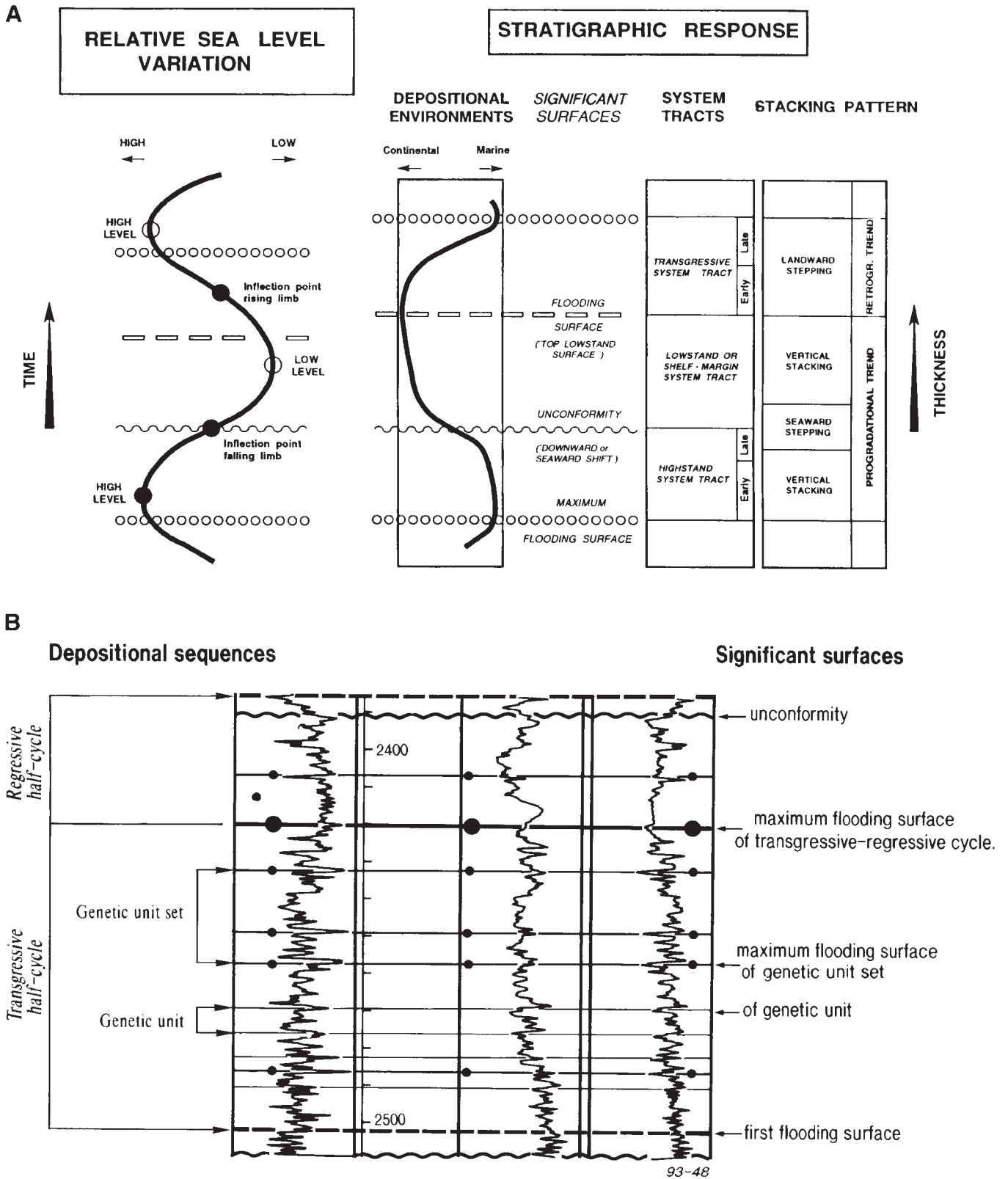


Figure 3. The basic principles of the stacking pattern method. (A) The stratigraphic response of a cycle of relative sea level variation (significant surfaces, relationship between systems tracts and stacking pattern). From Homewood et al., 1992. (B) Depositional sequence classification based on well logs (with the symbols identified for use in all figures).

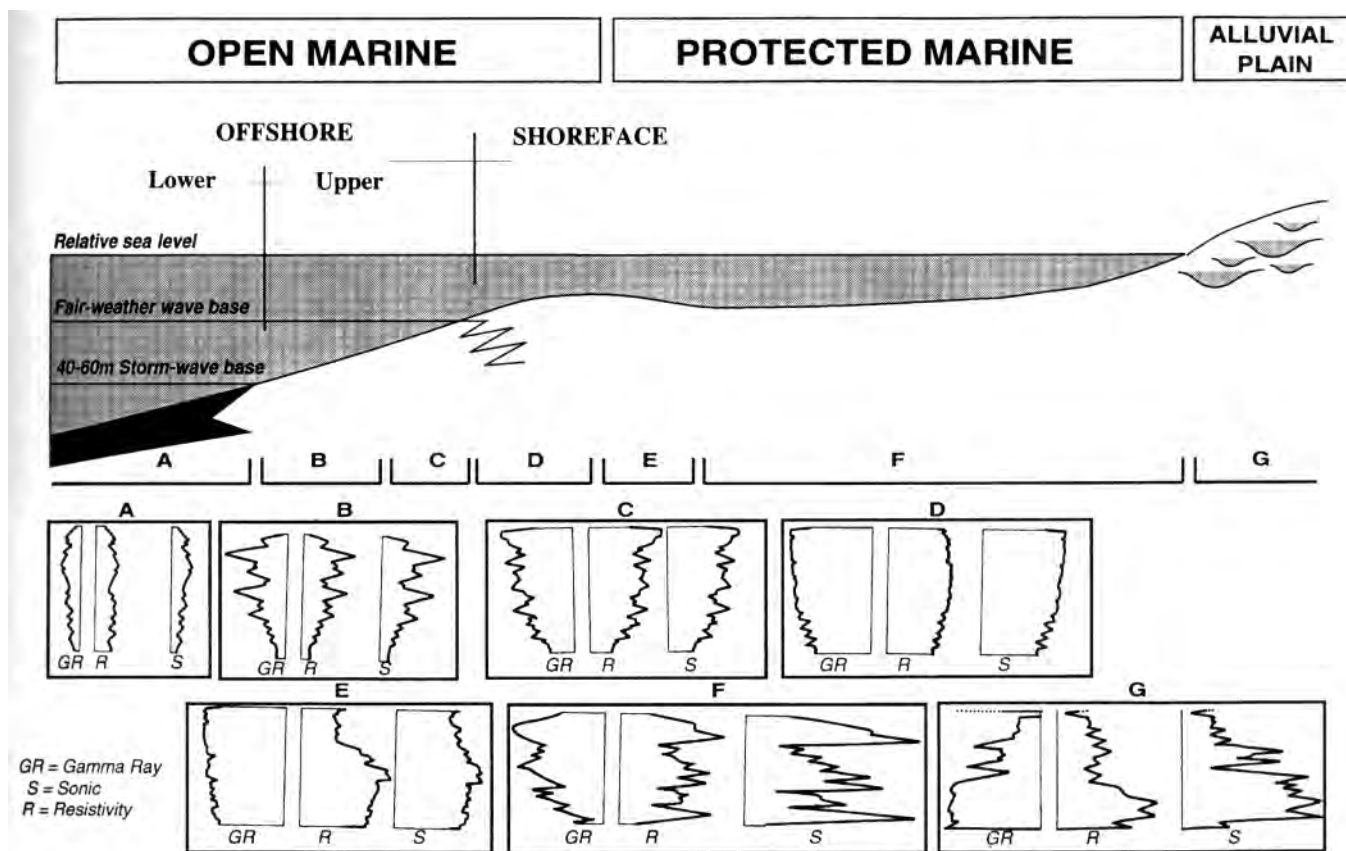


Figure 4. Typical wireline-log responses in the different depositional environments of the Liassic series.

The log patterns as defined above for marine shelf sediments are valid only if there is no organic matter present. Its presence modifies the log responses by increasing resistivity and sonic transit time. The GR response should, theoretically, not be altered because the radioactivity is not a physical property of the organic matter. In that case, the GR could be used alone as an indicator of shale content regardless of the presence of organic matter. In fact, there is a complex relationship between organic matter and radioactivity, but it is indirect and primarily due to uranium, thorium and potassium preferentially reflecting the proportion of shales (see discussions in Serra, 1984; Myers and Wignall, 1987).

The contribution of the three elements to the GR response was examined in the very few wells where an NGT was available, in order to discriminate between uranium and thorium-potassium. In the well shown on Figure 5 (located in the western part of the studied area), the CGR-SGR, thorium, potassium, and uranium logs are plotted with the TOC from the Carolog evaluation of the early and middle Lias interval. The total GR (SGR) is mainly dependent on the variations of thorium and potassium, as uranium is subordinate. In this predominantly carbonate-shale interval, the GR reflects primarily the variations in shale content, the less radioactive beds corresponding to car-

bonates. The FS (S1, L4, C6)* correspond to the base of increasing-upward shaly content intervals, whereas all the MFSs (H2, L1, C1, and D4) but one (D2) correspond to maximum shale content. It is also the case for the MFS of higher-order sequences like S1 to L2. The MFS D2 might be considered as a partial exception to this rule as the GR response is predominantly influenced by a high uranium content. This complex GR response is likely due to development of reducing conditions within a shaly depositional environment.

The above discussion demonstrates that, in this interval, the genetic units can be defined with confidence regardless of the organic matter content. Consequently, *comparisons can be made between the sequence stratigraphic framework and the occurrence of organic matter.*

In the Schistes Carton formation (early Toarcian), organic matter influences the resistivity and sonic responses. It has been shown by different studies, among them a study on the Jet Rock of Yorkshire (Myers and Wignall, 1987), that the total GR response is complex: in this interval, which is made up of calcareous shales, the response results from the combination

* All the surfaces are numbered to facilitate the discussion. The letters refer to their age, and the numbers are serial, without any reference to the type of surface.

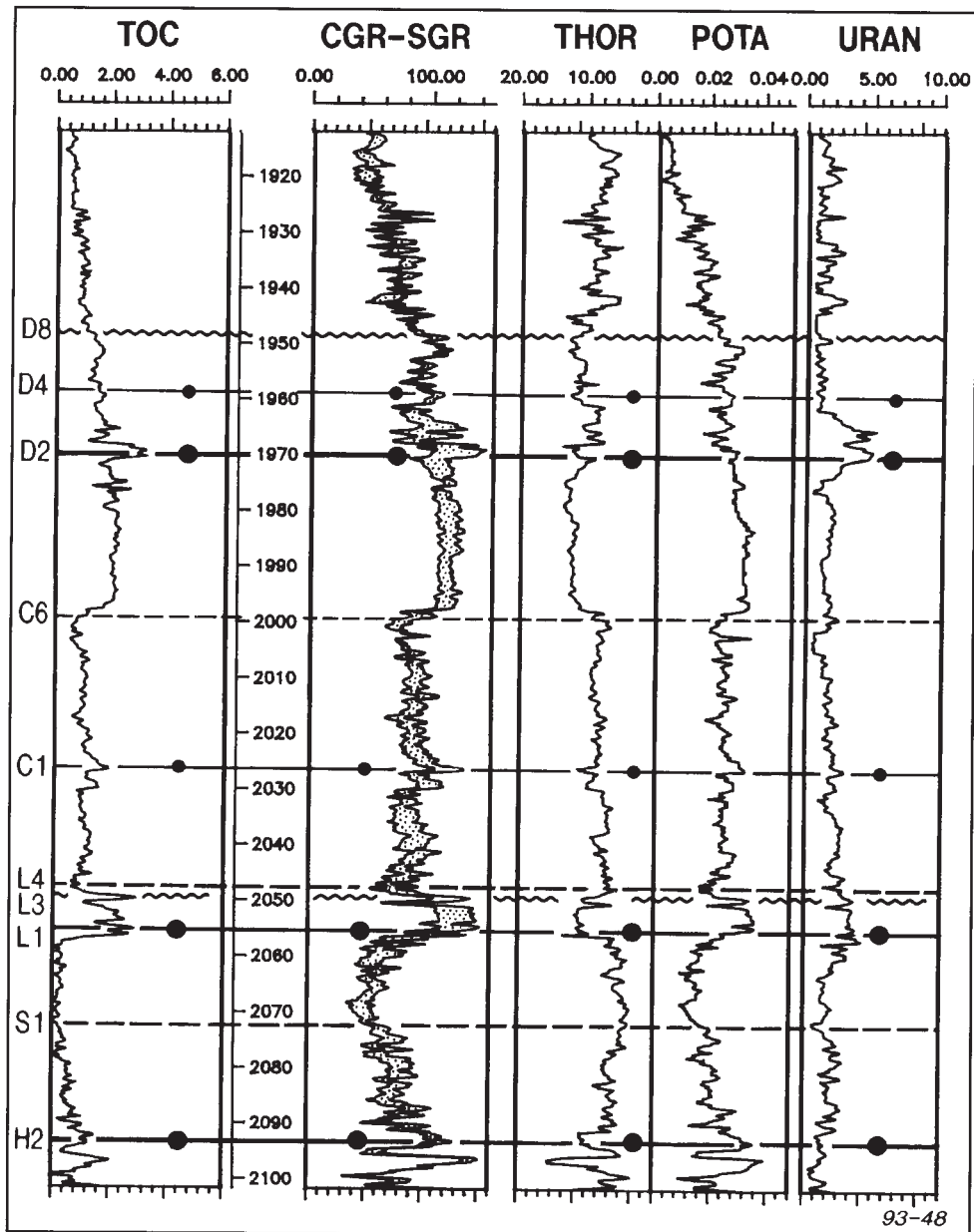


Figure 5. Comparison of a TOC log to the GR spectral response in the lower and middle Lias. See text for explanation of terms. Scale is in meters.

of variations in the clay fraction relative to the carbonate fraction (generally decreasing upward), and the predominant influence of uranium. Nevertheless, as shown in the four wells, several tens of kilometers apart, on the west-to-east cross section (Figure 6), the early Toarcian exhibits rather similar log patterns which may be interpreted as homogeneous vertical evolution of the depositional conditions. The correlation of these patterns, well by well and step by step, allowed the identification of surfaces T2 and T3; the T2 was placed at the top of a bed of low GR and sonic values, and the T3 was located at the first upward maximum of the GR. In the latter, this MFS cannot definitely

be interpreted as maximum shale content, but much more likely as corresponding to maximum anoxia.

In the Paris basin, the stratigraphic sequences were tentatively dated using ammonite zonation from the outcrops east and south of the basin, the Couy 1 stratigraphic well (Gely and Lorenz, 1991; Guillocheau et al., 1992), and scattered cores of old wells compiled by Serra (1971). That allowed reasonable durations to be proposed for the lowest-order sequences defined in this study and for some higher-order sequences. However, because of the heterogeneity and the scarcity of the data, the accuracy level was, in most cases, the ammonite zone, more rarely the ammonite subzone.

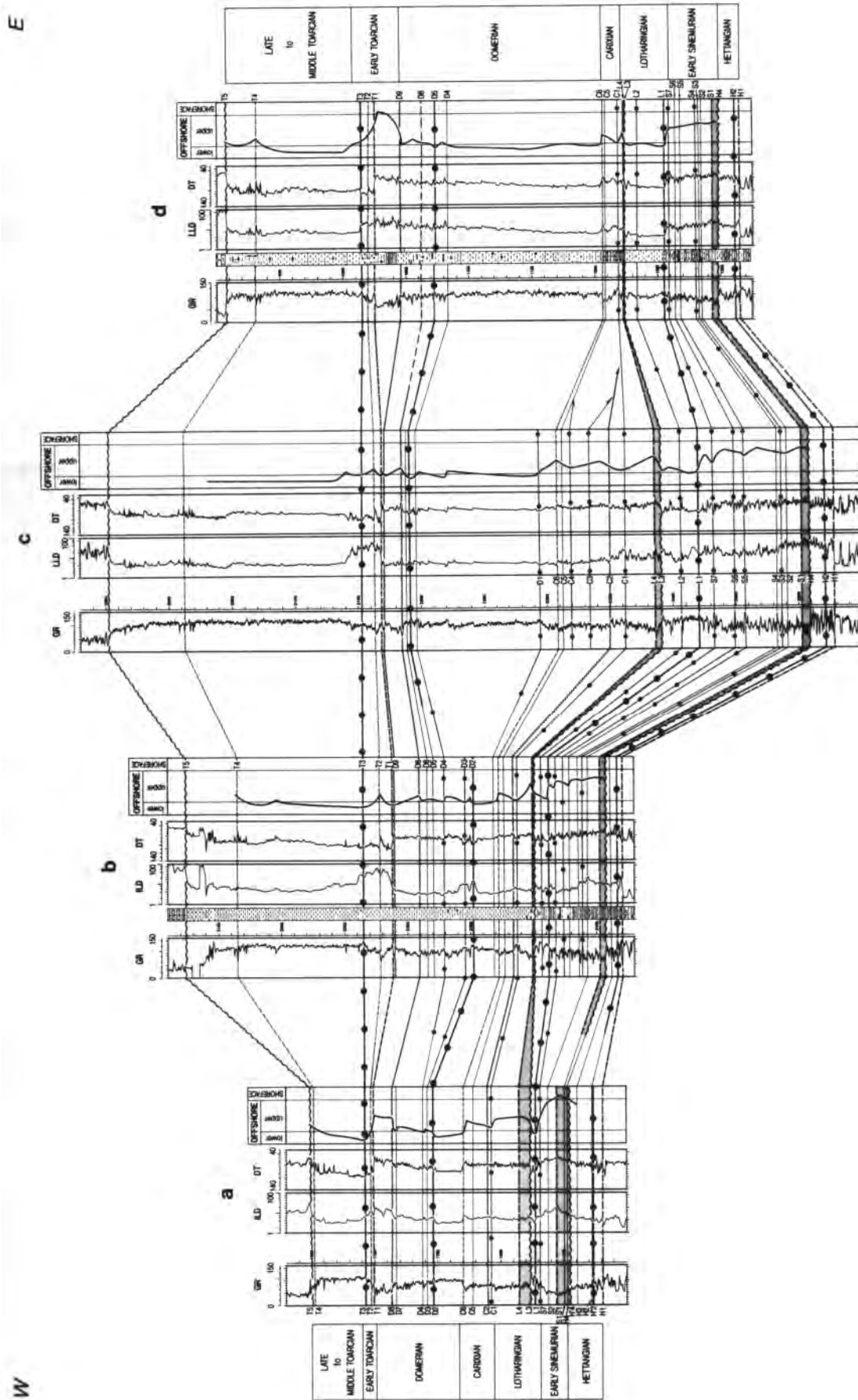


Figure 6. Cross section 2: logs from four representative wells showing the division of the Lias into the different order sequences and the depositional environments. The significant surfaces correspond to the minor T-R cycle order and the genetic unit set order. All of the genetic unit set surfaces are traced in the Sinemurian; in the Pliensbachian, only the most important or significant are drawn; only one appears in the middle-late Toarcian. (For the symbols of the significant surfaces, refer to Figure 3.) The MFS T3 is the datum. Vertical scale is in meters.

THE GEOLOGICAL AND GEOCHEMICAL SETTING OF THE PARIS BASIN

Geological Setting and Contributions of Sequence Stratigraphy

The Paris basin originated during the Permian–Triassic extensional phase (Perrodon and Zabeck, 1991) and developed over three major basement blocks—Ardennes, Morvan-Vosges, and Armorican massif—limited by major fault systems—Bray fault, Seine-Sennely fault, and St. Martin de Bossenay and other meridian faults (Figure 1). During the Lias, the faults were reactivated and the basin was down-warped in response to the geodynamic events which affected the areas bordering the basin (Tethys and Atlantic).

Previous study (Guillocheau, 1991) identified six major Mesozoic transgressive-regressive (T-R) cycles, corresponding to phases of acceleration of the subsidence. The Lias makes up the greater part of the third cycle, the Norian–Toarcian. This cycle was largely dominated in time as well as in volume by its transgressive phase which extended from the end of the Carnian to the early Toarcian. During this period, the sea progressed westward along the Ardennes massif which remained as an emergent northern edge. The sea progressively transgressed the Armorican block, first to the NNW until the Carixian, then to the southwest since the Domerian; the Massif Central was flooded since the early Sinemurian. The sediments were deposited in a continental to restricted marine environment during the Hettangian, rapidly grading upward into marine environments, from shoreface to lower offshore, during Sinemurian and Pliensbachian ages. The maximum transgression corresponds to the deposition of the Schistes Carton of early Toarcian age. The regressive phase is much shorter and ended with shaly to sandy clastics deposited in upper offshore to more and more proximal facies. The total thickness of the series never exceeds 600 m and the subsidence rates are moderate (<40 m/Ma), as expected for such an intracratonic basin. During the whole Lias, the climate was humid (Hallam, 1984), probably tropical (Rioult, 1968).

This sequence stratigraphic approach led to the definition of three orders of superimposed sequences within this major T-R cycle (from higher to lower frequency): (1) the genetic units, (2) the genetic unit sets (equivalent to parasequence sets of Mitchum and Van Wagoner, 1991), and (3) four so-called “minor” T-R cycles. The results will be discussed with reference to two cross sections (west to east and southwest to northeast), which cover the major tectonic features of the basin (Figure 1): the former cross section starts in a weakly subsident zone, the latter cross section runs through the set of longitudinal faults south of the basin, and both cross the Bray fault, the northward prolongation of the St.

Martin de Bossenay fault and the Marne faults. Due to lack of wells appropriate for Carbolog treatment, these cross sections only partly cover the major paleogeographic features, as they never reach the coastal areas.

1. Defined as the smallest traceable units at the basin scale, the genetic units (Figure 3B) do not always correspond to the same absolute duration nor to the same order value. They range from 0.1 to 0.4 m.y. in duration. Where the series is thickest, they can be subdivided into four or five smaller units. According to this duration and this ratio of superimposed higher-frequency sequences, they are comparable to Milankovitch cycles. Thus, they are of possible climatic origin (glacio-eustatic and/or fluctuation of carbonate productivity). They correspond to fourth to fifth order in Vail’s nomenclature (Vail et al., 1991).

2. The genetic unit sets (Figure 6) are made up of a varying number of genetic units arranged in progradational and retrogradational cycles, and they are bounded by two MFSs. They have a duration ranging from 0.6 to 1 m.y. and, consequently, they record sub-periodic cyclic variations of relative sea level. They could be of eustatic origin, and they correspond to third to fourth order in Vail’s nomenclature (Vail et al., 1991).

3. The four T-R minor cycles, bounded by FSs, result from the stacking of the previous sequences which are disposed in large cycles of increasing depth (transgressive phase), then decreasing depth (regressive phase) (Figures 6, 7, and 8). The first three cycles (Hettangian, Sinemurian, and Pliensbachian*) are strongly dominated by their transgressive phase (up to two times longer than the regressive phase), the fourth (the Toarcian cycle) is dominated by its regressive phase (Figure 9). This asymmetry also finds expression in significant thickness variations of the series, from a few tens to a few hundreds of meters.

The total duration of these cycles ranges from 5 to 8 m.y.; it is the “stage scale.” They correspond to the second order cycles in Vail’s nomenclature. They are clearly of tectonic origin. The southwest-northeast cross section (Figure 7) shows strong lateral thickness variations associated with the major faults in each cycle and shift of the depocenters from one cycle to another. It substantiates that the variations in the subsidence regimes inside the different tectonic blocks and the reactivation of the major basement faults which limit them are the main factors controlling the basin evolution at this order. These features are, presumably, a result of tectonic stress regime changes in the Paris basin. In contrast, the early and probably the middle Toarcian is characterized by a generally more homogeneous subsidence regime of flexural type within the whole basin, with only very minor lateral

* To make the discussion easier, the minor cycles will be given the name of the stage they mostly coincide with, even if their limits do not fit exactly with the standard stage limits.

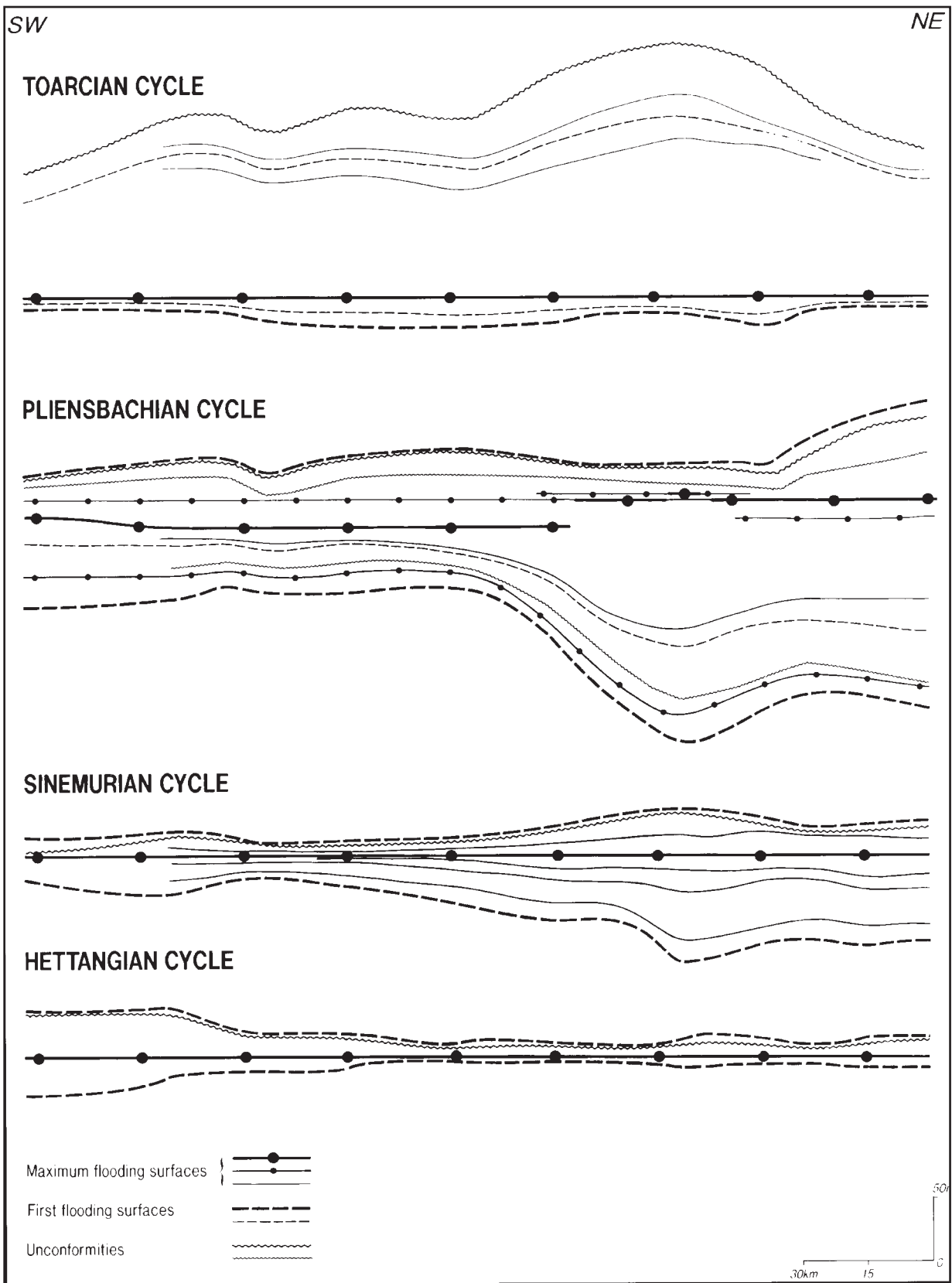


Figure 7. Schematic representation of the structural evolution, cycle by cycle, along cross section 1. The major MFS has been taken as the datum, assuming that, along the cross section, the variations in water depth can be reasonably considered as negligible with respect to the thickness variations of the undercompacted series.

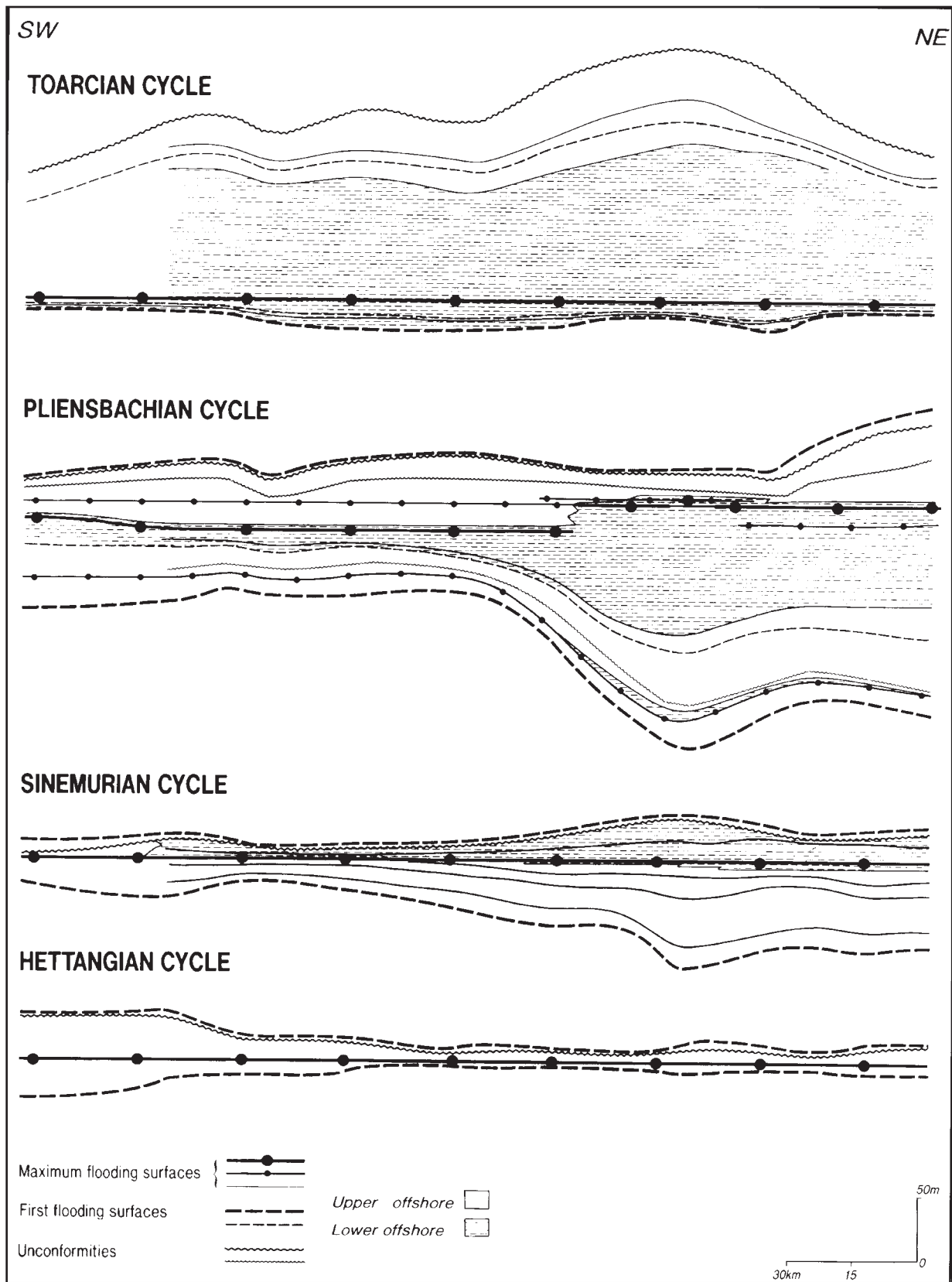


Figure 8. Schematic representation of the depositional environments, cycle by cycle, along cross section 1.

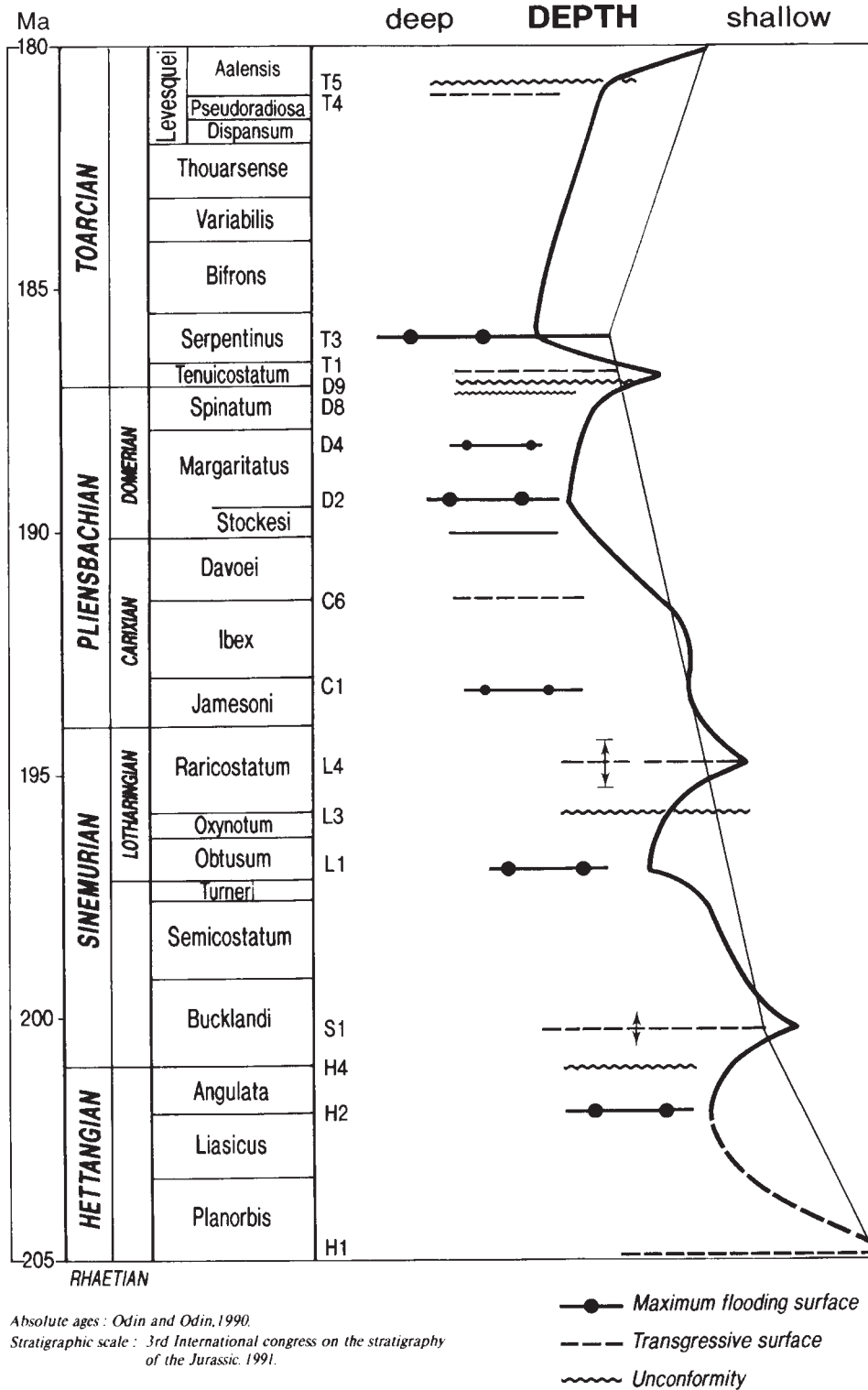


Figure 9. The four T-R minor cycles stacked within the Lias cycle.

variations. The faults are no longer active and the Schistes Carton onlaps both sides of the basin. The Toarcian T-R cycle ends with a disconformity with erosion of clearly tectonic origin, which marks the base of the next major T-R cycle of Bajocian–Bathonian age.

The maximum water depth of the Pliensbachian cycle occurred later in the northeast part of the basin

(near the top of *Margaritatus* zone—MFS D4/D5) than in the western area (top of *Stockesi* subzone (i.e., base of *Margaritatus* zone—MFS D2). This suggests a shift in time of the MFS of this T-R minor cycle which implies a decoupling in the tectonic regime of the blocks on either side of the Bray and St. Martin de Bossenay faults.

The Paris basin is also characterized by the lack of lowstand systems tract (LST) or shelf margin wedge during most of the Lias. A LST is only developed in the Pliensbachian cycle in the northeastern part of the basin, which originated in the tectonic decoupling previously invoked for the shift of the major MFS in this cycle (see discussion in Bessereau and Guillocheau, 1994).

Conclusions

As expected from this methodology, this study resulted in a consistent framework of superimposed sequences. Three orders were identified within the 25 m.y. duration T-R cycle of second order. This study, thus, resulted in a consistent chronostratigraphic framework for the Liassic series.

Although tectonics obviously control the minor T-R cycles, MFS can be considered as synchronous at basin scale during the Sinemurian and at the beginning of the Pliensbachian (its influence is very difficult to precisely estimate in the Hettangian as the series is very condensed). In the Sinemurian, it is essentially limited to condensation of the higher-order sequences in the weakly subsident zones or, to the contrary, to their development in the more subsident areas. Consequently the MFS of the Sinemurian cycle (L1) as well as most of the MFS of the genetic unit sets (S5, S6, S7, and L2) are considered as synchronous at the basin scale—the L1 is dated as the base of the *Stellare* subzone (base of *Obtusum* zone). This regime was still prevailing at the beginning of Pliensbachian cycle, up to the MFS C1, dated at the *Brevispina* subzone age. Above, the tectonic factors became dominant and controlled the vertical location of the Pliensbachian MFS from one tectonic block to another; consequently, this surface is no more synchronous at the basin scale, even if it is still expressed as the MFS of a higher-order sequence. In the early Toarcian, the faults were no longer active: the MFS T3, dated within the *Serpentinus* zone, which is also the maximum of the Lias transgression, can be considered as synchronous not only within the Paris basin but also in the northern European plate subjected to the global geodynamic events mentioned above.

This study also led to a more accurate approach to the physiography of the basin, which is important for organic matter sedimentology study.

The general morphology of the Paris basin was typical of epicontinental seas with shallow depths and with ramp-type margins. During the early and middle Lias, no sharp topographic variations were recorded in the profile of the basin: higher-order surfaces within each cycle do not present any progradational patterns (lack of downlaps), and variations of the depositional environments are recorded only from the shoreface to the lower offshore (Figures 7 and 8). Due to its general flexural pattern, the topography during the early Toarcian was also rather smooth; however, at the Domerian–Toarcian boundary, the presence of two “highs”—the first of limited extent located immediately east of Paris, the second approximately trending north-south from Reims to Dijon (Figure 14A)—is strongly suspected; the thinning of the overlying interval T1-T2 (wells a and d—Figure 6)

could represent the onlapping of the Schistes Carton facies onto these highs.

It can also be inferred from the depositional patterns that there is no development of a condensed section, in Exxon's model sense, in the basin center. Exxon's model postulates the development of a condensed section within the transgressive and distal highstand system tracts, related to the terrigenous supply starvation of the basin (Van Wagoner et al., 1988). Here, downlap geometries are absent and the sequences are dominantly aggrading in the basin centers, where they reach their maximum. Distal starvation may not have occurred here due to the relatively small width of the basin where fine sediments could readily reach the center.

Organic Matter in the Lias and Contributions of the Carbolog Method

Very few geochemical results have been published on the Lias of the Paris basin except the study by Espitalié et al. (1987) and a few papers on more limited areas and periods of time (Huc, 1976; Thomas, 1977; Hollander et al., 1991). The study by Espitalié et al. (1987) is a survey of the organic matter in the Lias in terms of TOC distribution and organic matter type characterization. The Schistes Carton formation was chosen as the standard reference for marine organic matter (type II of Tissot et al., 1974). The analyses performed on kerogens of other Liassic intervals concluded that the organic matter is of the same marine origin.

The Carbolog method was applied to assess the distribution of organic matter in the Liassic series of the Paris basin (Bessereau et al., 1992). This study confirms the results previously obtained. Along the southwest-northeast cross section (Figure 10), more than 200 km long, the TOC profiles show:

- strong vertical variations of TOC from less than 1% (part of Carixian, Domerian, and middle Toarcian) to almost 8% (Schistes Carton), within this 300 to around 600 m thick interval;
- the occurrence of three main organic-rich intervals besides the well-known Schistes Carton (early Toarcian): (1) the Lotharingian interval, (2) an interval near the base of the Carixian, and (3) a doublet of high TOC layers within the Domerian. All of these organic-rich intervals but one—the Domerian doublet—are continuous over the basin, with variations in thickness and in organic matter content. However, these lateral variations are of lesser amplitude when compared to the vertical variations.

These main basinal-scale results can be made up of smaller-scale observations, among them (Figure 11): the rapid alternation of organic-poor and organic-rich beds which characterize the early Sinemurian, the vertical complexity of the TOC pattern in the Lotharingian interval accompanied by significant lateral changes in the more distal wells (d for instance), the homogeneous pattern of low TOC in the Carixian interval, and the impressive uniformity of the lower part of the Schistes Carton

with, especially, the constant occurrence of an organic-poor bed near their base.

Thus, the Lias is characterized by a complex and varied distribution of its organic matter content. This complexity is much greater vertically than laterally. Moreover, this happens at the different scales of observation. This pattern does not really fit with a simple scheme of recurrent patterns of TOC proposed by Creaney and Passey (1993). At the basin scale (Figure 10), the repetitive occurrence of organic-rich beds is recognized within the early and middle Lias. However, these recurrent intervals exhibit different patterns in terms of TOC profiles. It should be noted that the Schistes Carton, which has been taken as representative of the so-called HTB ("highest TOC bed"—Creaney and Passey, 1993), is clearly not representative of the general pattern as it appears from the set of TOC profiles.

THE ORGANIC MATTER IN THE SEQUENCE STRATIGRAPHIC FRAMEWORK

The examination of the organic matter distribution relative to the sequence stratigraphic framework is made by simple superimposition of the sequence boundaries on the TOC profiles. This has been performed for the four T-R minor cycles and the genetic unit sets which offer an appropriate observation scale, compatible with a basinwide-scale study in the context of a low subsidence basin where the series is relatively thin. Two main types of results are obtained:

This approach provides a precise chronostratigraphic framework to the distribution of the organic matter. Whereas age dates in wells are often scarce or absent, this approach provides a homogeneous and dense set of age dates based on synchronous significant sequence surfaces. This allows chronostratigraphic correlations to be proposed at the basin scale with confidence for all the TOC values and especially for the organic-rich intervals. This, hence, allows interpretations in terms of organic matter depositional history.

This approach allows, then, the organic matter distribution to be examined in terms of sequence stratigraphy. Figures 10–12 provide clear evidence that the organic matter is not randomly distributed neither vertically in the series nor laterally in the basin, but is in keeping with the sequence stratigraphic framework defined in this study. Three main features are noted:

1. The organic-rich intervals roughly correspond to the MFS at all scales of cycles.
2. There are a few noticeable exceptions.
3. The organic content of an organic-rich interval is roughly correlated with its thickness.

These results will be successively discussed and compared to the present state of knowledge in organic sedimentology.

Organic Matter and MFS: The Role of Water Depth

The correlation between organic-rich intervals and MFS is well documented along the two cross sections (Figures 10 and 11) and thus, at the basin scale, for the MFS of minor T-R cycle order (H2, L1, and T3) as well as for the MFS of the genetic unit set order (S3, S5, S6, S7, L2 within the Sinemurian cycle, and C1 in the Carixian cycle). It is also well documented for the MFS of the Pliensbachian cycle, but only in the southwestern part of the basin (D2). In contrast, there is no organic matter associated with this MFS in the eastern and northeastern areas (D4/D5). In addition, there is no organic matter associated with the MFS C3 and C4 (Carixian age) or the MFS of D4 (Domerian age) in the southwestern area. All these organic-rich intervals exhibit lateral variation in thickness and in organic content.

More generally, the organic matter content follows a typical trend of vertical evolution, increasing from the FS up to a maximum in the late stage of retrogradation (i.e., end of the transgressive system tract [TST]) and early stage of progradation (i.e., beginning of highstand system tract [HST]). This is valid for the two sequence orders but is better expressed at the lower frequency; for example, in the Sinemurian cycle. The genetic unit set order is illustrated, for instance, by the MFS C1 and its underlying interval (L4-C1). This trend, well documented in the early and middle Lias, occurs within the Toarcian cycle, but with some specific differences. The whole TST is very organic rich, starting systematically at a very high TOC (values up to 8%) which marks a major break with the underlying organic-poor Domerian. Within this system tract, a continuous bed of low TOC is developed. It corresponds to a well-identified carbonate interval at the *wireline-log scale*. It has been interpreted as a sedimentary event of global character that is synchronous at the basin scale, and its top is identified as a FS (T2). Above the major MFS, the lower section of the HST exhibits various patterns of decreasing TOC which occur within a more or less thick interval.

Still considering the vertical trend of TOC, it can be noticed that, within the Lias cycle, the average TOC values associated with the MFS of each minor T-R cycle increase from the MFS L1 to the MFS D2 and up to the MFS T3, which is the MFS of Toarcian cycle. This MFS also corresponds to the maximum transgression in the Lias cycle. The TOC exhibits the same pattern at the genetic unit set order. Within the Sinemurian cycle, for instance, TOC is progressively greater from S2 to S4, to S7, and up to the MFS L1. This MFS also corresponds to the MFS of the minor T-R cycle of Sinemurian age. Thus, the sequence hierarchy seems to be reflected in the organic matter distribution. In other words, the amount of organic carbon stored in a sequence could be determined by the position of this sequence within the lower-order sequence.

Discussion

We suggest, as discussed hereunder, that these features can be interpreted with regard to two factors: the location of the sediments with respect to the SWB, and

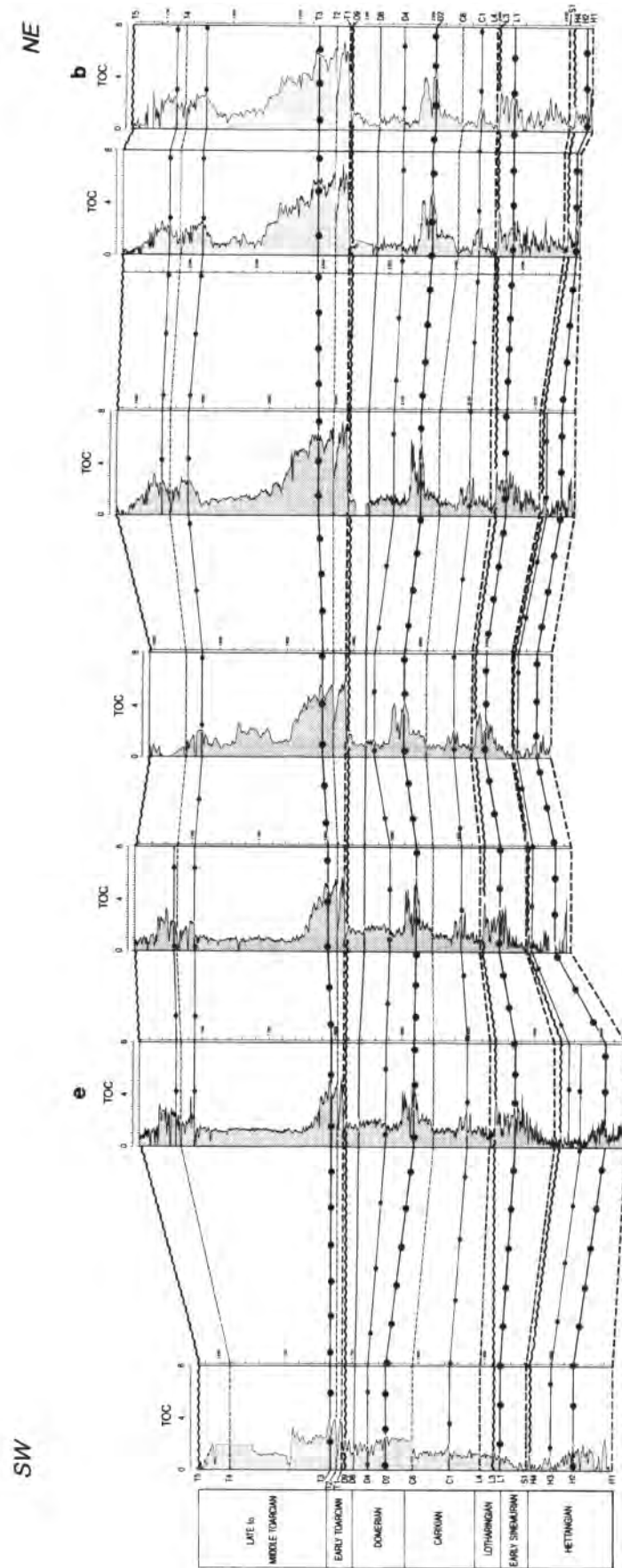


Figure 10. Organic matter distribution (present-day TOC) in the sequence stratigraphic framework along cross section 1 (for the symbols of the significant surfaces, refer to Figure 3). The FS T1, which can be identified from wireline logs prior to any interpretation, has been chosen as the datum. Vertical scale is in meters.

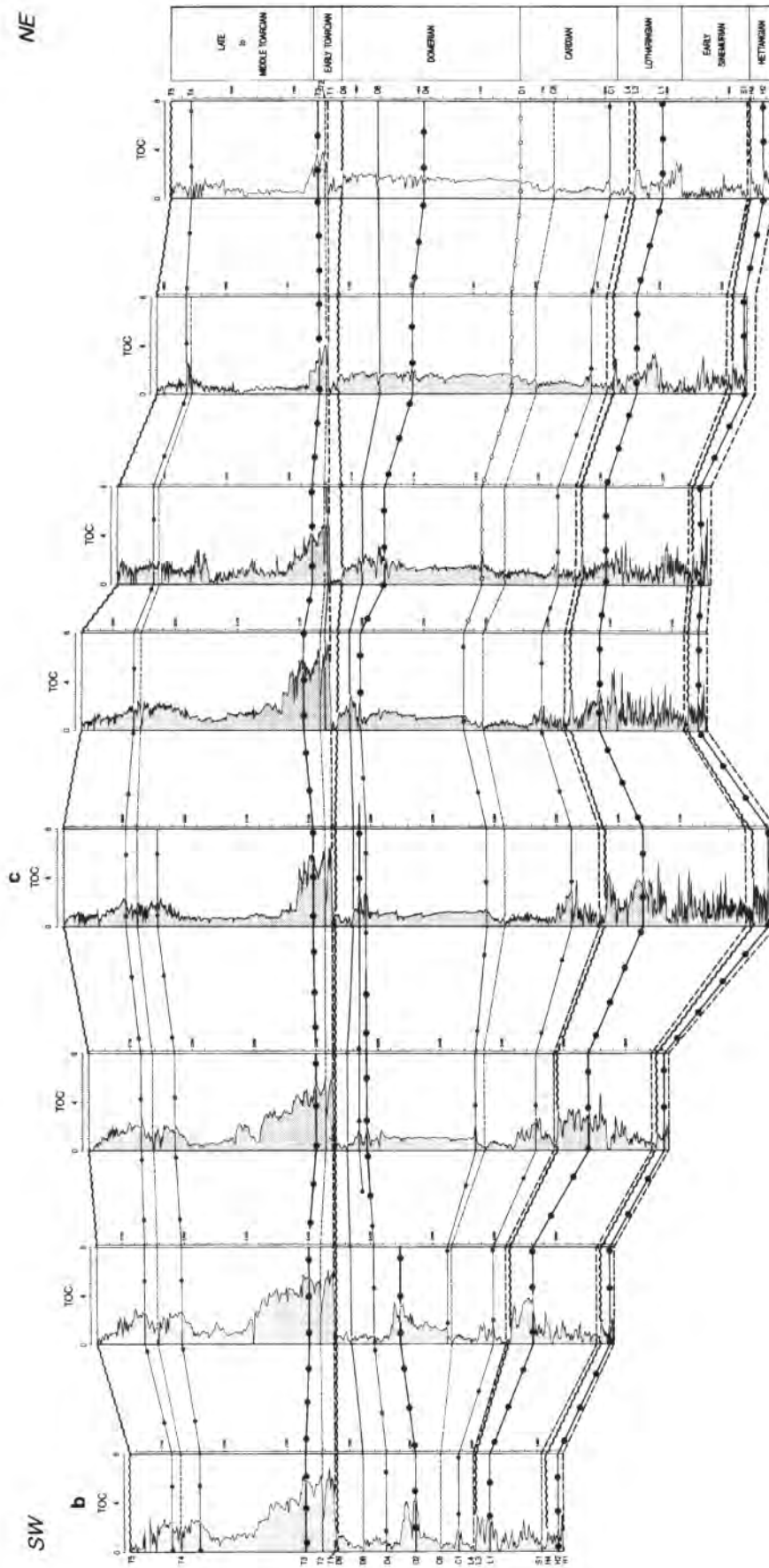


Figure 10 (continued).

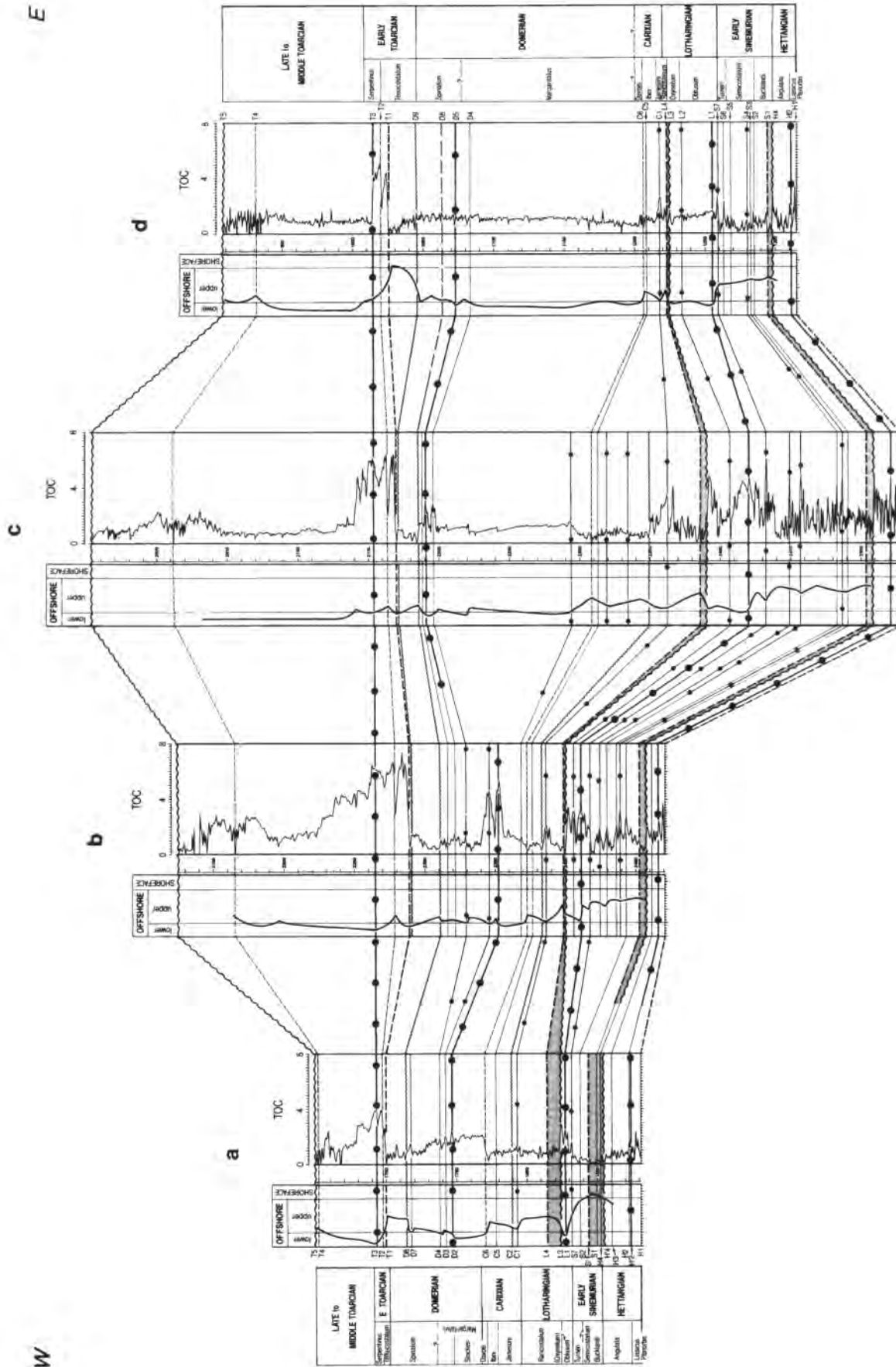


Figure 11. Cross section 2: logs from four representative wells showing the organic matter distribution (initial TOC) in the stratigraphic framework and the depositional environments (for the symbols of the significant surfaces, refer to Figure 3). The MFS T3 has been chosen as the datum. Vertical scale is in meters.

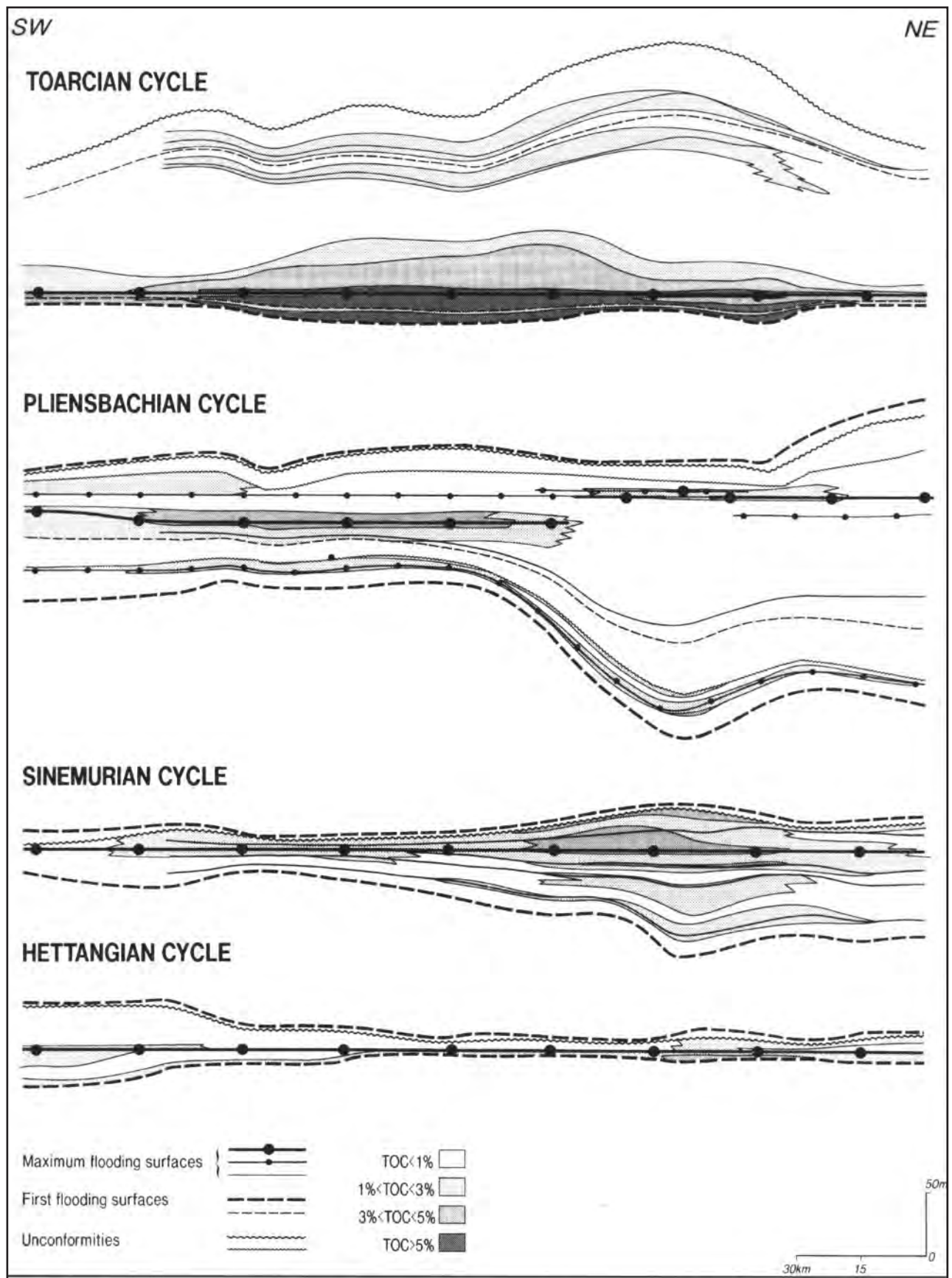


Figure 12. Schematic representation of the organic matter distribution cycle by cycle (initial TOC), along cross section 1.

the degree of oxygen deficiency. The occurrence of organic matter is related to sediments deposited below the SWB which directly depends on the water depth. Moreover, the organic content is interpreted, in this sedimentary interval, as mainly governed by the degree of oxygen deficiency, which in turn is proposed to be primarily controlled by water depth.

From Sinemurian to late Toarcian, sedimentation occurred in a shallow epicontinental sea, characterized, according to sedimentological data from outcrops and cores, by a "zero" fair-weather energy and low storm-wave energy (F. Guillocheau, 1994, personal communication). The SWB was, thus, a major hydrodynamic boundary which separated the upper offshore (dominated by waves and currents ensuring oxygenation in the water column and at the sea bottom) from the lower offshore (where the effects of storms are weak to absent). Consequently, it is a significant boundary for the occurrence of organic matter which can be preserved only if sediments were deposited below the SWB. Comparison of organic matter occurrence to the depositional patterns (Figures 8, 11, 12) demonstrates that all the organic-rich intervals actually correspond to sediments deposited in the lower offshore, whatever their facies—mixed terrigenous-carbonate deposits during Sinemurian, terrigenous (silt dominant) during early Pliensbachian, and marls to shales during Toarcian. This situation is encountered at the MFS and more widely at the end of retrogradation and the beginning of progradation. This is true for the MFS of Sinemurian (L1), Pliensbachian (D2) in southwestern area, and Toarcian (T3) minor cycles. This is also true for the MFS of the higher-order sequence, of Carixian age (C1) for instance. In contrast, there is no organic matter where the sediments were deposited in the upper offshore, even if they were associated with a MFS: for instance, Carixian MFS C3 and C4. There is also no organic matter associated with the Pliensbachian MFS (D4/D5) in the eastern part of the basin where it occurs within the lower offshore: a difference in the depositional environment does not account for this noticeable exception.

The vertical TOC trends can also be partly explained by this factor. The most noticeable example is the Toarcian transgressive half-cycle where the sediments of the organic-rich TST were deposited in the lower offshore immediately above the FS (T1). However, this factor alone cannot account for the vertical organic content variations observed, in a same well, in the organic-rich intervals associated with the MFS of minor T-R cycles (L1, D2, and T3).

These vertical variations in organic content can be related either to variations of the biomass productivity or to variations of the organic matter preservation. Biomass productivity partly controls the organic input and interacts with some preservation factors. Preservation of organic matter is clearly related to the development of anoxic conditions in the water column and in the first centimeters of the sediments (Demaison and Moore, 1980; Pratt, 1984).

In the present study, the productivity factor is poorly documented. However, some information is available on the Schistes Carton formation, which cor-

responds to the major transgression in the Lias cycle. Most of the models which have been proposed to explain the accumulation of this formation and its equivalents primarily call for an increase in preservation, even if productivity might play some role (see discussion and references in Hollander et al., 1991). We assume that this hypothesis could be considered as reliable for the other comparatively less rich organic intervals. Such an assumption is based on the fact that, during the Lias, the Paris basin, even if it moved slightly northwestward, remained located in the subtropical realm (Rioult, 1968; Parrish and Curtis, 1982; Parrish et al., 1982; Hallam, 1984). This suggests that the climatic factors might not be significantly modified when considering *very long term climate changes*; that is, from early to late Lias. These considerations lead to the proposal of a scenario where productivity did not play a predominant role in the control of organic matter accumulation.

Are anoxic conditions developed below the SWB? In the early Toarcian (Schistes Carton), the deposition of organic matter in the lower offshore was associated with the development of strong anoxic conditions which, according to Hollander et al. (1991), prevailed at the sea bottom and within the water column, maybe up to the base of the euphotic zone. This model, substantiated from a single well, can be applied to the whole studied area, considering the vertical regularity of the TOC profiles in the interval T1-T3 (Figures 10 and 11) which suggest very homogeneous conditions for the deposition of this highly organic-rich interval. Anoxic conditions are documented from the base of the interval T1-T2. The low TOC bed at the top of this interval is related to the reoxygenation of the depositional environment due to a decrease in the water depth, followed by renewed euxinic conditions linked to a new increase in this water depth (FS T2). In the other organic-rich intervals, the sedimentological, biological, and mineralogical data which are required to precisely address this question are rare due to scarcity of cores. However, the general lithologic data, combined with the utilization of uranium content and more particularly of the so-called "authigenic" uranium as an indicator of benthic oxygen level (Myers and Wignall, 1987; Wignall and Myers, 1988), show that the degree of oxygenation of the environment might be different: oxic during deposition of the gray, silty calcareous shales of the organic-rich interval associated with the Sinemurian MFS (L1) or the Carixian MFS (C1), and slightly anoxic during deposition of the bituminous shales of the Pliensbachian MFS (D2) interval. These results suggest that different levels of oxygen deficiency might have prevailed during the deposition of organic-rich intervals.

In a regime of rather constant organic input, development of anoxia will be primarily related to oxygen supply, which depends on water circulation. During the Lias, a specific paleoceanographic system characterized by the lack of ocean-driven currents prevailed in the Paris basin. Its location within the northwestern European plate accounts for this feature (Hallam, 1975). Hence, in this storm-dominated, shallow, epi-

continental sea, the episodic injections of surficial oxygenated water below the SWB can likely be considered as decreasing as water depth increases. This results in a gradient of increasing oxygen deficiency with water depth. In this scenario, preservation of organic matter, and so organic content, will increase with water depth. This scenario is in agreement with the concomitant increase of organic content within the organic-rich intervals, and the deepening of the basin recorded within the major Lias cycle from early Sinemurian to middle Toarcian. It could also account for the variations recorded within the Sinemurian and Pliensbachian (western area) minor cycles (Figure 11).

Thus, in this basin, water depth might play a major role in controlling not only the occurrence of organic matter in sediments below the SWB, but also the development of dysaerobic to anaerobic conditions favorable to the preservation of organic matter. However, other factors like sedimentation rate might also contribute to organic matter preservation. Moreover, the influence of productivity on the preservation must not be totally excluded.

A Few Exceptions: The Role of Sedimentation Rate

It has been mentioned above that there is no organic-rich interval associated with the major MFS of Pliensbachian cycle in the eastern part of the basin. As

exhibited on Figure 13, the occurrence of an organic-rich interval is limited to the western part of the basin where it is well developed (MFS D2). Eastward, the organic-rich interval is still present within a restricted area, but it is much thinner and organic poorer, and located higher in the series (MFS D4/D5). Beyond, it completely disappears and the whole Pliensbachian becomes uniformly organic poor.

Discussion

For a same mass of organic material introduced per unit time, the organic content measured in a given interval will be higher when the sedimentation rate is low ("concentration" effect) and lower when sedimentation rate is higher ("dilution" effect). This general and reliable relationship can be modified to some degree by possible interaction between high organic sedimentation rate and increase in preservation (see discussion in Muller and Suess, 1979; Stein, 1986).

In the Paris basin, the bulk sedimentation rates recorded at the minor T-R cycle scale are rather low: from 10 m/m.y. to a few tens of meters/m.y. (raw averages on undecomposed series). However, significant variations are registered between the slowly subsiding western area and the more subsident eastern area. Within the Pliensbachian T-R minor cycle, the sedimentation rate above FS C6 exceeds 40 m/m.y. in the northeastern area, which is almost three times

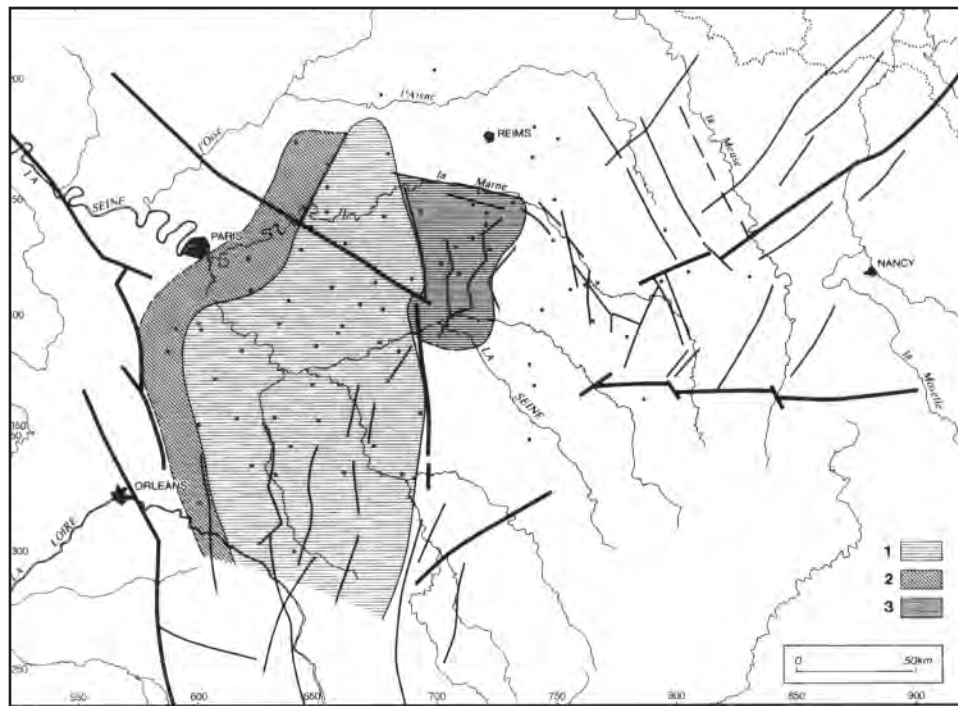


Figure 13. Areal distribution of the organic matter associated with the MFS of the Pliensbachian cycle: (1) areal extension of the organic matter bed associated with the MFS D2; its eastern limit corresponds to St. Martin de Bossenay fault and its extension northward; (2) area where the MFS D2 is defined but the organic matter bed is very thin or absent; (3) areal extension of the organic matter bed associated with the MFS D4/D5.

higher than in the southwestern area. We estimate that this high sedimentation rate, in a series which is dominantly terrigenous, accounts for the lack of an organic-rich interval associated with the Pliensbachian MFS, even though sediments were deposited in the lower offshore. The limit between the western and eastern domains coincides with the faults which have been demonstrated as controlling the subsidence regime (Figure 13). In other words, we consider that the disappearance of this organic-rich interval is due to the dilution effect of the organic input related to higher sedimentation rate led by a higher subsidence regime.

The role of the sedimentation rate factor has only been correlated with rather good confidence in the Pliensbachian. For other organic-rich intervals, especially of higher-order sequences, the required basic data are very imprecise (e.g., initial depositional thickness, decompacted series, accurate age dates) or even not documented (evaluation of time gaps).

The sequence stratigraphic approach postulates that maximum space is created during the maximum rate of relative sea level change (Cross, 1988). At that time, proportionally more sediment is stored in a continental environment, and the flux to marine environments is reduced. This may lead to the formation of a condensed interval. Consequently, all the other conditions being equal, the organic content will be higher in this interval. That could account, to a certain extent, for the increase of organic content from FS to the MFS, but it is not really documented.

Thickness and Organic Matter Content: The Role of Hydrodynamic Processes

In the Paris basin, a condensed section does not occur in the basin center where the sequences reach their maximum thickness. This increase in sediment thickness is combined with an increase in organic richness, as exhibited on the cross sections. This is well documented for the intervals associated with the MFS of minor T-R cycles and the MFS of some genetic unit sets like the MFS C1. This result will be examined in detail for the Toarcian and Sinemurian minor T-R cycles. Discussion is focused on organic-rich intervals associated with the major MFS.

The Toarcian Example

Only the transgressive half-cycle (interval T1-T3) will be discussed. Above the MFS (T3), the sequence stratigraphic study was unsuccessful in proposing realistic and chronostratigraphically reliable boundaries within this shaly, dominantly aggrading interval. The transgressive half-cycle presents a simple pattern of organic matter distribution (Figure 14): this is regular and centripetal with average TOC from <2% up to 5.5–6%, slightly elongated SSW-NNE and centered east of Paris, between the Aisne and Seine rivers; eastward, a second area of higher TOC begins, centered in the Luxembourg country (Megnien, 1980). Comparison of this distribution with the isopach map shows a good general correlation between the two areas of higher TOC and the two depocenters. Furthermore,

the thinnest areas are also the organic poorest. This pattern is much simpler than the following one.

The Sinemurian Example

A cross section (Figure 15a) comprising five wells illustrates the different organic matter profiles associated with the MFS. It extends from the southwestern area (total thickness of the cycle = 25 m) to the more subsident northern area (total thickness > 120 m) (Figures 15B, C). It contains distal offshore to proximal offshore facies but does not reach the coastal areas. Along this transect, the organic-rich interval ranges from 3 m thick (TOC = 2.3%) in well a, to 6 m (TOC = 3%) in well b, to 18 m (TOC = 4%) in well c; in well d, no well-marked organic-rich interval is associated strictly with the MFS, but a 3 m bed (TOC = 2%) is located a few meters below this MFS. This last well is representative of the situation recognized in a wide zone (striped area on Figure 15C) in the northern part of the studied area (see also cross section 1—Figure 10). Thus, the general pattern for this organic-rich interval is complex: it corresponds primarily to a concomitant increase in organic content and in thickness basinward, up to a zone where this pattern is no longer observed.

Discussion

Lateral distribution of organic matter in a given basin is governed by sediment transport rules. The organic matter tends to accumulate in the depocenters of lower energy, in the deeper parts of these basins (Huc, 1987, 1988). This results in centripetal patterns which are known in some modern examples like the Caspian Sea or Lake Bogoria in Kenya, where these hydrodynamic processes are well documented.

The early Toarcian pattern can be compared to these examples. Accordingly, this pattern could result from the combination of the anoxic conditions previously discussed, and the redistribution of the organic-rich sediments in the most central part of the basin by hydrodynamic processes. However, an alternative scenario can be proposed, based on possible diachronic expansion of black shales from inherited topographic lows onto "highs." Such a scenario, called by Wignall (1991) the "expanding-puddle" model, could account for the thinning patterns observed within the interval T1-T2; however, it cannot be proved owing to the lack of accurate age dates. This model can hardly be applied to the overlying interval T2-T3, because it would presuppose reactivation of the topographic "highs." It would also require substantiation, by a sedimentological approach, that the areas where the interval is the thinnest correspond to permanent shallower areas, and hence, to more oxygenated areas with less favorable preservation conditions. Therefore, we promote a model where the combination of preservation and redistribution tends to favor the accumulation of organic matter in the depocenters. In addition, we assume that the areal general homogeneity of the organic content pattern at the basin scale should be connected to the quite homogeneous depositional settings created by the flexuring of the basin.

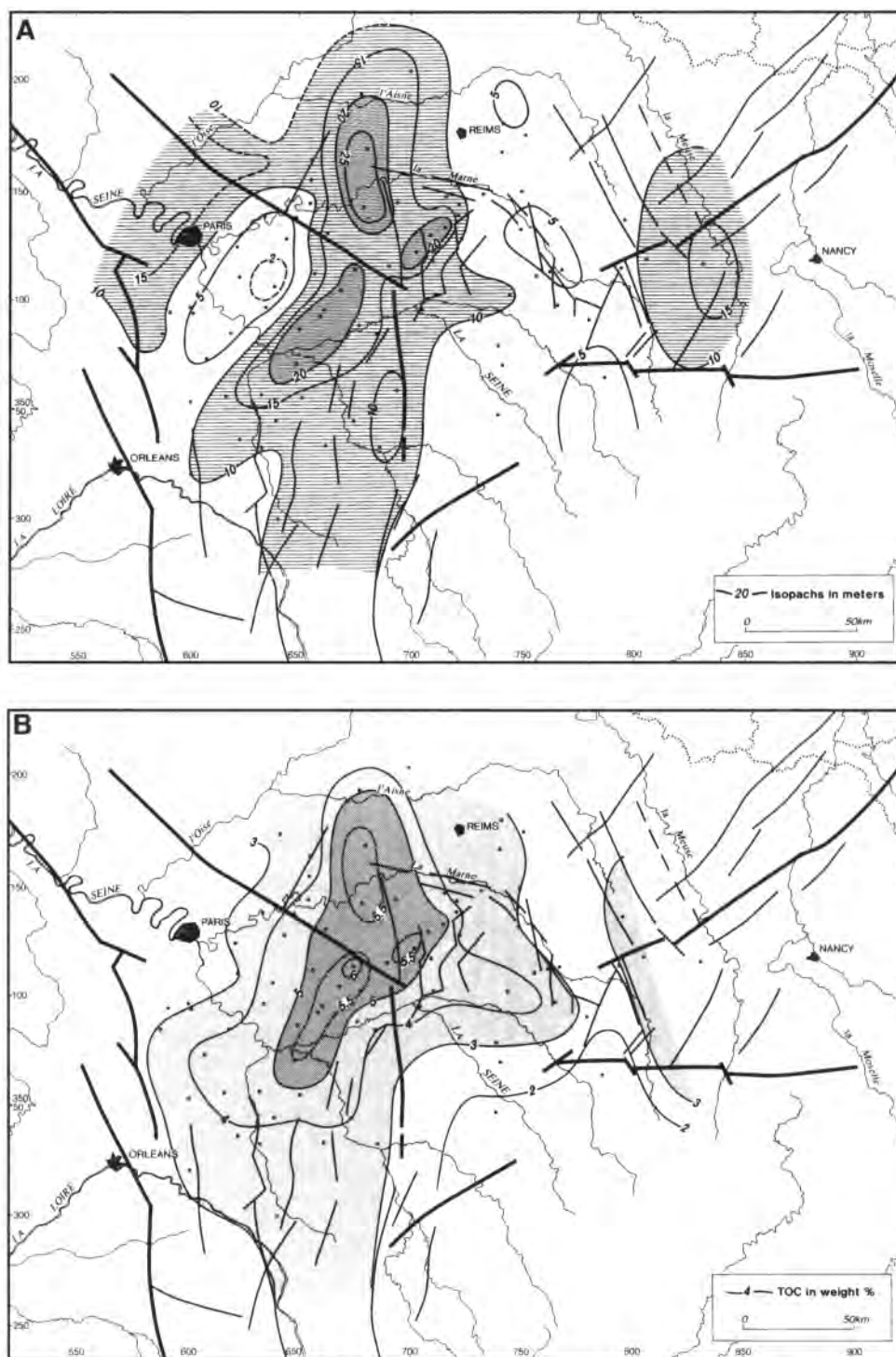


Figure 14. (A) Isopachs of the transgressive Toarcian half-cycle; (B) areal distribution of organic matter (initial TOC).

In the Sinemurian, deposition occurs below the SWB during the MFS, in possibly oxic sea-bottom conditions. This situation characterizes the whole studied area (Figure 15C). There is no indication of development of euxinic conditions in the central part of the basin. Besides, the lack of organic matter in the north-eastern zone cannot be explained by a dilution effect:

the section is in the same range of thickness as the organic-rich area. Hence, we suggest that hydrodynamic processes account for the different patterns of organic matter distribution observed in the basin. Paleogeographic data (C. Robin, in preparation) led to the hypothesis that there were different patterns of currents, supplying organic-poor sediments from the

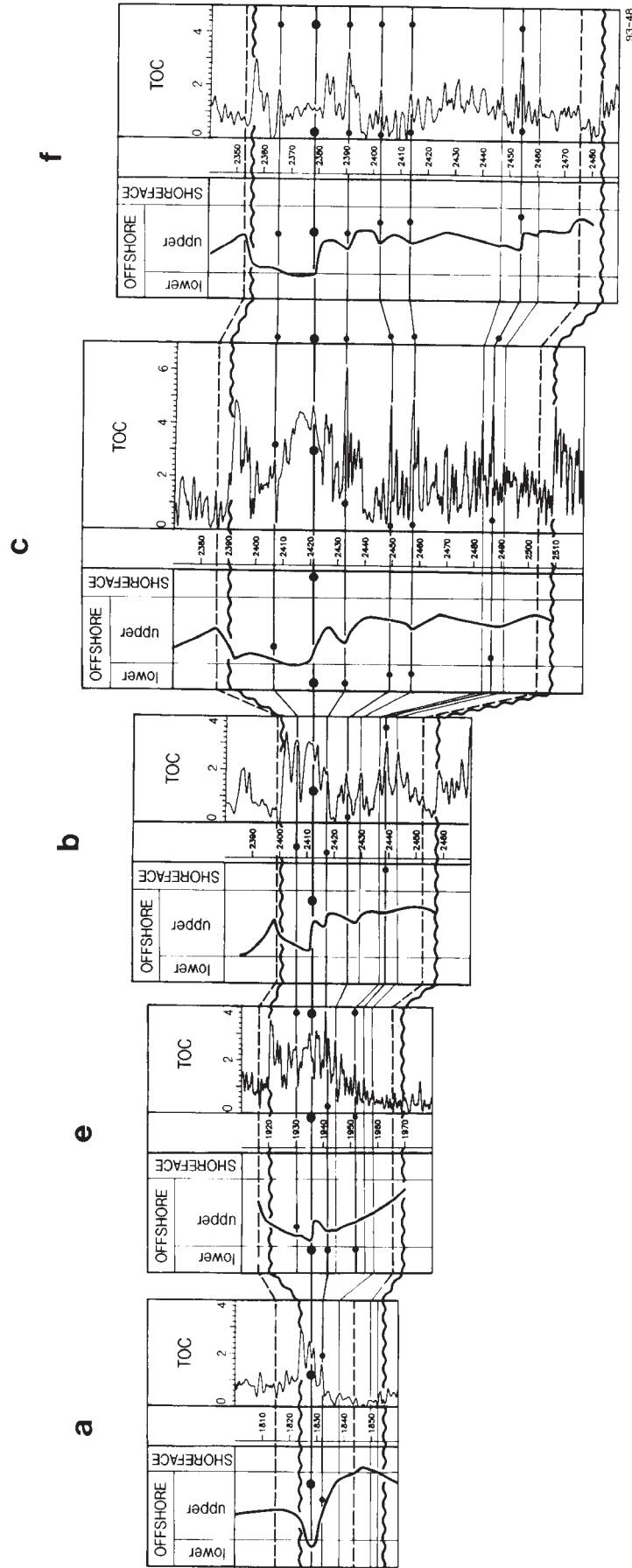


Figure 15A. Distribution of organic matter within the Sinemurian cycle in five significant wells. Vertical scale is in meters.

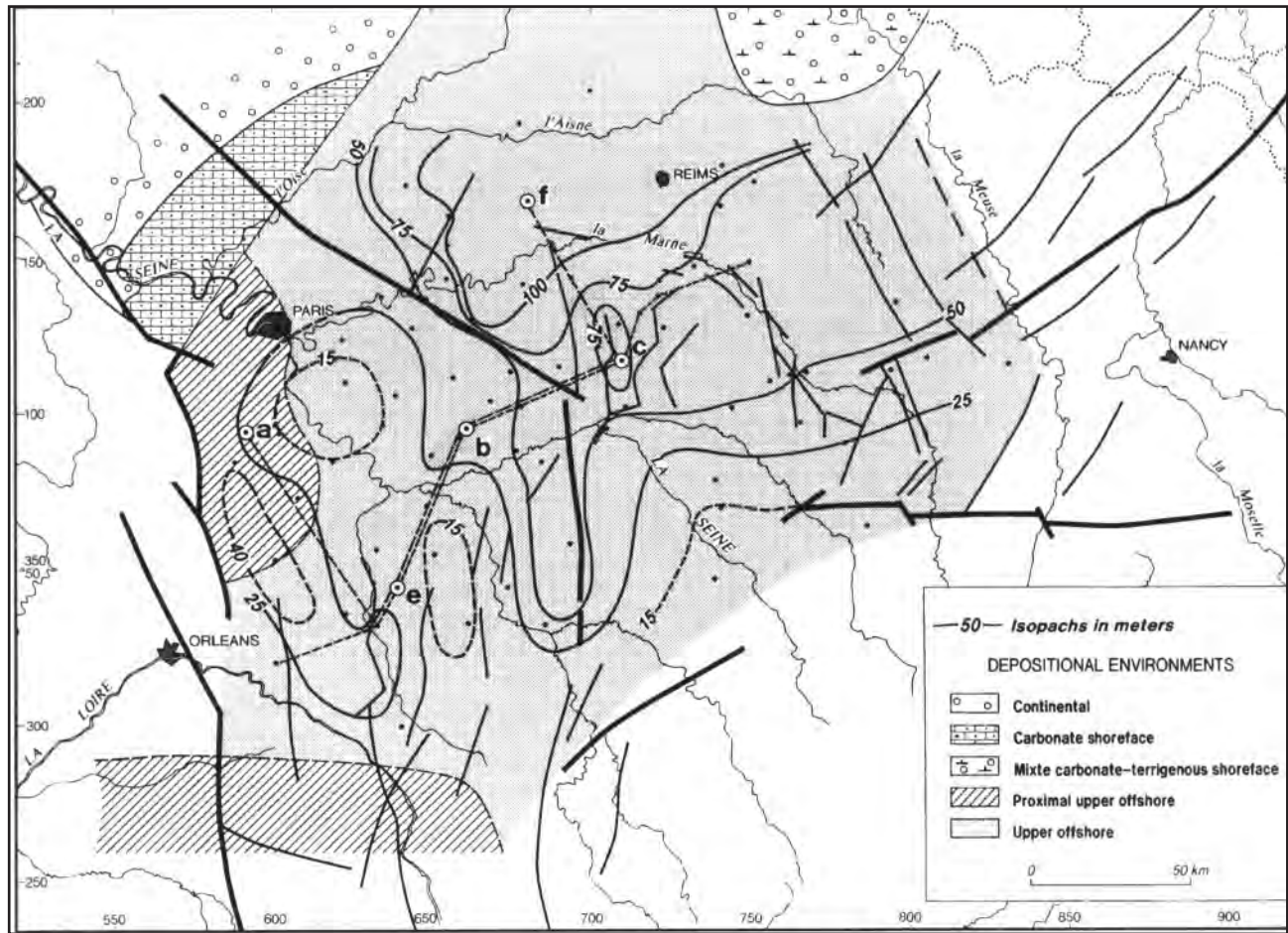


Figure 15B. Isopach map of the Sinemurian transgressive half-cycle (S1-L1 interval).

Ardennes area, and organic-rich sediments from the south of the basin; both were controlled by the rather complex physiography of the basin.

These two examples demonstrate that organic-rich intervals present basinward variations which, generally, combine increase of sediment thickness and increase of organic richness. We suggest that this pattern is primarily controlled by hydrodynamic processes even if the role of the preservation factors must not be excluded. The differences observed between the two examples might be relevant to differences in physiography related to different tectonic settings.

SUMMARY AND CONCLUSIONS

The Lias of the Paris basin exhibits significant vertical and lateral variations in the organic matter distribution, as well evidenced by use of the Carbolog method. This study shows that a correspondence exists between this distribution and the analysis of the series in terms of sequence stratigraphy, at different sequence orders (from 0.6 to 25 Ma), and at the basin scale. This study, then, shows that the features issued from this comparison can be interpreted

regarding the state of knowledge in organic sedimentology, the geological framework of the basin, and the implications of the sequence stratigraphic framework in terms of basin-fill history. The consistency of the tentative explanations proposed with *at once* all of these parameters allows these features to be *validated*.

1. The vertical distribution of organic matter is complex. It can be related to the superimposition of different orders of depositional sequences. Its lateral distribution is comparatively simpler. It results from a rather homogeneous geological setting at the basin scale. The eustatic and tectonic causes which originate the sequences control the water depth, the physiographic pattern, and the sedimentation rate, which have been identified as the main factors for organic matter accumulation.

2. The organic-rich intervals are associated, at all cycle scales, with the MFS and more widely with the end of the retrogradation and the beginning of the progradation, *as long as deposition occurs below the SWB*. In addition, a hierarchy in the organic content of the organic-rich intervals can be observed from the genetic unit set order to the T-R cycle order; their organic content also depends on the position of

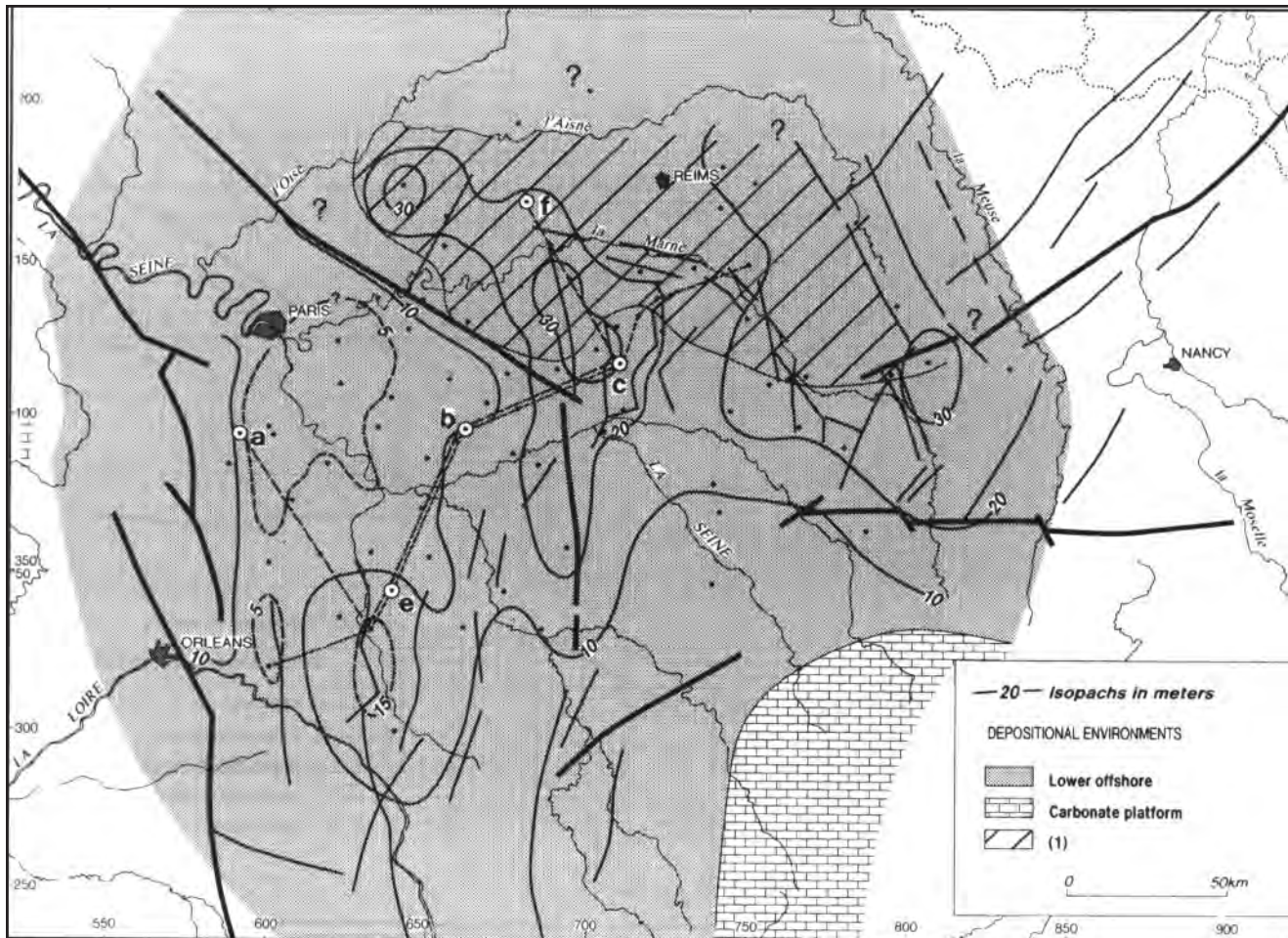


Figure 15C. Isopach map of the Sinemurian regressive half-cycle (L1-L3 interval). (1) Area where no well-marked organic-rich interval is associated with the MFS.

the sequence considered within the lower-order sequence. These variations are tentatively related to the differences in the degree of oxygen deficiency which are observed below the SWB. Although the contribution of additional factors to the organic matter preservation must not be excluded, water depth might be the primary factor controlling the vertical organic matter accumulation patterns.

3. However, a high rate of sedimentation can lead to the dilution of the organic input and the disappearance of the organic-rich interval (e.g., Pliensbachian). This factor is controlled by tectonics, whose predominant role in the organic matter accumulation patterns is well demonstrated at the T-R cycle scale (5 to 8 m.y.). Tectonics directly influence the physiography of the basin. It accounts for the lack of progradational wedge with downlap, the necessary conditions to get significant condensed levels at third- to second-order sequences. Maximum anoxia (e.g., Schistes Carton) occurs when the basin is a huge flexure.

4. Increase in organic richness is generally associated with the increase of sediment thickness basinward. Hydrodynamic processes, possibly com-

bined with some preservation factors, primarily account for this pattern.

Sequence stratigraphy provides a consistent and chronostratigraphic framework to correlate the organic matter distribution patterns at a basinal scale. It also provides a framework for predicting these patterns. Some specific features have been identified at the third- and second-order sequences. They can be considered as general rules in spite of the existence of some exceptions, which are linked to local factors; these factors act within the sequence stratigraphic framework but may impose a predominant influence. Thus, we believe that the occurrence of the organic-rich intervals can be predicted using these general rules after a careful examination of the local conditions. This approach is especially fruitful at the "stage" scale where the organic-richest intervals occur. Furthermore, we believe that the *relative* organic content of these intervals can also be predicted considering their rank within the sequence stratigraphic framework. This study also shows that any organic matter study should integrate several superimposed sequence orders, up to the sequence order which

controls the organic-rich levels significant in terms of petroleum potential of the basin.

This approach definitely appears to be a powerful tool for predicting organic matter distribution. However, the extrapolation of the "rules" identified in this study to clearly different tectonic settings, like passive margins, is highly doubtful. Most of the organic matter accumulation patterns are directly or indirectly controlled by tectonic features characteristic of an intracratonic basin. Besides, productivity has been considered as subordinate with regard to the other factors which control the organic matter accumulation. In a case of a stronger climatic influence, for instance, the productivity could not be considered as subordinate and might interfere with the other processes involved in the accumulation of organic matter. However, we still consider that it would play a subordinate role, probably in modifying the organic matter content more than the organic matter occurrence. This assumption is valid if the organic matter is predominantly of continental origin, as its accumulation is not so dependent on the preservation factors (Cowie and Hedges, 1991). Consequently, this approach involves a preliminary examination of the general geological setting of the basin considered.

REFERENCES CITED

- Barlow L.K. and Kauffman E.G., 1985, Depositional cycles in Niobrara formation, Colorado Front Range: SEPM Field Trip Guide Book, n. 4.
- Bessereau G. and Guillocheau F., 1994, Sequence stratigraphy and organic matter distribution in the Lias of the Paris basin, in A. Mascle, ed., *Hydrocarbon and Petroleum Geology of France: Special Publication of E.A.P.G.*, n. 4, Springer Verlag, p. 107–120.
- Bessereau G., Huc A.Y., and Carpentier B., 1992, Distribution of organic matter in the Liassic series of the Paris basin: an example of organic heterogeneity in a source rock interval: Special publication of the E.A.P.G., t. 2, p. 117–125.
- Calvert S.E. and Pedersen T.F., 1992, Organic carbon accumulation and preservation in marine sediments: how important is anoxia?, in J. Whelan and J.W. Farrington, eds., *Productivity, accumulation and preservation in recent and ancient sediments*: New York, Columbia University Press, p. 231–263.
- Carpentier B., Huc A.Y., and Bessereau G., 1991, Wireline logging and source rocks—estimation of organic carbon content by the Carbolog method: *The Log Analyst*, v. 32, n. 3, p. 279–297.
- Carpentier B., Huc A.Y., Gely J.P., and Blanc-Valleron M.M., 1993, Geological and geochemical modeling, an approach for understanding organic cyclic sedimentation in evaporitic sequences. Application to the Mulhouse basin (France): *Organic Geochemistry*, v. 20, n. 8, p. 1153–1163.
- Cowie G.L. and Hedges J.I., 1991, The role of anoxia in organic matter preservation in coastal sediments: relative stabilities of the major biochemicals under oxic and anoxic depositional conditions: *Organic Geochemistry*, v. 19, n. 1–3, p. 229–234.
- Creaney S. and Passey Q.R., 1993, Recurring patterns of total organic carbon and source rock quality within a sequence stratigraphic framework: *AAPG Bulletin*, v. 77, n. 3, p. 386–401.
- Cross T.A., 1988, Controls on coal distribution in transgressive-regressive cycles: *SEPM Special Publication* 42, p. 371–380.
- Cross T.A., Baker M.R., Chapin M.A., Clark M.S., Gardner M.H., Hanson M.S., Lessenger M.A., Little L.D., McDonough K.-J., Sonnenfeld M.D., Valasek D.W., Williams M.R., and Witter D.N., 1993, Applications of high-resolution sequence stratigraphy to reservoir analysis, in R. Eschard and B. Doligez, eds., *Subsurface reservoir characterization from outcrop observations: I.F.P. Exploration and Production Research Conferences*, Technip, p. 11–34.
- Curiale J.A., Cole R.D., and Witmer R.J., 1992, Application of organic geochemistry to sequence stratigraphic analysis: Four Corners Platform area, New Mexico, U.S.A.: *Organic Geochemistry*, v. 19, n. 1–3, p. 53–75.
- Demaison G.J. and Moore G.T., 1980, Anoxic environments and oil source bed genesis: *AAPG Bulletin*, v. 64, p. 1179–1209.
- Espitalié J., Marquis F., Sage L., and Barsony I., 1987, *Géochimie organique du Bassin de Paris: Revue de l'Institut Français du Pétrole*, v. 42, n. 3, p. 271–302 (in French).
- Galloway W.E., 1989, Genetic stratigraphic sequences in basin analysis I: architecture and genesis of flooding-surface bounded depositional units: *AAPG Bulletin*, v. 73, p. 125–142.
- Gely J.P. and Lorenz J., 1991, Analyse séquentielle du Jurassique (Hettangien à Callovien) du sondage de Couy (bassin Parisien): *Comptes-rendus de l'Académie des Sciences de Paris*, 313, Série II, p. 347–353 (in French).
- Guillocheau F., 1991, Mise en évidence de grands cycles transgression-régression d'origine tectonique dans les sédiments Mésozoïques du bassin de Paris: *Comptes-rendus de l'Académie des Sciences de Paris*, 312, Série II, p. 1587–1593 (in French).
- Guillocheau F., Dromart G., Merzeraud G., Bessereau G., Van Buchem F., and Derasse S., 1992, Sedimentology and genetic stratigraphy of the GPF well Couy: Sequence Stratigraphy of European Basins, Dijon, May 18–20, 1992, abstract (registered Société Géologique de France, Paris).
- Hallam A., 1975, *Jurassic environments*: Cambridge University Press, 260 p.
- Hallam A., 1984, Continental humid and arid zones during the Jurassic and Cretaceous: *Palaeogeography, Palaeoclimatology, Palaeoecology*, v. 47, p. 195–223.
- Herbin J.-P., Muller C., Geysant J.R., Mélières F., and Penn I.E., 1991, Hétérogénéité quantitative et qualitative de la matière organique dans les argiles du Kimméridgien du Val de Pickering (Yorkshire, UK): *Revue de l'Institut Français du Pétrole*, v. 6, p. 675–711 (in French).

- Herbin J.-P., El Albani A., and Geyssant G., 1992, A tentative approach of the sequence stratigraphy of the source rocks deduced from the study of upper Jurassic in Dorset (UK), Yorkshire (UK) and Boulonnais area (France): Paleogeography—paleoclimate and source rocks: IFP/AAPG International Research Conference, Paris, July 7–10, 1992.
- Herron S.L., 1986, A total organic carbon log for source rock evaluation: Society of Professional Well-Log Analysts 27th Annual Logging Symposium Transactions, 11 p.
- Herron S.L. and Le Tendre J., 1990, Wireline source rock evaluation in the Paris basin, in A.Y. Huc, ed., Deposition of organic facies: AAPG Studies in Geology 30, p. 57–72.
- Hollander D.J., Bessereau G., Belin S., Huc A.Y., and Houzay J.P., 1991, Organic matter in the early Toarcian shales, Paris basin, France: a response to environmental changes: *Revue de l'Institut Français du Pétrole*, v. 46, n. 5, p. 543–562.
- Homewood P., Guillocheau F., Eschard R., and Cross T., 1992, High resolution correlations and genetic stratigraphy: an integrated approach: *Bulletin des Centres de Recherches Exploration-Production Elf-Aquitaine*, n. 16, 2, p. 357–381.
- Huc A.Y., 1976, Mise en évidence de provinces géochimiques dans les schistes bitumineux du Toarcien de l'est du Bassin de Paris: *Revue de l'Institut Français du Pétrole*, v. 31, p. 933–953 (in French).
- Huc A.Y., 1987, Aspects of depositional processes of organic matter in sedimentary basins: *Organic Geochemistry*, v. 13, p. 263–272.
- Huc A.Y., 1988, Sedimentology of organic matter, in F.H. Frimmel and R.F. Christman, eds., *Humic Substances and Their Role in the Environment*: Chichester, p. 215–243.
- Mann U. and Muller P.J., 1987, Source rock evaluation by well-log analysis, lower Toarcian, Hils syncline: *Organic Geochemistry*, v. 13, p. 109–119.
- Megnien C., 1980, Synthèse géologique du bassin de Paris: *Mémoire du BRGM*, n. 101 (in French).
- Meisner F.F., 1978, Petroleum geology of the Bakken formation, Williston basin, North Dakota and Montana: Reprinted from the Williston Basin Symposium, 1978, Montana Geological Society, 24th Annual Conference, Billings, Montana.
- Meyer B.L. and Nederlof M.H., 1984, Identification of source rocks on wireline logs by density/resistivity and sonic transit time/resistivity crossplots: *AAPG Bulletin*, v. 68, n. 2, p. 121–129.
- Mitchum R.M. and Van Wagoner J.C., 1991, High-frequency sequences and their stacking patterns: sequence stratigraphic evidence of high-frequency eustatic cycles: *Sedimentary Geology*, v. 70, p. 131–160.
- Muller P.J. and Suess E., 1979, Productivity, sedimentation rate and sedimentary organic content in the oceans, 1. Organic carbon preservation: *Deep-Sea Research*, 26A, p. 1347–1362.
- Myers K.J. and Wignall P.B., 1987, Understanding Jurassic organic-rich mudrocks—new concepts using gamma-ray spectrometry and paleoecology: examples from the Kimmeridge Clay of Dorset and Jet Rock of Yorkshire, in J.K. Legget and G.G. Zuffa, eds., *Marine Clastic Sedimentology*: Graham and Trotman, p. 172–189.
- Odin G.S. and Odin C., 1990, Echelle numérique des temps géologiques: *Géochronique*, n. 35, p. 12–21 (in French).
- Parrish T.J. and Curtis R.L., 1982, Atmospheric circulation, upwelling and organic-rich rocks in the Mesozoic and Cenozoic: *Palaeogeography, Palaeoclimatology, Palaeoecology*, v. 40, p. 31–66.
- Parrish T.J., Ziegler A.M., and Scotese R., 1982, Rainfall patterns and the distribution of coals and evaporites in the Mesozoic and Cenozoic: *Palaeogeography, Palaeoclimatology, Palaeoecology*, v. 40, p. 67–101.
- Pasley M.A., Gregory W.A. and Hart G.F., 1991, Organic matter variations in transgressive and regressive shales: *Organic Geochemistry*, v. 17, n. 17, p. 483–509.
- Passey Q.R., Creaney S., Kulla J.B., Moretti F.J., and Stroud J.D., 1990, A practical model for organic richness from porosity and resistivity logs: *AAPG Bulletin*, v. 74, p. 1777–1794.
- Perrodon A. and Zabek J., 1991, Paris basin: *AAPG Memoir* 51, p. 633–679.
- Posamentier H.W., Jervey M.T., and Vail P.R., 1988, Eustatic controls on clastic deposition I—Conceptual framework: *SEPM Special Publication* 42, p. 109–124.
- Pratt L.M., 1984, Influence of paleoenvironment factors on the preservation of organic matter in Middle Cretaceous Greenhorn Formation, Pueblo, Colorado: *AAPG Bulletin*, v. 68, p. 1146–1159.
- Riout M., 1968, Contribution à l'étude du Lias de la bordure occidentale du Bassin de Paris: Thesis, University of Caen, France (in French).
- Serra O., 1971, Apports des sondages pétroliers à la connaissance du Lias du bassin de Paris: *Mémoire du BRGM*, n. 75, p. 481–488 (in French).
- Serra O., 1984, Fundamentals of well-log interpretation, 1. the acquisition of logging data: *Developments in Petroleum Science*, Elsevier Science Publishers B.V.
- Stein R., 1986, Organic carbon and sedimentation rate. Further evidence for anoxic deep-water conditions in the Cenomanian/Turonian Atlantic ocean: *Marine Geology*, v. 72, p. 199–209.
- Thomas M., 1977, Les schistes bitumineux du Toarcien de Franche-Comté. Etude géologique, caractérisation géochimique et estimation du potentiel pétrolier: Thesis, Faculté des Sciences et Techniques de l'Université de Franche-Comté, France (in French).
- Tissot B., Durand B., Espitalié J., and Combaz A., 1974, Influence of nature and diagenesis of organic matter in formation of petroleum: *AAPG Bulletin*, v. 58, n. 3, p. 499–506.
- Vail P.R., Audemart F., Bowman S.A., Eisner P.N., and Perez-Cruz C., 1991, The stratigraphic signatures of tectonics, eustasy and sedimentology—an

- overview, *in* G. Einsele et al., eds., *Cycles and events in stratigraphy*: Berlin, Springer-Verlag, p. 617–659.
- Van Buchem F.S.P., McCave I.N., and Weedon G.P., 1994, Orbitally induced small scale cyclicity in a siliciclastic epicontinental setting, Cleveland basin, lower Lias Yorkshire, U.K., *in* P.L. De Boer and D. Smith, eds., *Orbital forcing and cycle sedimentary sequences*: International Association of Sedimentologists Special Publication, 19, p. 345–366.
- Van Wagoner J.C., Posamentier H.W., Mitchum R.M., Vail P.R., Loutit J.F., and Hardenbol J., 1988, An overview of fundamentals of sequence stratigraphy and key-definitions: SEPM Special Publication 42, p. 39–45.
- Van Wagoner J.C., Mitchum R.M., Campion K.M., and Rahmanian V.D., 1990, Siliciclastic sequence stratigraphy in well logs, cores and outcrops: concepts for high-resolution correlation of time and facies: AAPG Methods in Exploration 7, 55 p.
- Weedon G.P. and Jenkins H.C., 1990, Regular and irregular climatic cycles and the Belemnite Marls, Pliensbachian, Lower Jurassic, Wessex basin: *Journal of the Geological Society of London*, v. 147, p. 915–918.
- Wignall P.B., 1991, Model for transgressive black shales?: *Geology*, v. 19, p. 167–170.
- Wignall P.B. and Myers K.J., 1988, Interpreting benthic oxygen levels in mudrocks: a new approach: *Geology*, v. 16, p. 452–455.

The Organic Carbon Distribution in Mesozoic Marine Sediments and the Influence of Orbital Climatic Cycles (England and the Western North Atlantic)

F. S. P. van Buchem
Institut Français du Pétrole
Rueil-Malmaison, France

P. L. de Boer
University of Utrecht
Utrecht, The Netherlands

I. N. McCave
University of Cambridge
Cambridge, U.K.

J.-P. Herbin
Institut Français du Pétrole
Rueil-Malmaison, France

ABSTRACT

The distribution of organic carbon in marine sediments is commonly characterized by cyclicity at different time scales. A detailed analysis of such cyclicity in three case studies of Liassic and Kimmeridgian age in England and of Cenomanian age in the northwestern Atlantic Ocean shows that specific processes playing at different time scales control the storage of organic matter. Two scales are distinguished: (1) large-scale trends (>3 m.y., 2nd- and 3rd-order cycles) are caused by plate tectonics affecting paleogeography and topography, long-term eustatic sea level, and climatic changes (“ice-house” and “green-house”); they define the storage of organic matter worldwide by influencing productivity and ventilation of deep water; and (2) small-scale trends (<3 m.y., 4th- and 5th-order cycles) are caused by orbitally induced high-frequency glacio-eustatic and other oceanographic and/or climatic changes. If general conditions are favorable, the impact of these changes is a high-frequency signal of oxygenation/dilution cycles, whose particular expression strongly depends on the local sedimentary environment.

A consequence of the orbitally induced climatic/oceanographic control of high-frequency sedimentary cycles is that it has a regional (to worldwide)

expression, and is thus a powerful tool to reconstruct basin in-fill patterns and to establish detailed correlations between basinal (source rock) and margin (reservoir) successions. Once established, a high-resolution framework provides the necessary stratigraphic control for detailed geochemical studies and allows a quantitative approach of the geochemical sediment budget, as well as interpolation and extrapolation to time-equivalent sequences.

INTRODUCTION

Organic carbon in marine sediments is typically related to rhythmic bedding patterns, that is, regular alternations of organic-rich and organic-poorer layers with commonly parallel variations of other constituents (CaCO₃, silica, clay minerals, etc.). Some successions showing this pattern have a low (<1%) average organic carbon content and classify as normal marine deposits (e.g., Vandenberghe, 1978; McCave, 1979a; Fischer et al., 1985; Tribovillard and Cotillon, 1989; van Echenpoel and Weedon, 1990; van Buchem et al., 1994), while others have a high (>1%) average organic carbon content and classify as source rocks (e.g., de Boer, 1983; Herbin et al., 1987, 1991; Weedon and Jenkyns, 1990; Droste, 1990).

Basic prerequisites for the storage of organic matter are the primary production of organic matter in surface waters and water conditions which preclude a complete oxidation before burial can take place. Moreover, terrestrial organic matter introduced into the oceanic system may contribute to or dominate organic matter stored in marine sediments. In the long run, over millions of years, such conditions depend on larger-scale trends defined by plate tectonics affecting oceanography, geography and topography, and long-term eustatic sea level and climatic changes ("ice-house" and "green-house" states), the interplay of which allows or stimulates organic matter to be stored. On shorter time scales, once conditions are suitable for organic matter preservation, high-frequency (<500 k.y.) climatic changes *modulate* the degree to which organic matter is produced and preserved.

A simple and elegant explanation for high-frequency cyclicity gaining increasing support and attention is the theory of astronomical forcing of climatic changes. Astronomical forcing has now been recognized in sediments throughout the Phanerozoic, and in almost every sedimentary environment (de Boer and Smith, 1994a). The production and distribution of marine and terrestrial organic matter can be directly influenced by orbitally induced climatic and oceanographic changes in a sufficiently sensitive sedimentary environment (de Boer and Smith, 1994b). Such changes in atmospheric and oceanographic processes affect the character and the amount of organic matter produced and the amount which is oxidized before burial into the sedimentary column.

Detailed datasets are a first requisite for addressing specific questions about the factors influencing the

storage of organic carbon in different marine sedimentary environments. Densely spaced geochemical profiles quantifying the vertical changes in mineralogical composition and variations in quantity and quality of the organic matter are needed. They should be collected in a tightly controlled time framework, with, if possible, a regionally documented physico-chemical sedimentological history. Such an approach has been advocated by Kauffman (1988), his "high-resolution event stratigraphy," and more recently by Arthur and Dean (1991) in what they call a "holistic approach to geochemistry."

Here we present three case studies, compiled from the literature and our work, for which detailed physico-chemical sedimentological profiles are available within a regionally controlled biostratigraphic framework. All three examples are from the Mesozoic: the Lias and Kimmeridgian in England, and the Cenomanian in the northwestern Atlantic. We will analyze the hierarchy of the different cyclicities in these case studies, document the lateral variations, and discuss the relative importance of anoxia versus productivity.

HIGH-FREQUENCY CYCLICITY: SCALE IN TIME AND SPACE

For a full understanding of the sedimentary system, and thus the conditions under which organic carbon is produced and preserved, a clear notion of the scales at which different sedimentary processes act is critical. Three scales are distinguished, the basin scale, the facies scale, and the layer scale, each characterized by specific time and space values, processes, and theoretical models (Figure 1, top). This hierarchical subdivision is based on a process-oriented approach to sedimentary sequences, introduced—among others—by Matthews (1984) and Aigner (1985). High-frequency cyclicity in open marine sedimentary systems occupies the intermediate position, the facies scale, which explains its relevance for both basin-scale and diagenetic studies (Figure 1).

A subdivision of the petroleum play in a similar way helps to select the relevant geological disciplines to solve petroleum geological problems (Figure 1, bottom). The distribution of reservoir units and source rocks is studied at the scale of the sedimentary basin. Heterogeneities in reservoir architecture and heterogeneities in quality and quantity of organic matter become apparent at the facies scale. The petrophysical

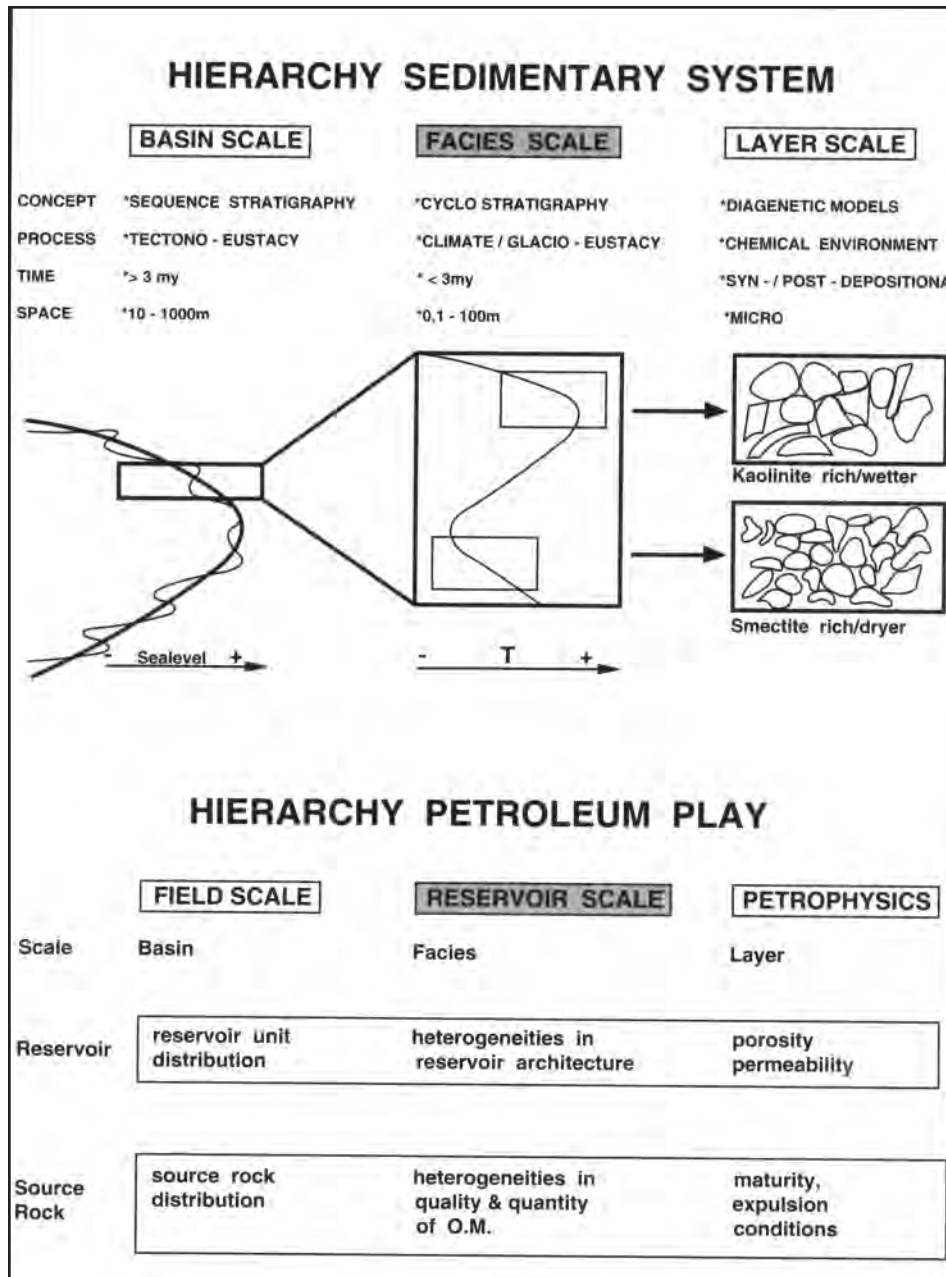


Figure 1. The hierarchy of the sedimentary system and the petroleum play follow the same scales, each characterized by specific dimensions, time duration, processes, and concepts. T = temperature, Micro = microscopic scale.

analyses (porosity and permeability) and the maturation and expulsion of organic matter take place at the smallest level, the layer scale.

The basin scale deals with facies sequences on the order of several tens to thousands of meters, and the time span involved varies from a few million years to tens of millions of years. The modern stratigraphic/sedimentological concept used at this scale is *sequence stratigraphy*, which has developed mainly from seismic studies of the subsurface (e.g., Van Wagoner et al., 1988; Vail et al., 1991). The main processes are tectono-eustatic changes in relative sea level, long-

term changes in climate, paleoceanography, paleogeography, and paleotopography.

The facies scale is superimposed on the long, basin-scale trends. It is characterized by allocyclic and autocyclic mechanisms affecting the temporal and spatial distribution of sediments working within a certain range of adjacent depositional environments (e.g., climate-controlled variations in relative sea level, storm activity, runoff, and lateral shifting of delta lobes). They produce typical cyclical patterns at a high frequency (<3 m.y.), expressed as lithological alternations at a scale between 0.1 and 100 m. The modern strati-

graphic/sedimentological concept applied at this scale is *cyclostratigraphy* which developed from detailed outcrop observations of sedimentary sequences and from subsurface correlations of well logs (e.g., Melnyk and Smith, 1989; Smith, 1989; Fischer et al., 1990; Van Wagener et al., 1990; Mitchum and Van Wagener, 1991; Fischer and Bottjer, 1991; de Boer and Smith, 1994b; Melnyk et al., 1994). Increasingly, examples of cyclic sequences are being described in which astronomical forcing is assumed or shown to be the driving force behind cycles in the range of 10 k.y. to 2 m.y.; that is, the Milankovitch domain (cf. de Boer and Smith, 1994b). Astronomically forced changes of climate do indeed directly affect terrestrial sedimentary systems. Indirectly, by influencing oceanography and the input of terrestrial sediment into the marine domain, they can produce cyclic sequences in the marine setting.

The layer scale deals with sediment texture and sediment composition as defined by the physical and chemical environment during and after deposition. The processes involved are relatively short-term "events" (hours to thousands of years) like the production of sediment beds by storms, tides and seasonal cycles, biologically induced sediment aggregation and accumulation, the effects of periodic chemical conditions at the sea bottom such as oxygen deficiency, etc. The amount of sediment affected may vary from concretionary layers up to a meter thick to decimeter thick storm beds and millimeter thick lithological alternations. Modern concepts about the preservation of organic matter at this scale are based on observations in modern-day environments and processes together with theoretical geochemical models (e.g., Froelich et al., 1979; Berner, 1981; Maynard, 1982; Einsele et al., 1991).

CASE STUDIES

The three case studies have been selected for their different types of environmental setting, and for which both very detailed geochemical profiles (20 to 30 samples per meter) documenting the high-frequency cycles and a good to excellent (bio-) stratigraphic control are available. They are:

1. Three adjacent epeiric subbasins in the Lower Jurassic of England; the studied interval is of Pliensbachian age and represents a transgressive phase in Northwest Europe (Sellwood, 1972; Donovan et al., 1979; Bradshaw and Penney, 1982; Hallam, 1988), but not a period of worldwide organic matter deposition.
2. A hemipelagic basin with a strong topographic relief in the Kimmeridgian of England; it represents a period of worldwide sea level highstand and widespread organic carbon storage (Cornford, 1984; Grace and Hart, 1986; Grant et al., 1988).
3. The Cenomanian–Turonian boundary event in a pelagic setting in the North Atlantic and along its western passive margin; it represents a period of worldwide sea level highstand, and is known for

its extensive organic carbon reserves (Jenkyns, 1985; Herbin et al., 1986; Thurow and Kuhnt, 1986; Arthur et al., 1987; Schlanger et al., 1987; Kuhnt et al., 1990; Stein, 1986).

The Lower Lias of England

The excellent biostratigraphy of the British Lias (Cope et al., 1980) offers the opportunity to choose a short stratigraphic interval (the *Uptonia jamesoni* ammonite zone of the Pliensbachian stage) showing clear cyclicity over a distance of at least 450 km through different sedimentary environments (Figures 2 and 3). Figure 4 schematically shows the paleogeographic situation. In the Dorset coastal outcrops marl-limestone cycles occur in a hemipelagic setting (Weedon and Jenkyns, 1990), with total organic carbon (TOC) values up to 5.5%. Over the Mendips high, in Oxfordshire, at the same time green/gray mudstone cycles were deposited in a setting just below storm-wave base (Horton and Poole, 1977). The Cleveland basin in Yorkshire, north of the Market Weighton block, shows a cyclicity of mudstones and siltstones, with generally low TOC (0.4–1.4%) values and an estimated water depth around storm-wave base (Sellwood, 1970; van Buchem and McCave, 1989; van Buchem et al., 1992, 1994). The Dorset and Yorkshire sites have been studied in detail in outcrop sections and their datasets have been analyzed with Fourier analysis. For a more in-depth discussion of the Fourier analysis technique and the results, the reader is referred to Weedon (1991, 1993), and the original publications on the Dorset (Weedon and Jenkyns, 1990) and Yorkshire sites (van Buchem et al., 1992, 1994).

Yorkshire

The *Polymorphites polymorphus* subzone (*U. jamesoni* zone) of the Banded Shales exposed in Robin Hood's Bay in Yorkshire (Figure 3A) has been sampled by van Buchem et al. (1994) in 5 cm intervals and analyzed for organic and inorganic geochemistry, grain size, and organic matter composition (Figure 5). Paleontological observations are from Tate and Blake (1876) and Sellwood (1970).

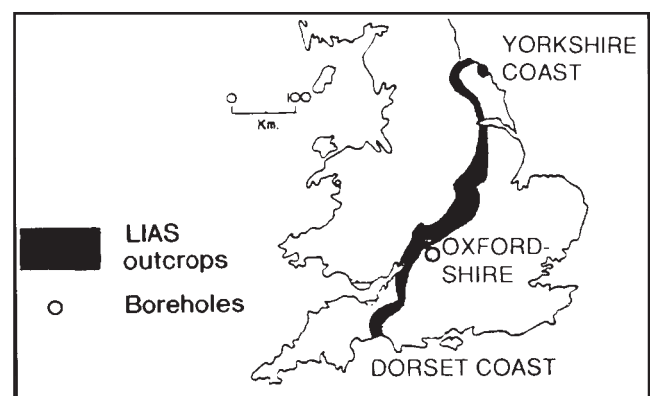


Figure 2. Map of Lias outcrops in England.

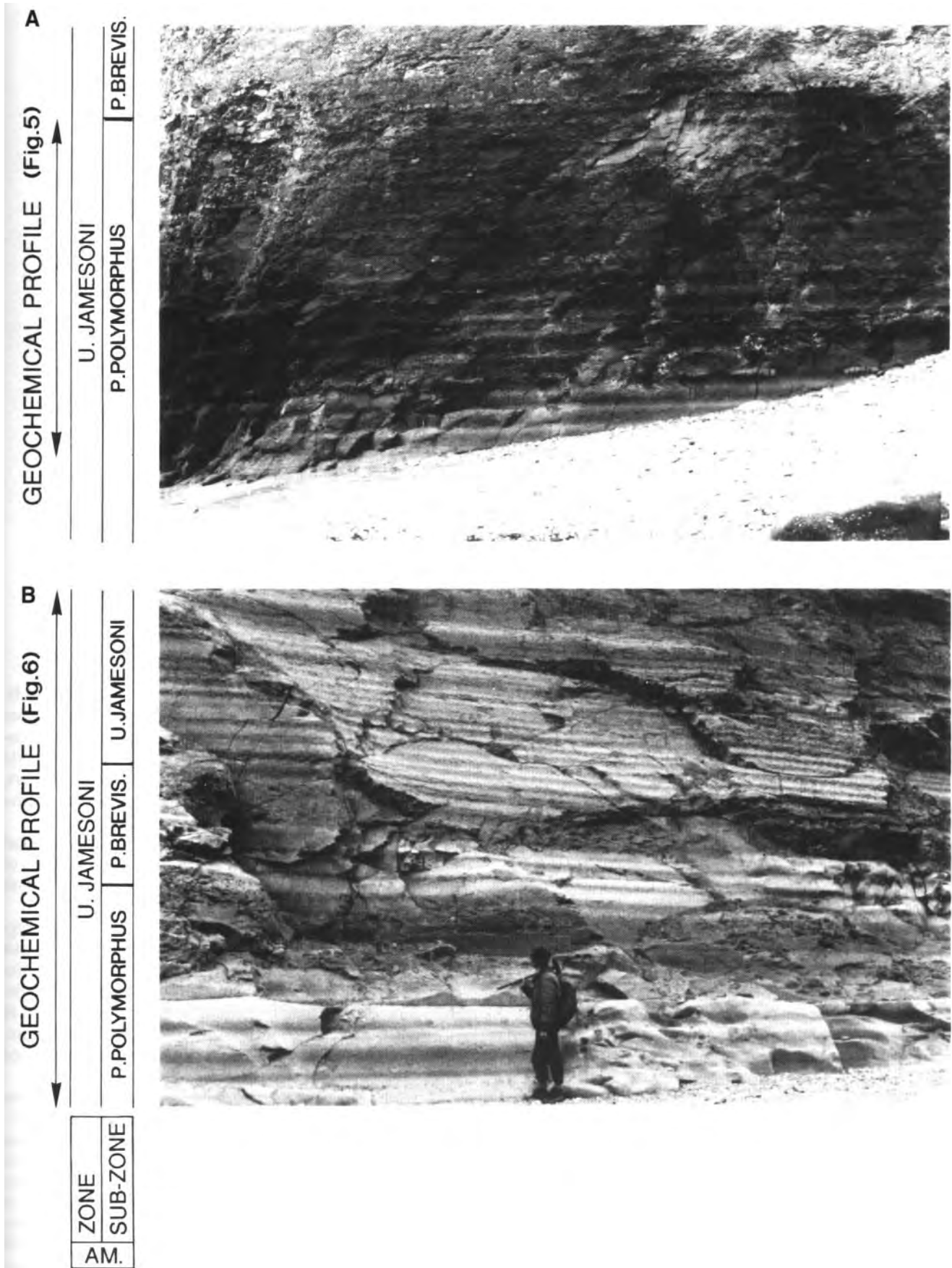


Figure 3. Outcrop pictures of high-frequency cyclicity in the *U. jamesoni* ammonite zone in Yorkshire (A) and Dorset (B; by courtesy of G.P. Weedon). Intervals sampled for geochemical analyses have been indicated.

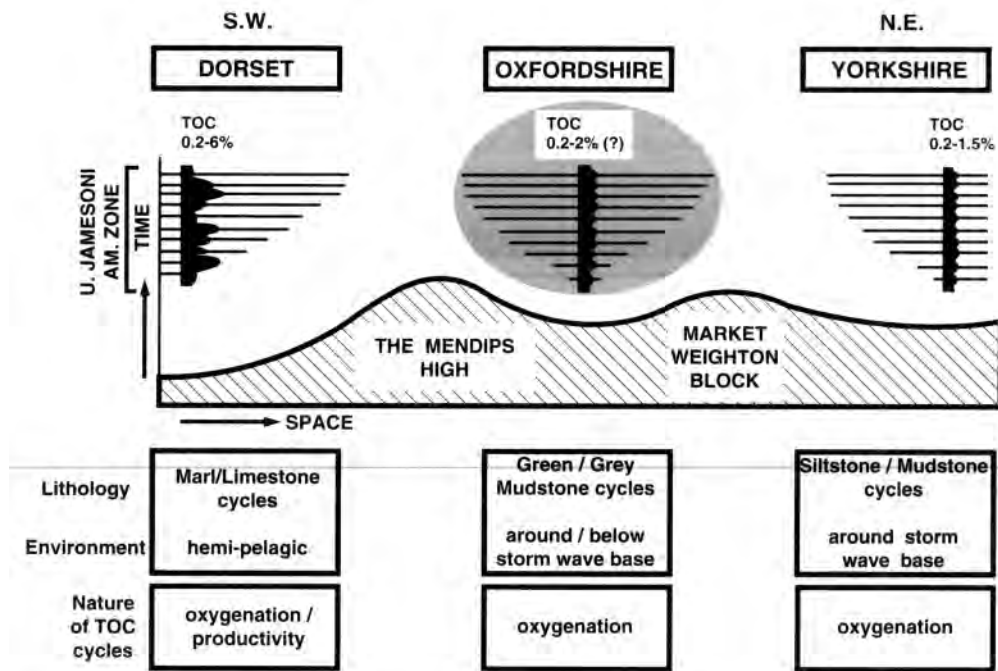


Figure 4. Schematic cross section through three adjacent Liassic epeiric sub-basins in England at *U. jamesoni* times. High-frequency cyclicality has been observed in all of them, but is expressed in different lithologies due to the different sedimentary environments. The TOC preservation potential varies accordingly. Gray marking: the TOC values for Oxfordshire have been extrapolated (see text).

The stratification pattern is the result of a variation of the quartz silt (33 to 55%) versus clay (39 to 59%) content. TOC values are low (between 0.4 and 1.4%), but vary inversely with the grain-size variations. The darker colored layers are TOC and clay rich, and have a poor fauna (small, thin-shelled, protobranch and lucinoid bivalves). The organic matter fraction is isotopically lighter (more marine) and consists of 75% type III (less plant tissue; for organic petrological data see van Buchem et al., 1994). The lighter colored layers are TOC poor, silty, and have a diverse macrofauna (belemnites, thick-shelled pectinids, *Pinnas*, *Grypheas*), and an organic matter fraction that is isotopically heavier (less marine) and consists of 85% type III (more plant tissue; for organic petrological data see van Buchem et al., 1994).

The average cycle thickness in the *Uptonia jamesoni* zone is 37.5 cm, and total thickness is 24 meters with 64 cycles. Fourier analysis of grain size and TOC time series revealed power at wavelengths of 50 cm and 83 cm.

Dorset

The *U. jamesoni* ammonite zone of the Belemnite Marls exposed along the Dorset coast near Charmouth (Figure 3B) has been sampled by Weedon and Jenkyns (1990) at 3 cm intervals and analyzed for TOC and CaCO₃ content (Figure 6).

The cyclicality is a result of a variation of the TOC content (0.5 to 5.5%) and the CaCO₃ content (30 to 65%); they show a nonlinear inverse correlation. The organic-rich marl layers are poor in carbonate content,

laminated, and contain scarce faunal elements (Sellwood, 1970, 1972). Organic-poor layers are carbonate rich, bioturbated, and contain a rich fauna. Trace fossils, laminated shales, and TOC values suggest oxic conditions during deposition of the limestone layers, and subanoxic conditions during deposition of the marls in a generally hemipelagic setting.

The average cycle thickness is 27.6 cm and total thickness is 10.5 m with 38 cycles. Fourier analysis of the TOC and carbonate time series gave two dominant wavelengths: 37.5 cm and 300 cm.

In both cases, the cyclicality is directly linked to a regular variation of the level of oxygenation at the sea floor, as expressed by the variations in intensity of bioturbation, the diversity and abundance of faunal elements, and the distribution of organic matter. Yet, in none of these cases is there strong indication of complete anoxia with black, pyritic organic-rich laminated shales with no trace fossils or body fossils.

To what extent productivity is involved in this cyclicality varies for both sites. In Yorkshire, the TOC-rich layers are isotopically lighter than the TOC-poor layers, indicating a higher content of marine organic matter. An analysis of the palynofacies (van Buchem, 1990) showed that the bulk of the organic matter in both layers represents type III, 75% for the organic-rich, and 85% for the organic-poor layers. Type III organic matter is characteristic of hydrogen-poor land-derived plant material (Tissot and Welte, 1984). Since a 50 to 300% difference in TOC values (0.4 to 1.4%) can not be explained by a 10% difference in the amount of

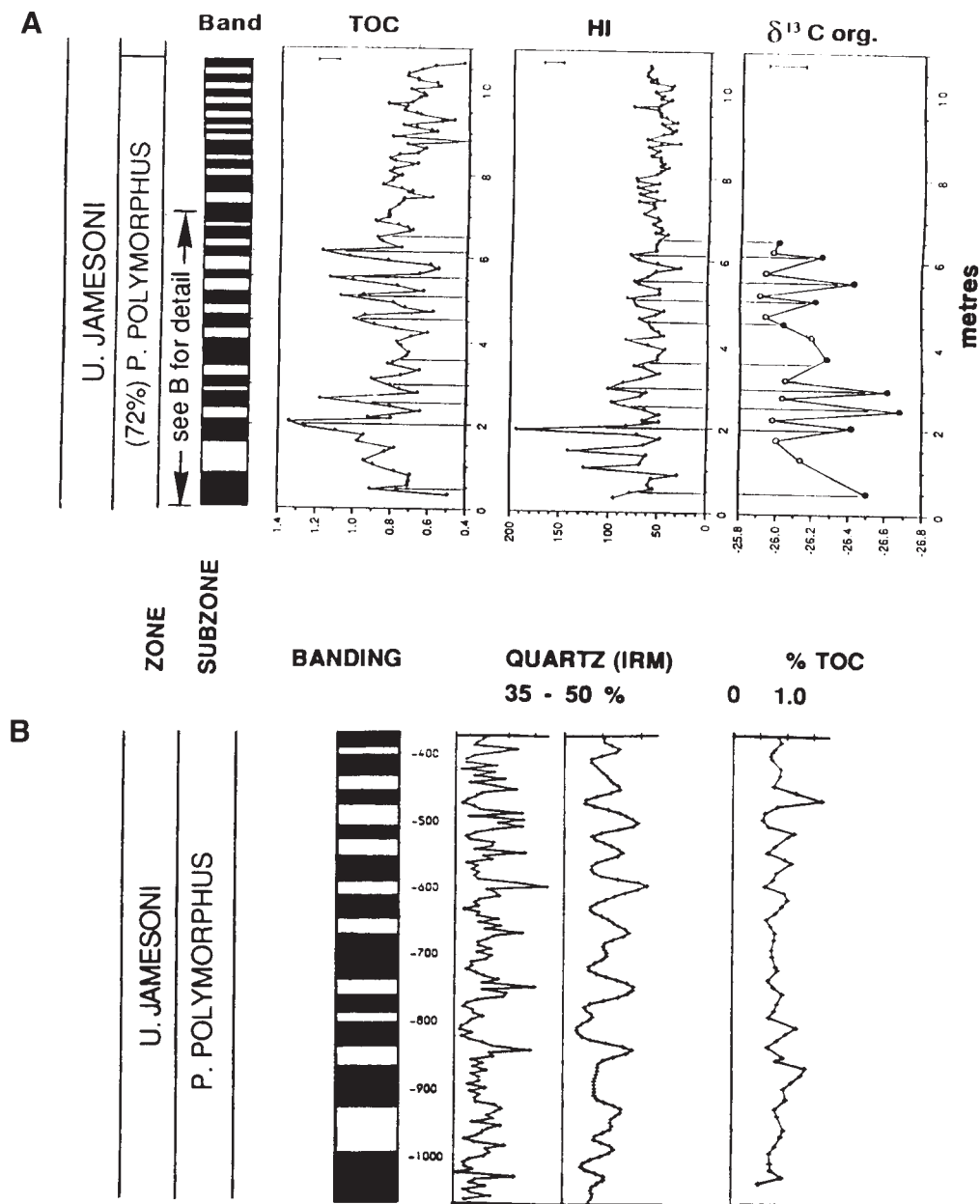


Figure 5. Geochemical profiles from the *U. jamesoni* ammonite zone (Pliensbachian) of the Banded Shales in Yorkshire (after van Buchem et al., 1994). The section was sampled at 5 cm intervals. (A) Variations in quantity and quality of the organic matter fraction. Organic matter was analyzed by Rock-Eval. Horizontal lines represent stratigraphic position of the dark layers. Standard error bars have been indicated. TOC = total organic carbon in %; HI = hydrogen index in mg hydrocarbon/g TOC; $\delta^{13}\text{C}_{\text{org}}$ = organic carbon stable isotopes in ‰; Band = alternation of dark and light layers as observed in outcrop. (B) Variations in grain size and TOC in the same interval as (A). IRM (isothermal remanent magnetization) has been used as an indicator of the relative concentration of quartz versus clay (see van Buchem et al., 1994, for details).

the marine organic matter fraction alone, this implies that marine productivity can be excluded as the prime reason for TOC variations in Yorkshire. The possibility of varying amounts of organic-matter influx from the land is unlikely, since detailed clay-mineralogical analyses showed no correlation between the land-

derived kaolinite distribution and the TOC variations (van Buchem et al., 1994). This leaves oxidation as the primary control on the TOC preservation in Yorkshire, and explains the difference in palynofacies assemblage as a result of selective oxidation of the vulnerable marine fraction. Combining these observations with

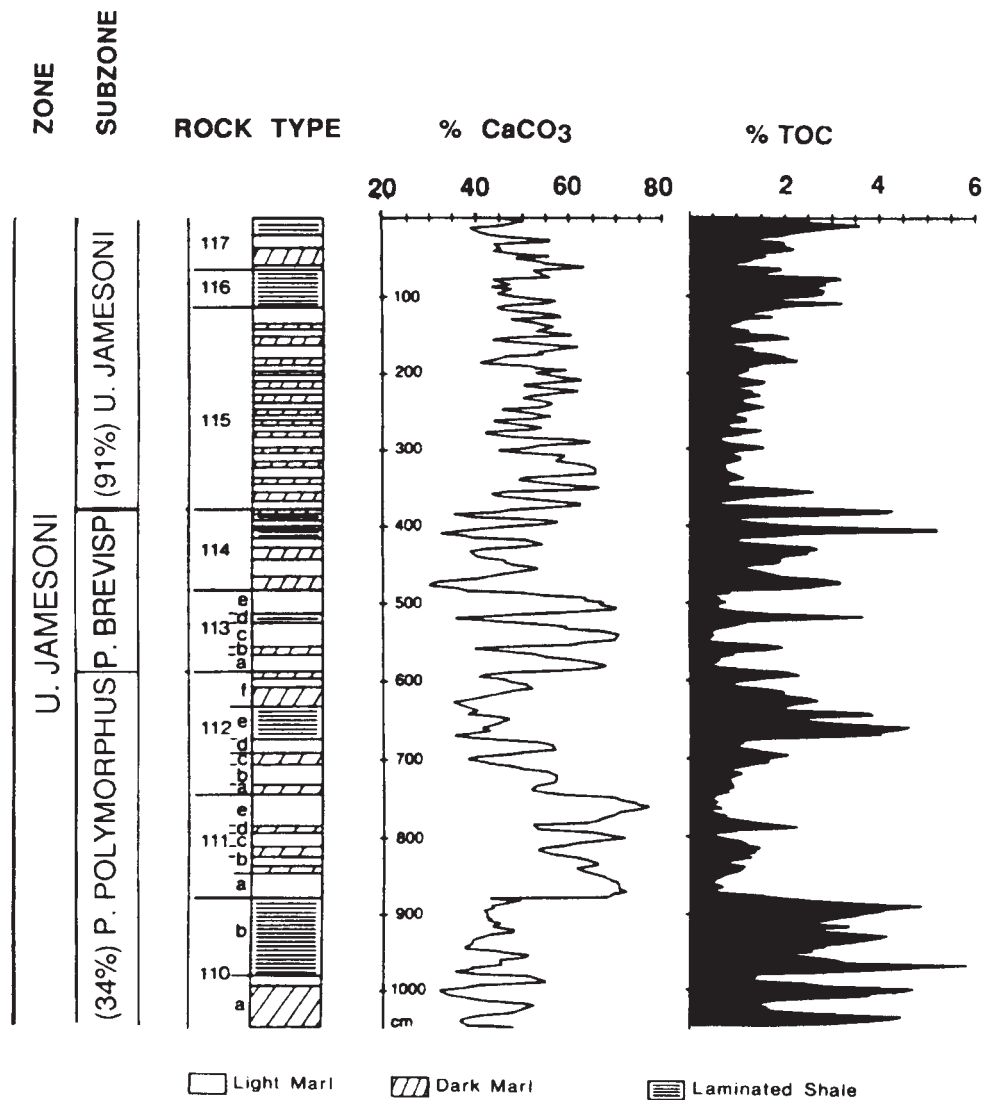


Figure 6. Geochemical profiles for 10 meters of the *U. jamesoni* ammonite zone (Pliensbachian) of the Belemnite Marls in Dorset (after Weedon and Jenkyns, 1990). The section was sampled at 3 cm intervals for TOC and carbonate carbon analysis. Scale is in meters.

the variations in the mud/silt ratio, the preferred explanation is that variations in the relative frequency and strength of storms, acting in a sedimentary environment around storm-wavebase, are the main control on the degree of oxidation of the sea floor and thus the preservation of organic matter (van Buchem and McCave, 1989; van Buchem et al., 1994).

In the hemipelagic Dorset setting, there is no indication of a grain size variation. Here, the cyclicity may (partly) be caused by the regular variation in productivity of carbonate-walled versus organic-walled plankton, causing dysaerobic conditions at the sea floor at times of abundant organic-matter supply. The data are however not sufficient to confirm this.

The TOC values found in Yorkshire (0.4–1.4%) are generally lower than those found in Dorset (0.5–5.5%). This is probably a result of both the better oxygenation and a generally higher sedimentation rate in the Yorkshire setting (couplets are about 30% thicker; Table 1).

Although the Dorset and Yorkshire Lower Jurassic sections are among the world's biostratigraphically best-studied sections (Tate and Blake, 1876; Simpson, 1884; etc. to Cope et al., 1980), a precise estimation of the cycle duration is difficult. In Table 1 the different options are presented. Two time scales have been used: one is based on the average length of a Jurassic ammonite subzone of 433 k.y. (144 subzones in the zonation scheme of Cope et al., 1980; for 62.5 m.y. in Harland et al., 1990); and the other is based on the duration of a Liassic ammonite zone of 1500 k.y. (20 zones in Cope et al., 1980; for 30 m.y. in Harland et al., 1990). The subzone scale gives values of 18.4 and 25.6 k.y. for the average duration of the cycles; for the zone scale these values are 11.2 and 17 k.y. If we consider the duration of the cycles in the individual subzones, a large variation is particularly apparent between the *Platypleuroceras brevispina* and *P. polymorphus* cycles in Dorset (11.0 to 72 k.y.) and to a lesser extent also in

Table 1. Overview of cycle thicknesses and duration of the four subzones constituting the *U. jamesoni* ammonite zone of Yorkshire and Dorset.

| Subzone | Yorkshire | | | | | Dorset | | | | |
|-----------------------|---------------|--------|---------------------------|-------------|-----------------------|---------------|--------|---------------------------|-------------|-----------------------|
| | Thickness (m) | Cycles | Aver. Cycle Thickness (m) | Time (k.y.) | Cycle Duration (k.y.) | Thickness (m) | Cycles | Aver. Cycle Thickness (m) | Time (k.y.) | Cycle Duration (k.y.) |
| <i>U. jamesoni</i> | — | — | — | — | — | (1.35)* | — | — | — | — |
| | 8.85 | 33 | 0.27 | 433 | 13.1 | 3.95 | 18 | 0.22 | 394 (91%) | 21.8 |
| <i>P. brevispina</i> | 4.50 | 11 | 0.41 | 433 | 39.4 | 2.00 | 6 | 0.33 | 433 | 72.0 |
| <i>P. polymorphus</i> | 10.65 | 20 | 0.53 | 312 (72%) | 15.6 | 4.65 | 13 | 0.35 | 147 (34%) | 11.3 |
| | (5.00) | — | — | — | — | (9.00) | — | — | — | — |
| <i>P. taylora</i> | (21.00) | — | — | — | — | (3.20) | — | — | — | — |
| Total | 24.00 | 64 | 0.37 | 1,178 | 18.4 | 10.50 | 38 | 0.28 | 974 | 25.6 |
| Total Zone | " | " | " | 720+ (48%) | 11.25 | " | " | " | 645+ (43%) | 17.0 |

* Thicknesses in parentheses represent intervals not showing cyclicity.

+ Duration is based on % thickness of the *U. jamesoni* Zone (as compared to the numbers based on a subzone time length given above).

Yorkshire. In the light of the hypothesis of an orbital control of the cycles this needs an explanation. There are three options: (1) a large number of cycles is missing in the *P. brevispina* subzone, (2) the boundary between the two is placed too high, or (3) ammonite subzones do not represent equal amounts of time. There is no sedimentological evidence for the first possibility, considering the regularity of the cycle thicknesses in both subzones and the absence of erosional surfaces. The fact that the *P. brevispina*/*P. polymorphus* boundary is renowned for its unreliability and is often difficult to locate (Wilson and Manning, 1978; Gaunt et al., 1980; Cope et al., 1980) may support both the second and third options. This problem can be circumvented by taking the two subzones together. In that case we arrive at an average cycle duration of 30.5 k.y.

Because of the difficulties in defining the absolute time span of the cycles, spectral analysis has been applied to decide if orbital parameters have been involved in the generation of the cycles. For the Cleveland basin, three sets of time series have been analyzed (outcrop geochemical profile, outcrop gamma-ray log, and Felixkirk borehole gamma-ray log). The outcrop geochemical time series gave two dominant frequencies: 50 cm and 83 cm. The wavelength ratios all compare well to the orbital wavelength ratios predicted by Berger et al. (1989) for the Early Jurassic, giving support to the idea that precession, obliquity, and eccentricity parameters influenced the sedimentation pattern in Yorkshire (see van Buchem et al., 1994, for details). Spectral analysis of the time series in Dorset showed two dominant wavelengths, 37 cm and 300 cm, of which the smaller one has been suggested to be the precession cycle (Weedon and Jenkyns, 1990). The difference in thickness of the precession cycle in both settings must be due to the difference in sedimentation rate. In Yorkshire, the average cycle is 30% thicker than in Dorset (37 cm versus 28 cm), which is exactly the same rate as the two wavelengths (50 cm and 37 cm). This difference in sedimentation rate, and the absence of the obliquity cycle in Dorset, may lie in the fact that it represents a hemipelagic setting, where sedimentation may have been more influenced by ocean currents, water temperature, and primary productivity, whereas the shallow marine siliciclastic Yorkshire setting was more directly influenced by epicontinental features such as sensitivity to storm magnitude and frequency, and by changes on the land affecting weathering intensity and runoff.

If we accept the hypothesis of orbitally forced climatic changes as the cause for the cyclicity in the Yorkshire and Dorset sections, then we may expect to find a similar type of cycles in the Oxfordshire area located between the two other sites (Figures 2 and 4). Cyclicity has indeed been observed by Horton and Poole (1977) in cores of the *U. jamesoni* zone of three boreholes (Apley Barn in Witney; Steeple Aston; and Withcombe Farm in Banbury). They described a rhythmic bedded interval with cycles showing the following organization (Horton and Poole, 1977):

The ideal rhythm commences above a well-defined burrowed surface. This is overlain by a

very thin shell-bed which may be pyritic. Thin pavements of disarticulated bivalves occur above in pale grey, rather blocky, slightly calcareous mudstones. Fine plant detritus may be present near the base. The proportion of shells and shell debris decreases upward and the unit terminates in a very thinly laminated fissile, greyish and olive-grey mudstone with immature bivalves and some fish debris. This uppermost bed is mottled by bioturbation such as is produced by *Chironidites* and may also contain both irregularly inclined and U-shaped burrows.

The cycles start at the base with a shell bed and burrowing which indicate relatively high wind stress and a probably related sufficient aeration of the water column for scavengers to colonize the sea floor. Then, through the rest of the cycle, the gradual diminution of the shell beds, absence of burrowing, and lamination at the top suggest a general decrease of wind stress and deterioration of living conditions at the sea floor (suboxic). The biostratigraphic control, the sedimentological characteristics of the cycles, and the position in between the Yorkshire and Dorset areas strongly suggest that sedimentation in the Oxfordshire area was controlled by similar processes as in the Yorkshire and Dorset sites.

To summarize, the Lias case illustrates the following points.

1. High-frequency cycles find expression in very different sedimentary settings over a distance of 450 km in the same small time interval (approx. 1 m.y.).
2. The total amount of organic matter stored in each environment may vary (e.g., Dorset and Yorkshire), but all TOC profiles follow the high-frequency cycles.
3. The cycles are caused by high-frequency climatic variations which controlled the degree of oxygenation at the sea floor, as expressed by the faunal and sedimentological features. The climatic variations are most likely orbitally forced (precession cycle).

The Kimmeridgian of England

The Upper Jurassic Kimmeridge Clay Formation (Kimmeridgian) is an important source rock of the North Sea oil province, and the formation's onshore extension provides a unique opportunity to study the variability of its organic carbon content. The classic outcrop location in Kimmeridge Bay, Dorset, has been studied in great detail for sedimentological, geochemical, and biostratigraphic aspects (Gallois, 1976; Cox and Gallois, 1981; Tyson, 1987; Oschmann, 1988, 1990; Wignall, 1989).

Here we discuss the study by Herbin et al. (1991, 1993) of the onshore subsurface Kimmeridgian in Yorkshire, approximately 450 km north of the Dorset outcrops. The four continuously cored boreholes cover a 35 km long transect which represents the transition from basin to shelf in an epicontinental setting (Figure 7). The Kimmeridgian reaches a thickness of 200 m

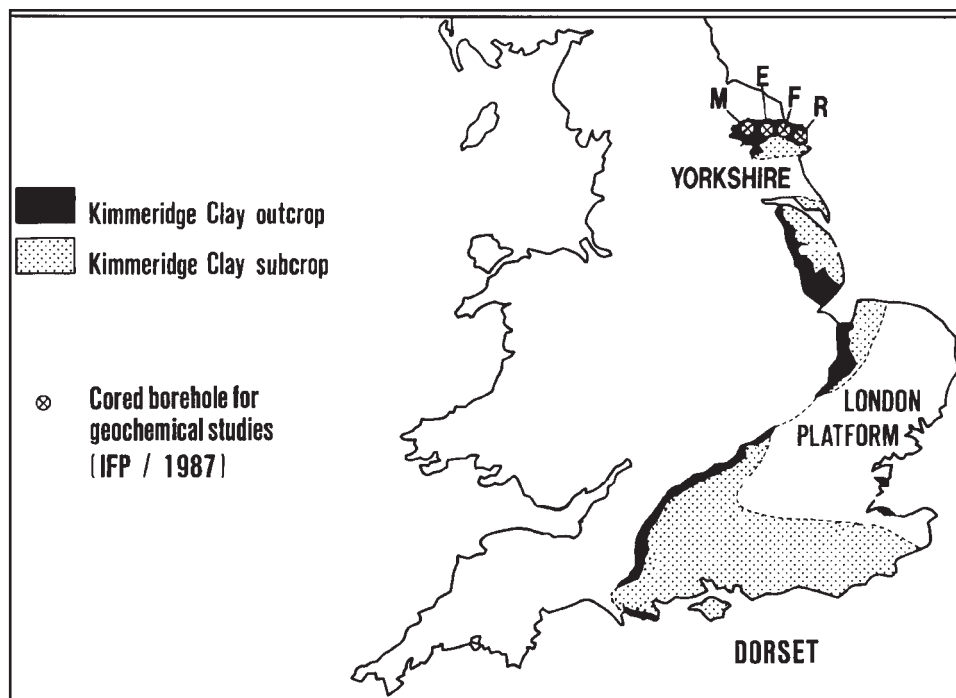


Figure 7. Location of the outcrop and subcrop of the Kimmeridge Clay in England, and the four IFP boreholes in the Yorkshire area (M = Marton, E = Eberston, F = Flixton, R = Reighton).

and ranges in age from the *Rasenia cymodoce* Zone to the top of the *Pectinatitus pectinatus* Zone. This study is unique in that very detailed geochemical analyses of the mineralogical content (sample spacing 4 m) and organic matter content (sample spacing 10 to 50 cm) have been carried out for all four wells over the whole interval. The sonic, density, and resistivity logs were then calibrated with the organic carbon percentages to obtain a continuous curve for the organic carbon distribution (Carpentier et al., 1991). Due to the relatively small variations in mineralogy, it is very hard to visually distinguish the cyclicity in the core material. Only extensive weathering, such as in Kimmeridge Bay, can bring out the cycles. This is important to realize, since it urges the need for detailed geochemical sampling of cored source rock intervals.

The sediment is mainly composed of clay minerals (70–80%), TOC (1–20%), and accessory biogenic calcite (coccoliths), quartz, and pyrite (Herbin et al., 1991). High-frequency variations in TOC are in phase both with the kaolinite content (23 to 45 total clay %; Bachaoui and Ramdani, 1993) and carbonate content (16 to 20 total weight %; Belin and Brosse, 1992). The TOC distribution shows strong vertical variations, with maximum values up to 40% in the most extreme case (well Marton 87), and is organized at three scales (Figure 8). The entire organic-rich interval (*R. cymodoce* to *P. pectinatus* zone) falls in a long-term trend that set the scene worldwide for organic carbon storage: the general Kimmeridgian eustatic sea level rise (Haq et al., 1987). Superimposed on this trend there are two smaller orders of cyclicity: the *medium-scale cycles* (decametric, 23 cycles of 330 k.y., 4th order), which are

each composed of approximately ten *small-scale cycles* (metric, 250 cycles of 30 k.y. each, 5th order). The time estimations are based on the ammonite zonation scheme of Cope et al. (1980) and the time scale of Harland et al. (1990) (74 ammonite zones in 62.5 m.y.).

The *small-scale cycle* forms the basic unit. It is characterized by couplets of an organic-poor layer (0.5–5% TOC) with a scarce dysaerobic fauna of thin-shelled bivalves (Oschmann, 1988; Herbin et al., 1993), and an organic-rich layer (5–40% TOC) which in the organic-richest levels is devoid of faunal elements, has no trace fossils, and has a fine lamination. The faunal content shows that conditions at the sea floor were generally dysaerobic, but that the organic-rich layers were deposited under conditions more hostile to life at the sea floor than in the organic-poor layers, and that they were probably anoxic. These conditions were at least continuous at the scale of the cross section, as suggested by the bed by bed correlation potential of the individual small-scale cycles (Figure 9).

The organic geochemical analysis of the extracts by Herbin et al. (1993) showed that the origin of the organic matter throughout the metric cycles is constant and of autochthonous marine type II. A plot of the hydrogen index (HI) and oxygen index (OI) values of cycles in a basinal section in a van Krevelen diagram shows, however, that organic-rich layers are much hydrogen richer than organic-poor layers (Figure 10). Two explanations are possible: (1) either they reflect variations in the state of preservation of the stable residue (oxidation control), indicating a better preservation in the anaerobic, organic-richer layers (high HI and low OI) and a degradation in the more oxic,

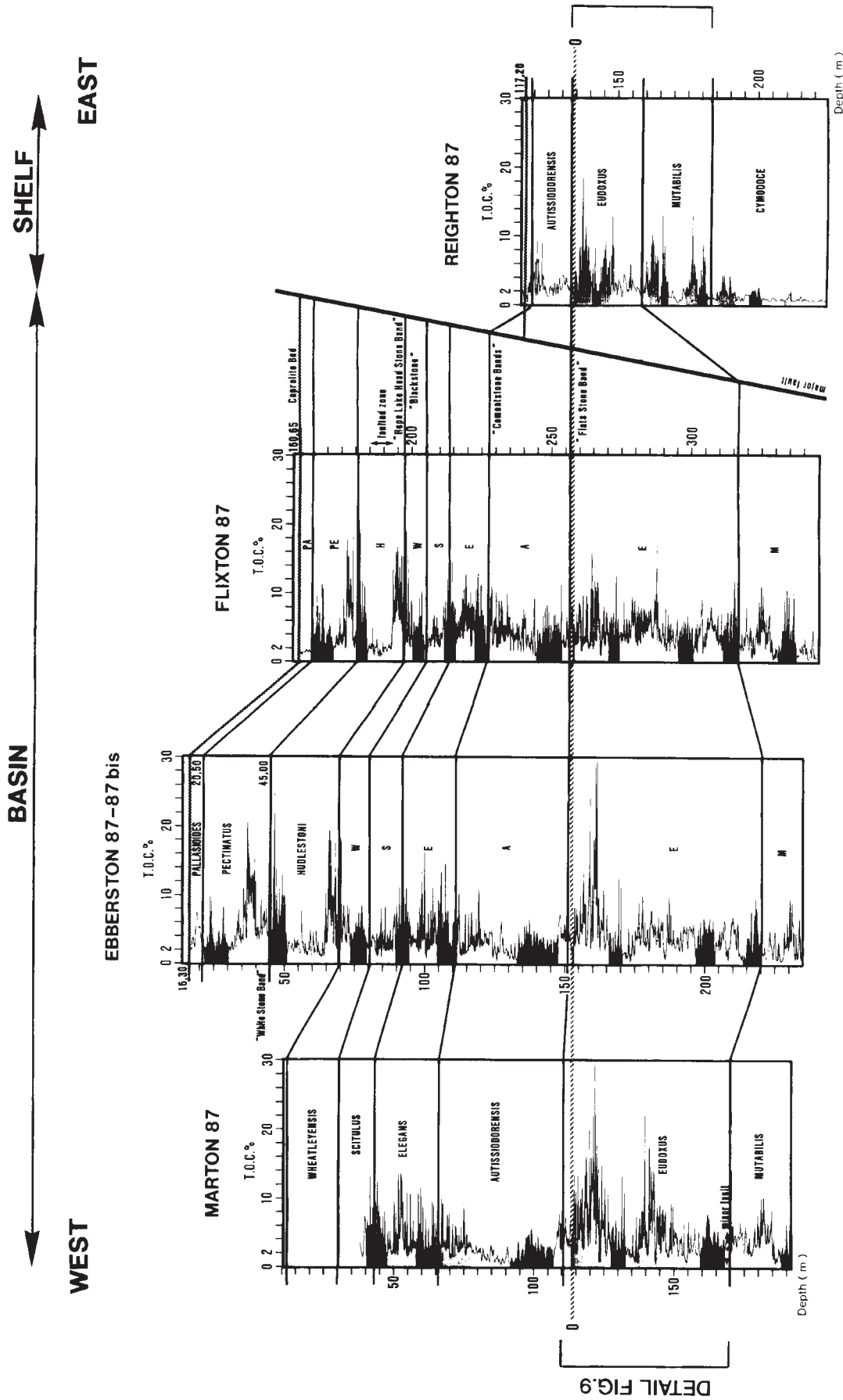


Figure 8. Ammonite biostratigraphic framework and total organic carbon distribution for the Kimmeridge Clay Formation of the four Yorkshire boreholes (after Herbin et al., 1991). The names of the ammonite zones are indicated. Black and gray-colored intervals are correlatable decameter-thick sequences. Note the reduced thickness of the Reighton 87 section on the shelf. Figure 9 shows a detailed correlation of the high-frequency cycles in the *A. eudoxus* zone. See Figure 7 for borehole locations.

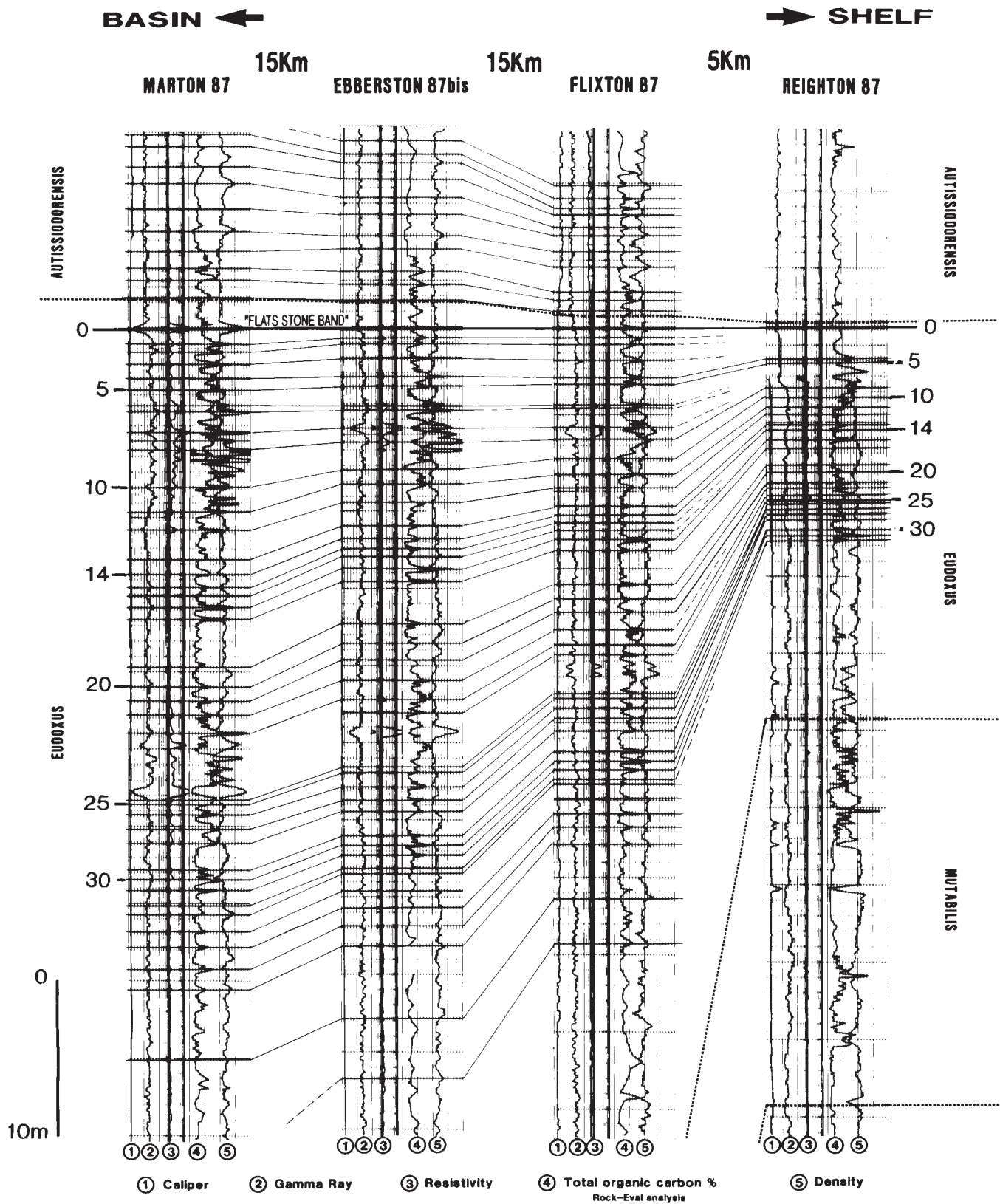


Figure 9. Detailed correlation of the high-frequency cyclicality in the *A. eudoxus* zone of the Kimmeridge Clay in the Yorkshire boreholes (after Herbin et al., 1991). The correlation is based on wireline logs (caliper, gamma ray, resistivity and density) and measured TOC content (Rock-Eval). Decametric-scale sequences can be traced from basin to shelf (numbers 0, 5, 10, 14, 20, 25, 30) over a distance of 40 km, while the highest frequency cycles often pinch out against the topographic relief (approximately 20 m). The Flats Stone Band is a geochemical marker bed roughly corresponding to the *A. eudoxus*/*A. autissiodorensis* ammonite zone boundary. See Figure 7 for borehole locations.

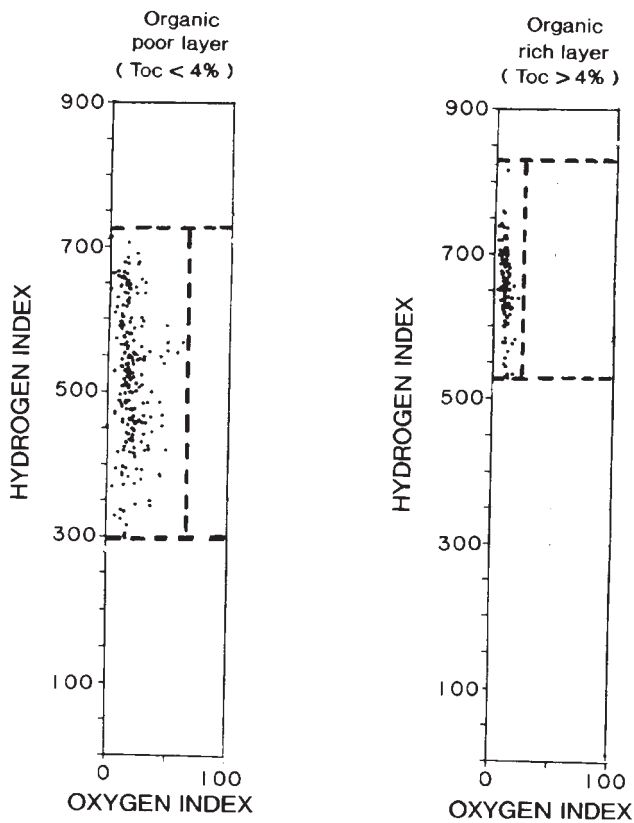


Figure 10. Hydrogen index/oxygen index diagrams for the Kimmeridge Clay cycles in the Marton 87 borehole in Yorkshire (after Herbin et al., 1991). Data are from the interval 113 to 156 m (see Figure 8) and have been presented for the organic-poorer and the organic-richer parts of the high-frequency cycles.

organic-poorer layers (low HI and high OI), or (2) they indicate a different primary composition of the algal types with different resistance against oxidation (productivity control). Detailed microscopic observations on two small-scale cycles confirmed that 80% of the organic matter is of marine origin (amorphous, fluorescing material), and showed an increased diversity of the marine organic matter with, notably, the appearance of a "new," brown-colored type algae for the organic-rich layers (Pradier and Bertrand, 1992; Ramanampisoa et al., 1992). Similar observations have been made by Belin and Brosse (1992), but they also showed that TOC enrichment is accompanied by the abundance of well-preserved fecal pellets consisting of coccoliths.

The diversification of the algal content (two types) and high concentration of the fecal pellets in organic-rich layers suggest an increased productivity at the time of their deposition. The increased organic matter flux may thus have enhanced or even caused the oxygen deficiency at the sea floor. A primary control of the productivity is also advocated by Bertrand and Lallier-Vergès (1993), Lallier-Vergès et al. (1993), and Tribouvillard et al. (1994), mainly based on geochemical arguments. The positive correlation of the TOC distri-

bution and the land-derived kaolinite implies that the variations in productivity were in phase with climatic changes affecting conditions on the land (Bachaoui and Ramdani, 1993).

The cyclic character and organization at three scales of the TOC distribution have been observed along a 3000 km north-south transect from the Dorset outcrops to the subsurface in the Barents Sea (Cornford, 1984; Dore and Gage, 1987; Ziegler, 1988). This implies that the mechanisms controlling the vertical variations in TOC were of a regional character and that they were more or less constant over a period of several million years. Concerning the metric- and decametric-scale cycles there is a broad consensus that they result from climatically controlled variations in sedimentary conditions (*Yorkshire*: organic geochemistry, Herbin et al., 1991, 1993; clay mineralogy, Bachaoui and Ramdani, 1993; *Dorset*: paleontology, Oschmann, 1988, 1990; paly-nology, Tyson, 1987, and Waterhouse, 1992; geochemistry, Mann and Myers, 1990; organic geochemistry, Huc et al., 1992; and clay mineralogy, Wignall and Ruffel, 1990). The exact mechanism by which climatic change influenced productivity and oxygenation is still a matter of debate (see review in Wignall and Hallam, 1991). It seems, however, that Oschmann's model (1988, 1990) accounts for most of the observations. He suggests that changes in the upwelling pattern related to monsoonal wind patterns caused a seasonal stratification of the water column and influenced productivity and runoff. The possibility of a direct relation to *high-frequency sea level changes* was tested in the marginal deposits of the Kimmeridgian in the Boulonnais (France), but showed no good correlation (Herbin and Geysant, 1993; Herbin et al., 1995).

An orbital control of these climatic changes seems likely considering the regional extent and the number and duration of the cycles (Oschmann, 1990; Herbin et al., 1991). An early attempt to search for orbitally induced cycles using spectral analysis was published by Dunn in 1974. He studied a 20 m thick section in the *Pectinatites wheatleyensis* and *Pectinatites hudlestoni* ammonite zones of the Dorset Kimmeridge Clay. Time series were constructed for 13 trace elements and TOC based on 25 cm interval sampling. Thirteen out of the 14 analyzed time series revealed high-amplitude harmonics (e.g., TOC, V, Cr, Zn, Mn, Rb, Li, Sc) representing a periodicity of 4 m (3.3–5.0 m). Depending on the choice of the time scale, this corresponds to a time span of 65 k.y. (Harland et al., 1990; ammonite scheme of Cope et al., 1980) or 119 k.y. (Haq et al., 1987; ammonite scheme of Cope et al., 1980) and falls roughly in the range of the eccentricity cycle. The spectral analysis of longer datasets and other intervals, such as the TOC curves and gamma-ray logs for the whole of the Kimmeridgian in Yorkshire (Herbin et al., 1991), are needed to confirm and possibly refine these results.

The *lateral* variation in TOC distribution in Yorkshire shows an important decrease from basin to shelf setting. The availability of a detailed ammonite bio-stratigraphy (down to the level of the subzone) and the presence of some very characteristic and regionally continuous dolomite beds (Flats Stone Band, Figures 8 and 9) provide an excellent frame-

work to evaluate these lateral variations at a fine scale. The topographic difference of 20 to 30 m over a distance of 40 km (Figure 8) shows a distinct thinning of the medium-scale cycles (4th order) and a decrease of TOC values on the shelf relative to the basin (basin 2–40%, shelf 1–0%). In the more detailed cross section for the *Aulacostephanus eudoxus* zone (Figure 9), the medium-scale cycles (4th order) can be followed from basin to shelf (numbers 5, 10, 14, 20, 25), while the small-scale cycles (5th order) are continuous between the basin sections, but disappear on the shelf with the general thinning (Reighton 87 well). Apart from the decrease in TOC, the HI and OI indicate that the organic matter on the shelves is hydrogen poorer in both the organic-rich and organic-poor layers (Herbin et al., 1993). This lateral trend in TOC distribution probably results from the combination of a better mixing of the water column on the shelf, ensuring fully oxic conditions, with the lower sedimentation rate being less favorable for organic matter preservation than the dys- to anaerobic conditions and higher sedimentation rate in the basin (Herbin et al., 1991). In other words, the lateral variation is explained as due to a preservation/oxygenation control related to the basin topography.

To summarize, the Kimmeridgian case illustrates

1. The *vertical trend* of the organic matter distribution, showing an *organization at three scales*. The large-scale trend is controlled by the Kimmeridgian eustatic sea level rise. Two types of high-frequency cyclicity are superimposed on this trend, and they are most likely caused by orbitally forced climatic changes. The organic matter distribution in these smaller-scale cycles is most likely the result of productivity-induced oxygenation cycles.

2. The *lateral distribution* of the organic matter is related to the basin topography, which influences the oxygenation at the sea floor and the sedimentation rate. In the hemipelagic basin, the stratigraphic sections are complete and the organic matter is better preserved and more abundant, while on the shelf, the stratigraphic sections are incomplete and condensed, and they contain less, and more degraded organic matter.

The Cenomanian–Turonian Boundary in the Western North Atlantic

The upper Cenomanian and lower Turonian have been recognized as a time of globally enhanced organic carbon storage. High TOC values for this interval have been found in very different settings such as Deep Sea Drilling Project (DSDP) sites in ocean basins (Herbin et al., 1986; Stein, 1986; Arthur et al., 1987), onshore pelagic sections (de Boer, 1983), and shelf settings (Jefferies, 1961, 1963; Thurow and Kuhnt, 1986; Kuhnt et al., 1990). The worldwide storage of the very great amount of organic matter enriched in ^{12}C has led to a positive excursion of the carbon-isotope ratio in biogenic carbonate at the Cenomanian–Turonian boundary (Scholle and Arthur, 1980; Jenkyns, 1980, 1985; de Boer, 1986; Schlanger et al., 1987; Gale et al.,

1993). The Cenomanian has also attracted attention for its high-frequency cycles, and orbital control has been suggested in several cases (e.g., McCave, 1979a; de Boer, 1983).

Here we discuss TOC trends and cyclicity in the upper Hatteras Formation (Cenomanian–Turonian) along an east-west transect through the western North Atlantic (DSDP sites 105, 603, 386, and 387). Figure 11 shows the geographical positions, and Table 2 summarizes the general sedimentological features of the different sites. At Site 386 the thickest and most complete Cenomanian section has been found (Tucholke et al., 1979; Müller et al., 1983). Toward the northwest, the Cenomanian section decreases dramatically in thickness. The estimated paleo-water depth of all four sites was between 3500 and 5000 m, with Site 386 being the shallowest (McCave, 1979b; Chenet and Francheteau, 1979). The biostratigraphic control of these sites (Müller et al., 1983; Herbin et al., 1987) does not have the same degree of resolution as the previous case studies, but is sufficient to place all the discussed intervals within the Cenomanian. A regionally recognized maximum in TOC values is dated as the upper Cenomanian to lower Turonian and corresponds to the Cenomanian–Turonian boundary event (CTBE). This organic carbon-rich interval terminates abruptly, and is overlain by the very organic poor (TOC <0.05%), multicolored, red mudstones of the Plantagenet Formation. The transition here is a regional event (Site 386/387 report, Tucholke et al., 1979), whereas in other places the CTBE has a symmetrical appearance (e.g., de Boer, 1982, 1983; Arthur et al., 1987; Schlanger et al., 1987; Stein, 1986).

Site 386 and Site 387

At Site 386 the most complete Cenomanian section is preserved with a thickness of 121 m (Tucholke et al., 1979; Müller et al., 1983). Site 387 is less complete, and has a Cenomanian section of about 48 m (Tucholke et al., 1979; Müller et al., 1983). The upper Cenomanian consists at both sites of decimeter-scale alternations of homogenous (burrow-mottled) green-gray mudstones (TOC < 0.5%) and pyrite-rich, sometimes laminated, black mudstones (TOC 1–5%) (McCave, 1979a; Kendrick, 1979). No graded units were found in the Cenomanian (McCave, 1979b), which excludes turbidites as a cause of the cyclicity. The distribution of the color and the burrow mottling suggest control of the cycles by oxygen availability in the deep water. Interesting is the preferred occurrence of centimeter-thick radiolarian sands in the black mudstone layers. They do not show any sorting, and the general absence of mud turbidites in this interval excludes transportation from adjacent highs (Figure 12). Since annual blooms of diatoms produce layers of about 2 mm (Calvert, 1964), the origin of layers of radiolaria, zooplankton with lower productivity, is attributed to “long blooms”; that is, several tens of years of very high productivity. They imply a correlation of the high-productivity events with the phases of black mudstone deposition.

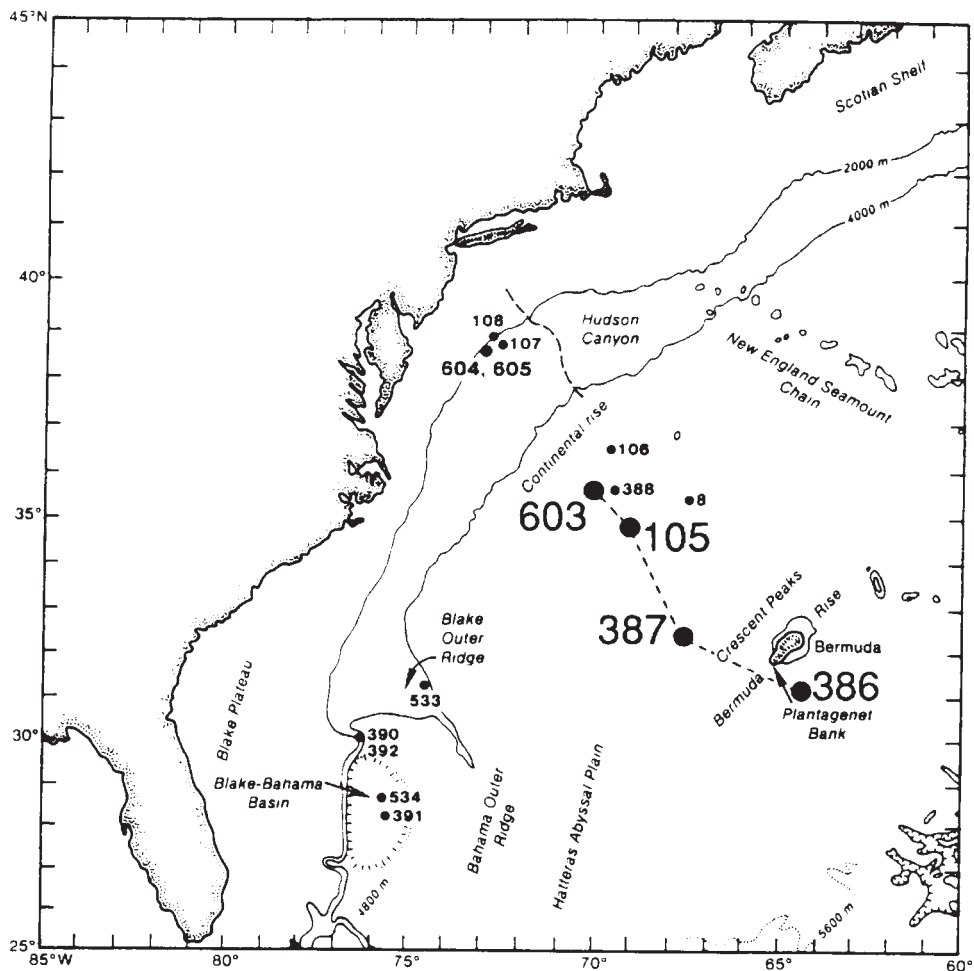


Figure 11. Geographical map of the location of DSDP sites 603, 105, 387, and 386 in the western North Atlantic Ocean.

Time calculations by McCave (1979a) for the duration of the cycles, based on biostratigraphic data (Tucholke et al., 1979), gave average values of 17 k.y. for Site 386 (based on 20 cycles), and, because of the less well constrained stratigraphic information, a range from 22–43 k.y. for Site 387 (based on 93 cycles).

Site 105

The Cenomanian (Upper Hatteras Formation) at DSDP Site 105 is 18 m thick (Hollister et al., 1972; Müller et al., 1983), and consists of an alternation of centimeter-thick, black organic carbon-rich (1–5% TOC) mudstones and decimeter-thick, burrowed, organic-poor (TOC <0.35%) olive-green mudstones (Herbin et al., 1987). Toward the top, in the upper Cenomanian, a change in the cyclicity pattern occurs. TOC values increase gradually and attain a maximum of 15% around 290.5 m (Figure 13). The composition of the organic matter also changes, from mainly detrital type III in the lower part, to a mixture of type II and III in the organic-rich upper part (Figure 13). Microscopic observations (Rüllkötter et al., 1987) showed that the marine organic matter has been structurally degraded and is mostly contained in fecal pellets, a phenomenon that has also been observed at

Site 603. The organization of the small-scale cycles changes from groups of 3 to 4 thin, black mudstones and pluri-decimeter green mudstone (section 5 and 6), to a dominance of the black mudstones and a reduction to millimeter-thick layers of green mudstones (sections 3 and 4; Figure 14).

The sedimentation rate at Site 105 was probably very low, and Müller et al. (1983) suggest a hiatus in the Cenomanian at this site. Herbin et al. (1987) recognized 41 cycles in the upper 5 m of the Cenomanian interval.

Site 603

The Cenomanian at Site 603 is approximately 6 m thick and is characterized by the alternation of organic-poor (TOC <1%), dusty yellow-green claystones with grayish yellow-green laminations (indicated by the odd numbers in Figure 14), and organic-rich (TOC 2 to 20%) laminated black claystones (indicated by the even numbers in Figure 14; Herbin et al., 1987). The organic matter distribution (Figure 9) shows variations at two scales: a long-term trend, covering the whole of the Cenomanian interval, and small, decimeter-scale variations (20 to 80 cm). The long-scale trend shows four characteristics

Table 2. Sedimentological characteristics of the upper Cenomanian in the western North Atlantic.

| Site | 603 | 105 | 387 | 386 |
|-----------------------|------------------------|--------------------------|-------------------------|---|
| Setting | Upper cont. rise | Lower cont. rise | Western Bermuda rise | Fracture valley on central Bermuda rise |
| Thickness Cenoman. | 6.5 m | 18 m | 48 m | 121 m |
| Cycle type (couplets) | Green-red M* Dark M | Olive green M Black M | Green-gray M Black M | Green-gray M Black M |
| TOC variations | | | | |
| Top Hatteras/CTBE | <20% | <25% | <14% | <12% |
| Base Hatteras | 0.2–3% | 1–5% | <5% | <5% |
| Radiolarians | rare | rare | common | abundant |
| TOC-Cycle† | 17 | 41 | 93 | 20 |
| Av. Thickness | 20–80 cm | 5–40 cm | 23 cm | 23 cm |
| Duration | 382 ka | ? | 22–43 ka | 17 ka |

Data from Hollister et al. (1972), Tucholke et al. (1979), McCave (1979a), van Hinte et al. (1987), and Herbin et al. (1987).

* M, mudstone.

† TOC-cycles represents the number of cycles showing a variation in TOC content.

(Figure 14): first, a gradual increase of TOC over the entire Cenomanian interval from low values around 0.5% at the base to values around 20% at the top; second, a change from dominantly hydrogen-poor type III, terrigenous organic matter (up to the base of section 5) to increasingly hydrogen-rich type II, marine organic matter in the upper part; third, a gradual increase in the thickness of the organic-rich layers; and fourth, a development from an asymmetric to a more and more symmetric distribution of the TOC and HI in the small-scale cycles. The organic geochemical analyses by Rüllkötter et al. (1987) and Meyers (1987), and geochemical analyses by Dean and Arthur (1987), all suggest that there is a background sedimentation of type III, terrigenous organic matter over the whole section (Albian to Cenomanian), but that in the Cenomanian, an increasing amount of marine, type II organic matter is added. Rüllkötter et al. (1987) also showed that the marine organic matter has been structurally degraded and is mostly present in the form of fecal pellets.

Assuming no major breaks in sedimentation occurred, an average duration of 382 k.y. is obtained for the 17 cycles in the Cenomanian interval (Cenomanian 6.5 Ma; Harland et al., 1990).

The organic geochemical data from all four sites show a distinct gradual increase of the organic matter content as well as an augmentation of the HI toward the Cenomanian–Turonian boundary. Both an increase in marine productivity and a reduced oxygen supply through more sluggish bottom water renewal may have caused this trend. Good evidence for a general increase in marine productivity exists at Site 386 where an abundance of radiolarian sands is found toward the top of the Cenomanian, and at Site 105 and

Site 603 where the high HI values are caused by the presence of marine organic matter occurring in the form of fecal pellets (confirmed by palynological observations). The correlation of radiolarian sands with black mudstones has also been observed in the upper Cenomanian of the Apennines in Italy (de Boer, 1983).

At a finer scale, all four sites are characterized by decimetric, high-frequency cycles. Bed by bed correlation from site to site, however, is not possible due to the poor stratigraphic control and partly incomplete and condensed sections (especially sites 105 and 603). A common feature of all cycles, however, is the changing degree of oxygenation of the sea floor as indicated by the alternation of laminated and burrowed intervals. The variations in TOC and HI are in phase (laminated: high TOC and high HI; burrowed: low TOC and low HI) and may be caused by (1) variations in productivity, (2) variations in the oxygenation of the bottom waters, or (3) a productivity-controlled oxygenation. In any case, no good evidence has been found for a continuous anoxic state of the ocean, which implies that the CTBE was not the result of an event, but rather was caused by gradually changing environmental conditions. Indeed, the observation that marine organic matter is deposited mainly as fecal pellets makes it unnecessary that the whole or most of the water column was anoxic (Site 105, Site 603; Rüllkötter et al., 1987). However, it is most probable that the bottom water was anoxic at the time of deposition of the black mudstone part of the cycles (Kendrick, 1979). Evidence for a possible orbitally forced climatic control (precession cycle) of the high-frequency cyclicity comes from sites 386 and 387, which have the best preserved records and dating.

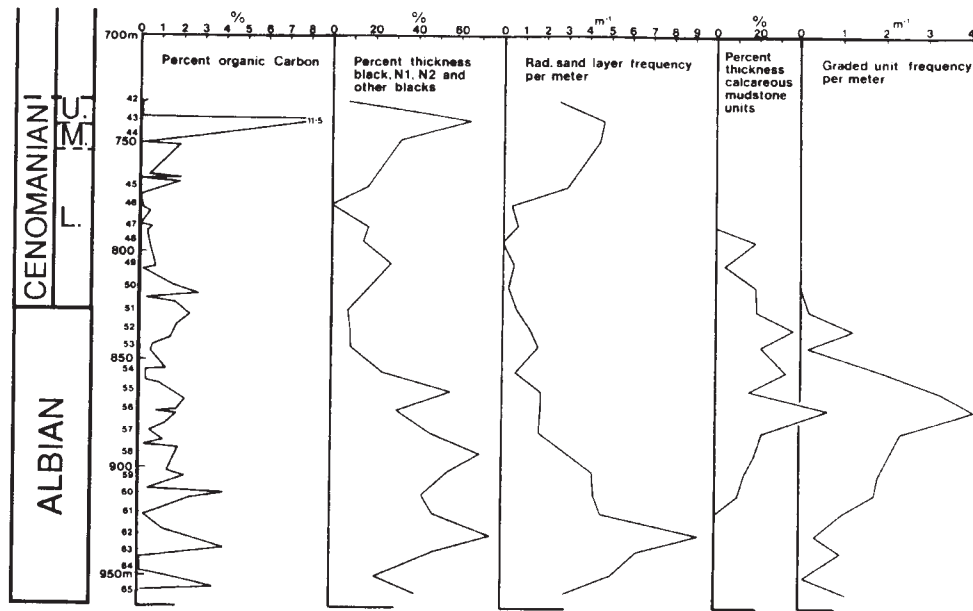


Figure 12. Downhole variation (Albian and Cenomanian) in parameters of the sediments in the green and black mudstones (unit 7) at DSDP Site 386 (after McCave, 1979a). Depth subbottom (m) and core numbers (midpoint) are shown. Note the disappearance of the graded units in the Cenomanian, and the peak in radiolarian sand frequency toward the top of the Cenomanian.

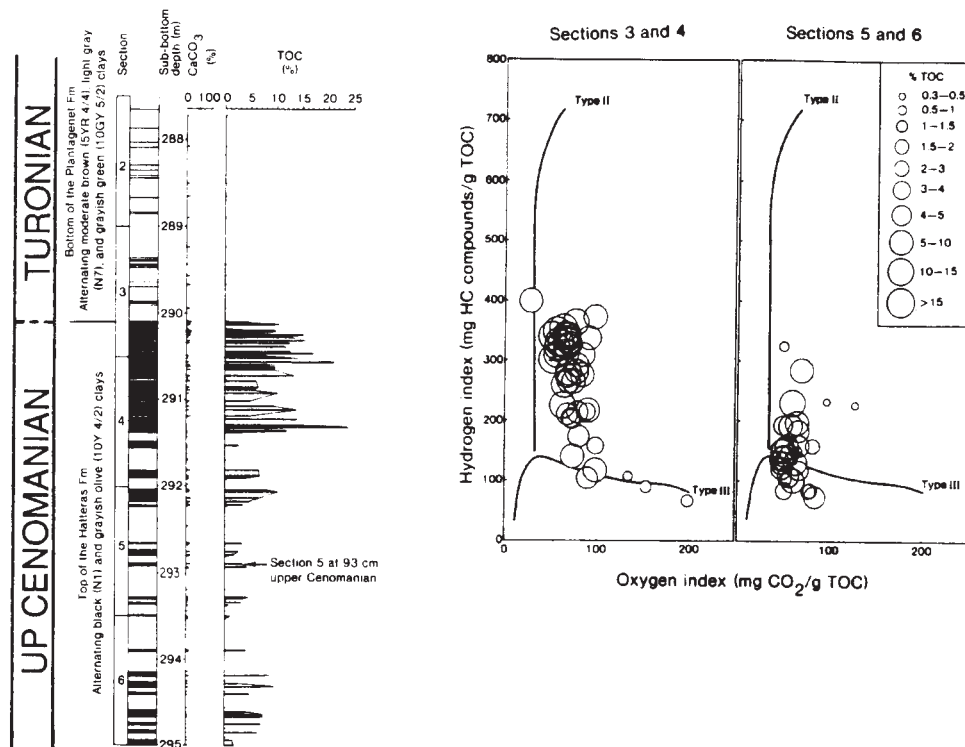


Figure 13. The stratigraphic distribution of TOC for the Cenomanian–Turonian boundary in DSDP Site 105 (sections 105-9-2 to 105-9-6) and the chemical characterization in HI-OI diagrams of the organic matter fraction (after Herbin et al., 1987). Sections 5 and 6 contain mainly type III organic matter, sections 3 and 4 contain a mixture of type III and type II. Measurements are made with a Rock-Eval apparatus.

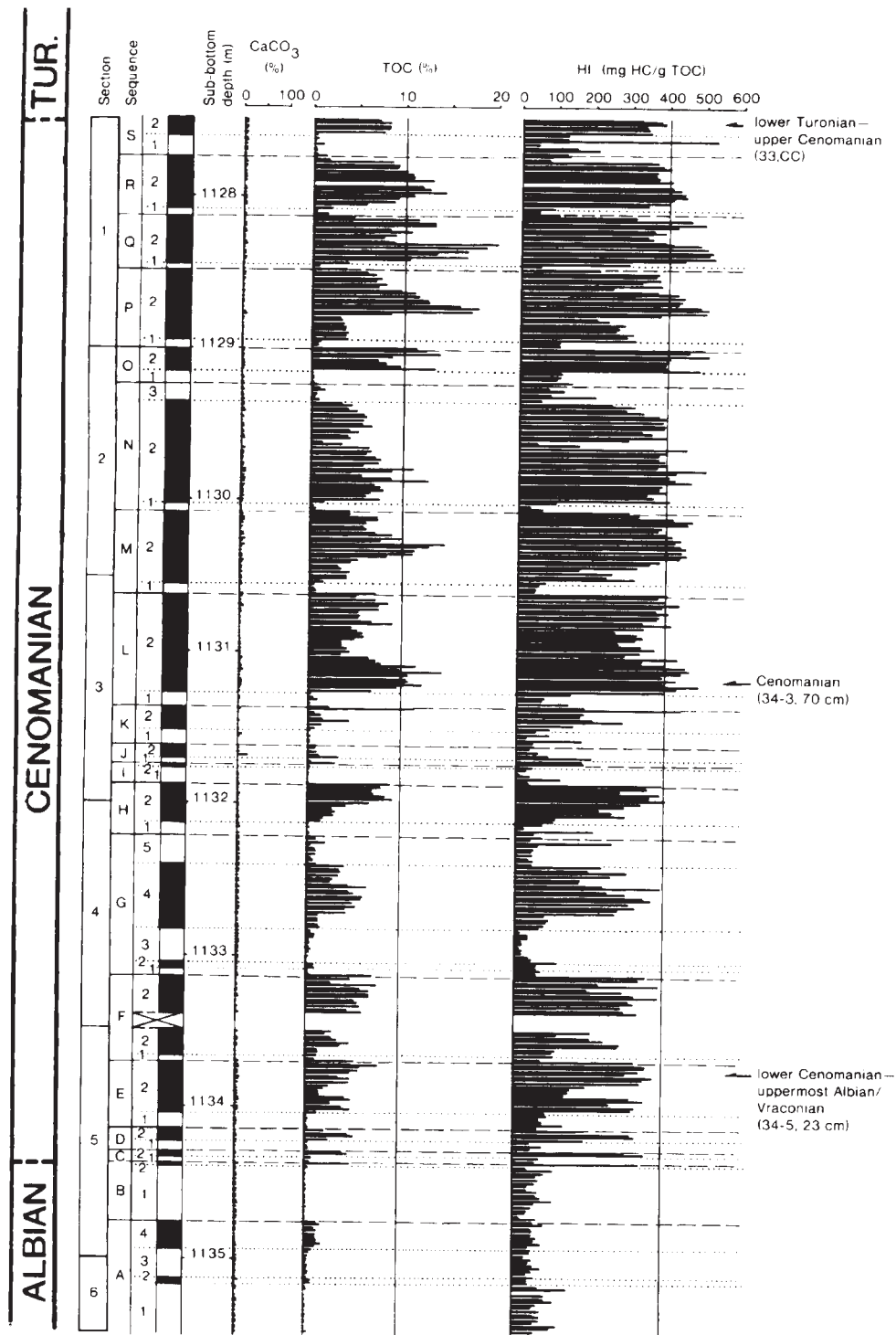


Figure 14. Total organic carbon and hydrogen index variations for the Cenomanian at DSDP Site 603, sections 603B-34-1 to 603B-34-6 (after Herbin et al., 1987). Note the stepwise overall increase and the development from asymmetric to symmetric high-frequency cycles in the TOC and HI curves. Organic matter composition gradually changes from mainly type III in the lower part of the section to a mixture of type III and type II in the upper part.

The lateral variation in sedimentation rate along this transect is due to several factors such as sea-floor topography, the paleo-water depth, the depth of the carbonate compensation depth (CCD) and the position

with respect to sediment sources (Hollister et al., 1972; Tucholke et al., 1979; van Hinte et al., 1987). A good example of the latter is the general diminution of radiolarians toward the west: radiolarian sands are abun-

dant at Site 386, radiolarians are common in the mudstones of Site 387, and at Site 105 radiolarians are scarce. This local distribution pattern is probably due to a zone of siliceous productivity associated with a circumglobal current across the central basin (Tucholke et al., 1979).

The Cenomanian case illustrates the points listed below.

1. Favorable conditions of organic matter storage, which culminated worldwide during the CTBE, developed gradually over the course of a number of high-frequency cycles.

2. This overall increase of TOC storage was accompanied by, and possibly due to, an increase of the marine productivity as suggested by the radiolarian sands and fecal pellets. However, the influence of a more sluggish ocean water circulation cannot be excluded.

3. The high-frequency cyclicity, superimposed on this long-term trend, is the result of a varying degree of oxygenation at the sea floor. This in turn may have been caused by high-frequency changes in productivity induced by some climate-related variable such as wind stress or nutrient supply.

DISCUSSION

The Relative Importance of Anoxia Versus Productivity

The amount and composition of organic matter preserved in marine sediments is determined by the interplay of three critical factors: production of biomass, its degradation, and its dilution (Huc, 1988; Stein, 1991). The first factor is the primary productivity of marine and terrestrial organic matter. During transport, grain size selection and early decomposition takes place, for example, when transported by river systems, longshore and oceanic currents, and sinking through the water column. Considering the conclusions of Bralower and Thierstein (1984), the time during which organic matter is exposed to predation and bacterial degradation processes is an important factor in the amount which arrives at the ocean floor. The small amount which does arrive at the sea floor is further degraded by microbiological activity in the sediment, which can be selective and variable in intensity. When it comes to deciding which of all these factors is the most important for organic carbon storage in the sediment, opinions vary between (1) anoxia caused primarily by low oxygen flux and (2) high carbon flux caused by primary production. Their relative importance is briefly discussed here.

Demaison and Moore (1980) advocate the opinion that an anoxic bottom-water environment is the essential condition for "source rock deposition." To understand the consequences of this statement, it is important to realize that the critical characteristic of a source rock is a high hydrogen content (HI) of the organic matter, but also that deposits with as little as 1% TOC can be classified as a source rock. In other

words, these authors look at a very particular type of organic matter, the preservation of which may be favored under anoxic conditions because of selective decomposition processes. Following Tissot (1979), they also observed that known marine oil source beds are not randomly distributed in time, but tend to coincide with periods of worldwide transgression and synchronous oceanic anoxia. Four main anoxic settings are distinguished: large anoxic lakes, anoxic silled basins, anoxic layers caused by abnormally high carbon flux under upwelling areas, and open ocean anoxic layers (Demaison and Moore, 1980).

Pedersen and Calvert (Pedersen and Calvert, 1990; Calvert and Pedersen, 1992) studied the distribution of organic carbon, regardless of its hydrogen content, and proposed that a high flux of organic matter through the water column to the sea bed, principally controlled by high primary productivity, was the most likely agent leading to the formation of organic-rich sediments and rocks. In their opinion, there is little evidence for the preferred accumulation or preservation of organic matter in sediments of anoxic basins when compared with oxygenated counterparts at equivalent sedimentation rates and water depths. They emphasize that a series of secondary oxidants, especially sulphate, is also involved in many continental margin environments when the small reserves of oxygen and nitrate are quickly exhausted, thereby continuing degradation of organic matter in anoxic environments. Implicit in this is a much more dynamic interaction of biological and chemical processes in the initiation of periods favorable for organic matter storage (algal blooms, change in wind stress causing upwelling favorable for organic matter production, and changes in atmospheric CO₂ pressure). They also keep the possibility open for dominance of local and regional factors creating conditions for high productivity and storage, rather than oceanwide phenomena.

A way to contribute to the above discussion is to look in close detail at some ancient examples where we have good control on the sedimentological conditions and their variations through time, both on a long scale and on a fine scale. We argue that the influence of factors controlling the organic matter storage varies with the different scales. And in particular, we believe that those environments which are sensitively poised so that they alternate between high and low preservation of organic matter under the climatic drive of Milankovitch-scale changes are likely to be most revealing of underlying controls.

With regard to the long-term trend (2nd- and 3rd-order cycles), the three case studies represent periods of eustatic sea level rise which, in the case of the Cenomanian and Kimmeridgian, coincides with abundant, worldwide organic matter storage. There is ample evidence that overall productivity increased during the Cenomanian and Kimmeridgian, but, as was stressed by de Boer (1991), a gradual change in the circulation velocity in oceanic systems may have caused similar effects. Two end members are distinguished, one with an extremely low circulation velocity where a lack of supply of oxygen to deep water leads to anoxia, also in case of a very low supply of organic matter, and the

other with upwelling/high-productivity conditions in surface waters, where the supply of organic matter exceeds the capacity of the oxygen available in deep water to oxidize the sinking organic matter (Figure 15). An important observation in the three case studies is that the major phases of organic carbon storage developed gradually with a superimposed rhythm of high-frequency oxygenation cycles. This means that conditions were never totally anoxic for a long time, but were always interrupted by periods of better oxygenation. In other words “oceanic anoxic events,” are not events, but rather phases exceptionally favorable for the widespread storage of organic matter.

A third factor which needs to be considered at a long time scale is that the storage of large amounts of organic carbon in the lithosphere may be linked to biogeochemical systems such as the carbon cycle (de Boer, 1983; Garrels and Lerman, 1984; Worsley and Kidder, 1991). An increased CO_2 pressure in the atmosphere, in combination with an increased long-term influx of nutrients into the ocean (de Boer, 1983, 1986), may have resulted in a (relative) increase of organic production and organic carbon storage in the overall low productive ocean (Bralower and Thierstein, 1984) in an effort to restore the chemical equilibrium. The role of the biological world, that is, the marine phytoplankton which represent a major proportion of the total global biomass, is in this context seen as the catalyst that allows the biogeochemical cycle to keep the balance in the CO_2 budget (cf. Lovelock, 1987, 1989). Interesting in this context are the results reported by Erba (1993) which demonstrate that there is, indeed, evidence that the marine plankton community changed before the actual phases of massive organic matter storage, and may possibly have reinforced it. Thus, a complex interactive network of feedback mechanisms involving the atmosphere, hydrosphere, biosphere, and lithosphere is believed to explain long-term periods of major organic matter storage.

At the small scale, the high-frequency cycles (4th and 5th order) are primarily controlled by a regular variation of the oxygenation level at the sea floor. In certain cases (Lias of Yorkshire), it appears that changes in the oxygenation level autonomously led to the deposition of redox cycles; in other cases (Kimmeridgian in Yorkshire, Cenomanian of the northwest Atlantic), the variation in primary organic productivity in surface waters may have led to temporary anoxia in deep water and increased levels of organic carbon content of the sediment. Turbidity currents as a cause of deposition of organic carbon-rich intervals (cf. Degens et al., 1986) seem to have been of minor or no importance in the examples discussed above. The link of this control to climatic variations is supported by the detailed observations on (1) *terrestrial influx*—for example, the Kimmeridgian cycles in Yorkshire show an increased influx of kaolinite in the TOC-rich layers suggesting a change of climatic and pedogenic conditions on the land, (2) *winnowing of the sea bed*—for example, the increased silt content and associated rich benthic faunas in the TOC-poor layers in the Lias of Yorkshire, and bioturbation in the Cenomanian examples, indi-

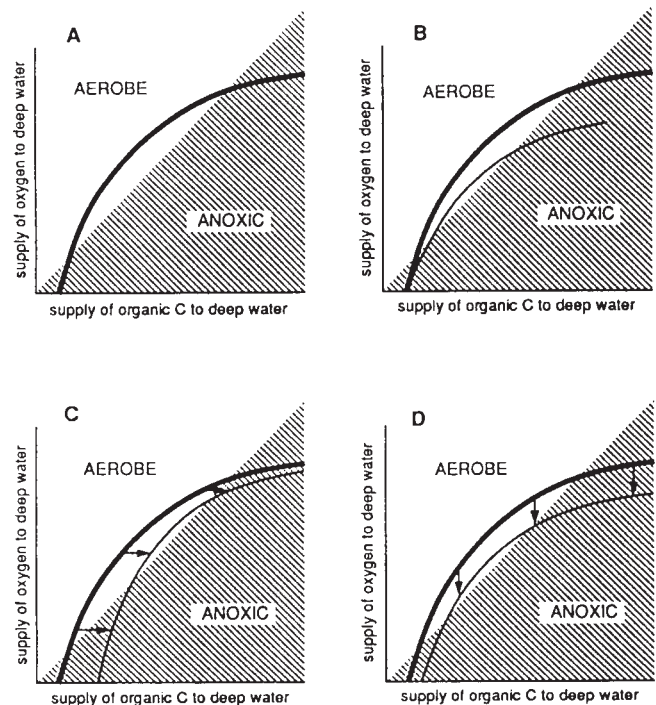


Figure 15. Oxygen versus organic carbon flux diagram for ocean systems representing four situations (de Boer, 1991). Oxygenation conditions of deep ocean water in response to the oxygen supply (vertical axis) and the organic carbon flux (i.e., organic matter supply, horizontal axis) to deep water. Both oxygen supply and production and preservation of organic matter depend on circulation intensity. (A) The present-day state. The solid line tentatively delineates the conditions met in present-day oceans: anoxia in deep water occurs in very strong or in very slow circulation (in the figure this corresponds with the upper right and lower left, respectively). Under “normal” conditions, with moderate circulation, deep waters are at present sufficiently aerated to oxidize the dead organic matter which descends (middle part of the curve). (B) In times of reduced circulation, the production of organic matter and the supply of oxygen to deep water are reduced. Thus, the values along both axes are compressed, making bottom waters depleted in oxygen to expand in volume (thin line) and anoxicity to become more obvious. (C) Input of terrestrial organic matter by rivers or winds will shift the curve toward the right into the anoxic part of the field. (D) In times of poor ventilation, due to decreased oxygen solubility in warm and saline waters (e.g., Cretaceous) or to a low oxygen content of the atmosphere (e.g., Paleozoic, Precambrian, Cambrian), the curve is depressed vertically downward. Reproduced courtesy of Springer-Verlag from *Cycles and Events in Stratigraphy*, Einsele et al., eds., 1991, p. 66.

cate a winnowing increase related to changes in climatic and oceanographic conditions affecting water circulation, depth of storm-wave base, frequency and intensity of storms, etc.; and (3) *variations in productio-*

ity—the environmentally very sensitive biological system is probably the first to react to climatic changes. The dominance of the algal fraction in the TOC-rich layers, associated variously with coccolith fecal pellets in the Kimmeridgian of Yorkshire and radiolarian blooms in the Cenomanian of the northwest Atlantic, suggests an increased biological activity during periods with increased organic carbon accumulation.

The most detailed sedimentary model proposed to explain these high-frequency fluctuations in organic-matter accumulation in modern and ancient black, organic-rich shale deposits is the one advocated by Oschmann (1990) and Tyson and Pearson (1991). Their “seasonal dysoxia-anoxia model,” which limits itself to epeiric seas such as during the Lias and Kimmeridgian in Yorkshire, is based on climatic changes driven by gradual variations in the *yearly seasons*. The key to this model is the length of the seasonal stratification period which may have shown cyclic changes between four and seven or more months of the year, over the course of tens of thousands of years. The force of this model is the direct link between the astronomical cycles and the climatic changes, since it is exactly in the domain of the seasonality and climate belt position that the orbital cycles influence the climate on earth (Table 3). Astronomically forced, high-frequency, climatic variations superimposed on longer-term global warming trends (related to the sea level rise) may have resulted in cyclic shifts toward climates characterized by earlier springs, longer summers, and less intense winter mixing (Herbert and Fischer, 1986). The combination of prolonged stratification, lower mixing, and higher oxygen demand would undoubtedly have resulted in summer dysoxia or anoxia being widespread throughout all the offshore areas of the epeiric sea during the appropriate parts of Milankovitch cycles. Such regular annual dysoxia and/or anoxia would have resulted in the widespread elimination of benthic faunas (Tyson and Pearson, 1991).

This model provides a mechanism linking orbital cycles to a number of environmental factors which are held responsible for the oxygenation cycles. However, the question of whether productivity in itself was the driving force behind the high-frequency cycles is still difficult to answer. Although not discussed in detail by Tyson and Pearson (1991), it should be realized that a number of factors influencing the seasonality and

stratification of the water column (temperature, wind stress, rainfall patterns, nutrient supply, etc.) will also affect the marine community, and by doing so, the productivity.

Returning here to the distinction between “source rocks” and organic carbon accumulations, it is clear from the studies by Pedersen and Calvert (1990), Calvert and Pedersen (1992), and the Kimmeridgian and Cenomanian examples discussed here, that anoxia is not an absolute necessity for the preservation of organic carbon, and demonstrates that the POC (particulate organic matter) flux can be the primary control of organic carbon preservation. However, for source rocks, hydrogen-rich organic matter needs to be preserved, and this is best achieved once the POC/O₂ flux has pushed the benthic system anoxic. So, it may be that the preservation of *any* organic matter is primarily determined by the POC flux, and “good” (hydrogen-rich) organic matter, the labile fraction requiring early preservation, is controlled by the oxygen flux. That is to say that in oxic settings you may have cyclicity in organic-matter distribution, but even if the POC flux pushes the system temporarily anoxic, it will be accompanied by much degradation of the labile organic-matter fraction and will thus not produce source rocks. Only restriction of O₂ supply to bottom water can allow that to happen, generally by silling and stratifying the basin.

The Vertical Trend

Cyclicity, that is, regular variations in the vertical distribution of the organic matter, is a prime characteristic of organic carbon distribution in marine sediments. Moreover, very often several orders of cyclicity can be distinguished. Based on the mechanisms which are the cause of the cycles, we can distinguish between long-term trends or lower-order cycles (2nd- and 3rd-order cyclicity, >3 m.y.) caused by long-term tectono-eustatic sea level changes, variations in topography, basin morphology, oceanography, and atmospheric conditions, and the higher-order cycles (4th and 5th order, with typical durations on the order of 20 to 400 k.y.) which are in the range of orbitally induced climatic and oceanographic changes.

The hierarchy of cycles and how they determine the stratigraphic expression of the organic carbon distri-

Table 3. Orbital forcing of climatic change. The variation in the distribution of the insolation (= received solar energy) per latitude and per season is differently influenced by the three orbital cycles.

| | |
|-----------------------------|---|
| Obliquity | <ul style="list-style-type: none"> • poles are affected in phase • increased seasonality • more uniform mean annual latitudinal distribution • position of the climate belts remains the same |
| Precession/ Eccentricity | <ul style="list-style-type: none"> • hemispheres 180° out of phase • the one: increased seasonality • the other: reduced seasonality • shift of the caloric equator causes shift of climate belt boundaries |

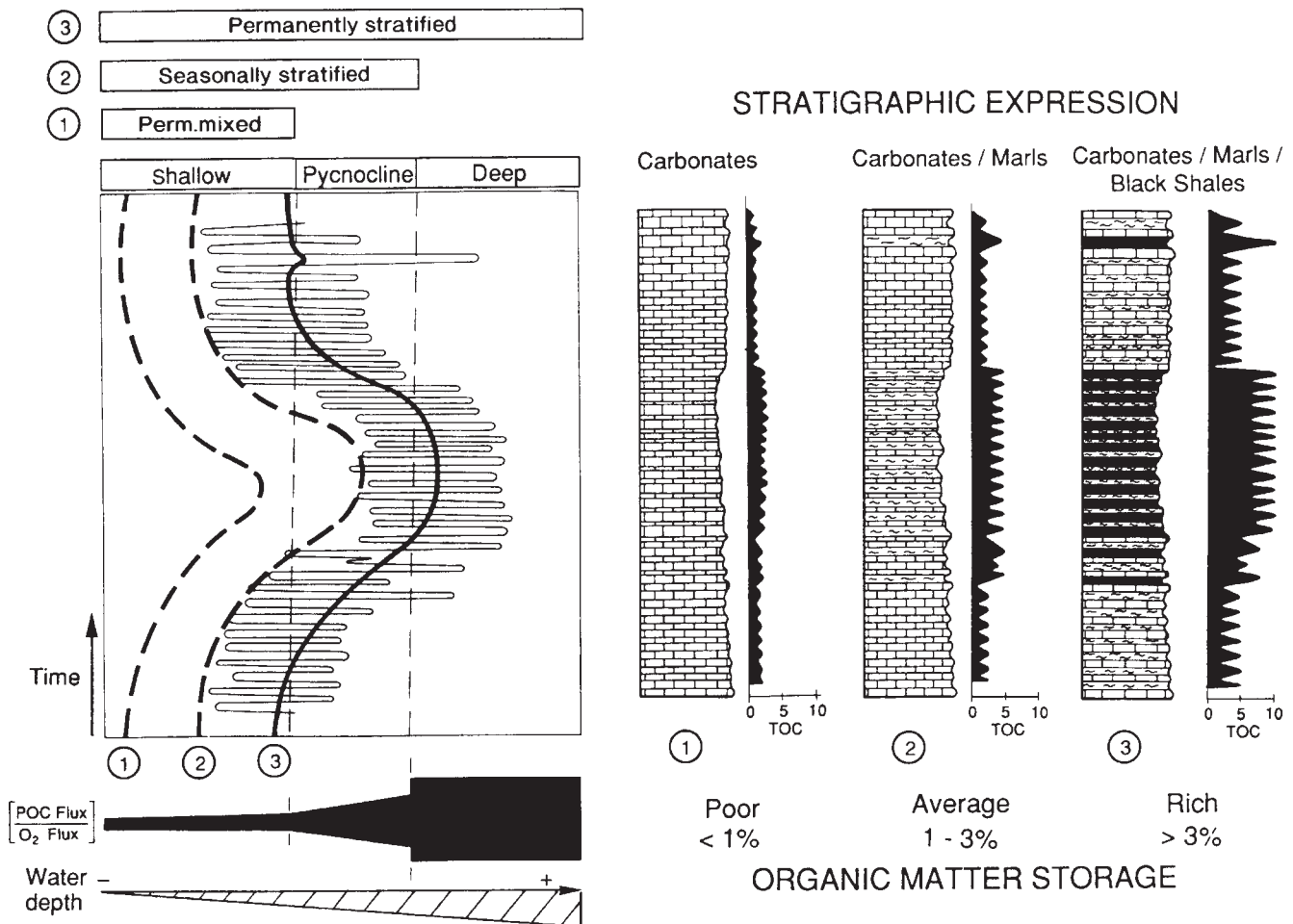


Figure 16. The vertical and lateral control of organic carbon distribution. The lefthand side of the diagram shows three orders of cyclicity. A *long-term trend* is represented by curves 1, 2, and 3. The curves represent the evolution of a system with a permanently mixed water column to a seasonally stratified water column and finally to a permanently stratified water column. This trend may develop through time, but may at the same time represent a lateral environmental variation. Superimposed on this long-term trend are *two higher orders of frequency*, which modulate the stratigraphic expression (and organic matter storage) of the long-term trend by pushing it over certain threshold boundaries (see text). The critical parameter for the organic matter storage is the ratio between the particulate organic carbon (POC) flux and the oxygen flux.

bution is shown in Figure 16. On the one hand, longer-term trends determine if conditions are favorable for the production and preservation of organic carbon in marine sediments (curves 1, 2, and 3). On the other hand, on a shorter time scale (<500 k.y.), the high-frequency climatic variations (superimposed on curves 1, 2, and 3) *modulate* the degree to which organic matter is produced and preserved, by pushing the sensitive sedimentary system over certain threshold conditions.

We have arbitrarily worked out an example where the ratio of POC flux/ O_2 flux near the sea bed is the critical factor determining the *variations* in organic-matter preservation. Three states of the water column are considered with increasingly favorable conditions for organic-matter storage when going from a permanently mixed water column (curve 1, Figure 16) to a seasonally stratified water column (curve 2, Figure 16) to a permanently stratified water column (curve 3, Figure 16). These three states are determined by a general

increase in water depth and represent, as such, the changing conditions during a long-term sea level variation. Then for each of these three situations, two orders of high-frequency (4th and 5th order) fluctuations in sea level, or any other climatic or oceanographic parameter of similar importance, are superimposed, and the corresponding expression in the stratigraphic record is shown.

The first scenario (curve 1, Figure 16) represents a shallow basin with a permanently mixed water column and two high-frequency variations in either relative sea level or storm activity. The conditions at the sea floor are always aerobic and support benthic communities. Consequently, very little organic matter is preserved (<1%), and the rock record commonly shows a poorly developed cyclicity due to minimal changes in sediment composition. Examples from the literature commonly show little or no regular cyclicity due to sufficient wind stress for winnowing and ero-

sion, and in many cases this leads to homogenous or randomly variable sedimentary sequences (e.g., Ricken, 1991). Exceptions may occur under special conditions, such as early diagenesis and precipitation of cement and authigenic minerals (e.g., carbonate, glauconite, chert) which enhance the cycles, for instance as observed in the Upper Cretaceous Chalk successions (cf. Zijlstra, 1994).

The second scenario (curve 2) represents a shallow sea which seasonally develops a density-stratified water column and sluggish circulation in the lower layer. The installation of dysaerobic to anoxic conditions at the sea floor hampers the growth of a benthic fauna and favors the storage of organic matter. High-frequency climatic changes then alternately amplify and suppress the production and preservation of organic matter, thus leading to a rhythmic deposition of organic-rich and organic-poor layers. The variation in sediment composition produces a clear stratigraphic expression of the cyclicity. This is the most common case, and examples are the Lias in England presented here, and others can be found in de Boer and Smith (1994b).

The third scenario (curve 3) represents the range of conditions from a permanently mixed water column, to a seasonally stratified water column, to a permanently stratified water column. "Permanently" refers here to part of a high-frequency cycle (i.e., 10 to 80 k.y.). A permanently stratified water column with stagnant, anoxic waters may be related to phases of maximum water depth, but other factors such as changing circulation patterns or the input of highly saline waters may as well favor such conditions. In this phase of reduced oxygen supply to the sea floor, an increased productivity may lead to exceptionally high TOC values and an exceptional preservation state of the organic matter (HI > 400), as observed in the Kimmeridgian and the Cenomanian examples.

The Lateral Trend

The three settings corresponding to the curves in Figure 16 can also be interpreted as lateral variations along a basin margin to basin center profile. The shallow environment along the basin margin (curve 1) is not favorable for organic-matter preservation due to the permanently mixed state of the water column. Cyclicity may, however, still be expressed through variations in the sediment composition, for instance as a result of fluctuations in the terrigenous sediment supply. In the more distal positions, the preservation potential of organic matter is much better due to the seasonally stratified water column (curve 2), while in the basin center, the permanently stratified water column provides best conditions for organic-matter storage (curve 3).

However, this ideal, lateral trend is often complicated by local effects, overprinting or obscuring the general pattern. The topography (water depth and basin shape) partly controls the degree of erosion, winnowing, and oxygen content of the water column. Reworking leads to intermittent erosion (and thus to an incomplete record) and inhibits organic-matter storage (e.g., the Yorkshire shelf in the Kimmeridgian).

Irregular sediment supply from adjacent highs (turbidites) may also distort the rhythmic pattern, but can significantly enhance organic-matter storage (e.g., DSDP Site 530, Angola Basin; Stow and Dean, 1984; Degens et al., 1986). A lack of sediment supply, on the other hand, may lead to condensed sections, in which a cyclic pattern may be unrecognizable. The paleogeography may also play a role in determining sites of major productivity in upwelling zones, or underneath circumglobal currents (Summerhayes et al., 1992).

Figure 17 illustrates three typical situations showing the potential and limitations of the lateral correlation of high-frequency variations in the distribution of organic carbon. The first one (Figure 17A) shows the influence of a basin margin to basin center topography in an epeiric setting, and is based on the Yorkshire Kimmeridgian example. A topographic difference of several tens of meters over a distance of about 30 kilometers (compare to Figure 9) is sufficient for the high-frequency cycles (5th order) to be winnowed out or condensed beyond recognition along the margin, while the signal of the medium-scale cycles (4th order) is strong enough to be preserved. The quality of the organic matter is best in the deeper part of the basin. The second situation represents different depositional environments in adjacent epeiric subbasins (Figure 17B) and is based on the Lias example. If the general conditions are suitable, high-frequency cyclicity is registered in all the subbasins. But in each basin the cyclicity (4th and/or 5th order) is expressed differently in the rock record due to the varying local conditions. The preservation of the organic matter fraction varies accordingly.

These two examples illustrate that while the oxygenation state of the sea floor may regularly vary through time, simultaneously lateral differences due to oceanographic differences, terrigenous sources, or topographic relief, for example, may lead to a different expression of such signals within different parts of a basin or between adjacent (sub)basins.

Spatial aspects playing over a longer time scale are shown in Figure 17C, which represents a situation in an oceanic, pelagic setting and is based on the Cenomanian example. It represents an organic matter depocenter formed during a phase of increased organic carbon burial which was terminated abruptly. The presumed source of the organic matter is algal blooms. The areal extent of the depocenter expands gradually and is a diachronous feature. The depocenter itself may also migrate laterally due to changing wind stress and deep water circulation. It shows a typical high-frequency stratification, which in cases where different orders of cyclicity are represented, display a predictable variation in the lateral and vertical distribution of the organic matter. This sort of complicated rhythmic patterns, which are the sum of the different orbital frequencies and amplitudes, are very suitable for correlations over great distances.

The Model

The factors involved in the storage of organic matter and the way in which they interrelate are represented in Figure 18. The essential idea is that local depositional

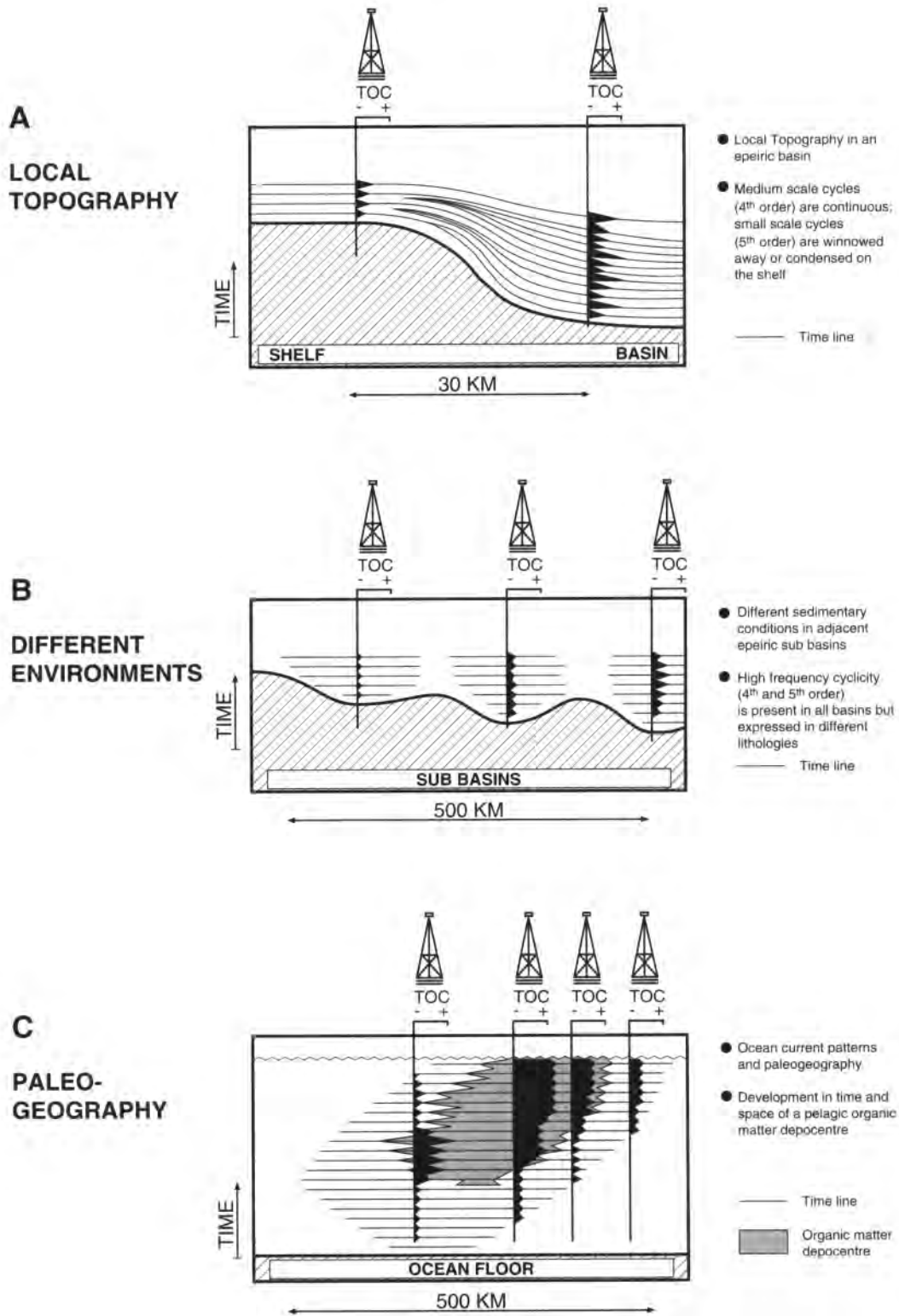


Figure 17. Lateral variations of high-frequency cyclicity and the influence on organic matter storage: (A) local topography in an epeiric basin, complete section preserved in the basin and good source rock qualities, winnowing and erosion on the shelf and little and more oxidized organic matter; (B) different environments in adjacent epeiric subbasins where local factors such as water depth, terrigenous influx, and water circulation determine the stratigraphic expression of the cyclicity and the distribution of the organic carbon; (C) paleogeography and ocean current patterns determine development and termination of organic matter depocentres. The figure shows an abrupt termination of the registration of cyclicity and organic matter storage.

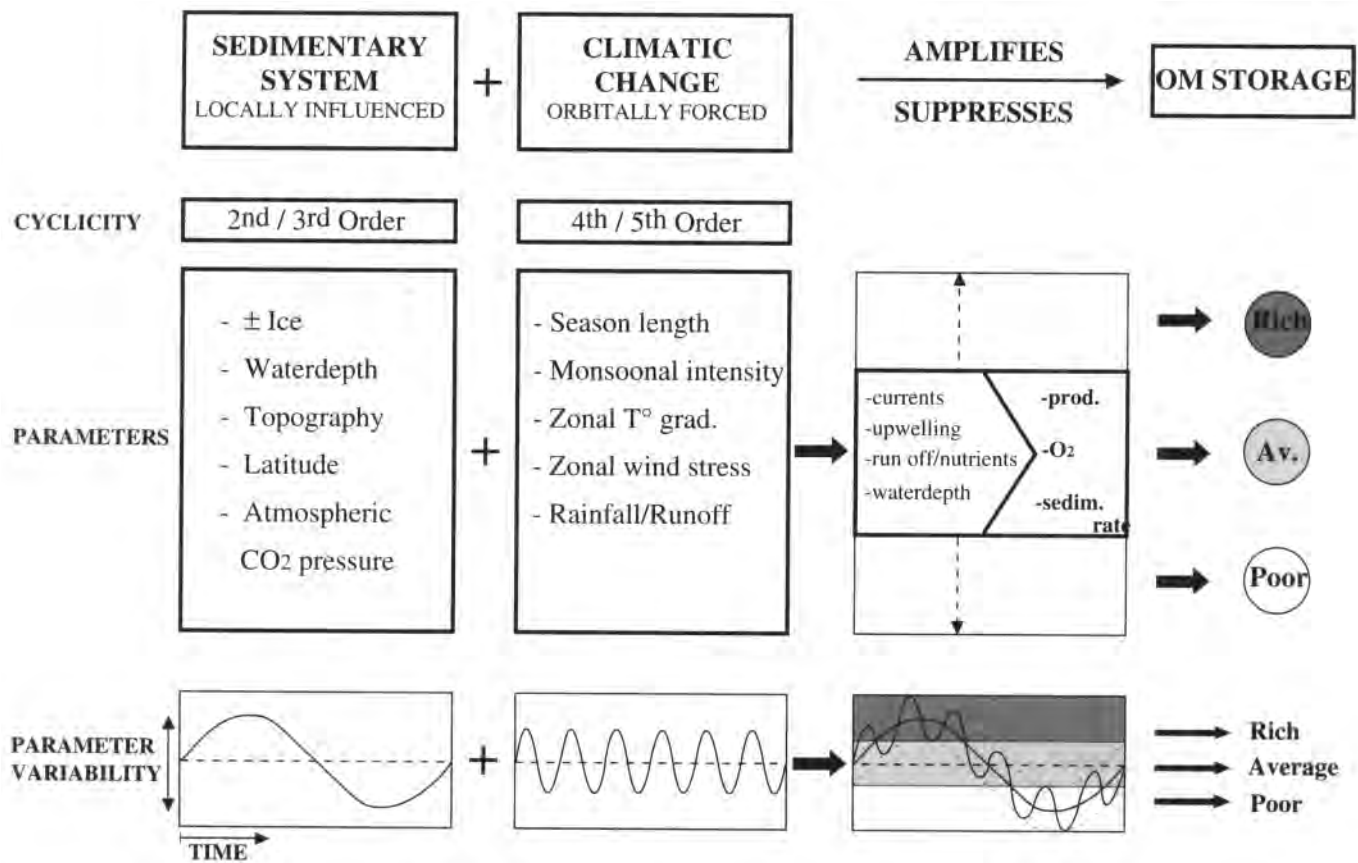


Figure 18. General "process" diagram explaining interaction between processes occurring at different scales and their influence on the organic matter storage (see text).

conditions are amplified or suppressed by the astronomically induced high-frequency climatic changes, which may or may not lead to organic matter storage. The figure specifies the critical parameters. First, the local setting depends on the general, global, environmental conditions determined by the presence or absence of ice caps, water depth, topography, latitude, and atmospheric CO₂ pressure. These parameters change on a long time scale (3rd and lower order). Secondly, the high-frequency (4th and 5th order) climatic changes affect the marine environment. The climate changes—season length, monsoonal intensity (in appropriate locations), zonal temperature gradient, rainfall and runoff patterns—suppress or amplify conditions existing in the local setting. Depending on the interplay of all of the above parameters, specific marine conditions are defined in terms of oceanic current patterns, upwelling zones, runoff/nutrient supply, and water depth. Together these features define the conditions which are critical for organic-matter storage (productivity, oxygen supply, sedimentation rate). Again, the main message is that there is a control at two scales, the shorter one of which works as an amplifier or suppressor of the longer one.

The Application

In the above discussion, we have distinguished between the various factors that determine the storage

of organic carbon in Mesozoic marine sediments. We have demonstrated the hierarchy in the different orders of cyclicality, pointed out the distinction between processes working at these different scales, and shown examples of the powerful lateral correlation potential of successions displaying high-frequency cyclicality. Here, we briefly examine some of the (potential) fields of application of cyclostratigraphy.

The important, and already known, practical message of the long-term vertical trends is that there are certain intervals in the stratigraphic record which are particularly enriched in organic matter (Tissot, 1979; Demaison and Moore, 1980). The periods during which these organic carbon-rich successions were formed are known as "oceanic anoxic events" (Jenkyns, 1985; Schlanger et al., 1987). But, as has been pointed out above, it is preferable to talk about "phases" favorable for the storage of organic matter, rather than the evocation of an oceanwide anoxia of a long duration. They are characterized by a positive excursion of the carbon isotope curve due to the strongly negative $\delta^{13}\text{C}$ values of the marine and terrestrial organic matter which was stored in the pelagic domain during such periods (e.g., Scholle and Arthur, 1980; de Boer, 1986). This feature can be used in two ways. As pointed out by Shackleton (1987), the carbon isotope curve may help to find other, as yet unidentified, intervals of great organic-matter storage. Besides, it may work as a rough chemostratigraphic tool with

the potential to link basin and carbonate platform successions (e.g., Vahrenkamp, 1994).

In the three Mesozoic case studies, the processes which led to such phases of enhanced storage of organic matter have been discussed, and one of the important conclusions is that only when involving the atmosphere, hydrosphere, biosphere, and lithosphere a complete picture of the driving mechanisms of these long-term trends appears. In other words, it is an ideal field for integrative studies of the Earth's history.

Three obvious applications of the high-frequency cyclicity (4th–5th order) patterns are discussed below.

1. The study of parameters influencing the organic-matter storage. The common presence of cyclicity in the marine domain (cf. the three case studies discussed in this paper, and examples such as Pratt et al., 1985; Hilgen and Langereis, 1989; Weltje and de Boer, 1993) indicates that the sedimentary system was sensitive to relatively weak, periodic variations of parameters such as water depth, terrestrial sediment supply, wind stress, biological productivity, oxygen supply, etc. Since these are the critical factors that also define the storage of organic matter, we believe that detailed physico-chemical sedimentological studies of samples in relation to their position within the different orders of sedimentary cycles are the best way to define the relative importance of the various features of influence. Moreover, this sort of detailed insight in the sedimentary system is needed to construct accurate computer models, and is thus required for all sedimentary environments.

2. Regional correlation of basinal sequences. High-frequency variations in organic-matter distribution are accurately reflected in wireline logs. Moreover, the combined treatment of gamma-ray, density, and sonic logs allows us to calculate the TOC present (cf. Carpentier et al., 1991). This, in combination with the theoretical considerations about the origin and the lateral continuity of the high-frequency cycles, may assist in basinwide and even regional recognition and correlation of cyclic, organic carbon-rich, marine mudstone series. The correlation potential of the cycles not only provides a high-resolution stratigraphic framework, but also allows reconstruction of the lateral changes in the amount and composition of organic matter stored, and determination of the spatial and temporal evolution of organic matter depocenters.

Examples of regional subsurface studies using such an approach are given by Stoakes (1980) for the Upper Devonian in the Western Canada shale basin, Melnyk and Smith (1989) for the middle Cretaceous in Italy, Plint et al. (1993) for the Cretaceous in Alberta, Bessereau and Guillocheau (1993, and this volume) for the Lias of the Paris basin, and Melnyk et al. (1994) for the Kimmeridgian of the Wessex basin. Along the same line, the vertical mapping of cycle frequencies (frequency contour maps) may help to detect lateral and vertical changes in patterns of (organic-rich) sedimentation (e.g., Melnyk and Smith, 1989; van Buchem et al., 1992; Grötsch, 1993; Melnyk et al., 1994). A still open field of study is the link between the different orders of high-frequency

cyclicity recorded in basin infill patterns and their seismic response.

3. Correlation of basin center with basin margin sequences. The recognition of high-frequency cycles in (organic-rich) basinal sediments invites attempted correlation with adjacent, shallow water coarse-grained siliciclastics and carbonates (the potential reservoir domain) where cyclicity is often well preserved.

An example from the subsurface comes from the Upper Jurassic Hanifa Formation on the Arabian Peninsula (Droste, 1990). The formation itself is positioned at the maximum deepening of the long-term Middle/Upper Jurassic "super cycle." An overall cross section through the formation shows a clear organization at two scales of the lateral distribution of the source rocks and shallow water carbonates (cf. Figure 2 in Droste, 1990). The cycles have been interpreted as driven by regional relative changes in sea level based on their correlatability over a wide area. At a finer scale, the basinal sections are characterized by a high-frequency cyclicity caused by oxygenation cycles (an alternation of laminated, organic-rich mudstones and bioturbated mudstones). Toward the basin margin they show a change in lithological composition and in places wedge out. The high-frequency cycles in the platform itself are not discussed in the paper.

The well-exposed mixed carbonate-siliciclastic platform of Carboniferous age in the Paradox basin (Goldhammer et al., 1991, 1994; Grammer et al., 1994) is another well-documented case of high-resolution stratigraphic basin center to margin correlations. Transgressive (4th order) black shales onlap the platform and provide excellent correlation levels which connect the basinal evaporite series and carbonate-siliciclastic cycles on the shelf. The 4th-order cycles in this system individually contain all elements of the petroleum system: mature source rocks onlap the shelf margin where the highly porous algal mounds are located, and evaporites and silty mudstones seal the system.

The Upper Devonian mixed carbonate-siliciclastic system in Western Canada also represents a petroleum system where source rocks, reservoir, and seal all occur in one long-term cycle. The beautifully exposed Frasnian buildups (Mountjoy, 1965, 1980) and surrounding organic-rich basinal shales were deposited in a long-term (2nd order) transgressive/regressive cycle. Four orders of cyclicity have been distinguished (2nd to 5th) which determine the facies distribution in the basin and on the buildups (Whalen et al., 1993). Best source rocks and reservoirs occur in the same two successive medium-scale sequences (3rd or 4th order) where organic-rich basinal sediments onlap the steep-sided, often erosional, dolomitized and highly porous margins of the buildups (van Buchem et al., 1994). At a finer scale (4th and 5th order), high-frequency shallowing-upward cycles in the buildup are matched by carbonate/shale cycles in the slope and basinal deposits.

A promising case for these types of correlations in a siliciclastic setting is the Upper Cretaceous of the

Western Interior Seaway in the U.S.A. Individual studies of the high-frequency cycles in the different sedimentary environments already exist: for marginal marine sandstones (Palmer and Scott, 1984; Wright, 1986; Devine, 1991; Eschard et al., 1993), subsurface wireline-log correlations (Molenaar and Baird, 1991), basinal shales (Pasley et al., 1993), and carbonates and organic-rich deposits along the eastern margin of the seaway (Pratt et al., 1985).

CONCLUSIONS

1. Cyclicity, regular variation in the vertical distribution, is a common characteristic of the organic carbon distribution in marine sediments. Two scales of cyclicity can be distinguished: large-scale cycles are of the 2nd or 3rd order and represent the evolution and decay of conditions favorable for the storage of organic matter; they involve more than 3 m.y. and sediment packages on the order of tens to hundreds of meters. Small-scale cycles are of the 4th and 5th order and have a duration of <3 m.y., but very often between 20 and 400 k.y. (Milankovitch cycles). The completeness of registration and the particular expression of the cycles are both strongly dependent on the local sedimentary environment.

2. Detailed studies of the cyclicity of the organic carbon distribution allow distinction between the influences of the different critical factors for organic-matter storage. First, a longer-term control (2nd to 3rd order) of the productivity and oxygenation of deep water is probably related to long-term processes such as tectono-eustatic sea level changes, atmospheric CO₂ pressure, and tectonic regime. These factors determine whether the organic matter stored will have source rock quality (high hydrogen content) or not. And secondly, a high-frequency (4th to 5th order) control of the oxygenation state of the sea floor may be induced or hampered by orbitally forced climatic variations. The small-scale cyclicity is superposed on the long-term trend. It modulates it by amplifying or suppressing the long-term variations in productivity and oxygenation of the deep water.

3. The correlation potential of the high-frequency cycles allows us to study in detail the infill patterns of basinal series and to correlate basin center and basin margin deposits (the potential source and reservoir domains) using classical wireline logs. A potentially unexplored field is the application of this type of high-resolution correlation to seismic lines.

4. High-resolution stratigraphic correlations established in this way provide a three-dimensional framework for detailed geochemical studies, and will thus allow a quantitative approach to the geochemical sediment budget.

ACKNOWLEDGMENTS

The manuscript benefited from the critical reading by Ph. Joseph, B. Carpentier, M.A. Pasley, and an unknown referee. We thank Y. Monteon and A. Nakou for drafting work.

REFERENCES CITED

- Aigner, T., 1985, Storm depositional systems—dynamic stratigraphy in modern and ancient shallow-marine sequences, series: Lecture Notes in Earth Sciences, 3: Berlin, Springer-Verlag, 174 p.
- Arthur, M.A., S.O. Schlanger, and H.C. Jenkyns, 1987, The Cenomanian–Turonian anoxic event, II. Palaeoceanographic controls on organic-matter production and preservation, *in* J. Brooks and A.J. Fleet, eds., Marine petroleum source rocks: Geological Society Special Publication 26, 401–420.
- Arthur, M.A., and W. E. Dean, 1991, A holistic geochemical approach to cyclomania: examples from Cretaceous pelagic limestone sequences, *in* G. Einsele, W. Ricken, and A. Seilacher, eds., Cycles and events in stratigraphy: Berlin, Springer-Verlag, 126–166.
- Bachaoui, E.M., and A. Ramdani, 1993, Evaluation de l'héritage et de la diagénèse dans deux cycles élémentaires de Marton-87 (Kimmeridge Clay Formation du Yorkshire, G.B.): relation avec la matière organique; Réunion du GDR 942 du CNRS, 7 Décembre Paris, Abstract, 7 p.
- Belin, S., and E. Brosse, 1992, Petrographical and geochemical study of a Kimmeridgian organic sequence (Yorkshire area, UK): *Revue de l'Institut Français du Pétrole*, 47, 711–725.
- Berger, A., M.F. Loutre, and V. Dehant, 1989, Astronomical frequencies for pre-Quaternary palaeoclimate studies: *Terra Nova*, 1, 474–479.
- Berner, R.A., 1981, A new geochemical classification of sedimentary environments: *Journal of Sedimentary Petrology*, 51, 359–365.
- Bertrand, P., and E. Lallier-Vergès, 1993, Past sedimentary organic matter accumulation and degradation controlled by productivity: *Nature*, 364, 786–788.
- Bessereau G., and F. Guillocheau, 1993, Stratigraphie séquentielle et distribution de la matière organique dans le Lias du Bassin de Paris: *Compte Rendue de l'Académie des Sciences de Paris*, 316, 1271–1278.
- Bradshaw, M.J., and S.R. Penney, 1982, A cored Jurassic sequence from north Lincolnshire, England: stratigraphy, facies analysis and regional context: *Geological Magazine*, 119, 113–134.
- Bralower, T.J., and H.R. Thierstein, 1984, Low productivity and slow deep-water circulation in Mid-Cretaceous oceans: *Geology*, 12, 614–618.
- Calvert, S.E., 1964, Factors affecting distribution of laminated diatomaceous sediments in the Gulf of California, *in* van Andel, T.J.H., and G.G. Shor, eds., Marine geology of the Gulf of California: AAPG Memoir 3, 311–330.
- Calvert, S.E., and T.F. Pedersen, 1992, Organic carbon accumulation and preservation in marine sediments: how important is anoxia?, *in* J.K. Whelan and J.W. Farrington, eds., Productivity, accumulation and preservation of organic matter in recent and ancient sediments, 231–263.
- Carpentier, B., A.Y. Huc, and G. Bessereau, 1991, Wireline logging and source rocks—estimation of organic carbon content by the carbolog method: *The Log Analyst*, 32, 279–297.

- Chénet, P.Y., and J. Francheteau, 1979, Bathymetric reconstruction method: application to the Central Atlantic Basin between 10°N and 40°N, in T. Donnelly, J. Francheteau, W. Bryan, P. Robinson, M. Flower, M. Salisbury et al., Initial Reports DSDP, 51, 52, 53, Pt. 2: Washington, U.S. Government Printing Office, 1501–1514.
- Cornford, C., 1984, Source rocks and hydrocarbons of the North Sea, in K.W. Glennie, ed., Introduction to the petroleum geology of the North Sea: Oxford, Blackwell, 197–236.
- Cope, J.C.W., T.A. Getty, M.K. Howarth, N. Morton, and H.S. Torrens, 1980, A correlation of Jurassic rocks in the British Isles, Part One, Introduction of the Lower Jurassic: Geological Society of London Special Report 14, 73 p.
- Cox, B.M., and R.W. Gallois, 1981, The stratigraphy of the Kimmeridge Clay of Dorset type area and its correlation with some other Kimmeridgian sequences: Institute for Geological Sciences, 80, 1–33.
- Dean, W.E., and M.A. Arthur, 1987, Inorganic and organic geochemistry of Eocene to Cretaceous strata recovered from the lower continental rise, North American Basin, Site 603, DSDP Leg 93, in S.W. Wise Jr. and J.E. van Hinte et al., Initial Reports DSDP 93: Washington, U.S. Government Printing Office, 1093–1197.
- de Boer, P.L., 1982, Cyclicity and storage of organic matter in Middle Cretaceous pelagic sediments, in G. Einsele and A. Seilacher, eds., Cyclic and event stratification: Berlin, Springer Verlag, 456–475.
- de Boer, P.L., 1983, Aspects of middle Cretaceous pelagic sedimentation in southern Europe: *Geologica Ultraiectina*, 31, 112 p.
- de Boer, P.L., 1986, Changes in the organic carbon burial during the Early Cretaceous, in C.P. Summerhayes and N.J. Shackleton, eds., North Atlantic Paleooceanography: Geological Society of London Special Publication 21, 321–331.
- de Boer, P.L., 1991, Pelagic black shale—carbonate rhythms: orbital forcing and oceanographic response, in G. Einsele, W. Ricken, and A. Seilacher, eds., Cycles and events in stratigraphy: Berlin, Springer-Verlag, 63–78.
- de Boer, P.L., and D.G. Smith, 1994a, Orbital forcing and cyclic sedimentary sequences, in P.L. de Boer and D.G. Smith, eds., Orbital forcing and cyclic sedimentary sequences: Special Publications of the International Association of Sedimentologists, 19, 1–14.
- de Boer, P.L., and D.G. Smith, 1994b, Orbital forcing and cyclic sedimentary sequences: Special Publications of the International Association of Sedimentologists, 19, 559 p.
- Degens, E.T., K-C. Emeis, B. Mycke, and M.G. Wiesner, 1986, Turbidites, the principal mechanism yielding black shales in the early deep Atlantic Ocean, in C.P. Summerhayes and N.J. Shackleton, eds., North Atlantic Paleooceanography: Geological Society Special Publication 21, 361–376.
- Demaison, G.J., and G.T. Moore, 1980, Anoxic environments and oil source bed genesis: AAPG Bulletin, 64, 1179–1209.
- Devine, P.E., 1991, Transgressive origin of channeled estuarine deposits in the Point Lookout Sandstone, northwestern New Mexico: a model for Upper Cretaceous cyclic regressive parasequences of the U.S. Western Interior: AAPG Bulletin, 75, 1039–1063.
- Donovan, D.T., A. Horton, and H.C. Ivimey-Cook, 1979, The transgression of the Lower Lias over the northern flank of the London Platform: *Journal of the Geological Society of London*, 136, 165–173.
- Dore, A.G., and M.S. Gage, 1987, Crustal alignments and sedimentary domains in the evolution of the North Sea, north-east Atlantic margin and Barentz Shelf, in J. Brooks and K. Glennie, eds., Petroleum Geology of North-West Europe: London, Graham and Trotman, 1131–1148.
- Droste, H., 1990, Depositional cycles and source rock development in an epeiric intra-platform basin: the Hanifa Formation of the Arabian peninsula: *Sedimentary Geology*, 69, 281–296.
- Dunn, C.E., 1974, Identification of sedimentary cycles through Fourier analysis of geochemical data: *Chemical Geology*, 13, 217–232.
- Einsele, G., W. Ricken, and A. Seilacher, 1991, Cycles and events in stratigraphy: Berlin, Springer-Verlag, 955 p.
- Erba, E., 1993, Calcareous nannofossils premonish Mesozoic anoxic events: Terra Abstracts, Abstract Supplement no. 1 to Terra Nova, 5, p. 688.
- Eschard, R., B. Tveiten, G. Desaubliaux, J.C. Lecomte, and F.S.P. van Buchem, 1993, High resolution sequence stratigraphy and reservoir prediction of the Brent Group (Tampen Spur area) using an outcrop analogue (Mesaverde Group, Colorado), in R. Eschard and B. Doligez, eds., Subsurface reservoir characterization from outcrop observations: Paris, Editions Technip, 35–52.
- Fischer, A.G., T.D. Herbert, and I. Primoli-Silva, 1985, Carbonate bedding cycles in Cretaceous pelagic and hemipelagic sediments, in L.M. Pratt, E.G. Kaufmann, and F.B. Zelt, eds., Fine-grained deposits and biofacies of the Cretaceous Western Interior Seaway: evidence of cyclic sedimentary processes: SEPM Excursion Guide, 1–10.
- Fischer, A.G., P.L. de Boer, and I. Primoli-Silva, 1990, Cyclostratigraphy, in R.N. Ginsburg and B. Beaudouin, eds., Cretaceous resources, events and rhythms: Reidel, NATO ASI ser. C, 139–172.
- Fischer, A.G., and D.J. Bottjer, 1991, Orbital forcing and sedimentary sequences: *Journal of Sedimentary Petrology Special Issue* 61, 1063–1252.
- Froelich, P.N., G.P. Klinkhammer, M.L. Bender, N.A. Luedtke, G.R. Heath, D. Cullen, P. Dauphin, D. Hammond, B. Hartman, and V. Maynard, 1979, Early oxidation of organic matter in pelagic sediments of the eastern equatorial Atlantic: suboxic diagenesis: *Geochimica et Cosmochimica Acta*, 43, 1075–1090.
- Gale, A.S., H.C. Jenkyns, W.J. Kennedy, and M.R. Corfield, 1993, Chemostratigraphy versus biostratigraphy: data from around the Cenomanian–Turonian boundary: *Journal of the Geological Society of London*, 150, 29–32.

- Gallois, R.W., 1976, Coccolith blooms in the Kimmeridgian Clay and the origin of North Sea oil: *Nature*, 259, 473–475.
- Garrels, R.M., and A. Lerman, 1984, Coupling of sedimentary sulfur and carbon cycles—an improved model; *American Journal of Science*, 284, 989–1007.
- Gaunt, G.D., H.C. Ivimey-Cook, I.E. Penn, and B.M. Cox, 1980, Mesozoic rocks proved by IGS boreholes in the Humber and Acklam areas: Report of the Institute of Geological Sciences, 79/13.
- Goldhammer, R.K., E.J. Oswald, and P.A. Dunn, 1991, Hierarchy of stratigraphic forcing: example from Middle Pennsylvanian shelf carbonates of the Paradox basin, in E.K. Franseen, W.L. Watney, Ch. G. St. C. Kendall, and W. Ross, eds., *Sedimentary modeling: computer simulations and methods for improved parameter definition: Kansas Geological Survey Bulletin*, 233, 361–414.
- Goldhammer, R.K., E.J. Oswald, and P.A. Dunn, 1994, High-frequency, glacio-eustatic cyclicity in the Middle Pennsylvanian of the Paradox Basin: an evaluation of Milankovitch forcing, in P.L. de Boer and D.G. Smith, eds., *Orbital forcing and cyclic sedimentary sequences: Special Publications of the International Association of Sedimentologists* 19, 243–285.
- Grace, J.D., and G.F. Hart, 1986, Giant gas fields of northern west Siberia: *AAPG Bulletin*, 70, 830–852.
- Grammer, G.M., G.P. Eberli, F.S.P. van Buchem, R. Eschard, P. Homewood, and G.M. Stevenson, 1994, Laterally discontinuous reservoir facies controlled by multiple orders of sea level change, Paradox basin, Utah, U.S.A. (abs.), in *Sequence stratigraphy of petroleum reservoirs and applications to development geology: AAPG Hedberg Research Conference*, Paris.
- Grant, A.C., L.F. Jansa, K.D. McAlpine, and A. Edwards, 1988, Mesozoic–Cenozoic geology of the eastern margin of the Grand Banks and its relation to Galicia Bank: *Proc. ODP*, 103, 787–807.
- Grötsch, J., 1993, Cyclostratigraphic analysis of a carbonate formation (Early Aptian, Oman): implications for sequence stratigraphic interpretation (abs.), in *Models for exploration and development: Geological Society of London Meeting on Carbonate Petroleum Reservoirs*.
- Hallam, A., 1988, A re-evaluation of Jurassic eustasy in the light of new data and the revised Exxon curve: *SEPM Special Publication* 42, 261–273.
- Harland, W.B., R.L. Armstrong, A.V. Cox, L.E. Craig, A.G. Smith, and D.G. Smith, 1990, *A geologic time scale 1989*: Cambridge University Press, 263 p.
- Haq, B.U., J. Hardenbol, and P.R. Vail, 1987, Chronology of fluctuating sea levels since the Triassic: *Science*, 235, 1156–1167.
- Herbert, T.D., and A.G. Fischer, 1986, Milankovitch climatic origin of mid-Cretaceous black shale rhythms in central Italy: *Nature*, 321, 739–743.
- Herbin, J.P., L. Montadert, C. Müller, R. Gomez, J. Thurow, and J. Wiedmann, 1986, Organic-rich sedimentation at the Cenomanian–Turonian boundary in oceanic and coastal basins in the North Atlantic and Tethys, in C.P. Summerhayes and N.J. Shackleton, eds., *North Atlantic Palaeoceanography: Geological Society Special Publication* 21, 389–422.
- Herbin, J.P., E. Masure, and J. Roucache, 1987, Cretaceous formations from the lower continental rise off Cape Hatteras: organic geochemistry, dinoflagellate cysts, and the Cenomanian/Turonian boundary event at sites 603 (Leg 93) and 105 (Leg 11), in J.E. van Hinte and S.W. Wise, eds., *Initial Reports of the DSDP, 93*: Washington, U.S. Government Printing Office, 1139–1162.
- Herbin, J.P., C. Müller, J.G. Geysant, F. Melieres, and I.E. Penn, 1991, Hétérogénéité quantitative et qualitative de la matière organique dans les argiles du Kimmeridgien du val de Pickering (Yorkshire, UK): *Revue de l'Institut Français du Pétrole*, 46, 675–712.
- Herbin, J.P., J.R. Geysant, F. Mélières, C. Müller, and I.E. Penn, 1993, Variation of the distribution of organic matter within a transgressive systems tract: Kimmeridge Clay (Jurassic) England, in B. Katz and L. Pratt, eds., *Petroleum source rocks in a sequence stratigraphic framework: AAPG Studies in Geology* 37, 67–100.
- Herbin, J.P., and J.R. Geysant, 1993, Ceintures organiques au Kimméridgien/Tithonien en Angleterre (Yorkshire, Dorset) et en France (Boulonnais): *Comptes Rendue de l'Académie des Sciences de Paris*, 317, 1309–1316.
- Herbin, J.P., J.R. Geysant, A. El Albani, J.P. Colbeaux, J.F. Deconinck, J.L. Fernandez-Martinez, J.N. Proust, and J.P. Vidier, 1995, Sequence stratigraphy of source rocks applied to the study of the Kimmeridgian/Tithonian in the northwest European shelf (Dorset/UK, Yorkshire/UK and Boulonnais/France): *Marine and Petroleum Geology*, 2.
- Hilgen, F.J., and C.G. Langereis, 1989, Periodicities of CaCO₃ cycles in the Pliocene of Sicily: discrepancies with the quasi-periods of the Earth's orbital cycles?: *Terra Nova*, 1, 409–415.
- Horton, A., and E.G. Poole, 1977, The lithostratigraphy of three geophysical marker horizons in the Lower Lias of Oxfordshire: *Bulletin of the Geological Survey GB*, 62, 13–24.
- Hollister, C.D., J.I. Ewing et al., 1972, *Initial Reports of the DSDP, 11*: Washington, U.S. Government Printing Office.
- Huc, A.Y., 1988, Sedimentology of organic matter, in F.H. Frimmel and R.F. Chrisman, eds., *Humic substances and their role in the environment: S. Bernard, Dahlem Konferenzen*, 215–243.
- Huc, A.Y., E. Lallier-Verges, P. Bertrand, B. Carpentier, and D.J. Hollander, 1992, Organic matter response to change of depositional environment in Kimmeridgian Shales, Dorset U.K., in J. Whelan and J. Farrington, eds., *Organic matter, productivity, accumulation and preservation in recent sediments*, 469–486.
- Jefferies, R.P.S., 1961, The palaeoecology of the Actinocamax Plenus subzone (lowest Turonian) in the Anglo-Paris basin: *Palaeontology*, 4, 609–647.
- Jefferies, R.P.S., 1963, The stratigraphy of the Actinocamax Plenus subzone (Turonian) in the Anglo-Paris basin: *Proc. Geol. Assoc.*, 74, 1–33.
- Jenkyns, H., 1980, Cretaceous anoxic events: from con-

- tinents to oceans: *J. Geol. Soc. London*, 137, 171–188.
- Jenkyns, H., 1985, The early Toarcian and Cenomanian–Turonian anoxic events in Europe: comparison and contrasts: *Geologische Rundschau*, 74, 505–518.
- Kauffman, E.G., 1988, Concepts and methods of high-resolution event stratigraphy: *Annual Review of Earth Sciences*, 16, 605–654.
- Kendrick, J.W., 1979, Geochemical studies of black clays from Leg 43, Deep Sea Drilling Project, in B.E. Tucholke and P.R. Vogt et al., Initial Reports of the DSDP, 43: Washington, U.S. Government Printing Office, 633–642.
- Kuhnt, W., J.P. Herbin, J. Thurov, and J. Wiedman, 1990, Distribution of Cenomanian–Turonian organic facies in the western Mediterranean and along the adjacent Atlantic margin, in A.Y. Huc, ed., Deposition of organic facies: AAPG Studies in Geology 30, 133–160.
- Lallier-Vergès, E., P. Bertrand, A.Y. Huc, B. Buckel, and P. Tremblay, 1993, Control on the preservation of organic matter by productivity and sulphate reduction in Kimmeridgian shales from Dorset (UK): *Marine and Petroleum Geology*, 10, 600–605.
- Lovelock, J.E., 1987, *Gaia—a new look at life on earth*, 2nd rev. ed.: Oxford University Press, 154 p.
- Lovelock, J.E., 1989, Geophysiology, the science of GAIA: *Reviews of Geophysics*, 27, 215–222.
- Mann, A.L., and K.J. Myers, 1990, The effect of climate on the geochemistry of the Kimmeridge Clay Formation, in Biomarkers in Petroleum, Memorial Symposium for W. Seifert: American Chemical Society, Division of Petroleum Chemistry, 139–142.
- Matthews, R.K., 1984, *Dynamic stratigraphy, an introduction to sedimentation and stratigraphy*, 2nd ed.: New Jersey, Prentice Hall, 489 p.
- Maynard, J.B., 1982, Extension of Berner's "New geochemical classification of sedimentary environments" to ancient sediments: *Journal of Sedimentary Petrology*, 52, 1325–1331.
- McCave, I.N., 1979a, Depositional features of organic-carbon-rich black and green mudstones at DSDP sites 386 and 387, western North Atlantic, in B.E. Tucholke and P.R. Vogt et al., Initial Reports of the DSDP, 43: Washington, U.S. Government Printing Office, 411–416.
- McCave, I.N., 1979b, Diagnosis of turbidites at sites 386 and 387 by particle-counter size analysis of the silt (2–40 microm.) fraction, in B.E. Tucholke and P.R. Vogt et al., Initial Reports of the DSDP, 43: Washington, U.S. Government Printing Office, 395–406.
- Melnyk, D.H., and Smith, D., 1989, Outcrop to subsurface cycle correlation in the Milankovitch frequency band: middle Cretaceous, central Italy: *Terra Nova*, 1, 432–436.
- Melnyk, D.H., D.G. Smith, and K. Amiri-Garroussi, 1994, Filtering and frequency mapping as tools in subsurface cyclostratigraphy, with examples from the Wessex Basin, UK, in P.L. de Boer and D.G. Smith, eds., *Orbital forcing and cyclic sedimentary sequences*: International Association of Sedimentologists Special Publication 19, 35–46.
- Meyers, P.A., 1987, Synthesis of organic geochemical studies, Deep Sea Drilling Project Leg 93, North American continental margin, in van Hinte, J.E., and S.W. Wise Jr. et al., Initial Reports DSDP, 93: Washington, U.S. Government Printing Office, 1333–1342.
- Mitchum, R.M., and J.C. Van Wagoner, 1991, High frequency sequences and their stacking patterns: sequence stratigraphic evidence of high frequency eustatic cycles: *Sedimentary Geology*, 70, 131–160.
- Molenaar, C.M., and J.K. Baird, 1991, Stratigraphic cross sections of upper Cretaceous Rocks in the Northern San Juan Basin, Southern Ute Indian Reservation, Southwestern Colorado, in R. Zech, ed., *Geologic framework and stratigraphy of Cretaceous and Tertiary rocks of the Southern Ute Indian Reservation, Southwestern Colorado*: U.S. Geological Survey Professional Paper 1505 B-C.
- Mountjoy, E.W., 1965, Stratigraphy of the Miette reef complex and associated strata, eastern Jasper Park, Alberta: *GSC Bulletin*, 110, 132 p.
- Mountjoy, E.W., 1980, Some questions about the development of Upper Devonian carbonate buildups (reefs), Western Canada: *Bulletin of Canadian Petroleum Geology*, 28, 315–344.
- Müller, C., A. Schaaf, and J. Sigal, 1983–1984, Biochronostratigraphie des formations d'âge crétacé dans les forages du DSDP dans l'Océan Atlantique Nord: *Revue de l'Institut Français du Pétrole*, Première partie, 38, 683–708, Deuxième partie, 39, 3–24.
- Oschmann, W., 1988, Kimmeridge Clay sedimentation—a new cyclic model: *Palaeogeography, Palaeoclimatology, Palaeoecology*, 65, 217–251.
- Oschmann, W., 1990, Environmental cycles in the late Jurassic northwest European epeiric basin: interaction with atmospheric and hydrospheric circulations: *Sedimentary Geology*, 69, 313–332.
- Palmer, J.J., and A.J. Scott, 1984, Stacked shoreline and shelf sandstone of La Ventana Tongue (Campanian), northwestern New Mexico: *AAPG Bulletin*, 68, 74–91.
- Pasley, M.A., G.W. Riley, and D. Nummedal, 1993, Sequence stratigraphic significance of organic matter variations: example from the Upper Cretaceous Marcos Shale of the San Juan basin, New Mexico: *AAPG Studies in Geology* 37, 221–242.
- Pedersen, T.F., and S.E. Calvert, 1990, Anoxia vs. productivity: what controls the formation of organic-carbon-rich sediments and sedimentary rocks?: *AAPG Bulletin*, 74, 454–466.
- Plint, A.G., B.S. Hart, and W.S. Donaldson, 1993, Lithospheric flexure as a control on stratal geometry and facies distribution in Upper Cretaceous rocks of the Alberta foreland basin: *Basin Research*, 5, 69–77.
- Pradier, B., and Ph. Bertrand, 1992, Etude à haute résolution d'un cycle du carbone organique de roche-mère du Kimmeridgien du Yorkshire (G.B.): relation entre composition pétrographique du contenu organique observé in situ teneur en carbone organique et qualité pétrologène: *C.R. Acad. Sci. Paris*, 315, 187–192.
- Pratt, L.M., E.G. Kaufmann, and F.B. Zelt, 1985, Fine-grained deposits and biofacies of the Cretaceous

- Western Interior Seaway: evidence of cyclic sedimentary processes: SEPM Field Trip Guidebook 4.
- Ramanampisoa, L., P. Bertrand, J.-R. Disnar, E. Lallier-Vergès, B. Pradier, and N.J. Tribovillard, 1992, Etude à haute résolution d'un cycle de carbone organique des argiles du Kimméridgien du Yorkshire (Grande-Bretagne): résultats préliminaires de géochimie et de pétrographie organique: C.R. Acad. Sci. Paris, 314, 1493–1498.
- Ricken, W., 1991, Variations of sedimentation rates in rhythmically bedded sediments: distinction between depositional types, in G. Einsele, W. Ricken, and A. Seilacher, eds., *Cycles and events in stratigraphy*: Berlin, Springer-Verlag, 167–187.
- Rüllkoter, J., P.K. Mukhopadhyay, and D.H. Welte, 1987, Geochemistry and petrography of organic matter from Deep Sea Drilling Project Site 603, Lower Continental Rise off Cape Hatteras, in J.E. van Hinte, S.W. Wise Jr. et al., DSDP 93: Washington, U.S. Government Printing Office, 1163–1176.
- Scholle, P.A., and M.A. Arthur, 1980, Carbon isotope fluctuations in Cretaceous pelagic limestones: potential stratigraphic and petroleum exploration tool: AAPG Bulletin, 64, 67–87.
- Schlanger, S.O., M.A. Arthur, H.C. Jenkyns, and P.A. Scholle, 1987, The Cenomanian–Turonian oceanic anoxic event. I. Stratigraphy and distribution of organic carbon-rich beds and the marine $\delta^{13}\text{C}$ excursion, in J. Brooks and A.J. Fleet, eds., *Marine petroleum source rocks*: Geol. Soc. Special Publication 26, 371–399.
- Sellwood, B.W., 1970, The relation of trace fossils to small scale sedimentary cycles in the British Lias, in T.P. Crimes and J.C. Harper, eds., *Trace fossils*: Geol. J. Spec. Issue 3, 489–504.
- Sellwood, B.W., 1972, Regional environmental changes across a Lower Jurassic stage boundary in Britain: *Palaeontology*, 15, 125–157.
- Shackleton, N., 1987, The carbon isotope record of the Cenozoic: history of organic carbon burial and of oxygen in the ocean and atmosphere, in J. Brooks and A.J. Fleet, eds., *Marine Petroleum Source Rocks*: Geological Society Special Publication 26, 423–434.
- Simpson, M., 1884, *The fossils of the Yorkshire Lias described from nature*, 2nd. ed.: Wheldon, London and Forth, Whitby.
- Smith, D.G., 1989, Stratigraphic correlation of presumed Milankovitch cycles in the Blue Lias (Hettangian to earliest Sinemurian), England: *Terra Nova*, 1, 457–460.
- Stein, R., 1986, Organic carbon and sedimentation rate—further evidence for anoxic deep-water conditions in the Cenomanian/Turonian Atlantic ocean: *Marine Geology*, 72, 199–209.
- Stein, R., 1991, Accumulation of organic carbon in marine sediments: *Lecture Notes in Earth Sciences*, 34, 217 p.
- Stoakes, F.A., 1980, Nature and control of shale basin fill and its effect on reef growth and termination: Upper Devonian Duvernay and Ireton Formations of Alberta, Canada: *Bull. of Can. Petr. Geology*, 28, 345–410.
- Stow, D.A.V., and W.E. Dean, 1984, Middle Cretaceous black shales at Site 530 in the southeastern Angola Basin: DSDP Initial Reports, 75, 809–815.
- Summerhayes, C.P., W.L. Prell, and K.C. Emeis, 1992, Upwelling systems: evolution since the early Miocene: Geological Society Special Publication 64, 519 p.
- Tate, R., and J. Blake, 1876, *The Yorkshire Lias*: London, J. van Voorst, 475 p.
- Thurrow, J., and W. Kuhnt, 1986, Mid-Cretaceous of the Gibraltar Arch area, in C.P. Summerhayes and N.J. Shackleton, eds., *North Atlantic Palaeoceanography*: Geological Society Special Publication 22, 423–445.
- Tissot, B., 1979, Effects of prolific petroleum source rocks and major coal deposits caused by sea level changes: *Nature*, 277, 463–465.
- Tissot, B.P., and D.H. Welte, 1984, *Petroleum formation and occurrence*: Berlin, Springer Verlag.
- Tribovillard, J.-P., and P. Cotillon, 1989, Relationships between climatically influenced sedimentation and salt diapirism in the French Western Alps based on evidence from organic and inorganic geochemistry: *Paleogeography, Paleoclimatology, and Paleocology*, 71, 271–280.
- Tribovillard, N.-P., A. Desprairies, E. Lallier-Vergès, P. Bertrand, N. Moureau, A. Ramdani, and L. Ramanampisoa, 1994, Geochemical study of organic-matter rich cycles from the Kimmeridge Clay Formation of Yorkshire (UK): productivity versus anoxia: *Palaeogeography, Palaeoclimatology, Palaeoecology*, 108, 165–181.
- Tucholke et al., 1979, *Initial Reports of the Deep Sea Drilling Project*, 93: Washington, U.S. Government Printing Office.
- Tyson, R.V., 1987, The genesis and palynofacies characteristics of marine petroleum source rocks, in J. Brooks and A.J. Fleet, eds., *Marine petroleum source rocks*: Geological Society Special Publication 26, 47–67.
- Tyson, R.V., and T.H. Pearson, 1991, Modern and ancient continental shelf anoxia: an overview, in R.V. Tyson and T.H. Pearson, eds., *Modern and ancient continental shelf anoxia*: Geological Society Special Publication 58, 1–26.
- Vahrenkamp, V., 1994, Improved age correlation in shallow water carbonate sequences with carbon isotope stratigraphy: the Aptian Shuaiba Formation, Oman and United Arab Emirates (abs.): AAPG Annual Convention, Denver, p. 274.
- Vail, P.R., F. Audemard, S.A. Bowman, P.N. Eisner, and C. Perez-Cruz, 1991, The stratigraphic signatures of tectonics, eustasy and sedimentology—an overview, in G. Einsele, W. Ricken, and A. Seilacher, eds., *Cycles and events in stratigraphy*, 617–659.
- van Buchem, F.S.P., 1990, *Sedimentology and diagenesis of Lower Lias mudstones in the Cleveland Basin, N.E. Yorkshire, U.K.*: Unpublished Ph.D. Thesis, University of Cambridge, 257 p.
- van Buchem, F.S.P., and I.N. McCave, 1989, Cyclic sedimentation patterns in Lower Lias mudstones of Yorkshire, G.B.: *Terra Nova*, 1, 461–467.
- van Buchem, F.S.P., D.H. Melnyk, and I.N. McCave,

- 1992, Chemical cyclicity and correlation of Lower Lias mudstones using gamma ray logs, Yorkshire, UK: *Journal of the Geological Society, London*, 149, 991–1002.
- van Buchem, F.S.P., I.N. McCave, and G.P. Weedon, 1994, Orbitally induced small scale cyclicity in a siliciclastic epicontinental setting (Cleveland Basin, lower Lias, Yorkshire, UK), *in* P.L. de Boer and D.G. Smith, eds., *Orbital forcing and cyclic sedimentary sequences: International Association of Sedimentologists Special Publication 19*, 345–366.
- van Buchem, F.S.P., G.P. Eberli, M.T. Whalen, O. Lerat, E.W. Mountjoy, and P. Homewood, 1994, Geometry and facies of reservoir and source rocks in the Upper Devonian carbonate system of Western Canada (abs.), *in* *Sequence stratigraphy of petroleum reservoirs and applications to development geology: AAPG Hedberg Research Conference*, Paris.
- Vandenbergh, N., 1978, Sedimentology of the Boom Clay (Rupelian) in Belgium: *Proceedings of the Koninklijke Akademie voor Wetenschappen Belgie*, 40, 1–137.
- van Echenpoel, E., and G.P. Weedon, 1990, Milankovitch cyclicity and the Boom Clay Formation: an Oligocene siliciclastic shelf sequence in Belgium: *Geological Magazine*, 127, 599–604.
- van Hinte, J.E., et al., 1987, Initial reports of the Deep Sea Drilling Project, 93: Washington, U.S. Government Printing Office.
- Van Wagoner, J.C., H.W. Posamentier, R.M. Mitchum, P.R. Vail, J.F. Sarg, T.S. Loutit, and J. Hardenbol, 1988, An overview of the fundamentals of sequence stratigraphy and key definitions, *in* C. Wilgus, B. Hastings, C. Ross, H. Posamentier, J. Van Wagoner, and L.G. St. C. Kendall, eds., *Sea-level changes—an integrated approach: SEPM Special Publication 42*, 39–45.
- Van Wagoner, J.C., R.M. Mitchum, K.M. Campion, and V.D. Rahmanian, 1990, Siliciclastic sequence stratigraphy in well logs, core and outcrops: concepts for high-resolution correlation of time and facies: *AAPG Methods in Exploration* 7, 55 p.
- Waterhouse, H.K., 1992, Unpublished Ph.D. Thesis, University of Southampton.
- Weedon, G.P., 1991, The spectral analysis of stratigraphic time series, *in* G. Einsele, W. Ricken, and A. Seilacher, eds., *Cycles and events in stratigraphy: Berlin, Springer-Verlag*, 840–854.
- Weedon, G.P., 1993, The recognition and stratigraphic implications of orbital-forcing of climate and sedimentary cycles: *Sedimentology Review*, 1, 31–50.
- Weedon, G.P., and H. Jenkyns, 1990, Regular and irregular climatic cycles and the Belemnite Marls (Pliensbachian, Lower Jurassic, Wessex basin): *Journal of the Geological Society of London*, 147, 915–918.
- Weltje, G.J., and P.L. de Boer, 1993, Astronomically induced paleoclimatic oscillations reflected in Pliocene turbidite deposits on Corfu (Greece): implications for the interpretation of higher order cyclicity in fossil turbidite systems: *Geology*, 21, 307–310.
- Whalen, M.T., G.P. Eberli, F.S.P. van Buchem, E.W. Mountjoy, and P. Homewood, 1993, Sequence stratigraphy and platform to basin correlation in a mixed carbonate-siliciclastic system, late Devonian, western Alberta (abs.): *GSA Meeting, Boston*.
- Wignall, P., 1989, Sedimentary dynamics of the Kimmeridge Clay: tempests and earthquakes: *Journal of the Geological Society, London*, 146, 273–284.
- Wignall, P.B., and A. Ruffel, 1990, The influence of a sudden climatic change on marine deposition in the Kimmeridgian of northwest Europe: *Journal of the Geological Society of London*, 147, 365–371.
- Wignall, P.B., and A. Hallam, 1991, Biofacies, stratigraphic distribution and depositional models of British onshore Jurassic black shales, *in* R.V. Tyson and T.H. Pearson, eds., *Modern and ancient continental shelf anoxia: Geological Society Special Publication 58*, 291–310.
- Wilson, H.E., and P.I. Manning, 1978, *Geology of the Causeway Coast: Mem. Geol. Surv. North. Irel., Belfast*.
- Worsley, T.R., and D.L. Kidder, 1991, First-order coupling of paleogeography and CO₂ with global surface temperature and its latitudinal contrast: *Geology*, 19, 1161–1164.
- Wright, R., 1986, Cycle stratigraphy as a paleogeographical tool: Point Lookout Sandstone, southeastern San Juan Basin, New Mexico: *GSA Bulletin*, 96, 661–673.
- Ziegler, P.A., 1988, *Geological atlas of Western and Central Europe: Shell International Petroleum Maatschappij B.V.*, 2 volumes.
- Zijlstra, J.J.P., 1994, *Sedimentology of the Late Cretaceous and early Tertiary tuffaceous chalk of Northwest Europe: Geol. Ultraict.*, 119.